VOL. 7

POLYMER

The Chemistry, Physics and Technology of High Polymers

BUTTERWORTHS
LONDON
1966

The Polymerization of Some Ethylene Oxides by the Diethylzinc – Water System

J. MALCOLM BRUCE and S. J. HURST

A kinetic study of the polymerization of several monosubstituted ethylene oxides by the diethylzinc–water system is described. The results are discussed in terms of possible mechanisms, and it is concluded that steric factors probably play a dominant role in determining the rate of polymerization. The polymerization of styrene oxide appears to be of a rather different character from that of the alkyl substituted ethylene oxides.

THE polymerization of ethylene oxides by products from the partial hydrolysis of dialkylzincs has been known for several years, and a recent study[1] of the polymerization of propylene oxide by the diethylzinc–water system has shown that when the molar ratio of water to diethylzinc is 0·4 the monomer is consumed in two stages, an initial fast one producing low molecular weight polymer, and a subsequent slower one yielding high molecular weight polymer. However, firm conclusions concerning the nature of the catalytically active species could not be drawn, and it was hoped that the use of other variously substituted ethylene oxides might afford indirect evidence relating to this problem. Polymerizations of ethylene oxide, four of its monoalkyl derivatives, and styrene oxide under conditions similar to those previously used for propylene oxide are described in the present paper, results for propylene oxide being included for comparison.

EXPERIMENTAL AND RESULTS

Ethylene oxide was dried over calcium hydride, distilled, and stored at 0°C. 1-Butene oxide was purified by preparative vapour phase chromatography. *t*-Butylethylene oxide[2], neopentylethylene oxide[2], and styrene oxide were fractionally distilled, the latter under reduced pressure. These monomers and propylene oxide were stored over calcium hydride. Other materials were purified as previously described[1], and reactants and solvents were transferred to the dilatometers used for the kinetic studies by the vacuum-line technique[1]. Polymerizations in dioxan using initial concentrations of monomer and diethylzinc of, respectively, 0·82 and 0·146 mole l^{-1}, and a molar ratio of water to diethylzinc of 0·4 were carried out in the dilatometers at 60°C, but, except for styrene oxide systems when 60°C was used, cathetometer readings of the meniscus levels were taken at 25°C, the rate of polymerization being negligible at this temperature. The densities of 1-butene oxide and neopentylethylene oxide at 25°C, and of styrene oxide at 60°C, required for interpretation of the dilatometric results,

were determined with a pyknometer and were, respectively, 0·830, 0·829 and 1·018 g cm^{-3}. Densities of the other monomers have been reported previously. The dilatometric results for neopentylethylene oxide were somewhat scattered above 20 per cent conversion, possibly due to precipitation of polymer. Reproducible results were not obtained for *t*-butylethylene oxide since separation of polymer commenced at an early stage, and the reaction was extremely slow.

In order to assess the rate of polymerization during the slow stage it was necessary to know the value of the dilatometric contraction (C_{100}) for 100 per cent polymerization, and the partial specific volume ($\bar{v}_2$) of the polymer in the polymerization mixture was therefore required. It was determined with a pyknometer at 25°C for dioxan solutions containing concentrations of polymer comparable with those produced in the dilatometer: for the polymers from ethylene-, propylene-, and 1-butene-oxide, respectively, $\bar{v}_2 = 0{\cdot}919$, 1·012, and 1·069 cm^3 g^{-1}. The solubility of poly(neopentylethylene oxide) was too low for comparable measurements to be made, and $\bar{v}_2$ was estimated to be 1·059 cm^3 g^{-1}. For poly(styrene oxide) $\bar{v}_2$ at 60°C, calculated from the volume contraction per gramme of polymer produced, was 0·874 cm^3 g^{-1}.

The rate of the initial fast reaction was determined from the slope of the tangent to the dilatometric contraction, C_t, versus time, t, curve at zero time, and the conversion during this stage was found by extrapolating the linear portion, corresponding with the slow stage, of a plot of $\log(C_{100} - C_t)$ versus t back to zero time.

Overall conversions were determined by isolation of the polymers as previously described[1]. Intrinsic viscosities, [η], were measured at 25°C for benzene solutions, except with poly(styrene oxide) when toluene was used as the solvent, and viscosity-average molecular weight ($\overline{M}_v$) were calculated for poly(ethylene oxide) using the equation[3] $[\eta] = 3{\cdot}97 \times 10^{-4}\,\overline{M}_v^{0{\cdot}686}$, and for

Table 1. Polymerization of ethylene oxides, R—CH(O)CH$_2$

R	*Fast stage*		*Slow stage*	*Overall*			
	$10^2 \times$ *Estimated initial rate, mole* $l^{-1}\,h^{-1}$	*Estimated conversion, %*	$10^3 \times$ *first order rate constant,* h^{-1}	*Polymerization time, h*	*Conversion, %*	$[\eta]$ $dl\,g^{-1}$	*Nature of product*
H	3·7 3·8	19 18	6·5 4·5	786 615	81 75	0·64 (*a*) 0·74 (*b*)	White powder
Me	2·1 1·8	8 8	5·1 4·1	275 277	77 71	(*c*) (*d*)	Rubber
Et	1·3 1·3	10 12	2·2 1·9	2 124 1 451	79 66	3·5 2·2	Tacky rubber
Bu^{t}CH$_2$	0·7	11	0·2	1 356	30	0·97	Tacky rubber
Bu^t	— —	— —	— —	2 793 2 606	15 14	— —	Viscous oil + fibrous material (*e*)
Ph	(*f*) (*h*)	— —	— —	497 49 (*i*)	90 79	0·56 (*g*) 0·53 (*j*)	Glass

(*a*) $\overline{M}_v = 48\,000$. (*b*) $\overline{M}_v = 58\,000$. (*c*) $\overline{M}_v = 480\,000$. (*d*) $\overline{M}_v = 450\,000$. (*e*) Combined polymeric products soluble in benzene at 25° had $\overline{M}_n = 650$. (*f*) $10^2 \times$Zero order rate constant = 1·48 mole l^{-1} h^{-1}. (*g*) $\overline{M}_v = 125\,000$; $\overline{M}_n = 1000$. (*h*) $10^2 \times$Zero order rate constant = 1·42 mole l^{-1} h^{-1}. (*i*) End of fast stage. (*j*) $\overline{M}_v = 120\,000$; $\overline{M}_n = 800$.

poly(styrene oxide) using the equation[4] $[\eta]=6{\cdot}79\times10^{-5}\,\bar{M}_v^{0{\cdot}766}$. Number-average molecular weights ($\bar{M}_n$) were determined for benzene solutions using a Mechrolab vapour pressure osmometer. Proton magnetic resonance spectra were measured with a Varian A-60 spectrometer for solutions in carbon tetrachloride at 40°C.

Duplicate experiments were usually performed, and the results are summarized in *Table 1*.

DISCUSSION

For the alkyl-substituted ethylene oxides listed in *Table 1* polymerization is characterized by an initial fast consumption of up to 20 per cent of the monomer followed by a slower consumption of the remainder, as has previously been reported[1] for propylene oxide. The slower stage is first order in monomer for ethylene-, propylene-, and 1-butene-oxide, and is probably first order for the neopentyl- and *t*-butyl-compounds also, although accurate assessments were not obtained in these cases owing to, respectively, the low solubility of poly(neopentylethylene oxide) which necessitated the use of an estimated value for $\bar{v}_2$, and the very slow polymerization of *t*-butylethylene oxide. Thus the qualitative features of the polymerization are not greatly altered by the substituent R. However, the rates of polymerization are appreciably dependent on it, and for both the fast and slow stages are in the order $R=H>Me>Et>Bu^tCH_2>Bu^t$. The most striking changes in the overall conversion rate occur for $R=Bu^tCH_2$ and, particularly, for $R=Bu^t$, and in the latter case the polymer eventually isolated is of comparatively low molecular weight.

Polymerization[5] of styrene oxide was initially much faster than that of the other monomers, and had proceeded to about 80 per cent conversion before the slow stage commenced, the rate then being similar to that of the slow stage for neopentylethylene oxide. The initial stage appeared to be zero order in monomer, and the overall features of the polymerization may be different from those of the alkyl-substituted ethylene oxides.

Precipitation of catalyst was not observed during any of the polymerizations. The mixture was colourless only for ethylene oxide, but for the other monomers it was yellow, the colour being particularly strong with styrene oxide. The influence of the phenyl group on the optical properties of a monomer–catalyst complex or an intermediate may be responsible for this effect. Alternatively, rearrangement of some of the monomer to a carbonyl compound, particularly likely with styrene oxide, followed by aldol or related condensations might account for the formation of coloured materials, but this seems unlikely since the colour was largely destroyed when the polymerization mixtures were treated with methanol. Also, the proton magnetic resonance spectra of the polymers were consistent with a polyether $-[OCH_2CHR]_n-$ formulation, and their i.r. spectra did not show carbonyl absorption.

The kinetic results can be discussed in terms of cationic active centre mechanisms[6] similar to those outlined[1] for propylene oxide. Thus if $X^{\oplus}$ represents a cationic site on the catalyst, initiation will probably involve coordination of monomer (as I) followed either by ring-opening to a

carbonium ion (II) to which further monomer becomes associated to give the hybrid (III ⟷ IV), or by ring opening *assisted* by a further monomer molecule to give (III ⟷ IV) directly. The polymer (V) would then be formed by repetition of one or both of these processes. Either mechanism

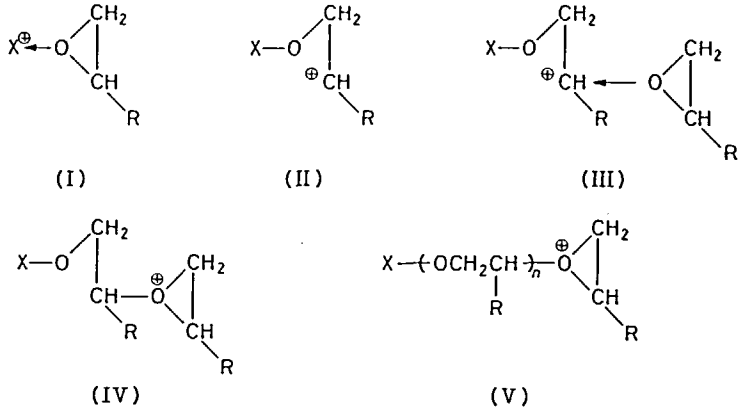

requires electron-donation from the monomer and/or stabilization of a secondary carbonium ion by the substituent R, and the expected order of rates of reaction would be R=Ph, Bu^t>Bu^{t}CH$_2$>Et>Me>H, which is the reverse of that observed. However, this argument neglects steric factors, which are particularly great when R=Bu^t since attack by monomer at the positive centre in (II) to give (III ⟷ IV), or alternatively the formation of (III ⟷ IV) directly by monomer-assisted ring-opening of (I) involves reaction at a neopentyl type of carbon atom, and therefore could account for the very slow polymerization of *t*-butylethylene oxide. Similar, though less severe, steric effects would operate for other R groups, and may be of greater importance in the overall consumption of monomer than the electronic effects.

The reaction with *t*-butylethylene oxide allows a distinction to be made between the formation of (III ⟷ IV) directly from (I) via a monomer-assisted process, or indirectly via the carbonium ion (II) since in the latter a 1,2-shift of a methyl group to give a more stabilized ion would be expected to occur more rapidly than attack of monomer on (II), and a product containing a carbon skeleton different from that expected from a normal epoxide polymerization would be formed:

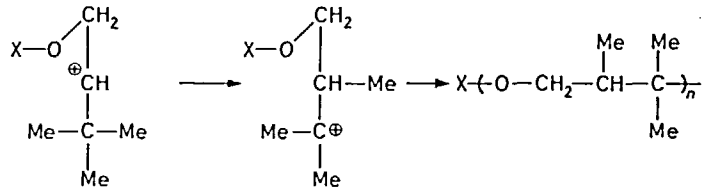

The proton magnetic resonance spectrum of the polymer from *t*-butylethylene oxide shows only a singlet at τ9·1 (relative intensity 3) and a

broad band centred at $\tau 6{\cdot}5$ (relative intensity 1), indicating that it should be formulated as $-[-OCH_2CHBu^t-]_n-$, and that if a methyl-shift occurs its extent is small. If a cationic mechanism operates, and solvent effects are not dominant, this implies that ring-opening of (I) does not occur spontaneously, but is assisted by monomer and leads directly to the oxonium ion (IV) as has been suggested previously[6].

The much greater initial rate for styrene oxide than for any of the alkyl-substituted ethylene oxides indicates that, at least in this case, factors other than steric ones are of considerable importance, and although stabilization of carbonium ions generated at the carbon atom carrying the phenyl group would be particularly marked, the differing kinetic features suggest that the polymerization of styrene oxide may not be mechanistically parallel to the polymerization of monoalkylethylene oxides.

Similar arguments can be applied to a coordinate anionic (insertion) mechanism[7] in which coordination of the monomer on to a catalyst site is followed by transfer of an anionic group from the catalyst to the coordinated monomer, with concomitant ring-opening, and, again, the sequence of rates observed for the monoalkylethylene oxides could be accounted for on steric grounds. In reactions of this type steric factors are likely to be large in the vicinity of an aggregated catalyst, particularly if it is producing isotactic polymer by an insertion mechanism. This lends support to the view[1] that polymerization of ethylene oxides by the diethylzinc–water system under the conditions outlined above involves two catalytically active species, and it could also indicate that polymer is produced in the initial fast stage by an oxonium ion mechanism, and in the later slow stage by an insertion mechanism.

We thank Dr C. Booth for helpful discussions, and Miss C. J. S. Guthrie and Mrs S. J. Hurst for experimental assistance.

Department of Chemistry,
The University,
Manchester 13

(*Received August 1965*)

REFERENCES

[1] BOOTH, C., HIGGINSON, W. C. E. and POWELL, E. *Polymer, Lond.* 1964, **5**, 479, and references therein
[2] HURST, S. J. and BRUCE, J. M. *J. chem. Soc.* **1963**, 1321
[3] PRICE, C. Personal communication
[4] ALLEN, G. and HURST, S. J. Unpublished work
[5] KERN, R. J. *Makromol. Chem.* 1965, **81**, 261
[6] COLCLOUGH, R. O. and WILKINSON, K. *J. Polym. Sci. Part C*, 1964, No. 4, 311
[7] Cf. PRICE, C. C. and OSGAN, M. *J. Amer. chem. Soc.* 1956, **78**, 4787

*The Crystallization and Melting of Copolymers I—The Effect of the Crystallization Temperature upon the Apparent Melting Temperature of Polymethylene Copolymers**

C. H. BAKER† and L. MANDELKERN

The apparent melting temperatures for a series of polymethylene copolymers were determined as a function of crystallization temperature and level of crystallinity. The copolymers contained from 1·2 to 6·4 mole per cent of either methyl or n-propyl side groups arranged in random sequence distribution. The data could be analysed to yield extrapolated equilibrium melting temperatures by assuming the formation and melting of finite size crystallites. The size of the crystallites is taken to be dependent solely on the crystallization temperature. In accord with the previous observations of Richardson, Flory and Jackson, based on directly observed melting temperatures, it is concluded that at equilibrium the crystalline phase remains pure for n-propyl side group copolymers while solid-solution occurs in the methyl copolymers.

STUDIES and analysis of the crystal–liquid equilibrium in copolymers and the constitution of the crystalline phase formed possess all the problems associated with classical binary systems. In addition, matters are further complicated by the paucity of information in regard to the solidus composition at the melting temperature, the finite size of the crystallites formed and compositional defects within the interior of the crystallites. It is not surprising, therefore, that many inconsistencies in interpretation exist even for a specific set of copolymers.

In the present series of papers we re-examine the crystallization and fusion properties of a series of polymethylene copolymers. We take advantage of the previous work on the melting temperature/composition relations reported by Richardson, Flory and Jackson[1] on the same samples, and the recent information on the formation and melting of a polymorphic form of polyethylene[2]. The construction of phase diagrams, based on liquidus composition, is the major concern of this paper. In the accompanying paper we critically examine the constitution of the crystalline state for these copolymers. All the experimental aspects of this work have been guided by a detailed study of the isothermal crystallization kinetics from the melt of the copolymers[3]. The basic data thus obtained set limits

*This work was supported by a contract with the Division of Biology and Medicine, Atomic Energy Commission.

†Present address: Research Department, ICI Fibres Ltd, Harrogate, Yorks.

on feasible crystallization temperatures with respect to the time involved and the levels of crystallinity attained. Conditions can then be prescribed which enable the crystallization process to be conducted both under controlled conditions and at the highest practicable crystallization temperature for each polymer.

EXPERIMENTAL

Materials—The copolymers studied were kindly supplied to us by Professor P. J. Flory and had been prepared by the copolymerization of diazomethane with the appropriate diazoalkane so as to give a polymethylene chain with randomly distributed methyl or *n*-propyl side groups. Complete details of the preparation and compositional analyses of the copolymers have been reported previously by Richardson, Flory and Jackson[1]. The compositions of the copolymers used in the investigation were as follows: four copolymers with methyl side groups were used, the composition in terms of CHR per 100 chain C atoms was 1·2 Me, 2·1 Me, 3·7 Me and 5·9 Me for copolymers M 1, M 2, M 3 and M 4 respectively. Copolymers containing *n*-propyl side groups had the compositions 2·0 Pr, 4·2 Pr and 6·4 Pr. These are denoted by the numbers P 7, P 8 and P 10 respectively.

Crystallization and melting procedures—The fusion curves and melting temperatures were determined utilizing dilatometric techniques. Because of the very small quantities of copolymer that were available, a slight modification to the usual form of the dilatometer was made so as to minimize the volume of mercury required. This modification consisted of using a spacer which was about 1 mm less in diameter than the internal diameter of the bulb, and which fitted all the way down into the horizontal bulb. Small pieces of bubble-free copolymer film were accommodated in a small saddle in the spacer, the ends of which were sealed around the ends of the bulb as shown in *Figure 1*. The stem of the dilatometer consisted

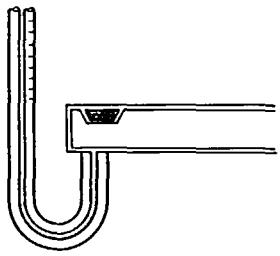

Figure 1—Schematic diagram of dilatometer

of a 25 cm length of 1 mm precision bore tubing graduated in millimetres along its length. About 0·3 g of copolymer and 20 g of mercury were used in each dilatometer. The dilatometers were evacuated and the polymer outgassed for several hours at about 160°C before the mercury was introduced. The weights of both copolymer and mercury in the dilatometer were determined in each case.

The crystallization of the copolymers was conducted in the following manner. Initially the sample under investigation was completely melted,

by immersing the dilatometer bulb for half an hour in a silicone oil bath above 160°C. The dilatometer was then swiftly transferred to another oil bath controlled at a preset temperature to better than 0·02°C. The copolymer was then allowed to crystallize isothermally for a time interval predetermined from studies of crystallization kinetics[3]. The times involved ranged from only a few minutes to forty days, depending on the composition and the crystallization temperature. Each sample was then heated, in the manner described below, to determine the apparent melting temperature. For subsequent crystallizations it was found necessary to heat the samples considerably above the apparent melting temperature in order to obtain crystallization kinetics and apparent melting temperatures which were reproducible. For purposes of the present study, the melting temperatures were deliberately determined utilizing a rapid heating rate. Melting temperatures so measured will be termed apparent melting temperatures, $T_m^{\ddagger}$, and should be distinguished from the equilibrium melting temperature of the copolymer, T_m, and from the corresponding homopolymer, T_m°. To determine the apparent melting temperature, the silicone oil thermostat was heated at a rate of 2°C per minute and the mercury level in the dilatometer stem recorded every degree, except in the immediate vicinity of the melting temperature. In this temperature range observations were made every half degree. Identical conditions with respect to heating rate, rate of stirring the oil bath and the positioning of the dilatometer were employed for each melting process for any one copolymer sample. This procedure rendered negligible the difference between the sample temperature and the temperature of the oil bath. The heating was continued to a temperature some 20°C above the melting point of the sample. An accurate extrapolation of the liquidus to lower temperatures could then be made, enabling the melting temperature to be more clearly identified[4]. A comparison of the liquidus on slow cooling, where true thermal equilibrium was established, with the liquidus determined on fast heating demonstrated that any error in the latter case was less than 0·5°C.

RESULTS

The maximum degrees of crystallinity $(1-\lambda)$ that were attained at the different crystallization temperatures for the seven copolymers studied are tabulated in *Table 1*, column (e). The constants necessary to calculate $1-\lambda$

Table 1. Crystallization times, degrees of crystallinity $(1-\lambda)$ and apparent melting temperatures $T_m^{\ddagger}$ for polymethylene copolymers

(a) *Copolymer*	(b) T_c °C	(c) t_i *min*	(d) t_{tot} *min* $\times 10^{-3}$	(e) $1-\lambda_{(max.)}$	(f) $T_m^{\ddagger}$ °C (*max.* $1-\lambda$)	(g) $T_m^{\ddagger}$ °C (*low* $1-\lambda$)
M1	121	600	55	18·2	134·5	131·75
(1·2% Me)	120	150	45	22·0	133·0	130·5
	119	120	50	25·4	133·0	
	117	20	14	29·5	132·0	128·5
	115	4·5	10	32·2	131·0	127·5
	113	2	10	35·0	130·5	
	110	1	10	36·9	129·7	

Table 1 (continued)

(a) *Copolymer*	(b) T_c °C	(c) t_i *min*	(d) t_{tot} *min* $\times 10^{-3}$	(e) $1-\lambda_{(max.)}$	(f) $T_m^{\ddagger}$ °C (*max.* $1-\lambda$)	(g) $T_m^{\ddagger}$ °C (*low* $1-\lambda$)
M2	113	200	50	2·4	125·5	124·0
(2·1% Me)	112	100	50	5·3	124·25	123·0
	110	15	50	14·2	123·0	120·5
	109	10	10	15·2	122·0	
	108	5	10	18·4	121·5	
	107	3	5	19·4	121·5	118·5
	106	2	5	21·4	120·5	
	105	2	6	23·1	120·5	118·0
	104	2	5	23·9	120·4	118·0
	102	1	4	26·0	120·0	118·0
	100	1	5	28·0	119·75	117·5
	98	1	5	29·2	119·25	
	96	1	4	30·9	119·0	
	93	1	4	32·1	119·0	
	90	1	4	33·2	118·75	
M3	100	150	21	4·8	111·0	
(3·7% Me)	98	40	20	7·9	109·5	
	96	6	20	10·4	108·75	
	94	33	9	13·1	108·5	
	92	2	9	15·3	107·5	
	90	2	9	17·0	107·5	
	85	1	9	21·1	106·5	
M4	75	50	30	1·0	84±1	
(5·9% Me)	72	15	10	1·7	83±1	
	70	10	10	2·6	83±1	
	68	3	10	4·2	82·3±0·5	
	66	2	10	5·8	82·3±0·5	
	64	1	5	7·2	82·1±0·3	
	60	1	5	10·5	82·0	
	56	1	2	12·9	81·5	
	52	1	2	14·8	81·0	
	48	1	2	16·1	80·0	
P7	104*			12·3	113·7	112·0
(2·0% *n*-Pr)	103	200	39	12·5	113·0	111·5
	102	70	30	14·4	111·5	110·5
	100	20	10	15·9	110·75	109·0
	98	7	15	18·3	109·0	108·0
	96	2	10	19·3	107·5	106·5
	94	1	10	20·9	107·5	106·5
	92	1	10	22·3	107·5	
	90	1	10	23·5	108·0	107·0
	86	1	10	25·4	108·0	
	80	1	10	27·1	107·25	

*isotherm not obtained

P8	78	30	30	2·7	89·0	
(4·2% *n*-Pr)	76	10	30	4·4	86·5	
	74	4	30	6·4	86·0	
	72	2	30	8·2	87·0	
	70	2	10	10·5	87·0	
	68	1	5	11·4	87·0	
	66	1	5	12·5	87·0	
P10	45	2	5	4·4	64±2	
(6·4% *n*-Pr)	40	2	3	6·6	64±2	
	35	2	5	9·0	64±2	

on a weight fraction basis have already been reported[1], and the additivity of the volumes of the two phases has been assumed. The time interval which elapses before crystallization is detected is also given in *Table 1*, column (c), while column (d) gives the approximate time required to attain the level of crystallinity indicated.

A typical set of fusion curves obtained on rapid heating is illustrated in *Figure 2* for copolymer P 7 after crystallization to the maximum attain-

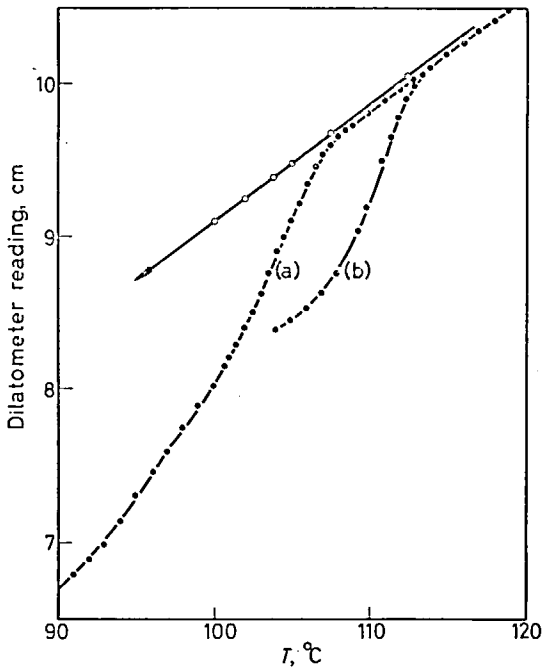

Figure 2—Dilatometer scale readings as a function of temperature for copolymer P 7 (2% *n*-Pr). Curve A crystallization temperature 90°C; Curve B crystallization temperature 104°C. Rapid heating •; slow cooling O

able levels at two different temperatures. The liquidus, re-established on slow cooling, is also illustrated. It is clear that any thermal non-equilibrium between sample and bath during rapid heating cannot exceed 0·5°C. Sigmoidal shaped fusion curves, typical of copolymers[4] are observed always. There is a definite inflection in the fusion curve for this sample after crystallization at 90°. This inflection cannot be attributed to any experimental discrepancy since its presence was confirmed in several repetitive crystallizations and meltings. The shape of the curve in *Figure 2* is suggestive of the melting of a crystalline species in the neighbourhood of 97°C in addition to the major melting which occurs at 108°C.

The apparent melting temperature $T_m^{\ddagger}$ (obtained on fast heating) is given in the last two columns of the table for each of the copolymers. The values listed in column (f) were obtained by melting the sample after the level of crystallinity in column (e) was reached. Melting temperatures characteristic of the low levels of crystallinity (about 20 per cent of the maximum attained) are given in column (g). The reproducibility of $T_m^{\ddagger}$,

for both high and low degrees of crystallinity, was usually better than ±0·2°C. However, for copolymers M 4 and P 10, where only very low levels of crystallinity could be attained, the uncertainty in $T_m^{\ddagger}$ was somewhat greater.

The apparent melting temperatures tabulated in column (f) are consistently greater than those in column (g). The effect of the degree of crystallinity upon $T_m^{\ddagger}$ is depicted in *Figure 3* for copolymer M 2 (2·1 per cent Me)

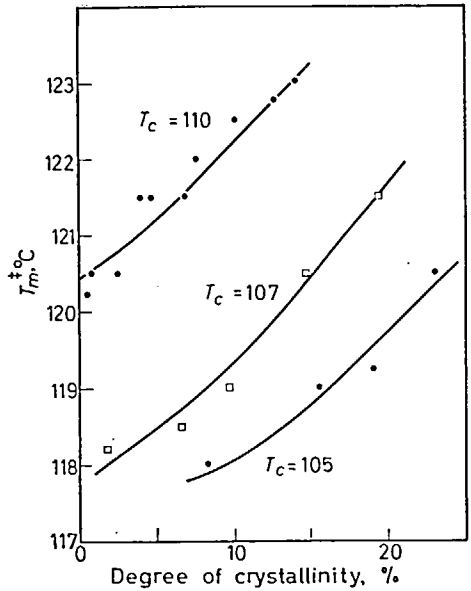

Figure 3—Plot of apparent melting temperature $T_m^{\ddagger}$ as a function of degree of crystallinity $1-\lambda$ for 2·1% Me copolymer (M 2) at indicated crystallization temperature

which was crystallized for various lengths of time at three different temperatures. A steady increase of about 3° is observed in $T_m^{\ddagger}$ as $1-\lambda$ is raised from just above zero to the practical maximum of about 0·20.

A comparison of the highest apparent melting points recorded utilizing a fast heating process with those obtained by Richardson, Flory and Jackson[1] after careful crystallization and subsequent slow heating is given in *Table 2.*

Table 2. A comparison of highest apparent melting temperatures obtained on fast heating and previous report utilizing slow heating

Sample		(a) $T_m^{\ddagger}$	(b) T_m
M 1	1·2% Me	134·5	135
M 2	2·1% Me	125·5	127
M 3	3·7% Me	111·0	112
M 4	5·9% Me	84±1	92
P 7	2·0% *n*-Pr	113·7	113
P 8	4·2% *n*-Pr	89·0	95
P 10	6·4% *n*-Pr	64±2	70

$T_m^{\ddagger}$ in this paper obtained by rapid heating at the rate of 2°C/min. T_m obtained by Richardson, Flory and Jackson[1] using slow heating rate of 1°C per day.

Higher values for the directly observed melting temperatures are invariably obtained when a slow heating process is utilized. The difference between the two kinds of melting temperatures becomes greater as the concentration of coingredient in either copolymer is increased. A significant amount of recrystallization on slow heating is thus indicated. The only advantage in the present method is that an extrapolation to the equilibrium melting temperature can be made.

DISCUSSION

Theoretical background—One of our major objectives was to estimate the equilibrium melting temperatures of the copolymers from the experimentally observed apparent melting temperatures. The underlying principle utilized is based on the assumption that the thermodynamic properties governing the stability of the crystallites are solely dependent on the crystallization temperature. Moreover it is assumed that the fusion process is conducted in such a manner that no changes in the constitution of the crystallites occur prior to melting. These concepts have been shown to be quite useful in studies of homopolymers[5] where the major factor is the finite size of the crystallites in the chain direction. To assess our results in terms of these concepts, we first extend the theory to include copolymers.

The methods used in the similar problem concerned with homopolymers are followed[5–7]. It is necessary to calculate the free energy of fusion of an internally perfect crystallite of finite size, formed from a copolymer chain. The copolymeric character of the chain, however, requires the specification of the composition and sequence distribution of each phase. It is shown in the Appendix that if for a binary copolymer comprised of A and B units, the probability P_A that an A unit selected at random is followed by another A unit independent of its predecessor* then the thermodynamic activity of the unit in any phase is equal to this probability. Hence

$$\mu^{(1)}_{A,c} - \mu^{(0,1)}_{A,h} = RT \ln P^0_A \tag{1}$$

Here $\mu^{(1)}_{A,c}$ is the chemical potential of the A unit in the copolymer melt and $\mu^{(0,1)}_{A,h}$ the corresponding quantity for the pure liquid homopolymer composed of A units at the same temperature and pressure. A similar expression, equation (2) can be written for the crystalline phase

$$\mu^{(c)}_{A,c} - \mu^{(0,c)}_{A,h} = RT \ln P^{(c)}_A \tag{2}$$

The superscript (c) denotes the crystalline phase and $P^{(c)}_A$ is the sequence propagation probability of an A unit in this phase. For the special case where the crystalline phase remains pure, admitting for example only A units into the lattice, $P^{(c)}_A$ is equal to unity.

From equations (1) and (2) and the corresponding equations for species B

$$\begin{aligned} \mu^{(1)}_{A,c} - \mu^{(c)}_{A,c} &= \Delta f'_{uA} = \Delta f_{uA} + RT \ln P^{(0)}_A - RT \ln P^{(c)}_A \\ \mu^{(1)}_{B,c} - \mu^{(c)}_{B,c} &= \Delta f'_{uB} = \Delta f_{uB} + RT \ln P^{(0)}_B - RT \ln P^{(c)}_B \end{aligned} \tag{3}$$

*This restriction is equivalent to considering copolymerization processes where only the terminal unit influences which of the two units will add to the growing chain.

Here, Δf_{uA} which equals $\mu_{A,h}^{(0,1)} - \mu_{A,h}^{(0,c)}$ is the free energy of fusion per repeating unit of the pure A homopolymer of infinite molecular weight. At the equilibrium melting temperature T_m of the copolymer both $\Delta f'_{uA}$ and $\Delta f'_{uB}$ must be zero. The resulting equation describes the equilibrium phase diagram in terms of the sequence propagation parameters of each phase. The analogy with the phase equilibrium of a binary monomeric system is apparent[8] with the *Ps* in the present case replacing the usual activities.

Our immediate concern, however, is the melting of crystals of finite size. The free energy change in forming a cylindrical crystallite, ρ sequences in cross section and ζ units long, is given by

$$\Delta F = n_A \Delta f'_{uA} + n_B \Delta f'_{uB} - 2\rho\sigma_e - 2\pi^{1/2}\zeta\sigma_u \tag{4}$$

Here σ_u is the lateral interfacial free energy per chain and σ_e the excess free energy (or interfacial free energy) attributable to a chain as it emerges from the 001 face of the crystallite. The number of A and B units in the crystallite is given by n_A and n_B. These latter quantities are equal to $\rho\zeta_A$ and $\rho\zeta_B$ respectively, where ζ_A and ζ_B are the numbers of A and B units in a crystalline sequence. Since ζ_A and ζ_B are equal to ζ equation (4) can be rewritten as

$$\frac{\Delta F}{\zeta\rho} = \frac{\zeta_A}{\zeta}\Delta f'_{uA} + \frac{\zeta_A}{\zeta}\Delta f'_{uB} - \frac{2\sigma_e}{\zeta} - \frac{2\pi^{1/2}}{\rho^{1/2}}\sigma_u \tag{5}$$

When the definitions of $\Delta f'_{uA}$ and $\Delta f'_{uB}$ given by equation (3) are used, the implicit assumption is made that the sequential distribution within the crystallite is the same as that for equilibrium. Hence equations (4) and (5) describe a crystallite whose properties, except for size, correspond to that for an equilibrium crystallite. At the melting temperature of the finite size crystal, $T_m^{\ddagger}$, $\Delta F(T_m^{\ddagger}) = 0$ so that

$$x_A \Delta f'_{uA}(T_m^{\ddagger}) + x_B \Delta f'_{uB}(T_m^{\ddagger}) = \frac{2\sigma_e}{\zeta} + \frac{2\pi^{1/2}\sigma_u}{\rho^{1/2}} \tag{6}$$

which can be rewritten as

$$\Delta f'_u(T_m^{\ddagger}) = \frac{2\sigma_e}{\zeta} + \frac{2\pi^{1/2}\sigma_u}{\rho^{1/2}} \tag{6'}$$

where $x_A = \zeta_A/\zeta$ and $x_B = \zeta_B/\zeta$ and the definition of $\Delta f'_u$ follows immediately. Comparison of those equations with equation (3) gives the depression from the equilibrium melting temperature of the finite size crystal.

For the special case where the crystalline phase remains pure, $x_B = 0$, equations (6) and (3) yield

$$\frac{T_m - T_m^{\ddagger}}{T_m} = \frac{1}{\Delta H_u}\left(\frac{2\sigma_e}{\zeta} - \frac{2\pi^{1/2}\sigma_u}{\rho^{1/2}}\right) \tag{7}$$

where ΔH_u is the heat of fusion per repeating unit of a homopolymer of A units. The similarity of equation (7) with the corresponding equation for a pure homopolymer is apparent[5]. When the lateral dimensions of the crystallite are very large, $\rho^{1/2} \longrightarrow \infty$, equation (7) can be reduced to

$$\frac{T_m - T_m^{\ddagger}}{T_m} = \frac{1}{\Delta H_u}\left(\frac{2\sigma_e}{\zeta}\right) \tag{8}*$$

In this development, there is no *a priori* need to prescribe the molecular nature of the interface. The analysis is based solely on the assumption of finite size crystals. If the relation for the melting temperature of a crystallite of the same size ζ and interfacial energy σ_e formed from an infinite molecular weight homopolymer is inserted into equation (8) together with the equilibrium melting temperature equation for the copolymer [obtained from equation (3)], the equation derived by Wunderlich[9] in an approximate and indirect manner is obtained.

In the treatment of homopolymers, it has been shown to be both useful and convenient to express the dimensions of the crystallite in terms of the critical nucleus dimensions $\rho^{\star}$ and $\zeta^{\star}$. The additional assumptions are often made[5] that the interfacial energies of these two entities are the same and that growth in the chain direction does not proceed significantly beyond $\zeta^{\star}$. Hence, in this approximation ζ and $\zeta^{\star}$ are equal. We shall initially utilize this approximation to develop the relations between the apparent melting temperature of a copolymer and its crystallization temperature.

The free energy surface described by equation (5) contains a saddle point, the coordinates of which define the dimensions of the critical sized nucleus. It is readily shown, since the composition of the crystallite is fixed, that

$$\rho^{\star 1/2} = \frac{2\pi^{1/2}\sigma_u}{\Delta f_u'(T_c)} \tag{9}$$

and

$$\zeta^{\star} = \frac{4\sigma_e}{\Delta f_\perp'(T_c)} \tag{10}$$

We note that the same form is obtained for $\rho^{\star}$ and $\zeta^{\star}$ as for an infinite molecular weight homopolymer with $\Delta f_u'$ in the above replacing Δf_u for the homopolymer† case[5]. It is again implicitly implied that the sequence distribution within the nucleus is identical to that for the equilibrium crystallite at T_m. By identifying $\zeta^{\star}$ with ζ and assuming the same σ_e for both crystallite and nucleus, equation (6′) becomes

$$\Delta f_u'(T_m^{\ddagger}) = \tfrac{1}{2}\Delta f_u'(T_c) \tag{11}$$

when ρ is large. If the entropy of fusion of the copolymer is independent of temperature over the temperature range of interest, then it is easily shown that

$$T_m^{\ddagger} = \tfrac{1}{2}(T_m + T_c) \tag{12}$$

in accord with the previous results for an infinite molecular weight homopolymer. Equation (12) therefore can be used as a guide to estimate or

*If the lateral interfacial energy σ_u is relatively small then of course the same equation results even if ρ does not become exceptionally large.

†The relations derived for copolymers in this paper are in the infinite molecular weight approximation. Extension to the case of chains of finite length follows along the lines previously given for homopolymers[10-13].

extrapolate to the equilibrium melting temperatures of copolymers. Within the limitations of the approximations made, it is not limited to copolymers whose crystalline phase remains pure.

Analysis of experimental data—In accordance with the suggestion of equation (12), the apparent melting temperature, $T_m^{\ddagger}$, is plotted in *Figures 4* and *5* as a function of the crystallization temperature for both types of

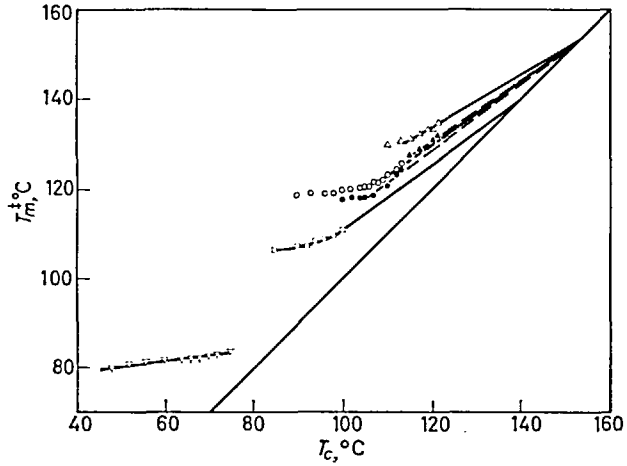

Figure 4—Plot of apparent melting temperature, $T_m^{\ddagger}$ as a function of crystallization temperature T_c for Me side group copolymers. 1·2% Me high crystallinity △, low crystallinity ▲; 2·1% Me high crystallinity ○, low crystallinity ●; 3·7% Me □; 5·9% Me ▽

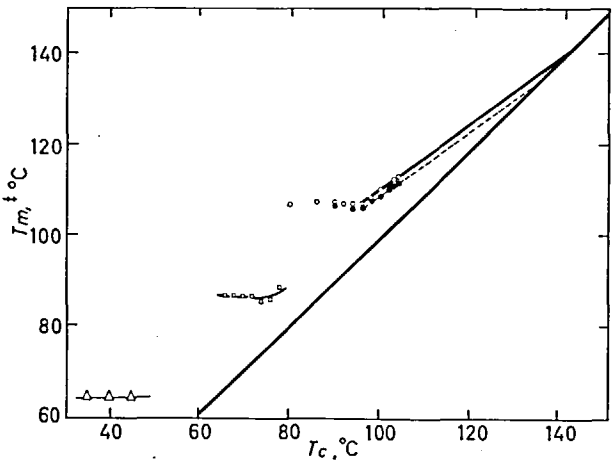

Figure 5—Plot of apparent melting temperature $T_m^{\ddagger}$ as a function of the crystallization temperature T_c for *n*-Pr side group copolymers. 2% *n*-Pr high crystallinity ○, low crystallinity ●. 4·2% *n*-Pr □; 6·4% *n*-Pr △

copolymers. There are, of course, two sets of values of $T_m^{\ddagger}$ for each crystallization temperature corresponding to the low and high degrees of crystallinity. The experimental data, in either case, can only be represented by a straight line at the higher crystallization temperatures where the crystallization rate is relatively slow. Below these temperatures $T_m^{\ddagger}$ is essentially independent of the crystallization temperatures. The extrapolated equilibrium melting temperature is then determined from the intersection of the linear portion of the plot with the straight line given by $T_m^{\ddagger}=T_c$. The values of T_m obtained in this manner are listed in the second column of *Table 3* for copolymers M 1, M 2, M 3 and P 7.

Table 3. Extrapolated equilibrium melting temperatures of polymethylene copolymers

Copolymer	*T_m from extrapolated plots of $T_m^{\ddagger}$ versus T_c °C*		*Slope*		*Theoretical* T_m °C*
	High 1−λ	*Low* 1−λ	*High* 1−λ	*Low* 1−λ	
M 1 1·2% Me	152	150	0·57	0·65	140·6
M 2 2·1% Me	152	150	0·69	0·72	137·4
M 3 3·7% Me	140		0·73		131·7
M 4 5·9% Me			0·13		123·7
P 7 2·0% Pr	140	135	0·73	0·74	137·8
P 8 4·2% Pr			0·2		129·9
P 10 6·4% Pr					122·2

*Calculated from relation $1/T_m-1/T_m^{\circ}=-R/\Delta H_u \ln X_A$ under the assumption that the crystalline phase remains pure. Here P_A equals the mole fraction of A units, x_A, for a random copolymer.

The increasing values of $T_m^{\ddagger}$ with increasing levels of crystallinity, at a fixed crystallization temperature, can be attributed in part to the change in composition and sequence distribution that occurs in the melt as isothermal crystallization ensues. Based on compositional changes alone, the crystallization process occurs at progressively decreasing undercoolings with time[13]. Larger, thermodynamically more stable crystallites thus result. A qualitatively similar effect has been observed for poly-chlorotrifluoroethylene[7] which because of its stereo-irregular character must be treated as a copolymer. However, similar effects are also observed in homopolyethylene during the course of isothermal crystallization[14,15]. In this case, the changing constitution of the melt as crystallization ensues must have an important influence. For present purposes, we are primarily interested in the dependence of the equilibrium melting temperatures of the copolymers on the liquidus composition. Hence, we shall be mainly concerned with the apparent melting temperature obtained after the development of small amounts of crystallinity.

The slopes of the linear portion of the $T_m^{\ddagger}$ against T_c are also given in *Table 3*. The slope for a given copolymer must by necessity lie between zero and unity. If crystallites of maximum stability are formed at each crystallization temperature, then $T_m^{\ddagger}$ would always equal T_m. At the other extreme, when the slope equals unity, $T_m^{\ddagger}$ will equal T_c and the crystallites will be inherently unstable. When all the assumptions leading to equation (12) are satisfied, then the slope of the linear region of *Figures 4* and *5* should be one-half. The slopes found for copolymers M 1, M 2, M 3 and P 7 are all very close to 0·7. These results thus indicate the formation of crystallites of lower thermodynamic stability than those consistent with the aforementioned requirements. Various possibilities suggest themselves to account for this apparent discrepancy. If the lateral dimensions of the crystallites do not become very large, as might be expected in random copolymers[16], then a slope greater than one-half could result[5]. The distinct possibility also exists that the interfacial energy σ_e of the crystallite will be greater than the nucleus from which it is formed. This effect will also lead to an increased slope[5]. Moreover, the derivation of equation (12) for copolymers is based on the proposition that the equilibrium sequence distribution is found within the nucleus and crystallite at T_c. This condition would be expected to be most difficult to fulfil for any real crystallization process. Its violation would lead to a reduced stability and increased slope. The various factors contributing to the observed deviations from the dictates of equation (12) cannot be separated at the present time. Hence, it must be recognized that although it is possible to estimate the equilibrium melting temperatures of copolymers by means of a linear extrapolation of the data of *Figures 4* and *5*, the equations derived for this purpose are not quantitatively obeyed.

Phase diagrams, based on the liquidus composition can be constructed from the equilibrium melting temperatures determined in the manner described above. The diagrams are given in *Figure 6*. In this figure the

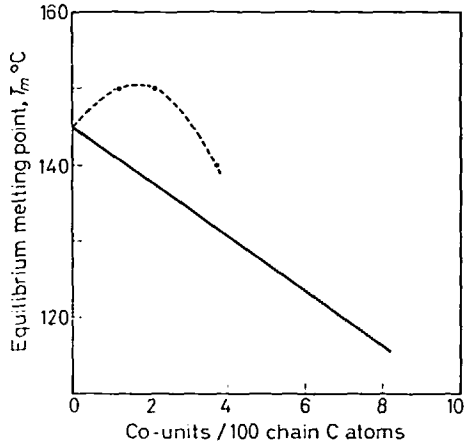

Figure 6—Plot of extrapolated equilibrium melting temperatures as a function of copolymer composition for methyl side groups ●, for *n*-Pr side groups ○. Solid line calculated for crystalline phase remaining pure

solid line represents the melting temperature/composition relation calculated on the basis that the crystal lattice contains only CH_2 units. The result for the *n*-propyl side group copolymer adheres remarkably well to this requirement. On the other hand, the results for the methyl side group copolymers are quite different. The plot of the data for this copolymer is similar to that previously reported by Richardson, Flory and Jackson[1] from their study of the same samples. In the latter work, the melting temperatures utilized were obtained on slow heating rather than the estimated equilibrium melting temperatures employed here. The initial elevation of the melting temperature with increased concentration of coingredient is strong evidence for solid-solution formation (or possibly compound formation). Hence for this copolymer a proportion of the methyl side groups are present in the crystal lattice as an equilibrium requirement.

The conclusion reached above with respect to the methyl side group copolymers is contrary to those previously reported by Wunderlich and Poland[17]. It was concluded, from apparently equilibrium thermodynamic reasoning, by the latter investigators that the $CHCH_3$ groups are non-crystallizable units which should not enter the polyethylene lattice. This deduction was based on the observation that the melting temperature continuously decreased as the concentration of coingredient was increased. Concomitantly, these investigators observed from x-ray diffraction measurements that the lattice parameters increased as the concentration of methyl side groups increased. They concluded, therefore, that the side groups were located in the crystal lattice as so-called 'amorphous defects'. These erroneous conclusions resulted from the failure to account properly for the melting of finite size crystals and the neglect of solid-solution formation as a possible equilibrium condition. As has been emphasized here and elsewhere[1], the fact that an experimentally observed melting temperature decreases with increasing copolymeric content does not necessarily mean that the crystalline phase is pure.

It has been noted, in discussing the plots of *Figures 4* and *5*, that for crystallization conducted at the lower temperatures (about 100°C or less) $T_m^{\ddagger}$ does not vary very much with T_c. One possible explanation of these observations is that the crystallization process is so rapid in this temperature range that the major portion of the crystallization always occurs at the same temperature and not at the temperature recorded. However, as can be noted from *Table 1*, the crystallization of copolymers M 4, P 8 and P 10 must be conducted below 80°C because of kinetic restrictions. The slopes from *Figures 4* and *5* range from 0·13 to 0·20. A linear extrapolation of the data yields equilibrium melting temperatures for M 4 and P 8 which are approximately 85°C and 90°C respectively. As is readily ascertained from the plots of *Figure 6*, these values are in complete disagreement with the melting points obtained by the introduction of small amounts of coingredients. It has been recently established, however, that a polymorphic crystalline form of polyethylene, whose melting temperature is below 100°C, will form under these crystallization conditions[2]. Hence, the distinct possibility exists that the copolymers which contain a higher proportion of side groups will develop a crystalline structure significantly different from

that found at the higher temperatures. This suggestion receives strong confirmation from the analysis of the wide-angle X-ray diffraction of these copolymers which will be discussed in the following paper[17a]. The inflection observed in the fusion curve of copolymer P 7 (*Figure 2*) subsequent to crystallization at 90°C can thus be attributed to the melting of the polymorphic structure developed under these crystallization circumstances.

In analysing the melting of copolymers, a key factor is the recognition that the thermodynamic activity of a chain unit, either in the liquid or crystalline phases, is determined by the sequence propagation probability. The activity depends on composition only through this latter quantity. The important distinction must then be made between the equilibrium requirements with respect to the constitution of the crystalline phase and the occurrence of non-equilibrium defects. It can be expected that a major source of non-equilibrium defects will involve the sequence distribution within the crystalline phase. The apparent discrepancies between the conclusions reached in this work, in regard to the constitution of the crystalline phase of polymethylene copolymers, and previous reports on the lattice structure[18–21] is discussed in detail in the following paper.

APPENDIX

We wish to calculate the thermodynamic activity of an A unit in a copolymer composed of A and B units. If it is assumed that during the polymerization reaction only the terminal group governs the selection of the adding monomer, then a unique parameter P_A exists. This quantity is the probability that an A unit selected at random will be followed by another A unit irrespective of the nature of the preceding units. In terms of the monomer reactivity ratios r_1 and r_2, P_A can be expressed as[22]

$$P_A = r_1 f_A / (r_1 f_A + f_B) \tag{13}$$

where f_A and f_B are the mole fractions of monomer in the reaction mixture.

In order to calculate the free energy difference between an A unit in the copolymer and in the corresponding homopolymer, the copolymer is treated as an ideal binary mixture. Hence we seek, Ω, the number of distinguishable ways in which the sequences of A and B units can be arranged in the linear chain. (This is analogous to the classical statistical derivation of Raoult's law in three dimensions. In this instance we seek the arrangement of sequences rather than units.) As Orr[23] has shown

$$\Omega = \frac{N_A! N_B!}{\prod_{\zeta_A=1}^{\infty} N_{\zeta_A}! \prod_{\zeta_B=1}^{\infty} N_{\zeta_B}!} \tag{14}$$

Here N_A and N_B are the total number of sequences of A and B units respectively; N_{ζ_A} is the number of sequences containing ζ A units and N_{ζ_B} is similarly defined. For this ideal system there is no enthalpic contribution to the free energy so that by invoking the Boltzmann relation[23]

$$\Delta F / kT = N_{0A} [(1 - P_A) \ln (1 - P_A) + \ln P_A - (1 - P_A) \ln P_A] \tag{15}$$

Only terms dependent on the number of A units in the chain, N_{0A}, are

included in equation (15). The other terms are of no importance for present purposes. The chemical potential of an A unit in the copolymer relative to that in a homopolymer, $\mu_{A,c}-\mu_{A,h}$ is given by

$$\mu_{A,c}-\mu_{A,h}=(\partial\Delta F/\partial N_{0A})_{N_{0B}}=RT\ln P_A \tag{16}$$

Equation (16), based on ideal mixing theory, represents the chemical potential of the A units in any phase. The chemical potential thus depends solely on the sequence propagation probability and only indirectly on composition. This equation can be applied directly to problems involving crystal–liquid phase equilibria of copolymers. For example, the equilibrium melting temperature T_m is defined as the temperature at which very long crystalline sequences melt. When the crystalline phase contains only A units then, since crystallite-end effects can be neglected, it immediately follows by applying the conditions for phase equilibrium that

$$1/T_m-1/T_m^0=(-R/\Delta H_u)\ln P_A \tag{17}$$

This equation has been derived previously by Flory[24,25] using other methods.

Department of Chemistry and
Institute of Molecular Biophysics,
Florida State University,
Tallahassee, Florida

(*Received August 1965*)

REFERENCES

[1] RICHARDSON, M. J., FLORY, P. J. and JACKSON, J. B. *Polymer, Lond.* 1963, **4**, 221
[2] FATOU, J. G., BAKER, C. H. and MANDELKERN, L. *Polymer, Lond.* 1965, **6**, 243
[3] BAKER, C. H. and MANDELKERN, L. To be published
[4] MANDELKERN, L. *Crystallization of Polymers*, p 93. McGraw-Hill: New York, 1964
[5] MANDELKERN, L. *Crystallization of Polymers*, p 321 ff. McGraw-Hill: New York, 1964
[6] MANDELKERN, L. *J. Polym. Sci.* 1960, **47**, 494
[7] HOFFMAN, J. D. and WEEKS, J. J. *J. Res. Nat. Bur. Stand.* 1962, **A66**, 13
[8] WILSON, A. H. *Thermodynamics and Statistical Mechanics*, p 410. Cambridge University Press: London, 1960
[9] WUNDERLICH, B. *Polymer, Lond.* 1964, **5**, 125
[10] MANDELKERN, L., FATOU, J. G. and HOWARD, C. *J. phys. Chem.* 1964, **68**, 3386
[11] FATOU, J. G. and MANDELKERN, L. *J. phys. Chem.* 1965, **69**, 417
[12] MANDELKERN, L., FATOU, J. G. and HOWARD, C. *J. phys. Chem.* 1965, **69**, 956
[13] GORNICK, F. and MANDELKERN, L. *J. appl. Phys.* 1962, **33**, 907
[14] WEEKS, J. J. *J. Res. Nat. Bur. Stand.* 1963, **67A**, 441
[15] GOPALAN, M. and MANDELKERN, L. Unpublished observations
[16] FLORY, P. J. *J. Amer. chem. Soc.* 1962, **84**, 2857
[17] WUNDERLICH, B. and POLAND, D. *J. Polym. Sci.* 1963, **1A**, 357
[17a] BAKER, C. H. and MANDELKERN, L. *Polymer, Lond.* 1966, **7**, in press
[18] WALTER, E. R. and REDING, F. P. *J. Polym. Sci.* 1956, **21**, 561
[19] EICHORN, R. M. *J. Polym. Sci.* 1958, **31**, 197
[20] COLE, E. A. and HOLMES, D. R. *J. Polym. Sci.* 1960, **46**, 147
[21] SWANN, P. R. *J. Polym. Sci.* 1962, **56**, 409
[22] FLORY, P. J. *Principles of Polymer Chemistry*, p 178 ff. Cornell University Press: Ithaca, 1953
[23] ORR, R. J. *Polymer, Lond.* 1961, **2**, 74
[24] FLORY, P. J. *J. chem. Phys.* 1949, **17**, 223
[25] FLORY, P. J. *Trans. Faraday Soc.* 1955, **51**, 848

Cocrystallization in Copolymers of α-Olefins II–Butene-1 Copolymers and Polybutene Type II/I Crystal Phase Transition

A. TURNER JONES

The cocrystallizing behaviour shown by copolymers of butene with a number of linear and branched α-olefins made with titanium trichloride–diethyl aluminium chloride catalysts has been investigated by x-rays over a range of copolymer compositions and the effect of copolymerization on the spontaneous polybutene Type II (PB II) to Type I (PB I) crystal phase transition has been studied in unoriented specimens and fibres. Degrees of crystallinity, crystal phase changes from those of the relevant homopolymers including lattice expansion and contraction and helix modification, and melting points have been observed. Pentene forms a highly cocrystallizing system based on PB I; propylene shows limited, and ethylene practically no 'isomerism of monomer units'. These three comonomers markedly accelerate the PB II/I transition, and in sufficient amount cause direct crystallization from the melt to PB I.

Hexene and octene units can enter the PB II lattice but α-olefins with C > 8 do not. Butene–3-methyl butene is a highly cocrystallizing system; 4-methylpentene and 4,4-dimethylpentene copolymers show limited and no cocrystallization respectively. Linear α-olefins with C > 5 and the branched comonomers retard the PB II/I transition and in sufficient amount stabilize the PB II form completely. For comonomers which enter the PB II lattice, stabilization is attributed to steric inhibition of the change from a PB II 11_3 (or more likely 40_{11}) helix to a more tightly coiled 3_1 (PB I) helix. For those that do not enter the lattice, it is believed that the large units act as 'stops' at the fold boundaries, which prevent the helical chains being drawn through the crystallites and thus inhibit the transition. The X-ray patterns of some of the copolymers show loss of short range order while preserving long range order. Phase separation and lack of randomness in the copolymers are discussed; the degree of copolymerization attained with this highly stereospecific catalyst system is shown to be related to the degree of cocrystallization possible in each copolymer.

THIS paper describes investigations on the cocrystallizing behaviour of isotactic copolymers of butene-1 with a number of α-olefin monomers branched and unbranched, namely ethylene, propylene, pentene, hexene, octene, nonene, decene, dodecene, octadecene, 3-methylbutene (3MB), 4-methylpentene (4MP) and 4,4-dimethylpentene (44DMP), over a wide range of copolymer composition. At each composition crystal phases were identified and unit cell dimensions, degrees of crystallinity and melting points measured on samples slow cooled at 6°C per hour from above their melting points. This was done with a view to obtaining information regarding the degree to which copolymerization had taken place, the way in which the comonomer units were distributed in the chains, randomly, or blocked to different degrees, the distribution of chain composition, the degree of cocrystallization, complete, partial or non-existent, and the structure of the crystalline phases in relation to copolymer composition.

The paper also describes the effect of copolymerization of these monomers in accelerating or retarding the transition from the polybutene Type II (PB II)[1,2] crystal form to the polybutene Type I (PB I) form[3]; this takes place spontaneously at ambient temperatures in butene homopolymers[1,4–6]. Sufficient amounts of comonomers can cause direct crystallization into PB I or stabilize the PB II form completely. A summary of the results given in this paper was presented at the IUPAC Conference on Macromolecular Chemistry in Prague, 30 August to 4 September 1965 and will be published in *Journal of Polymer Science*, Part C. Full experimental details (except for the butene–3MB system, which has been described separately[7]) are given here complete with results and discussion.

In Part I of this series of papers on copolymers with α-olefins[8] work by Natta and others in this field has been referred to, and some of the theoretical considerations involved in cocrystallization have been discussed and will not be repeated here. As for the 4-methyl pentene copolymers described in Part I, it is useful, in considering the likelihood of cocrystallization in any olefin copolymer system, to compare the homopolymer crystal phases of the different olefins from the points of view of their crystal symmetry and unit cell parameters, crystal density and melting point, together with their helical parameters, i.e. monomer units per turn, length parallel to the fibre axis per turn (l_t), and length parallel to the fibre axis c per monomer unit (l_m) and cross sectional area per chain (CSA). These parameters have been summarized in *Table 1*, and for convenience of reference many have been taken from *High Polymers* Volume XX, *Crystalline Olefin Polymers*[9].

At the high butene end of the composition ranges where the crystal phases observed are mainly those of polybutene homopolymer, or closely similar to them, modifications in the structure (helix type or lattice parameters) have been particularly investigated in relation to the effect of copolymerization and cocrystallization on the rate of the well known spontaneous transition from PB II to PB I and on rates of crystallization.

The spontaneous crystalline phase conversion from PB II to PB I shows an increase in rate from that at 20°C to a maximum at $\sim$ 40°C[4], and then decreases with rising temperature until no discernible change occurs at $\sim$ 100°C. The conversion must result from the difference in the free energies of the two forms. This difference results from several factors, amongst which are (*a*) the density difference between the forms (which at 20°C is large, 0·95 g/cm^3 and 0·90 g/cm^3 for PB I and PB II respectively), (*b*) the potential energies of the PB I 3·0 (3_1) helix (where all the chain bonds are staggered, either *gauche* or *trans*), and the PB II 3·667 (11_3) helix (where they are not staggered), (*c*) the different side-by-side packings of the two forms, and also (*d*) the mobility of the helices, which must be greater in the PB II form of lower density and lower melting point. Natta[13] has shown by conformational energy calculations that the energies of the two helices are not very different and suggests that the differences in stability in the crystalline state are mainly due to their packing efficiency. The conversion will take place if the thermal motions are

Table 1. Homopolymer crystal phases; unit cells and helical parameters

Phase		*Sym-metry*	*Unit cell constants* *a*	*b*	*c*		*Helix*	m_t	l_t	l_m	A^2	$d_{cryst.}$ g/cm³	*M.pt* °C
Polyethylene[9]		O	7·40	4·93	2·534					2·54	9·6	1·0	139
Polypropylene	α-form[9]	M	6·65	20·96	6·50	β=99·3	3_1	3·0	6·50	2·16	34	0·94	180
	β-form[10]	Trig.	6·36*	6·36*	6·49		3_1	3·0	6·49	2·16	35	0·92	150
Polybutene	Type I[9]	Trig.	17·7	17·7	6·5		3_1	3·0	6·5	2·17	44	0·95	134[12]
	Type II[9§]	Tet.	14·85	14·85	20·6		11_3	3·67	6·87	1·87	55	0·90	123·5[12]
					≈76		40_{11}	3·636	6·91	1·90			
Polypentene	Type I[15]	M	11·2†	20·85†	6·49		3_1	3·0	6·49	2·16	58	0·92	111[12]
	Type IIa[15]	M	19·3	16·9	7·08	γ=116°	4_1	4 0	7·08	1·77	74	0·90	80
Polyhexene[11]	either/	O	11·7	26·9	13·7		7_2	3·5	6·85	1·95	79	0·91	
	or	M	22·2	8·9	13·7	γ=94·5	7_2	3·5	6·85	1·95	98	0·73	
Polyheptene[11]					6·45		3_1						17
Polydecene[11]					13·2								34
Polydodecene[11]					13·2								49
Polyoctadecene[11]		O	7·5	70·4	6 7					1·68	264	0·95	71
Poly-3-methylbutene[9]		M	19·25	17·20	6·85	γ=116·5°	4_1	4·0	6·85	1·71	74	0·92	310
Poly-4-methylpentene[9]		Tet.	18·60	18·60	13·84		7_2	3·5	6·93	1·98	86	0·82	248
Poly-4,4-dimethylpentene‡		Tet.	20·35	20·35	7·01		4_1	4·0	7·01	1·75	104	0·90	> 350

M = monoclinic; O = orthorhombic; Trig. = trigonal; Tet. = tetragonal.
m_t = monomer units per turn; l_t = length parallel to c per turn.
l_m = length parallel to c per monomer unit; all lengths in Å.
A^2 = Transverse area per chain.
* = primitive cell; †a_0 and b_0 (a and b projected perpendicular to c); ‡unit cell derived from photographs of unoriented specimens.
§Now believed to be 40_{11} or possibly 29_8 (see later).

great enough to allow the energy barriers involved in the winding up of the helix from 3·667 to 3·0 and lengthening to $l_m = 2{\cdot}17$ Å from $l_m = 1{\cdot}87$ Å (*Table 1*) to be surmounted. It follows that the effect on the conversion of the presence in the chains of olefin units other than butene will depend on how the balance of these factors is adjusted. This in turn will depend on whether the copolymerized units enter the crystal lattice or are in the amorphous regions, and (if in the lattice) whether they can readily be incorporated in either of the two crystal forms, with or without lattice dimension changes, and the corresponding density changes. It will further depend on whether one of the butene helices is stabilized at the expense of the other; whether the melting points of the phases are raised or lowered, thus altering the mobility of the helices, and whether the units are randomly distributed in the chains or are present as runs of comonomer units which tend to take up the preferred helical conformation of their own homopolymers. The effect of copolymerization on the conversion is thus closely connected with the distribution of comonomer units in the chains, the extent to which cocrystallization takes place, and the crystalline phase changes in the copolymers, i.e. with the crystal structure of the copolymers which are discussed below. Later it will be shown in addition that comonomer units in the amorphous regions can also affect the rate of conversion.

EXPERIMENTAL

Copolymerizations were carried out with $TiCl_3$–$AlEt_2Cl$ catalysts by methods adapted for each pair of monomers, in particular by adjusting monomer ratios to take account of the different rates of polymerization and keeping the ratio constant throughout the reaction, but the results described below show that true random copolymerization was not achieved except possibly in the butene–pentene system. In some systems a large measure of copolymerization was obtained, in others a practically complete phase separation occurred with homopolymer chains developing separately (e.g. butene–44DMP). In the partially copolymerized systems chains may be present of varying composition and degrees of blocking, and the crystal phase behaviour may be very complicated especially in a highly cocrystallizating system. We have found that varying the polymerization procedures with a view to achieving greater randomness did not greatly influence the phase distribution observed. Some copolymers were prepared with catalysts that had been pretreated by homopolymerizing a small known amount of the comonomer, or of another monomer, before the copolymerization was carried out. The copolymer compositions given throughout refer to 'randomly' polymerized copolymer only. The small amounts of homopolymer do not affect the results significantly.

Copolymer compositions were measured by i.r. analysis. As each method is necessarily specific to each copolymer system, they will not be described here. The difficulties inherent in composition determinations in this type of copolymer where monomer sequences, helical conformations, crystal phase changes, degrees of crystallinity and cocrystallization are variable over the composition range were well recognized and the methods used were designed to be as far as possible independent of these

parameters. The composition data, which are given in moles per cent throughout, place the copolymers in order across the composition range. Particularly in the more complicated systems in the middle composition ranges the data are approximate, but this is not important in considering the general phase behaviour. The i.r. spectra of the copolymers always resembled in broad features a mixture of homopolymers, indicating that even where considerable copolymerization was shown to have taken place at least short homopolymer runs were present in the chains.

X-ray photographs were taken by Unicam 6 cm diameter cylindrical cameras and a Philips 11 cm diameter powder camera, and X-ray diffraction scans were obtained with Philips PW1010 or Hilger diffractometers, both with pulse height analysis.

In the work described in this paper the emphasis has been placed upon observing the change with copolymer composition in various factors such as degrees of crystallinity, rates of conversion from the Type I to the Type II crystalline form, and the rates of crystallization using X-ray techniques by methods which are both quick and simple to apply. This has necessarily been at a sacrifice of absolute accuracy, but usually it is the trend with copolymer composition and the variations with different α-olefin comonomers that is required and absolute accuracy is less important even if it were obtainable.

Determination of degree of crystallinity

Degrees of crystallinity were determined by methods similar to that used by Natta for polypropylene[11]; typical examples are illustrated in *Figure 1* which shows diffractometer scans from several copolymers obtained with the Philips diffractometer. In each case a linear background was drawn in and the area under the peaks was divided into amorphous (A) and crystalline (C) areas. The degree of crystallinity X was taken simply as $C/(A+C)$ with no further correction. Composite correction factors to take account of the effect of Lorentz, polarization and thermal factors on the relative areas were not considered very practicable or useful for the following reasons. This method is not absolute but the use of more absolute methods was ruled out by variations in composition, crystal phases and lattice parameters. Moreover the composition of the amorphous phase changes with comonomer content and this must give a progressively changing amorphous intensity distribution and replacement of monomer units by others in the crystal lattices necessarily creates imperfections giving rise to amorphous scattering which will be included in the amorphous regions. Where two or more crystalline phases are simultaneously present a large number of unresolvable peaks may be present, which makes difficult the fitting of the amorphous curve. Maximum consistency in the placing of the amorphous curve under the crystalline peaks was aimed at, and use made where possible of the distribution of intensity in the crystalline and fully amorphous homopolymers and copolymers where this was known. The degree of crystallinity must be regarded as relative not absolute, and care taken in comparing crystallinities where a sharp change of phase occurs.

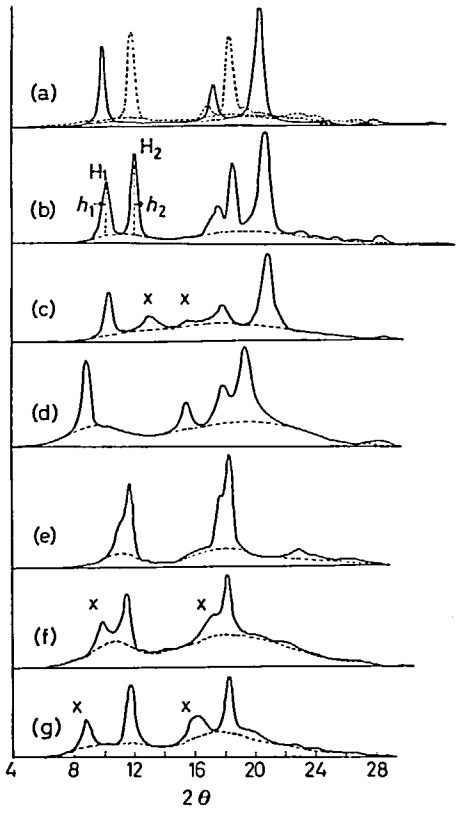

Figure 1—X-ray diffractometer scans of butene homopolymers and copolymers (all annealed). Major peaks of crystal phases other than PB I or II marked X: (a) PB I and PB II (dotted curve); (b) mixed PB I and PB II; (c) 44 per cent propylene ('PB I' and 'PPr'); (d) 77 per cent pentene ('PB I'); (e) 15 per cent 3MB (PB II_a and II_c)[7]; (f) 27 per cent 4MP ('PB II' and '4MP'); (g) 21 per cent 44DMP (PB II and 44DMP). Phases in parentheses show modified lattice dimensions

Rates of conversion from Type II to Type I polybutene

Rates of conversion from PB II to PB I were measured by an X-ray method similar to that of Zanetti[4] but developed independently with the aid of the Hilger diffractometer for which a heating oven had been designed. Measurements were made on a cylinder of about 2 mm diameter and 1·5 cm long cut from a moulded specimen of polymer. This fitted closely into a thin walled 2 mm diameter glass tube transparent to X-rays. The tube containing the copolymer was heated to 200°C for ten minutes and then quenched rapidly into water at 20° to 25°C and immediately transferred to the diffractometer and the diffracted intensity recorded at once over the 2θ range 7° to 14° to include the low angle peaks H_1 and H_2 at $2\theta = 10°$ and 11·8° which are due to Types I and II polybutene respectively [*Figure 1*(b)], and at appropriate intervals of time subsequently. The proportion of the total crystallinity in the Type II form was derived as described below. To investigate crystallization at higher temperatures the temperature of the oven, controlled by a thermistor controller, was set to the required crystallization temperature and the specimen quickly placed in it instead of being plunged into water; diffractometer scans were run as before.

Figure 1(b) shows an X-ray diffractometer scan of a butene homopolymer indicating Types I and II forms simultaneously. To derive the relative proportions of the two forms in the crystalline portion of the polymer an amorphous background curve is drawn in under the two peaks H_1 and H_2 at 10° and 11·8° of 2θ as shown, and their heights above this curve, h_1 and h_2, measured. The percentage in the Type II form of the total crystallinity (C_{II}), (i.e. $C_I + C_{II} = 100$) was taken as

$$C_{II} = h_2 \times 100/(h_2 + 2h_1)$$

It is appreciated that this may appear a somewhat arbitrary measure of relative proportions of Types I and II but it is simple and quick to apply. The justification for use of the above approximate formula came from earlier work when it had been found that C_I and C_{II} derived by methods involving resolution of the diffraction scans of butene homopolymer at various stages in the conversion from 100 per cent Type II to Type I, into the separate peaks of each form, gave results varying less than ±2 per cent from the values derived from the above formula, and it was a good approximation to take

$$C_I/C_{II} = 2h_1/h_2$$

The contraction or expansion of the polybutene homopolymer crystal lattice resulting from the inclusion of copolymerized units in the lattice causes a small shift of the Types I and II peaks at 10° and 11·8° of 2θ respectively; the maximum heights of the peaks above amorphous background were measured in each case, irrespective of the precise 2θ values at the maxima.

Rates of crystallization

In the course of the above rate of conversion experiments, the development of crystallinity was simultaneously measured at various times t from the start leaving the specimen undisturbed throughout. Immediately after the last short scan across H_1 and H_2, a full scan to give a final crystallinity X was obtained.

If h_1 and h_2 were the heights of peaks H_1 and H_2 on this scan, then the crystallinity X_t at any time t was taken as

$$X_t = X\,(2h_1' + h_2')/(2h_1 + h_2)$$

when h_1' and h_2' were the heights of the peaks at time t. When the time interval was reasonable the crystallinity scan was run when all the Type II had converted and h_2 was zero, as the crystallinity measurements are then more accurate. Comparisons of rates of crystallinity where crystallization was directly into the Type I form ($h_2 = 0$) are necessarily the most accurate.

COPOLYMERS SHOWING ACCELERATED POLYBUTENE TYPE II→I PHASE CONVERSION

Butene–pentene copolymer structure (6 to 84 per cent pentene)

Table 2 summarizes data relating to the crystallinity of copolymers of varying pentene contents. Crystallinity was observed throughout the whole

composition range but the series was unusual because only one phase was visible to X-rays over the range 0 to 84 per cent pentene, before and after annealing. This was basically the PB I phase, but with intensity changes due to the inclusion of pentene units and spacing changes due to a strictly linear increase with pentene content in the *a* cell dimension of the hexagonal cell from 17·6 Å in PB I to 20·1 Å at 84 per cent pentene while the *c* (fibre) axis remained constant at 6·5 Å. The degree of crystallinity dropped progressively to about 40 per cent at 50 moles per cent pentene and then remained approximately constant over the range where the 'PB I' form persists. There is thus a substantial degree of cocrystallization with pentene units substituting for butene units without causing a change to a polypentene (PPe) crystal phase even at 84 per cent pentene. This fact together with the absence of crystal phase separation, which is observed in the ethylene and propylene copolymers with butene, suggests that a much higher degree of randomness in the distribution of monomer units has been achieved in the polymerization. This may well be the result of rather similar rates of polymerization of the two structurally closely related monomers. *Figure 1*(d) shows the diffractometer scan of the 77 per cent pentene copolymer; the lateral lattice dimension changes from those of PB I homopolymer [*Figure 1*(a)] are clearly observable with the PB I peak at 20·3° of 2θ splitting into equatorial and first layer reflections at 17·8° and 19·3° respectively. Only at a level of 84 per cent pentene was PPe type crystallinity sometimes observed. Fibres of this copolymer drawn at 20°C showed oriented 'PB I' only, but those drawn at 100°C showed a little oriented PPe II also. Heating the latter fibre at 80°C for 20 hours converted all crystallinity to the 'PB I' phase in contrast to fibres of pentene homopolymer (II) which convert to PPe I under these conditions[15].

Within experimental error a linear reduction in final melting point of the 'PB I' phase with pentene content was also observed, so that in this phase the melting point varies linearly with crystal density (the density was calculated on the assumption that comonomer units are randomly distributed in the polymer chains in both amorphous and crystalline phases). This provides additional evidence for isomorphic cocrystallization of comonomer units largely randomly distributed. Melting points were measured by X-rays because the rather poor spherulitic texture gave rather lower values by the optical birefringence method; the latter indicated the presence of trace amounts of higher melting spherulites in the middle composition range. These must arise from small amounts of butene-rich chains. Otherwise these values confirmed that one crystalline phase only was present in slow-cooled specimens provided, of course, that any PB II initially present had converted to Type I. The rise in melting point between 84 and 100 per cent pentene corresponds to the crystal phase change from the 'PB I' phase to the pentene homopolymer phase and is reflected in an increase in crystal density (*Table 2*).

Butene–propylene copolymer structure (3 to 89 per cent propylene)

Table 3 gives crystallographic data and final optical melting points for copolymers of varying molar composition. Although the method of

Table 2. Butene-pentene copolymers—crystallographic data

Moles % *pentene*	*Crystal form**	*Crystal-linity*, %*	*PB I* *a-axis, Å**	$d_{cryst.}$ *†	*Transverse area/chain**	*M.pt°C** *X-ray*	*PB II* *a-axis (Å)§*	$d_{cryst.}$† *PB II*	Δd
0	PB I	65	17·6	0·96	44	135	14·85	0·90	0·06
6	PB I	61	17·80	0·952		128	14·96	0·900	0·052
16	PB I	55	18·15	0·940	46·5	123	15·11	0·904	0·036
21	PB I	54	18·30	0·935	48·5	121	15·21	0·903	0·032
32	PB I	51	18·55	0·931	49·5	115	15·36	0·909	0·022
51	PB I	39	19·15	0·915	53	95			
63	PB I	43				76			
77	PB I	40	19·85	0·90	57				
84	PB I	39	20·1	0·89	58·5	71			
100‡	PB I‡		20·6‡	0·875‡	61·5‡	55–60‡			
100	PPe I			0·92	58·5	111			
100	PPe II	50		0·90	74	80			

*Cooled 6°C/h from 140°C
†Calculated assuming comonomer units are randomly distributed and the crystallite and amorphous copolymer compositions are identical
‡Extrapolated to 100 per cent pentene
§Measured on partially converted, slow cooled samples

polymerization, which here involved feeding propylene at constant pressure into bulk butene, may favour a sliding composition, copolymers later made by improved methods did not differ significantly.

The crystallinity present at all compositions was basically that of the principal homopolymer phases and both PB I and polypropylene (PPr) type crystallinity occurred simultaneously in the middle composition range but with lateral cell dimension changes. The PPr α-form transverse lattice expands progressively with butene content to accommodate larger butene units and the PB I lattice contracts owing to inclusion of smaller propylene units. Microscope observation showed that two physically separate phases were present with different melting points, and this was confirmed by X-ray examination of fibres drawn at temperatures between 20°C and 100°C from specimens of $\sim 50/50$ composition where highly oriented PB I developed but the PPr phase remained unoriented.

The melting points and degrees of crystallinity showed a broadly eutectic behaviour. The cross sectional areas occupied per ternary helical chain in the two crystal phases are approaching each other in the copolymer composition of 44 per cent propylene, but cocrystallization does not occur, even into a third crystalline phase different from either homopolymer phase as has been observed in other copolymer systems. The results above are consistent with a heterogeneous system with butene-rich and propylene-rich, possibly blocked chains crystallizing in separate phases, together probably with more random polymer (non crystallizing). The difference in sizes between the polypropylene and polybutene side chains is too great to allow true isomorphous replacement and cocrystallization. It seems likely that comonomer units are increasingly accommodated in each of the crystal lattices as the overall proportion in the copolymer increases but in such a way that the change in lattice dimensions does not compensate to keep the density constant. The density falls until at a certain (as yet unknown) proportion of comonomer units the lattice is no longer stable. This suggests that a truly random (isotactic) copolymer would be amorphous in the middle composition range.

Table 3 also shows that in copolymers made by polymerizing propylene after the butene polymerization the two homopolymers crystallize separately—polybutene with unchanged melting point and *a* lattice dimension, and polypropylene with a small change probably resulting from copolymerization with residual butene, although the system was evacuated between the polymerizations.

Figure 1(c) shows a diffractometer scan of a copolymer containing 44 per cent propylene showing both phases with modified lattice dimensions (the propylene peak at $2\theta = 12{\cdot}95°$ is at $2\theta = 14°$ in the homopolymer).

Butene–ethylene copolymers (20 to 91 per cent ethylene)

Table 4 includes crystallinity and melting point data for copolymers of varying molar composition. Since crystallinity of both the polybutene type and polyethylene was present at all compositions examined except 91 per cent ethylene, and microscope observation confirmed that two

Table 3. Butene–propylene copolymers—crystallographic data

Moles % propylene	*Crystal forms**		*Crystallinity*, %	*Optical M.pt, °C** *PPrα*	*PB I*	*Cell dimensions, Å** *PPrα* $a \sin\beta$	*b*	*PB I* *a*	*Transverse area/chain, Å²* *PPrα*	*PB I*
0		*PB I*	63		135			17·65		45
3		*PB I*	60		129			17·55		44·5
12·5	PPrα†	*PB I*	56		125					
14	PPrα†	*PB I*	56		122			17·5		44
21·5	PPrα‡	*PB I*	51		120		≈23·0	17·4		43·5
44	PPrα	*PB I*	44	100	115	7·15	22·9	17·3	41	43
75·5	*PPrα*	PB I†	35	141		6·80	22·0		37·5	
89	*PPrα*		43	152		6·64	21·4		35·5	
100	*PPrα*			175		6·56	20·95		35	
'Block'										
24	PPrα	*PB I*		150	132			17·7		
36·5	PPrα	*PB I*	62	152	130	6·64	≈21·2	17·7		

*Slow cooled from 200°C at 6°C/h; †Trace; ‡Small amount. Major phases in italics.

physically distinct phases were present the polymerization clearly had not taken place randomly. Drawn fibres showed different degrees of orientation of polybutene and polyethylene crystallites thus confirming phase separation.

Table 4. Butene-ethylene copolymers

Moles % ethylene	*Crystal form*	*Crystallinity, %**	*M.pt, °C*	
			PB I	*PE*
20	*PB I*	24	111	
	PE (trace)			
33	*PB I*	16	~90	
	PE (little)			110
46	*PB I*	11	55	
	PE			122
62	PB I			
	PE	10		125
91	*PE*	34		126

Major phases in italics.
*Unannealed (annealed crystallinities were slightly lower).

No significant lattice dimension changes in the PBI form of the type observed in the copolymers of butene with propylene or pentene were observed; moreover the *a* cell dimension of the PE phase remained constant at 7·5 Å over the range examined showing, according to P. R. Swann[16], that not more than about 3·6 butene units per 100 carbon atoms are present in the lattice. Ethylene units would be expected to have a more marked effect than propylene in contracting the butene lattice, hence only a few units, probably solitary units, can be present in the polybutene crystalline phase. However, the low overall crystallinity and the loss of crystallinity in the middle composition range shows that a considerable degree of copolymerization had taken place without cocrystallization, and the relative proportions of the crystalline phases, degrees of crystallinity and melting points are consistent with a phase system of butene-rich block polymer and an ethylene-rich block polymer both crystallizing to a limited degree probably with varying block lengths and overall chain composition together with more random amorphous copolymer. The X-ray patterns of unoriented specimens and fibres of the butene-rich phases substantiate this; the relative intensities of the diffraction spots change with composition, the upper layer lines decreasing in intensity with respect to the equatorial layer while the spots remained sharp. This suggests good lateral order in the crystallites but limited order along the length of the chains, decreasing with ethylene content and therefore consistent with blocking. A high degree of cocrystallization between the two units is not likely owing to the considerable difference in cross sectional area occupied per chain in the polybutene and polyethylene crystal lattices; very short runs of non-helically disposed ethylene units in the butene rich-phase must disrupt the helical crystallization considerably.

Copolymers with ethylene, propylene and butene; PB II to PB I conversion

The structural investigations of these three copolymer systems have shown that PB I is the form preferentially involved in the cocrystallization

Table 5—PB II to PB I conversion and rates of crystallization for copolymers of butene with pentene, propylene and ethylene

Comonomer	*Comonomer mols %*	*% type II of total crystallinity*						*Crystallinity %*										*Slow cooled from 200°C**	*M.pt°C PB I slow cooled*
		Minutes after quench to 20–25°C			*Minutes after quench to 50°C*			*Minutes after quench to 20–25°C*					*Minutes after quench to 50°C*						
		5	30	240	5	30	240	2½	5	10	20	*Final†*	2½	5	10	20	*Final*†*		
—	0	100	100	94‡				37	38	39	40	51						62	
Pentene	6	100		96				31	32	33	34	50						61	128
	16	100	98	84								47						55	123
	21	98	89	53				25	27	29	32	46						54	121
	32	65	24					25	28	31	34	48						51	115
	51	—	0					0	1	5	25	37						39	95
	63	—	0					0	0	2	25	38						43	
	77	—	0					0	0	0	2	34						40	
Propylene	7·5	97	90	30				32	33	34	36	47						55	127
	12·5	9	3	0	86	71	62											56	125
	12·5	6	1	0	96	88		37	39	40	44	44	27	29	31	33	49	54	
	16·5	9	3	0	93	59		41	42	43	44	45					52	55	
	22	0	0	0	62	47	17	—	29	30	31	32	26	26	27	28	39	49	120
	26	0	0		50	28	8	18	20	23	27	32	11	21	26	30	42	51	
	29·5	0	0		8	1	0						1	21	24	27	34	52	
	30·5	0	2		18	7	1	11	20	23	24	33	4	12	21	24	36	53	122
	35	0	2		5	0	0	15	18	22	25	30	0	9	19	22	37	52	119
	37·5	0	1		0	0		15	22	23	24	30	0	11	20	23	33	51	116
	38	0	0		0	0		18	22	26	27	30	0	11	17	21	34	47	
(Block)	30	100	96	35‡															
Ethylene	20	94	78	12				0		12	12	24						24	111
	33	—	16	9				0	0	2	8	16						16	~ 90

*After specimens had regained room temperature.
†When crystallinity had reached a constant value and was predominantly PB I.
‡After 600 minutes.

Table 6—Copolymers showing stabilization of PB II—crystallinity, melting point and stabilization data

Comonomer	*Moles % comonomer*	*PB crystal forms (unannealed)*	*Crystallinity, % annealed* (PB II)*	*Final M.pt°C*† (PB II)*	*% PB II Days after annealing** 3	20	150	*% PB II Days after moulding‡* 10	50	200	*% PB II—moulding after compression dyne/cm²×10⁸* 1·1	2·2	*PB II stability in warm drawn fibres§*
None	0		~ 55	117				14	8	6	30	15	v. poor
Hexene	3·5	*I* trace II	45	108	89	68	10	20					poor
	7	*I* ,, ,,	42	102	97	96	88	97	92	76	60	35	poor
	13¶	*I* little II	35	98	97	96	95	100	100	100	82	73	good
	16·5	*I* II	25	89	92	91	90						mod. good
	41	I *II*	8										
	69	Amorphous	0										
Octene	3·5	I *II*	41	101	100	99	95	96	93	68	62	45	poor
	6·5¶	I *II*	27	96	100	98	93	100	100	100	88	70	good
	7¶	Little I *II*	32	92				100	100	100	96	93	good
	9·5¶	*I* II	22·5	95	100	98	98	100	100	100	97	89	
	13	*I* II	16	87	100	100	98						
	22·5	Trace I *II*	6		100	100	100						good
	48·5	Amorphous	0										
Nonene	2	*I* II	41	100	100		90	94	80	30	60	35	poor
	4¶	I III	33	93	100		92	100	100	100	92	75	mod. good
	6	I II	25	91	100		86						mod. good
	6¶	*I* II	24	92	100		81	100	100	100	94	94	good
Decene	2	*I* trace II	38	99	100	94	87	65	30	10	43	25	poor
	5·5¶	*I* ,, ,,	27	96	100	89	86	96	94	70		75	good
	7	I *III*	16	94	80	67	49	94	83	57	78	65	mod. good
	12	*I* trace II	9	78	80	59	42		Amorphous				mod.
Dodecene	3	I trace II	27	97	96	84	70	97	78	20	49	55	poor
	7¶	I ,, ,,	16	97				100	87	70	96	90	mod. good
	10·5	I ,, ,,	17	99	70	25	7						mod.
	12	I ,, ,,	12	93	70	29	10						mod.
Octadecene	1	I III	39	103	83	9	6	4	4	3	30	19	v. poor
	2	I III	27·5	100	70	11	4						poor
	3	I III	23·5	99	55	2	0	12	7	0	66	40	poor
4-Methyl pentene	3·5	I III	45	112	100	93	55						
	~ 5	I III	38	109	100	82	76	100	100	100	70	48	
	~ 7¶	*I* II			100	100	100	100	100	100	—	73	
	~ 11¶	*I* II	33	103	91	91	90	100	100	100	88	82	good
	14¶	I II	31	103	95	94	92	91	91	91	90	90	good
3-Methyl butene	4				81	20		92	68	36	42	30	poor
	4		55	117	96	78		99	95	82	53	38	poor
	8¶		55	129	100	100	100	100	100	100	97	92	good
	15¶		50		100	100	100	100	100	100	100	100	good

*Slow cooled at 6°C/h from 150°C (hexene–octadecene); from 250°C (4MP); from 200°C (3MB).
†Optical m.pt (hexene–decene) and 4MP; X-ray m.pt dodecene, octadecene, 3MB.
‡Compression moulding (10 min at 200°C, then quenched to 20°C); all samples in PB II form only immediately after moulding.
§Poor—PB II converts within a few days; moderate—partial or complete conversion in 1 to 2 months; mod. good—very slow conversion proceeding over ~ 9 months; good—effectively no conversion.
¶Moulding well stabilized (> 70 per cent PB II) on rapid compression to $2{\cdot}2\times10^8$ dyne/cm².
Major phases in italics.

and it was found that at high butene compositions, where the crystallinity is mainly that of polybutene, rates of conversion from PB II to PB I in all three copolymer systems were markedly increased compared with the average rate in butene homopolymers, even by quite small amounts of comonomer. *Table 5* gives the proportion of PB II crystallinity (of the total I+II crystallinity) present at various times from the start of crystallization after quenching the copolymers from 200°C to between 20° and 25°C and also to 50°C for copolymers with propylene. These data are taken from graphs of percentage PB II versus time. It will be seen that in all three copolymers the proportion of PB II initially produced becomes progressively lower as the overall comonomer content increases, until eventually crystallization takes place directly into the PB I form. The tables also show that as the proportion of PB II decreases the rates of crystallization also drop and progressively lower final crystallinities are attained. The latter were measured when the crystallinity was substantially converted to PB I.

The butene–propylene series of copolymers has been most extensively investigated so far. Up to ~ 10 per cent propylene the initial development of PB II on quenching to ~ 20°C and its conversion to PB II is somewhat variable, and probably reflects variations in the degrees of randomness of the copolymer due to differences in polymerization conditions. Above 10 per cent propylene crystallization occurs substantially directly into PB I with only a little PB II developing initially and traces developing in the course of crystallization. The initial rate of crystallization is still high (even at 30 per cent propylene) compared with the pentene series at the point where PB I develops directly, but the final crystallinities reached at 20°C were, as expected, considerably lower than those attainable by slow cooling with the difference increasing with propylene content. In a block polymer containing 30 per cent propylene (propylene polymerized first), the transition was only marginally accelerated compared with that in butene homopolymer showing that it is the randomly polymerized propylene that is effective. The relatively small accelerating effect of the blocked polypropylene is probably similar to that reported by Boor and Mitchell[17] in polybutenes to which small amounts of crystalline polypropylene had been added.

At a quench temperature of 50°C (*Table 5*) direct crystallization into PB I did not occur until much higher propylene contents (~ 25 per cent) were reached. The initial rate of crystallization, particularly at ~ 30 per cent propylene, had dropped considerably compared with the rate at room temperature and the copolymers were initially amorphous for several minutes. *Figure 2* shows the rate of conversion to PB I on one sample containing 22 per cent propylene at various temperatures up to 60°C; the rate drops progressively up to 50°C, but rather unexpectedly at 60°C a higher proportion of PB I develops initially although not much further conversion occurs.

In the butene-pentene series a considerably higher proportion of comonomer was required to effect direct crystallization into PB I. Rates of crystallization were much less reduced than in the butene–ethylene

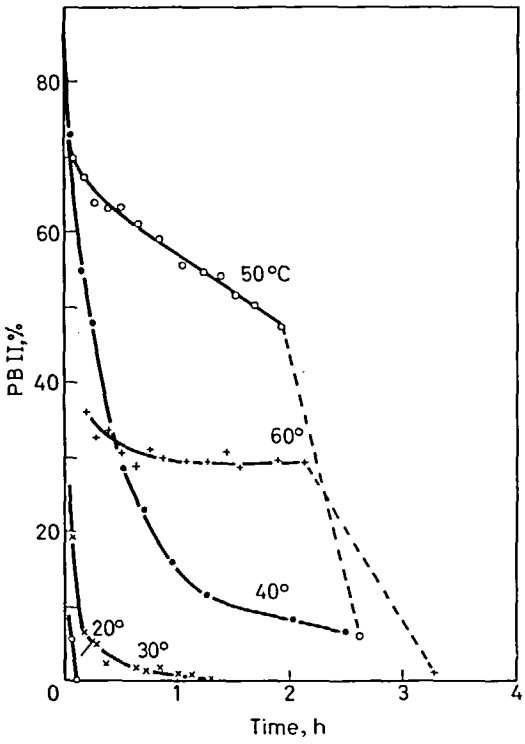

Figure 2—PB II–PB I conversions in 22 per cent propylene copolymer quenched to various temperatures. Dotted lines represent reversion to 20°C

copolymers at the same molar comonomer content and the final crystallinities eventually reached were much higher in line with the higher annealed crystallinities.

COPOLYMERS SHOWING STABILIZATION OF TYPE II POLYBUTENE. BUTENE–LINEAR α-OLEFIN COPOLYMERS

Table 6 lists crystallographic data obtained at several comonomer contents on the six copolymer systems of this series examined from hexene-1 to octadecene-1. Detailed examination was confined to copolymers of low comonomer content showing PB crystallinity only and where the crystallinity remained relatively high to provide evidence on the stabilization of PB II.

Stabilization in Type II form

In all these copolymer systems some degree of stabilization of PB II was observed. The degree of stabilization attained and the level of comonomer giving the highest stabilization was found to vary with the procedure used to measure it, and observations by several methods were made in order to make an overall assessment of each copolymer. The relative proportions of PB II and PB I crystallinity developed were measured by the method described in the experimental section and com-

pared with butene homopolymer treated under the same conditions (*a*) versus time in copolymers slow-cooled from 150°C at 6 degrees per hour, (*b*) versus time in compression mouldings quenched from 200°C (10 min) to 20°C (here the degree of crystallinity is, as expected, appreciably lower than in the slow-cooled specimens) and (*c*) in similarly prepared mouldings (1 in. × $\frac{1}{8}$ in. × $\frac{1}{8}$ in.) which were subjected immediately after moulding to rapidly applied and instantaneously released compressive forces of $1{\cdot}1 \times 10^8$ and $2{\cdot}2 \times 10^8$ dyne/cm^2, and (*d*) in fibres drawn at varying temperatures. Several copolymers, particularly those of lowest comonomer content showed considerable stability if left undisturbed by methods (*a*) and (*b*) but were still inherently unstable as they were appreciably converted if struck with a hammer or cut with a knife; it is well known that conversion of PB II is assisted by mechanical shock and by pressure[3,4] and method (*c*) was designed as a quick method of testing the stability of the copolymer in this respect. Where the mouldings were flexible this necessarily resulted in considerable deformation of the specimen.

If conversion to not less than 70 per cent PB II is taken as the criterion of good stabilization on mouldings examined by method (*c*) ($2{\cdot}2 \times 10^8$ dyne/cm^2) then those copolymers marked with a rubric are all well stabilized by methods (*a*), (*b*) and (*c*). Results on fibres are discussed below and are generalized in the last column. Octene and nonene copolymers show the best stabilization and require the lowest comonomer contents to produce effectively complete stabilization ($\sim$7 per cent octene and 4 per cent nonene) while 13 per cent hexene is required. Although 5 to 7 per cent decene and dodecene produce stabilization, a fall-off in stabilization is observed above $\sim$7 per cent. Octadecene shows only a small degree of stabilization.

Crystallinity and melting points

The relative proportions of PB I and PB II of the total crystallinity must be assessed alongside the overall degrees of crystallinity since the results are necessarily less accurate where the crystallinity is low. The degrees of crystallinity in the PB II form (immediately after slow cooling) fall off markedly and regularly with increasing amounts of comonomer and with increasing size of comonomer unit at comparable molar percentages. At the higher comonomer concentrations the crystallinity was sometimes decreased by slow cooling, presumably because crystallization from the melt is hindered by chain entanglements with the long side-groups. This effect was found in copolymers of 4-methyl pentene with linear α-olefins[8].

The melting points given (PB II form), which in each case are final melting points, decrease in a regular manner with comonomer content, and with increasing size of monomer unit for the lower α-olefin comonomers; with the higher α-olefins as comonomers (nonene upwards) melting takes place over a much wider temperature range, sometimes starting from room temperature, compared with the hexene copolymers where the melting points are much sharper. Hence, the final melting points can be rather misleading. Both crystallinity and melting point behaviour are consistent with appreciable copolymerization having taken place, but with increasing range of chain compositions as the α-olefin increases in size.

The retention of even a small amount of crystallinity in the hexene and octene copolymers containing >20 per cent comonomer suggest that possibly some degree of isodimorphic replacement of monomer units has taken place. This is consistent with the relatively sharp melting points of the hexene copolymers. It may alternatively be that, here too, there is a spread of chain compositions with butene-rich chains present which are more crystallizable than the remainder. No phase separation (except PB II $\longrightarrow$ I conversion) is observable under the microscope except at high contents of the larger comonomers (e.g. 12 per cent decene), but the spherulitic texture is poor and the melting points indistinct. The copolymers containing 7 per cent dodecene of final PB II m.pt 97°C gave a double melting point of 98°C (PB I—disperse phase) and 89°C (PB II—continuous phase) after partial conversion which is consistent with a butene-rich PB II crystalline phase converting first to PB I, leaving a less rich phase of lower melting point. No homopolymer of decene or dodecene is present since the X-ray diffraction scans of the copolymers containing 20 to 30 per cent by weight of comonomer do not show the typical low angle maxima at $2\theta = 5{\cdot}9°$ and $5{\cdot}5°$ 2θ respectively.

Table 7. Butene–linear α-olefin copolymers—equatorial lattice dimensions

Comonomer	*Mol. % comonomer*	*PB I a-axis, Å*	*PB II a-axis, Å*
None	—	17·65	14·85
Hexene	7	18·0	
	13	18·36	15·18
	16·5	18·37	15·25
Octene	6·5	17·98	15·01
	9·5	18·08	15·14
Nonene	6	17·85	15·09
Decene	5·5	17·85	15·01
	7	17·85	14·97
Dodecene	7	17·74	14·91

The hexene and octene copolymers showed a distinct increase in PB II and PB I lateral cell dimensions in slow cooled specimens (*Table 7*). It is doubtful whether the slight expansion of the lattices shown by copolymers with nonene and decene at ~ 6 per cent comonomer is significant, but certainly the 7 per cent dodocene copolymer shows no lattice expansion. These results are consistent with some hexene and octene units entering the lattice and this in part can explain the retention of crystallinity at high monomer contents. As expected a greater expansion of the more compact PB I lattice (44 Å^2 per chain) is found than in the PB II lattice (55 Å^2 per chain). Marked intensity changes in the PB I X-ray pattern from those of butene homopolymer are observed in both annealed and unannealed copolymers containing 16·5 and 13 per cent hexene, which must arise from the incorporation of hexene units in the lattice; at 7 per cent hexene there was little change and no intensity changes were observed at 9·5 and 13 per cent octene (as originally made) or 6 per cent nonene. Whilst it is clear copolymerization has also taken place in the nonene to octadecene copolymers, comonomer units do not

enter the PB crystal lattice in dodecene and octadecene, and probably not in decene or nonene either.

In general the physical texture of the copolymers varied according to their degree of crystallinity independently of comonomer content. At crystallinities of 30, or ~40 per cent (*Table 6*) they were received as white powders or relatively hard crepes which could be pressed into flexible mouldings. Below ~ 30 per cent crystallinity they were rubbers, becoming softer and sometimes sticky as the crystallinity decreased.

Fibres

It is well known that in fibres drawn from butene homopolymer, the conversion of any oriented PB II crystallinity formed initially is so rapid that it is difficult to get an X-ray photograph of a fibre showing appreciable PB II[1,2]. Fibres of this series of copolymers were cold drawn at ~20°C and warm drawn at ~70° to 100°C from copolymers at most of the compositions listed in *Table 6* and the development of PB II and its conversion to PB I were followed qualitatively by X-ray diffraction immediately after drawing and at various time intervals.

Cold drawn fibres of hexene copolymers showed oriented PB I predominantly up to 13 per cent hexene, but as the temperature of draw rose the proportion of oriented PB II increased and at 90° to 100°C PB II predominated initially in all specimens. The rate of conversion to PB I was slower in fibres drawn at 90°C from copolymers containing 3·5 and 7 per cent hexene, than in fibres of butene homopolymer, but very little PB II was left after one day. At higher hexene contents the PB II form became increasingly more stable and the 90°C fibre of a 16·5 per cent copolymer was only very slightly converted after six months.

A similar type of pattern was followed in all the copolymers of this series. In general cold-drawing at low comonomer contents favours the initial development of PB I, while development of PB II and stabilization in this form is favoured by higher temperatures of draw and by higher proportions of comonomer in both cold- and warm-drawn specimens, but stabilization tends to fall off beyond nonene. Both cold- and warm-drawn fibres from octene copolymers showed well stabilized PB II at all compositions above 3·5 per cent, as did also warm-drawn fibres from copolymers containing 6 per cent nonene; at 4 per cent nonene slow partial conversion took place. Well stabilized PB II developed in warm-drawn decene (5·5 per cent and 7 per cent) and dodecene (7 per cent) fibres, but there was evidence for a decrease in stability at higher comonomer contents in both copolymers as also shown by unoriented specimens; cold-drawn dodecene copolymer fibres also showed much higher initial PB I development than did the octene copolymers. Octadecene copolymers (1 to 3 per cent) showed very poor stabilization of PB II; PB I predominated in all fibres except the warm-drawn 3 per cent fibre and this converted to PB I predominantly after one day.

Warm-drawn fibres showed the highest orientation and in several copolymers sufficiently high orientation was obtained for a determination of the helical conformation of the chains to be made by the method of Cochran, Crick and Vand[18]; this in each case was $3{\cdot}636\ (40_{11})$ [see

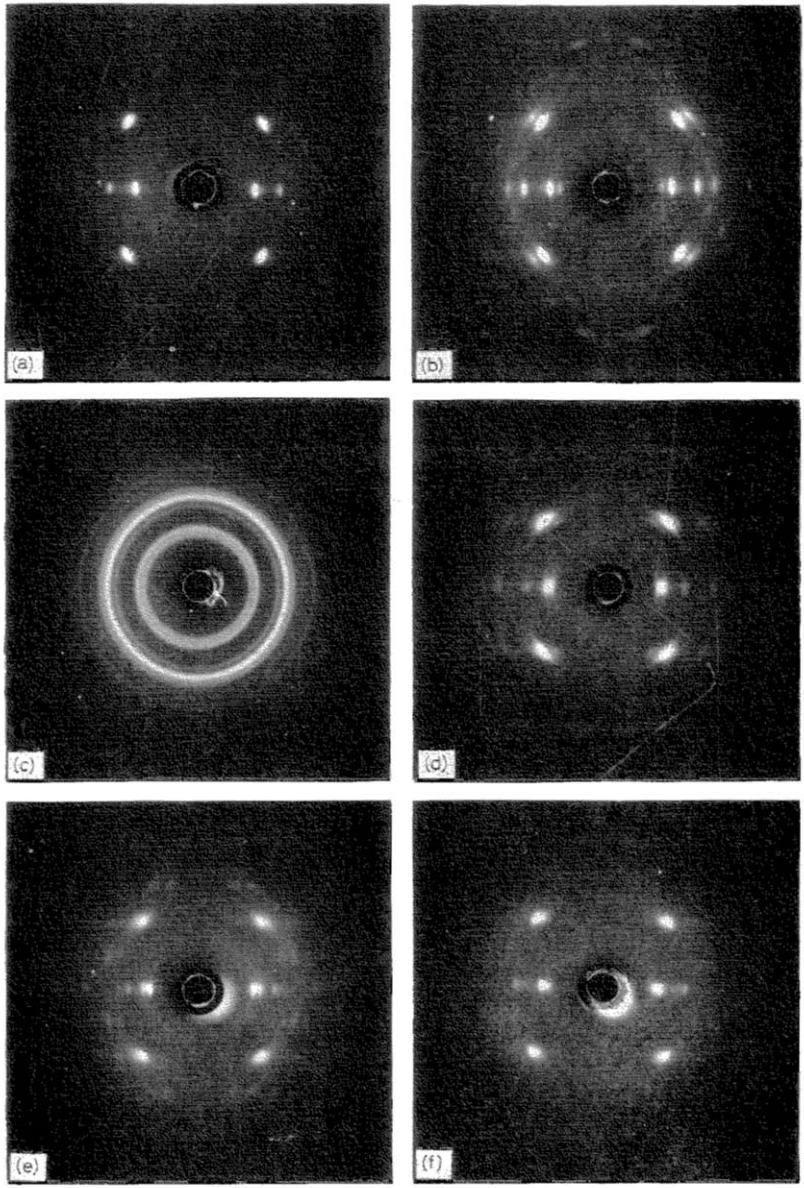

Figure 3—Butene homopolymers containing: (a) 15 per cent 3MB, fibre drawn $\sim$ 100°C (PB II_a form[7], 37_{10} helix); (b) 5·5 per cent decene, fibre drawn $\sim$ 100°C (PB II, 40_{11} helix, with some PB I); (c) 62 per cent 3MB, unoriented, annealed (P3MB chiefly); (d) 62 per cent 3MB, fibre drawn $\sim$ 120°C and annealed at constant length 120°C (PB II_b[7] chiefly, some P3MB); (e) 52 per cent 4MP, fibre drawn $\sim$ 180°C (P4MP chiefly and PB II with weaker layer lines missing); (f) 32 per cent 4MP, fibre drawn $\sim$ 180°C (PB II chiefly—weaker layers just present and P4MP—weaker layers missing)

Figure 3(b)] although the distinction from a 3·625 helix (29_8) is not always certain. As the proportion of comonomer increased the X-ray fibre photographs showed increasing signs of disorder in the crystal lattice. The helical conformations and the lattice disorder are considered later in the discussion.

COPOLYMERS SHOWING STABILIZATION OF TYPE II POLYBUTENE. BUTENE-BRANCHED α-OLEFIN COPOLYMERS

Butene–3-methylbutene (4 to 96 per cent 3MB)

This system has already been described[7]. The crystal forms of poly-3MB and polybutene are crystallographically quite different (*Table 1*), so that true isomorphism is not possible; nevertheless this system showed a high degree of cocrystallization and the crystallinity never dropped below 50 per cent in slow-cooled specimens even in the middle composition range. In this range several crystalline phases were observed which were related to the PB II crystal form but differed in helix and showed expanded tetragonal *a*-axis cell dimensions which must result from accommodation of monomer units of both types in the lattice; the melting points of the major crystalline phases rose with overall 3MB content in confirmation of this. *Figure 1*(e) shows a diffractometer scan of a 15 per cent 3MB copolymer (unoriented) showing such modified PB II phases (Types IIa and IIc principally[7]). Inclusion of 3MB units in the PB lattice caused marked stabilization of the PB II form, which was complete in fibres drawn at about 100°C at 10 to 15 per cent 3MB and in unoriented specimens at 8 per cent 3MB, while some degree of stabilization was effected by ~ 5 per cent 3MB as measured by a decreased rate of conversion to PB I. Stabilization results are included in *Table 6* for comparison with the other copolymers listed. At 8 per cent 3MB the helix was 3·667 (11_3) and at ~ 15 per cent 3MB is 3·70 (37_{10}), see *Figure 3*(a). The multiplicity of phases observed suggests that chains of variable composition and degree of blocking are present. Copolymers in the middle composition range can develop predominantly phases related to P3MB or to PB II depending upon their treatment. *Figure 3*(c) and *3*(d) show X-ray photographs of a copolymer containing 62 per cent 3MB annealed unoriented (P3MB type chiefly) and as a fibre drawn and annealed (PB IIb chiefly)[7].

Butene–4-methylpentene copolymers (3·5 to 92 per cent 4MP)

Table 8 gives crystallographic data on a number of copolymers selected to cover the full composition range from those examined. Basically two crystalline phases only were observed, those of P4MP and PB II (with Type I occurring at very low 4MP contents), but both phases were modified by inclusion of monomer units of the second type, which was shown by the gradual change in lateral (tetragonal) *a* unit cell dimensions of both forms (decrease and increase respectively) with overall composition and a gradual change in melting point of both forms. Crystallinity was observed at all compositions, but dropped in the intermediate range where both phases were present simultaneously. It was clear the polymerization had

Table 8. Butene–4MP copolymers—crystallographic data

Mol. % 4MP	*Crystal forms**	*Crystal-linity, %**	*Optical* m.pt°C*		*a-axis, Å**	
			P4MP	PB II	*P4MP*	*PB II*
0	*PB II/I*	~55		118		14·85
3·5	*PB II/I*	40		112		15·00
5	*PB II/I*	38		109		
7	*PB II*	40				15·1
11	*PB II*	33		103		15·15
14	*PB II*	31		103		15·2
27	4MP *PB II*	34			17·9	15·35
32	4MP PB II	30	196	~100	18·1	15·45
52	*4MP* PB II	35	226	~100	18·2	~15·6
79	*4MP*	45	235		18·4	
85	*4MP*	46	235			
92	*4MP*	57	240		18·5	
100	*4MP*	65	248		18·6	

*Slow cooled from 250°C. Major phases in italics.

resulted in the development of butene-rich and 4MP-rich chains which separated into two crystalline phases on slow-cooling. True cocrystallization did not occur, owing to the difference in size of the monomer units (compare the CSAs of the 4MP and PB II forms in *Table 1*), but a marked degree of replacement of monomer units occurred resulting in introduction of disorder into both phases, shown in X-ray photographs by loss of weaker reflections of both forms in both oriented and unoriented specimens. The *a* unit cell lengths were still very different in the middle composition range (*Table 8*).

In copolymers of high butene content the helical conformation of the chains in the crystallites deduced from X-ray fibre photographs was 3·636 (40_{11}) at ~5 per cent 4MP and at ~10 per cent 4MP was 3·625 (29_8) although the distinction between these two helices is rather fine. At 27 per cent 4MP, however, the weaker layer lines defining the PB II helical conformation had become very indistinct and the helix was uncertain, and at 52 per cent 4MP they had disappeared giving an apparent repeat of 6·9 Å corresponding to the pitch of the helix. This phase was now so disordered that only the three strongest reflections (two equatorial and one first layer, $c=6·9$) were still observed, but these were still strong and sharp. The cold-drawn fibres of the 52 per cent 4MP copolymers showed this highly oriented 'PB II' crystallinity, with some less well oriented P4MP. At higher draw temperatures 100° to 180°C the P4MP phase well oriented predominated, presumably because the less mobile 4MP-rich chains had now had opportunity to crystallize; the odd layer lines characterizing the 7_2 helix were weaker than in the homopolymer but still present [*Figure 3*(e)]. At 32 per cent 4MP 'PB II' predominated at all draw temperatures with intermediate layers very weakly present [*Figure 3*(f)], but the proportion of P4MP increased with temperature of draw and the odd layer lines were now missing in this phase (apparent repeat 6·9 Å) although annealing the fibres at constant length at 110°C developed these

layers weakly and increased the proportion of P4MP. The structures of the disordered phases are discussed later.

From what has already been said it will be apparent that the inclusion of 4MP units in the butene lattice stabilizes the PB II crystal form. *Table 6* includes results on butene–4MP copolymers (3·5 to 14 per cent 4MP) which have been investigated for PB II stabilization by the same methods as the butene–linear α-olefin copolymers. As before the level of comonomer conferring stabilization varies somewhat with the test method but in general from these results and others not recorded here, some degree of stabilization, as measured by a slower rate of change to PB I in annealed specimens and quenched mouldings, is present at 3·5 per cent 4MP, increased stabilization at 5 per cent, and good stabilization by all methods at 7 per cent and above. Some variation in stabilization was observed below ~7 per cent and could be due to variations in the degree of randomness in the distribution of 4MP units.

As in the butene–linear α-olefin series, drawn fibres showed a mixture of PB I and PB II at high butene contents, but the proportion of PB I developed initially decreased as the temperature of draw rose and as the 4MP content rose, and stabilization of PB II increased with increasing 4MP. At 14 per cent 4MP fibres drawn 120°C (PB II with a trace of I) showed only a small conversion after 18 days. At 26 per cent 4MP some PB I still developed on cold drawing, but not on drawing at 75° to 110°C and the latter fibres had remained completely stable in the PB II form after six months. Hence stabilization in fibres requires a somewhat higher content than unoriented specimens.

Butene–4,4-dimethylpentene copolymers (1 to 93 per cent 44 DMP)

All the copolymers were crystalline (*Table 9*) and showed the two normal homopolymer phases simultaneously in varying proportions with no change in lattice dimensions of either form (P44DMP is mainly

Table 9. Butene–44DMP copolymers—crystallographic data

Moles % 44DMP	*Crystal forms*[a]		*Crystallinity, %*[b]	*Optical m. pt °C*[b] *44DMP*	*PB II*
1	—	*PB II*, I†	51		110
3·5	44DPM†	*PB II*, I†			
5·0	44DPM†	*PB II*, I†			
8·5	44DPM	*PB II*	43	>350	103
21	44DPM	*PB II*	38	>350	99
50	*44DMP*	*PB II*	30	>350	91
78	*44DMP*	?	>47	>350	
93	*44DMP*	—	60	>350	
100	*44DMP*		61		

[b]Slow cooled from 350°C under nitrogen.
†Trace.
[a]Major phases in italics.

characterized by strong diffraction lines at $d = 10{\cdot}1$ Å and $d = 5{\cdot}55$ Å); this shows that 44DMP units are not entering the polybutene lattice, and

probably few butene units are entering the P44DMP lattice since lattice contraction would be likely to result. The presence of crystallinity of the minor component at very low levels shows that the copolymers are not random but must contain butene-rich and 44DMP-rich phases or mixtures of homopolymer chains or both. Under the microscope two physically distinct phases are seen confirming this. The melting points of the butene phase decrease with decreasing butene content suggesting that some copolymerization has taken place; the melting point of the P44DMP phase is always $> 350°C$.

Confirmatory evidence that copolymerization of some 44DMP units into the butene-rich phase has occurred, comes from the marked stabilization of the PB II form even at very low levels of 44DMP. Most specimens examined as made were in the Type III form of polybutene but on slow cooling from 200° to 250°C they showed good PB II stabilization. Even at only one per cent 44DMP no conversion to PB I had taken place after one year and only about half the PB II crystallinity present was converted to PB I by a sharp blow with a hammer. At ~ 3 per cent or more 44DMP the copolymers were completely stable in the PB II form and only a trace of PB I was produced on hitting with a hammer specimens containing 3·5 per cent and 5 per cent 44DMP. Quenched mouldings were equally stable. Fibres drawn $\sim 100°C$ from strips of pressed sheet of copolymers containing 3·5 per cent and 6 per cent 44DMP, showed oriented PB II crystallinity with only a little PB I and only slow conversion of a small part of the PB II crystallinity took place in 12 months. Fibres drawn at $\sim 100°C$ of copolymers containing 8·5 and 21 per cent 44DMP, showed oriented PB II mainly, some PB I and some much less well oriented P44DMP, and again substantially no conversion of the PB II took place in 12 months (the 21 per cent copolymer drawn $\sim 150°$ showed no PB I). The difference in the degree of orientation of the two phases confirms their physical distinctness. At higher 44DMP contents it was not possible to draw fibres.

As a large proportion of the 44DMP content is present as P44DMP-rich copolymer even at high butene contents it seems likely that never more than very few moles per cent 44DMP are present in the butene-rich phase and these are sufficient to cause PB II stabilization. Further information on this point should be gained from fractionation which is now proceeding.

DISCUSSION

Copolymer structure and polybutene Type II $\longrightarrow$ Type I phase transition

Consideration of *Table 1*, particularly the cross sectional areas (CSA) per chain of the homopolymers, which reflect the size of the side-groups, suggests that the greatest degree of isodimorphic replacement of monomer units is likely to occur in the butene–3MB and butene–pentene systems which in fact have shown the highest degree of cocrystallization as already described with butene–pentene copolymers showing one crystal phase only from 0 to 84 per cent pentene. The degree of cocrystallization falls as the size difference increases. The particular form of polybutene with which

cocrystallization takes place preferentially is likely to be that which lies closest in helical parameters and CSA with those of the homopolymers of the comonomer, and the degree of cocrystallization (complete, partial or non-existent) will depend upon the ease with which chains containing both monomers randomly disposed or partially blocked can adjust to a common helix and fibre repeat (possibly different from those of either homopolymer) and pack side-by-side in a stable array which in turn depends on whether the CSAs now occupied by each type of monomer unit are not too different.

Copolymers with linear α-olefin comonomers

The results given above show that in the butene–ethylene system only very limited accommodation of monomer units of the second type in the homopolymer phase can occur owing to the large difference in size. With the larger propylene units as comonomer, partial isomorphic replacement occurs with appreciable incorporation of propylene units in the polybutene lattice and vice versa and lattice dimension changes, but no true cocrystallization. The propylene units are more stable in the PB I form, the form with identical (3_1) helix and fibre repeat (6·5 Å) to the α-form of polypropylene, and produce a corresponding increased rate of PB II $\longrightarrow$ I conversion.

Copolymers with hexene and higher α-olefins of high butene content show a gradually decreasing ability to include comonomer units in the lattice. Hexene and octene units are already too large for true isodimorphic replacement but some units can enter the PB lattice as shown by the lattice expansion. It is doubtful if even a very few nonene or decene units can enter the lattice and dodecene-1 units do not. The PB II form primarily is involved and the effect of inclusion of these comonomer units is to inhibit the conversion to PB I and stabilize PB II, i.e. the lattice of lower density (higher CSA) which more readily accommodates the larger side-groups. Nevertheless stabilization of PB II increases up to octene and nonene and is still good up to dodecene. Hence, stabilization is not only effected by entry of larger units into the lattice but by copolymerized large groups in the amorphous regions also. The helical parameters (m_t, l_t and l_m) of polyhexene are closer to those of PB II than PB I (*Table 1*). *Table 10* summarizes the helical conformations observed in highly oriented fibres of copolymers showing stabilization of PB II. The helix is 3·636 (40_{11}) (or possibly 29_8) in all the linear α-olefin copolymers where sufficient orientation was obtained for a determination to be made[18], and this includes one per cent octadecene. *Figure 3*(b) shows an X-ray fibre photograph of the 5·5 per cent decene copolymer typical of those obtained. The distinction from the very similar helix 3·625 (29_8) is not completely certain as it rests entirely on very small changes in the ζ values of the first two observable layer lines and demands very high orientation. The distinction from a 3·667 (11_3) helix is quite unequivocal. Hence it seems very likely that PB II itself has a 40_{11} (or possibly 29_8) helix because decene, dodecene and octadecene units do not enter the lattice in unoriented specimens and modification of the PB II helix by these units seems unlikely even in fibre specimens, particularly at as low a level as one monomer

Table 10. Butene copolymers with PB II stabilizing monomers. PB II helical parameters from fibre photographs

Comonomer	*Comonomer mole %*	*Fibre repeat, Å*	*Helix*	m_t	l_t, Å	*M. pt, °C PB II**
3MB	4		40_{11}	3·636		
			or 11_3	3·667		
	8	21·0	11_3	3·667	7·0	129
	20	69·5	37_{10}	3·70	6·95	130
4MP	7	76·9	40_{11}†	3·636	6·99	
	11	55·5	29_8	3·625	6·94	103
Hexene	3·5		Not 11_3			108
	16·5	76·5	40_{11}†	3·636	6·97	89
	41	6·85	*c*		6·85	
Octene	3·5		*a*		6·93	101
	6·5		*a*			96
	13	6·85	*c*		6·85	87
Nonene	2	76·8	40_{11}†	3·636	6·98	100
	6		*b*			92
Decene	2	76·5	40_{11}†	3·636	6·97	99
	5·5	76·5	40_{11}	3·636	6·97	96
	12		*b*/*c*		6·93	78
Dodecene	3	76·0	40_{11}†	3·636	6·91	97
	12		*b*		6·93	93
Octadecene	1		40_{11}†	3·636		103

Intermediate layer lines ($\lambda/\zeta > 6·9$); *a* present, but orientation not high; *b* weakly present; *c* absent.
*Unoriented, slow cooled. †Possibly 29_8.

unit per 100, probably not even randomly distributed. It follows that hexene and octene units are accommodated without helix modification either. Further examination of the PB II fibre on which the original determination of an 11_3 helix for the homopolymer was made[2], suggests that 40_{11} is acceptable and even more likely than 11_3 although the orientation is not very high. Clearly helix modification by linear α-olefins to a more open helix (3·70) does not occur as it does in the 3MB copolymers, and this is certainly associated with the absence of branching close to the main chain as in polybutene itself.

The position occupied by pentene copolymers in this scheme is perhaps surprising. The CSAs of the chains in the two forms of polypentene are both larger than that of PB II, in line with their longer side-chain, hence cocrystallization with PB II and inhibition of the phase transition would seem likely. Type I PPe has a closely similar CSA to that of PB II but has a 3_1 helix like PB I, which makes a bad fit structurally, but there seems no reason why cocrystallization should not occur with Type II PPe which has similar helical parameters to P3MB (which gives a highly cocrystallizing system), more particularly as the PPe helix does not appear critical, and both 3_1 and 4_1 helices are stable; they could be expected to adjust closer to the 3·667 helix of PB II without much difficulty. Somewhat unexpectedly, however, chains containing both butene and pentene units crystallize in the PB I form with 3·0 helix, even up to pentene contents as high as 84 per cent, and the PB II $\longrightarrow$ I transition is correspondingly

accelerated by inclusion of pentene units. It appears that the preference for a 3·0 helix and a 6·5 Å repeat, as in both the Type I forms, is the dominating influence in the crystallization and the rather large difference in the CSAs of the homopolymers is accommodated by lateral expansion of the PB I lattice to accept the larger pentene units, but the occurrence of a phase closely related to PB I up to so high a level of pentene is surprising. It appears that a small proportion (16 per cent) of randomly distributed butene units is instrumental in causing the copolymer to crystallize into the 'PB I' phase in preference to the PPe II phase which is the form crystallizing directly from the melt in pentene homopolymers and in preference to the structurally more closely related PPe I with identical helix but different side-by-side chain packing. *Table 2* shows that at 84 per cent pentene-1 the transverse area occupied per ternary helix in the 'PB I' form has expanded to that occupied by the ternary helices in PPe I homopolymer. The crystal density is lower because of the presence in the lattice of 16 per cent of smaller butene units. Admittedly Danusso[19] has shown that PPe I is only formed with difficulty after prolonged heating above the melting point of the II form (15 days at 80°C) but this only makes it more unexpected that the copolymer crystallizes more readily at 84 per cent pentene into the related 'PB I' form of lower density, particularly as it would be expected that the larger pentene units would dominate the structure; this so far remains unexplained. In the middle range, ~ 50 per cent pentene, it is less surprising because the density of the 'PB I' forms is rising (*Table 2*).

We have calculated the effect on the lattice dimensions of the PB I structure of adding an extra carbon atom to the ethyl side groups in the *trans* position while twisting the chains slightly round their helical axes to preserve the same type of basic side-by-side chain packing as in PB I[3], and keep constant the interchain contact distances from these end carbon atoms of the side chains. On this basis the *a*-axis expands to 21·5 Å compared with the observed value of 20·6 Å (by linear extrapolation to 100 per cent pentene) (*Table 2*), an increase of 4 Å compared with an observed increase of 3 Å. Although of the right order, the 1 Å difference is large enough to suggest that the last C—C bond of the pentene side groups is not in the *trans* position.

If, as the evidence suggests, there is good cocrystallization in 'PB I' phase over the whole range of composition, then we have to explain the initial drop in crystallinity with introduction of pentene units followed by a levelling off to ~ 40 per cent crystallinity above 50 per cent pentene. The drop can be explained partially by loss of long range order as defined by Hosemann[20] owing to increasing numbers of imperfections in the lattice caused by two different randomly placed monomer units giving rise to X-ray scattering which is included in the amorphous scattering on the diffraction scans in the crystallinity determinations, together, possibly, with increased thermal movements at 20°C of the flexible side chains (particularly pentene) as the melting point drops. The X-ray photographs show a loss of the weaker reflections while the strong reflections, both equatorial and on the upper layers remain strong and sharp. No significant line broadening was observed over the whole range which is consistent

with long range order being preserved while thermal motions and imperfections increase. The levelling off above 50 per cent pentene might be accounted for by an increase in lattice perfection as the pentene units become the majority, countered by increased thermal motions as the crystal density and melting point continue to fall. Extrapolation of the 'PB I' parameters to 100 per cent pentene gives a crystal density of 0·875 g/cm^3 and melting point of 55 to 60°C both so appreciably lower than those of PPe II that it is not surprising pentene homopolymer has not been observed to exist in this lattice.

Accelerated Type II → I transition

Quantitative comparison of the relative effects of copolymerization of butene with ethylene, propylene and pentene on rates of crystallization and in accelerating the PB II → I transition is not possible because the ethylene and propylene systems are not homogeneous and contain ethylene-rich and propylene-rich chains and the comonomer content of the PB phase is necessarily lower than the overall composition while the pentene copolymers are substantially random. Nevertheless *Table 5* shows clearly that, mole for mole, pentene is the least efficient in accelerating the transition and causing direct crystallization, probably direct nucleation, into PB I. It also indicates that propylene is the most efficient, but it has already been shown that few ethylene units enter the PB lattice, and provided the responsible factor is units entering the lattice, then ethylene is more efficient than it appears.

Ethylene is certainly the most efficient comonomer in retarding the initial rate of crystallization (at 20°C, 20 moles per cent overall is sufficient to inhibit crystallization for several minutes) and propylene, particularly in view of the above remarks on composition, is more efficient than pentene. The decreased rate of crystallization is related to the melting points (reduced by copolymerization) of the PB phase of the slow-cooled copolymers (*Tables 2* to *5*) and also to the degree of cocrystallization points (reduced by copolymerization) of the PB phase of the slow-cooled specimens. Thus at 20 per cent ethylene where the rate of crystallization is very slow (0 per cent for 2½ minutes at least), the melting point has dropped to 110°C and the crystallinity is only 24 per cent and at 51 per cent pentene where the polymer also remains amorphous for several minutes after quenching the melting point has dropped to 95°C, although the maximum crystallinity is still 40 per cent. It will be noted that in these specimens crystallization takes place directly into the PB II form in the ethylene copolymer and into PB I in the pentene copolymer. The crystallinity attained in slow-cooled specimens is comparable in the 30 per cent pentene and propylene copolymers, i.e. when opportunity is given to the latter for crystal phase separation, and the greater inhibition to crystal growth on quenching to 20°C must be due to the interference with nucleation and growth from the melt of the PB phase by chains which are richer in propylene units and not therefore crystallizable in this phase, while the pentene copolymer chains are all capable of crystallizing this phase. In this connection it should be mentioned that the melting points of copolymers containing 30 per cent propylene crystallized at 20°C were only 70°C

compared with 115° to 120°C for slow-cooled specimens, and it was not found possible to regain the higher crystallinity or melting point by annealing near the 70°C melting point. This behaviour must be connected with the variation in chain compositions and the varying degrees to which chains of similar composition can phase separate at different temperatures of crystallization; it appears that at the low degree of mobility possible at the melting point of 70°C, the quenched material, which has not had time to phase separate during crystallization is still unable to do so. The decrease in the rate of crystallization with rising temperature in the propylene system must be the result of the decreased degree of supercooling, and the slower rate of PB II $\longrightarrow$ I conversion would appear to parallel the decreased rate of conversion in butene homopolymer above 40°C which in turn must result from changes in the relative free energies of the two forms with rising temperature.

The factors likely to influence the rate of PB II $\longrightarrow$ I conversion have been outlined in the introduction. Direct nucleation from the melt into either of the two forms will be subject to a similar balance of factors. Copolymerized ethylene units, which are most effective in disrupting crystallinity, because cocrystallization is not possible, can do so at comonomer levels where the butene runs are still sufficiently long to nucleate into PB II initially. The small cross-sectional area of the ethylene units included in the lattice and the more extended chain natural to ethylene sequences together with the reduction in melting point, aid, as expected, the conversion to the more extended PB I helix of smaller CSA. Propylene units reduce the initial rate of crystallization less than ethylene units since they can enter the PB II and PB I lattices to a limited extent without disrupting crystallinity, but in so doing alter the relative stabilities, i.e. free energies, of the forms and accelerate the conversion to PB I, because, it seems reasonable to assume, the instability caused by gaps in the structures due to inclusion of smaller methyl, instead of ethyl, side-groups is less in the PB I structures of higher density and lower CSA than in PB II, and because the natural helical configuration and repeat unit are identical; short runs of propylene units will naturally attempt to form a 3·0 helix. The reduced melting points of the two forms also would be expected to aid the conversion. Pentene units readily enter the PB lattice, in both forms, and hence (at high butene contents) reduce the rate of crystallization less than do propylene or ethylene units. Also, as already discussed, it appears that a structural or morphological preference for a 3_1 helix (as in the propylene system) seems to be the dominating factor in causing an increased rate of PB II to PB I conversion, together with reduction in melting point. Nevertheless, mole for mole, the effect is less than for propylene units, and hence the larger size of the side-groups deriving from the pentene units appears to offset the structural effect to some extent, and direct crystallization into PB I is not attained until high pentene contents are reached ($\sim$ 50 per cent), where the rate of crystallization has also been markedly reduced owing to reduced melting point. It is interesting to note that as the pentene content rises, the difference in densities of the PB I and PB II forms at 20°C (measured on samples half

converted; *Table 2*) decreases: the density of the PB II form increases only slightly with increasing pentene content. Hence it is not the density component of the free energy difference between the two forms that accelerates the conversion, but the structural component, together with the increased mobility of the chains, as outlined above.

Copolymers with branched comonomers

The degree of isodimorphism observed in copolymers of butene with 3MB, 4MP and 44DMP falls progressively with the size of the comonomer units as expressed by the CSAs of the homopolymer crystal forms (*Table 1*). With 3MB a highly cocrystallizing system is formed, although several crystal phases are observed, partly due to heterogeneity of chain composition. With 4MP partial isomorphic replacement of monomer units in the two homopolymer crystal phases is observed, with lattice dimension changes. With 44DMP both homopolymer phases occur, physically separate, without lattice dimension changes although some units of the second type are copolymerized into each phase. In each case at the high butene end the PB II phase is involved in the cocrystallization, i.e. the phase which besides having the greatest room for inclusion of larger side groups also has a helix [3·667 (11_3) or more likely 3·636 (40_{11}) as already discussed] closer in all parameters (*Table 1*) to the 4·0, 3·5 and 4·0 helices of the 3MB, 4MP and 44DMP homopolymer phases. The steric effect of increasing numbers of 3MB units in the PB II chains is to cause uncurling of the helix to 3·667 (11_3) at $\sim$ 8 per cent 3MB and further to 3·70 (37_{10}) at 15 to 20 per cent 3MB (*Table 10*) nearer to the 4·0 helix of P3MB, which itself results from steric interaction between the methyl branches close to the main chain and the main chain itself. The difference in the positions of the first two visible layer lines for a 37_{10} and a 40_{11} helix is seen in *Figures 3*(a) and *3*(b). The inclusion of 4MP units results in a 3·636 (40_{11}) helix at 7 per cent 4MP, which now probably does not involve any modification from the PB homopolymer helix, and a 3·625 (29_8) helix at 11 per cent 4MP, although the distinction between a 40_{11} and a 29_8 helix is rather fine; a slight coiling up towards the 3·5 helix of P4MP is possibly indicated. The inclusion of cocrystalline 3MB units results in an increase in PB II melting point, but inclusion of 4MP units reduces the melting point, which suggests that the expected increase in melting point from inclusion of a larger side-chain branched in the 4-position is more than offset by the imperfections introduced into the PB II crystal lattice because the 4MP units are not truly isomorphous, and by the lattice expansion, both factors reducing the melting point. The reduction in melting point by inclusion of copolymerized 44DMP units is the normal result of copolymerization without cocrystallization. Good stabilization of PB II occurs at progressively lower overall comonomer contents as the size of the unit rises and is complete in unoriented specimens at $\sim$ 8 moles per cent 3MB, 7 moles per cent 4MP and 3 moles per cent 44DMP. Owing to the production of butene-rich and 44DMP rich chains during polymerization the amount of 44DMP causing complete stabilization is likely to be less than three per cent.

Mechanism of stabilization of the Type II crystal form

The transition from PB II to PB I involves a coiling up and lengthening of the helix, with reduction in the CSA per chain (*Table 1*). Theoretically, therefore, provided we can assume that in bulk crystallized PB crystalline lamellae occur as have been demonstrated in bulk crystallized polyethylene[21] and polypropylene[22], it is morphologically possible for the change to take place by a simple thickening of the lamellae to provide for the helix extension and contraction followed by rearrangement of the lateral lattice on which the helices are arranged. (Holland and Miller[23] have shown the crystallographic relationship between the two packings by observing the conversion in single crystals by electron diffraction.) Alternatively the rearrangement may involve passage of the chains along their lengths through the lattice and a readjustment of chain folds, which thus need not necessarily increase in thickness even though the length along the chain per monomer unit has increased.

Stabilization of PB II occurs in 44DMP copolymers even though 44DMP units do not enter the lattice. The same is true of the dodecene and probably decene copolymers also. It is clear, therefore, that copolymerized large groups can effect stabilization while being incorporated in the amorphous regions only. It thus appears that the rearrangement does not just involve an increase in fold length keeping the large groups in the amorphous regions, but, at least in unoriented specimens, involves passage of chains through the crystallites; stabilization is effected because these large groups act as 'stops' as they are too large to be drawn through the lattice. Since much greater amounts than the 8 per cent 3MB causing good stabilization can readily enter an expanded PB II lattice[7], the stabilization by 3MB units cannot be by the 'stop' mechanism, but must be due to their incorporation into the lattice, which locally prevents the extension of the helix and lateral contraction of the lattice. This may be attributed to the steric effect of the inclusion of isopropyl side-groups, branched close to the main chain, which cannot be incorporated into a 3_1 helix without overcrowding, and indeed have the opposite effect of modifying the PB II helix towards the more open 4·0 helix of P3MB itself. The movement of chains through the lattice may also be hindered by these side-groups so that a similar mechanism to that operating in the 44DMP copolymers may play some part. The increased melting point of the PB II form will also hinder the conversion; indeed all these effects are co-related.

Both mechanisms may operate simultaneously in the 4MP, hexene and octene copolymers where comonomer units enter the PB II lattice to some extent. The decrease in melting point with increasing monomer content in these series (and indeed in all the stabilized copolymers except 3MB) must offset the stabilizing effect to some degree owing to increased thermal motions which could facilitate passage of the large groups through the lattice. The fall in PB stabilization shown by the decene and dodecene copolymers at comonomer contents > 7 per cent might then be explained by their considerably lowered melting points, which tip the balance towards conversion. This would imply that the side groups arising from the decene and dodecene units can pass through the lattice provided the thermal motions are sufficiently large, and this will undoubtedly be helped

by the linearity of the side-groups. The PB II phase remains well stabilized at 50 per cent 4MP (overall) even though the melting point has been reduced to 91°C (*Table 8*) which suggests that the branched side chain cannot pass through the lattice. However, in comparing the stabilities of the copolymers of *Table 5* in relation to their melting points, it must be remembered that the values quoted are *final* melting points, and more particularly with the larger linear α-olefin comonomers and as the comonomer content rises, the melting points are gradual and the end points indistinct, indicating a spread of compositions and less random copolymerization; the bulk of the material melts appreciably lower than the final melting points, while, for instance, in the hexene series the melting points are much sharper.

The failure of octadecene to produce more than a marginal stabilizing effect at the three per cent level could be due to blocking of the octadecene portion or failure to copolymerize. Hexene and octene units should be able to pass through the PB lattice as readily as decene or dodecene units, and hence their greater stabilizing effect at comonomer levels producing much lowered melting points must arise because the units are incorporated in the lattice. The rather lower stabilizing effect of hexene than octene reflects the fact that the next smallest monomer (pentene) has the opposite effect and accelerates the conversion.

The mechanism of stabilization in drawn fibres has yet to be discussed. In general the degree of stabilization is higher in warm-drawn as opposed to cold-drawn fibres and parallels that in unoriented specimens but good stabilization occurs at a slightly higher comonomer content. This is similar to the effect in PB homopolymers where drawing fibres causes very rapid conversion, presumably because tension aids the elongation of the helix. It is reasonable to suppose that stabilization by comonomer units that enter the lattice is by a similar mechanism to that in unoriented specimens, but in copolymers where the 'stop' mechanism has been postulated, a different mechanism must operate if a fringed micelle type of morphology can be accepted for highly oriented fibres drawn at elevated temperatures. Here passage of chains along the folds of the crystal lamellae cannot occur. It seems possible that some large groups may become trapped and frozen into the crystallites in the drawing process and inhibit the transition, and in support of this the lateral cell dimensions of drawn fibres are usually larger than those of annealed unoriented specimens. However, the mechanisms of stabilization in these copolymers, unoriented and oriented warrant much further study. It is only possible here to put forward a few ideas arising from the relatively qualitative results so far obtained.

Since the 'stop' mechanism of stabilization operates by the presence in the amorphous regions of large copolymerized groups which cannot pass through the crystal lattice, then it follows that other α-olefins yielding large branched or ringed side-groups which can be satisfactorily copolymerized with butene are also likely to stabilize PB II. In confirmation of this many such comonomers have now been shown to be effective, among which are 3-methylpentene, 5,5-dimethylhexene, styrene, allylcyclohexane, allylbenzene and vinylcyclohexane.

Lattice imperfections and thermal motions

Table 10 shows that as the amount of copolymerized linear α-olefin rises the weaker layer lines on the X-ray photographs which define the helical conformation and the weaker reflections gradually disappear, but the strong PB II reflections on the equator 200 and 220, and on the strongest layer line corresponding to the pitch of the helix ($\lambda/\zeta=6{\cdot}9$) i.e. that indexed 123 (213) on the 11_3 helix, remain sharp and strong as for example in *Figure 4*. The apparent repeat unit is thus reduced to $\sim 6{\cdot}9$Å. The same effect is seen in the intermediate composition range in both phases of the 4MP–butene system. In the α-olefin series it occurs at roughly progressively lower comonomer contents as the length of the α-olefin rises, but the particular level at which it occurs is undoubtedly complicated by the simultaneous increasing spread in chain composition.

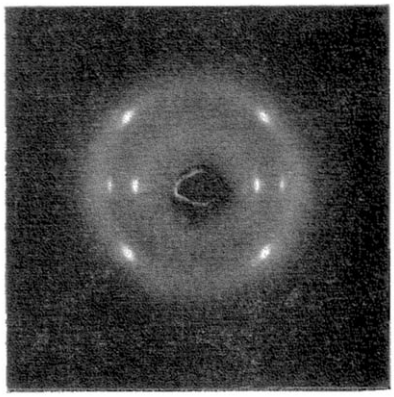

Figure 4—Fibre drawn ~110°C, of copolymer containing 23 per cent octene; strong reflections only present

The loss of weak reflections while preserving these strong, sharp reflections suggests loss of short range order while preserving long range order as discussed by Hosemann[20]. The loss of short range order can arise either from imperfections in the lattice arising from incorporation of two different monomer units, more particularly where no true isomorphous replacement occurs, and the lattice has to expand to accommodate the larger units, or from increased thermal motions resulting from reduction in melting point, or both. From *Table 10* it is seen that the pitch of the helix (l_t) remains constant at $\sim 6{\cdot}9$ both when the helix is 40_{11} and when the intermediate layer lines are disappearing. Preservation of long range order requires that the axes of the helices are effectively parallel and linear. The X-ray patterns thus demand good lateral correlation of parallel helices of constant pitch and good longitudinal correlation between helically arranged main chain atoms of the type required to give rise to a sharp strong reflection on the layer line corresponding to the pitch of the helix. This is schematically illustrated in *Figure 5*. The number of monomer units per turn of the helix (not shown in the diagram) need not be constant either between chains or within one chain, and indeed is likely to vary slightly depending upon the precise sequence of the two monomer

units, particularly where some degree of blocking is present and short runs of each type may occur. Thus the helix could vary from 3·5 (as in polyhexene itself or P4MP) to the helix of PB II. Provided the pitch is constant the 'grooves' in the helices (considered as grooved cylinders) will still fit and permit an ordered side-by-side packing, with some lateral lattice expansion. The precise disposition of the side-groups will be controlled by adjacently packed side-groups of the same chain, which may be derived from either type of monomer unit, and may thus vary relative to the helical axis and add to the imperfections caused by the presence of two kinds of monomer units and variations in numbers of monomer units per turn. Increased thermal motions, while preserving the basic lattice, reduce still further the short range order. Where the comonomer units do not enter the lattice, then it is suggested that increased thermal motions, as evidenced by lowered melting points, are largely responsible for the loss of weaker reflections and of intermediate layer lines.

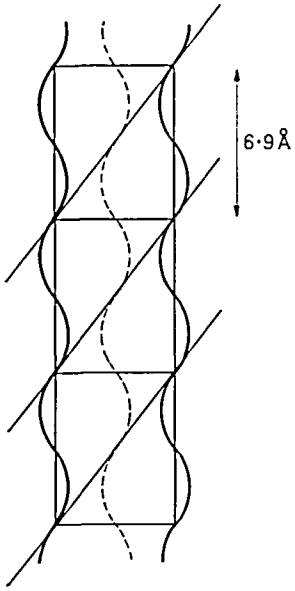

Figure 5—Diagrammatic representation of packing of helices of pitch 6·9 Å (side chains, which may vary in number, not shown) giving rise to strong reflection on layer corresponding to 6·9 Å from planes indicated

Phase separation during polymerization

From the foregoing it appears that using the $TiCl_3$–$AlEt_2Cl$ catalyst system, the degree to which isomorphism and cocrystallization between butene and comonomer units occurs is inversely related to the degree to which butene-rich and comonomer-rich chains are produced in the polymerization process. Thus with the highly isodimorphic 3MB unit, a largely copolymerized (even if somewhat blocked) system is produced while with 44DMP, where no isodimorphism and very little copolymerization occurs, P44DMP and PB chains are produced containing very few units of the second type, giving rise to complete phase separation. In both cases allowance was made in the polymerization for the very different rates of polymerization of butene and 3MB or 44DMP to their homo-

polymers. In the butene–4MP system, which shows partial isomorphism of monomer units, butene-rich and comonomer-rich chains crystallizing in physically distinct phases are produced, but both are far more copolymerized than the 44DMP system.

It appears that in the polymerization process, the crystal or helical structure of the growing chains can influence the acceptance or rejection of incoming monomer units. This concept has been treated theoretically by Ham[24] and discussed by Coover[25]; it is postulated that a growing isotactic polymer chain is helical as it leaves the catalyst surface and that the addition of the next unit is governed by the steric contacts it makes with the monomer unit to which it is adding and the preceding one, and probably with the units completing at least one turn of the helix; a correctly oriented monomer unit (giving isotactic placement) is accepted much more readily than one giving atactic placement. Coover suggests how this leads to phase separation in copolymerization of α-olefins, where the two α-olefins have different helical chain conformations, since a growing isotactic helix of one monomer will not only reject monomers in atactic placement but also will reject comonomer units which do not readily fit into the same helix. We would take this a stage further and say that while this is true when the helical conformation and dimensions of the homopolymers are so different that no isodimorphism occurs, nevertheless a large measure of copolymerization can occur when the helices of the two homopolymers are different provided isodimorphic replacement of comonomer units and cocrystallization can occur, if necessary by helix modification, because the side-groups are of comparable size.

Thus in contrast to the 44DMP–butene system, a growing polybutene helix in butene–3MB copolymerization can accept 3MB units, and similarly a P3MB helix can accept butene units and, provided the relative proportions of the comonomers are adjusted so far as possible to take account of the much greater ease of addition of linear butene units than branched 3MB units, copolymers over the whole range of composition should be obtainable as we have observed. Even when complete cocrystallization is theoretically possible some degree of phase separation is likely where the steric configuration close to the double bond is very different, because it is not possible in a single polymerization system to adjust concentrations to take account of all the different rates of addition of the two monomer units to the various terminal helical monomer sequences which are possible. For example, in attempting to make a 50/50 copolymer using an adjusted high 3MB concentration, a terminal helical sequence of butene units P—BBB— or P—BBBB— may still preferentially accept another butene unit to a 3MB unit, while the likelihood of adding a 3MB unit might be relatively higher for a P—(3MB) BB— or P—(3MB) BBB— sequence and higher still for a P—$(3MB)_2$B— sequence; possibly also an initial sequence of 3MB units might tend to propagate a 3MB-rich chain even though it would be expected that a butene unit would add readily on steric grounds. This will lead not only to chains of different composition, but also to blocked chains. The i.r. spectra of these copolymers indicate that at least short

runs of each comonomer unit are present because the general features are typical of a mixture of homopolymers.

A similar situation can be envisaged in the 4MP–butene system, but owing to the much lower compatibility of the two units, propagation of 4MP rich and butene-rich chains, leading to phase separation, becomes more likely.

The linear α-olefin series of copolymers is somewhat different from the branched α-olefin series, because the steric configuration at the double bond is identical in all the α-olefins and only the length of the 'tail' varies. In the butene–pentene series, the similar rates of polymerization of two very similar monomers, and their ability to cocrystallize as already discussed, makes this a nearly ideal system for random copolymerization. As the length of the α-olefin rises the rate of polymerization decreases relative to butene, but provided the latter is allowed for in the high butene-containing copolymers, there is no steric reason why random polymerization should not occur because the same helix, 3_1, is theoretically open to all linear α-olefins although the higher α-olefin homopolymers are not helical[11]. Nevertheless the spread in chain compositions increases as the comonomer unit becomes longer, so that the large size of the unit and its failure to enter the polybutene lattice appears to be having some effect. Local variation in monomer concentrations and diffusion of the two monomers may also play a part and failure to keep the correct relative concentrations in the system.

Similar remarks apply to the butene–propylene system as for the butene–4MP system. The butene–ethylene system is different because the question of stereoregularity does not arise with polyethylene and ethylene units polymerize readily on almost any site. Hence, although cocrystallization is not possible, marked copolymerization does occur.

From the foregoing it seems likely that this sort of phase separation will occur in copolymerizations with any highly stereospecific catalyst, and that increased randomness is likely to be achieved with less stereospecific catalysts only at the expense of isotaxy as suggested by Coover[25].

The question of solubles has been left out of the above discussion, but these in many cases do not amount to more than about five per cent. Where the soluble portion was much higher than this ($\geqslant 10$ per cent) it was usually necessary to work up the whole polymer to isolate it satisfactorily. Clearly fractionation is necessary to characterize more precisely the various phases produced in the polymerization.

The author's thanks are due to Dr K. J. Clark who made the copolymers, Mr R. P. Palmer for optical melting point data, Messrs H. A. Willis and M. E. A. Cudby for i.r. composition data and to them all for useful discussions, and to Mr D. R. Beckett and Mrs J. M. Sefton for their assistance in experimental work and calculations.

I.C.I. Plastics Division,
Welwyn Garden City, Herts.

(Received September 1965)

REFERENCES

[1] NATTA, G., CORRADINI, P. and BASSI, I. W. *Atti Accad. Lincei,* 1955, **19,** 404
[2] TURNER JONES, A. *J. Polym. Sci.* 1963, **B1,** 455
[3] NATTA, G., CORRADINI, P. and BASSI, I. W. *Nuovo Cim. Suppl.* 1960, **15,** 52
[4] ZANETTI, R., MANARESI, P. and BUZZONI, G. C. *Chim. e Industr.* 1961, **43,** 735
[5] BOOR, J. and MITCHELL, J. C. *J. Polym. Sci.* 1963, **A1,** 59
[6] DANUSSO, F. and GIANOTTI, G. *Makromol. Chem.* 1963, **61,** 139
[7] TURNER JONES, A. *J. Polym. Sci.* 1965, **33,** 591
[8] TURNER JONES, A. *Polymer, Lond.* 1965, **6,** 249
[9] *Crystalline Olefin Polymers,* pp 582–3. High Polymers Volume XX, Part 1. Ed. RAFF, R. A. V. and DOAK, K. W. Interscience: New York, 1965
[10] TURNER JONES, A., AIZLEWOOD, J. M. and BECKETT, D. R. *Makromol. Chem.* 1964, **75,** 134
[11] TURNER JONES, A. *Makromol. Chem.* 1964, **71,** 1
[12] DANUSSO, F. and GIANOTTI, G. *Makromol. Chem.* 1964, **80,** 1
[13] NATTA, G., CORRADINI, P. and GANIS, P. *J. Polym. Sci.* 1962, **58,** 1191
NATTA, G., CORRADINI, P. and GANIS, P. *R. C. Accad. Lincei,* 1962, **33,** 200
[14] NATTA, G., CORRADINI, P. and CESARI, M. *R. C. Accad. Lincei,* 1957, **22,** 11
[15] TURNER JONES, A. and AIZLEWOOD, J. M. *J. Polym. Sci.* 1963, **B1,** 471
[16] SWANN, P. R. *J. Polym. Sci.* 1962, **56,** 409
[17] BOOR, J. and MITCHELL, J. C. *J. Polym. Sci.* 1962, **62,** 570
[18] COCHRAN, W., CRICK, F. M. C. and VAND, V. *Acta cryst., Camb.* 1952, **5,** 581
[19] DANUSSO, F. and GIANOTTI, G. *Makromol. Chem.* 1963, **61,** 164
[20] BONART, R., HOSEMANN, R., MOTZKUS, F. and RUCK, H. *Norelco Reptr,* 1960, **7,** 81
[21] PALMER, R. P. and COBBOLD, A. J. *Makromol. Chem.* 1964, **74,** 174
[22] GEIL, P. H. *J. appl. Phys.* 1962, **33,** 642
[23] HOLLAND, V. F. and MILLER, R. L. *J. appl. Phys.* 1964, **35,** 3241
[24] HAM, G. E. *J. Polym. Sci.* 1960, **46,** 475
[25] COOVER, H. W. *J. Polym. Sci.* 1963, **C4,** 1511

Notes and Communication

A Reversible Change in Long Period Spacing with Temperature

THEORETICAL treatments of the chain fold length in polymer crystallites have been presented from a kinetic viewpoint by Lauritzen and Hoffman[1], Price[2], and Frank and Tosi[3], while a thermodynamic theory was proposed by Peterlin and Fischer[4]. Both treatments predict that the fold period should become longer with increasing temperature, but according to the kinetic theory no change should occur upon lowering the temperature, whereas the thermodynamic treatment predicts that the equilibrium fold length should decrease when the temperature is reduced.

There is considerable evidence that the long period increases at higher temperatures, and recently Hoffman and Weeks[5] showed that the fold length increases during isothermal ageing at the crystallization temperature. This demonstrates that the intermolecular forces in the crystal are weak enough to permit a chain to be pulled through the crystal by Brownian motion. Hence one might expect that, although the first fold period formed is dictated by crystallization kinetics, the final state may be governed by thermodynamic considerations. However, in no previous case has the fold period been observed to decrease upon lowering the annealing temperature. We present an example of this behaviour.

The sample studied was a crosslinked Neoprene HC film, which was cast and vulcanized by a procedure described elsewhere[6]. The sample was clamped in a frame at relative elongation $\alpha = 1{\cdot}9$, melted, and crystallized at 24°C. Measurements were performed using a Rigaku-Denki low angle diffractometer, Geiger counter, and heated sample holder. The variation of the long period spacing L with annealing temperature is represented by the filled circles in *Figure 1*. From measurements to be reported elsewhere, we estimate the thermodynamic melting point for this elongation to be 70°C. These data clearly resemble those obtained for other polymers. However, prior to this series of measurements, and immediately after the sample had been crystallized at 24°C, the measured spacing was 170 Å, as indicated by the open circle marked 1 in *Figure 1*. The sample temperature was increased to 40°C, and after 24 hours the observed spacing was 260 Å, as represented by open circle 2. The temperature was then reduced to 22°C, and after one day $L = 190$ Å, as shown by open circle 3. After collecting these results, the data represented by the filled circles were obtained by further measurements at 47°, 22° and thence at the intermediate temperatures. After each change of temperature, the sample was maintained at a fixed temperature for at least one day prior to measurement. Thus, there appears to be no doubt that the long period

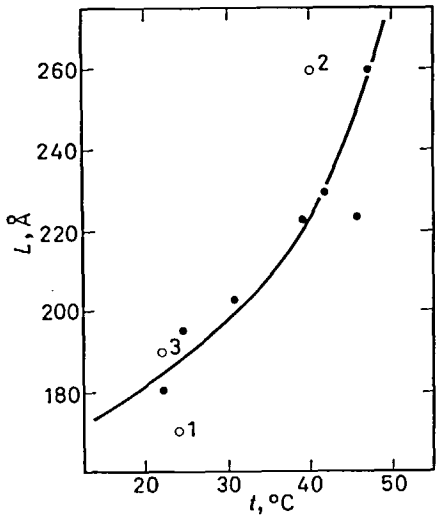

Figure 1—Temperature dependence of the long period spacing, L, for a polychloroprene vulcanizate at relative elongation $\alpha=1{\cdot}9$

observed for this polymer changes in a reversible manner with temperature.

Several explanations might be offered for this observation. First, polychloroprene may have a bundle-like, rather than a folded chain, morphology. Neoprene HC is, in fact, a copolymer containing about 10% *cis* units, and recent n.m.r. evidence[7] has indicated considerable H—T and H—H isomerism. The crystallinity probably did not exceed 30 per cent during our measurements. On the other hand, the available X-ray evidence does suggest a well-ordered, lamellar crystalline structure. *Figure 2* illustrates low angle data obtained at 25°C for a similar vulcanizate at three elongations. L is found to vary linearly with $1/\cos\chi$, where χ is the angle between the fibre axis and the plane containing the incident and diffracted beams. This suggests an ordered array of thin lamellae. Furthermore, a wide angle study[6] has revealed that the c axis (chain axis) aligns along the fibre axis, so the chains run along the thin dimension of

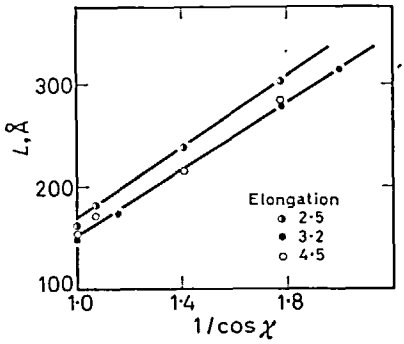

Figure 2—Variation of the long period spacing L with angle χ for polychloroprene at three values of the relative elongation α

the lamellae. This evidence is certainly suggestive of a chain-folded crystal morphology.

Support of this work by the U.S. Army Research Office (Durham) under grant 31-124-G580 is gratefully acknowledged.

W. R. KRIGBAUM
Y. I. BALTA
G. H. VIA*

Department of Chemistry,
Duke University, Durham, N.C.

REFERENCES

[1] LAURITZEN, J. I. and HOFFMAN, J. D. *J. Res. Nat. Bur. Stand.* 1960, **64A**, 73
HOFFMAN, J. D. *SPE Trans.* 1964, **4**, 315
[2] PRICE, F. P. *J. chem. Phys.* 1961, **35**, 1884
[3] FRANK, F. P. and TOSI, M. *Proc. Roy. Soc. A*, 1961, **263**, 323
[4] FISCHER, E. W. *Z. Naturforsh.* 1959, **14a**, 584
PETERLIN, A. *J. appl. Phys.* 1960, **31**, 1934
PETERLIN, A. and FISCHER, E. W. *Z. Phys.* 1960, **159**, 272
PETERLIN, A. and REINHOLD, CHR. *J. Polym. Sci.* 1965, **A3**, 2801
[5] HOFFMAN, J. D. and WEEKS, J. J. *J. chem. Phys.* 1965, **42**, 4301
[6] KRIGBAUM, W. R. and ROE, R. J. *J. Polym. Sci.* 1964, **A2**, 4391
[7] FERGUSON, R. C. *J. Polym. Sci.* 1964, **A2**, 4735

*Present address: Esso Research and Engineering Company, Box 121, Linden, New Jersey.

Proton Resonance Spectra and Tacticity of Poly-2-vinylpyridine

APPLICATION of high resolution nuclear magnetic resonance spectroscopy to polymers in solution can supply information on their tacticity. Among vinylaromatic polymers, poly-α-methylstyrene is a favourable case since the α-methyl group peak is split into three, ascribed to the iso-, hetero- and syndio-tactic configurations[1] but in polystyrene little or no difference in the spectra has been observed as a function of tacticity because the peaks of the α and β hydrogens are not quite resolved[2].

In poly-2-vinylpyridine, however, the electron attracting power of the nitrogen atom reduces the electron density on the α-hydrogen. So the α-hydrogen peak is expected to be shifted to lower field with respect to the β-hydrogen peak allowing a better separation between them. It therefore seems possible to study the stereochemical configuration of various samples of that polymer by high resolution nuclear magnetic resonance spectroscopy and to characterize one obtained in acidic medium. Such a sample should be mostly syndiotactic since F. A. Bovey prepared syndiotactic polymethylacrylic acid by polymerization of the monomer in basic medium[3].

the lamellae. This evidence is certainly suggestive of a chain-folded crystal morphology.

Support of this work by the U.S. Army Research Office (Durham) under grant 31-124-G580 is gratefully acknowledged.

W. R. KRIGBAUM
Y. I. BALTA
G. H. VIA*

Department of Chemistry,
Duke University, Durham, N.C.

REFERENCES

[1] LAURITZEN, J. I. and HOFFMAN, J. D. *J. Res. Nat. Bur. Stand.* 1960, **64A**, 73
HOFFMAN, J. D. *SPE Trans.* 1964, **4**, 315
[2] PRICE, F. P. *J. chem. Phys.* 1961, **35**, 1884
[3] FRANK, F. P. and TOSI, M. *Proc. Roy. Soc. A*, 1961, **263**, 323
[4] FISCHER, E. W. *Z. Naturforsh.* 1959, **14a**, 584
PETERLIN, A. *J. appl. Phys.* 1960, **31**, 1934
PETERLIN, A. and FISCHER, E. W. *Z. Phys.* 1960, **159**, 272
PETERLIN, A. and REINHOLD, CHR. *J. Polym. Sci.* 1965, **A3**, 2801
[5] HOFFMAN, J. D. and WEEKS, J. J. *J. chem. Phys.* 1965, **42**, 4301
[6] KRIGBAUM, W. R. and ROE, R. J. *J. Polym. Sci.* 1964, **A2**, 4391
[7] FERGUSON, R. C. *J. Polym. Sci.* 1964, **A2**, 4735

*Present address: Esso Research and Engineering Company, Box 121, Linden, New Jersey.

Proton Resonance Spectra and Tacticity of Poly-2-vinylpyridine

APPLICATION of high resolution nuclear magnetic resonance spectroscopy to polymers in solution can supply information on their tacticity. Among vinylaromatic polymers, poly-α-methylstyrene is a favourable case since the α-methyl group peak is split into three, ascribed to the iso-, hetero- and syndio-tactic configurations[1] but in polystyrene little or no difference in the spectra has been observed as a function of tacticity because the peaks of the α and β hydrogens are not quite resolved[2].

In poly-2-vinylpyridine, however, the electron attracting power of the nitrogen atom reduces the electron density on the α-hydrogen. So the α-hydrogen peak is expected to be shifted to lower field with respect to the β-hydrogen peak allowing a better separation between them. It therefore seems possible to study the stereochemical configuration of various samples of that polymer by high resolution nuclear magnetic resonance spectroscopy and to characterize one obtained in acidic medium. Such a sample should be mostly syndiotactic since F. A. Bovey prepared syndiotactic polymethylacrylic acid by polymerization of the monomer in basic medium[3].

EXPERIMENTAL

Three samples of poly-2-vinylpyridine have been prepared.

Sample 1

Polymerization, initiated by phenylmagnesium bromide, was performed under nitrogen atmosphere, at 45°C[1]. The acetone insoluble fraction of the polymer was used.

Sample 2

The outgassed monomer was polymerized in bulk with AIBN at 60°C in sealed bulb. The polymer dissolved in benzene was precipitated in hexane and dried.

Sample 3

10 g 2-vinylpyridine, dissolved in 50 ml 2M hydrochloric acid, was heated at 50°C with 0·1 g ammonium persulphate, in an atmosphere of nitrogen. The viscous solution was diluted with an equal volume of water and poured into ammonia solution. The polymer was then filtered and dried.

Three samples of poly-4-vinylpyridine were also prepared in the same way.

Nuclear magnetic resonance spectra were obtained with a Varian spectrometer operating at 60 Mc/s on 10 weight per cent solutions of poly-2-vinylpyridine in deuterochloroform at room temperature. Resolution was not better in benzene or pyridine, even at 80°C.

With poly-4-vinylpyridine, 10 weight per cent solutions in pyridine were used.

RESULTS AND DISCUSSION

The region of the spectra between $\delta=1$ and 3 from TMS is reproduced on *Figure 1*(a), (b) and (c) for samples 1, 2 and 3 of poly-2-vinylpyridine respectively. The peak at $\delta=2{\cdot}25$ is ascribed to the α hydrogen and the one at $\delta=1{\cdot}77$ to the β hydrogen.

With sample 1 [*Figure 1*(a)] the α hydrogen peak amounts to about one third of the whole (29 per cent). With samples 2 and 3 [*Figure 1*(b) and (c)], however, the same peak is only 13 per cent and 8 per cent of the whole so that it corresponds to part of the α hydrogen peak. According to the argument developed for the α-methylgroup of poly-α-methylstyrene[1], the α hydrogen peak in poly-2-vinylpyridine is expected to be split into three, associated from lower to higher field with the iso-, hetero- and syndio-tactic combinations of stereoisomers.

The peak at $\delta=2{\cdot}25$ from TMS must then be assigned to the first of these. This is supported by the fact that sample 1 is known to be isotactic[1]. Consequently, sample 3 is the least isotactic of the three and could be mostly syndiotactic, as suggested by the method of polymerization used: the terminal carbon atom of the chain being planar, when reaction occurs with a new monomer, a syndiotactic configuration with respect to the penultimate monomer unit must be favoured because of coulombic repulsions between pyridinium cations. Sample 2 is intermediate between

samples 1 and 3 and can be called atactic in a qualitative way. It is highly probable that three peaks could be observed for the α hydrogen in poly-β,β-dideutero-2-vinylpyridine and that a quantitative determination would be possible.

Spectra of poly-4-vinylpyridine samples show only one broad peak, associated with unresolved α and β hydrogens. Even a qualitative estima-

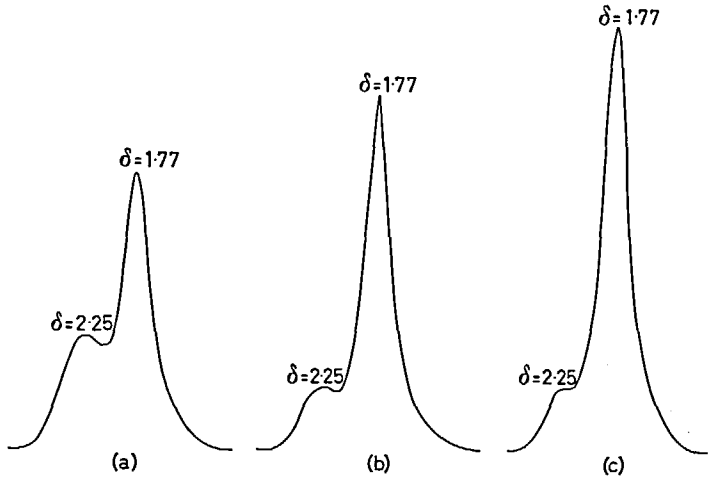

Figure 1—Proton resonance spectra of poly-2-vinylpyridine: (a) Sample 1 polymerized by phenylmagnesium bromide at 45°C, (b) Sample 2 polymerized with AIBN at 60°C, (c) Sample 3 polymerized in hydrochloric acid at 50°C

tion of tacticity based on the proton resonance spectra is excluded, although the sample prepared according to G. Natta's procedure[4] could be isotactic since it differs from others by its insolubility in chloroform.

We are very grateful to Professor L. de Brouckère for her interest in this work. We are also much indebted to Professor R. H. Martin for access to a proton magnetic resonance spectrometer and to Miss Defay and Mr Polain for recording the spectra.

G. GEUSKENS, J. C. LUBIKULU and C. DAVID
Service de Chimie Générale II,
Faculté des Sciences,
Université Libre de Bruxelles, Belgium

(*Received September 1965*)

REFERENCES

[1] BROWSTEIN, S., BYWATER, S. and WORSFOLD, D. J. *Makromol. Chem.* 1961, **48**, 126
[2] BROWNSTEIN, S., BYWATER, S. and WORSFOLD, D. J. *J. phys. Chem.* 1962, **66**, 2067
[3] BOVEY, F. R. *J. Polym. Sci.* 1963, **1A**, 843
[4] NATTA, G., MAZZANTI, G., LONGI, P., DALL'ASTA, G. and BERNADINI, F. *J. Polym. Sci.* 1960, **46**, 59

The Cold Drawing of Polyethylene Terephthalate

EXPERIMENTS on the relationship of the birefringence and modulus to the draw ratio in a drawn polymer[1,2] have indicated that the development of anisotropy can be approximately interpreted in terms of orientation functions which derive from the affine deformation theory of rubber elasticity. This leads one to consider whether the deformation of a polymer in the drawing process, even at temperatures below the glass-rubber transition, may be related to some network structure which exists within the polymer. In this correspondence an attempt will be made to relate some relatively simple ideas on network deformation to the process of cold drawing.

Several investigators[3,4] have reported that the 'natural draw ratio' of a cold-drawn polymer is strongly dependent upon the amount of orientation which is introduced into the sample prior to drawing. In this context, the natural draw ratio is defined as the new length to which a unit length is extended as the sample is cold drawn. Experiments of this type have been carried out either by 'pre-orienting' samples by stretching them at temperatures above their glass transition and then measuring their natural draw ratios or by producing spun fibres of given orientation and then measuring their draw ratios. In either case birefringence has been used as a measure of orientation and the results have been presented in the form of plots of birefringence versus natural draw ratio. A typical curve of this type for polyethylene terephthalate is presented in *Figure 1*. The striking feature of this curve is the fact that a relatively small amount of pre-orientation, as determined by the birefringence, has an extremely large effect on the natural draw ratio. A total birefringence of about 200×10^{-3} units may be introduced into polyethylene terephthalate by large extensions. However, a small fraction of this orientation ($\Delta n = 10 \times 10^{-3}$) apparently reduces the natural draw ratio by about a factor of two.

Let us assume that the deformation process which occurs in the glassy state is simply the stretching of a network system. The natural draw ratio can then be thought of as corresponding to the maximum extension which the network can undergo without breaking down. This particular extension of the network would then be a function of the original geometry of the network and the nature of the links of which it is comprised. Increments of strain applied to the system should be additive and the maximum extension should not depend on the way in which strain is applied as long as the junction points which hold the network together are not ruptured nor the links in the chain broken. Thus the ratio of the extended to unextended lengths of the network should be a constant which is independent of the route taken between these two states.

Andrews[4] has previously considered the possibility that cold drawing might involve the extension of a network to an ultimate value, but his experimental results for polystyrene did not substantiate this.

To test the hypothesis that the dimensions of the fully extended network should bear a constant relationship to the dimensions of the unstrained

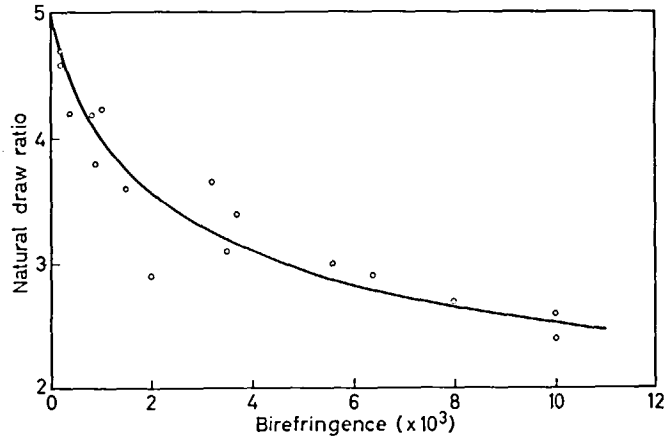

Figure 1—Natural draw ratio/birefringence curve

network, the natural draw ratios and the shrinkage characteristics of several melt-spun polyethylene terephthalate fibres of different initial birefringences were examined. This combination of draw ratio and shrinkage measurements was necessary since the samples contained an amount of pre-orientation which depended on the spinning conditions (melt through-put, wind-up speed, etc.). Thus the dimensions of the unstrained network could only be measured by shrinking the pre-strained network back to its original state.

Since the assumption is made that the deformation of the network is 'affine', changes in the dimensions of a macroscopic sample can be used as

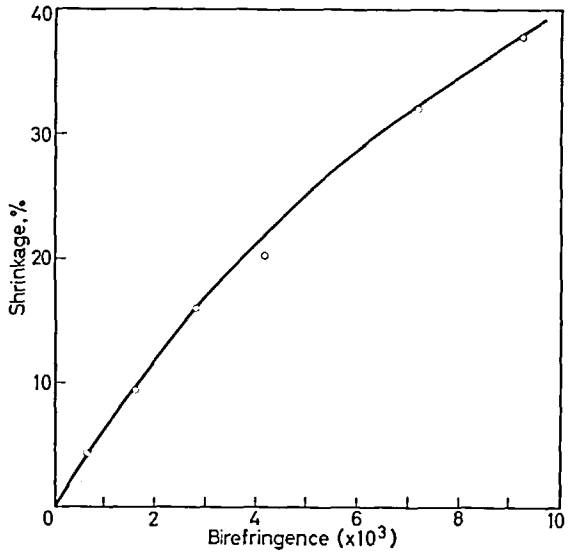

Figure 2—Shrinkage/birefringence curve

a direct measure of the microscopic deformation of the network itself.

The drawing was carried out at room temperature and at an extension rate of about 50 per cent/minute. The natural draw ratios were calculated directly from diameter measurements made on the drawn and undrawn fibres. Shrinkage measurements were made according to the method described elsewhere[5]. The birefringence/draw ratio and birefringence/shrinkage curves derived from these experiments are shown in *Figures 1* and *2*.

The relationship between the natural draw ratio, shrinkage and the dimensions of the network system can best be described with reference to *Figure 3*. A sample as prepared has an original length l_1, and an original

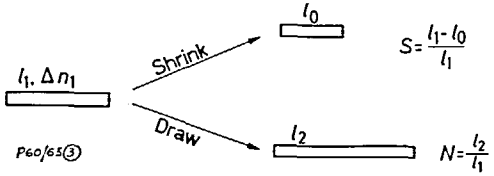

Figure 3—A representation of the shrinking and drawing processes

amount of pre-orientation (as measured by the birefringence) of Δn_1. If the sample is allowed to shrink back to its unoriented state, it will then have a length l_0. The amount of shrinkage (S) is thus

$$S=(l_1-l_0)/l_1 \tag{1}$$

Similarly, if a sample of length l_1 and birefringence Δn_1 is drawn to its natural draw ratio, it will have a new length, l_2, which is related to the natural draw ratio (N) by

$$N=l_2/l_1 \tag{2}$$

By a simple manipulation of equations (1) and (2) it can be shown that

$$l_2/l_0=N/(1-S) \tag{3}$$

Since l_2 and l_0 are assumed to be simply related to the deformed and undeformed network, respectively, we thus have a direct measure of the value of the ratio. Furthermore, by measuring the values of N and S for samples produced under different conditions and having differing amounts of pre-orientation, we can obtain a good indication of how this ratio depends upon pre-orientation.

Table 1 gives an outline of the results obtained in these experiments. The natural draw ratios and shrinkages were measured for samples which varied in original birefringence from $0{\cdot}45\times10^{-3}$ to 10×10^{-3}. The measured draw ratios varied between 4·2 and 2·6 and the shrinkages between 4 and 37·8 per cent. In this range, however, the ratio $N/(1-S)$ remained nearly constant at a value of about 4·0. This gives some support to these ideas about the deformation of a network structure.

The fact that Andrews' results for polystyrene did not support a similar

Table 1. Values of $N/(1-S)$ for samples of differing amounts of pre-orientation

$\Delta n_1 \times 10^3$	N	S	$(1-S)$	$N/(1-S)$
0·65	4·25	0·042	0·958	4·44
1·6	3·70	0·094	0·906	4·08
2·85	3·32	0·160	0·840	3·96
4·2	3·05	0·202	0·798	3·83
7·2	2·72	0·320	0·680	4·01
9·2	2·58	0·378	0·622	4·14

hypothesis, may well be attributed to the fact that the pre-orientation was carried out at temperatures about 60°C above the glass transition. At such high temperatures molecular rearrangement might allow destruction of the network system.

It should be noted that the $N/(1-S)$ ratio for the sample of nearly zero birefringence is somewhat greater than for the rest of the samples. This is an indication of the very strong curvature of the birefringence/draw ratio relationship at very low values of pre-orientation birefringence. Apparently a secondary effect occurs at extremely low degrees of pre-orientation which cannot be explained on the basis of these elementary ideas of network deformation.

S. W. ALLISON
P. R. PINNOCK
I. M. WARD

I.C.I. Fibres Ltd,
Hookstone Road,
Harrogate, Yorkshire

(Received November 1965)

REFERENCES

[1] WARD, I. M. *Proc. phys. Soc. Lond.* 1962, **80**, 1176
[2] PINNOCK, P. R. and WARD, I. M. *Brit. J. appl. Phys.* 1964, **15**, 1559
[3] MARSHALL, I. and THOMPSON, A. B. *Proc. Roy. Soc. A*, 1954, **221**, 541
[4] ANDREWS, R. D. and WHITNEY, W. Textile Division, Department of Mechanical Engineering, Massachusetts Institute of Technology *Report No. TD-123-64*, May 1964
[5] PINNOCK, P. R. and WARD, I. M. *Trans. Faraday Soc.* In press

*The Crystallization and Melting of Copolymers II—Variations in Unit-cell Dimensions in Polymethylene Copolymers**

C. H. BAKER† and L. MANDELKERN

Lattice spacings have been determined for polymethylene copolymers containing either methyl or n-propyl side groups in random sequence distribution. Unique to this study are the varied and controlled crystallization conditions, based on independent crystallization kinetic measurements, and the subsequent determination and comparison of the Bragg spacings both at room temperature and at the crystallization temperature.

For a given methyl copolymer the lattice spacings are essentially independent of crystallization conditions and the basal plane of the orthorhombic unit cell expands as the side group concentration increases. These observations are in accord with the thermodynamic analysis of the melting temperatures for this system wherein it was concluded that solid-solution formation occurs. In contrast, the spacings observed for the n-propyl copolymers depend markedly on the crystallization conditions. Under conditions conducive to the formation of the most stable crystallites, lattice spacings approaching those of the pure homopolymer are observed for copolymers containing small concentrations of side groups. For higher concentrations of both types of side groups, strong evidence exists for the crystallization of a lower melting polymorph in relatively high proportion. The Bragg spacings attributed to this structure obscure the analysis of the dimensions of the orthorhombic unit cell.

THE construction of phase diagrams representing the melting temperature/composition relations for copolymers is complicated by the great difficulty in establishing the solidus composition in equilibrium with the liquid at the melting temperature. Consequently, melting temperature/composition relations have been usually based solely on the liquidus composition with a paucity of direct information being available as to the composition and sequence distribution existing within the crystalline phase at the melting temperature. In addition, it is necessary to distinguish between the equilibrium state expected and the state actually observed as a result of a particular set of crystallization procedures.

Richardson, Flory and Jackson[1] have recently investigated the fusion process of polymethylene copolymers containing varying amounts of either methyl, ethyl or *n*-propyl side groups arranged in random sequence distribution. From an analysis of the melting temperature/composition relations they concluded that while small quantities of the methyl side groups are incorporated into the crystalline phase at equilibrium, the larger side groups are excluded. A subsequent study of the melting temperatures of

*This work was supported by a contract with the Division of Biology and Medicine, Atomic Energy Commission.

†Present address: Research Department, ICI Fibres Ltd, Harrogate, Yorks.

the same copolymers, using a semi-empirical procedure to estimate equilibrium melting temperatures[2], has substantiated this conclusion.

These conclusions appear to be disputed however, by wide-angle X-ray diffraction studies of copolymers of similar composition. Various investigators[3-6] have reported that the basal plane of the unit cell is expanded or distorted as the concentrations of either methyl, ethyl, *n*-propyl or *n*-butyl side groups are increased. This expansion of unit cell dimensions is interpreted as resulting from the presence of the coingredient in the crystalline phase. Although the results for the methyl side group copolymers are in harmony with the thermodynamic analysis, an apparent discrepancy clearly exists for the other cases. It should be noted that the X-ray diffraction measurements previously reported have been carried out at room temperature (far removed from the melting temperature) on samples whose crystallization was not controlled. Hence, the distinct possibility exists that the discrepancy arises from equilibrium considerations on the one hand and measurements on a crystalline phase which drastically departs from these conditions on the other.

To investigate this major discrepancy and the possible explanation offered above, we have taken advantage of studies of the kinetics of crystallization from the melt of these copolymers at various temperatures[7]. Data of this kind allow for well-defined crystallization procedures to be established and set the time/temperature requirements for crystallization to be conducted at elevated temperatures. These conditions are the most conducive for the formation of the more thermodynamically perfect crystalline phase[8]. We have, accordingly, measured the lattice spacings of polymethylene copolymers crystallized from the melt by different procedures. In addition to performing X-ray diffraction measurements at room temperature after attaining the maximum extent of crystallinity, measurements were also made at the crystallization temperature, while crystallization ensued isothermally.

EXPERIMENTAL

Materials—The copolymer samples utilized in this investigation were kindly supplied to us by Professor P. J. Flory and included those used in the studies of the melting temperature and crystallization kinetics[2, 7]. The details of the preparation and analysis of these samples have been described previously[1] and the methods of synthesis yielded copolymers which are in random sequence distribution.

Crystallization procedures—In preparation for the X-ray diffraction studies, the samples were first formed into thin uniform films 0·25 mm thick by use of a heated compression mould. After the initial moulding at about 170°C, the samples were allowed to cool down slowly in the press with the absence of any applied pressure. In order to minimize possible orientation, the samples were again reheated to 170°C in the mould, still under no pressure, and again allowed to cool gradually to room temperature. The samples were then wrapped individually in aluminium foil and crystallized from the melt in one of several prescribed ways.

In order to afford the copolymer the best opportunity to develop large

crystallites, crystallizations of the various films were conducted isothermally at temperatures as high as practical for periods up to five or six weeks. This was accomplished by simply transferring the foil-wrapped sample from a silicone oil bath at 165° to one set at a predetermined crystallization temperature, the temperature being controlled to better than 0·1°C. Prior knowledge of the times necessary at various temperatures to develop a certain degree of crystallinity was available from crystallization kinetic studies. After this initial isothermal crystallization, the samples were gradually cooled to room temperature at a rate of 2°C per day for the first seven days and then at rates of 10°C per day.

In another crystallization procedure, the samples of each copolymer were crystallized, after initially being melted at about 160°C, by very gradual cooling from 135°C to 45°C at the rate of 1°C per day.

Crystallizations were also conducted under conditions removed as far as practicable from equilibrium by rapidly transferring the films from a silicone oil bath set at 160°C into liquid nitrogen.

X-Ray diffraction measurements—X-Ray diffraction measurements were made on the samples using both flat-plate camera and Geiger-counter techniques, with Ni filtered Cu K_α radiation. The first series of measurements were made at room temperature with a Norelco flat-plate camera. An internal standard of silver was used in order to enable the sample–film distance to be accurately assessed. This took the form of a piece of very thin silver foil placed against one face of the copolymer film which was then mounted in a specially constructed brass holder. Exposures were made for about 24 hours with a 35 kV 15 mA X-ray beam. The exposed films were subsequently measured using a Nikon Comparator. The *d* spacings were reproducible to within 0·005 Å for the non-quenched samples and to better than 0·015 Å for the quenched samples.

Another series of measurements were made using a Norelco diffractometer with a Geiger-counter detection system. Measurements were made both at room temperature and at the temperatures of crystallization for selected samples. The measurements at elevated temperatures were performed using a specially constructed specimen holder, shown in *Figure 1*, which could be attached to the diffractometer in place of the normal radiation shield.

The specimen holder consisted essentially of a cylindrical aluminium block M, 2 in. in diameter and $2\frac{1}{4}$ in. in length, which had a slot $\frac{9}{16}$ in. in width and $1\frac{1}{8}$ in. in depth cut out. Below the slot a hole $\frac{1}{2}$ in. in diameter was drilled and plugged with a cylinder of copper C. This copper cylinder was in turn drilled so as to accommodate a cylindrical 50 W heater H, the end of which extended to $\frac{1}{8}$ in. below the surface of the copper block.

A slit $\frac{15}{16}$ in. wide and $\frac{1}{8}$ in. deep was cut out along the axis of the aluminium block so as to be parallel with the surface of the copper block C. A copolymer sample S in its individual frame could then be inserted into the apparatus and be held in position by two copper springs. The position of the copper core C was adjusted so that the upper surface of the copolymer sample S would lie along the axis of rotation R of the diffractometer arm and the axis of the aluminium cyclinder M. Two more

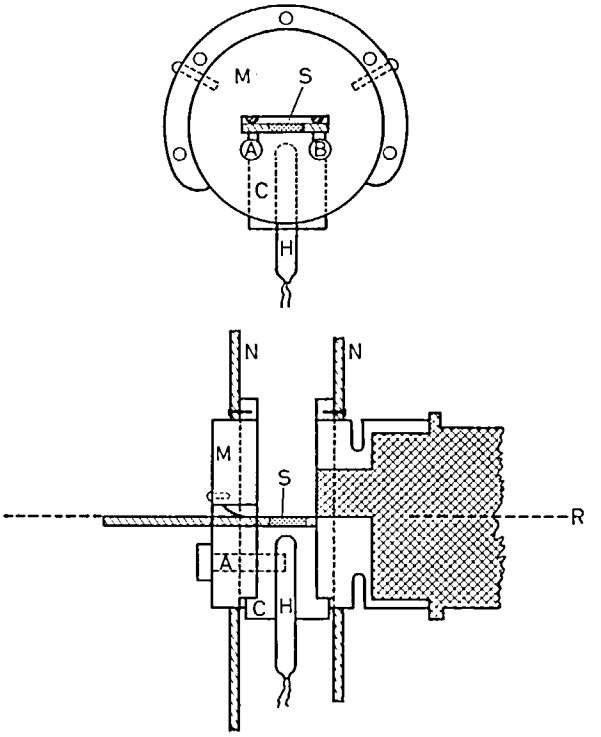

Figure 1—Schematic diagram of high temperature specimen holder for diffractometer

holes A and B were then drilled parallel to the axis of the cylinder M to accommodate a thermometer holder and thermistor respectively. These were situated so that the sample, thermometer and thermistor were all equidistant ($\frac{1}{8}$ in.) from the heating element H.

Two thermally insulated radiation shields N, 7 in. in diameter, were mounted on the aluminium body of the sample holder, as shown in *Figure 1*, to afford protection from any scattered radiation. The whole specimen holder was then mounted on the diffractometer unit in the same way as the customary Norelco radiation shield.

Since long periods of time were necessary to develop any substantial crystallinity at elevated temperatures, the copolymer samples were isothermally crystallized in a silicone oil bath for several days before X-ray diffraction measurements were made. Before transfer of the sample from the oil-bath to the specimen holder took place, the latter was heated and thermostated some 3 or 4 degrees above the crystallization temperature. During the transfer, which took less than 5 seconds, heat loss from the sample was minimized by an insulating sleeve which slipped over the frame containing the copolymer sample. Diffractometer scans were then made over the angular range $2\theta = 18°$ to 26° at about 3°C above the crystallization temperature, and then at a series of progressively lower temperatures.

RESULTS AND DISCUSSION

The Bragg spacings obtained from the flat-plate camera photographs at

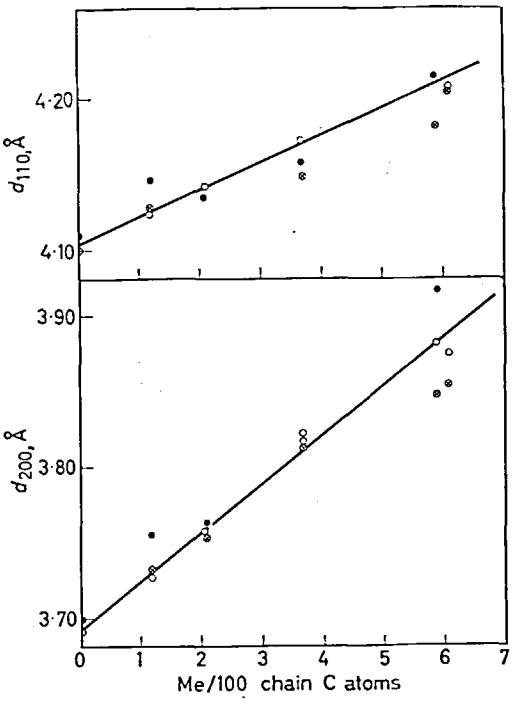

Figure 2—Plot of d_{110} and d_{200} spacings (Å) for methyl side group copolymers determined by flat-plate camera at room temperature. Isothermally crystallized and then cooled ○; gradually cooled at 1°C/day ⊗; quenched in liquid nitrogen ●

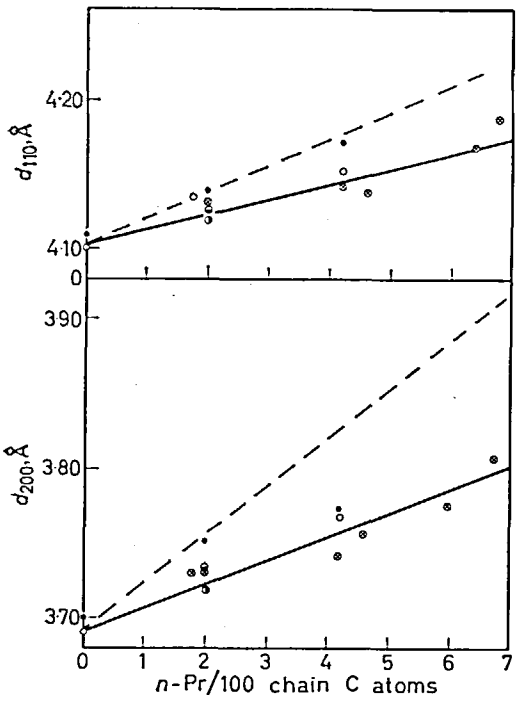

Figure 3—Plot of d_{110} and d_{200} spacings (Å) for *n*-propyl side group copolymers determined by flat-plate camera at room temperature. Isothermally crystallized and then cooled ○; gradually cooled at 1°C/day ⊗; quenched in liquid nitrogen ●; isothermally crystallized at 100°C ◒; isothermally crystallized at 103°C ◑. Dashed line, results for Me copolymers

room temperature are summarized in *Figures 2* and *3*. *Figure 2* illustrates the variation of the d_{110} and d_{200} spacings (for the orthorhombic unit cell) with increasing concentration of methyl side groups. The room temperature crystalline samples were obtained from the melt by either (*a*) cooling subsequent to prolonged isothermal crystallization at low undercooling, (*b*) very gradual cooling from the melt at the rate of 1°C per day or (*c*) quenching as previously described. A steady increase is apparent in the value of the spacings with increasing side-group concentration. The crystallization procedure has only a very slight effect on the observed spacings for the copolymers containing up to four per cent methyl side groups. However, at the higher concentrations of the coingredient, there is an indication that the crystallization conditions could be affecting the spacings. The slowly cooled samples appeared to have the smallest unit cell dimensions. The patterns obtained for these specimens are not as well-defined as those for the lower concentrations and hence, the possibilities of measuring errors cannot be dismissed.

A similar plot for the *n*-propyl branched copolymers is given in *Figure 3*. The results from *Figure 2* for the methyl copolymers are also indicated in this diagram by the dashed straight lines. The differences in the results for the two sets of copolymers are easily discerned in the figure. Moreover, the spacings observed for the *n*-propyl copolymers depend on the crystallization conditions. When the lower concentration *n*-propyl branched copolymers are rapidly crystallized from the melt by quenching, the unit-cell dimensions are similar to those of the methyl branched copolymers. However, if the crystallization is conducted more slowly, particularly at the elevated temperatures, the unit-cell dimensions definitely decrease. This effect is especially evident in the two per cent and four per cent copolymers. The analysis of the X-ray patterns of the quenched samples containing high concentrations of side groups is severely hampered by the presence of an intense halo which completely obscures measurements of the crystalline reflections. (This difficulty can be overcome with the diffractometer type of analysis, see below.) However, if the crystallization process is conducted very slowly, accurate measurements of the reflections obtained in this concentration range are possible. Under these circumstances a definite contraction in the unit-cell size, relative to that of the corresponding methyl copolymer, takes place. Hence, for the *n*-propyl copolymers, over the complete composition range studied, the lattice spacings are significantly less than those for the corresponding methyl copolymers and are definitely dependent upon the crystallization condition. This latter point is emphasized by the behaviour of the two per cent *n*-propyl copolymer (sample P 7). As is indicated in *Figure 3*, when this sample is crystallized at 103°C and then slowly cooled, smaller spacings are measured than if the sample is crystallized at 100°C and then similarly cooled. We should note that at both these temperatures, relatively long times are required for crystallization. The results just described are typical of the behaviour of *n*-propyl copolymers and suggest that, in contrast to the methyl copolymers, as crystallization conditions approach those which would favour development of the equilibrium state, the lattice spacings approach those for pure homopolyethylene.

A major difficulty in interpreting the results described above is that the specimens must be cooled from the high temperature of crystallization to room temperature. As is shown in *Table 1*, the relatively low levels

Table 1. Degree of crystallinity attained at crystallization temperature and at room temperature for various copolymer samples

Copolymer	*% Side group*		T_c °C	*% Degree of crystallinity*	
				at T_c[2]	*at 30°C*[1]
M 1	1·2	Me	120	22	55·4
M 2	2·1	Me	112	5·3	50·0
M 3	3·7	Me	100	4·8	(~ 40)
M 4	5·9	Me	~ 70	~ 2·6	(~ 19)
M 5	6·1	Me	~ 70	(~ 2·5)	17·1
P 6	1·8	*n*-Pr	~ 104	(~ 12·5)	41·0
P 7	2·0	*n*-Pr	103	12·5	(~ 40)
P 8	4·2	*n*-Pr	78	2·7	23·4
P 10	6·4	*n*-Pr	~ 45	~ 4·4	10·0

of crystallinity obtained at the crystallization temperature become substantially enhanced on cooling to room temperature. The relative increase in the level of crystallinity upon cooling becomes more pronounced as the concentration of coingredient is increased. Hence, by necessity, the diffraction pattern observed at room temperature must represent the state wherein a significant portion of sample has crystallized under conditions well removed from equilibrium. This effect is accentuated for the samples containing the higher concentration of coingredient.

To alleviate the difficulties cited above, experiments were performed at elevated temperatures utilizing the diffractometer equipped with the heated specimen holder. The results of these experiments are summarized

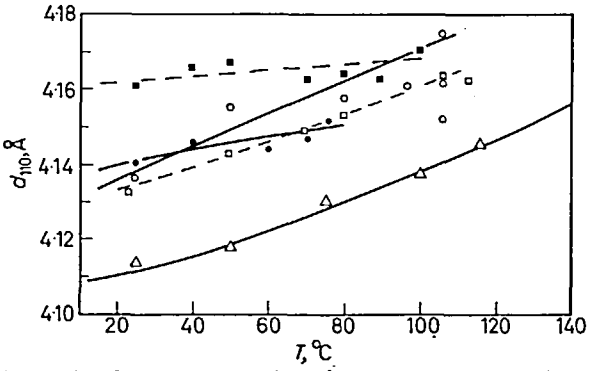

Figure 4—Plot of d_{110} spacing (Å) for linear polyethylene and copolymers determined by diffractometer at indicated temperatures. Marlex-50, crystallization temperature 130°C △; 2·1% Me copolymer, crystallization temperature 111°C □; 3·7% Me copolymer, crystallization temperature 98°C ■; 2% *n*-Pr copolymer, crystallization temperature 101°C ○; 4·2% *n*-Pr copolymer, crystallization temperature 76°C ●

in *Figure 4*. The highest temperature indicated for each copolymer represents the d_{100} spacing at the crystallization temperature; the spacings observed at the lower temperature are a consequence of the subsequent cooling of the specimens. To compare the various samples and to allow for the normal thermal contraction of the crystal lattice, a reference curve was obtained by measuring the d_{110} and d_{200} spacings of an unfractionated homopolyethylene sample (Marlex-50). By crystallizing at 130° for a long period of time a specimen of very high density was obtained[9,10] and the spacings measured over the temperature interval between 25° and 120°C. The results for the 200 spacing (not shown) gave an expansion coefficient for the *a* dimension of the unit cell which was in excellent agreement with the results reported by Cole and Holmes[5]. These in turn are consistent with Takayanagi's results over a limited temperature range[11].

The temperature coefficient of the d_{110} spacing of the 2·1% Me copolymer (M 2) is very similar to that of the homopolymer although the spacings themselves are displaced upward by about 0·02 Å at all temperatures. For the 3·7% Me copolymer an additional upward displacement of 0·01 Å is observed at the crystallization temperature. However, the apparent thermal expansion coefficient is significantly reduced for this copolymer. Hence, at room temperature the *d* spacing is displaced about 0·06 Å from that of the homopolymer in accord with the results of *Figure 2*. The role of the crystallinity developed at the lower temperatures in affecting the lattice spacings is quite clear and the possible difficulties in interpreting the room temperature results are indicated. An explanation of these results is that as the crystallization temperature is lowered, crystallization occurs under conditions farther removed from equilibrium and from a melt which now contains a higher proportion of coingredient than in the completely molten polymer. Hence, for both these reasons a progressively higher concentration of side groups will be expected in the lattice as the temperature is lowered.

A similar but more accentuated situation is observed during the crystallization of the 2% *n*-Pr copolymer. As is indicated in the figure, the initial measurement of the spacing at very low values of crystallinity at 101°C gives a value close to that of the homopolymer at this temperature. This indicates that for the *n*-Pr copolymers, in this concentration range, the crystalline phase remains pure as equilibrium conditions are approached. However, the other experimental points indicated in the diagram at this temperature were obtained as further crystallization ensued. A definite and distinct increase in the *d* spacings is observed with isothermal crystallization. Subsequent cooling then produced a series of points paralleling the locus for homopolyethylene but the spacings were about 0·03 Å larger. It is clear that if the initial crystals formed could be cooled without further crystallinity developing, then the spacing in this copolymer would be virtually identical to that of the homopolymer. The expansion coefficient of the 4·2% *n*-Pr copolymer is very similar to that for the 3·7% Me although the spacings themselves are significantly smaller.

As has been indicated previously, an analysis of the quenched copolymers of higher *n*-Pr concentration was virtually impossible with the flat-plate camera at room temperature. However, an analysis was accomplished with the diffractometer. The results for the quenched samples are summarized

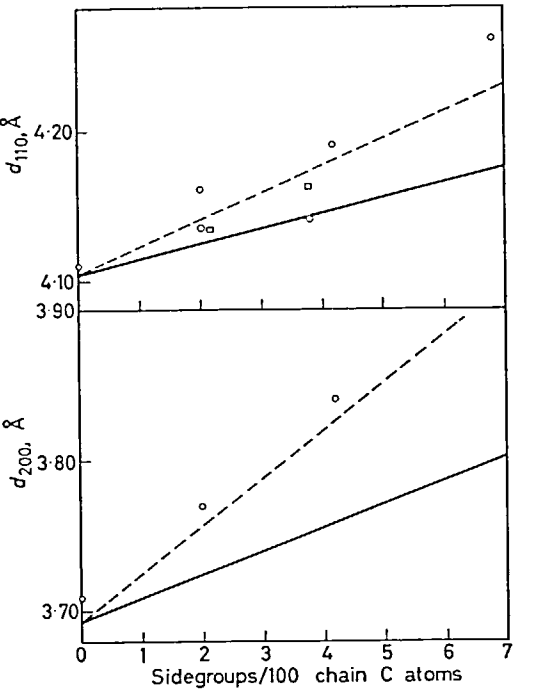

Figure 5—Diffractometer results at room temperature for copolymers. Slowly cooled Me copolymers □; slowly cooled *n*-Pr copolymers ○; quenched *n*-Pr copolymers •; flat-plate results for Me copolymers – – –; flat-plate results for *n*-Pr copolymers ————

in *Figure 5* together with other pertinent data which are helpful for comparative purposes. The obvious differences between the quenched and well-crystallized *n*-Pr copolymers are now clearly discernible. The spacings for the quenched samples are virtually identical to those for the Me branched copolymers, while those for the more slowly crystallized *n*-Pr copolymers are approaching the homopolymer values. These results thus reinforce the previous conclusions obtained from the data of *Figures 2* and *3*.

Another complication that exists in interpreting the reflections for these copolymers is the simultaneous development of another crystalline form. It has been shown that in homopolyethylene, another crystalline modification identified as triclinic by Teare and Holmes[12] will form at temperatures below about 90°C and will melt[13] in the range of 90° to 100°C. For the polymethylene copolymers containing the higher concentration of side groups, the crystallization must be conducted at large undercoolings in order to develop a measurable amount of crystallinity[2]. The crystallization temperatures are thus in the range where the formation of the polymorphic form can be anticipated. The apparent melting temperatures of the copolymers containing 5·9% methyl (M 4) and 4·2% *n*-Pr (P 8) are consistent with the formation of the triclinic form in relatively high proportion. The fusion curves for copolymer P 7 (2% *n*-Pr) initially crystallized at 90°C and then cooled gives evidence for the melting at about 95°C of this crystalline form. Further evidence for the formation of the polymorphic form in the copolymers studied here is found in the X-ray diffraction photographs taken at room temperature.

The polymorphic form in the homopolymer is characterized by a strong reinforcement of the diffraction ring found within the 110 orthorhombic reflection. This reflection has been attributed[14] to the 010 plane of the triclinic structure with a Bragg spacing of about 4·56 Å. The other reflections characteristic of this polymorph have been listed elsewhere[12–14]. A similar reinforcement of the innermost diffraction ring has been definitely observed for copolymers P 10 and P 11, 6·4 and 6·8% *n*-propyl respectively and is suggested by the photographs obtained for M 4, 5·9% Me. *Table 2* summarizes the relative intensities of the three innermost main diffraction rings for the various copolymers and a typical unbranched polymethylene. Column (a) is for the 010 reflection of the triclinic form; (b) is for the 110 reflection of the orthorhombic form; (c) is for the reflection in the range 3·70 to 3·85 Å which can be assigned to either the 200 reflection of the orthorhombic form or the 100 reflection of the triclinic form. The intensity of the innermost diffraction ring, typical of the triclinic form, relative to the d_{110} orthorhombic reflection increases appreciably as the concentration of coingredient increases. The value of the spacing itself increases for the Me copolymers with increasing copolymeric content, but remains essentially unchanged for the *n*-Pr copolymers. Hence, this form appears in concentrations which are significantly greater than those previously observed in undeformed polyethylene. For copolymers crystallized from the melt below 80°C, this reflection is particularly pronounced and is consistent with the kinetic conditions required for the formation of the low melting polymorph and the fusion curves[2].

The reflection assigned to the d_{200} spacing of the orthorhombic form in *Figures 2* and *3* varies from 3·75 to 3·88 Å for the copolymers which were crystallized below 80°C. However, the d_{100} spacing of the triclinic form has been calculated and observed to be 3·80 Å for the homopolymer and its calculated intensity should be weaker than the d_{010} spacing of the same form[14]. The data in the last column of *Table 2* show continuous diminution

Table 2. Variation of the intensities of the three innermost diffraction rings obtained by the flat-plate camera technique and *d* spacings corresponding to the innermost reflection

Sample	*% Side group*	*Diffraction ring intensities*			
		(a) *innermost*		(b) [110]	(c)
Polymethylene	Unbranched	vw	4·56 Å	vs	vs
M 1	1·2 Me	vw	4·55	vs	vs
M 2	2·1 Me	vw	4·57	vs	s
M 3	3·7 Me	w	4·60	vs	s
M 4	5·9 Me	w	4·62	s	w
M 5	6·1 Me	m	4·64	s	vw
P 6	1·8 *n*-Pr	vw	4·58	vs	s
P 7	2·0 *n*-Pr	vw	4·54	vs	s
P 8	4·2 *n*-Pr	w	4·56	s	m
P 9	4·6 *n*-Pr	w	4·59	s	m
P 10	6·4 *n*-Pr	m	4·58	m	vw
P 11	6·8 *n*-Pr	m	4·59	m	vw

vs = very strong; s = strong; m = medium; w = weak; vw = very weak.

of the intensity of this reflection while it progressively increases in position from 3·70 to 3·85 Å. At the same time the intensity of the innermost reflection is increasing. These observations further support the concept that the concentration of the triclinic modification increases appreciably with copolymeric content. Hence it can be concluded that the observed spacings result not only from any possible distortions of the orthorhombic unit cell but also from the presence of the polymorphic form.

A summary of the room temperature spacings in ethylene copolymers as reported by other investigators is given in *Figure 6*. Eichorn's[4] results

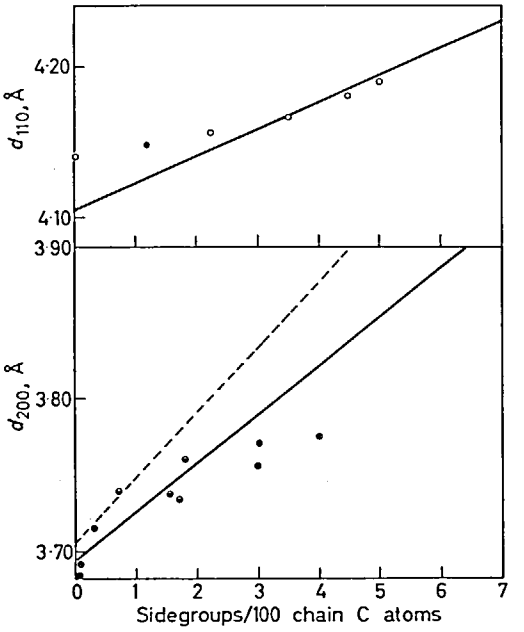

Figure 6—Compilation of results of different investigators for lattice spacings of polymethylene copolymers. Flat-plate results for Me copolymers, this work (*Figure 2*) ———; flat-plate results for quenched 1·2% Me copolymer, this work (*Figure 2*) •; Eichorn's results for Me side groups[4] O; Swann's results for Me side groups[6] – – – –; Swann's results for ethylene–olefin copolymers[6] ⊖; Walter and Reding's results for Me side groups[3] ⊗

for methyl branched polyethylenes are in good agreement with the data reported here. It is interesting to note that the point representing the d_{100} spacing of the quenched 1·2% Me copolymer which is off the line in *Figure 2* fits very well with Eichorn's data. There is, however, a large discrepancy between our data for unbranched polyethylene and those of Eichorn. The extrapolation of the copolymer spacings to those for an unbranched polyethylene agrees very well with our independent measurements on several Marlex-50 and unbranched polyethylene samples, as well as with Bunn's[15] reported values of 4·106 Å and 3·696 Å for the 110 and 200 reflections of the orthorhombic unit cell.

Swann's results[6] for methyl branched polyethylenes have a steeper slope than those reported here. This could be accounted for by slight discrepancies in the side-group concentrations or by a non-random sequence distribution in his case. The points representing Swann's results for samples with larger side groups lie fairly close to the line representing our results for

the methyl copolymers and the quenched *n*-propyl copolymers. This is the expected result since no effort was made to crystallize these samples under optimum conditions. The points representing the Walter and Reding data[3] for methyl branched copolymers are similarly distributed around our results.

The results of the X-ray diffraction analyses can now be compared with the conclusions drawn from the studies of the melting temperature/composition relation for the two series of copolymers. The differences in crystallization behaviour between the methyl and *n*-propyl copolymer have been confirmed and further emphasized. The phase diagram of the methyl copolymers, based on liquidus composition, is consistent with solid-solution formation in that a proportion of the side groups enters the lattice as an equilibrium condition. This conclusion is confirmed by the continuous expansion of the basal plane of the unit cell with increasing methyl group concentration, and the independence of the lattice spacings on crystallization conditions.

For the *n*-propyl copolymer the extrapolated equilibrium melting temperatures monotonically decrease with increasing concentration of coingredient[1,2]. This result is consistent with a phase diagram in which the crystalline phase remains pure. It is not necessarily an unequivocal demonstration of this. However, the experimentally extrapolated melting temperatures for the 2% *n*-Pr copolymers are in virtual agreement with the value calculated on this basis. The analysis of the X-ray pattern indicates that, in contrast to the methyl copolymer, the lattice spacings for all the *n*-Pr copolymers are very sensitive to the crystallization conditions. For the 2% *n*-Pr copolymers the lattice spacings approach those of the homopolymer as equilibrium crystallization conditions are approached. This supports the contention set forth above of the crystalline phase being pure at equilibrium. However, the ease with which non-equilibrium compositional defects can be developed within the crystalline phase of this copolymer is also apparent.

For copolymers containing higher concentrations of *n*-Pr side groups, comparable crystallization conditions cannot be experimentally achieved. The lattice spacings continually decrease as the crystallization conditions become more favourable and their values are less than the corresponding methyl side group copolymers. The analysis of the lattice parameters in this composition range is complicated by the reflections from the polymorphic form. Though the purity of the crystalline phase at equilibrium, for the higher concentration *n*-Pr side group polymers, cannot be definitely established, the observations cited are indicators that under appropriate conditions spacings comparable to those for the homopolymers would be achieved. The theoretical possibility still exists for a small concentration of *n*-Pr side groups to be accommodated in the crystalline phase at equilibrium.

Department of Chemistry and
Institute of Molecular Biophysics,
Florida State University,
Tallahassee, Florida

(*Received August 1965*)

REFERENCES

[1] RICHARDSON, M. J., FLORY, P. J. and JACKSON, J. B. *Polymer, Lond.* 1963, **4**, 221
[2] BAKER, C. H. and MANDELKERN, L. *Polymer, Lond.* 1965, **7**, 7
[3] WALTER, E. R. and REDING, F. P. *J. Polym. Sci.* 1956, **21**, 561
[4] EICHORN, R. M. *J. Polym. Sci.* 1958, **31**, 197
[5] COLE, E. A. and HOLMES, D. R. *J. Polym. Sci.* 1960, **46**, 147
[6] SWANN, P. R. *J. Polym. Sci.* 1962, **56**, 409
[7] BAKER, C. H. and MANDELKERN, L. To be published
[8] MANDELKERN, L. *Crystallization of Polymers.* McGraw-Hill: New York, 1964
[9] MANDELKERN, L., POSNER, A. S., DIORIO, A. F. and ROBERTS, D. E. *J. appl. Phys.* 1961, **22**, 1509
[10] FATOU, J. G. and MANDELKERN, L. *J. phys. Chem.* 1965, **69**, 417
[11] TAKAYANAGI, M. *Mem. Fac. Engng, Kyushu Univ.* 1963, **23**, 41
[12] TEARE, P. W. and HOLMES, D. R. *J. Polym. Sci.* 1957, **24**, 496
[13] FATOU, J. G., BAKER, C. H. and MANDELKERN, L. *Polymer, Lond.* 1965, **6**, 243
[14] TURNER-JONES, A. *J. Polym. Sci.* 1962, **62**, 553
[15] BUNN, C. W. *Trans. Faraday Soc.* 1939, **35**, 483

The Fractional Crystallization of Poly(ethylene oxide)

C. BOOTH and C. PRICE

Poly(ethylene oxide) has been fractionated by crystallization from dilute solution in several solvents. Fractionation with respect to molecular weight is slight: there is a tendency for lower molecular weight polymer to crystallize first. The mechanism of crystallization of poly(ethylene oxide) from dilute solution is discussed briefly, and the application of fractional crystallization to both nominally crystalline and partially crystalline polymers is considered.

THE use of fractional crystallization in the separation of stereoisomers of high polymers is an established procedure. Such separation is possible because of variation in melting point (and perhaps in heat of fusion) which accompanies the introduction of disorders into an otherwise regular chain. Provided the molecular weight is high (i.e. provided the melting point of the polymer is not depressed by end effects) it is usually assumed that the fractionation is influenced solely by the degree of stereoregularity. Indications are that this assumption is justified: we have found that there is little or no variation in molecular weight or molecular weight distribution from fraction to fraction when high molecular weight poly(propylene oxide) is crystallized from dilute solution[1]. Nevertheless, theoretical arguments concerning the crystallization of high polymers from solution suggest that the solubility should be slightly dependent upon molecular weight[2], and for this reason one might expect fractionation to occur with respect to both molecular weight and degree of stereoregularity. Unfortunately, in theoretical studies, account has not been taken of the fact that the nucleation temperature might be several degrees lower than the equilibrium melting temperature, nor of the possibility that the crystals might grow via a diffusion controlled mechanism. We have therefore carried out an empirical investigation of this problem.

In order to avoid the complexities involved in the use of polymers of varying degrees of stereoregularity we have used linear, high molecular weight poly(ethylene oxide). In particular we have prepared dilute solutions of samples of poly(ethylene oxide) having wide molecular weight distributions, and have precipitated successive crystalline fractions. Measurements of the intrinsic viscosities of the various fractions could then be used to detect differences in solubility caused by the variation of molecular weights in the original polymer.

EXPERIMENTAL

Materials

The samples of poly(ethylene oxide) were 'Polyox' WSR–205 resins prepared by Union Carbide Ltd, Chemicals Division. Two samples designated A and B were used: A (code number FC 2075) had a slightly

higher intrinsic viscosity than B (commercial resin). Sample A was fractionated above the melting point by successive addition of quantities of iso-octane to a dilute solution in benzene. The *liquid* phases so obtained

Table 1. Fractionation of poly(ethylene oxide) A at 65°C
Initial concentration 1 g l^{-1}, $[\eta]=5{\cdot}64$ dl g^{-1}

Fraction	*Weight* (%)	$[\eta]$ (*dl* g^{-1})	*Fraction*	*Weight* (%)	$[\eta]$ (*dl* g^{-1})
1	8·9	16·4	5	11·8	1·67
2	15·1	11·5	6	22·7	0·73
3	17·3	5·2	7	14·9	0·15
4	9·3	3·1			

Weight-average $[\eta]=4{\cdot}77$ dl g^{-1}

were separated by syphoning off the dilute phase. The results of this fractionation are given in *Table 1*; the molecular weight distribution is

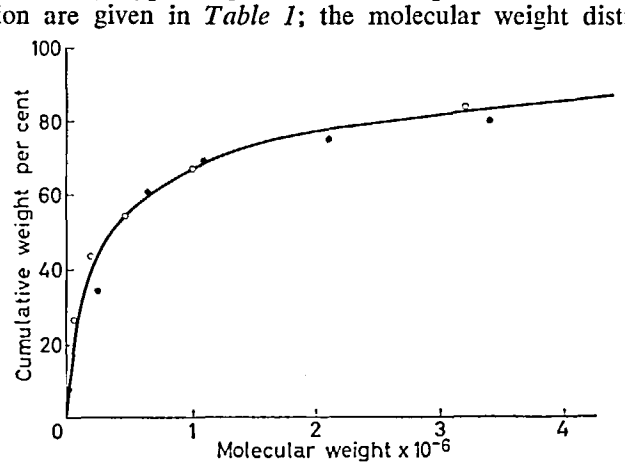

Figure 1—Molecular weight distribution of poly(ethylene oxide) A obtained by fractionation at 65°C (○) and at temperatures in the range 37° to 24°C (●)

seen to be wide (see also the *Figure 1*) and there is about 20 wt % of low molecular weight polymer. Sample B was shown to have a similar molecular weight distribution, although it contained rather more (some 30 wt %) low molecular weight polymer.

The solvents used in the crystallization experiments were commercial samples which had been dried and distilled; an exception was xylene which was shaken with concentrated sulphuric acid and then washed with water before the drying and distillation were carried out. The benzene used in the determination of dilute solution viscosities was obtained by drying and distilling analytical reagent grade solvent. Antioxidants of the hindered phenol type were added to all solvents at a concentration of one to two per cent of the polymer concentration.

Fractional crystallization

Dilute solutions (1 to 2 g l^{-1}) of the samples of poly(ethylene oxide) were placed in pear-shaped flasks and held at a controlled temperature

(±0·01°C) by immersion in a water bath. The solutions were stirred as the temperature was lowered to a value at which polymer was known to precipitate. After allowing crystallization to proceed for a given period of time (which varied from a few hours to several days depending upon the solvent and the temperature) the supernatant liquids were removed through a glass wool plug. The process was repeated to obtain further fractions. The crystalline precipitates were dissolved in benzene and freeze dried.

Intrinsic viscosity

Dilute solution viscosities in benzene at 25°C were measured by means of modified Desreux–Bischoff viscometers of low shear stress. Viscosity-average molecular weights were calculated by use of the relationship[3]

$$[\eta] = 3{\cdot}97 \times 10^{-4} M_v^{0{\cdot}686}$$

RESULTS

Representative results of fractional crystallizations from dilute solutions in ethyl alcohol, methylethyl ketone and xylene are given in *Tables 2* to *4*. Similar results were obtained in ethylbenzene. In each case more than one fractionation was performed. The solvents chosen were those for which crystallization occurred in the temperature range 20° to 40°C.

Table 2. The fractional crystallization of poly(ethylene oxide) A from ethanol
Initial concentration 1·59 g l^{-1}, $[\eta]$=4·98 dl g^{-1}

Precipitation temperature (°C)	*Weight* (%)	$[\eta]$ (*dl g*$^{-1}$)
32·5	18·5	4·83
32·0	7·7	4·96
31·5	25·9	5·18
31·0	26·8	5·65
Residue	21·1	3·96

Weight-average $[\eta]$=4·97 dl g^{-1}

Some degradation of the polymer occurred, especially in methylethyl ketone and xylene; values of the weight-average intrinsic viscosities of the fractions are quoted in the tables and can be compared with the intrinsic viscosity of the whole polymers before fractionation. Nevertheless, in all solvents, it is clear that fractionation of the high molecular weight

Table 3. The fractional crystallization of poly(ethylene oxide) B from methyl ethyl ketone
Initial concentration 2·5 g l^{-1}, $[\eta]$=3·66 dl g^{-1}

Precipitation temperature (°C)	*Weight* (%)	$[\eta]$ (*dl g*$^{-1}$)
30·5	24·3	3·97
30·5	16·8	4·20
30·5	23·7	4·15
26·0	6·1	3·65
Residue	29·1	0·57

Weight-average $[\eta]$=3·04 dl g^{-1}

polymer with respect to molecular weight is slight. Moreover, there is a tendency for the lower molecular weight *crystallizable* molecules to precipitate first. This tendency is common to all solvents; though it is only in ethyl alcohol, where degradation is minimal, that the effect can be seen clearly from the raw fractionation data. In all solvents the residue

Table 4. The fractional crystallization of poly(ethylene oxide) B from xylene
Initial concentration 2 g l^{-1}, $[\eta]=3{\cdot}66$ dl g^{-1}

Precipitation temperature (°C)	*Weight* (%)	$[\eta]$ (*dl* g^{-1})
37·7	9·1	3·60
37·7	12·2	3·75
37·7	15·1	3·86
37·7	9·7	3·38
2·3	23·1	2·77
Residue	31·1	1·87

Weight-average $[\eta]=2{\cdot}92$ dl g^{-1}

consisted of low molecular weight polymer: this material had a lower melting point than the other fractions and this would be expected for a fraction consisting mainly of molecules in the molecular weight range 5 000 or less. In every solvent it was possible to precipitate all the polymer except the low molecular weight residue by allowing the solution to stand for a prolonged time at the temperature of separation of the first fraction.

DISCUSSION

The process of crystallization is one of nucleation followed by growth. Since our data relate to the precipitation of large fractions we can assume that the growth process alone is important in determining the nature of the polymer precipitated. This growth process includes the diffusion of polymer molecules to the crystal/solution interface and the incorporation of molecules at the interface into the crystal. If processes of diffusion are of primary importance in determining the rate of growth of a crystal then it is to be expected that lower molecular weight polymer will precipitate more rapidly: if interfacial processes are rate-determining, in the sense that the incorporation of each polymer chain into the crystal involves a distinct nucleation process, then it is to be expected that higher molecular weight polymer will precipitate more rapidly. The data presented earlier, especially those obtained with ethyl alcohol as solvent when degradation was not a problem, indicate that processes of diffusion control the nature of the polymer incorporated into crystals of poly(ethylene oxide) when they are precipitated from a dilute solution of the high molecular weight, heterogeneous polymer. It is not possible to conclude that the overall rate of growth is controlled by diffusion; the data would be consistent with the suggestion[4] that the rate of growth is determined by slow secondary nucleation processes, while the bulk of polymer crystallizes by rapid addition to the growing lamellae: measurements of the rate of crystallization, from dilute solution, of fractions of high molecular weight poly(ethylene oxide) are in hand at the present time.

:he fractionation with respect to molecular weight is slight and it is sible that there is a balance between nucleation and diffusion as has n suggested by others[2]. Whatever the explanation these data support finding that the fractionation of poly(propylene oxide) with respect to ree of stereoregularity is not influenced measurably by the molecular ght of the high polymer. The small effect of molecular weight on :ipitation noted here [we assume that poly(propylene oxide) and poly-ylene oxide) have similar characteristics] would be swamped by the :e changes in solubility which accompany even minor changes in degree stereoregularity. In this way our results add weight to the general mption that molecular weight has negligible influence upon the tional crystallization of partially crystalline polymers.

inally these results confirm the widely held view that crystallization ot a useful process of fractionation with respect to molecular weight. he fractional crystallization of a linear, highly crystalline polymer such poly(ethylene oxide) gives such poor results, then the method can be ounted for all *high molecular weight* polymers.

APPENDIX

fractional crystallization of poly(ethylene oxide) from a mixture of octane and benzene.

/e have crystallized poly(ethylene oxide) from a mixture of 32% vol octane and 68% vol of benzene at temperatures in the range 37° to 2. Typical data are given in *Table 5*. Here fractionation occurs on

ble 5. The fractionation of poly(ethylene oxide) A from iso-octane and benzene
Initial concentration 1 g l^{-1}, $[\eta]=5{\cdot}64$ dl g^{-1}

ecipitation temperature (°C)	*Weight* (%)	$[\eta]$ (*dl* g^{-1})
37·0	19·3	15·8
35·0	1·6	12·1
33·7	8·5	8·6
31·7	2·3	5·6
28·3	14·3	3·88
24·2	38·6	2·00
Residue	15·3	0·21

Weight-average $[\eta]=5{\cdot}43$ dl g^{-1}

basis of molecular weight, although the fractions obtained were :alline solids. These fractionation data are very similar to those ined by liquid–liquid phase separation above the melting point *le 1*) and almost identical molecular weight distributions are obtained : the data of *Tables 1* and *5* (see *Figure 1*).

ıe similarity of the two sets of data, coupled with the wide tempera-range over which precipitation takes place (characteristic of liquid :r than crystal phase separation), implies that the mechanism is that quid phase separation even though a crystalline phase is recovered*.

ɔssible explanation of this phenomenon is that in this solvent the temperature of liquid phase ation is lower than the equilibrium melting point of the polymer in solution but higher than the :rature at which nucleation takes place. Given the condition that the concentrated liquid phase higher nucleation temperature (because of the greater concentration of polymer) then the possibility that a crystalline phase separates. Moreover, if the activation energy for continued growth from solution is similar to that for nucleation then only the highest molecular weight polymer will llize and separate.

This type of fractional crystallization is considered an exceptional case which will occur only when the temperature of liquid phase separation is at or about the melting point of the polymer in solution. However, in interpreting the results of a fractional crystallization, the possibility of a hybrid separation of this type should be borne in mind.

We wish to thank Miss C. J. S. Guthrie, Mrs J. A. Hurst, Mr F. Pezzano and Mr D. St J. Smyth for practical assistance; and to acknowledge the help and advice of Dr G. Allen.

Department of Chemistry,
University of Manchester

(*Received August 1965*)

REFERENCES

[1] ALLEN, G., BOOTH, C. and JONES, M. N. *Polymer, Lond.* 1964, **5**, 257
[2] FLORY, P. J. *Principles of Polymer Chemistry.* Cornell University Press: New York, 1953
KAWAI, T. *J. Polym. Sci.* 1965, **3C**, 83
[3] PRICE, C. To be published
[4] See, for example, GEIL, P. H. *Polymer Single Crystals.* Interscience: New York, 1963

The Influence of the Molecular Size Distribution within a Liquid on the Viscous Flow of the Liquid

A. POWELL

It is proposed that an empirical correction be applied to the Maxwell equation to take account of the distribution of relaxation times. Literature data are advanced to suggest there is a definite relationship between viscosity measurements in oscillatory shearing and those in continuous shearing.

IN considering a polymer melt, Ferry *et al.*[1] represented the distribution of relaxation times by an empirical function, which could only be determined by a complicated method of successive approximations; the viscous flow of the melt was expressed in terms of this distribution of relaxation times. Tobolsky and Eyring[2], considering a polymer melt, represented it by a network structure comprising three types of flow unit; the viscosity of the melt was expressed in terms of the relative numbers of these units and their characteristic relaxation times. The parameters in the equations presented by the above workers are not easily determined. In the present work, relatively simple equations are presented for the viscosity of a liquid in terms of the molecular size distribution within the liquid. The necessity to determine the distribution of relaxation times is avoided, and the number of parameters introduced is small. The equations in this present work permit simple mathematical treatment.

In the present work, considering a liquid in which the molecules have similar shapes and do not ionize, the liquid is represented by a model made up of a viscous component

$$s=\eta_0\dot{e} \tag{1}$$

and an elastic component

$$\dot{s}=G_\omega\dot{e} \tag{2}$$

where ω is equal to $(2\pi f)$ and is called the angular frequency; f is the oscillatory shear frequency; η_0 is the viscosity of the liquid at zero frequency; s is the stress; $\dot{e}$ is the rate of strain; $\dot{s}$ is the rate of change of stress with time; G_ω is the rigidity modulus at angular frequency ω. The rates of strain for these two components are added together to give for the complete model

$$\dot{e}=\dot{s}/G_\omega+s/\eta_0 \tag{3}$$

Equation 3 differs from the Maxwell model, in which the rigidity modulus is a constant, in that G_ω in equation 3 is given by

$$G_\omega=G\,(\lambda\omega)^{1-F} \tag{4}$$

where

$$F=(M_n/M_m)^x \tag{5}$$

G and λ are the values of the rigidity modulus and relaxation time which would be observed, for a liquid whose viscosity is η_0 at zero angular frequency, if all the molecules were identical, each molecule having a weight equal to the viscosity average weight. Thus

$$\lambda = \eta_0 / G \tag{6}$$

λ is called the representative relaxation time for a liquid of viscosity η_0 at zero angular frequency; M_n is the number average weight and M_m is the weight average weight of the molecules; x is a constant for the particular molecular species. Equations 4 and 5 are empirical. The reasons for introducing equations 4 and 5 into this model for the liquid are as follows.

(*i*) In a liquid comprising molecules each of which is the same shape and size, and at any frequency of shearing, all the molecules of the liquid will be responding elastically to the stress cycle; since the number of molecules responding elastically to the stress remains the same, the rigidity modulus (G_ω) should be the same at all values of ω. For such a liquid $(M_n/M_m)=1$ and equations 4 and 5 give $F=1$ and $G_\omega=G$, as expected.

(*ii*) In a liquid comprising molecules of the same shape, and a size distribution specified by the representative relaxation time λ and a value less than one for the ratio (M_n/M_m), the number of molecules responding elastically to the stress cycle will depend on the frequency; as the frequency increases, the duration of the stress cycle becomes less, and the period of time in which the molecule can respond elastically decreases. As this time decreases, the maximum size of molecule which can respond elastically becomes less, and the total number of molecules contributing to the elasticity becomes less. Thus as the frequency ω increases the rigidity modulus should increase; this is predicted by equation 4 which shows that as ω increases G_ω increases.

(*iii*) In liquids with the same value for η_0 and for λ, and containing molecules of the same shape, variation of molecular size distribution is accounted for by parameter F. At a particular frequency (or value of $\omega\lambda$), widening the distribution should increase the number of molecules which can respond elastically and increase G_ω. In equations 4 and 5, a widening of the size distribution [that is, a decrease in the value of the ratio (M_n/M_m)] is seen to result in a decrease of F and an increase in the value of G_ω, as expected.

(*iv*) In liquids with the same value for η_0 and for λ, and with the same size distribution, the molecular shape is taken into consideration by parameter x. The introduction of bulky side groups or chains along the length of the molecule will hinder the contraction of the molecule and limit the elastic response, hence increasing the value of G_ω. Thus the introduction of bulky side groups or chains along the molecule is considered in this interpretation to decrease slightly the value of x and therefore of F (equation 5), thus increasing the value of G_ω in equation 4.

For a liquid represented by equation 3 subjected to oscillatory shearing at angular frequency ω, equation 7 is obtained.

$$\eta_\omega = \eta_0 / \{1 + (\omega\lambda)^{2F}\} \tag{7}$$

where η_ω is the viscosity at angular frequency ω, η_ω is equal to (g/ω) where g is the imaginary part of the complex shear modulus. Equation 7 has been tested using viscosity data from oscillatory shearing experiments on glycerol[3], mineral oils[4], silicones[4,5] and polystyrene[6], log $\{(\eta_0/\eta_\omega)-1\}$ being plotted against log ω. Straight line plots are obtained for each of these materials in agreement with equation 7. Typical plots obtained are those

Table 1. Values of parameter F obtained from viscosity measurements

Material	*Viscosity average molecular weight*	*Temperature, °C*	F	$\left(\frac{M_n}{M_m}\right)$
Glycerol		−42·0 −34·0 −26·0 −18·0	1·00 1·00 1·00 1·00	1·00
LVI mineral oil* MVI(N) mineral oil* HVI mineral oil*	460	30·0 30·0 30·0	0·55 0·50 0·55	0·65
Polydimethylsiloxane MS200 silicone oil A MS200 silicone oil B DC200 silicone	$2{\cdot}6\times10^4$ $6{\cdot}4\times10^4$ 6×10^4	30·0 30·0 −49·5 −13·7 52·0	0·28 0·34 0·41 0·41 0·42	0·4
Polystyrene	$2{\cdot}4\times10^5$	200	0·26	
Polyisobutylene (Vistanex B100) dissolved in decalin at concentrations w/w 20 13 8 5	$1{\cdot}1\times10^6$	25·0	0·42 0·42 0·42 0·42	0·4
Polyethylene (Tenite 826F)	6×10^4	200	0·50	0·5

*The LVI oil is a Southern conventional oil, of Redwood viscosity index 260 sec at 140°F. The MVI(N) oil is a Southern Edeleanu oil, of Redwood viscosity index 170 sec at 140°F. The HVI oil is a Colon Duosol oil, of Redwood viscosity index 330 sec at 140°F.

for glycerol (*Figure 1*) and DC200 silicone oil (*Figure 2*). The values obtained for parameter F are given in *Table 1*. It is seen from the data for glycerol and for DC200 silicone that the parameter F is independent of temperature, as is suggested by equation 5. With glycerol, $F=1$ and equation 7 is then identical with the Maxwell equation.

An equation is derived for a polymer solution subjected to oscillatory shearing; equation 7 is used to represent the dependence of viscosity on ω for the polymer component, and the solvent viscosity (η_s) is assumed to be independent of the shear frequency. Adding together these two viscosity contributions gives the following equation for η_m, the viscosity of the polymer solution at angular frequency ω.

$$\eta_m=\eta_s+\{(\eta_m)_0-\eta_s\}\,/\,\{1+(\omega\lambda_p)^{2F}\} \tag{8}$$

or

$$(\omega\lambda_p)^{2F}=\{(\eta_m)_0-\eta_m\}\,/\,\{\eta_m-\eta_s\} \tag{9}$$

where $(\eta_m)_0$ is the viscosity of the polymer solution at zero frequency; and λ_p is the representative relaxation time for the polymer component in the solution. Equation 9 has been tested using data at 20°C for a solution of polyisobutylene of viscosity average molecular weight $6{\cdot}2 \times 10^4$, in cetane[7].

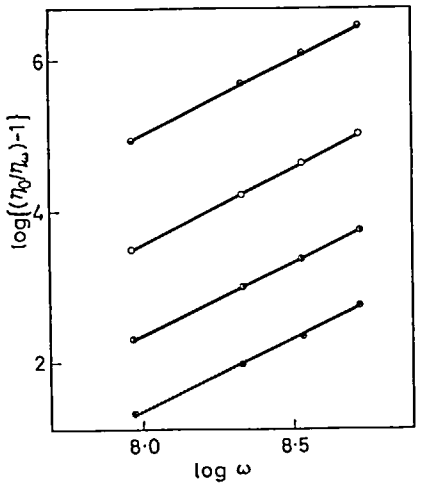

Figure 1—Glycerol at −42·0°C (⊖), −34·0°C (○), −26·0° C (◑), and −18·0°C (⊕)

$\log[\{(\eta_m)_0-\eta_m\}/\{\eta_m-\eta_s\}]$ being plotted against $\log\omega$. A straight line graph is obtained in agreement with equation 9.

Equations 10 and 11 below have been found to describe the experimental behaviour of a polymer melt and a polymer solution, respectively, when subjected to continuous shearing

$$\eta_D=\eta_0/\{1+(D\gamma)^{2F}\} \tag{10}$$

$$\{(\eta_m)_0-(\eta_m)_D\}/\{(\eta_m)_D-\eta_s\}=(D\gamma_p)^{2F} \tag{11}$$

where η_D and η_0 are the viscosities of the polymer melt at rates of continuous shear D and zero, respectively; γ is the relaxation time for the

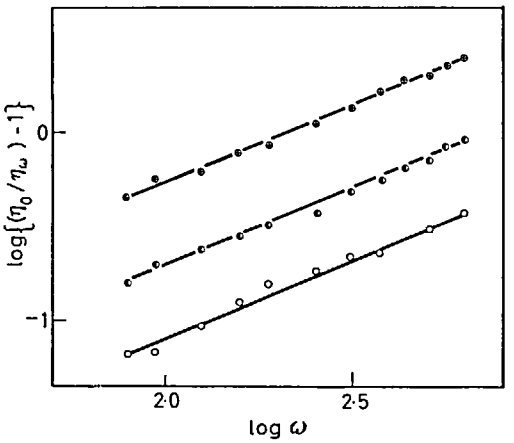

Figure 2—DC200 silicone oil at −49·5°C (⊕), −13·7°C (◐) and 52·0°C (○)

polymer molecule in the melt for continuous shearing; $(\eta_m)_D$ and $(\eta_m)_0$ are the viscosities of the polymer solution at rates of continuous shear D and zero, respectively; γ_p is the relaxation time of the polymer in the solution. Data have been obtained by Horio, Onogi and Ogiwara[8] in oscillatory and in continuous shearing experiments for molten polyethylene (Tenite 826F) at 200°C, and by De Witt, Markovitz, Padden, Jr. and Zapas[9] for solutions

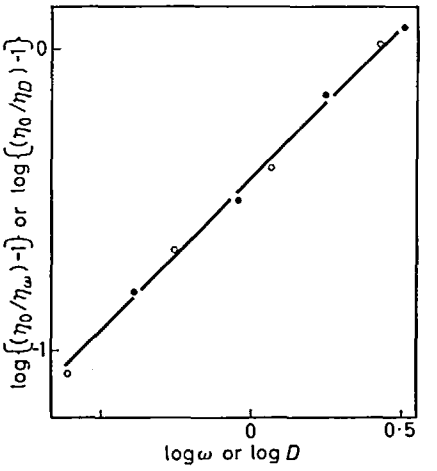

Figure 3—Polyethylene (Tenite 826F) at 200°C; log $\{(\eta_0/\eta_\omega)-1\}$ versus log ω (⊕); log $\{\eta_0/\eta_D)-1\}$ versus log D (○)

of polyisobutylene (Vistanex B100) in decalin at 25°C. *Figure 3* shows the data for the polyethylene, log $\{(\eta_0/\eta_\omega)-1\}$ being plotted against log ω for oscillatory shearing (equation 7), and log $\{\eta_0/\eta_D)-1\}$ being plotted against log D for continuous shearing (equation 10). *Figure 4* shows the data for the solutions of polyisobutylene in decalin, log $[\{(\eta_m)_0-\eta_m\}/\{\eta_m-\eta_s\}]$

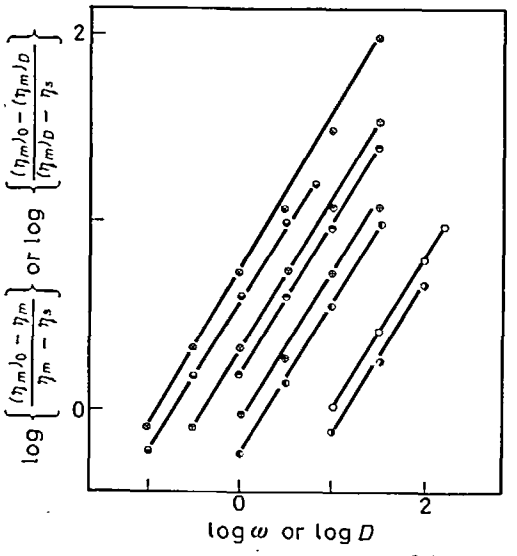

Figure 4—Solutions of polyisobutylene (Vistanex B100) in decalin at 25°C, log $\left\{\frac{(\eta_m)_0-\eta_m}{\eta_m-\eta_s}\right\}$ versus log ω for polymer weight concentrations of 5% (○), 8% (⊕), 13% (⊗) and 20% (⊗); log $\left\{\frac{(\eta_m)_0-(\eta_m)_D}{(\eta_m)_D-\eta_s}\right\}$ plotted against log D for polymer weight concentrations of 5% (◑), 8% (◐), 13% (⊖) and 20% (⊖)

being plotted against $\log \omega$ for oscillatory shearing (equation 9), and $\log [\{(\eta_m)_0 - (\eta_m)_D\} / \{(\eta_m)_D - \eta_s\}]$ being plotted against $\log D$ for continuous shearing (equation 11). In *Figure 3* and also in *Figure 4* the plots for oscillatory shearing have the same slopes as the plots for continuous shearing; thus, for each of these two materials, the viscosities in oscillatory shearing and in continuous shearing must be expressible in terms of the same molecular weight distribution parameter F. The values of F for the solutions of polyisobutylene (Vistanex B100) are given in *Table 1*, and are seen to be independent of polymer concentration, in accordance with equation 5.

Equations 7 and 10 which apply to a molten polymer, and equations 9 and 11 for a polymer in solution imply that the viscosity at oscillatory shear frequency ω will be equal to the viscosity at rate of continuous shear D, when $\omega = (\gamma/\lambda) D$ for the molten polymer, and when $\omega = (\gamma_p/\lambda_p) D$ for the polymer in solution. From the data plotted in *Figure 3*, the ratio (γ/λ) is seen to be approximately unity for the polyethylene. The data plotted in *Figure 4* give, for the polyisobutylene in solution, a value of 1·4 for the ratio (γ_p/λ_p).

Equation 10 has also been tested using viscosity data[10] from continuous shearing experiments at 18°C on polydimethylsiloxane, of viscosity average molecular weight 10^5. A plot of $\log \{(\eta_0/\eta_D) - 1\}$ against $\log D$ is found to give a straight line graph, in agreement with equation 10.

Equation 11 for a polymer solution has been tested further by applying it to continuous shearing data for a number of polymers in solution for which the ratio (M_n/M_m) is not known. Continuous shearing data for solutions of polystyrene in benzene[11], polydimethylsiloxane in toluene[12], and polybutadiene in benzene[13] were used, $\log [\{(\eta_m)_0 - (\eta_m)_D\} / \{(\eta_m)_D - \eta_s\}]$ being plotted against $\log D$, for each of these solutions. A straight line graph was obtained for each solution, as would be expected from equation 11. Equations 9 and 11 for a polymer in solution assume that η_s, the viscosity of the pure solvent, is independent of the oscillatory shear frequency and of the rate of continuous shear; this assumption is justifiable over the frequency or rate of shear range normally used.

The available values for (M_n/M_m) are given in *Table 1*, together with the corresponding values for F. These values suggest that as the molecular weight distribution widens, that is, as (M_n/M_m) changes from one to zero, the value of F changes from one to zero. The dependence of parameter F on the weight distribution and on the species of molecule does, however, require further investigation, and work is now in progress to this end.

The evidence presented does suggest that there is a definite relationship between viscosity measurements in oscillatory shearing and those in continuous shearing, through equations 7 and 10 for a molten polymer, and equations 9 and 11 for a polymer in solution. Also, the data for the mineral oil suggest that equation 7, and possibly equation 10, can be applied to liquids in which the constituent molecules are relatively small.

John Dalton College of Technology,
Chester Street, Manchester

(*Received September 1965*)

REFERENCES

[1] FERRY, J. D., FITZGERALD, E. R., GRANDINE Jr, L. D. and WILLIAMS, M. L. *Industr. Engng Chem. (Industr.)*, 1952, **44**, 703

[2] TOBOLSKY, A. and EYRING, H. *J. chem. Phys.* 1943, **11**, 125

[3] PICCIRELLI, R. and LITOWITZ, T. A. *J. acoust. Soc. Amer.* 1957, **29**, 1009

[4] BARLOW, A. J. and LAMB, J. *Proc. Roy. Soc. A*, 1959, **253**, 52

[5] HARPER Jr, R. C., MARKOVITZ, H. and DE WITT, T. W. *J. Polym. Sci.* 1952, **8**, 435

[6] COX, W. P., NIELSEN, L. E. and KEENEY, R. *J. Polym. Sci.* 1957, **26**, 365

[7] PORTER, R. S. and JOHNSON, T. F. *Amer. chem. Soc. (Divn Petrol. Chem.)*, **1959**, 215

[8] HORIO, M., ONOGI, S. and OGIWARA, S. Special issue of *J. Jap. Soc. Testing Materials*, **1961**, 350

[9] DE WITT, T. W., MARKOVITZ, H., PADDEN Jr, F. J. and ZAPAS, L. J. *J. Colloid Sci.* 1955, **10**, 174

[10] BENBOW, J. *Polymer, Lond.* 1961, **2**, 429

[11] KRIGBAUM, W. R. and FLORY, P. J. *J. Polym. Sci.* 1953, **11**, 37

[12] PHILIPOFF, W. *Industr. Engng Chem. (Industr.)*, 1959, **51**, 883

[13] TSVETKOV, V. N., PETROVA, A. I. and PODDUBNY, I. Y. *Rubb. Chem. Technol.* 1953, **26**, 81

Network Scission Processes in Peroxide Cured Methylvinyl Silicone Rubber

D. K. THOMAS

Stress-relaxation studies show that network scission in peroxide cured methylvinyl silicone rubbers at temperatures up to 250°C is largely the result of hydrolytic reactions in the main chain polymer. There are indications that at 250°C and above oxidative scission of crosslinks makes a significant contribution to the observed rate of continuous stress-relaxation. There is no indication that acidic byproducts of the vulcanization reaction catalyse the hydrolysis of siloxane bonds in the polymer.

SILICONE rubber vulcanizates are extremely stable when subjected to conventional heat ageing tests at temperatures up to 250°C. In these tests the specimens are aged in a relaxed state in an air circulating oven. In contrast the heat ageing of silicone rubbers at high temperatures in a confined space, where there is no opportunity for the diffusion of gases or vapours inwards or outwards from the system, leads to reversion. At temperatures above 250°C this process gradually reduces the rubber to a useless material of a soft cheesy nature.

In a rubber vulcanizate the loss of rubbery properties during ageing is largely due to reactions leading to network scission, network formation (i.e. crosslinking), or to a combination of both. The embrittlement which occurs in silicone rubbers after long exposure to air at temperatures above 200°C is presumably due to oxidative crosslinking reactions resulting from oxidation of the methyl side groups of the main chain polymer. The softening which occurs during confined heat ageing must be largely the result of network scission reactions; in general the rubber will be subject to both processes and the net effect on properties will be determined by the relative amounts of scission and crosslinking occurring. Commercial silicone rubbers usually contain high concentrations of fine silica, the presence of which may influence the heat ageing processes. In addition, the crosslinks in hot vulcanized silicone rubber may be of various types each having its having its own level of oxidative stability.

In the present work an attempt is made to identify those processes making the most significant contribution to network chain scission in a peroxide cured methylvinyl silicone at temperatures up to 250°C. If this can be done the prospects for improving the performance of silicone vulcanizates in respect of reversion can be properly assessed.

EXPERIMENTAL

Materials

The polymer used throughout was a methylvinyl silicone containing 0·2 mole per cent of vinyl groups. The crosslinking reagent, bis-1,4-dichlorobenzoyl peroxide was used throughout.

Compounding and vulcanization

The silicone polymer and organic peroxide were mixed on a laboratory mill; where reinforcing fillers were used processing aids were employed. Sheets of 0·015 in. thickness were moulded for stress-relaxation work and they were cured under pressure for 20 minutes at 120°C followed by an oven cure of 3½ hours at 250°C.

Stress-relaxation measurements

The technique of continuous stress-relaxation was used for following network scission processes; the apparatus used has been described fully elsewhere[1]. In order to obtain 'dry' and 'moist' atmospheres of a reproducible kind the procedure of Lewis and Turner[2] was used. The rate of air flow through the relaxometer envelope was 0·76 litre per minute in both cases.

RESULTS AND DISCUSSION

The crosslinking of a methylvinyl silicone with bis-1,4-dichlorobenzoyl peroxide (DCBP) occurs mainly through the vinyl groups and this results in the majority of crosslinks being of the type

$$=CH—CH_2—CH_2—CH=$$

In addition aryloxy radicals may abstract hydrogen from some of the methyl groups on the polymer and form crosslinks of the type:

$$=CH—CH_2—CH_2 \quad \text{and} \quad —CH_2—CH_2—$$

In a silicone rubber containing crosslinks of this type there are a number of reactions which can lead to network changes during heat ageing, for example: (*i*) siloxane bond interchange, (*ii*) hydrolysis of siloxane bonds, (*iii*) oxidation of hydrocarbon groups in the crosslinks and (*iv*) oxidation of hydrocarbon groups on the polymer main chain.

Process (*i*) does not affect the overall network chain concentration but leads to stress-relaxation in constant strain experiments and creep in constant stress experiments. Processes (*ii*) and (*iii*) result in a change in network chain concentration but the silanols formed as a result of (*ii*) may re-condense to form new network chains and a dynamic equilibrium will be established whose position is determined by the concentration of water in the system. Process (*iv*) will lead to crosslinking and hence to an increase in network chain concentration. It is possible that all these reactions occur simultaneously at high temperature.

By making use of stress-relaxation techniques it is possible to study chain scission processes in isolation from crosslinking reactions. Thus in a stress-relaxation experiment in which the rubber is held in continuous extension it can be assumed, at least over the initial stages of ageing, that the observed rate of relaxation is determined only by network scission processes. Any new network chains are formed while the network is in its equilibrium configuration, and they will not, therefore, support any stress at the instant of their formation.

In terms of the silicone rubbers under test this means that the observed rate of relaxation in a continuous stress-relaxation experiment will be due

to processes (*i*), (*ii*) and (*iii*). These processes will now be discussed in the light of the experimental results.

Siloxane bond interchange

Siloxane bond interchange was proposed[3] to account for the stress-relaxation in silicone rubbers at fairly low temperatures in dry air and dry nitrogen. This process does not lead to a change in network chain concentration and is thought to occur as follows:

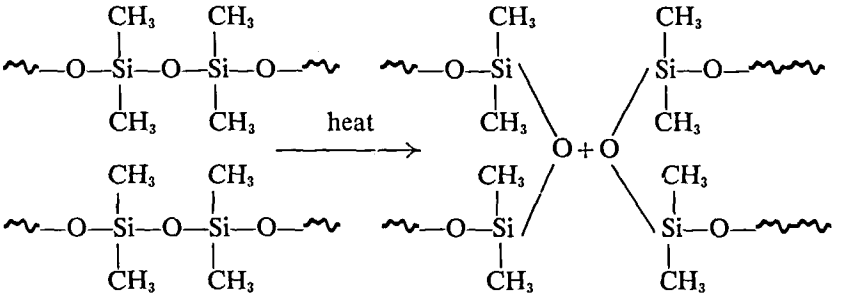

This reaction was shown to occur with an activation energy of 22·8 kcal/mole when uncatalysed and 5·1 kcal/mole when catalysed by bases, and it occurred with equal facility in the presence or absence of oxygen. The fact that this reaction does not require the presence of oxygen means that it can be separated from reactions (*ii*) and (*iii*) by measuring the rate of continuous stress-relaxation of an outgassed sample *in vacuo*. This has been done at 250°C at which temperature the reaction should proceed rapidly; the results (see *Figure 1*) show that with peroxide-cured methyl-

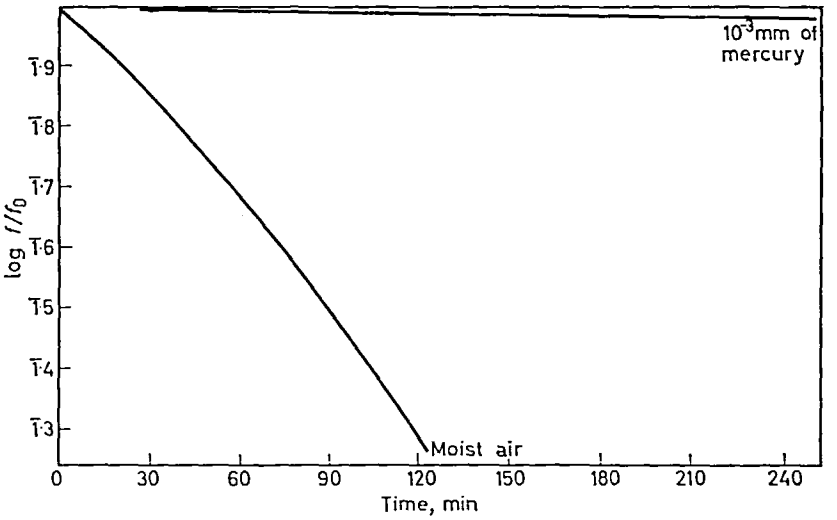

Figure 1—Effect of environment on the rate of continuous stress-relaxation at 250°C of an unfilled methylvinyl silicone rubber crosslinked with 0·6 per cent DCBP

vinyl silicone rubber siloxane bond interchange does not appear to make a significant contribution to the observed rate of continuous stress-relaxation. The vulcanizate used was unfilled but unextracted and so contained impurities arising from the polymerization and crosslinking reactions. There is still the possibility that in the presence of moisture a reaction of this kind will occur, i.e. with water acting as a co-catalyst. However, such a reaction could equally well be described as a base-catalysed hydrolytic reaction, the hydrolysis being followed by a condensation of silanol groups formed on adjacent network chains.

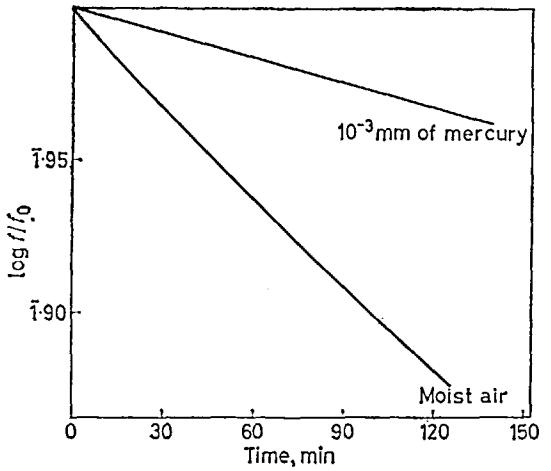

Figure 2—Effect of environment on the rate of continuous stress-relaxation at 250°C of a silica filled methylvinyl silicone rubber crosslinked with 0·7 per cent DCBP

An identical experiment carried out on a silica-filled vulcanizate showed a significant amount of stress-relaxation *in vacuo* (see *Figure 2*); this is presumably due to water being evolved from the filler at high temperature and causing hydrolytic scission.

Hydrolysis of siloxane bonds

The elimination of siloxane bond interchange as a process making a significant contribution to the observed rate of continuous stress-relaxation means that network scission is due almost entirely to hydrolysis of siloxane bonds, oxidation of crosslinks, or both. Hydrolysis proceeds as follows:

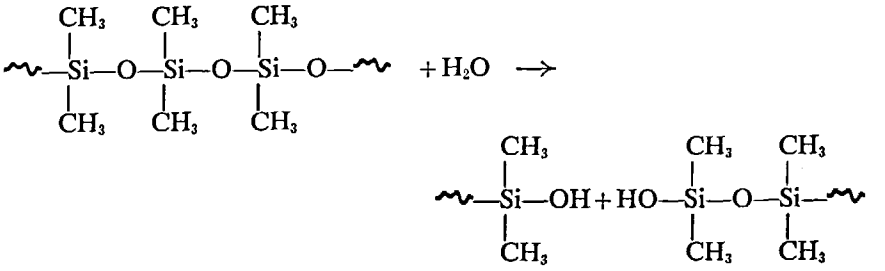

The rate of scission will be proportional to water concentration and the position of equilibrium will be determined by the water content of the system. The rate of scission due to this reaction should be at a maximum when the environment is saturated with water vapour, and perhaps under such conditions hydrolysis will be the major cause of stress-relaxation.

Experiments have been carried out in air saturated with moisture at temperatures up to 250°C and the continuous stress-relaxation data always fell on reasonable straight lines when $\log f_t/f_0$ was plotted against time. This allows the rate of relaxation to be characterized by a 'relaxation rate constant' k; the values obtained are shown in *Table 1.*

Table 1. Relaxation rate constants for methylvinyl silicone rubber in moist air at elevated temperatures

Temperature, °C	*k, unextracted*	*k, extracted*	*Temperature, °C*	*k, unextracted*	*k, extracted*
120	$6{\cdot}39\times10^{-5}$	—	172	—	$2{\cdot}65\times10^{-4}$
140	$1{\cdot}03\times10^{-4}$	$1{\cdot}19\times10^{-4}$	180	$6{\cdot}10\times10^{-4}$	$6{\cdot}10\times10^{-4}$
150	—	$1{\cdot}28\times10^{-4}$	200	$9{\cdot}04\times10^{-4}$	$9{\cdot}58\times10^{-4}$
160	$2{\cdot}50\times10^{-4}$	$2{\cdot}36\times10^{-4}$	250	$6{\cdot}96\times10^{-3}$	$4{\cdot}70\times10^{-3}$
161	$2{\cdot}04\times10^{-4}$	—	275	$1{\cdot}91\times10^{-2}$	—

When $\log k$ is plotted against $1/T$ a reasonable straight line is obtained (see *Figure 3*), and at all temperatures below 250°C no significant difference exists between the results for extracted and unextracted vulcanizates.

These results suggest that the effects of a single process are being

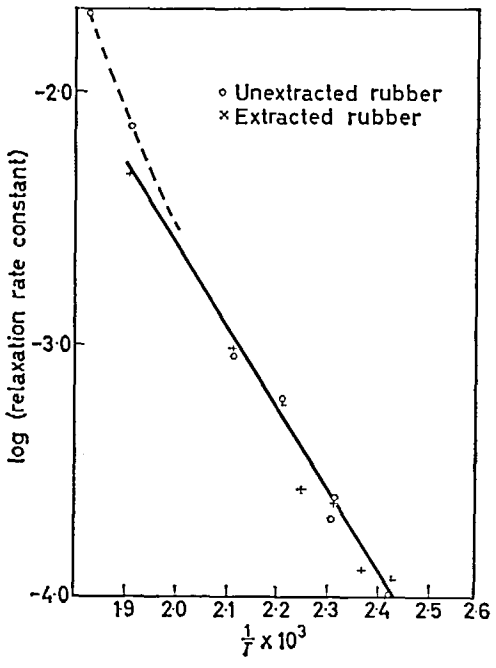

Figure 3—Arrhenius plot for 'relaxation rate constants' in unfilled methylvinyl silicone rubber crosslinked with 1·5 per cent DCBP

observed at temperatures up to 200°C, and in view of the conditions under which the experiments are being conducted this process is probably one of hydrolytic scission in the main chain polymer. The coincidence of results for extracted and unextracted vulcanizates shows that dichlorobenzoic acid is not catalysing hydrolytic scission over this temperature range. At 250°C extraction of the vulcanizate results in a significant decrease in rate of relaxation.

Oxidative scission in the crosslinks

It can be shown that added antioxidants reduce the rate of continuous stress-relaxation in methylvinyl silicone vulcanizates at 250°C (see *Figure 4*). If one accepts Tobolsky's postulate that crosslinks formed during ageing do not contribute to the tension during a continuous relaxation

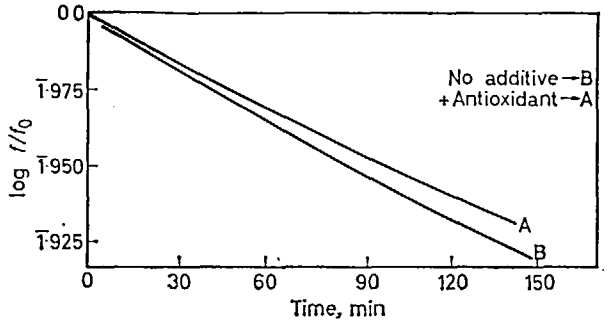

Figure 4—Effect of added antioxidant on the rate of continuous stress-relaxation at 250°C of a silica filled methylvinyl silicone vulcanizate in air

experiment, the effect of an antioxidant can only be to reduce the rate of oxidative scission in the primary crosslinks. The fact that solvent extraction reduces the values of the relaxation rate constant k at 250°C sufficiently to bring it on to the Arrhenius plot for the hydrolytic scission reaction could be interpreted as evidence that the high value for k is due to a contribution from acid-catalysed oxidative scission of crosslinks.

At temperatures of 200°C and below this process does not make a significant contribution to the rate of continuous stress-relaxation in unextracted vulcanizates.

CONCLUSIONS

In what appeared to be a complex system it transpires that network scission in methylvinyl silicone rubbers at temperatures below 250°C is due largely to hydrolytic reactions in the main chain polymer. At temperatures of 250°C and above there are indications that a significant amount of scission arises from oxidative reactions in the crosslinks, and that this reaction is catalysed by acidic residues in the rubber.

In conventional heat ageing tests in which the rubber remains in an unstrained condition the effects of hydrolysis will only be observed if the concentration of water in the system is allowed to rise. Under these

circumstances softening will occur due to a shift in the position of equilibrium in the reaction

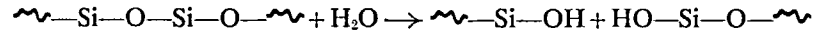

On ageing the material in a well ventilated situation the effects of hydrolysis are not seen and the silicone rubber becomes brittle after long exposure at high temperature. This embrittlement must result from additional crosslinking caused by oxidative reactions in the methyl groups of the main chain polymer. When the rubber is used in compression or tension hydrolytic scission will affect performance, and in applications of this sort it is important to dry out the rubber before use and prevent access of moisture to the component during use. With filled rubber the silica filler is a further source of moisture and drying needs to be carried out at elevated temperatures immediately prior to use. In order to improve the confined heat ageing performance of silicone rubber an alternative filler to fine silica is needed which does not have the same affinity for water. It may be, however, that ability to reinforce silicone rubber and affinity for water are inseparable.

The author is indebted to Mr R. Sinnott and Mr J. Day for their preparation of silicone vulcanizates.

Chemistry, Physics & Metallurgy Department,
Royal Aircraft Establishment,
Farnborough, Hants.

(*Received October 1965*)

REFERENCES

[1] ATKINSON, A. S. *R. A. E. Tech. Note No. Chem. 1393.* January 1963
[2] TURNER, M. J. and LEWIS, J. *Proc. 4th Rubber Technology Conference, London,* May 1962
[3] OSTHOFF, R. C., BUECHE, A. M. and GRUBB, W. T. *J. Amer. chem. Soc.* 1954, **76**, 4659

Some Solvent Effects on the Cobalt-60 Gamma-ray Initiated Polymerization of Isobutene in the Presence of Zinc Oxide

(Miss) J. A. BARTLETT and F. L. DALTON

n-Hexane has been added to isobutene–zinc oxide mixtures in order to study monomer dilution behaviour during radiation-initiated polymerization. The results obtained may be understood within the framework of a previously proposed reaction scheme if Fontana–Kidder type kinetics are assumed for the propagation and transfer reactions of the polymerization.

WE HAVE recently published[1] a number of observations on the cobalt-60 γ-ray initiated polymerization of isobutene and discussed a selection of papers on this subject[2–9]. An obvious extension of our own work was the addition of solvent to the system in order to gain further insight into the mechanism of the reaction. It was decided to use a hydrocarbon solvent of low dielectric constant for these experiments and *n*-hexane was arbitrarily chosen for this purpose. In view of our previous suggestion[1] that initiation occurs at the zinc oxide surface and that the energy absorbed in the zinc oxide is responsible for the observed polymerization, a fixed concentration (3·50 mole/l.) of zinc oxide of 0·17 m^2/g surface area was used throughout this work, and the concentrations of solvent and monomer in the liquid phase varied. Under these conditions measurements were made of the variation of polymerization rate and molecular weight of the polymer produced as functions of monomer concentration, both at −78°C and at 0°C: the purpose of this communication is to report and discuss the data obtained.

EXPERIMENTAL

The preparation and purification of zinc oxide and isobutene, and the methods used for preparing samples and measuring polymerization rates have been given previously[1,10]. Some modifications to the vacuum system were made for this work, in particular the substitution of all metal stopcocks (BiPL valves, Scientific Instrument and Model Co., Ross-on-Wye, Herefordshire) for the rubber diaphragmed stopcocks used previously. This was necessary since hexane swelled the rubber of the diaphragms. Isobutene was finally dried by co-distillation with sodium vapour as described by Plesch[11]; this was found more convenient than our earlier technique and was shown to give identical results. Arrangements were also made to introduce both solvent and monomer into dilatometers as liquids from burettes instead of as gases as has been done previously; this change again was a matter of convenience rather than principle.

Hexane was obtained as 'Research grade' 99·96 mole per cent pure material from Phillips Petroleum Co., Bartlesville, Oklahoma, the most probable impurity being methyl cyclopentane. It was outgassed, roughly

fractionated under high vacuum, co-distilled three times with sodium vapour, and finally vacuum distilled from residual sodium prior to use.

RESULTS

The rate and molecular weight data obtained from a series of runs carried out at −78°C, at a zinc oxide concentration of 3·50 mole/l. and a nominal intensity of 390 r/h* are given in *Table 1*, while the variation of rate and

Table 1

Temperature °C	*Monomer concentration mole/l.*	*Rate of polymerization mole l^{-1} sec^{-1}*	*Viscosity average molecular weight*	*Temperature °C*	*Monomer concentration mole/l.*	*Rate of polymerization mole l^{-1} sec^{-1}*	*Viscosity average molecular weight*
−78	11·89	$1{\cdot}27\times10^{-3}$	$6{\cdot}47\times10^{5}$	−78	1·50	$9{\cdot}63\times10^{-5}$	$1{\cdot}77\times10^{6}$
−78	11·57	$1{\cdot}84\times10^{-3}$	—	−78	1·19	$8{\cdot}95\times10^{-5}$	$1{\cdot}34\times10^{6}$
−78	11·27	$1{\cdot}77\times10^{-3}$	—	0	11·21	$1{\cdot}24\times10^{-3}$	$1{\cdot}10\times10^{5}$
−78	10·68	$1{\cdot}66\times10^{-3}$	—	0	8·94	$1{\cdot}19\times10^{-3}$	$1{\cdot}26\times10^{5}$
−78	9·49	$1{\cdot}35\times10^{-3}$	—	0	7·96	$1{\cdot}17\times10^{-3}$	$1{\cdot}27\times10^{5}$
−78	8·30	$1{\cdot}12\times10^{-3}$	$4{\cdot}68\times10^{5}$	0	5·99	$1{\cdot}21\times10^{-3}$	$1{\cdot}35\times10^{5}$
−78	7·10	$8{\cdot}97\times10^{-4}$	$4{\cdot}30\times10^{5}$	0	4·96	$8{\cdot}95\times10^{-4}$	$1{\cdot}27\times10^{5}$
−78	5·93	$7{\cdot}43\times10^{-4}$	$3{\cdot}39\times10^{5}$	0	3·92	$5{\cdot}51\times10^{-4}$	—
−78	4·72	$5{\cdot}17\times10^{-4}$	$3{\cdot}40\times10^{5}$	0	3·93	$6{\cdot}00\times10^{-4}$	$1{\cdot}25\times10^{5}$
−78	4·15	$3{\cdot}91\times10^{-4}$	$2{\cdot}64\times10^{5}$	0	2·97	$3{\cdot}04\times10^{-4}$	—
−78	3·56	$2{\cdot}39\times10^{-4}$	$2{\cdot}54\times10^{5}$	0	2·98	$2{\cdot}42\times10^{-4}$	$1{\cdot}29\times10^{5}$
−78	3·56	$1{\cdot}65\times10^{-4}$	—	0	1·99	$1{\cdot}26\times10^{-4}$	$1{\cdot}13\times10^{5}$

molecular weight with monomer concentration is shown in *Figure 1*. It should be mentioned that all conversion versus time plots were linear, and that reaction was generally continued to about ten per cent conversion of monomer to polymer. Data obtained at 0°C under otherwise identical conditions are also given in *Table 1*, while *Figure 2* shows plots of polymerization rate and molecular weight as functions of monomer concentration at this temperature.

DISCUSSION

In view of the variety of explanations of the polymerization of isobutene which have been considered in the literature, we shall here confine discussion to an attempt to link our present experiments with our own earlier suggestions. We have previously suggested that the polymerization of isobutene in a γ field might be due to the following processes. Initiation may be caused by the formation by the radiation of positive holes and electrons in the zinc oxide followed by the reaction of an adsorbed isobutene molecule at the surface of the zinc oxide with a migrating positive hole. The resulting adsorbed isobutene ion may either begin to polymerize and desorb into the liquid layer, or it may be neutralized rapidly by an electron in the zinc oxide. If desorption occurs the molecule continues to grow, undergoes several conventional chain transfers to monomer, and the kinetic chain eventually terminates by neutralization with an electron at the surface of a zinc oxide particle. Such a mechanism would suggest that at concentrations of monomer and solvent such that a relatively small proportion of each is adsorbed on the zinc oxide, the polymerization rate should show simple

*By nominal intensity is meant the intensity measured by the Fricke dosimeter ($G = 15{\cdot}5$) when a sample was placed in the position of the dilatometer bulb.

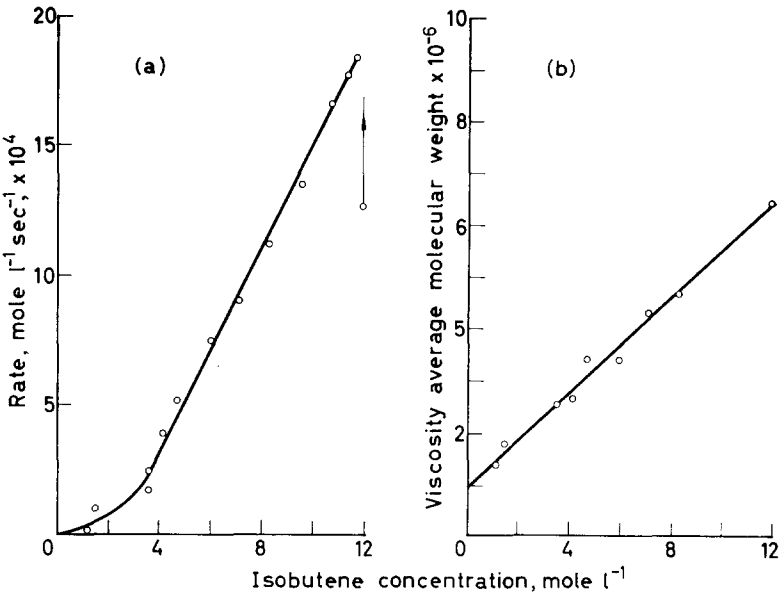

Figure 1—(a) Rate of polymerization as a function of monomer concentration at −78°C (zinc oxide concentration 3·50 mole/l.); (b) Molecular weight as a function of monomer concentration at −78°C (zinc oxide concentration 3·50 mole/l.)

dilution behaviour, and reference to *Figure 1* shows that at −78°C this is indeed so. After an initial sudden increase in rate when very small quantities of hexane are added to the isobutene, which is possibly caused by a more rapid initiation process when hexane is present in the surface layer, the rate falls linearly with dilution until low isobutene concentrations are

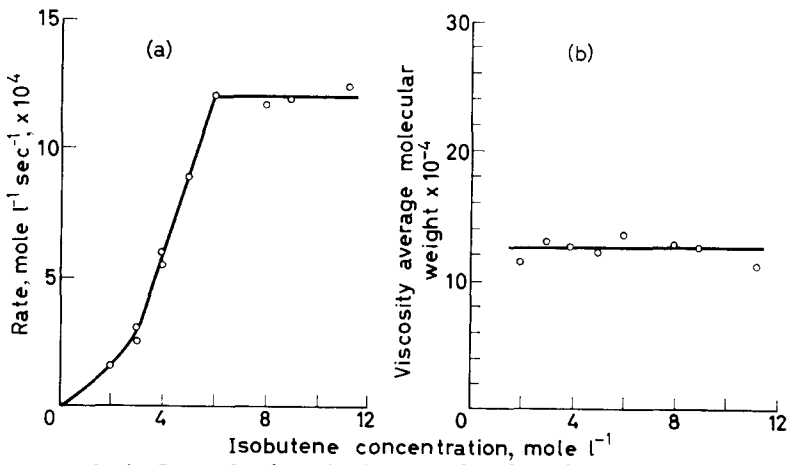

Figure 2—(a) Rate of polymerization as a function of monomer concentration at 0°C (zinc oxide concentration 3·50 mole/l.); (b) Molecular weight as a function of monomer concentration at 0°C (zinc oxide concentration 3·50 mole/l.)

reached, when a curvature due to the adsorption of a considerable fraction of the monomer by the zinc oxide is observed. If the temperature is raised to 0°C, the rate is independent of monomer concentration until the monomer concentration falls to about 6 mole/l.: further dilution leads to a linear fall in rate with dilution to low concentrations when a curvature is observed. It should be pointed out that at both temperatures no sharp change of rate with dilution occurs at the solvent concentration at which the polymer becomes completely soluble in the liquid layer, suggesting either that a growing polymer chain terminates (by transfer) before it has time to precipitate even in solvent-free monomer, or alternatively that the precipitated polymer coil is sufficiently extended to be readily accessible to monomer molecules.

On the assumption that propagation and transfer occur in a conventional manner in the liquid phase it would be expected that the rate of propagation would be given by

$$R_p = k_p [M^+] [M] \tag{1}$$

where R_p is the rate of propagation, $[M^+]$ and $[M]$ are the concentrations of growing cations and monomer respectively, and k_p is the propagation rate constant. Since polyisobutene ions do not undergo transfer to hexane[12], and the molecular weight of the polymer in the absence of solvent is transfer controlled, the effective rate of chain breaking should be

$$R_{tr} = k_{tr} [M^+] [M] \tag{2}$$

where R_{tr} is the rate of transfer to monomer and k_{tr} is the rate constant for the reaction, so that the degree of polymerization, DP, should be given by

$$DP = \frac{R_p}{R_{tr}} = \frac{k_p [M^+] [M]}{k_{tr} [M^+] [M]} = \frac{k_p}{k_{tr}}$$

that is, the molecular weight should be independent of monomer concentration.

It will be seen from *Figure 2* that this represents the molecular weight data obtained at 0°C, but that at −78°C the system is less simple. As shown in *Figure 1*(b) the molecular weight is a linear function of monomer concentration having a positive intercept on the axis at zero monomer concentration.

The observed linearity of molecular weight with monomer concentration at −78°C would seem to require the existence of two distinct propagation processes rather than the generally accepted propagation described above, since in the general case

$$DP = \frac{\Sigma \text{ Propagation processes}}{\Sigma \text{ Termination processes}}$$

If it is accepted that termination is predominantly by transfer to monomer according to equation (2) and the usual propagation according to equation (1) occurs, then it is necessary to postulate a second propagation process

dependent on the square of the monomer concentration to give an expression for *DP* of the type

$$DP = \frac{k_p [M^+] [M] + k'_p [M^+] [M]^2}{k_{tr} [M^+] [M]} = \frac{k_p}{k_{tr}} + \frac{k'_p}{k_{tr}} [M]$$

which is required by the molecular weight data. However, two simultaneous propagation processes of this form are not consistent with the linear variation of rate with monomer concentration which is observed experimentally over wide limits. This difficulty may be met if a unimolecular mechanism of the type first envisaged by Fontana and Kidder in the polymerization of propene[13] occurs for both propagation and transfer, the second propagation process now being first order in monomer concentration. The degree of polymerization is then given by

$$DP = \frac{k_p [M^+] + k'_p [M^+] [M]}{k_{tr} [M^+]} = \frac{k_p}{k_{tr}} + \frac{k'_p}{k_{tr}} [M]$$

and the rate by

$$R_p = k_p [M^+] + k'_p [M^+] [M]$$

and these expressions are in agreement with the observed data if the deviations of the rate from linearity at very low and very high monomer concentrations are due to the adsorption effects mentioned earlier. It also follows that over the linear region $[M^+]$, the concentration of growing polymeric ions, is independent of monomer concentration which suggests that electron neutralization of (isobutene)$^+$ ions formed in the surface layers of the zinc oxide is not significant under these conditions, since a competition between this process and desorption following addition of further isobutene molecules would lead to an increase in $[M^+]$ with increasing monomer concentration.

At 0°C, the assumption of a single propagation reaction and a transfer controlled termination, both proceeding by a unimolecular mechanism, leads to a DP independent of monomer concentration and equal to k_p/k_{tr} and to a rate also independent of monomer concentration and equal to $k_p [M^+]$. This is an adequate description of the molecular weight data and can explain the constancy of rate with dilution down to an isobutene concentration of 6 mole/l. Below this concentration the rate falls linearly with monomer concentration and it may be that in this region the mobility of electrons in the zinc oxide is sufficiently high to enable them to neutralize some isobutene ions formed on the zinc oxide surface and the number of such ions which desorb after addition to an isobutene molecule and lead to polymerization becomes dependent on monomer concentration: i.e. $[M^+]$ is no longer independent of monomer concentration.

Summarizing, it appears possible to understand the effect of hexane as a diluent on the radiation initiated zinc oxide catalysed polymerization of isobutene in the terms given previously for the behaviour of the solvent-free system if it is assumed that two propagation processes can occur simultaneously at low temperatures and that unimolecular kinetics may be applied to the propagation and transfer reactions at both 0° and −78°C. The results presented do not enable any firm conclusions to be drawn as to the

actual nature of the two propagation processes, though even if an alternative general kinetic scheme were adopted it would still seem necessary to postulate their existence.

Wantage Research Laboratory (AERE),
Wantage, Berkshire

(Received July 1965)

REFERENCES

[1] DALTON, F. L. *Polymer, Lond.* 1965, **6,** 1
[2] DAVISON, W. H. T., PINNER, S. H. and WORRALL, R. *Chem. & Ind.* **1957,** No. 38, 1274
[3] WORRALL, R. and CHARLESBY, A. *Internat. J. appl. Radiation and Isotopes,* 1958, **6,** 8
[4] DAVISON, W. H. T., PINNER, S. H. and WORRALL, R. *Proc. Roy. Soc. A,* 1959, **252,** 187
[5] COLLINSON, E., DAINTON, F. S. and GILLIS, H. A. *J. phys. Chem.* 1959, **63,** 909
[6] WORRALL, R. and PINNER, S. H. *J. Polym. Sci.* 1959, **34,** 229
[7] CHARLESBY, A., PINNER, S. H. and WORRALL, R. *Proc. Roy. Soc. A,* 1960, **259,** 386
[8] DAVID, C., PROVOOST, F. and VERDUYN, G. *Polymer, Lond.* 1963, **4,** 391
[9] DAVID, C., PROVOOST, F. and VERDUYN, G. *J. Polym. Sci. C,* 1964, **4,** 1135
[10] DALTON, F. L., GLAWITSCH, G. and ROBERTS, R. *Polymer, Lond.* 1961, **2,** 419
[11] BIDDULPH, R. H. and PLESCH, P. H. *J. chem. Soc.* **1960,** 3913
PLESCH, P. H. *The Chemistry of Cationic Polymerization,* p 676. Pergamon: Oxford, 1963
[12] PLESCH, P. H. *The Chemistry of Cationic Polymerization,* pp 146 and 183. Pergamon: Oxford, 1963
[13] FONTANA, C. M. and KIDDER, G. A. *J. Amer. chem. Soc.* 1948, **70,** 3745

The Homogeneous Polymerization of Butadiene Catalysed by Rhodium Salts

C. E. H. BAWN, D. G. T. COOPER and A. M. NORTH

A study has been made of the solution polymerization of butadiene, to predominantly trans *1,4 polymer, catalysed by rhodium salts. The reaction is accelerated by protonic acids (including water) and by those reducing agents which in aqueous systems would be capable of reducing* Rh^{III} *to* Rh^{I}. *Ligands such as organic amines, and also bromide and iodide anions, tend to retard or even inhibit the reaction. The overall process appears to be a chain reaction, but is not free radical in character. The mechanism which best fits all the observations is one in which the active species is a* π*-allylic rhodium hydride, initiation occurring by hydride shift and propagation occurring by a ligand displacement process.*

RHODIUM salts are known to exhibit high stereospecific control over the polymerization of butadiene. Most of the published reports[1-3], however, have dealt with emulsion systems in which mechanistic interpretation of kinetic data is extremely difficult. The accelerating effect of reducing agents in isomerization processes[4] and in butadiene polymerization[5], favours the existence of an active reduced state of rhodium. Possible organic complexes which might be intermediates and appear well substantiated include Rh^{I}-complexes[6-8] and Rh^{III}-hydride complexes[9,10].

In this paper are reported kinetic studies and mechanistic interpretations of the homogeneous solution polymerization of butadiene in the presence of certain rhodium compounds.

EXPERIMENTAL

Materials

Butadiene—from British Hydrocarbon Chemicals, was purified by passage over silica gel and magnesium perchlorate, and then condensed on to a sample of the same catalyst as used in kinetic polymerization experiments. The liquid monomer was outgassed, prepolymerized with ultra-violet light at $-30°C$ for 8 h, and monomer redistilled as required at $-40°C$.

Styrene—was washed with 10 per cent sodium hydroxide solution and then with distilled water. The monomer was dried over calcium chloride and then calcium hydride, and then distilled under dry nitrogen through a 3 ft column filled with Fenske helices. Prior to use aliquot samples were outgassed, prepolymerized by ultra-violet light, and residual monomer distilled into reaction vessels on the vacuum line.

NN-*dimethyl formamide*—was dried by azeotropic distillation with benzene and then redistilled over freshly ground barium oxide under reduced pressure. B.pt 48 °C at 30–32 mm Hg.

Rhodium salts—were prepared by alkali hydrolysis of potassium chlorrhodite to rhodium sesquioxide followed by treatment with the relevant acid.

The rhodium butadiene complex, ($Rh_2Cl_4C_{12}H_{18}$)—was prepared by saturating with butadiene a concentrated solution of rhodium trichloride in ethanol. After 24 hours at room temperature the yellow precipitate was collected, washed in petroleum ether, and dried.

Dichloro tetraethylene dirhodium, [$Rh_2Cl_2(C_2H_4)_4$]—was prepared by bubbling ethylene into a stirred solution of 0·74 g rhodium trichloride trihydrate in 1·5 ml water and 20 ml methanol. After three hours the orange/pink precipitate was collected, washed in methanol and ether, and dried under vacuum. The material was stored in a stoppered vessel in a refrigerator, and no decomposition was observed over eighteen months.

Techniques

All the operations involved in the preparation of the kinetic experiments were carried out under an air pressure less than 10^{-5} mm of mercury, using conventional vacuum procedures. Solid reagents were outgassed in solution.

Rates of polymerization were observed in conventional dilatometers, and unless stated otherwise all experiments were conducted at 71·5°C.

A frequently used polymerization composition contained 30 per cent v/v butadiene in dimethyl formamide. The solubility of *trans* polybutadiene in this system at 71·5°C is only 3 per cent w/w, so that deductions from kinetic observations were restricted to phenomena occurring at low conversions.

The molecular weights of the polymer samples were determined on a Mechrolab vapour pressure osmometer, and the isomer content calculated from infra-red spectra using the extinction coefficients of Hampton[11].

The density of dissolved monomer was determined dilatometrically, and that of polymer determined at the suspension point for a flotation/precipitation titration of absolute alcohol with water. Because the polymerization becomes heterogeneous at low conversions, accurate comparison of gravimetric and dilatometric observations could not be used to obtain absolute polymerization rates. For this reason rates of polymerization are relatively correct, although the absolute values may be in error by a quantity estimated as less than 30 per cent.

Kinetic observations of oligomer formation were made by carrying out the reaction in a glass vessel fitted with a serum cap and analysing samples at regular time intervals using a Perkin–Elmer 800 gas–liquid chromatograph fitted with flame ionization detector and temperature programmed at 3·3°C mm^{-1} from 50°C.

RESULTS

The effect of rhodium salts on free radical polymerization

It is conceivable that the three-valent rhodium salts might form, with solvent, a redox couple for the initiation of free radical polymerization. In order to test this hypothesis a series of rhodium salts were added to the solution polymerization of styrene initiated by azoisobutyronitrile. In no case was an enhancement of rate observed, and in every case involving three-valent rhodium effective retardation of free radical polymerization occurred. The results are summarized in *Table 1.*

Table 1. Effect of rhodium compounds on styrene polymerization. [Azoisobutyronitrile], $1{\cdot}0\times10^{-2}$ mole l^{-1}. Temperature, 40°C. [Styrene], 5·10 mole l^{-1}.

Solvent	*Rhodium compound*		$R_p\times10^5$
	Type	*Concentration* $\times10^4$ (*mole* l^{-1})	*mole* l^{-1} *sec* $^{-1}$
Dimethyl sulphoxide	$RhCl_3.3H_2O$	0·0	0·63
		0·0	0·71
		0·12	0·58
		48	0·38
		118	0·27
		206	0·18
Dimethyl sulphoxide	$RhCl_3$	0·93	0·28
Dimethyl sulphoxide	$Rh_2Cl_2(C_2H_4)_4$	0·0	0·62
		3·87	0·54
		4·14	0·65
Dimethyl formamide	$Rh(NO_3)_3.2H_2O$	0·0	0·58
		7·2	0·47

In the same way the addition of small quantities of butadiene did not accelerate the free radical polymerization of styrene in the presence of rhodium salts. Furthermore the rate of the rhodium catalysed polymerization of butadiene was not affected by traces of free radical inhibitors such as benzoquinone, hydroquinone, or oxygen.

The butadiene, dimethyl formamide, water, rhodium trinitrate system

The polymerization of butadiene in dimethyl formamide occurred in the presence of rhodium trinitrate and certain protonic compounds of which the commonest was water. When the concentration of each of the three reactants was varied independently, the polymerization rate was found to be proportional to the first power of the rhodium concentration, the square root of the water concentration and the first power of the monomer concentration (below 3·0 moles l^{-1}). At higher monomer concentrations the rate was essentially independent of monomer molarity. The relevant data are illustrated in *Figures 1* to *3*.

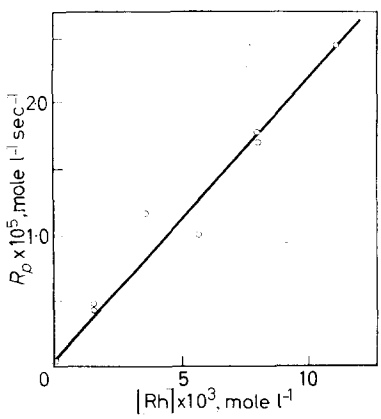

Figure 1—Rate of polymerization against concentration of rhodium trinitrate dihydrate in dimethyl formamide. Butadiene 2·56 mole l^{-1}, water 1·1 mole l^{-1}, 71·5°C

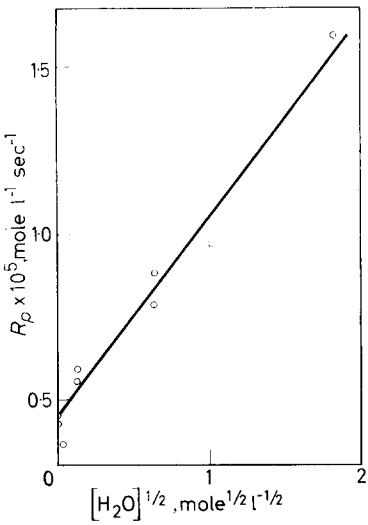

Figure 2—Rate of polymerization against the square root of total concentration of water in dimethyl formamide. Butadiene 2·56 mole l^{-1}, rhodium trinitrate dihydrate $6{\cdot}7 \times 10^{-3}$ mole l^{-1}, 71·5°C

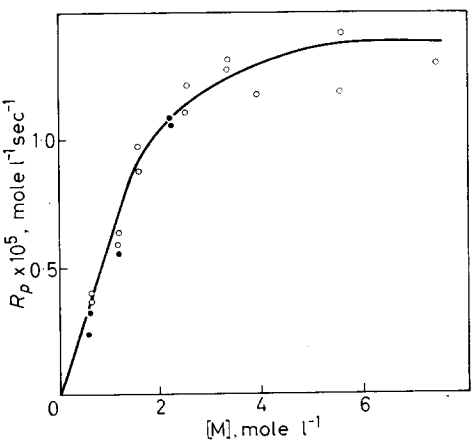

Figure 3—Rate of polymerization against monomer concentration in dimethyl formamide. ○ Rhodium trinitrate dihydrate $6{\cdot}7 \times 10^{-3}$ mole l^{-1}; water 1·1 mole l^{-1}; 71·5°C. ● solvent dimethyl formamide–*n*-hexane, total hydrocarbons 6·0 mole l^{-1}

That the levelling off in the rate against monomer plot at high hydrocarbon levels is not a dielectric effect was shown by examining the polymerization of varying concentrations of butadiene in a solvent containing *n*-hexane. The total hydrocarbon content was maintained above the threshold value (about 4·0 mole l^{-1}), but the rates of polymerization fell on the same curve as before; *Figure 3*.

The effect of added acids, reducing agents and ligands

Various protonic acids, added in concentrations from 10^{-4} to 1 mole l^{-1}, were found to increase the rate of polymerization by amounts up to a factor of ten. The increase was found to be proportional to the square root of the acid concentration, the effectiveness of the various acids falling in the sequence *p*-toluene sulphonic > formic > nitric > acetic. The very strong effect of formic acid seems to be due to its reducing properties.

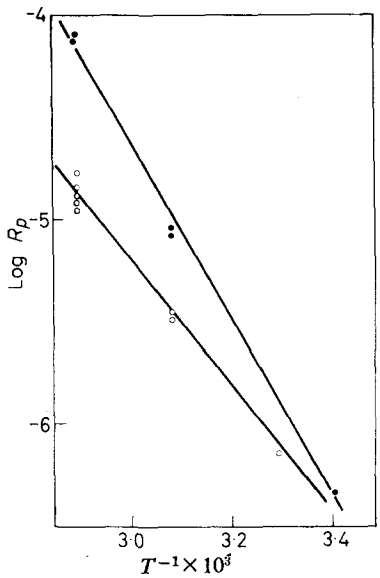

Figure 4—Temperature dependence of polymerization rate. ○ Monomer 2·56 mole l^{-1}, rhodium trinitrate dihydrate, $6{\cdot}7\times10^{-3}$ mole l^{-1}, water 1·18 mole l^{-1}. ● As above but with 0·36 mole l^{-1} formic acid catalyst

The addition of reducing agents to this system is particularly informative, since a cocatalytic effect is observed only with those substances for which the aqueous molar redox potential is less negative than that for the Rh^{III}–Rh^{I} transition (−1·20 V). Thus the effect of three organic aldehydes is illustrated in *Figure 5*, and of three transition elements in *Table 2*.

Table 2. Effect of soluble inorganic salts on polymerization rate. [Monomer], 2·39 mole l^{-1}; [rhodium trinitrate dihydrate], $6{\cdot}7\times10^{-3}$ mole l^{-1}; [water], 1·18 mole l^{-1}. Temperature 71·5°C.

Salt	*Redox potential* *V*	$\frac{[Salt]}{[Rh]}$	$R_p\times10^5$ *mole* l^{-1} *sec*$^{-1}$
None	—	—	1·16
$(CuCl)_2$	−0·153	0·14	2·28
$MnCl_2.4H_2O$	−1·51	0·40	0·06
		0·65	0·20
Cobaltous 2-ethyl hexoate	−1·81 (Co^{II}–Co^{III})	0·15	0·56

Reagents containing nitrogen had been reported to inhibit the emulsion polymerization of butadiene with rhodium catalysts[12]. In an attempt to elucidate a number of active coordination sites per rhodium atom that are required for this polymerization, a series of amine and diamine retarders was studied.

When rates of polymerization were plotted against the mole ratio [amine]/[Rh^{III}], graphs were obtained which could be considered linear, *Figure 6*. For ligands characterized by a very low instability constant (very

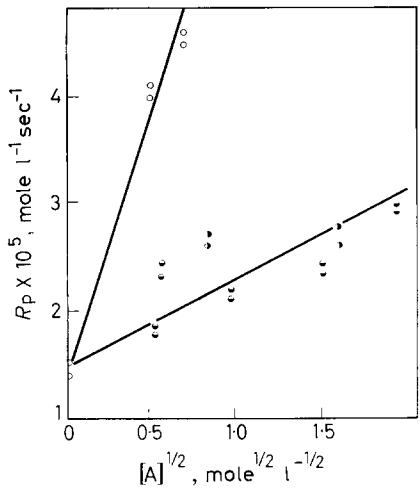

Figure 5—Effect of aldehydes on polymerization rate. Monomer 2·39 mole l^{-1}, rhodium trinitrate dihydrate $6{\cdot}66 \times 10^{-3}$ mole l^{-1}, water 1·18 mole l^{-1}. 71·5°C. ○ formaldehyde, ◒ acetaldehyde, ◑ propionaldehyde

large equilibrium constant for complex formation) a linear plot would be expected and extrapolation to zero rate would yield the ligand to rhodium

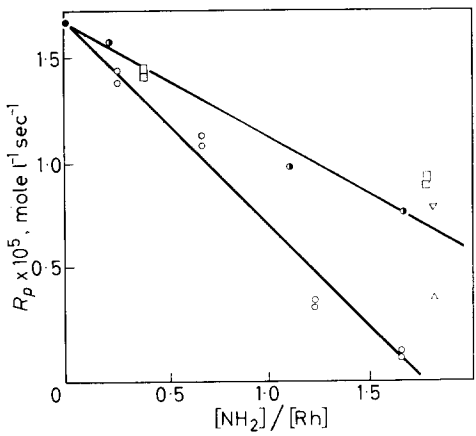

Figure 6—Effect of amines on polymerization rate. Monomer 2·40 mole l^{-1}; rhodium trinitrate dihydrate $6{\cdot}66 \times 10^{-3}$ mole l^{-1}; water 1·18 mole l^{-1}; 71·3°C. ○ σ-phenylene diamine, ◑ *m*-phenylene diamine, ◒ *p*-phenylene diamine, □ aniline, △ pyridine, ▽ triphenyl phosphine

ratio for complete blocking of polymerization sites. Of course it must be emphasized that this extrapolation is not valid for ligands which form complexes with large instability constants!

The 'inhibition ratios' found in this way are listed in *Table 3*.

Table 3. 'Inhibition ratios' of various ligands

Ligands	*Base strength* pK_A	*Inhibition ratio*
σ-Phenylene diamine	2·0	1·8
p-Phenylene diamine	3·2	2·4
Pyridine	5·2	2·4
m-Phenylene diamine	2·6	2·9
Triphenyl phosphine	—	3·3
Aniline	4·6	4·1

The addition of nitrate, iodide, bromide and chloride was also investigated. It was found that nitrate ions caused a very small rate acceleration, chloride ions precipitated the sparingly soluble rhodium chloride, but that the reducing ions bromide and iodide lowered the polymerization rate. When the halide/rhodium ratio was two, bromide and iodide ions lowered the rate to one fifth and one tenth of the original value respectively.

Chromatographic analysis of oligomer formation during polymerization

2 μl samples were withdrawn from a polymerizing reaction mixture after various times and were injected directly into the vapour phase chromatograph unit. Chromatograms of the type illustrated in *Figure 7* were

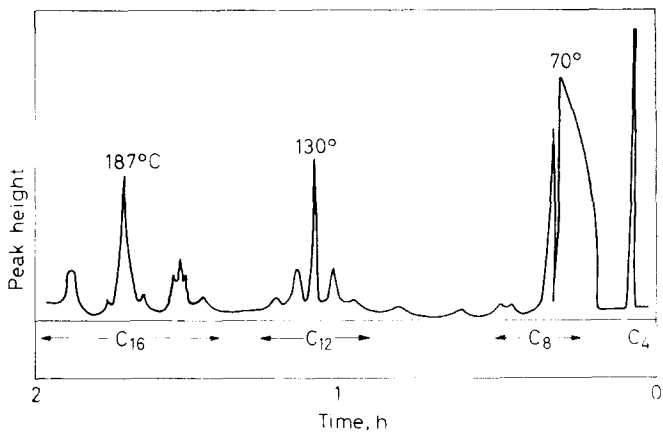

Figure 7—Typical vapour phase chromatogram of the low boiling components of a polymerizing mixture

obtained. The nature of the oligomers was ascertained by comparison of retention times with those for C_8, C_{12}, C_{16} and C_{22} unsaturated hydrocarbons.

The quantities of each oligomer were estimated by comparison of peak areas (normalized for the number of carbon atoms) with those of an added inert internal standard or with that of the solvent peak. It was found that the separate rates of formation of dimer, trimer and tetramer were proportional to the rhodium concentration and to the square root of the water concentration just as was the overall rate of polymerization. At very high water concentrations a peak due to dimethylamine appeared. The relative rates of formation of the oligomers $C_8 : C_{12} : C_{16}$ was in the ratio 3:2:1, and there was no evidence that the concentration of any oligomer passed through a maximum value during the reaction, *Figure 8*.

Infra-red analysis of the polybutadienes

Most of the polymers prepared had 1,4 *trans* isomer contents greater than 90 per cent, and many were greater than 95 per cent. However, the powerful cocatalysts cuprous chloride and formic acid gave polymers of 72 per cent and 77 per cent *trans* character respectively. Only those

polymers with greater than 77 per cent *trans* content exhibited crystallinity as evidenced by absorption bands at 8·1, 9·5 and 13·0 μ.

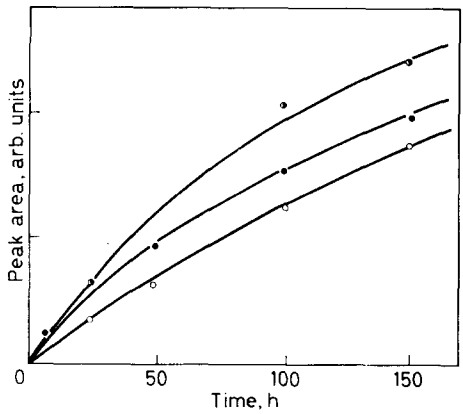

Figure 8—Oligomer concentration (VPC peak areas) as a function of time. ○ dimer, ● trimer, ◑ tetramer

The fact that the fastest polymerizations lead to polymer of lower stereospecificity raises the question as to whether the propagation reaction is stereospecific, or whether a random polymerization is followed by a rhodium catalysed isomerization of inert polymer. It was found that the *trans* content of polymer formed in a reaction mixture was independent of time. Furthermore, while polymer of very high *cis* content (96 per cent) is isomerized by rhodium nitrate trihydrate in this system, *Figure 9*, the reaction is strongly inhibited by butadiene and could not account for the high *trans* contents observed in practice.

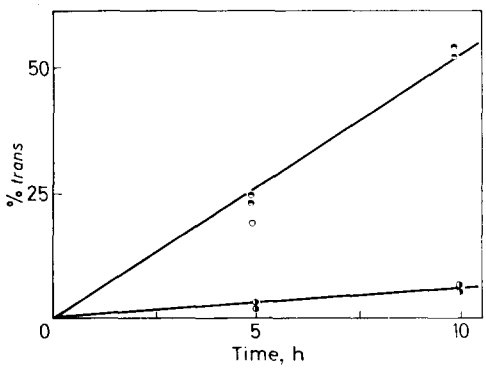

Figure 9—Isomerization of 96 per cent *cis*-1,4-polybutadiene. Rhodium trinitrate dihydrate $6{\cdot}66 \times 10^{-3}$ mole l^{-1}. Polymer 6·7 g l^{-1}; DMF benzene 40:60 v/v; ○ no further additive, ◒ plus acetic acid 0·25 mole l^{-1}, ◑ plus butadiene $2{\cdot}5 \times 10^{-3}$ mole l^{-1}

Some observations on rhodium butadiene complexes

Robinson and Shaw[13] first isolated and characterized the complex $[Rh_2Cl_4C_{12}H_{18}]$ which contains a trimer of butadiene as the organic ligand. Investigation of the catalytic properties of this complex showed that it is not the active intermediate in the formation of long chain polymers. However, reaction mixtures containing this complex rapidly converted butadiene to sweet-smelling oils believed (from VPC retention times) to be cyclic telomers.

The addition of iodide ions to this complex in the presence of butadiene resulted in the formation of a deep-red complex which was inactive.

An unstable complex was formed when liquid butadiene was allowed to stand over rhodium trinitrate dihydrate at temperatures below $-30°C$ for several weeks being periodically irradiated with ultra-violet light. This complex, which could be obtained only as a red, viscous oil, could be separated from excess butadiene by pumping at $-50°C$. On warming this complex to $-40°C$ decomposition occurred yielding gaseous monomeric butadiene. No further characterization of this unstable material has been possible. However, it seems probable that some unstable intermediate such as this must form the active polymerization intermediate.

A spectroscopic examination of the reaction mixture was carried out in an attempt to detect the presence of rhodium complexes as reaction intermediates.

The charge transfer absorptions of the Rh^{I} complex $[Rh_2Cl_4(C_2H_4)]$ and of rhodium trinitrate in dimethyl formamide both occur close to 272 mμ. Consequently even large equilibrium concentrations of any intermediate Rh^{I} complexes could be detected only if the two valence states had very different extinction coefficients. The characterization of the Rh^{I} d-d absorption was not possible owing to the low extinction coefficient of the absorption and the low solubilities of the stable Rh^{I} complexes available.

No absorption bands other than those directly attributable to Rh^{III} could be detected in polymerizing systems.

DISCUSSION

The mechanistic interpretation of a complicated reaction such as this, in which attempts to characterize a definite reaction intermediate have failed, is always a devious and unsatisfying process.

The most convincing statement that can be inferred from these studies is that this is not a simple free radical chain reaction. The retarding effect of rhodium complexes on other free radical reactions, the negligible effect of free radical inhibitors and the kinetic orders in catalyst concentration all point to a non-radical growth process. On the other hand the analysis of oligomer formation is in accord with a conventional chain reaction of some description. A stepwise growth or a process involving successive linking of all species present would require each oligomer to pass through a maximum in concentration, a time dependent phenomenon which was not observed.

These conclusions, together with the low polymerization rates and the lack of any ultra-violet or visible spectrum other than that of starting materials, suggests that we have a chain reaction propagated by a rhodium complex present only in trace quantities.

Since at least two types of rhodium–butadiene complex have been isolated in this work, and since one of these is a powerful catalyst for the telomerization of butadiene, the postulation of an active polymerization intermediate is not too fanciful. The remarkable effect of reducing agents suggests that a reduced form of rhodium must be responsible for the reaction, the most likely intermediates will be discussed in turn.

(a) *A* Rh^{I}*–butadiene* π*-allylic complex*

Rh^{I} is isoelectronic with Pd^{II} which is known to form a π-allylic complex by chloride ion migration. The incipient formation of a similar Rh^{I} complex might result in a reaction whereby monomer addition replaces the chloride ion migration at the ends of the π-allylic residue.

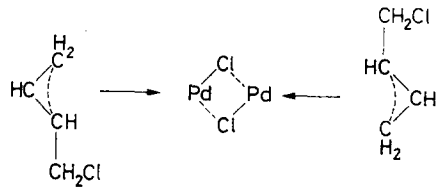

However, two observations are against this. In the first place aromatic amines are well known reagents for the detection of bridged complexes, and a base : transition ratio of 1 : 1 is usually observed. Here a ratio nearer 2 : 1 is required. Secondly the existence of a very small concentration of a binuclear complex in equilibrium with dissolved Rh^{III} would require a kinetic order of two with respect to the rhodium concentration. The value unity is observed. Of course it is possible to construct a reaction scheme involving several intermediates such that a stationary state concentration of one (binuclear) will obey the kinetics observed; but the critical application of Occam's razor leads us back to the picture of a reduced intermediate in a redox system in equilibrium (however established) with the oxidized form.

A highly unstable mononuclear Rh^{I} π-allylic complex can be postulated as the growth intermediate

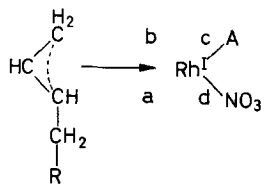

where the rhodium is assigned square planar coordination and A is a neutral ligand such as solvent or monomer. The reversible formation of such a complex in which A is monomer would explain the kinetic dependence on rhodium and monomer, although not the square root dependence on proton donors. If chain growth occurs by a mechanism such that monomer, complexed on the c position of the rhodium, adds to the a–b π-allylic ligand to form a new π-allylic group on the b–c positions, then three adjacent coordination sites are required. For such a reaction scheme only one amine ligand per rhodium should cause complete inhibition. Furthermore the initiation of chain growth is difficult to visualize.

The conclusion would seem to be that a square planar Rh^{I} complex does not completely fulfil all the requirements of the experimental observations.

(b) *A π-allylic* Rh^{III} *hydride*

It is immediately apparent that a Rh^{III}—H system is analogous in certain respects to $Rh^{I} + H^{+}$. Indeed Chatt and Shaw[6] first pointed out that the possibility of hydride formation must always be considered for a transition metal in the presence of a reducing agent in protonic media.

A six-coordinated Rh^{III}-hydride π-allylic complex containing butadiene monomer and the growing chain would explain all the experimental observations. The equilibrium concentration of such a complex would depend on the rhodium, acid, and reducing agent concentrations. Furthermore the initiation of chain growth would occur by a simple hydride shift to the ω-carbon atom of the first adsorbed butadiene molecule. Such a complex would require at least two nitrogen ligands to inhibit the growth reaction, which would occur by addition of complexed monomer to the π-allylic growing chain with concomitant 1,2 to 2,3 shift of the π-allylic bonding on rhodium.

Initiation

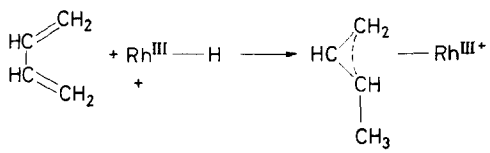

Propagation

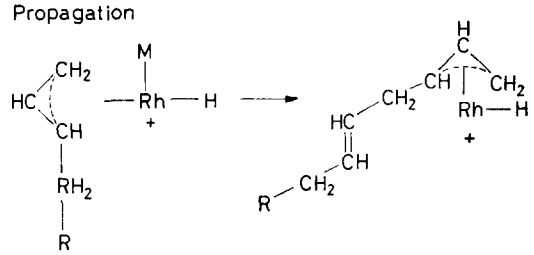

The effect of bromide or iodide ions can now be explained in either of two ways. They may function as ligands competing with monomer for coordination sites neighbouring the π-allylic growing chain. Alternatively they may form a stable ligand, but unfavourably alter the butadiene or growing chain bond strengths (or distances) by the so-called 'trans-effect'.

CONCLUSIONS

The kinetic observations of the rhodium catalysed homogeneous polymerization of butadiene are best explained by a chain reaction propagated by a reduced state of rhodium present in a very low stationary state or equilibrium concentration. The initiation and growth processes, and the inhibition by amines are best explained if the active intermediate is a six-coordinated Rh^{III} hydride containing the growing chain as a π-allylic complex and to which the monomer adds by prior π-complexing.

Donnan Laboratories,
University of Liverpool

(*Received November 1965*)

REFERENCES

[1] BERGER, R. S. and YOUNGMAN, E. A. *J. Polym. Sci.* 1964, **A1,** 357
[2] RINEHART, R. E., SMITH, H. P. and WITT, H. S. *J. Amer. chem. Soc.* 1961, **83,** 4864
[3] CANALE, A. J., HEWETT, W. A., SHRYNE, T. M. and YOUNGMAN, E. A. *Chem. & Ind.* **1962,** 1054
[4] DELEPINE, M. *C.R. Acad. Sci., Paris,* 1953, **236,** 559
[5] TEYSSIE, P. and DAUBY, R. *J. Polym. Sci.* 1964, **B2,** 413
[6] CHATT, J. and SHAW, B. L. *Chem. & Ind.* **1961,** 290
[7] RUND, J. V., BASOLO, F. and PEARSON, R. G. *Inorg. Chem.* 1964, **3,** 658
[8] RINEHART, R. E., SMITH, H. P., WITT, H. S. and ROMEYN, H. *J. Amer. chem. Soc.* 1962, **84,** 4145
[9] BATH, S. S. and VASKA, L. *J. Amer. chem. Soc.* 1963, **85,** 3500
[10] LAPLACA, S. J. and IBERS, J. A. *J. Amer. chem. Soc.* 1963, **85,** 3501
[11] HAMPTON, R. R. *Analyt. Chem.* 1949, **21,** 923
[12] TEYSSIE, P. and DAUBY, R. *C.R. Acad. Sci., Paris,* 1963, **256,** 2846
[13] ROBINSON, S. D. and SHAW, B. L. Cited in LYDON, J. E., NICHOLSON, J. K., SHAW, B. L. and TRUTER, MARY, R. *Proc. chem. Soc.* **1964,** 421

Limitations of the Tobolsky 'Two Network' Theory in the Interpretation of Stress-relaxation Data in Rubbers

D. K. THOMAS

Experiments have been devised which reveal shortcomings in the accepted method of interpreting the results of continuous and intermittent stress-relaxation measurements in terms of the Tobolsky 'two network' theory. In general the heat ageing of rubbers is a complex process and in such cases there is a likelihood that the results of stress-relaxation measurements will not be amenable to analysis by the 'two network' theory.

A POTENTIALLY powerful tool in the study of rubber ageing is the technique known as stress-relaxation; this is used in two ways, referred to as continuous and intermittent stress-relaxation, the combination of which can lead to basic information on the rates of rubber network scission and formation during the ageing process[1].

The usefulness of stress-relaxation measurements derives from the relationship between stress, strain, and network structure predicted by the kinetic theory of rubber-like elasticity

$$f = 2A_0C_1(\alpha - \alpha^{-2}) \tag{1}$$

where f is the force required to extend a strip of rubber of unstrained cross-sectional area A_0 to an extension ratio α. The quantity C_1 is equated to $\frac{1}{2}nkT$ by the Kuhn–Wall–Flory elasticity theory, n being the number of network chains per unit volume of vulcanizate. Substituting for C_1 in equation (1) gives

$$f = nkTA_0(\alpha - \alpha^{-2}) \tag{2}$$

Under conditions in which T, A_0 and α are kept constant f is directly proportional to n. This corresponds to the technique of continuous stress-relaxation, and at any elapsed time t during ageing

$$f_t/f_0 = n_t/n_0 \tag{3}$$

where f_t and n_t represent the force and network chain concentration at time t, f_0 and n_0 being the original unaged values.

This interpretation of continuous stress-relaxation measurements involves two major assumptions. First that the stress/strain relationship of equation (1) is valid, and secondly that f_t is determined solely by the fraction of the initial, or first, network remaining at time t, no account being taken of new network chains formed during ageing.

The first assumption pertaining to the validity of the stress/strain relationship for rubber networks in simple extension has been the subject of much

discussion. A consideration of this assumption is not the objective of the present work since it is felt that the second assumption, concerning new network chains formed during ageing, is likely to be the more misleading in the interpretation of continuous stress-relaxation measurements.

This second assumption is embodied in the 'two network' theory proposed by Andrews, Tobolsky and Hanson[2]. They suggested that crosslinks introduced in a strained vulcanizate could be regarded as building up a new network, interpenetrating but otherwise separate from the original one, and in equilibrium under the condition of its formation when the original network is under strain. The permanent set frequently observed in a rubber vulcanizate aged in tension is then due to the balancing of the retractive force of the first network and the extensive force of the second.

In the present work experiments are described which show that application of the 'two network' theory can lead to errors in the interpretation of continuous and intermittent stress-relaxation in terms of two interpenetrating, but otherwise independent, networks.

EXPERIMENTAL

Materials

The base polymer used throughout this work was the fluoroelastomer Viton B*; the crosslinking reagents used were hexamethylene diamine carbamate, *p*-phenylenediamine, and triethylene tetramine.

Compounding and vulcanization

All compounds were mixed on a small laboratory roll mill and they all contained 15 parts by weight of magnesium oxide. Thin sheets of thickness 0·010 in. were produced for the stress-relaxation work by moulding under pressure. Compounds containing hexamethylene diamine carbamate were vulcanized at 160°C in the press followed by an open post cure of 24 h at 200°C. Compounds containing triethylene tetramine were press cured for 1 h at 130°C only.

Stress-relaxation measurements

The technique used for stress-relaxation measurements has been described in full elsewhere[3]. Experiments were carried out in the temperature range from 130° to 250°C.

Equilibrium swelling measurements

About 0·2g of vulcanizate was weighed accurately and immersed in a large excess of acetone at 28°C. After a period of 48 h the rubber had reached its equilibrium swollen state. It was then withdrawn, surface dried, and weighed in a stoppered bottle. Finally it was dried to constant weight at room temperature. The fraction of soluble material was determined from the initial and final dry weights, and the volume of rubber in the swollen vulcanizate was calculated using values of 1·64 and 0·78 for the densities of polymer and solvent respectively.

*Du Pont trade name.

RESULTS AND DISCUSSION

There are several network change mechanisms which can lead to rubber ageing, and these can be of varying complexity, for example:

(*i*) Network scission only, in this case scission may occur in the crosslinks, in the main polymer chain, or in both.

(*ii*) Crosslink formation without network scission.

(*iii*) Crosslink scission with concurrent crosslink formation, both links being of the same chemical type.

(*iv*) Crosslink scission with concurrent crosslink formation, the new crosslinks being immune from further scission.

. . . . and so on.

In case (*i*) continuous stress-relaxation measurements will clearly give an unambiguous measure of the rate of removal of chains in the first network. In case (*ii*) in which additional crosslinks are introduced into an otherwise stable first network there seems no reason to suppose that the 'two network' theory is invalid.

Test of case (ii)

Experimental tests have been carried out by Berry, Watson and Scanlan[1]. They used peroxide cured natural rubber in an atmosphere of nitrogen as a system which approximates in behaviour on ageing to this case. Additional crosslinks were introduced during heat ageing by swelling dicumyl peroxide into the already vulcanized rubber, drying off the solvent, and heating the strained rubber at a temperature sufficient to cause thermal decomposition of the peroxide. Continuous stress-relaxation data obtained in this way, far from showing a lower rate of relaxation relative to the vulcanizate containing no additional peroxide, actually showed a significant increase in the rate of relaxation. Furthermore, the higher the concentration of peroxide introduced, the greater the rate of stress-relaxation. Hence although the results did nothing to cast doubt upon the validity of the 'two network' theory they were of limited value in view of the network scission which seemed to accompany peroxide initiated crosslinking. Berry, Watson and Scanlan also carried out experiments on this same system to show the extent of agreement between the observed permanent set in the rubber heated in tension, and the set calculated on the assumption that the 'two network' theory is valid.

Assuming that

$$f = GA\,(\alpha - \alpha^{-2}) \tag{4}$$

where G is equivalent to $2C_1$ of equation (1), then if f_0 and f_e are the tensions before and after introducing the crosslinks

$$\frac{f_e}{f_0} = \frac{G_e A_e(\alpha_e - \alpha_e^{-2})}{G_0 A_0(\alpha_0 - \alpha_0^{-2})} = \frac{G_e(\alpha_e^2 - \alpha_e^{-1})}{G_0(\alpha_0^2 - \alpha_0^{-1})} \equiv \frac{G_e}{G_0}\,\phi \tag{5}$$

where A_0, A_e are the original and final unstrained cross-sectional areas and α_0, α_e are the extension ratios at which crosslinks are introduced referred to the original length and set length respectively. Assuming that $f_e = f_0$ (i.e. assuming the 'two network' theory to be valid) then

$$\phi \equiv \frac{\alpha_e^2 - (1/\alpha_e)}{\alpha_0^2 - (1/\alpha_0)} = \frac{G_0}{G_e} \tag{6}$$

The experimental findings were that $G_e\phi$ was lower than G_0 approximately in the ratio 1 : 1·6; this is not particularly good, but again it must be remembered that the system studied was not ideal in that scission accompanied crosslinking in the strained state.

Viton, a copolymer of vinylidene fluoride and hexafluoropropylene, is an elastomer possessing outstanding heat stability[5]. It can be readily vulcanized at 130°C with triethylene tetramine (TETA) to give a reasonably heat stable rubber. This rubber undergoes network scission through oxidative reactions in the crosslinks, the rate of scission being measurable even at 130°C. An alternative crosslinking reagent for Viton is *p*-phenylenediamine (PPD), this is much less reactive towards the polymer and requires a temperature of 200°C to react at a reasonable rate. If a Viton compound is made up containing TETA and PPD and is press cured for one hour at 130°C only the TETA produces crosslinks (see *Table 1*).

Table 1. Vulcanization of Viton with TETA in the presence of PPD

Curing agent	*Cure conditions*	V_r *(in acetone)**
1·25%TETA	1 h at 130°C	0·26
1·25%TETA+4%PPD	1 h at 130°C	$0{\cdot}25_9$

*V_r is the volume fraction of rubber in the vulcanizate swollen to equilibrium.

If continuous stress-relaxation measurements are carried out at 200°C on the two vulcanizates listed in *Table 1* in an atmosphere of white spot nitrogen, the results shown in *Figure 1* are obtained. The rate of relaxation

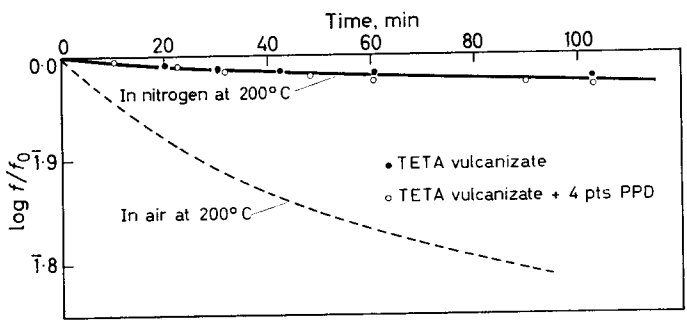

Figure 1—Continuous stress-relaxation in Viton vulcanizates at 200°C

of a TETA vulcanizate at the same temperature in air is shown by the dotted line. To within the limits of experimental error the rates of relaxation of the TETA and TETA + PPD vulcanizates are identical in nitrogen at 200°C. Swelling measurements carried out on these rubbers before and after the relaxation experiment shows that the TETA vulcanizate had suffered a

small amount of network scission, consistent with the relaxation data, while the TETA + PPD sample had experienced a large increase in crosslink density. The ratio of V_r before and after the relaxation experiment was 1·95 indicating a large increase in crosslink density. Despite this large change, the rate of continuous stress-relaxation remains the same. The small amount of network scission which occurs in nitrogen is thought to be due to traces of oxygen in the system.

These results are regarded as being conclusive evidence for the validity of the 'two network' theory in systems conforming to case (ii).

Test of case (iii)

This case has been treated theoretically by Flory[6], for the particular condition in which no change in crosslink density occurs, i.e. the original crosslinks introduced into the isotropic polymer undergo interchange in the strained state; a new crosslink being formed for each one dissociated. If k' represents the rate constant for this process Flory finds that

$$k't = \omega + \frac{\omega^2}{2 \times 2!} + \frac{\omega^3}{3 \times 3!} + \ldots . \tag{7}$$

where $\omega = -\ln (v_e/v)$, and $v_e = v$ at $t = 0$.

If the sample is maintained at constant elongation ω may be identified with $-\ln (f_t/f_0)$, where f_t is the stress at time t and f_0 that at $t = 0$.

If first stage crosslinks were destroyed without simultaneous formation of second stage linkages a first order decay of stress should occur.

No actual system is known which undergoes crosslink interchange in the manner required by Flory's treatment and hence no experimental test of the validity of his deductions is possible. However, his conclusion that at high percentage of interchange the stress will decay more slowly than required by the 'two network' theory seems a plausible one.

Test of case (iv)

The first instance in which serious doubt arises as to the validity of applying the 'two network' theory to the interpretation of continuous stress-relaxation measurements arises when scission and crosslinking (as distinct from bond interchange) occur simultaneously. Unfortunately in the heat ageing of rubbers this is a common occurrence. The only combination of scission and crosslinking which has received complete theoretical treatment is that represented by case (*iv*), in which scission occurs in the crosslinks. This is accompanied by crosslink formation, it being assumed that the new crosslinks are immune from further scission. The theoretical treatments of Flory[6] and Scanlan[7] both indicate that although the 'two network' theory is valid over the initial stages of reaction serious departures occur later. Both treatments show the decay in tension in a continuous stress-relaxation experiment to be less than that predicted by the 'two network' theory, the difference becoming significant as reaction exceeds twenty per cent based upon the first network. Scanlan's result for case (*iv*) as applied to stress-relaxation in simple extension is

$$f/f_0 = -[7 + 3q - 8 \exp (q/4)] \tag{8}$$

where f_0 is the original tension and f the value after a fraction q of crosslinks present in the first network have reacted.

Flory's result for the same case is

$$q = \omega - \frac{\omega^2}{2 \times 2!} + \frac{\omega^3}{3 \times 3!} - \frac{\omega^4}{4 \times 4!} \tag{9}$$

where $\omega = -\ln (f/f_0)$ for simple extension.

An experimental test of these predictions is now possible, again using the heat stable copolymer of vinylidene fluoride and hexafluoropropylene known as Viton. Viton can be crosslinked with hexamethylene diamine carbamate to give heat stable vulcanizates. The behaviour of these rubbers at high temperatures has been studied in conventional heat ageing tests and by the methods of continuous and intermittent stress-relaxation[5,8]. As expected, there was a reasonable correlation between the results of intermittent stress-relaxation and conventional heat ageing tests. The results obtained in continuous stress-relaxation experiments at temperatures up to 250°C were interesting in that they showed an exponential decay over the first 30 per cent of network scission but thereafter the rate fell below that expected for the first order process defined by this exponential region. The rate of continuous stress-relaxation is independent of crosslink density and dependent upon crosslink nature in such a way as to show that scission in the first network is occurring in and at the crosslinks. Intermittent stress-relaxation measurements show this crosslink scission to be accompanied by a crosslinking reaction of high efficiency ($\sim 80 \longrightarrow 90$ per cent), and further continuous relaxation measurements show that the new crosslinks formed are stable at 250°C, any further network changes being due to processes occurring very slowly in the main chain polymer.

It would appear, therefore, that in Viton crosslinked with hexamethylene diamine carbamate we have a system which, on heat ageing, conforms closely with that treated theoretically by Flory and Scanlan. In the first network at 250°C a rapid breakdown of crosslinks occurs, this is accompanied by the formation of new crosslinks (with only a small decrease in overall crosslink density) which are stable at 250°C and therefore are not subject to further reaction.

Making the reasonable assumption that the initial exponential portion of the continuous stress-relaxation curve (see *Figure 2*) represents the true rate of stress-relaxation due to crosslink scission in the first network, extrapolation (dotted line in *Figure 2*) allows one to obtain q as a function of time. Values of q from 0·1 to 0·9 have been introduced into equations (8) and (9) and the results are shown in *Figure 2*. In making calculations from equation (8) the exponential was not expanded to terms higher than q^2 and in equation (9) terms higher than ω^2 were neglected.

The agreement between theory and experiment shown in *Figure 2* is remarkably good, particularly with the Scanlan treatment, and it can be seen that this represents a breakdown of the 'two network' theory once about 30 per cent of the first network has been removed.

An extension of case (*iv*) arises if stable crosslinks are introduced in

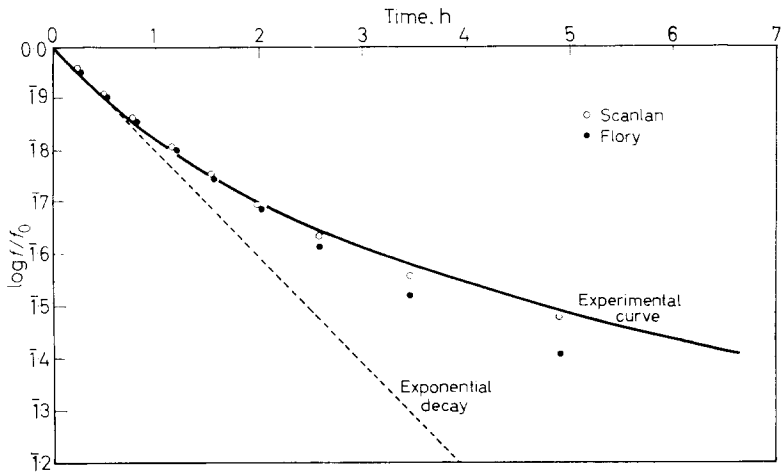

Figure 2—Continuous stress-relaxation in a conventional Viton vulcanizate at 250°C in air

excess of the number originally present in the first network. A system has been found in which this situation arises and this permits a striking demonstration of complete breakdown of the 'two network' theory as applied to the interpretation of continuous stress-relaxation measurements.

In this system a Viton elastomer is crosslinked with TETA and heat aged at 200°C in the presence of PPD. Viton is crosslinked effectively by TETA at 130°C but reaction with PPD requires a much higher temperature. If one uses both reagents in the same compound, heating at 130°C will cause vulcanization with the TETA but no reaction with the PPD. If this vulcanizate is heated in air at 200°C oxidative scission of the TETA crosslinks occurs. This is accompanied by the formation of a much more heat stable second network superimposed upon which is the appreciable amount of crosslinking due to reaction between the PPD and Viton. The crosslinks

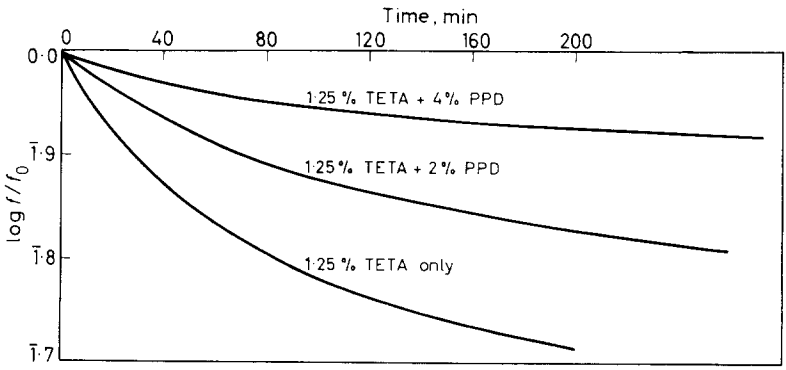

Figure 3—Continuous stress-relaxation in Viton vulcanizates at 200°C in air

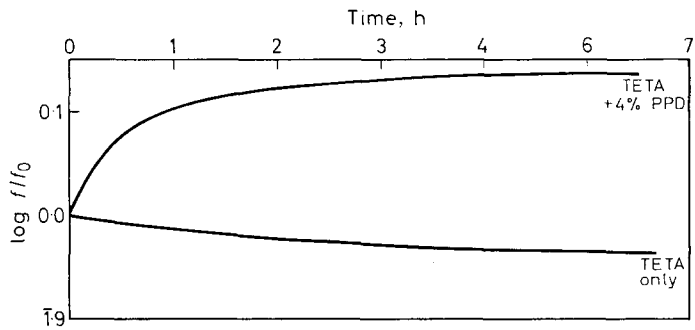

Figure 4—Intermittent stress-relaxation in Viton vulcanizates at 200°C in air

formed in this second reaction will be stable at 200°C as also will be the main chain polymer. The results shown in *Figure 3* illustrate the effect of various concentrations of PPD on the rate of continuous stress-relaxation at 200°C in a Viton–TETA network cured at 130°C.

Clearly the slope of these curves can be varied at will by a suitable choice of PPD concentration. Swelling measurements on these vulcanizates before and after the experiment showed that the presence of PPD resulted in a very large increase in crosslink density, the magnitude of the increase depending upon concentration. For example, in a Viton–TETA vulcanizate containing 4 per cent PPD, V_r in acetone had increased from $0{\cdot}25_9$ at the beginning of the experiment to a value of 0·41 after 160 minutes at 200°C. The intermittent stress-relaxation curves in *Figure 4* illustrate the effect of PPD on the heat ageing of Viton–TETA vulcanizates at 200°C. The fact

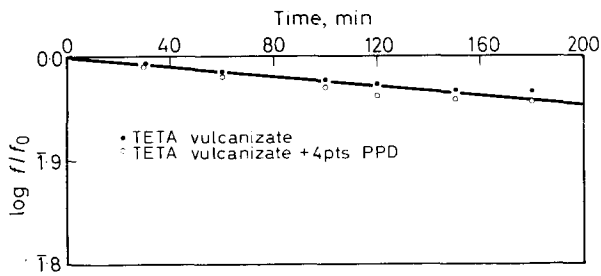

Figure 5—Continuous stress-relaxation in Viton vulcanizates at 130°C in air

that PPD is not behaving as an antioxidant in these experiments is shown by the relaxation curves in *Figure 5*. These show the PPD to have no effect on the rate of network breakdown of TETA vulcanizates in air at 130°C. At this temperature PPD is unable to produce crosslinks; if it were behaving as an antioxidant it would presumably be even more effective at 130° than at 200°C.

There is little doubt that PPD is affecting the form of the continuous

stress-relaxation curves in Viton–TETA vulcanizates at 200°C because it is producing a large number of stable crosslinks in the strained state. Furthermore it is having an effect from the commencement of the experiments and this represents a complete breakdown of the 'two network' theory in this system.

More complex cases

No theoretical treatment or experimental test has been possible on any of the more involved cases; however, in view of the results discussed under case (*iv*) caution must be exercised in applying the 'two network' theory to the interpretation of continuous stress-relaxation measurements in such systems.

The author is indebted to Mr R. Sinnott and Mr J. Day for their preparation of vulcanizates.

Ministry of Aviation,
Chemistry, Physics and
Metallurgy Dept,
R.A.E., Farnborough, Hants

(*Received December 1965*)

REFERENCES

[1] TOBOLSKY, A. V. *Properties and Structure of Polymers*, p 228. Wiley: New York, 1960
[2] ANDREWS, R. D., TOBOLSKY, A. V. and HANSON, E. E. *J. appl. Phys.* 1946, **17**, 352
[3] ATKINSON, A. S. *R.A.E. Tech. Note No. Chem. 1393*, January 1963
[4] BERRY, J., WATSON, W. F. and SCANLAN, J. *Trans. Faraday Soc.* 1956, **52**, 1137
[5] THOMAS, D. K. *J. appl. Polym. Sci.* 1964, **8**, 1415
[6] FLORY, *P. J. Trans. Faraday Soc.* 1960, **56**, 722
[7] SCANLAN, J. *Trans. Faraday Soc.* 1961, **57**, 839
[8] THOMAS, D. K., PHILLIPS, L. N., ATKINSON, A. S. and SINNOTT, R. *Rubber Plastics Age*, 1965, **46**, 1020

Electron Diffraction and Microscopy of Deformed Polymer Crystals III—Annealing

P. INGRAM, H. KIHO* and A. PETERLIN

Some aspects of annealing close to the vicinity of the melting point of spherulites and fibrils of polyethylene (PE) and single crystals and fibrils of polyoxymethylene (POM) are described. Electron diffraction and microscopy on deformed spherulites reveal considerable tilting of the molecules or lamellae resulting in a roof-tile stacking of the lamellae on annealing at 120°C. Electron diffraction on the same PE crystal before and after heating showed that phase changes induced by the deformation relax on annealing without reverse stress and are elastic. The striations appearing on fibrils pulled from the lamellae of PE and from single crystals of POM are thought to be associated with a folded chain lamellae-like structure in the unannealed fibrils. The change of striation periodicity was measured as a function of annealing time on the POM fibrils. After an initial jump from the periodicity found on unannealed fibrils, it was found to decrease. This depended on the heating rate used, the decrease only being observed when the sample was wrapped in aluminium foil. By comparison with the behaviour of single crystals on annealing, it is thought unlikely that tilting of the chains in the fibrils is responsible for the decrease in periodicity.

IT IS now well known that on annealing certain highly oriented polymers, particularly polyethylene (PE)[1-3] and polyoxymethylene (POM)[4, 5] close to their melting points, very conspicuous and sometimes highly regular morphological striations develop transverse to the direction of orientation. From studies on surfaces of bulk PE, it was suggested by Anderson[2] that these were the 'type II' lamellae previously reported by him[6, 7] and that they had their origins in epitaxial growth of lower molecular weight material fractionating and crystallizing. However, the fact that they have occasionally been seen on unannealed fibrils[8, 9] can by a variety of techniques be made manifest in unannealed fibrils that normally show no structure[5, 10] and be observed in fractions over a wide range of molecular weights[10] in annealed fibrils, strongly suggested that they may have some fundamental relationship to the mechanism of deformation[10] in the crystalline material. It is the purpose of this paper to discuss the significance of the annealing process in oriented crystalline material and to present results which seem to indicate that the appearance of striations may be related to the tilting behaviour of the molecular chains. Most of the work on PE has been performed on spherulites in order partly to be consistent with previous publications in this series[10, 11] and partly because it is the best defined mode of crystallization associated with the bulk state[12]. They have also been shown to resemble the behaviour of lamellae type single crystals in many respects both in morphology[13, 14] and deformation[11]. Although there is

*Present address: Kyoto University, Kyoto, Japan.

considerable evidence of similar morphology in POM single crystals and fibrils[4, 5], the preliminary measurements reported in the present paper with respect to the dependence of the fibril striation period on annealing time are different from those on PE. The relationship of this effect to tilting of chains in the original crystals is also considered.

EXPERIMENTAL AND RESULTS

Sample preparation

Single crystals and spherulites of PE were prepared from 0·1 per cent and 1 per cent xylene solutions respectively of a linear Fortiflex A60–500 polymer (trade mark of the Celanese Corporation of America) as described previously[10, 11]. However, in some cases single crystals grown from a 0·1 per cent solution of Alathon (trademark of E. I. du Pont de Nemours & Co., Inc.) in tetrachlorethylene by ambient cooling were used so that direct comparison could be made with earlier deformation studies[15].

The POM single crystals were multilayer structures[4] grown by ambient cooling of a saturated solution of Delrin (trademark of E. I. du Pont de Nemours & Co., Inc.) in bromobenzene.

All deformation was performed by depositing the polymer on to Mylar (trademark of E. I. du Pont de Nemours & Co., Inc.) film and then uniaxially stretching. This technique and the method of transferring the sample to the electron microscope has already been described in detail[1, 3, 16].

Samples were annealed in a test tube, except where stated, in a controlled temperature ($\pm 0{\cdot}1°C$) oil bath. Values of all periodicities and spacings were taken from the measurements plotted on distribution curves[5].

Annealing before deformation

Initially it was interesting to compare the morphology of annealed and unannealed undrawn spherulites of PE. It can be seen from *Figure 1* that only the 110 orthorhombic reflections appear on annealing at 120°C for one hour with the 200 reflections completely missing (compare Fig. 1, ref. 11). This means that tilting of the chains, which prior to annealing are approximately perpendicular to the lamellae in the spherulites, must be taking place; this tilting must be around the ⟨130⟩ direction such that the {110} planes are normal to the plane in which the lamellae lie. This is in general agreement with the work of Baltá Calleja *et al.*[17] on single crystal mats of PE who also found a slight decrease in the long period on annealing at 120°C. Furthermore there appears to be some significant change in the morphology of the sample. While retaining an overall similar appearance to the unannealed spherulites, some reorganization of lamellae has taken place and in certain regions there are groups stacked in a roof-tile fashion. Geil has also reported observations of this nature (see Chapter V of ref. 1).

Tilting is not observed on annealing POM single crystals at 170°C for one hour. Both before and after annealing prior to deformation the electron diffraction patterns remained essentially unchanged and dark field micrographs of the crystals are fairly uniform (excepting of course the holes). These are shown in *Figure 2*. This indicates that the molecules are normal

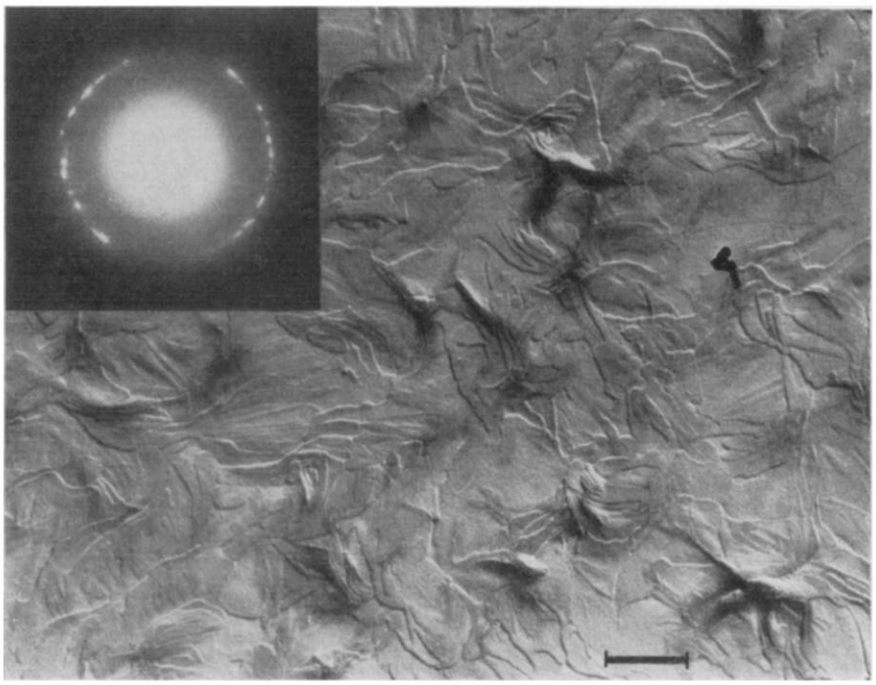

Figure 1—Electron micrograph and diffraction from undeformed PE spherulites annealed at 120°C for 1 h. Scale bar represents 1 micron

to the substrate and top surface of the crystals before and after annealing, much in contrast to the situation in PE.

When PE spherulites are drawn (in this case about 30 per cent) immediately after annealing at 120°C for one hour and cooling to room temperature, the same effects are obtained as in the deformation of unannealed material[11]. *Figure 3* shows that the usual phase change to a monoclinic unit cell occurs with the same orientation and chain tilting as in the unannealed case. The morphology remains similar to before deformation (*Figure 1*) with the additional appearance of some small fibrils between cracks in the lamellae (again cf. ref. 11).

Annealing after deformation

The annealing of single crystals of PE after deformation and the effects on the fibrils pulled from them has been the subject of extensive investigation and has been reported elsewhere[3–5]. We have therefore been concerned mainly with the morphology of spherulites of PE deformed and annealed under similar conditions. *Figures 4* to *6* show some aspects of this. The samples were all deformed 30 per cent and annealed at 125°C for one hour. As can be seen from *Figures 4* and *5* there is a much greater tendency for the lamellae to be stacked in a roof-tile fashion and the resemblance is very strong to the type II lamellae described by Anderson[2]. The electron diffraction pattern in *Figure 4* indicates that the molecules must be still oriented and tilted to a large extent from the vertical (to the substrate).

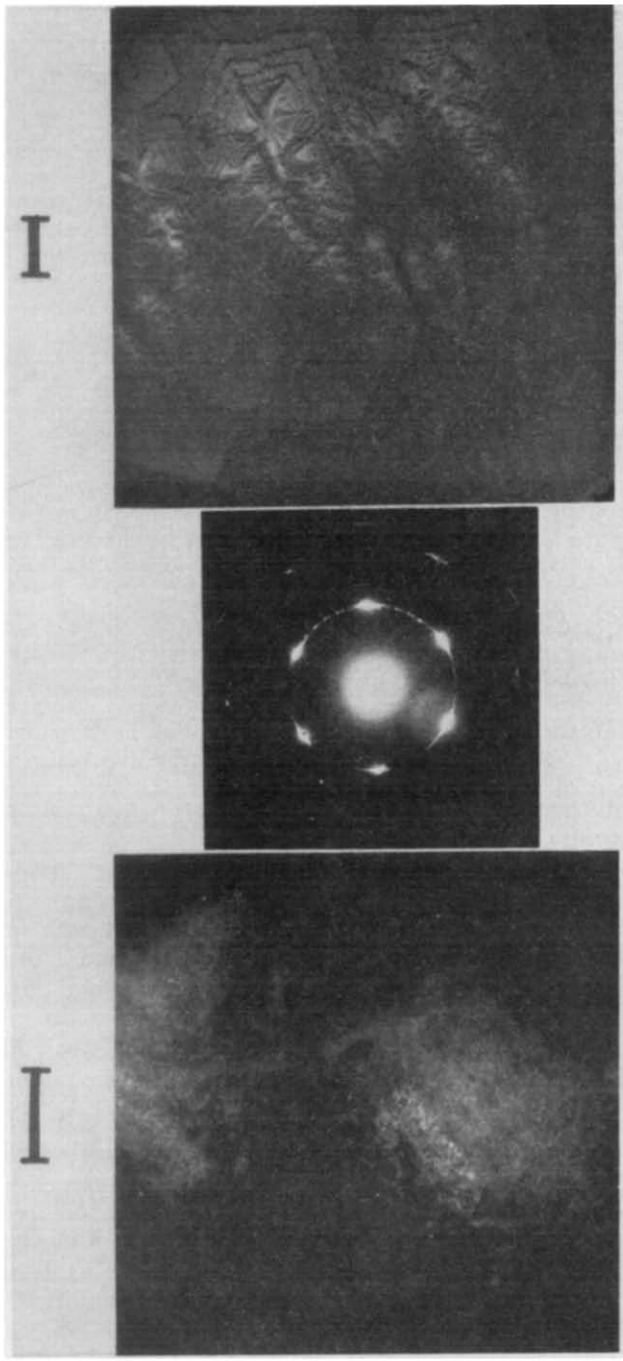

Figure 2—Electron diffraction and dark field micrographs of POM single crystals (of slightly dendritic shape) taken (a) before annealing, (b) after annealing for 1 h at 170°C. Scale bars represent 1·0 micron

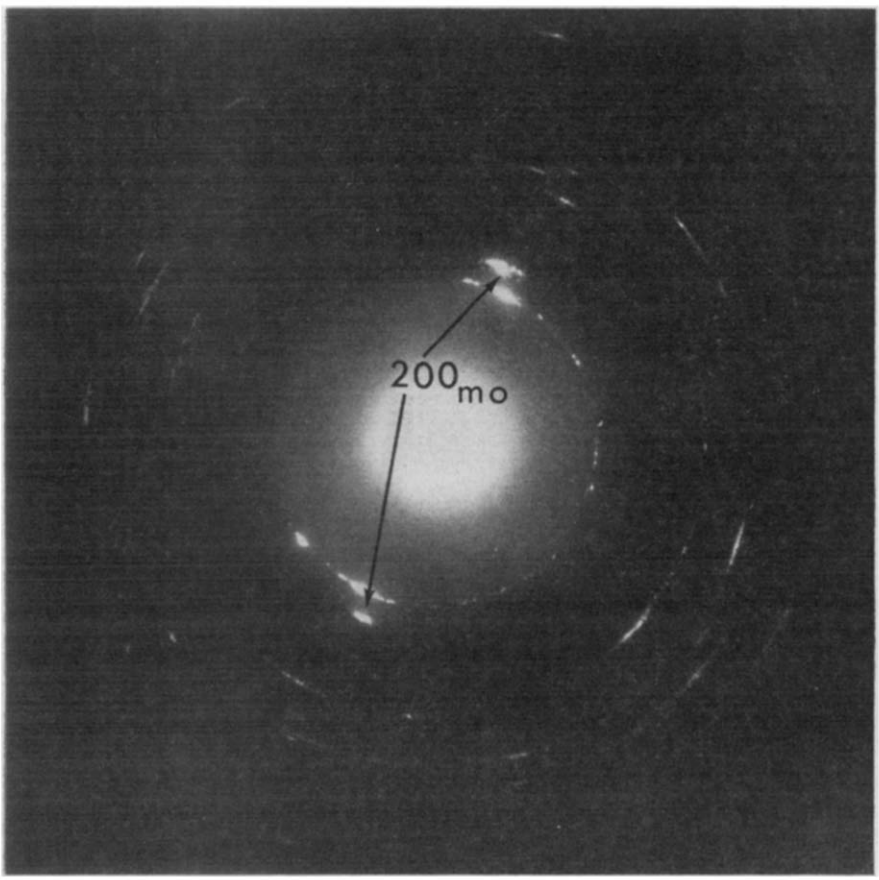

Figure 3—Electron diffraction from PE spherulites annealed at 125°C for 1 h and subsequently drawn about 30 per cent on Mylar film

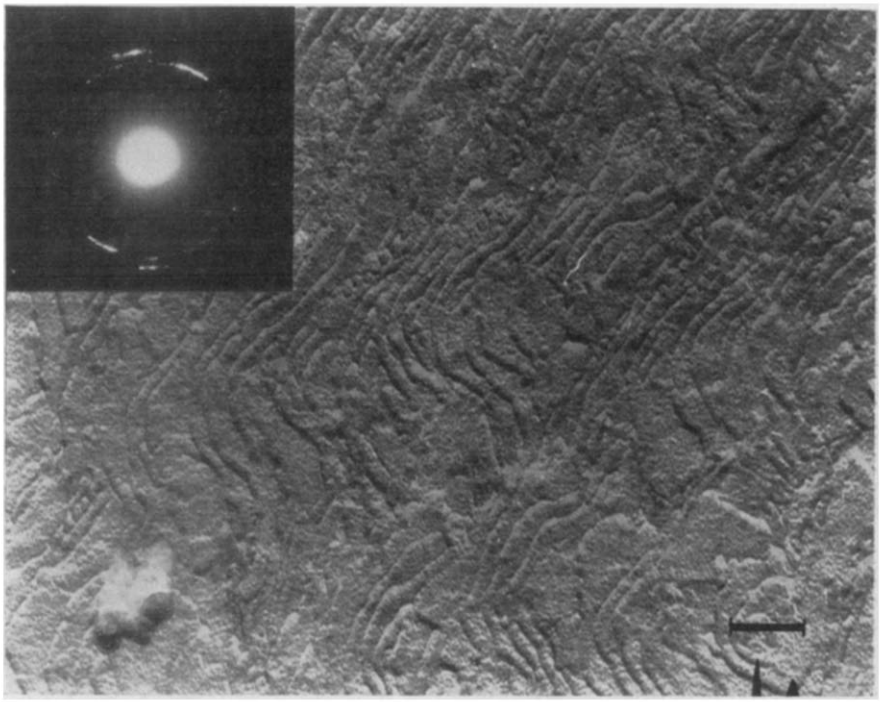

Figure 4—Electron micrograph and diffraction from a portion of a PE spherulite drawn 30 per cent and subsequently annealed at 125°C for 1 h. Note the apparent finite length of the lamellae. Scale bar represents 0·2 micron

Furthermore annealing has removed the monoclinic phase, only the 110_{or} and 200_{or} reflections remaining.

A similar effect is found on annealing deformed single crystals[3]. In that and subsequent studies[18] on relaxation at room temperature, it was suggested that if the monoclinic phase relaxed, a set of orthorhombic reflections would appear near the position for 110 twin reflections. We have therefore performed observations on the same deformed (unshadowed) single crystal before and after annealing on a heating stage in the electron microscope. *Figure 7* shows the results of this. The crystals had been deformed 25 per cent on Mylar film before transferring to a carbon substrate. It can be seen that after heating for one hour to 110°C both the monoclinic phase is removed and new reflections appear near the 110_{or} twin position. Also with more prolonged irradiation (even before heating) the 200_{or} reflections were found to have shifted into new positions such that hexagonal symmetry was evident. This is believed to be associated with an irradiation effect involving the liberation of radicals in the lattice which can, by rotation of the broken bonds or crosslinking, cause a new packing in the hexagonal phase[19, 32].

It will be noticed that there is some variation in what we have taken to be the 200_{or} reflections in *Figure 4* such that some diffraction appears inside

the 200 reflection; because of the multilayer nature of the lamellae in the spherulites we take this not to be due to a monoclinic phase, but rather to a slight broadening of the reflecting points from thin layers (in reciprocal space) where the diffracting planes are tilted very slightly out of their diffracting positions[20]. The Debye–Scherrer rings will then become ellipsoids thereby changing the spacing of the reflections. This effect can also be seen on the 110 reflections in *Figures 1* and *4*. In *Figure 5* the roof-tile

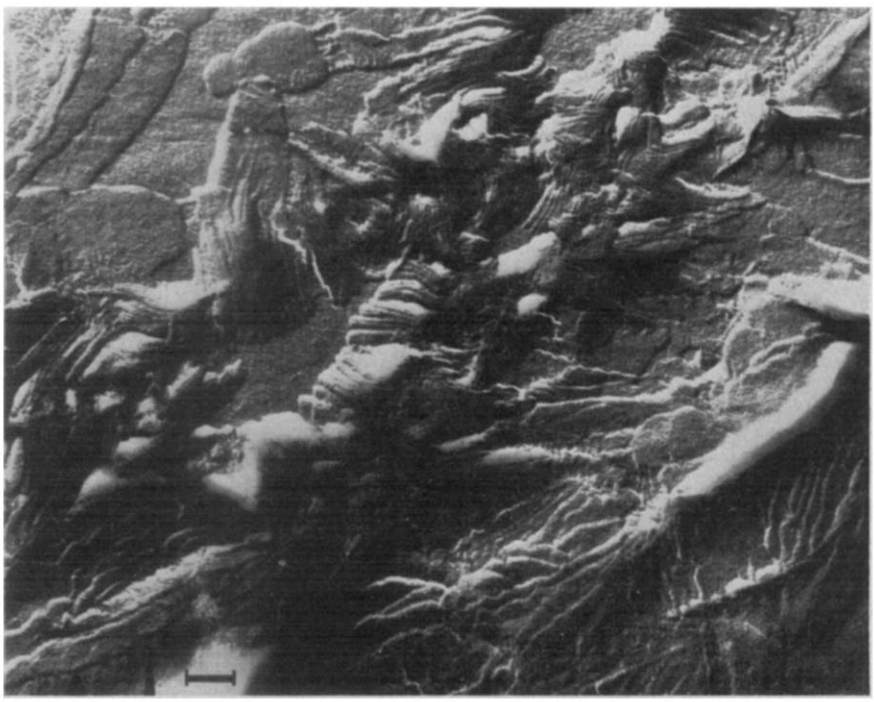

Figure 5—Another part of the same sample as in *Figure 4*. Unaffected lamellae can be seen in the upper left of the micrograph. 'Tilted' lamellae appear in the centre. Scale bar represents 0·2 micron

type lamellae appear better defined, together with the usual lamellae in the top left of the micrograph. A few striations are also evident on the latter. In these regions the chains probably have a slightly different tilt or orientation. In general it can be seen that there has been considerable reorganization in some regions of the spherulite, much more for example than in the undeformed case (cf. *Figure 1*). It was not possible to obtain electron diffraction from *Figure 5*.

Figure 6 shows the structure which appears on the fibrils pulled out between the boundaries of spherulites after annealing. This is the 'shish-kebab' type striation effect produced on fibrils from single crystals[3–5] and observed on oriented bulk material[2]. While the orientation of the striations is determined by that of the fibrils, it was not necessary that they were in

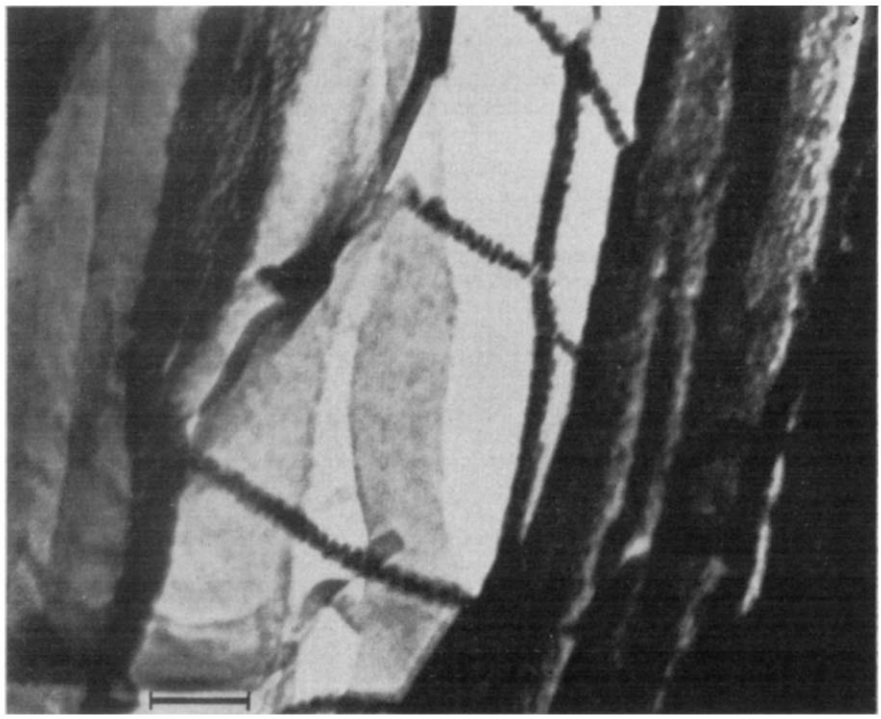

Figure 6—The 'shish-kebab' structure appearing on fibrils pulled from between the boundaries of spherulites, annealed at 120°C for 1 h. Scale bar represents 0·2 micron

contact with the substrate to show the effect (note the absence of shadows even though the sample was fairly heavily shadowed with platinum) in contrast to Geil's findings[8] for single crystals. However, all the fibrils we observed were fixed at both ends and could not be described as freely suspended, as in Geil's case[3]. Furthermore we have never been able to observe this type of 'freely suspended' fibril with no structure and the explanation for their appearance remains in doubt.

It has been shown in another publication[5] that the spacings (L) of the striations increases with annealing temperature between 163°C and 173°C in fibrils pulled from single crystals of POM. No definitive time dependence of annealing was found as might have been expected from long spacing measurements by X-ray diffraction in PE fibres[8] and POM single crystals[21]. However, if the heating rate was increased by wrapping and sealing the sample in aluminium foil and annealing in silicone oil, initial results showed that a larger value of L was attained than annealing in air in a test tube, and that there was an indication of a decrease in L with annealing time at 170°C. Annealing at different times has confirmed this and the results are shown in *Figure 8*. The type of morphology is almost identical to that of PE and can be seen in *Figure 9*. Also as previously reported[4,5] a striated effect is sometimes observed near holes, wrinkles and

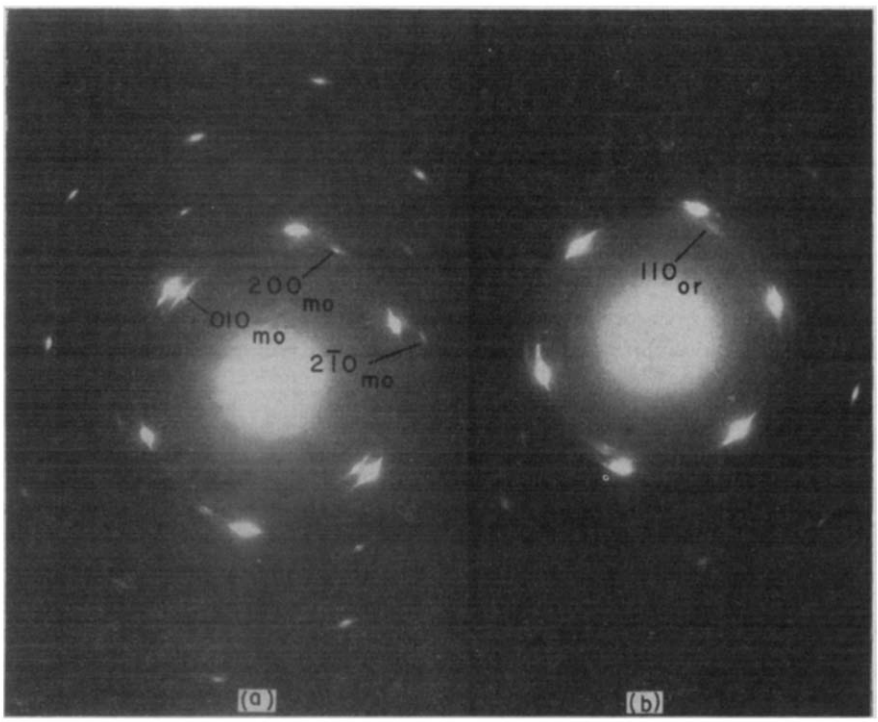

Figure 7—Electron diffraction from PE single crystals deformed 25 per cent on Mylar film (a) before and (b) after heating for 1 h to 110°C

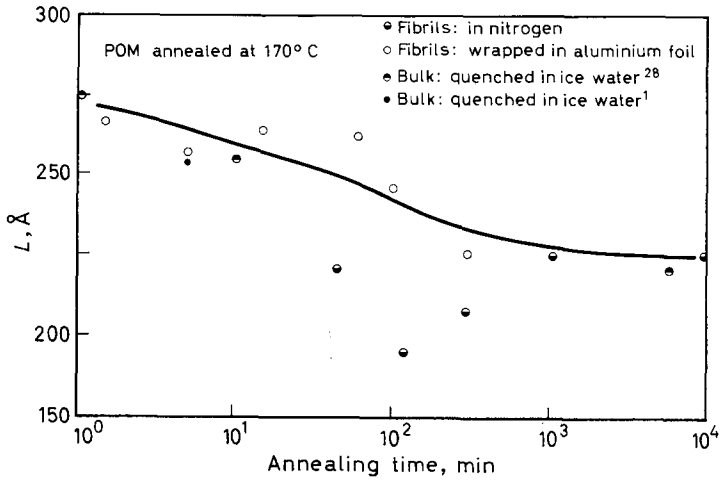

Figure 8—Periodicity of striations on POM fibrils as a function of time of annealing at 170°C. Crystals were deformed 100 per cent on Mylar film

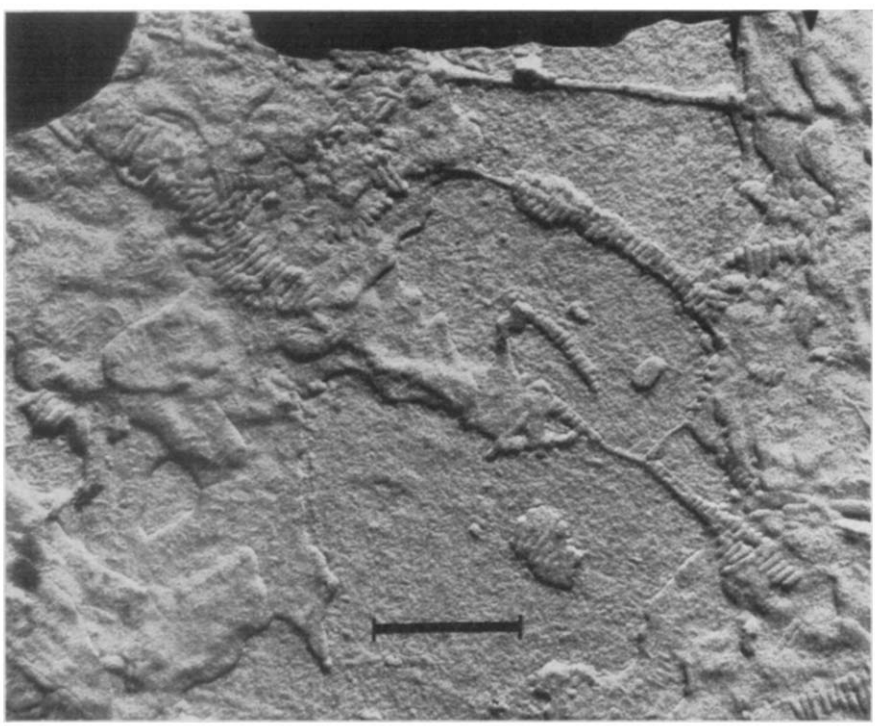

Figure 9—Striations on POM fibrils after annealing in air for 100 min at 170°C. Samples were wrapped and sealed in aluminium foil and immersed in silicone oil. Scale bar represents 0·5 micron

Figure 10—Striations near holes and wrinkles (indicated by arrows) on POM crystals drawn 100 per cent on Mylar film at room temperature and annealed for 60 min at 170°C in air. Scale bar represents 0·5 micron. Double arrow indicates draw direction

the edges of cracks with a spacing approximately the same as on the fibrils. This is shown in *Figure 10*.

DISCUSSION

As with drawn bulk[22] and single crystals of PE[3] the contribution to the deformation process in spherulites of a phase change from orthorhombic to monoclinic unit cell is completely removed on annealing. It has been shown that the original transformation is elastic[18]. However, it was suggested that the monoclinic III of ref. 15 could transform by the reverse of the type I phase change to the original orthorhombic phase by stress relaxation. The subsequent appearance of the 110_{or} reflections near the twin position by relaxation on annealing now unambiguously proves this point. (In ref. 18 it was written that the orthorhombic reflection near the 110 twin position could occur by the reverse of the *type III* phase change. From ref. 15 it is clear that this should be written as the monoclinic *III* transforming by the reverse of *type I*.) That the monoclinic phase is only stable under stress at least up to 110°C is further confirmed by the results of Magill[23] who succeeded in polymerizing linear polymethylene at temperatures below the glass transition and observed an irreversible change from triclinic to orthorhombic during warming to room temperature. Neverthe-

less there are indications from the recent work of Fatou *et al.*[24] that a monoclinic phase may crystallize slowly at temperatures greater than 100°C in bulk PE. It is not clear from their results whether the new phase is really stable at those temperatures. Although it has been shown that annealing undeformed crystals on a carbon substrate can induce phase changes in the crystals due to thermal stresses set up between crystals and substrate[19, 25], no effects due to this difference of coefficients of expansion were observed in the deformed crystals. This is because any phase change induced in this way would also relax above about 100°C[19].

The appearance of lamellae stacked in roof-tile fashion is the most striking phenomenon to occur on annealing deformed PE spherulites, and to a certain extent undeformed ones (*Figure 1*). A similarity exists both in appearance and spacing to the striations produced on fibrils after annealing. Anderson[2] has suggested that they are identical in both cases and has called them 'type II' lamellae, ascribing their formation as due to fractionation, and to epitaxial recrystallization of lower molecular weight polymer in oriented material (after annealing). While it is recognized that such a process is possible, there are two reasons why it seems unlikely. (*i*) Striations can be observed over a wide range of oriented fractionated material[5] from single crystals, and (*ii*) as has been pointed out before[3], there would not seem to be enough low molecular weight polymer present to account for all the material observed on the fibrils. In another paper of this series[5] it was suggested that the origin of these striations was in folded chain portions of the original lamellae being pulled out into the fibril. Subsequent annealing would induce more order into these regions and also incorporate the relaxed tie molecules[3]. It was therefore necessary to investigate the effect of temperature and time of annealing on the periodicity.

It has been shown by Fischer and Schmidt[8] for PE single crystals and by Hirai *et al.*[21] for POM single crystals, that the folded chain crystals show an increase in thickness (or long period) with temperature and time of annealing. (This dependence was also found on highly oriented bulk PE.) An increase in the striation periodicity in POM fibrils was found with temperature of annealing[5] which is very consistent with this model, and also in good agreement with small angle X-ray measurements[8]. Nevertheless little time dependence could be observed[5]. However, there did appear to be a dependence on heating rate in POM fibrils and either no time dependence (a result recently found for single crystals of PE[26, 27]) or possibly a slight decrease at short annealing times. From the results shown in *Figure 8* there clearly is a decrease at 170°C. Geil[28] has also found similar behaviour at this temperature on undeformed bulk POM. First it was thought that since in PE single crystals or spherulites tilting of the chains or lamellae occurs on annealing, this might be the cause of the decrease in spacing[17]. However, in POM single crystals the chains are generally everywhere normal to the lamellae surface as is shown in *Figure 2* by the uniform contrast[29] of the dark field image (taken from the {10·0} planes), and there appears to be little change on annealing. Consequently it is unlikely that this could be the explanation. There is no evidence from low angle X-ray data of any decrease in long spacing for drawn PE.

Another approach, however is possible. If we consider the measured

long period (L) in the fibril as the sum of an amorphous component (L_a) and a crystalline component (L_c), it could decrease if L_a is reduced by relaxation and retraction of the tie molecules between the crystals, for example. This would have the effect of drawing the crystalline components closer together. It is also possible that the crystals are not in thermodynamic equilibrium when in the fibril. According to current theory[30] folded chain crystals could be stable at a finite long period even close to the melting point. If there is a distribution of L_c some could be expected to be reduced on annealing in the direction of the position of minimum free energy[30]. There are also indications that the equilibrium melting temperature T_m decreases with time[27] which would be consistent with this view. Additionally there may be effects due to partial melting[31] of the crystals and recrystallization. Due to a reduction in the amorphous portion and increase in L_c the crystalline components would move closer together thereby decreasing L.

The experimental observation of a rapid rise of long period on annealing in PE[8] as well as in POM is suggestive of melt recrystallization taking place, and would not interfere with any of the above considerations. It seems unlikely that any one process is solely responsible for the change in long period on annealing, and the material used may be expected to influence the application of these processes. While it is known from diffraction contrast microscopy which part of the striated morphology is crystalline both before[10] and after annealing[4], it is clearly necessary to specify more precisely how and where the crystallinity changes in the fibrils during annealing.

The appearance of striations near holes and wrinkles in POM (*Figure 10*) is probably associated with molecular motion or melting on annealing when the lamellae thicken. Consequently the chains would be oriented in the direction of the motion, or at least highly tilted with respect to the substrate. The chains comprise new lamellae and may well be of the same origin as those observed in PE spherulites (*Figures 1*, *4* and *5*). In the undeformed spherulites some melting might have been expected to take place and new crystallization occurred with the tilted chains. The effect naturally would be more pronounced in the spherulites after deformation where that action had already induced considerable tilting. However, the identification of this type of morphology with the 'type II' lamellae observed[2] in fracture surfaces of unannealed undeformed bulk PE is by no means clear. There is no reason to suppose fractional melting and recrystallization or fractional crystallization should occur with a morphology any different from lamellae ('type I') crystals. Certainly single crystals from fractions do not appear significantly different from those from unfractionated material. The 'type II' lamellae in untreated PE may be 'type I' lamellae seen in cross section.

CONCLUSIONS

(*1*) In agreement with other work on PE single crystals there is considerable tilting of the chains on annealing spherulites which sometimes results in a change in morphology.

(*2*) This change is greatly emphasized on annealing after deformation,

the molecules remaining in a highly tilted state. Phase changes incurred on deformation relax on annealing without applied reverse stress and are elastic.

(*3*) Striations observed on annealed fibrils pulled from crystals of PE and POM are thought to originate from blocks of folded chains in the fibril before annealing.

(*4*) It is unlikely that any dependence of long spacing on annealing time of these striations, particularly the decrease observed in POM fibrils, is associated with tilting, since no tilting could be observed before or after annealing POM single crystals. Conversely no decrease in L has ever been observed in PE fibrils where tilting is evident.

(*5*) There are considerable differences in behaviour in long period of single crystals and fibrils on annealing and on subjection to different heating rates. Further investigations may reveal how important a role initial recrystallization plays in the early stages of annealing.

This work was supported by the United States Air Force, Aeronautical Systems Division, under contract AF-33(615)-2244 and the Camille and Henry Dreyfus Foundation.

Camille Dreyfus Laboratory,
Research Triangle Institute,
Durham, N.C., U.S.A.

(*Received November 1965*)

REFERENCES

[1] GEIL, P. H. *Polymer Single Crystals.* Interscience, Wiley: New York, 1963
[2] ANDERSON, F. R. Paper presented at American Physical Society Meeting, Philadelphia, March 1964
[3] GEIL, P. H. *J. Polym. Sci.* 1964, **A2,** 3835
[4] PETERLIN, A., KIHO, H. and GEIL, P. H. *J. Polym. Sci.* 1965, **B3,** 151
[5] INGRAM, P., KIHO, H. and PETERLIN, A. Paper presented at International Symposium on Macromolecular Chemistry, Prague, September 1965; *J. Polym. Sci.* To be published
[6] ANDERSON, F. R. *J. Polym. Sci.* 1963, **C3,** 123
[7] ANDERSON, F. R. *J. appl. Phys.* 1964, **35,** 64
[8] FISCHER, E. W. and SCHMIDT, G. *Angew. Chem.* 1962, **74,** 551
[9] HIRAI, H., KISO, H. and YASUI, T. *J. Polym. Sci.* 1962, **61,** S1
[10] PETERLIN, A., INGRAM, P. and KIHO, H. *Makromol. Chem.* 1965, **86,** 294
[11] INGRAM, P. and PETERLIN, A. *J. Polym. Sci.* 1964, **B2,** 739
[12] KEITH, H. D. and PADDEN, F. J. *J. appl. Phys.* 1964, **35,** 1270 and 1286
[13] KEITH, H. D. *J. Polym. Sci.* 1964, **A2,** 4339
[14] KELLER, A. and SAWADA, S. *Makromol. Chem.* 1964, **74,** 190
KAWAI, T. and KELLER, A. *Phil. Mag.* 1965, **11,** 1165
[15] KIHO, H., PETERLIN, A. and GEIL, P. H. *J. appl. Phys.* 1964, **35,** 1599
[16] GEIL, P. H. *J. Polym. Sci.* 1964, **A2,** 3813
[17] BALTÁ CALLEJÀ, F. J., BASSETT, D. C. and KELLER, A. *Polymer, Lond.* 1963, **4,** 269
[18] KIHO, H., PETERLIN, A. and GEIL, P. H. *J. Polym. Sci.* 1965, **B3,** 157
[19] KIHO, H. and INGRAM, P. To be published
[20] KELLER, A. Private communication
[21] HIRAI, H., TOKUMORI, T., KATAYAMA, T., FUJITA, S. and YAMASHITA, Y. *Rep. Res. Lab. Surf. Sci., Okayama Univ.* 1963, **2,** 91
[22] TANAKA, K., SETO, T. and HARA, T. *J. phys. Soc. Japan,* 1962, **17,** 873
[23] MAGILL, J. H., POLLACK, S. S. and WYMAN, D. P. To be published

[24] FATOU, J. G., BAKER, C. H. and MANDELKERN, L. *Polymer, Lond.* 1965, **6,** 243
[25] HOLLAND, V. F. *J. appl. Phys.* 1964, **35,** 3235
[26] TAKAYANAGI, M. and NAGATOSHI, F. *Mem. Fac. Eng. Kyushu Univ.* 1965, **24,** 33
[27] MEINEL, G. Private communication
[28] GEIL, P. H. Unpublished
[29] BASSETT, D. C., DAMMONT, F. R. and SALOVEY, R. *Polymer, Lond.* 1964, **5,** 579
[30] PETERLIN, A., FISCHER, E. W. and REINHOLD, CHR. *J. chem. Phys.* 1962, **37,** 1403
[31] NUKUSHINA, Y., ITOH, Y. and FISCHER, E. W. *J. Polym. Sci.* 1965, **B3,** 383
FISCHER, E. W. *Z. Naturforsch.* In press
[32] ORTH, H. and FISCHER, E. W. *Makromol. Chem.* 1965, **88,** 188

ANNOUNCEMENTS

CONFERENCE ON ADVANCES IN POLYMER SCIENCE AND TECHNOLOGY, LONDON, SEPTEMBER 1966

The second Conference to be organized jointly by the Plastics and Polymer Group of the Society of Chemical Industry, the Plastics Institute and the Institution of the Rubber Industry will be held at the Institution of Electrical Engineers, Victoria Embankment, London, W.C.2. on 20, 21 and 22 September. The Oil and Colour Chemists Association and the Society of Dyers and Colourists will participate. Papers will be preprinted and presented in summary form at the Conference which will consider: (1) Structures of polymeric systems; (2) Polymerization reactions, particularly polymerization and crosslinking reactions in films, and interaction with substrates and adhesion; (3) Physical and chemical changes in polymers with particular reference to long term ageing and load-bearing properties; (4) Practical implications of rheological measurements. Full details are obtainable from the Assistant Secretary, Society of Chemical Industry, 14 Belgrave Square, London, S.W.1, under reference 'Joint Plastics Conference'.

GORDON RESEARCH CONFERENCES

The 1966 Gordon Research Summer Conferences will be held during 13 June to 2 September in New Hampshire and from 20 June to 2 September in Enumclaw, Washington. Full details and application forms are obtainable from the Director, Dr. W. G. Parks, Gordon Research Conferences, University of Rhode Island, Kingston, Rhode Island 02881, U.S.A.

Polymers will be discussed at Colby Junior College, New London, New Hampshire during 4 to 8 July when four one-day seminars will be held on: (1) Structure–properties relationships; (2) Conducting polymers; (3) Polyelectrolyte polymers; (4) Coordinate polymerization, followed by discussions on 8 July.

The physics and physical chemistry of biopolymers will be considered at Tilton School, Tilton, New Hampshire during 1 to 5 August.

Thermodynamics of Mixing: Excess Volumes in Polyisobutylene–Solvent Systems

C. CUNIBERTI and U. BIANCHI

Measurements of excess volumes of polyisobutylene in eight solvents are reported. The heats of mixing are examined with a view to rationalization.

TRADITIONAL theories[1, 2] on liquid mixtures relate the heat of mixing to the difference in the interactions between like and unlike neighbouring molecules. On this account and assuming intermolecular forces to be of the London type[3], the heat of mixing ΔU_v^{mix} expected for non-polar polymer–solvent systems has been shown to be always positive (endothermic), being proportional to the square of the difference between polymer and solvent solubility parameters[1] (δ).

Experimental results have often given negative ΔH_p^{mix} values for various non-polar polymer–solvent mixtures[4–6]. It is, however, known that whereas experimental ΔH_p^{mix} values are measured at constant pressure, theoretical treatments give the change in energy ΔU_v^{mix} at constant volume; consequently a comparison between calculated and measured heats of mixing is equivalent to the unjustified assumption of an excess volume (change in volume on mixing) equal to zero. Simple thermodynamics shows:

$$\Delta H_p^{mix} = \Delta U_v^{mix} + T \left(\frac{\partial P}{\partial T} \right)_V \Delta V^{mix} + \ldots . \simeq \Delta U_v^{mix} + P_i \, \Delta V^{mix} \qquad (1)^*$$

where P_i is the internal pressure[7] of the solution. As P_i is of the order of 60 to 100 cal/cm^3 it is apparent that even a small change in volume ΔV^{mix} can result in a significant term $P_i \, \Delta V^{mix}$.

In an attempt to rationalize ΔH_p^{mix} values for polyisobutylene (PIB) in various solvents[8], we report here some results obtained in measuring excess volumes for PIB in eight organic solvents at 30°C. Measurements were made at high dilution (final polymer concentration less than one per cent) first because ΔH_p^{mix} values were measured in the same conditions, and secondly because for these concentrations ΔV^{mix} was expected to be independent of the amount of dissolved polymer.

EXPERIMENTAL PART

Materials

PIB was a fraction obtained from Enjay–Butyl Vistanex (LM–MS) in a previous fractionation[9]; its number average molecular weight is about

*ΔH_P^{mix}, ΔU_V^{mix} and ΔV^{mix} are all referred to a quantity of polymer equal to a mole of repeating unit (mole unit) dissolved in a very large amount of solvent (final concentration below one per cent).

5×10^4. The solvents (benzene, toluene, cyclohexane, methylcyclohexane, chlorobenzene, *n*-heptane, *n*-hexane and *n*-decane) were all reagent grade and were purified by fractional distillation.

Apparatus

The basic idea of our method to measure ΔV^{mix} is to convert volume changes into capacity changes which can be measured with very high precision by standard electronic circuits.

As the apparatus has been fully reported elsewhere[10], only the special dilatometer used to convert volume changes into capacity changes (*Figure 1*) is described briefly.

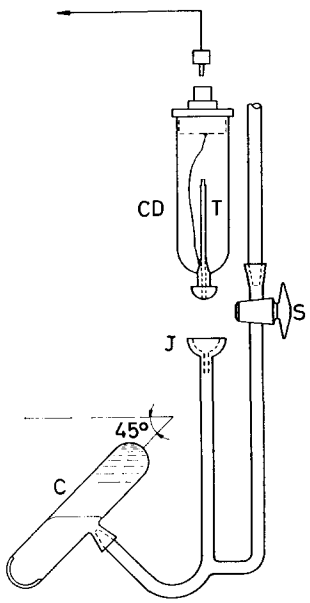

Figure 1—Mixing cell and dilatometer to measure ΔV^{mix}. C is the cell containing polymer (at the bottom) covered by mercury. T is the silver-coated capillary tube, which acts as a capacitor

A given amount of a PIB solution, containing from 0·02 to 0·1 g of polymer, is put in one end of the cell C; then the solvent is evaporated under vacuum, leaving a thin layer of polymer. With S closed, the dilatometer is joined through the spherical joint J to a vacuum line, carefully evacuated to 10^{-4} mm of mercury and completely filled with mercury. The solvent in which ΔV^{mix} has to be measured is then introduced into the cell (up to the level shown) by means of a syringe with a long Teflon tube passing through J. The dilatometer is then assembled with the capacity capillary device CD and the mercury level adjusted at about half way up the capillary T. T is externally silver-coated and thus acts as a capacitor whose dielectric is glass. With the temperature thermostatically controlled at 30° ±0·001°C, mixing is obtained by rotating the cell C through 180°.

Calibration was performed before each ΔV^{mix} measurement, by increasing the thermostat temperature (this producing a known thermal expansion of the cell contents) and measuring the corresponding capacity change[10].

RESULTS

Figure 2 shows ΔV obtained for PIB in various solvents as a function of the amount of polymer dissolved. As expected in the range of concentration studied, ΔV is proportional to the amount of polymer.

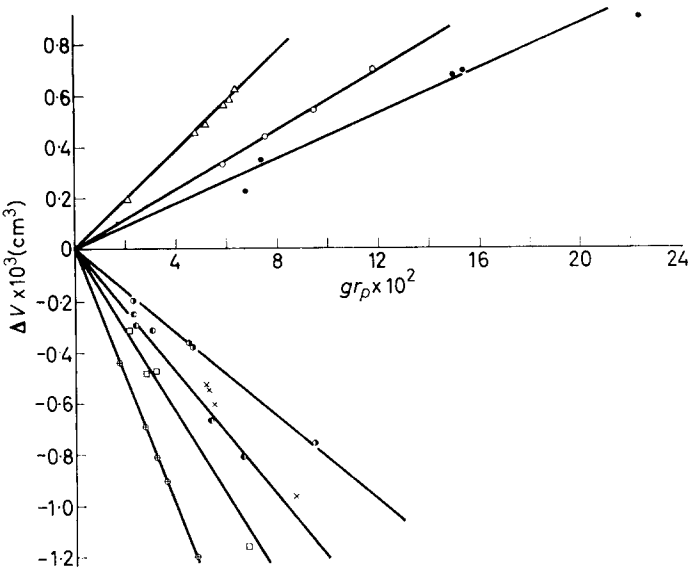

Figure 2—Plot of ΔV against amount of PIB used, in various solvents: ● chlorobenzene, ○ toluene, △ benzene, ◐ methylcyclohexane, ◑ cyclohexane, □ *n*-hexane, ⊕ *n*-heptane, × *n*-decane. Values shown for *n*-hexane (□) are multiplied by a factor 0·5

Table 1 summarizes the average values of ΔV^{mix}, referred to one gramme or to a mole of polymer repeating unit. Errors vary from system to system, reaching a maximum of ±5 per cent for PIB in chlorobenzene. It should be noted that this uncertainty corresponds to a relative change in volume of about one part per million.

Table 1. Average excess volumes at 30°C for dilute PIB solutions in the solvents indicated. One mole unit=56 *gr*

Solvent	$\frac{\Delta V}{gr_p} \times 10^3$ cm^3 (*g polymer*)$^{-1}$	ΔV^{mix} cm^3 (*m.u.*)$^{-1}$	*Solvent*	$\frac{\Delta V}{gr_p} \times 10^3$ cm^3 (*g polymer*)$^{-1}$	ΔV^{mix} cm^3 (*m.u.*)$^{-1}$
Chlorobenzene	+4·4	+0·24	Methylcyclohexane	−12·1	−0·68
Toluene	+5·8	+0·32	*n*-Hexane	−32·2	−1·80
Benzene	+9·6	+0·54	*n*-Heptane	−25·5	−1·43
Cyclohexane	−8·2	−0·46	*n*-Decane	−10·8	−0·60

DISCUSSION

We may now apply equation (1) to convert ΔH_p^{mix} into ΔU_v^{mix} data. The internal pressure P_i appearing in equation (1) should be that of the dilute

Table 2. Comparison between experimental ΔU_V^{mix} and calculated $\Delta U_{V\,(Hild.)}^{mix}$ values of the energy of mixing at constant volume: (a) values at 30°C obtained by using a Tian–Calvet microcalorimeter[12]; (b) estimated from the cohesive energy density

Solvent	ΔH_p^{mix} (*cal/m.u.*)	P_i, *cal/cm*^{3}	$P_i \Delta V^{mix}$, *cal/m.u.*	δ, (*cal/cm*^{3})$^{\frac{1}{2}}$	ΔU_V^{mix}, (*cal/m.u.*)	$\Delta U_{V\,(Hild.)}^{mix}$, (*cal/m.u.*)
Chlorobenzene	160	95[b]	23·5	9·5	136	240
Toluene	99·3[a]	84·8	27·5	8·9	72	116
Benzene	220[a]	90·5	49·0	9·2	171	171
Cyclohexane	−9·6	77·8	−36·0	8·2	26	29
Methylcyclohexane	−15·7	70·9	−48·0	7·85	32	7
n-Hexane	−34	57·1	−103·0	7·3	69	2·5
n-Heptane	−24	61·2	−87·5	7·4	63	~ 0
n-Decane	−7·3	67·0	−40·5	$7{\cdot}7_8$	33	5

polymer solution; it is, however, reasonable to expect that it would not differ significantly from the internal pressure of the pure solvent. We have shown[11] this to be so in two instances, where the P_i of a 0·5 per cent PIB solution in benzene and cyclohexane were measured (at 30°C) to be 92·8 and 79·1 cal/cm^3 respectively, whereas P_i of the pure solvents are 91 and 77·8 cal/cm^3. We have therefore used the P_i values of the pure solvents in what follows.

Table 2 collects all the data necessary to evaluate the energy change on mixing at constant volume.

The data of *Table 1* allow some interesting observations. The negative excess volumes found in paraffinic hydrocarbons (with an absolute value increased by decreasing the number of carbon atoms) is in agreement with previous work of Gee *et al.* on the system PIB–*n*-pentane[13].

The magnitude of this term is sufficient to convert the negative sign of ΔH_p^{mix} for PIB in cyclohexane, methylcyclohexane and paraffinic hydrocarbons into a positive (endothermic) value for ΔU_v^{mix} thus showing agreement with Hildebrand's expectations for such non-polar systems.

Moreover, ΔU_v^{mix} can be compared with the values calculated from the well known equation[1]

$$\Delta U^{mix}_{v(\text{Hildebrand})} = V_M (\delta_P - \delta_S)^2 \varphi_P \varphi_S \qquad (2)$$

where V_M denotes mixture volume, δ_P and δ_S are polymer and solvent solubility parameters, and φ_P and φ_S are polymer and solvent volume fractions. Assuming $\varphi_S \simeq 1$, $V_M \varphi_P \simeq gr$ of polymer/polymer density and, using for PIB[14] $\delta_P = 7{\cdot}5\ (\text{cal/cm}^3)^{\frac{1}{2}}$, we get the values reported in the last column of *Table 2*.

The density value used for PIB at 30°C was 0·94, as interpolated from the values at different temperatures reported by Bawn *et al.* in *Trans. Faraday Soc.* 1956, **52,** 1664.

In spite of the rather large uncertainty characterizing the $\Delta U^{mix}_{v(\text{Hild.})}$ values (δ_P values have been reported[15] in the range 7·5 to 7·8), one can see the calculated values to be in broad agreement with experimental ΔU_v^{mix} except perhaps the systems containing paraffinic hydrocarbons as solvent, where deviations seem to be outside the uncertainty involved.

New ideas[16, 17] about previously ignored contributions to the total heat of mixing in polymer–solvent systems could provide an explanation for these discrepancies and work is in hand to give a rational interpretation of existing heat of mixing measurements.

It is a pleasure to thank Professor C. Rossi for his interest in this work and Mr G. Parma for his collaboration during experimental work.

Istituto di Chimica Industriale,
Sezione V del Centro Nazionale di Chimica delle Macromolecole,
Università di Genova, Via Pastore 3,
Genova (Italy)

(*Received August 1965*)

REFERENCES

[1] HILDEBRAND, J. H. and SCOTT, R. L. *The Solubility of Nonelectrolytes.* Reinhold: New York, 1950
[2] FLORY, P. J. *Principles of Polymer Chemistry.* Cornell University Press: Ithaca, 1953
[3] ROWLINSON, J. S. *Liquids and Liquid Mixtures.* Butterworths: London, 1959
[4] FREEMAN, P. I. and ROWLINSON, J. S. *Polymer, Lond.* 1960, **1,** 20
[5] DELMAS, G., PATTERSON, D. and BÖHME, D. *Trans. Faraday Soc.* 1962, **58,** 2116
[6] BIANCHI, U., PEDEMONTE, E. and ROSSI, C. *Makromol. Chem.* In press
[7] ALLEN, G., GEE, G. and WILSON, G. J. *Polymer, Lond.* 1960, **1,** 456
[8] DELMAS, G., PATTERSON, D. and SOMCYNSKY, T. *J. Polym. Sci.* 1962, **57,** 79
[9] BIANCHI, U., DALPIAZ, M. and PATRONE, E. *Makromol. Chem.* 1964, **80,** 112
[10] LEVIALDI, S., WANKE, E., BIANCHI, U. and CUNIBERTI, C. *Rev. Sci. Instrum.* 1965, **36,** 1750
[11] Unpublished results
[12] BIANCHI, U. and LO GIUDICE, M. Unpublished results
[13] BAKER, C. H., BROWN, W. B., GEE, G., ROWLINSON, J. S., STUBLEY, D. and YEADON, R. E. *Polymer, Lond.* 1962, **3,** 215
[14] FOX, T. G. *Polymer, Lond.* 1962, **3,** 111
[15] MANGARAJ, D., PATRA, S. and RATH, C. *Makromol. Chem.* 1964, **67,** 75
[16] FLORY, P. J. *J. Amer. chem. Soc.* 1965, **87,** 1833
[17] BIANCHI, U. *J. Polym. Sci.* B. 1965, **3,** 1079

The Refinement of the Crystal and Molecular Structures of Polymers using X-Ray Data and Stereochemical Constraints

STRUTHER ARNOTT and A. J. WONACOTT

A general method is described for the automatic determination of the positions, orientations and conformations of molecules in crystals which best correspond to observed X-ray diffraction. The molecular conformations are described in terms of chain parameters, and standard bond lengths and angles are maintained during the refinement. For this reason the method is particularly suitable for establishing structures of polymers in crystalline fibres where the poor quality diffraction data requires to be supplemented by stereochemical information. Additional constraints which ensure that successive monomer units are linked appropriately are achieved by means of Lagrange multipliers. Refinement of the structures of Terylene and α-poly-L-alanine are used to illustrate successful application of this approach in the analysis of polymer structure.

IN THE solid state the highest degree of order attained by most polymers is in crystalline fibres. These may be considered to be arrays of microcrystals randomly arranged except that each has the same single axis parallel to the fibre length. The X-ray diffraction pattern therefore has the character of a single crystal rotation diagram, with the possibility of overlap of reflections on the layer lines. (Then, only the sum of the intensities in the group can be measured.) The quality of the data is frequently poor because of the difficulty of measuring intensities against a background of diffuse scattering from the non-crystalline regions of the fibre or from disorder within the crystallites. In addition, the parallelism of the crystallites is invariably imperfect and the diffracted intensities are distributed not in spots but along arcs the length of which increases with distance from the pattern centre. This dissipation of diffracted intensity over increasing lengths of arc implies a similar rise in the threshold for observation and even at moderate distances from the pattern centre all but the strongest intensities are merged in the background. The result is that the number of data is much less than that which could be obtained from a single crystal, and also that the resolving power of the data is low since it is the diffraction furthest from centre that defines the finer periodicities in crystals. (For Cu $K\alpha$ X-radiation of wavelength, $\lambda = 1{\cdot}5418$Å, a single crystal of Terylene theoretically could give 588 independent reflections with an *average* spacing of 1Å, while only 140 reflections occur in the observable region for the crystalline fibre, the *lowest* periodicity being 1·1Å.) This lack of resolving power in the diffraction data has limited or precluded the use of the powerful methods of conventional crystallography such as Fourier synthesis of electron density or least-squares refinement of atomic parameters since in the former, atomic positions would not be located, and in the latter, the calculated diffraction amplitudes are insufficiently sensitive to changes in individual atomic coordinates even

where there is a sufficient excess of data over parameters for the method to be undertaken. Consequently the usual method of structure refinement in such cases has been to incorporate knowledge of chemical sequence, bond lengths and angles in molecular models and then, by systematic trial and error, to adjust their conformations and crystal positions to obtain a good agreement between the observed amplitudes of diffraction, ${}_oF$, and the structure amplitudes, F, calculated from the model system. In the use of such methods it is difficult to decide that the best fit achieved is indeed the best fit possible and where competing model systems exist which give similar diffraction patterns it may, for that reason, be difficult convincingly to demonstrate that one system is preferable, and to what degree this is so.

In the following we describe a method for refining the positional and conformational parameters of model systems while retaining given stereochemical constraints. It is readily adaptable for automatic digital computers and is related to one studied for DNA fibres[1] and to others described for single crystals[2-5].

MATHEMATICAL ANALYSIS OF THE REFINEMENT

The 'best fit' considered to be that which minimizes

$$\Phi=\sum_1^M w_m\,({}_oF_m-F_m)^2=\sum_1^M w_m\Delta F_m^2 \tag{1}$$

where there are M observed diffraction amplitudes, ${}_oF_m$, and F_m are the corresponding amplitudes calculated for the model.

$$F_m=(A_m^2+B_m^2)^{\frac{1}{2}}\,.\,(1/K)\,.\exp\,(-B\rho^2/4) \tag{2}$$

where

$$A_m=\sum_1^P f_p\,(h_mk_ml_m)\cos\,2\pi\,(h_mx_p+k_my_p+l_mz_p) \tag{2a}$$

and

$$B_m=\sum_1^P f_p\,(h_mk_ml_m)\sin\,2\pi\,(h_mx_p+k_my_p+l_mz_p) \tag{2b}$$

when there are P atoms with fractional cartesian coordinates $(x_py_pz_p)$ in the crystal unit; $f_p\,(h_mk_ml_m)$ is the scattering power of the pth atom and $h_mk_ml_m$ are the indices of the X-ray reflection; K is the factor required to put the observations on an absolute scale; B is the average isotropic thermal vibration parameter which results in a radial fall-off of diffraction intensity; $\rho=2\,(\sin\theta)/\lambda$ where θ is the diffraction angle. w_m, the weight of each term in Φ, should be proportional to the reliability of ${}_oF_m$. Usually an analytic function $\{(1+a\,.\,{}_oF_m+b\,.\,{}_oF_m^2)\,.\,\rho\}^{-1}$ is satisfactory. a and b are chosen constants which result in the very intense reflections having low weights while ρ^{-1} reduces the weight of the reflections in the outer part of the diffraction pattern where observed intensities have large geometrical factors to convert them to ${}_oF_m$s. When a reflection is composite

$$F_m=(\sum_1^B F_{mr}^2)^{\frac{1}{2}}\,.\,(1/K)\,.\exp\,(-B\rho^2/4) \tag{2c}$$

where the F_{mr}s are the amplitudes of the reflections in the group.

If we begin with a model with N parameters $[u_n]$ we can obviously calcu-

late the value of Φ. If we change the parameters to $[u_n + \Delta u_n]$ the new value of Φ will be by Taylor's expansion

$$\Phi = \sum_1^M w_m \left\{ \Delta F_m([u_n]) - \sum_1^N \Delta u_n \frac{\partial F_m([u_n])}{\partial u_n} \right\}^2 \tag{3}$$

if the terms in $(\Delta u_n)^2$ are small, which will be so if the position represented by $[u_n - \Delta u_n]$ is close enough to $[u_n]$. The N values of $[\Delta u_n]$ which will minimize Φ are given by the N linear equations $\partial\Phi/\partial(\Delta u_n) = 0$, i.e. by N equations like

$$\partial\Phi/\partial(\Delta u_q) = -2\sum_1^M w_m \left\{ \Delta F_m - \sum_1^N \Delta u_n \frac{\partial F_m}{\partial u_n} \right\} \frac{\partial F_m}{\partial u_q} = 0 \tag{4}$$

They may be conveniently written in matrix notation (which also provides an indication of how they may be solved using standard computer routines)

$$\mathbf{F}.\mathbf{M} - \mathbf{U}.\mathbf{M}^T.\mathbf{M} = 0$$

i.e.

$$\mathbf{U} = \mathbf{F}.\mathbf{M}.(\mathbf{M}^T.\mathbf{M})^{-1} \tag{5}$$

where

$$\mathbf{F} \equiv [\sqrt{w_1}\Delta F_1 \ldots\ldots\ldots\ldots \sqrt{w_m}\Delta F_m] \tag{6}$$

$$\mathbf{M} \equiv \begin{bmatrix} \sqrt{w_1}\dfrac{\partial F_1}{\partial u_1} & \ldots\ldots\ldots & \sqrt{w_1}\dfrac{\partial F_1}{\partial u_N} \\ \vdots & & \vdots \\ \sqrt{w_m}\dfrac{\partial F_M}{\partial u_1} & \ldots\ldots\ldots & \sqrt{w_m}\dfrac{\partial F_M}{\partial u_N} \end{bmatrix} \tag{7}$$

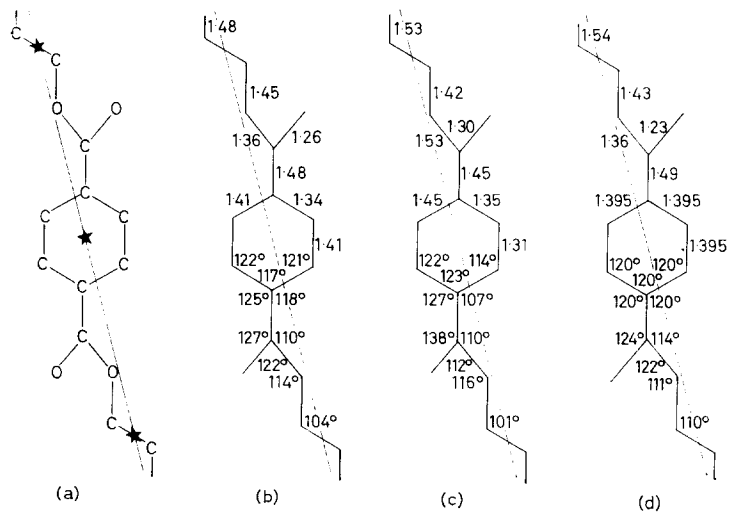

Figure 1—The refinement of Terylene. (a) the chemical constitution with stars indicating where molecular centres of symmetry coincide with ones in the crystal unit cell. The bond lengths and angles (b) calculated from the coordinates of Daubeny, Bunn and Brown[6] (c) after atomic coordinate refinement by least-squares and (d) used in the present constrained least-squares analysis

$$\mathbf{U} = [\Delta u_1 \ldots\ldots\ldots\ldots\ldots \Delta u_N] \tag{8}$$

In general equation (3) is an inadequate approximation (the $[\Delta u_n]$ are not small enough) and the parameters $[u_n + \Delta u_n]$ obtained after solving (5) will not give minimum Φ and the process has to be repeated with the new parameters and iterated until the $[\Delta u_n]$ are so small that Φ does not change significantly in successive cycles.

When the structure parameters refined are the fractional cartesian co-ordinates of the atoms in the crystal unit we have the case usual in single crystal analyses. What happens when this approach is used in refining the structure of Terylene is illustrated in *Figure 1*. There are 72 above threshold reflections, 23 parameters and even with this data/parameter ratio unusually favourable, convergence to a position with negligible shifts was achieved only after twenty refinement cycles from initial parameters given for the best published model[6]. In token of the inadequacies of the data for the reasons previously cited there are large estimated standard deviations in the coordinates, equivalent to 0·1Å in bond lengths and 6° in bond angles. Nevertheless no bond length or angle differs from the expected one by more than three times the standard deviation.

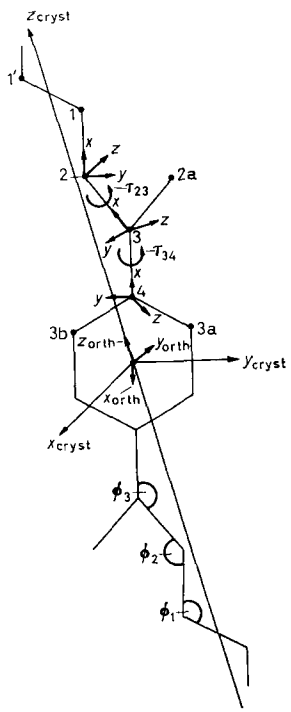

Figure 2—The chain geometry of Terylene. ϕ_1, ϕ_2 and ϕ_3 are bond angles along the chain

The scheme we have devised allows a set of standard bond lengths and angles to be included explicitly in the least-squares analysis. This is achieved in the manner indicated in *Figure 2* where Terylene is the example chosen. The unit in the Terylene molecule consists of four main chain atoms,

1, 2, 3, 4, and three substituents, 2a, 3a, 3b (for the moment hydrogen atoms will be ignored). Sets of axes may be set up at each atom of the main chain after the first in a systematic way such that in each case the x axis lies along the bond between atom n and atom $(n-1)$; the y axis is perpendicular to the x axis and lies within the obtuse angle formed by atoms $(n-1)$, n, and $(n+1)$ and is coplanar with them; the z axis completes a right-handed orthogonal set. The coordinates of atom 1 with respect to the set of axes at 2 are immediately known and are given by

$$\mathbf{X}_2=\mathbf{L}_{12}=\begin{bmatrix} l_{12} \\ 0 \\ 0 \end{bmatrix}$$

where l_{12} is the bond length between atoms 1 and 2. Its coordinates with respect to the next axial system at atom 3 are

$$\mathbf{X}_3=\begin{bmatrix} -\cos\phi_2 & -\sin\phi_2 & 0 \\ \sin\phi_2\cos\tau_{23} & -\cos\phi_2\sin\tau_{23} & \sin\tau_{23} \\ -\sin\phi_2\cos\tau_{23} & \cos\phi_2\sin\tau_{23} & \cos\tau_{23} \end{bmatrix}.\mathbf{X}_2+\begin{bmatrix} l_{23} \\ 0 \\ 0 \end{bmatrix}$$

i.e. $$\mathbf{X}_3=\mathbf{A}_{23}\mathbf{X}_2+\mathbf{L}_{23}=\mathbf{A}_{23}\mathbf{L}_{12}+\mathbf{L}_{23} \tag{9}$$

This transformation involves the stereochemical constants ϕ_2 and l_{23} together with angle τ_{23}, the dihedral angle between the plane formed by atoms 1, 2 and 3 and that formed by 2, 3 and 4. It is this angle which is regarded as a refinable parameter of the chain. A further similar transformation involving ϕ_3, τ_{34} and l_{34} will yield the coordinate of atom 1 with respect to the axial set at 4.

$$\mathbf{X}_4=\mathbf{A}_{34}\mathbf{X}_3+\mathbf{L}_{34}=\mathbf{A}_{34}\mathbf{A}_{23}\mathbf{L}_{12}+\mathbf{A}_{34}\mathbf{L}_{23}+\mathbf{L}_{34} \tag{10}$$

It is clear that the coordinates of all the atoms in the asymmetric unit of Terylene with respect to the axial set at 4 can be derived in a similar way as functions of the chain parameters τ_{23} and τ_{34} and the various bond lengths and angles. It remains only to relate them to the unit cell axes. Since crystal axes are not generally orthogonal it is convenient to define an orthogonal set which has $z_{\text{orthogonal}}$ coincident with z_{crystal}, $y_{\text{orthogonal}}$ in the same plane as y_{crystal} and z_{crystal}.

Coordinates can then be transformed to a set at 4 parallel to the crystal set by

$$\mathbf{X}_{\text{orthogonal}}=\mathbf{R}.\mathbf{X} \tag{11}$$

where

$$\mathbf{R}=\begin{bmatrix} 1 & 0 & 0 \\ 0 & \cos\theta_1 & -\sin\theta_1 \\ 0 & \sin\theta_1 & \cos\theta_1 \end{bmatrix}\begin{bmatrix} \cos\theta_2 & 0 & -\sin\theta_2 \\ 0 & 1 & 0 \\ \sin\theta_2 & 0 & \cos\theta_2 \end{bmatrix}\begin{bmatrix} \cos\theta_3 & -\sin\theta_3 & 0 \\ \sin\theta_3 & \cos\theta_3 & 0 \\ 0 & 0 & 1 \end{bmatrix} \tag{12}$$

θ_1, θ_2 and θ_3 are the Eulerian angles relating the orientation of the axial set 4 to the orthogonal crystal set. A final transformation

$$\mathbf{X}_{\text{crystal}}=\mathbf{C}.\mathbf{X}_{\text{orthogonal}}+\mathbf{T} \tag{13}$$

yields fractional crystal coordinates

$$\mathbf{C}=\begin{bmatrix} \dfrac{1}{a\sin\beta\sin\gamma^*} & 0 & 0 \\ \dfrac{1}{b\sin\alpha\tan\gamma^*} & \dfrac{1}{b\sin\alpha} & 0 \\ \dfrac{-(\sin\beta\cos\gamma^*+\tan\alpha\cos\beta)}{c\tan\alpha\sin\beta\sin\gamma^*} & \dfrac{-1}{c\tan\alpha} & \dfrac{1}{c} \end{bmatrix} \tag{14}$$

$$\mathbf{T}=\begin{bmatrix} u_1 \\ u_2 \\ u_3 \end{bmatrix} \tag{15}$$

u_1, u_2, u_3 are the fractional crystal coordinates of atom 4 and are the parameters necessary to define the position of the chain. For example, for atom 1

$$\mathbf{X}_{\text{crystal}}=\mathbf{C.R.A}_{34}\mathbf{A}_{23}\mathbf{L}_{12}+\mathbf{C.R.A}_{34}\mathbf{L}_{23}+\mathbf{C.R.L}_{34}+\mathbf{T} \tag{16}$$

and there are similar expressions for the coordinates of the other atoms.

For pendant atoms like 2a the first set of coordinates (with respect to axial set 3) would be

$$\mathbf{X}=\begin{bmatrix} \lambda l_{3\,2a} \\ \mu l_{3\,2a} \\ \nu l_{3\,2a} \end{bmatrix}$$

where $l_{3\,2a}$ is the length of the 3—2a bond and λ, μ, ν are the (stereochemically predetermined) direction cosines of 3—2a in the axial system 3.

This description of a chain molecule is entirely general and since it involves a set of systematic transformations in matrix form it is readily adaptable for automatic computation. The immediate advantages achieved, apart from the important one of maintaining predetermined bonded stereochemistry, are twofold: the number of parameters is reduced by a factor of two (in the case of Terylene) and since changes in these parameters will, in general, result in movements of large groups of atoms the lack of resolving power in the diffraction data becomes irrelevant.

To set up the least-squares equation the coefficients of $\mathbf{M}$, $\partial F_m/\partial u_n$, must be determined.

In equation (2) F_m is not an explicit function of τ_{23}, τ_{34}, θ_1, θ_2, θ_3, u_1, u_2, u_3 and it is desirable to use

$$\frac{\partial F_m}{\partial u_n}=\sum_1^P\left(\frac{\partial F_m}{\partial x_p}\frac{\partial x_p}{\partial u_n}+\frac{\partial F_m}{\partial y_p}\frac{\partial y_p}{\partial u_n}+\frac{\partial F_m}{\partial z_p}\frac{\partial z_p}{\partial u_n}\right) \tag{17}$$

since $\partial F_m/\partial x_p$ etc. and $\partial x_p/\partial u_n$ are easily calculated.

As it stands the analysis has one important deficiency: it does not ensure that the correct stereochemistry is maintained at the junction of successive chain units, i.e., in the Terylene example, it does not ensure that the implicit relationship will exist among τ_{23}, τ_{34}, θ_1, θ_2, θ_3, u_1, u_2, u_3 which will result in $l_{11'}$ and ϕ_2 having their normal values. Nor does it ensure that the benzene ring centre coincides with the origin of the crystallographic axes. It is not easy explicitly to ensure that the parameters refined are appropriately constrained. This may be done implicitly using Lagrange multipliers.

If there should exist H, $H < N$, implicit relationships $G_h = 0$, among the parameters $[u_n]$ then the best least-squares fit under these constraining conditions is obtained by minimizing

$$\Theta = \sum_1^M w_m \Delta F_m^2 + \sum_1^H \lambda_h G_h \tag{18}$$

As in equation (3), at a nearby point $[u_n + \Delta u_n]$,

$$\Theta = \sum_1^M w_m \left\{ \Delta F_m - \sum_1^N \Delta u_n \frac{\partial F_m}{\partial u_n} \right\}^2 + \sum_1^H \lambda_h \left\{ G_h + \sum_1^M \Delta u_n \frac{\partial G_h}{\partial u_n} \right\} \tag{19}$$

and the values of $[\Delta u_n]$ and $[\lambda_h]$ which will make Θ a minimum are given by N linear equations

$$\partial \theta / \partial (\Delta u_q) = -2 \sum_1^M w_m \left\{ \Delta F_m - \sum_1^N \Delta u_n \frac{\partial F_m}{\partial u_n} \right\} \frac{\partial F_m}{\partial u_q} + \sum_1^H \lambda_h \frac{\partial G_h}{\partial u_q} = 0 \tag{20}$$

and H linear equations

$$\partial \theta / \partial \lambda_r = G_r + \sum_1^N \Delta u_n \frac{\partial G_r}{\partial u_n} = 0 \tag{21}$$

$[\Delta u_n]$ and $[\lambda_h]$ can be obtained by a matrix process reminiscent of equation (5)

$$[\mathbf{U} \mid \mathbf{L}] \left[\begin{array}{c|c} \mathbf{M}^T.\mathbf{M} & \frac{1}{2}\mathbf{N} \\ \hline \frac{1}{2}\mathbf{N}^T & \mathbf{0} \end{array} \right] = [\mathbf{F}.\mathbf{M} \mid \tfrac{1}{2}\mathbf{G}] \tag{22}$$

In these partitioned matrices **F**, **M**, **U**, are defined by the conditions (6), (7) and (8)

$$\mathbf{L} = [\lambda_1 \ \lambda_2 \ldots\ldots\ldots\ldots \lambda_H] \tag{23}$$

$$\mathbf{N} = \begin{bmatrix} \frac{\partial G_1}{\partial u_1} & \ldots\ldots\ldots\ldots & \frac{\partial G_H}{\partial u_1} \\ \cdot & & \cdot \\ \cdot & & \cdot \\ \cdot & & \cdot \\ \frac{\partial G_1}{\partial u_N} & \ldots\ldots\ldots\ldots & \frac{\partial G_H}{\partial u_N} \end{bmatrix} \tag{24}$$

$$\mathbf{G} = [-G_1 \ldots\ldots\ldots\ldots -G_H] \tag{25}$$

In Terylene $H = 5$ and

$$G_1 = \phi_1 - 109{\cdot}5^\circ \tag{26}$$

$$G_2 = a^2x_1^2 + b^2y_1^2 + c^2(z_1 - \tfrac{1}{2})^2 + 2bc \cos\alpha\,(z_1 - \tfrac{1}{2})y_1 + 2ac \cos\beta\,(z_1 - \tfrac{1}{2})\,x_1 + 2ab \cos\gamma\, x_1 y_1 (0{\cdot}77)^2 \tag{27}$$

$$G_3 = a^2x_4^2 + b^2y_4^2 + c^2z_4^2 + 2bc \cos\alpha\, z_4 y_4 + 2ac \cos\beta\, z_4 x_4 + 2ab \cos\gamma\, x_4 y_4 - (1{\cdot}395)^2 \tag{28}$$

$$G_4 = a^2x_{3a}^2 + b^2y_{3a}^2 + c^2z_{3a}^2 + 2bc \cos\alpha\, z_{3a}y_{3a} + 2ac \cos\beta\, z_{3a}x_{3a} + 2ab \cos\gamma\, x_{3a}y_{3a} - (1{\cdot}395)^2 \tag{29}$$

$$G_5 = a^2x_{3b}^2 + b^2y_{3b}^2 + c^2z_{3b}^2 + 2bc \cos\alpha\, z_{3a}y_{3a} + 2ac \cos\beta\, z_{3a}x_{3a} + 2ab \cos\gamma\, x_{3a}y_{3a} - (1{\cdot}395)^2 \tag{30}$$

Equation (27) ensures that $l_{11'}=1{\cdot}54$Å and that (0 0 $\frac{1}{2}c$) is the centre of the 1—1′ bond; (28), (29) and (30) ensure that the benzene ring is centred on the unit cell origin.

RESULTS

A general computer programme capable of refining any long chain molecule with short side chains according to this scheme has been devised for the ATLAS computer. Using it a model of the Terylene structure was refined and a reduction of $\Phi=\Sigma w_m\Delta F_m^2$ from 14 617 to a minimum value 4 058 achieved after 12 cycles, each taking six seconds, by which time the shifts were less than a quarter of the estimated standard deviations in the parameters. The mean shift in θ was 1·7° and in τ, 10·1°, corresponding to changes in atomic position up to 1Å. The conventional crystallographic index of reliability, $R=\Sigma\mid\Delta F_m\mid/\Sigma_o F_m$, was reduced from 0·28 to 0·237 during the refinement. This value is not significantly inferior to that obtained previously[6] (0·19) whose model did not have standard bond lengths and angles, see *Figure 1*. R is of course much smaller (0·13) for the refinement of atomic parameters since the greater the number of variables the better the fit that can be achieved. The Daubeny, Bunn, Brown model (DBB) and the refined models have no non-bonded interatomic distance less than the accepted van der Waals distances. τ_{34} is expected to be approximately zero because of conjugation of the carboxyl group with the benzene ring; in the present study its value was found to be 7°, in DBB it was 12°. Further, although the hydrogen attached to atoms 1, 3a and 3b were ignored in this discussion, they were in fact included in the analysis as pendant atoms since no extra parameters are required once their relationship with the chain atoms is defined.

Terylene was unusual in providing more diffraction data than are normally available from crystalline fibres. In contrast only 61 X-ray reflections are observed for poly-L-alanine. Previous studies[7,8] have established that the molecule is a right-handed α-helix with 47 L-alanine residues in 13 turns of the helix. There is the equivalent of only 47 residues per unit cell but the crystal structure is apparently a statistical one with 'up-pointing' and 'down-pointing' molecules occurring at random (the α-helix possesses chain sense —CO . N H . CHR—). The statistical unit cell contains therefore 470 half atoms heavier than hydrogen and since the highest crystallographic symmetry present is a two fold axis relating 'up' and 'down' molecules, 705 atomic coordinates need to be determined. A least-squares analysis can only be undertaken when the number of data observed is greater than the number of parameters to be refined and this can be achieved here if the molecule is described as a regular helix and the structure amplitudes and their derivatives are expressed as functions of the atomic positions in the *molecular* asymmetric unit[9]. Then the data/crystal parameter ratio becomes 61/19 at most. (This assumes that 'up' and 'down' molecules have the same conformation, that their helix axes coincide and that only one translational and one rotational parameter are then required to fix their relative positions.) By describing the molecular conformation in terms of chain parameters (see *Figure 3*) only 11 crystal structure parameters are necessary and 5 constraints can be defined to ensure that the 1—2 bond is the helical repeat of

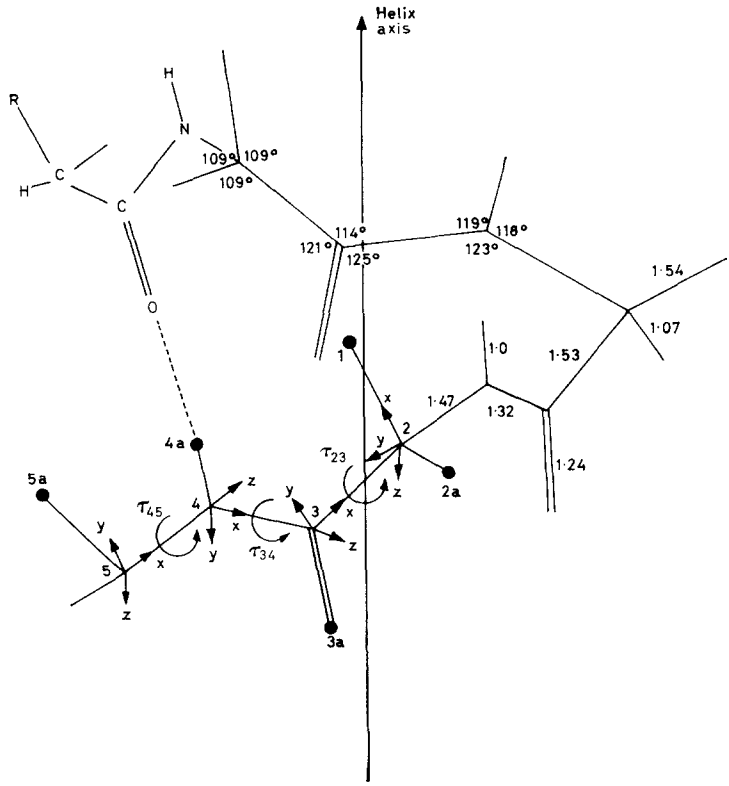

Figure 3—Four residues of an α-helix showing the chemical constitution, standard bond lengths and angles, and the chain geometry of poly-L-alanine. R denotes methyl

5a—5. The data/parameter ratio is then effectively increased to $61/(11-5)$ and a continuous α-helix with standard stereochemistry ensured.

It has been found convenient to have a separate programme for regular helical structures. Using it the structure of poly-L-alanine has been refined in eight cycles each taking 30 seconds. The initial model had $\Phi = 550/643$, $R = 0{\cdot}452$, the final one $\Phi = 164\,029$, $R = 0{\cdot}235$. The refined chain parameters result in the NH—O hydrogen bond having a length of 2·86Å and being very close to linear, the angle O—N—H being 13°. In addition $\tau_{3\text{-}1} = 179°$ with an estimated standard deviation of 10° so that the amide groups are planar. These results support the belief that the backbone is indeed a regular helix. However, it is necessary to postulate that the methyl groups are distorted on average up to 0·1Å from regular helical positions both to avoid short methyl–methyl contacts and to explain additional meridional reflections which could not be produced by a regular α-helix. This implies bond angle distortions averaging 3° which are possible without greatly increasing the energy of the system. The refined crystal structure can be used to predict the position and intensity of streaks in the diffraction pattern which result from the statistical nature of the structure and these

have been found to coincide with the observed ones. It is proposed to discuss the analysis and its result in more detail in a separate paper.

CONCLUSION

This analytical method is of completely general application in the refinement of molecular models with respect to X-ray data. The incorporation of chain parameters and constraints avoids meaningless changes in atomic parameters, while the resulting smaller number of parameters allows a sharper average to be drawn over errors in poor quality data. With fibres this is peculiarly important because of the smaller number of data. The reduction in the number of parameters avoids also the necessity of handling matrices of large order and since the parameters allow cooperative movement of large numbers of atoms the probability of poor initial models converging to the correct refined one is considerably increased.

We are obliged to Professor Sir John Randall, F.R.S., for provision of facilities, to Dr Arthur Elliott for help and encouragement and to the Science Research Council for a grant to A.J.W.

M.R.C. Biophysics Research Unit and
King's College London Dept. of Biophysics,
26–29 Drury Lane, London, W.C.2

(*Received November 1965*)

REFERENCES

[1] ARNOTT, S. and COULTER, C. L. *Acta cryst., Camb.* 1963, **16,** A175
[2] SCHERINGER, C. *Acta cryst., Camb.* 1963, **16,** 546
[3] ROLLETT, J. S. *Acta cryst., Camb.* 1963, **16,** A175
[4] BRÄNDEN, C-I., HOLMES, K. C. and KENDREW, J. C. *Acta cryst., Camb.* 1963, **16,** A175
[5] WASER, J. *Acta cryst., Camb.* 1963, **16,** 1091
[6] DAUBENY, R., BUNN, C. W. and BROWN, C. J. *Proc. Roy. Soc.* 1954, **226,** 531
[7] BROWN, L. and TROTTER, I. F. *Trans. Faraday Soc.* 1954, **52,** 537
[8] ELLIOTT, A. and MALCOLM, B. R. *Proc. Roy. Soc.* 1958, **249,** 30
[9] COCHRANE, W., CRICK, F. and VAND, V. *Acta cryst., Camb.* 1952, **5,** 581

The Dilute Solution Properties of Poly(propylene oxide)

G. ALLEN, C. BOOTH and C. PRICE

The dilute solution properties of several fractions of poly(propylene oxide) have been determined in two solvent systems; hexane at 46°C and iso-octane in the temperature range 46° to 89°C. In general these properties show no dependence on the degree of tacticity of the fractions. An exception is the second virial coefficient measured by light scattering in hexane at 46°C, which varies considerably from fraction to fraction. A tentative explanation, in terms of the incipient crystallization of the polymer, is advanced to account for this anomaly.

MOST studies of the influence of the degree of tacticity of a polymer upon its dilute solution properties lead to the view that the solution parameters do vary, but that this variation is seldom much greater than the errors involved in the measurements. The position has been summarized by Krigbaum *et al.*[1]. By contrast we have presented results which suggest that the dilute solution properties of poly(propylene oxide) in hexane at 46°C are greatly affected by the structural regularity of the polymer[2]. In that work the second virial coefficients of fractions of poly(propylene oxide), dissolved in hexane at 46°C, were shown to vary from $-1{\cdot}8 \times 10^{-4}$ cm^3 g^{-2} mole for the most isotactic fraction to $+4{\cdot}0 \times 10^{-4}$ cm^3 g^{-2} mole for the most atactic fraction. These data could only be explained in terms of dilute solution theory if the theta temperatures for the fractions ranged over 40 centigrade degrees[2]. Unfortunately it proved impossible to measure theta temperatures directly because most of the fractions available crystallized from hexane at relatively high temperatures; for this reason the interpretation of the data remained in doubt. In this work we have re-examined the dilute solution properties of poly(propylene oxide) in order to answer the question as to whether the properties of poly(propylene oxide) are exceptional or whether specific interactions, which are not accounted for by dilute solution theory, are playing an important role in the system.

We have chosen to repeat the measurements in hexane and also to use iso-octane as a solvent. Iso-octane is a poorer solvent for poly(propylene oxide) than is hexane and we hoped to observe theta conditions at temperatures high enough to preclude crystallization. An additional advantage was the higher boiling point of iso-octane, which enabled measurements to be made over a wide range of temperature. A disadvantage was the small difference in refractive index between iso-octane and poly(propylene oxide); the measurement of the dilute solution parameters by light scattering was more difficult on this account.

EXPERIMENTAL

Materials

The poly(propylene oxide) was prepared by means of the zinc diethyl–water catalyst using techniques developed by Powell *et al.*[3]. Briefly, pro-

pylene oxide (6·8 mole l^{-1}), zinc diethyl (0·52 mole l^{-1}) and water (0·48 mole l^{-1}) were mixed in dioxan under high vacuum conditions and allowed to polymerize at 25°C for one week. The reaction mixture was dissolved in benzene to which had been added a little methanol, and the catalyst residues were removed by centrifugation. The product was finally isolated by freeze drying. The conversion was better than 90 per cent.

The solvents used for fractionation and measurement of solution properties were dried and fractionally distilled. In order to minimize degradation of the poly(propylene oxide), hindered phenol antioxidants were added to the solutions at a concentration of about one per cent that of the polymer.

Intrinsic viscosities

The viscosities of dilute solutions were measured by use of modified Desreux–Bischoff viscometers of low shear stress. Intrinsic viscosities were obtained by extrapolation of data to zero concentration. Viscosity-average molecular weights could be calculated by means of the relationship established[4] for benzene at 25°C.

$$[\eta] = 1{\cdot}12 \times 10^{-4}\ \overline{M}_v^{0{\cdot}77}$$

Melting points

Melting points (T_m) were determined by means of a polarizing microscope fitted with a hot stage; crystallization temperatures of 40°C and a heating rate of 12 deg h^{-1} were used.

Fractionation

Poly(propylene oxide) was fractionated by cooling a dilute solution of the polymer in iso-octane, and separating the crystalline precipitates by filtration. Details of the technique have been given earlier[2].

Light scattering

Light scattering measurements were made over the temperature range 40° to 89°C using a Sofica photometer. Polymer solutions and solvents on which light scattering measurements were carried out were clarified by centrifugation. This was done in a No. 30 rotor of a Spinco Model L preparative ultracentrifuge for at least 1·5 h at 20 000 rev/min. The relatively large volume of dust-free solvent required for rinsing out glassware before each experiment was clarified by filtration through 100 mμ Millipore filters. Light scattering was performed with light of wavelength 546 mμ at ten angles between 30° and 150° for each of four dilutions. No significant depolarization of the scattered light was detected. The instrument was calibrated using benzene for which the Rayleigh ratio was known over a range of temperature[5]. For high temperature measurements it was found more convenient to use the glass reference standard, supplied by Sofica, which had been calibrated against benzene.

The second virial coefficient, A_2, the weight-average molecular weight, $\overline{M}_w$, and the z-average mean-square-radius of gyration $(\overline{S^2})_z$ were calculated using the equation

$$(Kc/R_\theta)_{\substack{c\to 0\\ \theta\to 0}} = (1/\overline{M}_w)\,[1 + \tfrac{1}{3}\mu^2\,(\overline{S}^2)_z^{\frac{1}{2}}] + 2A_2c \qquad (1)$$

where $\mu = (4\pi/\lambda)\sin\frac{1}{2}\theta$ and the other symbols have their usual meaning[6].

In order to evaluate the parameter K in equation (1) it was necessary to measure the refractive index increment, dn/dc. Since the light scattering study of poly(propylene oxide) in iso-octane was made over a range of temperature, dn/dc had to be known as a function of temperature. A Brice–Phoenix differential refractometer fitted with a lagged water jacket was used for the determination of refractive index increments up to 60°C. Above this temperature values of K were obtained by substituting known values of $\overline{M}_w$ into the equation

$$K = (R_\theta/\overline{M}_w c)_{\substack{c=0\\ \theta=0}}$$

RESULTS

Fractionation

A portion of the poly(propylene oxide), designated part A, was fractionated by crystallization from dilute solution. The fractionation data, which are given in *Table 1*, are similar to those presented earlier[2] with the exception of the molecular weights of fractions A7 and A8, which are higher than

Table 1. Fractionation data for poly(propylene oxide)—Part A

Fraction	*Crystallization temperature from iso-octane, °C*	*Wt %*	*$[\eta]$ dl g^{-1} (Benzene at 25°C)*	*T_m °C*
A1	47	2·99	6·82	69
A2	46	2·31	6·10	67
A3	45	1·72	6·78	66
A4	44	1·80	7·26	63
A5	43	1·12	7·0	63
A6	41	1·69	6·27	61
A7	41	1·03	9·61	58
A8	0	64·8	10·21	
Residue*	—	22·5		

*The residue was a low molecular weight fraction. Similar fractions have been shown to have $\overline{M}_n \simeq 700$.

anticipated. Since the fractional crystallization of high molecular weight poly(propylene oxide) almost certainly occurs solely on the basis of structural regularity[7], we conclude that the preparation conditions we used produced, inadvertently, a polymer having a dependence of structural regularity on molecular weight. Accordingly, a second portion of the poly(propylene oxide), designated part B, was degraded mechanically before fractionation. A solution containing 3%-wt of the poly(propylene oxide) and a little antioxidant in benzene was stirred using an Ultra-Turrax homogenizer rotating at approximately 20 000 rev/min. The temperature of the solution was kept below 35°C by surrounding the flask containing the solution with ice–water and switching off the homogenizer at ten-minute intervals. After a total stirring time of three hours the viscosity of the solution ceased to fall and the maximum amount of degradation possible under

these conditions had been achieved. The polymer was recovered from solution by freeze drying.

The fractionation data for part B are recorded in *Table 2*. The molecular structure no longer depends on the molecular weight; all the fractions of

Table 2. Fractionation data for poly(propylene oxide)—Part B

Fraction	*Crystallization temperature from iso-octane, °C*	*Wt %*	$[\eta]$ *dl* g^{-1} *(Benzene at 25°C)*	T_m *°C*
B1	45	2·43	3·77	69
B2	44	0·95	3·71	67
B3	43	1·32	3·83	66
B4	42	1·27	3·84	65
B5	41	2·01	4·03	62
B6	38	2·28	3·86	62
B7	36	4·02	3·40	59
B8	30	61·12	4·04	—
Residue	0	23·60	—	—

high molecular weight have similar intrinsic viscosities regardless of their melting point. We have demonstrated earlier[2] that a fractional crystallization of this type yields fractions of similar molecular weight distribution. With part B we can expect that this distribution will be fairly narrow, since it is formed by a mechanical degradation process in solution; we have evidence of this from the light scattering measurements. These measurements also show that no detectable amount of branching (or crosslinking) occurred during the degradation process. Thus the fractions isolated from part B were excellent material with which to study the dilute solution properties of poly(propylene oxide), since molecular weight, molecular weight distribution and branching had all been eliminated as variables.

Dilute solution properties

Light scattering data for fractions of poly(propylene oxide) in hexane at 46°C are given in *Table 3*; these data substantiate the claim that the second virial coefficient in hexane increases markedly as the structural regularity of the polymer decreases. By contrast the light scattering data obtained over a range of temperatures for selected fractions in iso-octane, given in *Table 4*, show little variation in A_2.

Table 3. Light scattering data: poly(propylene oxide) in hexane at 46°C

Fraction	$\overline{M}_w \times 10^{-6}$	$A_2 \times 10^4$ *cm³ g⁻² mole*	$\overline{(S^2)}_z^{\frac{1}{2}}$ *Å*
B1	0·783	0·46	535
B3	0·833	0·93	565
B5	0·881	1·18	578
B7	0·651	2·10	519
B8	0·901	4·50	503

Table 4. Light scattering data: poly(propylene oxide). Fractions in iso-octane

Fraction	*T*, °C	$A_2 \times 10^4$ $cm^3\ g^{-2}\ mole$	$(\overline{S^2})_z^{\frac{1}{2}}$ *A*
B8	48	0	348
	49	0	331
	53	0·26	344
	57·5	0·76	348
	64·0	0·91	351
	69·0	0·98	369
	71·5	1·40	364
	81·0	1·60	361
	85·0	1·58	375
B1	50	−0·25	358
	55	0·50	354
	60	0·65	365
	70·5	1·13	386
	76	1·56	392
	86	1·81	385
	89	1·72	398
B5	50	0·10	339
	59·0	0·46	361
	70	0·90	370
A8	46	−0·20	
	50	0·00	
A1	57·5	0·66	
	66·5	0·97	
	79·0	1·14	
	89·0	1·40	

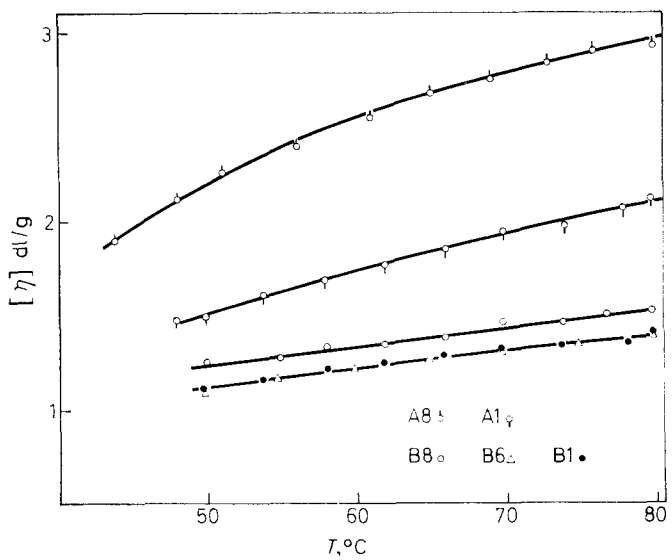

Figure 1—Temperature dependence of intrinsic viscosity of poly(propylene oxide) fractions in iso-octane

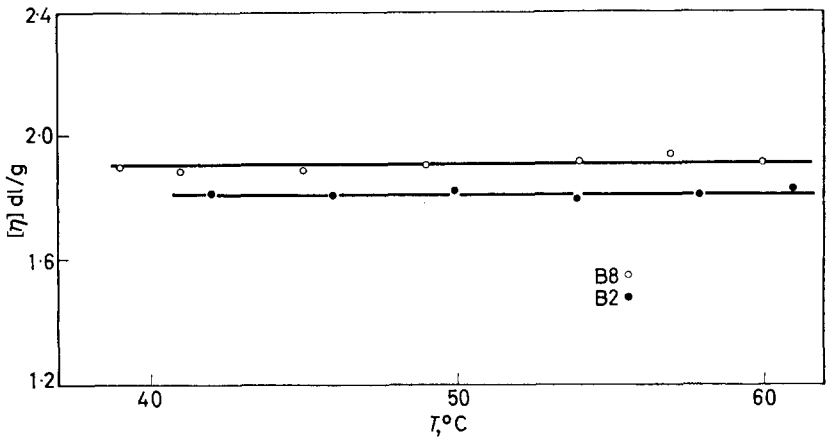

Figure 2—Temperature dependence of intrinsic viscosity of poly(propylene oxide) fractions in hexane

Intrinsic viscosities obtained over a range of temperature in hexane and in iso-octane are recorded in *Figures 1* and *2*. By comparing data for fractions having nearly the same molecular weight (i.e. B1, B6 and B8 in *Figure 1* and B2 and B8 in *Figure 2*), $[\eta]$ in both solvents is seen to be independent of structural regularity; such variations as do occur can be accounted for by the slight variation in molecular weight. However, $[\eta]$ is independent of temperature in hexane but dependent on temperature in iso-octane.

DISCUSSION

Current theories of the thermodynamic properties of dilute polymer solutions express the second virial coefficient (A_2) for a monodisperse polymer as[8]

$$A_2 = N_0 \beta n^2 h(\mathbf{z})/2M^2$$

where N_0 is Avogadro's number, β the excluded volume integral, n the number of equivalent statistical segments in the mathematical model, and M is the molecular weight of the polymer. The term $h(\mathbf{z})$ is a series expression in powers of $\mathbf{z}$, where

$$\mathbf{z} = (3/2\pi\overline{r_0^2})^{3/2}\beta n^2$$

and $\overline{r_0^2}$ is the unperturbed mean square end-to-end distance. The temperature dependence of A_2 is governed by the expression for the excluded volume integral, which is usually assumed to be of the form

$$\beta = 2v_1\psi_1(1 - \theta/T)$$

where v_1 is the volume of a solvent molecule and ψ_1 and θ are the entropy parameter and the theta temperature of Flory's dilute solution theory[9].

For high molecular weight polymers the intrinsic viscosity is given by the expression[9]

$$[\eta] = \Phi(\overline{r_0^2})^{3/2}\alpha^3/M$$

where Φ is the 'Flory–Fox parameter' and α is the coil expansion factor.

While the three parameters $\overline{r_0^2}$, Φ and α are all influenced by temperature, with polymer chains which are flexibly coiled the temperature dependence of $[\eta]$ is determined predominantly by the temperature dependence of α. Expressions for α vary, but are in agreement that α is a function of $\psi_1 (1 - \theta/T)$. For example, the Flory–Fox treatment would put

$$\alpha^5 - \alpha^3 = C\mathbf{z}$$

where C is a constant.

Thus, theory predicts that when a polymer solution is at or near its theta temperature, A_2 and $[\eta]$ increase rapidly with temperature, while at temperatures substantially higher than θ there is a region where A_2 and $[\eta]$ are essentially independent of temperature. The fact that our fractions are not monodisperse does not detract from these predictions.

In terms of these theories there is a clear contradiction between our light scattering and viscometric data in hexane solution. The intrinsic viscosity/temperature plots are characteristic of good solvent systems, while the light scattering data indicate that hexane is a poor solvent for the more isotactic fractions at 46°C (e.g. it would appear from the light scattering data that hexane is a theta solvent for fraction B1 a little below 46°C). On the other hand the iso-octane data are consistent; both indicate that iso-octane is a theta solvent for poly(propylene oxide) in the region of 50°C.

If we compare the data obtained for fractions B1 and B2 in the two solvents, a second inconsistency becomes apparent. For these fractions iso-octane at 50°C and hexane at a temperature a little below 46°C appear to be theta solvents if we take the evidence of the second virial coefficients at face value. One would expect that the dimension of the polymer chains measured in the two solvents at the temperatures in question would be very similar, since they should be the unperturbed dimensions in each case. In the same way one would expect the intrinsic viscosities in the two solvents to be similar, since $[\eta]$ is related to $\overline{r_0^2}$ by equation (3). In fact both these quantities differ considerably between the two solvent systems. This discrepancy is far too large to be explained in terms of the temperature dependence of the unperturbed dimensions.

Taken as a whole the data we have obtained suggest that hexane at 46°C is a thermodynamically good solvent for all the stereoregular modifications of poly(propylene oxide) we have isolated. We believe the explanation for the low values of A_2 obtained in this solvent for the more stereoregular fractions lies in some form of incipient crystallization.

According to nucleation theory, at a temperature somewhat above the equilibrium melting point of a crystallizable polymer, the crystallizing units form an equilibrium array of associates; as the temperature is lowered the size and number of associates increases, but irreversible growth to crystals will occur only when the temperature is lower than a critical nucleation temperature, i.e. at a temperature at which the size of the associates is sufficient to ensure stability. In dilute solution the majority of the associates will be intramolecular, but the proportion of intermolecular associates will increase as the concentration of polymer increases; only at infinite dilution will there be complete absence of intermolecular associates. If we now suppose that the formation of an intermolecular associate by two polymer

molecules leads effectively to their dimerization during the lifetime of the associate; then, since the associate need only contain small sequences of units, we may treat this dimer, to a crude approximation, as though it were a flexibly coiled polymer molecule having twice the molecular weight of the original polymer. Given certain simplifying assumptions, the effect of a small amount of association upon the apparent value of A_2 can be calculated; the results of such a calculation are given in *Figure 3*. The effect is seen to be that of lowering the apparent value of A_2 while changing the intercept, which gives the apparent value of $\overline{M}_w$, hardly at all.

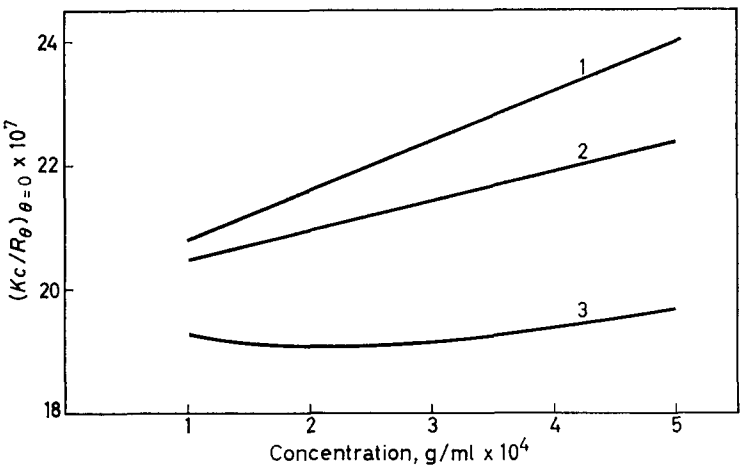

Figure 3—Effect of reversible dimerization ($2P \rightleftharpoons P_2$) on the light scattering plot. (Calculations are made on the assumption that the molecular weight of $P=5\times10^5$, that $A_2=4\times10^{-4}$ cm^3 g^{-2} mole for both P and P_2 and that equilibrium constants are (1) 0, (2) 5×10^4, (3) $2{\cdot}5\times10^5$ l mole^{-1}

Thus, a possible explanation of the different values of A_2 observed for the fractions of poly(propylene oxide) in hexane at 46°C is that these are a consequence of the different degrees of association in the solution; the latter difference is to be expected since the fractions crystallized from solutions at different temperatures. The insensitivity of the intrinsic viscosities of the fraction measured in hexane at 46°C, to the degree of tacticity is in accord with our explanation, since the intrinsic viscosity is a property of molecules at infinite dilution where intermolecular association is absent.

It remains to examine the light scattering data obtained in iso-octane. The theta temperatures of the poly(propylene oxide) fractions in iso-octane were determined from the intercepts of plots A_2 versus T upon the $A_2=0$ axis. No difference outside experimental error could be detected between the theta points of the different stereoisomers, which were found to be 50° ± 1°C. Also no meaningful difference in ψ_1 could be detected and, assuming $v_1N_0=165$ cm^3 and the partial specific volume of the polymer $=0{\cdot}94$ cm^3/g, the average value of ψ_1 was found to be 0·47. Below 50°C we found some evidence of association, although in this case we were unable to establish any consistent results. We cannot completely rule out the possibility that

some association was present above 50°C since the strong dependence of A_2 on temperature in this region could mask the effect. However, we incline to the view that 50°C is a good assessment of the theta temperature in iso-octane of all the structural modifications of poly(propylene oxide) we have investigated.

CONCLUSIONS

There is no measurable effect of tacticity on the thermodynamic properties of dilute solutions of poly(propylene oxide) in iso-octane.

There is a large effect of tacticity on the second virial coefficient of poly(propylene oxide) in hexane at 46°C, but the data are inconsistent with the established theories of dilute polymer solutions. We believe this discrepancy is due to specific interactions which must occur between small groups of crystallizing segments in the region of the critical nucleation temperature. It seems likely that the effects we have observed are general and that light scattering studies might be used to obtain insight into the molecular processes which occur just prior to nucleation.

We wish to thank Miss C. J. S. Guthrie and Mrs J. A. Hurst for their experimental assistance.

Chemistry Department,
University of Manchester

(Received December 1965)

REFERENCES

[1] KRIGBAUM, W. R., KURG, J. E. and SMITH, P. *J. phys. Chem.* 1961, **65,** 1984; see also W. R. KRIGBAUM, *Newer Methods of Polymer Characterization,* edited by B. KE. Interscience: New York, 1964
[2] ALLEN, G., BOOTH, C. and JONES, M. N. *Polymer, Lond.* 1964, **5,** 257
[3] BOOTH, C., HIGGINSON, W. C. E. and POWELL, E. *Polymer, Lond.* 1964, **5,** 479
[4] ALLEN, G., BOOTH, C. and JONES, M. N. *Polymer, Lond.* 1964, **5,** 195
[5] EHL, J., LOUCHEUX, C., REISS, C. and BENOIT, H. *Makromol. Chem.* 1964, **75,** 35
[6] PEAKER, F. W. *The Characterization of High Polymers,* Chapter 5, Edited by P. W. ALLEN. Butterworths: London, 1959
[7] BOOTH, C. and PRICE, C. *Polymer, Lond.* 1966, **7,** 85
[8] ZIMM. B. H. *J. chem. Phys.* 1946, **14,** 164
[9] FLORY, P. J. *Principles of Polymer Chemistry.* Cornell University Press: Ithaca, 1953

The Thermodynamic Analysis of the Effect of Pressure on the Glass Temperature of Polystyrene

G. GEE*

The applicability of the equations

$$dT_g/dP=\Delta\beta/\Delta\alpha=TV\Delta\alpha/\Delta C_p$$

is examined, and it is pointed out that an equivalent procedure is to compare the properties of two glasses formed under different pressures. A detailed analysis is given of published data on the isothermal compression of polystyrene, showing that the first equation fails because a glass formed at 1000 atm is approximately one per cent denser than one formed at atmospheric pressure. Measurements of ΔC_p suggest, however, that the two glasses probably do not differ correspondingly in energy and entropy. The bearing of these conclusions on theories of the glass temperature is briefly discussed.

RENEWED attention has been given in recent years to the possibility of a thermodynamic analysis of glass transitions in polymers, and in particular of the effect of pressure[1-10]. The present position appears extremely confused, different authors drawing contrary conclusions from the same experimental observations. Two major factors contribute to the confusion: lack of rigour in defining a glass temperature, and uncertainties in the interpretation of the measurements. In this paper we shall first present a definition unambiguously related to experiment, and then analyse in detail one of the most extensive bodies of data available.

(1) *Definition of T_g*

In a typical experiment a dilatometer is filled with polymer and volume measurements are started at a temperature high enough to ensure that the

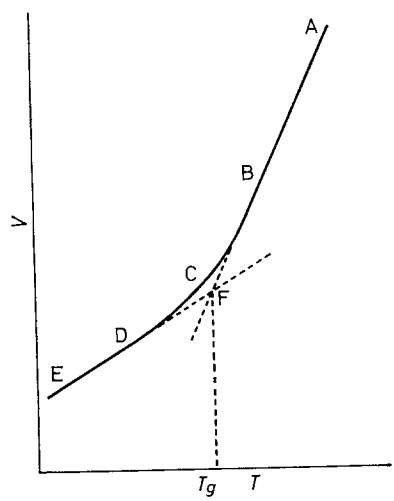

Figure 1—Definition of T_g

*University of Manchester. This analysis was carried out while the author was a fellow of the Michigan Foundation for Advanced Research, Midland, Mich., U.S.A.

polymer is fluid (Point A, *Figure 1*). The temperature is then lowered slowly, and the contraction observed. The word 'slowly' requires that the time scale shall be such that the volume is not time-dependent; in this region (A B, *Figure 1*) this condition is easily satisfied. Continued cooling takes the polymer into a region (point C) where the time factor is important and the shape and position of the curve depend somewhat on the patience of the experimenter. Beyond this region we come to a further one (DE) where time effects again disappear and the polymer is now in the glassy state. The line DE is not a unique property of the polymer, but depends on its history, i.e. on the way in which the transition BCD was accomplished. Nevertheless the line DE can be traversed reversibly and represents the actual behaviour of a real material, i.e. *the glass as it has been produced in this experiment.*

We now extrapolate the lines AB, ED to meet at F, and *define* this as the glass temperature. As is entirely proper for a thermodynamic definition, this avoids any discussion of mechanism, and relates directly to observations. It also focuses attention on the fact that T_g is a property of an experiment as well as of a material. Clearly a similar definition can be written for experiments in which variables other than V and T are used: the detailed study in §3 relates to isothermal compression.

In this definition we have implicitly assumed that there is only a single glass transition. Studies of cyclic deformation, using either dynamic mechanical or dielectric techniques, reveal the existence of several relaxation regions[1]. Of these, one can usually be associated unambiguously with the glass temperatures as observed in measurement of volume or heat capacity, while the others are not generally detected in such measurements. Our definition assumes the existence of regions of behaviour on each side of the glass transition, in which the property under investigation (e.g. volume) is not significantly influenced by relaxation phenomena. This condition appears to be generally satisfied.

(2) *Thermodynamic analysis*

We now wish to compare the properties of the polymer in the two states: liquid (AB) and glass (DE). We shall not discuss at all the time-dependent properties in the transition region. The two properties to be related are:

(*i*) the coefficient of cubical expansion $\alpha_L = (\partial \ln V/\partial T)_P$

(*ii*) the compressibility $\beta_L = -(\partial \ln V/\partial P)_T$

For the liquid region, these definitions suffice, for the volume is there uniquely determined by P and T. To describe the behaviour of the glass we need at least one further parameter, denoted by Z. Its necessary property is to be constant for a given glass (i.e. for the line DE in a particular experiment), and to vary with T (P) in the liquid region. In other words we assert that V depends on three variables T, P and Z, but that in a liquid, Z is uniquely determined by T and P. The physical significance of Z does not immediately concern us, but it may be thought of as a measure of order, or perhaps of free volume.

We can now define α_g and β_g for the glass:

$$\alpha_g = (\partial \ln V/\partial T)_{P,z} \; ; \quad \beta_g = -(\partial \ln V/\partial P)_{T,z}$$

where differentiation is to be carried out at *that value of Z which the liquid*

would have at T_g (point F). We shall be concerned with $\Delta\alpha \equiv \alpha_L - \alpha_g$; $\Delta\beta \equiv \beta_L - \beta_g$.

Consider the isothermal compression of the material. At constant T, V is a function of P and Z, so that

$$\delta \ln V = (\partial \ln V/\partial P)_{T,Z}\delta P + (\partial \ln V/\partial Z)_{T,P}\delta Z$$

In the liquid, P and Z both vary, and we have:

$$-\beta_L = \left(\frac{\partial \ln V}{\partial P}\right)_T = \left(\frac{\partial \ln V}{\partial P}\right)_{T,Z} + \left(\frac{\partial \ln V}{\partial Z}\right)_{T,P}\left(\frac{\partial Z}{\partial P}\right)_T$$

whence

$$-\Delta\beta = (\partial \ln V/\partial Z)_{T,P}(\partial Z/\partial P)_T \tag{1}$$

By an exactly similar argument:

$$\Delta\alpha = \partial \ln V/\partial Z)_{T,P}(\partial Z/\partial T)_P \tag{2}$$

Dividing (1) by (2) $$\frac{\Delta\beta}{\Delta\alpha} = -\left(\frac{\partial Z}{\partial P}\right)_T\left(\frac{\partial T}{\partial Z}\right)_P = \left(\frac{\partial T}{\partial P}\right)_Z \tag{3}$$

In these equations the derivatives $(\partial Z/\partial P)_T$, $(\partial Z/\partial T)_P$ and $(\partial T/\partial P)_Z$ are properties of the equilibrium *liquid*.

Equation (3) follows logically from the *assumed* properties of Z. To determine this derivative we must be in a position to compare experimentally two states of the material characterized by the *same* value of Z. It has been suggested that we can do this by determining the glass temperature at different pressures. We therefore repeat the experiment of *Figure 1* at a different (constant) pressure, obtain a new T_g, and assume that this corresponds with the same value of Z, so that

$$(\partial T/\partial P)_Z = \mathrm{d}T_g/\mathrm{d}P = \Delta\beta/\Delta\alpha \tag{4}$$

This is the equation whose applicability we shall examine, but it is clear, from this derivation, that there are no strong grounds to expect it to hold for experiments *carried out as described.* To ensure its validity, we should simply reverse the foregoing: the two experiments should start from two samples of the same glass (i.e. made under identical conditions) and all measurements in the glass region (ED) should be completed before the transition state is entered.

(3) *Isothermal compression of polystyrene*

Hellwege, Knappe and Lehmann[10] have carried out a detailed study of the isothermal compression of three polymers, up to 2 000 bars, over a wide temperature range; we select their polystyrene data for detailed analysis. In each experiment a sample of polymer was compressed isothermally, and the volume recorded every 200 bars. In the intermediate temperature range the polymer became converted from liquid to glass during the experiment, so the data can be used to determine glass temperatures as defined above. Plots of total volume against pressure, for this temperature range, are shown in *Figure 2*, and a highly significant feature is at once apparent. The vertical separation of the curves at zero pressure is of course a measure of the coefficient of expansion of the liquid. In the same way, one might

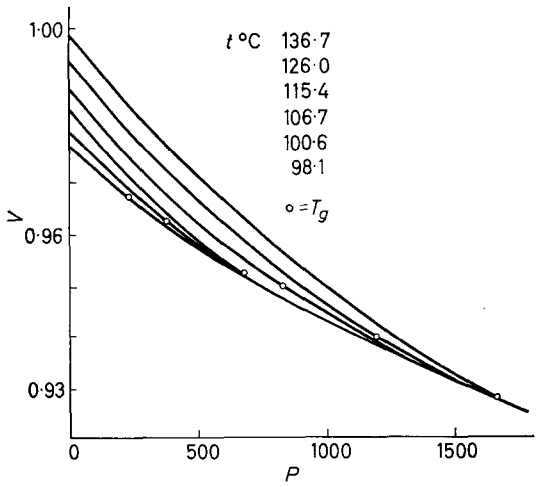

Figure 2—Isothermal compression curves[10] in the transition region. Temp. (°C): 1, 136·7; 2, 126·0; 3, 115·4; 4, 106·7; 5, 100·6; 6, 96·1. Points ○ transition, as located from *Figure 7*

expect to find a vertical spread at 1 800 bars, corresponding to the coefficient of expansion of the glass. Instead, all the curves are seen to converge to approximately the same volume. The circles on the six curves represent the glass temperatures (determined by a method described below), and it is evident that the properties of the glass are a function of the conditions of its formation. There is therefore no reason to expect equation (4) to hold, and our final conclusion will in fact be that it does not, in disagreement with the claim of the original investigators. To test the equation we have to analyse the data to obtain as reliably as possible the various quantities involved. As this is by no means a straightforward procedure, it seems essential to describe our methods in some detail. We need values extrapolated to the glass temperature, and have therefore sought empirical relationships. Those described below were adopted after a number of others had been examined and rejected.

(4) *Determination of compressibilities*

In agreement with Wood[11] and Nanda and Simha[12], we find the Tait equation to give an accurate description of the compression of liquid polystyrene. Using the equation in the form

$$V_0 - V = V_0 C \ln [1 + P/B] \tag{5}$$

the compressibility is given by

$$\beta = V_0 C / V (P + B) \tag{6}$$

Applying equation (5) over a pressure range ΔP, the compression, $-\Delta V$, is related to the mean pressure $\overline{P}$ by

$$-V_0/\Delta V = B/(C \,.\, \Delta P) + P/(C \,.\, \Delta P) \tag{7}$$

Using a pressure interval $\Delta P = 400$ bars, the result of applying (7) to the data at the highest temperatures is shown in *Figure 3*. The lines are drawn with a slope making $C = 0{\cdot}0894$, in accordance with Nanda and Simha's

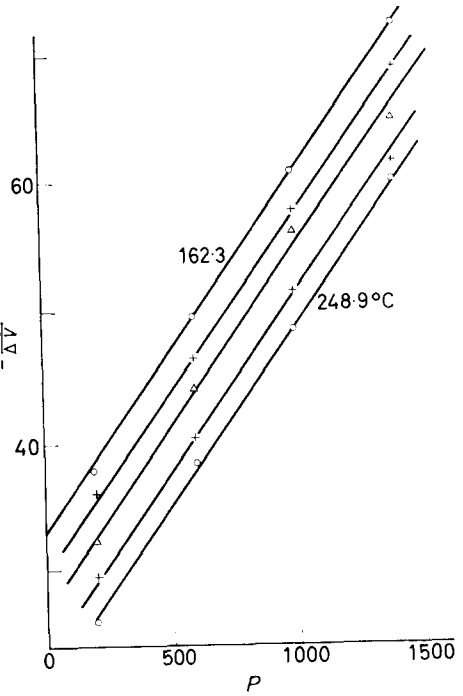

Figure 3—(Reciprocal) compressibility of liquid polystyrene as a function of pressure. Temp. (°C): 1, 162·3; 2, 178·7; 3, 202·9; 4, 229·0; 5, 248·9

conclusion[12] that this can be used as a universal value for hydrocarbon liquids and polymers. The fit is very satisfactory up to 1 600 bars, but values for the interval 1 600–2 000 bars are more scattered and generally somewhat lower; these have been ignored for the present analysis.

Taking C to be independent of temperature and applicable also to the glassy state, a further plot was made, subtracting the term $\bar{P}/(C \cdot \Delta P)$, and

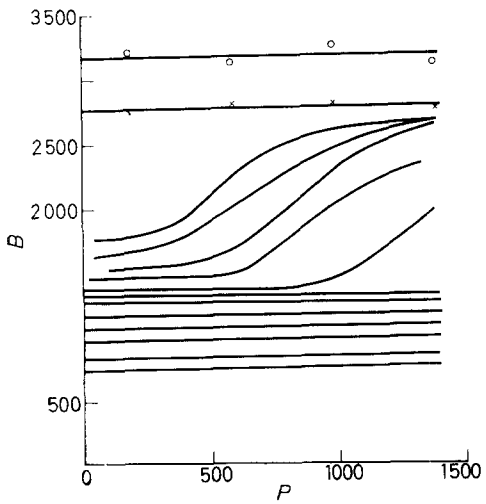

Figure 4—Estimation of Tait constant B from compressibility. Temp. (°C) (top to bottom): 1, 20·0; 2, 60·5; 3, 96·1; 4, 100·6; 5, 106·7; 6, 115·4; 7, 126·0; 8, 136·7; 9, 145·2; 10, 162·3; 11, 178·7; 12, 202·8; 13, 229·0; 14, 248·9

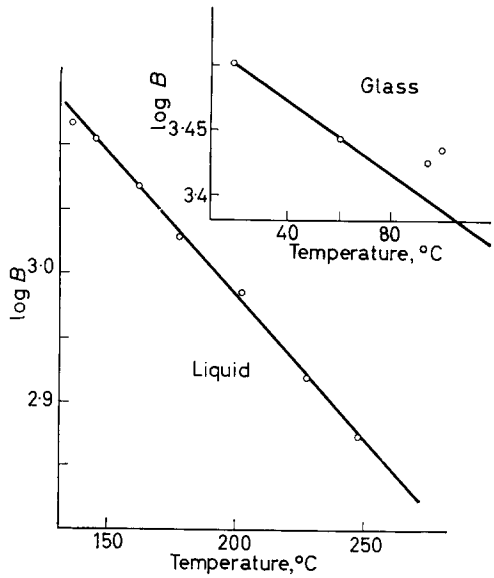

Figure 5—Temperature dependence of B

plotting B from equation (7) against $\bar{P}$. The result is shown in *Figure 4*, where the points shown for the two lowest temperatures confirm both this method of analysis and the value assigned to C. The intermediate curves show the transition, and it is possible to estimate approximate values of B for both liquid and glass at the same temperature. We shall need (below) the temperature dependence of B; *Figure 5* shows that this is well represented by a linear plot of log B versus T for the liquid, giving B_L (bars) = 10 560 exp ($0{\cdot}00506_5 T$). The glassy state presents a more difficult problem. The line drawn in *Figure 5* takes account only of the two lowest temperatures, and has been used to obtain $\mathrm{d} \ln B/\mathrm{d}T$. Data for higher temperatures are not directly comparable, since they refer to different glasses. In *Figure 4* all the intermediate curves appear to tend towards approximately the same limiting value at high pressures. It was therefore concluded that the most plausible assignment is $B \simeq 2\,700$ bars at the glass temperature, for each glass formed in this region, with $\mathrm{d} \ln B/\mathrm{d}T = -0{\cdot}00333$ deg^{-1}.

These values have been used, in conjunction with equations (5) and (6), to calculate the compressibilities given in §6.

(5) *Coefficients of expansion*

The coefficient of expansion at zero pressure is usually treated as a constant, though there is considerable evidence that it increases with temperature. Bueche[13] has deduced the relationship $\alpha = A\sqrt{T}$, and Flory *et al.*[14] a more complex equation giving a somewhat larger dependence. Simha and Havlik's general equation of state leads to polystyrene data[15] approximating to $\sqrt{\mathrm{T}}$ dependence, while Fox and Flory[16] found evidence of a change of coefficient (more or less sharp) for the same polymer at about 160°C. However, the present data are well represented (*Figure 6*) by a linear plot

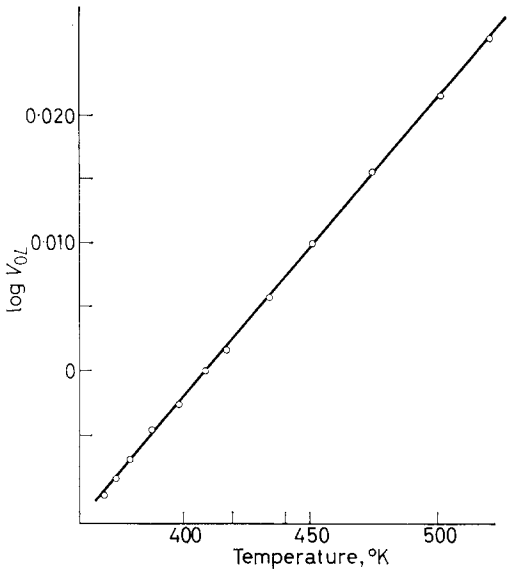

Figure 6—Cubical expansion of liquid polystyrene at $P=0$

of log V against T, and we have accordingly taken $\alpha_{0L}=5{\cdot}34\times10^{-4}$ deg^{-1}. Only two points are available to determine α_{0g}, which we therefore take as constant and equal to $2{\cdot}50\times10^{-4}$ deg^{-1}.

The pressure dependence of α follows from our analysis of the Tait equation. Differentiating equation (5) w.r.t. T we obtain

$$\alpha_L=\alpha_{0L}+P\beta_L\,(\mathrm{d}\ln B_L/\mathrm{d}T) \tag{8}$$

with a similar equation for α_g.

(6) *Numerical results*

The methods outlined in §§4 and 5 were used to evaluate the quantities required, at the temperatures and pressures corresponding to the assignment of T_g (§7). The results (*Table 1*) are not in good agreement with those deduced by Hellwege, Knappe and Lehmann. The main discrepancy is that they obtain much smaller values of $\Delta\beta$, so that their ratio of $\Delta\beta/\Delta\alpha$ is approximately 0·03. The present analysis is believed to be sound, but its precision could have been considerably improved had *P–V–T* measurements been made on the glasses formed under pressure.

Table 1

t	P	α_L	α_g	$\Delta\alpha$	β_L	β_g	$\Delta\beta$	$\frac{\Delta\beta}{\Delta\alpha}$
°C	bars		$deg^{-1}\times10^4$			$bar^{-1}\times10^5$		$\frac{deg}{bar^{-1}}$
*89·0	0	5·34	2·50	2·84	5·33	3·31	2·02	0·071
96·1	225	4·78	2·27	2·51	4·90	3·08	1·82	0·072
100·6	390	4·43	2·12	2·31	4·62	2·93	1·69	0·073
106·7	580	4·06	1·97	2·09	4·35	2·75	1·60	0·077
115·4	875	3·58	1·75	1·83	3·98	2·57	1·41	0·077
126·0	1250	3·06	1·52	1·54	3·59	2·35	1·24	0·081
136·7	1640	2·64	1·32	1·32	3·25	2·16	1·09	0·083

*Extrapolated.

(7) *Location of the glass transition*

The determination of T_g, in accordance with our definition, involves extrapolation of the liquid and glass curves, which can only be done reliably when the equations to these curves are known. Inspection of the raw V/P curves (*Figure 1*) fails to disclose any obvious breaks. Using the Tait equation constants already assigned, we therefore subtract from the measured volume the calculated volume of the liquid. So long as the polymer remains liquid the answer should be zero, but when the polymer becomes glassy the

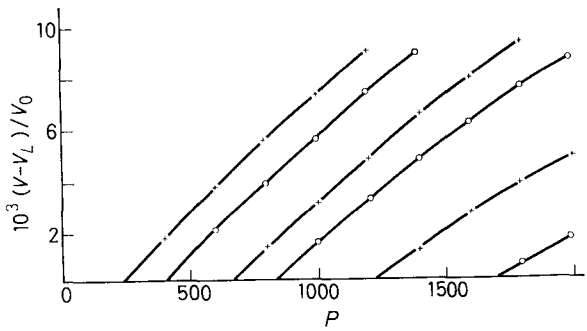

Figure 7—Location of glass temperature in isothermal compression. Temp. (°C) (left to right): 1, 96·1; 2, 100·6; 3, 106·7; 4, 115·4; 5, 126·0; 6, 136·7

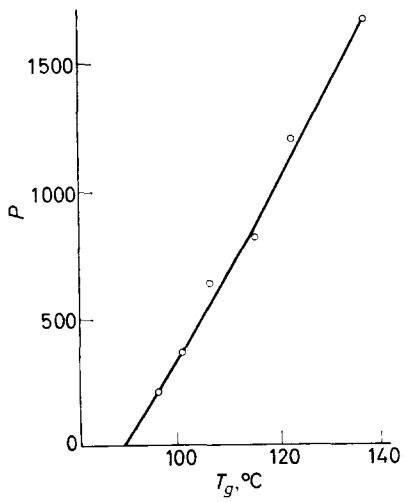

Figure 8—Relation of glass temperature to pressure

difference becomes positive, as shown in *Figure 7*. Extrapolation of the high pressure lines to $P=0$, ignoring curvature at low P, gives the results plotted in *Figure 8*. Smoothed values from *Figure 8* were used in *Table 1*, and agree well with those found by Hellwege, Knappe and Lehmann. They give $dT_g/dP \simeq 0{\cdot}03$ deg bar^{-1}, falling slightly with rise of P.

(8) *Discussion*

How far can we be sure of the results of these computations? The coefficients of expansion at $P=0$ of the fluid and of the low temperature glass should be reliable; so should the compressibility of the fluid. To make $dT_g/dP=\Delta\beta/\Delta\alpha$ at $P=0$ all the adjustment has therefore to be in β_g. This requires $B_g=2\,010$, compared with our value of 2 700. The admitted uncertainty in B_g is much less than this.

The coefficient of expansion of glass made at high temperature and pressure has been assumed equal to that of the low temperature glass; it may well be lower. An alternative assumption would be that the internal pressures of the various glasses are equal (at the same temperature). Since we have taken $B_g=2\,700$ for all glasses at their T_g, this makes α_{0g} proportional to $1/T$. The effect of this assumption would be to increase $10^4\Delta\alpha$ for the highest temperature from 1·32 to 1·61, reducing $\Delta\beta/\Delta\alpha$ to 0·068. The true value of $\Delta\alpha$ probably lies between these two extremes.

This analysis is therefore believed to show that equation (4) is *not* obeyed by the results analysed. It has already been pointed out that agreement was not to be expected, since the properties of the glass depend on the conditions of its formation. It is now possible to analyse this variation more quantitatively. *Figure 9* compares the temperature dependence of four volumes:

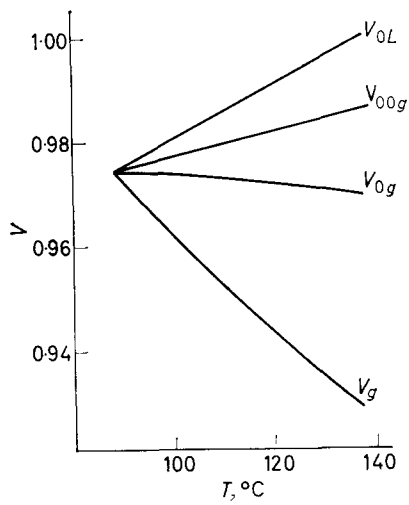

Figure 9—Comparison of measured and calculated volumes. V_{0L} denotes volume of liquid at $P=0$; V_g denotes volume of glass at transition temperature and pressure; V_{0g} denotes calculated volume of glass if decompressed at transition temperature; V_{00g} denotes calculated volume of glass if heated at $P=0$

V_{0L} denotes volume of liquid at $P=0$

V_g denotes volume at glass temperature and pressure

V_{0g} denotes calculated volume of glass at T_g but decompressed to $P=0$ without conversion to liquid

V_{00g} denotes volume of glass formed at $P=0$, heated without conversion to liquid.

Evidently V_{0g} and V_{00g} are hypothetical quantities incapable of experimental realization. The difference between them is, however, a measure

of the additional compression which the polymer has sustained as a result of the glass being formed under pressure.

An alternative estimate of this compression has been obtained by carrying through the following cycle of calculations. Start from glass at $T=20°C$, $P=0$ $V=0{\cdot}9574$

1. Heat through T_g (89°C) to 126°C $V=0{\cdot}9942$
2. Compress at 126°C to 1 250 atm (glass transition) $V=0{\cdot}9377$
3. Cool to 20°C at 1 250 atm $V=0{\cdot}9238$
4. Release pressure at 20°C $V=0{\cdot}9470$

Loss of volume $0{\cdot}010_4$

(Compare $V_{00g}-V_{0g}$ at 126°C $=0{\cdot}012_6$)

A cycle of this kind has in fact been carried through experimentally by Shishkin[17], who has confirmed directly the 'compression' resulting from glass formation at high temperatures and pressures.

(9) *Theoretical isobars and glass temperatures*

The results of dilatometric experiments at constant pressure are readily predicted from the *P–V–T* relations we have set up. If the experiment is carried out with *rising* temperature the glass is the same in each experiment, and its properties are those of the low temperature glass, for which $B=8\,420\exp(-0{\cdot}00333T)$. Glass temperatures were found 'experimentally' by plotting log V versus T for glass and liquid at $P=0$, 500 and 1 000 atm; these intersect at T_g. The data are summarized in *Table 2*.

Table 2

P	*Isobaric 'experiment'*			*Isothermal experiment (Hellwege)*		
		T_g (°C)			T_g (°C)	
	$\frac{\Delta\beta}{\Delta\alpha}$	*'obs.'*	*calc.*	$\frac{\Delta\beta}{\Delta\alpha}$	*'obs.'*	*calc.*
0	0·056	78·4	(78·4)	0·071	89·0	(89·0)
500	0·060	108	107·5	0·075	104·3	125·5
1 000	0·064	139	138·5	0·078	118·9	164

The agreement between 'observed' and calculated values in our paper experiment is easily shown to be a mathematical necessity. In other words, provided that the same glass is used in each experiment *and that it shows reversible P–V–T behaviour well below* T_g, *the relationship* $dT_g/dP=\Delta\beta/\Delta\alpha$ MUST hold. Observed genuine departures from this equation, in such experiments as those of Hellwege and co-workers, therefore reflect the dependence of glass properties on the conditions of formation.

(10) *A modified equation for isothermal experiments*

The analysis has shown that in Hellwege's experiments, a degree of compression occurs before glass formation, which is a function of T. We represent this as a fraction f of V_{0g}. It has also been observed that the Tait constant for each glass has the same value at its own glass temperature: denote this by $B^{\star}_{g}$. The condition for T_g is then $V_L=V_g$, which gives

$$V_{0L}[1-C\ln(1+P/B_L)]=V_{0g}(1-f)\,[1-C\ln(1+P/B_g^{\star})]$$

Differentiation with respect to T (remembering that $B_g^{\star}$ is a constant) leads to

$$\frac{dT_g}{dP}=\frac{\Delta\beta}{\alpha_L-\alpha_{0g}-\{d\ln(1-f)\}/dT} \tag{9}$$

Rearranging this as an equation for f

$$-\ln(1-f)\simeq f$$
$$=\int_{T_{g0}}^{T_g}[\Delta\beta/(dT_g/dP)+\alpha_{0g}-\alpha_L]\,dT \tag{10}$$

Table 3 gives values of f derived in this way, in comparison with our former estimate $f=(V_{00g}/V_{0g})-1$, and with a value f_s, calculated from Shishkin's value[17] of $df/dT_g=3{\cdot}3\times10^{-4}$ deg^{-1}. The agreement leaves no doubt that this compression is the origin of the observed departures from equation (4).

Table 3

T_g	$100f$(eq. 10)	$100f_s$	$100\left(\frac{V_{00g}}{V_{0g}}-1\right)$
89	(0)	(0)	(0)
96·1	0·26	0·24	0·16
100·6	0·43	0·39	0·35
106·7	0·65	0·59	0·56
115·4	0·98	0·88	0·87
126·0	1·38	1·23	1·30
136·7	1·79	1·59	1·71

Bianchi[9] has argued that equation (4) should be modified to take account of the fact that the volume at T_g is not a constant, and has proposed the equation

$$\frac{dT_g}{dP}=\frac{\Delta\beta}{\Delta\alpha-d\ln V_g/dT} \tag{11}$$

Table 4 shows that this is just as far out as equation (4), but in the opposite direction.

Table 4. Observed and calculated dT_g/dP

T_g (°C)	*Eq. (4)*	*Eq. (11)*	*Eq. (9)* $10^4\,df/dT_g=$ *3·30**	*3·70†*	*Exptl*
89·0	0·071	0·0144	0·033	0·031	0·031
96·1	0·072	0·0135	0·032$_5$	0·030$_5$	0·030$_5$
100·6	0·073	0·0129	0·032$_5$	0·030	0·030$_5$
106·7	0·077	0·0127	0·033	0·030$_5$	0·030
115·4	0·077	0·0117	0·032	0·029$_5$	0·029
126·0	0·081	0·0109	0·032	0·029	0·028
136·7	0·083	0·0102	0·032	0·028	0·027

*Shishkin's value. †Adjusted to fit dT_g/dP.

(11) *Comparison with other polymers*

Hellwege, Knappe and Lehmann also give data for polymethyl methacrylate (PMMA) and polyvinyl chloride (PVC). These have not yet been subjected to the same critical analysis as those for polystyrene, but a preliminary assessment is possible. The paper can be assumed to give reasonable values at $P=0$ for T_g, dT_g/dP and $\Delta\alpha$. Nanda and Simha[12] have estimated B as a function of T for both glass and liquid; except for the values for PMMA at 109° these are consistent with linear log B versus T plots, from which the following values are obtained:

Table 5. Comparison with PMMA and PVC

Material	*Glass*		*Liquid*	
	B_0	$-10^3 \frac{d \ln B}{dT}$	B_0	$-10^3 \frac{d \ln B}{dT}$
PMMA	11 820	4·23	31 500	7·50
PVC	7 270	2·56	26 400	7·00

Using these values, we obtain *Table 6.*

Table 6

Values at $P=0$	*PMMA*	*PVC*
(T_g) (°C)	111	75
$10^5 \beta_L$	5·07	3·89
$10^5 \beta_g$	3·84	3·00
$10^5 \Delta\beta$	1·23	0·89
$10^4 \Delta\alpha$	2·95	2·15
$\Delta\beta/\Delta\alpha$	0·042	0·041
dT_g/dP	0·023	0·0135
$\frac{\Delta\beta}{\Delta\alpha+df/dT}$	0·023	—

The value of $df/dT=2{\cdot}5\times10^{-4}$ used in the last line (*Table 6*) is taken from Shishkin's direct measurements[17].

It appears quite certain, from this preliminary survey, that both these polymers show the same kind of deviation from equation (4) as is shown by polystyrene.

(12) *Calorimetric evidence*

By an argument exactly parallel to that used in §2, a further relationship can be derived

$$dT_g/dP=TV\,\Delta\alpha/\Delta C_p \qquad (12)$$

where ΔC_p is the difference of heat capacity fluid–glass. O'Reilly[6] has collected data for a number of polymers which suggest that this relationship is at least approximately true.

Two independent studies of the specific heat of polystyrene have recently been published, giving the following results:

Authors	ΔC_p (cal g^{-1} deg^{-1})	T_g °K	$T_g V \Delta\alpha/\Delta C_p$ (deg. bar^{-1})
Abu-Isat and Dole[18]	0·0645	366	0·0375
Karasz, Bair and O'Reilly[19]	0·0708	362	0·0339

(The last column was calculated using our values of $V_g = 0{\cdot}974$, and $\Delta\alpha = 2{\cdot}84 \times 10^{-4}$ deg^{-1}.)

There are unexplained differences of detail between the two investigations, and the values both of T_g and of ΔC_p are somewhat dependent on the procedure used to obtain them from the data. For example, Abu-Isat and Dole give linear equations for C_p, both below and above T_g; when combined these give $\Delta C_p = 0{\cdot}2249 - 0{\cdot}417 \times 10^{-3} T$. Taking $T = 366$, this makes $\Delta C_p = 0{\cdot}0722$ and $T_g V \Delta\alpha/\Delta C_p = 0{\cdot}0335$. A similar method applied to the other set of data requires a quadratic equation below T_g, and leads to

$$\Delta C_p = 0{\cdot}1196 + 0{\cdot}0957 \times 10^{-3} T - 0{\cdot}637 \times 10^{-6} T^2$$

Moreover $T_g = 366$ seems more consistent with the data than the authors' own estimate of 362; at $T = 366$ we find $\Delta C_p = 0{\cdot}0689$ and $T_g V \Delta\alpha/\Delta C_p = 0{\cdot}0352$. A quadratic equation has also been fitted to the low temperature data of Abu-Isat and Dole; this gave $T_g = 368$°K, $\Delta C_p = 0{\cdot}0629$, and $T_g V \Delta\alpha/\Delta C_p = 0{\cdot}0385$.

This analysis of the two papers suggests that there is an uncertainty of at least ± 5 per cent in ΔC_p. Taking into account the uncertainty in $\Delta\alpha$, it cannot be claimed that $T_g V \Delta\alpha/\Delta C_p$ is known to better than ± 10 per cent. To this degree of precision, the conclusion must be

$$\frac{TV\Delta\alpha}{\Delta C_p} \simeq \frac{dT_g}{dP} < \frac{\Delta\beta}{\Delta\alpha}$$

The interpretation of this conclusion is less straightforward. A difficulty becomes apparent if we use these heat capacity data to evaluate the changes in energy and entropy in the cycle described in §8. There are no measurements of C_p under pressure but the relationship $(\partial C_p/\partial P)_T = -\alpha^2 VT$ shows that a pressure of 1 200 atm will at most depress C_{pg} by $2{\cdot}5 \times 10^{-4}$ cal g^{-1} deg^{-1}. Less certain is the effect of the higher density of glasses formed under pressure: in the absence of data, any such effect has been neglected. The calculations summarized in *Table 7* were carried out as follows:

$$\Delta U_1 \quad (\Delta U_3) = \int C_p \, dT - P\Delta V/41{\cdot}9$$

$$\Delta U_2 \quad (\Delta U_4) = \frac{1}{41{\cdot}9} \int \left(\frac{\alpha T}{\beta} - P \right) V \, dV$$

$$\Delta H = \Delta U + \frac{\Delta(PV)}{41{\cdot}9}$$

$$\Delta S_1 \quad (\Delta S_3) = \int (C_p/T) \, dT$$

$$\Delta S_2 \quad (\Delta S_4) = \frac{1}{41{\cdot}9} \int \frac{\alpha V}{\beta} dV$$

The equations of Abu-Isat and Dole were used for C_p.

Table 7

	State of polymer	T °K	P (bars)	ΔU cal g^{-1}	ΔH cal g^{-1}	ΔS cal g^{-1} deg^{-1}
	Glass	293	0	0	0	0
	Glass–liquid (T_{g_0})	362	0	21·75	21·75	0·0664
1	*Liquid*	399	0	16·12	16·12	0·0424
2	*Liquid–glass* (T_g)	399	1 250	−3·68	24·27	−0·0111
3	*Glass*	362	1 250	−13·25	−13·40	−0·0359
	Glass	293	1 250	−21·75	−22·01	−0·0664
4	*Glass*	293	0	1·30	−26·24	0·0055
	Overall cycle			0·49	0·49	0·0009
	Increment T_{g_0} *to* T_g			12·44	40·39	0·0313

Thus despite the considerable contraction during the cycle, the enthalpy and entropy return, at least approximately, to their original values. This conclusion is equivalent to Goldstein's argument[3] that the 'excess' quantities H_e and S_e are zero. The intuitive expectation would be $\Delta H \sim (\partial U/\partial V)_T \times \Delta V \sim -0{\cdot}8$ cal g^{-1}; $\Delta S \sim (\partial S/\partial V)_T \times \Delta V \sim -0{\cdot}0025$ cal g^{-1} deg^{-1}. It is in fact easily shown that these relationships would hold if $VT\Delta\alpha/\Delta C_p \sim \Delta\beta/\Delta\alpha$.

(13) *Conclusions*

This analysis illustrates the limited significance of questions as to the applicability of thermodynamic equations to glass transitions as observed experimentally. Discussions as to whether there is a limiting thermodynamic glass temperature, as suggested by Kauzmann[20] and Gibbs and DiMarzio[21], are not directly relevant to this issue. Any study of the pressure coefficients of a glass temperature involves two experiments, and our thermodynamic enquiry is equivalent to asking whether the glasses produced in these two experiments are identical. *Table 8* summarizes our tentative comparison of two polystyrene glasses made by cooling the liquid slowly at (a) $P=0$, (b) $P=1\,250$ atm.

Table 8. Properties of polystyrene glasses at $P=0$, $T=293$

Property	(*a*)	(*b*)
V (cm^3 g^{-1})	0·9574	0·9470
$10^4\,\alpha$ (deg^{-1})	2·50	(2·50)*
$10^5\,\beta$ (bar^{-1})	2·82	2·33
C_p (cal g^{-1} deg^{-1})	0·298	(0·298)*
$S^0_T - S^0_0$ (cal g^{-1} deg^{-1})	0·2945†	0·2954
$H^0_T - H^0_0$ (cal g^{-1})	42·45	42·94
Internal pressure (bar)	2 600	3 150

*Assumed. †Ref. 18.

This comparison is based entirely on indirect argument, and for two properties we have no comparison at all. The neglect of any difference in α and C_p necessarily affects the other quantities and limits their quantitative

significance. It is clear that a direct comparison of these materials would be much more reliable, and that for future work, such comparisons would be far more profitable than further studies of pressure coefficients of T_g.

These thermodynamic studies give no direct evidence as to the mechanism of glass formation, but a few comments may be added. It was pointed out in §1 that T_g is dependent on the experiment as well as on the material. It is therefore the more striking that values of dT_g/dP obtained in different ways show general agreement. In particular, from dynamic experiments $(\partial T/\partial P)_\tau$, has been found[6] independent of the relaxation time τ and equal to the 'static' value of dT_g/dP. This seems to leave no doubt[4] that the observation of the transition is determined by the correlation between relaxation time and the time scale of the experiment. The fundamental mechanistic problem therefore is how the relaxation time is influenced by temperature and pressure.

On the negative side, it is evident that the iso-free volume theory[1] is unacceptable in its simplest form, for the volume V_g at the glass temperature is seen to depend strongly on the pressure (*Figure 9*). It may be noted that V_g would still fall with rising pressure, even if equation (4) held, for we should then have $d \ln V_g/dP = \beta_L\beta_g\Delta\gamma_T/\Delta\alpha$, and $\Delta\gamma_T$, the change in thermal pressure coefficient (α/β) is observed to be negative.

Goldstein's suggestion[3], that the key is to be found in the zero values of 'excess' entropy and enthalpy, is interesting, but it is clear from the last line of *Table 7* that the values of U, H and S at the glass temperatures are far from constant. Any explanation of this kind therefore encounters the same kind of difficulty as that represented by the non-constant V_g.

Department of Chemistry,
University of Manchester

(Received January 1966)

REFERENCES

[1] BOYER, R. F. *Rubber Chem. Technol.* 1963, **36,** 1303
[2] BUECHE, F. *J. chem. Phys.* 1962, **36,** 2940
[3] GOLDSTEIN, M. *J. chem. Phys.* 1963, **39,** 3369
[4] GOLDSTEIN, M. *Modern Aspects of the Vitreous State,* Vol. III, p 90. Edited by J. D. MACKENZIE. Butterworths: London, 1964
[5] O'REILLY, J. M. *Modern Aspects of the Vitreous State,* Vol. III, p 59. Edited by J. D. MACKENZIE. Butterworths: London, 1964
[6] O'REILLY, J. M. *J. Polym. Sci.* 1962, **57,** 429
[7] HIRAI, N. and EYRING, H. *J. Polym. Sci.* 1959, **37,** 51
[8] WUNDERLICH, B. *J. phys. Chem.* 1960, **64,** 1052
[9] BIANCHI, U. *J. phys. Chem.* 1965, **69,** 1497
[10] HELLWEGE, K. H., KNAPPE, W. and LEHMANN, P. *Kolloidzschr.* 1962, **183,** 110
[11] WOOD, L. A. *Polymer Letters,* 1964, **2,** 703
[12] NANDA, V. S. and SIMHA, R. *J. chem. Phys.* 1964, **41,** 3870
[13] BUECHE, F. *Physical Properties of Polymers,* p 86. Interscience: New York, 1962
[14] FLORY, P. J., ORWOLL, R. A. and VRIJ, A. *J. Amer. chem. Soc.* 1964, **86,** 3507
[15] SIMHA, R. and HAVLIK, A. J. *J. Amer. chem. Soc.* 1964, **86,** 197
[16] FOX, T. G and FLORY, P. J. *J. appl. Phys.* 1950, **21,** 581
[17] SHISHKIN, N. *Soviet Physics Solid State,* 1960, **2,** 322
[18] ABU-ISAT, I. and DOLE, M. *J. phys. Chem.* 1965, **69,** 2668
[19] KARASZ, F. E., BAIR, H. E. and O'REILLY, J. M. *J. phys. Chem.* 1965, **69,** 2657
[20] KAUZMANN, W. *Chem. Rev.* 1948, **43,** 219
[21] GIBBS, J. H. and DIMARZIO, E. A. *J. chem. Phys.* 1958, **28,** 373

ANNOUNCEMENT

Symposium on polymer degradation
1 July 1966

The Department of Chemistry and Biology of the Welsh College of Advanced Technology, Cardiff have arranged a one-day Symposium on Polymer Degradation on Friday 1 July 1966. The four papers to be presented are:

Thermal degradation, by N. GRASSIE (*Department of Chemistry, University of Glasgow*); Oxidative degradation, by N. URI (*Ministry of Aviation, Waltham Abbey*); Photochemical degradation, by H. R. COOPER (*Shirley Institute, Manchester*); and Radiolytic degradation, by A. J. SWALLOW (*Christie Hospital and Holt Radium Institute, Manchester*).

Further details may be obtained from the Organiser of Short Courses, Welsh College of Advanced Technology, Cathays Park, Cardiff.

Note and Communication

Thermal Stability of Amine-cured Epoxide Polymers

THE purpose of work described herein was to determine effects of positions of amino groups on thermal stability of corresponding epoxide polymers. It was thought that thermal stabilities of diaminobenzene–epoxide polymers would decrease in the order of *o*-, *m*-, and *p*-diamino-benzenes because of decreasing crosslink densities between the amino groups. This was not the case, however, as will be shown later.

Three crosslinked epoxide polymers were prepared by causing stoichiometric amounts of *m*-phenylenediglycidyl ether (MPDE) to react with *o*-, *m*-, and *p*-diaminobenzenes.

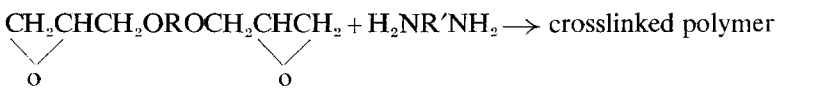

by way of epoxide and amino groups as shown below for ethylene oxide and an amine. R and R′ denote an ortho-, para-, or meta-phenylene group.

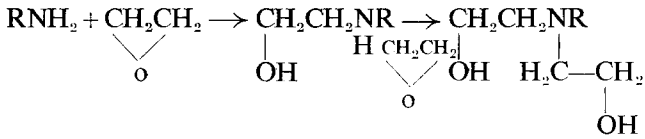

A linear epoxide polymer was prepared from stoichiometric quantities of *m*-phenylenediglycidyl ether and aminobenzene. Highly purified materials were used throughout. The crosslinked epoxide polymers were cured in a nitrogen atmosphere as follows: 96 hours at 100°C, 48 hours at 125°C, 24 hours at 160°C, 6 hours at 200°C, and 0·75 hour at 250°C. Differential thermometric (DT) apparatus was used to cure the linear polymer from 25° to 185°C at a heating rate of 2·5 deg C/min. Thermogravimetric[1] and differential thermometric[2] apparatus described previously was used to determine thermal stabilities.

Thermogravimetric curves for the four polymers are shown in *Figure 1*. Each curve is an average of three experiments. Curves for the MPDE–*o*-diaminobenzene, MPDE–*m*-diaminobenzene, and MPDE–aminobenzene polymers practically coincide. These results indicate that the three polymers have about equal thermal stabilities. It is remarkable that the linear MPDE–aminobenzene polymer is as stable as the crosslinked MPDE–diaminobenzene polymers. The curve for the MPDE–*p*-diaminobenzene polymer differs from the others by breaking at a lower temperature and by showing a larger residual weight. On the basis of residual weight, this polymer is more stable; on the basis of temperature of initial decomposition, it is less stable.

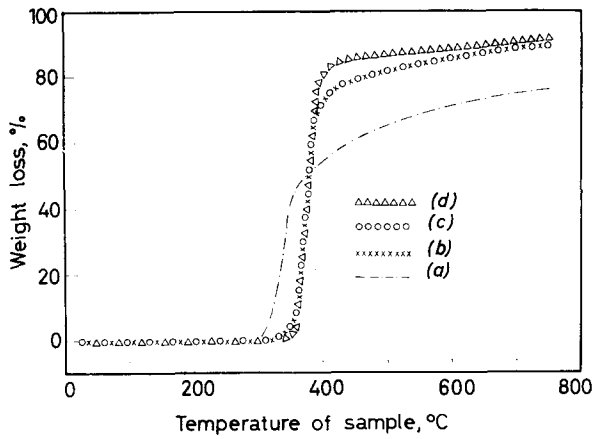

Figure 1—Thermogravimetric (TG) curves of cured *m*-phenylenediglycidyl ether–amine polymers: (*a*) *p*-diaminobenzene; (*b*) *o*-diaminobenzene; (*c*) *m*-diaminobenzene; and (*d*) aminobenzene. Heating rate: 5 deg C/min *in vacuo*

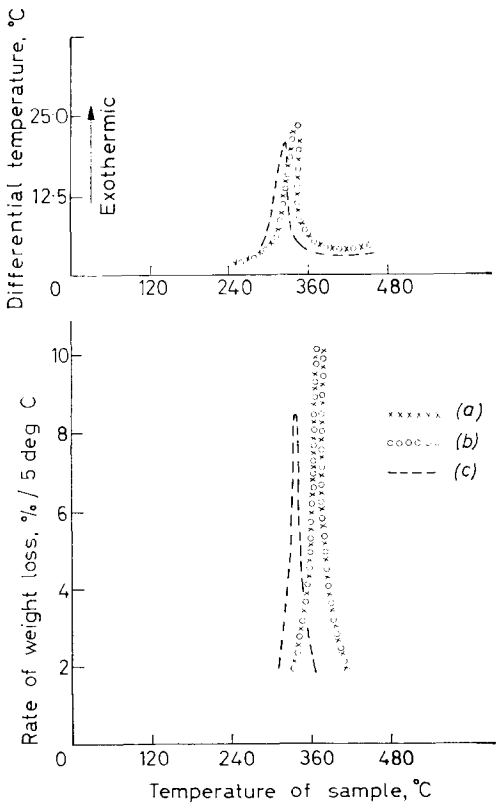

Figure 2—Differential thermogravimetric (DTG) and thermometric (DT) curves of *m*-phenylenediglycidyl ether–diaminobenzene polymers: (*a*) ortho; (*b*) meta; and (*c*) para. Heating rates: DTG *in vacuo*, 5 deg C/min; DT in air, 2·5 deg C/min

As a check on the thermogravimetric results for the three crosslinked polymers, differential thermometric experiments were performed. In *Figure 2*, the resulting DT curves are compared with the corresponding differential thermogravimetric curves. Each set of curves shows that the MPDE–*p*-diaminobenzene polymer has a lower maximum rate of decomposition than the other two polymers. This maximum also occurs at a lower temperature in both cases. The differential thermometric results, therefore, enhance the validity of the thermogravimetric data. Different heating rates caused the two sets of curves in *Figure 2* to appear in different temperature ranges[3, 4]. Exothermic DT peaks in the decomposition range are due to exothermic isomerization of residual epoxide groups[5, 6].

Two findings lead to the conclusion that crosslinking is not a major factor in the thermal decomposition of the epoxide polymers studied. They are: (*1*) Order of thermal stability for the three crosslinked polymers did not correlate with crosslink densities between amino groups; (*2*) The linear polymer was just as thermally stable as the crosslinked ones. It would be informative to make a similar study of the *o*-, *m*-, and *p*-phenylenediglycidyl ether cured with an aromatic diamine.

H. C. ANDERSON*

Chemistry Research Department,
Polymer Research Group,
U.S. Naval Ordnance Laboratory,
White Oak, Silver Spring, Maryland 20910

(Received November 1965)

*Present address: Exploratory Research Division, National Research Corporation, 70 Memorial Drive, Cambridge, Massachusetts, 02142.

REFERENCES

[1] ANDERSON, H. C. *J. appl. Polym. Sci.* 1962, **6,** 484
[2] ANDERSON, H. C. *Analyt. Chem.* 1960, **32,** 1592
[3] ANDERSON, H. C. *J. Polym. Sci.* 1964, **C6,** 175
[4] FRIEDMAN, H. L. *J. Polym. Sci.* 1964, **C6,** 183
[5] ANDERSON, H. C. *Polymer, Lond.* 1961, **2,** 452
[6] LEE, L. H. *J. appl. Polym. Sci.* 1965, **9,** 1981

On the Reliability of the Gradient Column Method for Measuring Densities of Polymer Single Crystals

THE degree of crystallinity of polymer crystals grown from dilute solutions is a very important property of those samples since the structure of the so-called 'single crystals' is not yet completely elucidated. The simplest and most convenient method for determination of crystallinity is the measurement of density. With polyethylene different values are reported in the literature. One group of authors[1–4] found values in the region of 0·97 indicating an amorphous fraction of about 20 per cent. On the other hand Kawai and Keller[5] obtained a value very close to the ideal crystallographic density and concluded that no appreciable amount of an amorphous phase is present. The reasons for this discrepancy are still unknown.

There are two types of observations supporting the lower value of crystallinity. First, the amorphous content can also be detected by other methods, e.g. by X-ray scattering (literature is cited in ref. 6); secondly, the crystal-

As a check on the thermogravimetric results for the three crosslinked polymers, differential thermometric experiments were performed. In *Figure 2*, the resulting DT curves are compared with the corresponding differential thermogravimetric curves. Each set of curves shows that the MPDE–*p*-diaminobenzene polymer has a lower maximum rate of decomposition than the other two polymers. This maximum also occurs at a lower temperature in both cases. The differential thermometric results, therefore, enhance the validity of the thermogravimetric data. Different heating rates caused the two sets of curves in *Figure 2* to appear in different temperature ranges[3, 4]. Exothermic DT peaks in the decomposition range are due to exothermic isomerization of residual epoxide groups[5, 6].

Two findings lead to the conclusion that crosslinking is not a major factor in the thermal decomposition of the epoxide polymers studied. They are: (*1*) Order of thermal stability for the three crosslinked polymers did not correlate with crosslink densities between amino groups; (*2*) The linear polymer was just as thermally stable as the crosslinked ones. It would be informative to make a similar study of the *o*-, *m*-, and *p*-phenylenediglycidyl ether cured with an aromatic diamine.

H. C. ANDERSON*

Chemistry Research Department,
Polymer Research Group,
U.S. Naval Ordnance Laboratory,
White Oak, Silver Spring, Maryland 20910

(Received November 1965)

*Present address: Exploratory Research Division, National Research Corporation, 70 Memorial Drive, Cambridge, Massachusetts, 02142.

REFERENCES

[1] ANDERSON, H. C. *J. appl. Polym. Sci.* 1962, **6,** 484
[2] ANDERSON, H. C. *Analyt. Chem.* 1960, **32,** 1592
[3] ANDERSON, H. C. *J. Polym. Sci.* 1964, **C6,** 175
[4] FRIEDMAN, H. L. *J. Polym. Sci.* 1964, **C6,** 183
[5] ANDERSON, H. C. *Polymer, Lond.* 1961, **2,** 452
[6] LEE, L. H. *J. appl. Polym. Sci.* 1965, **9,** 1981

On the Reliability of the Gradient Column Method for Measuring Densities of Polymer Single Crystals

THE degree of crystallinity of polymer crystals grown from dilute solutions is a very important property of those samples since the structure of the so-called 'single crystals' is not yet completely elucidated. The simplest and most convenient method for determination of crystallinity is the measurement of density. With polyethylene different values are reported in the literature. One group of authors[1–4] found values in the region of 0·97 indicating an amorphous fraction of about 20 per cent. On the other hand Kawai and Keller[5] obtained a value very close to the ideal crystallographic density and concluded that no appreciable amount of an amorphous phase is present. The reasons for this discrepancy are still unknown.

There are two types of observations supporting the lower value of crystallinity. First, the amorphous content can also be detected by other methods, e.g. by X-ray scattering (literature is cited in ref. 6); secondly, the crystal-

linity of the so-called single crystals increases by annealing. We have shown[2] that this increase is connected with the growth of the long period L by the relation

$$\rho = \rho_c - A/L \tag{1}$$

where ρ is the density of the single crystal mat measured by the gradient column method, ρ_c approaches the ideal crystallographic density and A is a constant.

Referring to our publication Kawai and Keller[7] pointed out that the method of density gradient can give erroneous results due to the additional interfacial free energy gradient present in the column. Taking into account this effect they found for the apparent density $\rho_{\text{app.}}$ the equation

$$\rho_{\text{app.}} = \rho_t - K/l \tag{2}$$

where ρ_t is the true density, l is the thickness of the crystals, and K is a constant. On the basis of the similarity between equations (1) and (2) the authors suggested that the values of ρ measured by the gradient method may not be directly related to changes of density.

Our previous results[2] gave strong evidence that the increase of density was really caused by annealing of the 'single crystals'. It was found that the constant A in equation (1) depends strongly on the temperature of annealing, whereas the constant K in equation (2) is proportional to the interfacial energy gradient and therefore, of course, dependent on the history of the sample. In this note we present additional proof that the gradient column method gives reliable results for polyethylene single crystals.

We compared the specific volumes measured by means of that method with the heat content of the same samples. 'Marlex–50' was crystallized from dilute solutions under different conditions and annealed at various temperatures. Some parts of the samples were used for repeated density measurements, other parts for measuring the heat content by differential thermal analysis (DTA) with a modified commercial apparatus (Gebr. Netzsch 404). The areas under the fusion curves of the polyethylene samples were calibrated by the heat of fusion of $CO(NH_2)_2$ and indium[8]. The reproducibility of the data is very good, the relative error is about one per cent. Details of DTA measurements and sample preparation will be reported in a subsequent publication on the analysis of the melting behaviour of single crystals. The mean square fluctuation of the density data is 0·002 as stated in our previous report[3].

In order to take into account the energy content of the surface of the crystals the measured values of $\Delta H'$ have to be corrected according to $\Delta H' = \Delta H - 2\sigma_e/\rho_c l$, where ΔH is the true heat of fusion of the crystalline fraction of the sample and σ_e is the specific surface enthalpy of the longitudinal boundaries of lamellar crystals[9]. The crystal thickness l can be estimated from the long periods measured by X-ray small angle scattering from the same samples. Choosing a value[9] of $\sigma_e = 60$ erg/cm^2 the corrections amount to 1 to 4 cal/g. These corrections and the choice of σ_e do not affect the qualitative conclusions described below.

In *Figure 1* the heat of fusion ΔH per gramme is plotted as a function of the specific volume measured at 30°C in the gradient column. From

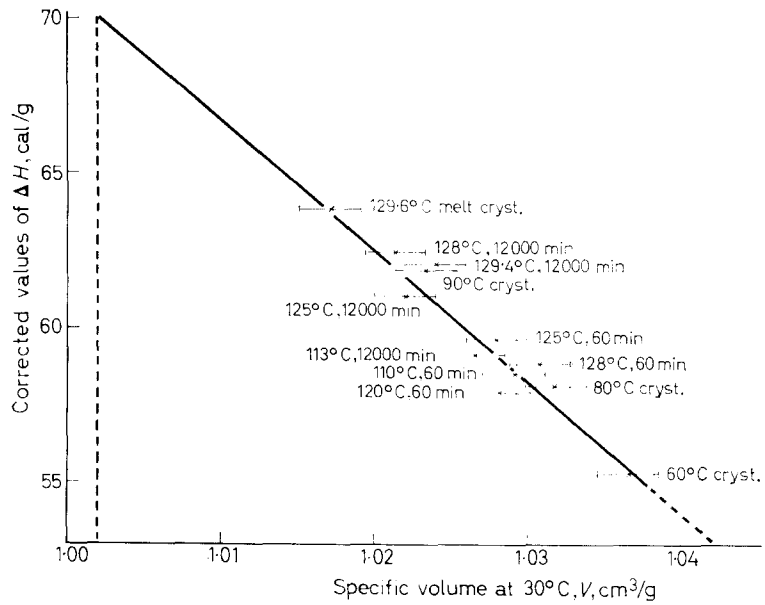

Figure 1—Plot of corrected values ΔH of heat of fusion against the specific volume measured at 30°C by means of a density gradient column. Single crystal samples have been crystallized from 0·01 per cent xylene solution. Specifications of temperature and time indicate annealing conditions of crystals grown at 80°C

these results the following conclusions can be drawn:

(1) The data are reasonably represented by a linear relationship between heat of fusion and specific volume. This verifies the assumption that the values of specific volume measured by the gradient method are determined by the crystallinity of the samples and not by the interfacial energy gradient present in the column. Indeed, degrees of crystallinity calculated either from specific volume or heat content data do agree for almost all samples within the limits of experimental error. This fact also excludes the possibility of there being an appreciable content of voids in our samples.

(2) The heat of fusion of the untreated crystals, for example crystallized at 80°C from xylene, indicates an amorphous content of about 20 per cent in agreement with other calorimetric data[10, 11, 16]. There is no doubt that polyethylene crystallized from the melt (for example at 129·6°C) can yield higher heat of fusion than the samples crystallized from dilute solutions.

(3) The heat of fusion of the single crystals increases by annealing at temperatures below 130°C. This result proves our previous conclusions from density measurements that the overall order of crystal mats can be improved by annealing[2, 6].

(4) The extrapolation to a 100 per cent crystalline sample ($v_c = 1{\cdot}002$ cm³/g at 30°C) yields a heat of fusion of 70 cal/g in excellent agreement with data reported recently by Mandelkern *et al.*[8]. This value does not depend strongly on the choice of surface energy. It changes ± 1 cal/g within reasonable limits of σ_e, but the extrapolation to the specific volume

of a completely amorphous sample ($\Delta H = 0$) reveals rather different values depending on σ_e. For the value of 60 erg/cm^2 used in *Figure 1*, a specific volume $v_a = 1{\cdot}17$ cm^3/g is obtained in agreement with the data of Chiang and Flory[12] and other authors. Making use of $\sigma_e = 0$, 30, or 90 erg/cm^2, however, extrapolation yields $v_a = 1{\cdot}10$, $1{\cdot}12$ or $1{\cdot}20$ cm^3/g respectively. So $\sigma_e = 60$ erg/cm^2 seems to be a reasonable estimate of heat content of the crystal surface. It may be mentioned that the data of drawn polyethylene samples do not fit into the plot of *Figure 1*, the points are placed considerably above the straight line. This indicates the strain imposed on the molecule sequences in the amorphous regions of drawn material[13].

In connection with the basic question for the crystallinity of the so-called polyethylene single crystals it should be mentioned that Martin and Passaglia[14] recently repeated the density measurements by the pyknometer method used by Kawai and Keller[5]. They found values close to those of other authors[1-4] and significantly less than the crystallographic density. It may or may not be that there are two different kinds of single crystals as was suggested by Keller[15] and that one kind possesses 100 per cent crystallinity. This suggestion has yet to be tested. From the measurements reported here, however, it can be concluded that Kawai's and Keller's considerations on the irrelevance of density data obtained by the gradient method cannot be applied to polyethylene crystal mats.

The authors are indebted to Professor H. A. Stuart for his encouragement of this work and to Dr G. F. Schmidt for his helpful advices.

E. W. FISCHER
and G. HINRICHSEN

Laboratorium für Physik der Hochpolymeren am Institut für Physikalische Chemie der Universität Mainz, Germany.

(*Received December 1965*)

REFERENCES

[1] WUNDERLICH, B. and KASHDAN, W. H. *J. Polym. Sci.* 1961, **50,** 71
[2] FISCHER, E. W. and SCHMIDT, G. F. *Angew. Chem.* 1962, **74,** 551
[3] FISCHER, E. W. and LORENZ, R. *Kolloidzschr. u. Z. Polym.* 1963, **189,** 97
[4] JACKSON, J. B., FLORY, P. J. and CHIANG, R. *Trans. Faraday Soc.* 1963, **59,** 1906
[5] KAWAI, T. and KELLER, A. *Phil. Mag.* Ser. VIII, 1963, **8,** 1203
[6] FISCHER, E. W. *Faserforschung u. Textiltechnik,* 1964, **15,** 545
[7] KAWAI, T. and KELLER, A. *Phil. Mag.* Ser. VIII, 1963, **8,** 1973
[8] MANDELKERN, L., FATOU, J. G., DENISON, R. and JUSTIN, J. *J. Polym. Sci. B,* 1965, **3,** 803
[9] HOFFMAN, J. D. *S.P.E. Trans.* 1964, **4,** 315
[10] KARASZ, F. E. and HAMBLIN, D. J. *Report* of National Physical Laboratory Teddington, May 1963. Her Majesty's Stationery Office, London
[11] KILIAN, H. G. Private communication
[12] CHIANG, R. and FLORY, P. J. *J. Amer. chem. Soc.* 1961, **83,** 2857
[13] PETERLIN, A. and MEINEL, G. *J. appl. Phys.* 1965, **36,** 3028
[14] MARTIN, G. M. and PASSAGLIA, E. *J. Res. Nat. Bur. Stand.* In press
[15] KELLER, A. 'Some basic issues concerning the structure of polymer crystals from solution and melt'. Main Lecture (II/6) at The Prague International Symposium on Macromolecular Chemistry 1965 [International Union of Pure and Applied Chemistry]
[16] ILLERS, K. H. Frühjahrstagung der DPG, Bad Nauheim 1965

*An Infra-red Study of the Interaction of Polyamides with Iodine in Iodine–Potassium Iodide Solution**

IKUO MATSUBARA† and J. H. MAGILL

The infra-red spectra of thirty one polyamides of different structures have been examined. The spectral changes which occur on iodine sorption in iodine–potassium iodide solutions and the accompanying changes on iodine desorption with sodium thiosulphate solution have been studied. The spectral observations have been analysed in relation to the changes in the polymer structures. Results show that polyamides of similar structural types, i.e. 'even-even', 'odd-odd', etc., usually conform to a given pattern of behaviour. It is concluded from the spectral evidence that iodine is involved in complex formation with polyamides as the tri-iodide ion.

X-RAY studies of polyamides (Nylons) have revealed that these polymers exist in different crystal forms which depend not only on the type of polymers, but sometimes on the method of sample preparation. The α and β forms were initially proposed by Bunn and Garner[1] for Nylon 6.6 and Nylon 6.10. These triclinic structures consist of sheets of fully extended chains joined by hydrogen bonds. More recently another structure designated as the γ form was found by Kinoshita[2] for Nylon 7.7. In this structure the molecular chains are slightly contracted because of internal rotation around the single bonds adjacent to the amide groups along the chains. The plane of these amide groups makes an angle of about 30° with the polymer chain axis. The unit cell of this form is found to be pseudo-hexagonal. A further structure described as the δ form was proposed by Miyake[3] for polyamides such as Nylon 6.9 and Nylon 7.6. However, other studies revealed that the δ form is likely to be a mixture of the (α, β) and the γ structures[4], so that all known polyamides exist in the (α, β) or the γ form or mixtures of these structures‡.

Infra-red (i.r.) measurements have been made in the medium frequency range (4 000 to 400 cm^{-1}) for a variety of polyamides[3, 5–8], but a detailed analysis of the relation between the spectra and the chain conformations of the polymers has been lacking until recently. Miyake[3] first observed and realized that the amide V (N–H out-of-plane bending) frequency was associated with the change in crystal modification in polyamides; the characteristic absorption occurs at about 690 cm^{-1} in the α form and at about 725 cm^{-1} in the γ form. A detailed i.r. and X-ray work by Arimoto[9, 10] deals with the $\alpha \longrightarrow \gamma$ transformation in Nylon 6. This author attributed the 692 cm^{-1} band of the α form and the 708 cm^{-1} band of the γ form of Nylon 6 to the amide V vibration characteristic of each

*Paper presented at the 16th Pittsburgh Conference on Analytical Chemistry and Applied Spectroscopy, Pittsburgh, March 1965.

†Present address: Central Research Laboratories, Toyo Rayon Co. Ltd. Sonoyama, Otsu, Japan.

‡In this paper we simply use the term α form when referring to both α and (α, β) structures.

structure[9, 10]. He also assigned the 578 cm^{-1} band of the α form and the 619 cm^{-1} band of the γ form to the amide VI (C=O out-of-plane bending) mode of each structure[10]. Schneider *et al.*[11] also studied Nylon 6 and Nylon 6.6 in this respect. Recently, one of us (I.M.)[12] has studied the spectra in the lower frequency region (800 to 200 cm^{-1}) of several polyamides of the diamine–diacid type and of ω-amino acid class. In this work the following structure/frequency correlations have been established:

	α form	γ form
Amide V	*ca.* 690 cm^{-1}	*ca.* 710 cm^{-1}
Amide VI	*ca.* 580 cm^{-1}	*ca.* 620 cm^{-1}

Furthermore the band appearing in the 400 to 200 cm^{-1} region was tentatively assigned to amide VII (CO—NH torsion) and the frequency shift of this band was discussed in relation to the polymer structures.

In the present study, measurements were made in the medium frequency i.r. region (4 000 to 400 cm^{-1}) on the widest variety of polyamides so far examined, and also in the lower frequency region (400 to 33 cm^{-1}) on some of the polyamides. It concerns the effect of sorption and desorption of iodine–potassium iodide solutions in these polymers and the subsequent changes in chain conformation accompanying this treatment. Earlier published works also dealt with this topic in a limited sense[9–11, 13]. The spectrum of the potassium tri-iodide complex of a model compound, *N*-methylacetamide, which was studied previously by Doskočilová and Schneider[14], has been re-investigated and confirmed in the present study.

EXPERIMENTAL

Materials

Twenty three polyamides of the diamine–diacid type and eight of the ω-amino acid type were examined. The polyamides of the diamine–diacid type, $-[NH(CH_2)_xNHCO(CH_2)_{y-2}CO]_n-$, are sub-divided into the following groups:

(*1*) 'even-even' polyamides, 2.10, 6.6, 6.8, 6.10, 8.6, 8.8, 10.6 and 10.10;

(*2*) 'even-odd' polyamides, 2.9, 4.9, 6.7, 6.9 and 10.9;

(*3*) 'odd-even' polyamides, 5.6, 7.6, 7.8, 7.10 and 9.6;

(*4*) 'odd-odd' polyamides, 5.7, 7.7, 7.9, 9.7 and 9.9.

Polyamides of the ω-amino acid type, $-[NH(CH_2)_{z-1}CO]_n-$, where z is 4, 6, 7, 8, 9, 10, 11 and 12, were studied.

Polymer films of suitable thickness for i.r. measurements were cast from formic acid solution. Traces of formic acid were removed at temperatures mostly below 100 °C on a hot plate.

Iodine treatment of samples

Polyamide samples were treated for different periods (a quarter of an hour to 200 h) with aqueous iodine–potassium iodide solutions. Concentrations of iodine, in aqueous potassium iodide solution from 0·25N to 4N were used. Some of the polymers were also treated with saturated solutions of iodine–potassium iodide in methanol, chloroform, cyclohexane and acetonitrile.

Iodine removal

Iodine was removed from the iodine–potassium iodide treated samples with aqueous sodium thiosulphate solutions. It was sometimes necessary to warm this thiosulphate solution to remove the iodine completely from the sample. Complete removal of iodine was judged from the colour of the films and also from the appearance of the i.r. spectra.

Infra-red spectra

The i.r. spectra in the region 4 000 to 400 cm^{-1} of the polymer films and the model compounds were taken using a Beckman IR-9 spectrophotometer. The lower-frequency spectra of Nylons 6.6, 7.7 and 6 and of the model compounds were also measured in the region 400 to 33 cm^{-1} with a Beckman IR-11 spectrophotometer.

Measurements on the polymer films were made before and after iodine treatment and then after iodine removal.

RESULTS

Iodine sorption and desorption

The efficacy of iodine sorption from iodine–potassium iodide solution was shown qualitatively (by i.r. spectra) to depend on (*a*) specimen, (*b*) concentrations of iodine and potassium iodide, and (*c*) time of treatment.

In general, the extent of iodine sorption decreases as the methylene chain length increases (e.g. the change occurs with greater ease in Nylon 6 than in Nylon 11). The extent of iodine sorption was influenced by changing the potassium iodide concentration, but no detailed measurements were made at this stage of the investigation.

The ease of iodine desorption also depends on the nature of the sample and time of treatment.

Infra-red spectra

'Even-even' polyamides—All the polyamides of this series exhibit the same behaviour (as assessed by i.r. measurements) except Nylon 2.10. Typical spectra before and after iodine treatment as well as after iodine removal are illustrated for Nylon 6.6 in *Figure 1*(a). The atypical spectrum of Nylon 2.10 after similar treatment is shown in *Figure 1*(b). The characteristic amide V and amide VI frequencies for untreated polymers are listed in *Table 1*.

Table 1. Amide V and amide VI frequencies for 'even-even' polyamides

Polymer	*Amide V* cm^{-1}	*Amide VI* cm^{-1}	*Predominant structure*
6.6	692	581	α
6.8	692	581	α
6.10	689	583	α
8.6	691	582	α
8.8	689	581	α
10.6	689	581	α
10.10	687	582	α
2.10	706 sh*	630	γ

*sh denotes shoulder.

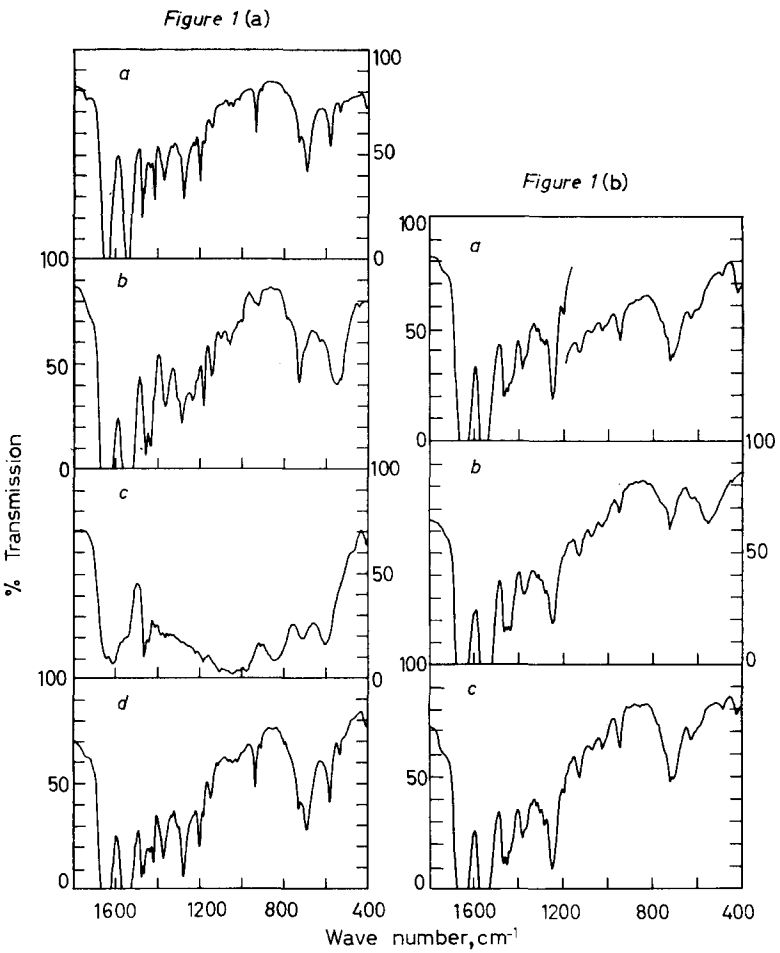

Figure 1(a)—The i.r. spectral changes in Nylon 6.6: (*a*) untreated sample, (*b*) moderate iodine treatment, (*c*) severe iodine treatment, (*d*) iodine removed

Figure 1(b)—The i.r. spectral changes in Nylon 2.10: (*a*) untreated sample, (*b*) moderate iodine treatment, (*c*) iodine removed

With the exception of Nylon 2.10 all the polyamides exhibit the amide V and VI bands around 690 and 580 cm^{-1}, respectively, before iodine treatment and after iodine was removed, showing that the polymer chains take the α conformation in these polyamides. In Nylon 2.10 the amide V band appears at 706 cm^{-1} as a shoulder on the 723 cm^{-1} CH_2 rocking band and the amide VI band occurs at 630 cm^{-1}. Therefore, the γ structure must be predominant in this polyamide.

A sequence of spectral changes occurred on complexing these polyamides in iodine–potassium iodide solution. At first the amide V band of the untreated samples decreased in intensity and a broad band appeared in the range 570 to 550 cm^{-1}. This band is assigned to the amide V vibration of

the complex itself. On more severe treatment (for longer periods or in more concentrated solutions) this band moves towards higher frequency to about 605 cm^{-1}. The amide VI band appears to remain unchanged throughout this treatment but it is sometimes partially obscured by the broad band of the complex in the 610 to 550 cm^{-1} region. More specifically, when Nylon 6.6 was treated with a 2N iodine–potassium iodide solution for less than four hours, amide V shifted from 692 to 550 cm^{-1} (*Figure 1*(a)*b*). However, on more severe treatment (four hours to 70 hours in this solution) an upward shift in frequency to about 605 cm^{-1} occurred (*Figure 1*(a)*c*). Noteworthy too in such circumstances are the changes wrought at the amide I (1 640 cm^{-1}) and the amide II (1 540 cm^{-1}) frequencies. Both these bands are reduced in intensity and a new stronger band appears at 1 610 cm^{-1}. At the same time some broad, strong absorption occurred in the 1 200 to 900 cm^{-1} region accompanied by a weaker one at about 840 cm^{-1}. The amide A (N—H stretching) absorption which occurs at about 3 300 cm^{-1} in untreated material moved to around 3 360 cm^{-1} after complete complex formation. After iodine was desorbed, Nylon 6.6 showed the same spectrum as the original one regardless of whether the sample had undergone a moderate or severe iodine treatment. This behaviour is followed by all the other polyamides.

The spectrum of Nylon 6.6 in the CH_2 scissoring frequency region shows four distinct bands at 1 476, 1 467, 1 438 and 1 418 cm^{-1}. On complexing the polymer with iodine–potassium iodide, however, the bands at 1 476 and 1 418 cm^{-1} decreased in intensity, while the 1 438 cm^{-1} band increased in intensity. Only two peaks with comparable intensities are observed at 1 463 and 1 440 cm^{-1} on complete complex formation. When iodine was removed from the polymer, the original four peaks reappeared. All the other even-even Nylons, except Nylon 2.10, behaved as Nylon 6.6 in this respect, though the spectral changes were less pronounced with the polyamides having longer methylene chains.

'Even-odd' polyamides—The significant amide V and amide VI fre-

Table 2. Amide V and amide VI frequencies for 'even-odd' polyamides

Polymer		*Amide V* cm^{-1}		*Amide VI* cm^{-1}		*Predominant structure*
2.9	b*	715 sh†	—	630	—	γ
	a	—	—	—	—	—
4.9	b	715 sh	693	—	582	α
	a	712 sh	—	621	—	γ
6.7	b	716 sh	696 sh	634	590 sh	γ
	a	716	—	637	—	γ
6.9	b	712 sh	692	620 sh	584	α
	a	~710 sh	—	622	—	γ
10.9	b	~710 sh	—	622	—	γ
	a	~710 sh	—	620	—	γ

*b denotes before iodine treatment; a, after iodine has been removed from the iodine treated sample.
†sh denotes shoulder.

quencies before iodine treatment and after iodine desorption are listed in *Table 2*. The polyamides of this series appear to exist as mixtures of the α and the γ structures. The observed spectra depend on which of the two structures is predominant in each polymer. Thus Nylons 4.9 and 6.9 exhibit the amide V and amide VI peaks at about 690 and 580 cm^{-1}, respectively, which shows that the α form is predominant in these polyamides. The fact that weaker shoulder bands are observed around 715 and 620 cm^{-1} suggests that the γ form also exists as a minor component. Typical spectra are shown for Nylon 6.9 in *Figure 2*(a). The spectra of

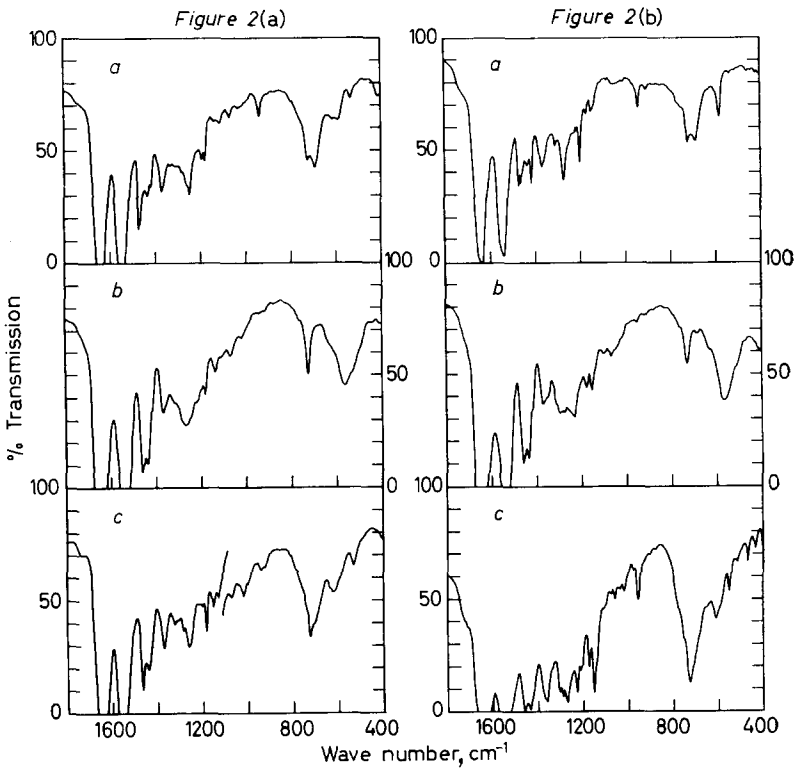

Figure 2(a)—The i.r. spectral changes in Nylon 6.9: (*a*) untreated sample, (*b*) moderate iodine treatment, (*c*) iodine removed

Figure 2(b)—The i.r. spectral changes in Nylon 7.8: (*a*) untreated sample, (*b*) moderate iodine treatment, (*c*) iodine removed

Nylons 2.9, 6.7 and 10.9 resemble those of the 'odd-odd' polyamides (see below). The amide V and amide VI bands appear around 715 and 630 cm^{-1} respectively, showing that the γ structure is predominant in these polymers. Nylon 6.7 must contain a small fraction of the α form, because it exhibits weaker shoulders at about 690 and 590 cm^{-1}.

When the polyamides were subjected to iodine treatment, the amide V band decreased in intensity or disappeared on severe treatment, and a new band appeared in the 610 to 550 cm^{-1} region which is the same as

found in the 'even-even' series. When iodine was desorbed, amide V and amide VI of all the polyamides appeared around 715 to 630 cm^{-1} respectively, showing that they take only the γ structure irrespective of whether the α or the γ form is predominant in the untreated polymers.

Nylon 4.9 and Nylon 6.9 show four CH_2 scissoring bands around 1 475, 1 465, 1 440 and 1 420 cm^{-1}. On iodine treatment of the polymers, the 1 475 and the 1 420 cm^{-1} bands decreased in intensity, while the 1 440 cm^{-1} band increased in intensity. On complete complex formation, the polyamides show two peaks with comparable intensities around 1 460 and 1 440 cm^{-1}. These bands remained unchanged when iodine was removed from the sample. On the other hand, Nylons 2.9, 6.7 and 10.9 have only two peaks around 1 460 and 1 440 cm^{-1}, and this structure of two peaks was retained throughout the process of iodine treatment and subsequent iodine removal.

'Odd-even' polyamides—The amide V and amide VI frequencies before iodine treatment and after iodine desorption are listed in *Table 3*.

Table 3. Amide V and amide VI frequencies for 'odd-even' polyamides

Polymer		*Amide V* cm^{-1}		*Amide VI* cm^{-1}		*Predominant structure*
5.6	b*	713 sh†	693	—	580	α
	a	710 sh	—	614	—	γ
7.6	b	712 sh	690	—	581	α
	a	710 sh	—	~590 *b*‡		γ
7.8	b	—	691	—	583	α
	a	710 sh	—	612	—	γ
7.10	b	—	688	—	583	α
	a	710 sh	—	620	—	γ
9.6	b	—	689	—	580	α
	a	~705 sh	—	~590 *b*		γ

*b denotes before iodine treatment; a, after iodine has been removed from the iodine treated sample.
†sh denotes shoulder.
‡*b* denotes broad.

Typical spectral changes found after iodine sorption and desorption experiments are illustrated for Nylon 7.8 in *Figure 2*(b). Before iodine treatment the amide V and amide VI bands appear at about 690 and 580 cm^{-1} respectively. This shows that the α structure is predominant in the untreated polyamides. However, the existence of weaker satellite bands around 715 and 630 cm^{-1} suggests that the γ structure also exists as a minor component.

On iodine treatment of the polyamides, amide V disappeared and a new band appeared in the 610 to 550 cm^{-1} region. After iodine was desorbed, amide V was observed around 710 cm^{-1} as a shoulder on the 725 cm^{-1} CH_2 rocking band and amide VI appeared in the 620 to 590 cm^{-1} region, showing that all the polyamides take the γ structure under this condition.

All the polymers of this series have four CH_2 scissoring bands around 1 475, 1 465, 1 440 and 1 420 cm^{-1}. When the polymers were subjected to

iodine treatment, the 1 475 and 1 420 cm^{-1} bands decreased in intensity. Only two peaks were observed around 1 460 and 1 440 cm^{-1} on complete complex formation, and they remained the same after the iodine was removed.

'Odd-odd' polyamides—All the polyamides of this series show similar i.r. spectra before iodine treatment and after iodine removal. The amide V and VI frequencies for untreated polymers are listed in *Table 4*. Typical

Table 4. Amide V and amide VI frequencies for 'odd-odd' polyamides

Polymer	*Amide V* cm^{-1}	*Amide VI* cm^{-1}	*Predominant structure*
5.7	710	634	γ
7.7	718 sh*	633	γ
7.9	717 sh	624	γ
9.7	716 sh	635	γ
9.9	~718 sh	624	γ

*sh denotes shoulder.

spectra before and after iodine treatment as well as after iodine removal are illustrated for Nylon 7.7 in *Figure 3*(a). The amide V band appears

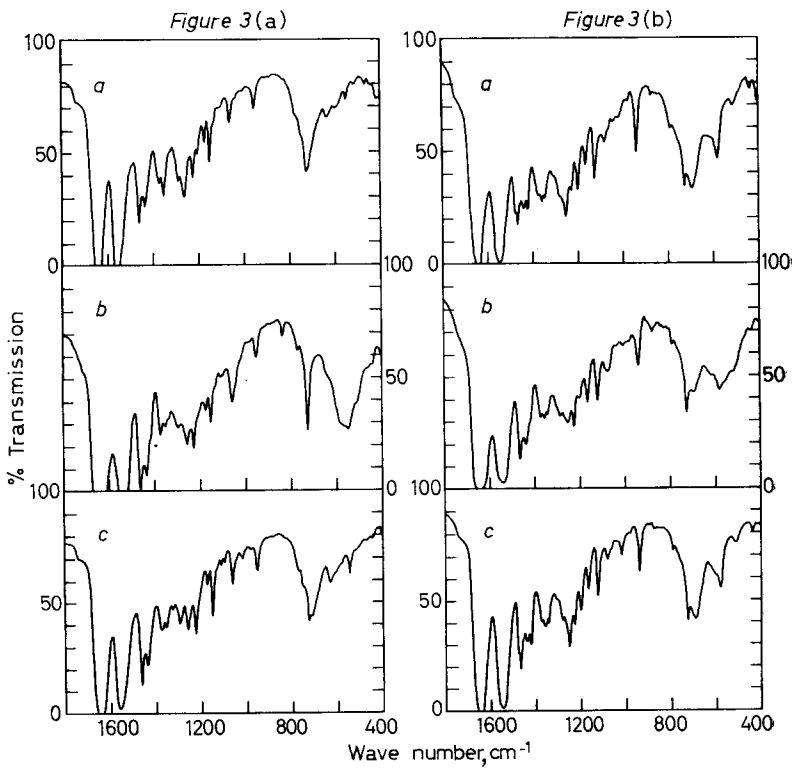

Figure 3(a)—The i.r. spectral changes in Nylon 7.7: (*a*) untreated sample, (*b*) moderate iodine treatment, (*c*) iodine removed

Figure 3(b)—The i.r. spectral changes in Nylon 7: (*a*) untreated sample, (*b*) moderate iodine treatment, (*c*) iodine removed

around 715 cm^{-1} as a shoulder on the 725 cm^{-1} CH_2 rocking band and amide VI is observed at about 630 cm^{-1}. This shows that all these polyamides take the γ structure.

On iodine treatment of the polymers, amide V disappeared and a new band appeared in the 610 to 550 cm^{-1} region.

All the polyamides of this series exhibit only two CH_2 scissoring bands around 1 460 and 1 440 cm^{-1}, and no change in frequency nor in intensity of these bands was noted throughout the course of complex formation with iodine–potassium iodide and subsequent iodine removal.

Polyamides of the ω-amino acid type—Table 5 lists the amide V and

Table 5. Amide V and amide VI frequencies for ω-amino acid type polyamides

Polymer		*Amide V* cm^{-1}		*Amide VI* cm^{-1}		*Predominant structure*
4	b*	—	694	—	576	α
	a	—	693	—	575	α
6	b	712 sh†	692	623 w‡	579	α
	a	712	—	623	—	γ
7	b	~710 sh	691	620 w	581	α
	a	~705 sh	691	~610 sh	582	α
8	b	714 sh	690	633 w	583	α
	a	714 sh	—	631	—	γ
9	b	—	690	—	582	α
	a	~710 sh	690	621 w	583	α
10	b	714 sh	—	627	—	γ
	a	714 sh	—	623	—	γ
11	b	—	690	~625 w	584	α
	a	~710 sh	690	622 w	584	α
12	b	712 sh	—	627	—	γ
	a	714 sh	—	626	—	γ

*b denotes before iodine treatment; a. after iodine has been removed from the iodine treated sample.
†sh denotes shoulder.
‡w denotes weak.

amide VI frequencies of the polyamides of this series before iodine treatment and after iodine removal. These polyamides may be classified into the following three sub-groups according to the positions of the amide V and amide VI bands and their frequency changes when the polymers are subjected to iodine sorption and desorption treatments.

(1) Nylons 4, 7, 9 and 11 exhibit the amide V and VI bands around 690 and 580 cm^{-1} respectively, showing that the α form is predominant in these polyamides.

On iodine treatment of these polymers the amide V band decreased in intensity and a new band appeared in the 610 to 550 cm^{-1} region, although the spectral changes become less pronounced with the increasing methylene number of the polymers. When iodine was removed, amide V moved

back to the original position of 690 cm^{-1}. In Nylons 7, 9 and 11 weaker bands were observed around 710 and 620 cm^{-1} both before iodine treatment and after iodine desorption. This suggests that the γ structure also exists as a minor component in these polymers. Typical spectral changes are shown for Nylon 7 in *Figure 3*(b).

Nylons 7, 9 and 11 show four CH_2 scissoring bands at about 1 475, 1 465, 1 440 and 1 420 cm^{-1}, except that the 1 475 cm^{-1} band appears only as a shoulder to the 1 465 cm^{-1} one in Nylon 9 and Nylon 11. When the polyamides were subjected to iodine treatment, the 1 475 and 1 420 cm^{-1} bands decreased in intensity, while the 1 440 cm^{-1} one became more intense. When iodine was removed, the spectra of all the polyamides resumed the original structure of four peaks. Nylon 4 has three peaks at 1 473, 1 451 and 1 417 cm^{-1} and a weak shoulder around 1 440 cm^{-1}. The frequency of the second band, 1 451 cm^{-1}, is noticeably lower than the value of 1 465 cm^{-1} of the other polyamides.

(*2*) Nylon 6 and Nylon 8 exhibit the amide V and VI peaks around 690 and 580 cm^{-1} respectively, which shows that the α form is predominant in these polyamides. However, the existence of two weaker bands around 715 and 630 cm^{-1} is evidence that a considerable portion of the polymer chain takes the γ structure.

When the polyamides were subject to iodine treatment, both the 690 and 715 cm^{-1} amide V bands disappeared and a new band appeared in the 610 to 550 cm^{-1} region. On iodine desorption, amide V and amide VI appeared at about 715 and 630 cm^{-1}, respectively, but no band was observed around 690 nor 580 cm^{-1}. This means that only the γ structure exists under this condition. Typical spectral changes are illustrated for Nylon 8 in *Figure 4*(a).

These polyamides exhibit four CH_2 scissoring bands around 1 475, 1 465, 1 440 and 1 420 cm^{-1}. On iodine sorption and desorption treatments of the polymers, these bands behaved in the same way as in the 'odd-even' polyamides.

(*3*) Nylon 10 and Nylon 12 exhibit amide V around 715 cm^{-1} as a shoulder on the 725 cm^{-1} CH_2 rocking band and amide VI at about 630 cm^{-1}, showing that these polyamides exist in the γ form.

On iodine treatment of the polyamides, amide V behaved in the same way as in the 'odd-odd' polyamides, and returned to the original position when iodine was removed. Typical spectral changes are shown for Nylon 10 in *Figure 4*(b).

These polyamides have only two CH_2 scissoring bands around 1 460 and 1 440 cm^{-1}, and this structure of two peaks is retained throughout the process of iodine treatment and subsequent iodine removal.

Iodine treatment in solutions other than water—Nylon 6 treated with saturated iodine–potassium iodide in methanol showed a similar but less pronounced change in the spectra than that observed when the sample was treated with an aqueous iodine–potassium iodide solution for a comparable period. Nylons 6, 10.6, 4.9 and 9.7 are unaffected by saturated iodine–potassium iodide in dry acetonitrile, chloroform or cyclohexane solutions respectively.

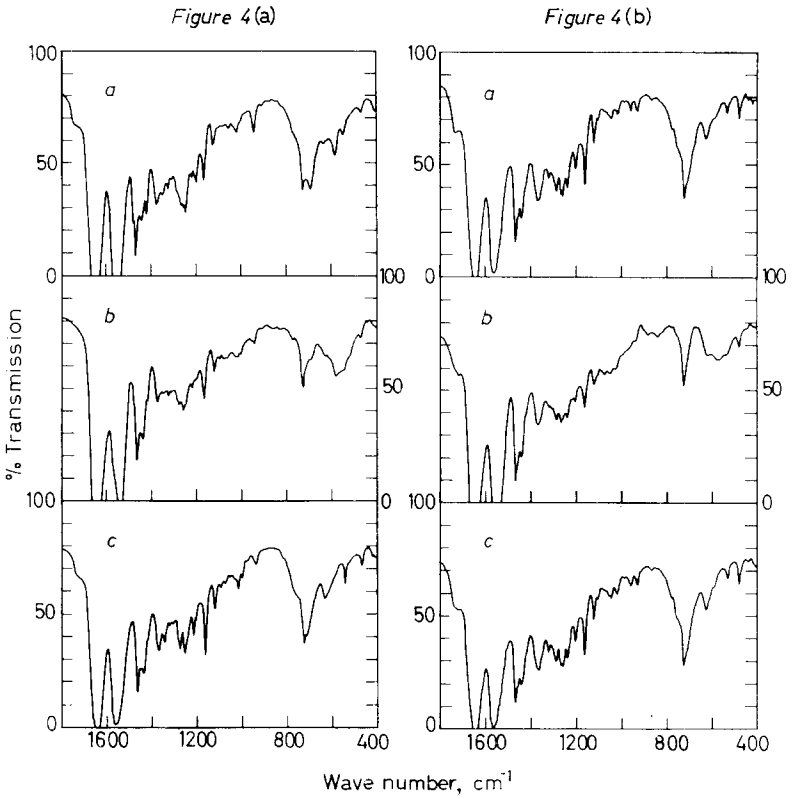

Figure 4(a)—The i.r. spectral changes in Nylon 8: (*a*) untreated sample, (*b*) moderate iodine treatment, (*c*) iodine removed

Figure 4(b)—The i.r. spectral changes in Nylon 10: (*a*) untreated sample, (*b*) moderate iodine treatment, (*c*) iodine removed

N-*methylacetamide complex*

Characteristic amide frequencies of *N*-methylacetamide and its potassium tri-iodide complex are shown in *Table 6*. The results are essentially the same as those reported by Doskočilová and Schneider[14].

Table 6. Amide frequencies of N-methyl acetamide and its potassium tri-iodide complex

Band	N-*methyl acetamide** cm^{-1}	*Complex*† cm^{-1}
Amide A	3310	3374
I	1659	1650
II	1566	1548
III	1300	1294
IV	629	638, 627
V	720	547
VI	602	—

*Capillary film between caesium iodide plates at *ca.* 30°C.

†Nujol mull between caesium iodide plates.

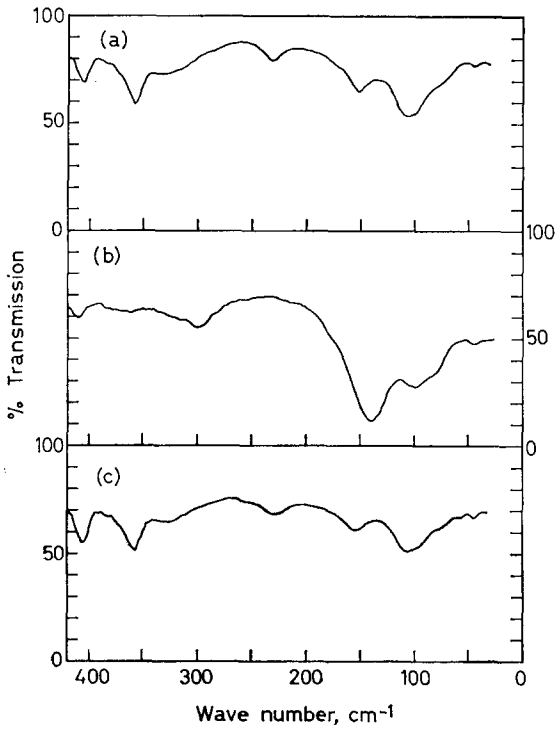

Figure 5 — Lower - frequency i.r. spectra of Nylon 6.6: (a) untreated sample, (b) iodine treated, (c) iodine removed

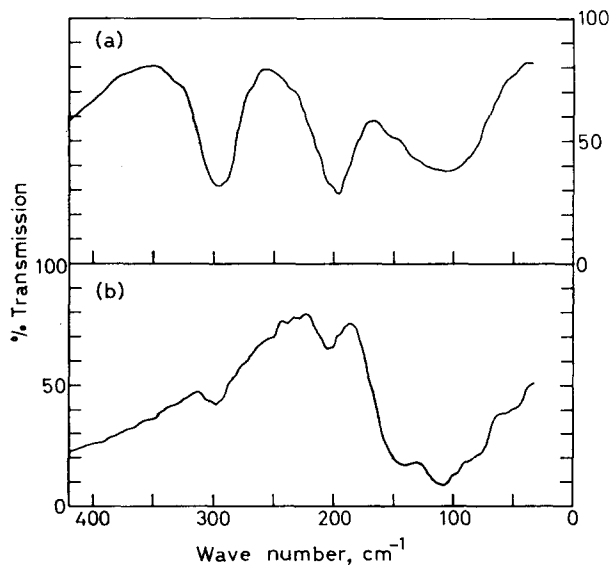

Figure 6—Lower-frequency i.r. spectra of the model compounds: (a) *N*-methylacetamide (film between polyethylene plates), (b) potassium tri-iodide complex of *N*-methylacetamide (Nujol mull between polyethylene plates)

Lower-frequency i.r. spectra

All of the three different polyamides so far examined (Nylons 6.6, 7.7 and 6) exhibit the same behaviour in the lower-frequency region (400 to 33 cm^{-1}) when treated with iodine–potassium iodide solution. Typical spectra are illustrated for Nylon 6.6 in *Figure 5*. When the polyamides are treated with iodine–potassium iodide solution, a strong band appears at 140 cm^{-1} which is not observed in untreated materials. This is so even when the polyamide complex with iodine–potassium iodide is not fully formed. The band at 140 cm^{-1} remained unchanged after the sample had been pumped out under a vacuum (10^{-4} to 10^{-5} mm of mercury) for a few days. This band disappeared after iodine was removed from the sample with sodium thiosulphate solution.

The spectra of the model compounds, *N*-methylacetamide and its potassium tri-iodide complex, are shown in *Figure 6*. The complex exhibits a strong band at 140 cm^{-1} which is not observed in *N*-methylacetamide. The band of the complex observed at 110 cm^{-1} may have the same origin as the broad band of *N*-methylacetamide at 115 cm^{-1}.

DISCUSSION

The nature of the iodine complex

Polyamides form complexes with an aqueous iodine–potassium iodide solution, but not in non-aqueous media, as judged from the i.r. spectral observations. Evidence presented in this paper indicates that iodine forms complexes with polyamides as the tri-iodide ion and not as the molecular species[15] as has been suggested[9].

The strong band observed at 140 cm^{-1} in the iodine–potassium iodide treated polyamides must correspond to some vibration of complexed iodine in these polymers. It is believed that this band is due to the tri-iodide ion because caesium tri-iodide exhibits a strong band at 149 cm^{-1} which is assigned to the I—I stretching vibration of tri-iodide ion. The i.r. inactive vibration of molecular iodine at 213 cm^{-1} becomes i.r. active in the presence of a strong donor molecule such as pyridine[16] giving an absorption band above 180 cm^{-1}. This frequency is considerably higher than the 140 cm^{-1} band found for the polyamide complexes. This fact, together with the observed similarity between the spectra of iodine treated polyamides and the tri-iodide complex of *N*-methylacetamide[14], is in accord with the presence of I_3^- ions in these polymer complexes.

X-ray evidence from polyamide complexes[9, 17] reveals a shortening of the molecular repeat distance with the concomitant appearance of new meridional reflections which must be attributed to the presence of halogen. These results (which were obtained on oriented fibres) usually refer to comparatively short periods of treatment with aqueous iodine–potassium iodide solution. The diffuse nature of the X-ray pattern for fully complexed polymers (as judged from the i.r. spectra) arises because of the powerful scattering effect of the large halogen ion compared with the polymer itself. Radiation other than CuKα which is less strongly scattered may be used with particular reference to the halogen spacing in the complex. West[18] proposed (on the basis of dichroic and X-ray measurements on oriented specimens) that the halogen was present as 'polymeric iodine' but this

explanation has been refuted by Tranter and Collins[17] who find no evidence for this type of structure.

From the observations that the amide I (C=O stretching) frequency decreases by about 10 cm^{-1} and the amide A (N—H stretching) frequency increases by about 60 cm^{-1} when Nylon 6 is complexed in aqueous iodine–potassium iodide solution, Arimoto[9, 10] assumed that the hydrogen bond between the amide groups was weakened or broken and iodine was co-ordinated to the amide oxygen to form a halogen-molecule bridge. However, the decrease of the amide V frequency by almost 170 cm^{-1} on complex formation of the polymer, which is much larger than would correspond to the weakening of the hydrogen bond, led Doskočilová and Schneider[14] to conclude that the halogen ion is coordinated to the nitrogen of the amide groups. The additional fact, in the present work, that the amide I at 1 640 cm^{-1} moved down to 1 610 cm^{-1} and some broad, strong bands appeared in the 1 200 to 800 cm^{-1} region in polyamides which had undergone drastic treatment (i.e. complete complex formation) suggests that protonation occurred (as K^+ or H^+) at the oxygen atom[19]. The ingress of the large halogen ion into the polyamide structure can occur only after the original hydrogen bonded network has been disrupted by protonation of the carbonyl oxygen in the aqueous ionized medium and is accompanied by a concomitant zig-zag type chain contraction to facilitate the entrance into the network of tri-iodide ions, which have a strong affinity for the amide groups. Because of space requirements this large and linear or nearly linear tri-iodide ion[20] must be aligned predominantly in the direction of molecular chains. At the same time, a 'bridge' is formed between an amide nitrogen atom and a protonated carbonyl group in adjacent 'crumpled' or distorted polymer sheets. When the iodine is removed, the amide groups re-form hydrogen bonds with the neighbours of the adjacent sheets which may differ from the original ones. A similar kind of structure has been independently proposed for the hydrochlorides of Nylon 6.6 and Nylon 6.10[21].

The incorporation of tri-iodide ions into the polyamide is also accompanied by an increase in density as witnessed by the different flotation properties of untreated and iodine treated polymer films. Furthermore, the fully complexed polymer films are plastic and have elastomeric properties arising from their modified structures on iodine treatment. After iodine is desorbed from these films they are mechanically weaker than the untreated samples.

Structural changes in polyamides

Amide V and VI bands—Tables 1 to *4* summarize the predominant structural forms of the polyamides before complex formation and after iodine desorption. The assignment of these conformations is based on the correlations between the amide V and VI frequencies and the crystal structures of the polyamides[12]. Those polymers which have the α structure show the definite amide V and VI absorption bands at about 690 and 580 cm^{-1} respectively. All the polymers existing in the γ form have the amide V and VI frequencies at about 715 and 630 cm^{-1} respectively. Consistent behaviour is noted, in respect to these bands, for the wide variety of polyamides examined, though there are some exceptions to the general

classification of polyamides according to polymer classes such as 'even-even', and so on.

Except for Nylon 2.10, the 'even-even' series of polyamides which have originally the α structure with fully extended molecular chains, revert to this structure after iodine is desorbed from the complex. In the complexed condition a twisted chain conformation exists. This conformation is independent of the original polymer structure (i.e. whether α or γ forms). The α form must be the more stable form in the 'even-even' series since it allows maximum hydrogen bonding. On the basis of molecular models, complete hydrogen bonding is possible in the linear or extended chain form of Nylon 2.10. However, the short diamine sequence in this polymer may impose some restrictions on the molecular chain conformation (especially in the hydrogen bonded state) which makes it energetically more feasible for this polymer to form pleated hydrogen bonded sheets in preference to the sheets of fully extended chains present in the other members of this series. To test this suggestion, it would be necessary to examine Nylon 10.2 or some other polyamide possessing a comparable long and short sequence in the molecular chain.

All the 'even-odd' polymers in *Table 2* exist in the γ form after the Nylon complex is freed of iodine, suggesting that the γ structure is the more favourable conformation. During this desorption process, the polymer chains are probably facilitated into states of lower chemical potential with complete hydrogen bonding. This process must be accompanied by a contraction of the chains from their dilated condition in the complex. An inspection of *Table 2* reveals that some of these polymers have been obtained initially in the α form during the film preparation. Under suitable conditions it is believed that all of these 'even-odd' polymers can be obtained in the α form even though this molecular arrangement may not be the one of lower chemical potential. Miyake[3] has reported that Nylons 4.9, 6.7, 6.9 and 10.9 exist in the δ structure when prepared from formic acid or benzyl alcohol solution. However, this structure is believed to be a mixture of the α and the γ forms[4].

The 'odd-even' polyamides, illustrated in *Table 3*, follow a consistent pattern and proceed from the $\alpha \longrightarrow \gamma$ conformation on desorption of iodine.

'Odd-odd' polyamides do not undergo a conformational change, but retain their original γ structure after iodine is removed. Arimoto[13] also finds that Nylon 5.7 and Nylon 5.9 retain their γ conformation under the above circumstances. Miyake[3] reports that Nylons 7.7, 7.9 and 9.9 exist in the γ structure when cast from formic acid solution in agreement with our results.

At first sight, the poly-ω-amino acid series presents a complicated pattern but, on closer inspection, some uniformity is observed. The even members of the series with longer methylene chains usually have the γ conformation before and after iodine sorption and desorption treatment, but the odd members generally exist in the α form. Nylon 6 and Nylon 8 represent an intermediate stage of behaviour and undergo an $\alpha \longrightarrow \gamma$ transformation. Nylon 4 either behaves anomalously, or else marks the beginning of a trend where $\alpha \longrightarrow \alpha$ transformations are predominant in polymers with

short methylene sequences and $\gamma \longrightarrow \gamma$ changes are prevalent when these sequences are longer and more capable of forming twisted structures. In this respect, it must be stated that Nylons 3, 4 and 10 have been prepared in the α form[3] though it is anticipated that the α form of Nylon 10 would change to the γ structure on complex formation with iodine–potassium iodide solution and subsequent iodine removal.

The fine structure of CH_2 *scissoring bands*—The fine structure of the CH_2 scissoring bands in the 1 500 to 1 400 cm^{-1} region is also related to the change in chain conformation of the polyamides with iodine sorption and desorption treatment. Miyake[3] noticed earlier that the peak around 1 415 cm^{-1} appears only when amide V absorbs at 690 cm^{-1} and suggested that it may correspond to the scissoring vibration of the CH_2 groups adjacent to the amide group. On the basis of a detailed analysis of the spectra of Nylon 6.6 and some of its analogues deuterated in the α-position to the amide group, Heidemann and Zahn[22] assigned the 1 474 cm^{-1} and the 1 416 cm^{-1} bands to the scissoring vibration of the N-vicinal and the CO-vicinal CH_2 groups, respectively, and the 1 460 cm^{-1} band to the scissoring vibration of the other CH_2 groups. They also concluded that the scissoring frequencies of the N-vicinal and the CO-vicinal CH_2 groups coincide at 1 435 cm^{-1} as a result of the rotation of the —CH_2—CONH—CH_2— group out of the ideal *trans* conformation. The assignment is in conformity with our observation that the polyamides of the α form which, like Nylon 6.6[1], have the *trans* planar chain conformation around the amide group, exhibit four peaks at about 1 475, 1 465, 1 440 and 1 420 cm^{-1}, one of which at 1 440 cm^{-1} is much weaker than the others, while all the polyamides of the γ form which have twisted chain conformation around the amide group as does Nylon 7.7[2] exhibit only two peaks at about 1 460 and 1 440 cm^{-1}. All the iodine–potassium iodide complexes of polyamides have only two absorption bands around 1 460 and 1 440 cm^{-1}. This is a further indication that the polymer molecules, when combined with tri-iodide ions, have a twisted chain conformation around the amide group regardless of the original chain conformation of the molecule.

CONCLUSIONS

The complex formed when polyamides are treated with iodine–potassium iodide in aqueous solution involves the tri-iodide ion (I_3^-), not molecular iodine (I_2).

The tri-iodide complexes of polyamides are characterized by i.r. bands at about 3 360 cm^{-1} (N—H stretching), 1 460 and 1 440 cm^{-1} (CH_2 scissoring), 570 cm^{-1} (N—H out-of-plane bending) and 140 cm^{-1} (I_3^- ion). Complexes formed on more severe iodine treatment exhibit i.r. bands at about 1 610 cm^{-1} (C=O stretching), 605 cm^{-1} (N—H out-of-plane bending) and an overlapping of several broad absorptions in the 1 200 to 800 cm^{-1} region, which are probably due to protonation at the amide oxygen atom.

Polyamides of the diamine–diacid type generally conform to the following pattern of behaviour before and after iodine sorption and desorption:

Polyamide	*Before iodine treatment*	*After iodine desorption*
even-even	α	α
even-odd	α	γ
odd-even	α	γ
odd-odd	γ	γ

The ω-amino acid type polymers usually change from α to γ structures with the increasing methylene sequence length. Those with short methylene sequences generally undergo $\alpha \longrightarrow \alpha$ transformations whereas with longer sequences the change is $\gamma \longrightarrow \gamma$ transformations, while Nylon 6 and Nylon 8 are intermediate in character.

J. H. Magill expresses indebtedness to the Office of Naval Research for support under contract no. Nonr 2693(00) during the course of this investigation. I. Matsubara acknowledges his appreciation to the National Science Foundation for the support of this work through Grant GP–1628. Thanks are due to Dr F. A. Miller for his interest in this work and helpful comments on the manuscript.

Mellon Institute, Pittsburgh,
Pennsylvania 15213, U.S.A.

(Received May 1965)

REFERENCES

[1] BUNN, C. W. and GARNER, E. V. *Proc. Roy. Soc. A*, 1947, **189,** 39
[2] KINOSHITA, Y. *Makromol. Chem.* 1959, **33,** 21
[3] MIYAKE, A. *J. Polym. Sci.* 1960, **44,** 223
[4] MAGILL, J. H. *J. Polym. Sci.* 1965, **A3,** 1195
[5] CANNON, C. G. *Spectrochim. Acta*, 1960, **16,** 302
[6] TRIFAN, D. S. and TERENZI, J. F. *J. Polym. Sci.* 1958, **28,** 443
TERENZI, J. F. Ph.D. Thesis, Princeton University, 1959
[7] TOBIN, M. C. and CARRANO, M. J. *J. chem. Phys.* 1956, **25,** 1044
[8] BRADBURY, E. M. and ELLIOTT, A. *Polymer, Lond.* 1963, **4,** 47
[9] ARIMOTO, H. *J. Polym. Sci.* 1964, **A2,** 2283
[10] ARIMOTO, H. *Kobunshi Kagaku*, 1962, **19,** 101, 205, 456
[11] SCHNEIDER, B., SCHMIDT, P. and WICHTERLE, O. *Colln. Czech. chem. Commun. Engl. Edn*, 1962, **27,** 1749
[12] MATSUBARA, I., ITOH, Y. and SHINOMIYA, M. *J. Polym. Sci.* 1966, **B4,** 47
[13] ARIMOTO, H. *Kobunshi Kagaku*, 1962, **19,** 461
[14] DOSKOČILOVÁ, D. and SCHNEIDER, B. *Colln. Czech. chem. Commun. Engl. Edn*, 1962, **27,** 2605
[15] MELLOR, J. W. *A Comprehensive Treatise on Inorganic and Theoretical Chemistry*, Vol. II. p 110 ff. Longmans, Green: New York, 1922
GOULD, E. S. *Inorganic Reactions and Structure*, Revised ed., p 210 ff. Holt, Rinehart and Winston: New York, 1962
[16] BRIEGLEB, G. *Elektronen–Donor–Acceptor–Komplexe*, p 98. Springer: Berlin, 1961
[17] TRANTER, T. C. and COLLINS, R. C. *J. Text. Inst. (Trans.)* 1961, **52,** T88
[18] WEST, C. D. *J. chem. Phys.* 1947, **15,** 689
[19] COOK, D. *Canad. J. Chem.* 1963, **41,** 2794; 1964, **42,** 2721
[20] WELLS, A. F. *Structural Inorganic Chemistry*, 3rd ed., p 326 ff. Clarendon: Oxford, 1962
[21] STACE, B. C., TRANTER, T. C. and COLLINS, R. C. Private communication
[22] HEIDEMANN, G. and ZAHN, H. *Makromol. Chem.* 1963, **62,** 123

Model Polyethers II—Synthesis by Polycondensation of Glycols in the Presence of Alcohols

T. P. HOBIN and R. T. LOWSON

The acid-catalysed condensation of glycols in the presence of alcohols has been investigated as a potential synthesis for model polyethers $H[(CH_2)_xO]_n(CH_2)_xH$ *where* $n=2$, *3, 4, etc. The method proved to be satisfactory where* $x=6$ *and 10 but failed where* $x=4$ *and 5.*

THE use of the Williamson reaction for the stepwise synthesis of model polyethers was described in Part I[1]. A batch synthesis yielding a homologous series of model polyethers was required and a possible method of achieving this was by a polycondensation of glycols in the presence of alcohols; the latter to provide terminal alkoxy groups on the condensed glycols.

Earlier work by Hibbert and Perry[2] had shown that ethylene glycol would undergo polycondensation in the presence of iodine to give a homologous series of model polyethylene glycols; the same catalyst was also effective for the depolymerization of polyethyleneglycol. Later, Rhoad and Flory[3] reported that sulphuric acid catalysed the polycondensation of 1,10-decanediol but decomposed lower glycols. Subsequently, Lal and Trick[4] found that sulphuric acid used in conjunction with borontrifluoride etherate was a successful catalyst for the polycondensation of both 1,6-hexanediol and 1,10-decanediol.

The various catalysts used by the previous workers were tried in the course of the present work. Optimum conditions for condensation were ascertained from a preliminary study of the condensation of *n*-hexanol to di-*n*-hexylether. These conditions were employed in attempts to achieve polycondensation of glycols, both alone and in the presence of alcohols.

EXPERIMENTAL

(1) *Optimum conditions for the condensation of* n-*hexanol*

n-Hexanol was heated with the catalyst in a two-necked flask. A thermometer with a ground-glass conical joint was inserted into one of the necks of the flask to record the temperature of the reactants. A Dean and Stark apparatus, inserted into the other neck of the flask, was used to isolate the water produced in the reaction. A series of experiments was carried out using various concentrations of several catalysts (sulphuric acid alone and sulphuric acid, sulphamic acid or *p*-toluene sulphonic acid in conjunction with borontrifluoride etherate).

Some results are summarized in *Table 1*. The yields quoted were only approximately reproducible because the rise in temperature as the *n*-hexanol was converted to di-*n*-hexylether was not necessarily the same in

all the experiments and because the composition of the condensate in the Dean and Stark separator was not controlled. In all cases some unreacted hexanol remained in the separator at the end of the experiment. The following conclusions were drawn from the results.

Efficiency of the catalysts—Comparison of half-reaction times for runs 5, 11 and 12 shows that in the presence of borontrifluoride etherate the order of catalytic activity was sulphuric acid > *p*-toluene sulphonic acid > sulphamic acid. Comparison of runs 2, 4, 6 and 7 shows that the presence of borontrifluoride etherate had very little effect on the rate of reaction or on the yield of hexylether.

Effect of catalyst concentration—Comparison of the half-reaction times for runs 8, 9, 10 and 4 shows that increase of catalyst concentration increased the rate of reaction.

Effect of temperature—The temperatures at half-conversion ranged from 162° to 181°C. This range of temperature is therefore adequate for the condensation. In the later stages of the reactions, however, the temperatures rose as high as 208°C but at the same time there was some loss of *n*-hexylether, presumably by acid-catalysed degradation (compare runs 2 to 5). In keeping with this it was observed that there was considerable darkening of the reaction mixtures when the temperatures exceeded 180°C.

By-products—In all cases a small amount of hexene was obtained (average 1·7 per cent, maximum 3·0 per cent) and an involatile residue remained after distillation of the products (average 6·7 per cent, maximum 10 per cent). In addition, reactions in the presence of borontrifluoride etherate produced a white deposit in the condenser. The latter contained both silicon and fluorine but it had no catalytic activity.

(2) *Attempted polycondensation of glycols*

(i) *Catalysis by iodine*—Some preliminary experiments showed that iodine is a general catalyst for the condensation of glycols. 1,4-butanediol and 1,5-pentanediol, when heated with half per cent by weight or iodine, were readily converted into cyclic ethers. Under the same conditions, 1,6-hexanediol and 1,10-decanediol were converted into low polymers. The latter developed a yellow colouration on storage.

(ii) *Catalysis by sulphuric acid*—Sulphuric acid was found to be a more active catalyst than iodine for the condensation of glycols but it caused some charring of the products (less darkening was observed when the reactions were carried out under vacuum). Catalyst concentrations of half per cent by weight and a reaction temperature of 180°C were found to be suitable for the polycondensation of both 1,6-hexanediol and 1,10-decanediol, although, with the former, about ten per cent of the glycol was converted to cyclic ether. All the polymers, after decolourization with charcoal, exhibited no discolouration on storage.

Table 1. Condensation of *n*-hexanol to di-*n*-hexylether
Runs 1 to 10 Sulphuric acid catalyst
Run 11 *p*-Toluenesulphonic acid catalyst
Run 12 Sulphamic acid catalyst

Run	*Catalyst (% by wt)*		*Half-reaction position*		*Final position*		*Yields %*	
	Acid catalyst	BF_3, Et_2O	*Time, h*	*Temp. °C*	*Time, h*	*Temp. °C*	*Hexyl-ether*	*Water*
1	0·6	0·9	—	—	15	172	84	93
2	0·6	0·9	12	169	20	180	86	88
3	0·6	0·9	—	—	25	194	74	95
4	0·6	0·9	12	181	30	208	64	77
5	0·6	0·9	13	168	63	210	68	94
6	0·6	—	—	—	20	180	86	95
7	0·6	—	12½	178	32	204	65	81
8	0·1	0·3	104	175	129	181	62	87
9	0·2	0·3	39	162	56	190	83	64
10	0·4	0·6	20	165	52	206	70	96
11	1·2	0·9	25½	174	73	213	42	59
12	0·6	0·9	45	178	72	208	57	66

Two solvents were tried namely, *n*-decane (b.pt 171° to 175°C) and, for the reactions involving hexanediol, di-*n*-hexylether (b.pt 223°C). There was no evidence that these interfered with the reactions, except for the expected reduction in rate. Two comparative experiments were carried out in *n*-decane for the purpose of ascertaining the effect of borontrifluoride etherate on the polycondensation of 1,6-hexanediol. In these 1,6-hexanediol (75g) and *n*-decane (50 ml) were reacted with sulphuric acid (0·45g) in one case and sulphuric acid (0·45g)+borontrifluoride etherate (0·9g) in the other. The rate at which water collected was found to be the same in both experiments and both reactions approached completion after five hours. In each case about 7 g of hexamethylene oxide and 52 g of low polymer were obtained.

(3) *Attempted polycondensation of glycols in the presence of alcohols*

(i) *Butanediol*—1,4-Butanediol (1 mole), *n*-butanol (2 mole) and sulphuric acid (1·5 g) reached 118°C on heating and steadily evolved a vapour which passed over at 95° to 100°C. Most of the reactants had been converted to product after eight hours. The distillate contained *n*-butanol, tetrahydrofuran and water.

(ii) *Pentanediol*—1,5-Pentanediol (1 mole), *n*-pentanol (2 mole) and sulphuric acid (1·5 g) attained 140°C at reflux and evolved water at the rate of 1 g/h. A considerable quantity of tetrahydropyran was formed (b. pt 88°C) and because this tended to lower the temperature of the reactants it was distilled over and collected from time to time. The reaction was stopped after 40 h when 19 g of water had been collected. The product was neutralized with aqueous sodium carbonate solution and on fractional distillation yielded the following: *n*-pentanol (118 g), tetrahydropyran

(48 g), di-*n*-amylether (7 g), pentyloxypentanol (7 g) and a higher-boiling residue (7 g).

(iii) *Hexanediol*—The ease of condensation of *n*-hexanol at its boiling point (158°C) and the reluctance of 1,6-hexanediol to undergo intramolecular condensation contributed to the success of attempts to prepare model hexamethylene oxide polymers from condensations involving 1,6-hexanediol and *n*-hexanol. The results of two experiments are given in *Table 2*.

Table 2. Condensation of hexanediol (1 mole) with hexanol. Sulphuric acid catalyst (0·6% by wt)

Hexanol (moles)	*Final position*			*Crude yields (g)*							
	Time, h	*Temp. °C*	*Water formed g*	*Hexene, 70°-90° (760 mm)*	*Cyclic ether, 105°-125° (760 mm)*	*Hexanol, 140°-160° (760 mm)*	*Hexanediol, 250°-265° (760 mm)*	*Monoether, 200°-225° (760 mm)*	*Diether, 140°-160° (2 mm)*	*Triether, 190°-220° (2 mm)*	*Tetraether, 250°-275° (2 mm)*
5	15	180	50	4·6	6·5	148	—	234	60	38	21
3	11	190	34	15	7	25	20	160	68	34	21

It can be seen that increase in the ratio of hexanol to hexanediol from 3 : 1 to 5 : 1 did not appreciably affect the yields of diether $H[(CH_2)_6O]_2(CH_2)_6H$, triether or tetraether but produced a substantial increase in the yield of di-*n*-hexylether. The crude diether and triether referred to in *Table 2* were at least 80 per cent pure by vapour phase chromatography (VPC). The ethers were further purified by repeated fractional distillation from sodium and characterized by boiling point and refractive index (diether 135°C/1 mm $n_D^{20}=1{\cdot}4381$, triether 190°C/0·7 mm $n_D^{20}=1{\cdot}4457$ and tetraether 240°C/0·4 mm $n_D^{20}=1{\cdot}4511$). The diether and triether were also mixed with the same compounds prepared by the Williamson method[1] and subjected to VPC; the mixtures were unresolvable.

(iv) *Decanediol*—As might have been expected, model decamethylene oxide polymers were satisfactorily obtained by the polycondensation of 1,10-decanediol in the presence of *n*-decanol. A mixture of decanol (1 mole), decanediol ($\frac{1}{2}$ mole) and sulphuric acid (0·6% w/w) at 180°C gave 12 g water in eight hours. The product was neutralized with aqueous sodium carbonate solution and all material of boiling point less than 180°/5 mm was distilled off and discarded. Fractional distillation of the residue gave the following:

180° to 190°C/5 mm	28 g	(decylether)
172° to 220°C/1 mm	10 g	
235° to 240°C/1 mm	29 g	(diether)
240° to 300°C/1 mm	5·5 g	
300° to 305°C/1 mm	15·5 g	(triether)
Residue	32 g	(tetraether, etc.)

The diether $H[(CH_2)_{10}O]_2(CH_2)_{10}H$ and triether were fractionally distilled several times from sodium and characterized by melting points, boiling point

and refractive index (diether m.pt 40°C, b.pt 235°/0·4 mm, $n_D^{60} = 1{\cdot}4366$, triether m.pt 50°C, b.pt 305°/1·0 mm, $n_D^{60} = 1{\cdot}4416$). The values of these physical constants agree with those of the analogous compounds prepared by the Williamson reaction.

DISCUSSION

The preliminary experiments on the condensation of *n*-hexanol had indicated that in order to minimize degradation of the products the least quantity of sulphuric acid catalyst consistent with a convenient time scale should be employed (e.g. 0·5 per cent H_2SO_4 w/w) and that the temperature should not be allowed to rise much above 180°C. This was satisfactorily achieved by the use of *n*-decane (b.pt 171° to 175°) as a carrier for the removal of water from the reactants. Rhoad and Flory[3] used more drastic conditions (2 per cent H_2SO_4, 200°C) and so it is perhaps understandable that 1, 6-hexanediol decomposed in their experiments. Lal and Trick[4] apparently did not try sulphuric acid alone; they used a mixture of sulphuric acid with borontrifluoride etherate but did not explain why they used this combination. The polycondensation of 1, 6-hexanediol is accompanied by some intramolecular condensation to hexamethylene oxide and it is known that borontrifluoride is a catalyst for the polymerization of some cyclic ethers[5]. There have been no reports, however, of hexamethylene oxide having been so polymerized. The nearest cyclic ether to have been polymerized is tetrahydrofuran and the polymerization of this has a ceiling temperature of 83°C[6]. The ceiling temperature for the polymerization of hexamethylene oxide would have to be well above 200°C (the temperature used by Lal and Trick) for there to be any appreciable polymerization at this temperature. In the present work it was found that the same quantity of hexamethylene oxide was formed whether borontrifluoride etherate was used or not. In fact borontrifluoride etherate was found to have very little effect on the sulphuric acid catalysed condensation of either *n*-hexanol or of 1, 6-hexanediol. There is a theoretical objection to the use of borontrifluoride in that it might conceivably be converted to boric acid which is known to be an excellent reagent for the conversion of alcohols to olefins[7], the yield of 1-hexene from *n*-hexanol in reaction with boric acid is of the order of 90 per cent.

The possibility of obtaining high-molecular-weight polyethers by the acid catalysed condensation of diols is doubtful. The experiments on the condensation of hexanol showed that some hexene was formed in the reaction; a similar reaction in a diol during polycondensation would produce inactive end-groups which would result in limitation of the molecular weight. Another snag is that towards the end of the reaction the ratio of catalyst to hydroxyl groups increases rapidly and at this stage degradation of the ethereal products becomes significant. This might possibly be overcome by first preparing and purifying the low polymer and then applying very low catalyst concentrations and extended reaction times in an attempt to convert the low polymer to material of higher molecular weight.

The main objective of the present work, the synthesis of model polyethers from glycols and alcohols, was successfully achieved with 1,6-hexanediol and 1,10-decanediol. The method failed for 1,4-butanediol and

1, 5-pentanediol, not because these diols resisted condensation but because of their preference for intramolecular condensation. On this basis it is expected that the synthesis would be satisfactory for all diols higher than hexane diol.

The author is grateful to Mr I. Tunstall of the E.R.D.E. Analytical Section for carrying out VPC analysis.

Explosives Research and Development Establishment,
Waltham Abbey

(*Received September 1965*)

REFERENCES

[1] HOBIN, T. P. *Polymer, Lond.* 1965, **6,** 403
[2] HIBBERT, H. and PERRY, S. Z. *Canad. J. Res.* 1936, **14B,** 77
[3] RHOAD, H. J. and FLORY, P. J. *J. Amer. chem. Soc.* 1950, **72,** 2216
[4] LAL, J. and TRICK, G. S. *J. Polym. Sci.* 1961, **50,** 13
[5] EASTHAM, A. M. *Advanc. Polym. Sci.* 1960, **2,** 18
[6] SIMS, D. *J. chem. Soc.* **1964,** 864
[7] BRANDENBERG, W. B. and GALAT, A. *J. Amer. chem. Soc.* 1950, **72,** 3275

Model Polyethers III—Acid-catalysed Condensation and Degradation Reactions of Hydroxyl-terminated Ethers

T. P. HOBIN

Alkoxyalcohols, $H(CH_2)_xO(CH_2)_xOH$, *where* $x=4$, *5, 6 and 10, undergo acid-catalysed condensation at 180°C to give triethers* $H1[(CH_2)_xO]_3(CH_2)_xH$. *In addition, where* $x=4$ *and 5, simultaneous degradation takes place to give cyclic ethers, lower alcohols, and lower model polyethers. Under comparable conditions triglycols show a similar pattern of behaviour. Some conclusions have been drawn regarding the stability of polyalkylene ethers to acids.*

FOLLOWING the methods of synthesis of model polyethers described in Parts I and II[1,2] the present investigation was undertaken with the specific objective of the synthesis of alkylene triethers from alkoxyalcohols

$$2H(CH_2)_xO(CH_2)_xOH \longrightarrow H[(CH_2)_xO]_3(CH_2)_xH + H_2O$$

When it had been found that in some cases the alkoxyalcohols were prone to degradation, the acid-catalysed reactions of triglycols were investigated to ascertain whether they exhibited a similar pattern of behaviour.

EXPERIMENTAL

(1) *Characterization of model polyethers*

For simplicity, the model polyethers $H[(CH_2)_xO]_n(CH_2)_xH$ will be referred to as diethers where $n=2$ and as triethers where $n=3$. In all cases below where it is stated that a particular model polyether was obtained it is implied that the product, after distillation from sodium until no longer reactive to sodium, gave a fraction of sharp boiling point which was identical to the corresponding model polyether prepared by the Williamson method[1]. The criteria used to establish identity were boiling point, refractive index and infra-red (i.r.) spectra. In addition, vapour phase chromatography (VPC) was used to establish that mixtures of the model polyether with the corresponding material prepared by the Williamson method were not resolvable.

(2) *Apparatus and technique*

In general two methods were used for the condensation reactions.

Method 1—The reactants were heated in a flask connected to a Dean and Stark apparatus for the isolation of the water produced in the reaction. In this method there was a steady flow of condensate back into the reactants.

Method 2—The reactants were heated in a flask with a short distillation head and the volatile products were condensed and collected. Because there

was a continuous transfer of volatiles away from the reaction mixture it was arranged that the distillation took place slowly so that the loss over the period of the reaction was relatively small.

In all cases the products were neutralized with aqueous sodium hydroxide solution and washed with water prior to fractional distillation.

(3) *Reactions of alkoxyalcohols*

The alkoxyalcohols used were those described in Part I[1].

(A) *Butoxybutanol*—Butoxybutanol (73 g 80 per cent pure by VPC), *n*-decane (15 g) and sulphuric acid (0·7 g) were reacted by Method 2 for two hours at 175°C. The following fractions were obtained:

60° to 75°C (mainly tetrahydrofuran)	10 g
116° to 122°C (mainly *n*-butanol)	6 g
170° to 175°C (*n*-decane)	12 g
180° to 230°C (crude butoxybutanol)	4 g
234° to 238°C (diether)	8 g
238° to 310°C (diether and triether)	5 g
310°C (triether)	24 g

The tetrahydrofuran fraction after several distillations from sodium and fractionation gave a liquid b. pt 64° to 66°C, $n_D^{20} = 1{\cdot}407$. These results agree with those expected for tetrahydrofuran.

The *n*-butanol fraction gave a 3,5-dinitrobenzoate which melted at 63° to 64°C. The expected melting point for *n*-butyl-3,5-dinitrobenzoate is 64°C.

(B) *Pentyloxypentanol*—(*i*) Pentyloxypentanol (300 g, 99 per cent pure by VPC), di-*n*-amyl ether (150 g) and sulphuric acid (1·8 g) were reacted by Method 1 for 21 hours at 188°C. 5 ml water was obtained after five hours; this rose to 8·2 ml after 21 hours. The following fractions were obtained:

75° to 90°C (mainly tetrahydropyran)	33 g
90° to 137°C	10 g
138°C (*n*-pentanol)	46 g
180° to 190°C (di-*n*-amyl-ether)	143 g
270° to 300°C (diether)	86 g
180°C/1·0 mm (triether)	50 g

The tetrahydropyran fraction, after several distillations from sodium, distilled at 88°C. The i.r. spectra and refractive index ($n_D^{20} = 1{\cdot}420$) were in agreement with those of a known specimen of tetrahydropyran.

The *n*-pentanol fraction gave a 3,5-dinitrobenzoate which melted at the required temperature (46°C).

(*ii*) Pentyloxypentanol (348 g), di-*n*-amyl ether (180 g) and sulphuric acid (2·5 g) were reacted by Method 2 at 186°C for two hours. Fractionation, as above, gave 74 g tetrahydropyran fraction, 67 g *n*-pentanol fraction, 165 g di-*n*-amyl ether, 57 g diether fraction and 71 g triether fraction.

(C) *Hexyloxyhexanol*—(*i*) Hexyloxyhexanol (40 g, 97 per cent pure by VPC) and sulphuric acid (1 g) were reacted by Method 2 for two hours at 180°C. The following were obtained:

100° to 260°C		1·2 g
260° to 290°C	(mainly hexyloxyhexanol)	5·0 g
130° to 150°C/1·5 mm	(crude diether)	3·0 g
150° to 180°C/1·5 mm	(diether and triether)	1·5 g
180° to 220°C/1·5 mm	(crude triether)	20 g
Residue		2 g

(*ii*) Hexyloxyhexanol (30 g), *n*-decane (50 ml) and sulphuric acid (0·2 g) were reacted by Method 1 at 172°C for eight hours. The following were obtained:

150° to 160°C (crude hexanol)	0·4 g
170° to 180°C (*n*-decane)	49·0 ml
200° to 260°C	0·5 g
260° to 290°C (mainly hexyloxyhexanol)	15·5 g
310° to 320°C (crude diether)	0·5 g
190° to 200°C/0·8 mm (triether)	9·3 g
Residue	1·1 g

The hexanol fraction gave a 3,5-dinitrobenzoate which melted at 58°C. The same derivative from a known sample of *n*-hexanol melted at 59°C. The mixed m. pt was 58·5°C.

(*iii*) Hexyloxyhexanol (44 g), di-*n*-hexyl ether (50 ml) and sulphuric acid (1·5 g) were reacted by Method 2 at 180° for two hours. The following were obtained:

150° to 165°C	(crude hexanol)	2 g
220° to 225°C	(di-*n*-hexyl ether)	46·0 ml
230° to 300°C	(crude hexyloxyhexanol)	8 g
140° to 180°C/2 mm	(mainly diether)	7 g
180° to 210°C/2 mm	(diether and triether)	1·5 g
210° to 220°C/2 mm	(mainly triether)	14 g

(D) *Decyloxydecanol*—Decyloxydecanol (50 g, 98 per cent pure by VPC), *n*-decane (50 ml) and sulphuric acid (1·5 g) were reacted by Method 1 at 175°C for two hours. Difficulties in phase separation during the aqueous washing process resulted in some loss of product. After removal of materials boiling up to 200°C/2 mm, the dark residue was dissolved in ether, treated with decolourizing charcoal and filtered. The ether was removed from the filtrate by distillation and the residue was vacuum distilled. The following were obtained:

190° to 210°C/2 mm (decyloxydecanol)	6 g
210° to 300°C/2 mm	4 g
310° to 330°C/2 to 3 mm (triether)	15 g

There was no trace of decanol in the original volatiles and no trace of diether in the residue.

(4) *Reactions of triglycols* $OH[(CH_2)_xO]_3H$

The triglycols used were those described in Part I[1].

(A) *Tri-decamethylene glycol*—This underwent a slow, steady polycondensation at 180°C in the presence of one per cent of sulphuric acid (w/w). There was no evidence of any significant degradation beyond the usual darkening of the reactants.

(B) *Tri-hexamethylene glycol*—This reacted at 180°C, in the presence of one per cent sulphuric acid (w/w) in a manner analogous to tri-decamethylene glycol.

(C) *Tri-pentamethylene glycol*—(*i*) Tri-pentamethylene glycol (25 g) and iodine (0·1 g) were reacted by Method 2 at 200°C for four hours. A distillate was obtained which contained 2 ml of tetrahydropyran and 0·2 ml water. The residue contained unreacted triglycol (180° to 190°C/1 mm) and 2 g of a higher boiling liquid (200° to 300°C/0·5 mm).

(*ii*) Tri-pentamethylene glycol (17 g) and sulphuric acid (0·5 g) were reacted by Method 2 at 200°C. After half an hour only a small amount of charred residue remained. The distillate consisted of tetrahydropyran and water.

(*iii*) Tri-pentamethylene glycol (10 g), 1,5-dipentyloxypentane (11·5 g) and sulphuric acid (0·1 g) were reacted by Method 2 for two hours at 180°C. The distillate consisted mainly of tetrahydropyran. The residue, on vacuum distillation, gave 10 g of 1,5-dipentyloxypentane (120°C/0·3 mm) and 5 g of higher boiling residue.

(*iv*) Tri-pentamethylene glycol containing 0·5 per cent w/w of sulphuric acid was reacted by Method 2 at 180°C. The reaction was stopped when about one third had been converted to cyclic ether (about one hour). The residue was neutralized and vacuum distilled. A small amount of unreacted triglycol was obtained, but nothing of lower boiling point. The polymeric residue was crystallized several times from methanol–water to give a waxy solid m. pt 37·5°C.

(D) *Tri-tetramethylene glycol*—Tri-tetramethylene glycol (5 g) and sulphuric acid (0·1 g) were reacted by Method 2 at 180°C. After ten minutes, 2 ml of distillate (mainly tetrahydrofuran) had collected. The residue was poured into methanol–water to give low molecular weight polytetramethylene glycol as a viscous oil.

(5) *Other reactions*

(*i*) The triether $H[(CH_2)_5O]_3(CH_2)_5H$ was heated with 0·5 per cent sulphuric acid (w/w) by Method 2 at 180°C. After six hours, although considerable darkening had occurred, there had been no loss in weight (i.e. no volatile degradation products). Most of the triether was recovered.

(*ii*) Hexamethylene oxide was heated under reflux (120°C) with 0·5 per cent w/w sulphuric acid. Considerable darkening occurred but most of the cyclic ether was recovered after six hours.

EXPERIMENTAL RESULTS SUMMARIZED

The following generalizations refer to reactions in the region of 180°C and in the presence of catalytic quantities of sulphuric acid:

(I) All the alkoxyalcohols and triglycols which were investigated exhibited some degree of intermolecular condensation.

(II) Alkoxyalcohols and triglycols with six or more recurring methylene groups did not undergo any appreciable degradation and did not yield any cyclic ethers; they gave high yields of condensation products.

(III) Alkoxyalcohols and triglycols with sequences of four or five methylene groups underwent significant degradation to give cyclic ethers. Other degradation products were water in the case of the triglycols and lower alcohols in the case of alkoxyalcohols.

(IV) The alcohols produced by degradation reacted with alkoxyalcohols to give diethers. This could be prevented to some extent by removal of the alcohols as they were formed, e.g. by using Method 2 rather than Method 1.

(V) Under comparable conditions, the model polyethers

$$H[(CH_2)_xO]_3(CH_2)_xH, \text{ where } x = 4 \text{ or } 5,$$

did not undergo any significant degradation in the time required for the complete degradation of the corresponding triglycols, even when mixed with the triglycols.

DISCUSSION

It is well-known that the stability of polyoxymethylene can be considerably improved by the replacement of terminal hydroxyl groups by alkoxy groups[3]. It is perhaps not surprising, therefore, that alkoxy-terminated tetramethylene ethers and pentamethylene ethers were more stable to acids than their hydroxyl-terminated counterparts. The degradation of the latter to cyclic ethers presumably occurred by the formation of a transient ring structure at the end of the chain, a process not sterically favoured for higher alkylene ethers. This agrees with the results given in Part II[2] where it was shown that butane-1,4-diol and pentane-1,5-diol underwent intramolecular condensation under conditions in which hexane-1,6-diol and decane-1,10-diol reacted by intermolecular condensation. It can be inferred that the stability of polytetramethylene glycol and polypentamethylene glycol to acids should be considerably improved by replacement of hydroxyl end-groups by alkoxy groups; copolymerization with hexamethylene glycol or higher glycol might also be expected to arrest the degradation process.

The cleavage of ethers has been reviewed by Burwell[4]. It is generally believed that any process which results in a net transfer of positive charge to the oxygen atom will increase the tendency to cleavage by attack by a nucleophilic species. Dilute aqueous acids cleave ethers slowly, probably as follows

$$R_2\overset{+}{O}H + H_2O \rightleftharpoons ROH + R\overset{+}{O}H_2 \qquad (1)$$

With sulphuric acid, although the acidity is high the bisulphate ion has low tendency to nucleophilic displacement and so cleavage does not readily occur. The water molecule likewise has low nucleophilic reactivity.

These generalizations agree with the present observations that the ethers were not easily cleaved by traces of sulphuric acid under anhydrous conditions. It is possible that some ether cleavage occurred, thus, in the reactions involving hexyloxyhexanol both hexanol and diether were found but no trace of cyclic ether was detected. The yields of these byproducts were increased when di-*n*-hexylether was used as solvent, presumably by acidolysis of this solvent. In this particular case there was probably a mass action effect because of the high concentration of ether at the start of the reaction when the rate of water production by condensation was at its greatest. In most of the other reactions, however, the ether concentration was zero at the start and did not become appreciable until after the rate of water formation had decreased considerably. This might explain why very little cleavage was detected in these cases.

The reactions involving hydroxy compounds were much more rapid; they presumably took place as follows:

$$\ldots\ldots (CH_2)_xOH + \overset{+}{H} \rightleftharpoons \ldots\ldots (CH_2)_x\overset{+}{O}H_2 \qquad (2)$$

followed by

(*a*) Condensation

$$\ldots\ldots (CH_2)_x\overset{+}{O}H_2 + \ldots\ldots (CH_2)_xOH \longrightarrow \ldots\ldots (CH_2)_xO(CH_2)_x \ldots\ldots + \overset{+}{H_3}O \qquad (3)$$

(*b*) Degradation (where $x = 4$ or 5)

$$\ldots\ldots (CH_2)_xO(CH_2)_x\overset{+}{O}H_2 \longrightarrow \ldots\ldots (CH_2)_x\overset{+}{O}H_2 + (CH_2)_xO \qquad (4)$$

The degraded species produced by reaction (4) would then either condense or degrade in a similar manner. With triglycols most of the condensation reactions would involve triglycol or higher glycol as one of the reactants and so very little accumulation of diols lower than triglycol would be expected. This is in agreement with the experimental observations.

If the above mechanism is correct then it can be inferred that cleavage by reaction (1) did not occur to any appreciable extent because the ROH_2^+ ion so produced would be expected to degrade to cyclic ether [as in reaction (4)] with both tetramethylene ethers and pentamethylene ethers, and this would have been contrary to observations. It may have been that the hydroxy compounds acted as proton scavengers so that fewer protons were available for a cleavage reaction; this might also explain the observations recorded in Part II that better yields of ethers were obtained when the condensations were not allowed to go to completion. Obviously, as the hydroxyl concentration decreased during the condensation there would be more and more protons available for other reactions and more ethers available to take part in such reactions.

The author is grateful to the E.R.D.E. Analytical Section for i.r. and VPC measurements.

Explosives Research and Development Establishment,
Waltham Abbey, Essex

(*Received September 1965*)

REFERENCES

[1] HOBIN, T. P. *Polymer, Lond.* 1965, **6,** 403
[2] HOBIN, T. P. and LOWSON, R. T. *Polymer, Lond.* 1965, **7,** 217
[3] KERN, W. and CHERDRON, H. *Makromol. Chem.* 1960, **40,** 101
[4] BURWELL, R. L. *Chem. Rev.* 1954, **54,** Pt 2, 615

Thermal Degradation of Piperazine Polyamides II—Poly(terephthaloyl piperazine), Poly(terephthaloyl 2-methylpiperazine) and Poly(isophthaloyl trans-*2, 5-dimethylpiperazine*

S. D. BRUCK*

The thermal degradation of poly(terephthaloyl piperazine), poly(terephthaloyl 2-methylpiperazine) and poly(isophthaloyl trans-*2,5-dimethylpiperazine) is discussed, thus extending the previously published work on poly(terephthaloyl* trans-*2,5-dimethylpiperazine) and poly(oxalyl* trans-*2,5-dimethylpiperazine). The results are discussed in terms of rates, activation energies and degradation products. These piperazine polyamides may be arranged according to the following order of decreasing thermal stability in a vacuum: poly(terephthaloyl piperazine) > poly(terephthaloyl* trans-*2,5-dimethylpiperazine) > poly(terephthaloyl 2-methylpiperazine) > poly(oxalyl* trans-*2,5-dimethylpiperazine) > poly(isophthaloyl* trans-*2,5-dimethylpiperazine). The data indicate that methyl substitution of the piperazine rings of the polymers* decreases *the thermal stability of the system in a vacuum, whereas the presence of terephthaloyl moieties (polycondensation in the* para *positions of the acid component)* increases *the thermal stability in comparison with the system having isophthaloyl moieties in the polymer chains (polycondensation in the* meta *positions of the acid component). The high activation energies, the nature of the volatile degradation products, and the character of the rate curves indicate essentially random thermal breakdowns. However, the degradation is influenced by competing hydrolytic processes, especially with poly(isophthaloyl* trans-*2, 5-dimethylpiperazine).*

IN A previous publication the thermal degradation of two heterocyclic polyamides, poly(terephthaloyl *trans*-2,5-dimethylpiperazine) and poly(oxalyl *trans*-2,5-dimethylpiperazine) was discussed[1]. The present study deals with the thermal degradation in a vacuum of three other piperazine polyamides in the series, namely poly(terephthaloyl piperazine), poly(terepthaloyl 2-methylpiperazine) and poly(isophthaloyl *trans*-2,5-dimethylpiperazine). The objects of this investigation were: (*1*) to study the effects arising from systematic structural variations of the polymers on their thermal stability; (*2*) to determine the rates, activation energies, and the nature of the volatile degradation products; and (*3*) to establish a correlation between structural parameters and thermal stability of the piperazine polyamides.

EXPERIMENTAL DETAILS

Materials

The piperazine polyamides were prepared by the low-temperature solution condensation method of Morgan and Kwolek[2] in chloroform with

*Present address: IBM Research Center, P.O. Box 218, Yorktown Heights, New York 10598, U.S.A.

excess diamine as the acceptor. The inherent viscosities of the polymers were as follows: (*a*) poly(terephthaloyl piperazine) = 1·06; (*b*) poly(terephthaloyl 2-methylpiperazine) = 0·83; (*c*) poly(isophthaloyl *trans*-2,5-dimethylpiperazine) = 2·77. The number-average molecular weights of these polymers are in the range of 14 000 to 38 000 as indicated by end-group/viscosity data and by the results of osmotic measurements as well as differential vapour pressure lowering[3,4].

Polymer melting points

The polymer melting points were estimated from differential thermal analysis data (heating rate 30°C/minute, nitrogen-bleed) obtained with a du Pont 900 Differential Thermal Analyzer using the Standard Cell Assembly.

Viscosity measurements

The inherent viscosities $[(\ln \eta_{rel.})/c$, where $c = 0{\cdot}5$ g/100 ml] were determined in *m*-cresol at 30°C ± 0·05° with Cannon–Fenske viscometers. Intrinsic viscosities ($[\eta] = \lim_{c \to 0} \eta_{inh.}$) were determined in a 40 : 60 mixture by weight of sym-tetrachlorethane : phenol at 30°C ± 0·05° with Cannon–Ubbelohde semi-micro dilution viscometers.

Thermogravimetry

The thermogravimetric studies were carried out in a vacuum ($\sim 10^{-5}$ mm of mercury) with 3 to 5 mg samples using a Cahn RG electrobalance. The method was described in detail in previous publications[5–8].

Mass spectrometric analyses of volatile degradation products

To prevent contamination of the collected gaseous products by materials which may be adsorbed on the electronic components of the electrobalance, separate degradation experiments were carried out with approximately 10 mg samples of the polymer. Each sample was first pre-heated at 100°C for 30 minutes under a vacuum of $\sim 10^{-5}$ mm of mercury with continuous pumping to remove moisture and adsorbed gases; while maintaining this vacuum, the collection vessel was sealed and the sample pyrolysed at 475°C for one hour. During the pyrolyses the collection vessel was cooled with liquid nitrogen to facilitate rapid diffusion of the volatile degradation products from the hot zone and thereby minimize the occurrence of secondary reactions. As in the previous work[1], a fractionation technique was used (liquid nitrogen, dry ice–acetone) in admitting the volatile degradation products into the mass spectrometer.

RESULTS

The general scheme for the preparation of the piperazine polyamides discussed in this paper may be illustrated by the following reactions:

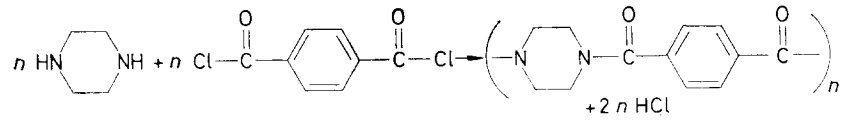

+2 *n* HCl

Poly(terephthaloyl piperazine)
m.pt >450°C

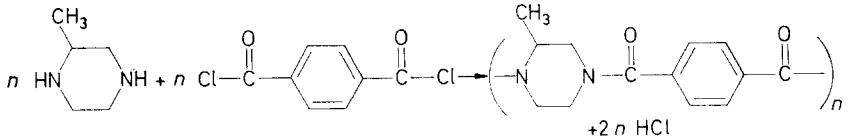

+2 *n* HCl

Poly(terephthaloyl 2-methyl-piperazine)
m.pt* : 430°-460°C

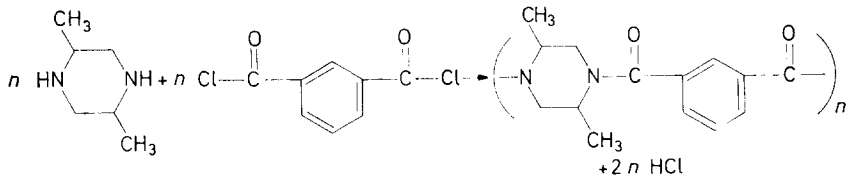

+2 *n* HCl

Poly(isophthaloyl *trans*-2,5-dimethylpiperazine)
m.pt* :380°-420°C

*The first value represents the beginning of the endotherm, the second the maximum.

As the first step in the thermal degradation study of the above polymers, experiments were carried out by programmed thermogravimetry at a heating rate of 4°C/minute in a vacuum ($\sim 10^{-5}$ mm of mercury). The results, illustrated by *Figure 1*, indicate that no appreciable weight loss occurs up to approximately 400°C. However, poly(isophthaloyl *trans*-2,5-dimethylpiperazine) starts to lose weight rapidly at about 420°C (Curve C), whereas poly(terephthaloyl 2-methylpiperazine) and poly(terephthaloyl piperazine) are quite stable up to approximately 440°C and 450°C respectively (Curves B and A). This behaviour of poly(terephthaloyl piperazine) is very similar to that of poly(terephthaloyl *trans*-2,5-dimethylpiperazine), reported earlier[1].

To study the kinetics of the thermal degradation, experiments were also carried out under isothermal conditions in a vacuum between 462°C and 390°C. *Figures 2* to *4* show, respectively, the percentage volatilization as a function of time at various temperatures for poly(terephthaloyl piperazine), poly(terephthaloyl 2-methylpiperazine) and poly(isophthaloyl *trans*-2,5-dimethylpiperazine). Since thermal equilibrium was reached usually within 15 to 20 minutes from the time the pre-heated furnace was positioned around the sample tube, zero time denotes the start of the isothermal heating period. The small weight losses that occur prior to the attainment of isothermal conditions are possibly due to loss of moisture. Whereas poly-(isophthaloyl *trans*-2,5-dimethylpiperazine) almost completely volatilizes

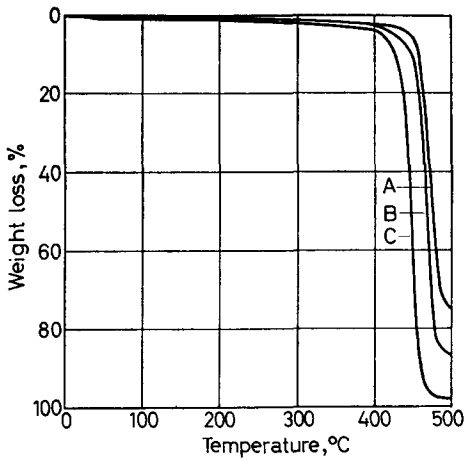

Figure 1—Thermal degradation of (A) poly(terephthaloyl piperazine), (B) poly(terephthaloyl 2-methylpiperazine), and (C) poly(isophthaloyl *trans*-2, 5-dimethylpiperazine) in a vacuum by programmed thermogravimetry of 4°C/minute

at the higher temperatures, both poly(terephthaloyl 2-methylpiperazine) and poly(terephthaloyl piperazine) leave small quantities of residue. Programmed temperature thermogravimetric experiments (*Figure 1*) also confirm these results.

The rates of degradation were obtained from the slopes of the volatilization versus time curves with the aid of an electronic computer, and are characterized by the appearance of distinct maxima, as illustrated in *Figures 5* to *7*. With poly(terephthaloyl piperazine) these maxima occur between 15 and 20 per cent conversion, whereas with poly(terephthaloyl 2-methylpiperazine) and poly(isophthaloyl *trans*-2,5-dimethylpiperazine) they appear at somewhat higher conversions.

The activation energies were calculated from the maximum rates of degradation using the Arrhenius relationship $k = S \exp(-E/RT)$, where k is the rate constant, S is the frequency factor, E is the activation energy,

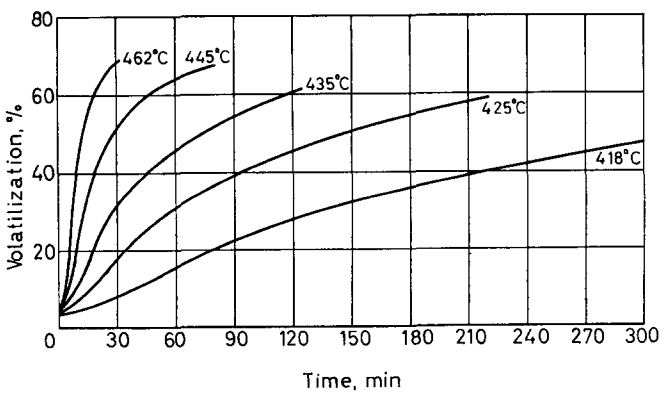

Figure 2—Thermal degradation of poly(terephthaloyl piperazine) at various temperatures in a vacuum

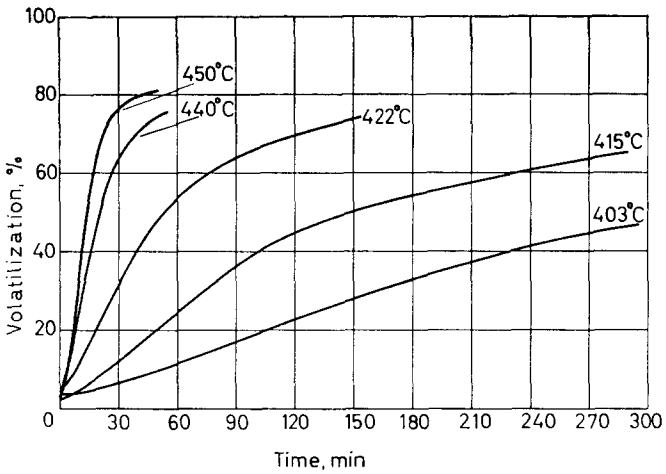

Figure 3—Thermal degradation of poly(terephthaloyl 2-methylpiperazine) at various temperatures in a vacuum

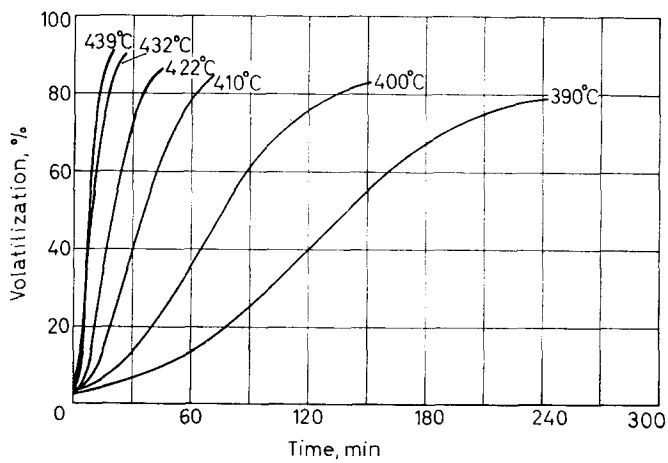

Figure 4—Thermal degradation of poly(isophthaloyl *trans*-2,5-dimethylpiperazine) at various temperatures in a vacuum

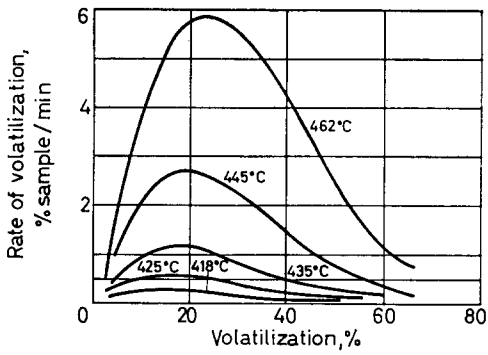

Figure 5—Rates of thermal degradation of poly(terephthaloyl piperazine) at various temperatures in a vacuum

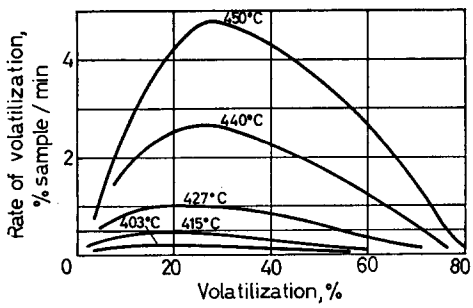

Figure 6—Rates of thermal degradation of poly(terephthaloyl 2-methylpiperazine) at various temperatures in a vacuum

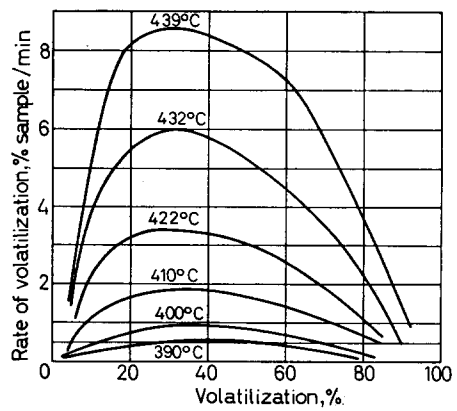

Figure 7—Rates of thermal degradation of poly(isophthaloyl *trans*-2,5-dimethylpiperazine) at various temperatures in a vacuum

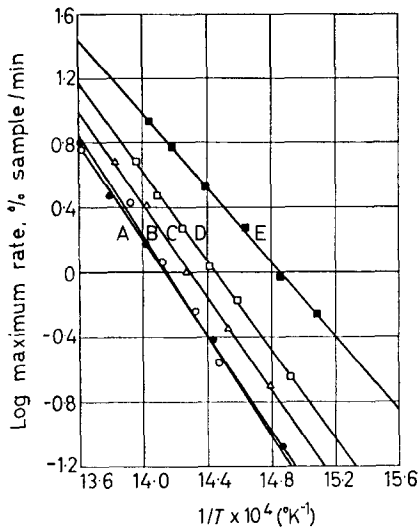

Figure 8—Arrhenius plot for the thermal degradation in a vacuum of (A) poly(terephthaloyl *trans*-2, 5-dimethylpiperazine), (B) poly(terephthaloyl piperazine), (C) poly(terephthaloyl 2-methylpiperazine), (D) poly(oxalyl *trans*-2, 5-dimethylpiperazine), and (E) poly(isophthaloyl *trans*-2, 5-dimethylpiperazine)

R is the gas constant, and T is the absolute temperature). *Figure 8* illustrates the straight-line relationships which were obtained by plotting the logarithm of the maximum rates (expressed in sample volatilized per minute) against the inverse of the absolute temperatures. These are Arrhenius plots for poly(terephthaloyl piperazine), poly(terephthaloyl 2-methylpiperazine) and poly(isophthaloyl *trans*-2,5-dimethylpiperazine), and also for poly(terephthaloyl *trans*-2,5-dimethylpiperazine) and poly(oxalyl *trans*-2,5-dimethylpiperazine), reported earlier[1]. It should be noted that the activation energy of poly(terephthaloyl *trans*-2,5-dimethylpiperazine) was found to be slightly higher (68 kcal/mole) than the value reported previously (64 kcal/mole). The maximum rates of degradation and the activation energies for the five piperazine polyamides are summarized in *Table 1*.

The nature of the degradation products volatile at room temperature was determined by mass spectrometry, following separate pyrolysis experiments in a closed system which had been evacuated to approximately 10^{-5} mm of mercury prior to sealing. *Table 2* summarizes the results in mole per cent. As in the previous studies[1], the chief volatile degradation product is carbon monoxide, with lesser amounts of carbon dioxide, hydrogen, hydrocarbons, pyrazines, pyrroles and ammonia. Water is not considered to be a product of the pyrolytic degradation but rather to originate from adsorbed moisture held in the polymer by hydrogen bonds. Hydrogen chloride was not detected among the volatile degradation products most likely due to the hydrolysis of the acid chloride end-groups prior to the thermal degradation experiments. The data in this and the previous paper[1] indicate that increased methyl substitution of the piperazine rings increases the yield of those degradation products which are volatile at room temperature and decreases the residue remaining in the combustion tube.

Table 1. Maximum rates and activation energies for the thermal degradation of piperazine polyamides in a vacuum

Polymer	*Pyrolysis* °C	*Max. rate* % *sample/min*	*Activation energy* kcal/mole	*Reference*
Poly(Pip-T)	462	5·800		
	445	2·700		
	435	1·170	71	This paper
	425	0·580		
	418	0·280		
Poly	462	6·342		
(*t*-2, 5-DMePip-T)	452	3·000		
	440	1·500	68 (64)	(1)
	420	0·388		
	400	0·084		
Poly(2-MePip-T)	450	4·800		
	440	2·680		
	427	1·000	67	This paper
	415	0·450		
	403	0·200		
Poly	445	4·920		
(*t*-2, 5-DMePip-2)	437	3·000		
	430	1·880	64	(1)
	421	1·110		
	412	0·678		
	397	0·229		
Poly	439	8·600		
(*t*-2, 5-DMePip-I)	432	6·000		
	422	3·400	53	This paper
	410	1·900		
	400	0·940		
	390	0·560		

Legend:
Poly(Pip-T) = Poly(terephthaloyl piperazine)
Poly(*t*-2, 5-DMePip-T) = Poly(terephthaloyl *trans*-2, 5-dimethylpiperazine)
Poly(2-MePip-T) = Poly(terephthaloyl 2-methylpiperazine)
Poly(*t*-2, 5-DMePip-2) = Poly(oxalyl 2, 5-dimethylpiperazine)
Poly(*t*-2, 5-DMePip-I) = Poly(isophthaloyl *trans*-2, 5-dimethylpiperazine)

DISCUSSION

As seen in *Table 1* the activation energies of the thermal degradation of the piperazine polyamides are considerably higher than the 24 to 43 kcal/mole reported for aliphatic polyamides[9]. According to Straus and Wall[9], the low activation energies which characterize the thermal degradation in a vacuum of aliphatic polyamides suggest that a hydrolytic scission of the amide links competes with thermal free radical (random) cleavage. Such hydrolytic processes can be promoted by relatively small quantities of water (held tightly by hydrogen bonds) which cannot be removed by ordinary drying procedures. Simha and Wall[10] have shown on theoretical grounds that for a random type breakdown, the rates versus conversion curves display maxima at about 26 per cent conversion. It is known, however, that the maxima do not always occur at 26 per cent conversion but could shift to higher (or lower) conversions if the polymer breakdown is a

Table 2. Mass spectrometric analysis of degradation products volatile at room temperature of piperazine polyamides during pyrolysis in a vacuum (475°C, 1 h, $\sim 10^{-5}$ mm of mercury)

Component	*Poly(pip-T)** *Mole %*	*Poly(2-MePip-T)†* *Mole %*	*Poly(t-2,5-DMePip-I)‡* *Mole %*
Carbon monoxide	18·7	37·8	43·4
Carbon dioxide	9·2	9·1	11·3
Water	41·3	19·3	12·3
Ammonia	7·0	7·9	0·4
Hydrogen	10·5	6·1	8·8
Methane	3·6	8·7	12·2
Ethane	1·3	2·2	2·9
Propylene	0·5	0·6	1·6
Butane	—	1·2	1·5
Butylene	—	0·8	—
2, 5-Dimethylpyrazine	—	—	1·3
2-Methylpyrazine	—	2·9	0·8
Pyrazine	4·8	—	—
Pyrrole	1·0	0·2	0·3
2-Methylpyrazine	0·2	0·9	0·3
Benzoic acid	—	—	0·2
Benzaldehyde	0·4	0·3	0·1
Xylene	—	—	0·2
Benzonitrile	0·3	0·2	0·2
Benzene	0·4	0·7	1·5
Phenol	0·4	0·1	—
Toluene	0·4	0·6	0·7
Acetylene	—	0·4	—
Total volatiles at room temperature, %	33·3	42·5	20·5
Total non-volatiles at room temperature, %	45·6	46·2	73·8
Residue, %	21·1	11·3	5·1

*Poly(terephthaloyl piperazine)

†Poly(terephthaloyl 2-methylpiperazine)

‡Poly(terephthaloyl *trans*-2, 5-dimethylpiperazine)

non-random one. Such a situation may arise if the degradation process is influenced by so-called 'weak-links' in the polymer, or if a competing degradation process, such as hydrolytic cleavage, is also operative. It is interesting to note that with poly(terephthaloyl piperazine) and poly(terephthaloyl 2-methylpiperazine) the maxima in the rates versus volatilization curves appear between 15 and 25 per cent conversion, but with poly(isophthaloyl *trans*-2,5-dimethylpiperazine) the maxima shift to 30 to 40 per cent conversion. Furthermore, the activation energy of the overall degradation of this latter polymer is significantly lower (53 kcal/mole) than that found for the other members in the series (64 to 68 kcal/mole). The shift of the maximum rates to higher conversions and the reduced activation energy of 53 kcal/mole are probably effects of a hydrolytic breakdown of the amide groups, which competes with a random free-radical cleavage. Such a hydro-

lytic type breakdown will also promote the formation of carbon dioxide according to the following reaction

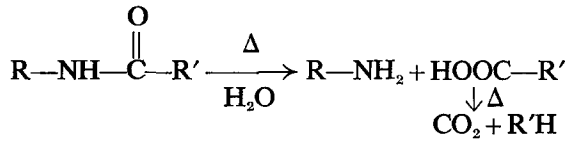

Mass spectrometric analyses (*Table 2*) of the degradation products indicate the presence of large quantities of carbon monoxide and lesser amounts of carbon dioxide, in addition to other materials. The appearance of carbon monoxide has also been reported in the previous study[1] with poly(terephthaloyl *trans*-2,5-dimethylpiperazine) and poly(oxalyl *trans*-2,5-dimethylpiperazine). This is unlike the situation with aliphatic polyamides where pyrolysis in a vacuum produces large amounts of carbon dioxide but only trace amounts of carbon monoxide[9]. The view that polyamides may be influenced by a hydrolytic type thermal breakdown gains further support from the observation that special drying procedures and extraction of acidic catalysts from Nylons prior to pyrolysis in a vacuum increased their activation energy and diminished the evolution of carbon dioxide[11]. However, other workers attribute the production of carbon dioxide to crosslinking and branching reactions involving the amide links and end-groups[12].

With the piperazine polyamides, large quantities of *carbon monoxide* are produced in addition to lesser amounts of carbon dioxide. This observation, coupled with the high activation energies and the general character of the rate curves, points to an essentially random breakdown during pyrolysis in a vacuum which, however, may be influenced by a hydrolytic type cleavage of the amide groups, especially with poly(isophthaloyl *trans*-2,5-dimethylpiperazine).

The appearance of small quantities of ammonia in the volatile degradation products suggests the participation of end-groups in the overall degradation process, as was proposed in the previous publication[1]. Such a process will yield, in addition to ammonia, hydrogen and carbon dioxide according to the following scheme:

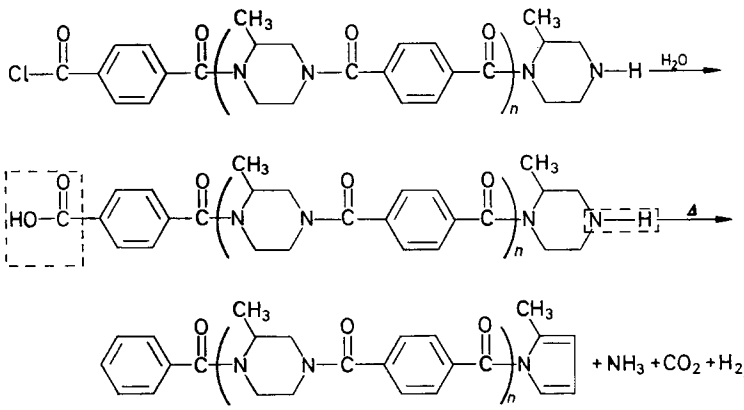

Considering the available experimental evidence, the piperazine polyamides described in this and the previous paper[1] may be arranged according to the following order of decreasing stability: poly(terephthaloyl piperazine > poly(terephthaloyl *trans*-2,5-dimethylpiperazine) > poly(terephthaloyl 2-methylpiperazine) > poly(oxalyl *trans*-2,5-dimethylpiperazine) > poly(isophthaloyl *trans*-2,5-dimethylpiperazine).

It is apparent that methyl substitution of the piperazine rings *decreases* the thermal stability of the polymers in a vacuum. On the other hand, the presence of terephthaloyl moieties (polycondensation in the *para* positions of the acid component) *increases* the thermal stability, in comparison with the system having isophthaloyl moieties in the polymer chains (polycondensation in the *meta* position of the acid component).

This work was supported by the Bureau of Naval Weapons, Department of the U.S. Navy, under Contract NOw 62–0604–c.

The author thanks Professor Joseph Silverman of the Department of Chemical Engineering, University of Maryland, College Park, Maryland, for permission to use the du Pont 900 Differential Thermal Analyzer, and Mr S. J. Burdick and Mr H. E. Bair for technical assistance in some phases of this work. The mass spectrometric analyses were performed by Mr William H. Dorko of the National Bureau of Standards, Washington, D.C.

Applied Physics Laboratory,
The Johns Hopkins University,
8621 Georgia Avenue,
Silver Spring, Maryland, U.S.A.

(Received October 1965)

REFERENCES

[1] BRUCK, S. D. *Polymer, Lond.* 1965, **6**, 483
[2] MORGAN, P. W. and KWOLEK, S. L. *J. Polym. Sci. A*, 1964, **2**, 181
[3] BRUCK, S. D. and BAIR, H. E. *Polymer, Lond.* 1965, **6**, 447
[4] BRUCK, S. D. *Polymer, Lond.* In press
[5] BRUCK, S. D. *Polymer, Lond.* 1964, **5**, 435
[6] BRUCK, S. D. *Polymer, Lond.* 1965, **6**, 49
[7] BRUCK, S. D. in *Vacuum Microbalance Techniques*, Vol. IV (edited by P. M. WATERS). Plenum Press: New York, 1965
[8] BRUCK, S. D. *J. chem. Educ.* 1965, **42**, 18
[9] STRAUS, S. and WALL, L. A. *J. Res. Nat. Bur. Stand.* 1958, **60**, 39
[10] SIMHA, R. and WALL, L. A. *J. phys. chem.* 1952, **56**, 707
[11] STRAUS, S. and WALL, L. A. *J. Res. Nat. Bur. Stand. A*, 1959, **63**, 269
[12] KAMERBEEK, G., KROES, H. and GROLLE, W. 'Thermal degradation of polymers', *Soc. Chem. Ind. Lond. Monogr. No. 13*, p 357, 1961

The Crosslinking of Methylvinyl Silicones with Organic Peroxides

D. K. THOMAS

*A study of the crosslinking efficiency of selected organic peroxides in a methylvinyl silicone polymer and of the mechanical properties, heat stability and processing of the vulcanizates indicates that 2,5-dimethyl-2,5-di-*tert*-butylperoxy hexane is to be preferred to the dichlorobenzoyl peroxide normally used. Vulcanizates produced with this peroxide give a better all round level of properties at high temperatures with a much more economical cure cycle.*

AN OUTSTANDING feature of silicone rubbers is their heat stability. In view of the reported sensitivity of silicone polymers to traces of acidic[1,2] and basic[3] impurities at high temperatures it is important, when a rubber component is being made for high temperature use, to ensure that the process of vulcanization does not leave residues of this nature in the rubber.

Hot vulcanization of methylvinyl silicone polymers involves the use of an organic peroxide to initiate crosslinking; this peroxide is commonly bis-1,4-dichlorobenzoyl peroxide which leaves an acidic residue in the vulcanizate. There are other peroxides which, from a technological standpoint, appear as suitable as bis-1,4-dichlorobenzoyl peroxide (DCBP) for the crosslinking of methylvinyl silicones, and which do not leave acidic residues in the vulcanizate. Two such materials are dicumyl peroxide (DCP) and 2,5-dimethyl-2,5-di-*tert*butylperoxy hexane (VX).

The present work is concerned with the evaluation of the three peroxides DCBP, DCP and VX, as crosslinking reagents in a methylvinyl silicone polymer. They are compared in terms of crosslinking efficiency, and the corresponding vulcanizates are compared in respect of their mechanical properties and behaviour on heat ageing in the relaxed state, in tension and in compression.

EXPERIMENTAL

Materials

The polymer used in this work was a methylvinyl silicone containing about one vinyl group for every 500 methyl groups. The molecular weight of the polymer as determined by solution viscosity measurements was 6×10^5. The organic peroxides were all commercially available materials dispersed in inert mineral powders for processing safety.

Compounding and vulcanization

All compounds were mixed on a laboratory roll mill. A low molecular weight hydroxy terminated silicone polymer (ESP.2436) was used as processing aid in the preparation of silica-filled compounds for mechanical and compression testing; it was introduced on the mill during the mixing of the raw polymer and fine silica filler. Rubbers for compression tests contained 40 parts by weight of fine silica, and those for conventional heat

ageing tests 20 parts. Sheets of thickness 0·010 in. were moulded for stress-relaxation experiments.

In those cases where crosslinking efficiencies were being determined the compounds were heated for a time sufficient to decompose the peroxide virtually completely, this amounted to at least eight half-lives.

Rubbers for mechanical testing received a press cure of one hour at 160°C and in some cases this was followed by a post cure of three and a half hours at 250°C in an air-circulating oven. Thin sheets for stress-relaxation studies were cured for one hour at 160°C in the press only.

Equilibrium swelling measurements

About 0·2g of vulcanizate was weighed accurately and immersed in a large excess of benzene at 28°C. After a period of 48 hours the rubber had reached its equilibrium swollen state; it was then withdrawn, surface dried, and weighed in a stoppered bottle. Finally it was dried to constant weight at 40°C. The fraction of soluble material was determined from the initial and final dry weights, and the volume fraction of rubber in the swollen vulcanizate was calculated using values of 1·08 and 0·876 for the densities of polymer and benzene respectively.

Stress-relaxation measurements

The apparatus used for stress-relaxation measurements has been described elsewhere[4]; only continuous stress-relaxation measurements were made and these were performed in a moist atmosphere. The moist atmosphere was obtained by bubbling air at a constant rate (0·76 litres per minute) through a saturated solution of sodium chloride at room temperature[5], it was then pre-heated before being passed into the relaxometer envelope.

Mechanical testing

Measurements of tensile strength, elongation at break, and modulus were made in the temperature range from 20° to 250°C, six specimens (C- type dumbells) being tested at each temperature.

Compression testing

Compression set tests were carried out at 160°C on filled and unfilled vulcanizates and also on rubbers which had been subjected to different curing cycles. The tests were based on *B.S.903* in which discs of rubber 0·25 in. thick and 0·564 in. in diameter are compressed by 25 per cent of their original thickness. After release from compression the specimens are allowed to recover for ten minutes at 160°C and ten minutes at room temperature before being measured. Compression set is then defined as $(\epsilon_0 - \epsilon_s) \times 100/0{\cdot}25\ \epsilon_0$, where ϵ_0 is the original uncompressed thickness and ϵ_s the final uncompressed thickness.

Heat ageing tests

C-type dumbells were suspended in an air-circulating oven at 200°C and groups of six specimens were periodically withdrawn for mechanical testing at room temperature.

RESULTS AND DISCUSSION

Crosslinking efficiency of the peroxides

Flory and Rehner[6] have related the degree of swelling of rubber vulcanizates in a swelling liquid to network structure in the following way

$$-\ln(1-V_r)-V_r-\mu V_r^2=2V_0C_1R^{-1}T^{-1}V_r^{\frac{1}{3}} \quad (1)$$

In this equation V_r is the volume fraction of rubber in the vulcanizate swollen to equilibrium, V_0 is the molar volume of the swelling liquid, μ is the interaction parameter for the polymer and solvent in question, R is the gas constant and T the absolute temperature. The quantity C_1 is the elastic constant which elasticity theory relates to the concentration of network chains per unit volume of vulcanizate (n).

$$C_1=\tfrac{1}{2}nkT=(\rho RT/2M_c)(1-2M_c/M) \quad (2)$$

where ρ is the density of the polymer of initial molecular weight M, and M_c is the number average molecular weight between crosslinks.

The value of μ is known to be 0·53 for the system methylvinyl silicone–benzene at 28°C[7] and hence the crosslink density can be calculated from the experimentally determined values of V_r.

The peroxides used in this work are known to undergo first order homolytic scission on heating and their half-lives for decomposition have been well defined over a range of temperatures. It is therefore possible to determine the number of molecules of peroxide which decompose in a given time at any temperature and the number of crosslinks which they produce. In the present work the system was always heated for a time sufficient to decompose almost all of the peroxide thus allowing the amount of peroxide decomposed to be identified with the initial concentration.

A striking feature of the results is the strong dependence of crosslinking efficiency on peroxide concentration, the values usually falling below 30 per cent at a concentration of greater than two weight per cent of peroxide. It can be seen from *Figure 1* that, to within the limits of experimental error, results for all three peroxides fall on a common curve. The plateau at higher concentrations in *Figure 1* indicates that for this particular methyl-

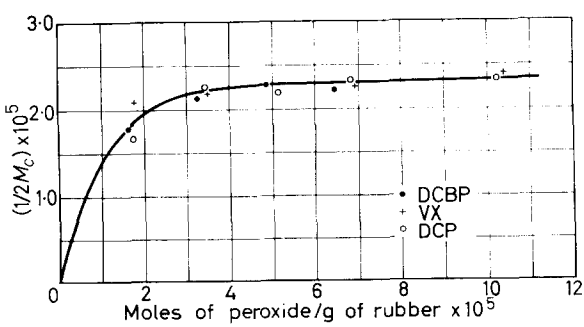

Figure 1—Crosslink density ($1/2M_c$) as a function of peroxide concentration

vinyl polymer there is an upper limit of crosslink density, and therefore modulus, which can be achieved in the vulcanizate. This limit is presumably set by the concentration of vinyl groups in the raw polymer, and the only consequence of using high concentrations of peroxide will be to cause an accumulation of decomposition products which may have a harmful effect upon the thermal stability of the vulcanizate.

Therefore, as far as their ability to produce crosslinks is concerned there is nothing to choose between DCBP, DCP and VX.

Thermal stability of the rubber networks

Two techniques have been used in a study of network stability; first, network scission reactions have been followed by means of continuous stress-relaxation measurements, secondly the overall effect of scission and crosslinking has been assessed by means of equilibrium swelling measurements.

In order that a fair comparison of network stability may be made it is necessary to use vulcanizates of closely similar crosslink densities. Where stress-relaxation measurements are used they should be carried out in a controlled environment. These requirements are met by using 1·5 weight per cent of DCBP, 1·0 weight per cent of DCP, and 2·0 weight per cent of VX, and observing the rate of relaxation in moisture-saturated air at any particular temperature. In addition the reinforcing filler is omitted as it may obscure differences in thermal stability which may exist between the gum vulcanizates.

The results of continuous stress-relaxation measurements at 160°, 200° and 250°C are shown in *Table 1* as relaxation rate constants (k), which correspond to the slope of the $\ln f_t/f_0$ against time (in minutes) plots, f_0 and f_t being the values of the force required to extend the rubber to the same extension ratio λ at zero time and at time t.

Table 1. Relaxation rate constants (k) for continuous stress-relaxation in unfilled methylvinyl silicone rubber in moist air

Curing agent	*Weight % of curing agent*	*160°C*		*200°C*		*250°C*	
		k unextracted	*k extracted*	*k unextracted*	*k extracted*	*k unextracted*	*k extracted*
DCBP	1·5	$2{\cdot}5\times10^{-4}$	$2{\cdot}4\times10^{-4}$	$9{\cdot}1\times10^{-4}$	$9{\cdot}5\times10^{-4}$	7×10^{-3}	$4{\cdot}8\times10^{-3}$
DCP	1·0	$4{\cdot}3\times10^{-5}$	$9{\cdot}4\times10^{-5}$	$7{\cdot}9\times10^{-4}$	$8{\cdot}9\times10^{-4}$	$9{\cdot}7\times10^{-3}$	$1{\cdot}6\times10^{-2}$
VX	2·0	$1{\cdot}6\times10^{-4}$	$1{\cdot}7\times10^{-4}$	$7{\cdot}6\times10^{-4}$	$9{\cdot}2\times10^{-4}$	$9{\cdot}7\times10^{-3}$	$1{\cdot}0\times10^{-2}$

The results at 160° and 200°C fit into a pattern in that for unextracted materials the least heat-stable network is that produced by DCBP, while solvent extraction has no effect upon the rate of network scission in DCBP systems but produces an increase in the rate of scission in DCP and VX networks. At 250°C the situation is changed, the most stable unextracted network is now that produced by DCBP; solvent extraction produces a small decrease in stability of DCP and VX networks and a larger increase in stability of the DCBP network, with the result that the latter is substantially more stable with respect to network scission than the other two.

It has previously been shown that network scission in peroxide-cured methylvinyl silicone rubber at temperatures below 250°C can be accounted

for largely in terms of a hydrolytic reaction in the main chain polymer[8]. At and around 250°C oxidative reactions in the crosslinks make a significant contribution to the rate of network scission. In conventional heat ageing tests at 160° and 200°C methylvinyl silicone rubbers show an extremely slow increase in modulus; in these tests the rubber is in a relaxed state throughout and the values for the modulus are an indication of the change in crosslink density. Increases in crosslink density in these systems must result largely from oxidative reactions in the methyl side groups and it would appear therefore that such reactions also proceed very slowly below 200°C. Undoubtedly the most rapid reactions occurring in this temperature range are those of hydrolysis in the main chain polymer and re-condensation of the silanols thus formed, and these reactions will determine the performance of silicone rubbers in tests in which they are continuously under strain. It follows that the resistance to compression set of the unfilled vulcanizates over fairly short periods at 160°C should correlate with the 'relaxation rate constants' obtained from continuous stress-relaxation measurements at this temperature. Reference to the data in *Table 2* shows that this is so.

Table 2. Correlation of compression set resistance at 160°C with relaxation rate of constants from continuous stress-relaxation measurements at 160°C

Curing agent	*Weight % of curing agent*	*Cure conditions*	*Test duration, all at 160°C*	*Compression set %*	*Relaxation rate constant*
DCBP	1·5	1 h at 120°C	24 h	50·9	$2{\cdot}5\times10^{-4}$
			48 h	Specimen broken up	
VX	2·0	1 h at 160°C	24 h	22·7	$1{\cdot}6\times10^{-4}$
			48 h	42·8	
			72 h	53·5	
DCP	1·0	1 h at 160°C	24 h	14·3	$4{\cdot}3\times10^{-5}$
			48 h	17·0	
			72 h	26·9	

At 250°C a similar correlation would not be expected because of the high rate of oxidative crosslinking which occurs at this temperature; indeed these crosslinking processes may dominate compression set behaviour at such high temperatures. This is confirmed by the value of 160 per cent obtained for the compression set of an unfilled DCBP vulcanizate after 24 hours compression at 250°C.

The combined effect of scission and crosslinking is shown by results of swelling measurements on unfilled vulcanizates which had been exposed to air at 250°C (see *Figure 2*). A marked difference is now apparent between the three systems; the rate of embrittlement is DCP $>$ DCBP $\gg$ VX.

The overall picture which emerges from this work on network stability is that the DCBP system is inferior to the others at temperatures below 250°C. At the lower end of the temperature scale, where oxidative reactions proceed relatively slowly the most heat-stable network is obtained with DCP, the VX system coming a close second. At temperatures near 250°C, where oxidative reactions are important the most stable network is obtained with

VX, DCBP and DCP systems being much inferior. The effect of solvent extraction upon the relaxation rate constants for continuous stress-relaxation at 160°, 200° and 250°C serves to emphasize the bearing which byproducts of vulcanization can have upon network stability.

Mechanical properties and conventional heat ageing tests

When silicone rubber articles are produced commercially they are always filled with fine silica; in addition to a press cure they are often subjected to a high temperature post cure, and this is frequently three and a half hours at 250°C. The effect of this post cure treatment on vulcanizates produced from all three peroxides is shown by the results of mechanical tests (see *Table 3*) and compression set tests (see *Table 4*).

Table 3. Mechanical properties of filled silicone vulcanizates before and after post-cure treatment

Temperature	*DCBP*		*VX*		*DCP*	
	Press cure	*Press+post cure*	*Press cure*	*Press+post cure*	*Press cure*	*Press+post cure*
	Tensile strength (lb/in²)					
20	821	673	817	676	984	679
100	447	543	562	456	634	390
150	445	405	439	315	545	374
200	316	341	332	296	347	241
250	270	226	242	182	292	197
	100 per cent modulus (lb/in²)					
20	181	240	191	240	146	265
100	186	226	179	231	169	228
150	204	213	180	191	179	235
200	195	199	174	205	169	230
250	197	180	153	200	167	220
	Breaking elongation (%)					
20	465	275	487	315	557	273
100	375	235	365	220	410	183
150	265	203	315	170	352	165
200	180	180	210	148	245	108
250	140	127	127	82	193	93

Reference to the data in *Table 3* shows that the effect of high temperature post cure on all three vulcanizates is to increase the modulus and hence the crosslink density by substantial amounts. This is presumably the result of oxidative reactions and is reflected in the increase in modulus and decrease in breaking elongation of the vulcanizates. It is interesting to note that by far the greatest rise in modulus and greatest fall in breaking extension occurred in the DCP vulcanizate, this being consistent with the results of heat ageing in unfilled vulcanizates in air at 250°C (see *Figure 2*).

The strength and elastic properties of all three vulcanizates fall off in a similar way as the temperature is raised, the rubbers that were not post cured always showing a higher strength and breaking extension at 250°C. On the basis of mechanical properties over the range 20° to 250°C there is

Table 4. Compression set tests on post cured silica filled methylvinyl silicone vulcanizates

Curing agent	*Weight % of curing agent*	*Duration of press cure, all at 160°C*	*Duration of post cure, all at 250°C*	*Test duration, all at 160°C*	*Compression set %*
DCBP	1·5	1 h	3½ h	24 h	69·2
				48 h	75·3
				72 h	80·7
DCBP	1·5	1 h	24 h	24 h	29·1
DCP	1·0	1 h	3½ h	24 h	34·4
				48 h	46·4
				72 h	48·4
				168 h	57·0
DCP	1·0	1 h	24 h	24 h	35·9
VX	2·0	1 h	3½ h	24 h	31·0
				48 h	37·6
				72 h	43·3
				168 h	54·3
VX	2·0	1 h	24 h	24 h	38·9
		1 h	None	24 h	33·0

little to choose between the three systems whether in the post cured condition or without post cure.

The compression set data in *Table 4* show up some interesting differences which may be of practical significance. The results for silica-filled DCBP vulcanizates show that for the best resistance to compression set the rubber must receive a prolonged post cure treatment of 24 hours at 250°C. With DCP and VX vulcanizates the prolonged high temperature post cure has no effect upon resistance to compression set at 160°C, furthermore the values for compression set in the compounds that were not post cured are virtually the same as the value shown by the fully post cured DCBP vulcanizate.

Viewing the results in *Tables 3* and *4* together it is clear at this stage that a good all round level of properties can only be attained with DCBP compounds if they receive a post cure of 24 hours at 250°C; however, if DCP or VX is used there is no necessity for a post cure, the best level of properties being obtained after press-curing. With DCP vulcanizates the

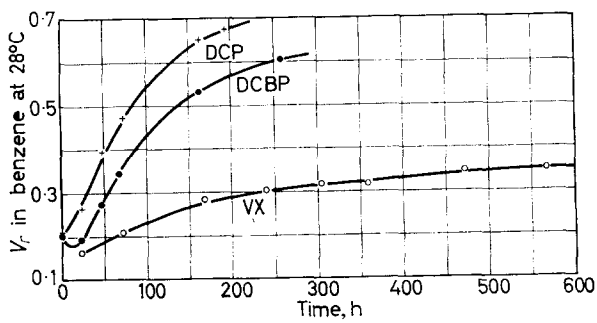

Figure 2—Volume fraction of rubber (V_r) in the swollen vulcanizates as a function of time of exposure to air at 250°C

results shown in *Figure 2* give a warning that the behaviour of these materials on ageing at temperatures above 200°C may not be good. Conventional heat ageing tests have been carried out on DCBP and VX vulcanizates at 200°C and the results are summarized in *Table 5*.

Table 5. Conventional heat ageing tests on filled vulcanizates in air at 200°C

Time, days	*T.S.* $(lb/in)^2$		*M.100* $(lb/in)^2$		*EB%*	
	DCBP	*VX*	*DCBP*	*VX*	*DCBP*	*VX*
0	560	620	118	114	390	448
30	497	510	216	205	195	228
60	437	498	273	265	156	177
90	450	490	325	267	146	167
120	403	463	364	298	105	147
150	407	456	350	282	110	143
180	384	414	328	311	103	126
210	—	393	—	330	91	110

The rate of increase in modulus is noticeably lower with the VX compound and this is in qualitative agreement with the results of heat ageing on unfilled vulcanizates.

CONCLUSIONS

A study of the crosslinking of a methylvinyl silicone polymer by three different organic peroxides, and of the properties of the vulcanizates over a range of temperature from 20° to 250°C reveals no good reason why DCBP should be specially favoured. Of the peroxides used the best would appear to be VX, and the case for using it is especially strong in view of the processing advantage it appears to have over DCBP. Thus a vulcanizate having the best possible all round properties can be obtained without subjecting the rubber to a long high-temperature post-cure; with DCBP vulcanizates the best all round properties for high temperature applications are only achieved after a post cure of 24 hours at 250°C.

The author is indebted to Mr R. Sinnott and Mr J. Day for preparing the vulcanizates and carrying out the heat ageing programme.

Chemistry, Physics and Metallurgy Department,
Royal Aircraft Establishment,
Farnborough, Hants.

(*Received November 1965*)

REFERENCES

[1] LEWIS, C. W. *J. Polym. Sci.* 1958, **33**, 153
[2] KUČERA, M. and LANIKOVA, J. *J. Polym. Sci.* 1961, **54**, 375
[3] KUČERA, M. and LANIKOVA, J. *J. Polym. Sci.* 1961, **53**, 301
[4] ATKINSON, A. S. *R.A.E. Tech. Note No. Chem. 1393*, January 1963
[5] TURNER, M. J. and LEWIS, J. *Proceedings of the Fourth Rubber Technology Conference, London*, May 1962
[6] FLORY, P. J. and REHNER, J. *J. chem. Phys.* 1950, **18**, 108
[7] THOMAS, D. K. *Polymer, Lond.* 1964, **5**, 463
[8] THOMAS, D. K. To be published

Book Reviews

The Macromolecular Chemistry of Gelatin

A. VEIS. Volume 5 in Molecular Biology Series edited by B. HORECKER, N. O. KAPLAN, H. A. SCHERAGA. Academic Press: London and New York, 1964. x+433 pp. 6¼ in. by 9 in. 103*s* 6*d*

UNTIL the publication of this book, the most useful starting point for a study of the available data on collagen and gelatin was the 1956 monograph *The Chemistry and Reactivity of Collagen*, by K. H. Gustavson. As the author is very willing to point out, Gustavson's work provides an excellent background to a complex topic which has not been correlated since the 1920s. Such a correlation was needed; the excellence of this book makes it doubly valuable.

The current concepts of the chemistry and structure of collagen, the main component of animal connective tissue, are reviewed, with particular emphasis on the recently developed concepts of the collagen-fold formation, and the details of the transitions between collagen and gelatin. A major part of the book is devoted to methods used for the molecular characterization of gelatin, in which it is considered as a high polymer, a polyelectrolyte, and as a protein; the techniques of molecular weight determination (and their relative value), titration studies, and configurational studies by optical rotation measurements are discussed in relation to these concepts.

Methods of conversion of collagen to gelatin are then described: this is probably the weakest portion of the book, since the behaviour of two idealized cases (conversion of acid-soluble tropocollagen and of purified insoluble collagen to gelatin) only are considered. The general principles of commercial manufacture of gelatin are presented soundly—published data are notably scanty in this field, as the author is aware, although perhaps he is less aware that frequently the paucity of information is often due to the ignorance of gelatin manufacturers, rather than to commercial secrecy. It is indeed here that the contribution of a book such as this can be most valuable, with its emphasis on elucidation of basic principles from much generalized data. Many such empirical data exist, but their organization is frequently rudimentary.

Much important information obtained in studies of hydrolytic and enzymatic degradation of gelatin is discussed in relation to data obtained in the great amount of work on cleavage of the gelatin chain with a variety of oxidizing agents. The rest of the work is devoted to an extensive study of the gelatin-to-collagen transformation, and of the stability and rheology of gelatin gels.

The work is recommended to biochemists, biophysicists, and molecular biologists—it is also to be warmly commended to polymer chemists as an excellent treatment of a difficult and rewarding topic which still presents many unsolved problems. The book is well produced and printed, but suffers from a number of misprints, notably amongst the references.

C. A. FINCH

Crystalline Olefin Polymers

R. A. V. RAFF and K. W. DOAK (Editors). High Polymers, Volume XX—Part 1. Interscience: New York, 1965. 1003 pp. 7 in. by 10 in. 249*s*

THIS book is a recent addition to the firmly established Interscience series on High Polymers. Volume XX will consist of two parts which together supersede Volume XI on Polyethylene published in 1956. The complete new volume is about 3½ times the length of the old one.

The increased length is due partly to the inclusion of other olefin polymers, particularly polypropylene. It is mainly due to the great advances in the past nine years in the knowledge and understanding of polyethylene itself.

Naturally, much of this new information concerns the practice and theory of stereospecific polymerization but it is pleasing that the progress made in studying and interpreting the physical properties of partly crystalline polymers has been very well covered in the text.

Unlike Volume XI, which had only two authors, the new one is the work of a large team. Twenty eight have contributed to Part 1. This has allowed each topic to be treated by experts and has led to a gain in the depth and breadth of the treatment. It has led also to some loss of coherence in the book as a whole. There is some overlapping of chapters, for example the simple basis of monomer reactivity ratios in copolymerization is given three times. This is nowhere very serious but is most marked in chapters 3, 5 and 8 when polymerization on Ziegler–Natta catalysts is being discussed.

Occasionally different authors express apparently conflicting views. For example excellent cases are presented in separate chapters for the anionic mechanism and for the radical-ion mechanism of propagation on heterogeneous catalysts. This makes it difficult for the inexpert reader to formulate his own opinion clearly.

The most serious weakness in the book is that whereas some chapters were obviously written for the benefit of generally well-informed polymer scientists others were equally clearly directed towards specialists in individual fields. They would not be fully comprehended by a wide range of potential readers.

It is impossible in a short review to deal adequately with each of the sixteen chapters. The first two follow closely those in Volume XI with the addition of material on higher olefins. Chapters 3, 5, 6, 7 and 8 deal with polymerization in various ways. Chapters 5 and 6 can be especially recommended as readable accounts of topics which are very difficult to summarize at the present time. Despite a misleading title, Chapter 4 is a good logical presentation and explanation of stereoregularity of polymers in general. It is marred by a rather poor English style and some loose remarks about entropy. Chapters 9 and 11 deal with dilute solutions in relation to molecular weights and distributions (Chapter 11) and to branching and stereoregularity (Chapter 9). Their order would be better reversed. Chapter 11 is an excellent basic account with special emphasis on the study of crystalline polymers. Chapter 9 is a highly sophisticated account by specialists for specialists. Chapter 12 gives an orthodox survey of polymer crystallinity with examples chosen from poly-olefins. Chapters 10 and 13 are mainly qualitative accounts of the effects of chemical structure, molecular weight distribution, branching and crystallinity on melt viscosity, viscoelasticity, transitions and tensile properties. The chapters are pleasant to read and show that much more research is required in these areas. Chapter 14 contains about 100 pages on infra-red, n.m.r. and mechanical relaxation spectra of poly-olefins. About 40 pages is spent on basic theory. Although very well written it would be hopeless to try to learn about such complex phenomena from so compressed an account. The remaining 60 pages are a fine review of the mass of published data on polyethylene and polypropylene. It is more valuable to experts than to beginners. Chapters 15 and 16 deal with the breakdown and change of poly-olefins by heat, halogens, oxidation (Chapter 15) and radiation (Chapter 16). Chapter 15 is only a brief sketch but Chapter 16 is systematic, exhaustive, and not easy to read. Neither of these chapters seems really to belong in Part 1 and might have been better placed at the beginning of Part 2.

The title of the book is not quite accurate. 'Crystallizable' would have been better as many matters unconnected with crystallinity are discussed. It is well styled and produced but printed on paper which reflects too much light. Regular purchasers of this series will certainly wish to have this volume and it can also be recommended to all who are interested in poly-olefins and in crystallizable polymers generally.

P. MEARES

Polymers: Structure and Bulk Properties

P. MEARES. Van Nostrand: New York and London, 1965. xi+381 pp. 6¼ in. by 9 in. 70*s*

AS A result of our increased understanding of the microstructure of polymers in recent years an important consideration is the relation between bulk properties of polymers and their fine structure. Where possible the present volume lays emphasis on this relationship and, in general, is a well produced and readable account of most aspects of bulk properties.

Unlike Volume XI, which had only two authors, the new one is the work of a large team. Twenty eight have contributed to Part 1. This has allowed each topic to be treated by experts and has led to a gain in the depth and breadth of the treatment. It has led also to some loss of coherence in the book as a whole. There is some overlapping of chapters, for example the simple basis of monomer reactivity ratios in copolymerization is given three times. This is nowhere very serious but is most marked in chapters 3, 5 and 8 when polymerization on Ziegler–Natta catalysts is being discussed.

Occasionally different authors express apparently conflicting views. For example excellent cases are presented in separate chapters for the anionic mechanism and for the radical-ion mechanism of propagation on heterogeneous catalysts. This makes it difficult for the inexpert reader to formulate his own opinion clearly.

The most serious weakness in the book is that whereas some chapters were obviously written for the benefit of generally well-informed polymer scientists others were equally clearly directed towards specialists in individual fields. They would not be fully comprehended by a wide range of potential readers.

It is impossible in a short review to deal adequately with each of the sixteen chapters. The first two follow closely those in Volume XI with the addition of material on higher olefins. Chapters 3, 5, 6, 7 and 8 deal with polymerization in various ways. Chapters 5 and 6 can be especially recommended as readable accounts of topics which are very difficult to summarize at the present time. Despite a misleading title, Chapter 4 is a good logical presentation and explanation of stereoregularity of polymers in general. It is marred by a rather poor English style and some loose remarks about entropy. Chapters 9 and 11 deal with dilute solutions in relation to molecular weights and distributions (Chapter 11) and to branching and stereoregularity (Chapter 9). Their order would be better reversed. Chapter 11 is an excellent basic account with special emphasis on the study of crystalline polymers. Chapter 9 is a highly sophisticated account by specialists for specialists. Chapter 12 gives an orthodox survey of polymer crystallinity with examples chosen from poly-olefins. Chapters 10 and 13 are mainly qualitative accounts of the effects of chemical structure, molecular weight distribution, branching and crystallinity on melt viscosity, viscoelasticity, transitions and tensile properties. The chapters are pleasant to read and show that much more research is required in these areas. Chapter 14 contains about 100 pages on infra-red, n.m.r. and mechanical relaxation spectra of poly-olefins. About 40 pages is spent on basic theory. Although very well written it would be hopeless to try to learn about such complex phenomena from so compressed an account. The remaining 60 pages are a fine review of the mass of published data on polyethylene and polypropylene. It is more valuable to experts than to beginners. Chapters 15 and 16 deal with the breakdown and change of poly-olefins by heat, halogens, oxidation (Chapter 15) and radiation (Chapter 16). Chapter 15 is only a brief sketch but Chapter 16 is systematic, exhaustive, and not easy to read. Neither of these chapters seems really to belong in Part 1 and might have been better placed at the beginning of Part 2.

The title of the book is not quite accurate. 'Crystallizable' would have been better as many matters unconnected with crystallinity are discussed. It is well styled and produced but printed on paper which reflects too much light. Regular purchasers of this series will certainly wish to have this volume and it can also be recommended to all who are interested in poly-olefins and in crystallizable polymers generally.

P. MEARES

Polymers: Structure and Bulk Properties

P. MEARES. Van Nostrand: New York and London, 1965. xi+381 pp. 6¼ in. by 9 in. 70*s*

AS A result of our increased understanding of the microstructure of polymers in recent years an important consideration is the relation between bulk properties of polymers and their fine structure. Where possible the present volume lays emphasis on this relationship and, in general, is a well produced and readable account of most aspects of bulk properties.

The conditions of polymer formation have an important bearing on polymer properties; the preparation and characterization of polymers is covered in the first three chapters, dealing in turn with methods of polymerization, microstructure and molecular weights and their distributions. Inclusion of such accounts is very useful in a book of this type, although the chapters covering polymer formation and molecular weights cannot be considered as comprehensive. The bulk properties of polymers are described in the remaining ten chapters, the first two of which are devoted to polymer crystal structures, crystallinity, the thermodynamics of fusion and kinetics of crystallization. An excellent treatment of elastomers in the following three chapters discusses the thermodynamics of rubber elasticity, statistical thermodynamics of networks and practical aspects such as thermo-elastic phenomena and the effects of plasticizers. The nature of viscoelasticity is the subject of Chapter 9, followed by a discussion of the glassy state and the glass transition, including the effect of polymer structure on the transition temperature. There follows a description of mechanical models of viscoelastic behaviour and a molecular interpretation of viscoelasticity. The next chapter is rather unconventional in a book of this type, but is useful in showing how diffusion studies help in the study of molecular mobility in polymers. Finally, there is a discussion of irreversible deformations.

As a textbook this volume will be of considerable use to students taking advanced courses on polymer physics, to postgraduate students and other research workers who require a good grounding in this field. It contains a wide selection of references and gives a good coverage of the most important aspects of this branch of polymer science.

G. C. EASTMOND

Proceedings of the Natural Rubber Producers' Research Association Jubilee Conference Cambridge 1964

L. MULLINS (Ed.). London: Maclaren, 1965. 250 pp. 42*s*

AT A time when scientific progress is taking place at a truly remarkable rate twenty five years can seem a very long time. It is now difficult to realize how little was known of the science of rubber in those days, just prewar, when the then British Rubber Producers' Research Association was founded. The technology had advanced with little help from any basic scientific knowledge and the BRPRA's aim was to lay a firm scientific foundation upon which further technological advance could be based. In this aim it has had outstanding success and it is by no means an accident that such tremendous progress has been made during its lifetime.

The purpose of the present book is to record the proceedings of the Research Association's Jubilee Conference held in Cambridge in April 1964. After interesting background Plenary lectures by Sir HARRY MELVILLE, Professor MARK and Professor BONNER, the conference was subdivided into two concurrent symposia on 'Rubber biosynthesis' and 'The relation between chemical structure and mechanical properties'. To a mere physical scientist like the present reviewer the section on biosynthesis is of great interest, especially when viewed, as it must be, against the background of man's difficulties in producing stereospecific rubbers synthetically.

Before reading the proceedings of the second symposium I was apprehensive lest I should find a mere repeat of sections from the earlier excellent book written by members of the Association's staff*. These fears were groundless; there is of course some overlap but the subjects covered have been emphasized rather differently, new material has been introduced where available and, in general, a more detached and critical view of sections of a field have been taken. The introductory paper by Professor GEE is of particular interest reviewing, as it does, the various theories of rubber elasticity, their successes and failures. One is perhaps, however, wrong in singling out separate chapters, all the papers reprinted are well worth reading and no rubber scientist can afford to overlook this book.

The volume concludes with the closing remarks of Dr. BATEMAN and a list of participants; this list seems rather superfluous but is a very minor blemish in a very well-produced book.

L. D. LOAN

**The Physics and Chemistry of Rubberlike Substances.* Edited by L. BATEMAN. Maclaren: London.

The Temperature Dependence of Viscoelastic Behaviour in Polyethylene Terephthalate

P. R. PINNOCK and I. M. WARD*

Dynamic mechanical measurements of unoriented crystalline polyethylene terephthalate fibres have been made over the temperature range of the glass/rubber transition. The results have been compared with previously reported creep data. A consistent representation of both sets of data can be obtained using first-order approximation methods and defining the transition temperature as that for which tan δ *is a maximum.*

DYNAMIC mechanical measurements on polyethylene terephthalate fibres of different physical structure have been reported in a previous publication[1] which was primarily concerned with the anisotropy of elastic and viscoelastic behaviour in oriented fibres. The present paper deals particularly with the frequency/temperature relationships for these fibres, and the earlier work has been extended in several ways. First, the dynamic mechanical measurements have been extended to lower frequencies by construction of an apparatus with a working range of 10^{-3} to 10 c/s. Secondly, the dynamic measurements are compared with extensional creep data obtained elsewhere[2] and previously reported dielectric loss[3] and dilatometric measurements[4].

The previous dynamic mechanical measurements[1] were restricted to a narrow range of frequencies, and it was found adequate to describe the frequency/temperature behaviour as that of a constant activation energy system. The extensional creep data[2] for unoriented crystalline fibres, on the other hand, showed shift factors which could be fitted to the Williams–Landell–Ferry relationship[5]. It also appeared that the dielectric loss and dilatometric measurements were consistent with this representation. It is, however, not easy to distinguish between the WLF representation and a constant activation energy over a narrow range of frequencies, particularly at high frequencies. It is therefore of interest to examine dynamic mechanical measurements over a wide range of frequencies for crystalline unoriented fibres, together with the creep data, to see if a consistent representation of both can be obtained.

EXPERIMENTAL

Preparation of samples

The fibres were made by the conventional melt-spinning process in which molten polymer is extruded through small orifices to produce non-crystalline fibres with a very low degree of molecular orientation. These fibres were then subjected to a heat-crystallization process. The latter

*Present address: H. H. Wills Physics Laboratory, University of Bristol.

process is necessary to stabilize the samples before subjecting them to the range of temperatures encountered during the dynamic mechanical testing.

Physical characterization of samples

A detailed investigation of the molecular structure of the samples was not undertaken. However, it was of value to obtain empirical measures of crystallinity and molecular orientation, recognizing the arbitrary nature of these types of measurement.

The measure of crystallinity was an X-ray diffraction method devised by Farrow and Preston[6], which compares the integrated intensity of the sharp X-ray reflections from crystalline material with the integrated intensity of the diffuse reflections from the non-crystalline material.

A measure of the overall molecular orientation was obtained from the optical birefringence. This is the difference between the refractive indices of the fibres, along and at right angles to the fibre axis, and was measured using polarized light and a Berek compensator.

Measurement of dynamic extensional modulus (Young's modulus)

The apparatus used in the measurement of extensional modulus is shown diagrammatically in *Figure 1*. It is identical in principle to that described in a previous publication[1] but possesses a wider frequency range (10^{-3} to

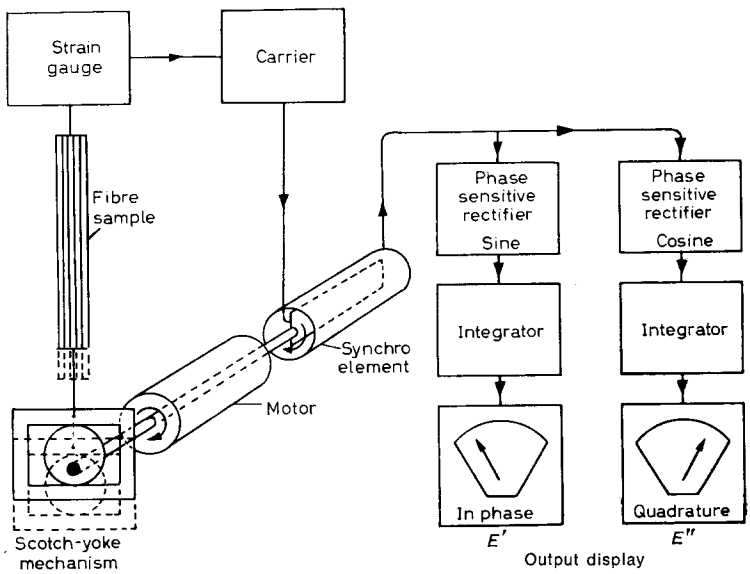

Figure 1—Schematic diagram of the dynamic mechanical apparatus

10 c/s). It was also found to produce results with greater accuracy and reproducibility than had proved possible using the earlier apparatus.

The sample is subjected to a sinusoidal strain of fixed amplitude, which

is provided by a Scotch-yoke mechanism driven by a servo-controlled motor. The stress is measured by a non-bonded strain gauge transducer attached to the other end of the sample. Simultaneous comparison of stress and strain is made electronically using a Servomex Transfer Function Analyser (TFA).

The TFA provides a servo-controlled motor which, in addition to providing a means for a sinusoidal strain, rotates a loop in a high frequency (ω_c) alternating magnetic field (2 kc/s). Since the loop rotates at a very low frequency (ω_m), i.e. the test frequency, this produces a carrier modulated at the rotational speed of the form

$$K \sin \omega_m t \cos \omega_c t \quad \text{for} \quad \omega_c \gg \omega_m$$

which can then be fed to the system under test. However, in our application the mechanical signal is used and consequently the return signal presented to the measuring system by the transducer will be of the form

$$K_1 \sin (\omega_m t + \delta) + N$$

where δ is the angular phase shift produced by the system under test and N represents unwanted elements such as harmonics, random noise, etc. At this stage a carrier is introduced and the signal is then multiplied simultaneously but separately by $\sin \omega_m t$ and $\cos \omega_m t$. This multiplication at the modulation frequency, ω_m, is carried out by a synchro element with resolver type windings. This element is directly coupled to the same motor shaft which drives the Scotch-yoke and the rotor winding is fed with the signal from the transducer plus carrier. The two stator windings are at 90° to each other and from these are derived the sine and cosine functions.

These two signals after being demodulated to remove the carrier frequency component are of the form

$$\begin{aligned} & K_2 \sin (\omega_m t + \delta) \sin \omega_m t + N \sin \omega_m t \\ & = \tfrac{1}{2} K_2 [\cos \delta - \cos (2\omega_m t + \delta)] + N \sin \omega_m t \end{aligned}$$

and

$$\begin{aligned} & K_2 \sin (\omega_m t + \delta) \cos \omega_m t + N \cos \omega_m t \\ & = \tfrac{1}{2} K_2 [\sin \delta + \sin (2\omega_m t + \delta)] + N \cos \omega_m t \end{aligned}$$

These signals are then integrated over a complete cycle to remove all unwanted terms. Two steady signals are then obtained which are proportional in magnitude and polarity to the real and imaginary parts of the system output at the fundamental frequency, i.e.

$$\int_0^{1/\omega_m} \tfrac{1}{2} K_2 \cos \delta \, dt \quad \text{and} \quad \int_0^{1/\omega_m} \tfrac{1}{2} K_2 \sin \delta \, dt$$

It is essential that the Scotch-yoke mechanism be as free from noise as possible and this was largely achieved by making the eccentric collar of Nylon which, in turn, rotates in contact with polished stainless-steel surfaces. Provision was also made for aligning the eccentric Nylon collar with respect to the loop thereby avoiding any constant additional phase difference between the loop and the strain.

As in the previous apparatus a sinusoidal strain of $\pm 0{\cdot}25$ mm, i.e.

$\pm 0{\cdot}25$ per cent on the 10 cm sample, was chosen, having already established that this is within the range of the linear viscoelastic behaviour. The sample was also subjected to a static strain of approximately 0·25 mm to prevent it going slack. The fibre is connected to both the Scotch-yoke mechanism and to the strain gauge by German-silver tubing connections.

The fibre is surrounded by an annular copper can through which heated air may be passed. The copper can in turn is insulated by a Thermos jacket enabling the temperature of the fibre to be controlled to within 1 deg. C.

Creep measurements

The creep data discussed in this paper were all obtained in a previous investigation which has been reported fully elsewhere[2]. The creep measurements were confined to unoriented monofilaments which had been heat-crystallized by heating at 180°C for one hour. These samples were therefore exactly equivalent to the unoriented crystalline fibres used for the dynamic mechanical measurements.

The reader is referred to the previous publication for details, but to summarize, the creep compliance of unoriented crystalline polyethylene terephthalate was measured in the linear viscoelastic range from 65 to 115·5°C, isothermal creep data being obtained at nine fixed temperatures.

THEORY

Linear viscoelastic behaviour

There are several equivalent ways of determining the mechanical behaviour of a linear viscoelastic system. These are broadly of two types, the first being the response of the system to transient stress or strain, and the second its response to dynamic stress or strain. The results of transient measurements define a relaxation modulus or a creep compliance and the dynamic measurements define a complex modulus or compliance.

A convenient starting point for consideration of the transient type measurements is the Boltzmann superposition principle. For uniaxial creep, this relates the final strain $e(t)$ to the elemental increments of stress $\mathrm{d}\sigma(\tau)$ applied at times τ.

Thus

$$e(t) = \frac{\sigma}{E_0} + \int_{-\infty}^{t} J(t-\tau) \frac{\mathrm{d}\sigma(\tau)}{\mathrm{d}\tau} \mathrm{d}\tau$$

where $J(t)$ is the creep compliance, and similarly for stress relaxation

$$\sigma(t) = E_0 e + \int_{-\infty}^{t} E(t-\tau) \frac{\mathrm{d}e(\tau)}{\mathrm{d}\tau} \mathrm{d}\tau$$

where $E(t)$ is the stress relaxation modulus, E_0 is the instantaneous elastic modulus and $\mathrm{d}e(\tau)$ are the elemental strain increments.

From the dynamic mechanical approach, consider the system to be subjected to a sinusoidal stress

$$\sigma = \sigma_0 \sin \omega t$$

Then the sinusoidal strain produced will be given by $e = e_0 \sin(\omega t - \delta)$ where δ defines the phase lag between stress and strain. The ratio between strain and stress e/σ defines the complex compliance $J^* = J' + iJ''$. Alternatively, we may define the complex modulus $E^* = E' + iE''$, from the reciprocal ratio of stress to strain.

The mathematical relationships between the creep compliance, the stress-relaxation modulus and the dynamic compliance and modulus, have been discussed in detail by Gross[7] and others. These relationships are complex and involve, for example, recourse to the methods of Fourier or Laplace transforms to relate transient to dynamic quantities. Although it is possible to compute exactly one quantity from another, provided that a sufficient time-scale is covered, this is rarely profitable for considerations of the viscoelastic behaviour of polymers. In the first place, the viscoelastic behaviour can rarely be determined experimentally with sufficient accuracy, and secondly the behaviour normally changes fairly slowly with change in frequency. It is therefore often adequate to resort to approximate methods, and these will be discussed in the next section.

Use of approximate methods

The relaxation modulus can also be expressed as

$$E(t) = E_0 + \int_{-\infty}^{\infty} H(\tau)\, e^{-t/\tau}\, \mathrm{d} \ln \tau \tag{1}$$

where $H(\tau)$ is a function defining the relaxation spectrum (see, for example, ref. 8, p 41).

A similar generalization for creep gives the creep compliance in terms of a 'retardation-time' spectrum, $L(\tau)$.

$$J(t) = J_0 + \int_{-\infty}^{\infty} L(\tau)\,(1 - e^{-t/\tau})\, \mathrm{d} \ln \tau$$

where J_0 is the instantaneous elastic compliance.

The real and imaginary parts of the dynamic modulus can also be expressed in terms of $H(\tau)$.

$$E'(\omega) = E_0 + \int_{-\infty}^{\infty} \left[\frac{H(\tau)\, \omega^2 \tau^2}{1 + \omega^2 \tau^2} \right] \mathrm{d} \ln \tau \tag{2}$$

and

$$E''(\omega) = \int_{-\infty}^{\infty} \left[\frac{H(\tau)\, \omega \tau}{1 + \omega^2 \tau^2} \right] \mathrm{d} \ln \tau \tag{3}$$

The approximations to be used in this paper all derive from approximate methods to obtain $H(\tau)$.

Equation (1), which has the form of a Laplace transform, can be used to evaluate $H(\tau)$ to various orders of approximation, as has been extensively discussed in the literature (see, for example, ref. 8, p 44).

The first-order approximation was proposed by Alfrey and is generally known as the Alfrey approximation.

It gives

$$H(\tau)=[-\mathrm{d}E(t)/\mathrm{d}\ln t]_{t=\tau}$$

and can be considered to arise by approximating the intensity function $e^{-t/\tau}$ which goes from 0 at $\tau=0$ to 1 at $\tau\longrightarrow\infty$ by a step function going from 0 to 1 at $\tau=t$.

Second-order and higher-order approximations can be obtained involving the first derivative and higher derivatives of $E(t)$ with respect to $\ln t$.

As discussed in detail by Staverman and Schwarzl[8] and others the first-order Alfrey approximations hold provided that the relaxation spectrum or retardation spectrum do not change very rapidly with frequency. In mathematical terms this requires that the second- and higher-order derivatives should be small compared with the first-order derivative.

The analysis of the creep and dynamic data presented here suggests that first-order approximations are adequate. Furthermore this will be shown to be expected from examination of the creep data alone.

Thus we shall assume that the relaxation spectrum is given by

$$H(\tau)=[-\mathrm{d}E(t)/\mathrm{d}\ln t]_{t=\tau}$$

To a similar degree of approximation equations (2) and (3) can be shown to give

$$H(\tau)\simeq\left[\frac{\mathrm{d}E'(\omega)}{\mathrm{d}\ln\omega}\right]_{1/\omega=\tau}=\frac{2}{\pi}[E''(\omega)]_{1/\omega=\tau} \tag{4}$$

From the latter approximations it follows that

$$\mathrm{d}\ln E'(\omega)/\mathrm{d}\ln\omega=(2/\pi)\tan\delta \tag{5}$$

In a similar manner it can be shown that

$$\mathrm{d}\ln J'(\omega)/\mathrm{d}\ln\omega=(2/\pi)\tan\delta \tag{6}$$

It is also noted that $E(t)=E'(\omega)$ and $J(t)=J'(\omega)$ for $\omega=1/t$.

Frequency/temperature equivalence and the definition of 'transition temperatures'

The discussion has so far only been concerned with the variation of mechanical properties with time or frequency at a fixed temperature. This paper is, however, primarily concerned with the temperature dependence of the viscoelastic behaviour. With transient measurements, it is fairly straightforward to obtain the frequency/temperature dependence by comparison of data obtained at different fixed temperatures. The procedure is to obtain a 'master creep curve' or a 'master stress-relaxation curve' by superposition of the isothermal data. The linear frequency shifts corresponding to shifts in temperature are thus obtained directly.

It is, however, not so obvious how to obtain shift factors directly from the dynamic mechanical data, obtained at constant frequency over a range of temperatures, because each set of data for the real and imaginary parts

of the modulus or compliance does not in itself define a particular temperature. Strictly, the measurements of E' and E'' at constant frequency over a range of temperatures should be used to construct plots of E' and E'' at constant temperature for a series of frequencies. These plots can then be superimposed to obtain the shift factors. A similar procedure, of course, can be applied to measurements of J' and J'' at constant frequency, with an identical result.

A somewhat simpler procedure has been used in this paper, which will be shown to be adequate. It is based on the following considerations.

The previous dynamic mechanical measurements[1] showed that to a first approximation change in temperature produced a uniform shift on a logarithmic time scale. However, the creep data show that this is not strictly true over a wide time scale, since the so-called WLF equation gives a better fit to the shift factors than one with a constant activation energy. However, the difference between these two representations is not large for a restricted time scale.

It follows from equation (4) that a peak in the relaxation spectrum (which will correspond to a 'transition') occurs when $dE'(\omega)/d\ln\omega$ and $E''(\omega)$ have a maximum value. In a system with a constant activation energy A then time is related to temperature θ by the equation

$$\tau(\theta) = \tau(0)\exp(A/R\theta)$$

Hence for measurements at constant frequency a possible definition of the transition temperature is the temperature at which $dE'(\theta)/d\theta$ and $E''(\theta)$ have a maximum value. For reasons of experimental convenience, this definition was adopted in one of our previous publications[1] and used to define transition temperatures for extensional and torsional viscoelastic behaviour. Similarly an alternative definition can be the temperature when $dJ'(\theta)/d\theta$ and $J''(\theta)$ have a maximum value. A further definition, following from equation (5) and (6), is that the transition temperature is the temperature for a maximum value of $\tan\delta$, which is equivalent to that for a maximum in $d\ln E'(\theta)/d\theta$ and $d\ln J'(\theta)/d\theta$.

These three definitions of transition temperature give appreciably different values for that temperature. This was remarked in the previous paper[1], and shown to follow very simply from the standard linear solid representation which was considered adequate for the previous investigation in a very narrow frequency range. In particular, it is to be expected that the maximum in $\tan\delta$ will occur at a temperature intermediate between the maximum in $dE'(\theta)/d\theta$ or $E''(\theta)$ and that in $dJ'(\theta)/d\theta$ or $J''(\theta)$.

The aim of our simplified procedure can now be defined. It is to select one point from the $E'(\theta)$, $E''(\theta)$, $J'(\theta)$, $J''(\theta)$ or $\tan\delta(\theta)$ results and observe how this point shifts with change of frequency. Since our frequency shifts must be identical whether we use modulus or compliance results it would suggest the best approximation will be obtained by defining the transition temperature as the temperature of the maximum in either $\tan\delta$, $d\ln E'(\theta)/d\theta$ or $d\ln J'(\theta)/d\theta$.

RESULTS

Typical results for the variation of the measured quantities E' and E'' are

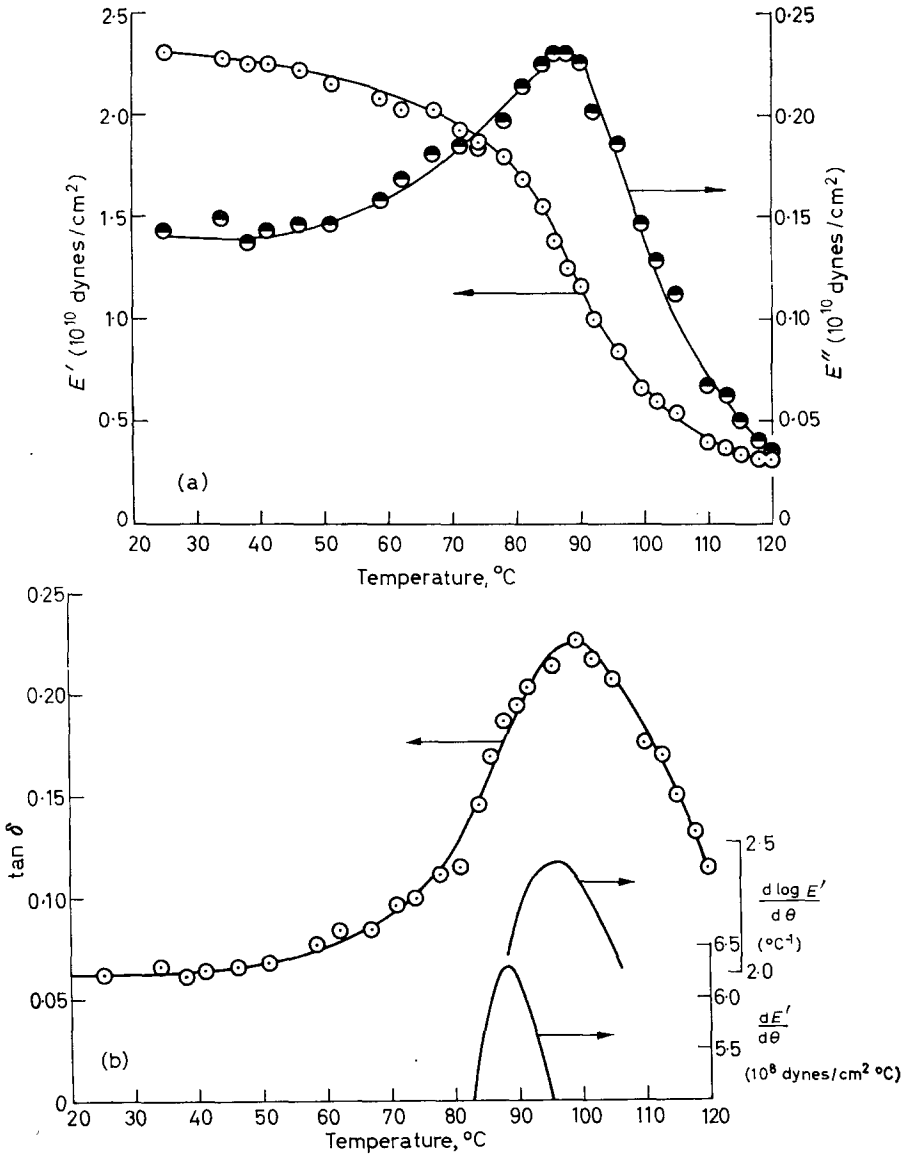

Figure 2—Typical measurements made at 0·1 c/s (a) E' and E'', (b) tan δ, $dE'/d\theta$ and $d \log E'/d\theta$

Table 1. Transition temperatures for unoriented crystalline PET fibres

Birefringence	*X-ray crystallinity* %	*Temperature, °C for maximum*				*Dynamic frequency, c/s*
		E''	$dE'/d\theta$	tan δ	$d \log E'/d\theta$	
0	33	79	84	92	92	0·01
0	33	86	88	97	96	0·1
0	33	89	93	103	100	1
0	33	95	95	110	104	10

shown in *Figures* 2(a) and 2(b), together with the derived quantities $dE'/d\theta$, $\tan\delta$ and $d \ln E'/d\theta$. Values of the transition temperatures defined by the temperature at which these quantities have a maximum value are given in *Table 1* for various frequencies. *Table 1* also includes the X-ray crystallinity.

DISCUSSION

Dynamic mechanical data

The results in *Table 1* show that, to a good approximation, the maxima in $dE'/d\theta$ and E'' occur at the same temperature and similarly the maxima in $d \ln E'/d\theta$ and $\tan\delta$ also occur at the same temperature, although the latter temperature is appreciably higher than the former. These similarities in temperature substantiate to a large extent the approximations made earlier which resulted in equations (4), (5) and (6).

The transition temperatures which are defined as the temperatures for maximum $\tan\delta$ have been plotted as a function of log frequency in *Figure 3* in a way suitable for fitting to the WLF equation. The value of T_g needed to give agreement between these data and the equation (also shown in *Figure 3*) is 79°C. As will be remembered this form of the WLF universal equation was formulated such that the fitting temperature T_g should be similar to the dilatometrically-measured transition temperature. This is certainly verified here where previous dilatometric measurements[4] gave a value of 81°C for crystalline polyethylene terephthalate polymer. It should also be noted that it was not possible to fit the temperatures for maximum E'' to the WLF equation.

Further justification for use of first-order approximations

Further justification for the use of the first-order approximations can be obtained directly from the creep data.

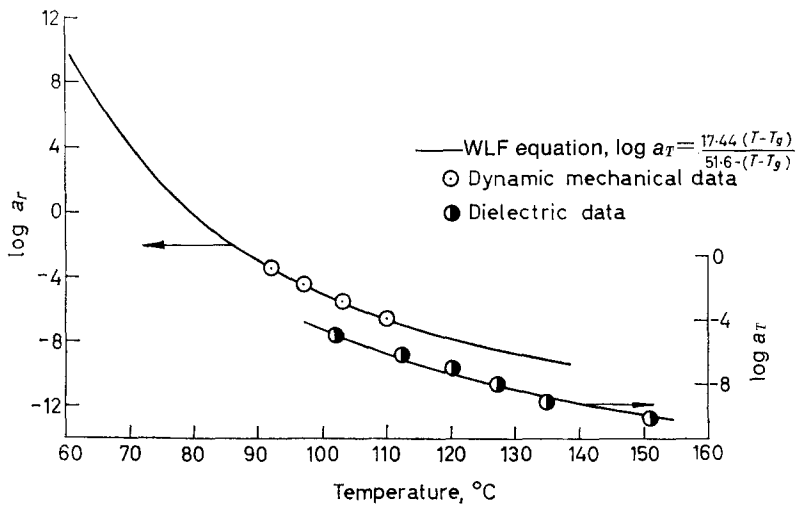

Figure 3—Temperatures for $(\tan\delta)_{max.}$ at various frequencies fitted to th WLF equation

The master creep compliance curve (Figure 4 in Ward[2]) shows that the creep compliance $J(t)$ is, to a good approximation, a linear function of $\ln t$ over the time range 10^5 to 10^{14} sec. This range corresponds to creep data obtained in the time interval 10 to 10^4 sec over the temperature range 84·4° to 115·5°C. Over this range it therefore follows that $dJ(t)/d\ln t$ is approximately constant and that $d^2J(t)/d\ln t^2$ and higher derivatives are zero, giving direct justification for the first-order approximation.

Outside this range, i.e. from 10^{-4} to 10^5 sec on the master curve, the first-order approximation is not satisfactory, particularly at the lowest times. This range covers creep data obtained at the three lowest temperatures only (65·0°C, 70°C and 76·6°C). It will be noted that the shift factors from these results do not, in fact, fit on to the WLF curve (Figure 5 in Ward[2]). Over the central and higher range of the creep data, however, where the link with the dynamic data is being established, the approximation holds and a good fit is obtained to the WLF equation.

Comparison of dynamic mechanical and creep data

Using the approximations described earlier it is possible to check the internal consistency of the dynamic mechanical data and the previously published creep data. From the creep measurements (Figure 3 in Ward[2]) E' was computed over a range of temperatures at a number of fixed frequencies (times) by assuming that $E'(\omega, \theta) = 1/J(t, \theta)$ with $t = 1/\omega$. These derived dynamic data are given in *Figure 4* where $\log E'(\omega)$ is shown as a function of temperature for four frequencies, viz. 10^{-4}, 10^{-3}, 10^{-2}, 10^{-1} c/s. The transition temperatures which are defined as those at the point of maximum $d\ln E'/d\theta$ are also included in the figure. Comparison of these with corresponding dynamic data of *Table 1* shows reasonable agreement confirming the equivalence of the creep and dynamic mechanical measurements and the validity of the approximate procedures.

Figures 5(a) and 5(b) show the shift factor a_T as a function of temperature, these data being obtained from the previous creep measurements. The curve shown in *Figure* 5(a) is similar to that obtained in the previous work where no correction was made for changes in the unrelaxed modulus (or the factor $\rho T/\rho_0 T_0$) with temperature. Although such factors are extremely small in polyethylene terephthalate where the creep compliance changes markedly with temperature recent work by Morris and McCrum[9] prompted us to attempt such a correction. On the basis of the high frequency results of Thompson and Woods[10] it was estimated that the change in the unrelaxed modulus was approximately 0·2 per cent per deg. C. New shift factors were then obtained from the previous data, taking into account this correction factor. The data can again be fitted to the WLF equation, and the value of T_g is slightly reduced, to 82°C from 85°C [*Figure* 5(b)].

This value of 82°C is in excellent agreement with both the dynamic T_g of 79°C and the dilatometric transition temperature of 81°C. This confirms the expectations of the theoretical discussion that definition of dynamic transition temperature as that for the maximum in $\tan\delta$ is necessary to produce a consistent shift factor for both creep and dynamic data.

Over this wide frequency range, there is a definite divergence of the

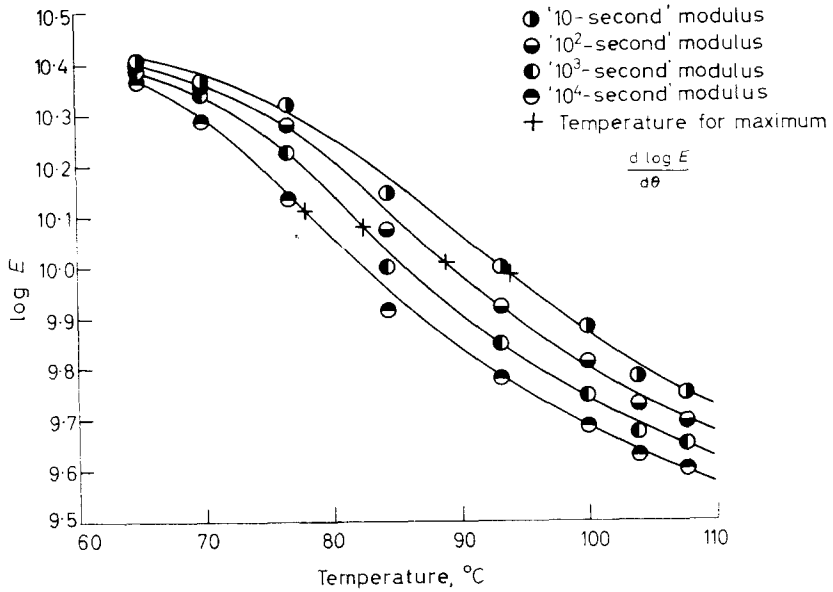

Figure 4—Modulus measurements at different times and temperatures derived from previous creep data

frequency/temperature behaviour of the dynamic data from that of a constant activation energy system. The fit to a WLF equation for the dynamic data alone is probably not completely conclusive, but it would certainly appear that this representation gives a consistent fit for both dynamic and transient data.

Comparison with dielectric measurements

In the paper on creep measurements, it was noted that the dielectric loss measurements were consistent with the WLF equation. The shift factors were obtained by Reddish[8] from the dielectric data by measuring the frequency at which the tan δ maximum occurs at a given temperature and are also plotted in *Figure 3*. The consistency of the dielectric and mechanical data is further confirmed by the present work, although it may be possible that the best fit for the dielectric data does involve a small vertical displacement with respect to the dynamic data. This displacement would not affect the choice of the T_g, although it is to be noted that there is not a significant difference between the WLF equation and a constant activation energy at high frequencies.

CONCLUSION

It is concluded that dynamic mechanical data on polyethylene terephthalate are consistent with the WLF equation relating time-temperature equivalence. Consistency between our previous creep data and the dynamic results

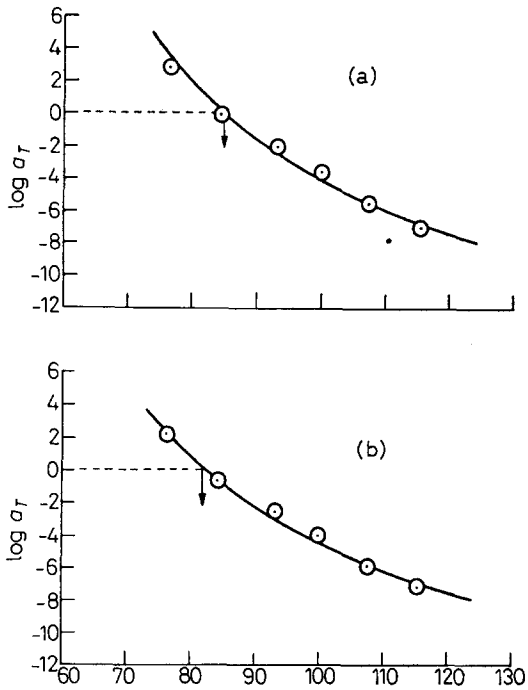

Figure 5—Shift factors obtained from creep data fitted to WLF equations, (a) uncorrected data, (b) data corrected to account for the change in the unrelaxed modulus with temperature

can be obtained if the transition temperature is defined from the dynamic data by the temperature at which tan δ is a maximum.

Research Department,
Imperial Chemical Industries Fibres Limited,
Harrogate, Yorkshire

(*Received December 1965*)

REFERENCES

[1] PINNOCK, P. R. and WARD, I. M. *Proc. phys. Soc.* 1963, **81,** 260
[2] WARD, I. M. *Polymer, Lond.* 1964, **5,** 59
[3] REDDISH, W. *Trans. Faraday Soc.* 1950, **46,** 459
[4] KOLB, H. J. and IZARD, E. F. *J. appl. Phys.* 1949, **20,** 564
[5] WILLIAMS, M. L., LANDELL, R. F. and FERRY, J. D. *J. Amer. chem. Soc.* 1955, **77,** 3701
[6] FARROW, G. and PRESTON, D. *Brit. J. appl. Phys.* 1960, **11,** 353
[7] GROSS, B. *Mathematical Structure of the Theories of Viscoelasticity.* Hermann: Paris, 1953
[8] STAVERMAN, A. J. and SCHWARZL, F. *Die Physik der Hochpolymeren,* Band IV. (Ed. H. A. STUART), Springer: Berlin, 1956
[9] MORRIS, E. L. and MCCRUM, N. G. *J. Polym. Sci. B,* 1963, **1,** 393
[10] THOMPSON, A. B. and WOODS, D. W. *Trans. Faraday Soc.* 1956, **52,** 1383

Limiting Viscosity Number versus Molecular Weight Relations for Polyoxacyclobutane

KAZUHIKO YAMAMOTO, AKIO TERAMOTO and HIROSHI FUJITA

Relations between limiting viscosity number $[\eta]$ *and molecular weight for polyoxacyclobutane* ($[O—(CH_2)_3]_n$) *in benzene, carbon tetrachloride and acetone at 30°C were determined over a range of weight-average molecular weight* M_w *from 3 000 to 30 000. It was found that the osmotic second virial coefficients of this polyether in these solvents were abnormally large, being of the order of* 10^{-3} *in c.g.s. units. The data for* $[\eta]$ *as a function of* M_w *were analysed in terms of the equation derived by Stockmayer and Fixman. The results yielded* $\sigma=1{\cdot}43$, *where* σ *is a parameter which represents the hindrance to the internal rotation of the successive bonds of a polymer chain in a theta solvent relative to that obtained for a freely rotating chain. Comparison of this* σ *value with those reported for the first, second and fourth members of this polyether series and that for linear polyethylene indicates that among these polymers the molecular chain of polyethylene oxide has the least hindrance to internal rotation and thus may be said to be most flexible.*

THE flexibility of a polymer chain is expressed in terms of a parameter σ, which is defined as the root mean square end-to-end distance of the chain in a theta solvent relative to its value which would be obtained if the hindrance to the rotation of successive bonds were absent except for the bond angle restrictions[1]. It is of interest to compare the values of this parameter for polymers whose structural units vary in a systematic fashion. An excellent example pertinent to this problem is the series of polyethers represented by $[O—(CH_2)_m]_n$. Recently, the first[2], second[1] and fourth[3] members of this series have been studied in various solvents, and their σ values have been evaluated from the viscosity versus molecular weight relations obtained. In the present paper we report a similar study on the third member of the series, i.e. polyoxacyclobutane.

EXPERIMENTAL

Polymer

The monomer oxacyclobutane was prepared by the method of Rose[4]. One mole of propane-1,3-diol and one mole of acetyl chloride were mixed in a glass tube at $-80°C$, the tube was sealed, and the mixture was stood overnight in an ice-bath. The tube was then heated at 100°C for eight hours. The product formed was neutralized with an aqueous solution of potassium carbonate and distilled under reduced pressure (14 mm of mercury). The distillate (b.pt 66·5° to 68°C at 14 mm of mercury), which is 1-acetoxy-3-chloropropane, was converted to oxacyclobutane by distillation in the presence of fused potassium hydroxide. The boiling point of the product was 47·9° to 48·0°C. Its purity, when estimated by gas chromatography, was 99·5 per cent.

A 40 m mole portion of the oxacyclobutane so prepared was dissolved in one of the following organic solvents: *n*-heptane, toluene, methylene chloride or ethylene bromide. The solution was cooled to −80°C, four m moles of a borontrifluoride ether complex was added, and the tube containing the mixture was sealed. Polymerization of oxacyclobutane was allowed to proceed by keeping the tube at various temperatures (−80° to 20°C) and for various intervals of time (10 to 100 hours), depending on the degree of polymerization desired. The polymer formed was dissolved in a mixture of aqueous ammonia and methanol, the solution was dried, and the residue was twice precipitated from a methanol solution by the addition of cold water. The final product was freeze-dried from a benzene solution and stored in a freezer. From a number of polyoxacyclobutanes so prepared, fifteen samples were chosen for the present study.

Solvent

The solvents used for the physical measurements were benzene, carbon tetrachloride, acetone and methylethyl ketone. These were dried with molecular sieves and fractionally distilled before use.

Number-average molecular weight M_n

The values of M_n of the fifteen samples chosen were determined using a Mechrolab vapour pressure osmometer (Model 301A) with benzene at 37°C as solvent. The osmometer was calibrated with the systems benzene–benzil, carbon tetrachloride–benzil, and acetone–benzil. Additional measurements were made on three samples in carbon tetrachloride at 37°C and one in acetone at 37°C. In each case, the plot for inverse apparent molecular weight versus polymer concentration c (g/dl) was linear within experimental uncertainty, and the desired values of M_n and the osmotic second virial coefficient A_2 were evaluated from the ordinate intercept and the slope of the linear plot obtained.

Weight-average molecular weight M_w

Four samples were chosen and the M_w of each was evaluated by sedimentation equilibrium experiments with methylethyl ketone at 25°C as solvent. Plots of M_w/M_n against M_n derived from these data showed a definite correlation between M_w and M_n. We therefore drew a smooth curve fitting the plotted points and, with this as the calibration line, calculated M_w of all other samples from their M_n values obtained in benzene at 37°C.

For the sedimentation equilibrium experiments we used a Spinco model E ultracentrifuge equipped with the Rayleigh interference optical system. No bottom liquid was introduced into the cell. The thickness of the solution column in the cell was adjusted to 2 to 3 mm. The partial specific volume of the polymer in methylethyl ketone at 25°C was 0·956 ml/g, and the specific refractive index increment of this solution, measured by a Brice–Phoenix differential refractometer, was 0·0946. The highest molecular weight sample among the four chosen was examined with the ultracentrifuge for two initial concentrations c_0, while the other three were studied at

only one c_0 (0·3 to 0·5 g/dl). The apparent (weight-average) molecular weights M_{app} obtained for the last three samples were substituted into the equation[5] $1/M_{app} = (1/M_w)(1 + 2A_2' M_w \bar{c})$ to evaluate the M_w values of the respective samples. Here $\bar{c}$ is the average concentration between the meniscus and the bottom of the cell, and A_2' is the light-scattering second virial coefficient of the solution. It was assumed that the A_2' value estimated from the data for the highest molecular weight sample was applicable to the others.

Viscosity

Values of the limiting viscosity number $[\eta]$ were obtained for all 15 samples in benzene, for 11 samples in carbon tetrachloride, and 7 samples in acetone, all at 30°C. The measurements were made with a capillary viscometer of the Ubbelohde type (suspended-meniscus) that had an upper bulb of about 2 ml capacity and an efflux time of 404·0 sec for benzene at 30°C. The water bath for the viscometer was regulated to within ±0·01°C of the desired temperature.

RESULTS AND DISCUSSION

$[\eta]$ *versus molecular weight relation*

Table 1 summarizes the numerical results obtained. One can see that the samples of polyoxacyclobutane we prepared cover a range of M_n from 2 000 to 16 000. Efforts to obtain a sample of higher M_n were unsuccessful.

Table 1. Summary of numerical results obtained for solutions of polyoxacyclobutane

	Thermodynamic			Viscometric		
Sample No.	$M_n \times 10^{-3}$ *(benzene)*	$A_2 \times 10^3$ *(ml mole/g²) (benzene, 37°C)*	$M_w \times 10^{-4}$ *(butanone)*	*Limiting viscosity number (dl/g) at 30°C*		
				Benzene	CCl_4	*Acetone*
1	$1·9_3$	2·3	$2·8_6$	0·105	0·107	0·085
2	$3·0_3$	2·7	$4·5_1$	0·159		
3	$3·1_6$	2·3	$4·7_2$[d]	0·155	0·147	0·116
4	$3·2_5$	2·2	$4·8_4$	0·150	0·154	
5	$4·6_3$ ($4·7_0$)[a]	3·2 (1·5)[a]	$6·9_5$	0·202	0·158	0·141
6	$5·0_8$	3·9	$7·6_7$	0·253		
7	$6·0_0$	3·2	$9·1_2$	0·251	0·238	0·168
8	$7·4_6$ ($7·2_5$)[b]	2·8 (2·9)[b]	11·8[d]	0·302	0·285	0·200
9	$8·0_0$	3·2	12·4	0·338		
10	10·0	4·5	15·9	0·402	0·392	
11	10·0 (10·1)[b]	3·5 (3·2)[b]	15·9	0·412	0·377	
12	11·1	3·3	18·0	0·464	0·442	0·264
13	11·8 (11·2)[b]	3·5 (3·1)[b]	19·1[d]	0·466	0·443	0·265
14	14·3	3·4	24·7	0·554	0·528	
15	15·6	3·6 (0·15)[c]	28·1[d]	0·590		

(a) Data in acetone at 37°C.
(b) Data in carbon tetrachloride at 37°C.
(c) Data in methylethyl ketone at 25°C determined from sedimentation equilibrium measurements.
(d) Determined directly by sedimentation equilibrium experiment.

Where comparison can be made, the M_n obtained in different solvents are in good agreement, suggesting that our M_n data are probably reliable. The most striking feature exhibited by *Table 1* is the fact that the indicated A_2 values are abnormally large. They are of the order of 10^{-3} (in ml mole

g^{-2}) and thus about ten times as large as the values which are usually encountered with ordinary polymers in good solvents. It can be noted that the values of A_2 in benzene solutions decrease appreciably as M_n becomes smaller than about 4 000. Elias and Lys[6] and independently Yamada *et al.*[7] have observed a similar trend of A_2 for polyethylene oxide (the second member of the polyether series considered) in benzene and in acetone.

The data for $[\eta]$ as a function of M_w are plotted double-logarithmically in *Figure 1*. The corresponding plots for log $[\eta]$ versus log M_n may be

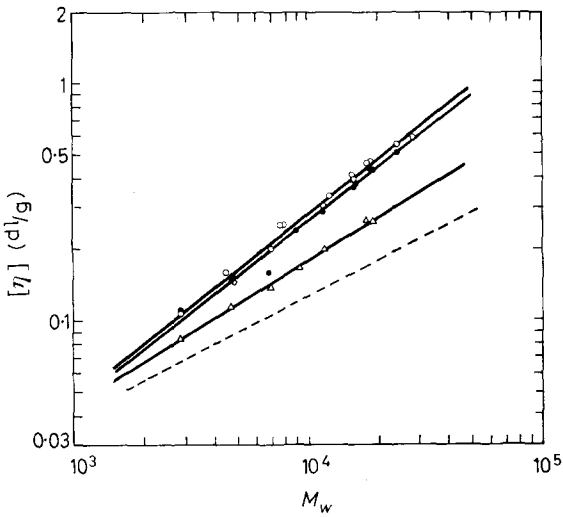

Figure 1—Double logarithmic plots of limiting viscosity number $[\eta]$ (dl/g) versus weight-average molecular weight M_w for polyoxacyclobutane $[O—(CH_2)_3]_n$ in various solvents at 30°C. ○ in benzene; ● in carbon tetrachloride; △ in acetone. Dashed line represents the relation expected under theta conditions

constructed from the data given in *Table 1*, but they will not be shown here because $[\eta]$ is a quantity which is related more closely to M_w than to M_n. The plots for each of the three solvents are fitted reasonably well by a straight line over the range of M_w indicated. The resulting Houwink–Mark–Sakurada relations for polyoxacyclobutane in benzene, carbon tetrachloride, and acetone, all at 30°C, are as follows:

$$\left.\begin{aligned} [\eta] &= 2{\cdot}1_9 \times 10^{-4} M_w^{0{\cdot}78} \quad \text{(benzene)} \\ [\eta] &= 2{\cdot}6_7 \times 10^{-4} M_w^{0{\cdot}75} \quad \text{(carbon tetrachloride)} \\ [\eta] &= 7{\cdot}6_0 \times 10^{-4} M_w^{0{\cdot}59} \quad \text{(acetone)} \end{aligned}\right\} \qquad (1)$$

It should be noted that the exponents in the Houwink–Mark–Sakurada equations for benzene and carbon tetrachloride are as high as about 0·8 in the region of relatively low molecular weight studied in this work. This feature must be related to the fact that the A_2 values in these solvents are abnormally large, as has been remarked above.

Evaluation of the parameter σ for polyoxacyclobutane

As has been done for the first, second and fourth members of the polyether series considered, we now analyse our viscosity data on polyoxacyclobutane in terms of the equation derived by Stockmayer and Fixman[8]. The appropriate expression is

$$[\eta]/M_w^{1/2} = K + BM_w^{1/2} \tag{2}$$

where K is a constant characteristic of a given polymer (precisely speaking, it depends slightly on temperature and solvent), and B is a parameter associated with the long-range interference between segments on the polymer chain and should be independent of molecular weight. Tests of equation (2) with the present data on polyoxacyclobutane are shown in *Figure 2*. One can see that the linear relation between $[\eta]/M_w^{1/2}$ and $M_w^{1/2}$

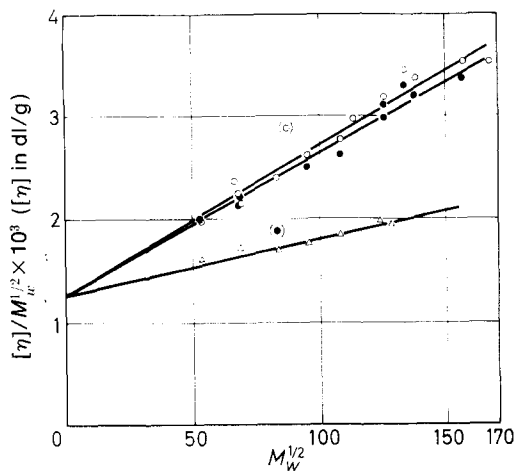

Figure 2—Stockmayer–Fixman plots for polyoxacyclobutane in benzene (○), in carbon tetrachloride (●), and in acetone (△), all at 30°C

predicted by equation (2) is well obeyed in any of the three solvents studied. Moreover, the plots for the three solvents give an identical ordinate intercept, in agreement with the requirement that K in equation (2) is independent of the solvent used (to a good approximation). Thus the present study yields $1{\cdot}26 \times 10^{-3}$ (dl mole$^{1/2}$ g$^{-2/3}$) for the K of polyoxacyclobutane.

Once the value for K is known, the desired value of σ for the given polymer can be calculated by the well-established method[1] with a relevant value being taken for the Flory constant Φ. To be consistent with the previous calculations of σ for other members of the series, here we use $2{\cdot}5 \times 10^{21}$ for Φ. Then the result is $\sigma = 1{\cdot}43$.

Comparison of σ values for members in the polyether series

Table 2 summarizes the values of K and σ for the first four members of the polyether series and those for linear polyethylene[9]. The data for the last polymer are cited here, since this polymer may be regarded as the limiting case of the polyether series in which the number of carbon atoms,

m, between ether oxygen atoms becomes indefinitely large. *Table 2* also includes, for comparison, the data for polypropylene oxide, the isomer of polyoxacyclobutane, which have been derived from the article of Moacanin[9]. *Figure 3* shows σ as a function of m. It is seen that among the members

Table 2. Values of K and σ for polyethers$[(CH_2)_m—O]_n$

Polyether	$K \times 10^3$ ($dl\ mole^{1/2}/g^{3/2}$)	σ[f]
$m=1$: polyoxymethylene	3·8[a]	2·43
$m=2$: polyethylene oxide	1·10[b]	1·38
$m=3$: polyoxacyclobutane	1·26	1·43
$m=4$: polytetrahydrofuran	1·96[c]	1·58
$m=\infty$: polyethylene	2·95[d]	1·81
		1·92 (at 30°C)[g]
Polypropylene oxide	1·15[e]	1·59

(a) Stockmayer and Chan[3].
(b) Taken from Kurata and Stockmayer[1].
(c) Kurata, Utiyama and Kamada[4].
(d) Chiang[10].
(e) Moacanin[9].
(f) Calculated assuming the Flory constant Φ to be $2{\cdot}5 \times 10^{21}$.
(g) The value 1·81 refers to 161°C, and the value at 30°C is derived from this, assuming[11] $-1{\cdot}2 \times 10^{-3}$ deg^{-1} for $d \ln \langle r^2 \rangle_0 / dT$, which is equal to $d \ln \sigma^2 / dT$. The σ values for other polymers refer to room temperature.

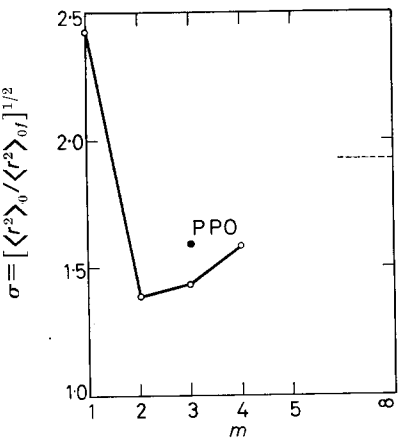

Figure 3—σ values for the polyethers as a function of m, the number of CH_2 groups between ether oxygen atoms. ●, polypropylene oxide (isomer of polyoxacyclobutane); – – –, linear polyethylene ($m=\infty$)

of the series concerned the molecular chain of polyethylene oxide has the least hindrance to internal rotation. It would be of interest to investigate, by performing similar viscometric studies for members higher than polytetrahydrofuran, the manner in which σ approaches the level for polyethylene as m increases. Finally, we wish to remark that in this polyether series the third member has the lowest melting temperature[12].

We wish to thank Professors Kurata and Inagaki of the Institute for Chemical Research, Kyoto University, for their helpful discussion. Thanks

are also due to Mr Umehara of this Department who helped us with the preparation of the polymer samples.

Department of Polymer Science,
Osaka University,
Toyonaka, Japan

(Received December 1965)

REFERENCES

[1] KURATA, M. and STOCKMAYER, W. H. *Fortschr. Hochpolym.Forsch.* 1963, **3,** 196
[2] STOCKMAYER, W. H. and CHAN, L.-L. Unpublished data
[3] KURATA, M., UTIYAMA, H. and KAMADA, K. *Makromol. Chem.* 1965, **88,** 281
[4] ROSE, J. B. *J. chem. Soc.* **1956,** 542
[5] FUJITA, H. *Mathematical Theory of Sedimentation Analysis,* Chap. V. Academic Press: New York, 1962
[6] ELIAS, H.-G. and LYS, H.-P. *Makromol. Chem.* 1964, **80,** 229
[7] YAMADA, N., YOKOUCHI, N., SATO, H. and NAKAMURA, R. *Repts Progr. Polym. Phys. Japan,* 1965, **8,** 27
[8] STOCKMAYER, W. H. and FIXMAN, M. *J. Polym. Sci.* 1963, **C1,** 137
[9] MOACANIN, J. J. *J. appl. Polym. Sci.* 1959, **1,** 272
[10] CHIANG, R. J. *J. phys. Chem.* 1965, **65,** 1645
[11] FLORY, P. J., CIFERRI, A. and CHIANG, R. *J. Amer. chem. Soc.* 1961, **83,** 1023
[12] LAL, J. *J. Polym. Sci.* 1961, **50,** 13

Some Polymers of Substituted Acetylenes

B. J. MACNULTY

Polymers of low molecular weight have been prepared from methyl propiolate, propiolamide and cyano-acetylene. These have been briefly examined for heat resistance and semiconductive properties.

RECENT Russian work[1] reports that heat treatment of polyacrylonitrile gives rise to a product with semiconducting properties. Vosburgh[2] describes a fireproof fabric obtained by heat-treating an acrylic fibre (Orlon) at temperatures between 150° and 300°C in the presence of oxygen. The Russian work suggested the following scheme of reaction:

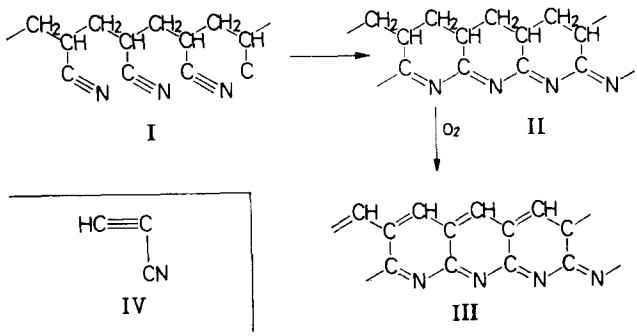

Vosburgh suggests a similar mechanism for the formation of the textile fibre. Both are in agreement with earlier suggestions of Houtz[3] and the more recent work of Grassie and McNeil on the structure of heat-treated acrylonitriles[4–7]. If the structures proposed for these materials are substantially correct then polymerization of cyano-acetylene (IV) should give a polymer possessing heat resistance and semiconductive properties similar to heat-treated acrylonitrile (III). This possibility has been investigated and polymers have been prepared from cyano- and other substituted acetylenes.

EXPERIMENTAL

Raw materials

Propiolic acid—manufactured by L. Light & Co.

Methyl alcohol—Analytical Reagent grade.

Infra-red spectra

These were obtained on a Grubb Parsons S3A double beam spectrometer with sodium chloride optics. Band frequencies are quoted in cm^{-1}.

Methyl propiolate, propiolamide and cyano-acetylene were all prepared by the method of Moureu and Bongrand[8] with only minor alteration as regards quantities.

Methyl propiolate ($CH{\equiv}C{\cdot}COOCH_3$)—B.pt 103° to 104°C at 762 mm
Infra-red bands: 3 337, 2 940, 2 146, 1 712, 1 446, 1 266, 1 190, 1 124, 990, 859, 756.

Propiolamide ($CH{\equiv}C{\cdot}CONH_2$)—The method was changed so that instead of lixiviating the reaction mixture with ether, the mixture was ground up and extracted with sodium-dried ether by shaking in a closed vessel.

M.pt 61·5°C Found: C 52·4, H 4·9, N 20·5 per cent; C_3H_3ON requires: C 52·17, H 4·35, N 20·3 per cent.
Infra-red bands: 3 400, 3 300, 3 200, 2 120, 1 670, 1 620, 1 590, 1 460, 1 385, 1 130.

Cyano-acetylene ($CH{\equiv}C{\cdot}CN$)—M.pt 5°C.
Found: C 69·1, H 2·7, N 27·0 per cent; C_3HN requires: C 70·59, H 1·96, N 27·45 per cent.
Infra-red bands: 3 940, 3 311, 2 940w, 2 262, 2 080, 1 316, 1 299.

Polymethyl propiolate

Method I—Methyl propiolate (1 g) was added in 0·05 g portions to triethylamine (1·2 g) (redistilled b.pt 89·5° to 90·5°C), over a period of 20 to 30 minutes. At each addition the temperature rose about 5 deg.C and the flask was cooled to room temperature. A dark brown product started to precipitate immediately. After two hours at room temperature the volatile fraction, pure triethylamine, was removed under a vacuum and collected in a liquid nitrogen trap. The residue, a dark sticky resinous mass, was extracted for 30 minutes with dry ether (2 × 20 ml) leaving a dark resinous material which was dried in a vacuum over sulphuric acid for 14 days. [Yield 60 per cent; Found: C 57·9, H 6·6, N 2·4 per cent.] The product, a brown powder, was soluble in acetone and methyl alcohol and insoluble in diethyl ether and benzene.

Method II—Triethylamine (0·36 g) was added in 0·02 g portions to methyl propiolate (5 g), the flask being thoroughly shaken between additions. At each addition, a temperature rise of 10° to 15°C occurred and the reaction vessel was cooled to below 25°C. The reaction mixture darkened steadily and was finally a thick almost solid black mass which was dissolved in 200 ml of a 1 : 1 : 1 acetone–ethyl alcohol–benzene mixture and precipitated with 3·5 litres of diethyl ether. The dark brown solid was filtered, washed with dry diethyl ether (3 × 150 ml) and dried in a vacuum over phosphorus pentoxide.

The product was soluble in acetone, methyl alcohol and chloroform in the cold, slightly soluble in warm benzene and insoluble in diethyl ether and petroleum ether.

On heating at about 3 deg.C/min it sintered slightly at 180°C to 190°C; sintering became marked at 220°C. At 254°C there were distinct signs of melting, but the product looked like a firm tar at 280°C. [Yield 50 per cent on monomer. Found: C 57·4, H 4·9, N 0·8 per cent; $(C_4H_4O_2)_n$ requires: C 57·14, H 4·76 per cent.]

Infra-red bands: 3 000, 2 950, 1 730, 1 630, 1 400, 1 370.

Polypropiolamide

Triethylamine (0·1 g) was added with shaking in 0·02 g portions, allowing an interval of several minutes between additions, to molten propiolamide (3·0 g). The reaction proceeded quietly until the final addition, when it became violent and about 0·5 g of amide was lost. The product, a black sticky solid, was Soxhlet-extracted with methyl alcohol until the extracting portion was pale orange in colour. (The main bulk of the solvent was then coloured deep claret.) The undissolved residue was ground with methyl alcohol, filtered and washed successively, with alcohol, a 1 : 1 methyl alcohol–ether mixture, and ether. The final liquid was colourless. On heating at about 3 deg.C/min the product appeared stable up to 310°C when a small amount of material distilled out of it; there was some sintering at 330°C leaving a black granular product which was unchanged at 360°C. Found: C 52·0, H 4·9, N 17·7 per cent $(C_3H_3NO)_n$ requires: C 52·2, H 4·4, N 20·5 per cent. Infra-red bands: 3 400, 3 226, 1 670, 1 610, 1 430.

Poly-cyano-acetylene

In a dry nitrogen atmosphere about 0·1 g of triethylamine was added a drop at a time, allowing several minutes between additions, to cyano-acetylene (2 g) at about 6°C. The reaction started immediately and occasionally became quite violent, when considerable amounts of the reactant were lost due to its high volatility. The product, a black sticky solid, was washed with acetone, and poured into a crystallizing dish where it dried out to a hard glassy brittle coating which could be broken up with some difficulty with a spatula. On heating it showed slight shrinkage above 320°C which was progressive, but there was no sign of softening or melting up to 400°C. It appeared to decompose at approximately 600°C. The black shiny powder was insoluble in benzene, methyl alcohol, diethyl ether, petroleum ether 40/60, chloroform, glacial acetic acid and water. It was unattacked by hydrochloric acid, only slightly attacked by concentrated sulphuric acid, but more readily by concentrated nitric acid or aqua regia. Some preparations were fairly soluble in acetone, probably due to a high proportion of low molecular weight material, but the best preparations were insoluble.

The reaction also took place in the vapour phase since when the reaction became violent the whole of the inside of the apparatus to a distance of several feet from the reaction vessel became coated with a hard black product that was very difficult to remove. Found: C 69, H 5·8, N 23 per cent; $(C_3HN)_n$ requires: C 70·59, H 1·96, N 27·45 per cent. Infra-red bands: 3 570, 2 222, 1 704w, 1 630, 1 200, 1 149.

Polymer A

Methyl propiolate (5 g) was poured rapidly into 0·88 ammonia (15 ml), allowed to stand for one hour and evaporated to dryness in a draught of air. The glassy solid was ground to a fine powder and dried at 105°C overnight; the treatment was repeated daily until after standing one hour in a closed weighing bottle the powder did not smell of ammonia. The product, an orange or yellow powder (the exact colour seemed to depend

on particle size), appeared to soften at about 135° to 136°C but did not liquefy below about 150°C. Found: C 44·9, H 5·7, N 16·7 per cent; $H[CH{=}C(CONH_2)]_2OH$ requires: C 46·15, H 5·13, N 17·95 per cent. Infra-red bands: 3 400, 3 200, 1 670, 1 590, 1 400, 1 250, 1 100.

Polymer B

This was obtained by heating polymer A for four weeks or more at 105°C. The product appeared to sinter at 170°C and decomposed giving tarry products at about 180°C. Found: C 52·5, H 5·7, N 16·7 per cent; $(C_3H_3NO)_n$ requires: C 52·17, H 4·35, N 20·29 per cent. Infra-red bands: 3 333, 3 279, 1 670, 1 600, 1 520.

DISCUSSION

Although numerous partially successful attempts have been made to polymerize acetylene compounds[9–23], in many cases[9–12,18] ring compounds were obtained and most linear polymers were low molecular weight oligomers[13–17]. In some cases high molecular weight polymers have been claimed[16,19–22] but these were insoluble intractable materials for which no figure was quoted. Molecular weights have never been quoted in excess of about 1 200, which is low compared to polymers in successful use.

The three compounds methyl propiolate, propriolamide and cyano-acetylene have not previously been polymerized. Meriwether and co-workers[18] mention the last two compounds amongst seven which they failed to polymerize with dicarbonyl-bis-(triphenylphosphine). In general the polymerizations seemed to occur by an ionic mechanism. Although satisfactory molecular weights have not been obtained consideration of the analysis of the present polymers indicates molecular weight no higher than those obtained with other polyacetylenes.

In their preparation of propiolamide Moureu and Bongrand[8] mentioned the production of a considerable amount of yellow oil as a byproduct. We also found this yellow oil (Polymer A) and from the conditions of its formation concluded that it was a polymer of propiolamide, methyl propiolate, or a copolymer of the two and that the polymerization was initiated either by the ammonium or hydroxyl ion. Analysis for carbon, hydrogen and nitrogen indicated an oligomer of the amide initiated by a hydroxyl, with an approximate formula $H[CH{=}C(CONH_2)]_nOH$.

On the basis that concentrated aqueous ammonia initiated a polymerization reaction under suitable conditions, the effect of an organic base on cyano-acetylene was tried. Triethylamine was chosen because its volatility would facilitate removal of excess from the product and because it was hoped that the relatively bulky group at the end of a chain would hinder the formation of cyclic compounds. A black solid, partially soluble in acetone, was obtained. When the triethylamine was added to solid nitrile, which is snow white, the rapid formation of oligomer could be followed by the expansion of a black area arising from the point of contact of the initiator. The polymerization was, however, only completed if a considerable amount of triethylamine was added and the reaction could be made to stop at any time by ceasing to add triethylamine. However, the polymer,

as denoted by acetone solubility, had a molecular weight in inverse proportion to the amount of triethylamine added.

Triethylamine successfully initiated polymerization of both propiolamide and methyl propiolate. At about the same time as these experiments were started it was reported[24] that tertiary amines dimerized methyl propiolate and that when triethylamine was used a considerable amount of black polymer was produced.

The assumed structure of the polymers was confirmed by infra-red spectra, none of which shows bands in the region of 2 100 cm^{-1} (C≡C) and all show indications of a band in the 1 630 cm^{-1} region corresponding to a carbon–carbon double bond. Consideration of the carbon hydrogen nitrogen analyses, which were difficult to obtain as most of the polymers resisted combustion, and of possible end groups, indicated chains containing between four and ten conjugated double bonds.

Much larger molecules could be present if they existed as stabilized biradicals such as $^{\bullet}[CH{=}CR]_n{}^{\bullet}$, which has been suggested by Berlin[25].

Conductivity and e.s.r. measurements were carried out on my behalf at Nottingham University by Miss Pamela Wynne-Thomas and Professor Eley. The polymers were ground to a fine powder and pressed into discs 13 mm in diameter and 0·1 mm to 1·0 mm thick under a pressure of 10 000 kg/cm^2. The disc was mounted in the conduction cell and the resistance measured using a d.c. voltage and a Vitron electrometer, after heating in a vacuum for 12 hours. The method is fully described[26] and will be referred to in papers now being prepared at Nottingham. *Tables 1* and *2* give the results which are typical of polyconjugated systems with unpaired

Table 1. Conductivity results for polyvinylenes

Polymer	$\log R_{293°C}$	$\log \rho_{293°C}$	$\log \sigma_0$	E_A (eV)
A	14·08	15·11	19·18	2·00
B	16·73	18·16	12·07	1·81
C	16·88	17·96	9·34	1·59
D	15·57	16·75	8·85	1·49
E	17·36	18·68	3·61	1·29

Table 2. Electron spin resonance results for polyvinylenes

Polymer	*Colour*	*Free spins per gramme*	*H (Gauss)*
A	Orange	$0{\cdot}48 \times 10^{17}$	8·0
B	Brown	$2{\cdot}29 \times 10^{17}$	10·0
C	Brown	$3{\cdot}37 \times 10^{17}$	6·5
D	Black	$9{\cdot}95 \times 10^{17}$	7·5
E	Brown	$1{\cdot}56 \times 10^{18}$	8·0

Polymer C is polymethyl propiolate.
Polymer E is polypropiolamide.
Polymer D is poly-cyano-acetylene.
E_A denotes energy of activation for the conduction process. $= \frac{1}{2}E_g$.
R = resistance in ohms.
$\sigma = \sigma_0 \exp(-E_g/2kT)$, where σ is conductivity and $\rho = 1/\sigma$, denotes resistivity.
σ_0 is an exponential constant.

electrons delocalized over the chains. Treatment of the conductive process by the potential box model[27,28] indicates that the polymers only have five

to ten conjugated bonds per chain[21] as has been deduced from carbon hydrogen nitrogen determinations, and that the measurements are in accord with the theories of Berlin[25].

The elemental analyses, infra-red spectra, and conductivity measurements all indicate that polymers A and B are both oligomers of polypropiolamide differing only in chain length and end groups.

Of the polymers prepared, that from cyano-acetylene is the most heat resistant (decomposition about 600°C) and nearly possesses semiconductor properties, $E_g = 3{\cdot}18$ eV, and electron spin concentration of 1×10^{18} g^{-1}, compared to Topchiev's values of 1·7 eV and 1·7 to 15×10^{18} g^{-1} for heat-treated polyacronylonitrile. The infra-red spectra are very similar to those published for heat-treated polyacronylonitrile[29, 30]. The material, although promising and possessing properties close to those expected for a compound having the structure of a heat-treated acrylonitrile (III), is brittle and intractable, probably due to its relatively low molecular weight. If means could be found to produce a polymer of high molecular weight a most useful product could be expected. The most likely route to such a polymer seems to lie in a thorough investigation of the initiators and catalysts for polymerizing acetylenes and their oligomers and a study of the mechanisms of their action, such as is being undertaken by Evans[31] and by Angelescu[32].

In a recent publication[33] a preparation of poly-cyano-acetylene is described using sodium cyanide as catalyst in dimethyl formamide. The product appears to be similar to our preparation but its total solubility in acetone would indicate a low molecular weight.

It should be noted that the combined vapours of methyl propiolate and ammonia have a marked anaphylactic effect on the skin, which should be rigorously protected from contact.

The author wishes to thank his colleagues, Mr H. E. Poupard for some repeat preparations, Mr G. Howell for infra-red spectra, Mr W. H. G. Wright for micro-analyses, and Miss Pamela Wynne-Thomas and Professor Eley of Nottingham University for conductivity and e.s.r. measurements.

Ministry of Aviation,
Explosives Research and Development Establishment,
Waltham Abbey, Essex.

(Received December 1965)

REFERENCES

[1] TOPCHIEV, A. V., GEIDERIKH, M. A., DAVYDOV, B. E., KARGIN, V. A., KRENTSEL, S., KUSTANOVICH, I. M. and POLAK, L. S. *Dokl. Akad. Nauk S.S.S.R.* 1959, **128,** 312; *Chem. & Ind.* **1960,** 184

[2] VOSBURGH, W. J. *Text. Res. (J.)*, 1960, **30,** 382

[3] HOUTZ, J. *Text. Res. (J.)*, 1950, **20,** 786

[4] GRASSIE, N. and MCNEIL, I. C. *J. chem. Soc.* **1956,** 3929

[5] GRASSIE, N. and MCNEIL, I. C. *J. Polym. Sci.* 1958, **27,** 207; 1958, **30,** 37; 1958, **33,** 171
[6] GRASSIE, N. and MCNIEL, I. C. *J. Polym. Sci.* 1959, **39,** 211
[7] GRASSIE, N. and HAY, J. N. *J. Polym. Sci.* 1962, **56,** 189
[8] MOUREV, C. and BONGRAND, J. C. *Ann. Chim.* 1920, **14,** 47
[9] REPPE, W. and SCHWECKENDICK, W. J. *Liebigs Ann.* 1948, **560,** 104
[10] ROSE, J. D. and STATHAM, F. S. *J. chem. Soc.* **1950,** 69
[11] HARRIS Jr, J. F., HORDER, R. J. and SOUSEN, G. N. *J. org. Chem.* 1960, **25,** 633
[12] SAUER, J. C. and CAIRNS, T. L. *J. Amer. chem. Soc.* 1957, **79,** 2659
[13] CHAMPETIER, C. and MARTYNOFF, M. *Bull. Soc. chim. Fr.* **1961,** 2083
[14] LUTTINGER, L. B. *J. org. Chem.* 1962, **27,** 1591
[15] GREEN, M. L. H., NEHME, M. and WILKINSON, G. *Chem. & Ind.* **1962,** 562
[16] NATTA, G., MAZZANTI, G. and CORRADINI, P. *Atti Accad. Lincei Cl. Sci. Fis. Mat. Nat.* 1958, **25,** 3
[17] BERLIN, A. A., CHERKASHIN, M. I., SEL'SKAYA, O. G. and LIMANOVA, V. E. *Vysokomol. Soedineniya,* 1959, **1,** 1817
[18] MERIWETHER, L. S., COLTHUP, E. C., KENNERLY, G. W. and REUSCH, R. N. *J. org. Chem.* 1961, **26,** 5155
[19] BERLIN, A. A. and CHERKASHIN, M. I. *Izvest. Akad. Nauk S.S.S.R, Ser. Khim.* **1964,** 565
[20] BARKALOV, I M., GOLDANSKII, V. I. and HO MIN-KAO. *Dokl. Akad. Nauk S.S.S.R.* 1964, **155,** 883
[21] NATTA, G., PINO, P. and MAZZANTI, G. *Ital. Pat. No. 530 753* (1955)
[22] NATTA, G., MAZZANTI, G., PREGAGLIA, G. and PERALDO, M. *Gazz. chim. ital.* 1959, **89,** 465
[23] BAWN, C. E. H., LEE, B. E. and NORTH, A. M. *J. Polym. Sci. B,* 1964, **2,** 263
[24] WENKERT, E., ADAMS, K. A. H. and LEICHT, C. L. *Canad. J. Chem.* 1963, **41,** 1844
[25] BERLIN, A. A. *J. Polym. Sci.* 1961, **55,** 621
[26] WYNNE-THOMAS, PAMELA. 'Semiconductors in organic macromolecules'. *Ph. D. Thesis.* University of Nottingham, 1965
[27] ELEY, D. D. and PARFITT, G. D. *Trans. Faraday Soc.* 1955, **51,** 1529
[28] ELEY, D. D. and WILLIS, M. R. Symposium on Electrical Conduction in Organic Solids. Duke University, Durham, North Carolina, April 1960. Sponsored by Office of Ordnance Research, U.S. Army, Office of Naval Research, U.S. Navy, and Office of Scientific Research, U.S. Air Force. Papers edited by H. KALLMANN and M. SILVER. Interscience: New York, 1960
[29] BURLANT, W. J. and PARSONS, J. L. *J. Polym. Sci.* 1956, **22,** 249
[30] TAKATA, T., HIROI, I. and TANIYAMA, M. *J. Polym. Sci. A,* 1964, **2,** 1567
[31] EVANS, A. G. and PHILLIPS, B. D. *J. Polym. Sci. B,* 1965, **3,** 77
[32] NICOLESCU, I. V. and ANGELESCU, E. M. *J. Polym. Sci. A,* 1965, **3,** 1227
[33] MANASSEN, J. and WALLACH, J. *J. Amer. chem. Soc.* 1965, **87,** 2671

*Irradiated Polyethylene I—Free Radical Formation**

I. AUERBACH

Several aspects of alkyl and allyl free radical formation in Marlex 50 polyethylene are examined. The free radicals were generated with ^{60}Co γ-rays and examined qualitatively and semiquantitatively by electron spin resonance techniques. Irradiations were performed at −196°C. The following conclusions are derived from this study: (1) the alkyl radical is relatively stable in the glassy amorphous region of polyethylene and relatively unstable in the viscous-elastic region. Alkyl radical decay takes place by a diffusion process; (2) in the decay process, few of the alkyl radicals, if any, are transformed to allyl radicals, and (3) preliminary results suggest that allyl radical formation at room temperature involves an intermediate other than the alkyl radicals.

Conclusion (1) is derived from the following: (a) isochronal measurements of the relative alkyl to allyl radical concentrations, as a function of temperature, decrease markedly as the temperatures go through the glass transition range; (b) a 12 kcal/mole activation energy value for alkyl radical decay, obtained from data above the glass transition temperature, T_g, is the same as that obtained from diffusion studies in polyethylene at higher temperatures; and (c) temperatures below T_g provide a linear relationship between the specific heat, C_p, for amorphous polyethylene and the decay rate. This relationship indicates that the molecular motions which determine the value for C_p also govern diffusion. Conclusion (2) is derived from a comparison of the residual allyl radical concentration at room temperature, following alkyl radical decay, with the initial alkyl radical concentration for radicals formed at −196°C. The comparative concentrations show that a very small fraction of allyl radicals remains following alkyl radical decay. Conclusion (3) is suggested from a comparison of the larger G values for allyl radical formation at room temperature irradiations with the smaller G values for alkyl and/or allyl radical formation at −196°C irradiations.

FREE radical formation in polyethylene by high energy radiation has been a subject for a large number of studies in recent years. Many of these investigations have used electron spin resonance (e.s.r.) techniques as the experimental basis for obtaining an understanding of the free radicals that are formed. The subject of free radical formation in polyethylene, studied by methods other than e.s.r. spectroscopy, is reviewed and discussed by Bovey[1], Charlesby[2], and Chapiro[3].

The e.s.r. techniques have provided not only quantative estimates of the free radicals formed but have shown qualitatively that three distinct radicals exist[4–18]. The literature is in general agreement that the alkyl radical, $-CH_2-\dot{C}H-CH_2-$, is one of the first observable products formed in irradiated polyethylene at very low temperatures. It has a sextet e.s.r. spectrum and it was evident in this study at temperatures below the glass transition temperature, T_g.

Polyethylene samples irradiated at room temperature possess an e.s.r.

*This work was supported by the United States Atomic Energy Commission. Reproduction in whole or in part is permitted for any purpose of the U.S. Government.

This paper, in part, was presented at the Fall Meeting of the American Chemical Society, 1962, Atlantic City, New Jersey.

septet spectrum which may have overtones of the alkyl radical sextet spectrum[4–8, 10–12, 14–17]. The septet spectrum is generally associated with the allyl radical, —CH=CH—$\dot{C}$H—CH_2—. The extent to which each species is present is dependent on the type of polyethylene, the administered dose, and the time that has lapsed from radiation to measurement.

A third radical which has been observed by Lawton, Balwit and Powell[3] and by Ohnishi, Ikeda, Sugimoto and Nitta[6, 14] possesses a singlet spectrum. A conjugated polyene structure adjacent to the unpaired electron, —CH_2—$\dot{C}$H—$(CH{=}CH)_n$—CH_2—, has been postulated for this radical. Doses of several hundred Mrads are required before this radical is evident in the e.s.r. spectra. The formation of conjugated double bond systems in irradiated polyethylene associated with this radical has been studied by Fallgatter and Dole[18] using u.v. spectrophotometric techniques.

In this study the effect of temperature on the e.s.r. spectrum is re-examined. It is shown that the disappearance of the alkyl radical can be correlated with the transition of the amorphous glassy state to the viscous-elastic state. Evidence is provided which indicates that an alkyl to allyl radical transformation cannot account for all of the allyl radicals formed during room temperature irradiations. The effect of matrix condition on the type of free radicals formed will also be discussed.

These conclusions were derived from the following experiments. (1) Marlex 50 polyethylene samples were irradiated in a ^{60}Co source at $-196°$C and the derivative spectrum recorded at a series of temperatures. (2) Alkyl radical concentrations were determined for samples irradiated at $-196°$C and measured at $-185°$C. The allyl radicals remaining when these samples were allowed to warm up to room temperature were also determined. The ratios obtained by dividing the initial alkyl radical concentrations into the resultant allyl radical concentrations were determined as a function of dose.

EXPERIMENTAL METHODS

Linear polyethylene in rod form (3/16 in.) was used for this study. It was prepared from a Marlex 50 stock which has a density of 0·96 and a melt index of 0·9. The rod is supplied by Allied Resinous Products Inc. and is listed as Resinol Type F polyethylene. The polyethylene specimens were irradiated in tubes which were evacuated for 24 hours at 10^{-5} to 10^{-6} Torr.

The ^{60}Co source consists of a 13 cm diameter cylindrical configuration of ^{60}Co slugs in 12 capsules. The capsules are 8 cm in height. The dose rate was approximately 6 Mrad/h at the time of this study. Ceric sulphate, nitrous oxide, cobalt glass and ionization chamber techniques provided dose rate calibration data. These calibration materials gave consistent results.

The free radical e.s.r. spectra were obtained with a Varian Model 4500 X-Band EPR Spectrometer which was equipped with a variable temperature cavity. Temperature control was maintained within $\pm 0{\cdot}05°$C. The microwave power supplied to the cavity was 0·5 mW.

Radical concentrations in arbitrary units were obtained by double integration of the derivative spectral form. The first integration which

provided the absorption spectrum was obtained electronically by passing the e.s.r signal into an *RC* analogue type integrator. A second integration was performed with a planimeter using the absorption curve realized from the first integration.

RESULTS AND DISCUSSION

Effect of temperature on the e.s.r. spectra

The relative concentrations of the alkyl and allyl radicals were determined as a function of temperature for constant doses and constant decay times in the present study. Lawton *et al.*[7,8], Kashiwabara[10] and Ohnishi *et al.*[14–17] have investigated the changes in the e.s.r. spectra of Marlex 50 as a function of radiation dose, radiation temperature and decay time. Their data, however, do not lend themselves well to the objectives of this study.

The alkyl radical is far less stable than the allyl radical. Any ratios of their concentrations would, therefore, be time dependent. The following experimental procedure was, therefore, adopted to determine the relative concentrations of the alkyl and allyl radicals as a function of temperature. Samples were irradiated with 12 Mrad doses at -196°C. The samples were then placed in the spectrometer cavity which was maintained at various temperatures and allowed to equilibrate over a 15 minute period before the spectra were recorded. Because alkyl radical decay took place during this period, the resultant spectra represent an isochronal picture of the relative radical concentrations.

Examples of the derivative spectra that were obtained at the various temperatures are shown in *Figure 1*. The multiplication factor represents attenuation. *Figure 1*(a) to (c) represents the alkyl radical sextet. The integrated form of this radical's spectrum is shown in *Figure 2*(a). The derivative form of the allyl spectrum is shown in *Figure 1*(e). The integrated form of the allyl spectrum, *Figure 2*(b), appears to be devoid of the fine structure depicting the five lines. The lack of structure is due to the condensed scale common to both spectra. Although forms of these spectra have been published elsewhere[7,8,10,14–18], they are presented here again so that the analytical technique for estimating the relative concentrations of the alkyl and allyl radicals may be adequately described. The technique provides an easy but approximate method for determining the relative concentrations of these two coexistent radicals.

The premise for this analytical technique is that the heights of the e.s.r. component bands are proportional to the concentrations of the respective species represented by the bands. The centre band of the derivative sextet spectrum, h_1 in *Figure 1*(a), and those bands marked off with dashed lines in *Figures 1*(b) and (c), correspond to the symmetrical depression on the integrated spectrum, *Figure 2*(a). Conversely, the centre band of the septet spectrum in the derivative form, also designated as h_1 and marked off by the dashed lines in *Figure 1*(e), corresponds to its centre band on the integrated form, *Figure 2*(b), rather than the absence of a band as in *Figure 2*(a). Therefore, h_1 represents the difference of two bands, $h_1' - h_1''$, where h_1' and h_1'' represent the height of the centre bands in the sextet

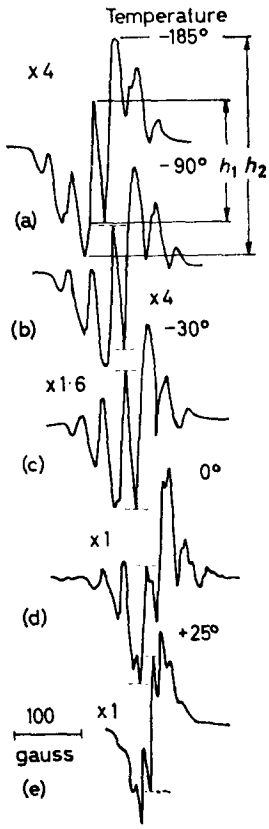

Figure 1—E.s.r. spectra of alkyl and allyl radicals at several temperatures. The spectra represent the following: (a) to (c), alkyl radical; (e), allyl radical and (d), an intermediate stage in the spectral transformation. The multiplication factors represent attenuation

and septet spectra, respectively. Also, h'_1 is always negative since it represents the absence of a band. As the sextet spectrum disappears with increasing temperature and the septet spectrum takes its place, h_1 (absolute value) will approach a minimum and then increase. Although the spectroscopic splitting factors (g) for these spectra are not quite equal, they are sufficiently close to cause overlapping of these bands.

In addition to the spectral conversion which takes place, the total radical concentration decreases due to radical decay. Changes in the value for h_1, therefore, reflect changes in concentration as well as the sextet–septet spectral transformation. An approximate method for normalizing concentration variations and one which still makes it possible to follow the variation in h_1 is obtained by studying the ratio $h_1/h_2=(h'_1-h''_1)/(h'_2+h''_2)$ where h'_2 and h''_2 represent the height of the component bands next to the centre band in the sextet and septet spectra; both have positive values since they represent the presence rather than the absence of bands in the integrated spectra. As the spectral transformation proceeds, h_1/h_2 (absolute value) will also go through a minimum. The effects of superimposing the radical spectra and the resultant observed spectrum are illustrated graphically by Lawton *et al.*[7] in their Figure 5.

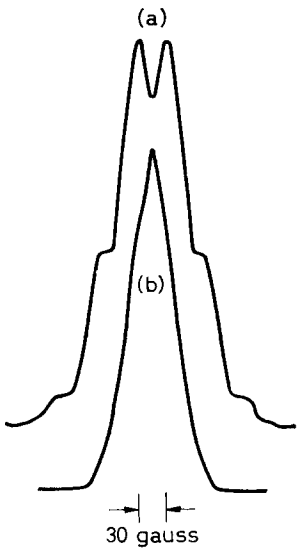

Figure 2—Integrated forms of the e.s.r. spectra for the alkyl radical, (a), and the allyl radical, (b)

Values for h_1/h_2 are instructive when the natural logarithm for h_1/h_2 is plotted against $1/T$, *Figure 3*. T is the absolute temperature. It shows the relative concentrations of the alkyl and allyl radicals as a function of temperature. The linear relationship for values of $1/T$ greater than 6 ($-106°C$), section (a) of the plot, may be due to motional narrowing of the spectral bands. As the temperature increases beyond this point, h_1/h_2 decreases [section (b)] indicating that the relative allyl radical concentration is increasing. These results do not necessarily imply that alkyl radicals

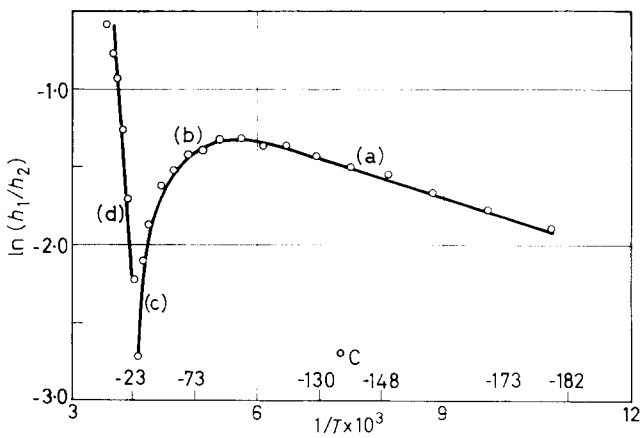

Figure 3—Relationship between temperature and the ratio of the peak-to-peak amplitude for the centre depression in the alkyl radical, h_1 (see *Figures 1* and *2*), with the peak-to-peak amplitude for the bordering spectral bands, h_2

are being converted to allyl radicals, however. The apparent results may, rather, be a reflection of the more rapid decay of the alkyl radical at these temperatures. The relatively more stable allyl radical would, therefore, constitute a higher percentage of the total residual radical concentration.

The decreasing values for $\ln(h_1/h_2)$ approach a linear relationship with $1/T$ [section (c)]. The very low values realized for h_1/h_2 and the apparent minimum [sections (c) and (d)] are the result of the depression being replaced in the alkyl radical spectrum, *Figure 2*, by the centre band of the allyl radical spectrum which has been described. Thus, sections (a), (b) and (c) correspond to h_1/h_2 values where the alkyl radical spectrum is predominant after the 15 minute equilibration period. Similarly, section (d) corresponds to the predominance of the allyl radical in the centre band of the spectrum.

The absolute values for the slopes of the linear portions of the two plots, sections (c) and (d), are equal. The equality emphasizes the interpretation that h_1/h_2 has the same significance in both plots. It was estimated that the slope in section (c) becomes constant at temperatures above $-36°C$.

An activation energy can be obtained from sections (c) and (d) of the Arrhenius plot in *Figure 3*, which reflects the energetics involved in the decay process. A value of 12 kcal/mole was realized. This value compares with a value of 12·2 kcal/mole which was obtained from the diffusion study of octadecane in polyethylene over the temperature range of 40° to 90°C[19]. The comparable activation energy values indicate that alkyl radical decay is a diffusion process and that the same matrix is involved in both systems and temperature ranges. The temperature at which the slope in *Figure 3* becomes constant in the range where decay takes place, $-36°C$, is of significance since it corresponds to the maximum temperature in the glass transition temperature range noted by Wunderlich[20], $-36°C$. The constant slope above this temperature indicates that diffusion is taking place in a matrix that is not changing form.

Evidence that the increase in decay rate with respect to temperature, section (b), is related to the glass transition is found in the relationship of h_1/h_2 to the specific heat, C_p, of amorphous polyethylene. C_p is a convenient parameter for this comparison since it also changes rapidly in this temperature range. The linear relationship is shown in *Figure 4*. Experimental values for h_1/h_2 and the C_p data of Wunderlich[20] were used for this plot. Although the range of values covered in this plot is small, it covers all of the h_1/h_2 data in the curved portion of *Figure 3*, section (b), and all of the C_p data in the glass transition range reported by Wunderlich[20].

The relationship probably arises from the fact that the specific heat is a measure of the motional freedom of the polymer molecules. The decay rate being a diffusion process is also dependent on molecular motion and, therefore, is related to the transition of the polymer molecules from the glassy state to the viscous-elastic state. The fact that the relationship is linear over the entire range of section (b) in the *Figure 3* plot shows that a relatively simple relationship is involved.

The gradual increase in the activation energy in section (b) is probably

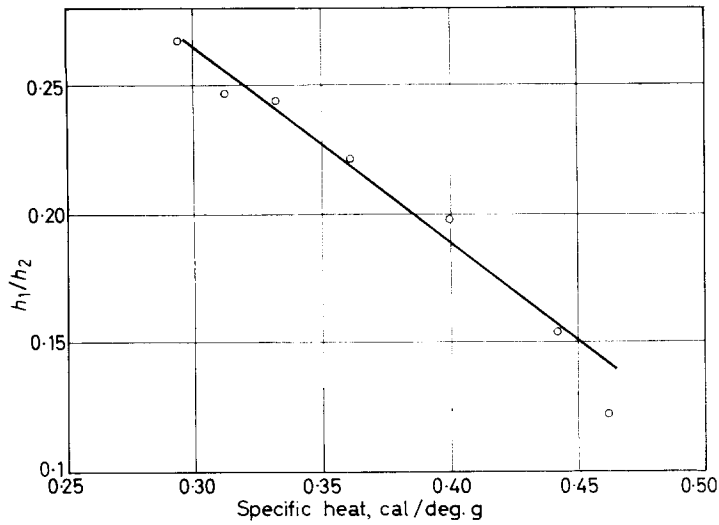

Figure 4—Relationship between h_1/h_2 and specific heat, C_p, in the range of 183° to 238°K

due to the fact that two competitive processes are involved, (1) the motional narrowing of the spectral lines which increases h_1/h_2, and (2) the decay process which decreases h_1/h_2. As the temperature increases, increasing molar quantities of the radicals are involved in the decay process. The latter process with its higher activation energy therefore becomes more prominent over the former process as the temperature increases. These results provide added evidence for a diffusion-controlled decay process which is dependent on the phase transition of the amorphous state.

Very little, if any, alkyl radical decay involves an alkyl–allyl radical transformation. This conclusion is derived from a series of experiments in which alkyl radical concentrations, in arbitrary units, were determined by double integration of the e.s.r. signal at −185°C immediately following irradiation at −196°C. The samples were then allowed to remain at room temperature for one hour after which alkyl radicals were not observed. The allyl radical concentration was then measured by double integration.

The absence of alkyl radicals after the one hour decay period was indicated by the observations that the allyl radical septet spectra showed no overtones of the sextet alkyl radical spectrum. In addition, the residual allyl radicals showed no measurable decay over a period of several hours. These results suggest that any allyl radicals formed directly at the lower temperatures or by a radical transformation process were also measured at room temperature.

The conclusion that very little, if any, alkyl radical decay involves an alkyl–allyl radical transformation is derived from *Figure 5* where the concentration ratios of allyl radicals/alkyl radicals are plotted against dose. It is evident that only a few per cent of the alkyl radicals could have been converted to allyl radicals. *Figure 5* also shows that the ratio is at its maximum at the lowest dose. It is of interest that the reverse process, allyl

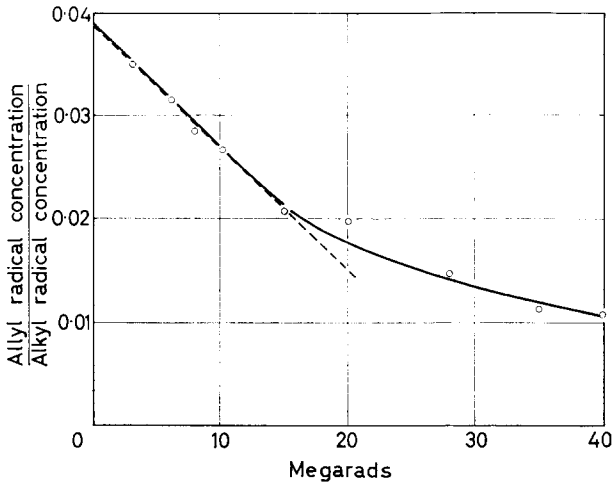

Figure 5—Relationship between dose and the ratio of the residual allyl radical concentration following alkyl radical decay to that of the alkyl radical concentration following irradiation at −196°C

to alkyl radical transformation, can be induced by ultra-violet irradiation[17]. Ohnishi, Sugimoto and Nitta[17] provide no explicit evidence that the forward process is also induced by u.v. irradiation.

The allyl radical/alkyl radical ratios obtained in this study compare favourably with those obtained from the data of Ohnishi[14]. His G values for allyl and alkyl radical formation, 0·3 and 6·4, respectively, provide a ratio of 0·047. This compares with an initial ratio value of 0·039 obtained in the present study.

It is of interest that Ayscough and Evans[21] also report that significant amounts of allyl radicals remain when the alkyl radicals of straight chain terminal olefins disappear. They state that it has never been possible to establish whether the allyl radicals were initially present or not. The results of the present study are, therefore, in general agreement with those of Ayscough and Evans[21]. They show a similarity in behaviour of Marlex 50 with lower molecular weight olefins.

A corollary to the observation that few, if any, alkyl radicals formed at −196°C are converted to allyl radicals is the probability that allyl radicals formed at room temperature do not involve an alkyl–allyl radical transformation. This conclusion is derived from a comparison of the G values for alkyl radical, $G(M)$, and allyl radical, $G(A)$, formation for the two sets of irradiation conditions, those described above and those involving allyl radical formation by irradiation at room temperature. Ohnishi[14] provides a $G(M)$ value of 6·4 for Marlex 50 irradiations in the 0 to 15 Mrad range at −196°C. Assuming that allyl radicals are formed initially from vinyl groups on a 1:1 basis, then the initial G value for vinyl group disappearance provided by Dole, Milner and Williams[22], 9·6, is sufficiently larger than $G(M)$ to indicate that another mechanism for allyl radical formation is operative.

The basis for assuming a 1 : 1 relationship between allyl radical formation and vinyl group disappearance lies in a consideration of the comparative rate constants for the two processes. Dole *et al.*[22] provide a first order rate constant for vinyl disappearance of $1{\cdot}61 \times 10^{-21}$ g/eV. In a subsequent publication it will be shown that the first order rate constant for allyl radical formation, in the dose range where vinyl groups disappear, is $1{\cdot}77 \times 10^{-21}$ g/eV.

The evidence for a non-alkyl radical intermediate in allyl radical formation which is provided by the above comparative G values is supported by the data in *Figure 5*. They show that the allyl radicals remaining at room temperature following alkyl radical decay are a very small percentage of the radical concentration at $-185°C$.

The possibility exists that the high $G(A)$ value at room temperature is due to a difference in behaviour of (1) alkyl radicals formed at $-196°C$ and then raised to room temperature, and (2) alkyl radicals formed initially at room temperature. This possibility is remote. Instead, the prevalence of different radicals is probably due to a difference in behaviour of a radical precursor at these different temperatures. At low temperatures, the precursor forms alkyl radicals which decay at temperatures above T_g, whereas at the higher temperatures it is involved in allyl radical formation.

The results of the present study are interpreted in the following manner. The formation of allyl radicals at very low doses, where the relative yield is highest, presumably involves vinyl groups since vinylene groups are initially not present in Marlex 50. The vinyl groups are probably present to a large extent in the amorphous portion of the polymer since they represent defects and are probably rejected by the lamellae during the crystallization process.

Vinylene groups are formed during the radiation process and are also available for allyl radical formation. The vinylene groups may be in amorphous regions since the regions in which they are formed may have received sufficient radiation to be converted to amorphous material. They may, however, also be present in the crystalline regions.

It is believed that the state of the amorphous region, i.e. glassy or viscous-elastic, influences the type of radical formed, i.e. alkyl or allyl radical, hence, the emphasis which has been placed on the vinyl and vinylene groups being present in amorphous regions.

These results can be explained if it is assumed, as Ayscough *et al.*[21,23] suggest, that allyl radicals are formed by the transfer of hydrogen as an atom or proton from the β-carbon relative to the double bond to an ion or an unsaturation site. In the glassy state such transfers would be highly restricted because of the mobility limitations. In the viscous-elastic state, greater mobility is possible and the hydrogen can diffuse to another site.

The glass to viscous-elastic transition affects the radical processes in two ways. (1) Hydrogen atom or proton mobility, which is possible in the viscous-elastic state, permits allyl radical formation as described in the above paragraph. (2) Alkyl radical decay increases because of the similar freedom for mobility allowing for radical recombination.

The decay results would also suggest that most of the radicals in this

study were in the amorphous region. If radiation interaction with polyethylene is assumed to be random, then some of the radicals must have formed in regions which were formerly crystalline since Marlex 50 is approximately 80 per cent crystalline. The conditions through which these radicals are concentrated in amorphous regions could result if it is assumed that the radiation damage is sufficiently severe to create amorphous regions and trap the resultant alkyl radicals.

SUMMARY

Alkyl radicals in polyethylene, produced by γ-rays at −196°C, are relatively stable in the glassy state of the amorphous phase and unstable in the viscous-elastic state. Their decay is associated with the glass transition and is dependent on a diffusion process. Their decay does not proceed in large measure through an alkyl–allyl radical transformation. At −196°C alkyl radicals are formed predominantly whereas at room temperature allyl radicals are mainly formed. It is believed that the state of the amorphous phase determines the type of radical which is formed.

The author is grateful to Arthur W. Lynch for his technical assistance.

Sandia Laboratory,
Albuquerque, New Mexico 87115

(*Received December 1965*)

REFERENCES

[1] BOVEY, F. A. *Effects of Ionizing Radiation on Natural and Synthetic High Polymers,* Chap. 5. Interscience: New York, 1958
[2] CHARLESBY, A. *Atomic Radiation and Polymers,* Chap. 13. Pergamon: New York, 1960
[3] CHAPIRO, A. *Radiation Chemistry of Polymeric Systems,* Chap. 9. Interscience: New York, 1962
[4] SMALLER, B. and MATHESON, M. S. *J. chem. Phys.* 1958, **28,** 1169
[5] KORITSKII, A. T., MOLIN, YU. N., SHAMSHEV, V. N., BOUBEN, N. YA. and VOEVODSKII, V. V. *Vysokomol. Soedineniya,* 1959, **1,** 1182
[6] OHNISHI, S., IKEDA, Y., SUGIMOTO, S. and NITTA, I. *J. Polym. Sci.* 1960, **47,** 503
[7] LAWTON, E. J., BALWIT, J. S. and POWELL, R. S. *J. chem. Phys.* 1960, **33,** 395
[8] LAWTON, E. J., BALWIT, J. S. and POWELL, R. S. *J. chem. Phys.* 1960, **33,** 405
[9] LOY, B. R. *J. Polym. Sci.* 1960, **44,** 341
[10] KASHIWABARA, H. *J. phys. Soc. Japan,* 1961, **16,** 2494
[11] OHNISHI, S., IKEDA, Y., KASHIWAGI, M. and NITTA, I. *Polymer, Lond.* 1961, **2,** 119
[12] CHARLESBY, A., LIBBY, D. and ORMEROD, M. G. *Proc. Roy. Soc. A,* 1961, **262,** 207
[13] KASHIWAGI, M. *J. chem. Phys.* 1962, **36,** 575
[14] OHNISHI, S. *Bull. chem. Soc. Japan,* 1962, **35,** 254
[15] OHNISHI, S., SUGIMOTO, S. and NITTA, I. *J. chem. Phys.* 1962, **37,** 1283
[16] OHNISHI, S., SUGIMOTO, S. and NITTA, I. *J. Polym. Sci.* 1963 **A1,** 605
[17] OHNISHI, S., SUGIMOTO, S. and NITTA, I. *J. chem. Phys.* 1963, **39,** 2647
[18] FALLGATTER, M. B. and DOLE, M. *J. phys. Chem.* 1964, **68,** 1988
[19] AUERBACH, I., MILLER, W. R., KURYLA, W. C. and GEHMAN, S. D. *J. Polym. Sci.* 1958, **28,** 129
[20] WUNDERLICH, B. *J. chem. Phys.* 1962, **37,** 1203
[21] AYSCOUGH, P. B. and EVANS, H. E. *Trans. Faraday Soc.* 1964, **60,** 801
[22] DOLE, M., MILNER, D. C. and WILLIAMS, T. F. *J. Amer. chem. Soc.* 1958, **80,** 1580
[23] AYSCOUGH, P. B., MCCANN, A. P., THOMPSON, C. and WALKER, D. C. *Trans. Faraday Soc.* 1961, **57,** 1487

Rapid Turbidimetric Determinations of θ-Conditions

C. F. CORNET and H. VAN BALLEGOOIJEN

This paper describes rapid semi-empirical methods for the turbidimetric determination of θ-conditions. The θ-compositions and θ-temperatures thus obtained agree well with those found by other methods. The theoretical background of the methods is discussed.

A DILUTE polymer solution is said to be under θ-conditions if the second virial coefficient, A_2, is zero (see ref. 1, p 425). A single solvent or a mixture of solvents with a constant composition may have a θ-temperature for a certain polymer. Similarly, a mixture of solvents at constant temperature may have a θ-composition for a certain polymer. The knowledge of these θ-conditions is important for several obvious reasons.

Therefore we need rapid and simple methods to determine these conditions. Elias[2-6] has developed such a method for θ-compositions using turbidimetric titrations.

However, the knowledge of θ-compositions is usually only of importance when intrinsic vicosities must be measured at θ-conditions. Light-scattering, osmotic-pressure and ultra-centrifugation measurements in θ-mixtures may lead to erroneous results. Therefore we need the knowledge of θ-temperatures of single solvents for such measurements.

As far as we know no rapid method for the determination of θ-temperatures is as yet available. One must either measure the second virial coefficient, A_2, at several temperatures and find the θ-temperature by interpolation to $A_2=0$ or determine the θ-temperature by extrapolating the critical miscibility temperature of a polymer–solvent system to infinite molecular weight (see ref. 1, p 613). Both methods are very time-consuming.

We have now developed a rapid and simple semi-empirical method to determine θ-temperatures of polymer–single solvent systems, analogous to the one described by Elias[2-6] for the determination of θ-compositions.

The results of our theoretical work have also led us to modify Elias's procedure.

EXPERIMENTAL

Methods

(1) *Determination of θ-compositions*—Non-solvent is added to a stirred and thermostatically controlled dilute polymer solution until phase separation starts. This is done with various solutions, the polymer concentration ranging between about 1 and 0·001 per cent by weight. The volume fraction of non-solvent necessary for incipient precipitation is plotted versus the logarithm of the corresponding volume fraction of

polymer*, resulting in a linear dependence. Extrapolation to pure polymer gives the θ-composition.

We have found that the rate of addition of non-solvent must be below 1 ml/min if a 100 ml cuvette is used. Furthermore, the temperature must be kept constant within about 0·1 °C.

(2) *Determination of θ-temperatures*—A stirred dilute polymer solution is slowly cooled down until phase separation starts. This is done with several polymer concentrations between about 1 and 0·001 per cent by weight. The values of the reciprocal absolute temperatures of incipient turbidity are plotted versus the logarithm of the corresponding volume fraction of polymer, which results in a linear dependence. Extrapolation to pure polymer gives the reciprocal θ-temperature. The cooling rate must be below about 1 °C per minute.

Apparatus

A 100 ml cylindrical glass cuvette, which contains the solution under study, just fits in a thermostatically controlled brass jacket. A lamp, fed by a constant voltage unit and facing a hole in the jacket, illuminates the solution. A photocell is placed before a second hole in the jacket, opposite to the first hole. The photocell output is fed to one input of a two-pen $2\frac{1}{2}$ mV Brown recorder. The other input of the recorder is connected to an iron–constantan thermocouple placed in the solution. The solution is stirred magnetically at a rate of about 200 rev/min. A constant volume pump (a DCL micro-pump with a plunger head of the C type) supplies non-solvent through a stainless-steel injection needle. The tip of this needle is placed just above the bottom of the cuvette, and so the non-solvent is brought to the temperature of the solution while being passed through the needle. The temperature of the brass jacket is regulated by means of circulating water or alcohol originating from an outside thermostat (type: Haake, Kryotherm KT 62), whose temperature can be programmed. The appearance of any turbidity causes a change in the light transmission and thereby in the photocell output. The apparatus allows the 'first cloud point' of polymer–solvent systems with concentrations as low as about 0·001 per cent by weight of polymer to be detected with sufficient accuracy (see also ref. 5).

RESULTS

(A) *θ-temperatures*—We have determined the θ-temperatures of the systems:

(1) poly-α-methylstyrene (PAMS)–cyclohexane;
(2) polystyrene (PS)–cyclohexane;
(3) polyisoprene (IR)–methyl isobutyl ketone (MIBK).

Re (1): independent measurements on three samples of PAMS in cyclohexane gave experimental θ-temperatures for this system of 35·7°, 36·1° and 36·8 °C (see *Figure 1*). The real θ-temperature is therefore

*This is in contrast with Elias's procedure. He plots the *logarithm* of the volume fraction of non-solvent versus the logarithm of the *concentration* (in g/ml) of the polymer. From Elias's papers it appears that he extrapolates to a polymer *concentration* of unity, which concentration differs from pure polymer by a factor equal to the density of the polymer (see e.g. Figure 1 of ref. 3). See the theoretical part for further details.

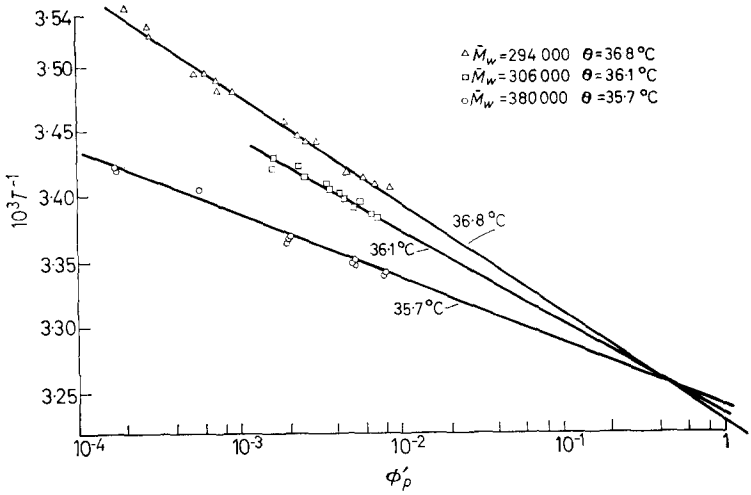

Figure 1—Turbidimetric determination of θ-temperature of system PAMS–cyclohexane $1/T$ versus $\log \phi'_p$

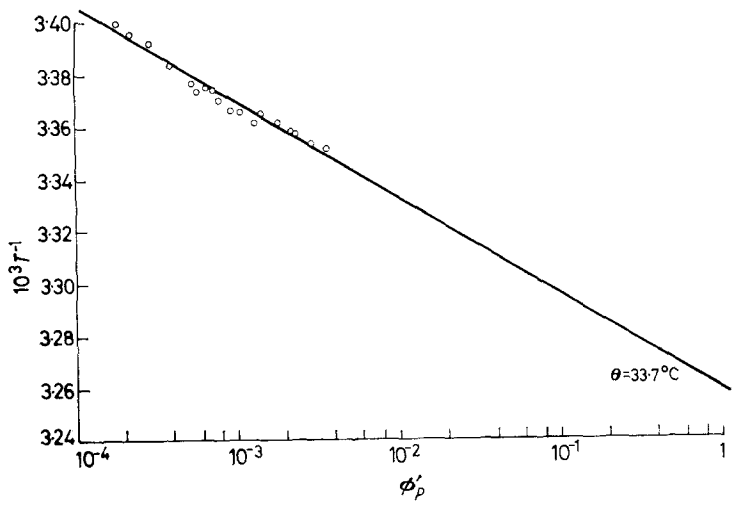

Figure 2—Turbidimetric determination of θ-temperature of system PS–cyclohexane $1/T$ versus $\log \phi'_p$. Sample: polystyrene Dow 666. $\theta = 33{\cdot}7$°C

expected to be 36·2° ± 1·0°C*. This value is in agreement with literature data. Kotera *et al.*[8] and Cottam *et al.*[9] reported 36°C and 38°C respectively.

Re (2): the θ-temperature of the system PS–cyclohexane was found to be 33·7°C (see *Figure 2*). This value is in good agreement with literature data (see e.g. ref. 1, p 615; refs. 10 and 11).

*This is in agreement with other experiments carried out in this laboratory. Mr H. Zeldenrust has measured the second virial coefficient of the system PAMS–cyclohexane at temperatures from 26° to 38°C by means of light-scattering experiments[7]. He found that $A_2 = 0$ at 35·5° ± 0·5°C.

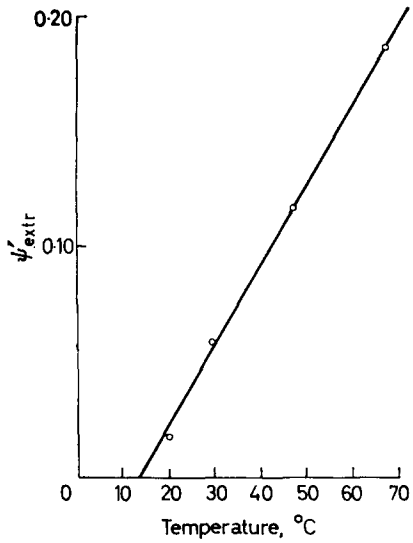

Figure 3—$\psi'_{extr.}$ versus titration temperature for the system polyisoprene–methyl isobutyl ketone–butanol-2. At $\psi'_{extr.}=0$, $t=13°C$

Re (3): the system IR–MIBK proved to be under θ-conditions at 13°C. An indirect measurement gave the same result (see the following section, re (2), the θ-compositions of IR–MIBK–butanol-2 mixtures at various temperatures, *Figure 3*).

(B) *θ-compositions*—We determined the θ-compositions of the following systems:

(1) PS–cyclohexane–*n*-heptane at 34°C;

(2) IR–MIBK–butanol-2 at various temperatures.

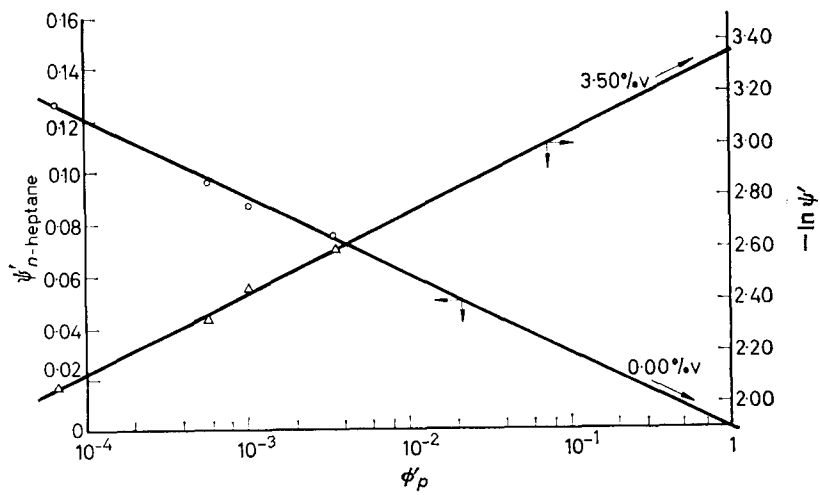

Figure 4—Turbidimetric titrations of polystyrene–cyclohexane with *n*-heptane at the θ-temperature of the PS–cyclohexane mixture (34°C). Extrapolation according to Elias gives an erroneous θ-composition

Re (1): as expected titrations performed in the system PS–cyclohexane at the θ-temperature (34°C) with *n*-heptane show that the θ-composition is equivalent to that of the pure θ-solvent (see *Figure 4*).

Re (2): we have measured the θ-composition of an MIBK–butanol-2 mixture for polyisoprene at various temperatures. A plot of θ-composition versus corresponding temperature gives a straight line, which extrapolates to the θ-temperature of the solvent at a θ-composition equivalent to that of the pure solvent (see *Figure 3*). The θ-temperature (of IR–MIBK) thus obtained agrees well with that found from direct measurements.

THEORETICAL BACKGROUND

(A) *Determination of θ-temperatures*

The rapid method to determine θ-temperatures was found empirically by searching for a method analogous to Elias's procedure for the determination of θ-compositions[2–6]. Elias's method is based on work by Patat and Träxler[12], who found that the composition of the gel phase precipitated in a polymer–solvent system is constant. However, later measurements by Männer[13] showed that the precipitate composition depends on the molecular weight and concentration of the polymer. Although Elias's theoretical explanation cannot therefore be entirely correct, his experimental results clearly show the practical value of his method. Since our method also gave good results, we have looked for a theoretical explanation. The results of this theoretical work have led to a few modifications in the evaluation of our experimental results and in the procedure as given by Elias[2–6].

Up till now it has not been possible to find a closed expression for the relation between the polymer concentration and the temperature of a polymer–solvent mixture which is on the verge of separating into two phases.

In order to find such a relation we have carried out numerical calculations in a way indicated by for example Flory (see ref. 1, p 545) and Tompa (see ref. 14, p 178). In the temperature/composition diagram of a polymer–solvent system a binodal line indicates the temperatures and compositions at which the system just separates into two phases. At equilibrium conditions the chemical potential of either component in one phase is equal to that in the coexisting phase.

The various theories on thermodynamics of polymer–solvent mixtures relate the chemical potentials of the components to the composition of the mixture, to the ratio between the molecular volumes and to a polymer–solvent interaction parameter. Combination gives two equations with three variables, viz. the two compositions and the polymer–solvent interaction parameter. By elimination of one of these variables a relation between the other two can be found.

We started from a modification of the Flory–Huggins expression for the Gibbs free energy of mixing, ΔG, as proposed by Holly[15]

$$\Delta G = kT\,[n_s \ln \phi_s + n_p \ln \phi_p + \chi_0 n_s \phi_p + \sigma n_s \phi_p^2] \qquad (1)$$

with

$$\phi_s = n_s/(n_s + mn_p) \text{ and } \phi_p = mn_p/(n_s + mn_p) \qquad (2)$$

where k is the Boltzmann constant, T is the absolute temperature, n_s and n_p are the numbers of molecules of solvent and polymer, ϕ_s and ϕ_p are the volume fractions of solvent and polymer, m is the ratio between the molecular volumes of polymer and solvent and χ_0 and σ are polymer–solvent interaction parameters. The chemical potentials of polymer and solvent are the partial derivatives of ΔG with respect to the numbers of polymer and solvent molecules.

When ϕ_p' and ϕ_p'' are related to the dilute and concentrated phases respectively, and m and σ are fixed, the relation between ϕ_p', ϕ_p'' and χ_0 can be found by numerical computation. This has been done for values of

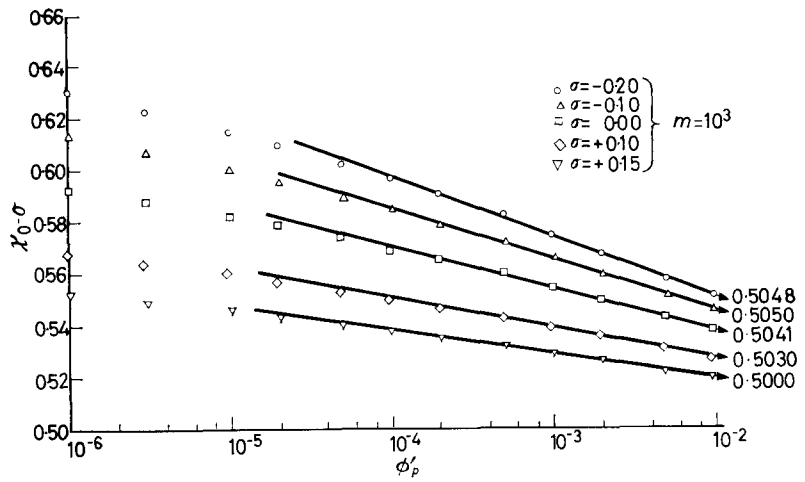

Figure 5—$\chi_0-\sigma$ as a function of $\log \phi'_p$

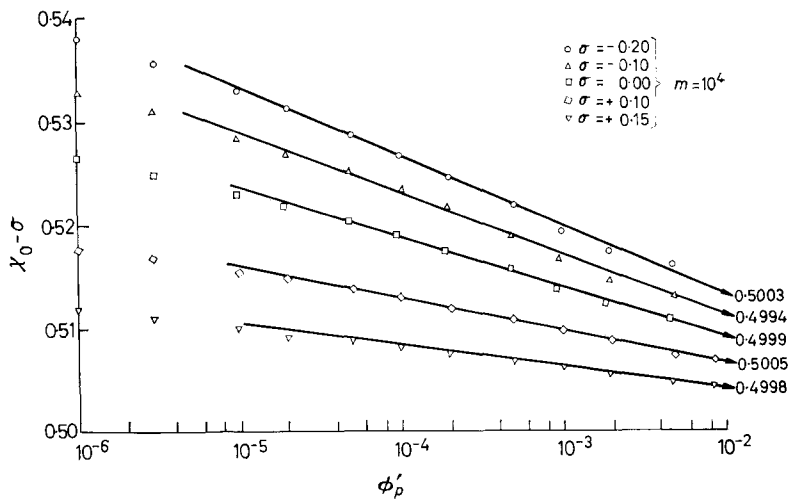

Figure 6—$\chi_0-\sigma$ versus $\log \phi'_p$

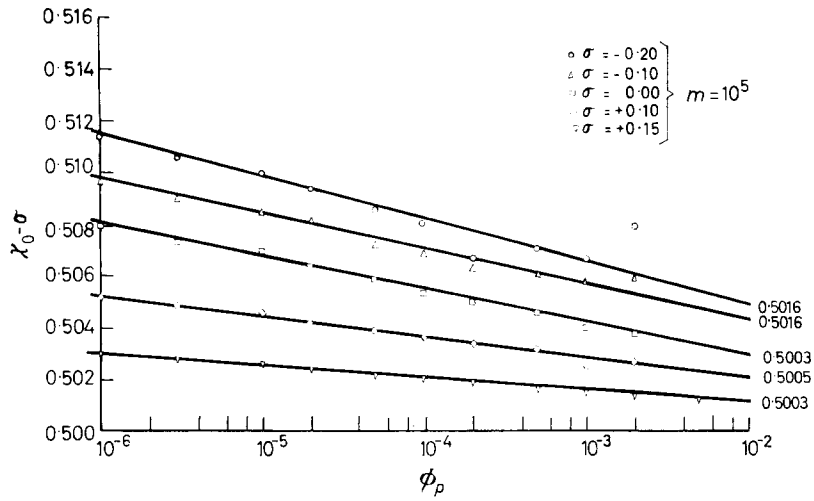

Figure 7—$\chi_0-\sigma$ versus $\log \phi_p' M = 10^5$

m ranging from 10^3 to 10^5 and values of σ ranging from $+0{\cdot}15$ to $-0{\cdot}20$*. The results of these calculations are shown in *Figures 5* to *7*.

When plotting $(\chi_0-\sigma)$ versus $\log \phi_p'$, we find that the part of the curve lying somewhere between $\log \phi_p' = -2$ and $\log \phi_p' = -5$ is approximately a straight line, which can be extrapolated to $(\chi_0-\sigma)=0{\cdot}50$ for $\log \phi_p' = 0$. Owing to the approximate character of equation (1) it seems useless to search for a curve which fits better. Following Flory (ref. 1, p 522), it can be shown that the condition $(\chi_0-\sigma)=0{\cdot}50$ corresponds to the θ-temperature, because $(\chi_0-\sigma-\frac{1}{2})$ is equivalent to $-\psi_1(1-\theta/T)$, where ψ_1 is an entropy parameter. Therefore $\chi_0-\sigma$ varies linearly with $1/T$ and $T=\theta$ if $\chi_0-\sigma=\frac{1}{2}$.

The extrapolation method as described above gives $(\chi_0-\sigma)$ values near 0·50 but not equal to 0·50. The most serious deviation δ, occurring with a low-molecular-weight polymer, is approximately 0·005. The deviation δ corresponds to an error in the θ-temperature, $\Delta\theta = \theta\delta/\psi_1$. As θ is usually about 300°K and ψ_1 may vary between 0·15 and 0·70, the deviation $\Delta\theta$ could according to these theoretical arguments reach a value up to 10°C. However, in polymers with a moderate or high molecular weight $\Delta\theta$ would usually be less than 1°C. Our experimental results indicate that only small errors are involved.

It must be remembered that this theoretical explanation is based on an approximate equation for the Gibbs free energy of mixing. However, our experimental results support the above arguments.

(B) *Determination of θ-compositions*

The analogon of a temperature/composition diagram of a polymer–single solvent system is a composition/composition diagram of a polymer–mixed-solvent system at constant temperature. Instead of the temperature, the

*We are indebted to Mr J. Ponstein who carried out the calculations with the aid of an IBM 7070 computer.

composition of the mixed solvent is plotted versus the volume fraction of polymer. The positions of coexisting phases relative to each other are not known for this diagram, because in general the compositions of the mixed solvent in these coexisting phases differ (see e.g. ref. 1, p 548 and ref. 14, p 192). As a rough approximation we can, however, neglect this difference and then it is possible to regard a solvent–non-solvent–polymer system as a quasi-single solvent system, where the polymer–solvent interaction parameter is now determined by the composition of the mixed solvent (see e.g. ref. 14, p 192). This apparent interaction parameter is given by

$$\bar{\chi} = \chi_{sp} + \psi_n (\chi_{np} - \chi_{sp} - \chi_{sn}) + \chi_{sn}\psi_n^2 \qquad (3)$$

where

$$\psi_n = \phi_n / (\phi_n + \phi_s)$$

and ϕ_n and ϕ_s are the volume fractions of non-solvent and solvent, respectively, and χ_{sp}, χ_{np} and χ_{sn} are the interaction parameters of the systems solvent–polymer, non-solvent–polymer and solvent–non-solvent respectively.

At constant temperature the parameter $\bar{\chi}$ is a function of ψ_n' only, because χ_{sn}, χ_{sp} and χ_{np} are then constant. In a sufficiently small range of ψ_n'-values the relation between $\bar{\chi}$ and ψ_n' is even approximately linear.

We now assume that $\bar{\chi}$ at constant temperature is equivalent to χ_0 in equation (1) and accordingly that a plot of $\bar{\chi}$ or ψ_n' versus $\log \phi_p'$ is equivalent to a plot of χ_0 or $1/T$ versus $\log \phi_p'$.

Extrapolation to $\log \phi_p' = 0$ in a $\bar{\chi}$ or ψ_n' versus $\log \phi_p'$ plot must then give a value of ψ_n' equal to $(\psi_n')_{extr.}$, and so $\bar{\chi} = \frac{1}{2}$ and the second virial coefficient is zero.

These qualitative arguments indicate that the results of turbidimetric titrations must not be plotted according to Elias[2–6], viz. $\log \phi_n'$ versus $\log \phi_p'$, but as described above, viz. ψ_n' versus $\log \phi_p'$. We have the following experimental evidence to support this statement. A turbidimetric titration on a polymer–θ-solvent–non-solvent system only produces the correct θ-composition, viz. the pure θ-solvent, if our extrapolation method is used (see *Figure 4*). If titrations are involved on systems whose θ-composition differs enough from zero, the two extrapolation methods give identical results.

Realizing that all χs are approximately linear functions of $1/T$, it can be seen from equation (3) that there must be a relationship between $(\psi_n')_{extr.}$ and the temperature T at which the titration has been carried out. In a sufficiently small temperature range the relation between $(\psi_n')_{extr.}$ and T is even approximately linear. Extrapolation to $(\psi_n')_{extr.} = 0$ must give a temperature equal to the θ-temperature of the polymer–solvent system and extrapolation to $(\psi_n')_{extr.} = 1$ must give the θ-temperature of the polymer–non-solvent system.

Part of these theoretical arguments is in agreement with our experimental results (see the measurements on the system IR–MIBK–butanol-2; *Figure 3*).

CONCLUSIONS

We have shown experimentally and theoretically that θ-conditions can be found by means of turbidimetric measurements. The logarithm of the

volume fraction of polymer in a dilute polymer solution at the beginning of phase separation is linearly related to the reciprocal absolute temperature or to the relative volume fraction of non-solvent. Extrapolation of this linear relationship to pure polymer (log volume fraction = 0) gives the θ-temperature or the θ-composition. The method appears to be rapid.

The knowledge of the relations between polymer concentration, temperature and solvent composition is indispensable to the use of a turbidimetric method as a means to characterize molecular-weight distributions and may be of great help when employing other fractionation techniques based on polymer solubility.

Koninklijke/Shell Laboratorium,
Amsterdam, Netherlands
Shell Research N.V.

(Received January 1966)

REFERENCES

[1] FLORY, P. J. *Principles of Polymer Chemistry,* Cornell University Press; Ithaca, 1953
[2] ELIAS, H. G. *Makromol. Chem.* 1959, **33,** 140
[3] ELIAS, H. G. *Makromol. Chem.* 1961, **50,** 1
[4] ELIAS, H. G. and GRUBER, U. *J. Polym. Sci. B,* 1963, **1,** 337
[5] GRUBER, U. and ELIAS, H. G. *Makromol. Chem.* 1964, **78,** 58
[6] ELIAS, H. G. and GRUBER, U. *Makromol. Chem.* 1964, **78,** 72
[7] ZELDENRUST, H. Private communication
[8] KOTERA, A., SAITO, T. and FUJISAKI, H. *Rep. Progr. Polym. Phys. Japan,* 1963, **6,** 9
[9] COTTAM, B. J., COWIE, J. M. G. and BYWATER, S. *Makromol. Chem.* 1965, **86,** 116
[10] SCHULZ, G. V. and BAUMANN, H. *Makromol. Chem.* 1963, **60,** 120
[11] OROFINO, T. A. and MICKEY Jr, J. W. *J. chem. Phys.* 1963, **38,** 2512
[12] PATAT, F. and TRÄXLER, G. *Makromol. Chem.* 1959, **33,** 113
[13] MÄNNER, E. 'Die Zusammensetzung der Gelphase und der Fraktionier-effekt bei der Fällfraktionierung des Polyisobutylen B 15'. *Thesis.* University of Munich, 1962
[14] TOMPA, H. *Polymer Solutions,* Butterworths: London, 1956
[15] HOLLY, E. D. *J. Polym. Sci. B,* 1964, **2,** 541

Contributions to Polymer

Papers accepted for future issues of POLYMER include the following:

Influence of the Dielectric Constant on the Rate of Solution Polymerization of Trioxan—M. KUČERA

Yield Stress Behaviour of Isotactic Polypropylene—J. A. ROETLING

Electron Microscope Studies of the Fracture of Glassy Polymers—R. J. BIRD, J. MANN, G. POGANY and G. ROONEY

Regular Alkylene Ether Copolymers—T. P. HOBIN

The Present Status of the Theory of Rubber Elasticity—G. GEE

The Infra-red Absorption Characteristics of Syndiotactic Poly(methyl methacrylate) from 1 050 cm^{-1} to 1 300 cm^{-1}—S. HAVRILIAK JR

Heat Capacities of Propylene Oxide and of Some Polymers of Ethylene and Propylene Oxides—R. H. BEAUMONT *et al.*

Thermal Degradation of Piperazine Polyamides III—S. D. BRUCK

The Dynamic Mechanical Properties of Some Polyethers—R. E. WETTON and G. ALLEN

A Comparison between Real Polymer Dimensions in Solution and the Behaviour Predicted from Models—A. J. HYDE

Polythioacetone—O. G. VON ETTINGSHAUSEN and E. KENDRICK

Polymerization of Styrene under Pressure—G. B. GUARISE

CONTRIBUTIONS should be addressed to the Editors, *Polymer*, c/o Butterworths, 125 High Holborn, London, W.C.1.

Authors are solely responsible for the factual accuracy of their papers. All papers will be read by one or more referees, whose names will not normally be disclosed to authors. On acceptance for publication papers are subject to editorial amendment.

If any tables or illustrations have been published elsewhere, the editors must be informed so that they can obtain the necessary permission from the original publishers.

All communications should be expressed in clear and direct English, using the minimum number of words consistent with clarity. Papers in other languages can only be accepted in very exceptional circumstances.

A leaflet of instructions to contributors is available on application to the editorial office.

Yield Stress Behaviour of Isotactic Polypropylene

J. A. ROETLING*

The tensile yield stress behaviour of isotactic polypropylene was measured over wide ranges of strain rate and temperature. As was found with amorphous materials studied previously, the yield stress behaviour could be described as the sum of the stresses due to two rate processes. One of these processes again appears to be the α-process (i.e. the process associated with the glass temperature, T_g) but the second process appears to be associated with the crystalline melting temperature (T_m). It is believed that the relaxation time of the usual β-process is too short for this process to make a significant contribution to the stress in the temperature region studied.

IN PREVIOUS papers[1,2] it was shown that the tensile yield stress behaviour of the amorphous polymers poly(methyl methacrylate) (PMMA) and poly(ethyl methacrylate) (PEMA) could be described by means of the Eyring viscosity theory. However, it was found that it was not possible to describe the data by means of a single process. To describe the observed behaviour over wide ranges of rate and temperature, it was necessary to assume that two rate processes were involved and that the stresses due to these two processes were additive. This not only permitted an excellent fit of the theoretical equation to the experimental data, but the activation energies obtained for the two processes were close to those obtained by means of dynamic mechanical and dielectric measurements. From this and other considerations it appears that the non-linear deformation processes involved at high stress levels are related to the linear processes which are observed at low stresses and that this relation is provided by Eyring's viscosity theory. The present paper describes the results obtained when the yield stress measurements were extended to isotactic polypropylene as an example of a crystalline polymer.

EXPERIMENTAL

The sample used in this investigation was a commercially available isotactic polypropylene sold under the trade name 'Profax'†. Test specimens were injection moulded bars of the type used in the previous investigations and the experimental procedure was the same as described previously.

The results of the tensile yield stress measurements on the polypropylene sample are shown in *Figure 1*, where the ratio of yield stress to absolute temperature (σ/T) is plotted as a function of the strain rate at each of several temperatures. The solid curves drawn through the data were calculated from the equation

$$(\sigma/T)=\sum_i (1/A_i)\sinh^{-1}\{(C_i\dot{\epsilon}/T)\exp(\Delta H_i/RT)\} \qquad (1)$$

*Present address: General Electric Co., M.S.D., P.O. Box 8555, Philadelphia, Pa 19101, U.S.A.
†Hercules Powder Company, Wilmington, Delaware.

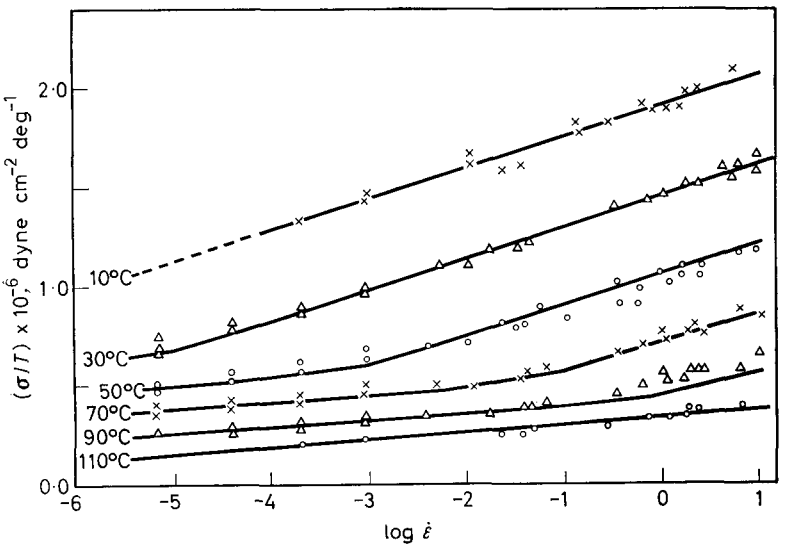

Figure 1—Measured ratio of yield stress to temperature as a function of rate of strain

where σ denotes yield stress (dyne cm^{-2}), $\dot{\epsilon}$ is strain rate (sec^{-1}), T is temperature (°K) and the A_i, C_i and ΔH_i are material constants. The values of these constants are given in *Table 1* and were chosen so as to result in a reasonably good fit of equation (1) to the data. As with previously studied materials, the equation describes the data quite well if it is assumed that two rate processes are involved.

Table 1. Polypropylene constants

Process (i)	α	ζ
ΔH_i (*kcal/mole*)	45·6	88·6
A_i	19×10^{-6}	62×10^{-6}
$\ln C_i$	−58·8	−90·4

DISCUSSION

Dynamic mechanical measurements[3,4] on crystalline polypropylene have shown the presence of at least three processes. These appear to be the usual α-process (i.e. the process associated with the glass transition temperature), a lower temperature process which will be referred to as the β-process, plus a third process which is associated with the crystalline melting point (T_m) and which will be referred to in this paper as the ζ-process. Considering the data presented in *Figure 1* and comparing them with similar data on PMMA and PEMA published previously, it will be noted that the yield stress at the higher rates and lower temperatures is relatively low for the polypropylene*. This lower yield stress together with a lower rate

*At the higher rates and lower temperatures PMMA and PEMA may fail before yield is reached. However, the yield stress may be calculated from equation (1) using the constants given for PMMA or PEMA.

of change of stress with increasing strain rate and the fact that only two processes are necessary to describe the data, suggests that one of the three processes observed in the dynamic (oscillatory) measurements is too rapid (i.e. the relaxation time is too short) to make a significant contribution to the stress in the range of rates and temperatures studied. The presence of at least one such rapid process will permit some relaxation at points of stress concentration and is possibly a characteristic of ductile polymers[5]. Of the three processes observed in the dynamic testing of polypropylene, one might expect that the β-process (i.e. the process associated with the lowest temperature loss peak) is too fast to contribute to the yield stress in this temperature range and that it is the remaining two processes which are observed in the yield stress measurement. This appears to be so, as will be noted from the considerations which follow.

The value of 62×10^{-6} obtained for one of the A constants (A_ζ) is unusually large compared to values previously obtained for either the α- or β-processes. A large value for A implies a large volume swept out as a segment jumps and this in turn means a larger segment, a longer jump distance, or both. This does not seem to be in accord with what may be expected for the relatively flexible polypropylene chain. On the other hand the value of 19×10^{-6} (A_α) is in line with previously obtained values of A for the α-process. Since the polypropylene sample was crystalline, large deformations may be expected to involve motion or deformation of crystallites or aggregates of segments. For a process consisting of the deformation of these larger entities a larger value for the constant A would be reasonable. Considering the values obtained for the activation energies, ΔH_α is much less than that observed for the α-process of previously studied polymers, but this could be the result of greater chain flexibility. Furthermore, if one of the observed processes does involve the deformation of crystallites as expected, this might be expected to be the higher energy process.

As a final consideration, it may be noted that dynamic measurements[9] on amorphous polypropylene show a broad, weak peak at 235°K and a much sharper peak at 270°K. These are probably the usual β and α process loss peaks respectively. For crystalline material these loss peaks are shifted to 240°K and 300°K respectively, and a peak corresponding to the crystalline melting point appears at 435°K. Making use of the constants given in *Table 1*, one may calculate the temperature at which the apparent Newtonian (i.e. linear behaviour region) viscosity of each of the processes involved in the yield stress is equal to that due to the α-process of, for example, PEMA when PEMA is at its glass temperature (65°C). If this is done we obtain a calculated temperature of 296°K for the process which is being referred to here as the α-process (of the polypropylene) and a value of 410°K for what is referred to as the ζ-process. These calculated temperatures are in good agreement with the observed temperatures at which the loss maxima occur in the dynamic mechanical measurements and this is taken as an indication that the correct assignment of the processes was made. That is, this calculation indicates that the process referred to as the ζ-process acquires a degree of mobility at T_m comparable to that

attained by the α-process at temperatures near T_g and hence is probably to be associated with T_m.

A similar calculation may be made, with essentially the same result, if the constants for PMMA[1] are used together with a T_g of 105°C for the PMMA. This calculation is similar to that done previously[2] to show that the glass temperature of PEMA could be calculated from the α-process constants. This calculation made use of the α-process constants of both PMMA and PEMA, a knowledge of the T_g of PMMA, and the assumption that the Newtonian viscosity due to the α-process was the same for the two polymers when each was at its glass temperature. This assumption is probably most valid when the polymers being compared are similar in structure.

The author is indebted to Mr W. W. Moore, III, for very capable assistance in the gathering and reduction of data and to Mr L. R. De Fonso for computational assistance.

Rohm and Haas Company,
Research Laboratories,
P.O. Box 219,
Bristol, Pa, U.S.A.

(*Received January 1966*)

REFERENCES

[1] ROETLING, J. A. *Polymer, Lond.* 1965, **6**, 311
[2] ROETLING, J. A. *Polymer, Lond.* 1965, **6**, 615
[3] SAUER, J. A., WALL, R. A., FUSCHILLO, N. and WOODWARD, A. E. *J. appl. Phys.* 1958, **29**, 1385
[4] SAUER, J. A. and WOODWARD, A. E. *Rev. mod. Phys.* 1960, **32**, 88
[5] STAVERMAN, A. J. *Proc. Roy. Soc. A*, 1964, **282**, 115

Electron Microscope Studies of the Fracture of Glassy Polymers

R. J. BIRD*, J. MANN†, G. POGANY† and G. ROONEY*

Electron microscopy of fracture surfaces has shown that polystyrene, styrene–acrylonitrile copolymer and polymethylmethacrylate behave with a good measure of similarity under conditions of fast flexural fracture. The surface detail is considered to be due mainly to plastic deformation and the size of this detail is slightly influenced by both the molecular weight of the polymer and the temperature at which samples are fractured. Polycarbonate, a tougher polymer, surprisingly shows less detail suggestive of plastic deformation.

In polystyrene, regions of different crack growth velocity have been shown to have characteristically different fracture surface appearance. Much of this may be due to differences in the extent of plastic deformation ahead of the propagating crack and the consequent differences in the radius of curvature of the tip of the crack.

ALTHOUGH electron microscopy has been used by other workers to study the fracture surfaces of brittle polymers[1–3], surprisingly little systematic work has been done in this field. The present authors found the technique valuable with rubber modified styrene–acrylonitrile copolymers (ABS polymers)[4] and they have now extended their studies to the pure styrene–acrylonitrile copolymer, polystyrene, polymethylmethacrylate, polycarbonate and, for comparison purposes, soda glass and sucrose sugar glass. The main object of the work was to establish whether fracture surfaces show characteristic surface detail, and to lay the foundation for more systematic work.

The work presented here may be divided into two parts. The first consists mainly of a comparison between the various materials under constant conditions of fast flexural fracture. With polystyrene, however, extra specimens were prepared at a second temperature to assess the temperature dependence of fracture surface detail. The second part of the work was carried out on a tensile specimen of polystyrene with the object of finding the effect of speed of fracture on surface detail, for this one material only.

EXPERIMENTAL

For the fast flexural fracture work specimens, mainly in the form of strips about 1·5 mm thick, were gripped between two pairs of pliers and bent sharply to fracture. For the high and low temperature experiments the pliers were correspondingly heated or chilled to minimize heat transfer.

The speed of fracture is something that cannot be closely defined and controlled in absolute terms. Indeed it is accepted that where slow fracture is attempted, a wide range of crack propagation rates occurs during the formation of a single fracture. We therefore used one specimen only, a

*Thornton Research Centre, Shell Research Ltd. Chester.
†Carrington Plastics Laboratory, Shell Research Ltd, Urmston, Manchester.

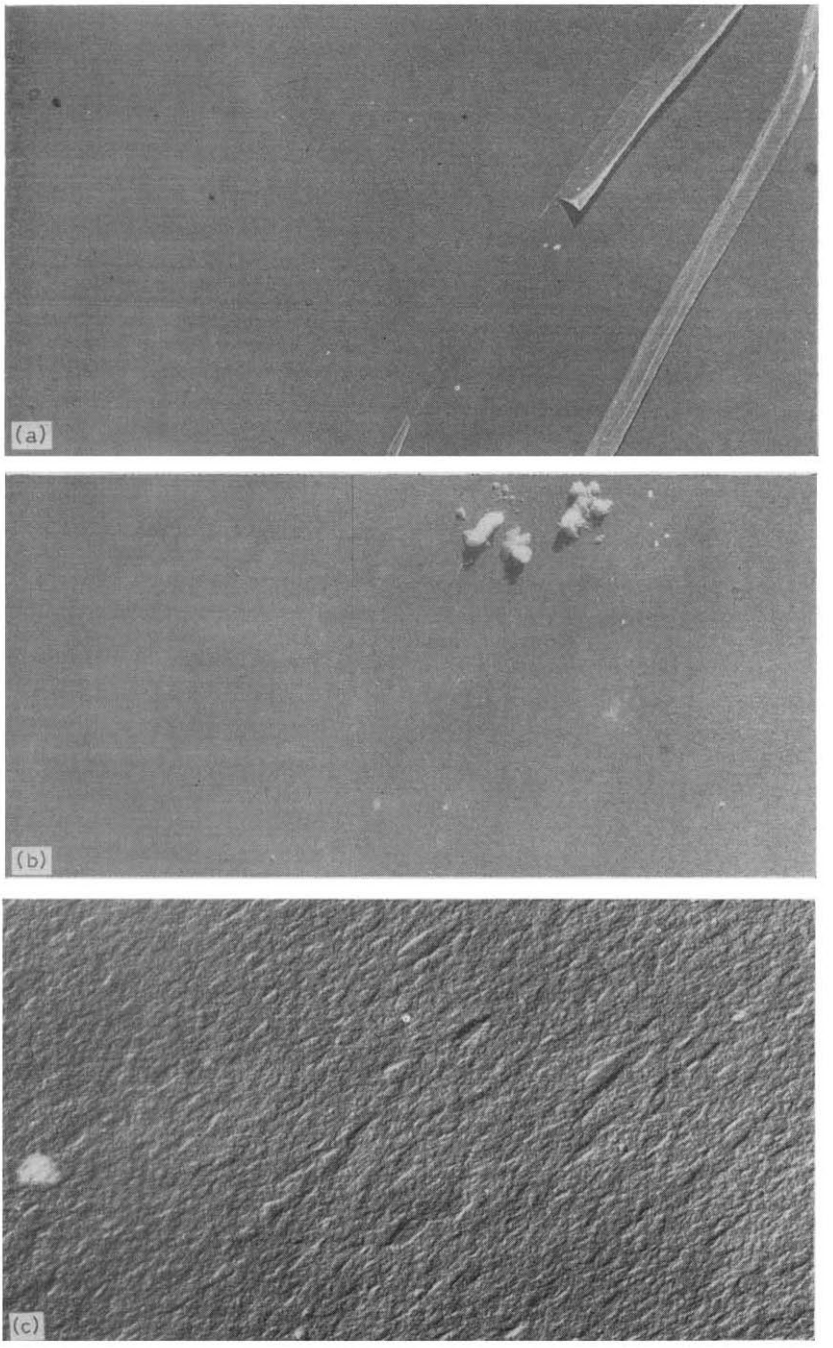

Figure 1—Brittle fractures. Magnification × 25 000; reduced 2/3 on reproduction.
(a) Glass at 300°C; (b) Sucrose; (c) Glass at 20°C

compression moulded strip of polystyrene pulled at an elongation rate of 0·01 min^{-1}, and on the fracture surfaces produced we selected regions of different appearances associated with different rates of crack growth.

The fracture surfaces were replicated by the preshadowed carbon technique due to Bradley. For the shadowing gold–palladium alloy was deposited at a mean angle of about 30°. After this a thicker layer of carbon was deposited at normal incidence. The samples were then immersed in methylethyl ketone to release the replicas by partial dissolution of the plastics. After release the replicas were washed in fresh solvent before collection for examination.

RESULTS AND DISCUSSION

The fracture surfaces of all the organic polymers show considerable amounts of detail compared with those of sucrose and the inorganic glass. Before discussing these results, however, it will be valuable to consider what is giving rise to the detail.

From the work of Berry[5–7] on polymethylmethacrylate and polystyrene we know that fracture produces plastic deformation of a thin layer at the surface generated, even at temperatures well below the glass transition point of the material (i.e. down to −190°C). Thus the structure we see on the fracture surfaces is likely to arise from plastic deformation. In support of this, the fracture surfaces of inorganic glass* and sucrose glass shown in *Figure 1* (a) and (b) are featureless. Of these, inorganic glass is generally held to approximate to ideal brittle fracture, and any plastic deformation is confined to an extremely thin surface layer[13]. Similarly we would not expect sucrose to give plastic deformation, since it behaves as a brittle material in all mechanical tests carried out at normal speeds. The fracture surfaces will, therefore, not give direct evidence of the structure of glassy polymers. They will give information on the plastic deformation which accompanies fracture and this may of course have structural implications.

(I) *Fast fracture in flexure*

(i) *Polystyrene—The effect of temperature on fracture surfaces*—The surfaces of a low molecular weight polystyrene fractured rapidly in flexure at −180°C and 19°C are shown in *Figure 2* (a) and (b). Both surfaces are covered with small hillocks of size 400Å to 800Å and there are occasional ridges of similar substructure. There is a suggestion of slightly larger hillocks at the higher temperature, which is maintained in other micrographs of these surfaces.

We imagine that the structure results from the fracture of a plastically deformed layer of material, which forms ahead of the tip of the fracture crack. This plastic deformation involves orientation of molecules perpendicular to the fracture surface. The structures which we observe are surprisingly rounded, suggesting that relaxation of the oriented material has occurred. The rounding is equally evident on fracture faces produced at −180°C and 20°C and this might suggest that any such relaxation is

*For this comparison the glass was fractured at 300°C so that it would be below its glass temperature by about the same amount as the plastics.

brought about by the heating associated with replica making, when the surface is bombarded with metal and carbon atoms. However, this now seems less likely since in later work (to be published) finer more intricate detail in polystyrene has satisfactorily survived the replica process.

(ii) *Polystyrene—The effect of molecular weight*—Molecular weight has no noticeable influence on the nature of the fracture surface at 19°C as

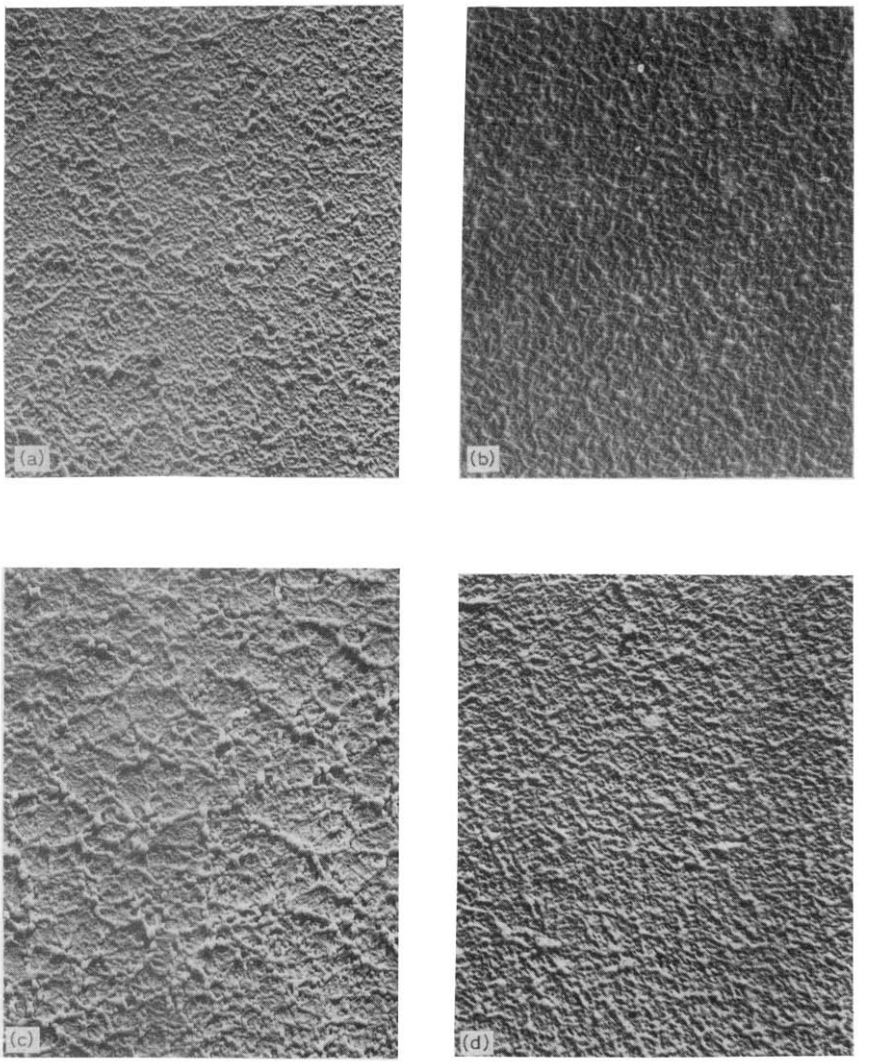

Figure 2—Polystyrene. Effects of molecular weight and temperature. Magnification × 25 000; reduced 6/10 on reproduction. (a) Low molecular weight polystyrene −180°C; (b) Low molecular weight polystyrene 19°C; (c) High molecular weight polystyrene −180°C; (d) High molecular weight polystyrene 20°C

can be seen by comparing *Figure 2* (b) and (d). At −180°C, however, there is slight evidence of increased hillock size for the high molecular weight material [compare *2* (a) and *2* (c)].

(iii) *Styrene–acrylonitrile copolymer*—Two samples of low and high molecular weight respectively were fractured at −180°C. These showed the same type of surface as polystyrene and again there was slight evidence of high molecular weight giving rise to larger hillocks [*Figure 3* (a) and (b)].

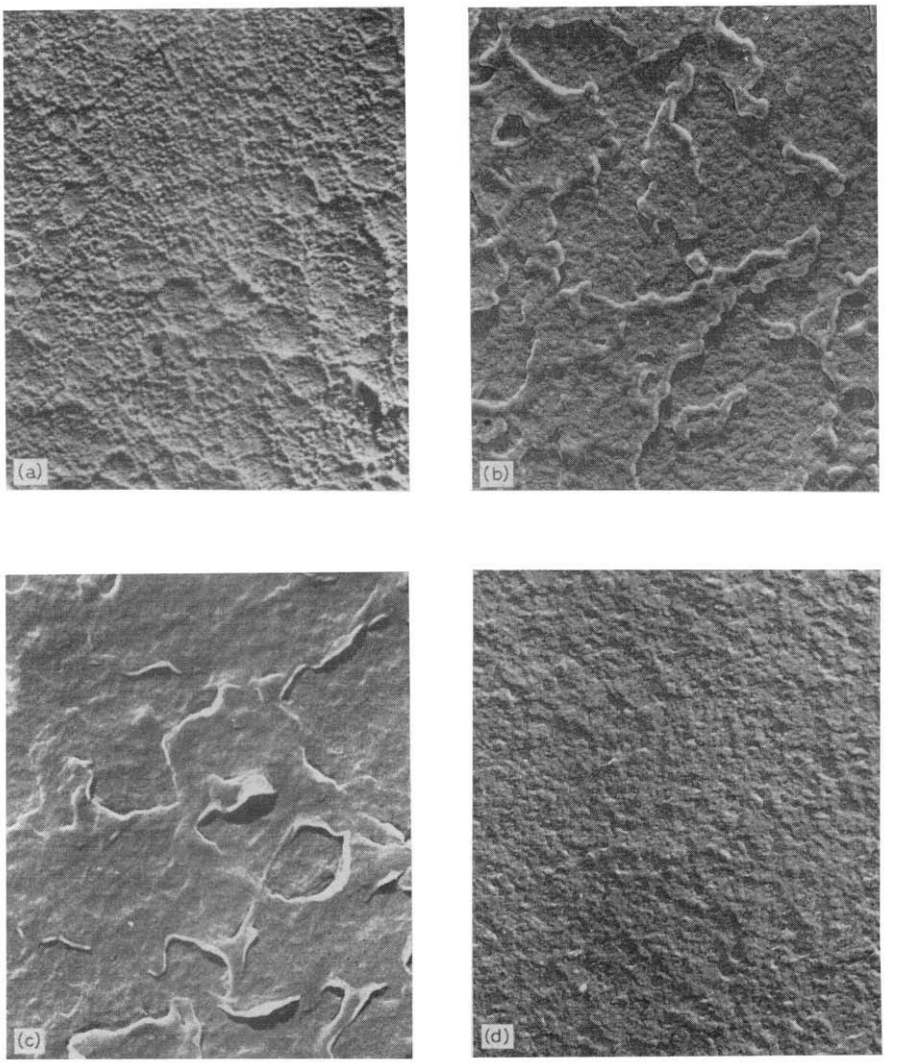

Figure 3—Styrene–acrylonitrile (ACN) and polycarbonate at −180°C. Magnification× 25 000; reduced 6/10 on reproduction. (a) Low molecular weight styrene–ACN copolymer; (b) High molecular weight styrene–ACN copolymer; (c) Polycarbonate; (d) Polycarbonate

(iv) *Polymethylmethacrylate*—Fractured at low temperature this material also largely resembled polystyrene though there were some areas of fracture surface where the fine detail was noticeably smoother (not illustrated).

(v) *Polycarbonate*—Since polycarbonate is a tough polymer and becomes brittle only below $-135°C$ we might expect that fracture surfaces of this polymer would show more pronounced indications of plastic deformation. This is not so, however, and much of the fracture surface has comparatively little fine detail as in *Figure 3* (c), though other parts do show detail more like that of polystyrene [*Figure 3* (d)].

(II) *The effect of speed of fracture in polystyrene*

The fracture surface of the specimen used for this work is shown diagrammatically in *Figure 4*. This appearance indicates that the fracture

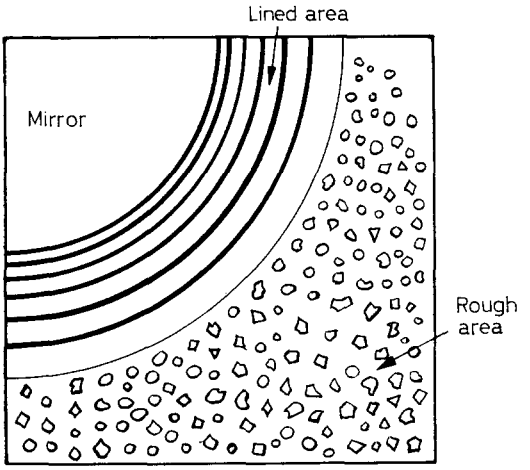

Figure 4—Diagrammatic representation of fracture surface of polystyrene

started at the corner contained by the mirror area. There is universal agreement that the rough area corresponds to a region of fast crack growth[8, 9]. The lined area, according to the studies of Schardin[10], corresponds to a region where the crack is accelerating. For the mirror area, all our observations agree with Sauer[1] in suggesting that the flat mirror area is a region of slow crack growth . This appears to be at variance with Berry's conclusions on polymethylmethacrylate that the flat mirror area is a region of fast crack growth. However, there may well be some confusion with terms since crack speeds cannot be quoted quantitatively, and there is a further difficulty in distinguishing crack growth from the growth of a craze[11]. A craze may form slowly, and subsequently the crack may progress through the affected region more rapidly.

Other work we have done shows that flat mirror surfaces are associated with fracture of crazed material, and we would suggest that this appearance

is not diagnostic of slow crack growth. We suspect it results from the fracture of crazed material or fracture where orientation of the material occurs well ahead of the crack tip.

One real difference exists between Berry's observations on polymethylmethacrylate and our own on polystyrene. Berry observed a deeply furrowed region before the mirror region, which we have never observed with polystyrene. It may be that in the latter material, this region is too small for easy observation.

Since we cannot define absolutely the speeds of crack growth occurring in our experiments, we shall discuss results in terms of the three areas of distinctive appearance to the unaided eye, and we postulate that in this experiment at least, these surfaces in order of increasing speed of crack growth are:

'mirror', 'lined', 'rough'.

(i) *Mirror area*—Representative micrographs of this region are shown in *Figures 5* and *6*. The most characteristic features are the grained appearance

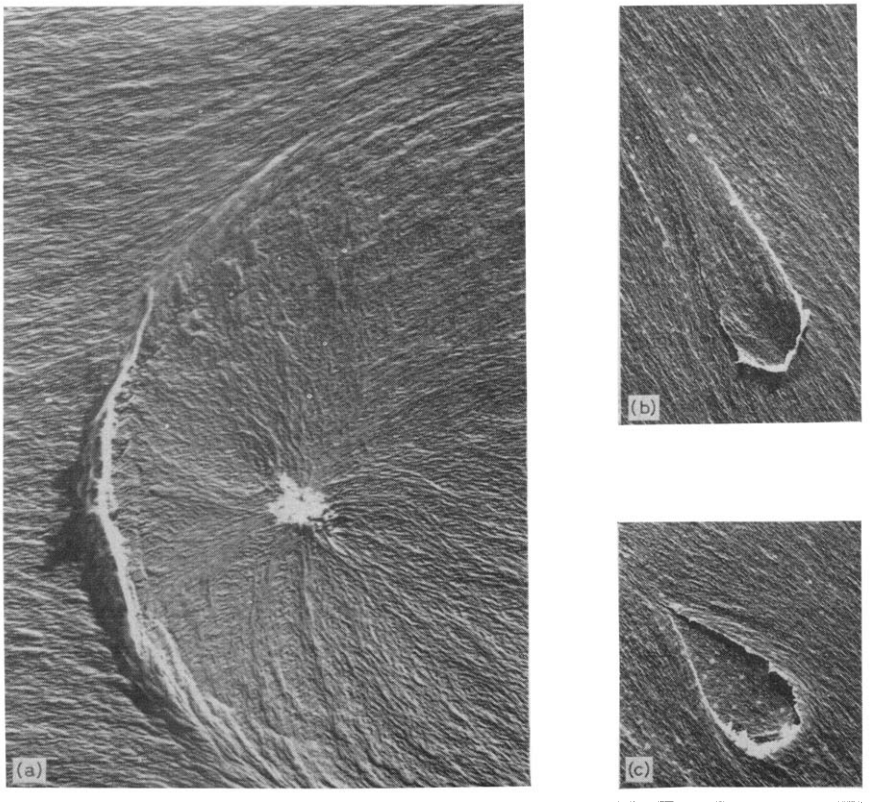

Figure 5—Polystyrene. Mirror area of fracture face. Magnifications (a)×25 000, (b) ×3 750, (c) ×3 750; all reduced 6/10 on reproduction

and the secondary fracture features. These latter are well known. Their outlines are formed by the meeting of the main crack front and those of the subsidiary cracks formed ahead of it. Frequently these outlines are parabolas resulting from the meeting of a straight main crack front and a circular secondary front travelling at about the same speed[12]. Many of the secondary fracture features we observe are not parabolas but closed pear-shaped figures. These must result from the main crack front travelling faster than the secondary fracture and overtaking it.

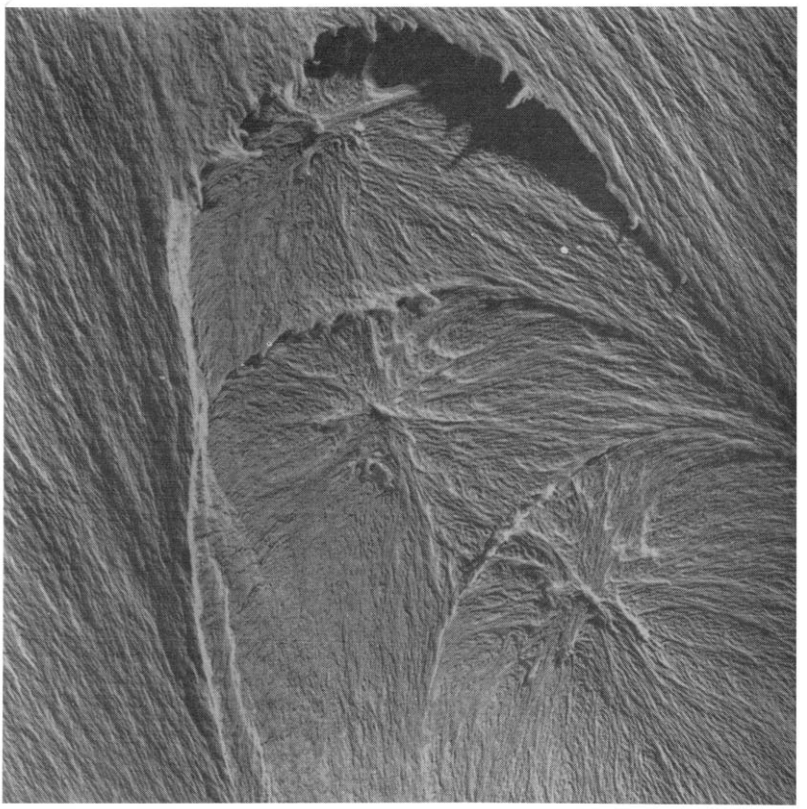

Figure 6—Polystyrene. Mirror area of fracture face. Magnification×25 000; reduced 6/10 on reproduction

The secondary fractures allow us to identify the direction of propagation of the main crack front. In *Figure 6* for example the main crack propagated from the upper left of the plate towards the lower right, while in *Figure 5* (b) it was in the reverse direction. The grain on the surface always lies along the direction of travel of the crack. It often changes direction close to secondary fractures, showing the influence of the latter on main crack propagation.

Plastic deformation is known to accompany fracture[5, 6], but apart from

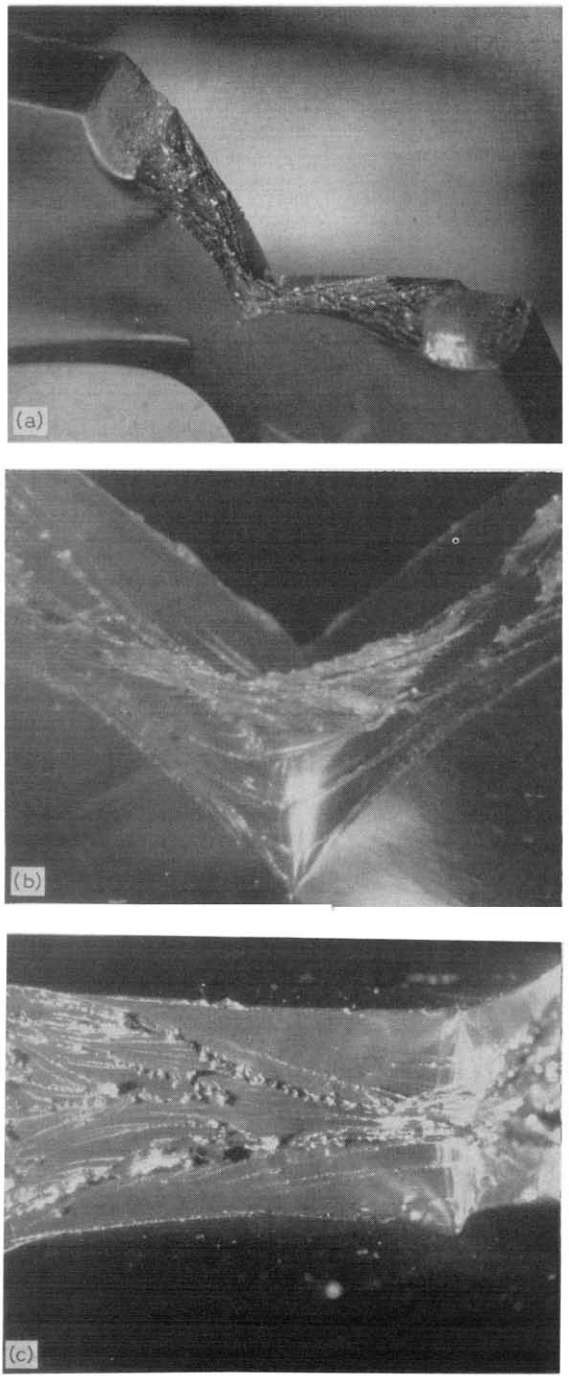

Figure 7—Polymethylmethacrylate fractured at elevated temperature. (a) General view. Magnification × 5·5; (b) Crack tip. Magnification × 25; (c) View of one face. Magnification × 16·8; all reduced 2/3 on reproduction

the edges of secondary fractures, and perhaps their points of initiation, there is little obvious sign of it on the fracture surfaces. The main feature of the fracture surfaces is the grain, however, and we must consider whether this could be formed by plastic deformation.

For brittle fracture the two fracture faces will be exact negative counterparts of one another. On one fracture face, therefore, we would expect to see roughly equal numbers of raised and sunken features of a given size. A grain which is clearly of this type is shown in *Figure 1* (c) for soda glass. When we turn to the grain on polystyrene, as on the left hand side of *Figure 6* for example, it is less easy to visualize the opposite fracture face being a negative counterpart. The raised and sunken features do not appear to be statistically equal in number and in size. This suggests that the grain is produced by plastic deformation accompanying fracture.

We have, with polymethylmethacrylate, obtained some evidence to support the view that the grain is a result of plastic deformation. A specimen of this material was heated above its glass transition temperature. It was then rapidly withdrawn from the oven and fractured in a room temperature environment. The conditions in this experiment should be similar to those in the fracture of polystyrene in that the material is capable, during fracture, of undergoing extension which will then be frozen in. The appearance of the resulting fracture surface is shown in *Figure 7*. It has much in common with the polystyrene results except that the grain is on a larger scale. The ridges on one fracture face correspond with ridges on the other. The drawing of material in the crack tip is shown at (b) and the rather ragged ridges (cooling was too rapid to allow relaxation) are best seen in (c). The progressive restriction of ridge formation to the middle part of the fracture face is also thought to be due to cooling of the specimen during fracture.

The precise mechanism by which the grain is formed in polystyrene is not clear, but we offer the following hypothesis based on the Griffiths ideas on cracking. We assume that, due to plastic deformation, the tip of the crack has a finite radius. We further assume that the material is not homogeneous on the microscopic scale, and that in some places the crack advances

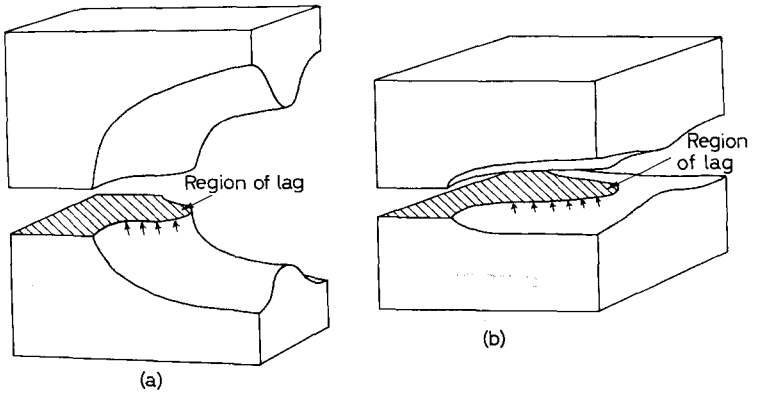

Figure 8—Suggested forms of crack tip. (a) Slow crack generating grained surface. (b) Fast crack generating stippled surface

slightly ahead of the mean crack front and in other places, regions of greater strength, it lags a little [see *Figure 8* (a)]. Places where lagging occurs will be flanked by newly generated surfaces which, because they have not yet relaxed to the horizontal, will still constitute part of the apex of the crack. The force on the lagging regions may, therefore, be thought of as being directed upwards and forwards with respect to the new surface. As the crack progresses regions of lead and lag will move about, and it is not difficult to imagine plastic deformation, in response to such stresses, giving rise to the system of short ridges all of one orientation, i.e. the grain. If the leading parts of a crack break through into a secondary crack, we might expect the lagging regions to give rise to drawn necks or fibrils: there is some evidence of this in *Figure 6*, for instance.

This type of reasoning can also be used to explain the change in surface appearance which is found as the crack speed increases. At slower speeds extensive plastic deformation occurs ahead of the tip of the crack, and this generates a crack tip radius which is larger than the inhomogeneities giving rise to the regions of lag and lead. When a fast crack develops,

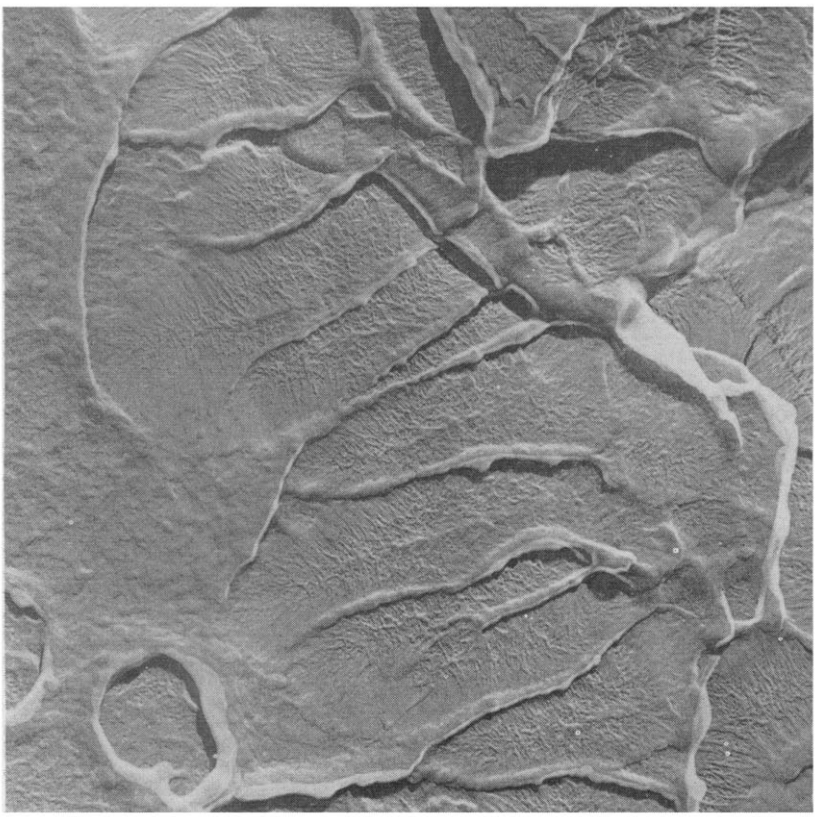

Figure 9—Polystyrene. Domains in lined area of fracture face. Magnification × 25 000; reduced 6/10 on reproduction

however, the plastic deformation ahead of the crack is much smaller, as is the radius of curvature of the crack tip. With a sufficiently small radius of curvature, the newly generated surfaces flanking the lagging parts of the crack front will be essentially horizontal, as in *Figure 8* (b). The stress on the lagging parts will then be normal to the adjacent surface, and we would no longer expect ridges to be pulled along the surface. Instead, we might well expect plastic deformation to take the form shown, for instance, in *Figure 2*.

(ii) *Rough area*—It is easier next to consider the rough area, the region of greatest crack speed. Its matt appearance, to the unaided eye, is caused by surface roughness on a scale upwards of a few microns. Nevertheless at electron microscope magnifications individual areas in this region are found to be relatively smooth as in *Figure 2* (c). They show merely a fine texture such as is seen on surfaces produced by fast flexural fracture as discussed in section I (i). This fine texture appears, therefore, to be characteristic of fast fracture over a wide range of temperature.

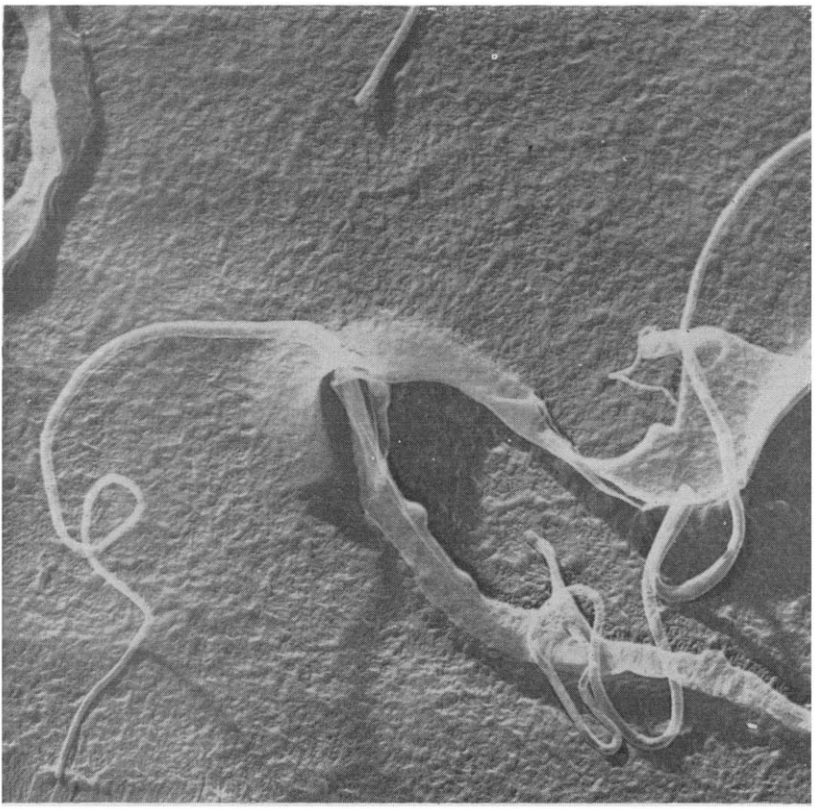

Figure 10—Polystyrene. Fibrils in lined area of fracture face. Magnification × 25 000; reduced 6/10 on reproduction

(iii) *Lined area*—Results on the lined area are less easy to interpret. This region exhibited a wide variety of surface texture due perhaps to local variations in crack speed and direction. Much of the surface had the fine texture invariably found in the 'rough' area. This suggests that for the most part crack speed in the lined area was also high. In many places, however, the surface had a more directional texture. This occurred in domains, as shown in *Figure 9*, but these were very variable both in size and the direction of the texture. These domains may perhaps have resulted from secondary fractures which, from our earlier discussions of surface texture, we would say propagated relatively slowly. Unfortunately, it was not possible to relate the microscopic detail to the lines and the areas between the lines as seen with the unaided eye.

Occasionally in the lined area long fibrils were found such as those shown in *Figure 10*. If these form by simple drawing of the material their lengths would suggest considerable local heating. However, consideration of several micrographs which show this type of feature suggests that the fibrils are in fact rolled up thin sheets or ribbons. These are probably formed where the main crack overtakes a secondary crack not quite in its own plane. This could happen in a purely brittle material such as glass, as suggested in *Figure 1* (a). It seems more likely, however, that with polystyrene they arise from plastic deformation of the thin sheet of material remaining between two such cracks.

Shell Research Ltd

(Received January 1966)

REFERENCES

[1] HSIAO, C. C. and SAUER, J. A. *J. appl. Phys.* 1950, **21,** 1071
[2] NEWMAN, S. B. and WALOCH, I. *Adhesion and Cohesion*, p 218. Editor WEISS, P. Elsevier: Amsterdam, 1962
[3] NEWMAN, S. B. *Polym. Engng Sci.* 1965, **5,** 159
[4] BIRD, R. J., ROONEY, G. and MANN, J. *Makromol. Chem.* 1966, **90,** 207
[5] BERRY, J. P. *J. Polym. Sci.* 1961, **50,** 107
[6] BERRY, J. P. *J. Polym. Sci.* 1961, **50,** 313
[7] BERRY, J. P. *J. Polym. Sci.* 1963, **1A,** 993
[8] WALOCH, I., KIES, J. A. and NEWMAN, S. B. 'Fracture phenomena in polymers', in *Fracture*, p 250. By B. L. AVERBACH, D. K. FELMAN, G. T. HAHN and D. A. THOMAS. Wiley: New York, 1959
[9] BERRY, J. P. *Nature, Lond.* 1960, **185,** 91
[10] SCHARDIN, H. 'Velocity effects in fracture', in *Fracture*, p 297. By B. L. AVERBACH. D. K. FELMAN, G. T. HAHN and D. A. THOMAS. Wiley: New York, 1959
[11] SPURR, O. K. and NIEGISCH, W. D. M. *J. appl. Polym. Sci.* 1962, **6,** 585
[12] SCHWARZL, F. and STAVERMAN, A. J. *Die Physik der Hochpolymeren*, Vol. IV, p 205. Springer: Berlin, 1956
[13] MARSH, D. M. *Proc. Roy. Soc. A*, 1964, **282,** 33

Thermal Degradation of Piperazine Polyamides III—The Effect of Ultra-violet Irradiation on Poly(isophthaloyl trans-*2,5-dimethylpiperazine)*

S. D. BRUCK*

The thermal degradation of ultra-violet irradiated films of poly(isophthaloyl trans-*2,5-dimethylpiperazine) was studied in terms of changes in the molecular weight, absorption spectra, rates and activation energies. Ultra-violet irradiation causes progressive yellowing of the samples and a rapid drop in their intrinsic viscosity from 2·91 to 1·25 during the initial ten hours; this is followed by a levelling-off in further degradation and increasing gelation. Films of the polymer which had been irradiated for 42·5 hours in a vacuum ($[\eta]$ of the sol fraction $\simeq$ 1·0) showed increased thermal stability, as evidenced by the reduction in the rates of degradation, and an increase in the activation energy from 53 kcal/mole to 78 kcal/mole, in comparison to* un-*irradiated control samples. The increased thermal stability of the irradiated system is attributed to the effect of crosslinks.*

IN previous publications[1, 2] the thermal degradation of a series of piperazine polyamides was discussed in terms of rates, activation energies and degradation products. It was shown that these polymers, in contrast to aliphatic polyamides, exhibit good thermal stability up to 400° to 450°C in a vacuum. Recent technological activities, especially in the aero-space area, created new demands for non-metallic materials which may be useful in a *combined* environment of heat and radiation. However, to understand properly the overall degradation process, it is desirable first to study each environmental effect separately. The behaviour of piperazine polyamides under both programmed temperature and isothermal conditions was previously reported[1, 2]. This paper deals with the thermal degradation of film samples of poly(isophthaloyl *trans*-2,5-dimethylpiperazine) that has been irradiated prior to pyrolysis by ultra-violet radiation in a vacuum.

EXPERIMENTAL DETAILS

Materials

Poly(isophthaloyl *trans*-2,5-dimethylpiperazine) was prepared by the low temperature solution condensation method described by Morgan and Kwolek[3], with excess diamine as the acceptor. The number-average molecular weight of this polymer was approximately 37 000 as determined from end-group/viscosity data, osmotic measurements, and by thermoelectric differential vapour pressure lowering[4]. Transparent films were cast from a 6·5 weight per cent solution of the polymer in chloroform with a micrometer-equipped 'doctor-knife'[5]. The thickness of the film samples was in the range of 0·001 to 0·0015 inch.

*Present address: Thomas J. Watson Research Center, IBM Corpn, P.O. Box 218, Yorktown Heights, New York 10598, U.S.A.

Viscosity measurements

The inherent viscosity [$\ln \eta_{rel}/c$), where $c = 0{\cdot}5$ g/100 ml] was determined in *m*-cresol at 30°C ± 0·05 with Cannon–Fenske viscometers. Intrinsic viscosity measurements ($[\eta] = \lim_{c \to 0} \eta_{inh}$) were made in a 40:60 mixture by weight of sym-tetrachlorethane–phenol at 30°C ± 0·05° with Cannon–Ubbelohde semimicro dilution viscometers. In the case of those irradiated samples which contained gel particles, the polymer solution was filtered through a medium porosity sintered glass filter by the application of a slight vacuum, the gel particles washed with a predetermined volume of the solvent, and the washings combined with the polymer solution. Because of the possibility that some of the sol-fraction might have been retained by the gel, the intrinsic viscosity of the sol fractions may be accurate only within ± 10 per cent. The percentage gel content was determined by weight after extraction with ethyl alcohol, followed by drying at 100°C for three hours in a vacuum oven.

End-group analyses

The carboxyl end-groups were determined by dissolving the polymer in a 90:10 mixture (by volume) of benzyl alcohol–methyl alcohol and titrating it with a 0·1 N methyl alcohol solution of potassium hydroxide using phenolphthalein as indicator. The amine end-groups were determined conductometrically in a 90:10 mixture (by volume) of benzyl alcohol–methyl alcohol with a 0·01 N aqueous solution of hydrochloric acid.

Ultra-violet irradiation

Film samples (0·001 to 0·0015 inch thick) of poly(isophthaloyl *trans*-2,5-dimethylpiperazine) were irradiated in a quartz cell under a vacuum of $\sim 10^{-5}$ mm of mercury by the unfiltered radiation of a Hanovia Type A-10 high pressure mercury lamp. Approximately 46 per cent of the total radiant energy of this lamp is emitted between 2 224 and 3 660 Å. The intensity of the radiation at the sample's position was 31 000 μwatt/cm^2 ± 10 per cent as measured by an Eppley thermopile.

Thermogravimetry

Thermogravimetric analyses were carried out in a vacuum ($\sim 10^{-5}$ mm of mercury) with 1 to 2 mg samples using a Cahn RG electrobalance by a method described in detail in previous publications[6–9].

Spectroscopy

Absorption curves in the ultra-violet and visible regions of the spectrum were obtained directly on the dry film samples with a Beckman DK-2A spectrophotometer. The attenuated total reflectance spectra (ATR) in the infra-red region were determined with a Beckman IR-7 spectrophotometer equipped with a Barnes Model 3 ATR unit.

RESULTS AND DISCUSSION

Poly(isophthaloyl *trans*-2,5-dimethylpiperazine) is prepared in chloroform according to the following reaction[3]

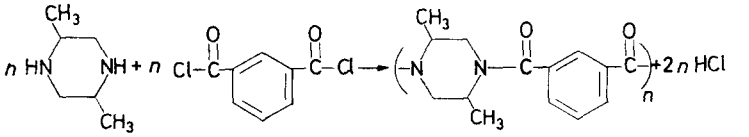

The polymer is soluble in various solvents including chloroform, formic acid, and a 90:10 mixture (by volume) of benzyl alcohol–methyl alcohol. This solubility behaviour was partly the reason for this piperazine polyamide being selected for the present studies over the other members of the series[1, 2]. The molecular weight of the polymer can be controlled by changing the diamine/diacid ratio[3]. With equimolar quantities of ingredients, a polymer with an intrinsic viscosity of 2·91 was prepared, whereas by changing the ratio of the diamine/diacid to 2·5, a polymer with an intrinsic viscosity of 1·05 was obtained. The relationship between intrinsic viscosities (measured in a 40:60 mixture by weight of sym-tetrachlorethane–phenol at 30°C ± 0·05°) and the inherent viscosities (measured in *m*-cresol at 30°C ± 0·05°) is illustrated in *Figure 1*.

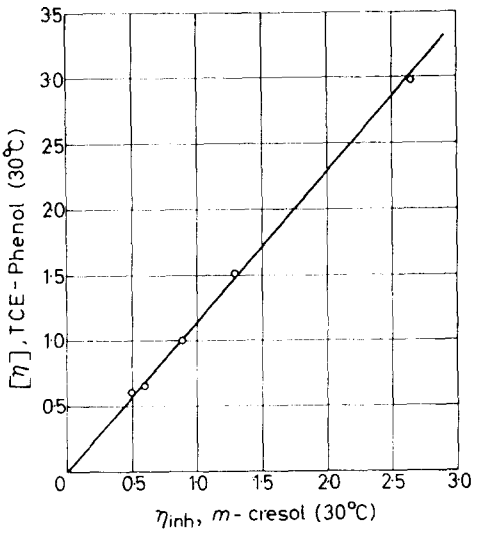

Figure 1—Relationship between intrinsic viscosity in sym-tetrachlorethane:phenol (40:60 wt %) and inherent viscosity in *m*-cresol of poly(isophthaloyl *trans*-2,5-dimethylpiperazine)

The number-average molecular weights of the *un*-irradiated polymer samples were determined by end-group analyses. The number-average molecular weight of the control sample having an intrinsic viscosity of 2·91 was also determined osmometrically (in chloroform) and by thermoelectric differential vapour pressure lowering (in 90 per cent formic acid). The agreement between end-group analyses, osmotic measurements and thermoelectric differential vapour pressure lowering was reasonably good, as seen from the following results: $\overline{M}_n$ (end-group analyses) = 36 700, $\overline{M}_n$ (osmotic pressure) = 38 000, and $\overline{M}_n$ (vapour pressure lowering) = 32 500. In contrast to the successful use of thermoelectric differential vapour pressure lowering[4]

in 90 per cent formic acid with Nylon 6 and poly(terephthaloyl *trans*-2,5-dimethylpiperazine), the lower molecular weight samples of poly(isophthaloyl *trans*-2,5-dimethylpiperazine) gave results which were considerably below those obtained from end-group analyses and expected from viscosity data. The substitution of chloroform for 90 per cent formic acid as solvent in the vapour pressure measurements did not change the situation to any significant extent. The problem is likely due to the formation of an excessively large fraction of low molecular weight material which apparently becomes entrapped in the precipitated polymer. Similar discrepancies were also reported by others[10] in the osmotic determination of the number-average molecular weights of 6–10 polyamides prepared by interfacial polycondensation.

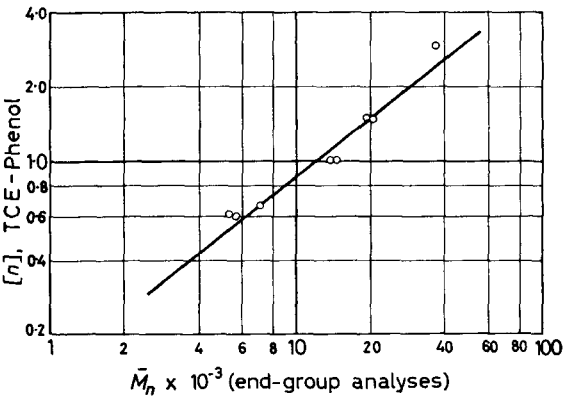

Figure 2—Relationship between intrinsic viscosity in sym-tetrachlorethane : phenol (40 : 60 wt %) and number-average molecular weight (end-group analysis) of poly(isophthaloyl *trans*-2,5-dimethylpiperazine)

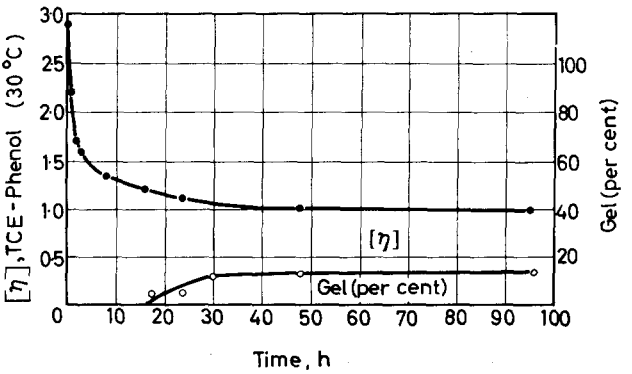

Figure 3—Degradation of poly(isophthaloyl *trans*-2,5-dimethylpiperazine) under ultra-violet irradiation

The relationshi$_\nu$ between intrinsic viscosities and the number-average molecular weights determined by end-group analyses for the *un*-irradiated samples of poly(isophthaloyl *trans*-2,5-dimethylpiperazine) is illustrated by *Figure 2*. The line yields an equation, $[\eta] = 5{\cdot}99 \times 10^{-4} (\overline{M}_n)^{0{\cdot}79}$.

To study the degradation of the polymer under ultra-violet irradiation, film samples were irradiated for various times in a vacuum by the unfiltered radiation of a Hanovia Type A-10 high pressure mercury lamp, with a total intensity of 31 000 μwatt/cm^2. The intrinsic viscosity of the samples after irradiation was determined in a 40:60 mixture by weight of sym-tetrachlorethane–phenol, but the samples which contained gel particles were first treated as described in the Experimental section. *Figure 3* illustrates the degradation of the polymer in terms of decreasing viscosities and increasing gelation. There is a large drop in the intrinsic viscosity of the polymer during the first 10 to 15 hours of irradiation, followed by a levelling-off. Gelation was observed only in those samples that had been irradiated for approximately 15 hours and the total amount of gel did not increase significantly beyond 48 hours of irradiation.

The ultra-violet and visible spectra of the film samples show progressively decreasing transmission between 290 and 600 mμ with increasing times of irradiation, as seen in *Figure 4*. The progressive decrease in percentage transmission was also evidenced by the yellowing of the samples. The attenuated total reflectance spectra (ATR) between 2·5 and 16 microns of the *un*-irradiated and irradiated samples showed no significant differences (*Figure 5* curves A and B).

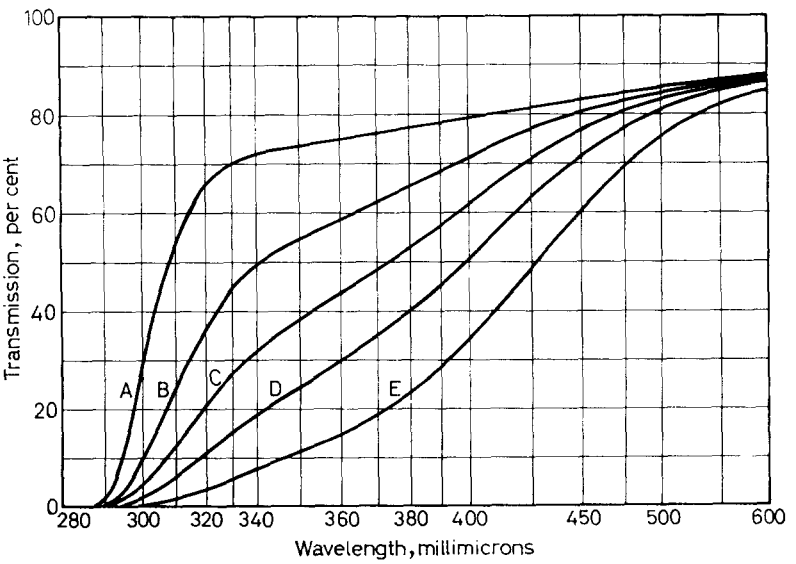

Figure 4—Change in per cent transmission in the ultra-violet and visible regions of the spectrum of poly(isophthaloyl *trans*-2,5-dimethylpiperazine) as a function of time of ultra-violet irradiation; A denotes zero time, B 2 h, C 6 h, D 12 h and E 30 h of irradiation

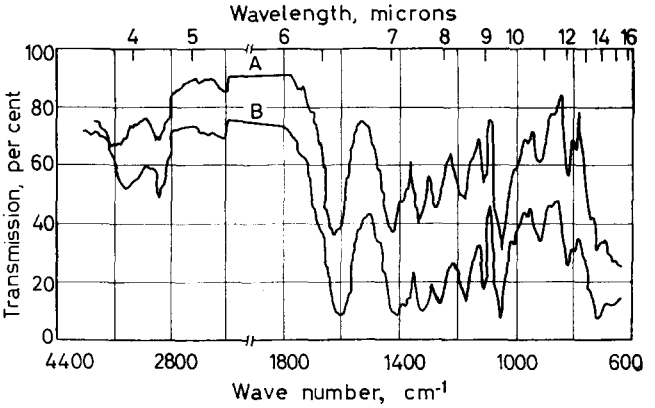

Figure 5—Attenuated total reflectance (ATR) spectra of A, *un*-irradiated and B, ultra-violet irradiated poly(isophthaloyl *trans*-2,5-dimethylpiperazine) in a vacuum for 42·5 h

To evaluate properly the effect of ultra-violet radiation on the mechanism of thermal degradation, experiments were carried out not only with the irradiated polymer but also with two *un*-irradiated samples having intrinsic viscosities of 2·91 and 1·05, respectively. Because of the drop in the intrinsic viscosity of the polymer from 2·91 to approximately 1·0 (sol fraction) after 42·5 hours of irradiation, the *un*-irradiated control sample having the lower viscosity served to screen out possible effects which may be attributable to a decrease in the molecular weight alone.

Thermogravimetric studies were carried out under isothermal conditions in a vacuum ($\sim 10^{-5}$ mm of mercury) between 440° and 380°C. *Figures 6*

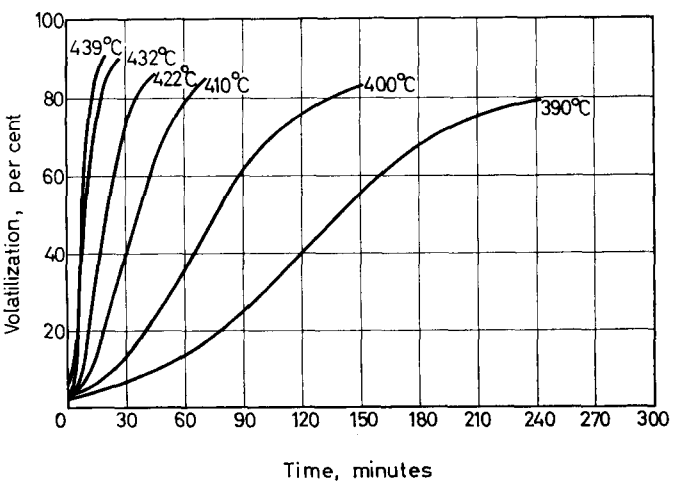

Figure 6—Thermal degradation of *un*-irradiated poly(isophthaloyl *trans*-2,5-dimethylpiperazine) in a vacuum (initial $[\eta]=2{\cdot}91$)

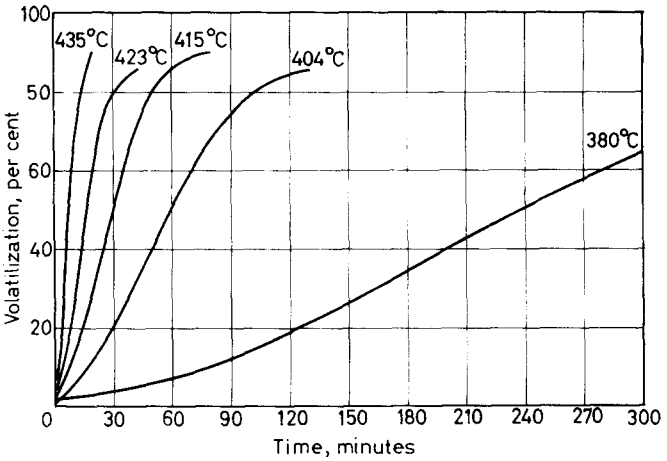

Figure 7—Thermal degradation of *un*-irradiated poly(isophthaloyl *trans*-2,5 dimethylpiperazine) in a vacuum (initial $[\eta]=1{\cdot}05$)

and *7* show the percentage volatilization as a function of time at various temperatures for the *un*-irradiated control samples of poly(isophthaloyl *trans*-2,5-dimethylpiperazine) having intrinsic viscosities of 2·91 and 1·05, respectively. Zero time denotes the start of the isothermal heating period which was usually reached within 15 to 20 minutes from the time the preheated furnace was positioned around the sample tube. The data indicate no appreciable difference in the behaviour of the two samples. The corresponding rates of degradation are illustrated by *Figures 8* and *9*. These rate

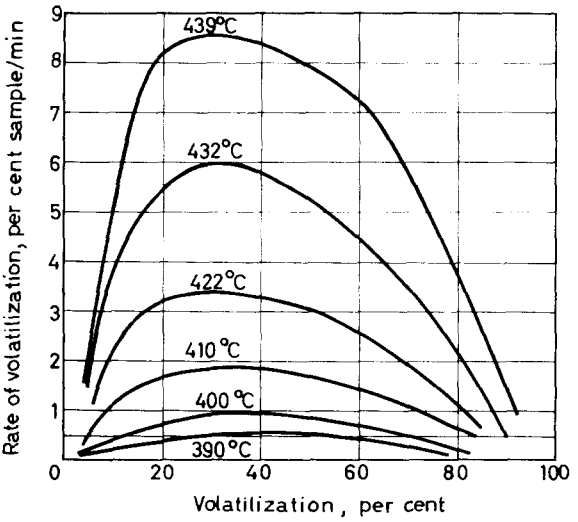

Figure 8—Rates of thermal degradation of *un*-irradiated poly(isophthaloyl *trans*-2,5-dimethylpiperazine) in a vacuum (initial $[\eta]=2{\cdot}91$)

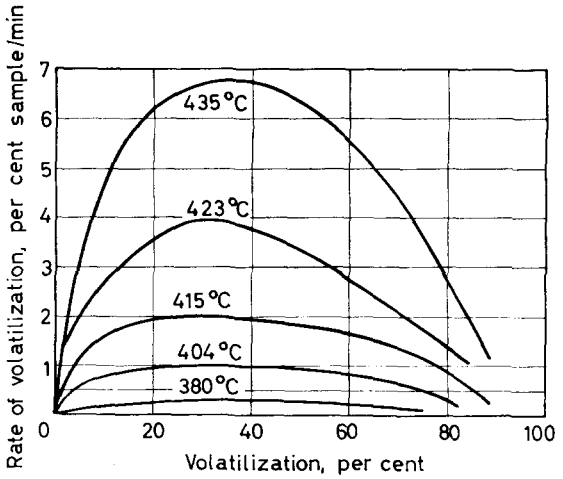

Figure 9—Rates of thermal degradation of *un*-irradiated poly(isophthaloyl *trans*-2,5-dimethylpiperazine) in a vacuum (initial $[\eta]=1{\cdot}05$)

curves were calculated (with an electronic computer) from the slopes of the volatilization versus time curves and are characterized by distinct maxima between 30 per cent and 40 per cent conversions. Here again, there is no significant difference in the rate curves between the two control samples.

Thermal degradation studies were carried out with a sample of poly(isophthaloyl *trans*-2,5-dimethylpiperazine) that had been irradiated for 42·5 hours with a total intensity of 31 000 μwatt/cm^2 by the unfiltered radiation of a Hanovia Type-A high pressure mercury lamp. The intrinsic viscosity of this sample prior to irradiation was 2·91, whereas that of the sol fraction after irradiation was approximately 1·0. The gel was not removed from the sample prior to the thermal degradation studies. These experiments were carried out under conditions similar to those employed for the two control samples.

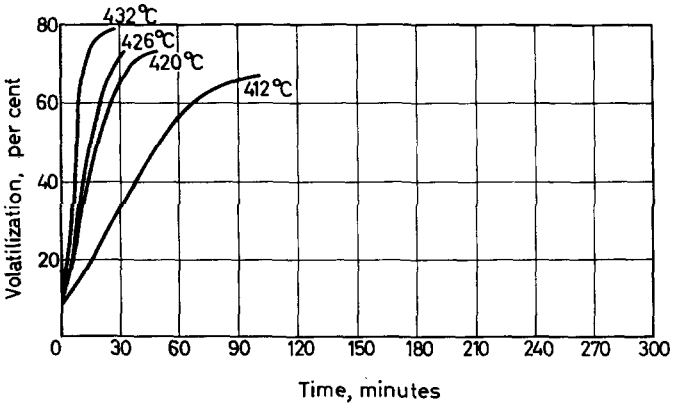

Figure 10—Thermal degradation of ultra-violet irradiated poly-(isophthaloyl *trans*-2,5-dimethylpiperazine) in a vacuum ([η] of sol fraction≃1·00)

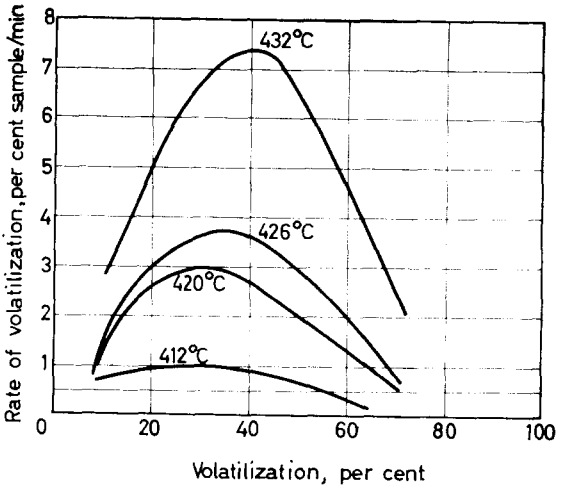

Figure 11—Rates of thermal degradation of ultraviolet irradiated poly(isophthaloyl *trans*-2,5-dimethylpiperazine) in a vacuum ([η] of sol fraction $\simeq$1·00)

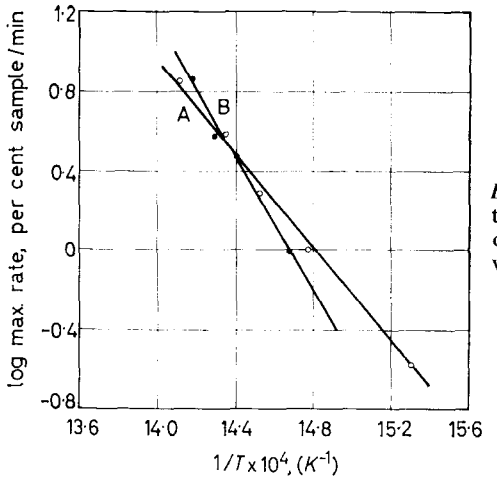

Figure 12—Arrhenius plots for the thermal degradation in vacuum of A *un*-irradiated and B ultraviolet irradiated poly(isophthaloyl *trans*-2,5-dimethylpiperazine)

Figure 10 shows the percentage volatilization as a function of time between 435° and 404°C. The corresponding rates of degradation are illustrated by *Figure 11*. Although the maxima in the rate curves occur between 30 per cent to 40 per cent conversion, the rates of degradation show a much greater decrease beyond the maxima, in comparison to the *un*-irradiated control samples. Apparently, the irradiated sample becomes stabilized due to the effect of crosslinks, which are produced by the irradiation. In the irradiated sample, thermal degradation experiments conducted at 380°C showed an abnormal pattern (not illustrated), suggesting that at the lower temperature competing reactions may predominate. Further work

must be carried out to explore the nature of this behaviour at lower temperatures.

Figure 12 shows Arrhenius plots which were constructed from the maximum rates of degradation of the irradiated polymer and one of the control samples ($[\eta]=1{\cdot}05$). A similar plot for the other control sample ($[\eta]=2{\cdot}91$) is not shown in *Figure 12* because the slope of the line was identical[2]. The activation energy of both control samples is 53 kcal/mole, whereas that of the irradiated sample is 78 kcal/mole. This large increase in the activation energy in the irradiated sample is most likely due to the formation of intermolecular C—C crosslinks, which stabilize the system.

In summary, poly(isophthaloyl *trans*-2,5-dimethylpiperazine) shows rapid degradation during the initial ten hours of ultra-violet irradiation from an intrinsic viscosity of 2·91 to approximately 1·25, followed by a sharp levelling-off, due to the stabilizing effect of crosslinking which competes with chain scission. The irradiated polymer shows increased thermal stability and a much higher activation energy than the *un*-irradiated control samples. These are attributed to the stabilizing effect of intermolecular crosslinks which are formed during the ultra-violet irradiation.

This work was supported by the Bureau of Naval Weapons, Department of the U.S. Navy, under Contract NOw 62-0604-c.

The author thanks Mr S. J. Burdick and Mr H. E. Bair for technical assistance in some phases of this work, and Mr Stanley Favin for the computer programming of the kinetic data.

Applied Physics Laboratory,
The Johns Hopkins University,
8621 Georgia Avenue,
Silver Spring, Maryland, U.S.A.

(*Received February 1966*)

REFERENCES

[1] BRUCK, S. D. *Polymer, Lond.* 1965, **6**, 483
[2] BRUCK, S. D. *Polymer, Lond.* 1966, **7**, 231
[3] MORGAN, P. W. and KWOLEK, S. L. *J. Polym. Sci.* 1964, **A2**, 181
[4] BRUCK, S. D. and BAIR, H. E. *Polymer, Lond.* 1965, **6**, 447
[5] SORENSON, W. R. and CAMPBELL, T. W. *Preparative Methods of Polymer Chemistry*, p 27. Interscience: New York, 1961
[6] BRUCK, S. D. *Polymer, Lond.* 1964, **5**, 435
[7] BRUCK, S. D. *Polymer, Lond.* 1965, **6**, 49
[8] BRUCK, S. D. *Polymer, Lond.* 1965, **6**, 319
[9] BRUCK, S. D. in *Vacuum Microbalance Techniques*, Vol. IV, pp 247–278 (edited by P. M. WATERS). Plenum Press: New York, 1965
[10] MORGAN, P. W. and KWOLEK, S. L. *J. Polym. Sci.* 1963, **A1**, 1147

The Dynamic Mechanical Properties of Some Polyethers

R. E. WETTON* and G. ALLEN

The dynamic rigidity moduli (G′ and G″) have been measured for a number of poly(ethers). Measurements were made in the frequency range 0·01 to 1 000 c/s at temperatures from −150°C to +100°C, on a new apparatus which is briefly described. At 1 c/s the G″ peak locations were as follows: Poly(methylene oxide) β peak −69·7°C; poly(propylene oxide) β peak −60·7°C; poly(ethylene oxide) β peak −55°C, with a tan δ *crystalline melting peak at +69°C; poly(tetramethylene oxide) γ peak −139°C, β peak −74°C,* tan δ *melting peak +38·5°C; poly(ethylvinyl ether) β peak −27°C. Correlation in loss peak positions is observed between G″ and ϵ″ and activation enthalpies are calculated therefrom. The variation of activation enthalpy and the width parameter (Fuoss and Kirkwood's β) with temperature are discussed. Poly(ethylvinyl ether) data are reduced by the WLF scheme over limited temperature ranges and the activation enthalpy variation explained by Bueche's theory. The discussion also deals with the effect of crystallinity on loss peaks, the origin of* tan δ *loss peaks at the crystalline melting point and the correlation between G″ and ϵ″ peaks.*

THE characteristic general features of the dynamic mechanical behaviour of high molecular weight amorphous polymers are well known and qualitatively understood. In particular, frequency/temperature measurements in the rubbery region can be correlated by the Williams, Landel and Ferry[1] expression and the molecular theories of Kirkwood[2], Rouse[3] and Bueche[4] meet with some success. The nature of the glass transition in polymers is still a subject of discussion and all treatments of dynamic behaviour become empirical as the glassy state is approached.

Partially crystalline polymers present a much more complex picture and even their simplest dynamic properties[5] cannot at present be treated theoretically with any success. The present work constitutes an experimental study of some polyethers, which, with one exception, were all partially crystalline. The aim of this work has been to obtain data on a single undisturbed specimen over wide frequency and temperature ranges in order to obtain approximations to relaxation spectra without recourse to time/temperature reductions. This has necessitated the use of measurements mainly under non-resonant conditions.

The specimens measured were: poly(methylene oxide) $[CH_2—O]_n$, two poly(ethylene oxide) samples $[CH_2—CH_2—O]_n$, two poly(propylene oxide) samples $[CH_2—CH(CH_3)—O]_n$, differing in crystallizability, poly(tetramethylene oxide) $[(CH_2)_4—O]_n$, and poly(ethylvinyl ether) $[CH_2—CH(O—C_2H_5)]_n$.

Dynamic mechanical, dielectric and n.m.r. data for some of these polymers have already been published. For example, extensive dielectric measurements have been made on poly(methylene oxide) by Williams[6], Read and Williams[7], Thurn[8], Ishida[9] and Mikhailov and Eidelnaut[10].

*Present address: Chemistry Dept, University of Technology, Loughborough.

Mechanical data covering a wide range of frequency and n.m.r. wide-line studies have been published by Thurn[8] and over a more limited range by McCrum[11] and by Read and Williams[7]. Nuclear spin lattice relaxation times of poly(ethylene oxide) were reported by Allen, Connor and Pursey[12] and these results together with mechanical and dielectric data have been reviewed by Connor, Read and Williams[13]. Ferry *et al.*[14] have made mechanical measurements on poly(ethylene oxide) networks above the melting point and McCrum[11] has presented mechanical data at one frequency over a wider temperature range. Other mechanical measurements at a single frequency have been made for the remaining polymers including work by Willbourn[15] [poly(tetramethylene oxide)], Woodward *et al.*[16], Schmeider and Wolf[17] [poly(ethylvinyl ether)] and Read[19] [poly(propylene oxide)]. Wetton and Williams[18] have reported dielectric loss measurements over a range of frequencies for poly(tetramethylene oxide).

EXPERIMENTAL

Data characterizing all the polymers are given in *Table 1*. Number average molecular weights, $\overline{M}_n$, were determined by osmometry, weight averages, $\overline{M}_w$, by the light scattering technique and $\overline{M}_v$ is the viscosity average.

Densities were measured by a flotation technique. Degrees of crystallinity were estimated from literature values for the densities of the purely amorphous and completely crystalline regions. Glass transitions, T_g, and melting points were determined dilatometrically using slow rates of heating.

Poly(methylene oxide)—was a commercial sample of Delrin 500. Hammer, Koch and Whitney's[20] values of 1·250 and 1·506 g. cm^{-3} for the densities of, respectively, the amorphous and crystalline regions were used to estimate the degree of crystallization. Polymer degradation at 180°C prevented a determination of the melting point.

Poly(ethylene oxide)—Two samples were used. The first (I) was Poly-ox F.C.118 and the second (II) was prepared by D. W. Farren in this department using a zinc diethyl–water catalyst[21].

Intrinsic viscosities were measured in water at 35°C and molecular weights were estimated from the relation[22]

$$[\eta]=6{\cdot}4\times10^{-5}M^{0{\cdot}82}$$

The amorphous density was estimated as 1·178 g. cm^{-3} by extrapolation from the density of the melt. Price and Kilb's[23] value of 1·23 g. cm^{-3} was used for the crystal density.

Poly(propylene oxide)—Two fractions of different degrees of crystallizability were obtained from a whole polymer prepared[24] by polymerization in dioxan using a zinc diethyl–water catalyst. The first fraction crystallized from iso-octane solution above 42°C while the second fraction precipitated between 39° and 42°C. There is now evidence that the first fraction is more stereoregular than the second one[25].

Densities of 1·002 g. cm^{-3} and 1·157 g. cm^{-3} were used[26] for respectively the amorphous and crystalline regions.

Poly(tetramethylene oxide)—was prepared by D. Sims using phosphorus pentafluoride (PF_5) as catalyst. The density of the crystalline regions has not been reported but a preliminary X-ray measurement based on the intensity of the amorphous halo indicates approximately 33 per cent crystallinity. We are grateful for the gift of this sample.

Poly(ethylvinyl ether)—D. W. Farren used borontrifluoride etherate in *n*-pentane at −80°C as the catalyst for this polymerization[27]. The polymer was amorphous and its molecular weight was determined in solution in butanone from the relation[28]

$$[\eta]=1{\cdot}37\times10^{3}M^{0{\cdot}54}$$

Table 1

Polymer	*Molecular weight*	*Density at 20°C (g. cm^{-3})*	*Crystallinity (approx. % by weight)*	T_g(°C)	T_M(°C)
Poly(methylene oxide)	$\overline{M}_n=4\times10^4$	1·424	70	−82	+180
Poly(ethylene oxide), I 'Poly-ox'	$\overline{M}_v=1{\cdot}4\times10^6$	1·203	44	−66·5	+66
Poly(ethylene oxide), II	$\overline{M}_v=4{\cdot}4\times10^5$	1·210	63	(−66·5)	+64
Poly(propylene oxide), high density	$\overline{M}_w=1{\cdot}2\times10^6$ $\overline{M}_n=3\times10^5$	1·086	54	(−75)	+70
Poly(propylene oxide), low density	$\overline{M}_w=1{\cdot}2\times10^6$ $\overline{M}_n=3\times10^5$	1·034	20	−75	+62
Poly(tetramethylene oxide)	$\overline{M}_w=5{\cdot}1\times10^5$	1·036	33	−84	+38·3
Poly(vinylethyl ether)	$\overline{M}_v=2\times10^5$	0·976	0	−43·6	—

Dynamic mechanical measurements

The instrument used was a much improved version of that described by Lord and Wetton[29]. A small cylindrical specimen was oscillated torsionally and the phase and amplitude of vibration used to compute the storage (G') and loss (G'') components of the complex dynamic rigidity modulus. Measurements could be made over continuously variable frequency and temperature ranges, which were 0·01 c/s to 1 kc/s and −150°C to +120°C respectively. Full details of the new apparatus are given elsewhere[30].

The instrument is shown in *Figure 1*. A cylindrical polymer specimen, P, was clamped rigidly at its lower end in a fixed pin vice, K, while the top end was firmly attached to a small coil, C. This coil was pivoted vertically

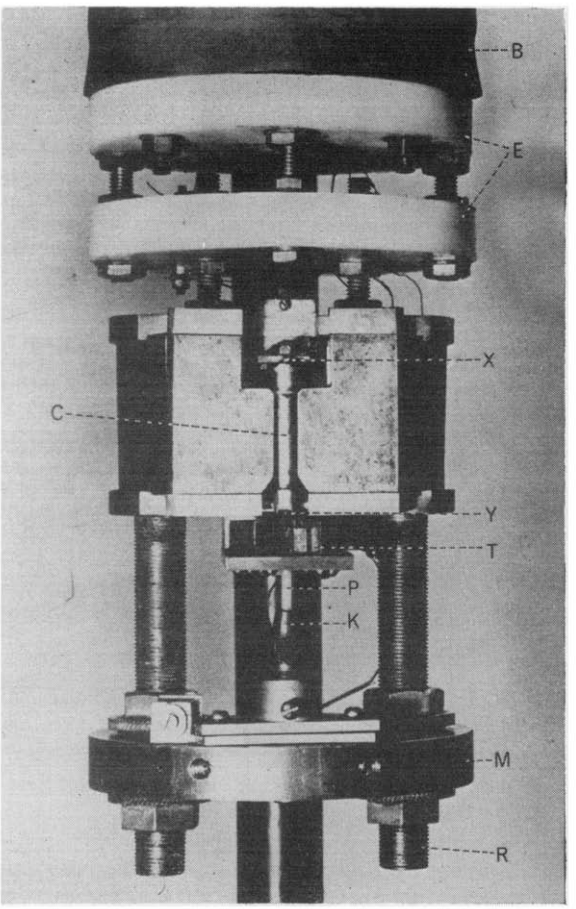

Figure 1—Photograph of apparatus with thermostat removed. B—cylindrical rubber block, C—former carrying copper coil, E—PTFE discs, K—pin vice, M—Brass platform, P—polymer specimen, R—support rods, T—transducer, X, Y—pivots

between the poles of a permanent magnet, so that an alternating current passing through the coil applied a sinusoidal torque to the specimen. The current was generated by a variable frequency oscillator and fed to the upper pivot of the coil, the lower one being earthed.

The angular oscillation of the coil and hence of the upper end of the specimen was followed with the aid of a capacitance change transducer, T in *Figure 1*. It is also shown schematically, in plan view, in *Figure 2*. The

transducer comprised a set of four radial vanes, which were mounted at the lower end of the coil so that they lay adjacent to a complementary set of fixed vanes. Rotation of the coil produced a change in the separation of adjacent vanes and hence a capacitance change proportional to the angular displacement. The stationary set of vanes were electrically connected to a capacitance meter[31], which produced an output voltage accurately proportional to the capacitance change in the transducer.

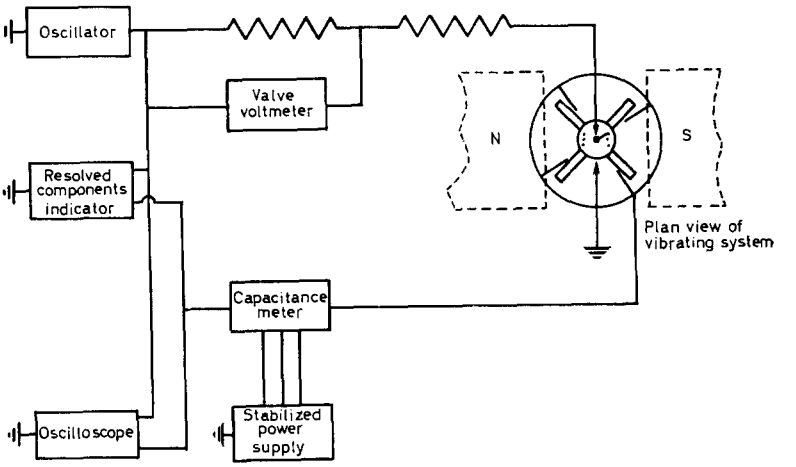

Figure 2—Block diagram of electrical circuits and transducer

A block circuit diagram is shown in *Figure 2*. The variable frequency oscillator (Solartron O.S.103) applied an attenuated voltage to a non-inductive resistance and hence on to the coil, the remote end of which was earthed. The r.m.s. current passing through the coil was determined from the voltage drop across a 100 ohm series resistance. The signal from the capacitance meter was applied to a resolved components indicator (Solartron V.P.253) which also received four phase reference signals from the oscillator. The resolved components indicator then read the amplitude of the output signal from the capacitance meter and its phase relative to the input driving voltage applied to the coil. Both input and output signals were monitored on an oscilloscope, which was used to make the necessary phase and amplitude measurements at frequencies below 0·5 c/s.

The most general equations relating dynamic moduli to the measured terms are:

$$G' = (Ni/kBV)\cos\beta + I\omega^2/k \tag{1}$$

$$G'' = (Ni/kBV)\sin\beta \tag{2}$$

where β is the phase lag of strain behind stress, i is the current through the coil, N is the proportionality constant between current and applied torque, obtained from initial calibrations, V is the output voltage from the capacitance meter, B is the proportionality constant between V and the angular

displacement, I is the inertia of the vibrating system, ω is the angular frequency of measurement and k is a geometrical factor incorporating the sample dimensions ($k = \pi a^4/2l$, where a is the radius and l the length).

At some high frequency ($\sim$1–2 kc/s) the vibrating system resonated and $\cos\beta = 0$, $\sin\beta = 1$. Using this condition, equation (1) gave an absolute measure of G', which, combined with a measurement of the half width of the resonance curve, gave an absolute value for G''. In equation (2) the only unknown constant B could be determined for the pertaining transducer setting. A more convenient procedure for determining B was to extrapolate lower frequency measurements of G' to the resonant frequency, where the absolute value was known. The extrapolation only extended results by a quarter of a decade and could normally be used with good accuracy.

Spurious phase shifts were introduced by the capacitance meter, particularly at high frequencies. To eliminate these and other instrumental errors as far as possible, a background calibration of phase shift versus frequency was obtained using specimens of zero loss. As no polymer has a sufficiently low loss for this purpose, a series of steel and copper wires was used. The required phase shift, β, for any polymer specimen was always taken as the difference between actual measurements and the background values*.

Specimen clamping is always a source of difficulty in mechanical measurements. In this work the cylindrical specimen was moulded with a short square cross-sectioned length at one end. The cylindrical end was clamped tightly in a pin vice with rounded jaws, while the square end was forced into a matching hole in the former of the coil and clamped on one side by a small grub screw. The length of the specimen used was normally of the order of 1 cm. When measurements were required under conditions in which the polymer could flow, pressure clamping was useless. In such cases a cylinder of polymer was stuck with Kodak Eastman adhesive between two brass jigs which could easily be clamped in position. Data obtained with the two different types of clamping agreed to better than ten per cent.

Temperature control was by an adiabatic vacuum system. The instrument was hung from an insulating support and surrounded by a double walled Dewar-like vessel, which could be evacuated. The temperature of the instrument could only change by heat transference between an external temperature bath, via the air inside the double walled vessel. After the vessel had been evacuated to a pressure lower than 10^{-2} mm of mercury, the instrument was essentially thermally isolated and its temperature remained constant to within $\pm 0{\cdot}3$°C, for at least an hour. Suitable external temperature baths were chosen to cover the range -150°C to $+120$°C. The two copper–constantan thermocouples used to measure the temperature were positioned just above and just below the specimen.

Several other unrelated points, which were fully considered, may be worth a brief mention. The maximum rate of energy dissipation by the electromagnetic drive was 5×10^{-3} W, which is sufficiently small to be negligible. The phase of driving current to driving voltage was slightly dependent on the mechanical impedance of the specimen. This effect was made negli-

*A recent modification has removed this spurious shift. The new results indicate that the true phase shift is obtained by the above procedure.

gible by incorporating an 800 ohm resistance in series with the coil. The frictional torque at the pivots was maintained at about 60 dyne cm, a sufficiently low value to be negligible compared to the loss components of the specimen. The pivots were supported on short leaf springs so that thermal expansion or contraction of the specimen could occur without producing high stresses in the pivots. Small phase angles could be measured with more accuracy by backing off the in-phase component with an exactly 180° out-of-phase signal and then measuring the quadrature component on a more sensitive range.

All the specimens, except one, for dynamic measurement were injection moulded and allowed to cool very slowly (about five hours) to room temperature, then they were stored under vacuum prior to measurement. Delrin was the only polymer not moulded, this polymer being easily machined to size.

RESULTS

Each polymer was measured in a similar manner. Measurements were made always in the direction of increasing temperature, results being obtained over the full frequency range of the apparatus at a series of constant temperatures at intervals of approximately 10°C. These data have been cross-plotted against temperature at selected frequencies, which were normally 10^{-2}, 10^{-1}, 10^{0}, 10^{1}, 10^{2} and 10^{3} c/s. We present the data in this form to give the most concise and easily interpretable summary. *Figures 3* to *11* show the results for all the polymers measured.

Poly(methylene oxide)—One broad transition occurs in the temperature range −110° to 0°C (*Figure 3*). At 1 c/s the maximum in G'' lies at −66·7 while at 0·02 c/s the very broad peak is located at about −83°C. This is close to the proposed glass transition temperature (−82°C). The high values of G' ($\sim 1{\cdot}3 \times 10^{10}$), which persist even above the β dispersion, are due to the high degree of crystallinity.

There is evidence in the 0° to 100°C temperature range of further loss peaks (in tan δ) occurring at low frequencies only. Complete presentation of these high temperature results is impossible because of the poor accuracy of our data in this region, but the low frequency results are similar to those of Read and Williams[7].

Poly(ethylene oxide)—The results for polymers I and II are shown in *Figures 4* and *5* respectively. In each sample there is one fairly broad transition at low temperatures. The location of this peak is the same for each sample. At the lowest frequency of measurement (0·01 c/s) the G'' maximum lies at −60·5°C supporting the assignment of −66·5°C as the dilatometric T_g for high molecular weight polymer.

At a temperature 2°C below the melting point of each sample the G' values drop very sharply as crystallites melt.

Above the melting point (66°C), the modulus of sample I has a value of 10^{7} dyne cm^{-2} at high frequencies over a considerable range of temperature. It seems that an $\bar{M}_v$ of $1{\cdot}4 \times 10^{6}$ is high enough to allow temporary entanglements to act as effective crosslinks at high frequencies. Rather surprisingly, the lower molecular weight sample II ($\bar{M}_v = 4{\cdot}4 \times 10^{5}$)

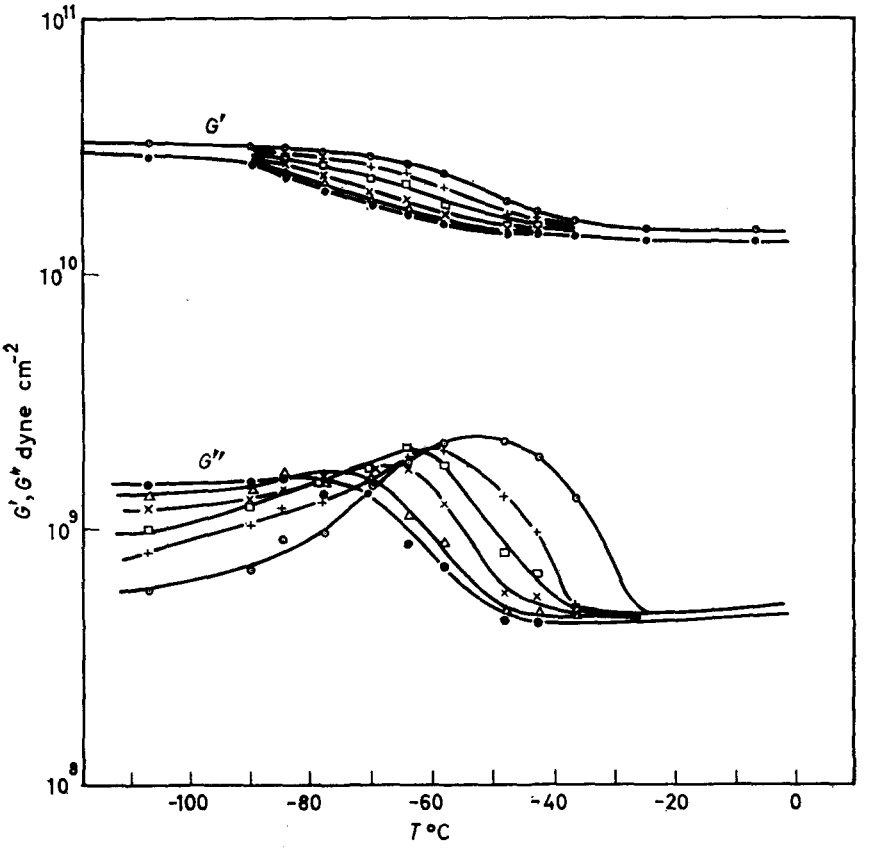

Figure 3—Dynamic rigidity moduli of poly(methylene oxide) as functions of temperature. ○ 1 kc/s, + 100 c/s, □ 10 c/s, × 1 c/s, △ 0·1 c/s, ● 0·02 c/s

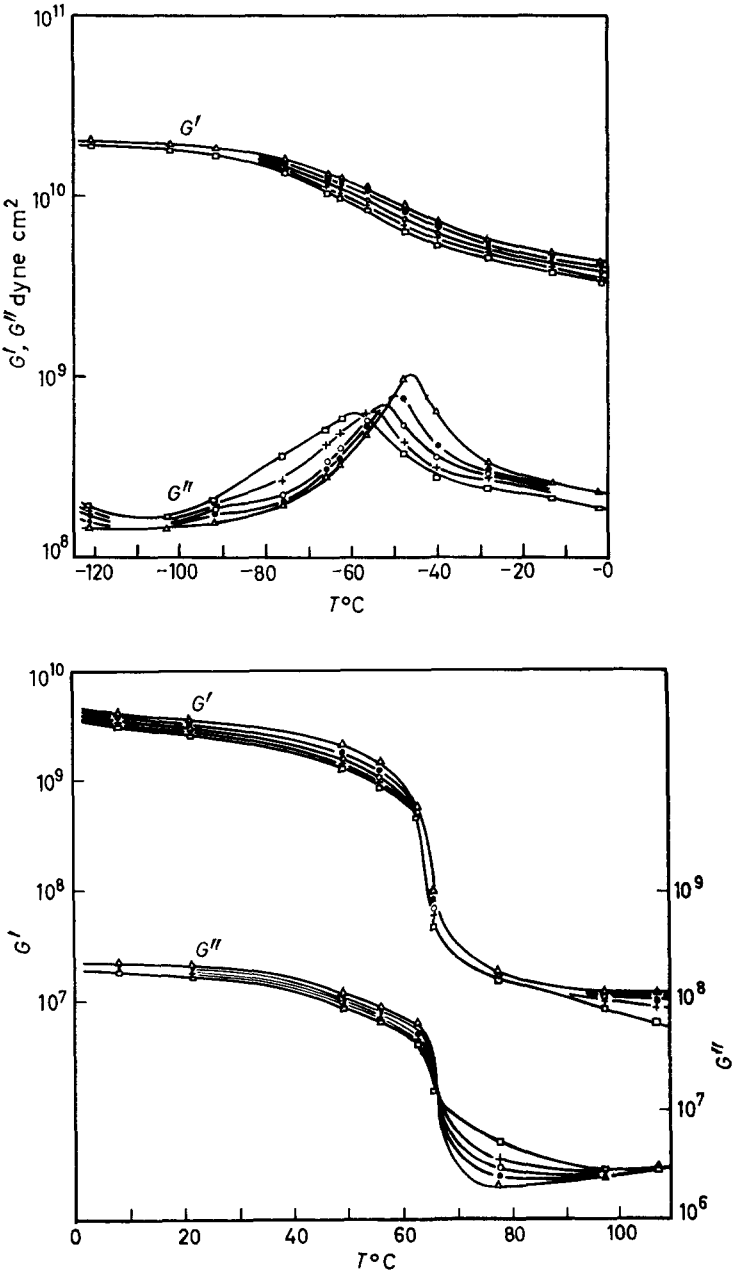

Figure 4—Dynamic rigidity moduli of poly(ethylene oxide) I as functions of temperature. △ 1 kc/s, ● 100 c/s, ○ 10 c/s, + 1 c/s, □ 0·2 c/s

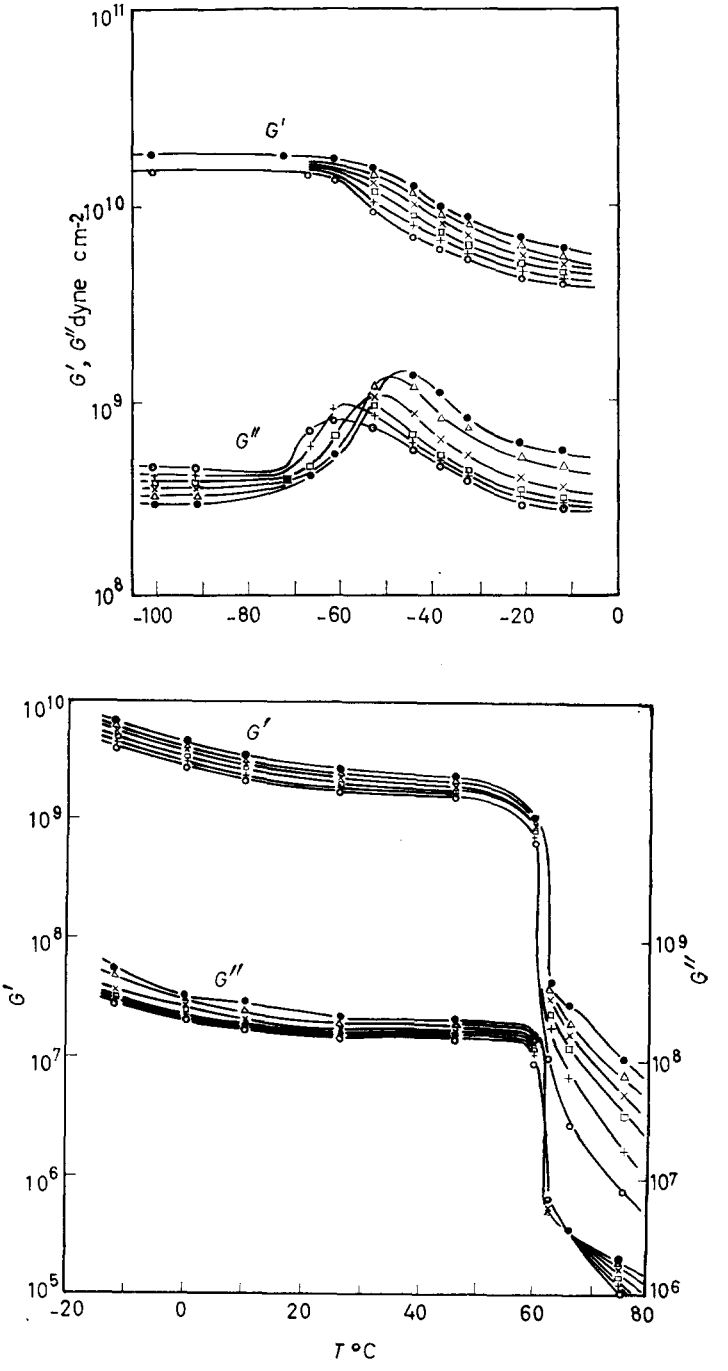

Figure 5—Dynamic rigidity moduli of poly(ethylene oxide) II as functions of temperature. ● 1 kc/s, △ 100 c/s, × 10 c/s, □ 1 c/s. + 0·1 c/s, ○ 0·02 c/s

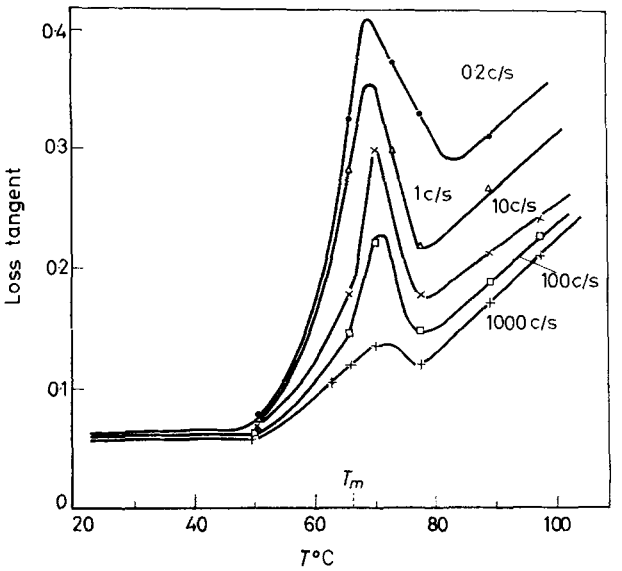

Figure 6—Loss tangent peaks at the melting point for poly(ethylene oxide) I. + 1 kc/s, □ 100 c/s, × 10 c/s, △ 1 c/s, ● 0·2 c/s

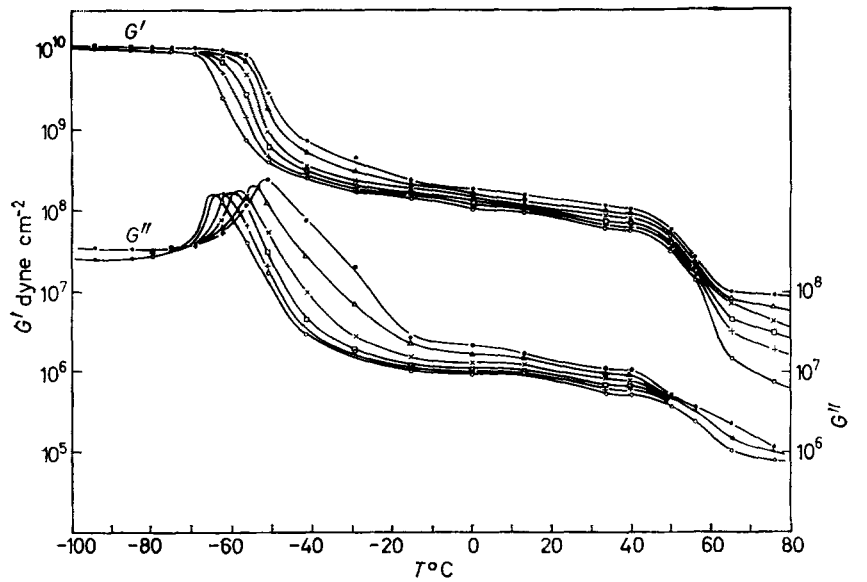

Figure 7—Dynamic rigidity moduli of low density poly(propylene oxide). ● 1 kc/s, △ 100 c/s, × 10 c/s, □ 1 c/s, + 0·1 c/s, ○ 0·01 c/s

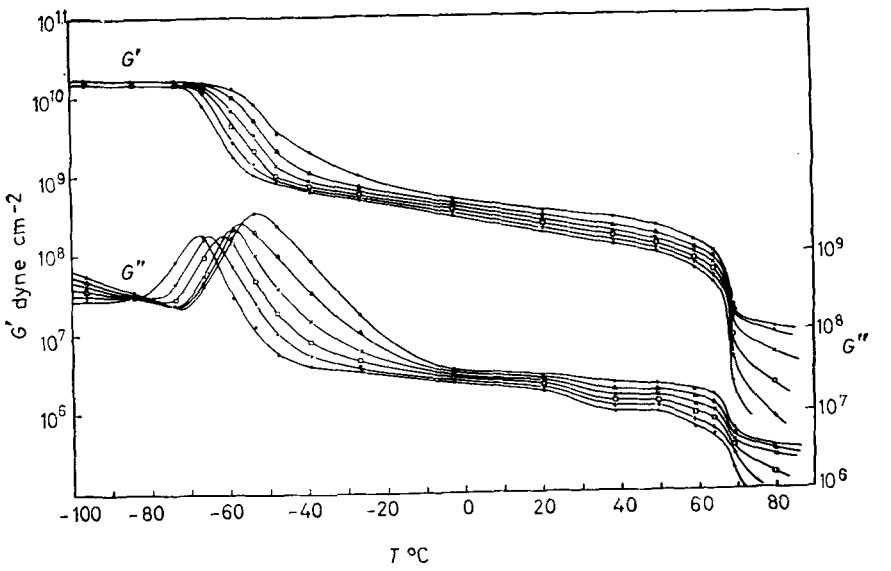

Figure 8—Dynamic rigidity moduli of high density poly(propylene oxide). Legend as *Figure 7*

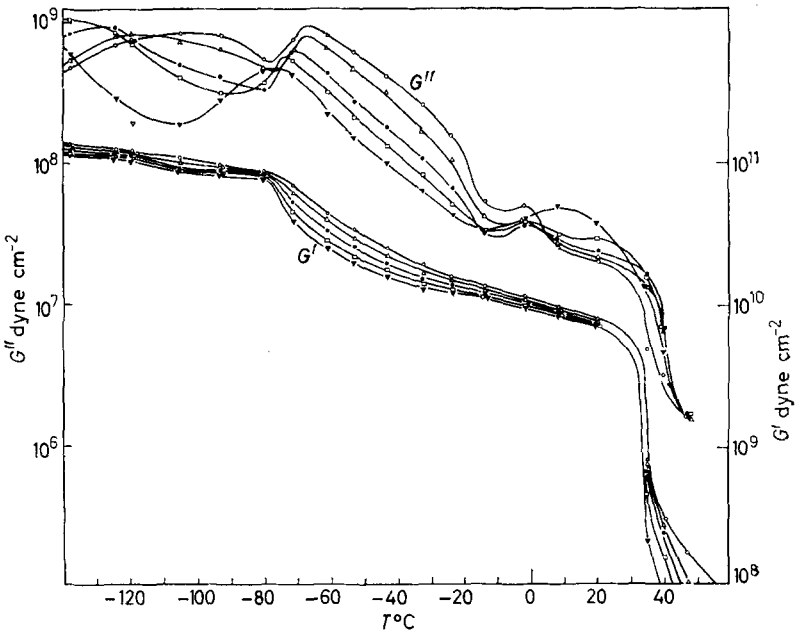

Figure 9—Dynamic rigidity moduli of poly(tetramethylene oxide).
● 1 kc/s, △ 100 c/s, × 10 c/s, □ 1 c/s, + 0·1 c/s, ○ 0·01 c/s

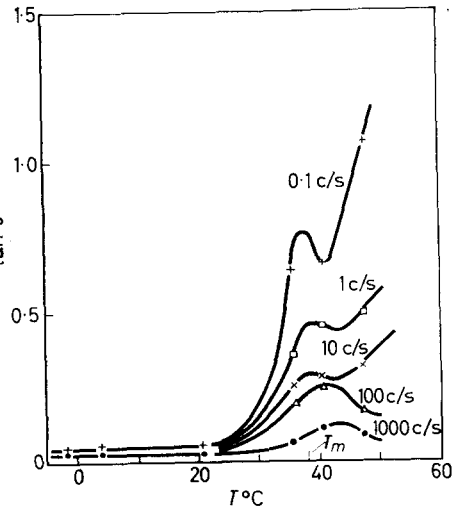

Figure 10—Loss tangent peaks at the melting point for poly(tetramethylene oxide). ● 1 kc/s, △ 100 c/s, × 10 c/s, □ 1 c/s, + 0·1 c/s

does not show a plateau region in G', the values of which decrease slowly with increasing temperature. This suggests that entanglement coupling is weakened at this molecular weight so that whole chains can move relative to each other within the time of stressing. Normally such behaviour would only be expected at $\overline{M}_v \sim 10^4$.

An extremely interesting observation with sample I is that although there are no maxima in G'' values in the melting range, a re-plot of the data as tan δ, in *Figure 6*, shows pronounced loss peaks centred precisely on the melting point.

There are signs of similar tan δ peaks in the experimental sample, but the behaviour is obscured by high tan δ values due to viscous flow in this lower molecular weight polymer. Dispersion behaviour in the melting range will be considered further in the discussion.

Poly(propylene oxide)—The two samples differ only in their tacticity and degree of crystallinity. The low temperature data, shown in *Figures 7* and *8*, reveal only one dispersion region. With the low density sample the peak in G'' moves from $-52°C$ at 1 kc/s to $-65°C$ at 0·01 c/s, the corresponding peaks in the high density sample being lower by about two degrees at each frequency.

The G' values decrease fairly rapidly a few degrees below the melting point of each sample. The decrease is sharper in the more tactic sample in keeping with its sharper melting point. In both sets of results G'' values decrease in sympathy with G' without a dispersion of any kind.

Poly(tetramethylene oxide)—This polymer exhibits two dispersions below 0°C, as can be seen in *Figure 9*. The temperature location of the lower dispersion shows the stronger frequency dependence, with the result that greater separation is achieved at lower frequencies. The locations of

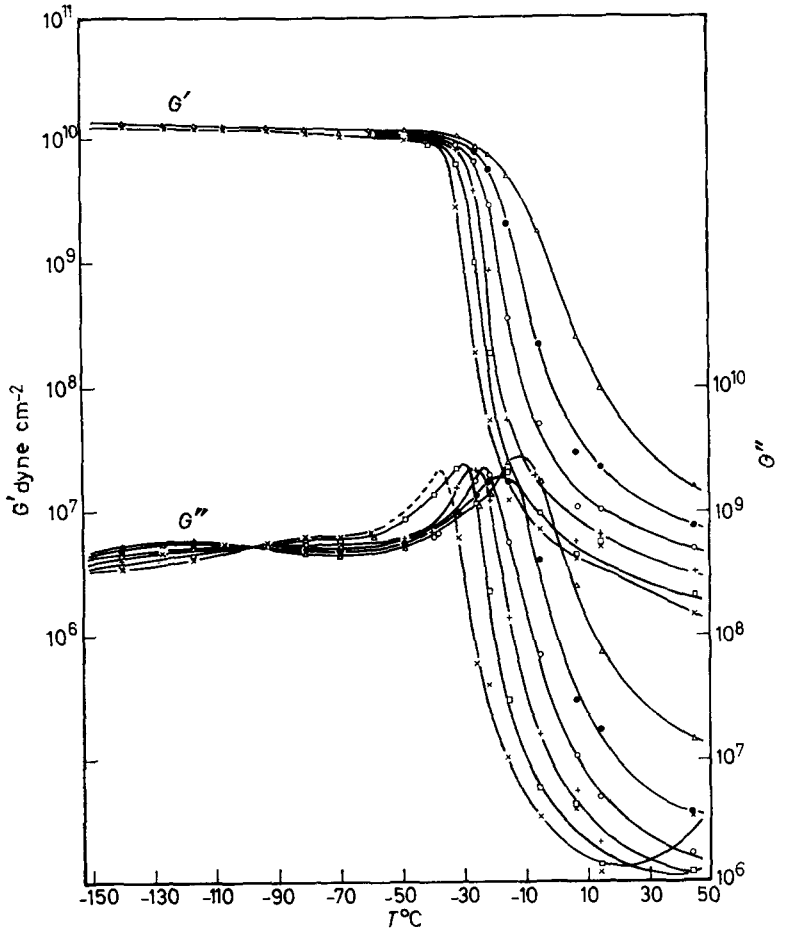

Figure 11—Dynamic rigidity moduli of poly(ethylvinyl ether). △ 1 kc/s, ● 100 c/s, ○ 10 c/s, + 1 c/s, □ 0·1 c/s, × 0·01 c/s

these two dispersions agree with those discussed by Willbourn[15]. The latter are included in *Figure 15* of the discussion.

The dispersion behaviour in the region of the melting point is not clear. More work is required to investigate the reality of G'' peaks just below the melting point. Centred on the melting point, however, there are certainly low frequency peaks in tan δ without accompanying G'' peaks. These tan δ peaks are similar (cf. *Figure 10*) to those for the poly(ethylene oxide) sample I, being much more pronounced at lower frequencies.

Poly(ethylvinyl ether)—This polymer was amorphous and un-crosslinked, with the consequence that the main glass–rubber transition was complicated on the high temperature side by viscous flow. Results are shown in *Figure 11*.

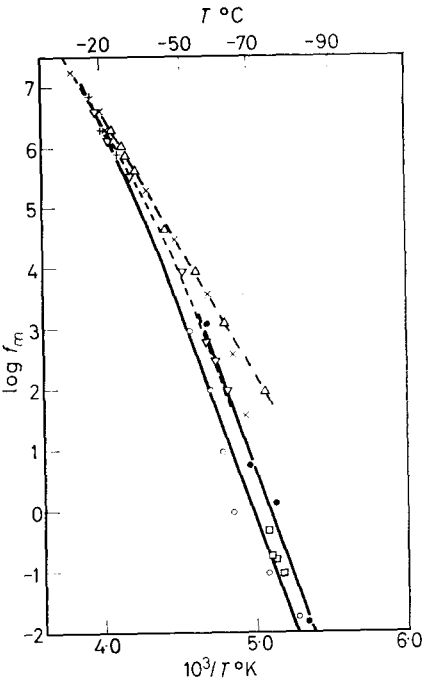

Figure 12—Locations of maxima of loss peak of poly(methylene oxide). ○ present (G''_f), ● present work (G''_T), Read and Williams[6] (G''_f), ▽ Read and Williams[6] (ϵ''_f), △ Read and Williams[6] (ϵ''_T), × Thurn[8] (ϵ''_f), + Thurn[8] (E''_f)

At 1 kc/s the main dispersion peak in G'' occurred at $-11°C$. The temperature of the peak decreases with decreasing frequency to attain a value of $-30°C$ at 0·1 c/s. The peaks are less asymmetric in the temperature plane than in the frequency plane.

Accuracy

Dynamic mechanical measurements using driven frequency techniques are less accurate than single frequency resonance methods. In the present work the limit of error on the absolute value of G' is approximately twelve per cent. The relative values of G' in any one set of measurements will be considerably better than this, i.e. changes in G' have an error of about two per cent.

Agreement of G' values with other published data bears out the order of magnitude of the absolute error. For example, the value of G' at $-120°C$ for poly(ethylvinyl ether) is given by Saba, Sauer and Woodward[16] as 10^{10} dyne cm^{-2} which compares with our value of $1{\cdot}2 \times 10^{10}$ dyne cm^{-2}.

The worst agreement between the present work and published data, where accurate comparison is possible, is with the low temperature storage moduli of McCrum[11] and of Read and Williams[7], who used closely similar torsion pendulums. A larger disagreement than expected from random error is found in the glassy state moduli, as the data in *Table 2* show.

Table 2

Polymer	*T(°C)*	*f(c/s)*	*G'(dyne/cm²)*	
			Present	*Torsion pendulum*
Poly(methylene oxide)	−110	0·3	$3·0\times10^{10}$	$3·7\times10^{10}$
Poly(ethylene oxide)	−120	1·0	$2·0\times10^{10}$	$2·5\times10^{10}$

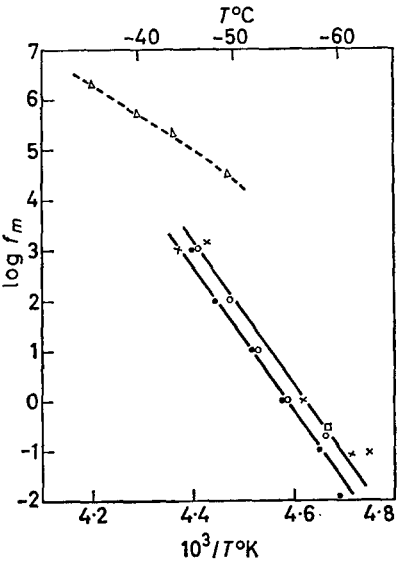

Figure 13—Locations of maxima of loss peak of poly(ethylene oxide). ● present work sample II (G''_f), + present work sample II (G''_T), ○ present work sample I (G''_f), × present work sample I (G''_T), △ Connor, Read and Williams[13] (ϵ'_f), □ Read[19]

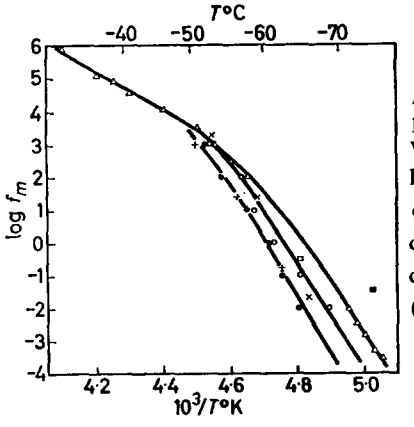

Figure 14—Locations of maxima of loss peak of poly(propylene oxide). ● present work less dense sample (G''_f), + present work less dense sample (G''_T), ○ present work more dense sample (G''_f), × present work more dense sample (G''_T), △ Williams[6] intermediate density (ϵ''_f), □ Read[19] intermediate density (G''_f), ■ Woodward and Sauer[16] syndiotactic(?) sample (G''_f)

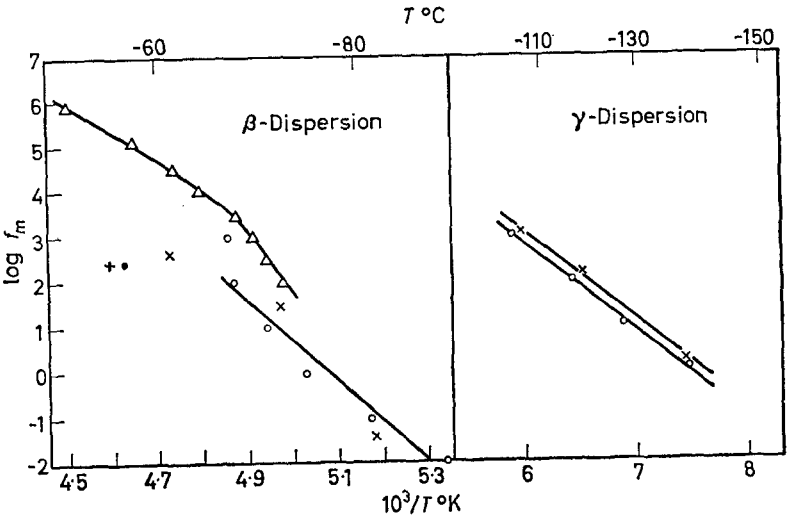

Figure 15—Location of maxima of loss peaks of poly(tetramethylene oxide). ○ present work (G_f''), × present work (G_T''), ● present work (tan δ_f), △ Wetton and Williams [18] (ϵ_f''), + Willbourn[15] (tan δ_f)

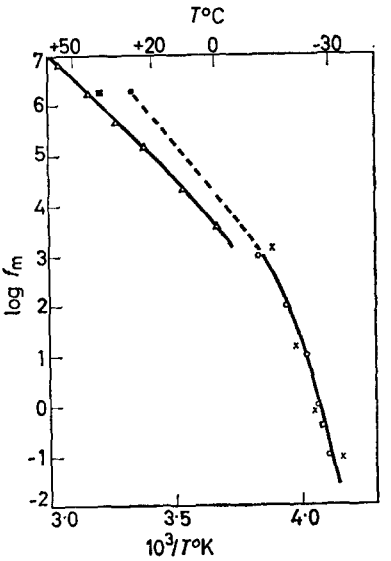

Figure 16—Location of maxima of loss peaks of poly(ethylvinyl ether). ○ present work (G_f''), × present work (G_T''), △ Wetton and Williams[18] ■ (ϵ_f''), Woodward and Sauer[16] (G_f''), ● Thurn and Wolf[38] (U.S. damping maxima)

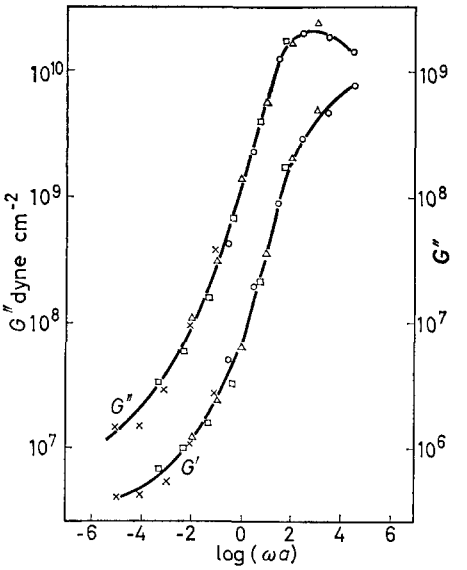

Figure 17—Reduction of the data for poly(ethylvinyl ether) to 257·0°K. ○ 250·7°K, △ 257·0°K, □ 266·9°K, × 278·7°K

Differences between the low temperature moduli are of the order of 20 to 25 per cent. Any one of the following explanations may be correct, but the last seems most feasible.

(*a*) Torsion pendulum amplitudes were a factor of 10^3 greater than those of the present work.

(*b*) Low temperature clamping might be at fault in the present work but no discontinuities were observed.

(*c*) The torsion pendulum data may be too high because the ends of the rectangular specimen were constrained always to be planar by the method of clamping. The geometric factor used in the torsion pendulum work overestimates the modulus by the factor[32] $2 \times (0{\cdot}43$ breadth/length). Taking the breadth to length ratio as one fifth we see that the modulus is overestimated by about 20 per cent.

The error in G'' is ± 5 per cent for values greater than $0{\cdot}1G'$ but this becomes progressively worse at lower phase angles.

The shape of relaxation spectra, as approximated by G'' versus $\ln(1/\omega)$, is dependent largely upon relative changes and should thus have fairly good accuracy. Good agreement of loss maxima loci with published data is obtained. This can be seen from *Figures 12, 16* and *17*, which show all available loss maxima locations.

DISCUSSION

Treatment of experimental data

(i) *Comparison of mechanical and dielectric loss peaks*—Mechanical compliance terms J' and J'' might be expected to be directly comparable with dielectric components ϵ' and ϵ'' since both are measured with respect to the applied potential (respectively stress and voltage). Alternatively one might expect agreement between locations of the maxima in tan δ values

obtained from mechanical and dielectric measurements since tan δ is dimensionless. In practice closest agreement is found between ϵ'' and G'' (or E'' the loss component of Young's modulus[46]). The mechanical response of a typical polymer system in modulus, compliance and tan δ is shown schematically in *Figure 18*. The exact shapes of the curves depend on the individual polymer system. Differences in location of the maxima occur also in the temperature plane and are less pronounced for weaker transitions. For example in the present work, the temperature difference, at 1 kc/s between the G'' and tan δ peaks was 9° for poly(ethylvinyl ether) but only 4° for Delrin.

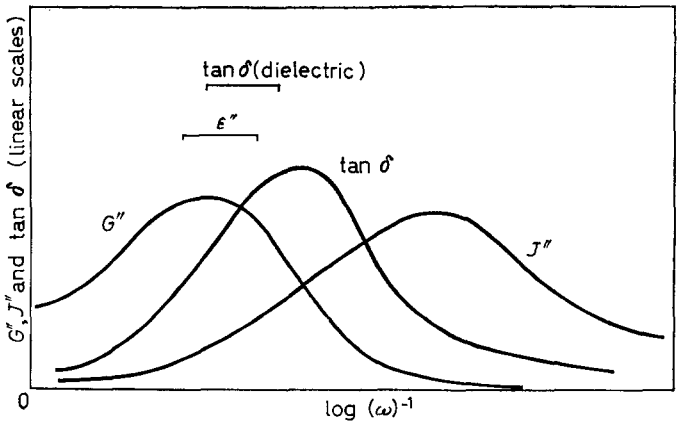

Figure 18—Typical mechanical loss peak and dielectric loss peak locations for the glass–rubber dispersion in the same polymer

The difference in position of the mechanical peaks is due to the different weightings imposed upon the basic time spectrum by defining it in terms of either modulus or compliance contributions. As the largest relaxation strength in terms of the modulus increment occurs with the small scale motions in a nearly glassy state, G'' is biased to emphasize short time effects. The opposite argument holds for J'' where the largest compliance change occurs with large scale chain motion in an essentially rubber-like state. A retardation spectrum at the same temperature will thus emphasize the long time scale end of the basic time spectrum. As tan δ is dimensionless, it does not suffer from arbitrary weighting distortions, and is probably the best indication of the spectrum of molecular motions contributing to mechanical energy dissipation.

In the dielectric case tan δ is the best indication of the spectrum of molecular motions contributing to dielectric energy dissipation. The dielectric retardation spectrum (ϵ'') although dimensionless is slightly distorted by the weighting given to dipole orientation as well as the time scale of individual processes.

Comparison of mechanical and dielectric spectra should, on the grounds of the above arguments, best be made in terms of tan δ in each case. In

fact the positions of the tan δ peaks do not coincide. The micro-Brownian molecular motions must be identical in both mechanical and dielectric cases since these are characteristic of the polymer not of the measurement and so we conclude that the molecular mechanisms most effective in dielectric energy dissipation have slightly faster motions than those most effective in mechanical energy dissipation. The agreement between G'' and ϵ'' loss peak locations may result fortuitously from the different weightings given to the slightly different basic time spectra.

A mechanical description of a dynamic system is given by reporting two of three possible parameters, G', G'' and tan δ ($\equiv G''/G'$) as functions of frequency and temperature. In this paper we have reported G' and G'' because they are, by definition, governed by the same relaxation time spectrum. Furthermore presentation of G'' facilitates comparison with dielectric results. tan δ is obtained readily from the results, if required. From the point of view of calculation of activation enthalpies and deducing relaxation time distributions there is little to choose between the convenience of using either tan δ or G'', but the presentation of G' with tan δ is inconsistent in the sense that they are governed by different distributions.

(ii) *Temperature dependence of relaxation processes*—The temperature dependence of relaxation phenomena is discussed either as an activated rate process or by the applicability of the WLF[1] empirical equation. This equation is most successful when the relaxation time spectrum is essentially independent of temperature. This condition holds for a rubber, where the relaxation spectrum is governed largely by the chance of cooperative modes of motion of statistical chain segments. It is not expected to hold at or

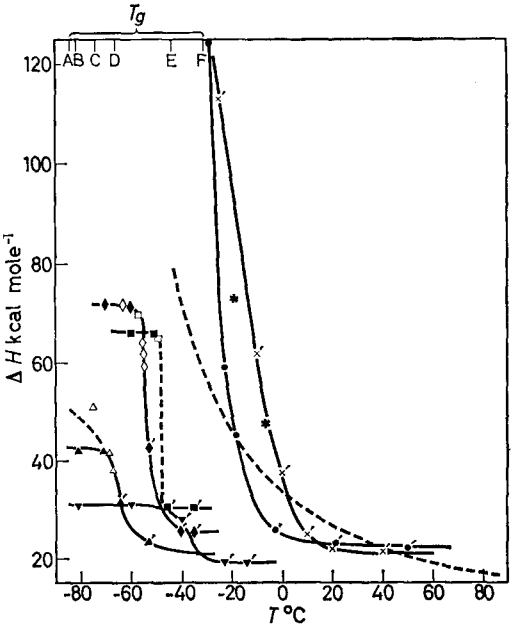

Figure 19—Variation of ΔH with temperature. ▲ Poly(tetramethylene oxide), T_g—A; ▼ Poly(methylene oxide), T_g—B; ◆ Poly(propylene oxide), T_g—C; ■ Poly(ethylene oxide), T_g—D; ● Poly(ethylvinyl ether), T_g—E; × Poly(acetaldehyde), T_g—F. Primed symbols refer to dielectric measurements, the others to mechanical results. Open symbols are results calculated from areas, ringed symbols are from shift procedures. The broken curve is the temperature variation required by the WLF equation for T_g—43·5°C

below the glass transition temperature, nor for systems having a distribution of relaxation times created in part by a distribution of activation enthalpies.

In the present discussion an average activation enthalpy (ΔH) defined by

$$\tau_{\text{av.}} = 1/\omega_m = A \exp(\Delta H/RT) \tag{3}$$

is used, where $\tau_{\text{av.}}$ is an average relaxation time characterized by the angular frequency (ω_m) for a maximum in G''. Although the results allow a distinction to be made between loss maxima in the temperature or frequency planes, the scarcity of data in the frequency plane necessitates the use of both sets of values and ΔH has been averaged from both sets of data. Equation (3) does not fit the results unless ΔH is, itself, a function of temperature. Thus ΔH pertaining at a particular temperature is determined from the instantaneous slope of $\ln(1/\omega_m)$ versus $1/T$ at that temperature. The physical significance of equation (3) is more uncertain when applied to systems having broad, asymmetric and temperature-dependent distributions of relaxation times since the nature of the average value of τ then changes with temperature.

An alternative approach uses the area method proposed by Read and Williams[34] which defines an average activation enthalpy as

$$(1/\Delta H)_{\text{av.}} = \{(G_U - G_R) R\pi\}/2 \int_0^\infty G'' \mathrm{d}(1/T) \tag{4}$$

This solves the problem of defining a specific average, because equation (4) is valid even for distributions changing with temperature. There still remains the practical problem, however, of estimating the area under a broad asymmetric peak.

(iii) *Characterization of relaxation time distributions*—The distributions of relaxation times required to describe the dielectric behaviour of polymers are much broader than that predicted by use of a single relaxation time in the modified Debye equation[42, 43]

$$\epsilon''_\omega/\epsilon''_m = \operatorname{sech}(\ln \omega\tau'_{\text{av.}}) \tag{5}$$

Here ϵ''_ω is the dielectric loss at frequency ω, ϵ''_m is the maximum value of ϵ''_ω in a frequency plane, and $\tau'_{\text{av.}}$ is the most probable retardation time defined as $1/\omega_m$ where ω_m is the angular frequency of maximum loss.

Fuoss and Kirkwood showed[43] that the broad distributions in a polymer system could be fitted by the expression

$$\epsilon''_\omega/\epsilon''_m = \operatorname{sech}(\beta \ln \omega\tau'_{\text{av.}}) \tag{6}$$

where β measures the breadth of the distribution, being unity for a single retardation time and zero for an infinitely broad distribution.

Read and Williams[7] have recently applied equation (6) to dielectric and dynamic mechanical data on Delrin. We have also employed this approach to obtain a quantitative comparison of the distributions of relaxation times

at different temperatures. The expression analogous to equation (6), relating shear moduli to the most probable relaxation time is

$$G''_\omega / G''_m = \text{sech}\,(\beta \ln \omega\tau_{\text{av.}}) \tag{7}$$

Read and Williams give three possible methods for determining β:

(a) Using

$$G''_m = (G'_U - G'_R)\,\tfrac{1}{2}\beta \tag{8}$$

when β can be found if the frequency coverage is great enough to obtain the limiting moduli values G'_u and G'_R.

(b) From

$$G''_\omega = [2G''_m\,(\omega\tau_{\text{av.}})^\beta]/[1+(\omega\tau_{\text{av.}})^{2\beta}] \tag{9}$$

log G''_ω versus log ω has a slope

$$-\beta \quad \text{when} \quad \omega \gg \omega_m$$

$$\text{and} \quad +\beta \quad \text{when} \quad \omega \ll \omega_m.$$

(c) Since

$$\cosh^{-1}(G''_m/G''_\omega) = \beta \ln (\omega\tau_{\text{av.}}) \tag{10}$$

a plot of $\cosh^{-1}(G''_m/G''_\omega)$ versus log ω, with a sign change at $G''_\omega = G''_m$ has a slope of 2·303 β over the whole frequency range.

A fourth method (d), not given by Read and Williams, has proved more useful than the others. It involves a measurement of the half width of the loss peak and uses the equation

(d)
$$\cosh^{-1} 2 = \beta \mid \ln (\omega_1/\omega_m) \mid \tag{11}$$

where ω_1 is the angular frequency at which G''_ω has dropped to $\frac{1}{2}G''_m$.

When dynamic behaviour only approximately conforms to equation (7),

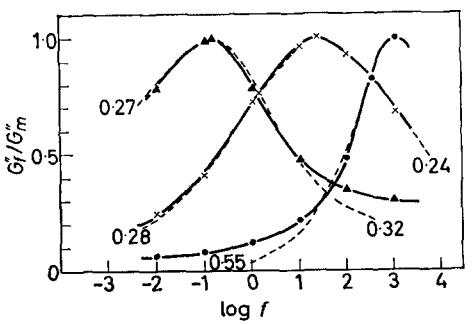

Figure 20—Frequency dependence of the reduced G'' for the less dense poly(propylene oxide) sample. β values are given for the high and low frequency sides of the loss peak. ● −51·2°C, ×−56·5°C, ▲−62·7°C

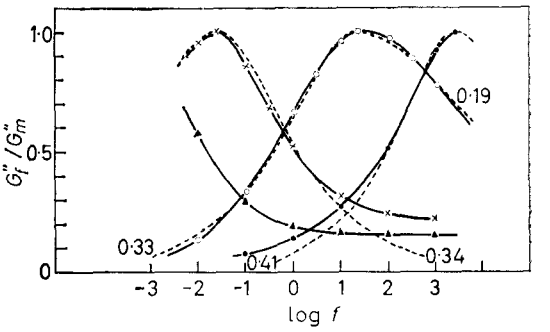

Figure 21—Frequency dependence of the reduced G'' for the more dense poly(propylene oxide) sample. β values are given for the high and low frequency sides of the loss peak. ●—53·3°C, ○—59·0°C, ×—66·4°, ▲—74°C

the most satisfactory value of β is obtained by reiterative curve fitting. *Figures 20* and *21* show the data for two different polypropylene oxide samples in the dispersion region with the best approximations of equation (7) to these curves. In assessing the most appropriate value of β required to fit any data, particular attention has been paid to exact correspondence near the maximum, where most of the relaxation occurs. More precisely the accuracy of fit at any frequency has been made roughly proportional to the relaxation strength at that frequency.

In fitting equation (7) to the experimental data, satisfactory agreement could only be obtained by using a different value of β for each side of the maximum. Thus the dispersion on opposite sides of a maximum has been characterized separately as if it were one half of a symmetrical distribution. There are no assumptions made here, we are merely seeking a quantitative description of the distributions.

Individual polymers

Poly(methylene oxide)—The relaxation spectrum of this polymer is broad and asymmetrical in the temperature range of the present measurements. The G'' peaks plotted against temperature are also very asymmetrical at low frequencies but become sharper and more symmetrical at higher frequencies. In fact the behaviour of the mechanical (G'') and dielectric loss (ϵ'')[7, 8] peaks is very similar. The changing asymmetry of the loss peaks at low temperatures makes conditions unfavourable for obtaining meaningful values of ΔH.

The locus of the G'' and ϵ'' loss peaks on the $\log f_m$ versus $1/T_m$ plot of *Figure 12* are in close agreement. In the temperature plane, extrapolation of the G'' data to meet those of Thurn[8] at high frequencies, gives a curve very close to the ϵ''_f locus. In the frequency plane agreement becomes progressively worse at lower temperatures. In this low temperature region

$$\Delta H \text{ (dielectric at constant } T) = 19{\cdot}4 \text{ kcal mole}^{-1}$$

compared with ΔH (mechanical) $= 31$ kcal mole^{-1}.

Curvature of the $\log f_m$ versus $1/T_m$ plots in the temperature plane cannot be attributed wholly to changing distributions in the mechanical case, as the slopes of plots in both the temperature and frequency planes are in

reasonable agreement at low temperatures. At higher temperatures the curvature can, with some certainty, be attributed to a variation in ΔH because of the sharper loss peaks and the parallel dielectric data. The most reasonable interpretation of the low temperature mechanical and dielectric relaxation in poly(methylene oxide) is of a single type of relaxation mechanism with a varying relaxation time distribution and an average activation enthalpy varying as shown in *Figure 19*. ΔH increases fairly sharply as the temperature is lowered and the mechanical data suggest that there is a limiting value at low temperatures of 31 kcal mole^{-1}. As these data are obtained entirely from loss peak positions, ΔH refers always to the same basic molecular relaxation process.

We assign this transition to the onset of cooperative main chain rotation in the amorphous phase in agreement with Read and Williams[7] and conclude, because all the dipoles in this polymer lie on the main chain, that the molecular process followed by mechanical and dielectric processes is probably the same. The transition is classified by Saito, Okano, Iwayanagi and Hideshima[35], as due to 'local mode' vibrations. This is an interesting possibility. However, the dependence of the temperature of maximum loss on molecular structure shown in *Table 3* seems to justify the assignment of the peak at $-65°C$ as the glass transition loss.

Table 3

Polymer	*Repeat unit*	*T for maximum in G″ and ϵ″ at 1 c/s*
Poly(tetramethylene oxide)	—$(CH_2)_4$—O—	−74°C
Poly(ethylene oxide)	—$(CH_2)_2$—O—	−55°C
Poly(propylene oxide)	—CH_2—CH(—CH_3)—O—	−60°C
Poly(acetaldehyde)	—CH_2—CH(CH_3)—O—	−30°C
Poly(methylene oxide)	—CH_2—O—	−65°C

Poly(ethylene oxide)—The low temperature behaviour of both the experimental and commercial samples is very similar. The only low temperature dispersion found is that due to the glass transition. The relaxation time distribution is broad ($\beta = 0{\cdot}25$), but in the temperature and frequency planes the loss peaks are reasonably symmetrical above 0·1 c/s. The plots of $\log f$ versus $1/T$ in both the temperature and frequency planes are shown for the two different samples in *Figure 13*. Frequency and temperature plane data are coincident for each sample and the plots linear. The loci of maximum loss differ by only half a decade for both polymers.

The torsion pendulum data obtained by Read[19] on a similar sample agree with our data in the location of the loss peaks, but the magnitudes of the loss peaks are less in the present work. If the change in storage modulus is small through the dispersion, then the area under the loss modulus curve

will be correspondingly small[34]. The magnitude of the loss peaks are also sensitive to water sorption and crystallinity.

The dielectric loss maxima[19] appear to be governed by a different activation energy in this region. The ΔH values are:

Dielectric (high temperature), 30·5 kcal mole^{-1}
Mechanical (low temperature), 66 kcal mole^{-1}

Using the total area beneath G'' over the temperature interval of major relaxation for the mechanical data we obtain a value of ΔH varying between 60 and 70 kcal mole^{-1}. By the same method Read[19] has obtained a value of about 35 kcal mole^{-1}. Yin, Lovell and Ferry[14] have obtained a value of 11·7 kcal mole^{-1} for the activation enthalpy between 70°C and 120°C (at these temperatures the polymer is above its melting point). From our values of ΔH at lower temperatures we would predict a value of 20 to 30 kcal mole^{-1} at 70°C. This is the only polymer used in our work for which correlation between G'' and ϵ'' loss peaks has not been demonstrated.

The behaviour at the crystalline melting point is discussed later in conjunction with the corresponding results for other polymers.

Poly(propylene oxide)—The two samples differed in their tacticity and crystallinity, but not in their molecular weight. The mechanical data give parallel log f versus $1/T$ plots for the two samples. Frequency and temperature plane data are coincident and the loci of loss peaks for the two samples are separated by less than a decade as shown in *Figure 14*. The activation enthalpy from these data is calculated as 72 kcal mole^{-1} at -60°C.

The G'' maximum from the torsion pendulum measurements of Read, Williams and Connor[13] is also shown in *Figure 14* together with a wide frequency range of dielectric loss maxima locations. The dielectric data refer to a sample differing only in its intermediate crystallinity. The close proximity of G'' and ϵ'' maxima leads us to postulate that the mechanical data at higher frequencies would lead to a curved locus for the mechanical loss maxima very similar to that obtained dielectrically. The corresponding variation of ΔH with temperature is shown in *Figure 19*. Activation enthalpies obtained by the area method also follow this trend.

Saba, Sauer and Woodward[16] have obtained torsion pendulum data on a sample claimed to be syndiotactic. At the same frequency our results for isotactic samples show the loss peak to be 11 deg C higher.

A low-temperature secondary (γ) dispersion of small magnitude ($\tan\delta = 0{\cdot}03$) has been reported[16] for this polymer at -150°C and 0·6 c/s. This is below the sensitivity obtainable in the present work.

Poly(tetramethylene oxide)—This polymer exhibits two definite low temperature mechanical maxima which are clearly shown in the temperature plane in *Figure 9*. The low temperature transition will be termed γ and the other, which is believed to be the glass transition, β. In terms of the mechanical relaxation spectrum, approximated by G'', the relaxations are of similar magnitude whereas in terms of the dimensionless spectrum, approximated by $\tan\delta$, the β relaxation is the larger. The storage rigidity modulus increment for the γ transition is $3{\cdot}5 \times 10^9$ dyne/cm^2 and for the β transition

$7{\cdot}2 \times 10^9$ dyne/cm^2. On this evidence the main glass transition is ascribed to the β peak because it is the stronger transition, i.e. $T_g = -84°C$.

The temperature loci of the loss peaks are complicated by the considerable overlap of the dispersions. At 1 kc/s the separation in the temperature plane is 37°C and in the frequency plane at $-80°C$ it is approximately four decades. Separation increases at lower temperatures and frequencies. The log f versus $1/T$ plots for both peaks are shown in *Figure 15*. Neither of these plots will give a precisely correct activation enthalpy because of the change in overlap with temperature. Consideration of the effect of changing overlap shows that the β peak locations in the frequency and temperature planes are shifted to higher frequencies and higher $1/T$ values respectively as $1/T$ decreases. The reverse is true of the γ peak locations.

Dielectric data have been obtained[18] on a closely similar sample of poly(tetramethylene oxide) and the locations of the ϵ'' maxima for the β dispersion are shown in *Figure 15*. The pronounced curvature at the low frequency end of the dielectric locus is due to the rapidly changing dielectric spectrum in this region. Again, there is fair agreement in the position of the ϵ'' and G'' maxima and this is taken to indicate that the mechanical and dielectric β-dispersions have the same molecular origins. The overall impression is that ΔH exhibits a small sigmoidal change as shown in *Figure 19*. Calculations using the area method agree reasonably well with low temperature values of ΔH but do not confirm the low temperature plateau in ΔH values. The dielectric data for this polymer can be resolved also into two loss peaks in the frequency plane, despite the appearance of only a single ϵ_f'' peak in the temperature plane. The β and γ dielectric (ϵ_T'') peaks correlate with the mechanical β and γ dispersions. Thus the low temperature process must involve some dipole motion. Onset of rotational freedom of some five or six main chain units, similar to that suggested (see ref. 33) by Schatzky is one possibility. 'Local mode' angular oscillation of the main chains about their equilibrium positions is an alternative explanation. Recent X-ray studies indicate that the chains have a zig-zag configuration in the crystalline phase. It is most probable that the short range amorphous configuration will also tend to a zig-zag. Rotational oscillation of any chain length greater than a single monomer would produce a dielectric transition of very low strength, because of the alternating dipole opposition along the main chain. We conclude that if local oscillations are responsible for the γ process, the basic unit involved approximates to the length of the monomer.

Poly(ethylvinyl ether)—This was a completely amorphous un-crosslinked polymer so that at low frequencies and at temperatures above T_g some viscous flow occurred. Fortunately flow interfered seriously only at temperatures well in excess of T_g so that the positions of the peaks themselves (in G'' in particular) were unaffected. Only one dispersion region associated, with the glass transition, was found in the temperature range studied. Secondary transitions due to side group motion, which have been reported[16,17] at low temperatures, were below the sensitivity of the apparatus.

The relaxation spectra for this polymer are relatively sharp ($\beta = 0{\cdot}4$) but the spectrum is broader on the high frequency than on the low frequency

side. The log f versus $1/T$ plot is shown in *Figure 16*. The locus in the temperature plane is well represented by a curved plot which is very nearly contiguous with the corresponding plot of dielectric loss (ϵ''). The curvature in this plot is ascribed to a temperature dependent activation enthalpy. In the frequency plane the limited data show considerable scatter. Also shown in *Figure 16* are loss peak locations found in other work. Dielectric data[38] at 2×10^6 c/s are consistent with the plot shown. The location of the maximum in the ultrasonic damping coefficient, also at 2×10^6 c/s, gives weight to the idea of a curved locus for the mechanical data, although it must be remembered that the G'' and damping coefficient maxima will differ slightly in their locations. Torsion pendulum data[16] at 0·43 c/s agree with our location of G'' at that frequency.

Using the combined dielectric and mechanical data, we calculate the variation of ΔH with temperature shown in *Figure 19*. At high temperatures the activation enthalpy varies only slowly with temperature. Forty degrees above T_g, ΔH increases fairly sharply with decreasing temperature.

Reduction of poly(ethylvinyl ether) data—In general accurate reduction was impossible for the partially crystalline polymers due to the changing distributions of relaxation times. The data for poly(ethylvinyl ether) can, however, be reduced over limited temperature ranges. The lower limit is set by approach to the glass transition temperature and the upper limit by onset of viscous flow. The results for G' and G'' reduced to 257°K are shown in *Figure 17*. No vertical shift was applied. The empirical frequency shift factors (a_T) are:

T°A	250·7	257·0	266·9	278·7
log (a_T)	1·5	0	−1·33	−3·04

Activation enthalpies calculated as $2{\cdot}303R[\mathrm{d}(\log a_T)/\mathrm{d}(1/T)]$ are shown in *Figure 19*. These show the same trend as the values obtained from peak positions but for a given temperature are 50 per cent higher. Such a divergence is not unexpected. McCrum and Morris[39] have recently pointed out that small errors in the vertical shift term, which was ignored in the present calculation, produce large errors in the activation enthalpy values. Furthermore, reduction of the results is concerned with parts of the spectrum removed from the peak. If a distributon of activation enthalpies is present the reduction factor will not be governed by the average value. In our reduction, emphasis was placed upon fitting the long time end of the spectrum which will involve the higher activation enthalpies.

Comparison of ΔH temperature dependence

The WLF universal reduction scheme has provided an adequate correlation between relaxation data obtained at different temperatures for amorphous polymers. This is equivalent[1] to an activated process with a temperature dependent ΔH of the form

$$\Delta H = \frac{2{\cdot}303R \;\; 17{\cdot}44 \times 51{\cdot}6 \;\; T^2}{(51{\cdot}6 + T - T_g)^2} \qquad (12)$$

An activation enthalpy varying according to equation (12) is shown in *Figure 19* for a T_g equal to that of poly(ethylvinyl ether), i.e. 43·5°C. The agreement between this calculated curve and the experimental data is reasonable when it is remembered that 'universal' constants were employed in equation (12). In the temperature range (T_g+20)°C to (T_g+120)°C the worst agreement between the curves is about 35 per cent which would not be detectable in most relaxation experiments.

Values of ΔH calculated from Williams's[40] dielectric results on poly(acetaldehyde) are also shown in *Figure 19*, and again follow the general form given by equation (10).

The variations of ΔH with temperature always occur more sharply than predicted from the WLF expression. For amorphous polymers the activation enthalpy tends to infinity with decreasing temperature. This is consistent with a kinetic theory of the glass transition since when the activation enthalpy is infinite (at T_g) the molecular process ceases. The limited amount of accurate data available supports this view for amorphous polymers. Becker[41], for instance, has reported ΔH variations similar to the amorphous cases shown in *Figure 19*, for poly(vinyl chloride), poly(styrene) and poly (methyl methacrylate).

With the partially crystalline polymers ΔH shows a similar sharp increase about 20 degrees above the dilatometric T_g. As the temperature approaches T_g, however, the activation enthalpy tends to assume a constant value.

Mechanical relaxation time distributions

Values of β calculated mainly by method (d) are shown in *Figures 22* and *23* for all polymers with the exception of poly(tetramethylene oxide) for which the results are confused by overlapping dispersions.

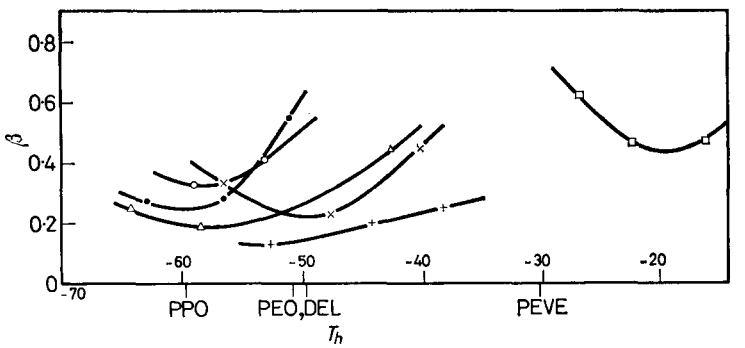

Figure 22—Variation with temperature of the width parameter β for the low frequency side of each spectrum. △ poly(methylene oxide), ○ poly(propylene oxide), high density, ● poly(propylene oxide), low density, × poly(ethylene oxide) I, + poly(ethylene oxide) II, □ poly-(ethylvinyl ether)

On the low frequency side of the maximum there is a trend to minimum values of β close to the temperature (T_h) at which ΔH has acquired a high value (*Figure 19*). The low frequency side of the spectrum originates from

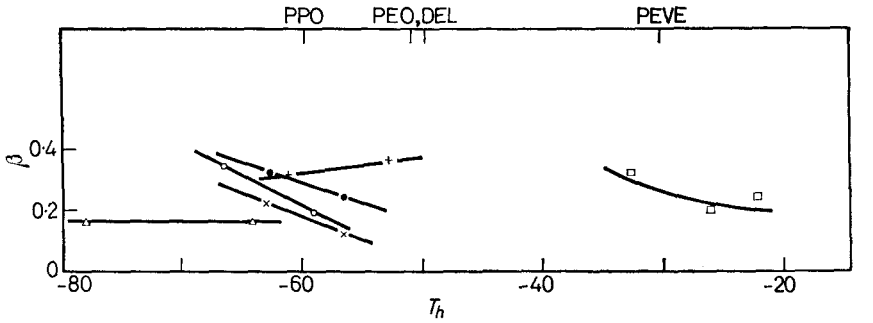

Figure 23—Temperature variation of β on the high frequency side of each spectrum. Legend: see *Figure 22*

the long relaxation times in the system. For polymer solutions this side of the mechanical spectra can be described by the theories of Rouse[3], Zimm[44] or Bueche[4]. These theories give qualitative agreement also with the long-time regions of spectra of bulk amorphous polymers. Thus, in the present context, the long-time side of the spectra might originate from a Rouse type of cooperative mechanism, with Gaussian segments as the basic units. For clarity this type of segment will be termed a 'Rouse segment'. However, this naïve idea cannot apply to the present system without modification.

Figure 24—A typical 50-bond 'Rouse segment'. X and Y are possible primary rearranging units

A typical Rouse segment is illustrated schematically in *Figure 24*. This has been drawn with 50 main chain σ bonds, since this is about the minimum length required for flexible chains to exhibit Gaussian distributions[45]. This segment must undergo rapid micro-Brownian motion through rearrangement of smaller units such as X and Y in *Figure 24*. Such units will be termed 'primary rearranging units', which might be roughly estimated at ten monomer units in length. It follows that any spectrum originating from the activation of primary rearranging units must lie at far shorter times than a spectrum originating from a Rouse mechanism. This means that if indeed a Rouse type of spectrum is being observed in any system

it cannot have contributions in the main region from relaxations of primary rearranging units.

All the systems shown in *Figure 22* exhibit a similar variation in width of the β plot with changing temperature. A spectrum produced completely by a Rouse mechanism would be shifted bodily along the time axis by changing temperature, without change in shape. We would expect this constancy of shape to hold even for a system loaded with rigid crystallites, as changing temperature merely alters the monomeric friction coefficient. The evidence thus points rather to the following interpretation. If the Rouse approach is employed the Gaussian segments must be replaced by smaller non-Gaussian segments which tend in the lower limit to the size of the primary rearranging units. There will now be contributions to the mechanical spectrum from both the cooperative modes of the small non-Gaussian segments and the individual relaxation times of the primary rearranging units.

The two different spectral contributions have similar time scales and the affected also by changing individual ΔH_1 to ΔH_n values as activation enthalpies governing the time scale of primary unit rearrangement.

Equation (3) represents an average relaxation time based on some average activation enthalpy. In fact there will be a large number of different possible primary rearrangements each characterized by its own activation enthalpy, giving rise to a set of relaxation times as follows:

$$\tau_1 = A_1 \exp(\Delta H_1/RT)$$
$$\tau_2 = A_2 \exp(\Delta H_2/RT) \quad \text{etc.} \ldots\ldots$$
$$\tau_n = A_n \exp(\Delta H_n/RT)$$

A natural consequence of the above set of relaxation times is that the spectrum should narrow as the temperature is raised. The increase in β values at higher temperatures shown in *Figure 22*, could be explained by a spread of activation enthalpies only ± 100 per cent from the average value. However, it is seen from *Figure 18* that the low frequency β values have been obtained in the same temperature range as that in which some average ΔH value undergoes rapid change. The spectrum will thus be affected also by changing individual ΔH_1 to ΔH_n values as activation becomes increasingly difficult at lower temperatures. At higher temperatures ΔH values are relatively constant and it is expected that β values will slowly increase with temperature as in the dielectric case[7, 43].

The slight upswing in β values shown in *Figure 22* at low temperatures may well be due to the progressive loss of spectral contributions from the modified Rouse spectrum as the temperature is lowered. Comparison of these absolute values of β shows that amorphous poly(ethylvinyl ether) has a considerably narrower spectrum than the partially crystalline polymers. Between themselves, however, the broad spectra of the partially crystalline polymers show no systematic trend with differing crystallinities.

On the high frequency side of each spectrum, it is apparent from *Figure 23* that the spectra are all broad and only slightly temperature dependent. There is a general trend for the width of the distributions to increase with increasing T. The Rouse theory does not provide even qualitative agree-

ment with the high frequency side of the relaxation spectra of bulk polymers. In this short-time region the spectrum will result predominantly from the ΔH distributions postulated above, with only minor contributions from Rouse effects. The values for poly(ethylvinyl ether) are similar to those of the partially crystalline polymers, again indicating that this side of the spectrum arises from very localized mechanisms in an environment which is basically glass-like on these time scales.

Crystalline melting transition

It has already been shown (*Figures 6* and *10*) that Polyox and poly(tetramethylene oxide) exhibit strong tan δ peaks at the crystalline melting points. They are similar to the crystalline melting peaks in the poly(ethylene) copolymers studied by Jackson, Flory, Chaing and Richardson[5]. These loss peaks are different in origin to the various crystal disordering transitions observed in many polymers well below the melting point[35], e.g. the tan δ peaks in the present work have no loss modulus peaks associated with them and are incapable of yielding peaks in the frequency plane. Moreover the peaks are centred on the crystalline melting point. The magnitude of the tan δ peaks increases with decreasing frequency, even when allowance has been made for the rapidly changing background due to viscous flow. From *Figures 6* and *10* it is evident that there is a small shift in loss peak location with frequency. Formally these shifts are described by equation (3), with activation enthalpies of 300 kcal mole^{-1} and 570 kcal mole^{-1} for poly(tetramethylene oxide) and Polyox respectively.

One explanation of these loss peaks is that localized crystallite melting may occur to relieve strain in neighbouring amorphous regions, with recrystallization occurring during the low stress part of the cycle. If recrystallization does not occur, then the system will change with time becoming more amorphous as cyclic stressing continues. The experimental facts so far known do not suggest this and it is difficult to understand also how this mechanism of elastic loss can persist even a few degrees above the accurately known thermodynamic melting points. No other explanation has been offered.

Effect of crystallinity on mechanical loss peaks

The two samples of poly(propylene oxide) measured were approximately 20 per cent and 50 per cent crystalline. The two poly(ethylene oxide) samples also differed in crystallinity. However, *Figures 13* and *14* show that neither polymer exhibits any significant change in loss peak location or in activation enthalpy with differing crystallinities. *Figure 22* shows that the low frequency breadth of the spectrum increases slightly with increasing crystallinity in the range 20 to 60 per cent. These facts show clearly that variation in crystallinity produces no significant change in mobility of the amorphous regions.

There has been a dispute in the literature as to the dependence of loss peak areas on the degree of crystallinity. In poly(ethylene) for example the area under the low temperature (γ) tan δ versus temperature peak is approximately proportional to the fraction of amorphous phase[47]. Illers *et al.*[48], however, consider that the G'' area is a more correct measure of

the strength of a transition. The γ peak in poly(ethylene), expressed as G'', shows little variation with crystallinity and so they consider that the process occurs equally in both crystalline and amorphous phases.

The analysis by Read and Williams[34] of loss peak areas for any relaxation process, provides an alternative approach to the problem. The following equations hold for a single relaxation time, but their form is unchanged for any temperature-independent relaxation time distribution.

$$\int_0^\infty G'' \quad \mathrm{d}(1/T) = (G_U - G_R)\, R\pi / 2\Delta H \tag{13}$$

$$\int_0^\infty \tan\delta \quad \mathrm{d}(1/T) = \{(G_U - G_R)\, R\pi\} / \{(G_U G_R)^{1/2}\, 2\Delta H\} \tag{14}$$

The left hand sides of equations (13) and (14) represent the areas under respectively G'' and tan δ versus $(1/T)$ loss peaks. Over limited temperature ranges the area under any peak versus T will follow the same variations as the data plotted against $(1/T)$. Now we find that for the present systems ΔH is independent of crystallinity. Thus in equations (13) and (14), ΔH is constant for a given polymer and the loss peak areas depend only on the unrelaxed (G_U) and relaxed (G_R) moduli on either side of the transition. With increasing crystallinity both G_U and G_R increase. However, for the main glass transition (β) peak G_U is usually $\sim 10^{10}$ dyne cm^{-2} while for low degrees of crystallinity G_R is usually 10^8 to 10^9 dyne cm^{-2}. Thus, from equation (13), the G'' loss peak area is dominated by the G_U value and as this increases with increasing crystallinity the peak area also should *increase*. This effect, which is contrary to that expected from a superficial examination, is clearly illustrated by both systems in *Table 4*. Even though the absolute values of crystallinity are uncertain the order of increasing crystallinity should be reliable since it follows the density of the material.

Table 4

Polymer	*G'' loss peak area at 100 c/s*	tan δ *loss peak area at 100 c/s*
PPO 20% cryst.	51·7 dyne cm^{-2} (°C)$^{-1}$	530 arb. units
PPO 50% cryst.	74·0 dyne cm^{-2} (°C)$^{-1}$	376 same units
PEO 40% cryst.	54·7 dyne cm^{-2} (°C)$^{-1}$	408 same units
PEO 60% cryst.	57·5 dyne cm^{-2} (°C)$^{-1}$	447 same units

The respective G_U and G_R values are listed in *Table 5*.

Table 5

Polymer	*G_U dyne cm^{-2}*	*G_R dyne cm^{-2}*
PPO 20% cryst.	$9{\cdot}7\times10^9$ (−70°C)	$2{\cdot}4\times10^8$ (−20°C)
PPO 50% cryst.	$1{\cdot}5\times10^{10}$ (−70°C)	$6{\cdot}0\times10^8$ (−20°C)
PEO 40% cryst.	$1{\cdot}6\times10^{10}$ (−80°C)	$4{\cdot}8\times10^9$ (−20°C)
PEO 60% cryst.	$1{\cdot}7\times10^{10}$ (−80°C)	$6{\cdot}0\times10^9$ (−20°C)

With the tan δ loss peak areas, equation (14) shows that since G_R undergoes the most rapid change (on a logarithmic scale) with varying crystallinity, the denominator will dominate the behaviour of the expression. By comparison $(G_U - G_R)$ varies slowly, because this term is dominated by G_U. Thus equation (23) predicts qualitatively that as G_R increases with increasing crystallinity the tan δ area will *decrease*. This is the behaviour frequently assumed in the literature. Examination of *Table 4*, however, shows that although this effect is exhibited by poly(propylene oxide), poly(ethylene oxide) does not conform. The cause of the failure of this latter system to obey the generalized prediction lies in the relatively high degree of crystallinity. At these levels of crystallinity, it can be seen from *Table 5* that G_R is 5×10^9 dyne cm^{-2}, which is no longer negligible compared to G_U in the $(G_U - G_R)$ term.

When G_U and G_R values are even closer in magnitude, as frequently happens in low temperature γ transitions, $(G_U - G_R)$ remains roughly constant with increasing crystallinity due to similar increases in both moduli. The term $(G_U \cdot G_R)^{1/2}$, however, always increases with increasing crystallinity so that equation (23) predicts a *decrease* in tan δ. This has been observed by McCrum[49] for the γ transition of poly(tetrafluorethylene), in which the variation of tan δ peak area with amorphous content was almost linear.

Summarizing, we can say that G'' loss peak areas will rarely increase with increasing amorphous content. On the other hand tan δ loss peak areas usually will increase with increasing amorphous content; particularly favourable conditions occur in small γ transitions and in β transitions at low degrees of crystallinity.

CONCLUSIONS

G'' and ϵ'' loss peaks are governed by similarly weighted spectra. A comparison of loss peak positions shows that the activation enthalpy increases with decreasing temperature and in partially crystalline polymers a limiting low temperature value is observed.

In general the WLF time/temperature reduction scheme cannot be applied to the partially crystalline polymers because of temperature dependent relaxation time spectra. These spectra are broad with different β values (~0·2 to 0·5) for the low frequency and high frequency sides of the loss peaks. This also applies to the poly(ethylvinyl ether) data. Logical arguments lead to the conclusion that on the low frequency side of mechanical spectra a modified Rouse spectrum operates with contributions also from a distribution of activation enthalpies. On the high frequency side the spectrum is dominated by the activation enthalpy distribution.

The state of polymer chains in the amorphous regions of partially crystalline polymers is still unexplored. Modulus calculations[5] based on Gaussian chains give completely erroneous results. This suggests that the chains between crystallites are under considerable tension, yet the present data indicate that changing crystallinity does not appreciably affect chain mobility in the amorphous regions. We have shown too that whereas tan δ loss peaks will in favourable cases increase with increasing amorphous fraction of a polymer, G'' loss peaks will rarely, if ever, vary in this way.

The β loss peaks associated with the glass transition of all the polymers measured lie below 0°C. In addition poly(tetramethylene oxide) has a low temperature γ peak in the -150°C to -120°C range which may well arise from a local mode mechanism. Poly(ethylene oxide) and poly(tetramethylene oxide) both exhibit tan δ loss peaks at their crystalline melting points.

Department of Chemistry,
University of Manchester,
Manchester 13.

(*Received March 1966*)

REFERENCES

[1] WILLIAMS, M. L., LANDEL, R. F. and FERRY, J. D. *J. Amer. chem. Soc.* 1955, **77,** 3701
[2] KIRKWOOD, J. G. *J. chem. Phys.* 1946, **14,** 51
[3] ROUSE Jr, P. E. *J. chem. Phys.* 1953, **21,** 1272
[4] BUECHE, F. *J. chem. Phys.* 1954, **22,** 603
[5] JACKSON, J. B., FLORY, P. J., CHAING, R. and RICHARDSON, M. J. *Polymer, Lond.* 1963, **4,** 237
[6] WILLIAMS, G. *Polymer, Lond.* 1963, **4,** 27
[7] READ, B. E. and WILLIAMS, G. *Polymer, Lond.* 1961, **2,** 239
[8] THURN, H. in *Festschrift Carl Wurster der B.A.S.F. Dez. 1960,* p 321
[9] ISHIDA, Y. *Kolloidzschr.* 1961, **174,** 162
[10] MIKHAILOV, G. P. and EIDELNAUT, M. P. *Vyosokomol. Soedineniya,* 1960, **10,** 1552
[11] MCCRUM, N. G. *J. Polym. Sci.* 1961, **54,** 561
[12] ALLEN, G., CONNOR, T. M. and PURSEY, H. *Trans. Faraday Soc.* 1961, **59,** 1525
[13] CONNOR, T. M., READ, B. E. and WILLIAMS, G. *J. appl. Chem.* 1964, **14,** 74
[14] YIN, T. P., LOVELL, S. E. and FERRY, J. D. *J. phys. Chem.* 1961, **65,** 534
[15] WILLBOURN, A. H. *Trans. Faraday Soc.* 1958, **54,** 717
[16] SABA, R. G., SAUER, J. A. and WOODWARD, A. E. *J. Polym. Sci. A,* 1963, **1,** 1483
[17] SCHMEIDER, K. and WOLF, K. *Kolloidzschr.* 1953, **134,** 149
[18] WETTON, R. E. and WILLIAMS, G. *Trans. Faraday Soc.* 1965, **61,** 2132
[19] READ, B. E. *Polymer, Lond.* 1962, **3,** 529
[20] HAMMER, C. F., KOCH, J. A. and WHITNEY, J. F. *J. appl. Polym. Sci.* 1962, **57,** 395
[21] POWELL, E. *Ph.D. Thesis,* University of Manchester, 1963
[22] BAILEY Jr, F. E., KUČERA, G. L. and IMHOF, I. D. *J. appl. Polym. Sci.* 1959, **1,** 56
[23] PRICE, F. P. and KILB, R. W. *J. Polym. Sci.* 1962, **57,** 395
[24] BOOTH, C., HIGGINSON, W. C. E. and POWELL, E. *Polymer, Lond.* 1964, **5,** 479
[25] ALLEN, G., BOOTH, C. and JONES, M. N. *Polymer, Lond.* 1964, **5,** 195 and 257
[26] ALLEN, G., BOOTH, C., JONES, M. N., MARKS, D. and TAYLOR, W. D. *Polymer, Lond.* 1964, **5,** 547
[27] BRUCE, M. J. and FARREN, D. *Polymer, Lond.* 1963, **4,** 407
[28] MANSON, J. A. and ARQUETTE, G. J. *Makromol. Chem.* 1960, **37,** 187
[29] LORD, P. and WETTON, R. E. *J. sci. Instrum.* 1961, **38,** 385
[30] WETTON, R. E. *Ph.D. Thesis,* University of Manchestesr, 1962
[31] ATTREE, V. H. *Electronic Engng.* 1955, **27,** 308
[32] TIMOSHENKO, S. and GOODIER, J. N. *Theory of Elasticity,* p 304. McGraw-Hill: New York, 1951
[33] Discussed by BOYER, R. F. *Rubber Chem. Technol.* 1963, **36,** 1303
[34] READ, B. E. and WILLIAMS, G. *Trans. Faraday Soc.* 1961, **57,** 1979
[35] SAITO, N., OKANO, K., IWAYANAGI, S. and HIDESHIMA, T. *Solid State Physics,* Vol. XIV, p 343 (Ed. SEITZ and TURNBULL). Academic Press: New York, 1963
[36] ILLERS, K. H. and JENKEL, E. *Rheol. Acta,* 1958, **1,** 322
[37] SLICHTER, W. P. *Makromol. Chem.* 1959, **34,** 67
[38] THURN, H. and WOLF, K. *Kolloidzschr.* 1956, **148,** 16

[39] McCRUM, N. G. and MORRIS, E. L. British Polymer Physics Group Meeting, Shrivenham, April 1964
[40] WILLIAMS, G. *Trans. Faraday Soc.* 1963, **59,** 1397
[41] BECKER, G. W. *Kolloidzschr.* 1955, **140,** 1
[42] DEBYE, P. *Polar Molekulen.* Springer: Leipzig, 1929
[43] FUOSS, R. M. and KIRKWOOD, J. G. *J. Amer. chem. Soc.* 1941, **63,** 385 and 2401
[44] ZIMM, B. H. *J. chem. Phys.* 1956, **24,** 269
[45] FLORY, P. J. *Principles of Polymer Chemistry,* Chapter X. Cornell University Press: Ithaca, N.Y., 1953
[46] KASTNER, S., SCHLESSER, E. and POHL, G. *Kolloidzschr.* 1963, **192,** 21
[47] DEELEY, C. W., KLINE, D. E., SAUER, J. A. and WOODWARD, A. E. *J. Polym. Sci.* 1958, **28,** 109
[48] ILLERS, K. H., KILIAN, H. G. and KOSFELD, R. *Ann. Rev. phys. Chem.* 1961, **12,** 49
[49] McCRUM, N. G. *J. Polym. Sci.* 1959, **34,** 355

Regular Alkylene Ether Copolymers

T. P. HOBIN

Mixed triglycols, $HO(CH_2)_xO(CH_2)_yO(CH_2)_xOH$, *where x is not less than six, undergo acid-catalysed polycondensation to give regular alkylene ether copolymers* $[(CH_2)_xO(CH_2)_yO(CH_2)_xO]_n$. *Melting temperatures and crystallization rate data have been obtained for several of these copolymers.*

α-ω-GLYCOLS with six or more linked methylene groups will undergo acid-catalysed polycondensation to give polyethers[1, 2]. It was anticipated, therefore, that the appropriate mixed triglycols would likewise yield mixed polyethers. Regular alkylene ether copolymers have not been reported previously. An earlier paper by Lal and Trick[3] compared melting and crystallization rate data for alkylene sulphide polymers and regular copolymers and alkylene ether homopolymers. The present work enables the comparisons to be extended to regular alkylene ether copolymers.

EXPERIMENTAL

Preparation of mixed triglycols

The diol $HO(CH_2)_xOH$ (3 moles) was stirred with boiling toluene (300 ml) while a solution of sodium hydroxide (2 moles) in water (50 ml) was added slowly over two hours. A Dean and Stark attachment was used to isolate the water which condensed from the vapours (approximately 50 ml). A solution of the dibromide $Br(CH_2)_yBr$ (1 mole) in toluene (100 ml) was added slowly during half an hour and the mixture finally stirred under reflux for one hour. The precipitated solids were removed by filtration through a sintered glass filter and the excess diol was removed by vacuum distillation. The residual crude triglycol was washed with small quantities of water and the aqueous phases extracted with ether to recover any dissolved triglycol. Pure triglycols were obtained by fractional vacuum distillation; they were white crystalline solids. Yields ranged from 40 to 50 per cent, based on the amount of dibromide used. There was always a higher-boiling residue of higher mixed glycols, amounting to 30 to 50 per cent by weight of the yield of the triglycol.

Preparation of regular copolymers

Mixed triglycol (20 g) and sulphuric acid (0·1 g) were heated together in a glass tube for 48 hours under vacuum (1 mm of mercury); the temperature being maintained at 180°C by an external *o*-dichlorobenzene vapour bath. A very fine nitrogen bleed was used to stir the mixture and to carry off the water produced during the polycondensation. The polymeric product was stirred with boiling methanol (100 ml), cooled, and the insoluble solids separated by filtration. These were treated with boiling methanol to dissolve out the lower-molecular-weight fractions. The residual polymers were hard brittle solids, brown in colour. The colouration developed slowly during the polymerization; it could be minimized by exclusion of light and air from the reactants.

Preparation of random copolymer

A copolymer containing approximately equal numbers of hexamethylene and decamethylene sequences was desired. Because about ten per cent of 1,6-hexanediol is converted to cyclic ether during polycondensation[1], ten per cent excess of this reagent was used. The two diols were heated with one half per cent by weight of sulphuric acid in *n*-decane for 24 hours to produce a low polymer; water was removed by a Dean and Stark apparatus. After washing with water and removal of *n*-decane by vacuum distillation the polymer was polymerized further by the sulphuric acid technique described above.

Characterization

Molecular weights of the triglycols were ascertained by acetylation. Intrinsic viscosities of the polymers were determined from measurements in benzene at 20°C over the concentration range 0·2 to 0·5 per cent. Melting points were measured in capillary tubes heated at 1°C per minute. For the copolymers melting points were also determined in dilatometers.

Dilatometric measurements

Dilatometers with inverted bulbs were used. The polymers, cast into sticks, were inserted into the open bulbs which were then sealed off while the portion of the bulb which contained the polymer was cooled in liquid nitrogen. The polymers were degassed by melting them in the bulbs under a high vacuum. After cooling, mercury was run into the bulbs without releasing the vacuum.

(a) *Melting temperatures*—The position of the mercury meniscus was measured as the temperature was raised by increments. From 10° below the melting temperature upwards, measurements at each temperature were checked at intervals until no change occurred in the course of an hour.

(b) *Crystallization rates*—These were measured at temperatures in the vicinity of 10°C below the melting temperatures. The time required for the volume to decrease to a value halfway between that of the liquid polymer (as read off from the extrapolated liquid cooling curve) and the solid polymer (read off from the melting curve) at the temperature of the measurement was ascertained. It was found that over the short range studied, the reciprocal of the half-time for crystallization was proportional to the temperature of crystallization and so the temperature corresponding to a half-time of crystallization of 30 minutes was readily calculated (T_{30}).

EXPERIMENTAL RESULTS

The experimental results are summarized in *Tables 1* and *2* and *Figures 1* and *2*.

DISCUSSION

The melting points of the copolymers were not very different from those of the corresponding triglycols. They are shown in relation to carbon/oxygen ratio in *Figure 1*. Curve *A* represents the homopolymers and is based on

Table 1. Mixed triglycols $HO(CH_2)_xO(CH_2)_yO(CH_2)_xOH$

x	y	M.pt °C	B.pt °C/mm Hg	Molecular weight		Microanalysis			
						Expected		Found	
				Calc.	Found	C	H	C	H
6	4	51	200/0·8	288	290	66·1	11·8	65·8	11·6
6	5	40	215/1·5	301	304	67·0	11·9	66·9	11·9
6	10	67	235/0·8	377	374	70·5	12·9	71·1	12·7
10	4	75	255/0·5	402	402	71·6	12·5	71·3	12·5
10	5	69	252/0·4	413	416	72·0	12·6	72·5	12·7
10	6	76	255/0·4	425	430	72·5	12·6	72·5	12·7

Table 2. Mixed polyethers $[(CH_2)_xO(CH_2)_yO(CH_2)_xO]_n$

x	y	M.pt °C		T_{30} °C	ΔT °C	C/O ratio	Intrinsic viscosity 20°C	Microanalysis			
								Expected		Found	
		Capillary	Dilato-meter					C	H	C	H
6	4	46–7	50·0	40·6	9·4	5·3	0·26	70·5	11·9	70·3	12·0
6	5	42–3	46·0	37·2	8·8	5·7	0·18	71·3	12·0	70·7	11·9
6	6	60	62·0	52·0	10·0	6·0	0·24				
6	10	64–65·5	67·5	57·4	10·1	7·3	0·26	74·1	12·5	74·6	12·6
10	4	71–2	73·2	63·5	9·7	8·0	0·41	74·9	12·6	75·1	12·4
10	5	70–71	72·3	61·3	11·0	8·3	0·20	75·3	12·7	75·5	13·0
10	6	74	76·5	65·5	11 0	8·7	0·25	75·7	12·7	75·6	12·8
Random 6/10		69	71·4	62·0	9·4	8·2	0·39			75·2	12·5

T_{30} denotes temperature at which half-crystallization occurs in 30 minutes.
ΔT denotes dilatometric m. pt$-T_{30}$.

the following melting points, polyethylene oxide 66°C[3], polytrimethylene oxide 38°C[4], polytetramethylene oxide 46°C[4] and polydecamethylene oxide 80°C[3]. The value used for polyhexamethylene oxide is given in *Table 2* ($x=6$, $y=6$). It is 4 deg. C higher than that obtained by Lal and Trick, who used the polarizing microscope technique on a sample of rather low molecular weight. Curve *B* represents copolymers containing only even-numbered sequences of methylene groups while curve *C* represents those

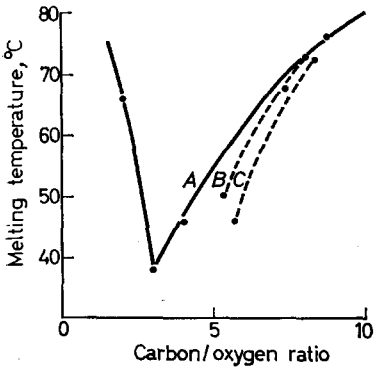

Figure 1—Melting points of the copolymers in relation to carbon/oxygen ratio—see text

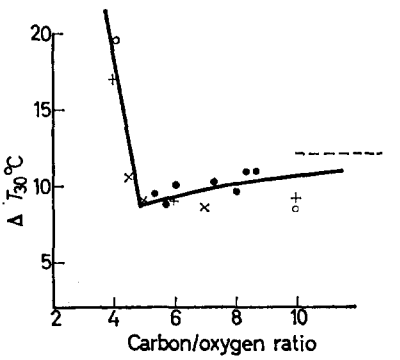

Figure 2—Rates of crystallization as measured by amount of supercooling to give a half-time of crystallization of 30 minutes versus C/O ratio: ● this work; ○ homopolyethers (Lal and Trick); + homopolysulphides (Lal and Trick); × sulphide copolymers (Lal and Trick); ----- ΔT_{30} polyethylene (Lal and Trick)

that contained some odd-numbered sequences of these. The result for the random 6/10 copolymer also lies on this curve. It can be seen that the regular copolymers had slightly lower melting points than the homopolymers but the differences decreased with increase in the C/O ratio and were insignificant when this ratio was greater than eight. The greater depression of melting point when the copolymer contained some odd-numbered sequences of methylene groups would appear to be another example of a general tendency for odd sequences to lower melting points[5].

The amount of supercooling to give a half-time of crystallization of 30 minutes (T_{30}) was used by Lal and Trick as a measure of rate of crystalliza-

tion. To enable a comparison, similar measurements were made on the present copolymers. The results plotted in *Figure 2* include Lal and Trick's data for polyethers and polysulphides (with the exception of their value for polyhexamethylene oxide, which has been omitted because of their low melting point result). It can be seen that most of the data lie within 1 to 2 deg. C of the drawn curve, which suggests that the amounts of supercooling required to give a half-time of crystallization of 30 minutes are much the same for corresponding polysulphides and polyethers irrespective of whether they are homopolymers or regular copolymers.

Explosives Research and Development Establishment,
Waltham Abbey, Essex

(*Received January 1966*)

REFERENCES

[1] HOBIN, T. P. and LOWSON, R. T. *Polymer, Lond.* 1966, **7**, 219
[2] HOBIN, T. P. *Polymer, Lond.* 1966, **7**, 225
[3] LAL, J. and TRICK, G. S. *J. Polym. Sci.* 1961, **50**, 13
[4] SIMS, D. Private communication
[5] BUNN, C. W. *J. Polym. Sci.* 1955, **16**, 323

*The Present Status of the Theory of Rubber Elasticity**

G. GEE

In this review a modified equation for the free energy of a single chain is proposed, based on a recent discussion of the excluded volume problem. A simple model of a network element is used to study departures from affine behaviour and the form of the stress/strain curve. Comparison with the Mooney equation suggests that the C_2 term cannot be explained in terms of excluded volume, and it is suggested that the packing problem requires further study. Energy and volume changes on elongation are reviewed and the need for further work emphasized.

(1) *Introduction*

IT IS not possible, in the course of a single lecture, to review all facets of the theory of rubber elasticity. Comments will therefore be centred on two topics of current interest: (*a*) the form of the stress/strain curve, and its dependence on chain statistics; (*b*) the volume and energy changes accompanying elongation.

The quantitative interpretation of rubber elasticity[1] rests firmly on the use of Gaussian statistics to describe the behaviour of a single chain. The elastic network is then treated as an assembly of chains, with the assumption —which can be justified for Gaussian chains—of affine deformation of the junction points. From time to time the suggestion has been made that some of the observed discrepancies between theory and experiment may have their origin in departures from Gaussian statistics. It is well known that a free chain, in a neutral environment, is not Gaussian, due to the excluded volume effect. In a dilute solution the overall dimensions depend upon the nature of the solvent, and much use has been made of theta solvents, defined[2] as those in which the laws of ideal solutions hold at finite (low) concentrations. Under these circumstances the net excluded volume effect is zero, the expansion due to this cause being balanced out by the contraction occurring in a thermodynamically poor solvent. It is also generally accepted[3,4] that in a bulk polymer, the effective excluded volume must be zero, because the local structure is determined by interactions of segments, in which it is a matter of indifference whether these belong to the same or to different molecules.

Quantitative analysis of the behaviour of networks of non-Gaussian chains raises two problems: (*1*) the description of the properties of a single chain, and (*2*) the study of possible departures from affine deformation. In this paper we make use of a recent treatment of the statistics of an infinite chain to define a parameter which can be used to describe departures from Gaussian statistics. The resulting free energy equation is then used in an accurate study of a 'network' of four chains, where departure from affine behaviour can be determined.

*This review was prepared during the tenure of a Fellowship of the Michigan Foundation for Advanced Research, Midland, Michigan, U.S.A., and was presented at the Great Lakes Conference on Polymer and Colloid Science, Detroit, Michigan, U.S.A., October 1965.

(2) *The single molecule*

The simplest theories of rubber elasticity[1] treat a linear molecule as a random chain, made up of n links of length l, in which there are no restrictions on orientation. If one end of the chain is fixed, the probability $P(r)$ of finding the other end in a specified volume element dv at a distance r is given by

$$P(r)\,dr=(\tfrac{2}{3}\pi nl^2)^{-3/2}\exp(-3r^2/2nl^2)\,dV \tag{1}$$

It is seen that $P(r)$ has a maximum at $r=0$, i.e. the most probable point at which to find the chain end is coincident with the beginning. The probability $W(r)$ of finding the end at a distance between r and $(r+dr)$ is then

$$W(r)\,dr=4\pi r^2P(r)\,dr \tag{2}$$

which has a maximum at $r_{max.}=(\frac{2}{3}nl^2)^{\frac{1}{2}}$. The mean square of r is easily shown to be

$$\langle r^2\rangle_0=nl^2 \tag{3}$$

This quantity $\langle r^2\rangle_0$ plays a central role in all theories of rubber elasticity and a reconsideration of its evaluation is one of the principal objectives of current work. Three factors have received attention, concerned with: (*a*) the recognition that the angle between consecutive links is fixed by valency considerations; (*b*) the fact that rotation about a single bond involves changes of energy, so that certain orientations are favoured; (*c*) the fact that molecules occupy a finite volume, so that conformations involving simultaneous occupation of a given volume element by two links are impossible. Of these the first introduces no modifications which cannot be allowed for by redefining n and l, subject to the condition that nl is the outstretched length of the molecule.

Energy barriers to rotation also leave the form of equation (3) unchanged, but $\langle r^2\rangle_0$ becomes a function of temperature. If we consider a chain in which each link has effectively a choice of two orientations, which differ in energy by ΔE, then[5]

$$d\ln\langle r^2\rangle_0/dT\approx\Delta E/RT^2 \tag{4}$$

The experimental study of this equation has been one of the most fruitful of recent developments. It will be noted that to maintain equation (3), if $\Delta E\neq 0$, n and l must be temperature dependent.

The effect of finite volume has proved difficult to treat quantitatively. Physically it is evident that exclusion of the more folded configurations must expand and broaden the distribution. Monte Carlo calculations on lattice models have led to the result[6]

$$\langle r^2\rangle_0\sim n^{1+\gamma} \tag{5}$$

where, for long chains, $0{\cdot}22>\gamma>0{\cdot}18$. Schatzki[7] has also tabulated distributions of end to end distances, from which it is possible to derive numerically[8] $P(r)$ and $W(r)$. These suffer from the fact that the particular lattice model chosen necessarily imposes a certain discontinuity, although Domb[9] has shown that all lattices give similar values of γ (equation (5)). Recently Edwards[10] has succeeded in obtaining an asymptotic solution in closed form for the position of the nth link of an infinite chain, which may

be written

$$P(r) \sim \exp\left[-(1{\cdot}35/nl^2)\,(r-0{\cdot}87n^{0{\cdot}6}la^{0{\cdot}2})^2\right] \tag{6}$$

where the volume excluded by a link is

$$v_{(ex.)} = al^3 \tag{7}$$

so that a appears in equation (6) as a numerical parameter. In the limit of $n \longrightarrow \infty$, this leads to a mean square end to end distance

$$\langle r^2\rangle_0 = 0{\cdot}755n^{1{\cdot}2}l^2a^{0{\cdot}4} \tag{8}$$

The exponent of n is here exactly $6/5$, giving γ (equation (5)) $= 0{\cdot}20$, in agreement with the lattice calculations.

For the purpose of this paper, it has been *assumed* that an equation of the form (6) is valid also for finite values of n. Although this will not be strictly true, it should suffice to indicate semi-quantitatively the consequences of departure from Gaussian statistics.

For application to the theory of elasticity, the distribution is conveniently expressed in terms of the configurational free energy of a chain whose ends are fixed at two specified points, a distance r apart. For a chain obeying Gaussian statistics, i.e. equation (1), this has the form

$$G = \text{const.} + (3kT/2nl^2)r^2 \tag{9}$$

If such a chain is deformed from an initial length r_i, to a final length r, the increase of free energy is then

$$\Delta G = (3kT/2nl^2)\,(r^2 - r_i^2) = (3kT/2nl^2)r_i^2(\lambda^2 - 1) \tag{10}$$

where λ is defined as r/r_i.

For non-Gaussian chains, G will no longer be linear in λ^2; numerical calculations have been reported[8] on the basis of Schatzki's work. If an equation of the form (6) holds, (9) and (10) must be replaced by

$$G = \text{const.} + (1{\cdot}35/nl^2)\,(r - r\star)^2 \tag{11}$$

$$\Delta G = (1{\cdot}35kT/nl^2)r_i^2\left[(\lambda - b)^2 - (1-b)^2\right] \tag{12}$$

If equation (6) held exactly we should have further

$$r\star = br_i = 0{\cdot}87\,la^{0{\cdot}2}n^{0{\cdot}6} \tag{13}$$

and we may guess that this is the correct limit as $n \longrightarrow \infty$.

The mean value of r^2 has been obtained as a function of b by numerical integration of

$$\langle r^2\rangle_0 = \frac{\int_0^\infty r^4 \exp\left[-(1{\cdot}35/nl^2)\,(r-r\star)^2\right] \mathrm{d}r}{\int_0^\infty r^2 \exp\left[-(1{\cdot}35/nl^2)\,(r-r\star)^2\right] \mathrm{d}r} \tag{14}$$

in terms of a further parameter $B = 1{\cdot}35r\star^2/nl^2$. The limiting form for $B \longrightarrow 0$ is readily shown to be

$$Y = \langle r^2\rangle_0/1{\cdot}111\,nl^2 = 1 + 0{\cdot}755\,\sqrt{B} = 1 + 0{\cdot}88\,b\,\sqrt{Y} \tag{15}$$

which may be compared with the known solution for small departures

from Gaussian statistics

$$\langle r^2\rangle_0/nl^2 = 1 + 0{\cdot}421\, a\sqrt{n} \tag{16}$$

Equating (15) and (16) (ignoring the factor 1·111) leads to

$$r^\star \longrightarrow 0{\cdot}48\, l\, a\, n \tag{17}$$

A general equation for $r^\star$, and therefore for b, should have equations (13) and (17) as limiting forms. For the purpose of this paper we simply treat b as a parameter which is some sort of measure of the excluded volume, becoming zero for Gaussian chains.

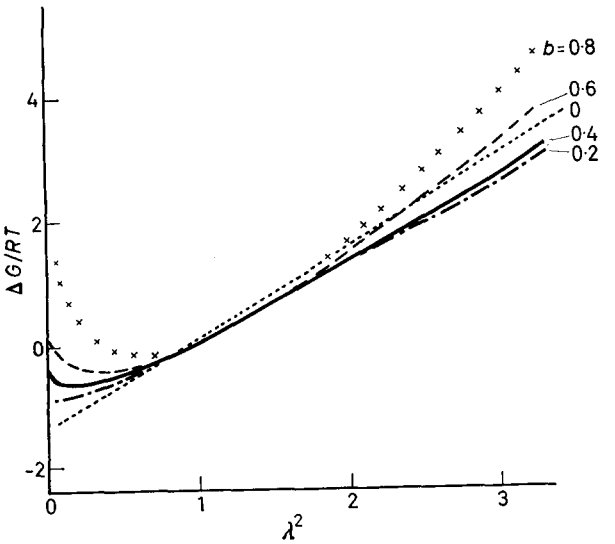

Figure 1—Effect of parameter b on chain free energy

Figure 1 gives a series of plots of ΔG against λ^2 for b between 0 and 0·8. The curves are qualitatively similar to those previously derived from Schatzki's data, but exact agreement is not expected, since in the latter elongation ratios were computed relative to $r_{max.}$, instead of to $\langle r^2\rangle_0$ (which is more difficult to estimate reliably). This has the effect of tilting the free energy curve; allowing for this, our calculations from Schatzki's data for $n=60$ give results very similar to those of *Figure 1* for $b=0{\cdot}6$.

(3) *The network*

In a normal crosslinking procedure, we start with a system consisting of a close-packed assembly of long molecules, free to move and to change shape and position subject to the requirement of constant volume. Chemical reagents are introduced and are molecularly dispersed uniformly throughout the system. Chemical reaction occurs, in which the effective reagent is a very small part of a polymer molecule, so that each molecule may possess (say) 10^4 reactive units. A small fraction (say one per cent) of these react, so that the chemical reaction is in no way influenced by the chain character

of the polymer. As a result of the chemical reaction the system now contains a large number of reacted points, and these will be randomly distributed in space. Each reacted point links together two of the original long molecules, and can now be thought of as a junction point from which four chains radiate. Most of these chains will terminate at some other junction point, and it is therefore convenient to speak of the length of molecule comprised between two junction points as a chain. A few chains will form a closed loop, returning to the same junction point. A number of chains equal to twice the original number of molecules will terminate in a free end. For most purposes, we can ignore both closed loops and free ends, and regard the structure as a perfect network.

When the body is deformed by the application of forces, the whole network must respond, and will of course do so in such a way that the increase of free energy is a minimum. It is frequently assumed that the network free energy is simply the sum of the free energies of the individual chains. If these are Gaussian, and a representative chain changes its end to end distance from r_i to r, the resulting free energy increase will be given by equation (10). To obtain an expression for the network free energy, we have still to solve two problems: to evaluate r_i; and to sum over all the chains.

The simplest forms of theory put $r_i^2 = \langle r^2 \rangle_0 = nl^2$, and thus obtain, for the representative chain,

$$\Delta G = 1{\cdot}5\, kT\, (\lambda^2 - 1) \tag{18}$$

The essential assumption involved in the summation is that each chain undergoes affine deformation, i.e. that its end to end distance changes proportionally to the bulk dimensions in the direction in which the chain lies. It then follows that if there are N chains in the network, and the total deformation is described by the three principal strains λ_1, λ_2 and λ_3, the total free energy of deformation is given by

$$\Delta G = 0{\cdot}5\, NkT\, (\lambda_1^2 + \lambda_2^2 + \lambda_3^2 - 3) \tag{19}$$

Wall and Flory[11] have argued that an additional term is required when the deformation involves a change of volume, to take account of the combination of the chains into a network; they modify (19) to

$$\Delta G = 0{\cdot}5\, NkT\, [\lambda_1^2 + \lambda_2^2 + \lambda_3^2 - \ln (\lambda_1\, \lambda_2\, \lambda_3) - 3] \tag{20}$$

The identification of r_i^2 with $\langle r^2 \rangle_0$ is based on the argument that any pair of segments in the linear polymer will on average be at this separation. When crosslinking occurs, the pair which form contiguous junction points become relatively fixed in position, and therefore retain this separation. This argument ignores a number of important considerations: (*a*) The value of $\langle r^2 \rangle_0$ which should be used is that appropriate to the conditions of crosslinking, which will typically involve a temperature much higher than that of the subsequent deformation. Unless $\langle r^2 \rangle_0$ is temperature-independent, chains which are at their most probable lengths when formed will no longer be so in the undeformed test piece used in a normal mechanical test. (*b*) Unless all the crosslinks are formed simultaneously, the growing fragments of network will tend to contract, thereby changing the statistics

of the chains already incorporated. The reality of this tendency to contract is illustrated by the observation that crosslinking in dilute solution may be followed by syneresis of free liquid. The equilibrium here involves a balance between network contraction and the swelling (osmotic) pressure of the liquid, which will be operative even if all the crosslinks are formed at the same instant.

Considerations such as these make it desirable to modify equation (19) [or (20)] by a factor $\langle r_i^2\rangle/\langle r^2\rangle_0$ which Tobolsky *et al.*[12] have called the 'front factor'. Recent discussion has been concerned with the temperature and volume dependence of this factor. From the foregoing argument $\langle r_i^2\rangle$ is seen to represent an average of the chains as they exist in a test sample at the *start* of a deformation experiment. If we compare one experiment with another under different conditions (of temperature, pressure or state of dilution by a swelling agent) it is reasonable to assume $\langle r_i^2\rangle \propto V_0^{2/3}$ where V_0 is the volume of the undeformed sample in a particular experiment. It is clear that $\langle r_i^2\rangle$ cannot change *during* an experiment, since it refers specifically to the initial conditions.

$\langle r^2\rangle_0$ refers to free chains as they would exist under the conditions of the experiment. It is an implicit assumption of the whole analysis that $\langle r^2\rangle_0$ will depend *only* on the temperature, and will therefore remain constant during any *isothermal* experiment. The most general form in which to express equation (20) is therefore

$$\Delta G = CV_0^{2/3}\, T\psi(T)\,[\lambda_1^2+\lambda_2^2+\lambda_3^2-\ln(V/V_0)-3] \tag{21}$$

where $\psi(T)$ accounts for the temperature dependence of $\langle r^2\rangle_0$. Applying this equation to simple elongation, $\lambda_1 = L/L_0$; $\lambda_2^2=\lambda_3^2=L_0V/LV_0$. If we also set $L_0^3 = V_0$, we obtain

$$\Delta G = CT\psi(T)\,[L^2+2\,V/L-\ln(V/V_0)-3] \tag{22}$$

For most purposes, the expansion accompanying elongation of a solid elastomer at constant pressure and temperature is entirely negligible, and the stretching force is then given by

$$f = 2\,CT\psi(T)\,[L-V/L^2] \tag{23}$$

where C is predicated to be independent of T and V.

Assuming the validity of this equation, we can use it in conjunction with standard thermodynamic equations to draw conclusions regarding the change in energy at constant volume, and the change in volume at constant pressure. Without further physical assumption, we obtain[3,13]:

$$f_e \equiv \left(\frac{\partial U}{\partial L}\right)_{T,V} = -fT\frac{\mathrm{d}\ln\psi(T)}{\mathrm{d}T} = fT\frac{\mathrm{d}\ln\langle r^2\rangle_0}{\mathrm{d}T} \tag{24}$$

and

$$\left(\frac{\partial V}{\partial l}\right)_{P,T} = \frac{\beta f}{\lambda^3-1} = 2\,\beta\,CT\psi(T)\,\lambda^{-2} \tag{25}$$

where β is the coefficient of compressibility.

The derivation of equations (21) to (25) has specificially assumed Gaussian statistics. If the representative chain is non-Gaussian, the analysis given is invalid. An attempt has been made[8] to investigate numerically the effect

of replacing equation (10) by a curve based on Schatzki's chain distribution data, retaining the crudest model of the network (three sets of mutually perpendicular chains). Uncertainties in the distribution curve made this inconclusive, but a similar analysis can now be made analytically by using equation (12). This leads straightforwardly to the result:

$$\phi \equiv \frac{f}{\lambda - \lambda^{-2}} = 0{\cdot}90\, NkT \frac{\langle r_i^2 \rangle}{nl^2} \left[1 - \frac{b\lambda^{1/2}}{1 + \lambda^{3/2}} \right] \tag{26}$$

This equation is of questionable significance, for any such analysis ignores a very important consequence of departure from Gaussian statistics: it is no longer permissible to assume affine deformation. To investigate this problem, some numerical calculations have been made on a simple model.

(4) *A tetrahedral model*

We consider four chains meeting at a junction point, with their other ends initially at the corners of a regular tetrahedron of volume V_0. A force (f) is now applied along the direction of one chain, so that the tetrahedron is deformed to a triangular pyramid of volume, $V = V_0 s^3$, and height λs times that of the tetrahedron. Denote by λ_1 the extension ratio of the axial

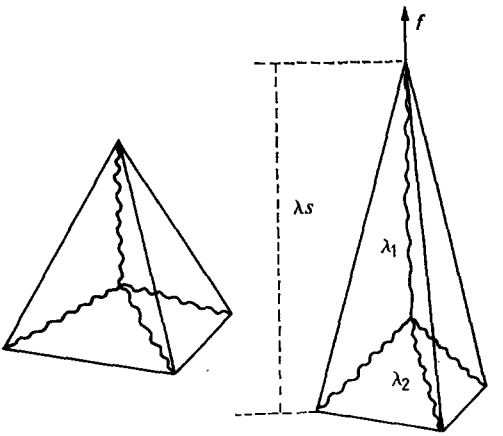

Figure 2—Tetrahedral model

chain, and by λ_2 that of the other three chains (*Figure 2*). The problems to be examined are: (*a*) the position of the junction point, and (*b*) the magnitude of the force.

The free energy is given by

$$\Delta G/C = (\lambda_1 - b)^2 + 3(\lambda_2 - b)^2 - 4(1 - b)^2 \tag{27}$$

and geometrical considerations require

$$\lambda_2^2 = (\tfrac{4}{3}\lambda s - \lambda_1)^2 + 8s^2/9\lambda \tag{28}$$

The position of the junction point will be such that $\partial G/\partial \lambda_1 = 0$, the solution to which is conveniently written in terms of $y = \lambda s - \lambda_1$

$$(4y+b)^2=\frac{9b^2\lambda\,(\lambda s+3y)^2}{8s^2+\lambda\,(\lambda s+3y)^2} \tag{29}$$

Since y is always small, this is easily solved numerically. The stretching force f is then given by:

$$f=(\partial G/\partial\lambda_1)_\lambda$$
$$=\frac{8s}{3}(\lambda_1-b)\left[1-\frac{s}{\lambda^2(4\lambda s-3\lambda_1)}\right] \tag{30}$$

These equations have been used in two series of computations:

(*i*) Taking $s=1$, $\lambda=\sqrt{6}$, ΔG has been plotted as a function of λ_1 (*Figure 3*) for several values of b. Affine deformation requires the minimum to occur at $\lambda_1=\lambda$; this is seen to apply for the Gaussian curve ($b=0$), but the other curves deviate substantially.

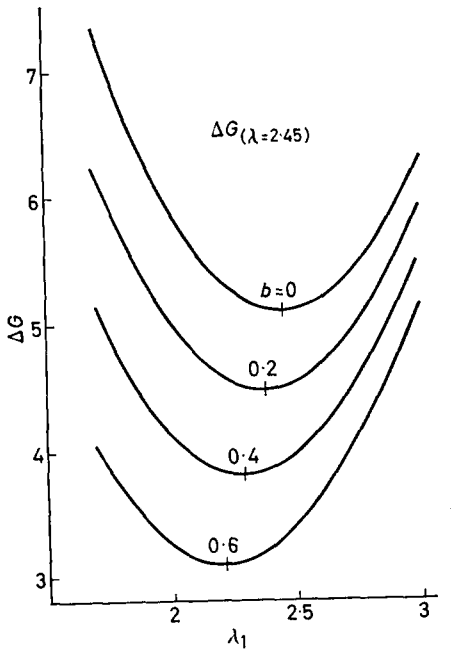

Figure 3—Dependence of ΔG on λ_1 at fixed $\lambda=2{\cdot}45$

(*ii*) Load/elongation curves were evaluated for a range of values of b and s. These are represented in *Figure 4* in the form of the function $\phi=fs^{-2}(\lambda-\lambda^{-2})^{-1}$, while the departure from Gaussian behaviour is shown in *Figure 5* by plotting $y/\lambda s$. It is easily seen, from the form of the equations, that these functions do not depend on b and s independently, but only on b/s. Thus while b will increase with dilution, its effect on the elastic behaviour of a network is compensated by the increase in s. For $\lambda>1$, $y/\lambda s$ shows a maximum at approximately 100 per cent elongation, representing a three per cent departure from affine deformation for $b/s=0{\cdot}2$. For the same b/s, the increase in ϕ from $\lambda=1$ is two per cent at $\lambda=2$, increasing to five per cent at $\lambda=3$, and eight per cent at $\lambda=4$.

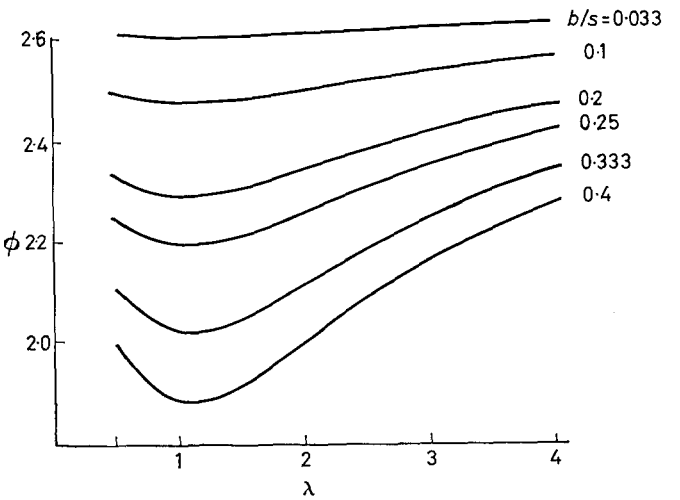

Figure 4—Dependence of ϕ on λ

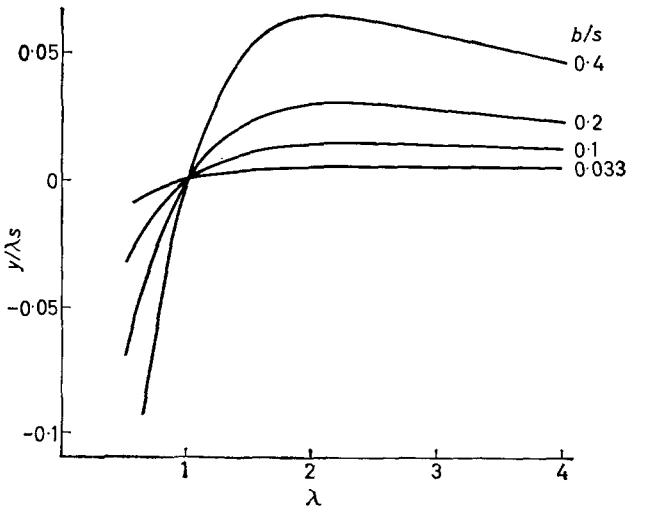

Figure 5—Departure from affine deformation

The Mooney equation—It is of interest to compare the results of these calculations with the observed behaviour of an elastomer. It has become customary to represent measurements made in simple elongation by means of the Mooney equation[14, 15]

$$f/2(\lambda-\lambda^{-2})=C_1+C_2/\lambda \tag{31}$$

which is generally found to hold fairly well over the range of elongation $1<\lambda<2$. If the polymer is swollen, the second term becomes less important, and the effect of swelling can be represented at least approximately by modifying equation (31) to the form[16]:

$$\phi = \frac{f\phi_2^{1/3}}{2(\lambda - \lambda^{-2})} = C_1 + \frac{C_2\phi_2^{4/3}}{\lambda} \tag{32}$$

where ϕ_2, the volume fraction of polymer in the swollen sample, is equivalent to $1/s^3$ in our analysis. The significance of the term C_2 has remained obscure, and some workers[17] have dismissed it as an experimental artefact.

It is not always sufficiently realized that the Mooney equation holds only over a very short range of λ. Combining Treloar's observations[18] on bi-axial deformation with Mullins's measurements[16] on elongation, two typical curves of ϕ versus $1/\lambda$ are reproduced in *Figure 6*, in which the

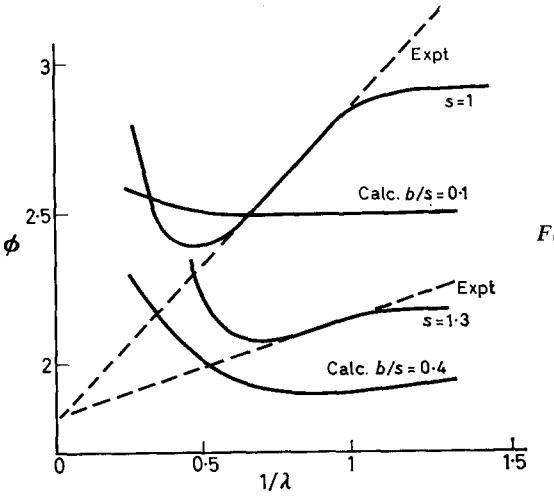

Figure 6—Dependence of ϕ on $1/\lambda$

broken lines represent equation (32). On the same figure are included two curves replotted from *Figure 5*. Comparison cannot of course be exact, since our model represents only a typical element of the network, deformed in a particular way. Nevertheless, two conclusions seem justified: (*1*) a very large ratio b/s would be needed to produce any detectable change in ϕ; (*2*) even with a large ratio b/s, the highly characteristic fall of ϕ from $\lambda=1$ to $\lambda=2$ is not reproduced at all. In the light of these observations, the suggestion made previously[8], that the C_2 term might be due at least in part to the excluded volume, must be withdrawn.

It is more difficult to make any positive contribution to the interpretation of C_2, more particularly since recent experimental work[19] has tended to contradict earlier evidence that C_2 does not vary widely. It may, however, be worthwhile to call attention again[20, 21] to the fact that the theoretical treatment ignores completely the problem of molecular packing in the solid state. This will greatly reduce the configurational entropy of the system, but will only contribute to the observed force if the packing free energy *changes* on deformation. DiMarzio[22] has recently concluded, on the basis of an admittedly crude analysis, that while this will indeed contribute to C_2, by itself it can account for no more than a small part of a typical value of

C_2. Before accepting this as a definitive result, it is pertinent to comment that the elastic free energy associated with the variation of ϕ in *Figure 6*, from $\lambda=1$ to $\lambda=2$, amounts only to 0·02 cal/cm³. This is only one tenth of the amount by which the entropy ($\times T$) of solid natural rubber has been estimated[23] (from solution thermodynamics) to fall short of the value for a random assembly.

(5) *Volume and energy changes on stretching*

For most purposes, it is a sufficiently good approximation to say that an elastomer elongates without change of volume. This cannot of course be strictly true, since the hydrostatic component of the tensile force must produce a dilation, whose magnitude is given, according to the network theory outlined above, by equation (25). Recently Tobolsky[24] has suggested that C in equation (23) may be volume dependent. The direct experimental determination of dilation is difficult, and equation (25) cannot yet be said to have been adequately tested. Strong, though indirect, evidence of its accuracy comes from a study of the thermoelastic behaviour of elastomers.

Equation (24) provides a basis for the interpretation of stress/temperature measurements; in conjunction with equation (4), valuable information becomes accessible on the energy differences between different rotational states of a chain. As it stands, equation (24) calls for temperature coefficients at constant *volume*, which have hitherto not been available. However, the constant pressure coefficients are readily converted, if the volume change is known. Assuming the dilation calculated from equation (25) to be correct, it is easily shown[3] that equation (24) is equivalent to

$$-\frac{\mathrm{d}\ln\langle r^2\rangle_0}{\mathrm{d}T}=\left[\frac{\partial\ln(f/T)}{\partial T}\right]_{P,L}+\frac{\alpha}{\lambda^3-1} \tag{33}$$

where α is the coefficient of cubical expansion. Flory and his co-workers have made a series of very careful measurements on a range of polymers, and have interpreted them by means of this equation. Their work may be illustrated by quoting some results[24] for atactic poly(isopropyl acetate):

λ	$-10^3\left[\frac{\partial\ln(f/T)}{\partial T}\right]_{P,L}$	$10^3\frac{\alpha}{\lambda^3-1}$	$10^3\frac{\mathrm{d}\ln\langle r^2\rangle_0}{\mathrm{d}T}$
1·134	1·78	1·50	0·28
1·214	1·07	0·87	0·20
1·256	1·00	0·70	0·30
1·305	0·81	0·56	0·25
1·364	0·68	0·45	0·23

The importance of the correction term $\alpha/(\lambda^3-1)$ is obvious, but the fact that the final column shows no systematic dependence on λ suggests that the dilation has been correctly estimated. Taken by itself, this evidence is far from compelling, as it is easily shown that a modification of equation (25) may change the figures in the last column without causing them to depend on λ. More convincing is the cumulative effect of a series of such investigations[25-29] in some of which an independent estimate of $\mathrm{d}\ln\langle r^2\rangle_0/\mathrm{d}T$

was obtained from dilute solution measurements. Moreover, the values obtained have several times been found consistent with calculations based on the energies of different chain conformations.

Current work should shortly lead either to complete confirmation of these conclusions, or to the need for a reassessment. Several investigators are re-examining the experimental problem of dilation measurements, with the hope of obtaining more definitive results. The direct measurement of temperature coefficients at constant volume has also been undertaken, but the preliminary results[30] which have been reported are not quite of the precision required.

SUMMARY AND CONCLUSIONS

The main stream of progress depends on a network theory in which the chains show Gaussian behaviour. This has achieved notable successes, but some caution is needed in accepting present evidence as a complete justification of all the details of the theory.

Perhaps the most striking recent advance is in the interpretation of the stress/temperature coefficient of a network in terms of the energy differences between rotational positions of a single chain. The good agreement found, both with measurements on dilute solutions and with theoretical values, is particularly convincing. It is clear, however, that this does no more than show the reality of this factor in determining the end to end distance of a chain; it is not by itself evidence concerning the distribution.

An attempt has been made here to assess the effects of departures from Gaussian behaviour consequent upon an excluded volume. Without claiming quantitative validity for the analysis, it seems justifiable to conclude that this would not modify the elastic properties of a network in the way empirically described by the C_2 term.

In principle, the most critical experiments which could be performed involve the use of samples swollen before and/or after crosslinking. There is evidence[31], however, that this introduces a new source of uncertainty, which is particularly important when we consider a polymer swollen to less than its saturation value, since the (negative) free energy of mixing is then large compared with that involved in network deformation. Closely related to this problem is the suggestion reiterated here that the C_2 term reflects, at least in part, changes of packing. It is clear that more detailed understanding of molecular arrangements in the solid polymer, both dry and swollen, is greatly to be desired.

I gratefully acknowledge discussion with S. F. Edwards of the use I have made of his work.

Department of Chemistry,
University of Manchester

(*Received January 1966*)

REFERENCES

[1] See, for example, TRELOAR, L. R. G. *The Physics of Rubber Elasticity*, Chapters 3 and 4. Oxford University Press: London, 1958.

[2] FLORY, P. J. *Principles of Polymer Chemistry,* p 425. Cornell University Press: Ithaca, 1953
[3] FLORY, P. J. *Trans. Faraday Soc.* 1961, **57,** 829
[4] BUECHE, F., KINZIG, B. J. and COVEN, C. J. *Polymer Letters,* 1965, **3,** 399
[5] FLORY, P. J., HOEVE, C. A. J. and CIFERRI, A. *J. Polym. Sci.* 1959, **34,** 337
[6] WALL, F. T. and ERPENBECK, J. J. *J. chem. Phys.* 1959, **30,** 634
[7] SCHATZKI, T. F. *J. Polym. Sci.* 1962, **57,** 337
[8] GEE, G. *Proceedings of the Natural Rubber Producers Research Association Jubilee Conference, Cambridge 1964,* p 125. Maclaren: Glasgow
[9] DOMB, C. *J. chem. Phys.* 1963, **38,** 2957
[10] EDWARDS, S. F. *Proc. phys. Soc., Lond.* 1965, **85,** 613
[11] WALL, F. T. and FLORY, P. J. *J. chem. Phys.* 1950, **18,** 108; 1951, **19,** 1435
[12] TOBOLSKY, A. V., CARLSON, D. W. and INDICTOR, N. *J. Polym. Sci.* 1961, **54,** 175
[13] KHASANOVICH, T. N. *J. appl. Phys.* 1959, **30,** 948
[14] MOONEY, M. *J. appl. Phys.* 1940, **11,** 582
[15] RIVLIN, R. S. and SAUNDERS, D. W. *Phil. Trans. A,* 1951, **243,** 251
[16] MULLINS, L. *J. appl. Polym. Sci.* 1959, **2,** 257
[17] CIFERRI, A. and FLORY, P. J. *J. appl. Phys.* 1959, **30,** 1498
[18] TRELOAR, L. R. G. *Proc. phys. Soc., Lond.* 1948, **60,** 135
[19] KRAUS, G. and MOCZVGEMBA, G. A. *J. Polym. Sci.* (*A*), 1964, **2,** 277
[20] GEE, G. *Trans. Faraday Soc.* 1946, **42,** 585
[21] VOLKENSTEIN, M. V. *Configurational Statistics of Polymeric Chains,* p 545. Interscience: New York, 1963
[22] DIMARZIO, E. A. *J. chem. Phys.* 1961, **35,** 658; 1962, **36,** 1563
[23] BOOTH, C., GEE, G., JONES, M. N. and TAYLOR, W. D. *Polymer, Lond.* 1964, **5,** 353
[24] TOBOLSKY, A. V. Private communication
[25] MARK, J. E. and FLORY, P. J. *J. Amer. chem. Soc.* 1965, **87,** 1423
[26] MARK, J. E. and FLORY, P. J. *J. Amer. chem. Soc.* 1965, **87,** 1415
[27] CIFERRI, A. HOEVE, C. A. J. and FLORY, P. J. *J. Amer. chem. Soc.* 1961, **83,** 1015
[28] OROFINO, T. A. and CIFERRI, A. *J. phys. Chem.* 1964, **68,** 3136
[29] MARK, J. E. and FLORY, P. J. *J. Amer. chem. Soc.* 1964, **86,** 138
[30] ALLEN, G., BIANCHI, U. and PRICE, C. C. *Trans. Faraday Soc.* 1963,**59,** 2493
[31] GEE, G., HERBERT, J. B. M. and ROBERTS, R. C. *Polymer, Lond.* 1965, **6,** 541

*The Infra-red Absorption Characteristics of Syndiotactic Poly(methyl methacrylate) from 1 050 cm^{-1} to 1 300 cm^{-1}**

S. HAVRILIAK, Jr and N. ROMAN

There are five (i.e. ν_1 to ν_5) infra-red absorption peaks associated with the ester group of s-poly(methyl methacrylate) while simple esters (i.e. methyl acetate) exhibit only one. These multiple absorption peaks do not arise because of specific intermolecular interactions because they persist in dilute solution. The multiple absorption peaks do arise because of specific intramolecular interactions because they disappear in copolymers of styrene. The implication being that a single ester group can be found in either one of two or perhaps four different rotational positions, each position is to be associated with a different force constant. The absorption characteristics could be described by the sum of seven Lorenz type dispersion functions each associated with a single absorption peak. From the Lorenz parameters the variation of integrated intensity (which is related to the population density in each environment) can be determined as a function of temperature. The integrated intensity was independent of temperature for all four peaks below the glass temperature: above the glass temperature they varied with temperature. However, the sum of the integrated intensities for peaks ν_1 and ν_2 as well as ν_3 and ν_4 was found to be independent of temperature over the entire experimental range. The implication is that the ester group can rotate from the environments associated with ν_1 to ν_2 or from ν_4 to ν_3 only above the glass temperature. Further experimental evidence indicates that the high temperature population distribution can be supercooled to room temperature. In addition, the dilute solution behaviour near room temperature is similar to the behaviour above the glass temperature for the solid polymer.

The location, relative intensity, polarization and sensitivity to polymer chain tacticity indicates that peaks ν_6, ν_7 may be associated with a planar zig-zag arrangement of the backbone carbon atoms.

THE infra-red (i.r.) absorption characteristics of poly(methyl methacrylate) (hereafter designated as PMMA) have been the subject of several investigations[1-5]. The object of most of these investigations was to describe the dependence of the i.r. absorption characteristics in terms of the stereoregular nature of the polymer chain. The differences in absorption characteristics between syndiotactic PMMA (i.e. *s*-PMMA) and isotactic PMMA (i.e. *i*-PMMA) were found to exist throughout the entire spectral region of 2 000 cm^{-1} to 650 cm^{-1}. The object of one investigation[1] was to sort out and identify which of these absorption peaks are due to C—H deformations. This object was achieved by a study of four differently isotopically substituted tactic polymers. These experiments clearly indicate which of the absorption peaks were associated with C—H deformations and to which chemical moiety each absorption peak belongs. Another set of absorption characteristics which were found to depend on the stereoregular nature of

*This paper was presented in part at the Phoenix American Chemical Society Meeting in January 1966: *Polymer Preprints*, 1966, 7, 253.

the polymer chain were the ester oxygen bands found between 1 050 cm^{-1} and 1 300 cm^{-1}. Although simple esters exhibit only one strong absorption peak centred at 1 200 cm^{-1} these polymer systems exhibit at least four peaks which are associated with the ester oxygen group. We set out, therefore, to investigate the origin of the multiple ester oxygen absorption peaks in *s*-PMMA.

EXPERIMENTAL

Polymers

The sample of *s*-PMMA from which the i.r. specimen was made was prepared by polymerizing pure methyl methacrylate monomer in liquid ammonia at $-80°C$ using the oxidation products of sodium as an initiator. The intrinsic viscosity in chloroform at 25°C indicated that the viscosity average molecular weight ($\overline{M}_v$) was $1{\cdot}93 \times 10^6$. The i.r. characteristics (*J* value)[5] indicated that the polymer sample was very highly syndiotactic. An n.m.r. study of the sample in chloroform indicated that at least 92 per cent of the monomer repeat triads[6] were syndiotactic. Solvent swelling with 4-heptanone crystallized the sample indicating the sequence of syndiotactic units to be very long.

A copolymer of methyl methacrylate (MMA) and styrene (S) was prepared by polymerizing a mixture of MMA and S in a 1:3 ratio. The reaction mixture was initiated free radically and terminated after a few per cent conversion was reached. This early termination allowed a study of the monomer addition sequence from their respective reactivity ratios[7]. The results of this analysis indicated the presence of two sequential MMA groups on the same chain to be below the i.r. level of detectability.

Instrumental

All the i.r. spectra were obtained using the Perkin–Elmer model 21 spectrophotometer under those conditions which would yield the maximum resolution, i.e. minimum slit width, maximum gain and slowest scan-speed. The spectra were usually obtained on an expanded scale.

Room temperature solution spectra were obtained using cells of matched thickness of conventional design (i.e. sodium chloride windows with lead spacers). Elevated temperature spectra of solutions were obtained by using similar cells mounted in a heated brass tube which is of conventional design. Solid phase spectra were obtained from specimens that were prepared by first filming a solution on to sheet silver chloride, followed by an evaporation of the solvent and finally drying *in vacuo* to romove traces of solvents.

The i.r. spectrum of *s*-PMMA exhibits six absorption peaks (designated as ν_1 to ν_6 inclusive in *Figure 1*) from 1 050 cm^{-1} to 1 300 cm^{-1}. The present results differ from those of Nagai[1] in that he did not observe peak ν_4 which is readily overlooked unless the spectrophotometer is operated under conditions of maximum resolution; otherwise the results appear to be identical. The polarization of peaks ν_1, ν_2, ν_5 and ν_6 are the same as those of Nagai; peak ν_4 is also sigma polarized. Nagai assigned peaks ν_1 and ν_2 to the coupled motion of the CCO group and peaks ν_3, ν_5 to the ester skeleton which also involved internal CH deformations. Peak ν_4 will be associated

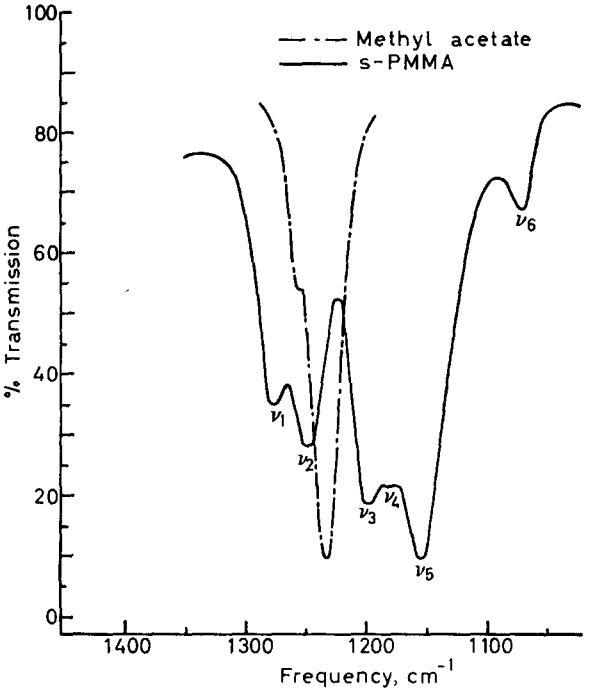

Figure 1—The i.r. spectrum of syndiotactic poly(methyl methacrylate) which is represented by the solid line exhibits at least five absorption peaks in the same region where methyl acetate which is represented by the dashed line exhibits a single absorption peak

with an ester vibration because of its location and relative intensity. These results, together with Nagai's tentative band assignments, are listed in *Table 1*.

Table 1. Absorption peaks in *s*-PMMA (1 050 cm^{-1} to 1 300 cm^{-1})

Peak designation	*Polarization*	*Frequency* cm^{-1}	*Nagai's tentative assignment*
ν_1	σ	1 268	ν_a(C—C—O) coupled with ν(C—O)
ν_2	σ	1 238	
ν_3	σ	1 192	Skeletal stretching coupled with internal C—H deformation
ν_5	σ	1 148	
ν_6	σ	1 060	Intramolecular
	Absorption peaks not observed by Nagai		
ν_4	σ	1 172	see text
ν_7	—	1 125	see text

Integrated peak intensity

The variation of the integrated peak intensity with temperature for the individual absorption bands was calculated from the temperature varia-

tion of the Lorenz parameters which were used to describe the absorption spectrum. These parameters were determined by first obtaining the i.r. spectrum at constant temperature under those conditions that would yield maximum resolution. The transmission was then calculated from the spectrum at 1·0 cm^{-1} intervals from 1 050 cm^{-1} to 1 300 cm^{-1} by assuming the scale to be linear, the specimen to be transparent at 1 600 cm^{-1} and 775 cm^{-1} and the zero per cent transmission determined by placing an opaque material in the sample beam. The absorbance was then calculated from the transmittance. The variation of the absorbance with frequency (from 1 050 cm^{-1} to 1 300 cm^{-1}) was calculated by assuming that each peak could be described by a Lorenz dispersion function[8] and that the absorbance at each frequency ν could be taken as the sum of all the absorption peaks absorbing at that frequency. The summation was performed on a Bendix G-15 computer, and the contribution from each peak at frequency ν was taken to be present. In other words

$$A_T(\nu)=\sum_i A_i(\nu)=\sum_i\{(\Delta\nu_i)^2 A_{0i}/[4(\nu-\nu_{0i})^2+(\Delta\nu_i)^2]\}$$

where $A_T(\nu)$ is the observed absorbance at frequency ν, $A_i(\nu)$ is the absorbance of peak i at ν, $(\Delta\nu_i)$ is the band width at half height, A_{0i} is the peak height which is located at frequency ν_{0i}. The initial values of the Lorenz parameters which were obtained by inspection of the absorption curve were varied until a minimum deviation between the calculated and observed absorbances was obtained.

The fit over most of the spectral region was found to be good except in two regions, namely 1 225 cm^{-1} and 1 125 cm^{-1}. The deviations in the 1 125 cm^{-1} were positive (i.e. observed values were larger than the calculated values). This difficulty was circumvented by postulating the existence of another absorption peak (ν_7) which is used to minimize the deviations between the observed and calculated absorbance values. It is not known whether this peak is real or whether ν_5 is unsymmetrical in this region. Assuming the existence of ν_7 is permissible for two reasons. First, an absorption peak at 1 120 cm^{-1} is consistent with the proposed model and second the integrated intensity is independent of temperature.

The second region of difficulty that was encountered (i.e. at 1 225 cm^{-1}) was thought at first to be serious because the deviations are in the middle of the ester group absorption region and the deviations are negative, i.e. the calculated values are larger than the experimental absorbances. However, extension of the measurements and data reductions to elevated temperatures revealed that these deviations (i.e. total area, band width and frequency) were independent of temperature and therefore presented no particular problem. The curves in *Figure 2* represent the extreme differences between the observed and calculated absorbances as a function of frequency at 30°C and 200°C. The magnitude and location of deviations observed at other temperatures are intermediate to these two. The average area associated with these negative deviations for all temperatures was found to be $3{\cdot}1 \pm 0{\cdot}2$ cm^{-1}. In *Figure 3* we have plotted the absorbance variation

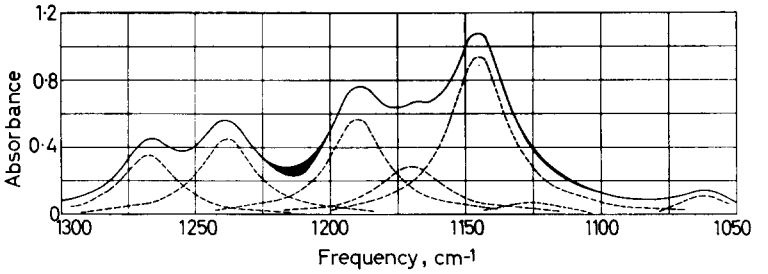

Figure 2—The absorption peaks of *s*-PMMA can be represented by seven Lorenz-type dispersion functions. The width of the line represents the difference between calculated and observed absorbance

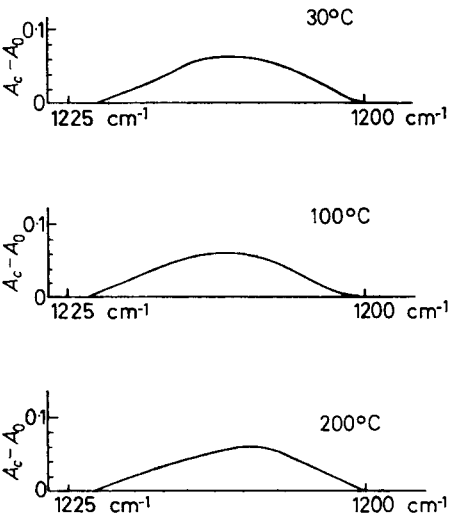

Figure 3—The difference between calculated and observed absorption is independent of temperature

with frequency from 1 300 cm^{-1} to 1 050 cm^{-1}, the width of the line represents the deviations between calculated and observed values (assuming the existence of ν_7). The Lorenz curves are represented by the dashed lines. The integrated intensity I_{0i} (ith peak) for a Lorenz absorption peak is given by[8]

$$I_{0i} = \tfrac{1}{2} \cdot 2{\cdot}303\pi \ \Delta\nu_i A_{0i}$$

The quantity A_{0i} is not the specific absorbance, therefore, I_{0i} is not the specific integrated intensity because no account was taken of the specimen thickness and area. This leaves A_{0i} unitless, therefore I_{0i} has the same units as $\Delta\nu_i$, namely cm^{-1}.

THE ESTER ASBORPTION (ν_1, ν_2, ν_3, ν_4 AND ν_5)

General background

In order to interpret the i.r. absorption characteristics of *s*-PMMA it is

necessary to review the structural nature of esters. Pauling and Sherman[9] observed that the esters are associated with much higher heats of formation than those computed from the corresponding ketones and ethers. They interpreted these higher heats in terms of a stabilization energy that was due to resonance. They reasoned that resonance would occur if the five atoms in the ester group maintained a planar conformation, there being two such arrangements, i.e.

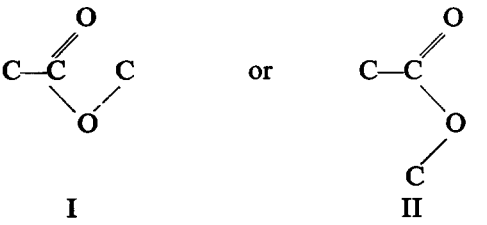

I II

Each of these two conformations would be associated with a different dipole moment, i.e. 1·8 *D* for structure I and 3·4 *D* for structure II. The experimental values of the dipole moment reported by Marsden and Sutton[10] for a wide variety of esters were found to be independent of temperature and fell in the range of 1·6 to 1·8 *D*, which supports structure I. In the compound γ-butyrolactone, conformation II is fixed by chemical bonds. The dipole moment[10] of this compound is 4·16, which is in fair agreement with the predicted value. The electron diffraction measurements of Schomaker *et al.*[11] on methyl acetate were interpreted in terms of a planar conformation for the five heavy atoms in the structure I arrangement. Further evidence for the ester group planarity was obtained by Wilmshurst[12] who interpreted the vapour phase i.r. absorption spectra of methyl formate and acetate in terms of a planar structure. The microwave measurements of Curl[13] on gaseous methyl formate and seven isotopically substituted species of the ester indicate that the ester group is planar with a type I arrangement.

Thompson and Torkington[14] have studied the i.r. spectra of esters of carboxylic acids and observed absorption bands at 1 160 and 1 185 cm^{-1} in the formates and analogous absorption bands at 1 245 cm^{-1} in the acetates. The weak absorption peaks at 1 185 cm^{-1} in the formates were readily interpreted by Korpovich[15] and Tabuchi[16] in terms of the existence of trace quantities of the planar II structure.

As a result of these observations, the ester group absorption spectrum of methyl acetate will be chosen as the basis of interpreting the ester absorption characteristics of the polymer and any deviations will be attributed to discrete structural considerations. In addition, it will be assumed that the ester group is a planar structure of form I with no possibility of internal rotations. The absorption characteristics of methyl acetate in the ester region are shown in *Figure 1* along with *s*-PMMA.

Multiple ester absorption peaks

In order to interpret the existence of five absorption peaks which are associated with the ester group in *s*-PMMA instead of the single peak observed in simple esters, we can proceed by considering the various ways

(environmental factors) which can cause multiple absorption peaks. For example, Stein[17] has shown that in crystalline polyethylene the single CH_2 wagging band observed in non-crystalline polyethylene is split into two components in crystalline polymer by means of intermolecular interactions. Therefore, in partially crystalline polyethylene it is possible to observe three absorption peaks which are associated with the CH_2 wagging vibration. Another source of peak splitting may come about from conditions similar to those described by Sutherland *et al.*[18] who have shown how the normal modes of vibration of the side group may be built up in terms of in-phase and out-of-phase vibrations in the zig-zag planar arrangement of the backbone carbon atoms. These are two of the several environmental factors by which a single absorption peak may be built up or split into several components. At this point it is convenient to divide the factors into two groups, i.e. intra- and inter-molecular factors. In each group one can list a variety of environmental factors, each of which is amenable to experimental verification.

Experimental results and discussion

In order to evaluate the intramolecular contributions as an environmental factor one need only compare the i.r. absorption characteristics of the polymer in a dilute solution with those of the polymer in the bulk phase. These spectra were obtained in a wide variety of solvents, among them are chloroform, chloroform-d, ethylene dichloride, toluene, benzene, benzene–cyclohexanol mixtures and carbon tetrachloride. In all cases the essential features of the i.r. spectra were the same, i.e. the five ester oxygen absorption peaks were always present. The solution spectrum of the polymer (0·5 per cent) in chloroform-d is reproduced in *Figure 4* because this solvent is transparent in the entire region of interest. As can be seen from

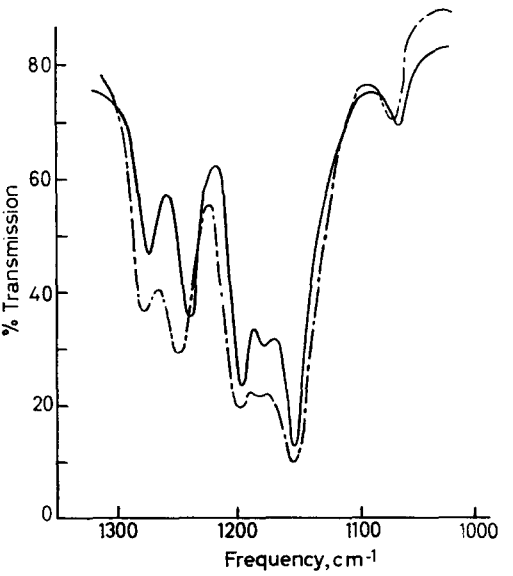

Figure 4—The solution spectrum of *s*-PMMA films which is represented by the solid line is similar to the absorption spectrum of films

that figure all the five ester oxygen absorption peaks are present. However, there has been an appreciable decrease in the band width indicating that intermolecular interactions are of the non-specific type.

In order to evaluate the intramolecular contribution as an environmental factor, one need only compare the spectrum of the MMA–S (1 : 3 mole ratio) copolymer to a blend of *s*-PMMA and PS in a ratio of 1 : 3. This copolymer was prepared in such a way that most of the ester groups along a single chain were separated from each other by phenyl groups. The i.r. spectrum of the copolymer is reproduced in *Figure 5*. As can be seen from this

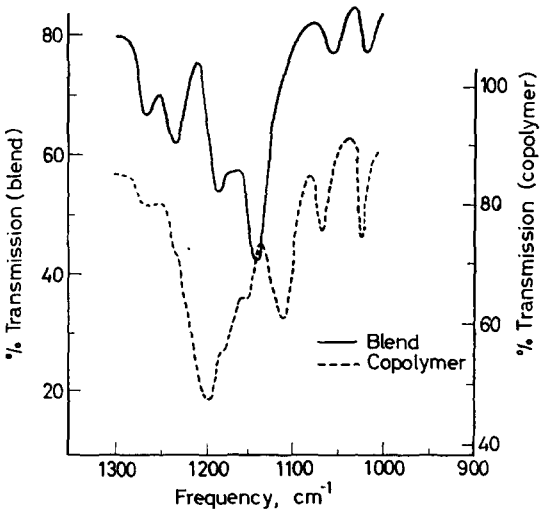

Figure 5—The multiple absorption peaks in *s*-PMMA disappear in the case of styrene–MMA copolymers

figure the four ester absorption bands have disappeared leaving only one ester oxygen absorption peak in the copolymer which is centred near 1 200 cm^{-1}. The reduction in the number of peaks indicates strongly that the perturbing causes for the multiple ester group absorptions are intramolecular factors.

Some information concerning the nature of these intramolecular factors can be obtained from thermal cycling measurements. The i.r. spectrum was obtained after allowing the specimen to come to thermal equilibrium. The data obtained in this way were free from any effects of hysteresis (open rings in *Figure 6*). The next experiment was to warm the i.r. specimen to 200°C followed by a quenching to dry ice temperature. The specimen was then allowed to warm to room temperature. The peak ratio was decidedly lower for the supercooled specimen, regardless of the length of time (days) the specimen was allowed to remain at room temperature. Another heating cycle was started and peak ratios determined from spectra obtained at constant temperature. The peak ratios (cross-hatched) remained lower than the original values (see *Figure 6*) until the glass temperature was reached. Above the glass temperature, the peak ratios were identical to the original values as they were for any succeeding cooling or warming runs (single hatched rings). The supercooled values could be obtained at will by quenching a heated specimen to dry ice temperatures. This experi-

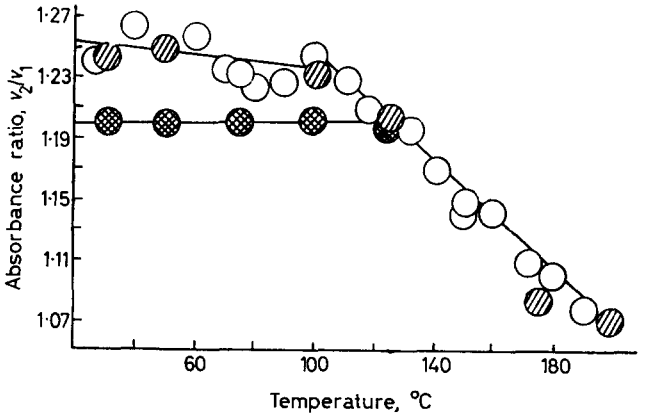

Figure 6—The absorbance ratios for the two peaks (ν_1/ν_2) are plotted as a function of temperature for slowly varying temperature studies and quenched studies

ment indicates that it is possible to supercool the high temperature ester conformation to room temperature, which evidence is consistent in terms of the side chain being found in either of two rotational sites but that the sites are no longer accessible to each other below T_g.

Additional information concerning the origin of four of these absorption peaks can be obtained from a study of the temperature variation of the integrated peak intensity. In the event that two absorption peaks are due to the same ester skeletal vibration, but the frequencies are different because the ester group can be found in either one of two different rotational positions which causes the force constants to be slightly different, the sum of the integrated intensities for the two peaks should be independent of temperature if the absorbance per ester group is the same for the two locations. On the other hand the ratio of the integrated intensities for the two peaks should vary with temperature as the number of ester groups increases in one of the sites at the expense of the number of ester groups in the other site. Therefore, a plot of $\log [I(\nu_1)/I(\nu_2)]$ versus $1/T$ should be a straight line if the population distribution between the two sites is controlled by Maxwell–Boltzmann statistics.

The observed behaviour of the ν_1, ν_2 pair of absorption peaks is just the predicted behaviour with a single variation. The average of the integrated intensities is $71{\cdot}3 \pm 0{\cdot}8\ \text{cm}^{-1}$ and independent of temperature. In addition the ratios of the integrated intensities (see *Figure 7*) varied from about 1·3 to 1·0 only above the glass temperature in what appears to be a linear fashion. Below T_g the ratio is independent of temperature. This observation implies that the rotational sites are accessible only above T_g while below T_g the sites are no longer accessible to each other.

The observed behaviour, and therefore the conclusions for the ν_3, ν_4 pair of absorption peaks is similar to that of the ν_1, ν_2 pair except that the experimental error associated with their determination is larger because of

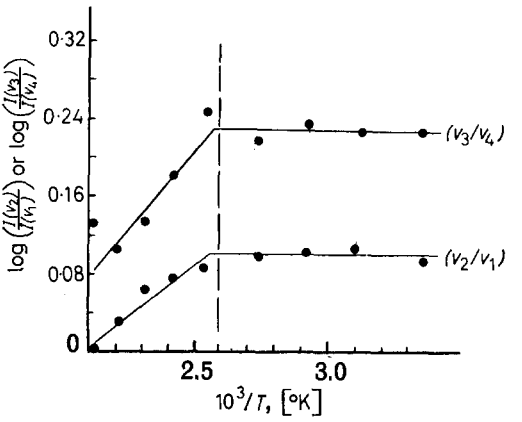

Figure 7—The variation of log absorbance ratio with reciprocal temperature is represented here

the greater overlap of the absorption bands (see *Figure 7*). In other words the average value for the integrated intensity of peaks ν_3 and ν_4 were independent ($77{\cdot}3 \pm 1{\cdot}4$) of temperature. In addition the ratio of the integrated intensity of the ν_3, ν_4 pair varied with temperature only above T_g.

The integrated intensity of peaks ν_5, ν_6 and ν_7 was found to be independent of temperature.

Some insight as to the nature of the forces restricting the reorientation of the ester side chain may be had from a study of the temperature dependence of the i.r. absorption characteristics in dilute solution. As before, in order to minimize the data reduction the ratio of peak heights (ν_2/ν_1) will be used. The measurements were made in matched thickness cells and the solvent was deuterated chloroform, because this solvent is transparent in the region of interest. The measurements were made at four temperatures between 25°C and 60°C, the results are shown in *Figure 8*. The

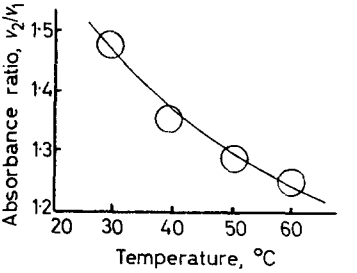

Figure 8—The variation of the absorbance ratio of the ν_2/ν_1 peaks determined in dilute solution is plotted against temperature

variation of this peak ratio in solution with temperature is similar to the variation observed above the glass temperature for the films. This observation indicates that the ester groups are redistributing themselves among the different sites below the glass temperature of the polymer, indicating that the restrictive forces are intermolecular and not intramolecular in this region.

Some insight as to the nature of the crystallization process for syndiotactic PMMA may be obtained by comparing crystallized with uncrystallized films. The crystallized films were prepared by first filming *s*-PMMA on to silver chloride backing material and then crystallizing the film with 4-heptanone. The solvent was then removed by evaporation. The i.r. spectrum is shown in *Figure 9*, along with the uncrystallized version. The

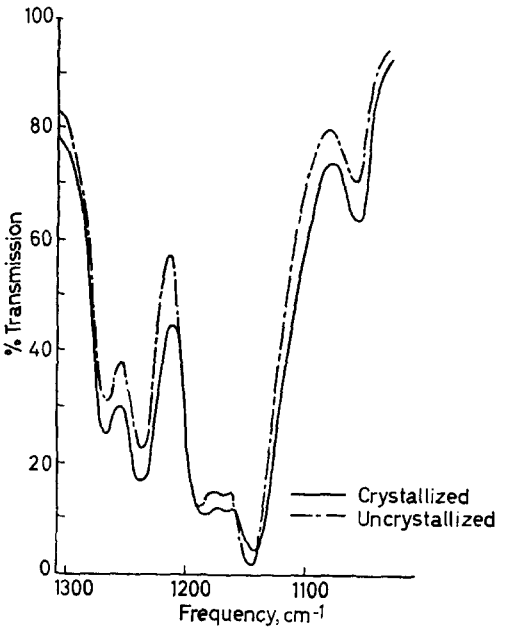

Figure 9—The absorption characteristics of crystallized and uncrystallized films are similar

film was stripped from its backing and an X-ray examination indicated the film to be crystalline. The fact that there are no major changes in the intensity ratio of the peaks ν_1, ν_2 indicates that there are no major changes in this population distribution upon crystallization.

THE C—C VIBRATIONS (ν_6 AND ν_7)

The reality of peak ν_7 is based on the fact that the absorbance variation with frequency could be described better by assuming the existence of an absorption peak in the 1 125 cm^{-1} region. The integrated intensity for both peaks ν_6 and ν_7 appears to be independent of temperature, although the scatter for ν_7 is considerably larger ($5{\cdot}8 \pm 0{\cdot}9$) than for ν_6 ($9{\cdot}16 \pm 0{\cdot}3$) because of the greater overlap of neighbouring peaks.

These two absorption peaks are probably best described in terms of zig-zag planar vibrations discussed by Sutherland *et al.*[18]. There are four observations which suggest this correlation: (*1*) the two bands observed are relatively weak, as are all C—C vibrations; (*2*) the observed frequencies are in good agreement with those calculated by Sutherland *et al.*[18], 1 125 cm^{-1} versus 1 137 cm^{-1} and 1·062 cm^{-1} versus 1 070 cm^{-1}; (*3*) the polarization of the 1 062 cm^{-1} band is σ, which is consistent with theory, the polarization of the 1 125 cm^{-1} band could not be measured; and (*4*) these two peaks are

very sensitive to changes to tacticity; they merge into one at 1 104 cm^{-1} for the isotactic polymer.

CONCLUSIONS

The crystal structure of *s*-PMMA is not known and therefore an interpretation of the i.r. spectrum in terms of three-dimensional structure is not possible. However, several structural features of this polymer system can be deduced from the i.r. behaviour. First of all peak ν_6 (and ν_7 if it exists) can be assigned to a planar zig-zag arrangement of the backbone carbon atoms. This arrangement for the backbone carbon atoms is not surprising in view of the fact that many syndiotactic polymers crystallize in this form. The planar conformation of simple esters together with the dichroisms of peaks ν_1 to ν_5 can be taken to mean that the plane of the ester group is perpendicular to the direction of the backbone axis. These remarks are represented schematically in *Figure 10*. The spectroscopic repeat unit can

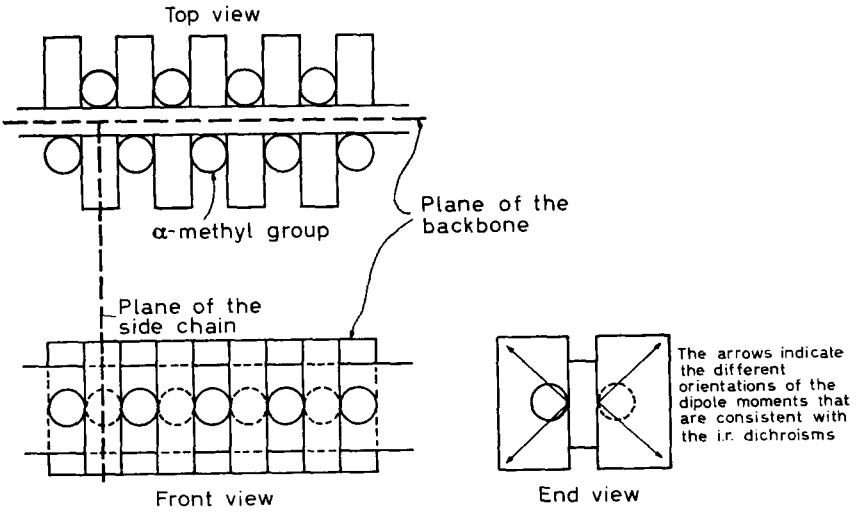

Figure 10—A simple schematic for the zig-zag planar model of *s*-PMMA is shown here

be taken as some element of a single polymer chain because intermolecular interactions are weak, if they do exist; furthermore no new bands are observed upon crystallization. Treating the ester and α-methyl groups as a structureless mass (*Figure 10*) the following elements of symmetry can be found: (*1*) a C_2 axis which coincides with the two-fold axis of the CH_2 group; (*2*) a mirror plane coincident with the plane of the ester group; and (*3*) a glide plane in which the carbon backbone atoms lie. These elements of symmetry place the polymer chain in the C_2v point group.

There are several different interpretations that can account for the multiple ester absorption peaks. First, the four ester peaks in *s*-PMMA can be considered as the successive splitting into four components of the single ester group observed in methyl acetate. The first splitting could be regarded as the in-phase and out-of-phase vibrations of the ester group in the spectro-

scopic repeat unit. This splitting could result in two components, one centred at 1 255 cm^{-1} and the other centred at 1 180 cm^{-1}. The fact that the sums of the integrated intensities [i.e. $I(\nu_1)+I(\nu_2)$ as well as $I(\nu_3)+I(\nu_4)$] are independent of temperature is consistent with this assignment as is the fact that the sums of the integrated intensities are approximately equal. The second source for the splitting comes from a consideration of nearest neighbour interactions based on triads. There are two arrangements of the ester group which are consistent with the σ dichroisms; i.e. the dipole moment of the carbonyl can be pointing up or down when the polymer is viewed end on as is shown in *Figure 10*. There are six different triads, but not all of these are equally probable. For example, the number of triads where the dipole moments are all up or all down will be very small, otherwise the polymer system would exhibit anomalous dielectric effects above the glass temperature or even in dilute solution which is not known to happen. The four remaining triads are not all different either; for example, the interactions at the central ester group in the udd and the duu (where u = up and d = down) triads should be the same as they are in the udu and the dud triads. Therefore, the udu and the dud can be attributed to one pair of peaks (i.e. ν_1, ν_4) while the udd and the duu triads can be identified with the other pair of peaks (i.e. ν_2, ν_3).

A second method for interpreting these four ester absorption peaks is to assume that the ester group can be found in any one of four rotational positions with respect to the plane of the backbone carbon atoms. This position must be arranged so as not to be inconsistent with the σ dichroisms observed in the stretched oriented films. In this arrangement it must be assumed that two of these sites are not accessible to the other two because the integrated intensities of $\nu_1+\nu_2$ and $\nu_3+\nu_4$ are independent of temperature.

Finally a third possibility presents itself by taking the band assignment of ν_6 to be wrong and the conformation of the polymer chain to be helical as was first suggested by Hughes and Stroupe[19]. With helical structures two conformations exist, namely left- and right-handed helices. Inspection of Fisher–Hirschfelder–Taylor molecular models reveals that the distances between nearest neighbouring ester groups are quite different for the two helices. Therefore, it is possible to assign one pair of absorption peaks which is associated with one helix in terms of two different rotational positions of the ester plane with respect to the backbone axis.

There are other models that can be proposed to account for the multiple ester absorption peaks but they are inconsistent with one of the observations, or they are related to very elaborate interactions; however, of the three trial structures that have been proposed, the first one appears to be the most likely. At any rate, any model that is used to account for the ester group peaks must take into consideration the possibility of freezing out high temperature population distributions by quenching them to low temperatures. This observation very strongly implies that the multiplicity of ester absorptions comes about because of discrete side chain arrangements with respect to one another or to the polymer backbone rather than minor changes in the specific absorbance with temperature.

The experiments recorded in *Figures 4* and *5* define the nature of the interactions that cause multiple ester group absorption peaks. For *s*-PMMA

the significant interactions are those along the chain with between the chain interactions being of a diffuse nature. The source of these interactions is probably the bond moment of the C—O—C group with the dipole moment of the adjacent ester groups in such a way as to alter the C—O—C force constant and hence the frequency at which maximum absorption occurs. Inasmuch as the interactions result in several discrete absorption peaks, the relative positions of ester groups along a single polymer chain must also be very discrete. In other words there must be considerable order or regularity along a single polymer chain without any or little order between chains. When *s*-PMMA crystallizes as defined by conventional X-ray techniques, two diffraction maxima are observed but no changes take place in the i.r. absorption characteristics. For this reason we can conclude that an ordering or alignment of chain axis must have occurred but without specific orientation about the chain axis of one chain with respect to its neighbouring chain. If this were to happen specific chain-to-chain interactions would have occurred. This division of polymer ordering into different levels has also been advanced by Statton[20] who found it convenient to recognize three levels of magnification in polymer ordering. The most primitive ordering is local ordering along a single chain. The next higher level of ordering is chain-to-chain ordering followed by chains ordering into aggregates.

Rohm & Haas Research Laboratories,
P.O. Box 219,
Bristol, Pa 19007

(*Received February 1966*)

REFERENCES

[1] NAGAI, H. *J. appl. Polym. Sci.* 1963, **7,** 1697
[2] NAGAI, H., WATANABE, H. and MISHIOKA, A. *J. Polym. Sci.* 1962, **62,** 595
[3] BAUMANN, U., SCHREIBER, H. and TESSMAR, K. *Makromol. Chem.* 1960, **36,** 81
[4] GOODE, W. E., OWENS, F. H., FELLMAN, R. P., SNYDER, W. H. and MOORE, J. E. *J. Polym. Sci.* 1960, **56,** 317
[5] FOX, T. G., GOODE, W. E., GRATCH, S., HUGGETT, C. M., KINCAID, J. F., SPELL, A. and STROUPE, J. D. *J. Polym. Sci.* 1958, **31,** 173
[6] BOVEY, F. A. and TIERS, G. V. D. *J. Polym. Sci.* 1960, **44,** 173
[7] ALFREY, T., BOHRER, J. J. and MARK, H. *Copolymerization.* Interscience: New York, 1962
[8] JONES, R. N. and SANDORFY, C. *Chemical Applications of Spectroscopy,* Vol. IX. Interscience: London, 1956
[9] PAULING, L. and SHERMAN, J. *J. chem. Phys.* 1933, **1,** 606
[10] MARSDEN, R. J. B. and SUTTON, J. E. *J. chem. Soc.* **1936,** 1383
[11] O'GORMAN, J. M., SHAND Jr, W. and SCHOMAKER, V. *J. Amer. chem. Soc.* 1950, **73,** 4222
[12] WILMSHURST, J. K. *J. molec. Spectrosc.* 1957, **1,** 201
[13] CURL Jr, R. F. *J. chem. Phys.* 1959, **30,** 1529
[14] THOMPSON, H. W. and TORKINGTON, P. *J. chem. Soc.* **1945,** 640
[15] KORPOVICH, J. *J. chem. Phys.* 1954, **22,** 1761
[16] TABUCHI, D. *J. chem. Phys.* 1958, **28,** 1014
[17] STEIN, R. *J. chem. Phys.* 1955, **23,** 734
[18] KRIMM, S., LIANG, C. Y. and SUTHERLAND, G. B. B. M. *J. chem. Phys.* 1956, **25,** 543
[19] HUGHES, R. and STROUPE, J. D. *J. Amer. chem. Soc.* **1958, 80,** 1768
[20] STATTON, W. O. American Chemical Society *Polymer Preprints,* 1966, **7,** No. 1, 31

Heat Capacities of Propylene Oxide and of Some Polymers of Ethylene and Propylene Oxides

R. H. BEAUMONT, B. CLEGG, G. GEE, J. B. M. HERBERT, D. J. MARKS, R. C. ROBERTS and D. SIMS

Adiabatic calorimeters were used to measure heat capacities from 80°K to 360°K. An approximate extrapolation procedure has been used to estimate absolute entropies. The properties of 100 per cent crystalline polypropylene oxide have been deduced from measurements on a 25 per cent crystalline sample. The following data are reported (all in cal, g, °K).

Material	Mol. wt	M. pt	ΔH fusion	S^0_{298}
Diglyme		209·11	31·7	0·628
Triglyme		229·35	31·8	0·661
Polyethylene oxide	750	303·0	39·5	
	4 000	332·9	46·1	
	20 000	336·0	44·5	0·372
Propylene oxide		161·25	27·1	1·176(*gas*)
Polypropylene oxide (100 per cent crystalline)	10^6	340	<31	0·394

The glass temperature of amorphous polypropylene oxide was found to be 198°K; $\Delta C_p = 0{\cdot}132$ cal. g^{-1} deg^{-1}.

Entropies of polymerization of ethylene oxide and propylene oxide (gas at 298°K, 1 atm) ⟶ 100 per cent crystalline polymer are estimated to be −41·5, −45·3 cal. $mole^{-1}$ deg^{-1} respectively.

AS PART of a general study of the chemistry and physics of polyethers we embarked some years ago on the measurement of heat capacities over the temperature range 80°K to room temperature or somewhat higher. Although omission of the range below 80°K precludes the exact determination of Third Law entropies, these can be evaluated to a modest degree of accuracy by an extrapolation procedure. Measurements of high precision on polymers are usually difficult to obtain in temperature regions where relaxation processes occur on a time scale comparable with that of the experiment, and there is inevitably some degree of arbitrariness in any procedure adopted to deal with this situation.

The materials to be studied were the simple cyclic ethers and their polymers. Data are already available for ethylene oxide. We now report measurements on propylene oxide, and on a number of polymers of these two monomers.

EXPERIMENTAL

The calorimeter

The calorimeter used for the propylene oxide–polypropylene oxide work was of conventional[1] low temperature adiabatic design and had a volume of 110 cm^3. Temperature was measured on a platinum resistance thermometer calibrated by the National Bureau of Standards, R_0 (=25 ohms) being determined using a triple point cell[2]. The thermometer and heating coil were housed in a re-entrant well—the base of the calorimeter from which eight radial vanes served to dissipate heat. Temperature rise and heat input were measured on a Smith's difference bridge and Vernier potentiometer respectively. The top, bottom and sides of the adiabatic shield were independently manually maintained at the temperature of the calorimeter. The calorimeter was calibrated in the range 90° to 360°K using benzoic acid[3] as a standard.

In view of the large temperature drifts encountered in the polypropylene oxide measurements and the practical difficulty of following these over long periods of time, another calorimeter was constructed for the polyethylene oxide measurements. This calorimeter of volume 90 cm^3 was essentially similar to the first but incorporated a transistorized automatic adiabatic shield control activated by ten series thermocouples between the calorimeter and shield. It could thus conveniently be used for continuous heating determinations. A Pyrotenax heating coil of large surface area was used as a heater inside the calorimeter and hence no vanes were included. In addition to benzoic acid calibrations, checks were also made at several temperatures using toluene, the heat of fusion of which was also determined to assess the reliability of such measurements. A value of 1 593 cal. $mole^{-1}$ was obtained which is 0·7 per cent greater than the literature[4] value.

Temperature increments were usually about five degrees and two degrees for the two calorimeters and the rate of energy input was varied to produce the desired increment in 20 minutes and one hour respectively. Curvature corrections were found to be insignificant as were corrections of the experimental specific heats to constant pressure conditions[5]. All samples were sealed in the calorimeter under a few millimetres pressure of hydrogen to aid conduction. Solids were carefully annealed before slowly cooling to the lowest temperature.

B.D.H. 'microanalytical' benzoic acid was used as obtained. 'AnalaR' toluene was purified by fractional distillation from sodium as were L. Light's diethylene glycol dimethyl ether (diglyme) and triethylene glycol dimethyl ether (triglyme). B.pt Diglyme 163·3° to 163·5°C/769
Triglyme 112·8° to 113·3°C/16

Polyethylene oxide (PEO) samples were obtained from the Shell Chemical Co. and the Union Carbide Co. They were characterized by vapour pressure osmometry and from intrinsic viscosity measurements in benzene at 25°C using the relation[6]:

$$[\eta] = 0{\cdot}0485\,\overline{M}_v^{0{\cdot}68}$$

P.E.O. 750 was a partially methylated low molecular weight soft wax having $\overline{M}_v \sim \overline{M}_n = 670$. P.E.O. 4 000 was methylated using sodium and methyl iodide in order to reduce the effects of the hydroxyl end groups. This, however, resulted in some chain scission.

Polymer as received	$\overline{M}_v \sim \overline{M}_n = 3\,300$	
Methylated polymer	$\overline{M}_v = 3\,600$	$\overline{M}_n = 3\,100$

P.E.O. 20 000 was used as obtained and had $\overline{M}_v = 19\,000$.

Propylene oxide (exBDH) was dried over calcium hydride, fractionated repeatedly, and finally distilled into the calorimeter *in vacuo*. Two samples of polypropylene oxide were prepared: (A) Using strontium carbonate as catalyst at 80°C, polymerization over a period of nine weeks gave a rubbery product which was separated into two fractions by cooling a methanol solution to −10°C. The quantity of precipitated 'crystalline' fraction (*ca.* 12 per cent) was too small to fill the calorimeter so measurements were made only on the 'amorphous' fraction. (B) A further polymer was obtained by use of a zinc diethyl–water catalyst over a period of one week at room temperature. A 'crystalline' fraction (33 per cent) was obtained by cooling a methanol solution to −15°C. Re-solution in benzene, followed by freeze drying gave a product which was too voluminous to load into the calorimeter; it was therefore consolidated by two passes through a water-cooled mixing mill with even speed rolls. The density of this material was determined by flotation to be 1·041 g. cm^{-3} from which it was estimated to be 25 per cent crystalline. Intrinsic viscosity measurements indicated a molecular weight of the order of 10^6. Dilatometric measurements gave a melting point of 340°K.

RESULTS AND DISCUSSION

I. POLYETHYLENE OXIDE

Specific heats

Observed values of the specific heats of diglyme and triglyme are shown in *Figures 1* and *2* respectively. Graphically smoothed values together with the derived values of enthalpy and entropy are given in *Tables 1* and *2*. Between 190°K and the melting points the data are extrapolated from the solid at lower temperatures to allow for the premelting. Observed values of the specific heats of P.E.O. 750, P.E.O. 4 000, and P.E.O. 20 000 are shown in *Figures 3, 4* and *5* respectively. In the melting region very large specific heats were observed for P.E.O. 4 000 and P.E.O. 20 000 and these are shown in *Figure 6*.

Observed values of the specific heats of P.E.O. 750 and P.E.O. 4 000 are given in *Tables 3* and *4* respectively. Smoothed values of the specific heat of P.E.O. 20 000, together with derived enthalpy and entropy values are given in *Table 5*. Between 290°K and the melting point the data are extrapolated from the solid at lower temperatures to allow for the premelting.

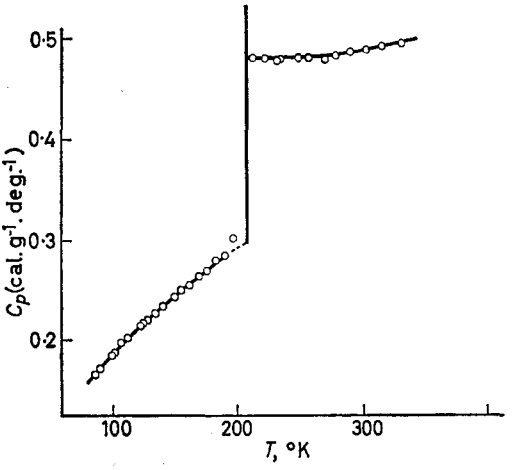

Figure 1—Observed specific heats of diglyme

Table 1. Smoothed values of the specific heat, entropy and enthalpy of diglyme

Temperature °K	C_p *cal.* g^{-1}. *deg.*$^{-1}$	$H_T - H_{90}$ *cal.* g^{-1}	$S_T - S_{90}$ *cal.* g^{-1}. *deg.*$^{-1}$
90	0·172	0	0
100	0·186	1·79	0·019
110	0·199	3·72	0·037
120	0·211	5·77	0·055
130	0·223	7·94	0·073
140	0·234	10·22	0·089
150	0·244	12·61	0·106
160	0·255	15·10	0·122
170	0·264	17·70	0·138
180	0·274	20·39	0·153
*190	0·283	23·17	0·168
*200	0·293	26·05	0·183
*209·11	0·300	28·75	0·196
209·11	0·484	60·40	0·348
210	0·483	60·83	0·349
220	0·481	65·65	0·372
230	0·480	70·46	0·393
240	0·480	75·26	0·414
250	0·480	80·06	0·433
260	0·481	84·86	0·452
270	0·483	89·68	0·470
280	0·484	94·52	0·488
290	0·486	99·37	0·505
298·16	0·488	103·3	0·519
300	0·489	104·2	0·522
310	0·491	109·1	0·538
320	0·493	114·1	0·553
330	0·496	119·0	0·569
340	0·498	124·0	0·583
350	0·500	129·0	0·598

*Extrapolated values.

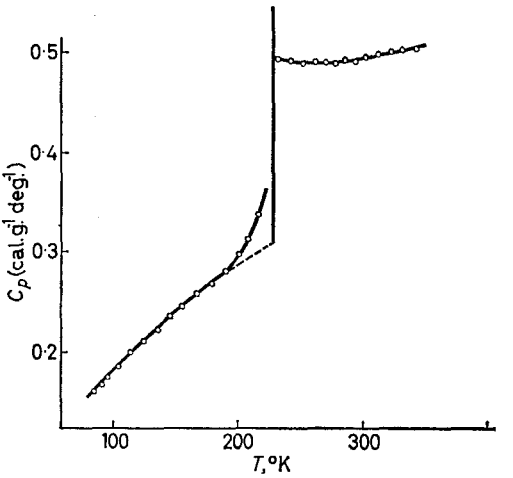

Figure 2—Observed specific heats of triglyme

Table 2. Smoothed values of the specific heat, entropy and enthalpy of triglyme

Temperature °K	C_p *cal.* g^{-1}. *deg.*$^{-1}$	$H_T - H_{90}$ *cal.* g^{-1}	$S_T - S_{90}$ *cal.* g^{-1}. *deg.*$^{-1}$
90	0·168	0	0
100	0·181	1·75	0·018
110	0·194	3·62	0·036
120	0·206	5·62	0·054
130	0·218	7·74	0·071
140	0·229	9·97	0·087
150	0·240	12·32	0·103
160	0·251	14·77	0·119
170	0·261	17·33	0·135
180	0·272	19·99	0·150
190	0·282	22·76	0·165
*200	0·292	25·63	0·180
*210	0·302	28·60	0·194
*220	0·312	31·67	0·208
*229·35	0·321	34·63	0·222
229·35	0·493	66·44	0·360
230	0·493	66·77	0·362
240	0·491	71·69	0·383
250	0·490	76·60	0·403
260	0·490	81·49	0·422
270	0·490	86·39	0·440
280	0·490	71·29	0·458
290	0·492	76·20	0·476
298·16	0·494	80·22	0·489
300	0·494	81·12	0·492
310	0·496	86·08	0·508
320	0·499	91·05	0·524
330	0·501	96·05	0·540
340	0·504	101·1	0·555
350	0·506	106·1	0·569

*Extrapolated values.

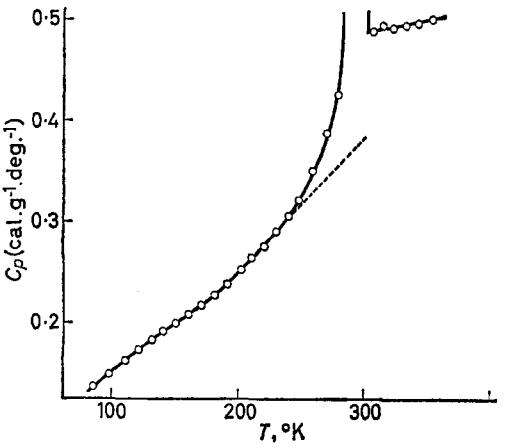

Figure 3—Observed specific heats of P.E.O. 750

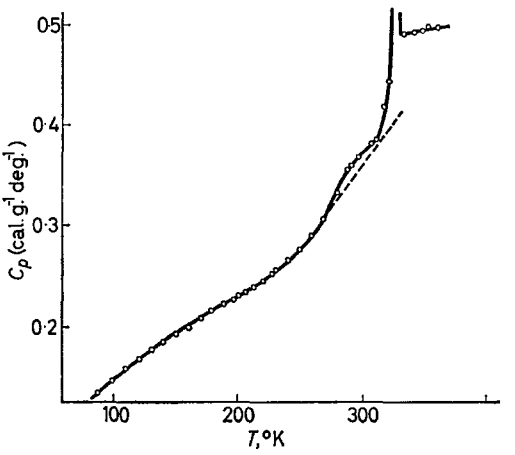

Figure 4—Observed specific heats of P.E.O. 4 000

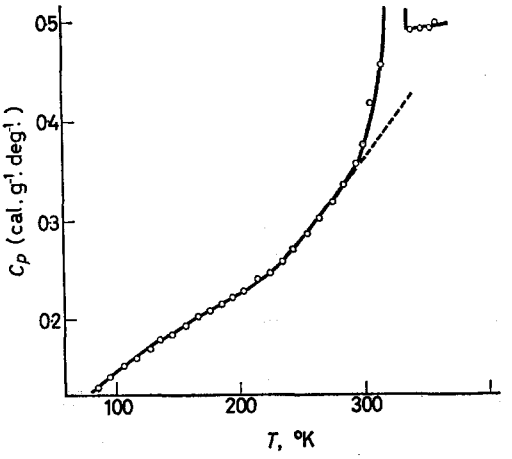

Figure 5—Observed specific heats of P.E.O. 20 000

Table 3. Specific heat of P.E.O. 750

Temperature °K	C_p *cal.* g^{-1}. *deg.*$^{-1}$	*Temperature* °K	C_p *cal.* g^{-1}. *deg.*$^{-1}$
84·6	0·135	286·6	0·843
96·9	0·149	288·2	1·11
109·8	0·162	289·5	1·35
120·6	0·173	290·6	1·54
130·1	0·182	293·5	2·14
140·9	0·191	294·9	2·32
150·4	0·199	296·1	2·56
161·2	0·207	297·2	2·92
171·3	0·216	298·2	3·44
181·9	0·226	299·1	3·57
192·2	0·238	299·9	4·06
201·9	0·252	300·6	4·20
211·1	0·265	301·4	4·10
219·9	0·277	302·2	3·38
230·2	0·291	303·4	2·00
239·6	0·306	306·6	0·490
249·1	0·322	314·9	0·496
259·8	0·352	324·4	0·496
270·5	0·388	334·1	0·498
279·8	0·427	344·4	0·500
284·6	0·628	355·0	0·504

Table 4. Specific heat of P.E.O. 4 000

Temperature °K	C_p *cal.* g^{-1}. *deg.*$^{-1}$	*Temperature* °K	C_p *cal.* g^{-1}. *deg.*$^{-1}$
86·9	0·134	292·8	0·359
97·9	0·146	297·1	0·365
109·1	0·158	298·5	0·367
120·4	0·169	309·7	0·381
130·2	0·177	311·9	0·383
139·7	0·185	320·5	0·417
150·3	0·193	323·4	0·441
160·0	0·199	326·4	0·562
170·0	0·208	330·4	3·75
179·2	0·215	331·1	7·62
188·2	0·221	331·5	12·81
197·4	0·226	331·8	17·51
202·4	0·230	332·0	22·33
206·1	0·233	332·1	26·33
211·5	0·238	332·3	28·79
219·9	0·244	332·4	29·19
228·1	0·252	332·6	22·92
230·3	0·255	332·9	7·49
240·2	0·265	333·6	4·59
249·9	0·275	336·0	0·490
260·0	0·290	344·9	0·491
270·3	0·306	349·9	0·492
280·2	0·331	355·3	0·496
288·7	0·355	360·5	0·495

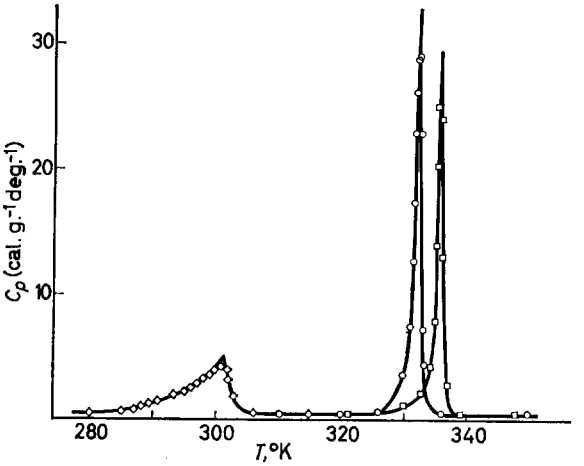

Figure 6—Specific heats of P.E.O. 750 (◇), P.E.O. 4 000 (○) and P.E.O. 20 000 (□) in the melting region

Table 5. Smoothed values of the specific heat, enthalpy and entropy of P.E.O. 20 000

Temperature °K	C_p *cal.* g^{-1}. *deg.*$^{-1}$	$H_T - H_{90}$ *cal.* g^{-1}	$S_T - S_{90}$ *cal.* g^{-1}. *deg.*$^{-1}$
90	0·135	0	0
100	0·146	1·41	0·015
110	0·156	2·92	0·029
120	0·165	3·52	0·043
130	0·174	5·22	0·057
140	0·182	7·00	0·070
150	0·190	8·86	0·083
160	0·198	10·80	0·095
170	0·205	12·81	0·108
180	0·212	14·90	0·119
190	0·219	17·05	0·131
200	0·227	19·28	0·143
210	0·234	21·58	0·154
220	0·242	23·96	0·165
230	0·252	26·42	0·176
240	0·264	29·00	0·187
250	0·278	31·71	0·198
260	0·295	34·57	0·210
270	0·311	37·60	0·221
280	0·328	40·80	0·233
290	0·344	44·16	0·244
298·16	0·358	47·02	0·254
300	0·361	47·69	0·256
310	0·378	51·38	0·268
320	0·394	55·24	0·281
330	0·411	59·26	0·293
336·16	0·421	61·82	0·301
336·16	0·488	106·3	0·433
340	0·489	111·2	0·438
350	0·492	116·1	0·453
360	0·495	121·0	0·467

Heats of fusion

The heats of fusion of the samples were determined from continuous heating runs started below the premelting region and ending some ten degrees above the melting point. Subtraction from the total heat input of the heat needed to raise the temperature of the calorimeter and solid contents from the initial temperature to the melting point and that needed to raise the temperature of the calorimeter and liquid contents from the melting point to the final temperature gave directly the heat of fusion of the sample in the calorimeter. In the calculation of the latter, in order to allow for the premelting, it was necessary to extrapolate the specific heat of the solid from below the premelting region to the melting point. Such extrapolations are shown in the figures. The results of the heat of fusion determinations are given in *Table 6*.

Melting points and purities

The melting points and purities of diglyme and triglyme were determined conventionally[7] from measurements of the equilibrium temperature when known fractions of the solids had been melted. The melting points of pure diglyme and triglyme are given in *Table 6*; the purities of the samples studied were found to be 99·62 and 99·44 mole per cent respectively. The melting points of the polymer samples were determined both dilatometrically using heating rates of 0·5°C per hour and from the specific heat measurements. The latter were not very suitable as it was difficult to locate the temperature at which the last traces of solid melted. Also, measurements in the melting region were thought to have lower precision than those elsewhere. The melting points so obtained are given in *Table 6*.

Table 6. Heats of fusion and melting points

Sample	*Observed* ΔH_m *cal.* g^{-1}	*Mean* ΔH_m *cal.* g^{-1}	*Melting point* °C *Calorimetric*	*Dilatometric*
Diglyme	**31·7, 31·6**	31·7±0·3	−64·05	
Triglyme	31·7, 31·8	31·8±0·3	−43·81	
P.E.O. 750	39·0, 40·0	39·5±0·4	30·0±1·5	29·8±0·2
P.E.O. 4 000	45·9, 46·2	46·1±0·5	59·6±0·4	59·7±0·2
P.E.O. 20 000	44·8, 44·3, 44·3	44·5±0·5	63·1±0·4	62·8±0·2

Discussion

Diglyme and triglyme behave physically and chemically as low molecular weight ethers. Simple physical properties of the liquids are known but little work has been done on the crystalline solids. It was found that on cooling, the liquids could be supercooled some 10° to 30°C below their melting points. An attempt was made to prepare a glass by shock cooling the liquids as quickly as possible to −196°C, but crystallization still occurred and there was no difference between the specific heat of the solid obtained in this way and that of the annealed sample on which the original measurements were made. Unfortunately, the maximum rate of cooling in

our apparatus was only about three degrees per minute and so the sample probably had time to crystallize fully.

Poly(ethylene oxide) is a highly crystalline linear polymer, crystallinities as high as 95 per cent being deduced[8] from n.m.r and X-ray measurements. The unit cell is monoclinic and contains two polymer chains, thought[9] to be 7_2 helices of repeat length 19·25Å. These in turn form crystalline aggregates in the form of helices which make up the radial arms of spherulites. Measured densities are usually much lower than the X-ray density[8] and this has been attributed to the formation of voids which are revealed in electron micrographs of cast films. For this reason, no attempt was made to measure the densities of the samples investigated. The dynamic mechanical and dielectric and the n.m.r. properties of PEO have recently been reviewed[10] and transitions are found to occur at about −60°C in both amorphous and crystalline regions. In addition, glass transitions of the quenched polymer have been found at −50°C from stiffness measurements[8] and at −67°C dilatometrically[11]. In an attempt to find such a transition calorimetrically, P.E.O. 20 000 was cooled as quickly as possible from 80°C to −80°C and a continuous heating run carried out between −80°C and −50°C. The specific heats obtained, however, were all identical with those previously obtained for the annealed polymer and no glass transition was detected; although here again the maximum rate of cooling was only three degrees per minute.

Specific heats

The experimental specific heats are generally as expected, decreasing as the molecular weight increases. It is thought that P.E.O. 20 000 will represent the lower limit for this decrease. It is interesting to note that the specific heat of PEO is intermediate between those of polyethylene and poly(methylene oxide). Below 200°K the specific heats will largely be determined by lattice vibrations, while the sharp rise above this temperature is due to the increasing contribution from carbon–hydrogen vibrations[12].

The specific heat of P.E.O. 4 000 is seen to exhibit a rather surprising point of inflection at 300°K. This is probably the result of a small amount of degradation which occurred during the methylation resulting in a slight broadening of the molecular weight distribution. The premelting of about one per cent of a lower molecular weight species would be sufficient to cause such an inflection.

Absolute entropies

Ideally one would like to measure specific heats using a liquid helium calorimeter when a small Debye extrapolation would enable absolute entropies to be determined by direct graphical integration of the C_p/T–T curves. Since the present results could not be extrapolated in this way, the Kelley, Parks, Huffman[13] method was used. S_{90} was estimated for diglyme and triglyme by comparison of the observed specific heats at 90°K and 120°K with the Kelley, Parks and Huffman standard and for P.E.O. 20 000 by comparison with the specific heat of poly(methylene oxide)[14]. Values so obtained for S_{90} and $S_{298\cdot16}$ are:

Diglyme	$S_{90} = 0{\cdot}142$ cal. g^{-1}. deg^{-1}	$S_{298\cdot16} = 0{\cdot}628$ cal. g^{-1}. deg^{-1}
Triglyme	$S_{90} = 0{\cdot}139$ cal. g^{-1}. deg^{-1}	$S_{298\cdot16} = 0{\cdot}661$ cal. g^{-1}. deg^{-1}
P.E.O. 20 000	$S_{90} = 0{\cdot}118$ cal. g^{-1}. deg^{-1}	$S_{298\cdot16} = 0{\cdot}372$ cal. g^{-1}. deg^{-1}

This method has been claimed to give values for S_{90} which are accurate to within five per cent and so the error in $S_{298\cdot16}$ should not exceed 0·01 cal. g^{-1}. deg^{-1} or 0·5 cal. deg^{-1} per repeating unit.

The absolute entropy at 25°C of ethylene oxide, calculated from specific heat data[15, 16] is 57·94 cal. mole^{-1}. deg^{-1} and subtracting this from the entropy of P.E.O. 20 000 gives an entropy of polymerization

$$\underset{\diagdown\ \text{O}\ \diagup}{CH_2{-}CH_2}\ (g) \longrightarrow \frac{1}{n}{-}(CH_2{-}CH_2{-}O)_n{-}\ (c)\quad \Delta S^0_{gc} = -41{\cdot}5 \text{ cal. mole}^{-1}. \text{deg}^{-1}$$

Similar values of ΔS^0_{gc} have been found for other related polymers; for poly(methylene oxide)[14] ΔS^0_{gc} -42 cal. mole^{-1}. deg^{-1}; for polyethylene $\Delta G^0_{gc} = -37{\cdot}7$ cal. mole^{-1}. deg^{-1}, for 'Rigidex 50', equivalent to $-41{\cdot}5$ cal. mole^{-1}. deg^{-1} for 100 per cent crystalline polyethylene.

Heats of fusion

The heat of fusion is not simply related to molecular weight. Diglyme and triglyme are seen to have the same heat of fusion, which is substantially less than those of the higher polymers. The heat of fusion of P.E.O. 4 000 was found to be greater than those of P.E.O. 750 and P.E.O. 20 000, suggesting that P.E.O. 4 000 must have the highest degree of crystallinity. It has been concluded[10] from both dynamic and X-ray measurements that the crystallinity of PEO has a maximum in the molecular weight region of 1 000. This effect is to be expected since the number of lattice defects and voids incorporated in a solid polymer will increase with increasing molecular weight while the lower molecular weight polymers will have a packing problem of the end groups. Mandelkern[17] has calculated the heat of fusion of PEO from measurements of the depression of the melting point by diphenyl ether and tetralin diluents obtaining values of 39·6 and 49·5 cal. g^{-1} respectively. A further estimate can be obtained from the variation of the melting point with applied pressure[18] using the relation

$$\Delta H_m = \Delta S_m \,.\, T_m = \Delta V_m \,.\, (\mathrm{d}P/\mathrm{d}T) \,.\, T_m$$

where ΔV_m and ΔS_m are the molar volume and entropy changes on fusion. Using the X-ray crystal density and the extrapolated liquid density[8] to calculate ΔV_m, a heat of fusion of 51·5 cal. g^{-1} at $T_m = 336$°K is obtained. These two methods give the heat of fusion of the 100 per cent crystalline polymer, ΔH^c_m, while the calorimetric value is simply the heat of fusion of the sample, ΔH^a_m, of degree of crystallinity, a. These are related: $\Delta H^c_m = \Delta H^a_m / a$. In the absence of any reliable data on the degree of crystallinity of the samples one can only conclude that the heat of fusion of 100 per cent crystalline PEO is greater than 46 cal. g^{-1} and probably less than 52 cal. g^{-1}.

II. PROPYLENE OXIDE

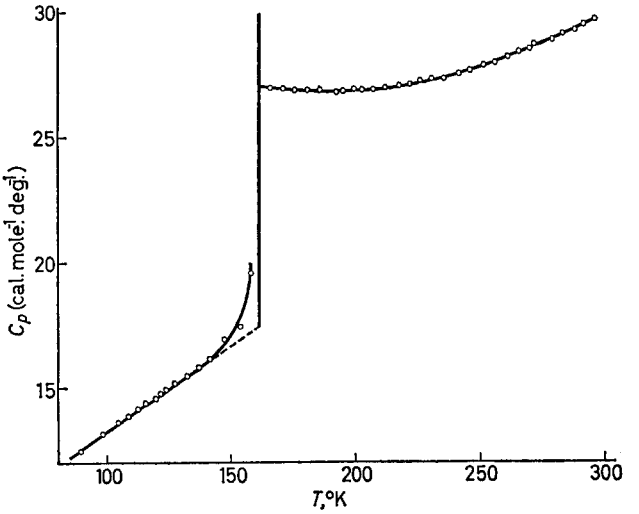

Figure 7—Observed specific heats of propylene oxide

Table 7. Smoothed values of the specific heat, enthalpy and entropy of propylene oxide

Temperature °K	C_p *cal.* g^{-1}. *deg.*$^{-1}$	$H_T - H_{90}$ *cal.* g^{-1}	$S_T - S_{90}$ *cal.* g^{-1}. *deg.*$^{-1}$
90	0·216	0	0
100	0·229	2·23	0·023
110	0·241	4·58	0·046
120	0·252	7·05	0·067
130	0·264	9·63	0·088
140	0·276	12·33	0·108
*150	0·289	15·16	0·128
*160	0·301	18·11	0·147
*161·25	0·303	18·49	0·149
161·25	0·466	45·59	0·317
170	0·465	49·66	0·341
180	0·463	54·30	0·368
190	0·463	58·93	0·393
200	0·464	63·56	0·417
210	0·465	68·20	0·439
220	0·468	72·87	0·461
230	0·471	77·56	0·482
240	0·476	82·29	0·502
250	0·481	87·08	0·522
260	0·486	91·92	0·540
270	0·493	96·82	0·559
280	0·500	101·8	0·577
290	0·508	106·8	0·595
298·16	0·514	110·9	0·609
300	0·516	112·0	0·612

*Extrapolated values.

Results of heat capacity measurements are plotted in *Figure 7*, and smoothed values of C_p, $H-H_{90}$ and $S-S_{90}$ listed in *Table 7*. The triple point was found to be 161·25°K, and the sample purity better than 99·9 moles per cent. The latent heat of fusion was determined in the same way as those of diglyme and triglyme, to be $1\,570 \pm 5$ cal. mole^{-1}, giving for the entropy of fusion $1\,570/161{\cdot}25 = 9{\cdot}74$ cal. mole^{-1}. deg^{-1}. Corresponding values for ethylene oxide are 1 237 cal. mole^{-1} and $1\,237/160{\cdot}6 = 7{\cdot}70$ cal. mole^{-1}. deg^{-1}. These comparative values are very nearly in the ratio of the molecular weights. $S_{90} - S_0$ was estimated as 0·200 cal. g^{-1}. deg, or 11·6 cal. mole^{-1}. deg^{-1}, by the method of Kelley, Parks and Huffman, using the known curves for ethylene oxide as standard.

The heat of vaporization is 6·67 kcal mole^{-1} and the boiling point $T = 308°$, giving $\Delta S_{vap} = 21{\cdot}7$ cal. mole^{-1}. deg^{-1} at 308°K or (approx.) 21·3 at 298°K. Hence, for the gas, $S_{298} - S_0 = 68{\cdot}2 \pm 2$ cal. mole^{-1}. deg^{-1}, or 1·176 cal. g^{-1}. deg^{-1}.

III. POLYPROPYLENE OXIDE

Heat capacity measurements on high polymers present severe experimental problems, especially where slow crystallization occurs. An amorphous polymer, below its glass temperature, is not in a state of internal equilibrium, and its behaviour on slow heating depends on its previous history. A sample which has been cooled rapidly will have a higher enthalpy than one cooled slowly. Conversely a sample which has been cooled slowly and is then heated rapidly may pass below the equilibrium H/T curve of the liquid, and subsequently 'catch up', producing a peak in the heat capacity curve which can be mistaken for evidence of a small first order transition. Crystallization adds further complications, for the transition is always spread over a wide temperature range. Rapid heating of a partially crystalline sample may induce melting, followed by re-crystallization. All these time-dependent phenomena are observed in calorimetric studies, as temperature drifts, which may continue for such long periods that it is impracticable to follow them in a calorimeter not specifically designed for such work. Some arbitrary decision is then needed as to how long the drift should be followed. Dainton and co-workers, in their very extensive survey[14], allowed only six or seven minutes after switching off the heater, before taking a reading, arguing that this virtual neglect of drifts would not influence their broad conclusions.

The substantial bulk of polymer used in this work precluded very rapid cooling, but care was taken to reduce the cooling rate to the order of one degree per hour when passing through transition regions. The points shown in the diagrams refer to several distinct series of measurements; these covered a total period of many weeks, and included periods at room temperature of up to two weeks. In the series of measurements on the amorphous sample, readings were generally taken half-an-hour after switching off the heater, but a further reading was taken ten minutes later to determine the temperature drift. This did not usually exceed 2×10^{-4} deg. min^{-1} (equivalent to 2×10^{-5} cal. deg^{-1}. g^{-1}. min^{-1} drift in the apparent C_p), but was much larger than this in the immediate region of the glass

temperature and in the region where crystallization was apparently occurring (see below). Rather less trouble was experienced with the 'crystalline' sample: the procedure adopted here was to follow the temperature until the drift was less than 4×10^{-4} deg. min^{-1}, the time required ranging from a few minutes to more than two hours. The extent of the scatter of experimental points is our only indication of the degree of success attained in recording significant results.

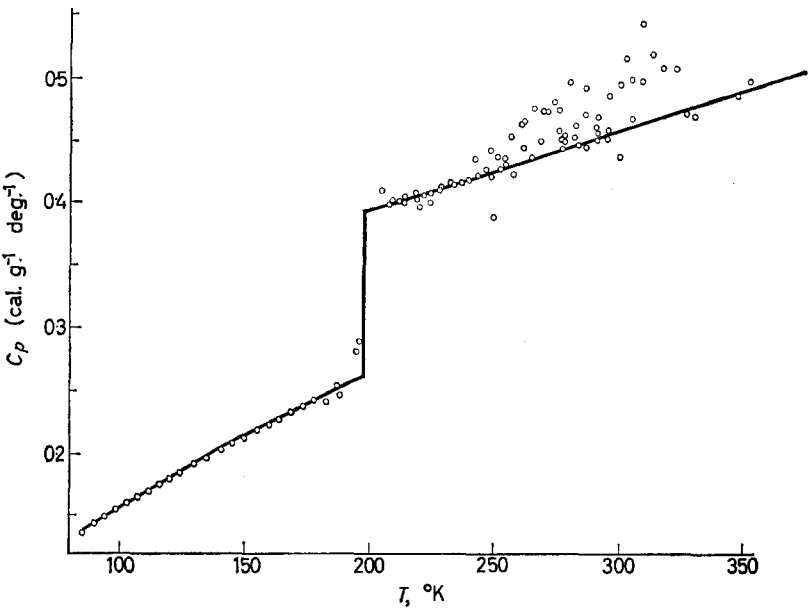

Figure 8—Observed specific heats of amorphous polypropylene oxide. Lines calculated from equations (1) and (2)

Heat capacity measurements for the amorphous sample are shown in *Figure 8*. Below the glass temperature there is negligible scatter, and the data, from 85°K to 180°K, are well represented by the equation

$$C_{pg} = 0{\cdot}0142 + 1{\cdot}556 \times 10^{-3}T - 1{\cdot}604 \times 10^{-6}T^2. \qquad (1)$$

A glass transition is seen to occur in the neighbourhood of 200°K; dilatometric measurements on a sample of the same polymer gave $T_g = 198$°K. By extrapolation, the heat capacity of the glass at 198°K is $0{\cdot}259_5$ cal. g^{-1}. deg^{-1}.

Measurements above T_g show very much more scatter, especially in the region 250° to 330°K. Comparison with the crystalline polymer (below) shows that this is almost certainly due to a minor degree of crystallization. In determining the heat capacity/temperature curve for the liquid, emphasis has therefore been placed on measurements (*a*) between 210° and 240°K, and (*b*) above 320°K, the latter being supplemented by data for the crystal-

line sample above its melting point. The line drawn in *Figure 8* has the equation

$$C_{pL} = 0{\cdot}263 + 0{\cdot}65 \times 10^{-3}\, T \qquad (2)$$

Extrapolating to $T = 198°$, the heat capacity of the liquid at T_g is $0{\cdot}391_5$ cal. mole^{-1}. deg^{-1}. This makes $\Delta C_p = 0{\cdot}132$ cal. g^{-1}. deg^{-1} or 7·65 cal. deg^{-1} per propylene oxide unit. To bring this into line with Wunderlich's generalization[19] that $\Delta C_p \simeq 2{\cdot}7$ cal. deg^{-1} per 'bead', it is evident that the bead must be one chain atom, either C or O.

Figure 9 shows the results of heat capacity measurements on the crystalline sample; these will be interpreted by making the usual assumption that the sample behaves as a simple mixture of atactic and tactic components, the latter being capable of 100 per cent crystallization. There is evidently a glass temperature at approximately the same temperature as in *Figure 8*, and this is attributed solely to the atactic component. Below T_g, the heat capacity curve drawn (AB) is calculated from equation (1). We conclude therefore that the heat capacity C_{p0} of the fully crystalline tactic component is identical with that of the glass, and extrapolate equation (1) to give an approximate heat capacity of 0·359 cal. g^{-1}. deg^{-1} at the dilatometric melting point of 340°K. This is a minimum estimate. If additional modes are excited in the crystal below the melting point, the heat capacity will of course increase, approaching more closely the value for the liquid. Above

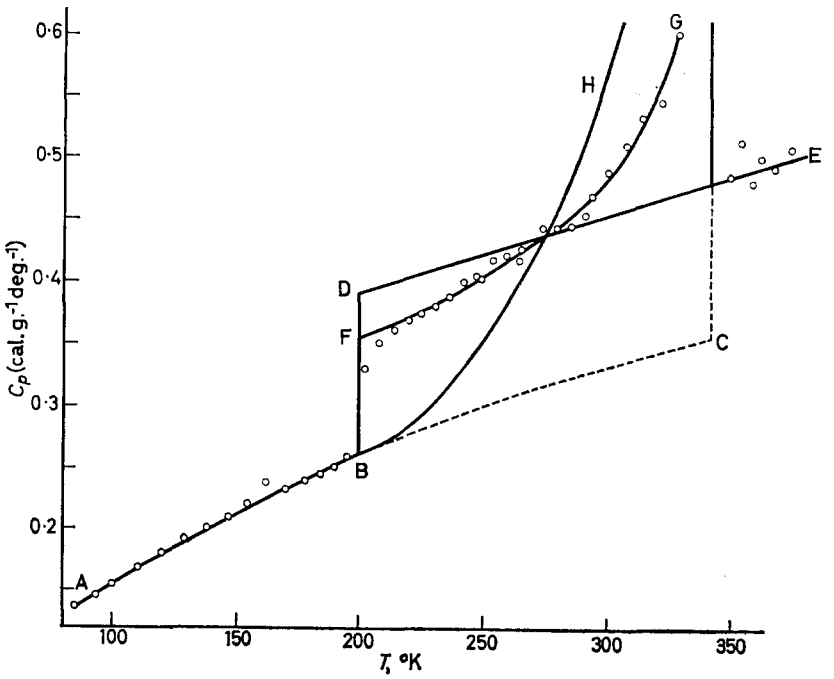

Figure 9—Observed specific heats of crystalline polypropylene oxide (ABFGE and points). ABC estimated curve in absence of melting; ABH estimated melting behaviour of 100 per cent tactic material

340°K, the points are in fair agreement with the line DE drawn [from equation (2)] for the amorphous sample. The scatter in this region is attributed to the fact that the calorimeter was designed for lower temperatures.

Between $T = 198°$ and 340°, the observed C_p (curve FG) is the sum of contributions from liquid and tactic components. Ignoring the diffuseness of the glass transition, extrapolation of the intermediate part of the experimental C_p curve back to cut BD at F gives an independent estimate of the per cent crystallinity in the sample (DF/DB). The curve drawn gives 27·3 per cent crystallinity, in good agreement with the estimate from density of 25 per cent. Using this figure, the heat capacity C_{pt} of the tactic component above 198°K is obtained from the equation

$$C_p = 0{\cdot}273\, C_{pt} + 0{\cdot}727\, C_{pL}$$

whence

$$C_{pt} = 3{\cdot}66\, C_p - 0{\cdot}702 - 1{\cdot}73 \times 10^{-3}\, T$$

Curve BH was calculated from this equation.

The latent heat of fusion of fully crystalline polymer can now be estimated from the area between curves BH and BC, i.e. $\int (C_{pt} - C_{p0})\, dT$. The important region between 325° and 340°K is very ill-defined, and our estimated area must be regarded as a minimum; this gives $L = 31$ cal. g^{-1}. Similarly, the entropy of fusion is given by $\int [(C_{pc} - C_{p0})/T]\, dT$, which is estimated as 0·0965 cal. g^{-1}. deg^{-1}. These data evidently include any contributions to H and S in the crystal from excitation of additional modes.

The absolute entropy of the 100 per cent tactic polymer at 90°K is estimated, by the Kelley, Parks and Huffman method, using Delrin[14] as standard, to be 0·118 cal. g^{-1}. deg^{-1}. Adding to this the entropy increment from 90° to 198°K [equation (1)] and 198° to 298°K (graphically from curve BH) gives $S_{298} = 0{\cdot}420$ cal. g^{-1}. deg^{-1}. If no melting occurred, equation (1) would apply up to 298°K, giving $S_{298\,(cr)} = 0{\cdot}394$ cal. g^{-1}. deg^{-1}. Combining with $S_{298} = 1{\cdot}176$ cal. g^{-1}. deg^{-1} for propylene oxide gas gives for $-\Delta S^0_{gc}$: (a) to fully crystalline polymer, 0·782 cal. g^{-1}. deg^{-1} or 45·3 cal. $mole^{-1}$. deg; (b) to 100 per cent tactic, but partially melted polymer, 0·756 cal. g^{-1}. deg^{-1} or 43·8 cal. $mole^{-1}$. deg^{-1}. These values seem reasonable, but in view of the indirect methods involved, their reliability is difficult to assess.

We acknowledge with thanks the assistance of Professor Geoffrey Allen in the direction of parts of this work and of C. Chernick in some of the measurements.

Department of Chemistry,
University of Manchester

(*Received February 1966*)

REFERENCES

[1] SOUTHARD, J. C. and BRICKWEDDE, F. G. *J. Amer. chem. Soc.* 1933, **55**, 4378
[2] STIMSON, H. F. *J. Wash. Acad. Sci.* 1945, **35**, 301
[3] GINNINGS, D. A. and FURUKAWA, G. T. *J. Amer. chem. Soc.* 1953, **75**, 523

[4] KELLEY, K. K. *J. Amer. chem. Soc.* 1929, **51,** 2738
[5] ASTON, J. G. and FRITZ, J. J. *Thermodynamics and Statistical Thermodynamics,* p 44. Wiley: New York, 1959
[6] SADRON, C. and REMPP, P. *J. Polym. Sci.* 1958, **29,** 127
[7] e.g. ROSSINI, F. D. *Chemical Thermodynamics,* p 294. Wiley: New York, 1950
[8] SMITH, K. L. and CLEVE, R. V. *Industr. Engng Chem. (Industr.),* 1958, **50,** 12
[9] MIYAZAWA, T. *J. Polym. Sci.* 1961, **55,** 215
[10] CONNOR, T. M., READ, B. E. and WILLIAMS, G. *J. appl. Chem. Lond.* 1964, **14,** 74
[11] MARKS, D. J. *Ph.D. Thesis* Manchester, 1961
[12] WUNDERLICH, B. *J. chem. Phys.* 1962, **37,** 1203, 1207
[13] KELLEY, K. K., PARKS, G. S. and HUFFMAN, H. M. *J. phys. Chem.* 1929, **33,** 1802
[14] DAINTON, F. S., EVANS, D. M., HOARE, F. E. and MELIA, T. P. *Polymer, Lond.* 1962, **3,** 263
[15] GIAUQUE, W. F. and GORDON, J. *J. Amer. chem. Soc.* 1949, **71,** 2176
[16] KISTIAKOWSKY, G. B. and RICE, W. W. *J. chem. Phys.* 1940, **8,** 618
[17] MANDELKERN, L. *J. appl. Phys.* 1955, **26,** 443
[18] FORTUNE, L. R. and MALCOLM, G. N. *J. phys. Chem.* 1960, **64,** 934
[19] WUNDERLICH, B. *J. phys. Chem.* 1960, **64,** 1052

Book Review

Polymer Handbook

Edited by J. BRANDRUP and E. H. IMMERGUT with the collaboration of H. G. ELIAS. Interscience: New York; Wiley: London, 1966. 147*s*

THIS book is primarily intended for polymer chemists and physicists in research and development laboratories. Its principal sections are concerned with polymerization by free-radical processes only, solid state properties, solution properties and physical data relating to polymers, oligomers, monomers and solvents. Included also, but in less detail, are data relevant to the thermal degradation of polymers, permeability, nuclear magnetic resonance etc. No attempt has been made to impart information of interest to polymer engineers or fabricators although a properties and price chart of some common thermoplastic materials has been included.

The various sections of the book have been compiled by known authorities. In some cases the tables have been taken from journals for publication as they are, without any modification or revision, example the section on copolymerization reactivity ratios is a reprint from *Copolymerization* by G. E. HAM (Interscience: New York, 1964).

The chapters on polymerization and solution properties of polymers are the most detailed and comprehensive and contain some very useful information. In addition to the basic kinetic and thermodynamic parameters, tables are included which are useful for emulsion polymerization and polymer fractionation studies. A serious criticism of this book is the total lack of reference to cationic, anionic and Ziegler type polymerization systems. A considerable amount of this information has been assembled in reviews and articles and it would have been worthwhile to have included some of this.

Solid state properties are treated reasonably well, and included in this chapter is an interesting table on the rates of crystallization of some common polymers at different temperatures and different molecular weights.

The chapter on the physical constants of important polymers is confined to cellulosive materials, polyethylene, polybutadiene, rubbers, polyacrylonitrile, polystyrene, polyhexamethylene adipamide and polyethylene terephthalate. Within the limits set by this chapter, it is very well done, but one would have liked to have seen more polymers included and such topics as the physical properties of monomers and solvents omitted; this information is readily available in organic chemistry texts.

The printing is inclined to be variable and there are errors, for example, the glass transition temperature for isotactic polystyrene is given as 100°C and that for atactic omitted; obviously this is a printing error. There is also a lack of information on polyvinyl chloride, Nylon 6, the higher Nylons and some of the newer materials such as polypyromellitimides. On balance, however, this is a reference book which is worth having and the price is not unreasonable.

D. G. H. BALLARD

Notes and Communications

cis-Polymerization by a Three-component System Containing Nickel (0)

MUCH information has recently been published on the polymerization activity for diolefins of catalysts containing zerovalent nickel. Thus it was shown that systems containing nickel carbonyl and molybdenum pentachloride gave a butadiene polymer of over 85 per cent *cis* content[1]. Similarly high *cis* polybutadiene has been prepared from olefinic nickel (0) complexes with Lewis acids[2] and from allylic nickel (0) complexes, with and without Lewis acids[3].

In our own investigations we have obtained a three-component system in which carbon is in no way bonded to any of the components by alkyl, allyl, π or carbonyl bond.

We have shown the complex $Ni(PCl_3)_4$, originally prepared by Wilkinson and Irvine[4], to polymerize butadiene completely and extremely rapidly in the presence of a number of transition metal halides, to a gelled product (*Table 1*). In particular $TiCl_4$ caused complete polymerization of 20 g butadiene in less than two hours. Isoprene was also polymerized by the system but in lower yields to give insoluble polymers. The addition of a third component to the catalyst, particularly $AlBr_3$ or $AlCl_3$, gave a controlled polymerization of butadiene with formation of hydrocarbon-soluble high-*cis* polymer

As with bis cyclooctadienyl nickel (0)–Lewis acid catalysts[2], microstructure appeared to be independent of transition metal halide but conversion varied considerably, ranging from 90 per cent with $TiCl_4$ to zero with insoluble halides such as $CoCl_2$. Polymerization could be carried out over a wide range of component ratios and down to extremely low catalyst levels (of the order of 1 millimole/litre monomer), in pure hydrocarbon solution between 0° and 80°C.

Tetrakis nickel phosphorus trihalides are known[5] to dissociate in solution

$$Ni(PX_3)_4 \rightleftharpoons [Ni(PX_3)_n] + (4-n)PX_3$$

and this leaves vacant sites for coordination of the initial olefin species. Interaction of $TiCl_4$ and $Ni(PCl_3)_4$ should also lead to redox process with the formation of Ti^{III} and Ni^{I} possibly as a halogen bridge complex. The instability of the nickel (1) complex may then result in the formation of an initiating allyl bonded butadiene. The most obvious role of the aluminium halide is to remove dissociated PCl_3 as a donor–acceptor complex, although at very low catalyst levels $TiCl_4$–$Ni(PCl_3)_4$ mixtures give gel free polymers in the absence of $AlCl_3$.

D. K. JENKINS
D. G. TIMMS
E. W. DUCK

Research and Development Laboratories,
The International Synthetic Rubber Co. Ltd,
Hythe, Southampton, Hants.

(*Received March 1966*)

Table 1. Polymerization of butadiene with catalysts containing $Ni(PCl_3)_4$ (8 oz bottles, 25 g butadiene, 25°C)

Catalyst components			*Mole ratios*	*Conc.* $Ni(PCl_3)_4$	*Solvent*	*Solvent: butadiene*	*Yield*	*Ultimate conversion*	*Inherent viscosity*	*Stereo-structure* cis *1,4 content*	
a	*b*	*c*	*a : b : c*	*mmole/litre*		*v : v approx.*	*g/mmole* $Ni(PCl_3)_4$ *per cent*	*18 h*	*dl/g benzene 25°C*	*per cent*	
$Ni(PCl_3)_4$	—	—	— — —	50	toluene	4:1	nil	—	—	—	
$Ni(PCl_3)_4$	—	—	— — —	50	hexane	4:1	nil	—	—	—	
$Ni(PCl_3)_4$	$TiCl_4$	—	1:1:—	25	toluene	4:1	ND*	very high	gelled	—	
$Ni(PCl_3)_4$	$TiCl_4$	—	1:1:—	25	hexane	4:1	ND	very high	gelled	—	
$Ni(PCl_3)_4$	$TiCl_4$	—	1:2:—	1	hexane	2:1	nil	—	—	—	
$Ni(PCl_3)_4$	$TiCl_4$	—	1:3:—	1	hexane	2:1	22	3·5	ND	94	some microgel
$Ni(PCl_3)_4$	$TiCl_4$	—	1:4:—	1	hexane	2:1	307	48	2·1	94	some microgel
$Ni(PCl_3)_4$	$TiCl_4$	—	1:5:—	1	hexane	2:1	282	44	2·2	94	some microgel
$Ni(PCl_3)_4$	$TiCl_4$	—	1:6:—	1	hexane	2:1	224	35	2·5	94	some microgel
$Ni(PCl_3)_4$	—	$AlCl_3$	1:—:1	25	toluene	2:1	0·6	—	—	Resinous hard	
—	$TiCl_4$	$AlCl_3$	—:1:1	25	toluene	2:1	0·2	—	—	—	
$Ni(PCl_3)_4$	$TiCl_4$	$AlCl_3$	1:1:1	10	toluene	2:1	57·5	90	0·85	94·5	completely soluble
$Ni(PCl_3)_4$	$TiCl_4$	$AlCl_3$	1:2:0·25	1	hexane	2:1	256	40	2·9	95	completely soluble
$Ni(PCl_3)_4$	$TiCl_4$	$AlCl_3$	1:1:0·05	2	hexane	2:1	176	55	2·1	95	completely soluble
$Ni(PCl_3)_4$	$CoCl_2$	—	1:1:—	25	toluene	2:1	nil	—	—	—	

*ND—not determined.

REFERENCES

[1] OTSUKA, S. and KAWAKAMI, M. *Angew. Chem.* 1963, **75**, 978
[2] DAWANS, F. and TEYSSIE, P. *Polymer Letters*, 1965, **3**, 1045
[3] PORRI, L., NATTA, G. and GALLAZZI, M. C. Paper to International Symposium on Macromolecular Chemistry, Prague 1965 (A593)
[4] WILKINSON, G. and IRVINE, J. W. *Science*, 1951, **113**, 742
[5] LETO, J. R. and LETO, M. F. *J. Amer. chem. Soc.* 1961, **83**, 2944

Observation of Crazes in ABS-Polymer and High-impact Polystyrene under the Electron Microscope

IT HAS been reported that crazes in amorphous thermoplastics such as polystyrene (PS) and polymethylmethacrylate (PMMA) induced under tensile stress are not mere cracks in the usual sense of open void cleavage. Rather they contain oriented polymer chains (craze matter) aligned in the direction of the tensile stress applied[1–3].

It was previously assumed that stress-whitening of rubber-toughened plastics was caused by a large number of small cracks[4]. Bucknall and

Figure 1—Electron micrograph of stress-whitened surface of compression-moulded sheet of HI-PS showing branched crazes. Direction of applied stress is perpendicular to main craze axis. Scale as *Figure 3*

REFERENCES

[1] OTSUKA, S. and KAWAKAMI, M. *Angew. Chem.* 1963, **75**, 978
[2] DAWANS, F. and TEYSSIE, P. *Polymer Letters*, 1965, **3**, 1045
[3] PORRI, L., NATTA, G. and GALLAZZI, M. C. Paper to International Symposium on Macromolecular Chemistry, Prague 1965 (A593)
[4] WILKINSON, G. and IRVINE, J. W. *Science*, 1951, **113**, 742
[5] LETO, J. R. and LETO, M. F. *J. Amer. chem. Soc.* 1961, **83**, 2944

Observation of Crazes in ABS-Polymer and High-impact Polystyrene under the Electron Microscope

IT HAS been reported that crazes in amorphous thermoplastics such as polystyrene (PS) and polymethylmethacrylate (PMMA) induced under tensile stress are not mere cracks in the usual sense of open void cleavage. Rather they contain oriented polymer chains (craze matter) aligned in the direction of the tensile stress applied[1–3].

It was previously assumed that stress-whitening of rubber-toughened plastics was caused by a large number of small cracks[4]. Bucknall and

Figure 1—Electron micrograph of stress-whitened surface of compression-moulded sheet of HI-PS showing branched crazes. Direction of applied stress is perpendicular to main craze axis. Scale as *Figure 3*

Smith[5], however, have concluded that stress-whitening is simply the same phenomenon as crazing based on the tensile behaviour of high-impact polystyrene (HI-PS) observed under the optical microscope.

In the present study, attempts have been made to observe stress-crazing (or stress-whitening) in ABS-polymer and HI-PS under the electron microscope so as to gain more insight into the behaviour of rubber-toughened plastics under stress. All the electron micrographs are taken by the methylcellulose/carbon two step replica method with Pt–Pd shadowing.

The electron micrograph of a stress-whitened surface of a compression-moulded sheet of HI-PS is presented in *Figure 1* to show characteristic stress-crazing as observed in PS and PMMA[3]. The stress-whitening evidently results from the stress-crazing of rubber-toughened plastics. In contrast with the straight crazes observed in PS and PMMA[3], however, branching is noted in crazes in HI-PS, which run in a direction perpendicular to the tensile stress applied.

The impact-fractured surface of ABS-polymer cleaved at a low temperature[6,7] is shown in *Figure 2*, the particles representing the rubber compo-

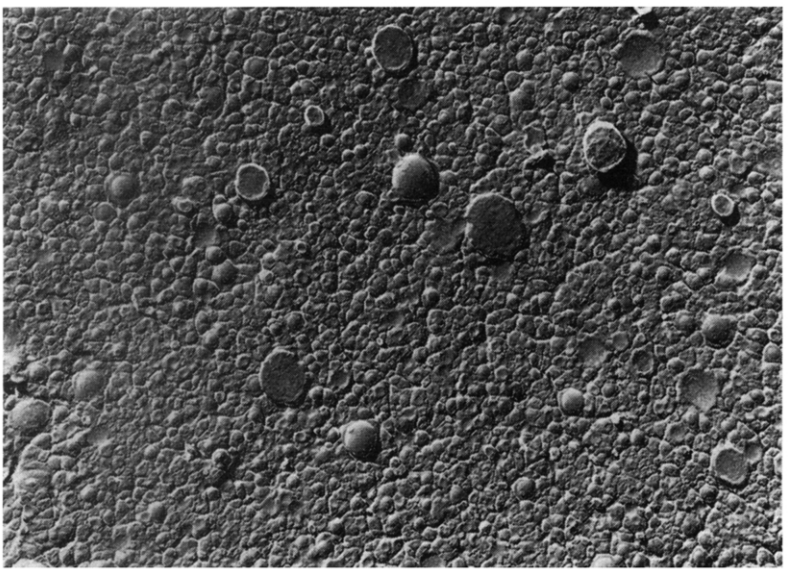

Figure 2—Electron micrograph of impact-fractured surface of ABS-polymer formed at a low temperature. Particles represent rubber components. Scale as *Figure 3*

nents (average radius *ca.* 0·3μ). Uni-axial tensile stress applied to this material causes stress-whitening. Branched crazes are observed in the whitened part as in HI-PS (*Figure 3*). It should be noted that the rubber particles are deformed along the direction of the applied stress.

A similar picture is also obtained at the stress-whitened surface of a compression-moulded sheet of ABS-polymer (*Figure 4*). Branched crazes

which run in a direction perpendicular to the applied stress are more clearly observable and crazes seem to propagate through the rubber particles.

When further stress is applied to the same specimen, denser whitening results and finally a crack starts at the most densely whitened portion. The electron micrograph of the whitened region at the tip of the crack is shown

Figure 3—Electron micrograph of whitening induced by a tensile stress applied to the specimen shown in *Figure 2*. Crazing associated with deformation of rubber particles is demonstrated. Arrow indicates direction of the applied stress

in *Figure 5*. Marked deformation throughout the structure including the rubber particles is clearly demonstrated and craze lines are no longer observable. The whole portion around the crack is rather covered with uniform craze matter.

Closer examination under the electron microscope reveals various steps of craze formation. Crazes, the widths of which are almost the same as the diameters of single rubber particles, are formed initially. Then, the rubber particles are deformed along the direction of the applied stress without reducing the radii in the direction perpendicular to the applied stress. The rubber particles often combine with each other along the direction of the applied stress during the coalescing process of craze lines.

The facts that the widths of the crazes in the initial stages correspond to the diameters of the rubber particles and that the crazes propagate into branches as they grow clearly imply that the presence of rubber particles

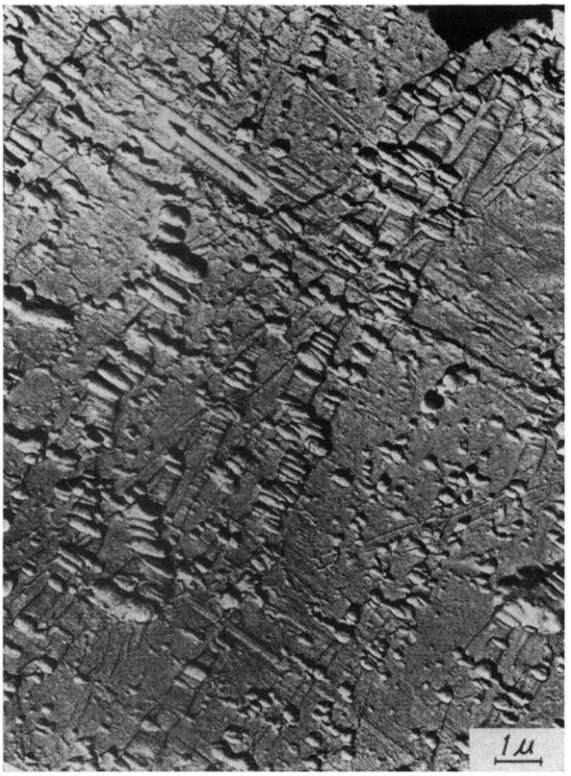

Figure 4—Electron micrograph of stress-crazing observed at compression-moulded surface of ABS-polymer. Arrow indicates direction of the applied stress

favours the initiation and development of crazes in a specimen under stress. As Nielsen[8] has previously suggested, the heat evolved due to the deformation of rubber particles would also play an important role in the craze formation.

The behaviour of ABS-polymer under stress may thus be visualized as follows:

(*1*) Since the modulus of rubber is approximately 0·001 that of the resin phase, rubber particles serve as voids or stress-concentrators, thus presenting a site for craze formation under stress.

(*2*) Crazes run through rubber particles in a direction perpendicular to that of the stress applied. Craze lines thus tend to branch out as the rubber particles are scattered in a random manner.

(*3*) Crazes broaden by themselves or coalesce with each other in the process of development. The whole portion under stress is ultimately covered with uniform craze matter.

(*4*) When the extension of craze matter reaches its limit or is interrupted by inhomogeneities such as dust particles and un-fused resin particles, a crack starts, and is closely followed by sudden rupture.

It should be noted that extensive crazing occurs before the start of true cracking and a considerable amount of energy is required in converting original polymer chains (random state) into craze matter (oriented state). It is, therefore, conceivable that the energy dissipation mechanism of rubber-

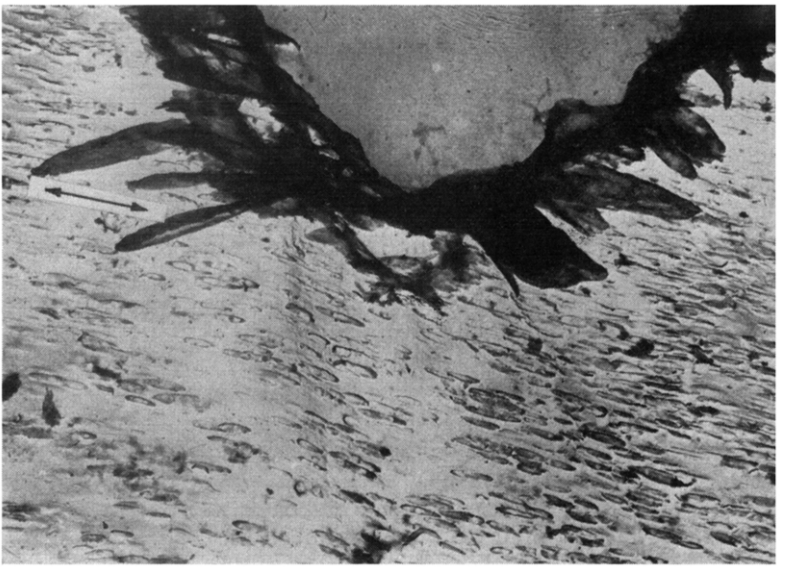

Figure 5—Electron micrograph of whitened region at the tip of true crack showing marked deformation throughout structure. Arrow indicates direction of the applied stress. Scale as *Figure 4*

toughened plastics should be interpreted in terms of the crazing process stimulated by the presence of rubber components rather than the process of crack propagation.

Though all the results reported in the present paper deal with the process of static tensile fracture, similar stress/strain relationships as well as whitening are noted in high-speed tensile fracture of ABS-polymer and HI-PS. It thus seems safe to apply the same energy dissipation mechanism to the impact fracturing process of rubber-toughened plastics.

The author wishes to thank Professor Y. Sato of Shinshu University for his kind suggestion and discussion, and Miss C. Nozaki for taking the electron micrographs.

Central Research Laboratory,
The Japanese Geon Company,
Daishigawara-Yako, Kawasaki City, Japan

MASATO MATSUO

(Received March 1966)

REFERENCES

[1] SAUER, J. A., MARIN, J. and HSIAO, C. C. *J. appl. Phys.* 1949, **20**, 507
[2] HSIAO, C. C. and SAUER, J. A. *J. appl. Phys.* 1950, **21**, 1071
[3] SPURR, O. K. and NIEGISH, W. D. *J. appl. Polym. Sci.* 1962, **6**, 585
[4] MERZ, E. H., CLAVER, G. C. and BAER, M. *J. Polym. Sci.* 1956, **22**, 325
[5] BUCKNALL, C. B. and SMITH, R. R. *Polymer, Lond.* 1965, **6**, 437
[6] BOTTY, M. C. *J. Polym. Sci. C*, 1963, **3**, 151
[7] SUEZAWA, Y., HOJO, H. and SAKAMOTO, S. *Journal of the Material Science Society of Japan*, 1964, **1**, 90
[8] NIELSEN, L. E. *Mechanical Properties of Polymers*, p 131. Reinhold: New York, 1962

Proton Spin–Lattice Relaxation in Polyethylene Oxide. Spin–diffusion and Methyl Group Rotation

PREVIOUS proton spin–lattice relaxation measurements on polyethylene oxide[1,2] (PEO) have indicated essentially a single motional minimum at all molecular weights although in the lower molecular weight materials ('Carbowaxes') it is difficult to dissociate the effects of the motional minimum from a coincident minimum due to the melting of the polymer. (This applies to measurements at 30 Mc/s; recently measurements at low frequency[3] in the rotating frame[4] have made it possible to separate the motional and phase change phenomena.) For the higher molecular weights ('Polyoxes': $\bar{M}_v > 2{\cdot}8 \times 10^5$) there is a motional minimum at $\sim 0°C$ and possibly another minimum associated with the softening point at $\sim 60°C$. All these results apply to polymers having hydroxyl end groups. However, methylation of these end groups leads to the appearance of a well defined motional minimum at low temperatures. Minima of this sort have been observed frequently in polymers containing a side chain methyl or ethyl group in their basic repeat unit[5–7] and have been ascribed to methyl group rotation, this assignment being confirmed by experiments on polymers containing deuterated methyl groups when the relaxation efficiency is reduced as expected[8]. However, it appears that in samples which contain only a small percentage of their protons in methyl groups, well defined motional minima can occur in the temperature range appropriate to methyl group rotation, and also that spin-diffusion is probably the important mechanism which allows nuclei in the bulk of the sample to relax.

Spin–lattice relaxation times of commercial samples[9] of PEO of molecular weights 550, 600, 750 and 6 000 were measured. Of these the 550 and 750 molecular weight samples had reputedly one OCH_3 end group and one OH end group. The precise amount of OCH_3 present was checked using a Varian HR 100 spectrometer and integrator, the relative areas of $—CH_2—$ ($6{\cdot}34\tau$) and $—CH_3$ ($6{\cdot}62\tau$) peaks being compared for the 550 and 750 samples. For the 550 sample the ratio was 0·061 (theoretical 0·064) and for the 750 sample 0·043 (theoretical 0·046), i.e. the OCH_3 concentration was slightly less than expected in both cases. The 600 and 6 000 samples did not contain detectable quantities of methyl groups. An unsuccessful attempt was made to methylate the OH end groups of the 6 000 sample. The measurements made on these samples are plotted in *Figure 1* as a function of $1/T \times 10^3$ [°K] and show the presence of shallow minima for the 550 and 750 samples at about 118°K, the 600 and 6 000 samples showing a steady increase in T_1 in this region as the temperature decreases. No non-exponential behaviour was observed in this region and it appears that the enhanced relaxation efficiency and occurrence of minima in the 550 and 750 samples must be due to the presence of the methyl groups, and that the bulk of the protons in the specimen are being relaxed by a spin-diffusion mechanism[8,10,11].

The theory of spin-diffusion has been discussed for paramagnetic impurities in alkali halides. In such systems relaxation depends on diffusion of nuclear polarization to the impurity centres which provide (via the large fluctuating local field due to the unpaired electron) efficient coupling with

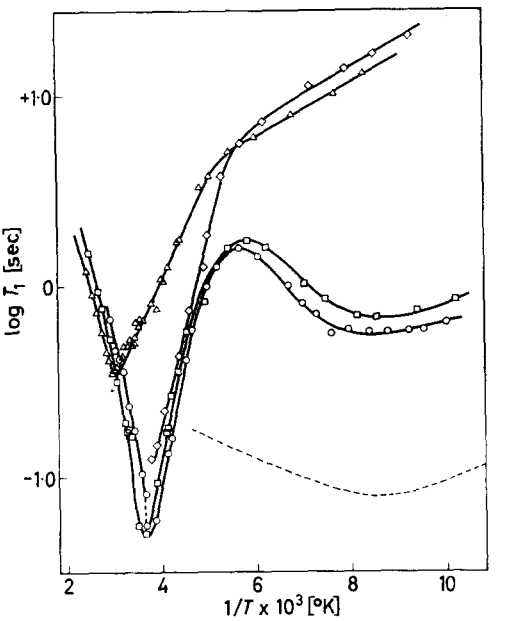

Figure 1—log T_1 versus $1/T \times 10^3$ (°K) for polyethylene oxide polymers. △ mol. wt 6 000, OH end groups; ◇ mol. wt 600. OH end groups; □ mol. wt 750 one OH and one OCH_3 end group; ○ mol. wt 550 one OH and one OCH_3 end group. Dotted line is theoretical curve from equation (4)

the lattice. In these experiments the most efficient coupling is apparently provided by a small percentage of protons present in rotating methyl groups.

Slightly modifying the theory of spin-diffusion as applied to the paramagnetic impurity case, we write for the contribution to relaxation due to spin diffusion

$$(1/T_1)_{S.D.} = 4\pi NbD \tag{1}$$

where N is the number of OCH_3 groups/cm³ and D is the diffusion constant for nuclear polarization defined approximately[8] as

$$D = Wa^2 \sim \{(\overline{\Delta\omega^2})^{\frac{1}{2}}/30\}a^2 \tag{2}$$

$(\overline{\Delta\omega^2})^{\frac{1}{2}}$ is the root second moment of the resonance line and a the mean distance within which there is a probability W of a spin exchange occurring. The length b may be defined[12] by the equations:

$$b \sim (C/D)^{\frac{1}{2}}$$

$$C = \frac{9}{40}\gamma^4\hbar^2\left[\frac{\tau_c}{1+\omega_0^2\tau_c^2}\,\frac{4\tau_c}{1+4\omega_0^2\tau_c^2}\right] \tag{3}$$

where ω_0 is the resonant frequency (30 Mc/s) and τ_c is the motional correlation time for the CH_3 group. For the theory to apply, the following inequalities must hold

$$b \ll R \ll L$$

where $R \sim N^{-\frac{1}{3}}$ and $L \sim R\,(R/b)^{\frac{1}{2}}$. These three quantities have the following significance[8] here; b is the scattering amplitude of a single methyl group, R the mean distance between methyl groups and L the diffusion length

during a relaxation time. Using reasonable values of the parameters involved [$(\overline{\Delta\omega^2})^{\frac{1}{2}}=5$ gauss, the value for polyethylene in this temperature range[13]; $a=2{\cdot}5$Å, a slightly greater distance than the CH_2 interproton distance of 1·8Å; unit density for PEO 750: $\omega_0\tau_c=0{\cdot}616$ at the T_1 minimum value] we find the values:

$$b=0{\cdot}43\text{Å} \qquad R=10{\cdot}8\text{Å} \qquad L=53{\cdot}9\text{Å}$$

which satisfy equation (4) reasonably well. It appears that no difficulty should occur on account of a diffusion barrier which exists in the paramagnetic impurity case[14] due to the large difference in Larmor frequencies of the nuclei and electrons. In the polymer the Larmor frequencies of the methyl group protons and the chain backbone protons will be almost equal, apart from the very small chemical shift difference. It seems therefore that equation (1) should be a reasonable approximation and combined with equation (3) gives

$$\left(\frac{1}{T_1}\right)_{\text{S.D.}}=4\pi N\left[\frac{9}{40}\gamma^4\hbar^2\left(\frac{\tau_c}{1+\omega_0^2\tau_c^2}\ \frac{4\tau_c}{1+4\omega_0^2\tau_c^2}\right)\right]^{\frac{1}{2}}D^{\frac{1}{2}} \qquad (4)$$

Using this equation and assuming an activation energy, Q, of 2 kcal[6] for τ_c and that $\omega_0\tau_c=0{\cdot}616$ at 118°K, values of T_1 are obtained whose temperature variation agrees reasonably well with the experimental curves in *Figure 1* but whose absolute values are much too low. Equation (4) here predicts a greater relaxation efficiency than is in fact observed. Theoretical T_1 values for PEO 750 in the low temperature region are shown as a dotted line in *Figure 1*, the values plotted being a factor of ten greater than those calculated. They still fall considerably below the experimental points, the theoretical and experimental values differing by two orders of magnitude. However, absolute calculations of T_1 using BPP theory [contained in the definition of C, equation (3)] frequently overestimate the efficiency of the relaxation process[15,16] and give values of T_1 which are too small, and it has been the practice to fit experimental values of T_1 using the minimum value of T_1 as one point on the theoretical curve[1,2,5-7], so a similar discrepancy here should not occasion surprise. Equation (4) reproduces the temperature variation of T_1 fairly well and predicts that the relaxation efficiency for PEO 550 should be greater than that for PEO 750, as is found.

However, a more stringent test of the theory would be provided by experiments at widely different frequencies, and relaxation measurements in the rotating frame[4,14] would be of interest from this point of view. It is difficult to envisage a mechanism other than spin-diffusion which will account qualitatively for these results, which show that the presence of quite small quantities of protons in methyl end or side groups can be detected by T_1 measurements.

T. M. CONNOR

Division of Molecular Science,
National Physical Laboratory,
Teddington, Middlesex.

(Received May 1966)

REFERENCES

[1] ALLEN, G., CONNOR, T. M. and PURSEY, H. *Trans. Faraday Soc.* 1963, **59,** 1525
[2] CONNOR, T. M., READ, B. E. and WILLIAMS, G. *J. appl. Chem.* 1964, **14,** 74
[3] HARTLAND, A. Private communication
[4] SLICHTER, C. P. and AILION, D. *Phys. Rev.* 1964, **135,** A1099
[5] CONNOR, T. M., BLEARS, D. J. and ALLEN, G. *Trans. Faraday Soc.* 1965, **61,** 1097
[6] CONNOR, T. M. and BLEARS, D. J. *Polymer, Lond.* 1965, **6,** 385
[7] POWLES, J. G., STRANGE, J. H. and SANDIFORD, D. J. H. *Polymer, Lond.* 1963, **4,** 401
[8] ABRAGAM, A. *The Principles of Nuclear Magnetism,* p 328. Oxford University Press: London, 1961
[9] *'Carbowax Polyethylene Glycols'* (Union Carbide Chemicals Co.) 1958
[10] BLOEMBERGEN, N. *Physica, 's Gravenhage,* 1949, **15,** 386
[11] DE GENNES, P. G. *J. Phys. Chem. Solids,* 1958, **7,** 345
[12] STEJSKAL, E. D. and GUTOWSKY, H. S. *J. chem. Phys.* 1958, **28,** 388
[13] MCCALL, D. W. and SLICHTER, W. P. *J. Polym. Sci.* 1957, **25,** 20
[14] GOLDMAN, M. *Phys. Rev.* 1965, **138,** A1675
[15] MONIZ, W. B., STEELE, W. A. and DIXON, J. A. *J. chem. Phys.* 1963, **38,** 2418
[16] MCCALL, D. W. and DOUGLASS, D. C. Private communication

Bulk Modulus Measurements on Polymers at High Temperatures

SOME measurements on the elasticity and anelasticity of polymethylmethacrylate by Kono reported[1] in 1960 were used by him as data to deduce a frequency shift versus temperature curve for bulk modulus but the course of this was highly and unexpectedly irregular. This suggested that it would be desirable to re-determine the data, preferably by another method.

A new method was developed based on some work by the writer in 1956. This used a small polymer specimen $\frac{9}{16}$ in. long, 1 in. diameter, cemented (by Araldite) into a cavity of similar dimensions in a sandwich type low velocity medium with two tapered aluminium blocks $2\frac{1}{2}$ in. in diameter, $2\frac{1}{4}$ in. long, similarly cemented to the circular faces of the specimen. Five zirconate piezoelectric transducer cylinders, each $\frac{1}{2}$ in. diameter, were fixed to the remote faces of these blocks to form a testing assembly suitable for transmitting (on an array of four transducers) and picking up 127 kc/s longitudinal mechanical waves which had travelled through the aluminium blocks and specimen. The sandwich type low velocity medium consisted of five $\frac{1}{16}$ in. thick plates of heavy metal (density about 17) cemented to four $\frac{1}{16}$ in. plates of laminated paper bonded with polymerized formaldehyde resin, the assembly having an axial velocity of about 1 350 m/sec together with a high attenuation so that almost no ultrasonic energy travelled other than via the specimen under test.

The assembly was heated up to about 160° C and was allowed to cool at the rate of about 1 deg. C or less per minute, the travel time of the mechanical waves being measured every 10 deg. C or so by methods described elsewhere[2] by the writer. A rectangular input electrical voltage wave one microsecond wide was used and the received signal was filtered via a series 20 mH coil and shunt load of 28 kΩ to guard against errors due to excessive high harmonics. The variation of velocity of longitudinal waves with temperature is plotted in *Figure 1,* and the data from the paper by Kono for $2\frac{1}{4}$ Mc/s waves are plotted as a dashed line on the same graph. Our velocity values are based on room temperature measurements on

REFERENCES

[1] ALLEN, G., CONNOR, T. M. and PURSEY, H. *Trans. Faraday Soc.* 1963, **59,** 1525
[2] CONNOR, T. M., READ, B. E. and WILLIAMS, G. *J. appl. Chem.* 1964, **14,** 74
[3] HARTLAND, A. Private communication
[4] SLICHTER, C. P. and AILION, D. *Phys. Rev.* 1964, **135,** A1099
[5] CONNOR, T. M., BLEARS, D. J. and ALLEN, G. *Trans. Faraday Soc.* 1965, **61,** 1097
[6] CONNOR, T. M. and BLEARS, D. J. *Polymer, Lond.* 1965, **6,** 385
[7] POWLES, J. G., STRANGE, J. H. and SANDIFORD, D. J. H. *Polymer, Lond.* 1963, **4,** 401
[8] ABRAGAM, A. *The Principles of Nuclear Magnetism,* p 328. Oxford University Press: London, 1961
[9] *'Carbowax Polyethylene Glycols'* (Union Carbide Chemicals Co.) 1958
[10] BLOEMBERGEN, N. *Physica, 's Gravenhage,* 1949, **15,** 386
[11] DE GENNES, P. G. *J. Phys. Chem. Solids,* 1958, **7,** 345
[12] STEJSKAL, E. D. and GUTOWSKY, H. S. *J. chem. Phys.* 1958, **28,** 388
[13] MCCALL, D. W. and SLICHTER, W. P. *J. Polym. Sci.* 1957, **25,** 20
[14] GOLDMAN, M. *Phys. Rev.* 1965, **138,** A1675
[15] MONIZ, W. B., STEELE, W. A. and DIXON, J. A. *J. chem. Phys.* 1963, **38,** 2418
[16] MCCALL, D. W. and DOUGLASS, D. C. Private communication

Bulk Modulus Measurements on Polymers at High Temperatures

SOME measurements on the elasticity and anelasticity of polymethylmethacrylate by Kono reported[1] in 1960 were used by him as data to deduce a frequency shift versus temperature curve for bulk modulus but the course of this was highly and unexpectedly irregular. This suggested that it would be desirable to re-determine the data, preferably by another method.

A new method was developed based on some work by the writer in 1956. This used a small polymer specimen $\frac{9}{16}$ in. long, 1 in. diameter, cemented (by Araldite) into a cavity of similar dimensions in a sandwich type low velocity medium with two tapered aluminium blocks $2\frac{1}{2}$ in. in diameter, $2\frac{1}{4}$ in. long, similarly cemented to the circular faces of the specimen. Five zirconate piezoelectric transducer cylinders, each $\frac{1}{2}$ in. diameter, were fixed to the remote faces of these blocks to form a testing assembly suitable for transmitting (on an array of four transducers) and picking up 127 kc/s longitudinal mechanical waves which had travelled through the aluminium blocks and specimen. The sandwich type low velocity medium consisted of five $\frac{1}{16}$ in. thick plates of heavy metal (density about 17) cemented to four $\frac{1}{16}$ in. plates of laminated paper bonded with polymerized formaldehyde resin, the assembly having an axial velocity of about 1 350 m/sec together with a high attenuation so that almost no ultrasonic energy travelled other than via the specimen under test.

The assembly was heated up to about 160° C and was allowed to cool at the rate of about 1 deg. C or less per minute, the travel time of the mechanical waves being measured every 10 deg. C or so by methods described elsewhere[2] by the writer. A rectangular input electrical voltage wave one microsecond wide was used and the received signal was filtered via a series 20 mH coil and shunt load of 28 kΩ to guard against errors due to excessive high harmonics. The variation of velocity of longitudinal waves with temperature is plotted in *Figure 1,* and the data from the paper by Kono for $2\frac{1}{4}$ Mc/s waves are plotted as a dashed line on the same graph. Our velocity values are based on room temperature measurements on

considerably larger blocks of the material under investigation and the fact that our check tests at higher frequencies agree within a fraction of one per cent of Kono's confirms that the materials used are very similar.

Comparison of the data from the two experiments shows good agreement at low temperatures but at high temperatures, where the velocity should be further maintained at the higher frequencies used by Kono, a

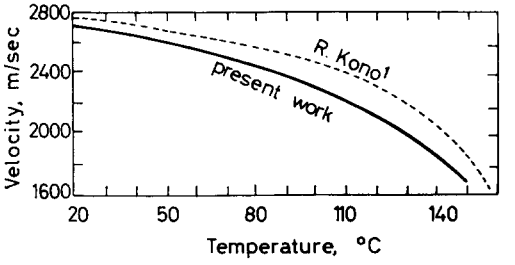

Figure 1—Variation with temperature of longitudinal wave velocity in polymethylmethacrylate (Perspex)

disagreement above 130° C is evident such that it is clear that the curves would cross at about 160° C. It is this rapid fall-off which is responsible for the anomalous course of the frequency-shift reported by Kono, an anomaly which is absent from his data on polystyrene[1] and his subsequent work[3] on polyvinylchloride. We therefore conclude that this anomaly is either absent or of considerably less extent than had been reported.

The writer wishes to thank the Director of the National Physical Laboratory for permitting him to use the equipment he had previously developed while working in those laboratories.

G. BRADFIELD*

Division of Molecular Science,
National Physical Laboratory,
Teddington, Middlesex.

(Received June 1966)

REFERENCES

[1] KONO, R. *J. phys. Soc. Japan,* 1960, **15,** 718
[2] BRADFIELD, G. National Physical Laboratory *Note of Applied Science No. 30,* 'Use in industry of elasticity measurements in metals with the help of mechanical vibration'. H.M. Stationery Office: London, 1964
[3] KONO, R. *J. phys. Soc. Japan,* 1961, **16,** 1793

*Now at University of Essex.

Studies on Radiation-induced Ionic Polymerization III—Polymerization of Styrene at Room Temperature*

K. UENO, K. HAYASHI and S. OKAMURA

The radiation-induced polymerization of styrene in an extremely dry system has been studied at room temperature. Sodium–potassium alloy was used as a drying agent. The kinetic results obtained were very different from those previously reported in which the radical reaction was predominant. A radical mechanism is precluded in a dry system for the following reasons: (a) *the addition of a small amount of water and ammonia caused a remarkable reduction in the rate of polymerization* (R_p); (b) *the activation energy for* R_p *was nearly zero between* $-20°$ *and* $+80°$ *C and* (c) R_p *was proportional to* $(\text{dose rate})^{0\cdot8 \text{ to } 1\cdot0}$, *while the molecular weight was independent of dose rate. To clarify the question whether the reaction mechanism in a dry system is cationic or anionic, copolymerizations of styrene with α-methyl styrene and with isobutyl vinyl ether were carried out and the results strongly support the suggestion of a cationic mechanism. This conclusion is also verified by the remarkable retardation of* R_p *by added ammonia and diethyl ether. Radical scavengers such as DPPH and oxygen also retarded the polymerization, so the existence of an ion-radical in the initiation step is supposed for the effect of above-mentioned scavengers. In an extremely dry system,* $G_{(\text{apparent initiation})}$ *is found to have a high value which may be attributed to a frequent monomer chain transfer. The polymerization mechanism based on free ions is described in detail.*

WHILE an ionic contribution to radiation-induced polymerization has been recognized and many researches have been carried out on several monomers such as isobutene[1], styrene[2] and butadiene[3], these studies have been largely confined to low temperatures. However, during the past few years, the radiation-induced polymerization of α-methyl styrene has been carried out by Williams *et al.*[4], and they have indicated the possibilities of ionic polymerization with dry monomers at room temperature. In general, it has been assumed that although electrons are ejected and cations are formed by the irradiation of monomers, the lifetime of ions is very short in a medium of low dielectric constant at room temperature, so that the radicals produced by charge recombination initiate a radical polymerization. Therefore, it seems that the studies of Williams *et al.*[4] indicate a new field of radiation-induced ionic polymerization, so the authors have investigated the polymerization of styrene in a rigorously dry system as part of a series of studies on radiation-induced ionic polymerization started in 1958[2]. This paper deals with the polymerization of styrene in bulk at room temperature and discusses the polymerization mechanism in detail[5].

*Parts I and II of this series; K. UENO, H. YAMAOKA, K. HAYASHI and S. OKAMURA, *Internat. J. appl. Radiat. Isotopes*, to be published.

EXPERIMENTAL

Materials

Commercial styrene was washed three times with ten per cent aqueous sodium hydroxide solution, three times with water, predried over anhydrous calcium chloride, and then dried over calcium hydride for a week. Before use, it was distilled under vacuum in a 60 cm helix packed column (25 mm mercury, 50°C). α-Methyl styrene was purified in a similar manner to styrene (25 mm of mercury, 67°C). Isobutyl vinyl ether was washed ten times with 20 per cent aqueous sodium hydroxide, washed with water, dried over potassium hydroxide for a week, and then distilled over fresh potassium hydroxide at 760 mm of mercury, 83°C. Sodium–potassium alloy (Na–K alloy) was prepared in dry cyclohexane in a ratio of 1 g of sodium to 2 g of potassium.

Sample preparations

The achievement of rigorous drying was a very important purpose of sample preparation. Purified styrene as mentioned above was stored in A of *Figure 1* and completely degassed. Na–K alloy, which was liquid above

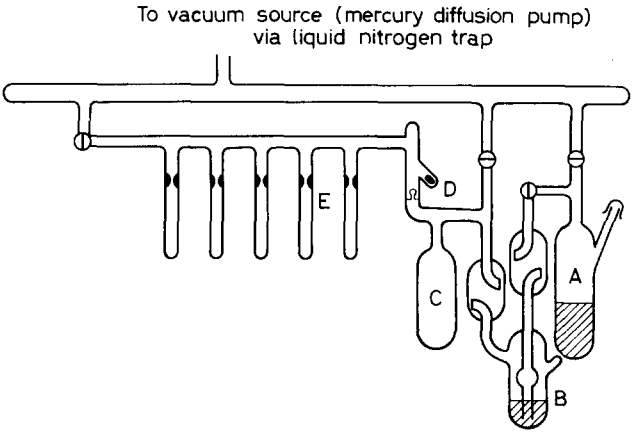

Figure 1—Apparatus for preparation of samples

−5°C, was poured into B, and sealed. The organic materials contained in the alloy were eliminated under high vacuum for 20 h, and then a small amount of the alloy was coated over the wall of the vessel. After the high vacuum line had been baked out, the middle fraction of A was distilled through fresh alloy into the reservoir of C kept at −80°C. After complete degassing in C, styrene was distilled into the polymerization ampoules through a breakable joint D, and finally sealed off in a vacuum of less than 10^{-5} mm of mercury. Ammonia was added using the apparatus shown in *Figure 2*. Commercial ammonia was distilled into a vessel containing Na–K alloy, stored for a week, enclosed in a break-seal vessel previously baked out, and then mixed with dried styrene which had been treated by the above method. The vapour pressure of ammonia was determined by a

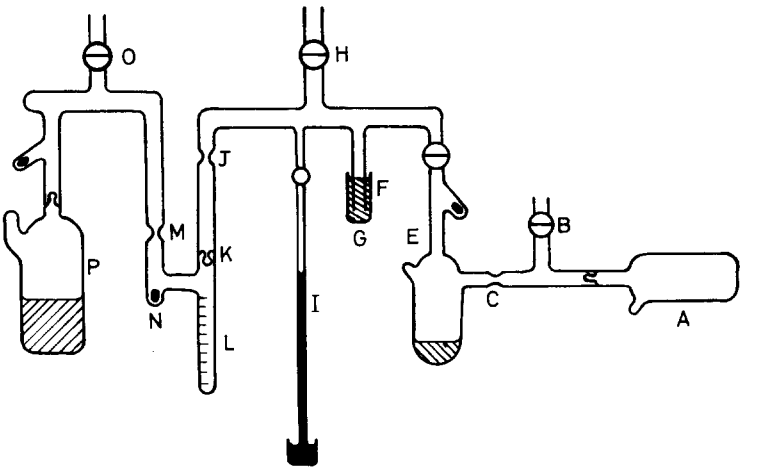

Figure 2—Apparatus for preparation of samples for styrene–ammonia system. A ammonia; B, H, O cock; C, J, M constriction; E, K breakable joint; F, G thermocouple gauge; I mercury manometer; L ampoule; N hammer; P styrene dried by Na–K

thermocouple vacuum gauge and a mercury manometer. Water was distilled from acidic aqueous potassium permanganate solution, aqueous sodium hydroxide solution, and finally without additive. The concentration of water was determined from the known saturated water vapour pressure at a particular temperature. Diethyl ether was dried over calcium hydride for 10 h, distilled into a vessel containing Na–K alloy, stored for a week, and finally enclosed in a break-seal vessel. Oxygen was passed through a spiral trap cooled by liquid nitrogen. DPPH was reprecipitated and dried under high vacuum at 70°C for 50 h. Zinc oxide and nickel oxide were baked under high vacuum at 300°C for 12 h. Samples for copolymerization studies, using the apparatus similar to that used for styrene bulk polymerization, were prepared as shown in *Figure 3*. For the purpose of comparison with a 'dry' system, 'wet' samples were prepared as follows. Pure monomers as mentioned under 'Materials' were transferred to the reaction ampoules by pipette and degassed under high vacuum. The water concentration was determined by the Karl Fischer method.

Polymerization and characterization of polymers

The activity of the ^{60}Co γ-ray source was 3 000 curies. Standard ferrous sulphate (Fricke) dosimetry was used in the determination of dose rates, employing a G value of 15·6 for the oxidation of ferrous sulphate. After irradiation, the ampoules were quickly opened, poured into a small amount of benzene, and added to a tenfold excess of methanol. After filtration, the polymer was dried to constant weight. An oily residue amounting to less than 0·5 per cent of the precipitated polymer was obtained after evaporation of the methanol used for precipitating and washing. Molecular weights were determined from intrinsic viscosity measurements

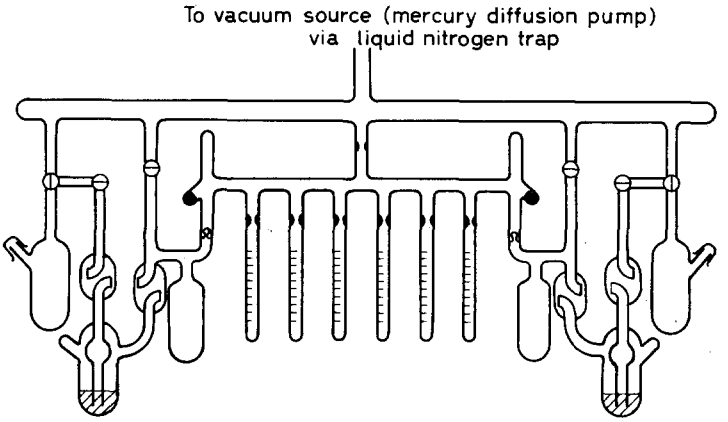

Figure 3—Apparatus for preparation of samples for copolymerization

in toluene at 30°C by means of an Ubbelohde viscometer, and the approximate number average molecular weight was calculated using Mayo *et al.*'s[6] equation (1).

$$\overline{M}_n = 1{\cdot}67 \times 10^5 [\eta]^{1{\cdot}37} \quad (1)$$

Yields of copolymerization were usually kept to less than ten per cent, and the molecular weight distributions were determined by a turbidimetric titration. The composition of styrene–α-methyl styrene units in the copolymer was determined from the ratio of optical densities of the infra-red absorptions at 1 380 cm^{-1} and 760 cm^{-1} using the potassium bromide method. For styrene–isobutyl vinyl ether copolymerization analysis, the use of 2 925 cm^{-1} and 700 cm^{-1} absorptions in carbon tetrachloride solution were adopted. The experimental errors were ± 5 per cent with St–αMeSt and ± 2 per cent in St–IBVE. Molecular weight distributions of polymers were measured by a turbidimetric titration apparatus[7] having an automatic recorder. The initial polystyrene concentration was 2 mg per 100 cm^3 of benzene, and methanol was used as a precipitating agent.

RESULTS

Polymerization of styrene

The radiation-induced polymerization in a rigorously dried system had very poor reproducibility, because it was very sensitive to the presence of

Table 1. Radiation-induced polymerization of 'pure' styrene

Sample and method	*Temp., °C*	*Dose rate rads/h*	*% conv. per 0·2 Mr*	M_n	$G(-m)$
Normal drying[10]	*ca.* 22	$1{\cdot}90\times10^5$	0·48	42 000	240
Normal drying[12]	*ca.* 20	—	0·52	—	260
Calcium hydride[9]	0	$1{\cdot}17\times10^6$	0·24	*ca.* 70 000	120
Silica drying[8]	0	$2{\cdot}24\times10^5$	11·2	78 900	5 600
Present result	24	$1{\cdot}90\times10^5$	69·1	42 000	34 400

traces of water. The results on the polymerization of pure styrene reported by several workers are summarized in *Table 1.* Metz and Johnson[8] obtained a very large rate of polymerization by the silica drying method, but our rate of polymerization achieved by Na–K alloy drying was further enhanced by a factor of between three and six. *Table 2* shows the results at different temperatures from −80°C to +37°C.

Table 2. Radiation-induced polymerization at various temperatures. Dose rate: 3 800 r/min

Code	*Temp., ° C*	*Physical state of monomer*	*Yield % per 0·2 Mr*	M_n
26*	−78	Solid	0·10	—
28*	−30·6	Solid–Liquid	1·46	—
37*	−21·0	Liquid	5·96	50 800
36**	0·0	„	28·4	44 600
35**	10·0	„	23·6	43 800
45***	−11·0	„	15·6	52 600
42***	0·0	„	29·0	44 200
40***	11·0	„	18·8	45 400
44***	33·0	„	20·1	42 200
41***	37·0	„	18·4	37 000

*, **, ***: the experiments having the same sign were made in the same run.

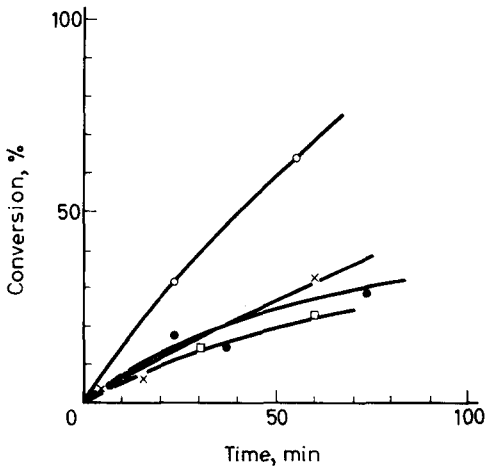

Figure 4—Polymerization of styrene. The experimental results having the same sign in the figure were made in the same run. Temp. 14° C. Dose rate 3 800 r/min. Na–K dried

In comparison with the data of Chen[9], it is obvious that water has almost no effect on the rate of polymerization at −80°C in the solid state. The rate in Chen's system indicated a maximum value in the neighbourhood of the melting point, where solid and liquid coexisted. On the other hand, in our 'dry' system, the rate increased remarkably, and no maximum value was obtained at the melting point. *Table 3* shows the results of polymerization at various temperatures. The activation energy from −20°C to 85°C was approximately zero, although accurate values could not be calculated because of poor reproducibility. Molecular weights showed reasonable

Table 3. Radiation-induced polymerization at various temperatures. Dose rate 2 100 r/min

Code	*Temp., °C*	*Yield % per 0·1 Mr*	M_n	*Code*	*Temp., °C*	*Yield % per 0·1 Mr*	M_n
233	20	16·7	46 000	227	59	21·8	34 500
237	28	13·1	45 000	232	73	23·2	32 500
235	35	19·3	37 000	229	83	15·5	—
236	47	21·0	38 000				

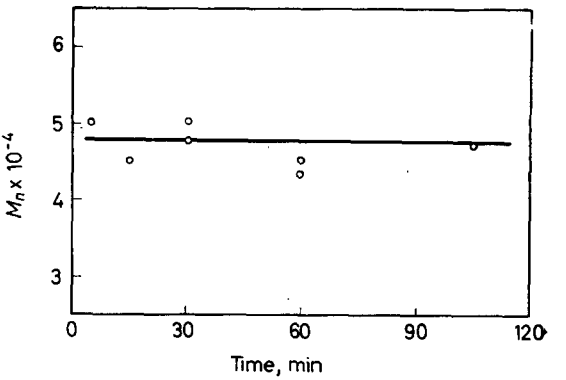

Figure 5—Dependence of molecular weight on polymerization time. Temp. 10° C. Dose rate 3 800 r/min. Na–K dried styrene

reproducibility and decreased slightly with increase of temperature. These results are very different from those of Ballantine *et al.*[10] in which the activation energy for the rate of polymerization is 6·7 kcal/mole, and the molecular weights increased with rise in temperature. *Figure 4* shows the relationship of polymerization yield and irradiation dose. If the preparation

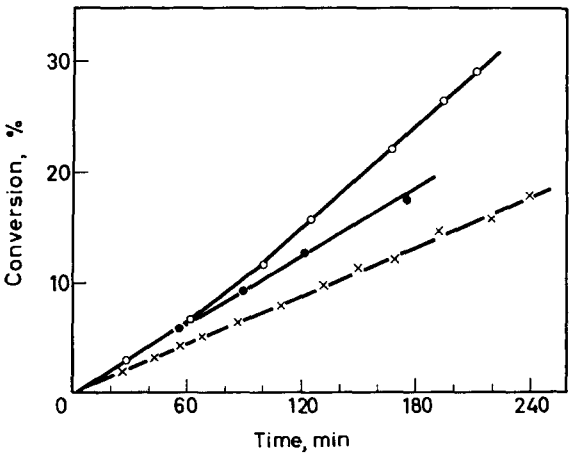

Figure 6—Time/conversion curve by dilatometry. Temp. 30° ±0·1° C. Dose rate 150 r/min. Dilatometer bulb volume 5·8 ml; capillary internal diameter 1·4 mm.
○ BaO dried; ●, ×, Na–K dried styrene

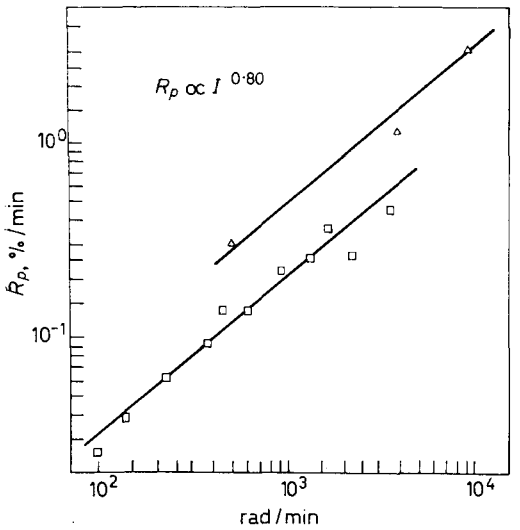

Figure 7—Dependence of rate of polymerization of styrene on dose rate. Points with same symbol represent same batch. Temp. 10° C. Na–K dried styrene. ^{60}Co γ-rays

batch was not the same, the reproducibility was very bad, so that it is essential to compare the results from the same batch. *Figure 5* indicates that molecular weights do not depend on the extent of conversion of polymer. Also, the molecular weights are nearly constant despite variations in rate. As shown in *Figure 6*, the polymerization started immediately after the system was irradiated with no induction period, and no marked acceleration was observed. *Figure 7* shows the dependence of polymerization rate on dose rate. The same symbol refers to the same batch. The rate of polymerization is proportional to the 0·8 power of dose rate, while in a 'wet' system, the rate depends on the square root of dose rate. *Figure 8* shows the dependence of the rate of polymerization on dose rate using electron irradiation by a Van de Graaff accelerator. At the higher dose

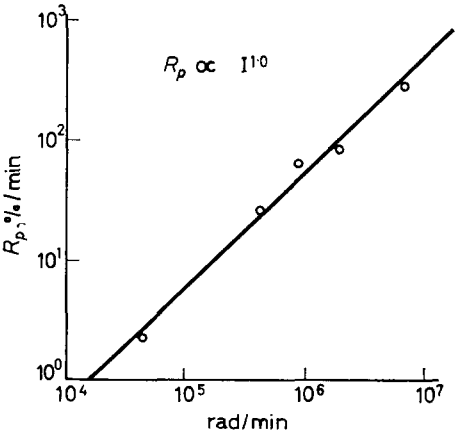

Figure 8—Dependence of rate of polymerization of styrene on dose rate. Temp. 0° C. Total dose 0·1 Mrad. Na–K dried syrene. 1·5 MeV electrons from Van de Graaff generator

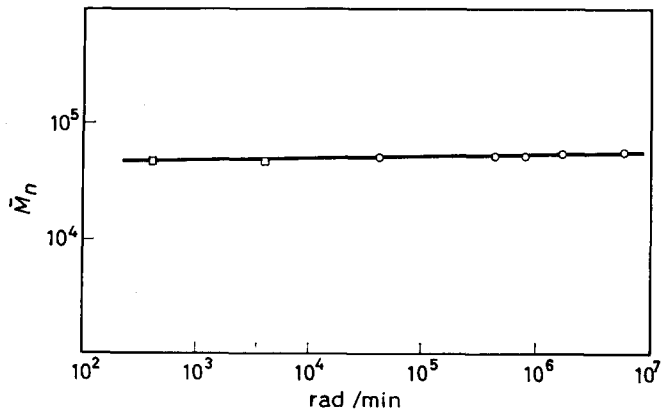

Figure 9—Dependence of molecular weight on dose rate. Temp. 0° C. □ ^{60}Co γ-rays. ○ 1·5 MeV electrons from Van de Graaff generator

rates, the rate of polymerization depends on the first power of dose rate, while in a 'wet' system, 0·5 order dependence was obtained[11]. *Figure 9* represents the relationship of molecular weights and dose in a 'dry' system and shows that molecular weights are independent of dose rate, although they increase slightly at higher dose rates. On the other hand, in a 'wet' system, they are proportional to the 0·5 power of dose rate[11].

Effect of additives

In order to investigate the polymerization mechanism, the usual radical scavengers such as DPPH and oxygen were used. They retarded the polymerization remarkably, as seen in *Table 4*. Molecular weights were little changed by additives. *Figure 10* shows the effect of oxygen and DPPH on the rate of polymerization. Even 1×10^{-4} mole/l. of these compounds induces a marked retardation. The effects of water, ammonia and diethyl ether were also investigated. *Figure 11* and *Table 5* show the effect of

Table 4. Effect of radical scavengers on polymerization of styrene. Temp., 16° C, dose rate 2 100 r/min

Code	*Radical scavengers mole/l.*	*Yield, %*	*Time, min*	R_p *%/min*	M_n
213	DPPH $4{\cdot}8\times10^{-3}$	1·24	1 449·5	0·0008	—
52	„ $3{\cdot}0\times10^{-3}$	0·00	100·0	—	—
214	„ $1{\cdot}0\times10^{-3}$	2·79	556·5	0·004	—
215	„ $6{\cdot}0\times10^{-4}$	3·92	556·5	0·007	53 000
216	„ $1{\cdot}1\times10^{-4}$	1·60	65·8	0·024	—
217	——	20·0	65·8	0·302	47 800
221	O_2 $2{\cdot}6\times10^{-2}$	4·75	556·5	0·0085	48 200
222	„ $4{\cdot}7\times10^{-2}$	15·2	1 425·9	0·0107	53 000
223	„ $4{\cdot}7\times10^{-3}$	5·2	390·7	0·0133	59 000
224	„ $1{\cdot}1\times10^{-3}$	9·3	390·7	0·0238	53 000
225	„ $1{\cdot}1\times10^{-3}$	23·8	1 425·9	0·0167	51 000

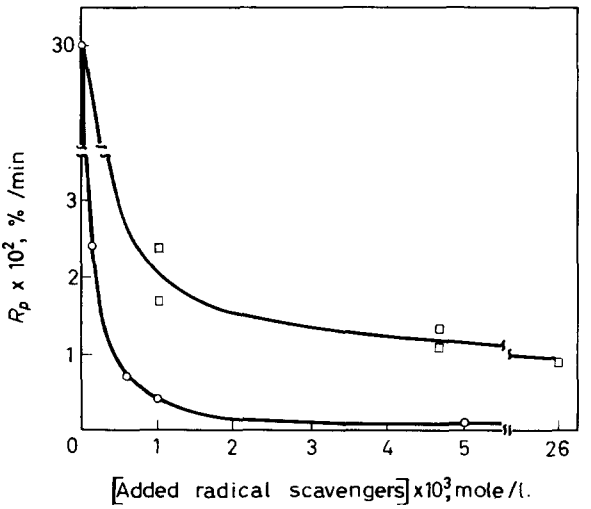

Figure 10—Effect of added oxygen and DPPH on rate of polymerization of styrene. □ O_2, ○ DPPH. Temp. 16° C. Dose rate 2 100 r/min

water on the rate of polymerization. A marked retardation was observed in the presence of water. The polymerization which is observed in the presence of more than 2×10^{-3} mole/l. of water may be due to a radical mechanism. The experimental technique used by Chen[9] might have been expected to give samples containing less than 1×10^{-3} mole/l. of water, but

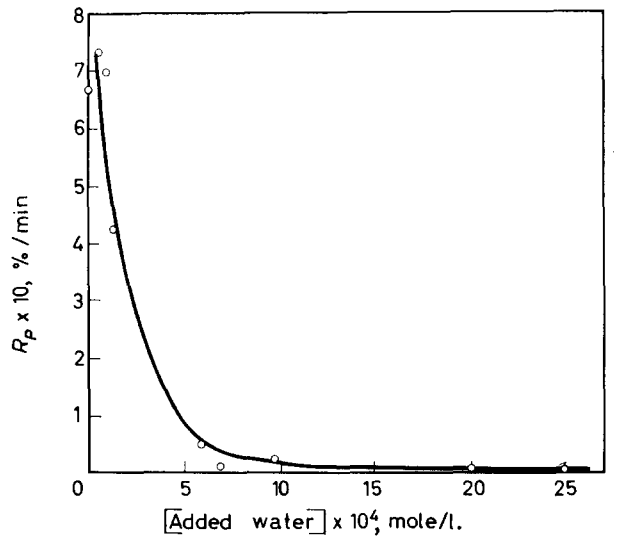

Figure 11—Effect of added water on rate of polymerization of styrene. Temp. 16° C. Dose rate 2 100 r/min

Table 5. Effect of added water on polymerization of styrene. Temp., 16° C, dose rate 2 100 r/min

Code	*Added water mole/l.*	*Yield %*	*Time, min*	R_p *%/min*	M_n
212	——	30·5	45·6	0·668	45 000
211	$4{\cdot}50\times10^{-5}$	39·8	54·6	0·730	40 000
201	$9{\cdot}00\times10^{-5}$	31·4	43·5	0·722	52 000
202	$1{\cdot}17\times10^{-4}$	19·6	45·6	0·430	49 000
206	$5{\cdot}70\times10^{-4}$	14·7	321·3	0·0458	48 000
207	$6{\cdot}80\times10^{-4}$	4·33	321·3	0·0135	50 000
204	$9{\cdot}75\times10^{-4}$	6·78	252·4	0·0269	55 000
208	$2{\cdot}00\times10^{-3}$	0·954	252·4	0·00378	60 000
209	$2{\cdot}50\times10^{-3}$	1·23	321·3	0·00458	—

Table 6. Effect of added diethyl ether on polymerization of styrene. Temp., 16° C, dose rate 2 100 r/min

Code	*Added diethyl ether mole/l.*	*Yield %*	*Time, min*	R_p *%/min*	M_n
254	$9{\cdot}00\times10^{-5}$	22·0	249·8	0·088	45 000
255	$1{\cdot}80\times10^{-4}$	4·9	755·2	0·0065	51 000

the results are very similar to those obtained in the 'wet' system of Chapiro[12], Ballantine[10] etc. Therefore, while it is obvious that water is usually the main cause of retardation, other impurities may also play an important role as mentioned already. The data of *Table 5* appear to show that the rate of polymerization is independent of water concentrations less than 1×10^{-4} mole/l. Nevertheless, samples dried by Na–K alloy showed poor

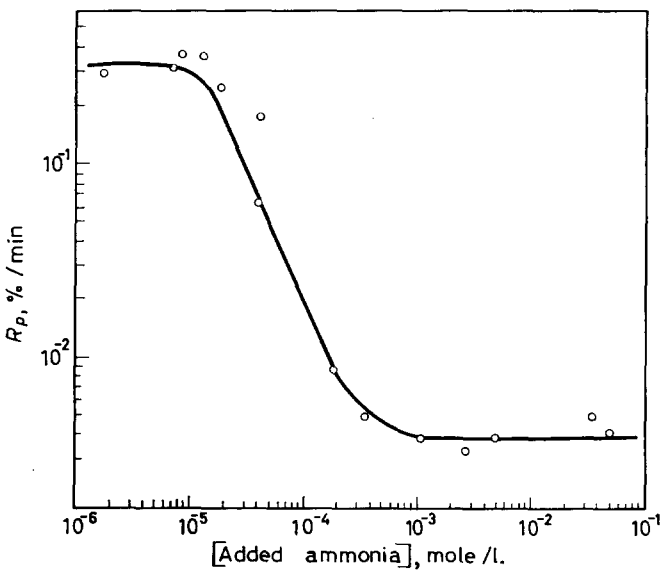

Figure 12—Effect of added ammonia on rate of polymerization of styrene. Temp. 20° C. Dose rate 2 100 r/min

reproducibility, and another experiment revealed that when a glass ampoule was not baked out, but only dried under vacuum at 10^{-5} mm of mercury for 5h, the rate of polymerization decreased remarkably. This latter result must be attributed particularly to the water adsorbed on the glass wall. It is well known that ammonia is a typical retarder of a cationic polymerization. Effects of ammonia in a 'dry' system are shown in *Figures 12* and *13*. Retardation by ammonia is even greater than that produced by the same concentration of water. The competition between polymerization and inhibition occurred in the range of from 10^{-4} to 10^{-5} mole/l. of ammonia concentration, and ammonia did not have an effect on the rate of polymerization in less than 10^{-5} mole/l. A cationic polymerization will be inhibited in more than 10^{-3} mole/l. and only a radical polymerization

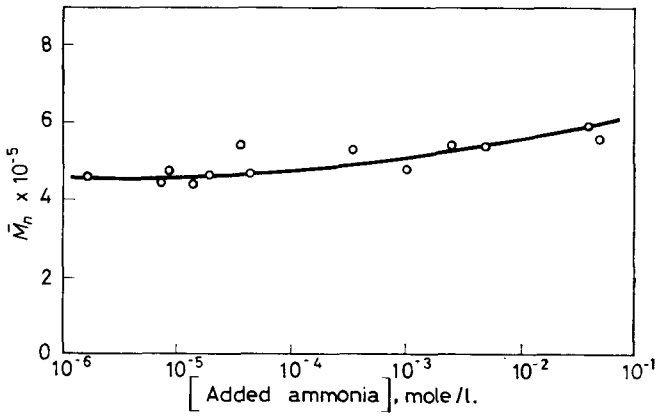

Figure 13—Effect of added ammonia on molecular weight. Temp. 20° C. Dose rate 2 100 r/min

will then be observed. On the other hand, the molecular weights increased only slightly in changing from a governing cationic polymerization to a radical polymerization. The results of experiments with dilatometers, as shown in *Figure 6*, do not appear to represent disappearance of impurities under irradiation. The effect of diethyl ether (Et_2O) is shown in *Table 6*. The retarder efficiency decreases in the series ammonia > diethyl ether > water which agrees with the order for the proton affinity of these

Table 7. Yield of methanol-soluble polymer. Dose rate 2 100 r/min. Temp. 16° to 20° C

Code	*Scavengers mole/l.*	*Methanol insoluble polymer, %*	*Methanol soluble polymer, %*
206	$H_2O: 5{\cdot}7 \times 10^{-4}$	14·7	0·2
207	$H_2O: 6{\cdot}8 \times 10^{-4}$	4·33	0·1
248	$NH_3: 1{\cdot}3 \times 10^{-5}$	30·4	0·2
249	$NH_3: 3{\cdot}6 \times 10^{-5}$	15·6	0·1
250	$NH_3: 3{\cdot}6 \times 10^{-4}$	3·88	0·3
254	$Et_2O: 4{\cdot}0 \times 10^{-5}$	22·0	0·3

scavengers[14]. Only methanol-insoluble polymers were considered in the above mentioned polymerization, but low molecular weight polymer which is soluble in methanol could be ignored in comparison with insoluble polymer, as shown by the results of *Table 7*. *Table 8* shows the effect of metal oxides, such as zinc oxide and nickel oxide. These metal oxides did not always enhance the rate of polymerization. It is often held that metal oxides serve to trap ejected electrons[15], but it might

Table 8. Effect of metal oxide on radiation-induced polymerization of styrene. Dose rate: 3 800 r/min, Na–K dried

Code	*Metal oxides wt %*	*Temp., °C*	*Yield % per 0·2 Mr*	M_n	$G(-m)$
54	None	10·0	27·2	50 400	13 600
46	ZnO 3·9	15·0	15·4	51 400	7 700
56	ZnO 6·2	15·0	87·1	60 000	43 500
57	ZnO 2·3	15·0	59·8	44 600	29 900
48	NiO 2·8	15·0	21·9	41 000	10 900

be considered that one of the roles of zinc oxide and nickel oxide as additives in this case is to act as drying agents for traces of water, because the highest $G(-m)$ obtained in this report was about 70 000 in drying by barium oxide as well as by Na–K alloy.

Copolymerization

As an attempt to elucidate the reaction mechanism, the copolymerization of styrene with α-methylstyrene was carried out with the results shown in *Figure 14*. The data in *Table 9* show that the rates of copolymerization

Table 9. Rate of copolymerization of styrene with α-methyl styrene. Dose rate $1{\cdot}0\times10^5$ r/h. Temp., 0° C

Code	*Drying method*	*Styrene mole fraction*	R_p *%/h*
66	Na–K	0·796	1·39
64	„	0·760	1·65
63	„	0·640	1·72
65	„	0·455	1·60
62	„	0·270	2·72
68	CaH_2	0·849	0·0324
69	„	0·627	0·0175
70	„	0·530	0·0089
80	„	0·403	0·0107
81	„	0·272	0·0041

in a 'dry' system are about fifty times as large as in a 'wet' system. From the results of *Figure 14*, monomer reactivity ratios are estimated to be $r_1(\mathrm{St})=0{\cdot}25\pm0{\cdot}25$, $r_2(\alpha\mathrm{MeSt})=8{\cdot}5\pm4{\cdot}0$ in a 'dry' system, while in a 'wet' system $r_1(\mathrm{St})=2{\cdot}2\pm0{\cdot}2$, $r_2(\alpha\mathrm{MeST})=0{\cdot}6\pm0{\cdot}2$. According to Tobolsky and Boudreau[16], the reactivity ratios are $r_1(\mathrm{St})=10{\cdot}5\pm0{\cdot}5$, $r_2(\alpha\mathrm{MeSt})=0{\cdot}08$

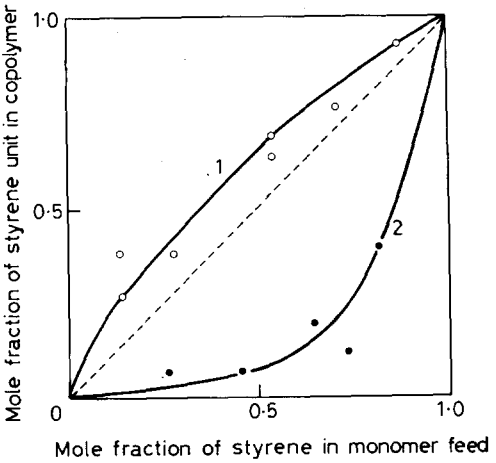

Figure 14—Copolymerization of styrene and α-methylstyrene. Temp. 0° C. Dose rate 3 800 r/min. ○ CaH_2 dried (water ~ 10^{-3} mole/l.). ● Na–K dried (no water). 1 r_1(St)= 2·2±0·2; r_2(αMSt)=0·6±0·2. 2 r_1(St) =0·25±0·25; r_2(αMSt)=8·5±4·0

±0·02 in the sodium–tetrahydrofuran system at 0°C, and $r_1=0{\cdot}54\pm0{\cdot}04$, $r_2=3{\cdot}6\pm0{\cdot}1$ in the titanium tetrachloride–toluene system at 0°C. As monomer reactivity ratios for radical polymerization in these systems have not been determined, they were calculated by the *Q.e* scheme and estimated to be r_1(St)=3·2, r_2(αMeSt)=0·2[17]. These facts indicate that the mechanism is cationic in a 'dry' system and radical in a 'wet' system. *Figure 15* represents the copolymerization results of styrene with isobutyl vinyl ether. The ratios r_1(St)=0·3±0·3 and r_2(IBVE)=10·0±4·0 are obtained for the 'dry' system, while r_1(St)=17·0±0·8 and r_2(IBVE)=0·1±0·1 apply to the 'wet' system. Rates of copolymerization in a 'dry' system were about twice as large as those in a 'wet' system (*Table 10*). The results are understandable in terms of a cationic mechanism, because it is well known that isobutyl vinyl ether is much more sensitive to cationic catalysts than styrene.

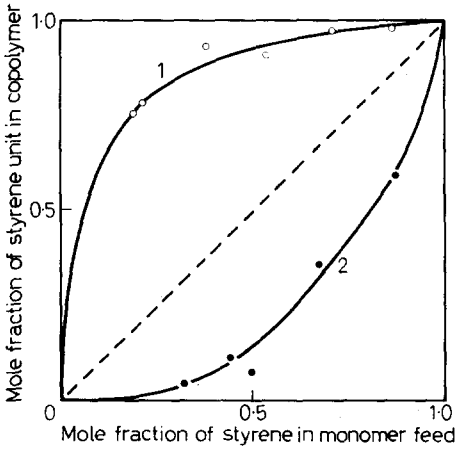

Figure 15—Copolymerization of styrene and isobutyl vinyl ether. Temp. 30° C. Dose rate 3 800 r/min. ○ KOH dried, water ~ 10^{-3} mole/l. ● Na–K dried, no water. 1 r_1(St)= 17·0±8·0; r_2(VE)=0·1±0·1. 2 r_1(St) =0·3±0·3; r_2(VE)=10·0±4·0

Table 10. Rate of copolymerization of styrene with isobutyl vinyl ether. Dose rate $1{\cdot}90\times10^5$ r/h. Temp., 30° C

Code	*Drying method*	*Styrene mole fraction*	R_p %/*h*
84	Na–K	0·860	0·71
89	,,	0·667	1·20
87	,,	0·490	4·25
83	,,	0·445	2·56
85	,,	0·320	4·38
86	,,	0·244	12·20
94	KOH	0·850	0·424
93	,,	0·696	0·374
92	,,	0·530	0·312
91	,,	0·361	0·228
90	,,	0·185	0·105

Williams *et al.*[18] found that the rate of polymerization for isobutyl vinyl ether increased remarkably in a 'dry' system, and estimated that a cationic polymerization had occurred. On the other hand, there are some reports about isobutyl vinyl ether[19] and α-methyl styrene[20] in a 'wet' system, which have suggested that the polymerization mechanism is radical. Methanol-soluble polymer has not been considered in these copolymerizations, because this represents less than three per cent of the methanol-insoluble polymer.

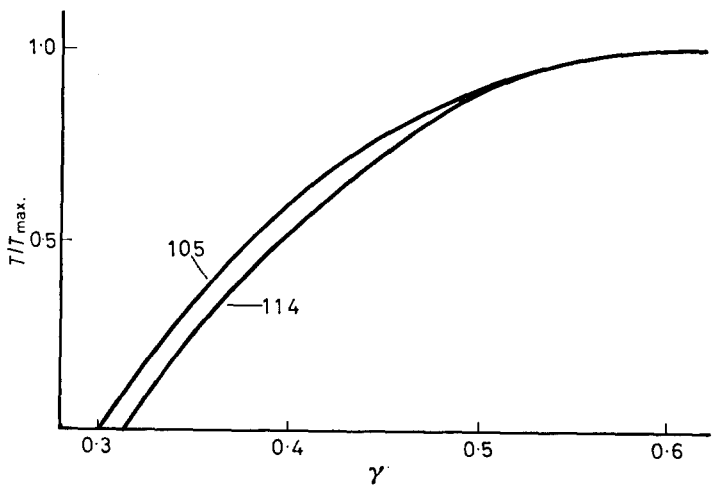

Figure 16—Turbidimetric titration curves of polystyrene

Code	*Temp.* ° *C*	*Dose rate r/min*	*Total dose Mr*	*Yield %*	*G(−m)*	M_n	*System*
105	24	3 170	0·0762	26·3	34 400	39 500	dry
114	24	3 170	8·70	19·8	227	39 500	wet

$T/T_{max.}$ ∽ f(M) dM γ=methanol/(methanol+benzene) ∽ M_w

Characterization of polymers

Viscosity average molecular weights obtained in a 'dry' system and a 'wet' system are very similar. The infra-red spectra of the polymers obtained in the two cases showed no difference, and both polymers softened at 135°C. *Figure 16* shows the results obtained for polymers prepared in the 'dry' and 'wet' systems as given by the turbidimetric titration method. The molecular weight distribution in a 'dry' system is very similar to that of a 'wet' system. Therefore, by these methods of characterization, there seems to be little or no difference in the polystyrenes formed in the radiation-induced ionic and radical reactions.

DISCUSSION

Styrene can be polymerized by radical cationic and anionic catalysts, so it is of much interest to clarify the polymerization mechanism in a 'dry' system. A radical mechanism is rejected for the following reasons.

(*a*) Addition of water in concentrations over 1×10^{-4} mole/l. results in a remarkable retardation.

(*b*) The rate of polymerization in a 'dry' system is proportional to the 0·8 to 1·0 order of dose rate in the range of 10^2 r/min to 10^7 r/min, while molecular weights are independent of dose rate.

(*c*) The activation energy for the rate of polymerization is nearly zero, while molecular weights are slightly larger at lower temperatures.

The above results show that polymerization in a 'dry' system is ionic. To answer the question whether the reaction mechanism in a 'dry' system is cationic or anionic, the following points are summarized.

(*d*) The rate of polymerization decreases markedly for ammonia concentrations exceeding 1×10^{-5} mole/l.

(*e*) Also, diethyl ether in concentrations over 1×10^{-4} mole/l. decreases the rate of polymerization.

(*f*) A large amount of methylene chloride does not decrease the rate of polymerization, while the molecular weights are enhanced (see Part IV)[21].

(*g*) The results of copolymerization of styrene with α-methyl styrene and of styrene with isobutyl vinyl ether support the view that a cationic polymerization occurs in a 'dry' system and a radical polymerization occurs in a 'wet' system.

The rate of polymerization in a 'dry' system is very sensitive to traces of water, while the molecular weights remain unchanged. A simple kinetic analysis on the effect of water is carried out as follows. The degree of polymerization in the absence of water is represented by equation (2).

$$\overline{DP} = k_p[M]/(k_{tm}[M] + k_t) \tag{2}$$

On the other hand, in the presence of water, equation (3) is obtained.

$$\overline{DP'} = \frac{k_p[\mathrm{M}]}{k_{tm}[\mathrm{M}] + k_{t'}[\mathrm{H_2O}] + k_t} \tag{3}$$

The apparent G_i for initiation is very large, so $G_{tm} = G(-m)/DP$ is much larger than the true $G_i(=G_t)$. And since $\overline{DP} \simeq \overline{DP'}$, then $k_{tm}[\mathrm{M}] \gg k_{t'}[\mathrm{H_2O}]$. These results are very different from behaviour in conventional cationic

polymerization, so it seems that water acts on the initiation process. The rate of polymerization in the absence of water is expressed by R_0 and in the presence of water by R_{H_2O}. On the assumption that water has an effect on the initiation step, Williams *et al.*[4] showed that equation (4) was obtained.

$$\log R_0/R_{H_2O} = \alpha[H_2O] \tag{4}$$

Assuming that when a water molecule is present in the distance x between ion and dipole, polymerization is inhibited completely in the initiation step, and also that the probability of inhibition obeys a Poisson distribution, x is estimated to be about 110Å in the styrene–water system. On the other hand, the intrinsic distance at which ion interacts with dipole is thought to be 15 to 30Å. Therefore, it is not clear whether water is effective in the initiation step only, because the distance of ion–dipole evaluated in these experiments is much larger than expected. Here, it is necessary to consider that the reproduction of active species occurs very frequently by chain transfer to monomer. If polymerization proceeds by free ions, which is very reasonable for radiation-induced ionic polymerization, G_i for the free ion is frequently less than 0·2[13, 22-24], so the number of polymer molecules produced by chain transfer after a single act of initiation becomes 500 as a maximum. By this means, it is possible to explain why the dependence of number average molecular weights on water concentration is within errors of molecular weight measurements, although water exerts a strong retardation effect. Moreover, when the water concentration is higher, the molecular weights of polymer produced by the radical mechanism must be considered. Therefore it is difficult to decide whether the effect of water is on the initiation or propagation step of polymerization, but it seems much more reasonable that this effect should be considered as the competition reaction between the growing chain end and water. Even in this case, the critical distance of ion–dipole calculated by equation (4) will represent a reasonable measure of inhibition; x is estimated to be about 190Å in the styrene–ammonia system, which shows that ammonia exerts a larger retardation than water, possibly because of the higher proton affinity of ammonia. Another factor favouring more effective retardation by ammonia than water may be the greater degree of association of the latter in hydrocarbons[25]. Experiments on diethyl ether are very few, but the order of retardation is ammonia > diethyl ether > water, which again agrees with the magnitudes of their proton affinities.

Now, the free ion mechanism is discussed for radiation-induced ionic polymerization. It is assumed that in ionic polymerization by catalysts, all the growing chain ends are closely associated with the counter ion having the opposite charge. In radiation-induced polymerization, counter ions certainly exist in the reaction vessel, but it is questionable whether they are localized in the vicinity of the growing centre without neutralization of charge, and have an effect on the propagation reaction. Two ions (or a carbonium ion and an electron) in solution will combine with high probability whenever they approach within a critical distance r_c, at which their mutual coulomb energy equals the energy of thermal migration kT. Then, $r_c = e^2/Ekt$ when e is the electronic charge and E is the dielectric constant

(for styrene; 2·43 at 25°C). For styrene at 25°C, r_c is evaluated to be 240Å. At closer distances, the ions drift towards one another at an accelerating rate, and the lifetime of ion pairs is too short for the polymerization of about 400 monomer units. It seems that polymerization induced by free ions is the more probable, because the lifetime of ion pairs is below 10^{-7} sec[22], while that of free ions is over 10^{-2} sec[23]. In addition the large effect of a small amount of additives is another reason in favour of the free ion mechanism. In catalytic ionic polymerization, the propagation step is thought to be[26]

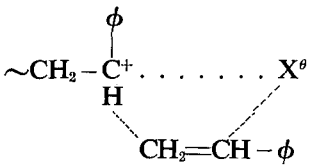

(5)

where X^{θ} denotes the counter ion. There the presence of the counter ion should be beneficial for the repulsion of additives of high proton affinity. Besides because the degree of freedom of the carbonium ion is small because of the counter ion[27], it seems that conventional ionic polymerization is not so sensitive to the presence of additives as is radiation-induced ionic polymerization. For example, the sensitivity of the latter system is such that even when the dose rate is increased from 10^2 r/min to 10^7 r/min, a remarkable retardation still appears, that is, the rate of polymerization at 10^7 r/min decreases to one thousandth with a water concentration of 10^{-3} mole/l. As well as a facile retardation by impurities, the absence of counter ions may greatly affect the chain transfer to monomer. It seems that electroconductivity measurements in saturated hydrocarbons by Allen and Hummel[23] clarify the polymerization mechanism by free ion initiation. The rate constant by the free ion mechanism is calculated as follows.

$$R_p = -\mathrm{d}[\mathrm{M}]/\mathrm{d}t = k_p[\mathrm{n}^{\star}]\,[\mathrm{M}] \tag{6}$$

This [n★] value is larger than the concentration of growing chain ends, and k_p calculated from equation (6) may give the minimum value. Assuming that the [n★] is approximately 10^{-10} mol/l., which is of the same order as the value estimated for ethyl benzene[28], k_p is calculated to be 10^6 l./mol. sec. Although this value is based on some bold assumptions, it is remarkably large in comparison with k_p values for conventional cationic polymerization. The propagation rate constants in conventional cationic polymerization have been obtained by several methods and they are less than 10^2 l./mol. sec[29-31]. The reason for the larger value of the propagation rate constant in radiation-induced polymerization can be explained by the free ion mechanism, for it has been shown by Szwarc *et al.*[32] that the propagation rate constant by free ions is five hundred times as large as that of ion pairs in the anionic polymerization of styrene in tetrahydrofuran.

It was found that polymerization in a 'dry' system was retarded remarkably by radical scavengers such as DPPH and oxygen. Although the action

of such scavengers may be ambiguous, this result suggests that the initiating process may occur by a radical-ion as follows.

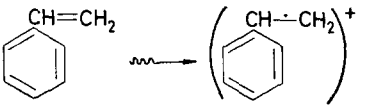

(7)

This cation-radical reacts very easily with another styrene monomer, because they have just the same π-electron configuration. Then they produce free cation and radical ends.

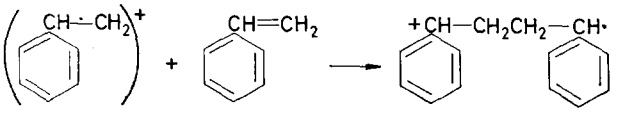

(8)

The propagation rate is very large for a free cation in comparison with radical propagation. Therefore in the absence of water, the free cationic propagation predominates. In the presence of water, the rate of polymerization is reduced and radical propagation plays the important role, because the cationic end is killed by traces of water. It is conceivable that DPPH has some retardation effect in an ionic polymerization as well as in radical polymerization. Inhibition by oxygen was also observed by Collinson *et al.*[33] in the radiation-induced ionic polymerization of isobutene at low temperature; while it is generally agreed that oxygen functions as an electron trap, their suggestion that O_2^- kills the carbonium ion before propagation can occur is inconsistent with the free ion mechanism.

Finally, the role of the negative ion (or electron) must be considered. Measurements of ion mobilities indicate that the mobility of negative ions is somewhat larger than that of positive ions[22, 28]. In addition Hamill *et al.*[34] have concluded from many studies on the absorption spectra of irradiated glasses at low temperature that electrons can be trapped as molecular anions. However, the concentration of negative ions does not appear to be so important in radiation-induced cationic polymerization of styrene and, from the dose rate dependence, the main termination reaction may be attributed to the reaction of carbonium ions with impurities.

The authors wish to acknowledge to Dr M. Katayama of the Faculty of Science of Hokkaido University for advice and assistance with experimental techniques.

Department of Polymer Chemistry,
Kyoto University,
Kyoto, Japan

(*Received November 1965*)

REFERENCES

[1] DAVISON, W. H. T., PINNER, S. H. and WORRALL, R. *Proc. Roy. Soc. A*, 1959, **252**, 187
[2] OKAMURA, S. and FUTAMI, S. *Internat. J. appl. Radiat. Isotopes*, 1960, **8**, 46
[3] ANDERSON, W. S. *J. phys. Chem.* 1959, **63**, 765
[4] BEST, J. V. F., BATES, T. H. and WILLIAMS, F. *Trans. Faraday Soc.* 1962, **58**, 192
[5] UENO, K., HAYASHI, K. and OKAMURA, S. *J. Polym. Sci. B*, 1965, **3**, 363
[6] MAYO, F. R., GREGG, R. A. and MATHESON, M. S. *J. Amer. chem. Soc.* 1951, **73**, 1691
[7] GOOBERMAN, G. *J. Polym. Sci.* 1959, **40**, 469
[8] METZ, D. J. and JOHNSON, C. L. American Chemical Society, Division of Polymer Chemistry, *Polymer Preprints*, 1963, **4**, 440
[9] CHEN, C. S. H. *J. Polym. Sci.* 1962, **58**, 389
[10] BALLANTINE, D. S., COLOMBO, P., GLINES, A. and MANOWITZ, B. *Chem. Engng Progr.* 1954, **50**, 267
[11] OKADA, T and SAKURADA, I. *Annual Report* of the Japanese Association for Radiation Research on Polymers, 1961, **3**, 103
[12] CHAPIRO, A. and WAHL, P. *C.R. Acad. Sci. Paris*, 1954, **238**, 1803
[13] BONIN, M. A., BUSLER, W. R. and WILLIAMS, F. *J. Amer. chem. Soc.* 1965, **87**, 199
[14] MUNSON, M. S. B. *J. Amer. chem. Soc* 1965, **87**, 2332
[15] WORRALL, R. and PINNER, S. H. *J. Polym. Sci.* 1959, **34**, 229
[16] TOBOLSKY, A. V. and BOUDREAU, R. J. *J. Polym. Sci.* 1961, **51**, S53
[17] ALFREY Jr, T. and PRICE, C. C. *J. Polym. Sci.* 1947, **2**, 101
[18] BONIN, M. A., CALVERT, M. L., MILLER, W. L. and WILLIAMS, F. *J. Polym. Sci. B*, 1964, **2**, 143
[19] OKAMURA, S., HAYASHI, K., NAKAMURA, Y. and NISHII, M. *Symposium on Radiation Chemistry*, p 11. Kyoto, Japan, 1960
[20] HIROTA, K., MAKINO, K., KUWATA, K. and MESHITSUKA, G. *Bull. chem. Soc. Japan*, 1960, **33**, 251
[21] UENO, K., HAYASHI, K. and OKAMURA, S. *Polymer, Lond*, 1966. **7**, 451
[22] WILLIAMS, F. *J. Amer. chem. Soc.* 1964, **86**, 3954
[23] ALLEN, A. O. and HUMMEL, A. *Disc. Faraday Soc.* 1963, **36**, 95
[24] FREEMAN, G. R. *J. chem. Phys.* 1963, **39**, 988
[25] WILLIAMS, F. *Disc. Faraday Soc.* 1963, **36**, 254
[26] OVERBERGER, C. G., AROND, L. H., TANNER, D., TAYLOR, J. J. and ALFREY Jr, T. *J. Amer. chem. Soc.* 1952, **74**, 4848
[27] KANOH, N., HIGASHIMURA, T. and OKAMURA, S. *Makromol. Chem.* 1962, **56**, 65
[28] HAYASHI, Ka., TAKAGAKI, T., HAYASHI, K. and OKAMURA, S. *Annual Report of the* Japanese Association for Radiation Research on Polymers, 1964–65, **6**, 135
[29] OKAMURA, S., KANOH, N. and HIGASHIMURA, T. *Chemy. high Polym.* 1962, **19**, 181
[30] PEPPER, D. C. Symposium über Makromolekulare Chemie in Wiesbaden 1959, III A-9. *Proc. Roy. Soc. A*, 1961, **263**, 58 and following papers
[31] LONGWORTH, W. R. and PLESCH, P. H. Symposium über Makromolekulare Chemie in Wiesbaden 1959, III A-11
[32] BHATTACHARYYA, N. D., LEE, C. L., SMID, J. and SZWARC, M. *Polymer, Lond.* 1964, **5**, 54
[33] COLLINSON, E., DAINTON, F. S. and GILLS, H. A. *J. phys. Chem.* 1959, **63**, 909
[34] RAO, P. S., NASH, J. R., GUARINO, J.P., RONAYNE, M. R. and HAMILL, W. H. *J. Amer. chem. Soc.* 1962, **84**, 500

Studies on Radiation-induced Ionic Polymerization IV—Polymerization of Styrene in Solution at Room Temperature

K. UENO, K. HAYASHI and S. OKAMURA

The radiation-induced polymerization of styrene in an extremely dry system has been studied in methylene chloride and toluene solution at room temperature. Under conditions of rigorous drying, far higher $G(-m)$ values have been obtained in comparison with those of normal conditions. Molecular weights of polystyrene formed in methylene chloride are higher than those obtained in bulk polymerization, which suggests strong confirmation of a cationic mechanism. Polystyrene obtained in methylene chloride at 10°C contained less than 0·3 chlorine atoms for each polymer molecule. In polymerization in toluene, the molecular weights of polystyrene decreased with increase of solvent concentration; this can be explained by chain transfer to toluene.

IN A previous paper[1] it was reported that the radiation-induced bulk polymerization of rigorously dried styrene proceeds by a cationic mechanism at room temperature. This paper describes the effect of solvents on the polymerization of styrene.

EXPERIMENTAL

Experimental procedures have been described in detail in previous papers, so only the drying methods used for the methylene chloride and toluene solvents are described. Methylene chloride was washed with ten per cent aqueous potassium carbonate, predried over phosphorus pentoxide, refluxed for five hours over fresh phosphorus pentoxide and then distilled. This was poured into A of *Figure 1*, agitated under high vacuum over calcium

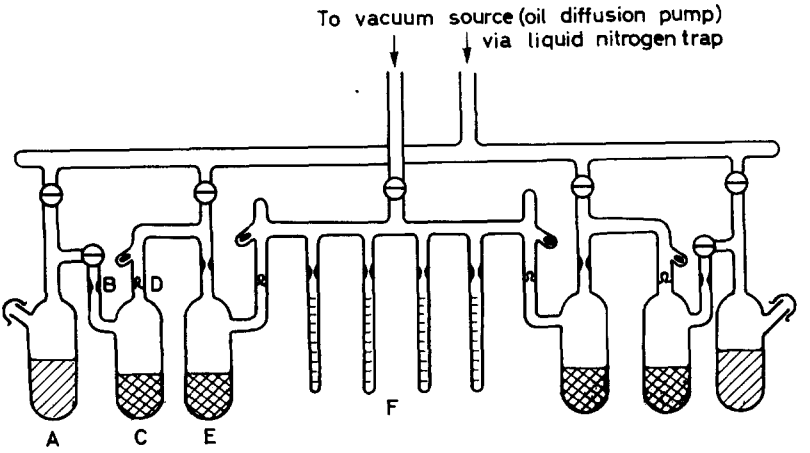

Figure 1—Apparatus for preparation of samples. A, CH_2Cl_2(or styrene), CaH_2; B, constriction; C, E, BaO, baked at 300°C under vacuum at 10^{-5} mm of mercury for 12 h; D, breakable joint; F, polymerizing ampoules

hydride for two days, distilled on to barium oxide which had been baked out under high vacuum at 330°C for 10 h, sealed off at the constriction of C, and stored for ten days. The middle fraction was distilled into the storage vessel containing baked barium oxide (E), stored for ten days in this vessel, and then distilled into the polymerization ampoules (F). Styrene was dried by the method previously mentioned[1]. Toluene was washed with concentrated sulphuric acid and then water, predried over calcium chloride for a day, refluxed over sodium metal for five hours and then distilled. This was dried by Na–K alloy, as described in the previous report[1], and also by barium oxide as already described for methylene chloride. The chlorine content of the polymer obtained in the styrene–methylene chloride system was determined by activation analysis[2]. Before analysis, the polymer was washed by dissolving in benzene and precipitating with methanol, and this procedure was repeated four times. Previously, these procedures were established to result in a complete purification of polymer. 50 mg of dried polymer was weighed accurately and packed with a sulphate paper. This was put into a polyethylene container with a standard sample consisting of a piece of filter paper containing ammonium chloride, and irradiated with thermal neutrons. After irradiation, the activities of the standard sample and the polymer were quickly determined by the use of a γ-ray scintillation spectrometer.

RESULTS

Figure 2 shows the effect of toluene on the rate of polymerization of styrene, which was much higher in a 'dry' system than in a 'wet' system. It was previously established that in the former case, the polymerization proceeds by a cationic mechanism, while in the latter system the reaction occurs by a radical mechanism. As shown in the relationship between styrene concentration and molecular weight in *Figure 3*, the lowering of

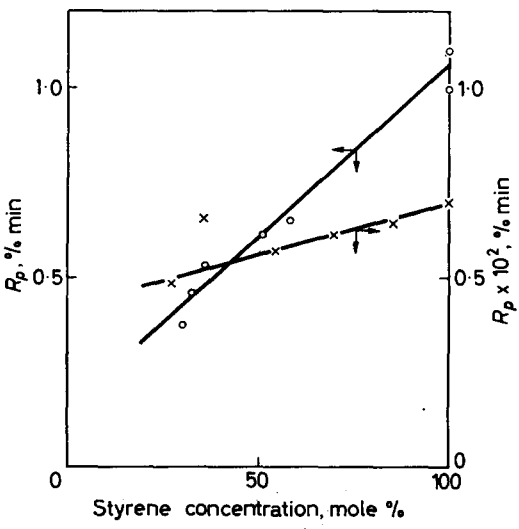

Figure 2 — Radiation-induced polymerization of styrene in toluene solution. Temp. 23°C. Dose rate 3 170 r/min. ○ Na–K drying (H_2O conc. none), × Normal drying (H_2O conc. 1×10^{-3} mole/l.)

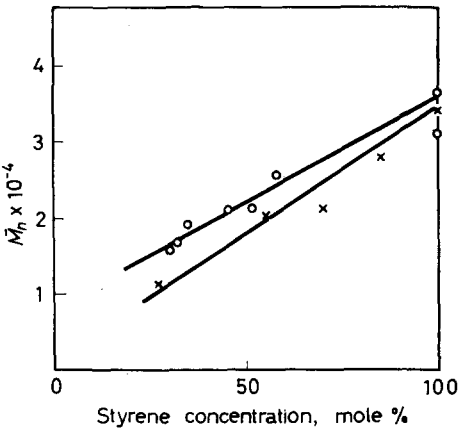

Figure 3—Radiation-induced polymerization of styrene in toluene solution; experimental conditions same as in *Figure 2*

molecular weight by addition of toluene was similar in both 'dry' and 'wet' systems. *Table 1* summarizes these results. The apparent G_i value was

Table 1. Radiation-induced polymerization of styrene in toluene solution*

Code	*Water conc. mole/l.*	*Styrene conc. mole/l.*	*Total dose Mr*	*Yield %*	M_n	$G(-M)$†	G_i‡
105	none¶	100	0·0762	26·3	42 000	34 400	86·5
102	none¶	58	0·0762	15·6	26 400	12 400	48·6
107	none¶	36	0·0762	12·8	16 200	6 550	42·1
101	none¶	32	0·0762	10·9	14 800	4 960	35·2
114	1×10^{-3}	100	8·70	19·8	39 500	227	0·600
113	1×10^{-3}	85	8·70	17·8	29 400	176	0·627
112	1×10^{-3}	70	8·70	17·0	20 500	141	0·720
111	1×10^{-3}	55	8·70	16·7	19 300	104	0·563
109	1×10^{-3}	27	8·70	11·4	8 400	44	0·552

*Temp., 24°C. Dose rate 3 170 r/min.
†Overall G value absorbed in solution per 100 eV.
‡Based on the assumption that $(G_i)_{\text{app. ion}}$ equals $(G_i)_{\text{app. radical}}$.
¶Na-K drying.

much higher in a 'dry' system than a 'wet' system, and the G_i of the former decreased with decrease of styrene concentration. *Figure 4* represents the effect of toluene concentration on the rate of polymerization in samples prepared by the barium oxide drying method. Although the conditions such as temperature and dose rate were different from those of the Na–K drying method, the rate of polymerization in this case was not lowered by the addition of about 40 mole per cent of toluene. Because of the different nature of the results obtained with the two drying agents, the dependence of the rate of polymerization on toluene concentration is not clear. However, the molecular weights attained under the two drying conditions are in much closer agreement. *Figure 5* shows the plots of $1/\overline{DP}$ against [S]/[M], according to Mayo's equation[3], from which are obtained $k_{tm}/k_p \fallingdotseq 0{\cdot}27\times10^{-2}$ and $k_{ts}/k_p \fallingdotseq 0{\cdot}22\times10^{-2}$ for the Na–K drying system, while the values $k_{tm}/k_p = 0{\cdot}24\times10^{-2}$ and $k_{ts}/k_p = 0{\cdot}16\times10^{-2}$ are deduced for the barium oxide drying system. In the system dried normally, in which a radical mechanism proceeds, Mayo plots based on *Figure 3* give $k_{tm}/k_p \fallingdotseq 0{\cdot}27\times10^{-2}$

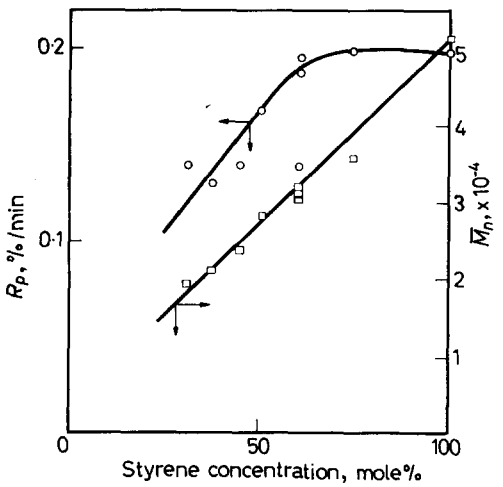

Figure 4 — Radiation-induced polymerization of styrene in toluene solution. Temp. 10°C. Dose rate 583 r/min. BaO dried. ○ Rate, □ Molecular weight

and $k_{ts}/k_p \fallingdotseq 0{\cdot}36 \times 10^{-2}$. In the catalytic polymerization, the chain transfer constant to toluene was estimated to be $k_{ts}/k_p \fallingdotseq 1 \times 10^{-2}$ for stannic tetrachloride[4] (cation), while $k_{ts}/k_p \fallingdotseq 3 \times 10^{-5}$ for azobisisobutyronitrile (radical)[5]. *Figure 6* shows the effect of methylene chloride on the rate of polymerization. The drying of methylene chloride by Na–K alloy did not change the rate of polymerization; however, drying by barium oxide enhanced the polymerization remarkably. It seems that the dependence of rate and molecular weight on monomer concentration is different in the 'dry' and 'wet' systems. The solution polymerization mechanism in a 'wet' system, which proceeds by a radical mechanism, has already been analysed kinetically in detail by Chapiro *et al.*[6] On the other hand, a

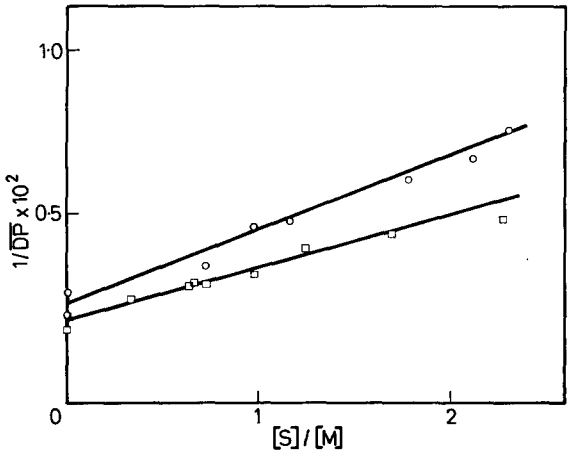

Figure 5—Relationship between degree of polymerization and monomer concentration. Experimental conditions same as *Figure 3* and *Figure 4*. ○ Na–K drying, □ BaO drying

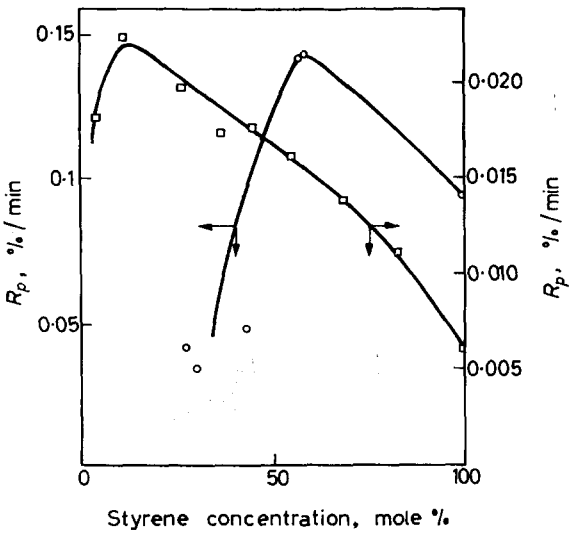

Figure 6—Rate of polymerization of styrene in CH_2Cl_2. Temp. 10°C. ○ BaO drying (H_2O conc. none); dose rate 583 r/min. □ Normal drying (H_2O conc. 1×10^{-3} mole/l.). Dose rate 467 r/min

kinetic analysis is difficult for the 'dry' system, because of poor reproducibility. *Figure 7* shows that molecular weights decreased with increase of methylene chloride in a 'wet' system, whereas the opposite effect occurred in a 'dry' system. These results are summarized in *Table 2*. Stannett *et al.*[7] have reported that the rate of polymerization in the styrene–methylene chloride system at −78°C is enhanced by drying, and we have obtained similar results. *Figure 8* shows the effect of water on the rate of polymerization in methylene chloride solution at −78°C. The initial rate of polymerization in a 'dry' system is twice as large as that obtained in a 'wet'

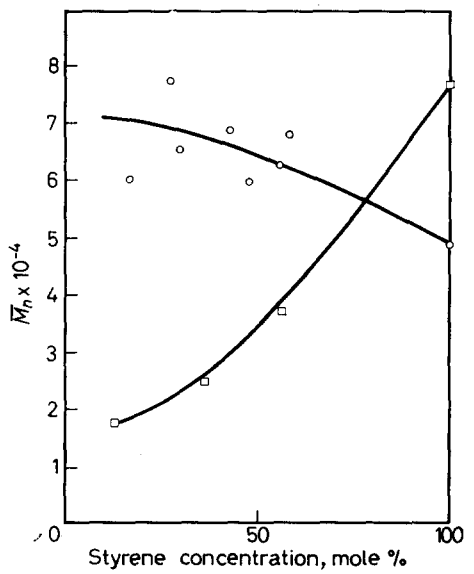

Figure 7—Polymerization of styrene in CH_2Cl_2. Temp. 10°C. ○ BaO drying (H_2O conc. none). Dose rate 583 r/min. □ Normal drying (H_2O conc. 1×10^{-3} mole/l.). Dose rate 467 r/min

Table 2. Radiation-induced polymerization of styrene in methylene chloride solution*

Code	*Water conc.* (*mole/l.*)	*Styrene conc.* (*mole%*)	*Dose rate* (*r/min*)	*Yield %*	$G(-m)$†	M_n	$G_{i_{app.}}$‡
154	none¶	100	583	19·8	15 500	49 000	32·8
151	none¶	58·2	583	31·2	15 400	68 000	21·4
155	none¶	57·0	583	25·6	15 200	63 000	25·2
152	none¶	43·3	583	8·68	4 040	69 000	6·11
153	none¶	30·1	583	7·25	1 980	65 000	2·92
182	1×10^{-3}	100	467	3·65	287	76 800	0·39
185	1×10^{-3}	56·3	467	11·9	570	36 800	1·61
187	1×10^{-3}	35·6	467	12·9	410	24 800	1·72
190	1×10^{-3}	12·2	467	16·6	190	17 800	1·10

*Temp. 10°C.
†Overall G value absorbed in solution per 100 eV.
‡Based on the assumption that $(G_i)_{app.\ ion}$ equals $(G_i)_{app.\ radical}$.
¶Barium oxide drying.

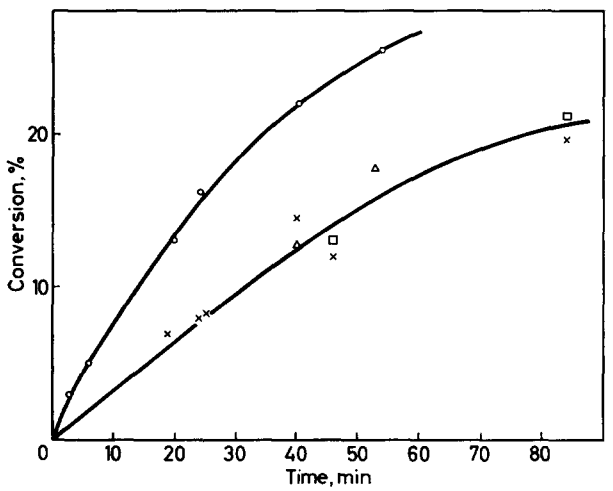

Figure 8—Effect of water on the polymerization of styrene in CH_2Cl_2 at −78°C. Dose rate $2{\cdot}0\times10^4$ r/h. Styrene conc. 3·28 mole/l. H_2O conc. ○ $<5\times10^{-5}$ mole/l., × 2×10^{-3} mole/l., △ 2×10^{-2} mole/l., □ 1×10^{-1} mole/l.

system, but in each case the rates decreased with the progress of polymerization. Experiments in a 'dry' system in methylene chloride showed very good reproducibility. Water concentrations exceeding 2×10^{-3} mole/l. did not further affect the rate of polymerization, because the solubility of water at −78°C is very small, the excess water adhering to the upper glass wall. *Figure 9* shows the molecular weights of the polymers obtained in the experiments of *Figure 8*. The molecular weights are generally slightly higher in the 'dry' systems than in the 'wet' systems. Therefore it is apparent that the increased rate of polymerization in a 'dry' system can be attributed to an increase of initiation efficiency. The chlorine atom content of the polymer obtained in the styrene–methylene chloride system was determined by activation analysis and the results are shown in *Table 3*.

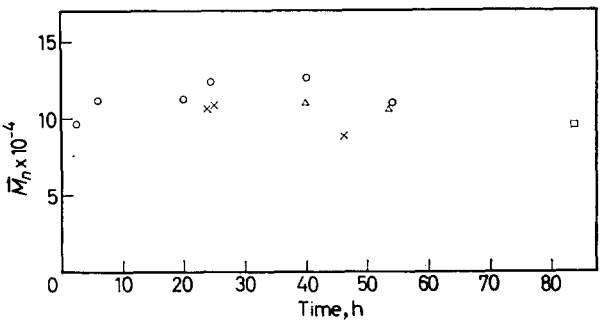

Figure 9—Effect of water on the polymerization of styrene in CH_2Cl_2 at −78°C. Dose rate $2{\cdot}0\times10^4$ r/h. Styrene conc. 3·28 mole/l. H_2O conc. ○ $<5\times10^{-5}$ mole/l., × 2×10^{-3} mole/l., △ 2×10^{-2} mole/l., □ 1×10^{-1} mole/l.

Table 3. Chlorine contents in polymers prepared in methylene chloride* by activation analysis method

Code	*Temp., °C*	*Styrene mole fraction*	*Dose rate r/min*	*Total dose Mr*
141	−78	0·36	300	0·360
143	−78	0·38	300	0·435
151	10	0·58	583	0·126
155	10	0·57	583	0·126

Yield %	*G (−m)*	M_n	*No. of Cl atoms per 1 g of sample*	*No. of Cl atoms per chain*
13·0	1 480	113 000	$2{\cdot}5\times10^{-5}$	2·8
16·1	1 700	125 000	$0{\cdot}95\times10^{-5}$	1·2
31·2	15 400	68 000	$4{\cdot}2\times10^{-6}$	0·29
25·6	15 200	63 000	$4{\cdot}5\times10^{-6}$	0·28

*Barium oxide drying.

The chlorine content of the polymer obtained at room temperature was very small, but for the polymerization at low temperature, chlorine atoms between one and three were found to be incorporated for the polymer molecule.

DISCUSSION

It seems that solution polymerization in a 'dry' system at room temperature proceeds by a cationic mechanism. Methylene chloride has a high dielectric constant and is suitable for a cationic polymerization, while toluene has a low dielectric constant and a similar molecular structure to that of styrene. Methylene chloride and toluene have different effects on the polymerization. At first, the effect of methylene chloride is discussed. In the previous paper[1], the polymerization mechanism was described as cationic. If the propagating ion is anionic, methylene chloride terminates polymerization or decreases the rate by chain transfer[8]. The effect of traces of water as shown in *Table 2* is strong evidence for a cationic mechanism. Methylene chloride increases the rate of polymerization and molecular weight. Such

behaviour is analogous to that found in conventional cationic polymerization. According to Maekawa and Hayashi[2], about two chlorine atoms are introduced into the polymer by chain transfer in the 'wet' styrene–methylene chloride system irradiated at 60°C. On the other hand, in the present work with a 'dry' system, chlorine atoms were not found in the polymer at room temperature, so this indicates a difference of polymerization mechanism.

Secondly, the styrene–toluene system is considered. To determine the exact role of chain transfer, the Mayo equation is used,

$$\frac{1}{\overline{DP}} = \frac{k_{tm}[\mathrm{M}] + k_{ts}[\mathrm{S}] + k_{tx}[\mathrm{X}]}{k_p[\mathrm{M}]} \tag{1}$$

where k_{tm}, k_{ts} and k_{tx} denote the rate constant of monomer transfer, solvent transfer and impurity transfer respectively. From the results of the previous paper[1], $k_{tm}[\mathrm{M}] + k_{ts}[\mathrm{S}] \gg k_{tx}[\mathrm{X}]$, so that, approximately,

$$\frac{1}{\overline{DP}} = \frac{k_{tm}}{k_p} + \frac{k_{ts}[\mathrm{S}]}{k_p[\mathrm{M}]} \tag{2}$$

$k_{tm}/k_p \fallingdotseq 0{\cdot}25 \times 10^{-2}$ and $k_{ts}/k_p \fallingdotseq 0{\cdot}19 \times 10^{-2}$ are evaluated for a 'dry' system. Thus, the lowering of molecular weight in toluene solution should be attributed to chain transfer to toluene.

The authors wish to express their gratitude to Professor I. Sakurada for his kindness in giving us the opportunity to carry out this study at the Osaka Laboratories, Japanese Association for Radiation Research on Polymers and to Dr Ff. Williams, University of Tennessee, for the helpful discussion of these works (Parts I-IV).

Department of Polymer Chemistry,
Kyoto University,
Kyoto, Japan

(Received November 1965)

REFERENCES

[1] UENO, K., HAYASHI, K. and OKAMURA, S. *Polymer, Lond.* 1966, **7**, 431
[2] MAEKAWA, T. and HAYASHI, K. Unpublished results
[3] MAYO, F. R. *J. Amer. chem. Soc.* 1943, **65**, 2324
[4] HIGASHIMURA, T. and OKAMURA, S. *Chemy. high Polym.* 1956, **13**, 397
[5] KATAGIRI, K., UNO, K. and OKAMURA, S. *J. Polym. Sci.* 1955, **17**, 144
[6] CHAPIRO, A. *J. chim. Phys.* 1950, **47**, 747 and 764
[7] STANNETT, V., BAHSTETTER, F. C., MEYER, J. A. and SZWARC, M. *Internat. J. appl. Radiat. Isotopes*, 1964, **15**, 747
[8] WEBB, R. L. *Proceedings* of the International Symposium on Radiation-induced Polymerization and Graft Copolymerization. Battelle Memorial Institute, November 1962, preprints 109 pp

A Comparison between Real Polymer Dimensions in Solution and the Behaviour Predicted from Models

A. J. HYDE

The variation of polymer coil dimensions with numbers of bonds in the chain for real polymers in solution is compared with the behaviour predicted by lattice random walk models. There appears to be agreement between one form, predicted by two independent methods from models, and the real behaviour of polymers.

IT HAS been suggested, on the basis of Monte Carlo sampling of self-avoiding walks on two and three dimensional lattices[1, 2], of exact enumeration of short self-avoiding walks on the same lattices[3, 4], and on the basis of a recent self-consistent field treatment[5], that the mean square end-to-end distance $\langle R^2 \rangle$ of such walks has the form

$$\langle R_n^2 \rangle = An^{1+\epsilon}$$

($\epsilon \sim 0{\cdot}2$ for three dimensions and $\epsilon \sim 0{\cdot}5$ for two dimensions).

On the basis of more recent Monte Carlo calculations[6, 7], Marcer has suggested that for three dimensions a more probable behaviour is given by

$$\langle R_n^2 \rangle = kn \ln n$$

The exact enumeration data for small walks may be fitted very closely by

$$\langle R_n^2 \rangle = k' (n + 1{\cdot}02\, n \log n)$$

but this expression would not be expected to remain correct for large values of n.

It is of interest to compare this suggestion with Rubin's[9] predictions of upper bounds for the limiting behaviour of self-avoiding walks in several dimensions. Rubin's upper bound for $n+1$ dimensions seems to approximate the limiting behaviour for n dimensions.

Marcer's suggestion is also to some extent compatible with the decreasing values of ϵ obtained from the Monte Carlo experiments as progressively larger walks on three dimensional lattices were examined[1, 2]. It was thought that it would be instructive to compare the predicted forms of behaviour of $\langle R^2 \rangle$ with some accurate experimental data[10, 11] on the behaviour of $\langle R^2 \rangle$—or to be more precise $\langle S^2 \rangle$, the mean square polar radius of gyration —for polyvinyl acetate and poly(2-vinyl pyridine).

THEORETICAL BEHAVIOUR

Curves of $\langle R_n^2 \rangle$ versus n are shown in *Figure 1* for the relationships

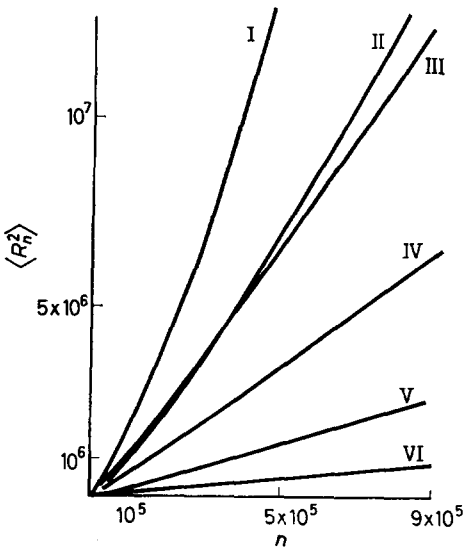

Figure 1—$\langle R^2 \rangle$ versus n. $\langle R_n^2 \rangle = n^{1+\epsilon}$; I, $\epsilon = 0{\cdot}25$; II, $\epsilon = 0{\cdot}20$; V, $\epsilon = 0{\cdot}08$; VI, $\epsilon = 0$; III, $\langle R_n^2 \rangle = n \ln n$; IV, $\langle R_n^2 \rangle = n + 1{\cdot}02\, n \log n$

$\langle R_n^2 \rangle = k\, n^{1+\epsilon}$ (with $\epsilon = 0{\cdot}25$, $0{\cdot}20$, $0{\cdot}08$ and $0{\cdot}00$), $\langle R_n^2 \rangle = k' n \ln n$, and $\langle R_n^2 \rangle = n + 1{\cdot}02\, n \log n$.

Over a large part of its range relevant to practical polymer sizes n log n may be approximated by n^β with β being about 1·16 for low values of n and decreasing to 1·12 for large values of n. Corresponding log $\langle R_n^2 \rangle$

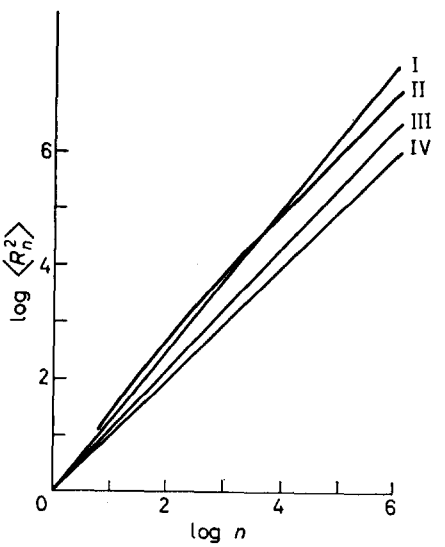

Figure 2—log $\langle R_n^2 \rangle$ versus log n. I, $\langle R_n^2 \rangle = n^{1{\cdot}25}$; II, $\langle R_n^2 \rangle = n \ln n$; III, $\langle R_n^2 \rangle = n^{1{\cdot}08}$; IV, $\langle R_n^2 \rangle = n$

versus log n curves are shown in *Figure 2*.

In many respects, however, the behaviour of $\langle R_n^2 \rangle$ as a function of n is a largely academic problem. The quantity related to the

linear molecular dimensions which is most easily measured (by light scattering methods) is $\langle S^2 \rangle_z$, the Z average mean square polar radius of gyration. It is therefore of interest to examine the behaviour of $\langle S^2 \rangle$ as a function of n. For a coil obeying the relationship $\langle r_{ij}^2 \rangle = k \mid i-j \mid^{1+\epsilon}$,

$$\langle S^2 \rangle = \frac{k\, n^{1+\epsilon}}{(2+\epsilon)\ (3+\epsilon)} = \frac{\langle R_n^2 \rangle}{(2+\epsilon)\ (3+\epsilon)}$$

A more realistic expression for $\langle R_{ij}^2 \rangle$ has also been used[12, 13] namely

$$\langle r_{ij}^2 \rangle = k'' \mid i-j \mid^{1+\nu} n^{\epsilon-\nu}$$

For this expression

$$\langle S^2 \rangle = \frac{k' n^{1+\epsilon}}{(2+\nu)\,(3+\nu)} = \frac{\langle R_n^2 \rangle}{(2+\nu)\,(3+\nu)}$$

If $\langle r_{ij}^2 \rangle = k''' \mid i-j \mid \log \mid i-j \mid$ then, from the second term of the angular light scattering function $P(\theta)$ for such a coil,

$$\langle S^2 \rangle = (6n \log n - 5n)/36$$

(assuming a Gaussian distribution for the r_{ij}s). Curves of $\langle S^2 \rangle$ as a function of n are shown in *Figure 3* for some intersegment distance relationships in *Figure 1*.

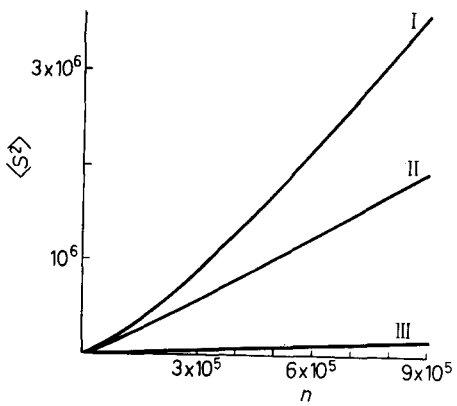

Figure 3—$\langle S^2 \rangle$ versus n. I, $\langle S^2 \rangle = n^{1.25}/3{\cdot}25 \times 2{\cdot}25$; II, $\langle S^2 \rangle = (n \ln n - 5/6)6$; III, $\langle S^2 \rangle = n/6$

In order to evaluate values of ϵ from experimental results, plots of $\log \langle S^2 \rangle$ versus $\log n$ are usually plotted and the slope of the line measured. Curves of this type for the theoretical relationships are shown in *Figure 4*. The curves for $\langle S^2 \rangle \propto n^{1+\epsilon}$ are naturally straight lines.

The log/log plot for Marcer's relation is seen to be *concave* towards the $\log n$ axis.

EXPERIMENTAL BEHAVIOUR

The experimental curves[10, 11] of $\langle S^2 \rangle$ versus M are convex towards the

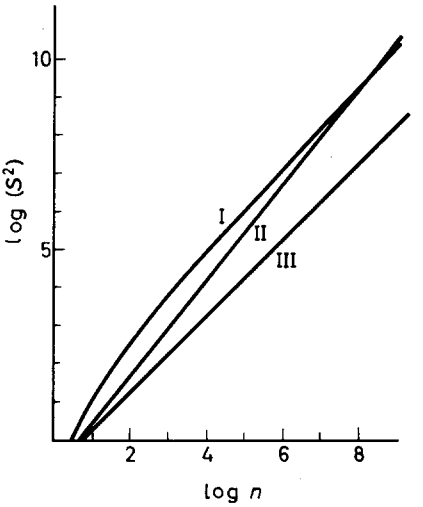

Figure 4—log $\langle S^2 \rangle$ versus log n. I, $\langle S^2 \rangle = (n \ln n - 5n/6)/6$; II, $\langle S^2 \rangle = n^{1.25}/3{\cdot}25 \times 2{\cdot}25$; III, $\langle S^2 \rangle = n/6$

molecular weight axis. Curves of log $\langle S^2 \rangle$ versus log M appear linear—it is just possible that they are slightly convex towards the log M axis—indicating a relationship between $\langle S^2 \rangle$ and M of the form

$$\langle S^2 \rangle = kM^{1+\epsilon} \quad (0 < \epsilon < 1)$$

For polyvinyl acetate in methylethyl ketone $\epsilon = 0{\cdot}16$, for poly(2-vinyl pyridine) in ethanol and an *n*-heptane–*n*-propanol mixture, $\epsilon = 0{\cdot}25$ and $0{\cdot}08$ respectively—as determined from least mean squares straight lines on the log $\langle S^2 \rangle$ versus log M plots.

DISCUSSION

The relation $\langle R_n^2 \rangle = kn \ln n$ was suggested from Monte Carlo sampling on very long lattice walks. The other methods of deriving such relations involve exact enumeration and evaluation of the relevant average property of all walks up to twelve or more steps[3] or a self-consistent field treatment[5].

It is of interest to examine the $n \log n$ relationship in the light of Fisher's[3] analysis. In order to estimate a value of γ (for the relationship $\langle R_n^2 \rangle = kn^\gamma$, where $\gamma = 1 + \epsilon$), the ratio $\langle R_{n+1}^2 \rangle / \langle R_n^2 \rangle = \xi_n$ is found and from this the value of $\gamma_n = n(\xi_n - 1)$ is obtained. The limiting value of γ_n as $n \longrightarrow \infty$ is required. Fisher and Hiley[3] suggested that the behaviour of γ_n was given by $\gamma_n = \gamma_\infty (1 + a/n + \ldots)$. A plot of γ_n versus $1/n$ will give the value of γ_∞ as intercept.

Values of $\langle R_n^2 \rangle = n \log n$ were found for values of n up to ten and values of γ_n evaluated and plotted against $1/n$. After the first two or three points (see *Figure 5*) the curve becomes linear and can be extrapolated towards an apparent γ_∞ of 1·23.

Since it can be shown that $\gamma_n \longrightarrow 1$ as $n \longrightarrow \infty$ for the relation $\langle R_n^2 \rangle \propto n \log n$, values of γ_n for $n = 20$, 100 and 200 were evaluated. The

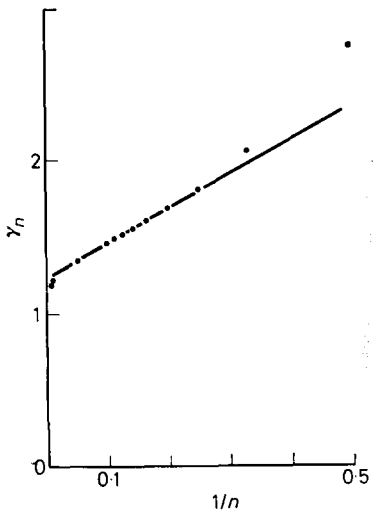

Figure 5—γ_n versus $1/n$ for Marcer's function

point for γ_{20} lay on the same straight line as the previous points but γ_{100} and γ_{200} lay off the line in a direction tending towards unity.

Similar considerations apply to the relation

$$\langle R_n^2 \rangle \propto n + 1{\cdot}02\, n \log n$$

It appears that it might be hazardous under certain circumstances to extrapolate to infinity from only the first 15 or so points in the above type of analysis. The apparent value of γ_∞ obtained above is not too far from the values obtained by both enumeration and sampling techniques.

The comparison between theoretical $\langle R^2 \rangle = \mathrm{f}(N)$ relations derived from lattice walks and the experimental relations for polymer solutions would seem to indicate that, if the theoretical relationships have relevance to polymer solutions, the relation $\langle R_n^2 \rangle = kn^{1+\epsilon}$ would seem preferable. ϵ will be a function of solvent–polymer and polymer–polymer interaction potentials. As Fisher and Hiley have shown for the lattice model and as is well known for practical systems, the introduction of large enough polymer–polymer attractive potentials will give $\epsilon = 0$ at the so-called θ point for a polymer solution.

Several recent papers [3, 5, 14, 15] have indicated that the distribution of end-to-end distances and intersegment distances is not Gaussian, at any rate for $\epsilon > 0$, and this will affect the theories of various polymer solution properties (light scattering, viscosity, etc.) which depend on chain conformations and will have some effect on the above considerations, but until the precise form of the distributions is known, it is not clear what the effect will be.

Physical Chemistry Section of the Department of Pure and Applied Chemistry,
University of Strathclyde,
Glasgow, C.1

(Received February 1966)

REFERENCES

[1] WALL, F. T., HILLER, L. A. and WHEELER, D. J. *J. chem. Phys.* 1954, **22,** 1036
[2] WALL, F. T. and ERPENBECK, J. J. *J. chem. Phys.* 1959, **30,** 634
[3] FISHER, M. E. and HILEY, B. J. *J. chem. Phys.* 1961, **34,** 1253
[4] FISHER, M. E. and SYKES, M. F. *Phys. Rev.* 1959, **114,** 45
[5] EDWARDS, S. F. *Proc. phys. Soc.* 1965, **85,** 613
[6] MARCER, P. J. *D.Phil. Thesis,* Trinity College, Oxford, 1960
[7] FLUENDY, M. A. D. and SMITH, E. B. *Quart. Rev. chem. Soc., Lond.* 1962, **16,** 260
[8] SMITH, R. P. *J. chem. Phys.* 1964, **40,** 2693
[9] RUBIN, R. J. *J. chem. Phys.* 1952, **20,** 1940
[10] SCHULTZ, A. R. *J. Amer. chem. Soc.* 1954, **76,** 3422
[11] TAYLOR, R. B. and HYDE, A. J. *Polymer, Lond.* 1963, **4,** 1
[12] HYDE, A. J., RYAN, J. H. and WALL, F. T. *J. Polym. Sci.* 1958, **33,** 129
[13] HYDE, A. J. *Trans. Faraday Soc.* 1960, **56,** 591
[14] MAZUR, J. *J. Res. Nat. Bur. Stand.* 1965, **69A,** 355
[15] DOMB, C., GILLIS, J. and WILMERS, G. *Proc. phys. Soc.* 1965, **85,** 685

Proton Acceptor Properties and Electrical Conductance of Deeply Coloured Cyclopentadiene Polymers

J. UPADHYAY, J. B. G. WALLACE and A. WASSERMANN

Equilibrium constants, K, of proton transfer from trichloracetic acid to deeply coloured cyclopentadiene polymers were measured in solvents methylene chloride and o-dichlorobenzene. Comparison with the results of previous experiments shows that the K values increase with increasing dielectric constant of the solvent. This is consistent with the assumption that the polymer trichloracetic acid adducts are ion pairs containing protonated polymer cations and trichloracetate anions. The results of electrical conductance tests confirm this conclusion.

IT HAS been shown[1,2] that coloured cyclopentadiene polymers, P, react in benzene solution with acids, HB, to produce bluish-black adducts according to

$$P + HB \overset{K}{\rightleftharpoons} \text{Adduct} \qquad (1)$$

In attempting to learn something about the influence of the dielectric constant of the solvent we have measured the equilibrium constant, K, of reaction (1), and the electrical conductance of the adduct in solvents methylene chloride and *o*-dichlorobenzene. In these experiments the species HB and P were trichloracetic acid and two coloured cyclopentadiene polymers, ref. design. A and A′.

EXPERIMENTAL

Methylene chloride and *o*-dichlorobenzene were dried over calcium hydride and fractionally distilled. The purification of benzene, trichloracetic acid and of polymer A has been described[1,2]. Polymer A′ is the alcoholic component of polymer A and was prepared as follows. A solution of polymer A (0·07M) and potassium hydroxide (0·14M) in benzene, containing ten per cent ethanol, was left under nitrogen for 12 hours at 20°C. The product, precipitated with ethanol (ten volumes) contained 84·5 per cent carbon and 8·60 per cent hydrogen; it was free of chlorine and its infra-red spectrum did not show the peak at 5·71μ, due to the carbonyl in the trichloracetate end group[1,2]. The number average molecular weight (benzene, 25°) was $1\,620 \pm 100$; the bromination indicated 20 ± 2 double bonds of which (according to the electronic spectrum in *Table 1*) 3 to 5 are conjugated. The optical densities d, d_0 and d_∞ [see equation (3)], back extrapolated[1,2] to the time of mixing, were measured at a wavelength close to 575mμ. The technique of the electrical conductance measurements has been described[2]. Molar electrical conductance, Λ, of the polymer acid adducts were calculated from

Table 1. Electronic spectrum of polymer A′ without and with trichloracetic acid

Solute	*Solvent*	$\lambda_{max.}$ ($m\mu$)	$10^{-3}\epsilon_{max.}$ (*l/mole polymer-cm*)
Polymer A′	Cyclohexane	260	4·1
,,	CCl_4	320	5·0
Polymer A′–	C_6H_6*	480	4·7
Cl_3CCOOH–Adduct	2M in CCl_3COOH	575	5·0

*In methylene chloride or *o*-dichlorobenzene the spectra of both polymers A and A′ are not significantly altered.

$$\Lambda = \{\kappa_{adduct} - (\kappa_{polymer} + \kappa_{acid})\}/c \qquad (2)$$

where κ is the specific electric conductance, corrected for the κ values of the solvent of the species indicated by subscripts, and c is the concentration of the adduct, obtained from the stoichiometric concentration of the addenda with the help of the K values of reaction (1). The solvent correction was below two per cent and $(\kappa_{polymer} + \kappa_{acid})$ was at the most 15 per cent of κ_{adduct}. In carrying out some optical density and conductance measurements atmospheric moisture was excluded with the help of a high vacuum technique and previously[1, 2] described apparatus. The results of these tests were not significantly different from those of the other experiments, done in a closed system, but without a high vacuum line. The evaluation of the conductivity measurements (see below) requires a knowledge of the viscosities, η, of the solvents. We found that η 25° (methylene chloride) is 0·00420 poise, and η 25·0° (*o*-dichlorobenzene) is 0·0109 poise.

RESULTS

In estimating the equilibrium constant of reaction (1) by the previously described[1, 2] techniques, we determined the ratio

$$\beta = \frac{\text{equilibrium concentration of adduct}}{\text{equilibrium concentration of polymer}} = \frac{d - d_0}{d_\infty - d} \qquad (3)$$

where d, d_0, and d_∞ are optical densities of solutions containing polymer and adduct, polymer without adduct, and adduct without polymer. The concentrations were varied in the range 10^{-4} to 10^{-3} M and the acid concentrations in the range 10^{-3} to 2 M. Plots of log β versus log [HB] were linear with slope $1·0 \pm 0·1$, which is consistent with the simple stoichiometry of reaction (1) and with the assumption that the ratio of activity coefficients $\gamma_{adduct}/\gamma_P \times \gamma_{HB}$ is close to unity. The log K values in *Table 2* are intercepts of log β/log [HB] graphs. The electrical conductance of these adducts studied in the solvents and in the concentration range specified in *Table 3* is due to the reaction

$$\text{Adduct} \overset{K_d}{\rightleftharpoons} PH^+ + \bar{B}$$

where the protonated polymer cations, PH, and the trichloracetate anions, $\bar{B}$, are the carriers of the current and K_d is a dissociation constant. The limiting electrical conductance, Λ_0, and the K_d values in *Table 3* were calculated with the help of Shedlovsky's method[5], using a computer programme.

DISCUSSION

The equilibrium constants of reaction (1) increase with increasing dielectric constant of the solvent (see *Table 2*) which is to be expected if these adducts are ion pairs[1, 2], having a stronger electrostatic field than the uncharged addenda. The ion pair hypothesis is, of course, consistent with the formation of the species $\overset{+}{P}H$ in reaction (4). In such cations the positive charge is spread over a sequence of conjugated double bonds[1, 2], as in authentic polyenes[6-9]. The charge density is thus decreased, which explains why the dissociation constants, K_d, in *Table 3* are larger than those of substituted ammonium salts[10, 11], in which the positive charge is localized.

Table 2. Equilibrium constants, K, of reactions between trichloracetic acid and coloured cyclopentadiene polymers, 20°

Ref. design of polymer	*Solvent*	*Mol. fraction* C_6H_6	*Dielectric const. (D) (20°)*	*No. of tests*	log K (K *in l./mole*)
	DCB*	0	9·8	13	2·0 ±0·1
	DCB–C_6H_6	0·318	7·7†	13	1·86±0·07
A	DCB–C_6H_6	0·562	5·8†	14	1·58±0·05
	DCB–C_6H_6	0·792	4·0†	8	1·26±0·05
	CH_2Cl_2	0	9·1	12	1·95±0·05
A′	CH_2Cl_2	0	9·1	12	1·5 ±0·1
	CH_2Cl_2–C_6H_6	0·205	6·7‡	12	1·86±0·05
A	CH_2Cl_2–C_6H_6	0·420	4·8‡	13	1·52±0·05
	CH_2Cl_2–C_6H_6	0·692	3·3‡	12	1·28±0·05
	C_6H_6	1·00	2·3	163§	1·0 ±0·1
A′	C_6H_6	1·00	2·3	10	1·15±0·05

*DCB denotes *o*-dichlorobenzene.
†These *D* values were estimated with the help of data in ref. 3.
‡Calculated from data in ref. 4.
§See ref. 2.

Table 3. Limiting electrical conductance, Λ_0 and dissociation constants K_d, of adducts from cyclopentadiene polymers (ref. design. A and A′) and trichloracetic acid, 25·0° C

Adduct from polymer	*Solvent*	*Conc.* Cl_3CCOOH* (*mole/l.*)	Λ_0 (*cm²/ohm-mole*)	$-\log k_d$ (K_d, *mole/l.*)
A	*o*-Dichloro-benzene	1·135	5·1±1·0	3·1±0·2
		0·300	7·0±1·0	3·4±0·2
		0·100	6·8±1·0	3·5±0·2
	Methylene chloride	1·100	31±4	4·3±0·2
		0·700	23±4	4·2±0·2
		0·500	17±3	4·0±0·2
		0·300	11±4	3·9±0·2
		0·100	10±2	3·7±0·2
A′		0·900	18±3	3·7±0·2

*At least eight experiments were carried out with each acid concentration, in which the polymer concentration was varied in the rage 10^{-3} to 10^{-4} M.

Financial support by the Central Electricity Board and experimental assistance by Mr J. Wajgras are gratefully acknowledged.

William Ramsay and Ralph Forster Laboratories,
University College, London W.C.1.

(*Received March 1966*)

REFERENCES

[1] FRENCH, P. V., ROUBINEK, L. and WASSERMANN, A. *J. chem. Soc.* **1961,** 1953
[2] UPADHYAY, J., GASTON, P., LEVY, A. A. and WASSERMANN, A. *J. chem. Soc.* **1965,** 3252
[3] MORGAN, S. O. and LOWRY, H. H. *J. phys. Chem.* 1930, **34,** 2385
[4] ERRERA, J. *Phys. Z.* 1926, **27,** 764
[5] SHEDLOVSKY, T. *J. Franklin Inst.* 1938, **225,** 70; cf. also FUOSS, R. H. and SHEDLOVSKY, T. *J. Amer. chem. Soc.* 1949, **71,** 1496; DAGGET, H. M. *J. Amer. chem. Soc.* 1951, **73,** 4977
[6] WASSERMANN, A. *J. chem Soc.* **1954,** 4329
[7] WASSERMANN, A. *J. chem. Soc.* **1955,** 585
[8] WASSERMANN, A. *J. chem. Soc.* **1958,** 1014 and 3228
[9] WASSERMANN, A. *J. chem. Soc.* **1959,** 986
[10] FUOSS, R. H. and KRAUS, C. A. *J. Amer. chem. Soc.* 1933, **55,** 2387
[11] BAIRD, J. H. and PLESCH, P. H. *J. chem. Soc.* **1964,** 4879

Polythioacetone

O. G. VON ETTINGHAUSEN* and E. KENDRICK

Pure monomeric thioacetone, m.pt −40°C, has been prepared in good yield by thermal dissociation of the cyclic trimer at reduced pressure over a hot wire. The monomer polymerized spontaneously to the linear polythioacetal between −20°C and +20°C. The highly crystalline polymers, m.pt 120° to 125°C, had molecular weights from 2 500 to 14 000. Ring opening polymerization of the cyclic trimer failed, and attempted copolymerizations with several polymerizable monomers were also unsuccessful. During this work, n.m.r. and mass spectroscopy revealed that the cyclic trimer, prepared from acetone, hydrogen sulphide and acid catalysts, contained small amounts of two isomers, an unsymmetrical cyclic disulphide and a cyclic thiol.

BAILEY AND CHU[1] recently prepared thioacetone monomer by pyrolysis of allyl isopropyl sulphide and reported its polymerization to linear polythioacetone of molecular weight 2 000. We have prepared substantially pure thioacetone monomer by pyrolysis of its cyclic trimer *in vacuo*. The monomer spontaneously gave linear polymers with molecular weights up to 14 000. This paper describes the characteristics of the cyclic trimers, the preparation and polymerization of the monomer, and the properties of the polymer.

THE CYCLIC TRIMERS

During this work it was found that the trimer prepared from acetone and hydrogen sulphide, using hydrochloric acid[2] or zinc chloride[3] as catalysts, contained in addition to I, the isomer II, and small amounts of III.

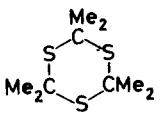

I

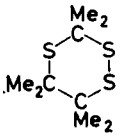

II

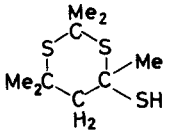

III

The intensities of some peaks in the mass spectrum of trithioacetone varied from sample to sample, and four in particular ($m/e=83$, 138, 157, 188) could not be assigned to fragments derived from I (*Table 1*).

The assignments shown were confirmed by precise mass measurements and by isotope distributions. The peak at $m/e=138$ corresponds to loss of C_6H_{12} from trimer, $m/e=83$ to C_6H_{11}, $m/e=157$ to loss of HS_2 from trimer. The peak at $m/e=188$, trimer less H_2S, is indicative of a thiol group.

*Present address: Erlenweg 7, 7970 Leutkirch, Germany.

Table 1. Mass spectra of trithioacetone

m/e	*Relative intensities* *Sample 1* ($ZnCl_2$)	*Sample 2* (HCl)	*Assignment*
59	39·4	37·9	74—CH_3
74	100·0	100·0	C_3H_6S (monomer)
83	1·0	1·1	C_6H_{12}—H
99	3·8	0·4	C_5H_7S
106	0·4	0·5	Trimer—$(C_3H_6)_2S$
113	4·7	0·6	C_6H_9S
116	6·4	6·4	Trimer—$C_3H_6S_2$
133	0·8	0·8	148—CH_3
138	7·6	6·1	Trimer—C_6H_{12}
148	25·6	22·0	Trimer—C_3H_6S
157	0·2	0·2	Trimer—HS_2
188	1·7	0·1	Trimer—H_2S
222	5·5	5·2	Trimer

Table 2. MS peaks due to trimer isomers

m/e	*Isomer indicated*	*Peak intensities relative to m/e 222=100* *Sample 1* ($ZnCl_2$)	*Sample 2* (HCl)	*Sample 3* (HCl) *Untreated*	*Quinone treated*
83	II	18·7	20·4	14·7	14·3
138	II	138·2	117·3	91·0	98·2
157	II	4·0	4·4	4·5	3·6
188	III	31·3	2·7	1·0	0·005

It was concluded that the trimer contained isomers with —CMe_2—CMe_2—, —S—S—, and —SH groups. Hence the presence of II and III was inferred. *Table 2* shows the variation of these peaks between samples.

The mass spectrum of thioacetone monomer showed a base peak at $m/e=59$ (loss of CH_3) and a parent peak intensity of 73 per cent.

Diffusion rates were measured in the mass spectrometer at m/e values 222, 148, 74 and 59. These showed that, at a sample temperature of 100°C, thermal decomposition was not significant. At higher temperatures thermal decomposition occurred, and the spectrum showed a much stronger peak at $m/e=59$.

Metastable peaks at $m/e=98{\cdot}7$ ($222 \rightarrow 148$) and $m/e=37{\cdot}0$ ($148 \rightarrow 74$) confirm that the $m/e=148$ and $m/e=74$ peaks are formed by ion fragmentation.

The major peak in the n.m.r. spectra of two trimer samples at $\tau=1{\cdot}68$ p.p.m. (measured from TMS internal reference) corresponded to the methyl groups on carbon atoms adjacent to two sulphur atoms. One sample showed additional peaks at 1·38 p.p.m. (singlet), 1·88 (doublet) and 5·55 p.p.m. (quadruplet). These peaks were only just discernible in the other sample. The 1·88 and 1·55 p.p.m. peaks were spin-coupled (J approximately 3 c/s), indicating a single proton with a methyl group in close proximity. Structure III is consistent with these observations as shown below.

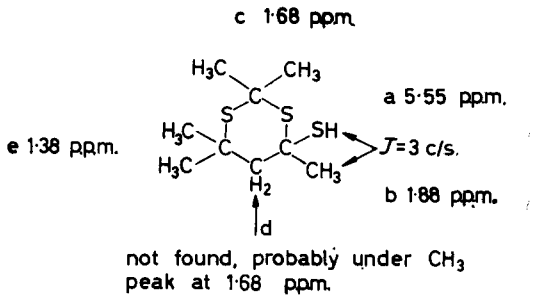

IV

The relative peak areas found agree reasonably with the proposed structure.

Proton	*p.p.m.*	*Area found*	*Area expected*
a	5·55	1·0	1·0
b	1·88	2·7	3·0
c, d	(1·68)	—	8·0
e	1·38	4·7	6·0

PREPARATION AND PROPERTIES OF POLYTHIOACETONE

Before proceeding with polymerization experiments, trithioacetone was

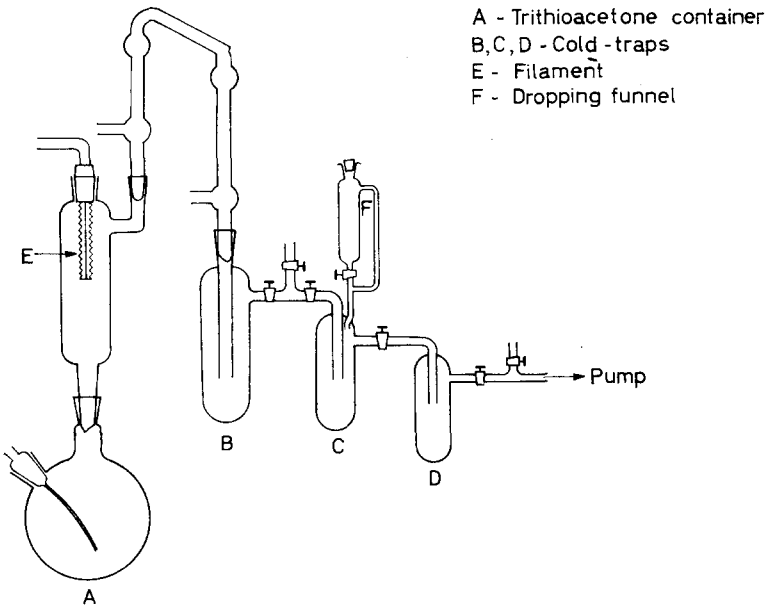

Figure 1—Apparatus for the thermal degradation of trithioacetone

stirred with benzoquinone to remove III, a possible source of chain terminating reagents, distilled and dried over alumina which reduced its water content to 20 p.p.m. Pyrolysis of the trimer under argon in a ketene apparatus[4], modified to function at 1 mm of mercury pressure (*Figure 1*), gave the monomer which collected in the cold traps as a brown liquid, or crystals m.pt −40°C. The monomer polymerized spontaneously when kept for four hours between −20°C and +20°C. After washing with ethanol, the crude polymer was taken up in the benzene and reprecipitated by ethanol; the overall yield from trimer being about 85 per cent. Molecular weights, determined in benzene solution by vapour pressure osmometry, are given in *Table 3*.

Table 3. Molecular weights of polythioacetone

Polymerization temperature °C	*Molecular weight*
20	2 500
0	6 500
−10	9 200
−20	14 000

The polymer was a white powder melting between 120° and 125°C. Its elemental analysis agreed with the required structure —$(CMe_2—S)_n$—.

Found:	C, 48·63	H, 8·15	S, 43·28
Calculated:	48·60	8·15	43·25

The reactivity of the monomer made gas chromatographic analysis difficult. Analysis of the vapour evolved by trithioacetone, when heated in a silica tube in an inert gas at atmospheric pressure, suggested an optimum degradation temperature of between 235°C and 245°C with a monomer purity of 98 per cent. Byproducts detected were hydrogen, lower olefins and C_1—C_3 mercaptans. The presence of these impurities was no doubt responsible for the low molecular weight of the resulting polymers. No methane or thioketene were detected.

The n.m.r. spectrum of the polymer showed a single peak at $\tau = 8{\cdot}1$ p.p.m. It was highly crystalline. The position and the relative intensities (RI) of the lines measured from an X-ray powder diagram of an unannealed sample are given in *Table 4* (see also *Figure 2*, A).

Table 4. X-ray powder diagram of polythioacetone

d, Å	*RI*	*d, Å*	*RI*	*d, Å*	*RI*
4·70	90	1·355	30	0·902	5
2·97	5	1·29	35	0·887	3
2·32	10	1·17	25	0·860	10
2·07	100	1·08	20	0·814	5
1·77	10	1·025	3	0·787	7
1·55	40	0·997	10		
1·47	40	0·938	20		

Attempts were made to copolymerize thioacetone with styrene, acrylonitrile, allyl formate, allyl acetate, methylvinyl ketone, and methylmethacrylate.

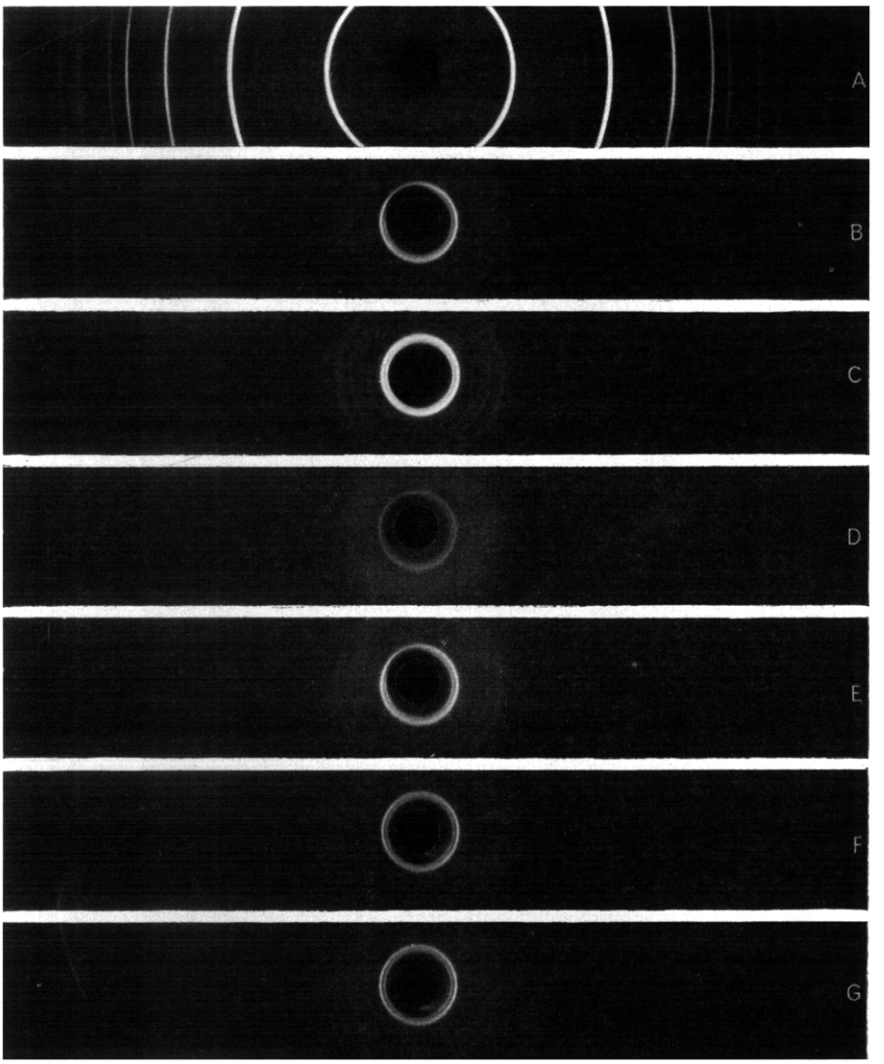

Figure 2—X-ray diagrams of polymer with comonomers—see text

These comonomers were added to the thioacetone monomer via the dropping funnel F (*Figure 1*). In each case almost 100 per cent of comonomer was recovered and no evidence of copolymerization detected. However, the presence of these comonomers reduced the crystallinity of the polythioacetone as shown in *Figure 2*, where the X-ray diagram B is that of polymer prepared in the presence of methyl methacrylate; C, acrylonitrile, D, methylvinyl ketone; E, allyl formate; F, allyl acetate; G, styrene.

In contrast to trioxan and trithian, trithioacetone did not undergo ring opening polymerization to true polythioacetone. Von Ettingshausen and

Marktscheffel[5] earlier found that treating trithioacetone with boron trifluoride etherate, and other Lewis acids, gave a few per cent of materials with molecular weights in the range 400 to 600, with a sulphur content of only 19 wt % (polythioacetone requires 43·3 per cent). Hydrogen sulphide and mercaptans were evolved during the reaction. This work was performed before the presence of the third isomer III was suspected.

Later work by Burnop and Latham[6] indicates that ring opening polymerization of purified trimer does not occur, and the product obtained by von Ettingshausen and Marktscheffel may be derived from III.

The authors wish to thank Dr F. Marktscheffel for valuable suggestions, Dr S. G. Perry for the gas chromatographic analyses and Mr J. Sparks for X-ray diffraction measurements.

Esso Research Ltd,
Abingdon, Berks.

(*Received February 1966*)

REFERENCES

[1] BAILEY, W. J. and CHU, H. Division of Polymer Chemistry, 149th Meeting of the American Chemical Society, Detroit, 5 April 1965
[2] FROMM, E. and BAUMAN, E. *Ber. dtsch. chem. Ges.* 1889, **22,** 1035, 2593
[3] BOHME, H., PFIEFFER, H. and SCHNEIDER, E. *Ber. dtsch. chem. Ges.* 1942, **75,** 900
[4] HANFORD, W. E. and SAUER, J. C. *Organic Reactions,* Vol. III, Chap. 3, p 133. Wiley: New York, 1946
[5] VON ETTINGSHAUSEN, O. G. and MARKTSCHEFFEL, F. Unpublished
[6] BURNOP, V. C. E. and LATHAM, K. G. To be published

Communication

Supermolecular Gels in Cellulose Nitrate Solutions

IN FORMER work[1-3] we had found that solutions of wood pulp nitrates in butyl acetate always contain a gel fraction of 10 to 15 per cent, depending on type of pulp as well as method of preparation and dissolution. Even for fractions, 10 to 20 per cent gel of about 20-fold molecular weight could be found, and obtained in spherolitelike form (*Figure 1*). Recently we have

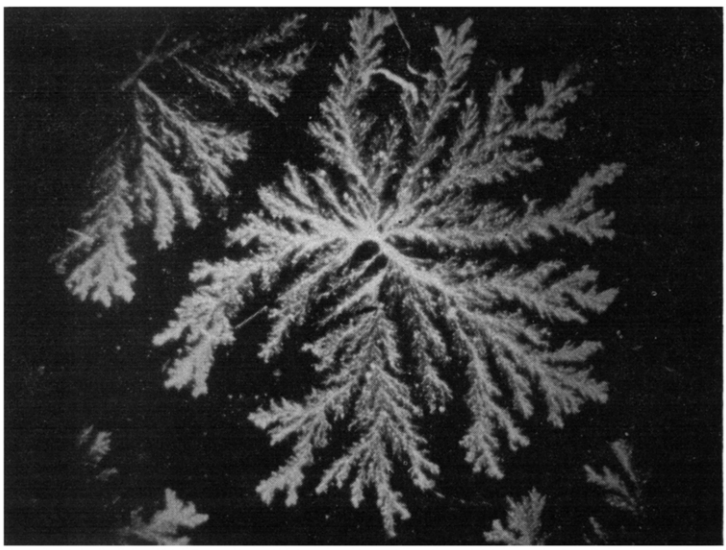

Figure 1—Spherolitelike cellulose nitrate gel (diameter about 0·5 mm, cf. ref. 1)

studied the gel phenomenon for the same wood pulp nitrates in acetone. In the following, a short preliminary account of our findings is presented.

(1) Wood pulp nitrates (from beech sulphite pulp 'Lenzinger Buche' with $M_w = 6 \times 10^5$) prepared in the usual way[4] contain a gel fraction of 8 to 16 per cent which is not detected by viscometric measurements. It can be isolated by pressure ultrafiltration (1 to 2 atm) through sintered glass filters of pore size $< 1\mu$ (Schott G5f), or wet membrane filters of pore size $< 0{\cdot}5\mu$ (Membranfiltergesellschaft). The isolated gels show a reduced nitrogen content of about 13·3 per cent as compared with 13·8 per cent for the total sample. In their X-ray pictures, residues of cellulose I reflections are observed: beside the reflection of cellulose nitrate, we note the A_4 and A_5 reflections of cellulose I, while A_4 of cellulose nitrate is shifted towards A_2 of cellulose I. Therefore, the gel particles may be residues of unreacted

cellulose I crystallites with intact bonding in the most strongly bonded A_2 direction[5].

Note. A referee pointed out that during nitration the trinitrate boundary moves through the cellulose from amorphous to highly crystalline regions. The surface of the crystalline domains may be nitrated, and thus the gel may go into solution with a cellulose I centre. This effect is possible for both wood and cotton cellulose. This opinion is in full agreement with our results.

(2) The isolated gels can be dissolved in acetone to yield solutions with positive yet low second virial coefficient ($B \leqslant 0{\cdot}6 \times 10^6$, as compared with $B \sim 10^7$ [erg $g^{-2}cm^3$] for molecular solutions). Their intrinsic viscosity is rather low (about 1 000 for $M \simeq 10^7$), and depends very weakly on the light scattering molecular weight according to

$$[\eta] = 1{\cdot}09 \times 10^1 \times M_w^{0{\cdot}293}$$

The low value of the exponent suggests that the gels are rather compact clusters. This explains why their viscosity contribution in molecular solutions (with exponent 1) is negligibly small, and expresses itself mainly in an erroneous concentration. Thus, gels will cause an apparent decrease in $[\eta]$. For gel-free solutions in acetone at 20°C we found $K = 1{\cdot}4 \times 10^3$ and $a = 1$; in the θ-solvent butyl acetate–ethanol 10:9 at 25°C, $K_\theta = 8{\cdot}5 \times 10^{-1}$ and $a = 0{\cdot}5$ (c always in g/cm^3). This K_θ, according to the Flory theory, would lead to an 'unperturbed' statistical chain element $A_m = 147$Å.

(3) In light scattering, the gels are detected by peaks in the $P(\vartheta)$ curve, which may be interpreted as Mie-scattering; and by an excess scattering over the linear response at small angles. If the latter is plotted in the way proposed by Wesslau[6], straight line diagrams are obtained. They allow the determination of $w_G M_G$ (w_G and M_G are the weight fraction and molecular weight of the gels). If we assume $w_G = 0{\cdot}14$ (from ultrafiltration), we can calculate M_G and M_M (for true macromolecules). The M values obtained from various methods agree reasonably, as shown in *Table 1* for one sample measurement.

Table 1

	Wesslau plot		*Direct measurement*		
	M	*R*, Å	*M*	*R*, Å	*w*, %
Macromolecules	7×10^5	650	6×10^5	770	86
Gels	11×10^6	1 350	$11{\cdot}5 \times 10^6$	2 000	14

R denotes radius of gyration.

An approximate reduction of a Guinier plot according to the graphical method by Jellinek *et al.*[7] yields the size distribution given in *Table 2*.

Table 2

R, Å	384	1 420	2 760	4 815
Wt %	79·5	10·4	8·86	1·24

The high radius of gyration, the relatively low intrinsic viscosity, and its weak dependence on molecular weight suggest for the gels a planar, disc-like shape, with little dependence of the ratio of the semi-axes on particle weight. Possibly they represent layers of cellulose nitrate chains, in which the glucose rings are threaded up plane-to-plane in the A_2-direction (cf. the 'radiator model' for cellulose[5]).

(4) Runs in an ultracentrifuge at 180 000 *g* showed the gel particles as small peaks preceding the main peak. After some time, the gel peak was split into two or three subpeaks. An approximate evaluation of the gel peak led to $M \simeq 13{\cdot}2 \times 10^6$.

(5) Preliminary experiments with cotton nitrates indicate that no gel particles are present here, but rather very large macromolecules due to either polymolecularity or a very large molecular weight of the whole sample.

Obviously, gels are typical of wood pulp nitrates. It is possible to remove them by ultrafiltration (glass sinter filters, however, are rapidly clogged thereby), or by ultracentrifugation (e.g. with 50 000 *g* for 1 h). In this way one may obtain strictly molecular-disperse solutions. On the other hand, the amount of gel found after a standard nitration may prove a new characteristic for wood pulps, important for their chemical processibility (e.g. for viscose production). It also may be an explanation for the old argument about the nature of cellulose nitrate solutions: if different workers find macromolecules in one case, and supermolecular particles in another, they simply have in hand solutions with different gel fractions. In future work on cellulose nitrate, a check on the absence of gels especially as regards removal prior to investigation, appears indispensable.

Institut für Physikalische Chemie,
Universität Graz, Austria

J. SCHURZ
H. TRITTHART

(*Received April 1966*)

REFERENCES

[1] SCHURZ, J. *Papier, Darmstadt,* 1961, **15,** 530
[2] SCHURZ, J. *Holzforschung,* 1964, **18,** 142
[3] SCHURZ, J. *Faserforschung u. Textiltechnik,* 1964, **15,** 598
[4] LANG, W. *Svensk Papp-Tidn.* 1956, **59,** 819
[5] SCHURZ, J. *Phyton (B Aires).* 1955, **5**(2), 53
[6] BURCHARD, W. *International Macromolecular Symposium, Prague,* 1965, Preprint P560 [A282]
[7] JELLINEK, M. H., SOLOMON, E. and FRANKUCHEN, I. *Industr. Engng Chem. (Anal.),* 1946, **18,** 172

ANNOUNCEMENT

SYMPOSIUM ON SPECTROSCOPY OF MACROMOLECULES

A Symposium on the Spectroscopy of Macromolecules is included in the XIII Colloquium Spectroscopicum Internationale to be held at Carleton University in Ottawa, Canada, on 19 to 23 June 1967. Joint sponsors are the Canadian Association for Applied Spectroscopy and the Society for Applied Spectroscopy (U.S.A.).

Papers of thirty minutes duration are now solicited and titles or requests for further information should be directed to:

Mr. A. W. Pross,
Central Research Laboratory,
McMasterville, Quebec, Canada.

Abstracts should be submitted by 1 October 1966 to:

The Secretary, XIII Colloquium Spectroscopicum Internationale,
National Research Council,
Ottawa 7, Ontario, Canada.

They should be 400 to 500 words in length in one of the official languages: English, French or German.

A Polymeric Enzyme Analogue Based on Nicotinamide

A. S. LINDSEY, S. E. HUNT and N. G. SAVILL

A polymeric nicotinamide system of defined structure and properties is described. Some preliminary studies of the effect of the structure of groups vicinal to the dihydronicotinamide system on its H*–donor properties and particularly on the rate of* H*–transfer are reported.*

IN THE long view synthetic polymeric enzyme analogues possess great potentialities for the construction of automatic synthesizing units for the production of organic compounds. However, the problems which need to be solved are complex and they are only being examined in a sporadic way at present. This partly stems from the small number of investigators in the field and partly from the very incomplete knowledge of natural enzyme structures and processes now available[1].

Recently a number of studies of the preparation and properties of various synthetic enzyme analogues have been reported[2] but they have not included an analogue based on the nicotinamide–dihydronicotinamide system. Polymers incorporating the simpler pyridine–dihydropyridine system have been reported, however[3]. The nicotinamide–dihydronicotinamide system has been established as the reactive component of coenzymes I, II and III (nicotinamide–adenine–dinucleotides) and is known to participate widely in the enzymic electron transport chain[1]. The theoretical examination by the Pullmans[4] of the orbital energy coefficients for NAD (nicotinamide–adenine–dinucleotide) indicate it to have strong electron acceptor but poor donor properties since both the lowest empty and the highest filled molecular orbitals are relatively low lying. However, in the reduced form, $NADH_2$, the values for both the lowest empty and the highest filled molecular orbitals are appreciably raised indicating the converse properties. Present views are that electrons are transferred from the dihydronicotinamide in the form of hydride ion (H^-) with concomitant or subsequent proton transfer[5, 6]. The transfer occurs rapidly and in a number of cases stereospecifically.

As part of our studies of electron exchange polymers we have recently examined the problem of synthesizing a polymeric nicotinamide system of defined structure and properties, and the results of this work are now reported here. We also report some preliminary studies of the effect of structure of groups vicinal to the dihydronicotinamide system on its H-donor properties and particularly on the rate of H-transfer.

At the outset it was established that pyridine would react with chlormethylated polystyrene, pre-swollen in anhydrous dioxan to give a polymer of empirical structure I. This polymer could readily be reduced to the dihydro-derivative and was then able to reduce methylene blue and thionine to their leuco forms and *p*–benzoquinone to quinol.

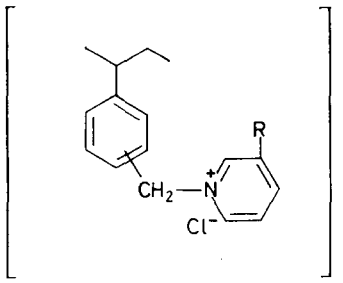

I R=H

II R=CONH$_2$

Nicotinamide also was found to react quantitatively with chlormethylated polystyrene to give a polymer of empirical structure II. Conversion to the dihydronicotinamide form on sodium dithionite reduction was confirmed by examination of the infra-red absorption spectra of the polymers and of the corresponding *N*-benzyl nicotinamide and dihydronicotinamide compounds. Previous work has established that sodium dithionite reduction of nicotinamide gives the 1,4-dihydropyridine derivative[7].

The dihydronicotinamide polymer was shown to reduce thionine, methylene blue and malachite green to their respective leuco derivatives as well as *p*-benzoquinone to hydroquinone. Experiment also indicated that the dihydropolymer would reduce anthrone and indophenol but side reactions complicated the course of the reduction. No observable reduction occurred with azobenzene or maleic acid as substrate.

An indication that the rate of hydrogen transfer from the dihydronicotinamide polymer to the substrate is diffusion controlled, was obtained by comparing the rates of reduction of equivalent amounts of dyes varying in molecular size and in oxidation-reduction potential. A modified Thunberg method was used and showed the reduction rates to decrease in the order thionine > methylene blue > malachite green. The results shown in *Table 1* indicate that the rate of reduction is related to the molecular size rather than the oxidation-reduction potential of the substrate.

Table 1

Dye	*Maximum molecular diameter Å**	E_m *(50 per cent reduction) pH=7·0 mV*	E_0 *(100 per cent reduction) pH=0 mV*	*Time for complete decolouration*
Thionine	10·6	63[8]	563[9]	30 *min*
Methylene blue	11·9	11[8]	534[9]	70 *min*
Malachite green	14·1	—	~ 700[10]	ca. 48 *h*

*Molecule assumed planar.

With simple *N*-substituted dihydronicotinamide compounds the work of Wallenfels and Gellrich[11] suggests that the rate of H-transfer is also dependent on the nature of the substituent. To confirm this with more certainty we have studied the rate of H-transfer from 1-benzyl dihydronicotinamide (III) and 1-(2,6-dichlorbenzyl) dihydronicotinamide (IV) respectively using benzoquinone as substrate. For comparison the rates of hydrogen transfer from Hantzsch's ester (V) to chloranil and benzoquinone were also measured.

These reactions are known to be bimolecular and to follow second order kinetics[12]. Application of the method of Koning and van Senden[13] to our own spectroscopic rate data for the chloranil–Hantzsch ester reaction confirmed the reaction kinetics to be second order. By rigorous exclusion of air from the reacting solutions reproducible values of the specific rate constant at 25°C were obtained giving a 'best' value of $k = 1{\cdot}53 \pm 0{\cdot}03$ l. mole^{-1} sec^{-1} and an average value of $k = 1{\cdot}57 \pm 0{\cdot}18$ l. mole^{-1} sec^{-1}. We consider this value to be more reliable than that ($k = 2{\cdot}60 \pm 0{\cdot}05$ l. mole^{-1} sec^{-1}) quoted elsewhere[12]. By a similar procedure the specific rate constants for the transfer of hydrogen from Hantzsch's ester to *p*-benzoquinone (10^2 $k = 0{\cdot}721 \pm 0{\cdot}045$ l. mole^{-1} sec^{-1}) and to the tetramethyl *p*-benzoquinone (10^2 $k = 0{\cdot}046$ l. mole^{-1} sec^{-1}; $t = 70$°C) were determined. In the latter instance the transfer reaction was very slow and consequently the k value given has lower reliability. However, the three results together lend support to the view[14] that the specific rate constants vary directly with the electron affinity of the quinone.

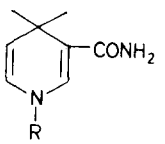

III R = $C_6H_5 \cdot CH_2$ —

IV R = 2,6-$Cl_2C_6H_3 \cdot CH_2$ —

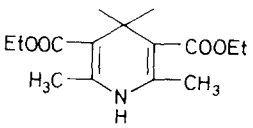

V Hantzsch's ester

We now measured the specific reaction rates of H-transfer from the benzyl dihydronicotinamides to benzoquinone. The general procedure of Wallenfels and Gellrich[11] was adopted except that phthalate buffer was used in preference to phosphate buffer to maintain the reaction mixture at pH = 7·0. This was done since Grishin and Yasnikov[15] have shown that nucleophilic addition of phosphate to *N*-benzyl dihydronicotinamide proceeds as a side reaction with a significant rate at pH = 7·0. However, in the case of phthalate the rate of addition to the dihydronicotinamide at pH = 7·0 was shown to be negligibly small. It was necessary to apply a correction factor to the optical density measurements to correct for the increase in optical density which was observed when benzoquinone was dissolved in the buffer.

The results of these measurements are given in the *Table 2* together with some of those of Wallenfels and Gellrich (starred). These results show that the rate of H-transfer from dihydronicotinamides depends on the

Table 2

H–*donor* (*dihydronicotinamide*) R–*group*	H–*acceptor*	*pH*	k l. *mole*$^{-1}$ *sec*$^{-1}$ *at 25°C*
Adenine–dinucleotide	*p*–benzoquinone	7·0	0·023★
1-(2,6-dichloro)benzyl	*p*–benzoquinone	7·0	10·7 (13·3★)
1-benzyl	*p*–benzoquinone	7·0	18·7

character of the group R attached to the ring nitrogen. However, further observations are necessary to decide whether the rate is influenced by structure in a regular way.

EXPERIMENTAL

General

Microanalyses were carried out by the Microanalytical Section of this Laboratory. Infra-red absorption spectra of solids dispersed in potassium chloride discs were taken on a Grubb–Parsons G.S.3 double-beam grating instrument; band wave numbers are correct to ± 3 cm^{-1} except those above 2 700 cm^{-1} which are correct to ± 5 cm^{-1}.

Ultra-violet absorption data were measured by means of an Optica CF4 automatic spectrophotometer which was fitted with a thermostatically controlled cell compartment.

Melting points are uncorrected.

Materials

Nicotinamide—This was of reagent grade quality m.pt 133° to 134°C, $\nu_{max.}$ 3 330, 3 120, 1 660, 1 606, 1 588, 1 574, 1 478, 1 384, 1 336, 1 222, 1 190, 1 144, 1 115, 1 090, 1 017, 968, 934, 826, 770 and 700 cm^{-1}.

Nicotinamide benzyl chloride—This was prepared according to the literature method[16] and recrystallized from ethanol as colourless plates m.pt 244°C (dec.), $\nu_{max.}$ 3 370, 3 260, 3 120, 2 930, 2 840, 1 698, 1 650, 1 630, 1 585, 1 500, 1 493, 1 450, 1 433, 1 387, 1 370, 1 350, 1 300, 1 268, 1 210, 1 180, 1 135, 1 104, 1 075, 1 026, 956, 890, 840, 825, 770, 734, 698 and 666 cm^{-1}.

1-Benzyldihydronicotinamide—This was prepared by sodium dithionite reduction of nicotinamide benzyl chloride[16], and recrystallized from aqueous methanol as orange prisms, m.pt 123°, (found: C, 72·6; H, 6·9; N, 13·1; $C_{13}H_{14}N_2O$ requires C, 72·9; H, 6·6; N, 13·1 per cent), $\nu_{max.}$ 3 455, 3 250, 3 100, 2 805, 1 670, 1 630, 1 550, 1 486, 1 420, 1 363, 1 338, 1 292, 1 214, 1 152, 1 083, 1 066, 1 023, 989, 970, 916, 869, 847, 793, 740, 718, 708 and 691 cm^{-1}.

1-[2,6-Dichlorbenzyl]-nicotinamide bromide—This was prepared by refluxing an acetone solution of 2,6-dichlorbenzyl bromide and nicotinamide for two hours[17]. The product was washed with acetone and had m.pt 250°, (found: C, 43·0; H, 3·0; N, 7·45; $C_{13}H_{10}BrCl_2N_2O$ requires C, 43·1; H, 3·1; N, 7·7 per cent), $\nu_{max.}$ 3 340, 3 285, 3 080, 3 045, 2 990, 2 930, 1 663, 1 596, 1 570, 1 556, 1 486, 1 454, 1 424, 1 394, 1 372, 1 310, 1 260, 1 174, 1 125, 1 111, 1 080, 968, 944, 895, 884, 832, 807, 763 and 670 cm^{-1}.

1-[2,6-Dichlorbenzyl]-dihydronicotinamide—This was prepared by alkaline dithionite reduction of 1-2,6-dichlorbenzyl-nicotinamide bromide[17], and recrystallized from methanol as yellow needles m.pt 170° (unsharp), (found: C, 55·1; H, 4·5; N, 9·9; Cl, 24·8; $C_{13}H_{12}Cl_2N_2O$ requires C, 55·1; H, 4·3; N, 9·9; Cl, 25·0 per cent), $\nu_{max.}$ 3 450, *ca.* 3 285, 3 110, 3 070,

2 945, 2 805, 1 677, 1 646, 1 556, 1 450, 1 423, 1 377, 1 356, 1 320, 1 294, 1 263, 1 217, 1 200, 1 174, 1 166, 1 072, 990, 975, 954, 925, 900, 870, 820, 793, 780, 763, 743 and 704 cm^{-1}.

2,6-Dimethyl-3,5-dicarboxyethyl-1,4-dihydropyridine (Hantzsch's ester)—This was prepared by the standard procedure[18] and purified by recrystallization from deoxygenated ethanol to give bright yellow needles m.pt 191°, (found: C, 61·7; H, 7·4; N, 5·4; $C_{13}H_{19}NO_4$ requires C, 61·6; H, 7·6; N, 5·5 per cent), $\lambda_{max.}$ (EtOH) 230 and 372 mμ (log ϵ 4·19 and 3·86 respectively).

Polystyrylmethylene chloride—Polystyrylmethylene chloride containing two per cent divinyl benzene was obtained in bead form (90/150 mesh size) from The Permutit Company Ltd, London. Preparatory to use it was immersed in methylethyl ketone for 24 hours, followed by slow gravity washes with (*i*) methylethyl ketone containing concentrated hydrochloric acid (five per cent by volume) and (*ii*) methylethyl ketone until the washings were acid-free. A sample was dried *in vacuo* and then analysed, (found: Cl, 22·80; $(C_9H_9Cl)_n$ requires Cl, 23·2 per cent), $\nu_{max.}$ 3 010, 2 905, 2 855, 2 685 (w), 1 598, 1 496, 1 430, 1 412, 1 340, 1 293, 1 250, 1 207, 1 150, 1 100, 1 006, 980, 908, 818, 734, 698 and 665 cm^{-1}.

*Polystyrylmethylene-pyridine-*N*-chloride*—Polystyrylmethylene chloride (5 g) was immersed in freshly purified dry dioxan (50 ml) for 16 hours. After addition of anhydrous pyridine (10 ml) the mixture was refluxed for 24 hours with continuous stirring. The recovered polymer beads were thoroughly washed first with hot then cold dioxan. A sample dried *in vacuo* was analysed, (found: C, 72·8; H, 6·4; N, 5·3; Cl, 14·9; $(C_{14}H_{14}NCl)_n$ requires C, 72·5; H, 6·1; N, 6·0; Cl, 15·3 per cent), $\nu_{max.}$ *ca.* 3 330, *ca.* 2 940, 1 616, 1 600, 1 473, 1 444, 1 420, 1 200, 1 140, 1 116, 1 044, 1 012, 858, 798, 768, 698 and 673 cm^{-1}.

*Polystyrylmethylene-*N*-1,4-dihydropyridine* — Polystyrylmethylene-pyridine-*N*-chloride (2·0 g) was immersed in a solution of sodium dithionite (13 g) and sodium carbonate (7 g) in water (50 ml) and maintained at 80° for three hours under nitrogen with continuous stirring. The reduced polymer beads were reddish in colour and were washed consecutively with deoxygenated distilled water, 2N hydrochloric acid, distilled water and dioxan. A sample was dried *in vacuo* and analysed, (found: N, 5·2; $(C_{14}H_{16}NCl)_n$ requires N, 5·98 per cent), $\nu_{max.}$ 3 410, 3 045, 2 960, 2 925, 2 858, 1 633, 1 615, 1 506, 1 490, 1 455, 1 427, 1 369, 1 292, 1 258, 1 220, 1 122, 1 084, 1 035, 949, 890, 874, 832, 805, 771 and 680 cm^{-1}.

*Polystyrylmethylene-*N*-nicotinamide chloride* — Polystyrylmethylene chloride (40 g) was immersed in freshly purified dry dioxan for 16 hours. Nicotinamide (35 g) was added and the reaction mixture was maintained at reflux temperature for 24 hours with continuous stirring. The polymer beads were separated from the reaction solvent and well washed with hot dioxan. A sample dried *in vacuo* was analysed, (found: C, 66·1; H, 5·6; N, 9·0; Cl, 13·1; $(C_{15}H_{15}ClN_2O)_n$ requires C, 65·6; H, 5·5; N, 10·2; Cl,

12·9 per cent), $\nu_{max.}$ 3 200, 3 090, 2 910, 2 845, 2 080, 1 685, 1 500, 1 438, 1 383, 1 282, 1 248, 1 194, 1 175, 1 113, 1 076, 1 040, 1 014, 890, 870, 820, 751, 703 and 673 cm^{-1}.

Polystyrylmethylene-N-1,4-dihydronicotinamide—Polystyrylmethylene-*N*-nicotinamide chloride (1 g) was immersed in a solution of sodium dithionite (5·2 g) and anhydrous sodium carbonate (2·6 g) in water (30 ml) for three hours at room temperature. The reduced polymer beads were orange in colour and after filtration under nitrogen were washed with oxygen-free water until the eluate was neutral. A sample was dried *in vacuo* and analysed, (found: C, 71·1; H, 6·2; N, 8·4; Cl, 0·6; $(C_{15}H_{17}N_2O)_n$ requires C, 74·7; H, 7·1; N, 11·6; Cl, 0·0 per cent), $\nu_{max.}$ 3 340, 3 180, 3 050, 2 900, 2 835, 1 680, 1 630, 1 546, 1 507, 1 440, 1 350, 1 283, 1 250, 1 172, 1 110, 1 072, *ca.* 1 027, 1 007, 886, 868, 812, 747, 670 cm^{-1}.

Reduction of p-*benzoquinone by means of polystyrylmethylene dihydronicotinamide*

Resublimed benzoquinone (100 mg) in AnalaR dioxan (70 ml) was refluxed with the dihydronicotinamide polymer (4 g) under nitrogen for seven hours. The mixture was filtered hot and the beads washed with hot dioxan (2 × 20 ml). Evaporation of the dioxan under reduced pressure afforded needle crystals of hydroquinone (80 mg), m.pt and mixed m.pt 172° and confirmed by comparison of the infra-red spectrum with that of an authentic specimen. It was noted that benzoquinone refluxed with wet dioxan yielded some quinhydrone, i.e. partial reduction occurred, but this was not observed under anhydrous conditions.

An attempted reduction of maleic acid by means of polystyrylmethylene dihydronicotinamide under anhydrous conditions led to the recovery of fumaric acid as sole product.

Reduction of dyes by means of polystyrylmethylene dihydronicotinamide

The aqueous dye solution (0·01M; 20 ml) was placed in a Thunberg tube and AnalaR dioxan (5·0 ml) added. The freshly reduced moist dihydronicotinamide polymer (=0·5 g dry polymer) was placed in the stopper cavity and the Thunberg tube was immediately evacuated. Each reduction experiment was run in duplicate. The evacuated Thunberg tubes were attached to a rotating clamp (~ 5 rev/min) which was housed in an oven thermostatically controlled at 80° ± 1°C. The time required for complete decolouration was noted. Duplicate experiments gave times in good agreement. Blank runs, carried out at the same time, showed no reduction. The results have been given in *Table 1*.

Kinetic measurements using Hantzsch's ester as hydrogen donor

The rate of the reaction between Hantzsch's ester and substrate at 25°C was determined by measuring the decrease with time in the absorption intensity at a suitable wavelength (see *Table 3*) of a solution containing equimolecular amounts of the two reactants. Anhydrous AnalaR benzene, which previously had been boiled and allowed to cool under nitrogen, was used as solvent. The reactants were separately recrystallized from this solvent and dried 24 hours prior to use.

The initial erratic results for the value of k were ascribed to traces of oxygen. However, by carrying out all the preparations and transfers of solutions within a 'dry nitrogen (oxygen free) box' reproducible values of k were obtained. By applying the method of Koning and van Senden[13] to the data obtained in the case of chloranil the order of the reaction was calculated to be 2·03, i.e. second order.

Table 3

Components	*Concentration* M	*Measurements made at* λ Å	*Total time observed* min	% *completion of reaction*	10^2k *l. mole*$^{-1}$ *sec*$^{-1}$	*t*°C
Hantzsch's ester tetrachloroquinone (1:4)	$2{\cdot}85\times10^{-4}$	3 950	130	78	153 ± 3	25
Hantzsch's ester benzoquinone (1:4)	$6{\cdot}32\times10^{-3}$	4 125	183	43	$0{\cdot}72\pm0{\cdot}05$	25
Hantzsch's ester tetramethylquinone (1:4)	$8{\cdot}42\times10^{-3}$	4 150	366	7	0·046	70

Kinetic measurements using 1-benzyl- and 1-2,6-dichlorbenzyl-dihydronicotinamides as hydrogen donors

Hydrogen transfer reaction rates at 25°C were determined spectrometrically by observing the change in the absorption intensity at 3 600 Å during the course of the reaction[11]. As in the previous kinetic experiments all preparation and transfer of solutions were carried out in a dry box with a nitrogen atmosphere. Solutions were prepared of benzoquinone in aqueous methanol (1: 1), and of the benzyl dihydronicotinamide in aqueous methanolic (1: 1) 0·014 M phthalate buffer (pH = 7·0). The reaction was made pseudomonomolecular by adding a suitable quantity of benzoquinone solution from a hypodermic syringe immediately prior to commencement of the spectrometric measurements, so as to ensure that the quinone was present in approximately tenfold excess.

Table 4

Components	*Concentration* M	*Total time observed* min	% *completion of reaction*	k *l. mole*$^{-1}$ *sec*$^{-1}$	*t*°C
1-Benzyldihydronicotinamide	$0{\cdot}296\times10^{-4}$	8	95	$18{\cdot}7\pm0{\cdot}5$	25
benzoquinone (1:4)	$2{\cdot}78\times10^{-4}$				
1-2,6-Dichlorbenzyl-		11	94	$10{\cdot}7\pm1{\cdot}3$	25
dihydronicotinamide	$0{\cdot}543\times10^{-4}$				
benzoquinone (1:4)	$4{\cdot}23\times10^{-4}$				

CONCLUSIONS

(1) A polymeric dihydronicotinamide can function as a hydrogen transfer agent and can be used to reduce substrates such as dyes and benzoquinone.

(2) The rate of hydrogen transfer from the polymer is probably diffusion controlled.
(3) The rate of hydrogen transfer from the monomeric *N*-substituted dihydronicotinamides is dependent on the nature of the substituent group.

We thank Mr H. M. Paisley for measurement of the infra-red spectra and Mr D. P. Biddiscombe for providing a full translation of reference 15. The work reported in this paper was carried out as part of the research programme of the former National Chemical Laboratory, D.S.I.R., Teddington.

Division of Molecular Science,
National Physical Laboratory,
Ministry of Technology,
Teddington, Middlesex

(*Received March 1966*)

REFERENCES

[1] LINDSEY, A. S. *Rev. pure appl. Chem.* 1964, **14,** 109 and references cited therein
[2] BRANDENBERGER, H. *Bulletin des Fermentations,* 1956, **11,** 237; MANECKE, G. *Pure and appl. Chem.* 1962, **4,** 507; LAUTSCH, W., BROSER, W., BIEDERMANN, W. and GNITCHEL, M. *J. Polym. Sci.* 1955, **17,** 479
[3] ADAMS, C. E. and KIMBERLIN, C. N. *U.S. Pat. No. 2 899 396* (1959); CASSIDY, H. G. *J. Amer. chem. Soc.* 1949, **71,** 402
[4] PULLMAN, A. and PULLMAN, B. *C.R. Acad. Sci., Paris,* 1959, **284,** 149
[5] WESTHEIMER, F. H. *The Enzymes,* Vol. I, p 278. Edited by P. D. BOYER, H. LARDY and K. MYRBÄCK. Academic Press: New York, 1959
[6] DITTMER, D. C. and FOUTY, R. A. *J. Amer. chem. Soc.* 1964, **86,** 91; ABELES, R. H., HUTTON, R. F. and WESTHEIMER, F. H. *J. Amer. chem. Soc.* 1957, **79,** 712
[7] PULLMAN, M., SAN PIETRO, A. and COLARICK, S. P. *J. biol. Chem.* 1954, **206,** 129; HUTTON, R. F. and WESTHEIMER, F. H. *Tetrahedron,* 1959, **3,** 73; KOSOWER, E. M. and BOWER, S. W. *J. Amer. chem. Soc.* 1960, **82,** 2191
[8] *Biochemists' Handbook,* p 88. E. and F. N. Spon: London, 1961
[9] CLARK, W. M., COHEN, B. and GIBBS, H. D. *Publ. Hlth Rep. Wash.* 1925, **40,** 1131
[10] KNOP, J. *Z. anal. Chem.* 1931, **85,** 253; ALLEN, M. J. and POWELL, V. J. *Trans. Faraday Soc.* 1954, **50,** 1244
[11] WALLENFELS, K. and GELLRICH, M. *Liebigs Ann.* 1959, **621,** 149
[12] BRAUDE, E. A., HANNAH, J. and LINSTEAD, R. P. *J. chem. Soc.* **1960,** 3249
[13] KONING, H. N. and VAN SENDEN, K. G. *Rec. Trav. chim. Pay-Bas,* 1962, **81,** 1024
[14] LINDSEY, A. S. *J. appl. Chem.* 1965, **15,** 161
[15] GRISHIN, O. M. and YASNIKOV, A. A. *Ukr. khim. Zh.* 1962, **28,** 707
[16] MAUZERALL, D. and WESTHEIMER, F. H. *J. Amer. chem. Soc.* 1955, **77,** 2261
[17] WALLENFELS, K. and SCHULZ, H. *Liebigs Ann.* 1959, **621,** 128
[18] SINGER, A. and MCELVAIN, S. M. *Org. Synth.* 1934, **14,** 31

*Estimation of Unperturbed Polymer Dimensions from Viscosity Measurements in Non-ideal Solvents**

J. M. G. COWIE

A critical examination of several graphical methods for obtaining unperturbed polymer dimensions from viscosity measurements has been made. The relative merits of each are discussed and a modified form of an equation proposed by Bohdanecky is presented. It is suggested that three of the equations be used in a complementary fashion to obtain accurate estimates of $(\bar{R}_0^2)^{1/2}$ *from data in non-ideal solvents.*

RECENT advances in the preparation of stereoregular polymers have stimulated the need to characterize their microtacticity and fine structure. It is of considerable interest, therefore, to derive information about the dimensions of a macromolecule in the absence of both inter- and intra-molecular interactions, such conditions being obtained when a polymer is dissolved in a theta solvent. However, as an ideal solvent is not always readily available and as certain stereoregular polymers have a tendency to crystallize out from poor solvents, techniques must be sought whereby the unperturbed dimensions may be obtained from measurements in non-ideal solvents.

Several graphical procedures have been proposed which require knowledge of the intrinsic viscosity of polymer fractions of known molecular weight. Flory, Fox[1] and Schaefgen were the first to put forward such a method; their equation was

$$[\eta]^{2/3}M^{-1/3} = K_\theta^{2/3} + K_\theta^{5/3}C_T M\,[\eta]^{-1} \tag{1}$$

and extrapolation gave $K_\theta^{2/3}$ as intercept from which the unperturbed root mean square end to end distance $(\bar{R}_0^2)^{1/2}$ could be obtained using

$$K_\theta = \Phi_0\,[(\bar{R}_0^2)/M]^{3/2} = \Phi_0 A^3 \tag{2}$$

where $\Phi_0 = 2{\cdot}87 \times 10^{21}$.

The relationship was found to be useful for only a limited number of systems[2] and several alternatives have been suggested. A modified form, which was applicable to polymers dissolved in 'good' and 'poor' solvents, was proposed by Kurata and Stockmayer[2] and was based on the solution theory of Kurata, Stockmayer and Roig[3]. The relationship

$$[\eta]^{2/3}M^{-1/3} = K_\theta^{2/3} + 0{\cdot}363\,\Phi_0 B\,[g(\alpha_\eta)\,M^{2/3}\,[\eta]^{-1/3}] \tag{3}$$

requires an initial estimation of K_θ by assuming $g(\alpha_\eta) = 1$ from which values of $[\eta]_\theta$, α_η and $g(\alpha_\eta)$ can then be obtained; subsequent replotting of the

*Issued as *N.R.C. No. 9233.*

data gives an accurate K_θ. Here $\alpha_\eta = ([\eta]/[\eta]_\theta)^{1/3}$, $g(\alpha_\eta) = 8\alpha_\eta^3 (3\alpha_\eta^2 + 1)^{-3/2}$ and $B = \beta/c^2m^2$, where β is the binary cluster integral, and cm is the molar weight of a chain 'segment'.

A much simpler form was proposed by Burchard[4], and by Stockmayer and Fixman[5]; the latter authors suggested the equation

$$[\eta]\, M^{-1/2} = K_\theta + 0{\cdot}51\Phi_0 B M^{1/2} \tag{4}$$

would be useful for all solvent–polymer systems, and this has indeed been one of the more successful relationships. The main weakness of equation (4) is that it is based on a closed expression for α^3 and the assumption that a similar expression will hold for α_η^3. This is apparently inadequate at high α_η and results in a non-linear plot when α_η exceeds $\sim 1{\cdot}5$. It is important, therefore, that a sufficiently wide range of molecular weights be examined so that an extrapolation can be made which does not result in an over-estimation of K_θ.

Inagaki, Suzuki and Kurata[6] have attempted to obtain a linear plot by using the Ptitsyn–Eizner equation relating α to z, the excluded volume parameter. They arrived at

$$[\eta]^{4/5} M^{-2/5} = 0{\cdot}786 K_\theta^{4/5} + 0{\cdot}950 K_\theta^{4/5} k^{2/3} M^{1/3} \tag{5}$$

where $k = 0{\cdot}33B\,[M/\langle\bar{R}^2\rangle_0]^{3/2}$ and B has now been defined above. The authors point out that their relationship can only be expected to afford an accurate value of K_θ in systems for which $\alpha > 1{\cdot}4$, and as such will be complementary to equation (4). The plots obtained were linear except at low α where an upward curvature was encountered.

While Inagaki *et al.* used an expression valid for high α in order to obtain a linear plot, Bohdanecky[7] proposed that the molecular weight dependence of the second virial coefficient should be considered. Starting from a semi-empirical equation derived by Krigbaum[8]

$$[\eta]\, M^{-1/2} = K_\theta + 5 \times 10^{-3} A_2 M^{1/2} \tag{6}$$

he arrived at the relation

$$[\eta]\, M^{-1/2} = K_\theta + 0{\cdot}762 K_\theta k^{7/10} M^{7/20} \tag{7}$$

This was accomplished by using the modified Flory–Orofino expression relating A_2 and z, from which equation (7) can be obtained using a graphical approximation for $z > 0{\cdot}5$. This form was found to give K_θ values which were too low and experimental evidence led to the modification

$$[\eta]\, M^{-1/2} = 0{\cdot}8 K_\theta + 0{\cdot}65 K_\theta k^{7/10} M^{7/20} \tag{8}$$

A somewhat different approach has been made by Cornet[9] who recently advanced a method of obtaining $(\bar{R}_0^2)^{1/2}$ which appears promising. He has shown that by determining the critical concentration in a plot of $\log \eta$ against $\log C$ for a polymer of known molecular weight, $(\bar{R}_0^2)^{1/2}$ can be calculated from

$$(\bar{R}_0^2)^{1/2} = 2{\cdot}84 \times 10^{-8}\, (M/C_{cr})^{1/3} \tag{9}$$

where C_{cr} is the critical concentration, defined as the concentration at which

$\log \eta$ ceases to curve and becomes a linear function of $\log C$. At this point it is assumed that the solution is sufficiently concentrated for the polymer molecules to adopt their unperturbed configuration. The results obtained are in good agreement with experimental results and the method has the added advantage that only one sample is required, in theory, for a determination.

APPRAISAL OF THE RELATIONSHIPS

It has been shown that equation (1) is not generally reliable[2], and as equation (3) requires successive approximations before suitable K_θ values are obtained, neither will be considered further here. For the purpose of comparing the relative merits of each equation, six polymer–solvent systems have been chosen for which data in both non-ideal and theta solvents, measured at the same temperature, are available.

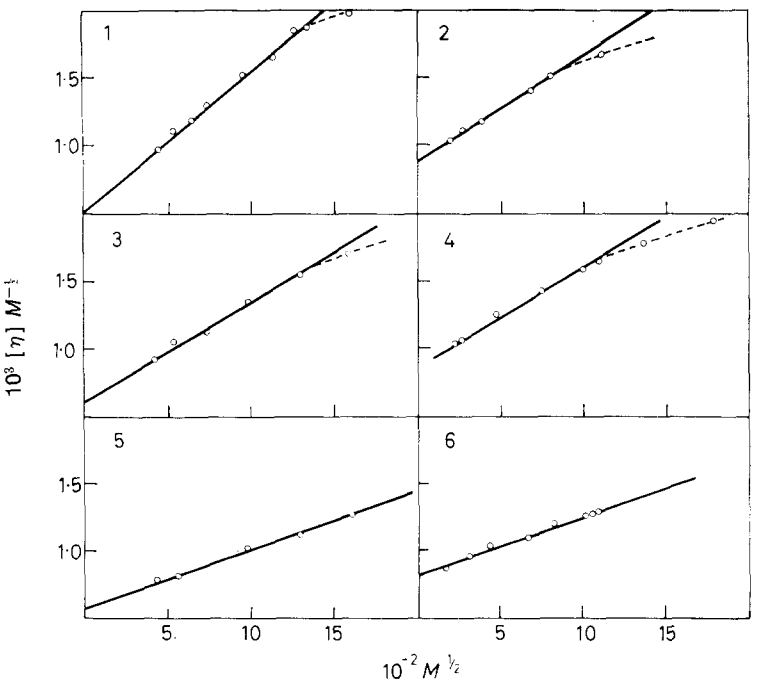

Figure 1—Plot of $[\eta] M^{-1/2}$ against $M^{1/2}$, equation (4), for various systems. Numbers correspond to systems in *Table 1*

The results, plotted according to equation (4), are shown in *Figure 1*. It can be seen that in the four examples for which ν lies between 0·7 and 0·8 the lines start to curve around $\overline{M}_w \sim 10^6$. Here ν is the exponent in the Mark–Houwink equation

$$[\eta] = K_m M^\nu \tag{10}$$

The two systems for which $\nu < 0{\cdot}7$ are linear over the range examined and present no great problem in extrapolation. Values of K_θ obtained are listed

Table 1. Comparison of experimental and calculated values of K_θ for several polymer–solvent systems

No.	Polymer	Solvent	Temp, °C	ν	$K_\theta \times 10^4$ expt.	$K_\theta \times 10^4$ eq. 4	$K_\theta \times 10^4$ eq. 5	$K_\theta \times 10^4$ eq. 8	$K_\theta \times 10^4$ eq. 23	Ref.
1	Poly ethyl methacrylate	Methyl ethyl ketone	23	0·79	4·7	4·9	4·3	3·4	4·5	(10)
2	Poly α-methyl styrene	Carbon tetrachloride	37	0·73	7·5	7·6	7·9	6·4	7·6	(11)
3	Poly methyl methacrylate	Toluene	34	0·73	6·3	6·1	6·9	5·1	6·1	(12,13)
4	Poly styrene	Toluene	35	0·70	8·6	8·5	8·9	7·8	8·8	(11,14)
5	Poly methyl methacrylate	Methyl isobutyrate	34	0·68	6·3	6·2	6·4	6·1	6·7	(12,13)
6	Poly vinyl acetate	Methanol	30	0·60	9·2	8·6	9·3	9·4	9·0	(15)

in *Table 1* and compare favourably with experimental results, the one possible exception being the polyvinyl acetate–methanol system.

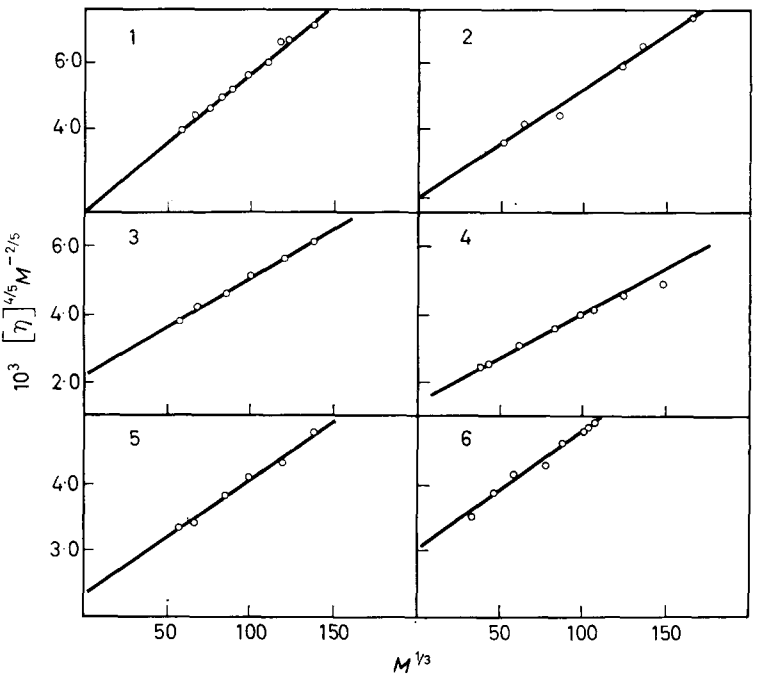

Figure 2—Test of equation (5) for systems numbered as in *Table 1*

The type of plot obtained using equation (5) is shown in *Figure 2*; these are linear with the exception of the polystyrene–toluene system which is slightly curved at high α. Results for K_θ are listed in *Table 1* together with those from equation (8), calculated from the lines shown in *Figure 3*. Comparison of graphical and experimental results indicates that agreement is good for equation (5), but not particularly good for equation (8) especially

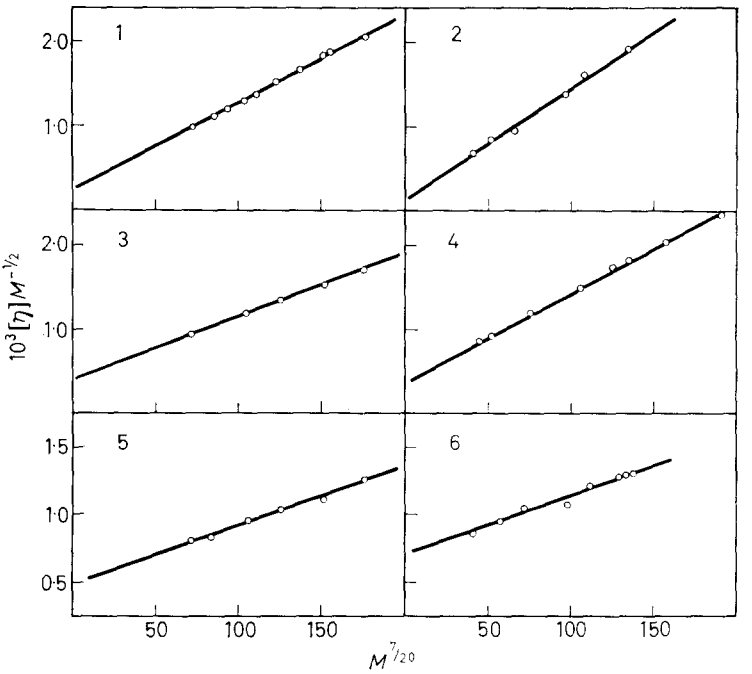

Figure 3—Data for systems listed in *Table 1* plotted according to equation (8)

at high ν. This latter relationship is also invalid in a theta solvent and this criticism can also be levelled at equation (5).

MODIFICATION OF EQUATION (8)

It can be seen from the results in *Table 1* that equation (8) is apparently inadequate in its present form, being both inflexible in non-ideal solvents and invalid under theta conditions. It was found possible to improve the relationship and produce a form applicable to 'good' and 'poor' solvents by modifying it in the following manner.

The semi-empirical relationship derived by Krigbaum[8] has the form

$$(\bar{R}^2)^{3/2}=(\bar{R}_i^2)^{3/2}+3\left(\frac{134}{105}\right)\left(\frac{3}{2\pi}\right)^{3/2}\frac{A_2}{N_A}M^2 \tag{11}$$

and this can be rearranged to

$$\left(\frac{\bar{R}^2}{\bar{R}_0^2}\right)^{3/2}=1+1{\cdot}263\,\frac{A_2}{N_A}\times\frac{M^{1/2}}{A^3} \tag{12}$$

The second virial coefficient A_2 as defined by Zimm is

$$A_2=\frac{1}{2}N_A\,B\,h(z) \tag{13}$$

where $h(z)$ is a molecular weight dependent function whose form is dependent on the theoretical treatment favoured by various authors[2]. By using the

modified Krigbaum–Flory–Orofino expression for $h(z)$, Bohdanecky arrived at the relation

$$z\,h(z) = 0{\cdot}479 z^{7/10} \tag{14}$$

which is a reasonable approximation except at very low z. The excluded volume parameter can be defined as

$$z = 0{\cdot}33\ \ B \times A^{-3} M^{1/2} \tag{15}$$

where

$$A = [(\overline{R_0^2})/M]^{1/2}$$

and substitution of (13), (14) and (15) in (12) yields

$$\left(\frac{\overline{R^2}}{\overline{R_0^2}}\right)^{3/2} = 1 + 0{\cdot}9166 z^{7/10} \tag{16}$$

To obtain equation (16) in terms of $[\eta]$ rather than $(\overline{R^2})^{3/2}$ one can use the equation

$$[\eta] = \Phi \left(\frac{\overline{R^2}}{M}\right)^{3/2} \times M^{1/2} \tag{17}$$

but as the statistical radius of the coil increases more rapidly than the hydrodynamic radius, a correction for this effect should be introduced in the conversion. Ptitsyn and Eizner[16] dealt with this problem by replacing equation (17) with

$$[\eta] = \Phi(\epsilon) \left(\frac{\overline{R^2}}{M}\right)^{3/2} \times M^{1/2} \tag{18}$$

where

$$\Phi(\epsilon) = \Phi_0(1 - 2{\cdot}63\epsilon + 2{\cdot}86\epsilon^2) \tag{19}$$

and ϵ is given by

$$R^2 = K_R M^{1+\epsilon} \tag{20}$$

The exponent ν is related to ϵ by

$$\nu = (1 + 3\epsilon)/2 \tag{21}$$

and thus $\Phi_0 = \Phi(\epsilon)$ in a theta solvent. Equation (16) can now be recast as

$$\frac{[\eta]}{[\eta]_\theta} \times \frac{\Phi_0}{\Phi(\epsilon)} = 1 + 0{\cdot}9166 z^{7/10} \tag{22}$$

or

$$\frac{[\eta]}{M^{1/2}} = \frac{\Phi(\epsilon)}{\Phi_0} K_\theta + 0{\cdot}9166 \frac{\Phi(\epsilon)}{\Phi_0} K_\theta k^{7/10} M^{7/20} \tag{23}$$

Thus equation (23), which now has a solvent-dependent factor modifying K_θ, will be valid in a theta solvent, unlike equation (8). The results for K_θ calculated from (23) are shown in the last column of *Table 1*, and are in good agreement with the experimental values.

LIMITS OF APPLICATION

In order to establish a range of α values in which the equations might be expected to hold, data for poly α–methyl styrene dissolved in toluene were examined. This system has been investigated[17, 18] at 30°C over a molecular weight range of 10^3 to 10^6 and a value of $K_\theta = 7{\cdot}68 \times 10^{-4}$ has been reported[19]

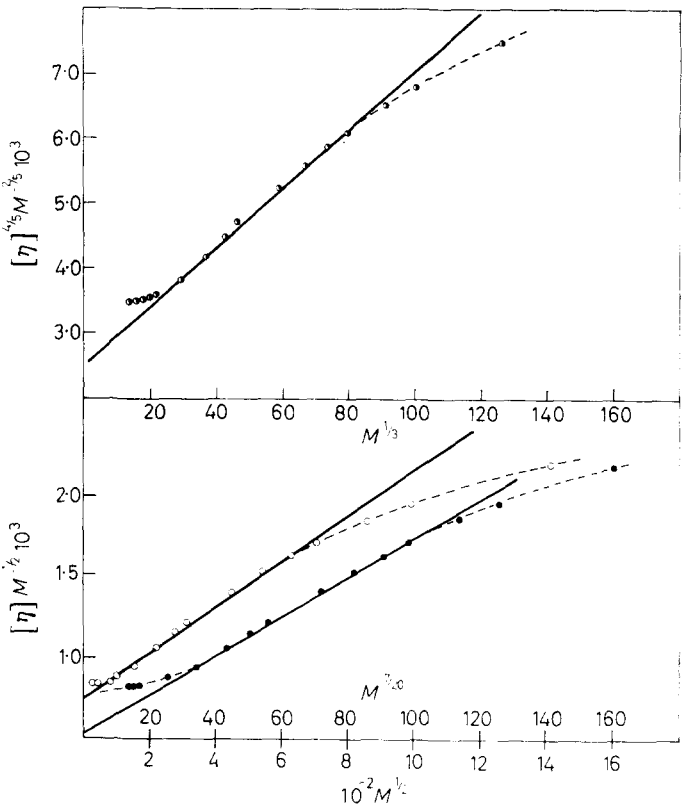

Figure 4—Results for system poly α-methyl styrene–toluene at 30° plotted using equations (4), (5) and (8) [or (23)]. Equation (4) ○, equation (5) ◑, equation (8) or (23) ●

for the polymer at 30°C. In *Figure 4* are shown the plots for equations (4), (5), (8) and (23); in no case was curvature eliminated entirely. With the exception of equation (8), there is good agreement between the calculated and experimental values of K_θ. These are shown in *Table 2* together with the range of α in which each equation was approximately linear. Equation (23) has a lower limit of $\alpha \sim 1{\cdot}2$ and an upper of $\alpha \sim 2{\cdot}5$, but as it can be used for theta-systems it may be considered to have a slightly greater range of application than the other equations.

Table 2. K_θ values for poly α-methyl styrene in toluene at 30° using various viscosity equations. Experimental $K_\theta = 7{\cdot}68 \times 10^{-4}$ and $\nu = 0{\cdot}71$

Equation	K_θ	*Range of application*
4	$7{\cdot}5 \times 10^{-4}$	$\alpha = 1{\cdot}0 \sim 2{\cdot}0$
5	$7{\cdot}5 \times 10^{-4}$	$\alpha = 1{\cdot}2 \sim 2{\cdot}5$
8	$6{\cdot}8 \times 10^{-4}$	$\alpha = 1{\cdot}2 \sim 2{\cdot}5$
23	$7{\cdot}8 \times 10^{-4}$	$\alpha = 1{\cdot}2 \sim 2{\cdot}5$

In this respect it is interesting to note that for poly α-methyl styrene in toluene, $\nu = 0{\cdot}71$ above $\overline{M}_w = 20\,000$, but below this value ν decreases and the $\log[\eta]/\log M_w$ plot approaches the theta line asymptotically. This is reflected in the line calculated from equation (23) where the points below $\alpha = 1{\cdot}2$ curve off and extrapolate to $K_\theta \sim 7{\cdot}8 \times 10^4$, thus the curvature shows the changing value of $\Phi(\epsilon)/\Phi_0$ (and of ν) as it approaches unity.

DISCUSSION

The results indicate that equations (4), (5) and (23) produce values of K_θ which are within eight per cent of the experimental values and in many cases the agreement is much better than this. Considering the semi-empirical nature of the relationships, based as they are on approximations, the results are surprisingly good. The most likely source of error is extrapolation of data which do not cover the desired range of α values for a particular equation, but even with good experimental results the uncertainties in extrapolation could lead to a possible error of from three to five per cent in K_θ. For these reasons the equations should be used to complement one another.

As the weaknesses in the various approaches are manifest in non-linear plots, it is interesting to note that Baumann[20] formulated a relation, similar to a form suggested by Burchard[4], which was linear over a wide range of α. Starting from the Fixman closed expression

$$\alpha^3 = 1 + 2z \tag{24}$$

he obtained

$$\left(\frac{\overline{R^2}}{\overline{M}}\right)^{3/2} = A^3 + BM^{1/2} \tag{25}$$

which produced A values in good agreement with data from other methods. Now both equations (4) and (25) are derived initially from (24); in the case of the Stockmayer–Fixman relationship it was suggested that α_η^3 could be used in (24) by assuming only a change in the numerical constant, whereas equation (25) follows directly from the Fixman relation. This might suggest that the weakness of the Stockmayer–Fixman equation lies in the method of relating α to α_η. However, use of the Kurata–Yamakawa[21] relation $\alpha^{5/2} \sim \alpha_\eta^3$ only reduces the power of M in equation (4) to 0·45 and produces little improvement in the linearity of the plot. To obtain a power of M closer to that in equations (5) or (8), which are linear over a wider α-range, would require the assumption that $\alpha^2 \sim \alpha_\eta^3$ and only then is linearity noticeably improved. The Krigbaum relation [equation (11)] can also be reduced to the form of equation (4) if higher terms in the expansion are neglected as they have been in the derivation of (8) and (23), and also if the function $h(z)$ is regarded as being unity. This latter condition is only true in the vicinity of the theta point, and non-ideal solvents require consideration of the $h(z)$ term which then modifies $M^{1/2}$ to $M^{7/20}$.

This apparently compensates in part for the neglect of higher terms in the α/z expression, by producing a plot which is linear over a higher and wider range of α_η. The fact that curvature is not eliminated entirely but is only shifted to a higher value of α_η suggests that the modification of the

linear α^3/z relation is inadequate; unfortunately the use of higher terms is impracticable.

The possibilities thus arise that either equation (25) is not linear over a wide range of α, although existing data do not support this conclusion, or compensation for differences in α and α_η, as formulated at present, is inadequate. The lack of suitable experimental evidence makes it difficult to decide which of the above propositions is correct, and it may even be a combination of effects rather than one alone.

Most linear synthetic polymers studied in dilute solutions conform to the restriction $0{\cdot}5 \leqslant \nu \leqslant 0{\cdot}8$ and the equations discussed above are valid only in this region, with the exception of equation (4). The reasons for this will not be discussed here. It is obvious from the foregoing that equations (5), (8) and (23) are no great improvement on the Stockmayer–Fixman relation, and that the modifications merely alter, and extend slightly, the α_η-range in which each is valid. Marked improvement in equation (4) might be better taken care of by introduction of a quadratic term, but as this cannot be done effectively, use of (4), (5) and (23) to complement each other could minimize the uncertainties in extrapolation introduced by non-linearity. In view of the limitations at low α_η in equation (5), the Stockmayer–Fixman relation is still the most versatile form.

The author wishes to thank Dr S. Bywater for helpful discussions.

Division of Applied Chemistry,
National Research Council,
Ottawa, Canada

(*Received April 1966*)

REFERENCES

[1] FLORY, P. J. and FOX, T. G. *J. Amer. chem. Soc.* 1951, **73,** 1904
[2] KURATA, M. and STOCKMAYER, W. H. *Fortschr. Hochpolym. Forsch.* 1963, **3,** 196
[3] KURATA, M., STOCKMAYER, W. H. and ROIG, A. *J. chem. Phys.* 1960, **33,** 151
[4] BURCHARD, W. *Makromol. Chem.* 1961, **50,** 20
[5] STOCKMAYER, W. H. and FIXMAN, M. *J. Polym. Sci. C,* 1963, **1,** 137
[6] INAGAKI, H., SUZUKI, H. and KURATA, M. *U.S.–Japan Seminar in Polymer Physics, Kyoto, 1965*
[7] BOHDANECKY, M. *J. Polym. Sci. B,* 1965, **3,** 201
[8] KRIGBAUM, W. R. *J. Polym. Sci.* 1955, **18,** 315
[9] CORNET, C. F. *Polymer, Lond.* 1965, **6,** 373
[10] CHINAI, S. N. and SAMUELS, R. J. *J. Polym. Sci.* 1956, **19,** 463
[11] BYWATER, S. and COWIE, J. M. G. To be published
[12] FOX, T. G. *Polymer, Lond.* 1962, **3,** 111
[13] SAKURADA, I., NAKAJIMA, A., YOSHIZAKI, O. and NAKAMAE, E. *Kolloidzschr.* 1962, **186,** 41
[14] COWIE, J. M. G. and BYWATER, S. *Polymer, Lond.* 1965, **6,** 197
[15] MATSUMOTO, M. and OHYAMAGI, Y. *J. Polym. Sci.* 1960, **46,** 441
[16] PTITSYN, O. B. and EIZNER, YU. E. *Soviet Phys.—Tech. Phys. (transl.),* 1960, **4,** 1020
[17] SIRIANNI, A. F., WORSFOLD, D. J. and BYWATER, S. *Trans. Faraday Soc.* 1959, **55,** 2124
[18] COTTAM, B. J., COWIE, J. M. G. and BYWATER, S. *Makromol. Chem.* 1965, **86,** 116
[19] OKAMURA, S., HIGASHIMURA, T. and IMANISHI, Y. *Chemy high Polym.* 1959, **16,** 244
[20] BAUMANN, H. *J. Polym. Sci. B,* 1965, **3,** 1069
[21] KURATA, M. and YAMAKAWA, H. *J. chem. Phys.* 1958, **29,** 311

Polymerization of Styrene under Pressure

G. B. GUARISE

The pressure effect on the kinetics of styrene polymerization up to 2 650 atm and at 80°C has been investigated. The results obtained with benzoyl peroxide show that the kinetics of polymerization under pressure follows the same mechanism as at atmospheric pressure. The rate of the peroxide-initiated polymerization depends on the peroxide concentration to the power 0·5. The thermal polymerization has also been examined. Activation volume values for thermal and peroxide-initiated polymerization are derived and discussed.

THE pressure is a powerful parameter for studying chemical reactions from the thermodynamic and kinetic points of view.

It is well known that the dependence of the rate constant k on temperature and pressure is:

$$\left(\frac{\partial \ln k}{\partial T}\right)_P = E/RT^2; \quad \left(\frac{\partial \ln k}{\partial P}\right)_T = -\Delta V^{+}/RT \qquad (1), (1')$$

where E is the activation energy and ΔV^{+} the activation volume, i.e. the difference in volume between the transition state and reactants.

Here we shall deal only with the isotherm (1').

According to equation (1') we can expect an accelerating effect of pressure on the rate of polymerization reactions. Bridgman and Conant[1] first observed this effect in polymerization of olefins. Further investigations on organic and inorganic polymerizations showed the general character of the pressure effect on these reactions.

FREE RADICAL POLYMERIZATION OF STYRENE

Styrene has been chosen for the following reasons:

(*i*) the mechanism of the polymerization is well understood at atmospheric pressure;

(*ii*) data regarding the polymerization under pressure are available in the literature and can be used for check purposes;

(*iii*) both monomer and polymer are easy to handle.

We refer to the polymerization mechanism proposed by Mayo *et al.*[2] for the free radical polymerization of styrene at atmospheric pressure. They write for the overall polymerization rate:

$$r^2 = k_p^2 \, (fk_d/k_t) \, [\mathrm{M}]^2 \, [\mathrm{I}] + r_{pt}^2 \qquad (2)$$

where [M], [I] are monomer and initiator concentrations, k_p, k_d, k_t are the rate constants for the propagation, initiator dissociation and termination steps respectively and f is the initiator efficiency. We neglect termination by disproportionation.

The contribution to the overall polymerization rate due to thermal poly-

merization corresponds to the term r_{pt}^2 of equation (2). In addition we consider

$$r_{pt} = k_p (k_i / k_t)^{\frac{1}{2}} [M]^2 \tag{3}$$

where k_i is the rate constant of the thermal initiation step, and

$$\frac{1}{\overline{P}} = \frac{k_M}{k_p} + \frac{k_t}{k_p^2 [M]^2} r + \frac{k_I}{k_p} \frac{[I]}{[M]} \tag{4}$$

where $\overline{P}$ is the average degree of polymerization and k_M, k_I are the rate constants for transfer reaction to monomer and initiator respectively[3, 4].

EXPERIMENTAL

The reaction vessel, designed to contain pressures up to 5 000 atm, is shown in *Figure 1*. The sample holders are PTFE bottles supported with a brass tube. The bottles are pressurized with the pressure-transmitting medium (Mil. H-5606 hydraulic oil). As pressure generator and pressure gauge a dead weight apparatus up to 3 000 atm is employed[5]. Temperature of the oil bath containing the pressure vessel is kept constant to $\pm 0{\cdot}1$ deg. C. Two minutes time is required to pressurize the system at 3 000 atm and pressure can be kept constant within less than 0·1 per cent.

Both styrene and benzoyl peroxide are C. Erba products. Styrene was purified from inhibitor by distillation under vacuum at 30°C. Only the middle fraction of the distillate was utilized.

Benzoyl peroxide was purified by precipitation with methanol from chloroform solution.

For each set of three or four runs new solutions of peroxide in freshly distilled styrene were prepared. To avoid additional polymerization, the samples were kept in liquid nitrogen before and after the run.

The yield of polymer was determined gravimetrically after precipitation of the polymer with methanol from benzene solution.

The molecular weights were derived from the intrinsic viscosity $[\eta]$ of benzene solutions, using the correlation[2, 6].

$$PM = 178\,000\,[\eta]^{1.37}$$

The origin of reaction time corresponds to the immersion of the reactor into the oil bath. In this way we include the preheating period in the reaction time. During this period (25 to 30 minutes), the pressure tends to rise owing to the thermal expansion of the pressurizing medium and a continuous pressure control is required. To take the preheating period into account, the zero point of the reaction times has been extrapolated in the yield versus time diagrams to zero yield. A similar procedure has been followed by Merrett and Norrish[7].

In order to control the temperature of the sample, especially during the preheating period, a thermocouple (Thermocoax, Chromel–Alumel 1 mm diameter) was inserted into the PTFE bottle as shown in *Figure 1*.

RESULTS

Measurements at atmospheric pressure

Table 1 shows the effect of the initiator concentration [I] on the poly-

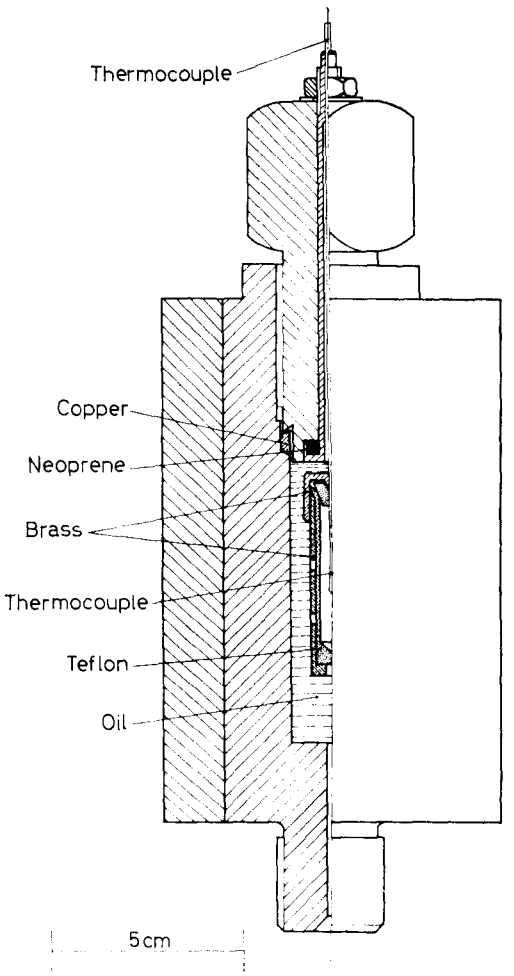

Figure 1—Reaction vessel up to 5 000 atm; capacity 40 cm³

merization rate r and the reciprocal degree of polymerization $1/\bar{P}$. Each value of r and $1/\bar{P}$ derives from at least four different yield and molecular weight determinations corresponding to different reaction times. The results have been found reproducible within about three per cent. To refer to initial conditions, especially for [I], the $1/\bar{P}$ values were obtained by extrapolating the intrinsic viscosity versus time curves to $t=0$. In these runs the PTFE containers were directly immersed into the oil-bath. The inserted thermocouple showed that the bath temperature was reached in about four minutes.

Only runs with yields less than ten per cent were considered and the polymerization rate was calculated assuming[8] $[M]=8{\cdot}17\times10^{-3}$ mole/cm³.

The results reported in *Table 1* differ by less than five per cent from the corresponding data of Bevington and Toole[9]. A similar agreement with data of Haward and Simpson[10] was found for the $[\eta]$ versus r correlation.

Table 1. Styrene polymerization at 80°C and 1 atm

$[I] \times 10^5$ mole/cm³	$r \times 10^7$ mole/cm³, sec	$[\eta]$ 100 cm³/g	$10^4/\bar{P}$
0·035	0·49	1·65	3·11
0·175	1·04	1·05	5·48
0·351	1·36	0·82	7·66
0·702	2·02	0·675	10·0

The application of equation (2) to the data of *Table 1* gives: $r_{pt} = 1{\cdot}27 \times 10^{-8}$ mole/cm³ sec compared with $1{\cdot}25 \times 10^{-8}$, $1{\cdot}09 \times 10^{-8}$, and $1{\cdot}08 \times 10^{-8}$ mole/cm³ sec according to Kromolicki[4], Haward and Simpson[10], Nozaki and Bartlett[11] respectively.

Measurements under pressure

Results at 1 400 and 2 650 atm are plotted in *Figure 3*. In both cases the extrapolations to zero yield show a delay time of about 21 minutes. It is apparent that the delay time is independent of pressure. The delay time at 740 atm was in fact found to be the same.

Since sample temperature versus time curves were available, we checked the value of the delay time with the following correlation:

$$\text{delay time} = \int_0^\infty \frac{r_0 - r}{r_0}\,dt = \int_0^\infty \left[1 - \exp\frac{E(-\Delta T)}{R(T_0^2 - T_0\,\Delta T)}\right] dt \qquad (5)$$

Subscript $_0$ indicates conditions of steady state (80°C).

Assuming 22 kcal/mole for the activation energy of the overall rate

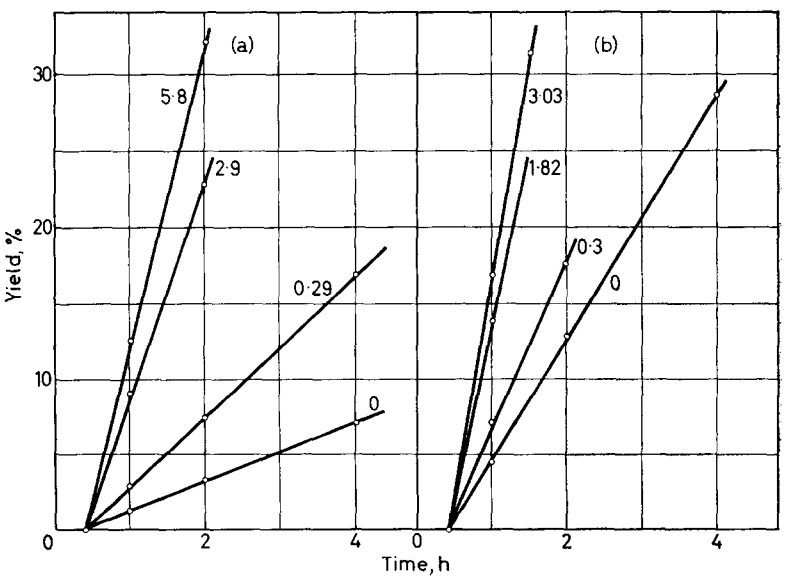

Figure 2—Polymerization of styrene at (a) 1 400, (b) 2 650 atm and 80°C. The parameter of the curves is $[I] \times 10^{-6}$ mole/cm³

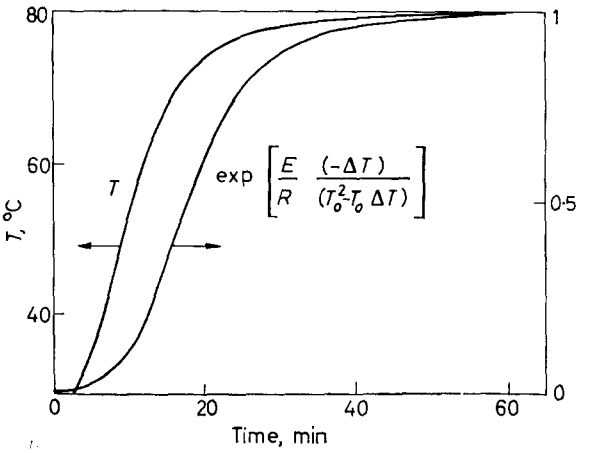

Figure 3.—Temperature versus time for the run: $P=1\,400$ atm, $[I]=2{\cdot}9\times10^{-6}$ mole/cm³, reaction time 4 h (not shown in *Figure 2*)

constant[12] and [M] and [I] independent of time we obtained a delay time of about 20 minutes, in good agreement with the extrapolated value.

The plots of polymer yield versus reaction time have been found to be linear up to about 30 per cent conversion. This behaviour has been reported by Merrett and Norrish[7] for peroxide-initiated polymerization at 60°C and by Gillham[13] for thermal polymerization of styrene at 100°C.

In the correlation $[\eta]$ versus r, shown in *Figure 4*, we chose for $[\eta]$ the value at 2 h reaction time. In this way the molecular weight should not be much affected by the higher molecular weight of the polymer formed during the preheating time. At the same time, the increase in the molecular weight noted at higher yield values should be negligible.

Table 2. Polymerization rate r and intrinsic viscosity $[\eta]$ as functions of pressure and initiator concentration [I]

P *atm*	$[M]\times10^3$ *mole/cm³*	$[I]\times10^5$ *mole/cm³*	$r\times10^7$ *mole/cm³. sec*	$[\eta]$ *100 cm³/g*	$10^4/\overline{P}$
740	8·619	0·279	2·01	1·33	3·94
1 400	8·946	—	0·51	2·88	1·37
1 400	8·946	0·029	1·13	2·70	1·50
1 400	8·946	0·290	3·48	1·83	2·56
1 400	8·946	0·580	4·85	1·43	3·56
2 650	9·330	—	1·94	3·03	1·28
2 650	9·330	0·030	2·82	2·79	1·43
2 650	9·330	0·182	5·71	2·47	1·73
2 650	9·330	0·303	7·14	2·40	1·77

The calculated values of r and [I] reported in *Table 2* were obtained by utilizing the $(\partial V/\partial P)$ data for styrene at 60°C[14]. We neglected the change in compressibility of styrene in the range 60° to 80°C, i.e. we considered $(\partial V/\partial P)_{60°C}\simeq(\partial V/\partial P)_{80°C}$.

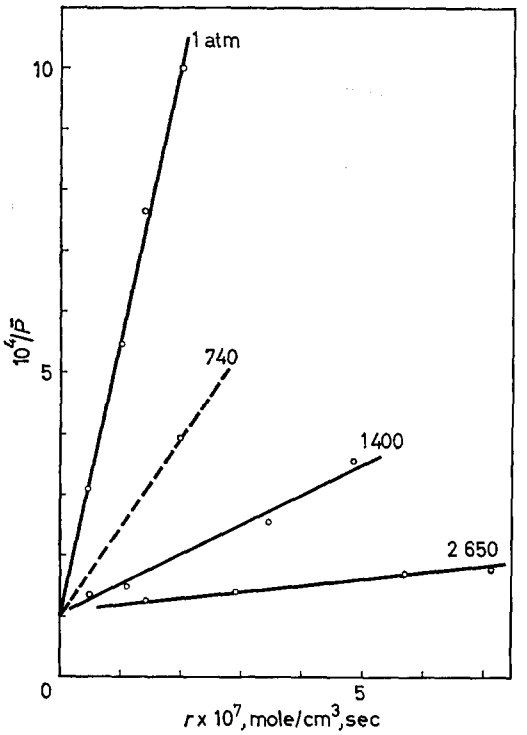

Figure 4—$1/\bar{P}$ versus r as a function of pressure at 80°C

DISCUSSION

Dependence of polymerization rate on initiator concentration

First of all we can calculate the constants of equation (2) from *Table 2*. Moreover, the exponent n of [I] can be obtained using the correlation

$$\log (r^2 - r_{pt}^2) = \text{constant} + 2n \log [\text{I}] \qquad (6)$$

The results are in *Table 3*, columns 2, 3, 4. It is evident that the pressure does not affect the dependence of the polymerization rate on [I], at least in the explored range of concentration.

Table 3. Pressure effect on rate constants

P *atm*	$(k_p^2 f\, kd/k_t) \times 10^4$ *cm³/mole. sec*	$r_{pt} \times 10^8$ *mole/cm³. sec*	n *eq. (6)*	k_t/k_p^2 *mole. sec/cm³*	$fk_d \times 10^5$ *1/sec*	$k_i \times 10^8$ *cm³/mole. sec*
1	0·85	1·27	0·48	0·297	2·5	1·1
740	1·9	2·7*	—	0·109	2·2	1·4
1 400	5·0	5·15	0·52	0·0385	1·9	1·6
2 650	18·0	19·0	0·51	0·0088	1·6	4·3

*Value interpolated according to equation (1') with ΔV_{pt}^{+} =const.

This result has been tested by application of equation (6) to the data of

Toohey and Weale[15] on styrene polymerization with benzoyl peroxide at 60°C. We found $n=0{\cdot}5\pm0{\cdot}02$ in the ranges: $[I]\leqslant 0{\cdot}35\times10^{-5}$ mole/cm^3 and $P\leqslant 4\,400$ atm. An analogous result came from the data of Merrett and Norrish[7] at 60°C, 2 910 atm and with $[I]\leqslant 1{\cdot}13\times10^{-5}$ mole/cm^3. At higher initiator concentrations, n tends to diminish. According to Merrett and Norrish this decrease should be related to a larger increase with pressure of transfer to initiator than that of termination by coupling. Toohey and Weale suggest that pressure should preferably accelerate the termination reaction with primary radicals from the initiator.

Nevertheless from our results this effect is not evident. It should become important only at high initiator concentrations. The plots of *Figure 4* test the absence of an appreciable termination by transfer to initiator, at least in the explored range of [I]. In fact, from the linearity of $1/\overline{P}$ versus r plots, we can argue that the last term of equation (4), due to transfer to initiator, is negligible.

Degree of polymerization

In *Figure 4* there is also evidence that the molecular weight of the polymer tends to become constant at pressures greater than 3 000 atm. The limiting value $1/\overline{P}$ is about 10^{-4} and corresponds to the transfer constant to monomer. This constant appears to be independent of pressure as would be expected from the similarity of the mechanisms involved in the propagation and the transfer-to-monomer reactions.

Nicholson and Norrish[6] showed that the decrease in slope of the $1/\overline{P}$ versus r plots with increasing pressure is due to the increase of viscosity of the medium. At high pressure the termination by coupling of radicals is diffusion controlled while the propagation still occurs in the kinetic region.

Polymerization rate

Analysis of the data in *Table 3* shows the different effects of pressure on the terms of the overall polymerization rate. At 2 650 atm the peroxide-initiated polymerization increases approximately fivefold while the thermal polymerization increases thirteenfold.

When the thermal polymerization term is neglected in equation (2), the 'apparent' exponent of [I] decreases with increasing pressure and $(\partial \ln k/\partial P)_T$ depends on [I].

The application of equation (1′) to the overall rate constants gives[16–19]:

$$\Delta V^{+}=\Delta V_{p}^{+}+\Delta V_{d}^{+}/2-\Delta V_{t}^{+}/2 \tag{7}$$

$$\Delta V_{pt}^{+}=\Delta V_{p}^{+}+\Delta V_{i}^{+}/2-\Delta V_{t}^{+}/2 \tag{8}$$

respectively for peroxide-initiated and thermal polymerization. Subscripts p, t, d, i, refer to propagation, termination, peroxide decomposition, thermal initiation respectively.

According to equations (7) and (8) the different effects of pressure on peroxide-initiated and thermal polymerization can be explained when considering the reactions which generate primary radicals in both cases. It is

understood that thermal initiation is due to a bi- or tri-molecular reaction among styrene molecules[20]. For reactions of this type we can expect an accelerating effect of pressure. On the other hand, the decomposition of benzoyl peroxide increases the number of molecules and a retarding effect of pressure is likely on this reaction[21–23].

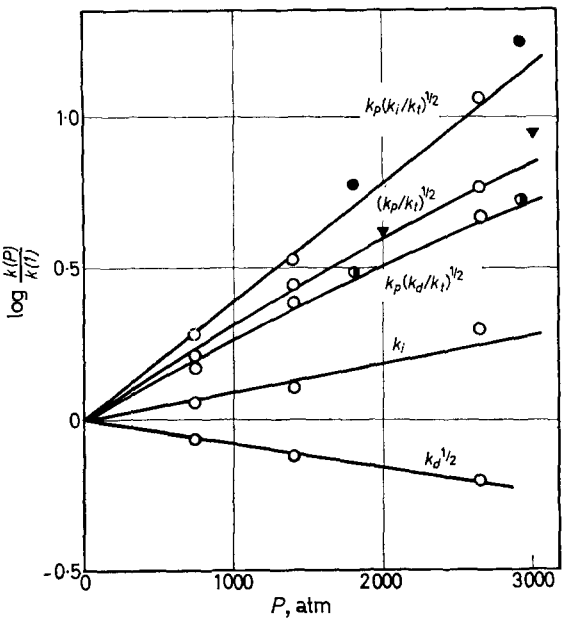

Figure 5—Rate constants for thermal and peroxide-initiated polymerization of styrene under pressure. ▼ Nicholson and Norrish's values[6] for $(k_p/k_t)^{\frac{1}{2}}$ at 30°C. ● ◑ Values of $k_p(k_i/k_t)^{\frac{1}{2}}$ and $k_p(k_d/k_t)^{\frac{1}{2}}$ respectively, as calculated from Toohey and Weale[15]

In *Figure 5* the rate constants for thermal and peroxide-initiated polymerization are plotted versus pressure. The overall constants have been calculated using equation (2) from the data of *Table 2*. The ratio $(k_p/k_t)^{\frac{1}{2}}$ is derived from the same data and equation (4). The k_d and k_i values plotted in *Figure 5* are also reported in the last columns of *Table 3*.

Toohey and Weale's[15] data shown in *Figure 5* have been obtained from their experimental values at 60°C by equation (2). The value of r_{pt} at 1 atm and 60°C is derived from our corresponding r_{pt} value at 80°C with $E = 21$ kcal/mole[12].

From *Table 3* and *Figure 5* the following activation volumes can be obtained:

thermal polymerization	$\Delta V_{pt}^{+} \simeq -25{\cdot}8$ cm³/mole
peroxide-initiated polymerization	$\Delta V^{+} \simeq -17$ cm³/mole
thermal initiation	$\Delta V_{i}^{+} \simeq -12{\cdot}6$ cm³/mole
peroxide decomposition	$\Delta V_{d}^{+} \simeq +5$ cm³/mole

The negative value of $\Delta V_i^{\ddagger}$ gives further evidence that the thermal initiation is a bi- or tri-molecular reaction.

Walling and Pellon's[23] value of ΔV_d^{+} is 4·8 cm³/mole for decomposition of benzoyl peroxide in acetophenone at 80°C, in good agreement with our value.

REMARKS

This work is of an introductory character to further research on styrene polymerization in a wider range of pressure; measurements are being carried out up to 40 000 atm. Some preliminary results regarding this research were presented at the 'Conférence Internationale sur les Hautes Pressions' held at Le Creusot, France, in August 1965[24].

This research is supported by C.N.R. (National Council for Research).

Istituto di Impianti Chimici,
Università di Padova, Via Marzolo, 9,
Padova, Italy

(*Received April 1966*)

REFERENCES

[1] BRIDGMAN, P. W. and CONANT, J. B. *Proc. nat. Acad. Sci., Wash.* 1929, **15,** 680
[2] MAYO, F. R., GREGG, R. A. and MATHESON, M. S. *J. Amer. chem. Soc.* 1951, **73,** 1691
[3] FLORY, P. J. *Principles of Polymer Chemistry,* p 138. Cornell University Press: Ithaca, New York, 1964
[4] KROMOLICKI, Z. *La Scuola in Azione,* Giugno, **1965,** 150
[5] GUARISE, G. B. *Ric. sci.* 1962, **32(II-A),** 172
[6] NICHOLSON, A. F. and NORRISH, R. G. W. *Disc. Faraday Soc.* 1956, **22,** 104
[7] MERRETT, F. M. and NORRISH, R. G. W. *Proc. Roy. Soc. A,* 1951, **206,** 309
[8] BLOUT, E. R. and MARK, H. *Monomers,* p 50. Interscience: New York, 1949
[9] BEVINGTON, J. C. and TOOLE, J. *J. Polym. Sci.* 1958, **28,** 413
[10] HAWARD, R. N. and SIMPSON, W. *Trans. Faraday Soc.* 1951, **47,** 212
[11] NOZAKI, K. and BARTLETT, P. D. *J. Amer. chem. Soc.* 1946, **69,** 2299
[12] FLORY, P. J. *Principles of Polymer Chemistry,* pp 124 and 132. Cornell University Press: Ithaca, New York, 1964
[13] GILLHAM, R. C. *Trans. Faraday Soc.* 1950, **46,** 497
[14] WEALE, K. E. Private communication
[15] TOOHEY, A. C. and WEALE, K. E. *Trans. Faraday Soc.* 1962, **58,** 2446
[16] GONIKBERG, M. G. *Chemical Equilibria and Reaction Rates at High Pressures,* p 95. I.P.S.T.: Jerusalem, 1963
[17] LAMB, J. E. and WEALE, K. E. *The Physics and Chemistry of High Pressures,* p 229. Society of Chemical Industry: London, 1963
[18] WEALE, K. E. *La Scuola in Azione,* Dicembre **1962,** 133
[19] WALLING, C. and PELLON, J. *J. Amer. chem. Soc.* 1957, **79,** 4776
[20] MAYO, F. R. *J. Amer. chem. Soc.* 1953, **75,** 6133
[21] EWALD, A. H. *Disc. Faraday Soc.* 1956, **22,** 138
[22] NICHOLSON, A. E. and NORRISH, R. G. W. *Disc. Faraday Soc.* 1956, **22,** 97
[23] WALLING, C. and PELLON, J. *J. Amer. chem. Soc.* 1957, **79,** 4786
[24] GUARISE, G. B. *Chim. e Industr.* 1965, **47,** 1262

Ageing Effects in Measurements of Polyacrylamide Solution Viscosities

N. NARKIS and M. REBHUN

A number of effects of solution age on viscosity were investigated. Viscosity and [η] of polyacrylamide solutions decreased with time to a constant value. Maintaining a high temperature did not shorten the time needed to reach the limiting viscosity values. It seems that this ageing effect cannot be attributed to degradation effects, but is instead related to disentanglement of the polymer molecules.

It thus appears that suitable standard conditions should be found for preparation of polyacrylamide solutions. These conditions should also be applied to determinations of $[\eta]=kM^a$, *so that consistent results can be found by various investigators.*

AS PART of an investigation of polyacrylamide molecular weights, viscosity was found to decrease with age for a given initial solution. This effect can result in a dependence of $[\eta]$ on the age of the test solution. Since, however, the molecular weight of the polymer is given by a unique value of $[\eta]$, an attempt was made to find an experimental technique to determine the true value.

Anomalous viscosity changes noted in tests of polymer solution viscosity with the aid of a capillary viscometer have been explained as being caused by adsorption on the capillary walls[1].

A decrease in the viscosity of a polymer solution on standing does not necessarily indicate degradation. The polymer molecules can be twisted internally or the molecules can become entangled during formation and growth of the polymer. The number of entanglements can increase because of complications of the macromolecules as a result of motion of segments. This motion can also be the cause of disentanglement and separation of the chains in dilute solutions. If tests of the intrinsic viscosity of the solutions show that $[\eta]$ remains constant, it is evident that the molecular configuration and not molecular weight has changed.

Since the chain entanglements are a function of the size and number of molecules in solution, the molecular weight and concentration of the dissolved polymer are important factors[2]. As the molecular weight increases, there is increasing probability of a large number of entanglements for the length of the chain[3]. In addition, as the concentration increases, the number of chains in a given volume increases, and the chances become greater for molecules to become entangled in loops of other molecules. The degree of entanglement in the solid or liquid state is larger than for dilute solutions[4].

A number of investigators[5-7] have shown that high shear rates cause disentanglement of polymer chains, either in solution or as liquids resulting in viscosity decrease.

The entanglement effect may be influenced by temperature, concentration,

shear rate and age. This article discusses the effects of solution age and polymer concentration on measured viscosity for solutions of certain polymers.

EXPERIMENTAL

Two polymers were used, both manufactured by the American Cyanamid Corporation; Cyanamer P-26, polyacrylamide (molecular weight $2{\cdot}24 \times 10^5$), Cyanamer P-250, polyacrylamide (molecular weight $1{\cdot}95 \times 10^6$).

The molecular weights given above were calculated using the equation[8] $[\eta] = 3{\cdot}73 \times 10^{-4} M^{0{\cdot}66}$, in normal sodium nitrate solution at $30^\circ \pm 0{\cdot}02^\circ$C as recommended by the manufacturer.

Each polymer sample was dissolved at room temperature in a 0·5 litre calibrated flask, by gentle shaking at regular intervals. (Mechanical stirring was avoided to prevent mechanical degradation of the polymer.) The effect of solution age on viscosity at various concentrations and on $[\eta]$ was checked by removing samples every few days. The viscosity of each sample was measured at 30°C, after which the sample was diluted in the viscometer for measurements as a function of concentration.

After being stored for 57 days, the polymer was precipitated by addition of acetone. The sample was redissolved in distilled water to remove traces of sodium nitrate, and precipitated again by use of acetone. Each sample was finally dried in a vacuum oven at 40°C for 24 hours and dissolved in normal sodium nitrate solution. After three days ageing time, $[\eta]$ was again measured.

Additional tests were performed on a solution of Cyanamer P-250 in normal sodium nitrate with solution preparation and ageing at a temperature of 55°C, under a nitrogen atmosphere to avoid oxidation. At various times, samples of this solution were removed and cooled to room temperature. The values of $[\eta]$ at 30°C were then determined.

ANALYSIS OF RESULTS

Viscosity measurements as a basis for determining polymer molecular weights, discussed in the introduction, will be considered first. *Figure 1* shows graphs of η_{sp}/c against c for Cyanamer P-250, with each line representing a different solution age. The rate of change of η_{sp}/c with time was greatest for the initial high concentrations, this rate decreasing for more dilute samples. After nine days storage at low concentrations there were no significant differences between corresponding values of η_{sp}/c. Similar values of $[\eta]$ were evident after nine days storage.

As the solutions aged from three to fifteen days, the value of $[\eta]$ decreased from 5·65 to 5·25, a difference of about eight per cent. Since molecular weight is proportional to $[\eta]^{1/0{\cdot}66}$, the corresponding error in molecular weight is 12 per cent. The results could be caused by degradation or disentanglement of the dissolved polymer.

The possibility of degradation was checked by precipitating the polymer, as explained above, and measuring $[\eta]$ again after ageing the new solution for three days. The experimental value of 5·6 was in excellent agreement with that obtained after ageing the initial solution for three days, thus showing that degradation had not taken place.

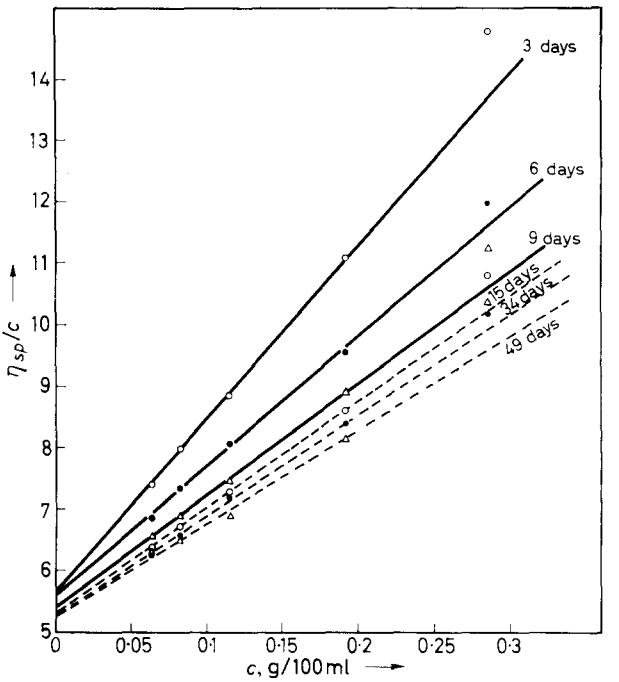

Figure 1—Reduced viscosity η_{sp}/c of Cyanamer P-250 in sodium nitrate solution for different storage periods at room temperature

According to the results reported, at least fifteeen days were required to achieve constant viscosity values. It was decided to check the effect on experimental viscosity values of high-temperature preparation and ageing of the polymer solution. Such an approach seemed reasonable in that heating is often used to speed polymer solution for viscosity measurements. *Figure 2* shows graphs of η_{ps}/c against c, with solution age at 55°C as parameter. Unexpectedly, maintaining a high temperature did not shorten the time needed to attain constant viscosity values. The final value of $[\eta]$ for this case was reached after at least 24 days of high-temperature storage. This final constant value was equal to that found for room-temperature ageing. The decrease in $[\eta]$ for this case as the solution aged between three and 24 days was from 6·37 to 5·20. Thus the observable difference amounts to about 22·5 per cent of the value of $[\eta]$, or about 38 per cent of the true molecular weight value. It should be stressed that the value of $[\eta]$ after three days was higher for high-temperature storage than for room-temperature storage.

An additional interesting effect in the high-temperature ageing of Cyanamer P-250 should be noted. The values of η_{sp}/c for the initial high-concentration solution were above the lines shown in *Figure 2*, especially for long storage times. The high values of η_{sp}/c are not plotted in *Figure 2*, but are given in *Table 1*.

As is evident from *Figure 2*, after the first dilution to 0·19 g/100 ml,

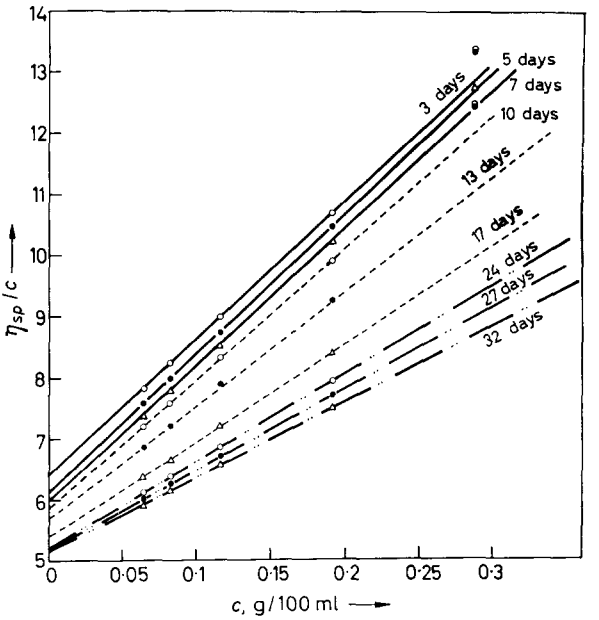

Figure 2—Reduced viscosity η_{sp}/c of Cyanamer P-250 in sodium nitrate solution for different storage periods at 55°C

the measured viscosity values corresponded to the straight lines in the figure. Since this increase was observed only for high-temperature ageing, we consider that this effect was caused by very weak intermolecular reactions due to the increased thermal activity. These interactions disappeared immediately after the first dilution.

Table 1. Comparison of experimental values of η_{sp}/c for initial high temperature Cyanamer P-250 solution and corresponding η_{sp}/c values from *Figure 2*. Concentration throughout 0·284 g/100 ml

Storage time at 55°C, days	η_{sp}/c *measured at 30°C*	η_{sp}/c *from Figure 2*	*Storage time at 55°C, days*	η_{sp}/c *measured at 30°C*	η_{sp}/c *from Figure 2*
3	13·3	12·85	17	17·6	9·97
5	13·35	12·70	24	29·1	9·35
7	12·8	12·45	27	31·1	8·98
10	12·5	12·00	32	33·2	8·68
13	12·5	11·07			

To test the assumption that the causes for the effects discussed would be important only for polymers of high molecular weights, additional tests were performed with Cyanamer P-26, with molecular weight $2{\cdot}24 \times 10^5$. As expected, the variation of viscosity with solution age for various concentrations was very small. Since the small differences would be difficult to demonstrate graphically, the results are presented in *Table 2*.

Table 2. Values of η_{sp}/c for solution of Cyanamer P-26 as a function of concentration and solution age

Concentration g/100 ml	η_{sp}/c *values after, days*					η_{sp}/c *values after precipitating and redissolving during three days*
	3	*9*	*15*	*37*	*57*	
0·804	2·32	2·16	2·16	2·14	2·14	2·49
0·536	1·94	1·865	1·865	1·85	1·85	2·15
0·402	1·805	1·715	1·72	1·73	1·72	2·02
0·321	1·69	1·62	1·65	1·66	1·62	1·90
0·229	1·53	1·515	1·52	1·52	1·53	1·77
0·178	1·47	1·47	1·44	1·43	1·44	1·67
$[\eta]$	1·262	1·262	1·260	1·250	1·262	1·47

For Cyanamer P-26, the viscosity values after three days storage were slightly higher than the other values in *Table 2*. For longer storage times, the viscosity values were for all practical purposes equal. The values of $[\eta]$ were equal for all measurements. *Table 2* also shows the results of measurements after precipitating and redissolving the polymer, as was done with the other solutions. The values obtained were higher than the initial values, evidently because of partial fractionation during precipitation, due to the relatively low molecular weight of the polymer.

The effect of solution age on measured values of viscosity and $[\eta]$ is to be explained not by degradation but probably by disentanglement of the polymer molecules, which is an integral part of the formation of a true polymer solution.

The change in configuration can be explained by the mechanism of entanglement formation during the original polymer growth. During preparation of a polymer solution, solvent molecules diffuse into the polymer chains and separate them. The separation is hindered by entanglements and by secondary chemical forces, such as strong hydrogen bonds in polyacrylamides. Thermal motion of segments of the molecule chains aids disentanglement. However, for a concentrated solution the free end of the molecule can undergo re-entanglement with a nearby molecule. Increasing the solvent cencentration can increase the chances for disentanglement. For such dilute solutions, a polymer chain that has succeeded in freeing itself from entanglements can move into the solvent without becoming entangled with another molecule.

Time is needed to achieve equilibrium between entanglement and disentanglement. The necessary time will increase with polyacrylamide size, since for higher molecular weights there are more entanglements that have to be freed for the chain length.

Entangled molecules increase the solution viscosity. Once equilibrium is reached, depending on concentration, the value of viscosity remains constant. Faster equilibrium is aided by decreasing concentration and molecular weight.

It has thus been shown that in testing polyacrylamide properties which

depend on viscosity measurements suitable standard conditions for preparation of solutions must be set in order to obtain reliable viscosity values. Heating does not shorten the time necessary for stabilizing the solution viscosity and in some cases can lead to mistaken values of $[\eta]$. In determination of the value of $[\eta]=kM^a$, it will be necessary to prepare the solutions according to these standard requirements so that the equation will correspond for the work of various investigators. If these precautions are not taken, large errors in measured values of molecular weight may result.

This work was partly supported by the U.S. Department of Agriculture, Grant No. FG-Is-148.

Technion—Israel Institute of Technology,
Sanitary Engineering Laboratories,
Haifa, Israel

(Received April 1966)

REFERENCES

[1] PATAT, F., KILLMANN, E. and SCHLIEBENER, C. *Fortschr. Hochpolym. Forsch.* 1964, **3,** 332
[2] CHINAI, S. N. and SCHNEIDER, W. C. *J. Polym. Sci. A,* 1965, **3,** 1359
[3] BUECHE, F. *Physical Properties of Polymers.* Interscience: New York, 1962
[4] GILLESPIE, T. *J. Polym. Sci. C,* 1965, **3,** 31
[5] LOHMANDER, U. and STRÖMBERG, R. *Makromol. Chem.* 1964, **72,** 143
[6] PORTER, R. S. and JOHNSON, J. F. *Trans. Soc. Rheol.* 1963, **7,** 241
[7] PORTER, R. S. and JOHNSON, J. F. *Polymer, Lond.* 1962, **3,** 11
[8] SORENSON, W. R. and CAMPBELL, T. W. *Preparative Methods of Polymer Chemistry.* Interscience: New York, 1961

The Temperature Dependence of Polymer Chain Dimensions and Second Virial Coefficients

G. DELMAS* and D. PATTERSON*

[η] and, using light scattering, $\langle S^2\rangle^{\frac{1}{2}}$ and A_2 have been measured from −15° to 76°C for polyisobutylene($\overline{M}_w = 9\times10^6$)–n-pentane (I), and from 0° to 140°C for PIB–dibutyl ether (II). For the exothermic mixture (I), these quantities decrease with increase of T, [η] and $\langle S^2\rangle^{\frac{1}{2}}$ attaining 'unperturbed' values, and A_2 becoming zero, at a θ-point, equal for this high molecular weight to the Lower Critical Solution Temperature (LCST). For (II), endothermic at room temperature, the quantities first pass through a maximum before decreasing. (The LCST at 204°C was not attained.) A maximum was observed in the swelling ratio of crosslinked polystyrene in cyclohexane as T passes from the Upper Critical Solution Temperature (UCST) of 34°C to the LCST of 210°C. For (I), χ_1 is not linear in 1/T in the region of the LCST. The observed temperature dependences of A_2 and the polymer dimensions are qualitatively predicted by the Prigogine theory of polymer solutions, which gives a new $\chi_1(T)$ dependence.

THE temperature dependence of the chain expansion factor, α, and of the second virial coefficient, A_2, arises almost entirely through the effect on the long-range interactions which are characterized by the parameter B in[1]

$$z = 0{\cdot}330\, A^{-3} B M^{\frac{1}{2}} \tag{1}$$

Here

$$A \equiv (\langle L_0^2\rangle / M)^{\frac{1}{2}} \tag{2}$$

and B is usually evaluated[2] by comparison with the Flory–Huggins theory and/or the theory of strictly regular solutions. Thus

$$B = 2\,(\tfrac{1}{2} - \chi_1)/V_1\rho^2 N \tag{3}$$

where V_1 is the solvent molar volume and ρ the polymer density. Equation (3) does not depend on a particular choice of the size of a polymer or solvent segment; however, the binary cluster integral given by $\beta = B/m_s^2$ depends on m_s the mass of the chosen chain element. If χ_1 has the well-known temperature dependence assumed by the Flory theory, then

$$B = B_0(1 - \theta/T);\quad B_0 = 2\psi_1/V_1\rho^2 N \tag{4}$$

The existence of *two* critical solution temperatures in polymer solutions shows that this form of ψ_1 cannot be general, and hence departures from equation (4) must be expected. According to the Prigogine theory of polymer solutions[3], χ_1 is given[4] by

$$\chi_1 = -(U/RT)\,\nu^2 + (C_p/2R)\,\tau^2 \tag{5}$$

*Present address: Department of Chemistry, McGill University, Montreal, Canada.

where U and C_p are the configurational energy and heat capacity of the solvent and ν and τ are molecular parameters. The first and second terms of χ_1 are positive and respectively decrease and increase with T, C_p going to infinity as the temperature approaches the vapour–liquid critical point. Thus χ_1 passes through a minimum as implied by the existence of the two critical solution temperatures. χ_1 decreases to $\frac{1}{2}$ as T rises to the θ-point, equal for infinite molecular weight to the Upper Critical Solution Temperature (UCST). Then it attains the minimum, B, α and A_2 being at their maximum values, and finally χ_1 increases to $\frac{1}{2}$, B becomes zero, and a second θ-point occurs, which, for infinite molecular weight coincides with the Lower Critical Solution Temperature (LCST). From the thermodynamics of critical points $\Delta\overline{H}_1$, $\Delta\overline{S}_1$ and Ψ_1 are positive at the UCST, but must have changed sign at the LCST. The inadequacy of equation (4) should thus appear as a decrease and change of sign of B_0.

The success of equation (4) over relatively wide temperature intervals above the θ-point seems to be due to the fact that the LCST usually lies above the boiling point of the solvent. However, a decrease of B_0 with temperature has in fact been found for polystyrene–decalin[5]. A minimum in $[\eta]$ versus T has been seen for certain systems[6], and an explanation was given in terms of a temperature dependence of A. This effect, and that of a possible transition[7] in the polymer chain should be rather small compared with that of the failure of equation (4) at temperatures approaching the LCST.

In the following, we study the temperature dependence of $[\eta]$, $\langle S^2\rangle^{\frac{1}{2}}$ and A_2, first in a system where the minimum of χ_1 lies below ordinary temperatures, so that the above quantities decrease monotonically with increase of T, and secondly, in an example of the more usual kind where the minimum of χ_1 lies above room temperature and the quantities pass through a maximum.

We also give, for a qualitative comparison, results on the swelling of crosslinked polystyrene in cyclohexane from the UCST at 34°C to the LCST at 210°C and beyond.

EXPERIMENTAL AND RESULTS

The systems chosen were: (I), polyisobutylene (PIB)–*n*-pentane, and (II), PIB–dibutyl ether. The first system has a negative value[8, 9a] of ΔH_M at room temperature and the LCST (see below and ref. 9a) for infinite molecular weight is only 76°. The second system has a small positive value[10] of ΔH_M at 25° and an LCST (see below) of 204° for infinite molecular weight which suggests that the minimum of χ_1 might be accessible, the boiling point being 142°.

Materials

The PIB, part of a generous gift from Enjay Inc., was twice fractionated. The $\overline{M}_w$ of the fraction used was determined by light scattering to be $9 \pm 1 \times 10^6$. $[\eta]_\theta$ in benzene at 24·5°C was found to be 3·2 dl/g, whence,

using compiled[1] values of K' and a, $\overline{M}_v = 9{\cdot}0 \times 10^6$. A light scattering determination[11] gave $\overline{M}_w/\overline{M}_n = 1{\cdot}3$. Gel permeation chromatography gave a value of 1·1 which is, however, too low since the largest molecules of this very high molecular weight fraction do not permeate the gel and pass with essentially the same retention time. $\overline{M}_w/\overline{M}_n = 1{\cdot}3$ is probably a fair estimate.

The pentane and dibutyl ether were reagent grade, dried and distilled. Swelling measurements were made with spherical beads of commercial Rohm and Hass emulsion polymerized polystyrene containing eight per cent divinylbenzene. The cyclohexane was spectrograde.

LCST

The LCST of systems (I) and (II) and of polystyrene–cyclohexane were measured as indicated elsewhere[4b,12]. Extrapolation of data on lower molecular weight fractions through that of $\overline{M}_w = 9 \times 10^6$ gives for infinite molecular weight: PIB–pentane, 76°; PIB–dibutyl ether, 204°. The first value compares with that of ref. 9a for a molecular weight of 2×10^6. A similar procedure with three fractions of anionically prepared polystyrene gave a LCST of 210° for the infinite molecular weight, as compared with a reported[9b] value of 180°. The shapes of the coexistence curves were also somewhat different from those given[9b] for polystyrene–cyclopentane, the minimum occurring around three per cent rather than at 10 to 20 per cent. Our experiments were done in sealed tubes, hence at the equilibrium vapour pressure, whereas the LCST result of ref. 9b is for zero pressure, but the difference still seems difficult to explain.

Viscosities

Sealed viscometers of Ubbelohde type and having negligible kinetic energy corrections were used. The solutions were thoroughly degassed to avoid degradation of the polymer at high temperature. After the measurement at the highest temperature, 140° in dibutyl ether, $[\eta]$ at 25° had decreased by three per cent. This variation, however, is very small compared with the temperature variation of $[\eta]$ and the use of an antioxidant was deemed unnecessary. The correction for finite shear rate[12] was found to be one per cent of $[\eta]_{sp}$ and was neglected. The results are shown in *Figures 1* and *2*.

Swelling measurements

The polystyrene beads were first leached and equilibrated with cyclohexane over several days, then placed in a cell, essentially a Teflon ring clamped between two glass windows, the mass of metal around the Teflon being large so as to provide a uniform temperature around the solution. The cell was wrapped in a resistance heater, the temperature of solution being read by a thermocouple calibrated by the melting points of standard substances placed in the cell. The dimensions of the beads were observed with a microscope of low magnifying power fitted with a Leitz screw micrometer; they were found to be accurately spherical and the volume was taken proportional to the (diameter)^3. Due to their small diameter, the beads came to equilibrium at any temperature within an hour. *Figure 3*

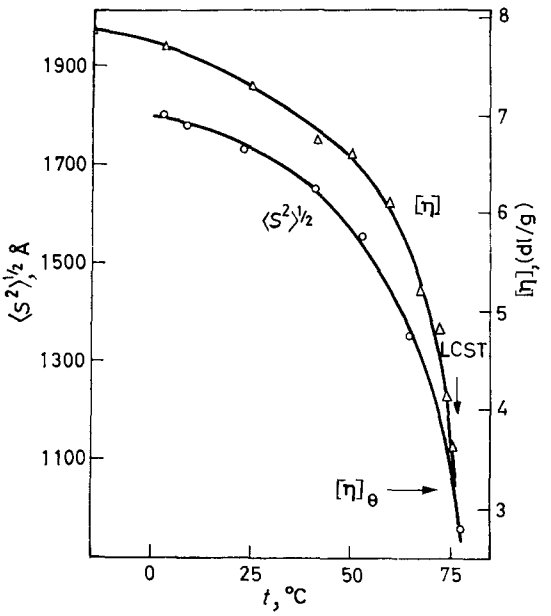

Figure 1—PIB–pentane: radius of gyration, and intrinsic viscosity versus temperature

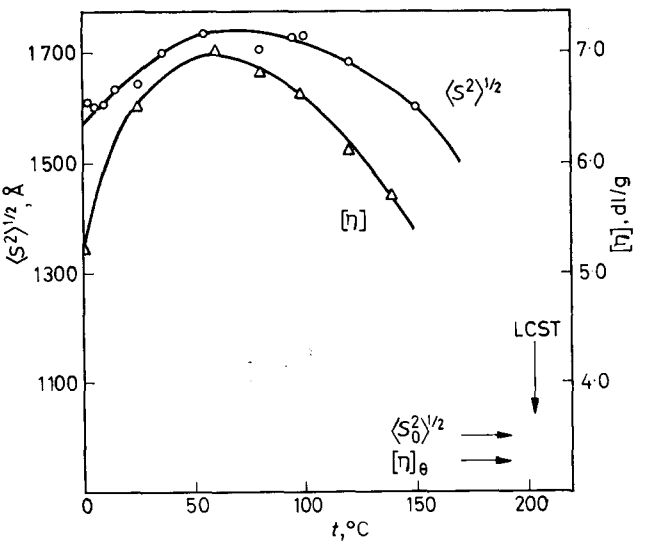

Figure 2—PIB–dibutyl ether: radius of gyration and intrinsic viscosity versus temperature

presents the temperature dependence of the swelling ratio, q, i.e. the swollen volume/dry volume. (In fact the dry volume was not measured as a function of T, but use was made of the fact that the thermal expansion coefficient of these networks is very close to that of the uncrosslinked polymer[13], which is known[13, 14].)

Light scattering

Refractive index measurements—We used a differential Brice–Phoenix refractometer equipped with a heating system for a cell which had been calibrated previously[15]. For the PIB–dibutyl ether system, we measured dn/dc at roughly 15 deg. intervals up to 120°. dn/dc varies linearly between 0·124 and 0·167 going from 22·5° to 120°. Using the formula

$$dn/dc = (n^P - n^S)/\rho^P \tag{6}$$

we find $dn/dc = 0{\cdot}128$ at 22·5° with $\rho^P = 0{\cdot}92$ and $n^P = 1{\cdot}515$. n^P was estimated by extrapolating the measured refractive indices of lower molecular weights. Using equation (6), leaving n^P independent of T, but taking into account the temperature variation[16] of n^S and [14] ρ^P we calculated $dn/dc = 0{\cdot}166$ at 120°. As good agreement exists at other temperatures than 22·5° and 120°, we use equation (6) to calculate dn/dc for the PIB–pentane system where measurements above the boiling point (36°) were inconvenient.

Calibration at different temperatures—The instruments used below 25° and between 25° and 140° were both of Sofica type[15]. A benzene standard was used for temperatures below 110°.

The variation of the Rayleigh ratio, R_B, with temperature is given by

$$\frac{R_B^t}{R_B^{25}} = \frac{I_B^t}{I_B^{25}} \left(\frac{n_B^t}{n_B^{25}} \right)^2 \tag{7}$$

where n_B and I_B are, respectively, the refractive index and the scattered intensity for benzene at a 90° angle. The relation between concentration and scattered intensity is[15]

$$\frac{2\pi^2 (n_B^t)^2}{\lambda^4 N R_B^t} \left(\frac{dn}{dc} \right)^2 \left(\frac{c}{I} \right) I_{B\ \theta=0\ c\to 0}^t = \frac{1}{\overline{M}_w} + 2A_2 c \tag{8}$$

Equation (8) substituted in equation (7) gives

$$\frac{2\pi^2 (n_B^{25})^2}{\lambda^4 N R_B^{25}} I_B^{25} \left(\frac{dn}{dc} \right)^2 \left(\frac{c}{I} \right)_{\substack{\theta=0 \\ c\to 0}} = \frac{1}{\overline{M}_w} + 2A_2 c$$

or

$$0{\cdot}506\, I_B^{25} \left(\frac{dn}{dc} \right)^2 \left(\frac{c}{I} \right)_{\substack{\theta=0 \\ c\to 0}} = \frac{1}{\overline{M}_w} + 2A_2 c \tag{9}$$

Equation (9) is valid for any temperature if I_B^{25} is kept constant (= 10 here) and the apparatus is set to give, for benzene at t°, a reading I_B^t given by equation (7). ($R_B = 16{\cdot}3 \times 10^{-6}$ at 25°, $\lambda = 5\,460$ Å.)

For temperatures above 110° a decalin standard (mixture of *cis* and *trans* isomers) was used in a similar fashion.

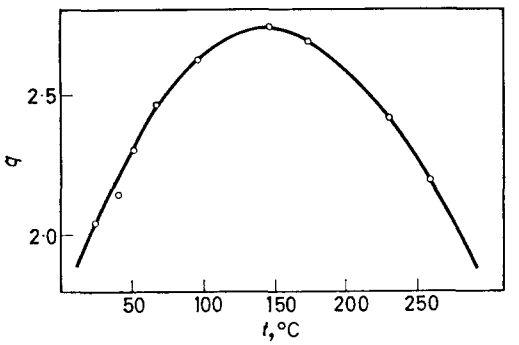

Figure 3—Crosslinked PS–cyclohexane: swelling ratio q versus temperature

Radius of gyration measurements—Instead of calculating $\langle S^2\rangle^{\frac{1}{2}}$ by the formula

$$\langle S^2\rangle^{\frac{1}{2}} = \frac{\lambda\sqrt{3}}{4\pi n}\left[\text{slope}\,\frac{c}{I}\,(\sin^2\tfrac{1}{2}\theta)\Big/\left(\frac{c}{I}\right)_{\substack{\theta=0\\c=0}}\right]^{\frac{1}{2}} \tag{10}$$

we have used the equivalent relation

$$\langle S^2\rangle^{\frac{1}{2}} = \frac{\lambda\sqrt{3}}{4\pi}\,(0{\cdot}506\overline{M}_w I_B^{25})^{\frac{1}{2}}\,\frac{\mathrm{d}n/\mathrm{d}c}{n}\left(\text{slope}\,\frac{c}{I}\right)^{\frac{1}{2}} \tag{11}$$

This choice was made because the value $(c/I)_{\theta=0}$ is very small and can bring about a large relative error in $\langle S^2\rangle^{\frac{1}{2}}$. However, since $P^{-1}(\theta)$ is a straight line as plotted against $\sin^2\frac{1}{2}\theta$, the slope is identified with the extreme difference of c/I giving better accuracy. This quantity diminishes considerably with temperature but is compensated in equation (11) by the rapid increase of $(\mathrm{d}n/\mathrm{d}c)/n$.

Figure 4 gives the Zimm plot for PIB–pentane at 77·5°. As the solution is very dilute, no phase separation has occurred, but A_2 is negative since the temperature is above the θ-point associated with the LCST.

Figures 1 and *2* show the variation of $\langle S^2\rangle^{\frac{1}{2}}$ with temperature for the

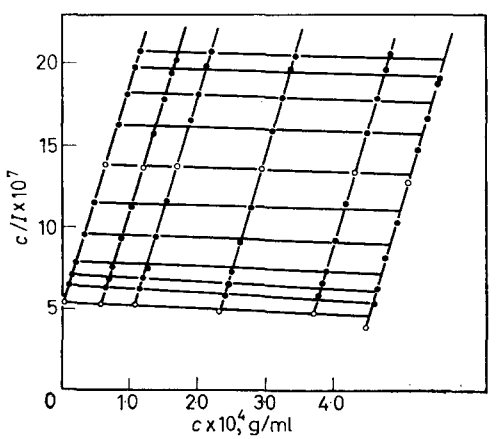

Figure 4—PIB–pentane: Zimm plot at 77·5°C, i.e. above the LCST

two systems and *Figure 5* the variation of A_2 as determined from the light scattering measurements.

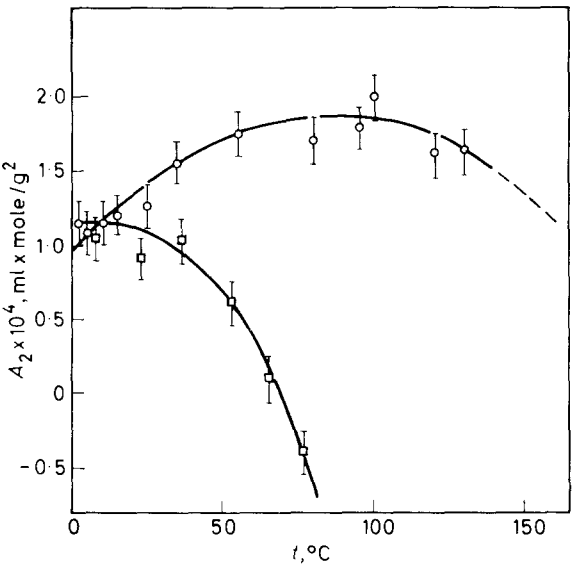

Figure 5—Virial coefficient as determined by light scattering versus temperature. ○, PIB–butyl ether; □ PIB–pentane

We have also obtained values of $\langle S^2\rangle^{\frac{1}{2}}$ using another method which does not require a knowledge of dn/dc, M or the temperature variation of the Rayleigh ratio of benzene [equation (7)]. Putting

$$0{\cdot}506\, I_B^{25}\left(\frac{dn}{dc}\right)^2 \frac{c}{I_\theta} = \frac{1}{M_w}\left[1 + \frac{1}{3}\langle S^2\rangle \frac{16^2}{(\lambda/n)^2}\sin^2\tfrac{1}{2}\theta\right]$$

and taking natural logarithms one sees that at a fixed concentration, $\langle S^2\rangle^{\frac{1}{2}}$ is given by the slope of ln I_θ with $\sin^2\frac{1}{2}\theta$ for $\theta \longrightarrow 0$. ln I_θ versus $\sin^2\frac{1}{2}\theta$ is not a straight line and only the first few angles may be used to determine the limiting slope; one extrapolates to zero concentration. For PIB–pentane, $\langle S^2\rangle^{\frac{1}{2}}$ at the LCST is found to be 950 Å in agreement with the 1 000 Å found by the other method. The values of $\langle S^2\rangle^{\frac{1}{2}}$ near room temperature are 20 per cent lower than found before. $\langle S^2\rangle^{\frac{1}{2}}$ for PIB–dibutyl ether presents a maximum at the same temperature as previously, but the values are $\simeq$ 20 per cent lower. It may be that due to the excluded volume effect far from the θ-point, $P^{-1}(\theta)$ should be taken proportional[17] to $(\sin^2\frac{1}{2}\theta)^\epsilon$ where $\epsilon \simeq 0{\cdot}8$.

Precision and accuracy—Different measurements of $[\eta]$ reproduced the same value to within ± 1 to 2 per cent. For $\langle S^2\rangle^{\frac{1}{2}}$ the slope of $(c/I)^{\frac{1}{2}}$ versus $\sin^2\frac{1}{2}\theta$ at zero concentration could be obtained to one per cent and $(dn/dc)/n$ was of comparable accuracy. Following equation (11) the same value of M_w, judged accurate to ± 10 per cent, was taken at each tempera-

ture. Thus the precision of the curve of $\langle S^2\rangle^{\frac{1}{2}}$ versus T should be ± 2 per cent but the accuracy possibly only $\simeq 15$ per cent or ± 250 Å; taking into account the lower values one gets using only the small angles (logarithmic method), the accuracy can be only 20 per cent far from the LCST. Using the usual equation (10) the scatter is much greater than when using equation (11), being $\simeq 60$ Å. The position of the maximum of $\langle S^2\rangle^{\frac{1}{2}}$ versus T for the PIB–dibutyl ether system is very sensitive to the value of the slope of $(c/I)^{\frac{1}{2}}$ and of $(\mathrm{d}n/\mathrm{d}c)/n$ which vary in opposite directions with change of T. The fair agreement between the positions of the maxima of $[\eta]$ and of $\langle S^2\rangle^{\frac{1}{2}}$ indicates that the present procedure is adequate. The precision of A_2 is $\pm 0{\cdot}15 \times 10^{-4}$ as shown in *Figure 5* and the accuracy is thought to be of the same order.

DISCUSSION

Intrinsic viscosities

For PIB–pentane, $[\eta]$ decreases with increasing rapidity as the temperature approaches the LCST at 76°. This is in accord[8] with the exothermic ΔH_M for high molecular weight PIB at 25° and with the prediction that the heat becomes more exothermic as the temperature increases. (An UCST has been reported[9a] for very low molecular weight (2 000) PIB–pentane at $\simeq -40°$. Here for a very high molecular weight $\mathrm{d}[\eta]/\mathrm{d}T$ is still negative at $-15°$.) In their original treatment of intrinsic viscosities, Fox and Flory[18] observed a decrease of $[\eta]$ with T for PIB–heptane. Since ΔH_M for this system is considerably less exothermic[8], the decrease of $[\eta]$ is much less apparent. This decrease was explained by a negative temperature coefficient of the parameter A, and by putting $\theta = 0°\mathrm{K}$.

A precise determination of $[\eta]$ at the LCST is difficult due to its rapid variation with T, but it is clearly of the same order as in benzene at 25°, 3·2 dl/g, showing that the polymer has attained unperturbed dimensions at this second θ-point (provided L_0 does not change drastically with temperature).

$[\eta]$ for PIB–dibutyl ether passes through a maximum as expected for a system having a positive ΔH_M at 25° as described above. There seems to be no reason to doubt that $[\eta]$ would fall to the value for a θ-solvent at 204°, the observed LCST for infinite molecular weight.

In the same way, the dimensions of the polystyrene gel swollen by cyclohexane attain a maximum at a temperature between the UCST and the LCST.

Radius of gyration

The picture presented by $\langle S^2\rangle^{\frac{1}{2}}$ is similar. For PIB–pentane, at 76° $\langle S_0^2\rangle^{\frac{1}{2}} \simeq 1\,000$ Å. Using[1] $(\langle L_0^2\rangle/M)^{\frac{1}{2}} = 7{\cdot}4 \times 10^{-9}$ cm/g$^{\frac{1}{2}}$ found at 91°, one calculates $\langle S_0^2\rangle^{\frac{1}{2}} = 940$ Å. This value would, however, be increased by about ten per cent assuming the molecular weight distribution to be characterized by $h \sim 3$. (The above value of $(\langle L_0^2\rangle/M)^{\frac{1}{2}}$ was calculated with the theoretical Kirkwood–Riseman value of $\Phi = 2{\cdot}87 \times 10^{21}$). It seems evident that $\langle S^2\rangle^{\frac{1}{2}}$ has attained its unperturbed value at the θ-point associated with the LCST.

$\langle S^2\rangle^{\frac{1}{2}}$ for PIB–dibutyl ether confirms the temperature variation of $[\eta]$.

We conclude that the θ-point at the LCST, like that at the UCST, confers unperturbed dimensions on the polymer, and that the chain statistics are the same at the two θ-points. This property might be of interest in studying polymers which are crystalline at ordinary temperatures. At both θ-points the tendency of the excluded volume between segments to expand the coil is balanced by an interaction with the solvent. At the UCST this is the positive heat of mixing with the solvent, while at the LCST it is a negative non-combinatorial entropy of mixing caused by a negative volume of mixing. It seems noteworthy that the chain statistics are the same in spite of the different thermodynamic origins of the θ-points.

In agreement with this, A_2 falls to zero at 76°for PIB–pentane, and that of system (II) appears to pass through a maximum (*Figure 5*).

Temperature dependence of B

Various theories are available for obtaining α, B and z from intrinsic viscosity results. The qualitative picture of $B(T)$ is not affected by the choice. We have calculated values of α for PIB–pentane from the relation[1]

$$\alpha^{2\cdot43} = \alpha_\eta^3 = [\eta]/[\eta]_\theta \tag{12}$$

using $[\eta]_\theta = 3{\cdot}2$ dl/g, and z was obtained through either

$$\alpha^5 - \alpha^3 = 134/105z \quad \text{(Flory–Stockmayer, see ref. 1)} \tag{13}$$

or

$$\alpha^3 - 1 = 2z \quad \text{(Fixman–Stockmayer[19])} \tag{14}$$

Using[19]

$$\alpha_\eta^3 - 1 = 1{\cdot}55z \tag{15}$$

gives an almost identical result to that found from equations (12) and (14). The small variation of A with T was ignored and a constant value of $7{\cdot}4 \times 10^{-9}$ was taken to translate z into B which is shown in *Figure 6* as a function of $1/T$.

Values of α found from $\langle S_0^2\rangle^{\frac{1}{2}} = 1\,000$ Å are larger than those found from $[\eta]$. This would be consistent with the much greater effect of polydispersity on the former values.

The Cassassa–Markowitz treatment was used to calculate B, as shown in *Figure 6*, from the A_2 values. This procedure gives a greater departure of $h(z)$ from unity than do the other well-known procedures which would therefore give smaller values of B.

Although the absolute magnitude of B differs depending on the method of evaluation, B is not linear in $1/T$ as the LCST is approached contrary to its behaviour approaching the UCST. Although equation (4) has been successful at low temperatures it has no real theoretical justification. It is evident from equation (5) that near the UCST where the first term is dominant, χ_1 or B should be approximately linear in $1/T$. However, approaching the LCST the second, or structural[3], term is the more important and C_p is an increasing function of T whose curvature increases with increasing T leading to the behaviour found here.

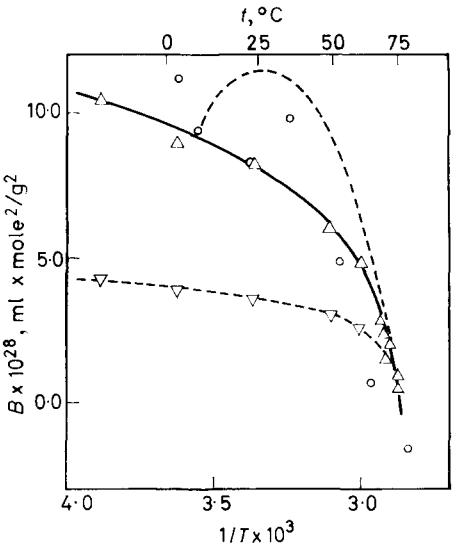

Figure 6—B values for PIB–pentane versus $1/T$, using $[\eta]$ with equation (13), △; with equation (14), ▽; using A_2 ○; from theory using equation (5), broken line

An additional argument comes from the curvature of B or A_2 with T. Taking B to be linear in $1/T$ near the UCST, and putting $\chi_1=0$, B and A_2 are concave downwards when considered as functions of T. If B were linear in $1/T$ near the LCST with a *constant* negative value of ψ_1, B and A_2 would be concave upwards in this region. It seems improbable, but of course not impossible, that this change of curvature would occur; our experiments show that B and A_2 are concave downwards throughout the temperature range.

χ_1 has been calculated for the present system, ignoring the first term of equation (5) which depends on the probably small 'chemical' differences between these two hydrocarbon components. τ has been evaluated elsewhere[4a], and C_p for pentane was obtained from that of heptane (which is known over a wide temperature range) and then applying the Law of Corresponding States[20]. The result of such a calculation appears[20] to give values of χ_1 which are generally too large. In *Figure 6* B calculated in this way is plotted with a constant added to fit $B=0$ at 76°. The similarity with the experimental curves seems to indicate that equation (5) gives a qualitatively correct temperature dependence of B.

Consistency with other measurements

The total heat of mixing[8] PIB of $M=30$ kcal with pentane to infinite dilution at 25° = −48 cal/base mole of 56 g, which gives an average value of the heat of dilution parameter $\kappa_1=-0{\cdot}15$. This is in agreement with a value obtainable from the temperature variation of activity data in ref. 9a, and which is valid for dilute solutions. Using χ_1 values obtained from viscosity values of B via equation (3) and

$$\kappa_1=-T\,\mathrm{d}\chi_1/\mathrm{d}T \tag{16}$$

we find κ_1 at 25°$\sim -0{\cdot}05$ or $-0{\cdot}02$ depending on whether equation (13) or

equation (14) is used, i.e. values much smaller than that found from the thermodynamic measurements.

B from A_2 varies more steeply with T in *Figure 6* than B from the viscosities, and could give κ_1 of about the right order. Values of $A_2M/[\eta]$ versus $(\alpha_\eta^2 - 1)$ are in line with those of other systems.

A lower molecular weight of 2×10^6 PIB was previously used[21] to obtain $[\eta]$ in a series of n-alkanes, including pentane. There a value of $\Phi = 2{\cdot}1 \times 10^{21}$ was used to obtain values of χ_1 by either equation (13) or the Kurata–Stockmayer–Roig treatment which is equivalent to equation (14). $\frac{1}{2} - \chi_1$ was found larger than at present; part but not all of the discrepancy is due to the present value of A which corresponds to $\Phi = 2{\cdot}87 \times 10^{21}$.

Use of an empirical formula for C_p

The temperature dependence of χ_1 in equation (5) may be predicted in a very approximate way by associating $-U$ with the energy of vaporization neglecting the correction for the imperfection of the gas in the calculation of the configurational energy. This procedure therefore cannot be accurate at high temperatures. Using the empirical formula for $-U$ and by differentiation, C_p

$$-U = -U_0/(1 - T/T_c)^m \qquad C_p = -U_0 m/T_c\,(1 - T/T_c)^{m+1} \tag{17}$$

where $-U_0$ and m are constants, the latter equal to 0·428 (see ref. 4a).

$$\chi_1/(-U/RT) = \nu^2 + \tfrac{1}{2}m\tau^2/(T_c/T - 1) \tag{18}$$

$$\kappa_1/(-U/RT) = [1 + m/(T_c/T - 1)]\,\nu^2 + \tfrac{1}{2}m\,(m+1)\,\tau^2\,(T_c/T - 1)^2 \tag{19}$$

Using equation (19), the parameters ν^2 and τ^2 were obtained for PIB–n-alkane systems from heat of mixing data at 25°C and it was assumed that τ^2 for PIB–dibutyl ether is the same as for PIB–nonane which has the same number of chain atoms; ν^2 was obtained from heat of mixing data[10]. These parameters were used to predict the LCST of PIB–dibutyl ether using equation (18) and $\chi = \frac{1}{2}$ giving 220° as compared with 204°; ν^2 plays only a small role at this high temperature. Setting $\kappa_1 = 0$, the temperature of minimum χ_1 was found to be 70° as compared with 60° from the $[\eta]/T$ curve. For the crosslinked polystyrene–cyclohexane system, τ^2 was obtained from the value of the LCST, 210°, the first term of equation (18) being neglected at this high temperature. ν^2 was then obtained using a value of κ_1 found from viscometric data[21] and the temperature of minimum χ_1 found to be 96° as compared with 140°. Equation (17) seems to have a semi-qualitative validity in spite of the adjusted parameters which tend to compensate for the inaccuracies.

CONCLUSIONS

The temperature dependence of $[\eta]$, A_2 and $\langle S^2 \rangle^{\frac{1}{2}}$ is as predicted by the Prigogine theory, i.e. these qualities fall towards the LCST, after passing through a maximum which may be easily observable above room temperature as for PIB–dibutyl ether. A linear dependence of χ_1 on $1/T$ is not general because of the presence of the structural term in χ_1 as seen in

equation (5). The two θ-points associated with UCST and LCST are similar in reducing the polymer molecule to its unperturbed dimensions.

We should like to thank Professor H. Benoit and his co-workers, Messrs Dick, Froehlich and Reiss for their interest and valuable advice.

Centre des Recherches sur les Macromolécules,
Strasbourg, France

(*Received May 1966*)

REFERENCES

[1] KURATA, M. and STOCKMAYER, W. H. *Fortschr. HochpolymForsch.* 1963, **3,** 196
[2] STOCKMAYER, W. H. *J. Polym. Sci.* 1955, **15,** 575
[3] PRIGOGINE, I. (with the collaboration of BELLEMANS, A. and MATHOT, V.). *The Molecular Theory of Solutions,* Chaps. 16 and 17. North Holland: Amsterdam, 1957
[4a] PATTERSON, D. and SOMCYNSKY, T. International Symposium on Macromolecular Chemistry, Prague, 1965 (Preprint A566)
[4b] PATTERSON, D., DELMAS, G. and SOMCYNSKY, T. To be published
[5] INAGAKI, H., SUZUKI, H. and KURATA, M. To be published
[6] KAWAI, T. and UEYAMA, T. *J. appl. Polym. Sci.* 1960, **3,** 227
[7] REISS, C. and BENOIT, H. International Symposium on Macromolecular Chemistry, Prague, 1965 (Preprint A466)
[8] DELMAS, G., PATTERSON, D. and SOMCYNSKY, T. *J. Polym. Sci.* 1962, **57,** 79
[9a] BAKER, C. H., BROWN, W. B., GEE, G., ROWLINSON, J. S., STUBLEY, D. and YEADON, R. E. *Polymer, Lond.* 1962, **3,** 215
[9b] ALLEN, G. and BAKER, C. H. *Polymer, Lond.* 1965, **6,** 181
[10] DELMAS, G., PATTERSON, D. and BOHME, D. *Trans. Faraday Soc.* 1962, **58,** 2116
[11] BENOIT, H., HOLTZER, A. M. and DOTY, P. *J. phys. Chem.* 1950, **18,** 635
[12] FOX, T. G, FOX, J. C. and FLORY, P. J. *J. Amer. chem. Soc.* 1951, **73,** 1901
[13] UBERREITER, K. and KANIG, G. *J. chem. Phys.* 1950, **18,** 399
[14] FOX, T. G and LOSHAEK, J. *J. Polym. Sci.* 1955, **15,** 379
[15] EHL, J., LOUCHEUX, C., REISS, C. and BENOIT, H. *Makromol. Chem.* 1964, **75,** 35
[16] TIMMERMANS, J. *Physicochemical Constants of Pure Organic Compounds,* Elsevier: Amsterdam, 1950
[17] BENOIT, H., WEILL, G. and LOUCHEUX, CL. *J. Chim. phys.* **1958,** 540
[18] FOX, T. G and FLORY, P. J. *J. Amer. chem. Soc.* 1951, **73,** 1909
[19] STOCKMAYER, W. H. and FIXMAN, M. *J. Polym. Sci. C,* 1965, **1,** 137
[20] BHATTACHARYYA, S. N., PATTERSON, D. and SOMCYNSKY, T. *Physica, 's Grav.* 1964, **30,** 1276
[21] BATAILLE, P. and PATTERSON, D. *J. Polym. Sci. A,* 1963, **1,** 3265

Polymer Fractionation at a Lower Critical Solution Temperature Phase Boundary

C. H. BAKER*, C. S. CLEMSON† and G. ALLEN

The influence of pressure on a lower critical solution temperature is much more pronounced than on an upper critical solution temperature. Accordingly it is possible to control phase separation at a LCST phase boundary under isothermal conditions by merely adjusting the pressure on the system. An apparatus has been constructed to investigate the isothermal fractionation of polyisobutene in which precipitation is controlled by pressure. Two samples of polyisobutene of $M_v = 1{\cdot}76 \times 10^6$ and $9{\cdot}0 \times 10^4$ have been fractionated in isopentane solution so as to yield up to six and nine fractions respectively. The integral molecular weight distribution curves thus obtained are compared with those obtained from conventional fractionations at an UCST. The sensitivity of the method is poor with regard to the separation of low molecular weight fractions and degradation occurs at the higher temperatures to an appreciable extent.

THE conventional methods used to fractionate polymers by liquid–liquid phase separation all employ upper critical solution temperature (UCST) phenomena. It has recently been shown[1,2] that when the temperature is raised some 20 to 100 degrees above the normal boiling point of the solvent polymer solutions can also separate into two phases at a phase boundary which has a lower critical solution temperature (LCST). The exact location of the LCST for a given polymer–solvent system depends upon the average molecular weight of the polymer, the effect of molecular weight on the LCST being similar in magnitude but opposite in sign to the effect on an UCST. This is shown in *Figure 1* in which the variation of the LCST of several polymer–solvent systems is plotted as a function of the molecular weight (as determined by viscometry).

It has already been noted[2] that fractionation of the polymer occurs across the LCST phase boundary and consequently this provides an alternative region for fractionation by liquid–liquid phase separation. We have also found that, compared with an UCST, a LCST is approximately one hundred times more sensitive to pressure‡ and that phase separation is readily reversed by increasing the pressure on the system by a few atmospheres. Thus the possibility exists of controlling the isothermal fractional precipitation of a polymer at a LCST phase boundary by simply varying the pressure. Furthermore the phase boundary curves at a LCST are flatter than those at UCST boundaries in polymer solutions and this offers scope for working at concentrations higher than those employed in conventional fractionations.

*Present address: I.C.I. Fibres Ltd, Harrogate, Yorkshire.

†Present address: Polymer Chemistry Laboratory, A.E.I., Trafford Park, Manchester, 17.

‡For this reason we shall define the LCST of a polymer solution (T_p) as the precipitation temperature measured at the saturation vapour pressure of the solution P_p. Precipitation temperatures measured at arbitrary pressures P_p will be designated with prime superscripts, i.e. T'_p.

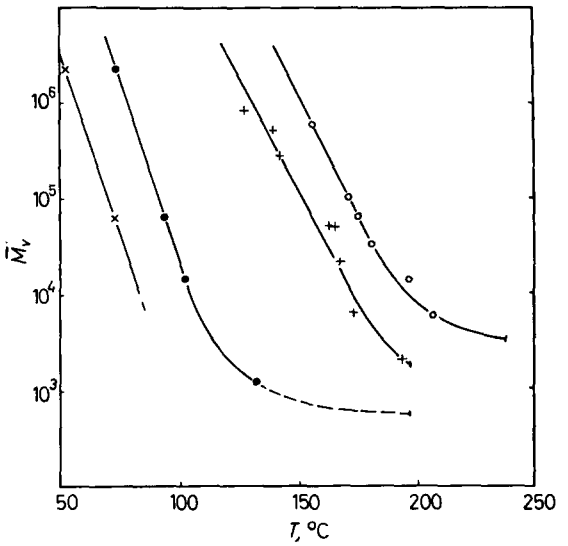

Figure 1 — Variation of LCST with viscosity-average molecular weight for various polymer–solvent systems: × polyisobutene–isopentane, ● polyisobutene–*n*-pentane, + polypropylene oxide–*n*-pentane, ○ polystyrene–cyclopentane

We have chosen to investigate the efficiency of fractionation at a LCST phase boundary using the system polyisobutene–isopentane because phase separation occurs at a conveniently low temperature and pressure, and also the dependence of the LCST upon pressure has been determined for this system[2].

EXPERIMENTAL

Materials

A commercial sample of iso-pentane was fractionally distilled to give a middle fraction which contained less than 0·5 per cent impurities as determined by vapour phase chromatographic analysis. The boiling point was 27·84° ± 0·02°C at 760 mm of mercury and the critical temperature was 187·30°C.

Two commercial samples, denoted by PIB 1* and PIB 2 were used. PIB 1 was Vistanex L100, the viscosity average molecular weight of which was found to be $1{\cdot}76 \times 10^6$. Viscosity measurements on this sample, and its fractions, were made in benzene solution at 24°C using an Ubbelohde dilution viscometer, the values of $\overline{M}_v$ being determined from the relation[3]

$$[\eta] = 1{\cdot}07 \times 10^{-3} \overline{M}_v^{\frac{1}{2}}$$

A reliable estimate of $\overline{M}_w$ could not be made from light scattering results because the sample contained a small amount of microgel.

PIB 2 was a sample of Oppanol B15 which had a viscosity average molecular weight of $9{\cdot}0 \times 10^4$. $\overline{M}_v$ measurements on this particular sample were performed in toluene solution at 30°C in a Desreux–Bischoff viscometer using the relation[4]

$$[\eta] = 2{\cdot}0 \times 10^{-4} M_v^{0{\cdot}67}$$

*In ref. 2 the sample designated PIB 1 was Vistanex L100 which had been subjected to a preliminary fractionation.

A value of $\overline{M}_w = 1{\cdot}3 \times 10^5$ was obtained from light scattering results.

Both samples were fractionated conventionally (under the guidance of Dr C. Booth) by precipitating fractions by the addition of methanol to a 0·25 per cent solution of polymer in benzene at 25°C. The results showed that the molecular weight distribution in each sample approximated to the 'most probable' distribution.

Apparatus

The original apparatus used for fractionation experiments at the LCST phase boundary has been described elsewhere[5]. A later modification is shown in *Figure 2*. Construction was mainly of brass although steel was used for the sections containing mercury and the pressure tubing connecting the various compartments was of copper.

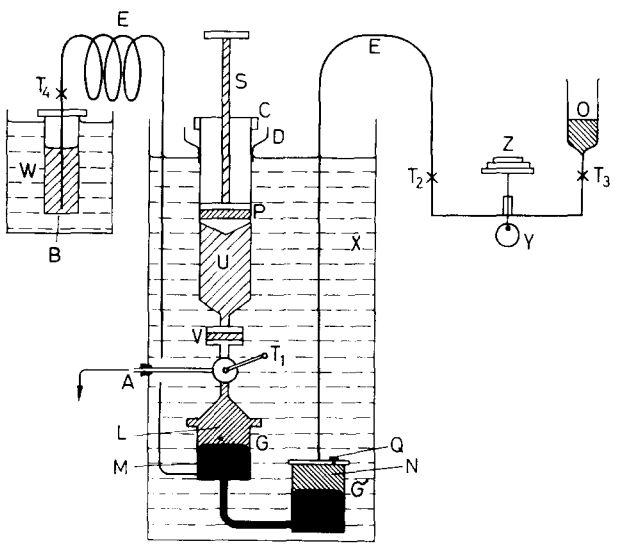

Figure 2—General arrangement of the Pressure Fractionation Apparatus: W Water bath for solvent reservoir, B Solvent reservoir, T_4 Klinger AB 10 cock, E Copper pressure tubing, A Outlet to collecting vessels and solvent recovery system, S Screw shaft of piston, C screw cap for upper cylinder, D 'Skirt' to prevent oil from bath creeping into cylinder, P Piston head packed with Teflon gasket, U Upper cylinder of fractionation apparatus containing dilute phase, V Perspex viewing window with brass housing, T_1 Klinger cock—initially a modified AB 10 but later a Klinger AB 12 two-way cock was fitted, L Lower concentrated phase of polymer solution, G Lower chamber of fractionation apparatus, M Mercury, G′ Mercury reservoir, N Transformer oil, X Oil or water thermostat bath. (Oil bath equipped with two 750W heaters, pump stirrer and cork lagging), T_2 and T_3 Budenberg needle valves, Y Excelsior Budenberg pressure balance, Z Pressure balance weights, O Oil reservoir, Q Air bleed valve

Reservoir B contained pure solvent. The polymer solution to be fractionated was contained in the cylinder U (volume 270 ml) which was sealed with a piston P. The piston was packed with Teflon and was driven by the screw S. The cylinder U was connected to the two steel reservoirs G (volume 200 ml) and G′ (volume 250 ml) via a Perspex viewing chamber V and a two-way tap T_1 (Richard Klinger Ltd, type AB 12). This tap could also connect U to a collecting vessel which was attached at the point A. The mercury reservoir G′ was connected via pressure tubing and the needle valve T_2 to an 'Excelsior' Budenberg pressure balance. The pressure balance was fitted with an oil reservoir O which could be isolated by means of the needle valve T_3. Neoprene gaskets were used on all seals except the Teflon-packed piston to make the apparatus pressure-tight so as to withstand up to 20 atmospheres.

The main section of the apparatus was immersed in an oil/water thermostat bath controlled to $\pm 0{\cdot}05$ deg C. The solvent vessel B was heated by a separate water bath.

Procedure

The solvent reservoir B was filled with solvent and isolated by valve T_4. The main section of the apparatus (U, V, G and G′) was then filled at room temperature and pressure as follows. The mercury reservoir G′ was filled with mercury so that the lower part of G also contained mercury. G′ was then sealed and the main section of the apparatus mounted in the empty thermostat bath. The pressure tubing between G′ and the pressure balance was filled with oil taking care to exclude any trapped air via a bleed valve Q on the top of G′. The oil reservoir O was filled with oil and the mercury level in G raised to near the top of G by transferring oil from O to G′. The two-way tap T_1 was opened to connect U and G and the piston P removed. About 200 ml of the polymer solution to be fractionated was then poured into U and allowed to drain through T_1 so as to fill the remainder of G, again care being taken to exclude all the air from being trapped in G. The piston P was chilled and inserted into U so as to rest upon the surface of the polymer solution. The apparatus was then sealed and tested for leaks. At all times during the subsequent experiment the relative volumes of polymer solution in G and U could be estimated from the length of the exposed part of the piston shaft S, and from the amount of oil in O.

The thermostat bath around U, G and G′ was then filled and controlled at the temperature required for the subsequent phase separation. This was generally some 6 to 7 deg. C above the 'normal' LCST of the system[2]. At this stage phase separation was prevented from occurring by the application of a pressure upon the solution some 15 lb/in^2 above the precipitation pressure for the particular temperature being employed. After thermal equilibrium had been established the pressure was gradually reduced in steps of 0·1 atm until phase separation, detected by the appearance of opalescence, was observed through V. The onset of phase separation was generally characterized by the increasing cloudiness associated with critical opalescence which could sometimes take on an intense brown colouration. Approximately one hour was required to allow the two phases to separate completely after which the phase boundary was located through V by

adjusting the relative volumes available in U and G. This was done by raising or lowering the piston, while maintaining a constant pressure on the system, by adjusting the volume of oil in the system by means of the pressure balance. The relative volumes of the two phases were estimated from the new position of the screw S and the change in oil level in O. From these measurements the movement of P necessary to push the phase boundary below T_1 was calculated and the operation then carried out. T_1 was then opened so as to connect U to a collecting vessel, at atmospheric pressure attached at A, whereupon the top phase was forced out of U by the vapour pressure of the solvent. As this operation was carried out at atmospheric pressure the solvent spontaneously volatilized in the collecting vessel and was collected in a cold trap. The polymer fraction so obtained was dried, weighed and its intrinsic viscosity measured.

To prepare for the next separation the temperature of the thermostat bath was lowered some 6 or 7 deg. C and the tap T_1 returned to the position in which it connected U to G. Pure solvent was then transferred from B to U and G by raising the temperature of the water bath around B to about 20 deg. C above that of the main thermostat, closing valve T_2 and opening valve T_4 and withdrawing P sufficiently. Valve T_4 was then closed and the new solution in U and G homogenized by pumping the solution between U and G several times by means of manipulating the piston P and the pressure balance. Further fractions were then obtained in a similar manner.

RESULTS

The phase diagram for the two polyisobutene–isopentane systems studied here have already been reported[2], the parameters of the LCSTs being as follows:

	T_p, °C	P_p atm	W_2	dT_p/dP deg. atm^{-1}
PIB 1	52	2·17	0·035	0·46
PIB 2	71	3·54	0·025	0·40

Fractionation of PIB 1

Three experiments were made with initial concentrations of polymer solution of about four per cent. In the first run at 56°C about 85 per cent of the polymer precipitated from the first top fraction because the temperature was too close to T_p to allow a suitable degree of control of phase separation by pressure variation. The second and third runs were carried out at 57·40° to 58·00° and 58·58° to 59·00°C respectively with the results shown in *Table 1*. In both cases the second fraction was of lower molecular weight than the first despite the expectation that precipitation would produce successive fractions of increasing molecular weight. From the point of view of molecular weight fractionation the third run is the most satisfactory. Six fractions were obtained with $\overline{M}_v$ ranging from 0·77 to $2{\cdot}71 \times 10^6$. In *Figure 3* the integral molecular weight distribution curve obtained from these results is compared with the distribution curve obtained from the results of the conventional fractionation at 25°C.

Later a run was attempted at 65°C using an initial solution of lower concentration but degradation was severe and the results were not significant.

Table 1. Fractionation data for PIB 1

Run 2

Fraction	*Wt* *g*	$\overline{M}_v$ $\times 10^{-6}$	T'_p °C	P'_p *atm*	*Relative volumes of phases* *lower phase* / *upper phase*
1	2·451	1·46	58·00	7·0	0·21
2	0·629	0·94	57·40	8·0	0·26
3	0·803	1·66	57·85	6·0	0·22
4	0·322	2·36	—	—	—

$W_i[\eta]_i = 1{\cdot}295$ $[\eta] = 1{\cdot}440$ for whole polymer

Run 3

Fraction	*Wt* *g*	$\overline{M}_v$ $\times 10^{-6}$	T'_p °C	P'_p *atm*	*Relative volumes of phases* *lower phase* / *upper phase*
1	0·666	0·79	59·00	6·0	0·70
2	0·393	0·77	59·00	7·0	0·55
3	1·147	1·16	58·50	10·0	0·21
4	0·405	1·50	58·50	10·0	0·25
5	0·266	1·75	58·50	13·0	0·11
6	0·509	2·71	—	—	—

$W_i[\eta_i] = 1{\cdot}219$ $[\eta] = 1{\cdot}440$ for whole polymer

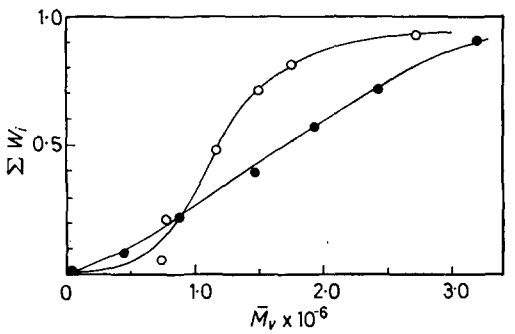

Figure 3—Integral Molecular Weight Distribution Curves for PIB 1, ○ Run 3, performed at 58·5°C, and a conventional fractionation ● at 25°C

Fractionation of PIB 2

Only two or three fractions could be isolated in preliminary experiments at 80°C. The results of three runs at 85°C are summarized in *Table 2.* Phase separation was readily controlled by pressure variation at this temperature and in the most extended experiment nine fractions were obtained. Unfortunately the time scale of the experiment was long and degradation was observed. For this reason the first run at 85°C is considered to be the

most satisfactory. A final attempt was made to improve fractionation by working at 90°C. Only four fractions were taken and although an anti-oxidant was incorporated to minimize degradation, degradation was very severe.

Figure 4 compares the results for PIB 2 obtained at 85°C with the integral molecular weight distribution curve obtained by precipitation at 25°C.

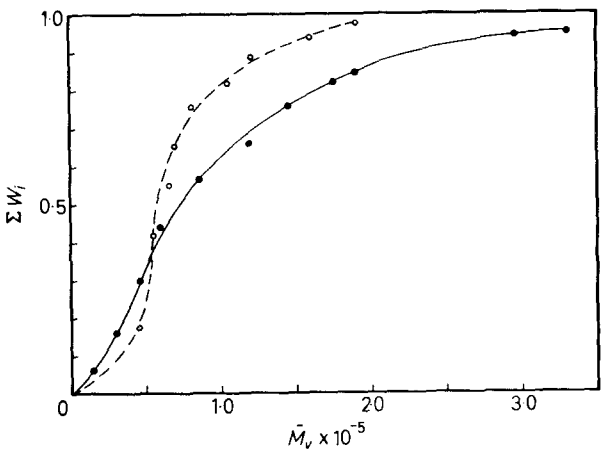

Figure 4—Integral Molecular Weight Distribution Curves for PIB 2, ○ Run III, performed at 85°C, and a conventional fractionation ● at 25°C

Table 2. Fractionation data for PIB 2 at 85·0°C

Run I

Fraction	*Wt* g	$\overline{M}_v$ $\times 10^{-5}$	P'_p atm
1	0·883	0·49	5·0
2	1·555	0·70	5·5
3	0·559	0·67	6·0
4	0·413	2·00	6·5
5	0·489	1·30	6·5

Recovery 92% $W_i[\eta_i]=0{\cdot}395$ $[\eta]=0{\cdot}416$

Run II

Fraction	*Wt* g	$\overline{M}_v$ $\times 10^{-5}$	P'_p atm
1	2·457	0·41	4·5
2	0·605	1·00	4·75
3	0·252	1·40	5·0
4	0·220	1·75	5·25
5	0·162	1·75	5·5
6	0·083	1·40	5·5

Recovery 91% $W_i[\eta_i]=0{\cdot}348$ $[\eta]=0{\cdot}416$

Run III *Table 2 (continued)*

Fraction	*Wt* *g*	$\overline{M_v}$ $\times 10^{-5}$	P'_p *atm*
1	1·279	0·44	4·5
2	0·553	0·54	4·75
3	0·377	0·67	5·0
4	0·410	0·70	5·25
5	0·339	0·81	5·50
6	0·189	1·04	5·75
7	0·251	1·40	6·25
8	0·175	1·60	7·00
9	0·112	1·89	7·00

Recovery 97% $W_i[\eta_i]=0{\cdot}356$ $[\eta]=0{\cdot}416$

DISCUSSION

Although our results show clearly that fractionation does occur at a LCST phase boundary, there is no doubt that the efficiency obtained in our experiments is quite inferior to that realized in the conventional fractionation at an UCST. Inspection of the results shows that a major factor is the difficulty encountered in, and the apparent insensitivity of the LCST method towards, the separation of the low molecular weight fractions.

The theory of polymer fractionation across a phase boundary leads to the result that for the polymer species of degree of polymerization x,

$$\phi'_x / \phi''_x = \exp(\sigma x)$$

where ϕ'_x is the volume fraction of x in the more concentrated phase and ϕ''_x that in the more dilute phase. In terms of Flory–Huggins solution theory the parameter $\sigma = f(\phi'_2, \phi''_2, \bar{x}_n, x)$. The fraction of species x remaining in the more dilute phase is $f''_x = (1 + [V'/V''] \exp[\sigma x])^{-1}$ where V' and V'' are the volumes of the two phases.

The object of our experiment was to enrich the dilute phase with species of low molecular weight and so obtain successive fractions of increasing molecular weight. Since σx is known to be positive, there will always be a larger fraction of the lower molecular weight species in the dilute phase and by making the volume of the dilute phase as large as possible an increased fraction of the smaller species will be retained in it. Thus it is advantageous to make the ratio:

$$\frac{V'}{V''} = \frac{\text{volume of lower phase}}{\text{volume of upper phase}}$$

as small as possible. If the initial volume fraction of polymer in solution is ϕ_2 then at equilibrium

$$(V' + V'')\phi_2 = V'\phi'_2 + V''\phi''_2 \qquad \text{whence} \quad \frac{V'}{V''} = \frac{\phi_2 - \phi''_2}{\phi'_2 - \phi_2}$$

and the ratio decreases as $\phi_2 \longrightarrow \phi''_2$. Clearly we should begin with a dilute solution and when working under isothermal conditions use pressure to adust the phase boundary in the T/ϕ_2 plane so that $\phi_2 \longrightarrow \phi''_2$.

Our experiments ranged over weight fractions of polymer in the initial solution from 4 to 0·5 per cent but no systematic improvement in efficiency was obvious. In all our experiments relatively high ratios of $V'/V'' > 0{\cdot}1$ were observed and this is one obvious reason for the inefficient fractionation. The results in *Table 2* are typical. The ratio V'/V'' is always highest for the first fraction and decreases to more favourable values as the fractionation proceeds (and the concentration of the solution in the pressure vessel declines). This explains, in part, the insensitivity to low molecular weight species. We conclude that in our apparatus control of pressure was too insensitive in the early stages of fractionation to give desirable results. It was for this reason that higher temperatures were used with PIB 2 to give more latitude in pressure variation but this effort was ruined by degradation. In all experiments it was difficult to assess the ratio V'/V'' quickly and a compromise between expediency and efficiency was required to minimize degradation.

This inherent inefficiency is augmented by the fact that the higher molecular weight polymer remains longer in the apparatus during fractionation and consequently these fractions are most susceptible to degradation. Apart from the basic disadvantage of degradation at the high temperature required for phase separation there is the further disadvantage of working above atmospheric pressure. On the other hand the factors in favour of the method are (*i*) the ability to fractionate at relatively high concentrations, (*ii*) the fact that the lower critical solution phenomenon is widespread in polymer solutions, and (*iii*) the potential ability to control the fractional precipitation in an isothermal system simply by pressure variation. It must be remembered, also, that this work represents one of the pioneering studies and improvements in technique will certainly enhance the usefulness of the method. For example a more efficient stirring device in the cylinder U would enable equilibrium to be attained more rapidly and further redesign of the apparatus could reduce the time scale of the experiment to one day. An alternative possibility would be the use of a continuous elution technique in which the eluting power of the solvent was gradually increased by progressively increasing the pressure on the system.

We wish to thank Dr C. Booth for his advice and assistance with the conventional fractionations. We also acknowledge a helpful discussion with Professor Gee.

The Chemistry Department,
The University, Manchester, 13

(*Received June 1966*)

REFERENCES

[1] FREEMAN, P. I. and ROWLINSON, J. S. *Polymer, Lond.* 1960, **1**, 20
[2] ALLEN, G. and BAKER, C. H. *Polymer, Lond.* 1965, **6**, 181
[3] FOX, T. G and FLORY, P. J. *J. Amer. chem. Soc.* 1951, **73**, 1909
[4] FOX, T. G and FLORY, P. J. *J. phys. Colloid Chem.* 1949, **53**, 197
[5] BAKER, C. H. *Thesis,* University of Manchester, 1962

Book Reviews

Polymer Mechanics, Vol. 1. No. 1, Jan.–Feb. 1965

THIS volume is the Faraday Press [84 Fifth Avenue, New York, N.Y. 10011] cover-to-cover translation of *Mekhanika Polimerov* published by the Russian Academy of Sciences. It is the first of a series of such publications and consequently a detailed assessment of the merits of each paper in this first volume would not be appropriate.

The idea behind the new journal is sound; it is that the great expansion of the industrial production of synthetic rubbers, plastics and fibres must be accompanied by a corresponding growth in polymer science, and especially in polymer physics, if rational choices are to be made among the myriad materials available or capable of synthesis. The journal under review is one of a number which have appeared recently to serve this branch of science, dealing in this case with work done in Russia and other parts of Eastern Europe.

The contents indicate that the preoccupations of polymer physicists and engineers are not so different east and west of the Iron Curtain. There are papers dealing with engineering design and testing of viscoelastic materials, the properties of composites, i.e. fibre-reinforced plastics and semi-crystalline polymers and others dealing with failure.

The general impression is of competent work but with nothing of outstanding significance. The translation is unobtrusive but explanation of the Soviet trade names would have been very useful.

E. R. HOWELLS

Testing of Polymers, Vol. I

Edited by J. V. SCHMITZ. Interscience: New York; London: Wiley, 1965. 479 pp. 147*s*

THIS book is announced as the first of a series to be devoted to polymer testing. In the preface the editor states that the series is intended not only for testing experts but also for polymer chemists and physicists and others who need to understand and apply test data. The plan of the series is not disclosed so volume I must be judged on its own with the realization that any criticisms of content may be disarmed by subsequent volumes.

There are 14 chapters written by 19 authors all with considerable experience, in industry or university, of polymers and test methods. The first two chapters set a very formal style dealing as they do with standards and specifications and with providing constant environmental conditions. The next two chapters provide an excellent introduction to mechanical testing. Professor Marin gives a very readable analysis of the many linear and non-linear relationships between load and deformation that arise in testing real materials. M. G. Sharma introduces theories of viscoelasticity that must inevitably arise when mechanical testing of polymers is discussed. Unfortunately after such an introduction to mechanical testing Volume I has no more to say on the topic.

The next five chapters discuss electrical testing. A brief introductory chapter, not so explicit as those on mechanical testing, is followed by four chapters on d.c. conductance, dielectric constant and loss, electrical resistivity, and high voltage testing. Electrical testing is therefore covered fairly thoroughly.

Four chapters follow on odd miscellaneous tests which seem to the suspicious mind of the reviewer to be in Volume I to make up the number. Chapter 10 deals with cavitation erosion, chapter 11 with odour and taste transfer testing, chapter 12 with indentation and compression testing of floor coverings and chapter 13 with the measurement of gas and vapour permeation.

The volume is brought back on to its wider view by a final chapter giving selected references to books and periodicals of relevance to the testing of polymers. It is perhaps unfair to pick on omissions from such a list (137 books, periodicals, handbooks, and dictionaries); the *British Journal of Applied Physics* and *Reports of Progress in Polymer Physics in Japan,* however, represent primary sources in their respective countries which should not be overlooked.

The writing style is of course variable but the editor seems to have succeeded in avoiding duplication and too wide a spread of style between his contributors; the book is therefore readable. It does in part fulfil the function set out in the preface and can be thoroughly recommended to all the classes of intended readers. If subsequent volumes are published to fill the gaps, a worthwhile and a well thumbed set of volumes will appear on library shelves; at 147*s* per volume they will be expensive for individuals.

K. W. HILLIER

Exposés de Chimie Macromoléculaire. Structure Chimique des Polyosides

J. NÉEL. 165 pp. Gauthier-Villars: Paris, 1965. *NF* 40

THE chemistry and terminology of sugars is a complex subject, fraught with difficulties for the inexperienced. There is, in spite of much devoted work, a considerable lack of correspondence between usages in different countries, and confusion can easily arise, even with small molecules, while with polymeric sugars greater problems arise.

This brief and clearly written text will do much to help anyone involved with interpretation of work in a difficult field. A 'polyoside' is taken to be a compound which, upon acid hydrolysis, yields one or more sugars, and, in certain cases, alcohols (usually methanol) or low molecular weight phenols. Throughout the book the term *'ose'* is used for 'sugar': the first half of the text is devoted to a clear and detailed account of the chemistry of monomeric sugars, including optical isomerism, classification, and cyclic formulae, and the chemical properties dependent on the presence of the carbonyl and hydroxyl groups, and their interactions.

The rest of the book follows on from this exposition, and describes the chemical structure of polyosides. Important natural polymers discussed include cellulose (with a particularly useful table relating structural characteristics to the methods and arguments by which they are established), starch, glycogen, polymannosides, polyfructosides (inulin), and more obscure polysaccharides and polyheterosides. Similarly, the polyuronides are more briefly discussed, including pectin, alginic acid, gum arabic, hyaluronic acid, blood polysaccharides, and the sulphur-containing polyuronides agar-agar, chondroitin sulphuric acid and heparin.

The book is a useful introduction to the difficult topic of sugar polymers. It contains adequate references, is well printed, and, although paper-backed, is not unreasonably priced.

C. A. FINCH

Thermoanalytical Methods of Investigation

PAUL D. GARN. Academic Press: New York, 1965. 606 pp. 156*s*

THIS book has been nicely produced with layout and illustrations of the usual high quality. It is a long book with 17 chapters. There is much repetition of material, in fact better organization of the topics could well have resulted in a reduction in size by a factor of two. One general characteristic which the reviewer found irritating is the style of writing which endeavours to strike a chatty, qualitative note when a simple and precise style might be more appropriate; this is of course very much a matter of personal preference.

The contents of the book make it most useful to the mineralogist and of less value to polymer scientists.

The volume is brought back on to its wider view by a final chapter giving selected references to books and periodicals of relevance to the testing of polymers. It is perhaps unfair to pick on omissions from such a list (137 books, periodicals, handbooks, and dictionaries); the *British Journal of Applied Physics* and *Reports of Progress in Polymer Physics in Japan,* however, represent primary sources in their respective countries which should not be overlooked.

The writing style is of course variable but the editor seems to have succeeded in avoiding duplication and too wide a spread of style between his contributors; the book is therefore readable. It does in part fulfil the function set out in the preface and can be thoroughly recommended to all the classes of intended readers. If subsequent volumes are published to fill the gaps, a worthwhile and a well thumbed set of volumes will appear on library shelves; at 147*s* per volume they will be expensive for individuals.

K. W. HILLIER

Exposés de Chimie Macromoléculaire. Structure Chimique des Polyosides

J. NÉEL. 165 pp. Gauthier-Villars: Paris, 1965. *NF* 40

THE chemistry and terminology of sugars is a complex subject, fraught with difficulties for the inexperienced. There is, in spite of much devoted work, a considerable lack of correspondence between usages in different countries, and confusion can easily arise, even with small molecules, while with polymeric sugars greater problems arise.

This brief and clearly written text will do much to help anyone involved with interpretation of work in a difficult field. A 'polyoside' is taken to be a compound which, upon acid hydrolysis, yields one or more sugars, and, in certain cases, alcohols (usually methanol) or low molecular weight phenols. Throughout the book the term *'ose'* is used for 'sugar': the first half of the text is devoted to a clear and detailed account of the chemistry of monomeric sugars, including optical isomerism, classification, and cyclic formulae, and the chemical properties dependent on the presence of the carbonyl and hydroxyl groups, and their interactions.

The rest of the book follows on from this exposition, and describes the chemical structure of polyosides. Important natural polymers discussed include cellulose (with a particularly useful table relating structural characteristics to the methods and arguments by which they are established), starch, glycogen, polymannosides, polyfructosides (inulin), and more obscure polysaccharides and polyheterosides. Similarly, the polyuronides are more briefly discussed, including pectin, alginic acid, gum arabic, hyaluronic acid, blood polysaccharides, and the sulphur-containing polyuronides agar-agar, chondroitin sulphuric acid and heparin.

The book is a useful introduction to the difficult topic of sugar polymers. It contains adequate references, is well printed, and, although paper-backed, is not unreasonably priced.

C. A. FINCH

Thermoanalytical Methods of Investigation

PAUL D. GARN. Academic Press: New York, 1965. 606 pp. 156*s*

THIS book has been nicely produced with layout and illustrations of the usual high quality. It is a long book with 17 chapters. There is much repetition of material, in fact better organization of the topics could well have resulted in a reduction in size by a factor of two. One general characteristic which the reviewer found irritating is the style of writing which endeavours to strike a chatty, qualitative note when a simple and precise style might be more appropriate; this is of course very much a matter of personal preference.

The contents of the book make it most useful to the mineralogist and of less value to polymer scientists.

The first three chapters contain a lengthy summary of the problems and effects in DTA; most of the topics raised here are duplicated later. There is some evidence of confusion in attempting to justify DTA as a more accurate method than conventional calorimetry; surely the two are different and the advantage of DTA is primarily that of speed of measurement.

The next three chapters contain useful and readable descriptions of DTA apparatus and the type of results obtainable.

Chapter 7 is an interesting account of the effect of the atmosphere around the sample on the thermogram obtained.

Chapters 8 to 14 contain material on TGA and miscellaneous topics all relevant to thermal analysis. This section of the book is, however, very drawn out.

The final chapters contain much important detail on the design of thermal analysis equipment and constitute profitable reading for all those intending to assemble their own apparatus.

The book contains extensive references and subject and author indices. It is likely to prove particularly useful as a reference work and for a general introduction to thermal analysis methods.

E. R. HOWELLS

Elastomer Stereospecific Polymerization

B. L. JOHNSON and M. GOODMAN. American Chemical Society: Washington, D.C., 1966. 155 pp. $5.50

THIS book contains eleven papers given at a symposium sponsored by the American Chemical Society in 1964. All are concerned with various aspects of stereospecific polymerization but the title of the book is somewhat misleading in that several of the papers relate to non-elastomeric polymers, and most are concerned with kinetics and mechanism of polymerization rather than with polymer properties. No outstanding development is recorded but the new information presented justifies its publication and its collection in one volume assures a permanent record of the proceedings. There is, however, no discussion and, from the diversity of subjects, publication in one of the established polymer journals would have been equally appropriate.

Seven of the papers deal with polymerization using coordination catalysts. There are several essentially practical accounts of the influence of catalyst structure and composition on the polymerization of isoprene, butadiene and propylene, the polymerization kinetics of 4-methyl pentene-1, and some interesting speculations on the mechanisms of polymerization of *trans* penta-1,3-diene to the isotactic and syndiotactic *cis* 1,4 forms, in the paper by Natta and Porri. Anionic polymerization receives attention in two short reviews by M. Morton and by Bywater and Warsfold. It is concerned with the mechanism and kinetics of lithium alkyl initiated polymerization of styrene, isoprene and butadiene. The two papers by Aggarwaal and co-workers on stereoisomerism and sequence length in polypropylene oxide are somewhat out of character with the other articles in this volume, being concerned with theories of melting and crystallization rather than with polymer synthesis. The remaining paper is a review of aldehyde polymerization by O. Vogl.

There is no clear theme that links all of the papers presented at this symposium and therefore the volume will tend to be used for reference by specialists for individual topics rather than to be read as a whole; the papers are fairly complete and have adequate bibliographies.

W. COOPER

A History of the Modern British Chemical Industry

D. W. F. HARDIE and J. DAVIDSON PRATT. Pergamon Press: Oxford, 1966. 380 pp. 21*s*

WITH the enormous growth of the chemical industry over the last two decades and the marked change of emphasis to processes where the basic intermediates are

The first three chapters contain a lengthy summary of the problems and effects in DTA; most of the topics raised here are duplicated later. There is some evidence of confusion in attempting to justify DTA as a more accurate method than conventional calorimetry; surely the two are different and the advantage of DTA is primarily that of speed of measurement.

The next three chapters contain useful and readable descriptions of DTA apparatus and the type of results obtainable.

Chapter 7 is an interesting account of the effect of the atmosphere around the sample on the thermogram obtained.

Chapters 8 to 14 contain material on TGA and miscellaneous topics all relevant to thermal analysis. This section of the book is, however, very drawn out.

The final chapters contain much important detail on the design of thermal analysis equipment and constitute profitable reading for all those intending to assemble their own apparatus.

The book contains extensive references and subject and author indices. It is likely to prove particularly useful as a reference work and for a general introduction to thermal analysis methods.

E. R. HOWELLS

Elastomer Stereospecific Polymerization

B. L. JOHNSON and M. GOODMAN. American Chemical Society: Washington, D.C., 1966. 155 pp. $5.50

THIS book contains eleven papers given at a symposium sponsored by the American Chemical Society in 1964. All are concerned with various aspects of stereospecific polymerization but the title of the book is somewhat misleading in that several of the papers relate to non-elastomeric polymers, and most are concerned with kinetics and mechanism of polymerization rather than with polymer properties. No outstanding development is recorded but the new information presented justifies its publication and its collection in one volume assures a permanent record of the proceedings. There is, however, no discussion and, from the diversity of subjects, publication in one of the established polymer journals would have been equally appropriate.

Seven of the papers deal with polymerization using coordination catalysts. There are several essentially practical accounts of the influence of catalyst structure and composition on the polymerization of isoprene, butadiene and propylene, the polymerization kinetics of 4-methyl pentene-1, and some interesting speculations on the mechanisms of polymerization of *trans* penta-1,3-diene to the isotactic and syndiotactic *cis* 1,4 forms, in the paper by Natta and Porri. Anionic polymerization receives attention in two short reviews by M. Morton and by Bywater and Warsfold. It is concerned with the mechanism and kinetics of lithium alkyl initiated polymerization of styrene, isoprene and butadiene. The two papers by Aggarwaal and co-workers on stereoisomerism and sequence length in polypropylene oxide are somewhat out of character with the other articles in this volume, being concerned with theories of melting and crystallization rather than with polymer synthesis. The remaining paper is a review of aldehyde polymerization by O. Vogl.

There is no clear theme that links all of the papers presented at this symposium and therefore the volume will tend to be used for reference by specialists for individual topics rather than to be read as a whole; the papers are fairly complete and have adequate bibliographies.

W. COOPER

A History of the Modern British Chemical Industry

D. W. F. HARDIE and J. DAVIDSON PRATT. Pergamon Press: Oxford, 1966. 380 pp. 21*s*

WITH the enormous growth of the chemical industry over the last two decades and the marked change of emphasis to processes where the basic intermediates are

derived from petroleum sources, it is of great interest to have before us a review of how industry has progressed from its modest beginnings in the pre-Victorian era to the stage of present day manufactures. All who are concerned with chemical science and technology should find the story as presented stimulating and perhaps, at times, salutary reading, especially when we consider how the efforts of our predecessors involved a great deal of empiricism, personal faith and business acumen.

The publishers present this book as the first of a series on specialized aspects of the industry and the authors, both of whom have long been associated with chemical manufacture, deal with their subject in a thoroughly competent and logical manner. Not only do they produce facts and figures but throughout the book give critical attention to the processes involved. After tracing the origins of the industry in this country, and dealing with those chemicals, particularly sulphuric acid, alkali, chlorine and tar products then required in increasing quantity by the glass, textile, soap and other manufacturers, the second chapter looks at a transition period and shows how discovery, chemical engineering, the 1914–18 war and company mergers all had their impact on technical and industrial development. A third chapter provides a comprehensive study of the modern industry: apart from covering heavy chemicals (both organic and inorganic), dyes, and pharmaceutical chemicals, a section on new materials deals with the origin and growth of polymers, showing their development from the early beginnings of celluloid and PF resins to the large scale manufactures of the wide range of important products currently used in plastics, rubbers and fibres.

In addition to a consideration of economic aspects and statistics, there is a fascinating chapter on companies of importance in the industry, wherein are traced their origins, growth and commercial interests, providing reminders of smaller companies now defunct in themselves but whose spirit still exists within the merged concerns. Concluding sections detail British trade associations and provide comprehensive indexes giving reference not only to chemicals and processes but to manufacturers past and present.

The book is well printed and produced and although paper-backed should be sufficiently robust to withstand considerable handling.

R. J. W. REYNOLDS

High Resolution Nuclear Magnetic Resonance Spectroscopy, Volume II

J. W. EMSLEY, J. FEENEY and L. H. SUTCLIFFE. Pergamon: Oxford, 1966. pp 665–1154. 105*s*

THE authors have attempted a comprehensive survey of the applications of high resolution nuclear magnetic resonance spectroscopy to the determination of molecular structure. The field is so vast that the book exceeds 1 150 pages and very sensibly has been divided into two volumes. Volume II reviews most of the experimental results which have been published up to the end of 1963 with comments on how well the measurements are explained by the theories described in Volume I. There are frequent cross references to Volume I.

Chapter 10, the first in Volume II, is concerned with correlation of proton resonance parameters with molecular structure. Large numbers of coupling constants and chemical shifts are tabulated, and where possible the shifts have been corrected so that they are relative to the same standard. This section will probably be useful, both to the theoretician who needs a convenient compilation of experimental data and to the structural chemist who wishes to interpret his spectra. There is a short section on the spectra of 'Large complex organic molecules'.

There have been comparatively few applications of *high resolution* n.m.r. to problems in polymer chemistry. However, in cases where suitable solvents can be found the spectra of polymers can be interpreted in much the same way as those of other large molecules, and extra information can often be obtained from the line widths. Examples of the use of n.m.r. to study segmental motion, structure, configuration and tacticity of polymers are discussed.

derived from petroleum sources, it is of great interest to have before us a review of how industry has progressed from its modest beginnings in the pre-Victorian era to the stage of present day manufactures. All who are concerned with chemical science and technology should find the story as presented stimulating and perhaps, at times, salutary reading, especially when we consider how the efforts of our predecessors involved a great deal of empiricism, personal faith and business acumen.

The publishers present this book as the first of a series on specialized aspects of the industry and the authors, both of whom have long been associated with chemical manufacture, deal with their subject in a thoroughly competent and logical manner. Not only do they produce facts and figures but throughout the book give critical attention to the processes involved. After tracing the origins of the industry in this country, and dealing with those chemicals, particularly sulphuric acid, alkali, chlorine and tar products then required in increasing quantity by the glass, textile, soap and other manufacturers, the second chapter looks at a transition period and shows how discovery, chemical engineering, the 1914–18 war and company mergers all had their impact on technical and industrial development. A third chapter provides a comprehensive study of the modern industry: apart from covering heavy chemicals (both organic and inorganic), dyes, and pharmaceutical chemicals, a section on new materials deals with the origin and growth of polymers, showing their development from the early beginnings of celluloid and PF resins to the large scale manufactures of the wide range of important products currently used in plastics, rubbers and fibres.

In addition to a consideration of economic aspects and statistics, there is a fascinating chapter on companies of importance in the industry, wherein are traced their origins, growth and commercial interests, providing reminders of smaller companies now defunct in themselves but whose spirit still exists within the merged concerns. Concluding sections detail British trade associations and provide comprehensive indexes giving reference not only to chemicals and processes but to manufacturers past and present.

The book is well printed and produced and although paper-backed should be sufficiently robust to withstand considerable handling.

R. J. W. REYNOLDS

High Resolution Nuclear Magnetic Resonance Spectroscopy, Volume II

J. W. EMSLEY, J. FEENEY and L. H. SUTCLIFFE. Pergamon: Oxford, 1966. pp 665–1154. 105*s*

THE authors have attempted a comprehensive survey of the applications of high resolution nuclear magnetic resonance spectroscopy to the determination of molecular structure. The field is so vast that the book exceeds 1 150 pages and very sensibly has been divided into two volumes. Volume II reviews most of the experimental results which have been published up to the end of 1963 with comments on how well the measurements are explained by the theories described in Volume I. There are frequent cross references to Volume I.

Chapter 10, the first in Volume II, is concerned with correlation of proton resonance parameters with molecular structure. Large numbers of coupling constants and chemical shifts are tabulated, and where possible the shifts have been corrected so that they are relative to the same standard. This section will probably be useful, both to the theoretician who needs a convenient compilation of experimental data and to the structural chemist who wishes to interpret his spectra. There is a short section on the spectra of 'Large complex organic molecules'.

There have been comparatively few applications of *high resolution* n.m.r. to problems in polymer chemistry. However, in cases where suitable solvents can be found the spectra of polymers can be interpreted in much the same way as those of other large molecules, and extra information can often be obtained from the line widths. Examples of the use of n.m.r. to study segmental motion, structure, configuration and tacticity of polymers are discussed.

A similar survey to that presented for protons in Chapter 10 is given for fluorine resonances in Chapter 11, and in Chapter 12 most of the published work on resonances of other spin $\frac{1}{2}$ nuclei is reviewed. Often the signals from such nuclei are too weak to be detected by normal techniques and the special experimental procedures necessary are briefly described.

In the preface it is predicted that with the rapid increases in the number of n.m.r. publications, it will soon be impracticable to cover the whole field in a single text. On reading the book, one suspects that this point may already have been reached. In Volume II a vast number of experimental data have been carefully collected and presented as clearly as possible, but discussion and comments are extremely brief. The book contains over 1 000 references to original papers, and there is an excellent index. It is a useful guide to the literature, but a serious disadvantage is that even the most recent work included is now at least two and a half years old.

J. G. KENWORTHY

The Identification of Plastics and Rubbers

K. J. SAUNDERS. London: Chapman and Hall, 1966. X+55 pp. 7*s* 6*d*

THIS small and modestly priced volume forms one of a series of paperbacks covering a diversity of subjects, and is based on a laboratory course given at the National College of Rubber Technology, where Dr Saunders is Senior Lecturer in Polymer Chemistry.

The analytical approach presented follows a scheme in which the sample is grouped as a rubber, thermoplastic or thermosetting material and subjected to a simple but effective initial examination covering such properties as colour, specific gravity and behaviour on heating, following which chemical tests designed to establish final identification are applied. Inorganic fillers and pigments are included in the scheme but not, unfortunately, plasticizers and other additives.

While there is good sense in the tests described and in the conclusions to be gained from them, the underlying physical and chemical principles could, with advantage, have been dealt with more fully. Again, although the polymers under study are well classified chemically, the text would perhaps have been made more interesting by the inclusion of some relevant trade names since these are often now widely used.

The book gives a number of references and recommendations for further reading but a brief chapter outlining the more sophisticated tools available to the modern experimenter and of invaluable assistance in analysis would have been useful. Few people these days rely solely on the sort of elementary approaches put forward; for initial teaching purposes these may be ideal but not for identification in general. Spectrographic techniques, for example, are now available to most of us, even in teaching laboratories, and there is everything to be gained by drawing them to the attention of a student at an early stage in his career.

In general the book will, as I think the author intends, serve as a useful practical introduction for students taking an interest in polymers and for those handling commercially established elastomers and plastics, although few people will wish to regard it as more than a preliminary guide to polymer identification.

R. J. W. REYNOLDS

Physics of Non-crystalline Solids

Proceedings of the International Conference, Delft, July 1964, under the auspices of the I.U.P.A.C. Edited by J. A. PRINS. Amsterdam: North Holland Publishing Co., 1965. xvii+667 pp. 6 in. × 9 in. 180*s*

THE International Conference on the Physics of Non-Crystalline Solids held in Delft in 1964, of which this book is the collected proceedings, was an attempt to produce a bridge between the groups working on inorganic and organic glasses. Consequently, the fifty three papers published in this volume, of which four are in French, eight in German and the rest in English, describe studies in a wide range of materials, using an equally wide range of techniques.

In the introductory paper Professor Prins discusses various models which have been used to describe the structures of non-crystalline solids, and lays the foundation

A similar survey to that presented for protons in Chapter 10 is given for fluorine resonances in Chapter 11, and in Chapter 12 most of the published work on resonances of other spin $\frac{1}{2}$ nuclei is reviewed. Often the signals from such nuclei are too weak to be detected by normal techniques and the special experimental procedures necessary are briefly described.

In the preface it is predicted that with the rapid increases in the number of n.m.r. publications, it will soon be impracticable to cover the whole field in a single text. On reading the book, one suspects that this point may already have been reached. In Volume II a vast number of experimental data have been carefully collected and presented as clearly as possible, but discussion and comments are extremely brief. The book contains over 1 000 references to original papers, and there is an excellent index. It is a useful guide to the literature, but a serious disadvantage is that even the most recent work included is now at least two and a half years old.

J. G. KENWORTHY

The Identification of Plastics and Rubbers

K. J. SAUNDERS. London: Chapman and Hall, 1966. X+55 pp. 7*s* 6*d*

THIS small and modestly priced volume forms one of a series of paperbacks covering a diversity of subjects, and is based on a laboratory course given at the National College of Rubber Technology, where Dr Saunders is Senior Lecturer in Polymer Chemistry.

The analytical approach presented follows a scheme in which the sample is grouped as a rubber, thermoplastic or thermosetting material and subjected to a simple but effective initial examination covering such properties as colour, specific gravity and behaviour on heating, following which chemical tests designed to establish final identification are applied. Inorganic fillers and pigments are included in the scheme but not, unfortunately, plasticizers and other additives.

While there is good sense in the tests described and in the conclusions to be gained from them, the underlying physical and chemical principles could, with advantage, have been dealt with more fully. Again, although the polymers under study are well classified chemically, the text would perhaps have been made more interesting by the inclusion of some relevant trade names since these are often now widely used.

The book gives a number of references and recommendations for further reading but a brief chapter outlining the more sophisticated tools available to the modern experimenter and of invaluable assistance in analysis would have been useful. Few people these days rely solely on the sort of elementary approaches put forward; for initial teaching purposes these may be ideal but not for identification in general. Spectrographic techniques, for example, are now available to most of us, even in teaching laboratories, and there is everything to be gained by drawing them to the attention of a student at an early stage in his career.

In general the book will, as I think the author intends, serve as a useful practical introduction for students taking an interest in polymers and for those handling commercially established elastomers and plastics, although few people will wish to regard it as more than a preliminary guide to polymer identification.

R. J. W. REYNOLDS

Physics of Non-crystalline Solids

Proceedings of the International Conference, Delft, July 1964, under the auspices of the I.U.P.A.C. Edited by J. A. PRINS. Amsterdam: North Holland Publishing Co., 1965. xvii+667 pp. 6 in. × 9 in. 180*s*

THE International Conference on the Physics of Non-Crystalline Solids held in Delft in 1964, of which this book is the collected proceedings, was an attempt to produce a bridge between the groups working on inorganic and organic glasses. Consequently, the fifty three papers published in this volume, of which four are in French, eight in German and the rest in English, describe studies in a wide range of materials, using an equally wide range of techniques.

In the introductory paper Professor Prins discusses various models which have been used to describe the structures of non-crystalline solids, and lays the foundation

for the general discussion. Subsequent papers extend the discussion to the nature of networks in organic and inorganic glasses separately, and consider factors controlling the properties of the networks, e.g. free ends and chain entanglements in organic polymer networks.

A few papers describe the use of various experimental techniques as probes for investigating the nature of non-crystalline solids. These include the applications of thermal conductivity, viscosity, inelastic neutron scattering, X-ray absorption fine structure and nuclear magnetic resonance pulse techniques. Most papers give accounts of results obtained on either organic or inorganic materials, but some papers show how narrow may be the gap between the two main fields. An example is the study of glass transition temperatures of sodium phosphate polymers, in which, if the polymer end-group is non-ionic, the dependence of T_g on molecular weight is the same as that found in many organic polymers, but, if ionic end-groups are present, the behaviour is profoundly different.

Studies on organic polymers include both mechanical and dielectric relaxation studies on methacrylates. Mechanical relaxation methods are also used to study the effects on transition temperatures in aromatic polyesters by restricting molecular mobility on the introduction of methyl groups into the polymer. The same technique is used to study relaxation processes in short-chain alcohols. There are corresponding papers on relaxation studies using a number of inorganic systems. Other studies on inorganic glasses include the distribution of ions and the determination of average coordination numbers, their optical and electrical properties, effects of radiation and fibre properties.

The volume is well presented and contains a short list of errors, most of which (and few others which have escaped notice) are trivial, and mainly slips in translation. Even if the original conference did not break down the barriers between the separate studies of inorganic and organic glasses, a view expressed both in the Foreword and in the Review Lecture, this book may help to achieve the aims of the conference, by providing a demonstration of the use of similar techniques in both fields and a comparison of the terminology of the two groups of workers. Any laboratory working on the structure and properties of non-crystalline solids should find this volume a useful addition to its library.

G. C. EASTMOND

The Polymerization of Trifluoracetaldehyde Initiated by Tertiary Bases; The Effect of Temperature on the Monomer–Polymer Equilibrium

W. K. BUSFIELD

Gaseous fluoral is polymerized very rapidly by traces of tertiary bases. There is no termination reaction. Measurement of equilibrium monomer pressures in the range 16° to 72°C has yielded the following values of the standard enthalpy and entropy of polymerization:

$$\Delta H^0_{gc} = -15{\cdot}43 \pm 0{\cdot}31 \text{ kcal mole}^{-1}$$

$$\Delta S^0_{gc} = -44{\cdot}6 \pm 1{\cdot}0 \text{ cal deg}^{-1} \text{ mole}^{-1}$$

They are compared with corresponding values for other aldehyde systems. Possible reaction mechanisms are discussed.

THE polymerization of gaseous fluoral (trifluoracetaldehyde) has not previously been studied. In this paper results are reported which show that gaseous fluoral at room temperature and pressures below atmospheric is stable in the absence of additives, polymerizes slowly in the presence of 2·0 mole per cent of formic acid and polymerizes extremely quickly in the presence of as little as 0·2 mole per cent of tertiary bases such as pyridine and trimethylamine. The latter system has been studied in some detail. It has been found ideal for studying the equilibrium between fluoral and its polymer.

EXPERIMENTAL

Fluoral

Fluoral hydrate (B.D.H. or produced by the reaction of trifluoracetic acid with lithium aluminium hydride[1]) was slowly dropped on to a mixture of phosphorus pentoxide and concentrated sulphuric acid at 95°C in about half an atmosphere of nitrogen and the product trapped at −196°C. The fluoral was purified by several bulb to bulb distillations from −78°C to −196°C the middle fractions being retained each time. Mass spectrometry indicated the absence of hydrate and the presence of less than 0·1 per cent of water. The infra-red spectrum was identical with that published[2].

Pyridine

Pyridine was dried over and distilled from potassium hydroxide pellets into a vacuum line and stored over solid calcium hydride. The mass spectrum of the vapour was identical with a standard spectrum and showed that the amount of water in the sample was less than 0·2 per cent.

Trimethylamine

This was obtained from a solution of trimethylamine in ethanol (B.D.H.) by distillation from a flask containing excess of potassium hydroxide pellets into a bulb containing potassium hydroxide pellets. After evacuation it was distilled from $-78°C$ to $-196°C$ three times, preserving the middle sample each time. It was stored in a vacuum over solid calcium hydride at $-196°C$ from which it was obtained for runs by warming the bulb. The mass and infra-red spectra were identical with standard spectra.

Apparatus and procedure

The reaction vessel was a 100 ml round bottomed flask surrounded by a water jacket through which water was cycled from a thermostat bath controlled at $\pm 0{\cdot}01$ deg. C over short periods but at $\pm 0{\cdot}05$ deg. C over 24 hours (the duration of some of the runs). The only outlet to the flask led to a glass spiral pressure gauge (sensitivity 1·47 cm of mercury per 1·00 cm of scale) and to a silicone-greased tap leading to the gas injection and sampling system and the vacuum line. The volume outside the thermostatically controlled jacket but enclosed in the reaction volume amounted to less than 4 ml; its walls were electrically heated to about 130°C.

The temperature of the water jacket was recorded with a calibrated mercury in glass thermometer housed in a thermometer well.

Monomer and initiator gases were admitted to the reaction vessel heated by a separate heater to about 90°C. At this temperature and at pressures below one atmosphere fluoral does not polymerize. Polymerization runs were started by switching on the pump circulating water through the reaction vessel jacket from the thermostat bath. At the same time the separate reaction vessel heater was turned off. Trial experiments showed that the reaction vessel at 90°C, filled with nitrogen and used as a constant volume thermometer, was within one centigrade degree of the thermostat bath at 25°C ten seconds after switching on the circulating pump. The total pressure was followed with time as the polymerization proceeded.

The stability of the polymers formed was examined by operating the thermostat at a suitable higher temperature. With the reaction vessel isolated, the change in total pressure indicated the rate and extent of depolymerization.

RESULTS

Polymerization

Typical pressure/time curves are shown in *Figure 1*. The stability of fluoral in the absence of initiator is demonstrated by run T. There was neither change in total pressure nor visual sign of solid polymer over 20 hours.

Although formic acid is known to polymerize formaldehyde rapidly[3], two mole per cent of formic acid (run B) promoted only a slow polymerization of fluoral with a half-life of about 12 hours (the decay curve is not first order).

On the other hand tertiary bases, which are known to polymerize liquid chloral rapidly[4], also promote a very fast polymerization of fluoral. In

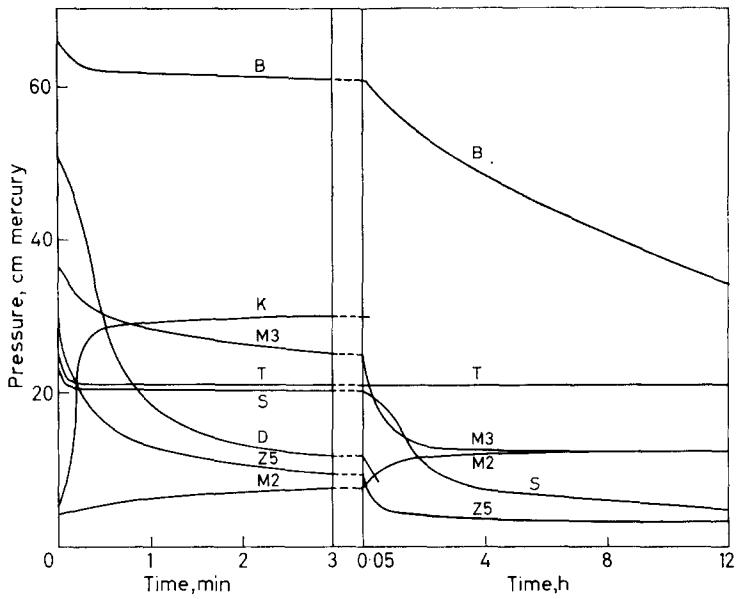

Figure 1—Total pressure/time curves. B, two per cent formic acid, 31°C; D, 0·2 per cent pyridine, 32°C; K, 5·8 per cent pyridine, 88°C; M2: 2·5 per cent pyridine, 45°C; M3: 2·5 per cent pyridine, 45°C; S, stable polymer (see text), 22°C; T, no catalyst, 21°C; Z5: 0·6 per cent trimethylamine, 30°C

run D, in the presence of as little as 0·2 mole per cent of pyridine, the half-life of the polymerization is about 35 seconds. Trimethylamine behaves similarly (run Z5).

The pressure/time curves did not follow any simple laws. Within the range 0·1 to 3 per cent of total pressure, the initiator pressure had little effect on the rate of polymerization. At lower concentrations there was sometimes an initial induction period of up to 30 seconds duration. This phenomenon was by no means reproducible, presumably because of the variable catalytic effects of the reaction vessel surface. Thereafter a fast polymerization ensued and the pressure approached a value independent of initiator and initial monomer concentration but dependent on the temperature. The pressure continued to fall very slowly until an equilibrium pressure was reached after 5 to 15 hours; run Z5, *Figure 1*, is typical.

Polymer stability

The polymer, made by pyridine or trimethylamine initiation, completely depolymerized at temperatures above 70°C in about three minutes to monomer and initiator (see gas analysis section). Run K is typical. Depolymerization runs exhibited no induction periods. In other respects and at temperatures below 70°C they were similar to polymerization runs with an initial fast depolymerization followed by a steady drift to an equilibrium total pressure. Evidently the polymer–monomer equilibrium is very mobile suggesting that the growing ends retain their activity. Both polymerization and depolymerization runs reach the same equilibrium total

pressure at the same temperature, see for example runs M2 and M3, *Figure 1*.

At each temperature there is a characteristic equilibrium pressure of fluoral. These values were measured in the temperature range 16° to 73°C and are listed in *Table 1*. In these experiments the initial initiator pressure

Table 1. Equilibrium fluoral pressures, *P*, at various temperatures

T, °C	*P*, cm mercury	*Initiator**	*Run from excess*
16·2	0·78	TMA	M
20·3	1·47	Pyr	M
20·5	1·29	Pyr	P
26·1	2·90	Pyr	M
29·7	3·02	TMA	M
32·2	4·10	Pyr	P
45·2	11·01	Pyr	P
45·2	11·78	Pyr	M
46·4	11·33	TMA	M
49·6	16·3	TMA	P
56·1	25·7	Pyr	M
58·6	28·2	TMA	P
59·5	26·5	Pyr	P
61·3	38·1	TMA	M
66·2	54·6	TMA	M
72·8	72·1	TMA	P

*TMA denotes trimethylamine; Pyr denotes pyridine; M denotes monomer; P denotes polymer.

was always less than two per cent of the total pressure. The presence of initiator was allowed for when calculating the equilibrium fluoral pressures, *P*. The estimated precision of *P* is ± 15 per cent at 16°C falling to $\pm 0{\cdot}2$ per cent at 73°C. These results will be discussed later in the light of the constitution of the gas and polymer phases.

Gas analysis

The fate of the initiator in the reaction was investigated by analysing samples of the gas phase at various times during the reaction by either mass spectrometry (AEI model 10) or infra-red gas analysis (Perkin–Elmer model 521 spectrophotometer). The analysis showed that only monomer and initiator were present in the gas phase in the reaction vessel before and after polymerization and depolymerization. There was no evidence for the presence of dimers or trimers which would have absorbed in the —C—O— or —O—H— stretching region of the infra-red spectrum or produced mass peaks above mass 98 in the mass spectrum.

Quantitative analysis of the gas samples, using peak heights in the mass spectra and optical densities in the infra-red spectra, coupled with the gas pressures in the reaction vessel led to the following generalizations. In the range of initial initiator pressures 2·1 to 41 per cent of the total pressure, polymer produced after one minute of the polymerization reaction contained 1·7 to 11 per cent (in terms of moles of initiator and moles of monomer in the polymer) respectively of initiator. The polymer remaining after 20 hours contained less than one per cent (usually the limit of measurement) of initiator over this whole range of initial initiator pressures.

In depolymerization experiments the first 20 per cent of polymer decomposed contained most of the initiator. The remaining polymer contained undetectable amounts. This demonstrates that at least two types of equilibria are taking part: a fast equilibrium between monomer and polymer and a slow one involving initiator also.

Polymer analysis

The polymer was formed as a thin film around the inner surface of the reaction vessel. It was quite stable in the presence of air as long as the equilibrium pressure of fluoral was maintained. The thin film could be peeled from the reaction vessel walls and had elastic properties. There seems little doubt that it is composed of polymeric molecules. When not in the presence of its equilibrium pressure of fluoral it very quickly depolymerized. A special infra-red cell attached to the reaction vessel was constructed to facilitate the recording of absorption spectra of polymer samples in the presence of the equilibrium pressure of fluoral. The samples were thin films formed on rock salt discs by preferential cooling. They scattered light badly especially in the near infra-red but gave some useful information.

The spectra were similar in most respects to those obtained with polyfluoral prepared in other ways[5]. Peaks characteristic of monomeric fluoral were present with optical densities of the order expected for the equilibrium pressure at room temperature and the length of the cell. In addition, for the polymer prepared from four mole per cent pyridine, there were seven small peaks in the region 1 450 to 1 700 cm^{-1}. The wavenumbers of six of the peaks corresponded with peaks in the spectra of pyridinium chloride and pyridine vapour. The other was not accounted for. The intensity agreement was not so good. It appears that the pyridine is present in the condensed polymer phase as pyridinium cations.

None of the polyfluoral samples absorbed in the 3 300 to 3 500 cm^{-1} region showing that either the end groups are not OH or that the degree of polymerization is large. Rosen and Sturm[6] observed no absorption in this region of the spectrum of $HO[CH.CHCl_2.O]_nH$ at a degree of polymerization of about 400.

The polymer can be stabilized by reaction with hydrogen chloride. For example, polymer made from four mole per cent of trimethylamine at room temperature completely depolymerized in 25 minutes at 58°C (there was insufficient polymer to reach the equilibrium pressure at this temperature). After repolymerization, reaction with 3 cm of mercury hydrogen chloride gas and evacuation, the polymer remained unchanged after 40 minutes at 58°C. Introduction of more trimethylamine gas destabilized the polymer immediately.

A stable polymer

During a series of about twenty experiments using pyridine as initiator, a thin film of a stable polymer grew on the surface of the reaction vessel which could not be removed by pumping at 95°C for five hours with a vacuum of 10^{-5} mm of mercury. This film still retained some catalytic activity for the polymerization of fluoral; see run S, *Figure 1*, which was

performed in the absence of gaseous initiator and presence of the thin film.

The film had a typical i.r. absorption spectrum of polyfluoral but with much sharper peaks than the unstable variety suggesting a higher degree of crystallinity. An X-ray diffraction photograph showed that the degree of crystallinity was similar to that produced by benzoyl peroxide initiation[5].

DISCUSSION

Since initiator is incorporated in the polymer as quaternary cations and since polymer activity is quenched by reaction with hydrogen chloride it is probable that the initiator forms the polymer end groups. Thus the initiator content of the polymer is a measure of the average degree of polymerization, if only straight chains are present.

The decrease in the initiator content of the polymer phase during the later stages of polymerization is probably due to reactions occurring between pairs of polymer molecule ends producing initiator molecules, which return to the gas phase, together with either cyclic polymers from intramolecular reactions or long chain polymers from intermolecular reactions. Depolymerization runs of suitable polymer samples showed that the stability of the polymer is not appreciably altered during this period. Since cyclic polymers would be more stable than linear polymers with active end groups, this evidence favours intermolecular reactions although some cyclization might occur concurrently. It is possible that the small fraction of stable polymer mentioned in the polymer analysis section may be composed of large cyclic structures. Attempts to extract any soluble crystallizable products such as cyclic trimers or tetramers from the polymer were unfruitful (parachloral is a crystalline solid soluble in many solvents[7]) and there was no evidence for any polymers, cyclic or straight chain, in the equilibrium gases. This indicates that the condensed phase after long reaction times is composed mainly of large cyclic structures or long chains in keeping with the elastic nature of the films. If the latter, then the average degree of polymerization must be at least 100 since the final polymer contained less than one mole per cent of initiator even from high initial initiator concentrations.

After long reaction times there is equilibrium between monomer vapour and high molecular weight active polymer molecules. The equilibrium monomer pressures, P, listed in *Table 1* are thus related to the standard free energy of polymerization of gaseous fluoral at one atmosphere pressure to solid polyfluoral:

$$\Delta G^0_{gc} = RT \ln P = \Delta H^0_{gc} - T\Delta S^0_{gc}$$

Log (P, cm mercury) is plotted against $10^3/T$ in *Figure 2*. The points lie on a reasonably straight line and least squares treatment yields the equation:

$$\log (P \text{ atm}^{-1}) = -(15{\cdot}43 \pm 0{\cdot}31 \text{ kcal mole}^{-1})/2{\cdot}303RT + (44{\cdot}6 \pm 1{\cdot}0 \text{ cal deg}^{-1} \text{ mole}^{-1})/2{\cdot}303R$$

Thus for the reaction:

$$CF_3CHO \text{ (g, 1 atm)} \longrightarrow (1/n)\,\ddagger C(CF_3)H.O\ddagger_n \text{ (solid, low crystallinity)}$$

$$\Delta H^0_{gc} = -15{\cdot}43 \pm 0{\cdot}31 \text{ kcal mole}^{-1} \quad \text{and} \quad \Delta S^0_{gc} = -44{\cdot}6 \pm 1{\cdot}0 \text{ cal deg}^{-1} \text{ mole}^{-1}$$

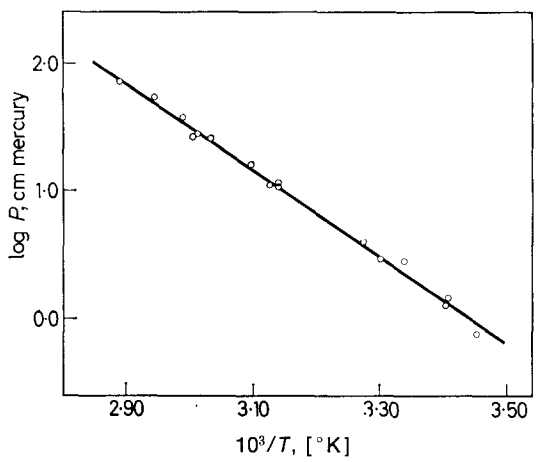

Figure 2—Graph of log (equilibrium fluoral pressure in cm of mercury) versus $10^3°K/T$

These values should be assigned to the mean temperature 45°C, but there is probably no significant error in assigning them to 25°C. The ceiling temperature, T^0_{gc}, is 73° ± 1°C.

North and Richardson[8] have emphasized the importance of the entropy of disorder of completely atactic polymers. The degree of stereoregularity of this polymer is unknown. If completely atactic then ΔS^0_{gc} for the formation of stereoregular polyfluoral will be $-46{\cdot}0$ cal deg^{-1} mole^{-1}. Values of ΔH^0_{gc}, ΔS^0_{gc} and T^0_{gc} for polyaldehydes are summarized in *Table 2*.

Table 2. Thermodynamic data for the polymerization of RCHO at one atmosphere pressure to solid polymer

R	$-\Delta H^0_{gc}$ *kcal mole*$^{-1}$	$-\Delta S^0_{gc}$ *cal mole*$^{-1}$ *deg*$^{-1}$	T^0_{gc} °C	*Polymer stereoregularity*	*Ref.*
H	14*	42·0	60	—	9
CH_3	11*	42	−10	high	8
C_2H_5	12*	44	5	high	8
CF_3	15·4	44·6	73	unknown	—
CCl_3†	16·4	44·1	98	unknown	4

*Estimated values.
†These values are calculated using the assumption that chloral forms an ideal solution in pyridine.

There is little variation in the entropy values as might be expected from a comparison with the polyolefin series[10] and from Trouton's rules on physical aggregation processes.

The reaction mechanism

Initiation can either occur in the gas phase or on the reaction vessel surface. In the gas phase some form of interaction between monomer and initiator molecules would be expected and the resulting complex might exhibit charge transfer bands in the ultra-violet or extra vibrational bands in the infra-red absorption spectrum. In fact the infra-red (400 to 4 000 cm^{-1}) and the ultra-violet (30 000 to 50 000 cm^{-1}) absorption spectrum of a 1 : 1 mixture of fluoral and trimethylamine, at pressures below the room temperature polymerization pressure, was simply the superposition of the spectra of the two separate gases. Secondly, if initiation and early growth occurred in the gas phase then most solid polymer might be expected to form at the bottom of the reaction vessel. The solid polymer was always

uniformly distributed around the surface. It seems probable therefore that both initiation and growth occur on the reaction vessel surface.

The mechanism of the initiation reaction poses some problems. In the presence of suitable proton donors, for example water, a mechanism similar to that proposed for the polymerization of chloral can be postulated[4]. However, no absorption in the OH stretching region of the infra-red spectrum of even low polymers was observed. Indeed the reagents were fairly rigorously dried. It is unlikely that sufficient proton donors are present as impurity to produce the low polymers observed early in the reaction.

In the absence of suitable proton donors one has to resort to structures involving large charge separations in the growing molecules.

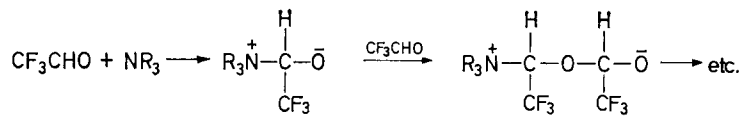

It is possible that the oppositely charged ends of adjacent growing polymer molecules are associated in the form of ion pairs, thus minimizing the electrostatic energy required for large charge separations in individual growing molecules.

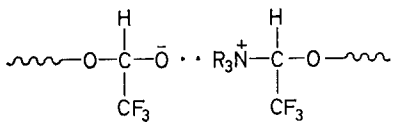

Recently Vogl and Bryant[11] have suggested a similar mechanism for the polymerization of aldehydes initiated by boron trifluoride.

Acknowledgements are made to Professor K. J. Ivin and colleagues in this department for stimulating discussion, and to Dr J. Iball for X-ray diffraction photographs.

Department of Chemistry, Queen's College,
University of St Andrews, Dundee

(*Received June 1966*)

REFERENCES

[1] BRAID, M., ISERSON, H. and LAWLOR, F. E. *J. Amer. chem. Soc.* 1954, **76,** 4027
[2] DODD, R. E., ROBERTS, H. L. and WOODWARD, L. A. *J. chem. Soc.* **1957,** 2783
[3] BEVINGTON, J. C. and NORRISH, R. G. W. *Proc. Roy. Soc. A,* 1951, **205,** 516
[4] BUSFIELD, W. K. and WHALLEY, E. *Trans. Faraday Soc.* 1963, **59,** 679
[5] BUSFIELD, W. K. and WHALLEY, E. *Canad. J. Chem.* 1965, **43,** 2289
[6] ROSEN, I. and STURM, C. L. *J. Polym. Sci. A,* 1965, **3,** 3741
[7] NOVAK, A. and WHALLEY, E. *Canad. J. Chem.* 1958, **36,** 1116
[8] NORTH, A. M. and RICHARDSON, D. *Polymer, Lond.* 1965, **6,** 333
[9] DAINTON, F. S., EVANS, D. M. and MELIA, T. P. *Polymer, Lond.* 1962, **3,** 263
[10] DAINTON, F. S. and IVIN, K. J. *Quart. Rev. chem. Soc. Lond. A,* 1958, **12,** 61
[11] VOGL, O. and BRYANT, W. M. D. *J. Polym. Sci. A,* 1964, **2,** 4633

Formation of New Crosslinkages in Proteins by Oxidation of the Tyrosine Residues with Potassium Nitrosyldisulphonate

C. EARLAND and J. G. P. STELL

Oxidation of wool fibres with potassium nitrosyldisulphonate increases their resistance to degradation by solutions of alkali and urea bisulphite and reduces their contraction in solutions of sodium bisulphite. Silk filaments have an increased tensile strength after treatment with the same reagent. This indicates that new crosslinkages have been introduced into these fibrous proteins and the available evidence suggests that oxidized tyrosine residues are involved in their formation. Although it is not possible to determine the structure of these new linkages, a melanin-type dimer or amino-substituted hydroquinone appears to be most probable. It is suggested also that potassium nitrosyldisulphonate crosslinks soluble and insoluble proteins by a common mechanism.

TEUBER AND RAU[1] found that potassium nitrosyldisulphonate (Frémy's salt) which in aqueous solution is dissociated into the free radical $\cdot ON(SO_3K)_2$ is able to oxidize phenols to quinones quantitatively. It has been suggested also that the insolubility of silk fibroin (*Bombyx mori*) after reaction with reagents such as potassium permanganate, sodium hypochlorite or chlorine dioxide is due to crosslinking via oxidized tyrosine residues[2]. Consistent with this suggestion, Earland *et al.*[3] found that potassium nitrosyldisulphonate was extremely effective for insolubilizing proteins. In addition to rendering silk insoluble in the usual solvents, potassium nitrosyldisulphonate precipitated insulin from solution as a reddish-brown solid in 100 per cent yield.

While reduction in the solubility of a protein is not in itself an unambiguous criterion of crosslinking, reliable methods exist for detecting the presence of new crosslinkages in fibrous proteins, and several such tests have been applied to wool and silk fibres oxidized with potassium nitrosyldisulphonate. It has been shown conclusively that the reagent has, in fact, introduced new crosslinkages into these structures and further evidence has been obtained which confirms that tyrosine residues are involved in the formation of these new linkages.

EXPERIMENTAL

Materials

Wool (70's quality) in the form of knitted fabric or Lincoln fibres was purified by scouring followed by ether and alcohol extraction. Raw silk (*Bombyx mori*) was purified as described previously[2].

Potassium nitrosyldisulphonate was prepared as described by Palmer[4],

iodometric titration showing the material to be 95 to 100 per cent pure. Peracetic acid was prepared by allowing glacial acetic acid (45 ml), 100 vol. hydrogen peroxide solution (55 ml) and concentrated sulphuric acid (0·56 ml) to stand for three days at 0° to 5°C. The concentration of peracid was approximately ten per cent. All other reagents were of AR grade.

Oxidation of wool and silk with potassium nitrosyldisulphonate

A known weight of potassium nitrosyldisulphonate was dissolved in 100 ml of 0·05 M sodium bicarbonate solution. Frémy's salt is reasonably stable in the pH range[5] 8 to 11 and sodium bicarbonate was regarded as a satisfactory buffering agent since in no experiment did the initial pH of 8·5 fall below 8·0 by the end of the treatment. It was necessary to avoid the use of solutions of pH appreciably greater than 8 or degradation of the protein would have occurred. One gramme of wetted out wool or silk was allowed to stand in the solution of the oxidant for 48 hours at 20°C in the dark, the contents of the flask being agitated occasionally. The protein was removed, washed in distilled water and air-dried.

Frémy's salt, although orange in the solid dimeric state, produces intensely purple aqueous solutions of the free radical. The reagent in solution was determined quantitatively with a Spekker photoelectric absorptiometer using a filter giving a maximum absorption at 550 mμ. The instrument was calibrated using solutions of 0·10 to 1·00 per cent concentration made from freshly prepared iodometrically pure reagent, the plot of concentration versus reading giving a straight line showing that dissociation was complete in the solutions used in this work. By determining the concentration of reagent in solution before and after reaction, it was possible to determine the maximum amount of reagent which had reacted. It should be emphasized that this gives the maximum possible uptake and because the decomposition of solutions of Frémy's salt is catalysed by its own degradation products, it is virtually impossible to correct for the decomposition of the reagent alone. Furthermore, although solutions in which decomposition has occurred may be estimated colorimetrically, this cannot be carried out titrimetrically since decomposition products interfere.

Oxidation of cystine residues in wool

Fabric was treated with 1·0 per cent aqueous peracetic acid solution (100 ml/g wool) for different lengths of time at 20°C, washed thoroughly in water and air-dried.

Susceptibility to degradation by alkali

Wool fabric was dried to constant weight at 110°C and cut into pieces approximately 1 cm × 1 cm. The loss in weight after treating with decinormal caustic soda (100 ml/g wool) at 65°C for one hour[6] was used as a measure of the susceptibility of the wool to attack by alkali.

Solubility in urea bisulphite solution

This was determined using the same conditions as in the previous test but replacing the solution of sodium hydroxide by one of pH 7·0 ± 0·1 containing 50g urea and 3g sodium metabisulphite[7] per 100 ml. It should be

emphasized that keratin is insoluble in all non-degradative solvents and the term 'solubility' merely expresses the loss in weight due to degradation by the reagent after the arbitrary time of treatment of one hour.

Contraction in sodium bisulphite solution

Tufts of fibres were treated for 30 min at 100°C in a five per cent (w/v) solution of sodium bisulphite[8]. The contraction in length, expressed as a percentage of the original, was determined immediately after removal from the solution and also after washing in cold water for 30 minutes. Measurements were made conveniently between two tie bands on the tufts.

Determination of cystine and tyrosine

Cystine analyses were performed by the method of Shinohara[9] using the phosphotungstic acid reagent of Folin and Marenzie[10]. Tyrosine was estimated by Lugg's method[11] using Millon's reagent. In both cases 0·40 g of wool was hydrolysed with 8·0 ml of 5N hydrochloric acid for eight hours in a sealed tube at 120° to 125°C prior to the determination.

Measurement of colour

The percentage reflectance from wool fabric before and after treatment with potassium nitrosyldisulphonate was measured over the wavelength range 380 to 700 mμ using an Optica C.F.4 double-beam recording spectrophotometer fitted with a reflectance attachment.

Mechanical properties of fibres

These were determined either on single wool fibres using a Cambridge extensometer or on bundles of 50 silk filaments using a Scott Serigraph yarn tester loading at 250g/min.

RESULTS

The increased resistance to chemical degradation of wool treated with potassium nitrosyldisulphonate

The solubility in both alkali and urea bisulphite solutions were used as measures of the resistance of wool keratin treated with potassium nitrosyldisulphonate to chemical degradation. It is seen from *Table 1* that after treatment, the solubility in both reagents is reduced considerably.

Table 1. Solubility of wool after treatment with $\cdot ON(SO_3K)_2$

$\cdot ON(SO_3K)_2$ *applied.* % *on wt of wool*	$\cdot ON(SO_3K)_2$ *reacted,* % *on wt of wool*	% *Solubility in* 0·10 N NaOH	% *Solubility in urea bisulphite solution*	
0	0	10·7	16·1	(28·5)
10	4	7·5	9·1	
25	10	5·8	4·8	
50	18	5·2	2·8	(1·6)
100	33	5·4	1·2	

The treated wool was a reddish-brown colour throughout, the depth of shade increasing with the degree of treatment. The values given in paren-

theses refer to another sample of wool and differ from the original because untreated wool contains small but varying amounts of lanthionine cross-linkages[12]. This in no way affects the validity of the urea bisulphite test but emphasizes its sensitivity.

Oxidation of the disulphide bonds of wool with peracetic acid increases its solubility in alkali due to a reduction in the number of crosslinkages and the formation of sulphonic acid groups. Subsequent treatment with Frémy's salt (25 per cent on the weight of wool), however, reduced considerably this increased solubility (*Table 2*).

Table 2. Solubility in alkali of oxidized wool treated with $\cdot ON(SO_3K)_2$

Time of oxidation with peracetic acid, min	*Cystine oxidized %*	$\cdot ON(SO_3K)_2$ *reacted, % on wt of wool*	*Solubility in* 0·10 N NaOH(%)	
			Before $\cdot ON(SO_3K)_2$	*After* $\cdot ON(SO_3K)_2$
0	0	10	10·5	6·0
30	46·3	16	34·4	24·4
60	71·0	17	73·0	38·3
120	75·0	17	88·0	36·4

A comparison of *Tables 1* and *2* shows that oxidized wool reacted with more potassium nitrosyldisulphonate than untreated wool. This is because after the severance of disulphide bonds, wool swells more readily in polar solvents, thus making the structure more accessible to reagents.

The contraction of wool fibres in sodium bisulphite solution

The contraction in boiling sodium bisulphite solution of wool fibres treated with Frémy's salt is shown in *Table 3*. It is seen that the reagent reduces considerably the contraction which occurs with untreated wool and that this diminution cannot be accounted for by the small amount of contraction produced by the reagent alone.

Table 3. The contraction in bisulphite solution of wool fibres treated with $\cdot ON(SO_3K)_2$

$\cdot ON(SO_3K)_2$ *applied, % on wt of wool*	*% Contraction after treatment*	*% Contraction in* $NaHSO_3$ *solution*	*% Contraction in* $NaHSO_3$ *solution followed by cold water for 30 min*
0	0	11·7	22·3
10	4·7	7·9	10·5
25	3·8	7·0	11·1
50	2·1	7·3	10·5
100	1·2	5·4	8·8

The cystine and tyrosine contents of treated wool

The diminution in the cystine and tyrosine contents of wool after treatment with potassium nitrosyldisulphonate is shown in *Table 4*.

For the treatment with 500 per cent of reagent, the wool was given five

Table 4. The losses of cystine and tyrosine from wool after treatment with $\cdot ON(SO_3K)_2$

$\cdot ON(SO_3K)_2$ *applied, % on wt of wool*	*Loss of cystine, %**	*Loss of tyrosine, %**
10	0	2·6
25	0	5·5
50	3·0	15·3
100	11·7	19·1
500	—	87·3

*The untreated wool contained 11·23 per cent cystine and 6·14 per cent tyrosine and from these data the percentage reductions were calculated.

separate 100 per cent treatments. This was to avoid excessive decomposition of the reagent due to the accumulation of decomposition products.

The mechanical properties of treated fibres

When single wool fibres were extended by 30 per cent in either pH 7 buffer solution or decinormal hydrochloric acid on the Cambridge extensometer no change in the work required to stretch the fibres after treatment could be detected. When, however, bundles of 50 silk filaments, wetted out in a solution of pH 7, were tested on the Scott Serigraph, appreciable changes in the breaking load and extension at break of the oxidized fibres were found (*Table 5*).

Table 5. The mechanical properties of silk treated with $\cdot ON(SO_3K)_2$

$\cdot ON(SO_3K)_2$ *applied, % on wt of silk*	*Breaking load of 50 filaments, g**	*Breaking load per filament, g†*	*Extension at break, %**
0	167·5	3·35	28·3
10	186·5	3·73	21·1
25	148·5	2·97	16·4
50	130·5	2·61	15·0

*Mean of five tests. †Maximum standard error of mean = $\pm 0{\cdot}10$ g.

Statistically, there is a very significant increase in breaking load when silk filaments are treated with ten per cent of potassium nitrosyldisulphonate. In view of the importance of these results, twenty further bundles of 50 filaments were tested, ten in the untreated state and ten after treatment with ten per cent of Frémy's salt. The untreated broke at a mean value of $3{\cdot}11 \pm 0{\cdot}09$g per filament with an extension of 27·9 per cent, whereas the treated broke at $3{\cdot}65 \pm 0{\cdot}07$g per filament with an extension of 20·4 per cent.

The colour produced by treatment with potassium nitrosyldisulphonate

Visually it was obvious that the intensity of the red-brown colour produced on wool and silk by potasssium nitrosyldisulphonate was related to the degree of treatment. A quantitative assessment of the colour was derived from the Kubelka–Munk treatment[13, 14] which relates the reflectance of a material to the concentration of coloured substance present.

Reflectance curves (per cent reflectance versus wavelength) were obtained for treated and untreated wool fabrics. From these curves, values for the fractional reflectance, R, were obtained at a given wavelength, and from

these the function $(1-R)^2/2R$, denoted by $[R]$, which gives a measure of the absorption was derived. Since,

$$[R]_{\text{treated}} - [R]_{\text{untreated}} = kC$$

where C is the concentration of the absorbing substance on the fibre, it was possible to calculate C in arbitary units. The full method of computation is shown in *Table 6*, which relates to the reflectance at 520 mμ.

Table 6. The reflectance at 520 mμ from wool treated with $\cdot ON(SO_3K)_2$

$\cdot ON(SO_3K)_2$ *applied, % of wt of wool*	0	10	25	50	100
R *(fractional)*	0·642	0·453	0·298	0·172	0·107
$[R]$	0·0998	0·330	0·827	1·999	3·728
$[R]_{\text{treated}} - [R]_{\text{untreated}}$	0	0·230	0·727	1·899	3·628
Ratio of concentrations $(kC_{10\%}=1)$	0 (0)	1·00 (1·0)	3·16 (3·3)	8·26 (8·2)	15·7 (15·6)

The values for C given in *Table 6* were obtained at one wavelength only, 520 mμ. These values were obtained also at 470 mμ, 570 mμ and 740 mμ, and the means of the four results are given in parentheses in *Table 6*. In point of fact the values of C varied but little with the wavelength and they are directly proportional to the amount of potassium nitrosyldisulphonate applied to the wool.

Reaction of modified fibroin with potassium nitrosyldisulphonate

Silk was methylated with a solution of diazomethane in ether as described by Rutherford *et al.*[15]. Methylation of the tyrosine hydroxyl groups was practically complete as the silk failed to form a red nickel nitroso complex[16] and gave only a very slight Millon reaction.

After treatment with 100 per cent of its weight of Frémy's salt for six hours, it was found that the untreated silk was the usual reddish-brown colour and only 1·6 per cent dissolved in calcium chloride–formic acid solvent[17]. The methylated fibroin, on the other hand, was only a pale pinkish buff colour after oxidation, and 97·8 per cent dissolved in the same solvent. The uptake of reagent was 2·2 and 28·9 per cent for the methylated and untreated proteins respectively.

DISCUSSION

The decreased solubility of wool in solutions both of alkali and of urea bisulphite after treatment with potassium nitrosyldisulphonate, coupled with its increased resistance to contraction in solutions of sodium bisulphite, suggests that new crosslinkages have been introduced into the keratin structure. This conclusion is supported by the finding that the greatly enhanced solubility of wool in alkali after the cystine residues have been ruptured with peracetic acid, is reduced considerably if the keratin be subsequently treated with Frémy's salt.

Although the lack of marked changes in the mechanical properties

of wool after treatment with potassium nitrosyldisulphonate may at first sight seem surprising, it has been suggested that this may occur if reaction takes place principally in amorphous rather than crystalline regions of the fibre[18]. This is known to occur when wool is treated with formaldehyde[19], although there is considerable evidence that crosslinking has, in fact, taken place[20]. It has been suggested, furthermore, that the increase in resistance to extension of wool fibres after treatment with other crosslinking agents, such as benzoquinone, is due not to true crosslinking, but to the deposition of polymer within the fibre[21]. Experiments on the highly crystalline silk fibroin, however, have shown that treatment with ten per cent of potassium nitrosyldisulphonate increases the breaking load of the filaments by 17 per cent and decreases the breaking extension by 27 per cent. There can, therefore, be no doubt that potassium nitrosyldisulphonate is capable of introducing new crosslinkages into fibrous proteins.

There is strong evidence in favour of modified tyrosine residues being involved in the new crosslinkages introduced into proteins by Frémy's salt. Prolonged treatment of wool with potassium nitrosyldisulphonate removes nearly all the tyrosine (*Table 4*) and blocking the hydroxyl group of these residues in silk fibroin completely inhibits the reaction. Furthermore, the coloration of the protein, which is directly proportional to the amount of Frémy's salt applied, shows indicator properties characteristic of quinone formation. Although coloration of proteins on oxidation may be associated also with the modification of tryptophan residues[22], insulin, which is devoid of these residues is coloured and completely insolubilized by potassium nitrosyldisulphonate. Furthermore silk, which contains approximately twice as much tyrosine as wool, but only half the amount of tryptophan, is coloured more intensely than wool. Finally there is the established efficacy of Frémy's salt to oxidize phenols to quinones[1]. Since potassium nitrosyldisulphonate takes several days to remove the tyrosine residues completely from insoluble proteins, it is hardly surprising that reaction is not confined exclusively to oxidizing these residues. Experiments on wool show that after the application of 50 per cent of reagent, cystine residues also are attacked (*Table 4*) and whereas ten per cent of Frémy's salt increases the strength of silk, further treatment decreases the strength indicating that degradation has occurred (*Table 5*).

It has been suggested previously that two possible crosslinkages could be formed when tyrosine residues in proteins are oxidized. These are a melanin-type dimer formed between two oxidized tyrosine residues[3] and the reaction product of a quinone with an amino group[2]. Since Zahn and Zuber[23] have shown that two tyrosine residues in silk fibroin may be bridged by bifunctional molecules such as *p,p'*-difluoro-*m,m'*-dinitrodiphenylsulphone, a melanin-type crosslinkage is stereochemically possible. On the other hand, the ease with which quinones react with amines at room temperature makes it difficult to eliminate the possibility that this will occur in proteins. A preliminary study of the infra-red absorption spectrum of wool oxidized with potassium nitrosyldisulphonate failed to show the presence of any new peaks which could be assigned to a possible crosslinkage, although this spectrum confirmed that some oxidation of cystine

to sulphonic acid groups had occurred. Although it is not possible at this stage to put forward a precise structure for these new crosslinkages the evidence from ultra-violet spectroscopy[3] suggests that both soluble and fibrous proteins are crosslinked in an identical manner.

The authors thank Mr E. Coates for helpful discussion on the reflectance data and Mr G. B. Benson and Mr D. E. Titheridge for experimental assistance.

Department of Textile Industries,
University of Bradford, England

(*Received May 1966*)

REFERENCES

[1] TEUBER, H. J. and RAU, W. *Chem. Ber.* 1953, **86,** 1036
[2] EARLAND, C. and STELL, J. G. P. *Biochim. biophys. Acta,* 1957, **23,** 97
[3] EARLAND, C., STELL, J. G. P. and WISEMAN, A. *J. Text. Inst.* 1960, **51,** T817
[4] PALMER, W. G. *Experimental Inorganic Chemistry,* p 281. Cambridge University Press: London, 1954
[5] MURIB, J. H. and RITTER, D. M. *J. Amer. chem. Soc.* 1952, **74,** 3394
[6] HARRIS, M. and SMITH, A. *J. Res. Nat. Bur. Stand.* 1936, **17,** 557
[7] LEES, K. and ELSWORTH, F. F. *Proceedings of the International Wool Textile Research Conference, Australia, 1955,* C363. C.S.I.R.O.: Melbourne, 1956
[8] SPEAKMAN, J. B. *J. Soc. Dy. Col.* 1936, **52,** 335
[9] SHINOHARA, K. *J. biol. Chem.* 1935, **109,** 665
[10] FOLIN, O. and MARENZIE, A. D. *J. biol. Chem,* 1929, **83,** 109
[11] LUGG, J. *Biochem. J.* 1937, **31,** 1422
[12] KRITZINGER, C. C. *J. Text. Inst.* 1960, **51,** T736
[13] KUBELKA, P. and MUNK, F. *Z. tech. Phys.* 1931, **12,** 593
[14] KUBELKA, P. *J. opt. Soc. Amer.* 1948, **38,** 448
[15] RUTHERFORD, H., PATTERSON, W. I. and HARRIS, M. *Amer. Dyest. Rep.* 1940, **29,** 583
[16] NILSSEN, B. *Symposium on Fibrous Proteins,* p 142. Society of Dyers and Colourists: Bradford, 1946
[17] EARLAND, C. and RAVEN, D. J. *Nature, Lond.* 1954, **174,** 461
[18] GHOSH, R. C., HOLKER, J. R. and SPEAKMAN, J. B. *Text. Res. (J.),* 1958, **28,** 112
[19] SPEAKMAN, J. B. and PEILL, P. L. D. *J. Text. Inst.* 1943, **34,** T70
[20] FRAENKEL-CONRAT, H. and OLCOTT, H. S. *J. biol. Chem.* 1948, **174,** 827
[21] STOVES, J. L. *Trans. Faraday Soc.* 1943, **39,** 301
[22] WARNER, R. C. and CANNAN, R. K. *J. biol. Chem.* 1942, **142,** 725
[23] ZAHN, H. and ZUBER, H. *Textilrdsch.* 1954, **9,** 119

Limiting Viscosity Number versus Molecular Weight Relations for Polyhexamethylene Oxide

KAZUHIKO YAMAMOTO and HIROSHI FUJITA

Relations between $[\eta]$ *and* $\overline{M}_w$ *were determined for polyhexamethylene oxide in benzene and in dioxan at 25°C, where* $[\eta]$ *is the limiting viscosity number and* $\overline{M}_w$ *is the weight-average molecular weight of the polymer. The samples studied ranged in* $\overline{M}_w$ *from the monomer to about* $1{\cdot}3 \times 10^4$. *Except for those of the monomer and the trimer, these values of* $\overline{M}_w$ *were determined from sedimentation equilibrium measurements in diethyl ketone at 25°C. Analyses of the viscosity data in terms of the Stockmayer–Fixman method, with* $2{\cdot}5 \times 10^{21}$ *assumed for Flory's* Φ *constant, yielded a value of* $1{\cdot}6_1$ *for the conformational parameter* σ. *Empirically, the values of* σ *so far obtained for the polyethers represented by* $[-O-(CH_2)_m-]_n$ *can be correlated in a linear fashion with the relative population of* CH_2-CH_2 *bonds in the chain,* $(m-1)/(m+1)$.

VALUES of the conformational parameter σ for the series of polyethers having the general structure $[-O-(CH_2)_m-]_n$ are now available for the first four members, polyoxymethylene[1] ($m=1$), polyethylene oxide[2] ($m=2$), polyoxacyclobutane[3] ($m=3$), and polytetrahydrofuran[4] ($m=4$), and for the limiting case of $m=\infty$, polyethylene[5]. All these values of σ have been estimated from the measured relations between $[\eta]$ and molecular weight by application of the method of Stockmayer and Fixman[6], with a suitable value (usually $2{\cdot}5 \times 10^{21}$) being assumed for Flory's Φ constant. Here $[\eta]$ stands for the limiting viscosity number. With the interest in obtaining further information on the flexibility of the polyether chain of this type, we have extended a viscometric study to the sixth member of the series, i.e. polyhexamethylene oxide. The results obtained are reported in this paper.

EXPERIMENTAL

Polymer sample

The monomer *n*-hexamethylene glycol was extracted by repeated crystallization from a commercial product dissolved in a 2/3 (by weight) acetone–ether mixture. Its melting point was 42·8°C, and the absence of isomers in it was checked by i.r. spectrum.

Polymerization was carried out in a reaction tube designed in accordance with the suggestions of Rhoad and Flory[7]. After 10 g of the monomer together with 0·2 to 0·3 g of concentrated sulphuric acid had been introduced, the tube was evacuated thoroughly. It was then heated at the boiling point (195·7°C) of ethylene glycol for three hours under a constant stream of dry nitrogen. Finally, the tube was further heated at the same temperature, but this time keeping its inside at a pressure lower than 1 mm of mercury. Samples of different degree of polymerization were produced by

varying the interval of this heating process. The product formed was dissolved in hot methanol (about 50°C) and precipitated by cooling the solution to room temperature (about 20°C). The precipitate, being coloured dark brown, was dissolved in hot ethanol with activated charcoal, filtered, and the white material precipitated was freeze-dried from a benzene solution. In this way, we prepared a number of samples, but no success was achieved in synthesizing a sample which had a weight-average molecular weight exceeding about 7 000. We therefore attempted extracting such a sample from a lower molecular weight sample by fractional precipitation. To this end, a sample of relatively high molecular weight was chosen, dissolved in methylethyl ketone at 30°C, and the solution was brought to phase separation at 28°C. The fraction extracted from the bottom phase, designated below as sample 611, was found to have a weight-average molecular weight over $1{\cdot}3 \times 10^4$.

In addition to the polymer samples prepared in this way, we chose the monomer and trimer as the objects of physical measurements. The trimer tri-hexane-1,6-diol was synthesized using the method of Hobin[8], and its purity was checked by both elemental analysis and i.r. spectrum.

Solvent

Benzene and dioxan were used for viscosity measurements and diethyl ketone for sedimentation equilibrium experiments. These were dried with molecular sieves and fractionally distilled before use; the boiling points of the fractions collected were 80·0° to 80·1°C for benzene, 101·0° to 101·5°C for dioxan, and 101° to 102°C for diethyl ketone.

Molecular weight determination

The molecular weight of the monomer was taken as its formula value. That of the trimer was determined by the method of freezing point depression, using benzene as solvent.

For all other samples their weight-average molecular weights $\overline{M}_w$ were evaluated from sedimentation equilibrium data taken in diethyl ketone at 25°C. Use was made of a Spinco model E ultracentrifuge equipped with the Rayleigh interference optical system. The short column technique was employed, with no bottom liquid being introduced. Rotor speeds were chosen in such a way that the ratio of the equilibrium concentrations at the ends of the solution column never exceeded three*.

For sample 611 the data were at two initial concentrations (0·3 to 0·5 g/dl), and the apparent molecular weights M_{app} obtained were extrapolated to zero concentration by making use of the relation[9] $1/M_{app} = 1/\overline{M}_w + 2A_2'\bar{c}$, where A_2' is the light-scattering second virial coefficient of the system and $\bar{c}$ is the arithmetic mean of the equilibrium solute concentrations at the ends of the solution column. The values obtained for $\overline{M}_w$ and A_2' were $1{\cdot}33 \times 10^4$ and $3{\cdot}8 \times 10^{-3}$ ml mole/g^2, respectively. For

*The partial specific volume $\bar{v}$ of the polymer in diethyl ketone at 25°C and the specific refractive index increment dn/dc of this polymer–solvent pair were 1·045 ml/g and 0·088 ml/g, respectively, when measured on sample 606. In the region of relatively low polymers, both $\bar{v}$ and dn/dc may vary with molecular weight but, for simplicity, these data obtained with a particular sample were used throughout for all molecular weight calculations.

each of the other samples the measurement was made only at one initial concentration, and the desired $\overline{M}_w$ was calculated by inserting the measured M_{app} into the above relation with $3{\cdot}8 \times 10^{-3}$ being assumed for A_2' irrespective of the magnitude of M_{app}. This convention may not be valid but, unless the variation of A_2' with molecular weight is too pronounced, the error introduced would be at most a few per cent in the region of $\overline{M}_w$ below 10^4.

Viscosity measurement

The measurements were performed at $25 \pm 0{\cdot}01$°C, using an Ubbelohde viscometer of the suspended-meniscus type which had an efflux time of 430·0 sec for benzene at 25°C. The desired value of the limiting viscosity number $[\eta]$ was determined as a common intercept of η_{sp}/c versus c, η_{sp}/c versus η_{sp}, and $(\ln \eta_{rel})/c$ versus c. Here η_{rel} is the relative viscosity, η_{sp} is the specific viscosity, and c is the solute concentration expressed in grammes per decilitre. The Huggins slope parameter k' was evaluated from the slope of the plot for η_{sp}/c versus η_{sp}.

RESULTS AND DISCUSSION

Limiting viscosity number versus molecular weight relations

Table 1 summarizes the numerical data obtained, and *Figure 1* shows the conventional double logarithmic plots for $[\eta]$ versus $\overline{M}_w$. The solid lines in

Table 1. Numerical results obtained for samples of polyhexamethylene oxide

Sample No.	$\overline{M}_w \times 10^{-3}$	$[\eta]$* *dioxan 25°C*	k'	$[\eta]$* *benzene 25°C*	k'
601	0·118†	$0{\cdot}016_5$	1·7	—	—
602	0·318‡	$0{\cdot}034_6$	$0{\cdot}6_1$	$0{\cdot}034_2$	0·58
603	1·09	$0{\cdot}059_2$	$0{\cdot}5_2$	$0{\cdot}062_8$	$0{\cdot}5_0$
604	1·72	$0{\cdot}086_2$	$0{\cdot}4_6$	$0{\cdot}092_5$	$0{\cdot}5_7$
605	2·60	$0{\cdot}098_7$	$0{\cdot}4_3$	$0{\cdot}10_9$	$0{\cdot}4_5$
606	3·40	$0{\cdot}11_1$	$0{\cdot}3_9$	$0{\cdot}12_3$	$0{\cdot}4_2$
607	4·18	$0{\cdot}12_5$	$0{\cdot}4_0$	$0{\cdot}13_8$	$0{\cdot}4_1$
608	4·39	$0{\cdot}13_4$	$0{\cdot}4_2$	—	—
609	6·69	$0{\cdot}16_3$	$0{\cdot}4_0$	$0{\cdot}19_0$	$0{\cdot}3_4$
610	6·86	$0{\cdot}16_6$	$0{\cdot}3_7$	$0{\cdot}19_5$	$0{\cdot}3_3$
611	13·3	$0{\cdot}24_7$	$0{\cdot}3_5$	$0{\cdot}30_4$	$0{\cdot}3_1$

*In dl/g.
†Formula value.
‡Determined cryoscopically with benzene as solvent.

the figure have been drawn to fit the plotted points for samples of $\overline{M}_w$ above 1 000, and can be represented by the following Mark–Houwink–Sakurada equations:

$$[\eta] = 1{\cdot}3_1 \times 10^{-3} \overline{M}_w^{0{\cdot}55} \quad \text{(in dioxan at 25°C)}$$

$$[\eta] = 8{\cdot}6_9 \times 10^{-4} \overline{M}_w^{0{\cdot}62} \quad \text{(in benzene at 25°C)}$$

Evaluation of the conformational parameter σ

The Stockmayer–Fixman plots obtained from the data of *Table 1* are

shown in *Figure 2*. Except for the point for the monomer, the data on either system are reasonably well fitted by a straight line having a common intercept on the ordinate axis. If, as before[3], we assume $2{\cdot}5 \times 10^{21}$ for

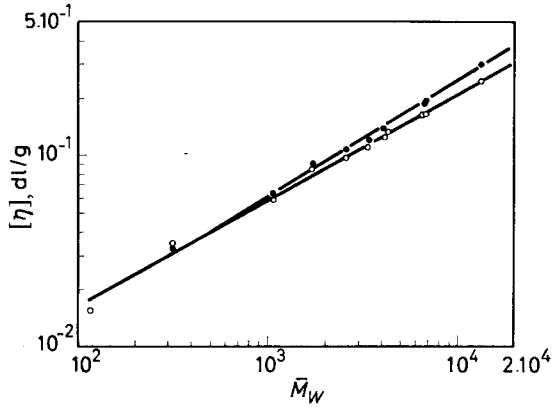

Figure 1—Double logarithmic plots for limiting viscosity number $[\eta]$ and weight-average molecular weight $\overline{M}_w$ on polyhexamethylene oxide in dioxan ○, and in benzene ●, both at 25°C

Flory's Φ constant, this intercept value ($1{\cdot}8_5 \times 10^{-3}$ dl mole/$g^{2/3}$) yields $1{\cdot}6_1$ for the conformational parameter σ of polyhexamethylene oxide. Here σ^2 is defined as the mean square end-to-end distance of a polymer chain in a theta solvent relative to that which would be obtained if the hindrance to internal rotation of the chain were absent except for the bond angle restrictions.

Figure 2 — Stockmayer–Fixman plots for polyhexamethylene oxide in dioxan ○, and in benzene ●, both at 25°C

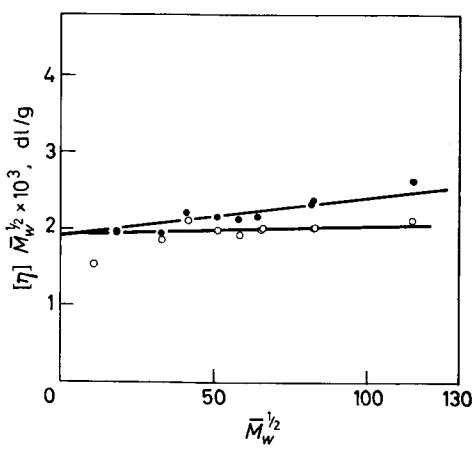

The validity of the σ value obtained above may be criticized because it is based on extrapolation from data for samples of $\overline{M}_w$ below $1{\cdot}3 \times 10^4$. In the ordinary sense, the samples used in this study may not belong to the category of typical high polymers when viewed in terms of their molecular weights. However, in terms of the number of single bonds constituting the backbone chain, even a sample of as low a molecular weight as 1 000 already contains 70 such bonds. Unless the internal rotation of each bond is restricted too much, this number of single bonds would be sufficient for

the chain to take a randomly coiled conformation. This implies that, at least in the region of $\bar{M}_w$ above 1 000, the viscosity data obtained above for samples of polyhexamethylene oxide manifest features characteristic of long-chain polymer molecules and thus may be analysed, with fair confidence, in terms of the theory of Stockmayer and Fixman to evaluate the conformational parameter for this polymer.

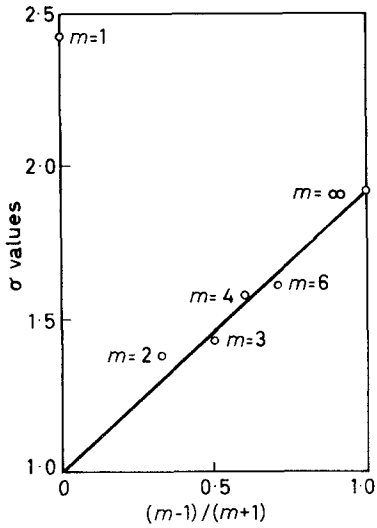

Figure 3—Correlation plots between σ and $(m-1)/(m+1)$ for the series of polyethers having the general structure $[-O-(CH_2)_m-]_n$. The σ values other than that for polyhexamethylene oxide ($m=6$) were taken from *Table 2* of ref. 3

Now the values of σ have become available for six members of the polyether series considered. It is of great theoretical interest to investigate, by the method of conformational statistics, how these values are correlated with the structural feature of each member, especially the number of methylene groups, m, intervening between ether oxygen atoms. In fact, an effort toward this problem is being made by Flory and Mark[10,11]. In this paper, we are content with pointing out that, as illustrated in *Figure 3*, the σs for members higher than polyethylene oxide appear to be related linearly to the relative population of CH_2—CH_2 bonds in the chain, i.e. $(m-1)/(m+1)$.

We wish to thank Dr A. Teramoto for his valuable discussion.

Department of Polymer Science,
Osaka University,
Toyonaka, Japan

(*Received July 1966*)

REFERENCES

[1] STOCKMAYER, W. H. and CHAN, L.-L. Unpublished data
[2] KURATA, M. and STOCKMAYER, W. H. *Fortschr. HochpolymForsch.* 1963, **3,** 196
[3] YAMAMOTO, K., TERAMOTO, A. and FUJITA, H. *Polymer, Lond.* 1966, **7,** 267
[4] KURATA, M., UTIYAMA, H. and KAMADA, K. *Makromol. Chem.* 1965, **88,** 281
[5] CHIANG, R. J. *J. phys. Chem.* 1965, **65,** 1645

[6] STOCKMAYER, W. H. and FIXMAN, M. *J. Polym. Sci. C*, 1963, **1**, 137
[7] RHOAD, M. J. and FLORY, P. J. *J. Amer. chem. Soc.* 1950, **72**, 2216
[8] HOBIN, T. P. *Polymer, Lond.* 1965, **6**, 403
[9] FUJITA, H. *Mathematical Theory of Sedimentation Analysis*, Chap. V. Academic Press: New York, 1962
[10] FLORY, P. J. and MARK, J. E. *Makromol. Chem.* 1964, **75**, 11
[11] MARK, J. E. and FLORY, P. J. *J. Amer. chem. Soc.* 1965, **87**, 1415

An Infra-red–Deuteration Study of the Grafting of Vinyl Polymers into Nylon Films

R. JEFFRIES and SUSAN HAWORTH

This paper describes an infra-red and deuteration study of films of Nylon 6.6 into which poly(acrylic acid) has been grafted. The results suggest that the grafted polymer penetrates all the regions of the Nylon accessible to deuterium oxide. The infra-red NH*-stretching band of the amide groups in the 'penetrated' regions is broadened by the presence of the polyacid and the rate of deuteration of these amide groups in deuterium oxide is increased. It is concluded that the amide–amide interactions in these accessible regions are weakened or disrupted by the presence of the polyacid. A few results are presented for Nylon 11 films, and on grafting polyacrylamide into Nylon films.*

THE study reported in this paper arose out of the recent work of Haworth and Holker[1] on the grafting of some vinyl polymers into Nylons using ceric salts as initiators. Its purpose was to investigate, by means of infra-red (i.r.) and deuteration techniques, the proportion of the Nylon structure penetrated by the grafted polymer, and the nature of any interaction between the two types of molecule. The principal system studied was poly(acrylic acid) grafted into Nylon 6.6; grafting of poly(acrylic acid) into Nylon 11, and polyacrylamide into Nylon 6.6, are dealt with only briefly.

EXPERIMENTAL

Preparation of Nylon films

Films of the Nylon (4 to 6 μ thick) were prepared from solutions of 0·6 g Nylon in a mixture of 95 ml formic acid, 5 ml water and 2 ml concentrated hydrochloric acid. Nylon 6.6 was soluble at room temperature and the films were cast on glass plates; Nylon 11 was soluble in hot solvent only, and films were formed as a skin on the solution during cooling. The films were freed from any residual formic acid by washing in water.

Grafting technique

Nylon film was treated for various times at room temperature in a 10 per cent v/v solution of acrylic acid in 0·01M ceric ammonium sulphate (the initiator)–0·2N sulphuric acid. The grafted films were rinsed in 2N sulphuric acid, followed by water. The proportion of grafted poly(acrylic acid) relative to Nylon was estimated by weighing the dried films (see *Table 1*).

Table 1

Time of treatment, h	0·1	0·2	0·5	1	3	24	24 (two treatments)
Per cent by wt grafted polymer	5	45	100	130	160	200	300

Sodium and calcium salts of the grafted polymer were prepared by immersing the film in solutions of sodium hydroxide and calcium acetate,

respectively, for 30 min, followed by rinsing in water.

Polyacrylamide was grafted into Nylon film by treating the film with a 10 per cent w/v solution of acrylamide in a solution of 0·01M ceric ammonium nitrate in 0·6N nitric acid; grafted films were washed and dried.

Preparation of film from solution of grafted polymer

Certain of the Nylon films containing grafted polymer were dissolved in formic acid and re-cast into films on microscope cover glasses. Film-casting was done initially on small plates of calcium fluoride, but in some circumstances this material is an unsuitable base for casting films (see below). With some of the grafted films it was necessary to warm the formic acid to achieve complete dissolution. Heavily grafted Nylon 11 samples were partially insoluble even in hot formic acid, and these films had to be re-cast from the decanted solutions.

Infra-red and deuteration techniques

Infra-red spectra were measured on a Grubb–Parsons double-beam spectrometer with a lithium fluoride prism. Samples of film were mounted in brass vacuum cells with calcium fluoride windows; the re-cast films were usually mounted and studied without being removed from the cover glass or calcium fluoride plate. Some spectra were obtained with air-dry samples, but most measurements (including all the spectra shown in the figures) were made on samples which had been dried by evacuation through a cold trap. Films were deuterated in the brass cells in the absence of air; deuteration was effected in deuterium oxide vapour (either saturated or at 75 per cent r.h., as indicated in the legends to the figures) at 20°C, the deuterated samples being dried by evacuation before i.r. study.

For clarity, it should be emphasized that in this paper the various features of the i.r. spectra are discussed in terms of peak intensity, peak frequency, and band width; integrated band intensities, as such, are not discussed.

RESULTS AND DISCUSSION

The i.r. and deuteration behaviour of untreated Nylon films has been discussed elsewhere[2-5]: for clarity in the subsequent discussion, however, it is first necessary to describe briefly the infra-red–deuteration behaviour of the untreated Nylon films used in this work. *Figure 1* shows i.r. spectra in the 3μ region of Nylon 6.6 film, in the undeuterated form and after deuteration for a short and a long period in saturated vapour at 20°C. The main features of interest in the spectrum of untreated films are the intensity and width of the NH-stretching band near 3 300 cm^{-1}, the relative intensities of the components of the 3 070 cm^{-1} overtone[4], and the resolution of the 2 870 cm^{-1} CH band. Decreasing the structural order in the film reduces the intensity and increases the width of the NH band, increases the intensity of the high frequency component of the overtone relative to that of the low frequency component, and decreases the resolution of the CH doublet. Deuterium oxide penetrates the less ordered parts of the polyamide structure, i.e. those parts containing the weaker and more 'disordered' amide–amide interactions, and $H \longrightarrow D$ exchange takes place on the amide NH

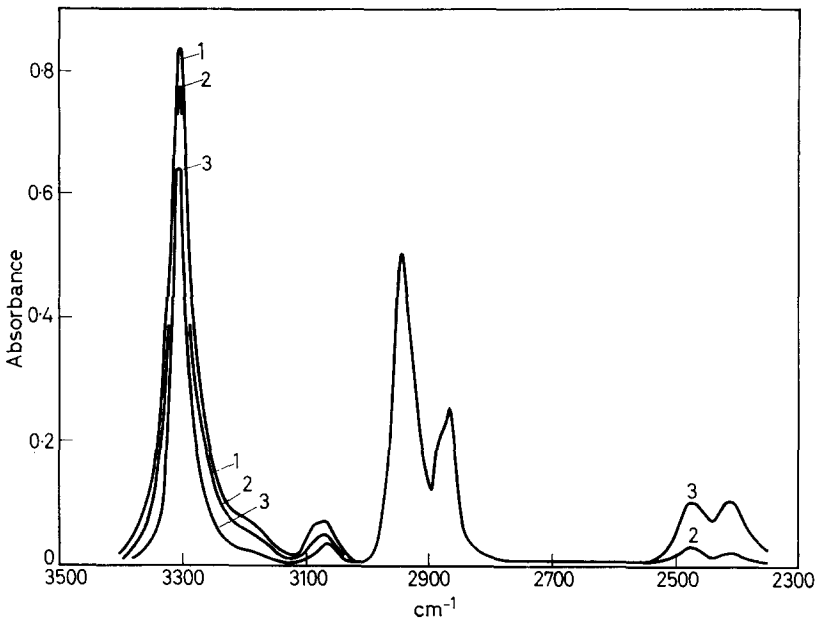

Figure 1—The deuteration of Nylon 6.6 film: 1, undeuterated; 2, deuterated half an hour in saturated vapour; 3, deuterated 10 days in saturated vapour. Sample dried by evacuation before each i.r. spectrum measured

groups in these regions. The extent of the isotopic exchange is thus a measure of the disorder in the structure[2,5]. These 'disordered' amide groups give rise to a broader NH-stretching band than the amide groups in the more ordered regions, and thus the effect of deuteration is to remove the broader component of the NH band, leaving the narrower component of the ordered, inaccessible, amide groups[5]. The effect of deuteration in reducing the intensity and the width of the NH band is clear in *Figure 1*. Deuteration also increases the intensity of the low frequency component of the 3 070 cm^{-1} overtone relative to the high frequency component, thus confirming the association between this relative intensity and order–disorder in Nylon. The doublet in the 2 400 cm^{-1} region, which increases in intensity as deuteration progresses, is not a simple ND-stretching band, as has been discussed elsewhere[2,3].

Nylon 6.6 films prepared by the present solvent-casting technique tended to vary slightly in degree of order: the intensity of the NH stretching band, relative to the intensity of the 2 935 cm^{-1} CH band, varied from sample to sample between 1·5 to 2, the more intense bands being the narrower; the fraction of the NH groups accessible to deuterium oxide, the relative intensities of the two components of the overtone at 3 070 cm^{-1}, and the resolution of the 2 870 cm^{-1} CH doublet, also varied slightly. A closer control of the conditions under which the solvent is evaporated would probably eliminate much of this variability.

Spectra of films cast on calcium fluoride plates and allowed to dry at room temperature exhibit unusual characteristics. The NH band contains

a distinctly broader component than the NH band of glass-cast film, or film dried down at 100°C on calcium fluoride; this broader component is rapidly removed by deuteration. With air-dry samples this broad component is associated with a shoulder on the high-frequency side of the NH band larger than that observed with glass-cast film; this shoulder, at least in glass-cast film, is due to absorbed water. These facts suggest that the film dried on calcium fluoride at room temperature is more disordered, and thus more moisture-sorptive, than glass-cast film. This difference in structure may be associated with the slight solubility of calcium fluoride in the solvent formic acid.

The infra-red–deuteration behaviour of Nylon 11 films is qualitatively similar to that of Nylon 6.6 films. The most obvious difference, as would be expected, is the lower intensity of the NH-stretching band relative to the intensity of the 2 935 cm^{-1} CH band (about 0·45 with the present Nylon 11 films).

Poly(acrylic acid) grafts

Figure 2 illustrates the spectra of Nylon 6.6 film into which 50 per cent and 200 per cent poly(acrylic acid) has been grafted, and the spectrum of poly(acrylic acid) itself; the very broad OH band of the latter, centred on about 3 100 cm^{-1}, is typical of that generally obtained with carboxylic acids.

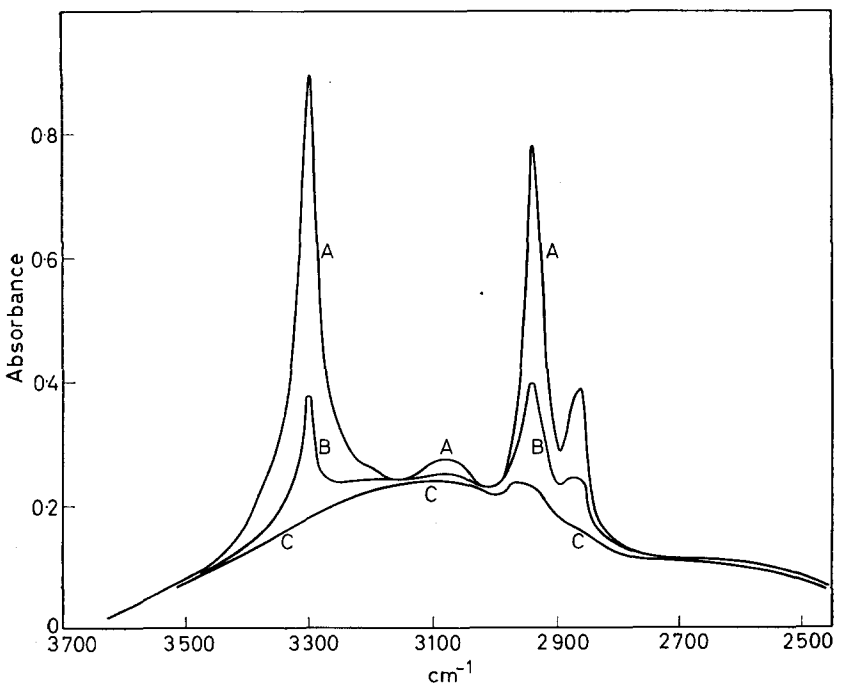

Figure 2—The i.r. spectrum of Nylon 6.6 film containing grafted poly(acrylic acid): A, 50 per cent poly(acrylic acid) on weight of Nylon; B, 200 per cent poly(acrylic acid) on weight of Nylon; C, poly(acrylic acid)

It is clear that the spectrum of grafted Nylon 6.6 in *Figure 2* is approximately a combination of the spectra of Nylon (*Figure 1*) and poly(acrylic acid) (*Figure 2*); this applies, in fact, to the whole spectrum of the grafted film, from 3μ to 15μ. In *Figure 2* the samples A and B are chosen to contain about the same weight per unit area of polyacid, i.e. to give a broad, 'polyacid' background of about the same intensity; the poly(acrylic acid) spectrum is also chosen to be at about this background level of intensity. Detailed examination of the spectra in *Figure 2*, however, shows that the well-defined NH band is reduced in intensity and width compared with that of untreated Nylon, particularly at the higher concentrations of polyacid (above about 200 per cent). [N.B. In estimating the intensity of the NH band relative to the CH band it is necessary to allow for the CH absorption of the polyacid.] The relative intensity of the two components of the 3 070 cm^{-1} overtone is also different, at least at the higher polyacid contents. The significance of these changes will be made clear below.

On deuteration of a film containing a large proportion of grafted polyacid (*Figure 3*) the broad background due to poly(acrylic acid) is rapidly removed, indicating that all of the OH groups in the polyacid are readily

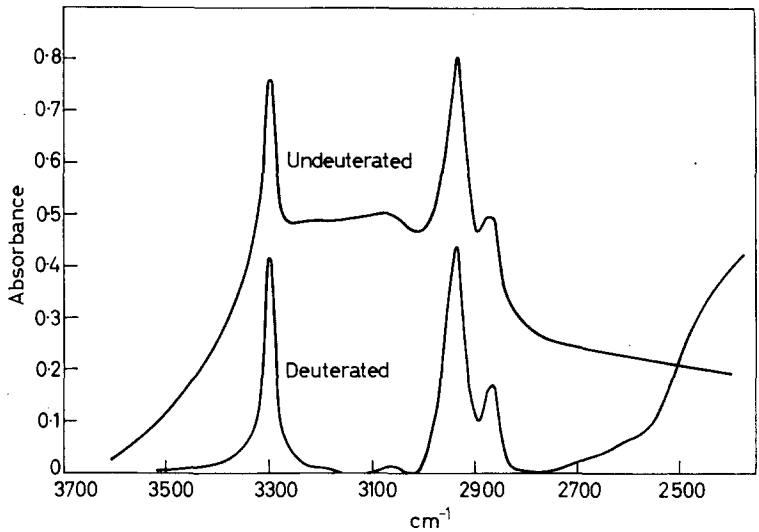

Figure 3—The deuteration of Nylon 6.6 film containing 200 per cent by weight of grafted poly(acrylic acid), deuterated for half an hour in saturated vapour

accessible to, and deuterated by, deuterium oxide. The spectrum of the deuteration-resistant material is similar in intensity and width of the NH band, and shape of the 3 070 cm^{-1} overtone, to that of ungrafted Nylon 6.6 after prolonged exchange (curve 3 in *Figure 1*), and also to the well-defined peaks on the spectrum of the grafted film before deuteration (*Figure 2*).

These i.r. and deuteration results support the hypothesis that the accessible regions in the original Nylon film (those which exchange after several

days in deuterium oxide vapour) are completely penetrated by the grafted polymer, at least at the higher concentrations. The effect of the polyacid may be either to weaken and disorder the amide interactions, or to replace them by interactions between the amide group and the carboxyl groups in the polyacid (hydrogen bonds involving both the carbonyl and the NH of the amide are possible). Modification of the amide interactions in the D_2O-accessible regions must clearly change the characteristics of their NH absorption. An increase in band width would be expected, causing this part of the NH band to merge into the broad OH background of the polyacid, but leaving unaffected the narrower NH band due to the amide groups in the 'ungrafted' regions (*Figure 2*). This lessening of the amide interactions also explains the high rate of NH $\longrightarrow$ ND exchange in heavily grafted co-polymer; all the NH groups in the grafted (D_2O-accessible) regions exchange within 10 to 15 min, compared with several days for ungrafted film. This behaviour suggests that the slow deuteration of the accessible regions of ungrafted film may be partly the result of the fairly high degree of amide interaction in these regions.

To confirm these conclusions, grafted film was dissolved in formic acid and then re-cast; spectra of the re-cast films are shown in *Figure 4*, for two levels of poly(acrylic acid) content. The NH band of film containing 200 per cent polyacid is very broad, almost merging with the broad OH background, and its peak frequency is distinctly higher than that of the NH band of ungrafted Nylon. Deuteration of this re-cast film (*Figure 4*) rapidly removes the broad NH and OH bands, i.e. all the amide groups are readily accessible and rapidly exchangeable. These results suggest that the polyamide chains in re-cast film are dispersed in a matrix of polyacid, so that amide–amide interactions are either weakened or replaced by amide–carboxyl interactions.

The NH band of a recast film from Nylon 6.6 containing about 100 to 130 per cent grafted polyacid is rather less broad than that of the '200 per cent' film (*Figure 4*), though still broader and of a higher peak frequency than the NH band of untreated Nylon film. This is presumably because the amide interactions are more numerous or stronger than in the higher concentration film; '100 per cent to 130 per cent' re-cast films, in fact, must sometimes contain a few strong amide interactions, since their spectra occasionally exhibit a small, narrow NH band (see, e.g., the spectrum in *Figure 4*). The NH groups in '100 per cent to 130 per cent' re-cast film deuterate rapidly, apart from the few strongly associated ones sometimes present.

When a re-cast film is washed in water, and then re-dried, a narrow, 'deuteration-resistant', NH band of moderate intensity reappears in its spectrum (*Figure 5*). The remaining, 'broad' part of the NH band also narrows somewhat, but still exchanges readily (*Figure 5*). Swelling the re-cast film in water must free the structure sufficiently to allow chain rearrangements and hence re-formation of regular, strong, amide interactions to occur.

As expected, formation of the sodium or calcium salt of the polyacid in a grafted film has an effect similar to deuteration, reducing the broad OH

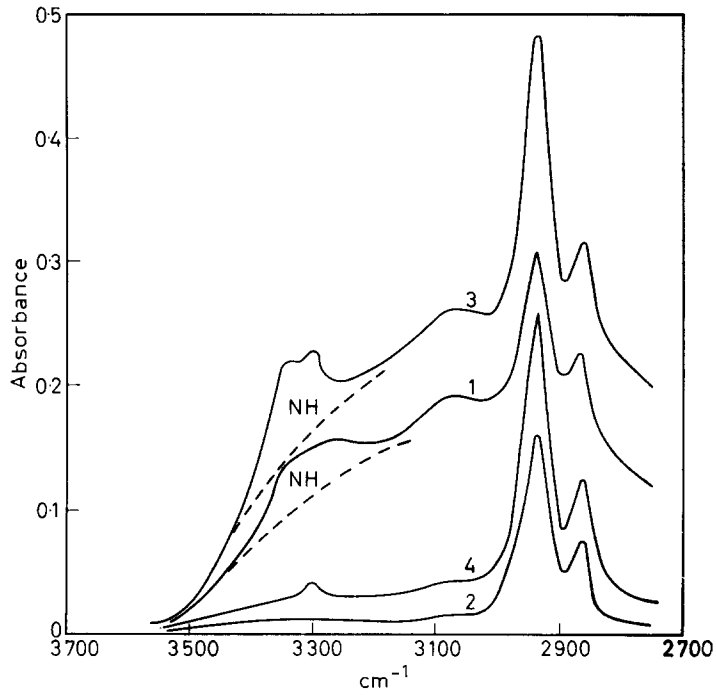

Figure 4—The i.r. spectrum of film of Nylon 6.6 with grafted poly(acrylic acid) re-cast from solution in formic acid: 1, Nylon 6.6+200 per cent poly(acrylic acid); 2, Nylon 6.6+200 per cent poly(acrylic acid), deuterated; 3, Nylon 6.6+100 to 130 per cent poly(acrylic acid); 4, Nylon 6.6+100 to 130 per cent poly(acrylic acid), deuterated. Samples deuterated in 75 per cent r.h. deuterium oxide vapour for three hours. ——————— estimated OH background due to the grafted poly(acrylic acid)

background in the spectrum of the dry film practically to zero. These films are very hydrophilic, to judge from the size of the shoulder on the high frequency side of the NH band of films in equilibrium with the atmosphere; this is particularly so with the sodium salts, in agreement with the moisture regain results of Magat and co-workers[8]. The free acid films are readily regenerated from the salt-form by treatment with dilute mineral acid.

The Nylon 11 plus poly(acrylic acid) system behaves in a qualitatively similar manner to the Nylon 6.6 plus polyacid system, as regards the general features of the spectra, and the effects of deuteration and of re-casting the grafted film.

Cannon[4], Barmby and King[6], and Wood and King[7] have described the effect of swelling agents (*o*-cresol, phenol, formic acid, antimony trichloride) on the 3μ-region spectrum of Nylon 6.6 and Nylon 6. The effect of the swelling agent was in general similar to that of the grafted poly(acrylic acid). Thus the sharp NH band at 3 300 cm^{-1} is gradually decreased in intensity as the concentration of swelling agent is increased and a broader

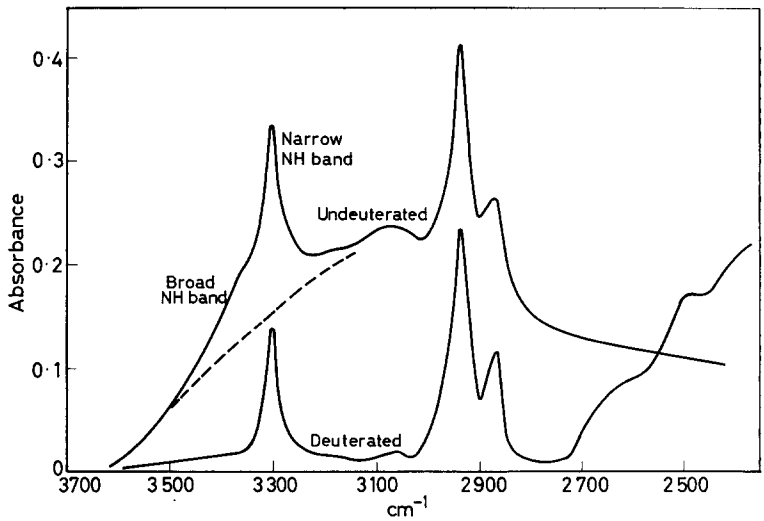

Figure 5—The effect of treatment with water on 're-cast' film of Nylon 6.6+200 per cent poly(acrylic acid). Deuterated three hours in 75 per cent r.h. deuterium oxide vapour. — — — — — — estimated OH background due to the grafted poly(acrylic acid)

NH band gradually appears at a higher frequency[6,7]. At a sufficiently high concentration of swelling agent the 3 300 cm^{-1} NH band eventually disappears, i.e. the whole of the polyamide structure is penetrated by swelling agent, whereas in the present work, only the D_2O-accessible regions are

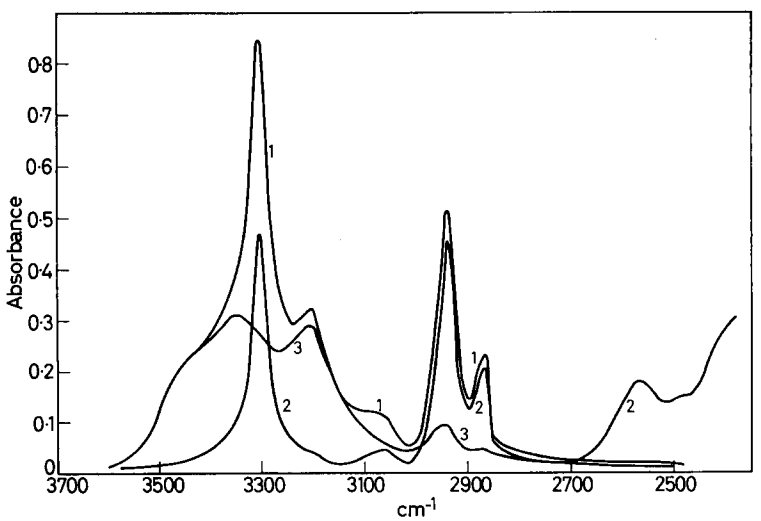

Figure 6—The i.r. spectrum of Nylon 6.6 film containing 100 per cent by weight of grafted polyacrylamide: 1, undeuterated; 2, deuterated quarter of an hour in saturated vapour; 3, polyacrylamide

penetrated by graft polymer, even at high concentrations of the latter. Dissolution of the grafted film and re-casting is necessary to produce a completely 'penetrated' structure.

Polyacrylamide

Some i.r. measurements were made on films of Nylon 6.6 into which polyacrylamide had been grafted. Unfortunately, it was not possible to graft more than 100 per cent by weight of the polyacrylamide into the Nylon, making comparison with poly(acrylic acid) difficult, since the effects of the polyacid on Nylon are most clearly defined at an add-on rather in excess of this value. As with the film containing grafted poly(acrylic acid), the i.r. spectrum of Nylon 6.6 film containing an equal weight of grafted polyacrylamide (*Figure 6*) can be approximately described in terms of the superposition of the spectra of Nylon and polyacrylamide. Deuteration of this grafted film causes rapid disappearance of the polyacrylamide component of its spectrum, hence the grafted polyacrylamide is clearly completely accessible to, and deuterated by, the deuterium oxide. Re-casting the graft copolymer from a solution in formic acid gives a film with a spectrum in the 3μ region which is not very different from that of the original grafted film; this behaviour contrasts strongly with film containing an equal weight of grafted polyacrylic acid, which after dissolution and re-casting gives a film with a very different spectrum (*Figure 4*).

The Cotton, Silk and Man-Made Fibres Research Association,
Shirley Institute,
Didsbury, Manchester

(*Received July 1966*)

REFERENCES

[1] HOLKER, J. R. and HAWORTH, S. *J. Soc. Dy. Col.* 1966, **82,** 257
[2] CANNON, C. G. *Spectrochim. Acta,* 1960, **16,** 302
[3] CANNON, C. G., STACE, B. C. and JEFFRIES, R. *Nature, Lond.* 1962, **196,** 436
[4] CANNON, C. G. *Mikrochim. Acta,* 1955, **2,** 555
[5] JEFFRIES, R. *J. Polym. Sci. A,* 1964, **2,** 5161
[6] BARMBY, D. S. and KING, G. *Proceedings* of the International Wool Textile Research Conference, Australia, 1955, *B,* 139
[7] WOOD, F. and KING, G. *J. Text. Inst.* 1963, **54,** T111
[8] MAGAT, E. E., MILLER, I. K., TANNER, D. and ZIMMERMAN, J. *J. Polym. Sci. C,* 1963, **1,** No. 4, 615

Initiation of Polymerization by Ammonium Trichloracetate in the Presence of Copper Derivatives — A Tracer Study

C. H. BAMFORD and V. J. ROBINSON*

The mechanism of the initiation of the free-radical polymerization of methyl methacrylate by ammonium trichloracetate in the presence of copper derivatives has been studied with the aid of ^{14}C labelling of the salt in the two positions. An earlier suggestion that the mechanism depends critically on the salt concentration has been confirmed. At low salt concentrations in the presence of $Cu(acac)_2$ *the initial radicals formed are exclusively* $\dot{C}Cl_3$ *[equation (2)]. At high salt concentrations, initiation by* CuCl *involves formation of* $\dot{C}OO^-$ *predominantly, but some production of* $\dot{C}Cl_3$ *may also occur [equation (5)]. High salt concentrations together with* $Cu(acac)_2$ *yield* $\dot{C}Cl_3$ *radicals [equation (9)]. It is suggested that, with high salt concentrations, termination by derivatives of* Cu^{II} *occurs, with formation of* Cu^{I}*, which may then react further. In this way cyclic processes involving alternate oxidation and reduction of copper may arise.*

IN A recent paper[1] we showed that the free-radical polymerization of methyl methacrylate may be initiated by ammonium trichloracetate in the presence of a suitable copper derivative, particularly cupric acetylacetonate. It was established that the nature of the initiation process depends on the concentration of ammonium trichloracetate, a comparatively simple kinetic mechanism at low concentrations ($< 10^{-3}$ mole l^{-1}) being replaced by a much more complicated reaction at higher concentrations ($> 10^{-2}$ mole l^{-1}). Although suggestions about the reaction mechanisms involved were advanced on the basis of kinetic evidence, the unusual behaviour of the system, particularly at high salt concentrations, made it desirable to obtain additional independent information about the reactions occurring. In the present paper we describe investigations with ammonium trichloracetate labelled with carbon-14; two specimens of the salt were employed, labelled at each carbon atom separately, i.e. $^{14}CCl_3COONH_4$ and $CCl_3{}^{14}COONH_4$. Since free-radical formation involves the reduction $Cu^{II} \longrightarrow Cu^{I}$ we have also studied the interaction between cuprous chloride and ammonium trichloracetate. The experiments consisted essentially in determining the extents to which the labelled groups become incorporated into the polymers during polymerization initiated by the different systems. Methyl methacrylate was the monomer used throughout the work.

EXPERIMENTAL

Materials

Methyl methacrylate was purified as described previously[1].

Cupric acetylacetonate was recrystallized from benzene or cyclohexane

*Present address: Department of Inorganic Chemistry, University of Manchester.

Analytical reagent grade cuprous chloride was used without further purification.

Inactive ammonium trichloracetate was prepared by neutralizing analytical reagent grade trichloracetic acid with analytical reagent grade ammonia (s.g. 0·880) and recrystallizing the product from water. The salt was dried *in vacuo* at room temperature. Labelled samples were prepared similarly from the respective acids $^{14}CCl_3COOH$, $CCl_3{}^{14}COOH$, obtained from the Radiochemical Centre, Amersham. The final activities of the materials used in the work described were $1{\cdot}35 \times 10^8$ and $2{\cdot}16 \times 10^8$ dis. mole^{-1} sec^{-1} for the CCl_3- and COOH-labelled samples, respectively.

Technique

Reaction mixtures were degassed by conventional freezing, pumping and melting cycles, and finally sealed under vacuum. All polymerizations were carried out in inactive (sodium) light. Rates of polymerization were generally determined dilatometrically. In all cases conversions were kept below ten per cent.

The polymers formed at high salt concentrations had rather low molecular weights and could not be isolated satisfactorily by precipitation into methanol, on account of the possibility of fractionation. The following procedure was therefore adopted. The reaction mixture was diluted with benzene, and all volatile materials (benzene and excess monomer) were removed by freeze-drying at room temperatures. The residue, containing polymer and unreacted ammonium trichloracetate, was again dissolved in benzene, and inactive ammonium trichloracetate added. The salt was then extracted with distilled water. Further inactive ammonium trichloracetate was added to the benzene solution, and the extraction repeated. After several repetitions of this process the benzene and water were removed by freeze-drying and the activity of the polymer measured. It was found that after three or four extractions the activity of the polymer had attained a constant value, showing that all the free labelled salt had been removed.

The polymers prepared at low salt concentrations had sufficiently high molecular weights to allow isolation by precipitation into methanol. This was followed by two or three further precipitations from chloroform solutions containing inactive ammonium trichloracetate.

Molecular weights of the polymers were measured viscometrically in benzene solution at 30°C, with the aid of the intrinsic viscosity/molecular weight relationship of Fox *et al.*[2]

$$[\eta] = 8{\cdot}69 \times 10^{-5} \overline{M}_n{}^{0{\cdot}76} \qquad (1)$$

Our lowest molecular weights lie outside the range for which this relationship has been established, but we do not think that any serious error is introduced by this extrapolation.

Activities were determined by internal sample liquid scintillation counting, using either an Isotope Developments Ltd 2022 counter or a Packard Tri-Carb scintillation counter. A conventional toluene-based organic scintillator solution was employed, and the counting efficiency (usually

about 80 per cent) was measured by the use of calibrated ^{14}C labelled *n*-hexadecane, obtained from the Radiochemical Centre, Amersham, as an internal standard.

RESULTS AND DISCUSSION

(1) *Low salt concentrations* ($<10^{-3}$ *mole* l^{-1})

We have previously shown[1] that in this concentration range the combination of $Cu(acac)_2$ and CCl_3COONH_4 is an active initiator at 80°C, whereas a mixture of CuCl and CCl_3COONH_4 is not active until the salt concentration exceeds 10^{-2} mole l^{-1}.

The results of experiments with the former system, given in *Table 1*, show that each polymer molecule contains approximately one CCl_3 group.

Table 1. Polymerization at 80°C initiated by $Cu(acac)_2$ and CCl_3COONH_4 at low $[CCl_3COONH_4]$*

$10^3[Cu(acac)_2]$ *mole* l^{-1}	$-10^4\frac{d[M]}{dt}$ *mole* l^{-1} *sec*$^{-1}$	*Conversion* %	$10^{-4}\bar{P}_n$	*Number of labelled groups per polymer molecule*
(a) $^{14}CCl_3COONH_4$				
8·31	1·20	2·12	1·096	0·94
8·67	0·91	3·30	1·429	0·82
8·67	0·79	4·74	1·603	1·11
				Mean 0·96
(b) $CCl_3{}^{14}COONH_4$				
5·41	1·15	2·07		$<0·1$
7·88	1·06	2·88		$<0·1$
8·87	0·97	3·48		$<0·1$
				Mean $<0·1$

*$[CCl_3COONH_4] = 2·22\times10^{-4}$ mole l^{-1} in all cases. M represents methyl methacrylate.

while the content of labelled COO^- is extremely low. They are therefore clearly consistent with initiation by $\dot{C}Cl_3$ exclusively; neither $\cdot\dot{C}O\bar{O}$ radicals, nor radicals containing both carbon atoms such as $\dot{C}Cl_2C\bar{O}\bar{O}$, play a significant part. These findings are in agreement with the mechanism previously postulated[1] on the basis of kinetic evidence in which $\dot{C}Cl_3$ radicals are formed by internal electron transfer in the 1:1 complex

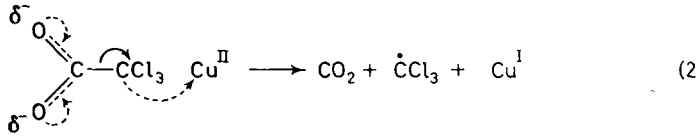

(2)

(It is assumed that at 80°C the termination reaction in the polymerization of methyl methacrylate occurs predominantly by disproportionation.)

(2) *High salt concentrations* ($>10^{-2}$ *mole* l^{-1})

(*i*) *Cuprous chloride system—Table 2* shows the dependence on salt concentration [S] of the rate of polymerization, the degree of polymeri-

zation P_n and the incorporation of activity in the polymer, measured as the number of labelled groups per polymer molecule. Although the results

Table 2. Polymerization at 60°C initiated by CuCl and CCl_3COONH_4 at high $[CCl_3COONH_4]$

No. of experiment	10^4 [CuCl] *mole* l^{-1}	10^2 [CCl_3COONH_4] *mole* l^{-1}	$-10^4 \frac{d[M]}{dt}$ *mole* l^{-1} *sec*$^{-1}$	$10^{-2}\overline{P}_n$	$(k_p k_t^{-\frac{1}{2}})_{apparent}$	*Number of labelled groups per polymer molecule*
$^{14}CCl_3COONH_4$						
1	1·21	1·37	1·77	7·94	0·043	0·35
2	1·21	2·75	1·25	9·25	0·039	0·19
3	1·21	4·12	1·28	8·67	0·038	0·29
4	1·21	5·50	1·53	8·02	0·040	0·24
						Mean 0·27
$CCl_3{}^{14}COONH_4$						
5	1·35	1·37	1·59	11·50	0·049	0·83
6	1·35	2·75	1·99	10·05	0·051	1·06
7	1·35	4·12	1·31	11·00	0·044	0·58
8	1·35	5·50	1·26	8·41	0·037	0·47
						Mean 0·73

show considerable scatter, it appears that neither the molecular weights nor the rates of polymerization are markedly affected by changes in [S] within the range shown. The rate is approximately proportional to the square root of the initial cuprous chloride concentration.

The data in the last column of *Table 2* suggest that the rates of incorporation of labelled CCl_3 and COO^- groups into the polymer are independent of [S] and also show that the mean rate of incorporation of COO^- is two to three times as great as that of CCl_3. Further, since the sum of the mean contents of the two types of group is unity, one group, either CCl_3 or COO^-, is built into each polymer molecule.

The value of the parameter $k_p k_t^{-\frac{1}{2}}$ in a free-radical polymerization may be calculated from the familiar equation

$$-\overline{P}_n (d[M]/dt) = (k_p^2/k_t)[M]^2 \qquad (3)$$

in which M represents monomer and k_p, k_t are the velocity coefficients for chain propagation and termination, respectively. Equation (3) is derived on the assumptions of bimolecular termination by disproportionation and negligible chain transfer or retardation. At 60°C we obtained a mean value of 0·14 mole$^{-\frac{1}{2}}$ $l^{\frac{1}{2}}$ sec$^{-\frac{1}{2}}$ for $k_p k_t^{-\frac{1}{2}}$ in the simple polymerization of methyl methacrylate initiated by azo-bis-isobutyronitrile, in the absence of other additives. Application of equation (3) to the present results gives much lower values of $(k_p k_t^{-\frac{1}{2}})_{apparent}$, as is evident from *Table 2*. Since the magnitude of the parameter $k_p k_t^{-\frac{1}{2}}$ is independent of the mechanism of initiation, it is clear that in these systems there must be considerable chain-transfer (or retardation), or a modified termination mechanism, or both. In an earlier publication[1] we showed that ammonium trichloracetate is a retarder of the polymerization of methyl methacrylate at 80°C, but subsequent work at 60°C has indicated that its activity in this respect is too small to be significant in the present case. Further, a considerable amount of chain-transfer by the salt would not be consistent with the observed independence

of $\overline{P}_n$ on [S]. We conclude, therefore, that the most important factor is a modification in the nature of chain termination, and we believe that bimolecular termination plays a minor role.

Polymethyl methacrylate radicals are known to react rapidly with oxidizing transition metal ions in non-aqueous solution[3]; Bengough and Fairservice[4] have recently shown that in dimethylformamide solution $CuCl_2$ is a powerful retarder of the methyl methacrylate polymerization, the rate constant for reaction with the growing chains being comparable to those of radical–radical reactions. In the medium of lower polarity used in the present work even higher rate constants might be anticipated[3]. It is therefore reasonable to suppose that a Cu^{II} derivative is responsible for chain termination. Cu^{II} is likely to be formed in the initiation process, and the retarding species might be $CuCl_2$ or $Cu(OOCCCl_3)_2$. In the latter case the termination process cannot incorporate $OOCCCl_3$ groups into the polymer to a significant extent, since this alone would introduce 1 COO^- and 1 CCl_3 group into each polymer chain, and hence would lead to activities greater than those recorded in *Table 2*. Further, a reaction in which only one type of labelled carbon atom becomes incorporated during termination with $Cu(OOCCCl_3)_2$ is improbable on chemical grounds. We shall see later that there is evidence that reaction between a growing chain and cupric trichloracetate leads to the addition of a trichloracetate residue to the chain; consequently we favour the view that the predominant retarder in the present system is $CuCl_2$.

If polymerization is prolonged, say for a period of half an hour, it may readily be shown from the data in *Table 2* that the molar yield of polymer exceeds (by a factor three, approximately) the initial concentration of cuprous chloride. Thus a recycling process must occur in which copper is alternately oxidized and reduced: $Cu^I \longrightarrow Cu^{II} \longrightarrow Cu^I$ etc. If the termination reaction involving $CuCl_2$ leads to the addition of Cl atoms to the polymer chains, the chloride ions would disappear progressively from the system, and recycling would be impossible (unless Cl^- can be replaced by $^-OOCCCl_3$, and we have given reasons for thinking this unlikely). Thus the termination reaction seems most likely to be that shown in equation (4).

$$\sim\!\!\sim CH_2\!-\!\underset{\displaystyle COOCH_3}{\overset{\displaystyle CH_3}{\overset{|}{\underset{|}{C}}}}\!\cdot + CuCl_2 \xrightarrow{k_2} \sim\!\!\sim CH_2\!-\!\underset{\displaystyle COOCH_3}{\overset{\displaystyle CH_2}{\overset{|}{\underset{|}{C}}}} + HCl + CuCl \qquad (4)$$

According to this view all the activity in the polymer originates in the initiation reaction. The two initiating radicals $\cdot COO^-$ and $\dot{C}Cl_3$ could arise from the following processes:

$$Cu^I + CCl_3COO^-NH_4^+ \begin{cases} \xrightarrow{k_1} Cu^{II} + CHCl_3 + \cdot COO^- + NH_3 & \text{(a)} \\ \xrightarrow{k'_1} Cu^{II} + \dot{C}Cl_3 + HCOO^- + NH_3 & \text{(b)} \end{cases} \qquad (5)$$

Both reactions follow simply from electron transfer; in (5a) the electron is transferred to the CCl_3 group and the process leads ultimately to the formation of chloroform through a subsequent proton transfer, while in (5b) electron transfer to COO^- (or COOH) occurs.

Although (5) may represent the course of the initiation process, in reality the latter is much more complicated, as is indicated by the unusual kinetic features already mentioned. The requirement for a high salt concentration may imply that the salt dimer is the reactive species, as discussed in the earlier paper[1], and the independence of the rate of polymerization on [S] would follow if Cu^I were associated with the dimer giving a complex which decomposes according to (5). The total rate of initiation in the steady state is thus $(k_1+k_1')[Cu^I]$, where k_1, k_1' are the first-order rate constants of the processes shown in (5). We have therefore:

$$-\frac{d[Cu^I]}{dt} = +\frac{d[Cu^{II}]}{dt} = (k_1+k_1')[Cu^I] - k_2[Cu^{II}][R\cdot] \qquad (6)$$

$$\frac{d[R\cdot]}{dt} = (k_1+k_1')[Cu^I] - k_2[Cu^{II}][R\cdot] - k_t[R\cdot]^2$$

in which k_2 is the rate constant of reaction (4) and R· represents a growing chain. If $k_2 \gg k_t$ bimolecular radical termination is always negligible, and $[R\cdot]=[Cu^{II}]$, since both species are formed and disappear in the same reactions. In these circumstances, (6), together with the steady state condition, leads to the relations in (7).

$$[R\cdot] = \{[(k_1+k_1')/k_2][Cu^I]\}^{\frac{1}{2}}$$

and

$$-d[M]/dt = k_p[M]\{[(k_1+k_1')/k_2][Cu^I]\}^{\frac{1}{2}} \qquad (7)$$

$$\bar{P}_n = -\frac{1}{(k_1+k_1')[Cu^I]}\frac{d[M]}{dt} = \frac{k_p[M]}{\{(k_1+k_1')k_2[Cu^I]\}^{\frac{1}{2}}}$$

Since [R·] is of the order of 10^{-7} to 10^{-8} mole l^{-1}, and $[Cu^I]_{initial}=10^{-4}$ mole l^{-1}, approximately, it follows that $[Cu^I]_{initial}$ and $[Cu^I]$ are very nearly equal. Thus (7) predicts that the rate of polymerization should be proportional to the square root of the initial concentration of cuprous chloride, in agreement with experiment. The number-average degree of polymerization is seen from (7) to be independent of [S], as observed. If the inequality $k_2 \gg k_t$ does not hold, bimolecular termination will occur in the early stages of the reaction, but will steadily decrease in importance as $[Cu^{II}]$ increases, until ultimately termination by Cu^{II} predominates, and $[Cu^I]$, $[Cu^{II}]$ become stationary. In this phase of the reaction an argument similar to that above shows that the rate of polymerization is approximately proportional to $[Cu^I]^{\frac{1}{2}}$. The final value of $[Cu^{II}]$ may, however, greatly exceed [R·]. The experimental indications are that the assumption $k_2 \gg k_t$ is probably a fair approximation.

According to the data in *Table 2*, $k_1/k_1' = 0{\cdot}73/0{\cdot}27 = 2{\cdot}7$.

(*ii*) *Cupric acetylacetonate system*—Results are presented in *Table 3*.

In the earlier paper[1] we showed that the rate of polymerization is sensibly independent of $[Cu(acac)_2]$, and recent results confirm this. The dependence

of rate on [S] is seen from *Table 3* to be complicated; at the lower concentrations the rate increases very rapidly with increase in [S]. The molecular weight changes comparatively little, but tends to increase with increasing [S].

Experiments with azo-bis-isobutyronitrile initiation at 80°C led to a value $k_p k_t^{-\frac{1}{2}} = 0{\cdot}18$ mole$^{-\frac{1}{2}}$ l$^{\frac{1}{2}}$ sec$^{-\frac{1}{2}}$. The values of $(k_p k_t^{-\frac{1}{2}})_{\text{apparent}}$ in *Table 3* [calculated with the aid of equation (3)] are considerably smaller than this, especially at the lowest salt concentration.

If termination involves the simultaneous occurrence of several different processes, then it may be shown that, in the absence of transfer, the fraction of radicals undergoing bimolecular termination f is given by

$$f = (k_p^2 k_t^{-1})_{\text{apparent}} / (k_p^2 k_t^{-1}) \tag{8}$$

We have already suggested that ammonium trichloracetate is not an active transfer agent at 60°C and reasons are given later for believing that transfer to salt does not play an important part in the present experiments. Thus we conclude from the low values of $(k_p k_t^{-\frac{1}{2}})_{\text{apparent}}$ in *Table 3* that bimolecular termination is negligible at the lowest salt concentration, but becomes increasingly important as [S] increases; at the highest [S] approximately 30 per cent of the radicals enter into bimolecular termination (*Table 3*).

Table 3. Polymerization at 80°C initiated by $Cu(acac)_2$ and CCl_3COONH_4 at high $[CCl_3COONH_4]$

No. of experiment	10^4 [Cu(acac)$_2$] *mole l^{-1}*	10^2 [CCl_3 $COONH_4$] *mole l^{-1}*	$-10^4 \frac{d[M]}{dt}$ *mole l^{-1} sec^{-1}*	$10^{-2}\bar{P}_n$	$(k_p k_t^{-\frac{1}{2}})_{apparent}$	*Percentage of chains terminated bimolecularly*	*Number of labelled groups per polymer molecule*
$^{14}CCl_3COONH_4$							
1	4·70	1·37	0·72	6·37	0·0247	1·5	0·74
2	7·83	2·75	5·67	6·76	0·071	16	1·40
3	7·44	4·12	7·54	6·97	0·0835	22	1·42
4	5·87	5·50	8·71	8·63	0·099	31	1·50
$CCl_3{}^{14}COONH_4$							
5	4·31	1·37	1·20	5·37	0·029	2·5	0·54
6	4·31	2·75	4·95	7·71	0·071	16	1·04
7	7·83	4·12	8·83	6·12	0·084	22	1·07
8	6·65	5·50	10·0	8·31	0·105	34	1·36

We believe that, as in the cuprous chloride system, an alternative termination reaction involves a derivative of Cu^{II}. $Cu(acac)_2$ is not a retarder, hence the retarding species must be generated during reaction. This could occur by direct reaction between the chelate and the salt. Alternatively, or additionally, initiation involving $Cu(acac)_2$ would produce Cu^{I}, which, by entering reactions of the type discussed earlier, would lead to Cu^{II}.

If, for the moment, we confine our attention to the experiments at the three higher salt concentrations in *Table 3*, we see that the total number of labelled groups per molecule is consistent with the incorporation of one such group by initiation and two by termination other than bimolecular termination, which does not incorporate any. Thus out of every 100 growing chains, 70 to 80 terminate with addition of 140 to 160 labels, giving a total number per molecule 2·4 to 2·6 in agreement with *Table 3*. The

balance between CCl_3 and COO^- is, however, different from that in the cuprous chloride system, the content of CCl_3 being higher in the present case. We therefore believe that initiation involves predominantly $\dot{C}Cl_3$ radicals, by (9) which is analogous to (2).

$$Cu^{II} + CCl_3COO^-NH_4^+ \longrightarrow \dot{C}Cl_3 + CO_2 + NH_4^+ + Cu^I \qquad (9)$$

The natures of the cupric and cuprous derivatives are not specified, and it should be remembered that the salt is probably involved as the dimer[1]. The rate-determining step is the thermal dissociation of this (probably giving $\overline{C}Cl_3$ as an intermediate), so that the rate of (9) is independent of $[Cu^{II}]$. It does not seem possible to construct any alternative radical-forming route involving cupric derivatives and ammonium trichloracetate. (This reaction has not been considered in the cuprous chloride system since it is probably much less important at 60°C. Its occurrence would imply that the importance of (5b), already a minor mode of initiation, has been overestimated.)

The termination reaction which is consistent with the above consideration is

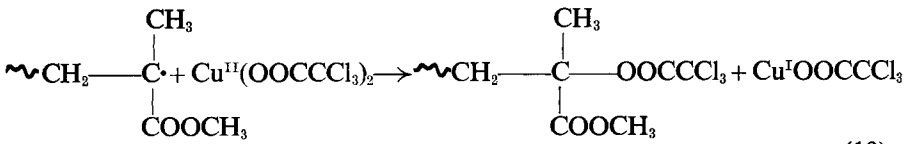

(10)

The occurrence of (9), (5), (10), with the assumption that 70 per cent of the growing chains terminate by (10) and 30 per cent by bimolecular interaction, leads to the following values for the content of labelled end-groups per polymer molecule: CCl_3, 1·34; COO^- 1·07. It would seem, therefore, that this mechanism is able to account for the experimental findings; more precise considerations are not possible at present, since the relative contributions of (9) and (5) cannot be assessed.

It seems likely that the active Cu^{II} derivative in (9) is formed by reaction between $Cu(acac)_2$ and ammonium trichloracetate. This view is consistent with the observation that the reaction is autocatalytic in its early stages. (The rates in *Table 3* are the stationary values after the acceleration period.) The derivative may well be cupric trichloracetate; its concentration may decrease with increasing [S], since (9) involves the salt dimer, and, since termination according to (10) also involves cupric trichloracetate, this could explain the trend towards higher molecular weights with increasing [S].

Three further points deserve consideration. First, chain transfer to salt would incorporate labelled end-groups in the polymer. Experiments with azo-bis-isobutyronitrile initiation, in the presence of labelled ammonium trichloracetate but without copper, showed that with $[S] = 5{\cdot}8 \times 10^{-2}$ mole l^{-1}, and a polymer molecular weight of $4{\cdot}8 \times 10^5$, each polymer molecule contained on the average 0·56 CCl_3 and COO^- groups. In experiments 4, 8 in *Table 3* the salt concentration is comparable, but the molecular weights are lower by a factor of six, approximately. The incorporation of labelled

ends arising from transfer to salt would therefore be less than 0·1 per polymer molecule in all the experiments in *Table 3*. This is therefore only a small effect; nevertheless, since it operates particularly at high molecular weights it would help to obscure any decrease in the content of labelled ends which might be expected to arise with increase in the proportion of bimolecular termination (*Table 3*). Secondly, experiments 1, 5 in *Table 3*, at the lower salt concentrations, reveal a low content of labelled groups, and also low molecular weights. We have referred earlier[1] to the difficulty of interpreting results obtained at this salt concentration. It would seem that [S] is not sufficiently high to allow rapid initiation by (9), hence the rate is comparatively low. At the same time, a retarding species must be responsible for the low molecular weights, and this appears to react with the growing chains without incorporation of labelled groups. In the earlier paper[1] we have suggested that an additional retarder is formed under these conditions. It is difficult to speculate about the nature of this retarder; it may be $Cu(acac)OOCCCl_3$, which at higher salt concentrations gives place to $Cu(OOCCCl_3)_2$. Thirdly, the rates of polymerization in *Table 3* are high at high [S], and the possibility of primary termination cannot be excluded. In experiments with azo-bis-isobutyronitrile at comparable rates, there was no evidence of primary termination, but this result is inconclusive, since different primary radicals are involved. Like chain-transfer to salt, primary termination would increase the content of labelled groups at high rates of reaction.

To summarize, we believe that the present results show that at high [S], $Cu(acac)_2$ leads predominantly to $\dot{C}Cl_3$, and CuCl to $\dot{C}OO^-$ radicals. Different termination mechanisms in the two systems also contribute to different activities of the resulting polymers; we have proposed that the difference in mechanism may arise from the presence of Cl^- in the CuCl system.

Department of Inorganic, Physical and Industrial Chemistry,
University of Liverpool

(*Received July 1966*)

REFERENCES

[1] BAMFORD, C. H., EASTMOND, G. C. and RIPPON, J. A. *Trans. Faraday Soc.* 1963, **59,** 2548
[2] FOX, T. G., KINSINGER, J. B., MASON, H. F. and SCHEULE, E. M. *Polymer, Lond.* 1962, **3,** 71
[3] BAMFORD, C. H., JENKINS, A. D. and JOHNSTON, R. *Proc. Roy. Soc. A,* 1957, **239,** 214
[4] BENGOUGH, W. I. and FAIRSERVICE, W. H. *Trans. Faraday Soc.* 1965, **61,** 1206

Book Review

Flammfestmachen von Kunststoffen
(Flameproofing of Plastics)

H. VOGEL. Alfred Hüthig: Heidelberg, 1966. 188 pages, 15 cm × 22½ cm. DM 17.80

THIS book is one of the technical series on the 'Technologie der makromolekularen Chemie' edited by Baum and Baumann: it is therefore technologically oriented.

The desirability that synthetic materials should have low flammability needs no emphasis, particularly in domestic articles and constructional materials. Dr Vogel first surveys briefly the phenomenology, dividing the synthetic polymers into: the more or less incombustible—phenoplasts, aminoplasts, silicones, PTFE, etc.; those which do not propagate flame—polyvinyl(idene) chlorides, polycarbonates, etc.; and those which burn—the rest, e.g. polyamides, polyesters, polyacrylates, polystyrene. Next follows a short descriptive section (18 pages) surveying in outline methods of reducing the flammability of the last group.

The book ends with a very short section on testing emphasising the difficulties of devising a test which has practical meaning; the author avoids all test detail, merely quoting the reference numbers of American and German standard methods.

The kernel of the book is a large central section—comprising two thirds of the text—on Methods. This is a literature survey of proposals for modifying the flammability of polymeric materials, with references to review articles in technical journals and to relevant patents, covering the post-1945 period to mid-1964. About one thousand patents are listed in a special index (with page references to the text abstract) and, so far as can be tested, this survey is reasonably complete in respect of substance. Like all literature surveys aiming at completeness, the section is uncritical, and a newcomer to the field will be left with very little indication as to which methods are used industrially and which of them will remain forever in limbo.

The author has taken particular care in this central section to give acceptable systematic names to the vast array of compounds mentioned—a virtue not always found in technical literature; for clarity, the text is enhanced with about two hundred numbered structural formulae.

The book can be recommended to all who desire to be informed of the vast amount of skilful and thoughtful work done in this field by preparative—mainly organic—chemists. Dr Vogel answers 'What?' questions admirably, but leaves almost untouched the 'How?' and 'Why?'. I hope the book will also be read by physical chemists, who might thereby be encouraged to improve, as is currently so desirable, our theoretical knowledge of mechanisms involved in the burning of solids based on carbon-containing polymers.

The book is well printed by an offset process on substantial matt paper—with excellent register of text on front and back of sheet. Choice of type face is good for a German book, and there are almost no printer's errors.

T. H. MORTON

Communication

Allotropy of Cyclic Tris(ethylene terephthalate)

CYCLIC tris(ethylene terephthalate) is of interest not only as the oligomer found in greatest abundance in equilibrium with molten poly(ethylene terephthalate)[1] but also because of the use made of it in assigning the infra-red absorptions in poly(ethylene terephthalate)[2]. Attempts to synthesize the cyclic oligomers of ethylene terephthalate have so far proved unsuccessful[3] and samples of the cyclic trimer have always been obtained for investigation by solvent extraction from the high molecular weight matrix[1,4,5]. However, the published data relating to cyclic tris(ethylene terephthalate) show discrepancies, notably in the infra-red absorption spectra published by Grime and Ward[2], Goodman and Nesbitt[1], and Seidel[5], and the X-ray data given by Goodman and Nesbitt[1] and by Zahn and Seidel[6].

We have now found that this oligomer can be obtained in two forms, giving distinct X-ray diffraction patterns and infra-red absorption spectra, and that this fact has not been recognized in previously published work, leading to the discrepancies in the data.

Several samples of the cyclic trimer were prepared by solvent extraction of poly(ethylene terephthalate) granules using the method of Goodman and Nesbitt[1]. Both 1,4-dioxan and *p*-xylene were used as solvents. Infra-red absorption spectra were obtained by incorporating the samples in potassium bromide discs and using a Beckman IR12 spectrophotometer. X-ray powder

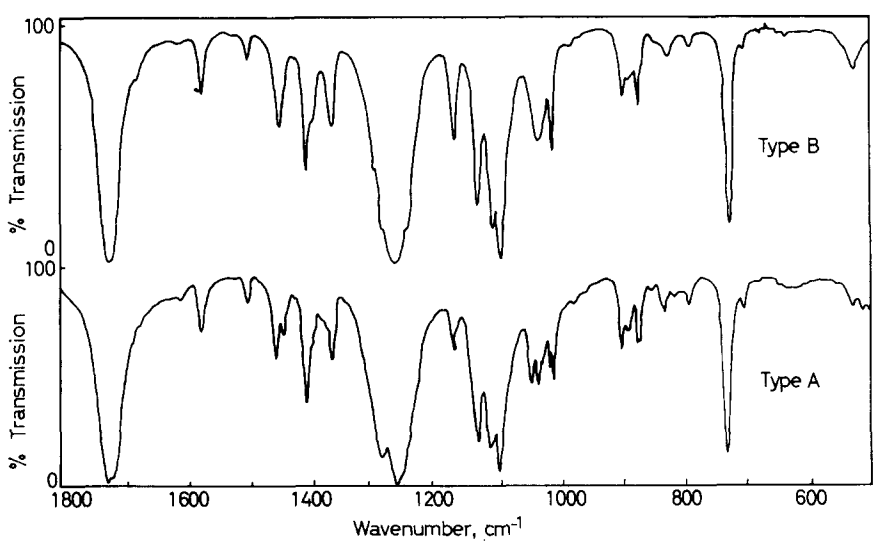

Figure 1—Infra-red absorption spectra of cyclic tris(ethylene terephthalate)

photographs of the samples were also taken using a 6 cm diameter cylindrical camera. All these samples, with one exception, showed the infra-red spectrum and X-ray powder pattern which we have designated Type A in *Figure 1* and *Table 1*. The exception was a sample which had accidentally been subjected to excessive heating during preparation. This sample showed the infra-red spectrum and X-ray pattern labelled Type B. On heating samples of Type A material to 200°C and cooling to room temperature, the infra-red spectrum and X-ray powder pattern were found to have changed to those of Type B. The reverse change was observed on recrystallizing the Type B material from ethyl acetate at temperatures below 80°C.

Table 1. X-ray powder photograph spacings and intensities

A-type structure

d, Å	2·74	2·92	3·10	3·44	3·65	3·87	4·24	4·84	5·28	6·37	6·67	8·60	9·88
$I/I_{max.}$	9	29	24	39	100	60	25	70	40	38	36	17	10

B-type structure

d, Å	3·17	3·35	3·45	3·63	4·05	4·33	4·50	5·05	5·58	6·10	7·62	11·6
$I/I_{max.}$	15	18	100	18	22	31	26	70	15	40	42	14

A sample of Type A material in a potassium bromide disc was then heated in a variable temperature infra-red cell and the absorption spectrum recorded as the sample was heated from room temperature. At about 150°C changes began to occur in the 1 050 cm^{-1} and 1 450 cm^{-1} regions of the spectrum, and at 200°C the spectrum had changed to that of Type B material. No further change took place on cooling to room temperature. Differential thermal analysis of a sample of Type A material revealed a broad endotherm at a temperature of about 195°C when the sample was heated from room temperature to its melting point (316°C) at a rate of 64 deg. C/min. No corresponding effect was observed as the sample cooled from the melt.

These results suggest that cyclic tris(ethylene terephthalate) can exist in two allotropic forms at room temperature. Only one form—Type B—appears to be stable above 195°C. The possibility that the change from Type A to Type B occurs at a slow rate at temperatures below 195°C has not been investigated, but a sample originally prepared in 1956 by Goodman and Nesbitt was obtained, and this showed the Type A characteristics after ten years storage at room temperature.

It is now apparent that the infra-red data given by Grime and Ward[2] and by Goodman and Nesbitt[1] refer to the form which we have designated Type B, whereas Seidel[5] and Zahn and Seidel[6] give infra-red and X-ray data corresponding to the Type A structure. The unit cell dimensions quoted by Farrow, McIntosh and Ward[7] agree with the d spacings of the powder lines on X-ray photographs of the Type A material.

Our work indicates that care is necessary in the preparation and handling of cyclic tris(ethylene terephthalate) if transitions between the two forms are to be avoided.

G. L. Binns, J. S. Frost, F. S. Smith and E. C. Yeadon

Research Dept, I.C.I. Fibres Ltd,
Hookstone Road,
Harrogate, Yorks.

(Received September 1966)

REFERENCES

[1] GOODMAN, I. and NESBITT, B. F. *Polymer, Lond.* 1960, **1,** 384–396
[2] GRIME, D. and WARD, I. M. *Trans. Faraday Soc.* 1958, **54,** 959–971
[3] ZAHN, H., BORSTLAP, C. and VALK, G. *Makromol. Chem.* 1963, **64,** 18–36
[4] ROSS, S. D., COBURN, E. R., LEACH, W. A. and ROBINSON, W. B. *J. Polym. Sci.* 1954, **13,** 406–407
[5] SEIDEL, B. *Z. Elektrochem.* 1958, **62,** 214–219
[6] ZAHN, H. and SEIDEL, B. *Makromol. Chem.* 1959, **29,** 70–92
[7] FARROW, G., MCINTOSH, J. and WARD, I. M. *Makromol. Chem.* 1960, **38,** 147–158

ANNOUNCEMENTS

TOXICITY IN PLASTICS

A two-day symposium on Toxicity in Plastics will be held at the Northern Polytechnic, Holloway, London N.7, on 6 and 7 December. The papers and speakers include:

Toxicity in plastics: the problem as typified by plastics packages. Mr J. M. J. ESTEVEZ, I.C.I. Plastics.

Safety evaluation of plastics for food packaging and other specific uses. Dr L. GOLDBERG, Director, British Industrial Biological Research Association.

Some problems created by the migration of plastics ingredients into food. Mr J. W. SELBY, British Food Industries Research Association.

Safety aspects of food packaging materials—a fabricator's viewpoint. Mr J. H. BRITTAIN, Metal Box Co.

Toxic hazards from the user's viewpoint. Mr. J. McL. PHILP, Unilever Research Laboratory.

Toxicological hazards from plastics toys. Dr P. S. ELIAS, Ministry of Health.

Some possible toxic hazards of plastics in medicine. Mr D. E. SEYMOUR, Smith & Nephew Research Ltd.

A review of legislation on toxic hazards in various countries. M. A. RODEYNS, Solvay et Cie.

For further information please write for the attention of STEWART LAURIE, Press Officer to the British Plastics Federation, 47–48 Piccadilly, London W.1.

FOURTEENTH CANADIAN HIGH POLYMER FORUM

The fourteenth Canadian High Polymer Forum will be held in Quebec City on 24 to 26 May 1967 at the Université Laval. Persons wishing to contribute papers should contact the Program Chairman, Dr D. M. WILES, Division of Applied Chemistry, National Research Council, Ottawa, Ontario. Titles, authors' names, and abstracts of 200 to 300 words should reach the Program Chairman no later than 15 February 1967.

Influence of the Dielectric Constant on the Rate of Solution Polymerization of Trioxan

E. HLADKÝ, M. KUČERA and K. MAJEROVÁ

The dielectric constant of the liquid phase is one of the factors having an influence on the overall reaction rate of the solution polymerization of trioxan. Since neglect of this effect can result in inaccurate conclusions, the authors have tried to determine the dependence of reaction rate of polymerization on the dielectric constant. Results show that the course of this relation is characteristic of the reactions of polar molecules or of ions with polar molecules and that it is influenced by the kind of solvent used. The value of the dielectric constant (and thus the rate constant) varies during polymerization of trioxan in a solvent which has a different value of dielectric constant from that of trioxan. An equation for the overall rate of solution polymerization of trioxan comprising factors having effects on this rate was deduced from the results of measurements and from the previous work of the authors.

IN REACTIONS between ions or polar molecules in a solution the reaction rate constant depends not only on the character of the reacting particles but also on the solvent. The solvent influences the value of the rate constant mainly by its polarity which is determined essentially by the dielectric constant (DC). It was found when studying the effect of the DC that the overall reaction rate was altered in the first place. The effect of the DC on the degree of polymerization can usually be neglected[1-3].

When studying the kinetics of the solution polymerization of trioxan, the effect of the DC on the polymerization rate constant cannot be neglected. Since the polymerization of trioxan is a precipitation reaction, the DC of the liquid phase is generally not constant (as the solvent has not the same DC as trioxan). Both the rate constant and the overall reaction rate will change during the polymerization because of this. This change is the larger the greater the difference between the DC of trioxan and that of the solvent. In our work we have tried to determine the dependence of the overall reaction rate on the DC of the liquid phase and to express the dependence of the change of the rate constant on the increase or decrease of the DC during the polymerization.

RESULTS

Exact evaluation of the effect of the DC on the rate constant of the polymerization of trioxan is difficult. The rate constant does not depend only on the DC; its value is a function of some further factors not directly related to the polymerization of trioxan. The decrease in initiator concentration[4]

is one of these factors; other factors are the dependence of the polymerization rate on the water content and the change of water concentration with conversion. These factors were previously investigated in the systems trioxan–*n*-heptane[5] and trioxan–*n*-heptane–nitrobenzene[6]. To widen our knowledge of polymerizations at higher dielectric constants we have studied the rate of formation of the polymer from trioxan in the presence of pure nitrobenzene, i.e. in a medium in which the DC grows with increase of conversion.

The dependence of the polymerization rate on the water concentration is shown in *Figure 1*. (The dependence was determined by graphic differentiation of the conversion curves at their points of inflection, i.e. at low

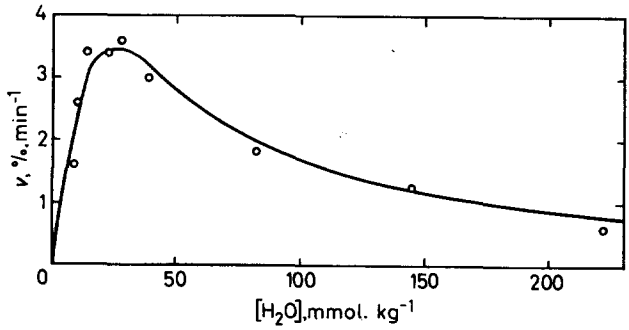

Figure 1—Dependence of rate of polymerization of trioxan in nitrobenzene on water concentration. Trioxan concentration 5·0 mole/kg, solvent concentration 5·0 mole/kg, initiator concentration $4{\cdot}3\times10^{-3}$ mole/kg, temperature 80°C

conversions when it is still realistic to neglect the change of DC and the loss of initiator.) It is evident from the plot that water has a great influence on the polymerization rate even in nitrobenzene. The form of the dependence agrees qualitatively with that found previously for the polymerization in *n*-heptane and in nitrobenzene–*n*-heptane mixtures. The dependence of the polymerization rate on water concentration is given by the following equation[5] even in this case

$$v=\frac{k'K_1[H_2O]}{1+K_1[H_2O]+\{K_1K_2/A\,.\,OH\}[H_2O]^2}\times[\text{init.}] \qquad (1)$$

The decrease of water in the polymerization of trioxan in nitrobenzene has qualitatively the same course as in *n*-heptane, as follows from *Figure 2*. The dependence of the instantaneous water concentration on conversion can be expressed in terms of the equation which has been derived for polymerization at lower dielectric constants[6].

$$\frac{[H_2O]}{[H_2O]_0}=\frac{1}{p+q}\left\{q+p\left[\frac{1-x}{(1-k_dx)^{1-a}}\right]^{\beta}\right\} \qquad (2)$$

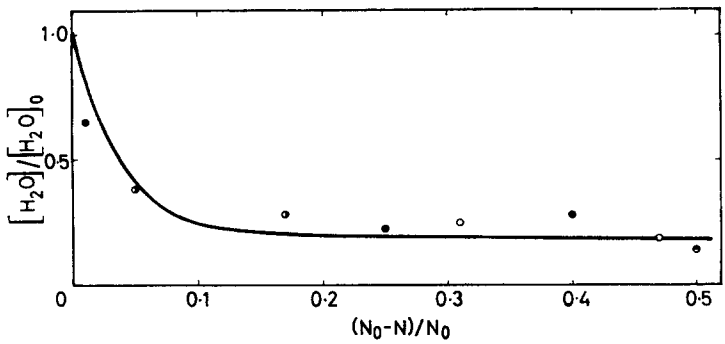

Figure 2—Water decrease during polymerization of trioxan in nitrobenzene. Trioxan concentration 5·0 mole/kg, initiator concentration $4{\cdot}3\times10^{-3}$ mole/kg, temperature 80°C. $[H_2O]_0$: ● 10·0 m mole/kg, ◑ 28·0 m mole/kg, ○ 38·4 m mole/kg, ◓ 82·0 m mole/kg

In equations (1) and (2) K_1 is the equilibrium constant in the reaction of formation of an active centre from the native initiator[5,6]

$$Ac^+B^- + H_2O \rightleftharpoons Ac^+ \,||\, B^-$$

K_2, A, p, q, α and β are constants which have been described earlier[5,6]; v is the polymerization rate in percentage of conversion/min; [init.] is the concentration of initiator. k_d is the constant expressing the loss of initiator[4,7]. $[H_2O]_0$ and $[H_2O]$ are the initial, and the instantaneous concentration of water, and x is the conversion.

The curves in *Figures 1* and *2* are calculated from equations (1) and (2) using constants whose values are summarized in *Table 1*. The experimental data are represented by separate points.

Table 1. Influence of the solvents on the values of constants in equations (1) and (5)

Solvent	*Ratio* TOX: *solvent vol.* %	*DC*	$K_1\times10^{-2}$	$\frac{K_1K_2}{A.\mathrm{OH}}\times10^{-3}$	*B*	*Note*
n-Heptane	30–70	4·2	7·6	3·8	−3·25	a
	50–50	7·1	6·0	8·0	−4·75	a
	85–15	13·0	5·1	5·1	−3·75	a
n-Heptane + nitrobenzene	50–50	15·6	0·03	1·8	0	b
Nitrobenzene	30–70	27·8	—	—	4·0	
	50–50	24·3	0·03	1·8	5·0	

a—see ref. 5
b—see ref. 4

The course of the polymerization of trioxan at different values of the DC is demonstrated by the conversion curves in *Figure 3*. These curves were obtained by polymerizing trioxan in nitrobenzene or *n*-heptane, or in their mixtures, at a constant initial water concentration in the polymerizing

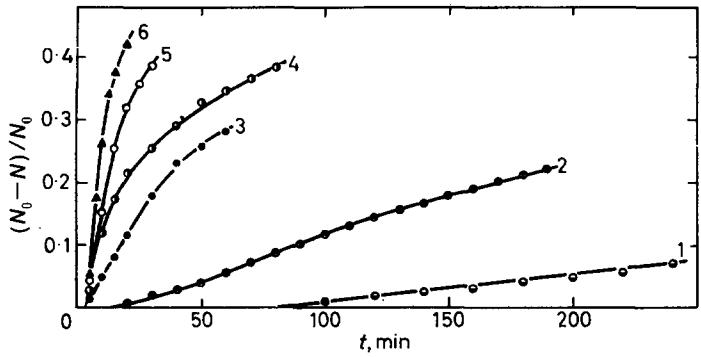

Figure 3—Influence of DC on the course of polymerization of trioxan in the presence of a solvent (*n*-heptane, nitrobenzene, and mixtures of them). Initiator concentration $8{\cdot}5\times10^{-3}$ mole/kg, water concentration 10·0 m mole/kg, temperature 80°C. $(DC)_0$: 1—4·2, 2—7·1, 3—13·0, 4—15·6, 5—23·7, 6—27·8

mixture. The effect of the DC can be seen in the figure. A more exact kinetic analysis, however, cannot be carried out without information as regards the change of DC of the liquid phase during polymerization. The dependence of the DC of the liquid phase on the conversion for the given systems of trioxan–solvent is shown in *Figure 4*.

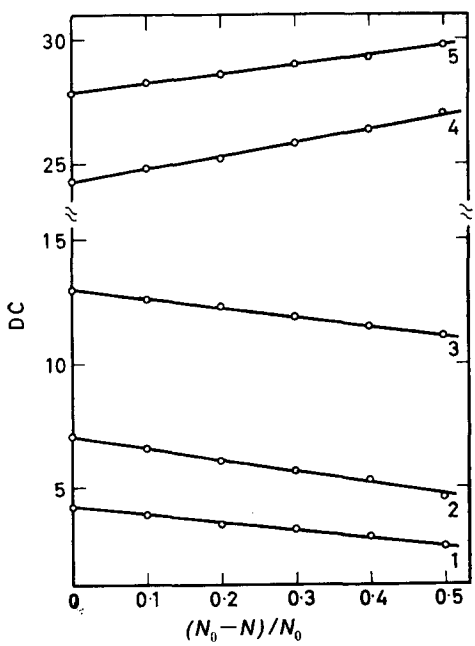

Figure 4—Dependence of DC on conversion in the polymerization of trioxan in *n*-heptane and nitrobenzene. Temperature 80°C. Solvent: 1—*n*-heptane 5·65 mole/kg, 2—*n*-heptane 3·65 mole/kg, 3—*n*-heptane 0·90 mole/kg, 4—nitrobenzene 5·00 mole/kg, 5—nitrobenzene 6·90 mole/kg

The reaction order with respect to monomer was found to be one[6] in our previous work where trioxan was polymerized in nitrobenzene–*n*-heptane

mixture, i.e. in a medium in which both solvent and monomer had the same DC. The reaction order was unity also with respect to the initiator[7]. For the overall polymerization rate we can write

$$-(1/G)(dN/dt) = k(N/G)[C]f(H_2O) \qquad (3)$$

where G (kg) is the weight of the liquid phase, [C] (mole/kg) is the initiator concentration, N is the number of trioxan moles and $f(H_2O)$ is a factor expressing the effect of a variable amount of water (cocatalyst) on the polymerization rate. If the values of N, G, [C] and $[H_2O]$ are made constant and the same in various systems while determining the rate, we can obtain the value of k and its dependence on the DC from equation (3). Experimental results are gathered in *Figures 5* and *6*.

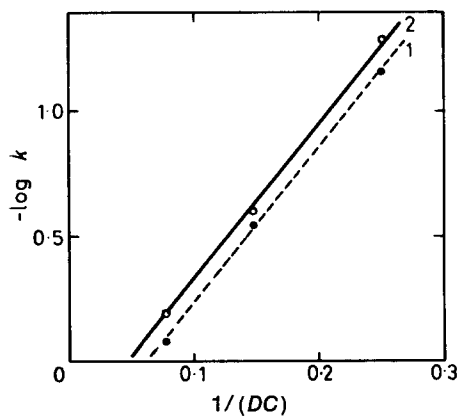

Figure 5—Dependence of rate constant of polymerization of trioxan in *n*-heptane on DC. Temperature 80°C. $[H_2O]_0$: 1—10·0 m mole/kg, 2—44·4 m mole/kg

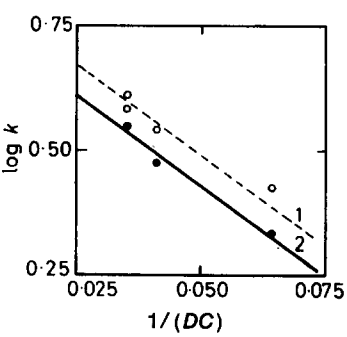

Figure 6—Dependence of rate constant of polymerization of trioxan in nitrobenzene on DC. Temperature 80°C. $[H_2O]_0$: 1—44·4 m mole/kg, 2—10·0 m mole/kg

It is evident from the figures that the results of the measurements agree well with theory which requires log k to be a linear function of the reciprocal of the DC[8]. Then we can write

$$\log k = \log k_0 + A/(DC) \qquad (4)$$

The constant k_0 has the significance of a rate constant at infinite dilution[8]. The values of k_0 and A in equation (4), read from *Figures 5* and *6*, are summarized in *Table 2*.

Table 2. Values of the constants in equation (4). They are independent of the concentration of the solvents

Solvent	$[H_2O]_0$ *m mole* kg^{-1}	$\log k_0$	A
Nitrobenzene	10·0	0·93	−7·35
	44·4	1·00	−7·35
n-Heptane	10·0	0·49	−6·25
	44·4	0·40	−6·25

DISCUSSION

The values of the constants in equation (4) differ for different solvents. The different water concentration can be made responsible for the change in k_0. It follows from the change in the A value that the rate constant does not depend only on the absolute value of the DC of the polymerizing mixture but that it is affected also by the character of the solvent used (e.g. by its solvation property).

Solvent affects also the values of the constants in equation (1) and thus even the quantitative effect of water on the rate of the polymerization of trioxan. This is demonstrated in *Table 1*.

The corresponding constants vary with the amount of solvent in polymerization in *n*-heptane, while they remain constant and do not depend on the amount of solvent in the presence of nitrobenzene.

The change of values of the equilibrium constants proves a direct interference of solvents with the structure of the solvation shell of the active centres. These observations agree with the experience of physical and organic chemistry. Hydrocarbons such as *n*-heptane are poor solvents of water. If, in addition to water, compounds of very polar character, as for example ion-pairs, are also dissolved in hydrocarbon, an interaction between water and these pairs can be expected, a 'drying' of *n*-heptane; the equilibrium constant of the interaction K_1 is high. Products of the interaction are active as initiating agents. The solubility of water is greater in more polar media; moreover nitrobenzene itself can participate in the solvation. Thus a lower value of K_1 can be expected. It seems that the presence of trioxan changes only quantitatively the conditions considered, by its polarity and concentration.

It follows from *Figure 4* that the change of the dielectric constant during polymerization is always directly proportional to conversion. This dependence can be expressed generally by the equation

$$(DC) = (DC)_0 + B[(N_0 - N)/N_0] \qquad (5)$$

where $(DC)_0$ is the initial value of the DC of the polymerization mixture, B is the constant and N_0 and N are the numbers of moles of trioxan at zero time and time t respectively.

Values of constants B in equation (5), read from *Figure 4*, are summarized in the penultimate column of *Table 1*. The constant B is positive or negative depending on whether the DC of the solvent is higher or lower than that of the monomer. However, its value is not the same for polymerization mixtures of any kind; it depends on the initial concentration of monomer and on the difference between the dielectric constants of the monomer and of the solvent.

It follows from equations (4) and (5) that the rate constants will change as a result of the change of DC during polymerization according to

$$k = k_0 \times 10^{A/\{(DC)_0 + B(N_0 - N)/N_0\}} \tag{6}$$

After substitution of equation (6) into equation (3) we can write

$$-\left(\frac{1}{G}\right)\frac{dN}{dt} = k_0 \times 10^{A/\{(DC)_0 + B(N_0 - N)/N_0\}} [C]\frac{N}{G} \tag{7}$$

Using a correction factor for the loss of initiator we obtain the following form of equation (7)

$$-\left(\frac{1}{G}\right)\frac{dN}{dt} = k_0 \times 10^{A/\{(DC)_0 + B(N_0 - N)/N_0\}} \frac{N}{R + MN} \cdot \frac{I_0}{G} \cdot \left[1 - k_d\left(\frac{N_0 - N}{N_0}\right)\right] \tag{8}$$

where R (kg) is the weight of the solvent, M (kg/mole) is the molecular weight of trioxan $\times 10^{-3}$, I_0 is the number of moles of initiator at zero time.

As $(N_0 - N)/N_0 = x$ (conversion), equation (8) can be rewritten

$$\left(\frac{1}{G}\right)\frac{dx}{dt} = k_0 \times 10^{A/\{(DC)_0 + Bx\}} \cdot \frac{(1-x)}{R + MN_0(1-x)} \cdot \frac{I_0}{G} \cdot [1 - k_d x] \tag{9}$$

Even this differential equation is rather complicated. We must also take into account the fact that the value of k_0 depends on the initial concentration of water (in the polymerizing system) which also varies with the conversion according to equation (2).

It is evident from the above that the mathematical description of the course of solution polymerization of trioxan in any solvent is remarkably complicated and difficult. This is illustrated in equation (7), which includes some factors having an influence on the reaction rate and thus also on the shape of the conversion curves. These factors must be accounted for in kinetic measurements and in considerations of the mechanism of the process. It is necessary to bear in mind that passing from one trioxan concentration to another in a solvent whose DC differs from that of trioxan, results in a change of the dielectric constant of the polymerizing mixture. Thus the change of the polymerization rate is due not only to the change of monomer concentration but also to that of the DC according to equation (8). We suppose that this fact is the cause of the high values of reaction order with regard to the monomer[9,10] and of differences in these values for various solvents.

EXPERIMENTAL

Trioxan was refined by rectification with sodium metal in a column with *ca.* 5 TP. The purity of trioxan was checked by gas chromatography.

After being washed with sulphuric acid *n*-heptane was dried by potassium hydroxide. It was also rectified with sodium metal before the polymerization.

Nitrobenzene was refined by vacuum distillation. A fraction taken at the temperature of 84·5° to 85·5°C and at a pressure of 10 mm of mercury was used for the polymerization.

A compound of the type [$\sim$ Si$\oplus$] [HSO$_4\ominus$], the preparation of which had been described previously[5], was used for initiation.

The water concentration in the polymerization mixture was determined by means of a modified Fischer method allowing measurement in p.p.m.[11].

The DC of the polymerization mixture was measured by the resonance method with a Schomandl DC-meter. The apparatus was calibrated using a dioxan–water mixture.

The course of the polymerization of trioxan in solution was measured with an automatic recording dilatometer also described previously[12].

CONCLUSION

We tried to elucidate further the complicating factors of the solution polymerization of trioxan, at least approximately. The polymerization rate is affected not only by the water concentration, as was shown earlier[13], but also by the DC and by the character of the solvent used. The dependence of the rate constant on the DC of the medium has a form characteristic of the reactions of polar molecules or ions with polar molecules. The DC is usually changed during the solution polymerization of trioxan. This change must be accounted for in kinetic measurements.

Research Institute of Macromolecular Chemistry,
Brno, Czechoslovakia

(*Received May 1965; revised April 1966*)

REFERENCES

[1] GEORGE, J. and WECKSLER, H. *J. Polym. Sci.* 1951, **6**, 725
[2] OVERBERGER, C. G. and ENDRES, G. F. *J. Polym. Sci.* 1955, **16**, 283
[3] PLESCH, P. H. (Ed.) *The Chemistry of Cationic Polymerization*, p 386. Pergamon: London and Oxford, 1963
[4] KUČERA, M., HLADKY, E. and MAJEROVÁ, K. *International Symposium on Macromolecular Chemistry, Prague, 1965.* P 24 (A 29)
[5] KUČERA, M. and HLADKY, E. *Coll. Czech. Chem. Commun.* In press
[6] KUČERA, M., HLADKY, E. and MAJEROVÁ, K. *Makromol. Chem.* 1966, **97**, 146
[7] KUČERA, M. *Thesis.* University of Brno, 1964
[8] JUNGERS, J. C., BALACEANU, J. C., COUSSEMANT, F., ESCHARD, F., GIRAUD, A., HELLIN, M., LEPRINCE, P. and LIMIDO, G. E. *Chemická Kinetika*, p 354, Prague, 1963
[9] ENIKOLOPYAN, N. S., IRYAK, V. I., KRAVCHUK, I. P., PLECHOVA, O. A., RAKOVA, G. V., ROMANOV, L. M. and SAVUSHKINA, G. P. *International Symposium on Macromolecular Chemistry, Prague, 1965.* P 297 (A 672)
[10] JAACKS, V. *Dissertation*, University of Mainz, 1959
[11] PRIBYL, M. and SLOVÁK, Z. *Mikrochim. Acta*, 1964, **6**, 1097
[12] KUČERA, M. and SPOUSTA, E. *Chem. Listy*, 1963, **57**, 842
[13] KUČERA, M. and SPOUSTA, E. *Makromol. Chem.* 1965, **82**, 60

Structural Changes and Molecular Forces in a Compressed Synthetic Polypeptide Monolayer

B. R. MALCOLM

It has been found that structural changes take place when a monolayer of poly-γ-methyl-L-glutamate is compressed. The first stage is the regular collapse of the α-helices in the monolayer to form a bilayer. Further compression appears to cause the formation of a third layer of molecules before the film starts to fold and collapse completely. During this process the molecules become aligned with the mean direction of their axes at right angles to the direction of compression. From the force required to produce a bilayer and the angle of contact of the polymer/liquid interface, the work of cohesion of the polymer has been calculated. Taking into account the molecular structure of the bilayer, and making certain assumptions, the mean work of cohesion per mole of residue pairs has been found to be 3·6 kcal.

EVIDENCE has been obtained to show that the monolayers of a number of synthetic polypeptides are in the α-helical conformation at the air/water interface (Malcolm[1,2]), whereas previous work based on the traditional methods of surface chemistry has led to extended conformations being proposed (Cheesman and Davies[3]). The hypothesis, that for certain synthetic polypeptides the α-helix is stable at the air/water interface, has been based not only on their surface chemistry but also on measurements of deuterium exchange rates and examination of collapsed films by infra-red spectroscopy. Further evidence (to be published), which supports the original conclusions, has since been obtained from electron diffraction examination of collapsed monolayers.

The α-helix is rigid and rodlike by comparison with most polymer conformations, so that the molecules in a monolayer must pack together in parallel groups. It appears that, as a consequence of the local order existing in the groups, when the molecules are compressed a bilayer is formed as a regular process. Since the pressure required to form the bilayer is dependent on the cohesive forces of the molecules of the polymer and the substrate, these observations lead to a new experimental approach to understanding molecular cohesion.

Results will be given here for poly-γ-methyl-L-glutamate to illustrate the process. A full account of the structure and properties of synthetic polypeptide monolayers, particularly in relation to their biological interest, will be given elsewhere.

EXPERIMENTAL

Poly-γ-methyl-L-glutamate with a reported intrinsic viscosity of 1·04 in dichloracetic acid was used, prepared by Yeda Research and Development Co. Ltd. The molecular weight was estimated by the makers to be

260 000 from viscosity measurements by comparison with measurements on poly-γ-benzyl-L-glutamate. Standard solutions for spreading monolayers were made by dissolving about 10 mg in 1 ml dichloracetic acid which was then made up to 10 ml by addition of chloroform. About 0·03 ml of solution was spread on a clean water surface in a fused quartz Langmuir trough. The work was greatly facilitated by the use of a new type of film balance (Malcolm and Davies[4]) consisting essentially of a bent metal strip with its lower edge in the interface. The deflection of the strip, which is proportional to the force on the film, is measured with a microscope. With a platinum–2% rhodium strip 0·003 in. thick, ¼ in. wide, 1 mm deflection corresponds to a force of 23 dyne cm^{-1} on the monolayer. The monolayer was compressed by a barrier moving continuously at the rate of 2 mm/min. All other experimental details, which followed the usual procedures of surface chemistry, were as given previously[2].

RESULTS AND DISCUSSION

Surface area measurement

The force/area curve for a monolayer spread on 0·01 N hydrochloric acid is shown in *Figure 1*. Similar results were obtained using a substrate

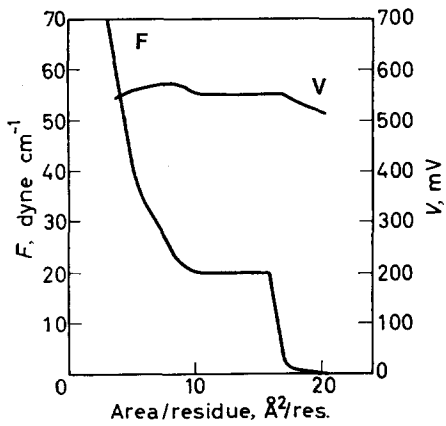

Figure 1—Force/area (*F*) and surface potential measurements (*V*) for a monolayer of poly-γ-methyl-L-glutamate on 0·01 N hydrochloric acid, 20°C

of distilled water. The monolayer, as prepared, is stable over many hours and the force/area curve unaffected by doubling the rate of compression. Extrapolation of the first steep rise of the force/area curve to zero pressure gives an area per residue of 17·5 ± 0·3 Å². At a pressure of 20 dyne cm^{-1} there is a yield point and under slow continuous pressure the film sustains an almost constant force until, at about 10 Å²/residue, the force on the film again rises until at 70 dyne cm^{-1} the film finally collapses. This is shown by irregular movements and rapid drifting of the film balance.

The area per residue of 17·5 Å² may be compared with 17·9 Å² calculated assuming that the molecules are in the α-helical conformation and packed at the same distance as in the solid state in a hexagonal cell with $a = 11{\cdot}95$ Å

and an increment of 1·5 Å per residue along the molecular axis[5]. Precise agreement is not to be expected since the packing of the molecules in a monolayer is not necessarily the same or as perfect as in the crystalline state. This evidence and measurements of deuterium exchange rates (to be published) are consistent with the assumption that the molecules are in the α-helical conformation. Without this hypothesis it is difficult to explain many of the observations.

An area of 10 Å^2/residue is too small to accommodate any reasonable conformation of this polymer in a monolayer and the plateau must therefore be associated with molecules being forced out of the surface and forming a second layer. The plateau does not quite extend to half the condensed area of a monolayer, which suggests that a proportion of the molecules in the monolayer are not in a regular arrangement and therefore require additional work in order to force them out of the surface. At this stage some might start to form a third layer. Over the extent of formation of the plateau, however, the collapse is probably propagated from points where isolated molecules are forced out of the surface. Adjacent molecules in the lower layer will then be in an asymmetric field and pulled upwards. They in turn will act on further molecules. The plateau has not, in any case so far examined, been found to extend to less than half the area of a close-packed monolayer. Its length and the pressure required to form it under given conditions appear to be quite reproducible and a characteristic of the polymer.

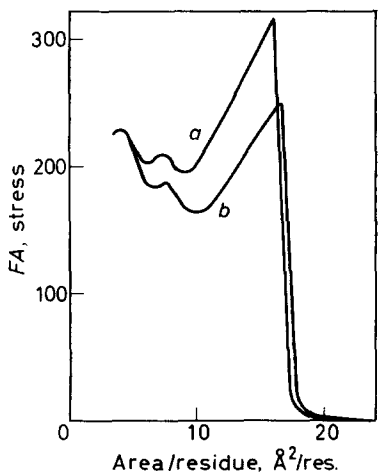

Figure 2—(*a*) Stress/area diagram derived from *Figure 1*, and (*b*) the effect of the addition of ½ per cent v/v isopropanol

The conventional force/area curve for a monolayer, as in *Figure 1*, is probably not the best way to present experimental data in which changes in the mechanical strength of the structure may be taking place. An alternative way is shown in *Figure 2*, in which the product of the force F (in dyne cm^{-1}) and the area A (Å^2/residue) is plotted against A. The product FA represents a quantity proportional to the force per unit cross-

sectional area (i.e. stress) that would be applied to a homogeneous material which increased uniformly in thickness as the area of the film decreased, so that the density remained constant. The deformation of the film as measured by the decrease in area, may be considered to represent the strain on the film and thus *Figure 2* is a form of stress/strain diagram. The collapse of the film to a bilayer is now shown as a continuous decrease in the stress sustained by the film until the process is complete. A further collapse is also indicated giving rise to a minimum at about 6 Å^2/residue, which is probably associated with the formation of a third layer of molecules. The peak of the curve at about 4 Å^2/residue is caused by the onset of folding and collapse of the film, though it may be mentioned that with poly-L-norleucine a further peak is observable before collapse, suggesting the formation of a fourth layer of molecules.

The stress, as calculated from the product FA, is only strictly meaningful when the film is of uniform thickness, i.e. after the formation of an integral number of layers. Nevertheless the fact that after what has been interpreted as a regular collapse is followed by an increase in the stress, as calculated, is a good indication that a transformation giving rise to an ordered structure has taken place. It will be seen that this type of analysis enables information to be obtained which may otherwise be hidden in the steep portions of a force/area graph. Finally, it should be pointed out that since the molecules are becoming orientated during compression (see below) a more detailed analysis of the data should take this into consideration.

Surface potential measurements

Above about 20 Å^2/residue the surface potential is non-uniform showing that the monolayer is condensed. Below 20 Å^2/residue it rises in proportion to the fractional decrease in area down to 17 Å^2/residue (*Figure 1*). This suggests that the dipoles contributing to the surface potential are not becoming reorientated, but simply pressed closer together. Between the yield point and 10 Å^2/residue the potential remains almost perfectly constant.

In the case of poly-L-alanine the surface potential arises entirely from a net reorientation of the water molecules consequent upon spreading the monolayer[2]. This is because, on account of its symmetry, the backbone of a long α-helix can have no dipole moment at right angles to its axis. If, however, as is the case here, the polymer has flexible side-chains, besides the component from the water, an additional contribution is to be expected in a monolayer arising from the dipoles in the side-chains. These will produce a direct component if the dipoles in the side-chains are not arranged in a symmetrical manner so that they cancel out, and an indirect component arising from interaction of some of the side-chain dipoles with the underlying water. It is not possible to judge how big these contributions are, but they appear largely to cancel each other out since the resultant potential is comparable in magnitude to poly-L-alanine. The second layer of polymer might reasonably be expected to have its side-chains in an approximately helical arrangement so that neither the side-chains nor the peptide groups of the second layer can give rise to a potential. If the horizontal plateau in the force/area curve is attributed

to the steady formation of a bilayer of α helices, the remarkable constancy of the surface potential below 17 Å^2/residue can therefore be understood. On the other hand, if the structure of the first layer were an extended polar structure, which underwent a reorientation or conformational change at the yield point, the surface potential would in general be expected to increase or decrease on further compression.

The mechanism of bilayer formation

The pressure required to form a bilayer is altered by not more than one per cent (approximately the limit of relative accuracy for two consecutive experiments) by raising the temperature from 20°C to 30°C or by changing the substrate from 0·01 N hydrochloric acid to distilled water. However, addition of half of one per cent by volume of isopropanol to the trough reduces the pressure required by 5 dyne cm^{-1} (*Figure 2*). This suggests that the pressure necessary is dependent on the work of adhesion of the monolayer to the substrate and gives a clue to the underlying physical process. The work done (if the conversion were 100 per cent) in forming 1 cm^2 bilayer at the observed pressure of 20 dyne cm^{-1} is clearly 20 ergs. Since this involves the removal of 1 cm^2 of monolayer from the water surface, energy must be supplied equal to the work of adhesion W_{SL} of the monolayer to the substrate. This may be calculated from Young's equation

$$W_{SL} = \gamma_{LA}(1 + \cos\theta)$$

where γ_{LA} is the surface tension of the liquid with respect to air and θ the angle of contact for the polymer/liquid interface[6]. θ has been measured by casting a thin clear film of polymer on a glass plate and using the usual dipping plate technique[7]. The value obtained, once the polymer has been dipped below the surface, is 58° ±2° for both distilled water and 0·01 N hydrochloric acid. Addition of half of one per cent isopropanol lowers θ by about 2°. A value 5° higher is obtained if the surface has not previously been wet; this type of hysteresis is not uncommon, but the reason for it in this instance is not known. Taking the value of 58° and $\gamma_{LA} = 72{\cdot}8$ dyne cm^{-1} the work of adhesion of the polymer to water is approximately 111 erg cm^{-2}. Since the mechanical work done in compressing the film is only 20 erg cm^{-2}, it follows that the additional energy for the formation of the bilayer, 91 erg cm^{-2}, is derived from the work of cohesion of the second layer of molecules on top of the first.

It is convenient to introduce here the term 'residue-pair' when discussing a bilayer meaning one residue from each layer. If the bilayer is taken to have a projected area per residue pair of 17·9 Å^2, from the figure above the work of cohesion per mole of residue pairs is 2·35 kcal. If it is assumed that the molecules pack in the same manner as in an infinite hexagonal cell, with the a and c axes parallel to the surface, two thirds of the total number of residues in an infinite structure may be considered to be involved in holding adjacent planes together (the remaining one third hold the molecules together within the plane as, we assume, in a monolayer). Thus the mean work of cohesion of all the residues in an infinite hexagonal

structure is 3·5 kcal/mole of residue pairs (subject to a small correction, see below).

This analysis neglects changes in the entropy of the molecules as a result of the formation of the bilayer. Since both before and after the transition they are presumed to be packed in parallel groups, the entropy change involved is likely to be very small and is neglected.

The assumptions concerning the way the molecules pack when the bilayer is formed require further justification since (*a*) when the bilayer starts to form, the monolayer is under pressure and occupying 16 Å^2/residue rather than 17·9 Å^2/residue as in an unstrained hexagonal cell, and (*b*) it has been assumed that in an unstrained bilayer the packing is hexagonal rather than, say, orthorhombic. A correction for (*a*) can be estimated from the additional work involved in compressing a bilayer from 17·9 Å^2/residue pair to 16·0 Å^2/residue pair. If this is taken as approximately twice the work done in compressing a monolayer over the same monolayer areas, the work done on a bilayer is 2 erg cm^{-2}. Thus the mechanical work done on a monolayer to convert it to an unstrained bilayer is reduced from 20 to 18 erg cm^{-2}. This increases the calculated work of cohesion to 3·6 kcal/mole of residue pairs. Assumption (*b*) is reasonable since there is fairly good agreement between the observed area per residue for an unstrained monolayer and the area expected assuming the same intermolecular distance as in a hexagonal cell, and also it is consistent with the results of electron diffraction examination of the collapsed multilayer (see below).

A further assumption is that the work of cohesion only involves nearest molecules, so that the work of cohesion between the planes of a bilayer is assumed to be the same as between similar planes in an infinite structure. A similar point arises in applying the angle of contact derived from measurements on a cast film of polymer to the calculation of the work of adhesion of a monolayer. In the absence of ionic interactions these are probably good approximations. A more difficult problem is to be sure that the angle of contact measured on the surface of a cast film is strictly applicable to a monolayer, where the structure of the film may be rather different. This may not be a serious limitation, but in the absence of any obvious experimental approach to justify this point, it should be borne in mind.

The corrected value for the work of cohesion per residue pair, 3·6 kcal/mole, appears reasonable. Interpenetration of the side-chains, for which there is direct electron diffraction evidence[8], must make an important contribution to this figure as a result of dipole and van der Waals interactions. However, it is not possible to suggest precise conformations remembering that the helices do not have an integral number of residues per turn and are probably packed with the peptide sequence of individual molecules running randomly in either direction with respect to the molecular axis. The figure is therefore an average value for the diversity of packing arrangements which must be present.

Observations using electron diffraction

If a film is further compressed after the point of final collapse, wrinkles develop which can be seen by oblique illumination of the surface. It can

then be removed as described previously[2] or picked up on electron microscope grids. The grids are dropped on to the film and the film and grids are then lifted off by means of a piece of Perspex, to which the film adheres, being gently placed on the surface. Optical microscope examination shows that in all cases so far examined, the molecules have become orientated with the mean direction of orientation at right angles to the direction of compression. Electron diffraction patterns (to be published) obtained with an Associated Electrical Industries E.M.6 electron microscope show clearly the main diffraction features of the α-helix including the meridional reflection at 1·5 Å. In the particular case of poly-γ-methyl-L-glutamate it is often possible to observe what approximates to a 'single crystal' diagram in that the diffracting crystals in the field (diameter 6μ) are not only all orientated with their molecular axes (c axis) in approximately the same direction but also with an a axis in the plane of the specimen. The diffraction pattern has therefore fewer reflections than the usual type of fibre diagram. This is good support for the hypothesis that the molecules are in the α-helical conformation in the monolayer, and for the interpretation of the surface chemistry data. It also suggests that the procedure used to prepare the specimens might be developed into a logical and precise method for preparing orientated polymer specimens for electron diffraction and other purposes.

CONCLUSIONS

Isemura and Hamaguchi have made observations on the surface chemistry of a number of polymers including poly-γ-methyl-L-glutamate. They appear to have observed a similar collapse phenomenon to the one described here in poly-DL-α-aminocaprylic acid and poly-DL-α-amino-capric acid[9], which, however, they attribute to a reorientation of the molecules and, in poly-γ-benzyl-L-glutamate and -DL-glutamate[10], without offering an explanation. Their data for poly-γ-methyl-L-glutamate appear to be seriously in error, possibly in part due to the use of pyridine as a spreading solvent. They consider the conformation to be that proposed by Ambrose and Hanby[11] for the α-structure, but in view of later work (Bamford, Elliott and Hanby[5]) and the work reported here, this seems unlikely.

It remains to be seen how general is the formation of a plateau in force/area curves of other polymers. So far, it has been found in the methyl, ethyl and benzyl esters of poly-L-glutamic acid, but only an inflection is observed in polypeptides with normal hydrocarbon side-chains unless the side-chain has four or more carbon atoms. It would, therefore, appear that the formation of a bilayer is facilitated by a measure of flexibility in the side-chains.

When it can be shown that the collapse of the polymer film is a regular process, as it is here, observations on synthetic polypeptide monolayers can evidently provide a direct quantitative experimental approach to understanding the cohesional forces between molecules. The information which might be obtained in this way is particularly important in relation to a proper understanding of the stability and conformational changes of proteins.

I am indebted to Mrs V. Bateman for technical assistance and to Dr G. H. Haggis for advice on electron diffraction methods.

University of Edinburgh, Department of Molecular Biology,
The King's Buildings,
West Mains Road, Edinburgh, 9

(*Received July 1966*)

REFERENCES

[1] MALCOLM, B. R. *Nature, Lond.* 1962, **195,** 901
[2] MALCOLM, B. R. *Surface Activity and the Microbial Cell,* p 102. Society of Chemical Industry: London, 1965
[3] CHEESMAN, D. F. and DAVIES, J. T. *Advanc. Protein Chem.* 1954, **9,** 439
[4] MALCOLM, B. R. and DAVIES, S. R. *J. sci. Instrum.* 1965, **42,** 359
[5] BAMFORD, C. H., ELLIOTT, A. and HANBY, W. E. *Synthetic Polypeptides,* p 239. Academic Press: New York, 1956
[6] YOUNG, T. *Phil. Trans.* 1805, **95,** 65
[7] ADAM, N. K. *The Physics and Chemistry of Surfaces,* p 178. Oxford University Press: London, 1941
[8] VAINSHTEIN, B. K. and TATARINOVA, L. I. *Soviet Physics—Doklady,* 1962, **6,** 663
[9] ISEMURA, T. and HAMAGUCHI, K. *Bull. chem. Soc. Japan,* 1952, **25,** 40
[10] ISEMURA, T. and HAMAGUCHI, K. *Bull. chem. Soc. Japan,* 1954, **27,** 125
[11] AMBROSE, E. J. and HANBY, W. E. *Nature, Lond.* 1949, **163,** 483

The Dissolution and Recrystallization of Polyethylene Crystals Suspended in Various Solvents

D. A. BLACKADDER and H. M. SCHLEINITZ*

The dissolution and recrystallization of crystals of polyethylene suspended in p-xylene, n-dodecane, and decalin, are described. It is shown that differential thermal analysis (DTA) can be applied to suspensions of polymer crystals to determine the dependence of dissolution temperature on concentration, temperature of crystallization, and solvent. In addition, DTA can be used to follow the course of isothermal recrystallization of a suspension as a function of time and temperature, as well as recrystallization occurring during heating at a constant rate. The results of DTA, coupled with those obtained by electron microscopy and low angle X-ray analysis, make it possible to present a general picture of the behaviour of suspended polyethylene crystals. Recrystallization normally occurs by a dissolution-redeposition mechanism, and evidence for thickening by creep-up is limited to certain special conditions. A detailed discussion of recrystallization is presented which involves both thermodynamic and kinetic arguments.

SINGLE crystals of many polymers have been prepared by crystallization from solutions[1-3], and the morphological forms have ranged from simple lamellae to complex lamellar aggregates resembling the spherulites characteristic of polymer crystallized from the melt. The conditions affecting the morphology have been studied extensively, and a considerable amount of attention has been given to the melting and annealing of polymer crystals in the absence of solvent.

Relatively few investigators have studied the reorganization or recrystallization of polymer crystals suspended in solvents. The purpose of this paper is to elucidate the changes which occur on heating polymer crystals in a solvent, and to interpret these changes in a phenomenological theory of recrystallization and annealing.

EXPERIMENTAL

Materials

Polyethylene—The polymer used throughout the investigation was Rigidex 50, batch F2609, supplied by Imperial Chemical Industries Limited in the form of extruded pellets. The suppliers quoted a number average molecular weight of 12 300 determined by ebulliometry, and a weight average molecular weight of 104 000 obtained by light scattering. The polyethylene was linear, having fewer than one side branch per 1 000 carbon atoms in the backbone chain, and it contained a small amount of very high molecular weight material.

*Present address: Plastics Department, Experiment Station, E. I. Du Pont de Nemours & Co., Wilmington, Delaware 19898, U.S.A.

Solvents—*n*-Dodecane, *p*-xylene and decalin, were chosen as being respectively poor, moderate and good solvents for polyethylene. Most of the experiments were carried out using *p*-xylene supplied by Imperial Chemical Industries Limited. The specification indicated a purity of not less than 99 per cent with the other isomers as the major contaminants (b.pt 138·0°C, m.pt 12·9°C). The solids content was determined by evaporation; the average of three determinations was 0·003 wt%. *n*-Dodecane was used as supplied by British Drug Houses (b.pt 218·1°C, m.pt −10·5°C). Decalin was also supplied by British Drug Houses who specified that more than 95 per cent of the sample distilled between 188°C and 194°C; the literature boiling points for *trans* and *cis* decalin are 185·5°C and 194·6°C respectively.

Sample preparation

Suspensions of polymer crystals in a solvent were prepared as follows. An appropriate weight of polyethylene pellets was first dissolved in the solvent by heating for two or three hours at 100°C to 140°C depending on the solvent. Crystals of the required type were obtained by quenching the solution in ice water, by cooling at approximately 20 deg. C/hour, or by isothermal crystallization for 1 000 minutes in an oil bath regulated to ±0·3 deg. C. At crystallization temperatures corresponding to less than 20 deg. C supercooling, a significant quantity of polymer remained in solution even after 1 000 minutes, and this precipitated on cooling to room temperature, complicating the morphology of the final crystals. This complication was eliminated as required by carrying out the crystallization (or annealing) process in a specially designed filter funnel which permitted separation of crystals and mother liquor *in situ* at the appropriate temperature. The crystals could then be cooled to room temperature in the absence of mother liquor and re-suspended in fresh solvent to give a suspension of the desired concentration. The precise concentration of the final suspension was determined by means of a mass balance which involved analysis of the mother liquor separated from the original suspension.

$$V_1\rho_1 w_1 = V_2\rho_2 w_2 + V_3\rho_3 w_3$$

Suffix 1 refers to the original solution or suspension, suffix 2 to the mother liquor or filtrate after crystallization, and suffix 3 to the final suspension in fresh solvent. V is volume, ρ density, and w weight fraction. V_3 had to be 5 ml for DTA and a value of 0·001 for w_1 ensured that simple lamellar crystals predominated in the samples. For all experiments other than those designed to show the effect of concentration a volume of 75 ml was used for V_1. If crystallization had been complete at the crystallization temperature ($w_2 = 0$), w_3 would have been exactly 0·015 but since it was not, the precise value of w_3 was determined in each experiment by use of the mass balance, assuming that these dilute suspensions or solutions had the same density. In these circumstances

$$w_3 = (0{\cdot}075 - 73w_2)/5$$

where $73 \pm 0{\cdot}5$ ml is the experimental value for V_2. The value of w_2 was obtained by gravimetric analysis of the filtrate which yielded further crystals of polymer on cooling to room temperature. A carefully weighed quantity

of this suspension was evaporated to constant weight in a porcelain crucible on a hot plate at an appropriate temperature between 90°C and 120°C. Calibration with suspensions of known solids content revealed that crystals retained 11 ± 3 per cent of their own weight of solvent, and a correction was therefore applied to all experimental results. Mother liquor analysis thus made it possible to determine the exact concentration of suspensions used for DTA, as opposed to the nominal concentration which assumed complete crystallization at the stipulated crystallization temperature.

Electron microscopy and diffraction

Samples for electron microscopy and diffraction were deposited on carbon substrates before being shadowed and transferred to electron microscope grids. Electron diffraction patterns could not be photographed under normal illumination but special procedures yielded satisfactory results. A 50 μ condenser aperture was inserted and the accelerating potential was reduced so as to lower the beam intensity at the specimen to approximately one hundredth of the level used for normal viewing. The specimen was barely visible on the fluorescent screen under this illumination. The microscope was focused with the objective aperture in place at a magnification of 8 000. It was then switched to diffraction, the objective aperture removed, and a 50 μ projector aperture inserted and aligned. The diffraction spot was expanded by increasing the magnification of the projector lens in order to select an area for diffraction. The diffraction pattern was obtained by reducing the magnification until the image was reduced to a spot once more, after which the condenser was defocused to reduce the intensity, and a photographic plate was exposed for between 30 and 60 seconds. The microscope was then switched to magnification, and the objective aperture was reinserted. The projector aperture limited the field of view to that area which had contributed to the diffraction pattern already obtained, and a photographic plate was slightly exposed to this image before withdrawing the aperture to photograph the whole specimen. The selected area was defined as an overexposed circle on the resulting electron photomicrograph.

Low angle X-ray diffraction

The low angle X-ray diffraction patterns were obtained by Dr. D. E. Henn at the National Physical Laboratory on the apparatus described by Franks[4]. Two orders or diffraction were observed for crystals prepared by isothermal crystallization, whereas samples which had been annealed appeared to be less regular in thickness.

Differential thermal analysis

The apparatus for DTA was designed in accordance with a theory of operation to be published elsewhere[5]. It consisted of a large heating block containing the cells for the reference material and sample, a controller for constant rate of heating, a potentiometer to measure the temperature of the centre of the reference, and an amplifier–strip chart recorder unit providing up to 10 μV/in. deflection to record the temperature difference between the reference and the sample. The heating block was machined from a 15·2 cm diameter cylinder of Dural 20·3 cm long. A large block was

used to damp out small fluctuations in the heating rate and to reduce heat transfer between the cells to a minimum. The block was non-inductively wound with two heaters and shielded with aluminium foil. The first heater, of 1 200 ohms, was connected to the controller, while the second, of 80 ohms, was controlled by a Variac to provide most of the power for heating the block. A thermocouple for the heating rate controller was located in a 3·2 mm diameter well drilled parallel to the axis of the block at a radius of 6·7 cm. Wells of diameter 1·6 cm at a radius of 2·5 cm accommodated the cells. The heating rate controller amplified the voltage difference between the control thermocouple–ice junction pair and a signal from a voltage divider regulated by a clock motor. The amplified signal difference was used to control a saturable reactor which provided the control heater with up to 250 V. Different heating rates were obtained by changing the clock motor, the rates being linear to within 0·2 per cent and reproducible to within 0·5 per cent. The voltage of the iron–constantan thermocouples was exactly proportional to temperature in the range of interest so the system provided a constant rate of temperature increase. The temperature around the circumference of the cells was naturally non-uniform, but for a heating rate of 2·35 deg. C per minute the maximum difference between any two points on the circumference was calculated to be only 0·071 deg. C. The cylindrical cells were machined from Dural for a close fit in the appropriate wells, and they had an internal diameter and depth of 1 cm and 12 cm respectively. The outer surfaces of the cells were coated with silicone grease to improve thermal contact with the block. The Dural cell tops were machined for a push fit in the cells and were accurately drilled axially to hold 2 mm twin-bore alumina tubes, secured with epoxy resin, to locate and insulate the thermocouples. The thermocouples were made from 36 s.w.g. iron and constantan wire electrically butt welded under paraffin oil to form beads less than 0·3 mm in diameter. Calibration showed that the thermocouples behaved identically. A block diagram of the DTA apparatus is presented in *Figure 1*. The voltage of the reference thermocouple–ice junction pair was measured intermittently and independently of the continuously recorded temperature difference between sample and reference. The parallel connections of the thermocouples ensured a precise indication, on the temperature difference record chart, of the moment in time at which

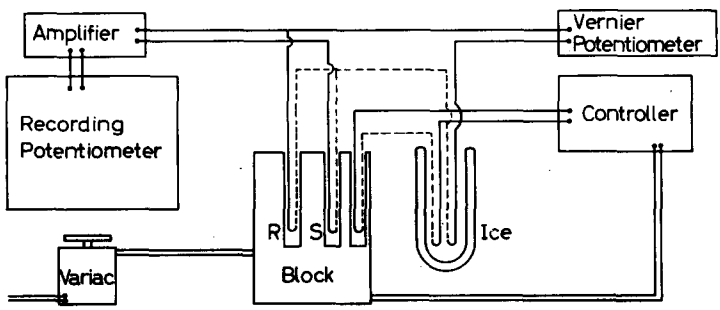

Figure 1—Block diagram of DTA apparatus. R is reference, S is sample

the reference thermocouple–ice junction potential equalled each potentiometer setting. As a consequence of the linear heating rate and of the direct proportionality between temperature and thermocouple potential, the temperature at the centre of the reference cell could be plotted accurately against the recorded temperature difference. The reference material was a polymer of dimethyl silicone, supplied by Midland Silicones, and designated ms 200/1 000 cps.

RESULTS

In experiments concerned with the dissolution of crystals suspended in a solvent it should be noted that the observed enthalpy changes are composite quantities. In addition to the enthalpy change associated with the breakdown of the crystal lattice they include the enthalpy of mixing molten polymer with solvent. The latter is relatively small (see Appendix), but in the interests of basing the discussion on thermodynamic quantities with a definite meaning the term heat of solution will be used here, rather than heat of fusion. For similar reasons the term 'melting' will be avoided although this has come to be used in the polymer literature for both dissolution and melting in the absence of solvent.

The effect of concentration

Although the morphology of polymer crystals is known to be affected by the concentration during crystallization there has been no complementary study of the influence of concentration on the dissolution process. DTA has made it possible to determine the dissolution temperature of polymer crystals suspended in solvent, and to obtain a measure of the heat of solution and of the thermal diffusivity of the system before and after dissolution.

Two sets of experiments were performed. The first concerned the effect of concentration on suspensions of identical crystals, using the technique of separation and re-suspension to obtain all the desired concentrations from material crystallized at a fixed concentration. In the second set of experiments, the required concentrations were obtained directly by crystallization of solutions of the appropriate concentration. Changes in morphology, known to be caused by changes in the concentration at crystallization[6], might be expected to affect the dissolution behaviour of these samples.

For the first group of experiments, single crystals were prepared by cooling a 0·1 wt% solution of polyethylene in 99 per cent *p*-xylene at about 0·3 deg. C per minute. The familiar diamond-shaped lamellae developed, many of which were thickened by spiral growth dislocations. The resulting suspension was filtered and the crystals used to prepare each of the final suspensions by re-suspension in the appropriate volume of fresh solvent. Concentrations of 0·375, 0·75, 1·00, and 1·5 wt% were used for DTA. The crystals in the suspension of lowest concentration were observed to settle slightly on standing. This matter of settling requires some comment because it has an important bearing on the range of concentrations over which reliable measurements are possible. It appears that at concentrations greater than 0·75 wt%, the suspended polymer crystals form an effectively continuous solid phase of very high porosity. Below this concentration, the

crystals settle in order to achieve a self-supporting structure leaving some clear supernatant liquid above. Such a separation is liable to upset DTA measurements if the sensing thermocouples are in the vicinity of the interface. DTA theory requires that heat transfer should be by conduction alone, and experiment has shown that this condition is not satisfied when the sample cell contains solution or solvent only. On the other hand, the thermal diffusivity of suspensions is close to the literature value for pure solvent at the same temperature. This implies that the extremely tenuous agglomerate of polymer crystals contributes little to the thermal diffusivity but restrains convection currents in the solvent. It would appear that in the absence of settling, a polymer suspension approximates closely to the behaviour of a homogeneous *solid* as required by theory.

Figure 2 shows thermograms to illustrate the effect of suspension con-

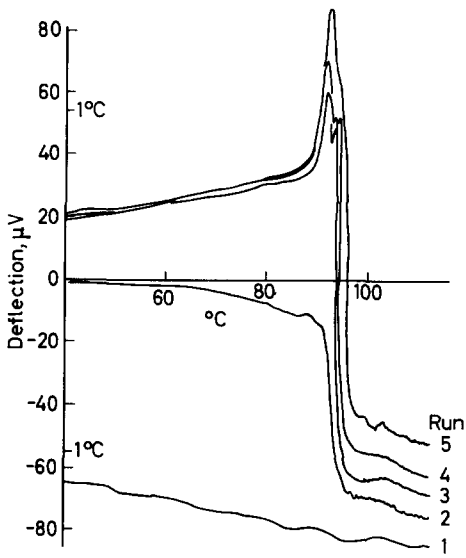

Figure 2—DTA of suspensions of single crystals at various concentrations

centration when the constituent crystals are of identical morphology. Concentrations in excess of about two weight per cent were not feasible because of the limited miscibility of molten polymer and solvent. *Table 1* gives the results corresponding to the traces in *Figure 2*. The dissolution peaks are fairly sharp, but once the maximum differential temperature is passed the fall-off is not rapid as one would expect for simple molecular substances, indicating that polymer crystals are dissolving over a range of temperatures. The dissolution temperature and the thermal diffusivities before and after dissolution were calculated using the new theory[5]. The area enclosed by a peak and the extension of the baseline from lower temperatures is most conveniently tabulated in units of (millivolts)^2.

It is apparent that the experimental values for the thermal diffusivities of the suspensions are considerably lower than the values for the corresponding solutions resulting from the dissolution process. It is therefore impos-

Table 1. DTA of suspensions of single crystals or axialites at various concentrations in *p*-xylene

Run	*Wt%*	T_s, °C	A $(mV)^2 \times 10^3$	D_H, cm^2/sec at 70°C	D_H, cm^2/sec at 110°C
1	0·00	—	—	0·00310	0·00490
2	0·375	89·2	0·4	0·00118	0·00376
3	0·75	91·2	4·1	0·00093	0·00298
4	1·00	91·0	5·6	0·00092	0·00269
5	1·50	91·2	10·4	0·00093	0·00310
6	0·375	92·0	—	0·00247	0·00389
7	0·75	92·0	—	0·00130	0·00307
8	1·00	92·4	5·0	0·00120	0·00242
9	1·50	92·4	12·4	0·00115	0·00167
Literature values for pure *p*-xylene				0·00083	0·00078

T_s is the dissolution temperature, A is the area under the peak, and D_H is the thermal diffusivity of the sample before (70°C) and after (110°C) dissolution. For runs 2 to 5, identical single crystals, prepared indirectly from dilute solutions of the same concentration, were used. For runs 6 to 9 the stated concentration was obtained directly by crystallizing solutions of the appropriate strength. Heating rate 2·35 deg. C/min throughout.

sible to find a reference material which will result in zero temperature difference between sample and reference both before and after dissolution. The thermogram for pure solvent (run 1, *Figure 2*) shows some oscillation about a straight line and some rather high frequency noise. These effects are probably associated with convective heat transfer, the former being due to a slow circulation of solvent in the cell, and the latter to small superimposed eddy motion. This interpretation is supported by the fact that the thermal diffusivity of pure *p*-xylene as determined by experiment is about four times larger than the literature value, indicating a considerable contribution to heat transfer from convection. As already noted, however, the presence of crystals in suspension has a restraining effect on the convection currents.

In the second set of experiments designed to show the effect of concentration, DTA was applied to suspensions which had been prepared at concentrations where axialites are the dominant morphological forms[6]. Axialite suspensions were prepared for DTA by cooling solutions of polyethylene in *p*-xylene at about 0·3 deg. C/min. Even the most concentrated suspension settled noticeably in a few hours, and in the more dilute suspensions, considerable settling took place in a few minutes, reducing the reliability of the results for peak areas. All the results appear in *Table 1*. The thermal diffusivities of the solutions resulting from the dissolution of equivalent amounts of axialites or single crystals were sensibly the same as one would expect, and the thermal diffusivity decreased with increasing concentration of dissolved polymer. The thermal diffusivities of both single crystal suspensions and axialite suspensions were independent of concentration above 0·75 wt% but for any given concentration the axialite suspension showed the higher thermal diffusivity. The axialites were presumably less effective in restraining convection than the same weight of single crystals, and gave an inflated experimental thermal diffusivity. The very large difference for the lowest concentration merely shows that the axialites had settled badly

being more compact than the corresponding weight of single crystals and less able to sustain a tenuous agglomerate structure.

For concentrations greater than 0·75 wt%, the dissolution temperature for suspensions of axialites was of the order of 1 deg. C higher than that for suspensions of single crystals.

The effect of crystallization temperature and the determination of the thermodynamic dissolution temperature

The thermodynamic melting point of solvent-free polymer crystals (T^0_m) is the temperature at which infinitely thick crystals are in equilibrium with pure molten polymer. It cannot be measured by direct experiment, but Hoffman and Weeks[7] showed that if the melting temperature of the most stable crystals is plotted against their crystallization temperature, extrapolation to the point where the two are equal gives T^0_m. The number distribution of crystal thicknesses is Gaussian with a sharp maximum at a thickness given by[8]

$$l^*_p = 4\sigma_e T^0_m / \Delta h_f (T^0_m - T_x)$$

l^*_p is the most probable step height, σ_e is the end surface free energy, Δh_f is the enthalpy of fusion per unit volume of crystal, and T_x is the temperature of crystallization. The thickness of the highest-melting crystals in a given sample is ζl^*_p, where the multiplier ζ increases from unity as the means of detecting the last trace of crystallinity becomes more sensitive. The melting temperature (T_m) can be expressed in terms of ζ:

$$T_m = T^0_m (1 - 1/2\zeta) + T_x/2\zeta$$

To distinguish between the melting of solvent-free crystals and the dissolution process considered in this paper, T^0_m and T_m will be replaced by T^0_s and T_s respectively. T^0_s is therefore the temperature at which an infinitely thick polymer crystal is in equilibrium with pure solvent, and it naturally depends on the polymer–solvent pair. DTA can be used to determine T_s and hence T^0_s for any polymer–solvent pair.

Polyethylene was crystallized for 1 000 minutes at 70°C, 80°C and 85°C from 0·1 wt% solution in *p*-xylene. At first the suspensions were cooled to room temperature without separating the crystals from the mother liquor. Electron photomicrographs showed typical lozenge-shaped crystals formed at the crystallizing temperature with the expected narrow borders, thinner than the rest of the crystal (*Figure 3*). The borders had formed, on cooling to room temperature, from polymer still in solution after 1 000 minutes of isothermal crystallization at the elevated temperature. During DTA of these suspensions at a nominal concentration of 1·5 wt% the thin borders dissolved over a range of temperatures below the dissolution temperature of the bulk of the material. The thermogram traces showed a small second peak in addition to the main peak. *Figure 4* shows the trace for the sample crystallized at 85°C. Recrystallization had clearly been enhanced by the presence of that material which had dissolved from the thin borders at an early stage of the DTA run and redeposited at a later stage as crystalline material with a higher and fairly sharp dissolution temperature. This

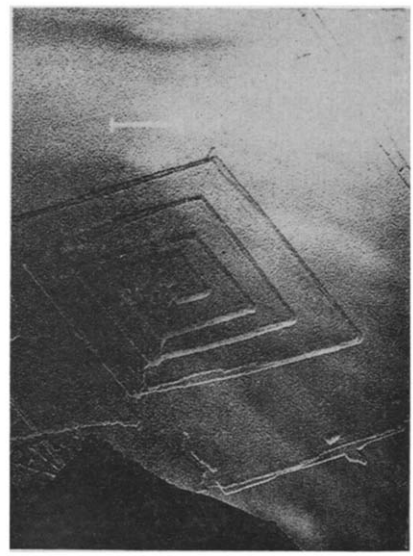

Figure 3—Crystal obtained from *p*-xylene. 0·1 wt % solution crystallized at 80°C for 1 000 minutes then cooled to room temperature without filtering. (Scale bar = 1μ for this and all other electron photomicrographs unless otherwise indicated)

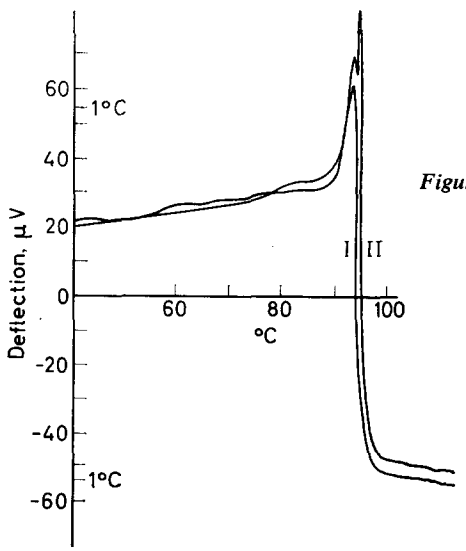

Figure 4—DTA of suspensions prepared at 85°C. I, filtered; II, unfiltered

interpretation was confirmed by filtering a suspension at 85°C after 1 000 minutes of crystallization and re-suspending the crystals in fresh solvent for DTA. The resulting crystals had no thin border (*Figure 5*) and the DTA trace showed only one peak (*Figure 4*). These essentially preliminary experiments established the desirability of isothermal separation of crystals in preparing samples for DTA and the identification of T_s. T_s^0 was therefore determined as follows.

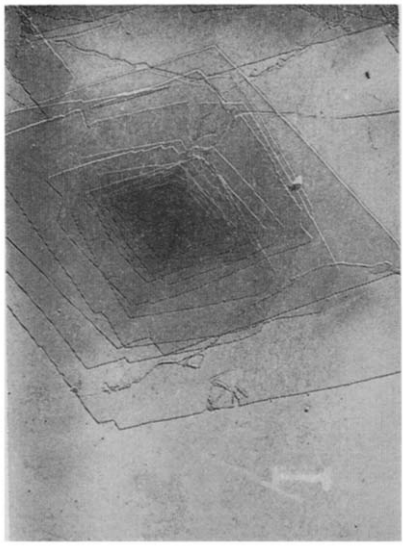

Figure 5—As *Figure 3* but separated at 80°C before cooling

Suspensions of crystals were prepared by isothermal crystallization from 0·1 wt% solution in *p*-xylene at 70°, 80° and 85°C; these crystals were separated off at the crystallization temperature after 1 000 minutes and resuspended in fresh solvent at room temperature to give a nominal concentration of 1·5 wt% suitable for DTA. Crystals characteristic of temperatures above 85°C were made by annealing, because no crystallization occurred even after 1 000 minutes at 90°C. (Annealing is considered in detail in the next section.) Suspensions made at 70°C, 80°C and 85°C were fully annealed at 90°, 92° and 94°C respectively, to provide three further samples. These too were separated at the annealing temperature and resuspended for DTA. The crystals were hollow with almost no trace of the original thickness.

DTA of these suspensions produced traces with only one peak if the heating rate was sufficient to prevent recrystallization during heating. At a rate of 2·35 deg. C per minute, only the crystals prepared at 70°C showed a second peak indicative of recrystallization. For all samples in this series, the peaks were sharper than for corresponding samples obtained by slow cooling from the crystallization temperature without isothermal separation, but even so the crystals undoubtedly dissolved over a narrow range of temperatures. A simulated DTA run in a Pyrex test tube heated at the appropriate rate in an oil bath showed that crystals were no longer visible to the naked eye at the temperature corresponding to the DTA peak, and that temperature may be taken as T_s though it is possible that a number of small, nearly perfect, crystals persist to a slightly higher temperature. The temperature at which the differential temperature on the thermograms falls to the level of the extended baseline may be a better measure of the dissolution temperature of the thickest crystals present. For completeness, both measures of T_s are reported, those of the latter type being designated T'_s (*Table 2*).

Table 2. DTA of suspensions of single crystals at a nominal concentration of 1·5 wt% prepared at various temperatures from dilute solutions in the stated solvent and re-suspended in the same solvent

Run	*Solvent*	T_x *or* T_a, °C	T_s, °C	T'_s, °C
10	*p*-Xylene	70	89·2	—
11	*p*-Xylene	80	90·6	—
12	*p*-Xylene	85	92·6	93·1
13	*p*-Xylene	90	94·2	95·5
14	*p*-Xylene	92	95·0	95·6
15	*p*-Xylene	94	95·9	96·7
16	*n*-Dodecane	95	104·3	105·5
17	*n*-Dodecane	100	105·5	106·2
18	*n*-Dodecane	102·5	105·7	107·0
19	*n*-Dodecane	105	107·2	107·9
20	Decalin	80	88·0	90·1
21	Decalin	84	89·1	90·8
22	Decalin	88	91·1	92·1

Heating rate 2·35 deg. C/min. T_x is the crystallization temperature and T_a the annealing temperature.

Similar techniques were used to find T_s for suspensions of polyethylene in *n*-dodecane. Suspensions were obtained at 95°C and 100°C. The crystals were laminar and resembled crystals prepared from dilute solution in octane[9] or higher paraffins (*Figure 6*). The *a* axis was truncated as in some

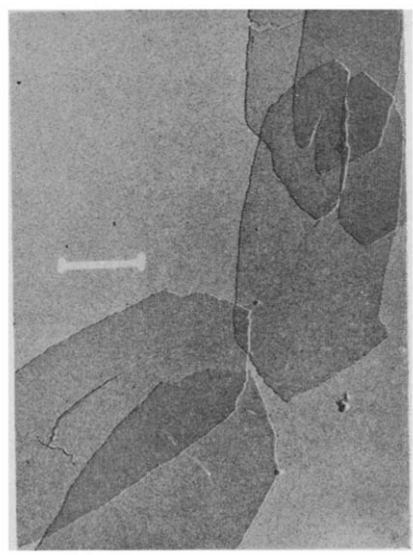

Figure 6—Crystals obtained from *n*-dodecane. 0·1 wt % solution crystallized at 95°C for 1 000 minutes then separated

crystals from *p*-xylene. The cracks and pleats in crystals dried out on the substrate were usually parallel to the *b* axis, suggesting that the crystals were pyramidal while in suspension. The splits in the crystals were analogous to those found in crystals from other solvents. The crack parallel to the (100) face in *Figure 6* is a simple fracture, but the one perpendicular to that direction has pulled fibrils of polymer out of the crystal lattice, indicat-

ing that the chain folds are parallel to the (100) growth face. The fold geometry is similar to that in the {100} sectors of truncated crystals from *p*-xylene. Additional suspensions in *n*-dodecane were obtained by annealing crystals prepared originally at 95°C. After prolonged annealing in the solvent at the elevated temperature the crystals were separated off, cooled to room temperature, and re-suspended in fresh solvent for DTA. The results appear in *Table 2*.

Finally T_s values were obtained for polyethylene in decalin. Isothermally crystallized samples were prepared at 80°C and 84°C and a sample characteristic of 88°C was obtained by annealing an 80°C sample in the solvent. The crystals were identical to those prepared from *p*-xylene. These results also appear in *Table 2*. *Figure 7* displays all the results concerning dis-

Table 3. Thermodynamic dissolution temperatures and values of ζ for polyethylene in various solvents

Solvent	*Best straight line*	T_s^0, °C	ζ
p-Xylene	$T_s=60{\cdot}9+0{\cdot}372T_x$ (or T_a)	96·8	1·35
p-Xylene	$T_s'=60{\cdot}4+0{\cdot}386T_x$	98·3	1·30
n-Dodecane	$T_s=78{\cdot}1+0{\cdot}275T_x$	107·6	1·82
n-Dodecane	$T_s'=82{\cdot}6+0{\cdot}240T_x$	108·5	2·10
Decalin	$T_s=56{\cdot}9+0{\cdot}388T_x$	92·8	1·29
Decalin	$T_s'=70{\cdot}0+0{\cdot}250T_x$	93·3	2·00

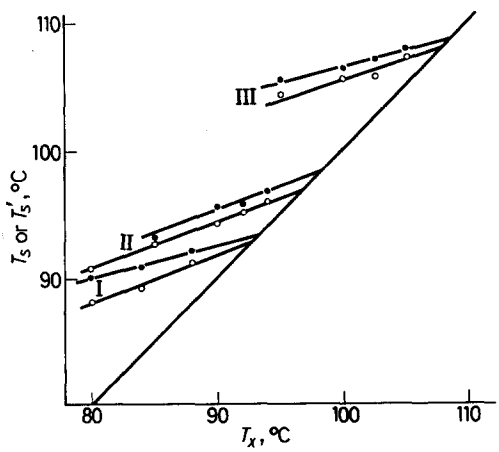

Figure 7—Dissolution temperature (T_s or T_s') as a function of crystallization temperature (T_x). I, decalin; II, *p*-xylene; III, *n*-dodecane

solution temperatures, and *Table 3* gives the equations of the best straight lines and other data.

The results for *p*-xylene in *Table 3* require comment. The best straight line for T_s neglects run 10; the point for this suspension lies well above the line for the other five, probably because crystals started to form before the original solution had reached the nominal crystallization temperature of 70°C. The extrapolation for T_s' similarly neglects the 70°C point and also the 80°C point. The DTA trace for the latter showed a shoulder due to recrystallization.

The thickness of polyethylene single crystals

The step heights of crystals from various suspensions were determined by low angle X-ray analysis. The measured thickness was essentially an average from a large number of crystals and the apparatus could not resolve the two distinct average step heights in certain annealed samples. The results appear in *Table 4*, and are in agreement with the general literature[10].

Table 4. Step heights of single crystals

Solvent	T_x *or* T_a, °C	*Height, Å*
p-Xylene	70	110±9
p-Xylene	85	118±8
n-Dodecane	100	144±10
n-Dodecane	105	152±9

Thickness and step height were shown to be identical by electron diffraction patterns, which indicated that the *c* (molecular) axis was perpendicular to the plane of the crystals. *Figures 8*, *9*, *10* and *11* provide examples of different conditions.

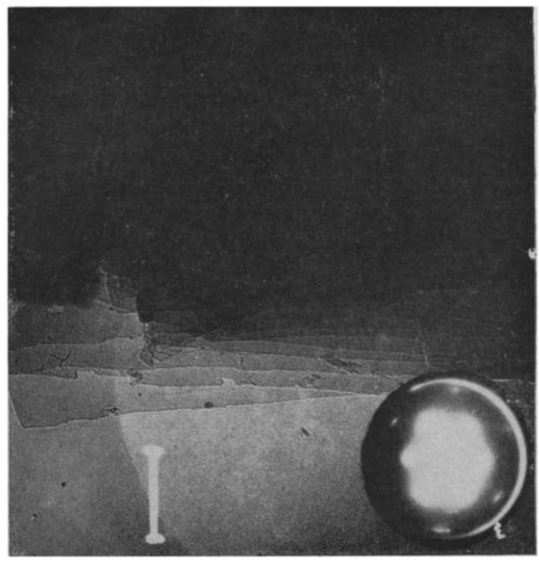

Figure 8—Selected area diffraction pattern of crystals from *p*-xylene (1 000 minutes at 85°C)

The isothermal annealing of single crystals in suspension

Polyethylene single crystals undergo considerable recrystallization when heated in a solvent to temperatures close to the expected dissolution temperature. Samples withdrawn at different stages of annealing can be subjected to DTA as a means of charting the process, provided that it is possible to eliminate or account for recrystallization during DTA. It is clear that polymer single crystals in suspension will recrystallize during DTA if the heating rate is slow enough. It was therefore necessary to document recrystallization occurring during DTA as a preliminary to experiments on annealing.

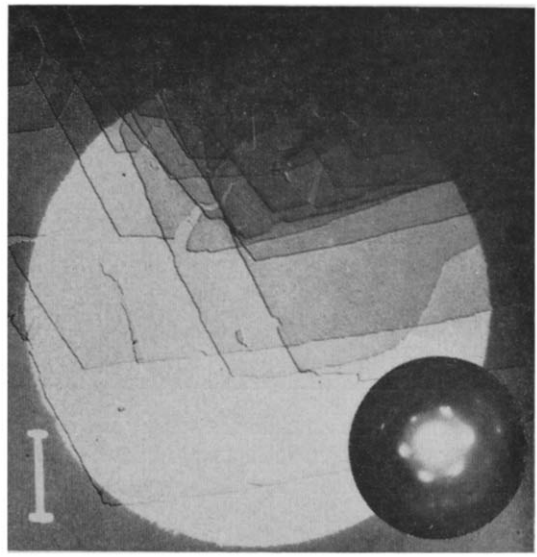

Figure 9—Selected area diffraction pattern of crystals from *n*-dodecane (1 000 minutes at 95°C)

Suspensions were prepared at 70°C, 80°C and 85°C, and subjected to DTA, especially at the lower heating rates. The suspensions were not filtered at the crystallization temperature so as to bring out every possible complicating feature of recrystallization during DTA. *Figure 12* shows typical results. The relative area of the second peak increased at lower heating rates, indicating a greater amount of recrystallization. The results are summarized in *Table 5*, and *Figure 13* shows that the total peak area was proportional to the rate of heating. For crystals prepared at 80°C, the

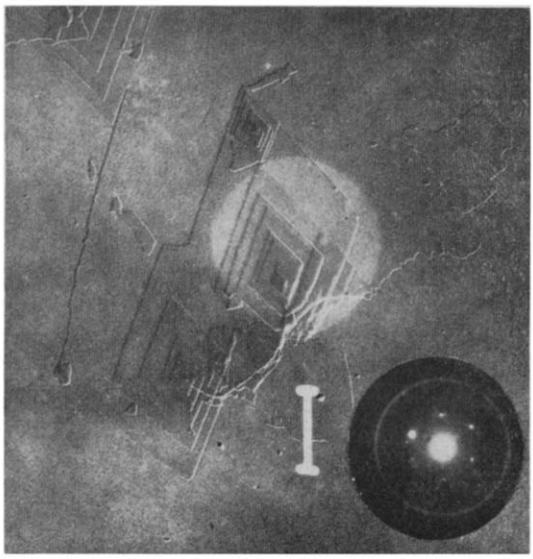

Figure 10—Selected area diffraction pattern of crystals from decalin (1 000 minutes at 80°C)

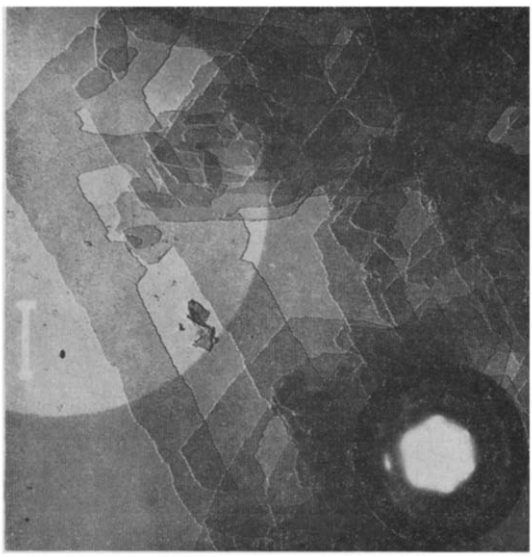

Figure 11—Selected area diffraction pattern of crystals from *n*-dodecane (1 000 minutes at 95°C, then 1 000 minutes annnealing at 105°C)

second peak was not significant at heating rates above 0·94 deg. C/min, and for crystals prepared at 85°C, it was not observed above 0·235 deg. C/min. The corrected temperature of the first peak was almost constant, but the temperature corresponding to the second peak increased as the rate of heating decreased.

From the results in *Table 5* the fraction of polymer which has recrystallized can be calculated from the ratio of the area of the second peak to the total area (*Figure 14*). In addition, the negative ratio of the post-dissolution slope on a DTA trace to the pre-dissolution slope is an index of the dissolution range of the material. A sample dissolving over a narrow range of temperatures will have a high index, and it is clear from *Table 5* that

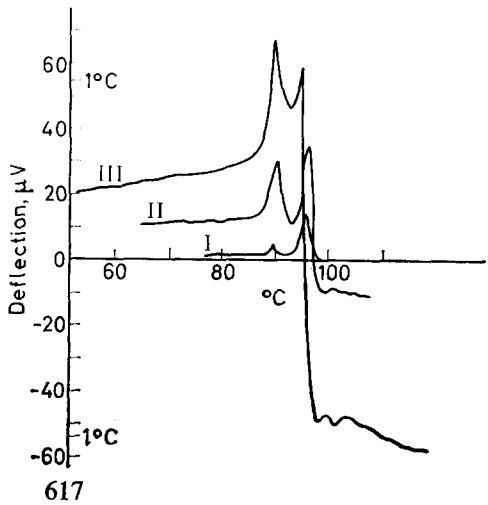

Figure 12—DTA of suspensions prepared at 70°C. Effect of heating rate: I, 0·235 deg. C/min: II, 0·94 deg. C/min; III, 2·35 deg. C/min

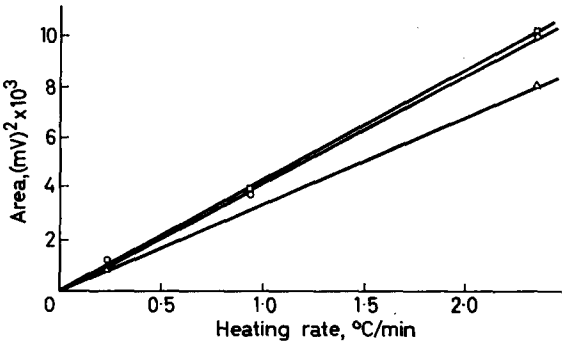

Figure 13—Total DTA peak area as a function of heating rate. Crystals prepared at various temperatures: ○, 70°C; □, 80°C; △, 85°C

Table 5. DTA of suspensions of single crystals in *p*-xylene at different rates of heating. Nominal concentration of suspensions 1·5 wt%

T_x, °C	*Heating rate, deg. C/min*	T_{s_1}, °C	T_{s_2}, °C	A_1 $(mV)^2 \times 10^3$	A_2	*Index*
70	2·35	89·3	94·5	7·6	2·3	21·0
70	0·94	89·8	95·4	1·87	1·87	2·9
70	0·235	89·5	95·6	0·12	1·10	1·2
80	2·35	90·8	—	10·1	—	—
80	0·94	90·8	95·0	3·84	0·4	5·5
80	0·235	90·6	96·2	0·49	0·76	1·9
85	2·35	92·6	—	8·0	—	—
85	0·235	92·9	96·7	0·76	0·07	6·9

T_{s_1}, T_{s_2}, are the dissolution temperatures associated with the first and second peaks respectively, having areas A_1, A_2. See text for explanation of last column.

for crystals prepared at a given temperature, the recrystallized material had a sharper dissolution temperature at higher rates of heating. Similarly, for a given heating rate, the material recrystallized from samples prepared at a higher temperature had a sharper dissolution temperature. These conclusions, based on DTA, were complemented by the results of electron micro-

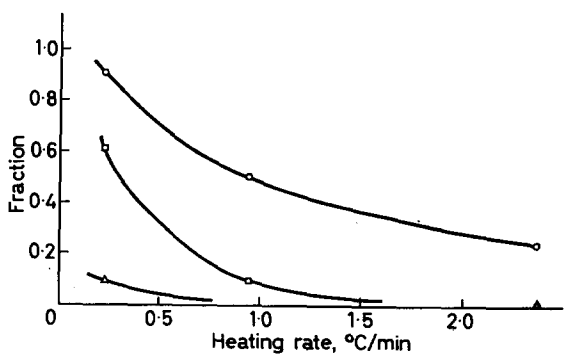

Figure 14—Fraction of material recrystallized during DTA as a function of heating rate. Crystals prepared at various temperatures; ○, 70°C; □, 80°C; △, 85°C

scopy. A suspension of crystals, prepared by quenching a 0·5 wt% solution of polyethylene in *p*-xylene was annealed at 85°C, and was then heated at 0·3 deg. C/min. Samples were withdrawn at temperature intervals of 1 deg. C and cooled by rapid dilution in tenfold excess of *p*-xylene at 20°C. The annealed crystals had thickened borders and no change occurred until 89°C when the edges began to dissolve. (The technique of dilution-cooling effectively prevents the formation of *thin* borders.) At higher temperatures, large single crystals were found after quenching. The centres of the original crystals and the thickened borders dissolved last of all (*Figures 15, 16, 17* and *18*). A similar experiment was performed with a suspension of crystals obtained by quenching a 0·5 wt% solution of polyethylene in *n*-dodecane. The suspension was annealed at 100°C. The morphological changes observed on heating the product at 0·3 deg. C/min were entirely analogous to those observed for crystals prepared and annealed in *p*-xylene.

When the above investigation of the occurrence and extent of recrystallization during DTA had been carried out it was possible to use DTA to follow the progress of annealing at a fixed temperature. Crystals prepared at 70°C were annealed in *p*-xylene at 90°C at a concentration of 0·1 wt%. The annealing was terminated at 6, 40, 100 or 1 000 minutes and the crystals were separated at the annealing temperature before cooling to room temperature for re-suspension in fresh solvent for DTA. In the initial stages of annealing the edges of the crystals dissolved (*Figure 19*) but later the dissolved polymer recrystallized on the edges of the original crystals with the thickness appropriate to 90°C, the annealing temperature, thus forming a thickened border (*Figure 20*). Finally, the centres of the crystals dissolved completely leaving picture frames consisting exclusively of material having a thickness appropriate to 90°C (*Figure 21*). Thermograms for the DTA analysis of the original, unannealed crystals, and the most fully

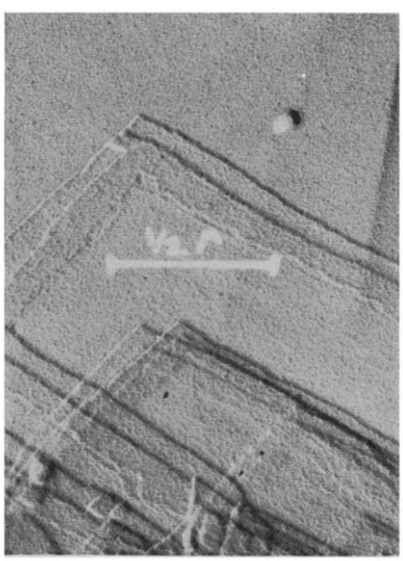

Figure 15—Crystals prepared by quenching a 0·5 wt% solution in *p*-xylene followed by annealing in the same solvent at 85°C

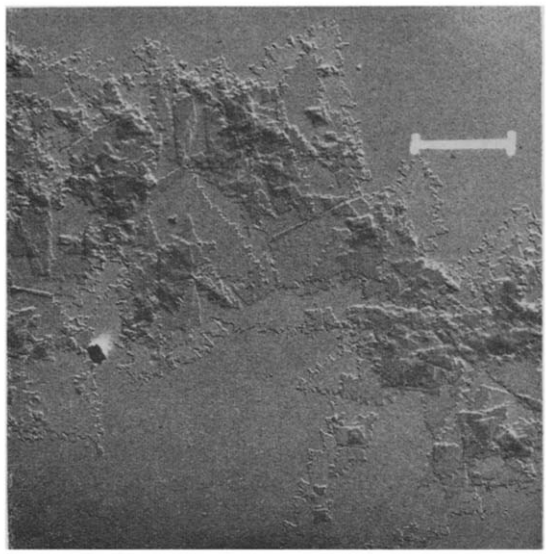

Figure 16—Changed morphology of crystals in *Figure 15* as a result of heating in suspension to 89°C at 0·3 deg. C/min; the edges have started to dissolve

annealed crystals, are shown in *Figure 22*. The original crystals gave two peaks, understandable in the light of the previous experiments. The first peak, at 89·2°C, originated from the dissolution of material having the original thickness or fold length, while the second peak, at 94·5°C, accounting for about 23 per cent of the sample, was due to recrystallization during DTA. Suspensions annealed for only 6 or 40 minutes also showed two peaks, but the area of the second increased relative to the total area due to

Figure 17—Further consequences of heating the crystals in *Figure 15* in suspension at 0·3 deg. C/min to between 89°C and 92°C; dissolved polymer has recrystallized on cooling to give regular lamellae once more

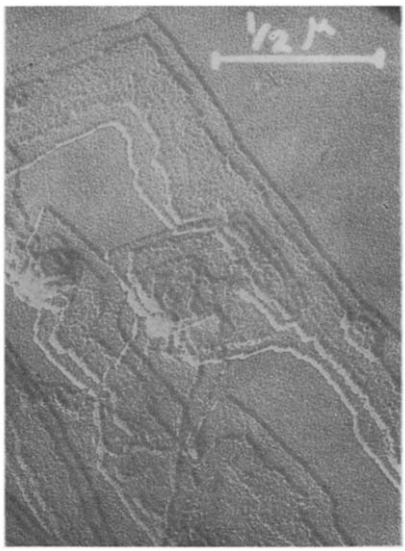

Figure 18—Final state of crystals shown in *Figure 15* after heating to 92°C at 0·3 deg. C/min; the centres have dissolved

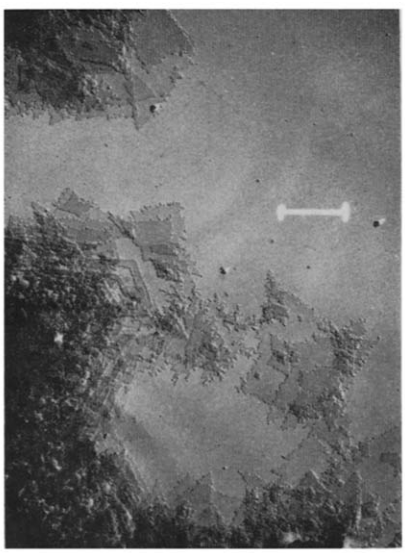

Figure 19—Crystals prepared from *p*-xylene at 70°C and annealed in the same solvent at 90°C for 6 min; the edges have started to dissolve

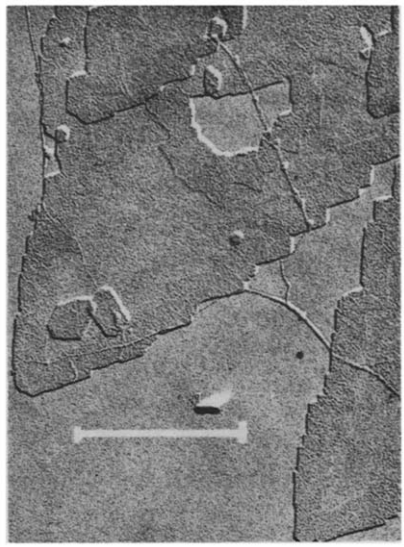

Figure 20—Crystals prepared from *p*-xylene at 70°C and annealed in the same solvent at 90°C for 40 min; thickened borders have started to form

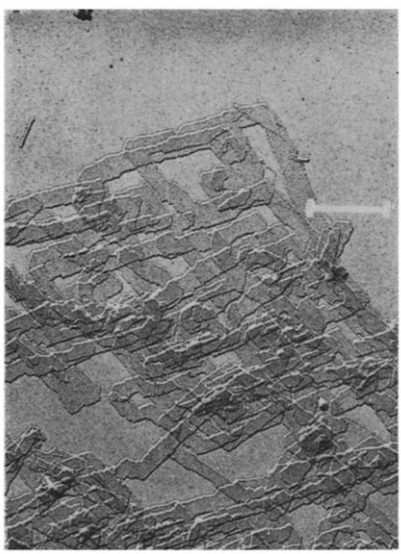

Figure 21—Crystals prepared from *p*-xylene at 70°C and annealed in the same solvent at 90°C for 1 000 min; the centres have dissolved leaving thickened 'picture frames'

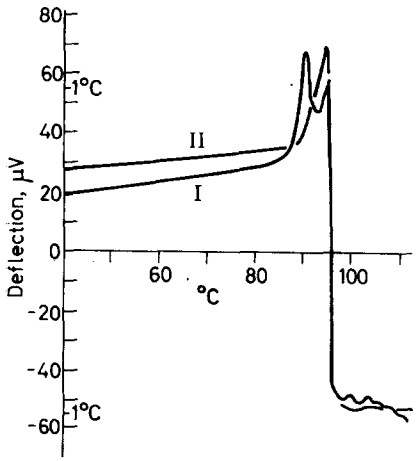

Figure 22—Effect of annealing on DTA trace; I, as prepared; II, annealed

recrystallization during the annealing process, augmented, though to a decreasing extent, by recrystallization during DTA. The results appear in *Table 6*. In a similar set of experiments, displayed in the same table, suspensions prepared at 85°C were annealed for 10, 30, 110 and 1 000 minutes at 93°C, a temperature 0·4 deg. C higher than the dissolution temperature of crystals characteristic of 85°C. The results are entirely analogous to those in the first set. The initial dissolution was more rapid and extensive, but the subsequent recrystallization was slower. The sequence of morphological changes in the annealing experiments at 93°C followed closely the results at 90°C but the thickened borders did not appear until the crystals had

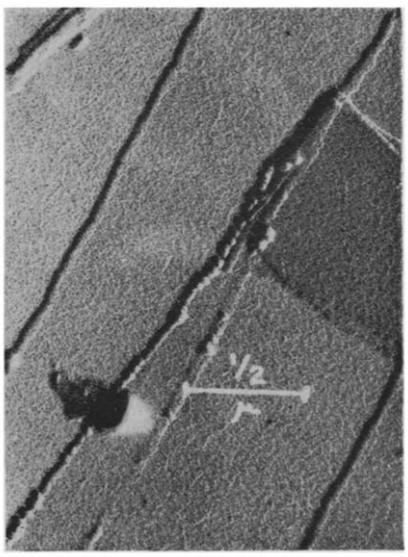

Figure 23—Crystals prepared from *n*-dodecane at 95°C and annealed in the same solvent at 105°C for 25 min

been annealed for 110 minutes. Several other miscellaneous experiments in *p*-xylene appear in *Table 6*.

Table 6. DTA of suspensions prepared and annealed at various temperatures in *p*-xylene or *n*-dodecane. Nominal concentration 1·5 wt%. Heating rate 2·35 deg. C/min; t_a is time of annealing

Solvent	T_x, °C	T_a, °C	t_a, *min*	T_{s_1}, °C	T_{s_2}, °C	A_1 $(mV)^2 \times 10^3$	A_2
p-Xylene	70	90	0	89·2	94·5	7·6	2·3
	70	90	6	89·6	94·8	5·7	3·5
	70	90	40	91·2	94·6	1·8	4·4
	70	90	100	—	94·2	0·42	3·8
	70	90	1 000	—	94·2	—	5·1
	85	93	0	92·6	—	8·0	—
	85	93	10	93·6	—	5·0	—
	85	93	30	93·4	—	4·1	—
	85	93	110	93·8	94·5	0·92	2·4
	85	93	1 000	—	94·5	—	3·8
	70*	85	1 000	89·6	93·5	8·9	1·2
	80	90	1 000	92·2	94·4	7·6	2·4
	80	92	1 000	—	95·0	—	2·9
	85	94	1 000	—	95·9	—	0·7
n-Dodecane	95	105	0	104·3	105·3	3·3	2·6
	95	105	25	105·3	106·6	0·98	1·25
	95	105	107	106·5	107·6	0·25	1·02
	95	105	1 000	—	107·3	—	2·75

*Showed an additional peak at 94·8°C of area 0·4.

Experiments on the annealing of suspensions in *n*-dodecane revealed certain new features. Dissolution again began from the edges but very few thickened borders were observed. Even after prolonged annealing few hollow crystals appeared and they seemed to have exceptional stability along the *b* axis. Many crystals had a series of small projections along the edges after moderate annealing; others had larger fragments of material on the surface (*Figures 23* and *24*, *Table 6*). The peak areas for DTA of suspensions in *n*-dodecane are of low accuracy because the traces deviated from a straight baseline several degrees before the onset of dissolution proper.

DISCUSSION

The effect of concentration on dissolution temperature

In the range of suspension concentrations over which settling is absent and where a homogeneous solution is formed, the observed dissolution temperature of *identical* single crystals is virtually independent of the concentration of the suspension. Flory's thermodynamic treatment[11] of solid polymer–solution equilibrium predicts a variation of 'solubility point' temperatures of about 0·5 deg. C over the range from 0·1 wt% polymer to 1·5 wt% polymer, though that treatment takes no account of the surface free energy term present in small crystals.

The results for axialite suspensions (*Table 1*) also show that the dissolution temperature is sensibly constant over the range considered, though the small rise may be genuine. The noteworthy point is that for any concentration, the dissolution temperature of a suspension of axialite crystals is about 1 deg. C higher than that of the corresponding concentration of single crystals. The results are similar to those of Jackson, Flory and Chiang[12],

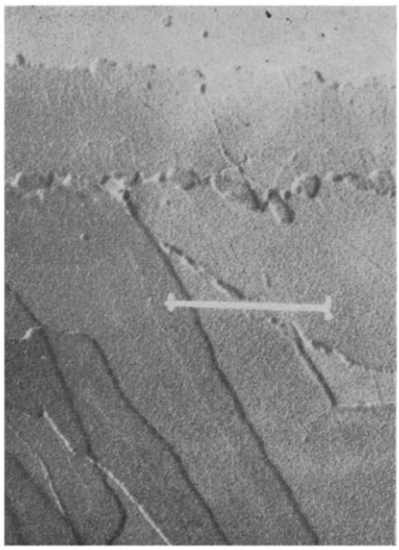

Figure 24—Crystals prepared from *n*-dodecane at 95°C and annealed in the same solvent at 105°C for 25 min

who compared the dissolution temperatures of mixtures of polyethylene and tetralin both for bulk-crystallized material and for single crystals prepared from solution. They found that for increasing dilution, the dissolution temperature of the solution-crystallized material fell further and further below that of the bulk-crystallized material, reaching about 13 deg. C in the limit. All of these findings are compatible with the idea that axialites occupy an intermediate position between the simplicity of lamellar crystals and the complexity of spherulites. There can be little doubt that axialites are composed of lamellae whose thickness is similar to that of single lamellar crystals prepared from the same solvent at the same temperature. The higher dissolution temperature of axialites noted in the present study might be due to either of two causes. The lamellar constituents of axialites are distinguished from simple lamellae in the form of lozenges, and also from splaying multilayer crystals, by the presence of a relatively large number of interlamellar tie molecules which bind adjacent lamellae into a contiguous packet[6]. (Spherulites are a natural consequence of the extension of lamellar binding.) Since dissolution of a crystal begins at the edges, it is quite likely that the presence of tie molecules in axialites impedes the dissolution, and that adjacent lamellae prevent the solvent from associating freely with polymer chains in the lamellar growth faces. The other possibility is that suspensions of axialites may tend to begin crystallizing at higher tempera-

tures during the preparation stage, thus causing a difference in dissolution temperature when compared with suspensions of single lamellar crystals.

The effect of crystallization temperature and the determination of the thermodynamic dissolution temperature

Table 3 and *Figure 7* show the results of using the extrapolation procedure for determining T_s^0, the procedure originally devised by Hoffman and Weeks[7] for melting in the absence of solvent. In *Table 7* the final results are compared with the findings of other workers.

The comparison of these data is greatly complicated by the present uncertainty concerning the effect of molecular weight[16,17], a difficulty which appears in all related attempts at a theoretical treatment. For example, Flory's discussion of the thermodynamics of polymer solutions[11] involves a polymer–solvent interaction coefficient, and this should become independent of molecular weight for sufficiently high degrees of polymerization. Wunderlich[18] has confirmed this prediction with *o*-xylene, but it is not in agreement with the results for *p*-xylene obtained by Trementozzi[19]. In the circumstances it is probably not very profitable to calculate T_s^0 from Flory's equations.

Holland's results[14] (*Table 7*) call for particular comment. A fraction of Marlex 50 with a viscosity average molecular weight of 135 000 was used in

Table 7. The thermodynamic dissolution temperature of polyethylene in different solvents

Solvent	*Method*	T_s^0, °C	ζ	*Reference*
p-Xylene	DTA	96·8, 98·3	1·35, 1·30	This work
n-Dodecane	DTA	107·6, 108·5	1·82, 2·10	This work
Decalin	DTA	92·8, 93·3	1·29, 2·00	This work
Xylene	Light scattering	100·0	0·995	Peterlin and Meinel[13]
Xylene	Slow heating	106·0	0·795	Holland[14]
Xylene	Hot stage microscope	96·0		Coran and Anagnostopoulos[15]
n-Dodecane	Hot stage microscope	109·5		
Decalin	Hot stage microscope	91·0		

The double entries for the present work are explained in Results.

his experiments. A 0·01 wt% suspension in xylene was heated at 1 deg. C per day, and the dissolution temperature of crystals of any particular thickness was taken as the maximum temperature at which that thickness could still be observed. It seems very probable that this approach involves an unreasonable neglect of kinetic considerations. The slow heating rate would certainly lead to the formation of thickened borders as stated in Holland's paper, but there is no guarantee that the thinner centre had been given enough time to dissolve away at the temperature where complete dissolution should have occurred. Once the edges of crystals have been blocked by the deposition of material with a new fold length appropriate to

a higher temperature, further dissolution from the centres of the crystals will be extremely slow. It would therefore be very easy to be misled into thinking that a portion of the original crystal had persisted because it was thermodynamically stable when in fact it was unstable, but restricted to a very slow rate of dissolution by kinetic factors.

It would appear that discrepancies between the results of different workers as shown in *Table 7* cannot be put down to one particular cause. On the other hand the general variation of T_s^0 from one solvent to another is wholly in harmony with intuitive expectation. Of the three solvents used in the present work decalin is a good solvent for polyethylene, *p*-xylene moderate, and *n*-dodecane poor. The corresponding mean values of T_s^0 (from T_s and T_s') are 93·1°C, 97·6°C and 108·1°C. The implication is that the fold surface free energy is not markedly dependent on the nature of the solvent present, a matter which figures in the next part of the discussion.

Estimation of the fold surface free energy

Lauritzen and Hoffman[8] derived an expression for the dissolution temperature of single crystals by the use of classical thermodynamics. They found that the dissolution temperature (T_s) could be represented:

$$T_s = T_s^0 (1 - 2\sigma_e / \Delta h_f l)$$

The original paper used T_m and T_m^0, but for reasons already given, the alternatives T_s and T_s^0 are preferred here. σ_e is the fold surface free energy, Δh_f is the heat of fusion of 1 cm³ of crystals, and l is the thickness of the crystal. Using the Lauritzen and Hoffman value of Δh_f it is possible to calculate σ_e from the data in *Tables 3* and *4*. The results appear in *Table 8*.

Table 8. Calculation of end surface free energy

Solvent	T_x, °C	T_s^0, °K	T_s, T_s' °K	l $cm \times 10^6$	σ_e erg/cm^2
p-Xylene	85	370·0	365·8	1·18	19
p-Xylene	85	371·5	366·3	1·18	23
n-Dodecane	100	380·8	378·7	1·44	11
n-Dodecane	100	381·7	379·4	1·44	12
Decalin	80	366·0	361·2	1·14	22
Decalin	80	366·5	363·3	1·14	14

$\Delta h_f = 2{\cdot}8 \times 10^8$ erg/cm³. The values of l for crystals from decalin were estimated from electron photomicrographs and the corresponding results for σ_e are of limited reliability.

Estimates of σ_e for polyethylene range from 20 erg/cm² to 180 erg/cm², and experimental values ranging from 57 erg/cm² to 140 erg/cm² have been reported by various authors[14, 20-22]. Recent investigations[13, 14] based on the thermodynamic melting point indicate that $\sigma_e = 50 \pm 10$ erg/cm² but a paper by Richardson[23] shows that lower values are to be expected at higher temperatures. He determined the value of σ_e as a function of temperature by

a precise calorimetric method and found that it decreased from 80 erg/cm^2 at 30°C to 25 erg/cm^2 at 100°C.

The values of σ_e obtained in the present investigation are lower than any obtained previously, but it is now clear that the problem of establishing reliable values involves a much more detailed specification of the conditions than was formerly supposed. In particular the effect of solvent is difficult to predict, though Richardson's mechanism for the gradual unloosening of sharp folds with increasing temperature suggests that the relatively small molecules of a solvent may assist the process so that a lower value of σ_e would result at any given temperature. Furthermore, Peterlin and Meinel[24] have shown that the fold surfaces of single crystals may be less compact than was previously supposed. The values of σ_e reported here are certainly not precise enough to justify further comment on the possible effect of solvent, even if the decalin results are neglected. Recent results of Kawai and Keller[9] are noteworthy in suggesting that even the long spacing is not independent of solvent, despite former beliefs to the contrary.

Isothermal annealing of single crystals in suspension

In this section of the discussion the experimental results on annealing are commented upon and related to the findings of other workers. Special features of recrystallization during annealing are discussed, but the formulation of a general mechanism to account for the behaviour of crystals in suspension is reserved for the final section.

The results of the experiments on isothermal annealing appear in *Table 6*. The general progress of annealing as a function of time can be followed by a combination of the DTA results in *Table 6* and mother liquor analysis. The latter gives the fraction of total polymer in solution, and the remaining polymer is allocated to unchanged or recrystallized fractions on the evidence of the respective DTA peak areas. *Figure 25* typifies the results obtainable

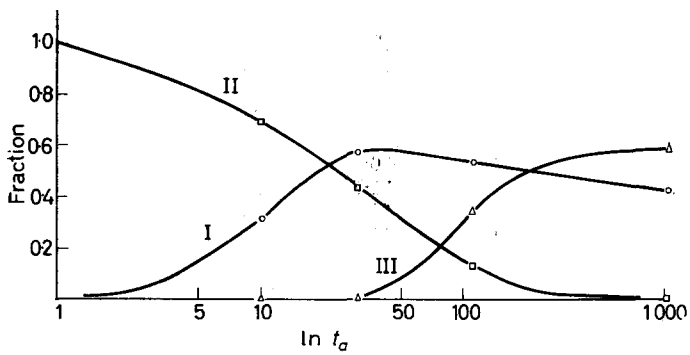

Figure 25—Distribution of polymer on annealing at 93°C in *p*-xylene; I, fraction in solution; II, fraction unaltered; III, fraction recrystallized

by this procedure. The results in *Table 6* show that the dissolution temperature of the unchanged material (T_{s1}) in a particular suspension is slightly increased as the time of annealing is extended. If the effect is genuine, it

could be that the recrystallized material provides an increasingly protective thickened border which makes the original material superheat a little before dissolving as a result of limited solvent access. Superheating of solvent-free crystals has been discussed by Zachmann[25] and by Hellmuth and Wunderlich[26]. Annealing for 1 000 minutes failed to remove all traces of the original thickness in a suspension, provided that the temperature lay below the expected dissolution temperature of the original crystals. Both DTA and electron microscopy revealed these persistent traces, perhaps the only techniques sensitive enough to do so. On the other hand annealing for 1 000 minutes at temperatures slightly above the expected dissolution temperature completely eliminated the original material and produced picture frame crystals with a new dissolution temperature (T_{s2}) characteristic of the annealing temperature. Dissolution undoubtedly begins at the edges but, once a thickened border has started to form, edge dissolution is not possible and the subsequent very much slower dissolution involves solvent attack on the centres of the crystals. The fact that thickened border formation is the preferred alternative to the formation of new crystals having the appropriate fold length is clear evidence that nucleation of the new fold length on existing, though thinner, growth faces requires less free energy than the formation of a free nucleus of the new fold length.

The results of the present work extend and largely substantiate the qualitative conclusions of other workers. Keller and Bassett[27] observed that when crystals were heated rapidly to above their crystallization temperature, the edges of the crystals, the (100) and (110) growth faces, began to dissolve. They also noted that crystals formed at a low temperature, heated to 83°C, and cooled without filtering, acquired new growths round the edges which were eliminated by filtering at the high temperature. Bassett and Keller[28] first reported the production of a thickened step on crystal edges as a consequence of partial dissolution and recrystallization. On prolonged annealing the centres of the crystals also dissolved but sector boundaries were noted to be especially resistant to dissolution. The {110} sectors were stated to be more stable than the {100} sectors, but the present work provides no support for these conclusions. The sector boundaries did not appear to be especially resistant to dissolution, and the above-mentioned sectors were of comparable stability. Holland's work on dissolution[14] confirmed the general pattern of thickened border formation followed by slow dissolution of centres. Peterlin and Meinel[13] used light scattering to follow the dissolution of extremely dilute suspensions of polyethylene in xylene. During isothermal annealing the scattered light intensity dropped very sharply indicating a high degree of dissolution followed by a slow recovery corresponding to recrystallization.

All of the above discussion referred to experiments using *p*-xylene or xylene as the solvent. The lower results in *Table 6* show the effects of annealing in *n*-dodecane. The electron photomicrographs (*Figures 23* and *24*) show certain features not observed in the xylene experiments. It is clear that the recrystallization of single crystals in suspension in *n*-dodecane proceeds in part by the dissolution–redeposition mechanism but, in addition, there is some evidence for the phenomenon of thickening by creep-up,

especially at the crystal edges. Many reports indicate that such a mechanism is responsible for the increase in long period when single crystals are annealed in the absence of solvent. Frank, Keller and O'Connor[29] showed that when crystals of poly-4-methyl-pentene-1 were heated, the appearance of holes was accompanied by the production of thickened portions, especially near the edges and sector boundaries. Bassett and Keller[28] showed substantial edge recrystallization in the absence of solvent. Hirai, Mitsuhata and Yamashita[30] have described the heating of dry crystals at 120°C. The crystals underwent considerable structural changes resulting in amoeba-like shapes, but no thickening was observed, though many dark portions extended inwards from the edges of the crystals. The authors suggest that the dark portions may be nuclei for the thickening process, these nuclei being 30 Å to 40 Å thicker than the rest of the crystal. Reneker[31] has devised a model by which these nuclei might form if folded molecules extend beyond the lattice from time to time as a result of thermal fluctuations. Molecules located in the growth faces are less securely bound than those elsewhere in the lattice, and nuclei are more likely to develop in consequence. A similar process seems to occur in crystals annealed in *n*-dodecane at 105°C although several investigators suggest that thickening in the dry state cannot occur by this mechanism at temperatures below 110°C. Fischer and Schmidt[32] and others noted that single crystals are stable at 105°C for 24 hours. N.m.r. measurements have shown that the number of chains with high mobility is greatly increased by annealing, but Thurn[33] and Slichter[34] point out that large scale mobility develops only above 108°C or 110°C. In order to explain how this sort of mechanism might operate in *n*-dodecane at 105°C it is necessary to invoke the idea that the lattice can be weakened by solvent. Kawai[35] has developed a theory to account for this, and it is certainly true that similar reductions in lattice forces occur in other systems. Kedzie[36] in particular has shown that low temperature mobility is due to solvent retention. Hoffman and Weeks[37] have reported the thickening of crystals maintained at the crystallization temperature itself.

It would seem that a creep-up mechanism for crystal thickening may always be possible for suspensions at temperatures as low as 105°C subject to the appropriate penetration of the crystal lattice by solvent. For a good solvent, however, it is likely that the contribution of the creep-up mechanism to crystal thickening will be completely overwhelmed by recrystallization brought about by the dissolution–redeposition process.

The mechanism of recrystallization

An acceptable mechanism for the dissolution and recrystallization of polymer single crystals suspended in a solvent must account for the following observations:

(*i*) Single crystals begin to dissolve from the growth faces. The temperature at which dissolution first becomes significant increases with the crystallization temperature T_x.

(*ii*) Dissolved polymer may recrystallize as a thickened border around the original crystals. This will normally occur on annealing at a tempera-

ture near T_s, but it will also take place during heating at a constant rate unless the rate is high.

(*iii*) After a thickened border has formed, a further increase in temperature *or* prolonged annealing (provided that $T_a > T_s$) results in the dissolution of the centre of the crystal.

(*iv*) The rate of recrystallization increases considerably at T_s. (T_s is of course the expected dissolution temperature of the original material.)

(*v*) The extent of the recrystallization during DTA is greatest at low heating rates and when the crystals are prepared at a low temperature.

(*vi*) The material recrystallized during DTA has its narrowest range of dissolution temperatures when the heating rate is high and when the crystals are prepared at a high temperature.

Holland[14] suggests that edges may be particularly susceptible to dissolution because they are composed of lower molecular weight material, because they are thinner, or because they contain more defects. In his experiments, the possible influence of molecular weight was minimized by using a narrow polymer fraction. Peterlin and Meinel[13] found that crystallization is relatively fast and complete with fractionated polymer of moderate molecular weight ($M_v = 85\,000$), but considerably slower with low and high molecular weight fractions or with the whole polymer. According to these authors considerable fractionation occurs during crystallization, and they suggest that the lower molecular weight material is the last to crystallize. Studies by Kawai and Keller[38] on the other hand, indicate that the later stages of crystallization involve the high molecular weight material of below average diffusivity. On this basis, the edge of a crystal would consist of the longer polymer chains after long crystallization times of the order of 1 000 minutes. It is difficult to see why such an edge should subsequently dissolve preferentially, but apparently ten per cent of the polymer remained in solution and crystallized only on lowering the temperature. These observations suggest that further work on the fractionation effect is essential.

Holland's second suggestion, that preferential edge dissolution occurs because the edges are thinner, is not in accordance with the evidence. Thin edges can be produced by slow cooling or eliminated by isothermal separation of crystals and mother liquor as desired, but in any event edge dissolution is observed. After isothermal crystallization it is generally agreed that, for a given polymer–solvent pair, the temperature alone determines the crystal thickness, not the distance from the centre of the crystal.

Holland's final suggestion concerns defects. He reports that Moiré patterns in ⟨110⟩ illumination show a large number of dislocations at the boundary of the thick portion of polyethylene crystals grown at 80°C and the thinner edges grown on subsequent cooling[39]. Similarly, Bassett and Keller[28] suggest that at crystal edges, especially where a border of different thickness has formed, an area of accommodation may occur or, more commonly, the edge or interface may contain extra discontinuities. In the present work there is no indication that defects are concentrated in the edges of crystals and there is no evidence in the literature[39,40] that such concentration occurs except at an interface between frames or sections of different fold length. If such interfaces are absent, then zones of high

defect concentration are probably absent. The crystallization theory of Frank and Tosi[41] can be shown to imply that defects should be most plentiful in the centre of a crystal, the chains having adjusted themselves to as near uniform fold length as possible, thereby introducing voids and other defects.

It would seem desirable to consider other explanations for preferential edge dissolution. A series of papers by Ueberreiter and Asmussen[42-45] describes the dissolution of amorphous polystyrene in terms of several distinct layers of solvent penetration. Although a similar mechanism cannot be expected to operate for polyethylene single crystals, it is undoubtedly necessary to consider the action of solvent as it disengages polymer chains from the crystal lattice. It seems entirely plausible that chains in the growth faces of single crystals, more lightly bound by the lattice and more exposed to association with the solvent, should enter solution more readily. This simple hypothesis provides a kinetic explanation for the preferential dissolution of crystal edges. Furthermore, it may be extended to account for the observation that dissolution of the centre of a crystal does occur given the opportunity. The dissolution of the centre of a crystal after the formation of a thickened border is probably initiated at large defects, a slower process than edge dissolution because of the increased difficulty of achieving polymer–solvent association. On the other hand, once a hole at a defect reaches a certain critical size, solvent access will be in no way inferior to that on the outside edge of the crystal. Current experiments on the rate of dissolution are expected to throw light on this matter.

To explain the remaining observations it is convenient to represent the crystallization and dissolution of polyethylene single crystals in the form of a chart. It must be emphasized that the curves are merely inferred from experiments and are essentially non-quantitative, but the device provides a suitable framework for the rest of the discussion (*Figure 26*). Curve X

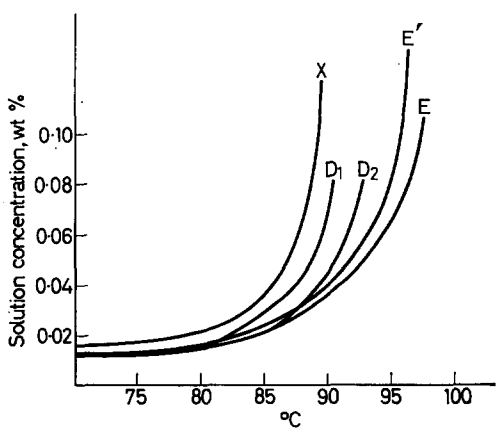

Figure 26—Polymer in solution as a function of temperature under various conditions (see text)

shows, as a function of temperature, the solution concentration required to bring about primary nucleation of crystals inside 1 000 minutes. In Ostwald's terminology[46], it represents the boundary between the labile and metastable regions. It was noted previously that after 1 000 minutes a

0·1 wt% solution had not crystallized at 90°C, but had substantially crystallized at 85°C. This implies that a little below 90°C a 0·1 wt% solution is just supersaturated enough to promote crystallization, and would be represented by a point on curve X. The general shape of curve X emphasizes the fact that the solution concentration of polymer required for nucleation increases very rapidly over quite a narrow range of temperatures. Curve E represents the equilibrium concentration of solution in contact with crystals of the fold length appropriate to each temperature. The curve turns up sharply at the thermodynamic dissolution temperature T_s^0. The temperature coefficient of solubility is evidently very large over a narrow range of temperatures, in sharp contrast to the behaviour of non-polymeric solutes.

In much of the region between curve X and curve E, growth on existing crystals is possible. There will be a curve E′, above curve E and probably quite close to it, which represents the minimum solution concentrations necessary for continued growth on existing crystals at each temperature. The reason is that a definite supersaturation will be required to provide for the two-dimensional nucleation of each new growth layer on existing growth faces, though this supersaturation may be small and partly dependent on the fold length of existing crystals. The results in *Table 9* cannot be far from curve E′ because after 1 000 minutes of crystallization the deposition had become very slow, and the supersaturation was probably only *just* sufficient to keep the crystallization going. At any rate, the region between curve E′ and curve E is one of metastable equilibrium in the classical sense.

Table 9. Polymer remaining in solution after 1 000 minutes of isothermal crystallization. Results based on filtrate analysis. Initial concentration 0·1 wt%

T_x, °C	70	80	85
Wt% in solution	0·014	0·016	0·028

The peaks shown by DTA of polymer suspensions indicate that the amount of polymer in solution increases sharply at the dissolution temperature of any given sample. The dissolution process is therefore more reminiscent of the melting of a non-polymeric substance than of the dissolution of such a substance. Curves D_1 and D_2 represent the amount of polymer in solution during DTA of suspensions prepared by isothermal crystallization at 80°C and 85°C respectively, *provided* that there is no recrystallization. They are not of course true equilibrium curves, because the crystals are unstable with respect to fold length at all temperatures above their crystallization temperatures. Nevertheless, curves D_1 and D_2 would be expected to cut curve E at 80°C and 85°C respectively, and in addition they would be expected to turn up sharply at their respective dissolution temperatures of 90·6°C and 92·9°C. It is important to note that as soon as a curve like D_1 or D_2 goes above curve E′, then redeposition on existing crystals with the new fold length may be expected to occur. This situation would be reached at an earlier stage if the original suspension of crystals had been prepared with the isothermal separation stage omitted. The polymer deposited on cooling to room temperature would redissolve

during the early stages of DTA heating and the corresponding curve of type D would be displaced to higher concentrations of polymer in solution, thus ensuring that redeposition would be possible earlier.

The processes involved in the annealing of polymer suspensions at a fixed temperature can also be explained very conveniently in terms of *Figure 26*. No recrystallization can occur until the amount of polymer in solution exceeds the amount required for deposition of thick borders of the new fold length characteristic of the annealing temperature. That is to say the concentration of polymer in solution must reach curve E′ before recrystallization begins. *Figure 25* shows this effect very clearly.

It is noteworthy that at high temperatures the rate of dissolution is far greater than the rate of crystallization. If the original crystals dissolve completely before recrystallization begins on their edges, the supersaturation required for the formation of new crystals is given by curve X. This explains why dilute suspensions cannot be annealed more than 1 deg. C or 2 deg. C above the dissolution temperature of the original crystals; there is not enough polymer in solution to initiate the crystallization. Near and slightly above the dissolution temperature recrystallization is extremely rapid and extensive. This too is understandable because curves like D_1 and D_2 sweep upwards near the dissolution temperature. In consequence, annealing at that temperature dissolves a good deal of polymer, much of which can redeposit with the new fold length on the remains of the original crystals.

The recrystallization which may occur during DTA has certain special features. Fast heating will eliminate recrystallization altogether if the amount in solution is nowhere great enough to exceed the concentration required for recrystallization (curve E′). Clearly, kinetic effects may be of paramount importance. It is quite possible for the concentration of polymer in solution to exceed the requirements of curve E′ at a particular temperature without noticeable crystallization if the *rate* of crystallization is too low. At lower rates of heating, recrystallization will begin to occur at that temperature where the critical concentration for redeposition is reached. It is a natural consequence of this interpretation that the lower the temperature at which a particular suspension was prepared, the lower will be the temperature at which recrystallization can begin for a given heating rate (e.g. curves D_1 and D_2). It was observed experimentally that dissolution occurs over an especially narrow range of temperatures at high heating rates or if the suspension had been prepared originally at a high temperature. Both of these conditions result in recrystallization being delayed with respect to time and temperature, these being equivalent at a constant rate of heating. The subsequent deposition of material over a narrower range of temperatures produces a narrower dissolution peak in the DTA trace when it finally dissolves again.

It is one of the great strengths of DTA of suspensions that it is possible to distinguish so clearly between the original material and that which has recrystallized, either by deliberate annealing or during DTA. Peterlin and Meinel[13,47] have shown that the dissolution temperature of suspensions of polyethylene crystals in *p*-xylene prepared at 85°C increases for heating

rates below 2·0 deg. C/min, but their light scattering technique could not distinguish between the dissolution of the original material and that which had recrystallized during heating. Dissolution measurements seem likely to form the basis of new methods of characterizing polymers[48,49], and DTA can play an important role.

CONCLUSION

DTA is a suitable and informative technique for the study of suspensions of polyethylene crystals in various solvents. The method is likely to be of general value and, in addition, the morphology of all polymeric substances is so similar that there is a good chance that the conclusions reached in this work have some validity for polymers other than polyethylene.

It is deduced that in moderate or good solvents, the recrystallization of suspended crystals proceeds by a dissolution–redeposition mechanism. Only in poor solvents is it likely that a creep-up thickening process makes a significant contribution to the observed changes in crystal morphology under annealing conditions. The general mechanism of dissolution and redeposition, even during heating, has a relatively simple explanation in terms of familiar kinetic and thermodynamic concepts.

The authors gratefully acknowledge the assistance of Dr D. E. Henn of the National Physical Laboratory who carried out the low angle X-ray analyses, the expert advice on electron microscopy provided by Mr J. M. Bell of the Cavendish Laboratory, Cambridge, and the guidance on electronic matters given by Mr. F. R. G. Mitchell of the Chemical Engineering Department. Thanks are due to the National Physical Laboratory for the use of certain facilities, and one of the authors (H.M.S.) thanks the U.S. National Science Foundation for a Fellowship.

Department of Chemical Engineering,
University of Cambridge

(*Received June 1966*)

APPENDIX

The enthalpy of dissolution of polyethylene single crystals suspended in p-*xylene*

Assuming that polyethylene crystals of the simplest lamellar type are 100 per cent crystalline, we may write the enthalpy of dissolution per cm³ of suspension (Δh_d) as follows:

$$\Delta h_d = \rho_s c \ \{\Delta h_f/\rho_c + \Delta h_m\}/100$$

ρ_s and ρ_c are the densities of suspension and crystalline polymer respectively, c is the concentration of the suspension in wt%, Δh_f is the enthalpy of fusion per cm³ of crystal at T_s, and Δh_m is the enthalpy of mixing 1g of molten polymer with the appropriate volume of solvent. A precise value of ρ_s is calculable from the expression $\rho_s = \rho_0 + c\,(\rho_1 - \rho_0)$ where ρ_0 is the density of pure solvent and ρ_1 is the density of a 1 wt% suspension. The effect of temperature is allowed for thus:

$$\rho_1 = 0{\cdot}8856 - 0{\cdot}0008448T$$
$$\rho_0 = 0{\cdot}8838 - 0{\cdot}0008562T \qquad (T \text{ in } °C)$$

Bunn[50] has obtained a value of 0·9897 g/cm³ for ρ_c at 90°C, and at that same temperature Lauritzen and Hoffman[8] have reported a value of $2{\cdot}8 \times 10^9$ erg/cm³ for Δh_f. The value of Δh_m can be calculated using the theory of polymer solutions. Flory[11] has shown that $\Delta h_m = kT\chi_1 n_1 v_2$ where k is Boltzmann's constant, T the absolute temperature, χ_1 the polymer–solvent interaction coefficient, n_1 the number of solvent molecules per gramme of polymer, and v_2 the volume fraction of polymer.

For the present calculation it is convenient to make use of the fact that v_2 has a value of 0·013 for a 1 wt% solution, and for values of c not too far from unity it may be assumed that $v_2 = 0{\cdot}013c$. Experiments by Trementozzi[19] suggest that 0·15 is an appropriate value for χ_1. In addition, n_1 may be written as $N(100-c)/M_w c$ where N is Avogadro's number and M_w is the molecular weight of the solvent. With these simplifications:

$$\Delta h_m = kT\chi_1 \frac{N}{M_w} 0{\cdot}013\,(100-c)$$

$$= 5{\cdot}62 \times 10^5\,(100-c)\ \text{erg/g at } 90°\text{C}.$$

In *Table 10*, values of Δh_d are calculated for three concentrations assuming that dissolution occurs at 90°C.

Table 10. Theoretical values of Δh_d (cal/cm³ of suspension)

c	$\rho_s c/100$	$\Delta h_f/\rho_c$	Δh_m	Δh_d
0·75	0·006067	$2{\cdot}829 \times 10^9$	$0{\cdot}056 \times 10^9$	0·417
1·00	0·008096	$2{\cdot}829 \times 10^9$	$0{\cdot}056 \times 10^9$	0·556
1·50	0·012170	$2{\cdot}829 \times 10^9$	$0{\cdot}055 \times 10^9$	0·836

It is clear that the contribution to Δh_d made by the heat of mixing is only one fiftieth of the contribution made by the heat of fusion. Nevertheless it is preferable to use Δh_d in all thermodynamic discussions of polymer dissolution.

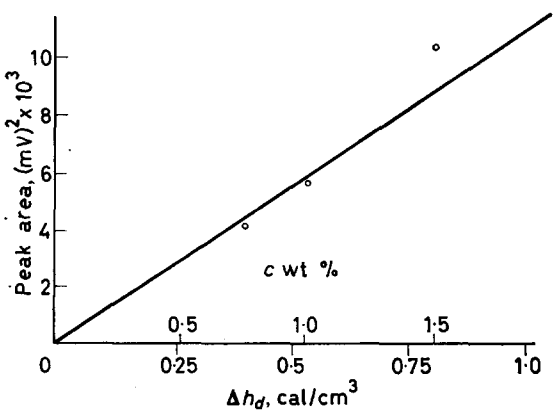

Figure 27—DTA peak area/enthalpy relationship. Solid line from calibration experiments. Experimental points from polyethylene suspensions

In *Figure 27*, peak areas observed by DTA are plotted against the corresponding theoretical enthalpies calculated in *Table 10*. The solid line is the relationship between peak area and enthalpic change established by

calibration of the apparatus[5]. It is clear that although DTA of suspensions affords a measure of the heat of dissolution, the method is not yet very precise. Refinements of technique are being investigated and will be reported in due course.

REFERENCES

[1] GEIL, P. H. *Polymer Single Crystals.* Interscience: London, 1963
[2] MANDELKERN, L. *Crystallization of Polymers.* McGraw-Hill: New York, 1964
[3] LINDENMEYER, P. H. *J. Polym. Sci. C,* 1963, **1,** 5
[4] FRANKS, A. *Brit. J. appl. Phys.* 1958, **9,** 349
[5] SCHLEINITZ, H. M. Unpublished results
[6] BASSETT, D. C., KELLER, A. and MITSUHASHI, S. *J. Polym. Sci. A,* 1963, **1,** 763
[7] HOFFMAN, J. D. and WEEKS, J. J. *J. Res. nat. Bur. Stand. A,* 1962, **66,** 13
[8] LAURITZEN, J. I. and HOFFMAN, J. D. *J. Res. nat. Bur. Stand. A,* 1960, **64,** 73
[9] KAWAI, T. and KELLER, A. *Phil. Mag.* Ser. VIII, 1965, **11,** 1165
[10] PETERLIN, A. *J. Polym. Sci. C,* 1965, **9,** 61
[11] FLORY, P. J. *Principles of Polymer Chemistry,* p 563. Cornell University Press: Ithaca, New York, 1953
[12] JACKSON, J. B., FLORY, P. J. and CHIANG, R. *Trans. Faraday Soc.* 1963, **59,** 1906
[13] PETERLIN, A. and MEINEL, G. *J. appl. Phys.* 1964, **35,** 3221
[14] HOLLAND, V. F. *J. appl. Phys.* 1964, **35,** 59
[15] CORAN, A. Y. and ANAGNOSTOPOULOS, C. E. *J. Polym. Sci.* 1962, **57,** 13
[16] KAWAI, T. *Kolloidzschr.* 1965, **201,** 15
[17] KAWAI, T. *Makromol. Chem.* 1965, **84,** 290
[18] WUNDERLICH, B., JONES, E. A. and TSAO-WUN SHU. *J. Polym. Sci. A,* 1964, **2,** 2759
[19] TREMENTOZZI, Q. A. *J. Polym. Sci.* 1957, **23,** 887
[20] MANDELKERN, L., POSNER, A. S., DIORIO, A. F. and ROBERTS, D. E. *J. appl. Phys.* 1961, **32,** 1509
[21] FUGIWARA, Y. and YASHIDA, T. *J. Polym. Sci. B,* 1963, **1,** 675
[22] BROWN, R. G. and EBY, R. K. *J. appl. Phys.* 1964, **35,** 1156
[23] RICHARDSON, M. J. *Trans. Faraday Soc.* 1965, **61,** 1876
[24] PETERLIN, A. and MEINEL, G. *J. Polym. Sci. B,* 1965, **3,** 1059
[25] ZACHMANN, H. G. *Kolloidzschr.* 1965, **206,** 25
[26] HELLMUTH, E. and WUNDERLICH, B. *J. appl. Phys.* 1965, **36,** 3039
[27] KELLER, A. and BASSETT, D. C. *J. R. micr. Soc.* 1960, **79,** 243
[28] BASSETT, D. C. and KELLER, A. *Phil. Mag.* Ser. VIII, 1962, **7,** 1553
[29] FRANK, F. C., KELLER, A. and O'CONNOR, A. *Phil. Mag.* Ser. VIII, 1959, **4,** 200
[30] HIRAI, N., MITSUHATA, T. and YAMASHITA, Y. *Chemy high Polym.* 1961, **18,** 33
[31] RENEKER, D. H. *J. Polym. Sci.* 1962, **59,** 539
[32] FISCHER, E. W. and SCHMIDT, G. F. *Angew. Chem.* 1962, **1,** 488
[33] THURN, H. *Kolloidzschr.* 1961, **179,** 11
[34] SLICHTER, W. P. *J. appl. Phys.* 1961, **31,** 1865
[35] KAWAI, T. *J. Polym. Sci. B,* 1964, **2,** 429
[36] KEDZIE, R. W. Reported in ref. 1
[37] HOFFMAN, J. D. and WEEKS, J. J. *J. chem. Phys.* 1965, **42,** 4301
[38] KAWAI, T. and KELLER, A. *J. Polym. Sci. B,* 1964, **2,** 333
[39] HOLLAND, V. F. *J. appl. Phys.* 1964, **35,** 1351 and 3235
[40] HOLLAND, V. F. and LINDENMEYER, P. H. *J. appl. Phys.* 1965, **36,** 3049
[41] FRANK, F. C. and TOSI, M. *Proc. Roy. Soc. A,* 1961, **363,** 323
[42] UEBERREITER, K. and ASMUSSEN, F. *J. Polym. Sci.* 1962, **57,** 187
[43] ASMUSSEN, F. and UEBERREITER, K. *J. Polym. Sci.* 1962, **57,** 199
[44] UEBERREITER, K. and ASMUSSEN, F. *Makromol. Chem.* 1961, **43,** 324
[45] ASMUSSEN, F. and UEBERREITER, K. *Makromol. Chem.* 1962, **52,** 164
[46] OSTWALD, W. *Lehrbuch,* Vol. II. Engelmann: Leipzig, 1896–1902
[47] PETERLIN, A. and MEINEL, G. *J. Polym. Sci. B,* 1964, **2,** 751
[48] CHIANG, R., RHODES, J. H. and HOLLAND, V. F. *J. Polym. Sci. A,* 1965, **3,** 479
[49] CHIANG, R. *J. Polym. Sci. A,* 1965, **3,** 2019
[50] BUNN, C. W. *Trans. Faraday Soc.* 1939, **35,** 482

Book Reviews

Conformations of Polyethylene and Polypropylene

A. OPSCHOOR. Rotterdam University Press: Rotterdam, 1966. 68 pp. 30*s*

THIS short monograph is a reprint of a Ph.D. thesis presented by A. Opschoor at the Delft Institute of Technology in 1965; naturally, therefore, the contents are almost wholly concerned with the author's own studies and opinions.

In the first three chapters, there is a clear well-written account of his theoretical studies on conformational problems associated with polyethylene and isotactic polypropylene. For both polymers values are predicted for the unperturbed dimensions and their temperature dependence.

The fourth chapter deals with the reliability of the various experimental techniques for determining unperturbed dimensions. The treatment here is surprisingly sketchy, and far better assessments of these techniques are to be found elsewhere.

In the fifth chapter, thermoelastic measurements at constant length and pressure are reported for amorphous crosslinked networks of polyethylene and isotactic polypropylene; details of the apparatus and of the methods used to prepare the samples are included. Since the author is forced to conclude that, contrary to current opinion, conformational information cannot be extracted from such measurements, the results obtained add little to the general understanding of conformational behaviour.

The monograph will be of most benefit to specialists in the field of conformational statistics, but it can also be recommended to other polymer scientists who wish to be well informed of current developments in this field of research.

C. PRICE

Mechanics of Polymer Melt Processing

J. R. A. PEARSON. 148 pp. Pergamon: Oxford, 1966. 35*s*

THE complaint that university workers do not concern themselves with technological problems is heard frequently. Less frequently is such a complaint refuted so comprehensively as by the appearance of this monograph, the style and substance of which leave little to be desired as a theoretical treatment of fabrication processes for polymers—rubbers and plastics.

This is a book for study rather than casual reading: it is a theoretical approach based on continuum mechanics to the problems of melt processing and some reasonable facility with mathematics is essential for full benefit. However, the serious student less well qualified mathematically will learn much from the approach even if he cannot follow the argument in detail. The 'theological equation of state' is mentioned—Chapter 1, page 1—but this is a book for down to earth mortals.

The opening two chapters, a short introduction and a comprehensive discussion of the flow behaviour of polymer melts, put the present position of the theory and practice of melt rheology into perspective and should be compulsory study for present and intending rheologists. Chapter 3 provides analyses for many continuous processes, including calendering, extrusion and fibre spinning, the treatments being based frequently on the lubrication approximation, that the flow route consists of a relatively narrow channel with defined boundaries. This assumption is at least approximately true for many of these processes and it will be interesting to see how far these theoretical deductions compare with practical operation and results. The analyses do serve, in any case, to draw together the similarities in the processes. The final chapter deals comparatively briefly with repetitive operations and underlines the empirical basis of injection moulding and blow moulding. Here again, analysing the operations in detail suggests numerous experimental measurements which would be desirable to provide a firmer basis for subsequent work.

In summary, this is a book with a difference as far as the polymer world is concerned, advancing the theoretical analysis of melt processing to a stage where accurate experimental data are required to check the theories and approximations employed.

A. W. BIRLEY

Organic Compounds with Nitrogen–Nitrogen Bonds
C. G. OVERBERGER, J.-P. ANSELME and J. G. LOMBARDINO.
Ronald: New York, 1966. 112 pp. $7.00

THIS book is a short review monograph in the series Modern Concepts in Chemistry. Various classes of nitrogen-containing molecules are briefly discussed and leading references to preparation, properties and uses are provided. Classification of the material falls under the following headings: Hydrazines, Azomethines, Azo compounds, Diazo compounds, Hydrazides, *N*-nitrosamines, and azides. Clearly there must be very large gaps in such a brief survey of so many types of organic molecule but the book is nevertheless useful, and provides a convenient starting point for anyone interested in the chemistry of these materials.

A. LEDWITH

Mechanisms of Electron Transfer

W. REYNOLDS and R. W. LUMRY. Ronald: New York, 1966. vi+175 pp. $7.00

DESPITE the plural in the title, this volume is a detailed account only of those one-electron transfer processes which occur between two transition element ions in solution. Inorganic oxidation reactions of complicated stoichiometry are not discussed, and all reactions involving electron transfer with organic intermediates are relegated to a few lines on the naphthalene radical anion. This latter bias is hardly justifiable under such a title, despite the fact that theoretical treatments are not so advanced in the organic sector.

Within the scope of the subject selected, however, this really is an excellent monograph. The current theories of so-called adiabatic and non-adiabatic electron transfer processes are discussed with lucidity, and the basic principles used in calculating the energies of dissolved ions are well set out. The documentation of reactions which have been studied experimentally is detailed, and is also presented in a readable fashion. There is no doubt that the book will occupy a most useful place in the libraries of chemists interested in chemical kinetics in general, and in the mechanism of inorganic reaction in particular. The material is probably rather detailed for undergraduate teaching (except for an advanced course on inorganic reaction mechanisms) but usefully fills a gap at post-graduate level.

A. M. NORTH

Notes

Thermodynamic Data for the System Formaldehyde–Polyoxymethylene

IN THE present work a critical examination of published equilibrium and thermochemical data for the system formaldehyde–polyoxymethylene has been made and 'best' values selected for the enthalpy, entropy and free energy changes associated with the polymerization of gaseous formaldehyde to crystalline polyoxymethylene. A new and more reliable value for the heat of formation of gaseous formaldehyde is also calculated.

The thermal decomposition of polyoxymethylene can be represented by the equation

$$H\text{-}[O\text{-}CH_2]_n\text{-}OH_{(solid)} \rightleftharpoons H\text{-}[O\text{-}CH_2]_{n-1}\text{-}OH_{(solid)} + CH_2O_{(gas)}$$

Several workers[1-6] have measured equilibrium pressures of gaseous formaldehyde over solid polyoxymethylene as a function of temperature. The early work[1,2] can be ignored since there is no certainty that equilibrium was established during the measurements. The results of more recent investigations[3-6] are contradictory as can be seen from the data of *Table 1*. One source of error is the variation in the crystallinity of the polymer specimens used.

Table 1. Heat and entropy changes associated with the polymerization of gaseous formaldehyde (one atmosphere pressure) to polyoxymethylene at 25°C, as obtained from equilibrium pressure data

$-\Delta H^0_{gc'}$ (kcal per CH_2O unit)	$-\Delta S^0_{gc'}$ (cal deg^{-1} per CH_2O unit)	*Reference*
12·2	30·7	3
14·3	—	4
16·3	41·8	5
17·2	43·8	6

Only Thompson[6] used a well characterized sample of high crystallinity. Consequently, in this work we shall accept his values, namely, $-\Delta H^0_{gc'} = 17{\cdot}2$ kcal per CH_2O unit and $-\Delta S^0_{gc'} = 43{\cdot}8$ cal deg^{-1} per CH_2O unit. Thompson's value for $-\Delta S^0_{gc'}$ is in good agreement with the value of 42·65 cal deg^{-1} per CH_2O unit derived from Dworjanyn's[7] value of 52·26 cal deg^{-1} $mole^{-1}$ for the entropy of formaldehyde gas at 25°C and one atmosphere pressure and Dainton, Evans, Hoare and Melia's[8] value of 10·61 cal deg^{-1} per CH_2O unit for the entropy of crystalline polyoxymethylene in its standard state. Thompson's data yield $-\Delta G^0_{gc'} = 4{\cdot}1$ kcal per CH_2O unit and a ceiling temperature of 133°C for the polymerization of gaseous formaldehyde.

The heat of formation of formaldehyde is based on rather old data[9]. A better value for this quantity may be obtained from Thompson's $-\Delta H^0_{gc'}$

value and the heat of formation of crystalline polyoxymethylene (−40·93 kcal per CH_2O unit) obtained by Parks and Mosher[10]. These yield the value −23·2 kcal $mole^{-1}$ for the heat of formation of formaldehyde. It is believed that this figure is more reliable than the presently accepted 'best' value for this quantity.

T. P. MELIA

Department of Chemistry and Applied Chemistry,
Royal College of Advanced Technology,
Salford 5, Lancs.

(Received July 1966)

REFERENCES

[1] NORDGREN, G. *Acta Path. Bicrobiol. scand.* (suppl.), 1939, **40,** 21
[2] NIELSEN, H. H. and EBERS, E. S. *J. chem. Phys.* 1937, **5,** 824
[3] DAINTON, F. S., IVIN, K. J. and WALMSLEY, D. A. G. *Trans. Faraday Soc.* 1959, **55,** 61
[4] WALKER, J. F. *Formaldehyde,* 3rd ed., p 180. Reinhold: New York, 1964
[5] IWASA, Y. and IMOTO, T. *J. chem. Soc. Japan,* Pure Chem. Sect. 1963, **84,** 29
[6] THOMPSON, J. B. (See WALKER, J. F.) *Formaldehyde,* 3rd ed., p 180. Reinhold: New York, 1964
[7] DWORJANYN, L. O. *Austral. J. Chem.* 1960, **13,** 175
[8] DAINTON, F. S., EVANS, D. M., HOARE, F. E. and MELIA, T. P. *Polymer, Lond.* 1962, **3,** 263
[9] VON WARTENBERG, H. and LERNER-STEINBERG, B. *Angew. Chem.* 1925, **38,** 591
[10] PARKS, G. S. and MOSHER, H. P. *J. Polym. Sci. A,* 1963, **1,** 1979

The Stabilization of Poly(vinyl chloride) by Organotin Maleates

ORGANOTIN derivatives of maleic acid are widely used to inhibit degradation of poly(vinyl chloride) by heat and light[1]. It has been suggested[1] that these compounds undergo Diels–Alder addition reactions with diene systems in the partially degraded polymer chains. There is no direct evidence for this and many of the stabilizers have been only vaguely described in the patent literature and are of uncertain composition.

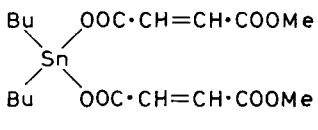

(I)

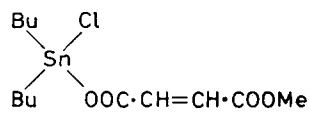

(II)

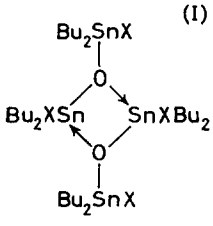

(III)

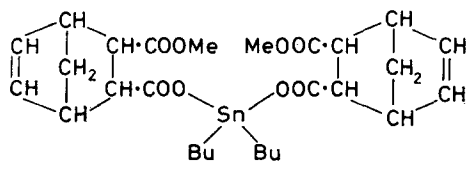

(IV)

value and the heat of formation of crystalline polyoxymethylene (−40·93 kcal per CH_2O unit) obtained by Parks and Mosher[10]. These yield the value −23·2 kcal $mole^{-1}$ for the heat of formation of formaldehyde. It is believed that this figure is more reliable than the presently accepted 'best' value for this quantity.

T. P. MELIA

Department of Chemistry and Applied Chemistry,
Royal College of Advanced Technology,
Salford 5, Lancs.

(Received July 1966)

REFERENCES

[1] NORDGREN, G. *Acta Path. Bicrobiol. scand.* (suppl.), 1939, **40,** 21
[2] NIELSEN, H. H. and EBERS, E. S. *J. chem. Phys.* 1937, **5,** 824
[3] DAINTON, F. S., IVIN, K. J. and WALMSLEY, D. A. G. *Trans. Faraday Soc.* 1959, **55,** 61
[4] WALKER, J. F. *Formaldehyde,* 3rd ed., p 180. Reinhold: New York, 1964
[5] IWASA, Y. and IMOTO, T. *J. chem. Soc. Japan,* Pure Chem. Sect. 1963, **84,** 29
[6] THOMPSON, J. B. (See WALKER, J. F.) *Formaldehyde,* 3rd ed., p 180. Reinhold: New York, 1964
[7] DWORJANYN, L. O. *Austral. J. Chem.* 1960, **13,** 175
[8] DAINTON, F. S., EVANS, D. M., HOARE, F. E. and MELIA, T. P. *Polymer, Lond.* 1962, **3,** 263
[9] VON WARTENBERG, H. and LERNER-STEINBERG, B. *Angew. Chem.* 1925, **38,** 591
[10] PARKS, G. S. and MOSHER, H. P. *J. Polym. Sci. A,* 1963, **1,** 1979

The Stabilization of Poly(vinyl chloride) by Organotin Maleates

ORGANOTIN derivatives of maleic acid are widely used to inhibit degradation of poly(vinyl chloride) by heat and light[1]. It has been suggested[1] that these compounds undergo Diels–Alder addition reactions with diene systems in the partially degraded polymer chains. There is no direct evidence for this and many of the stabilizers have been only vaguely described in the patent literature and are of uncertain composition.

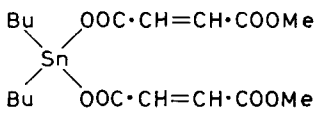

(I)

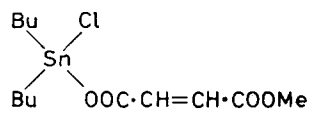

(II)

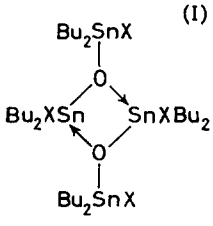

(III)

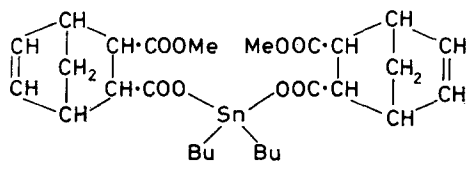

(IV)

In recent work[2] on the mechanism of stabilization of poly(vinyl chloride) dibutyltinbis(methyl maleate) (I), prepared[3] from dibutyltin dichloride and potassium methyl maleate, was used but no details of this compound were reported.

An attempt to repeat this preparation gave dibutylchlorotin methyl maleate (II), m.pt 41° to 43°C as the sole product. Compound I was, however, prepared from dibutyltin oxide and methyl hydrogen maleate and isolated as an oil n_D^{23} 1·4930 which could not be distilled without decomposition. An attempt to convert I to its 2,2′-bipyridyl derivative using the aqueous ethanolic conditions described by Huber *et al.*[4] caused hydrolysis to (III, X=OOC·CH=CH·COOMe) m.pt 91° to 94°C (similar compounds where X=CH_3·COO are well known[5]). Compound I interacted with dienes such as 2,3-dimethylbuta-1,3-diene but the products were gums and difficult to purify. However, with cyclopentadiene the crystalline Diels–Alder adduct IV m.pt 56° to 58°C was obtained.

Further studies on the mechanism of stabilization of poly(vinyl chloride) by organotin compounds are in progress.

(All the compounds described had satisfactory elemental analyses and infra-red spectra; compound III had molecular weight (found) 1 450, (required) 1 480.)

A. S. MUFTI
R. C. POLLER

Department of Chemistry,
Queen Elizabeth College,
Campden Hill Road, London, W.8

(*Received October 1966*)

REFERENCES

[1] CHEVASSUS, F. and DE BROUTELLES, R. *The Stabilization of Polyvinyl Chloride.* Edward Arnold: London, 1963
[2] FRYE, A. H., HORST, R. W. and PALIOBAGIS, M. A. *J. Polym. Sci. A,* 1964, **2,** 1 765, 1 785, 1 801
[3] FRYE, A. H. and HORST, R. W. *J. appl. Radiation and Isotopes,* 1964, **15,** 169
[4] HUBER, F., ENDERS, M. and KAISER, R. *Z. Naturf.* 1966, **21b,** 83
[5] POLLER, R. C. *J. Organometal. Chem.* 1965, **3,** 321

Classified Contents

ABS-polymer, observation of crazes in, under the electron microscope, 421
Acid-catalysed condensation [of model polyethers] and degradation reactions of hydroxyl-terminated ethers, 223
Ageing effects in measurements of polyacrylamide solution viscosities, 507
Allotropy of cyclic tris(ethylene terephthalate), 583

Bulk modulus measurements on polymers at high temperatures, 429
Butadiene, homogeneous polymerization of, catalysed by rhodium salts, 113
Butene-1 copolymers and polybutene type II/I crystal phase transition, 23

(Fourteenth) Canadian High Polymer Forum, 586
Cellulose nitrate solutions, supermolecular gels in, 475
Cocrystallization in copolymers of alpha olefins II—Butene-1 copolymers and polybutene type II/I crystal phase transition, 23
Cold drawing of polyethylene terephthalate, 66
Comparison between real polymer dimensions in solution and the behaviour predicted from models, 459
Conformations of Polyethylene and Polypropylene, review of, 638
Crosslinking of methylvinyl silicones with organic peroxides, 243
Crystalline Olefin Polymers, review of, 251
Crystallization and melting of copolymers I —Effect of crystallization temperature upon apparent melting temperature of polymethylene copolymers, 7
— II—Variations in unit-cell dimensions in polymethylene copolymers, 71
Cyclopentadiene polymers, proton acceptor properties and electrical conductance of deeply coloured, 465

Dilute solution properties of poly(propylene oxide), 167
Dissolution and recrystallization of polyethylene crystals suspended in various solvents, 603
Dynamic mechanical properties of some polyethers, 331

Effect of crystallization temperature upon apparent melting temperature of polymethylene copolymers, 7
Elastomer Stereospecific Polymerization, review of, 537
Electron diffraction and microscopy of deformed polymer crystals III—Annealing, 135
Electron microscope studies of the fracture of glassy polymers, 307
Epoxide polymers, amine-cured, thermal stability of, 193
Estimation of unperturbed polymer dimensions from viscosity measurements in non-ideal solvents, 487
Ethylene oxides, polymerization of some, by the diethylzinc–water system, 1
Exposés de Chimie Macromoléculaire. Structure Chimique des Polyosides, review of, 536

Flammfestmachen von Kunststoffen, review of, 582
Formaldehyde–polyoxymethylene system, thermodynamic data for, 640
Formation of new crosslinkages in proteins by oxidation of the tyrosine residues with potassium nitrosyldisulphonate, 549
Fractional crystallization of poly(ethylene oxide), 85
Fracture of glassy polymers, electron microscope studies of, 307
Free radical formation in irradiated polyethylene, 283

Heat capacities of propylene oxide and of some polymers of ethylene and propylene oxides, 401
High Resolution Nuclear Magnetic Resonance Spectroscopy, Vol. II, review of, 538
(*A*) *History of the Modern British Chemical Industry*, review of, 537
Homogeneous polymerization of butadiene catalysed by rhodium salts, 113

(*The*) *Identification of Plastics and Rubbers*, review of, 539
Influence of the dielectric constant on the rate of solution polymerization of trioxan, 587
Influence of molecular size distribution within a liquid on the viscous flow of the liquid, 91
Infra-red absorption characteristics of syndiotactic poly(methyl methacrylate) from 1 050 cm^{-1} to 1 300 cm^{-1}, 387
Infra-red–deuteration study of the grafting of vinyl polymers into nylon films, 563
Infra-red study of interaction of polyamides with iodine in iodine–potassium iodide solution, 199

Initiation of polymerization by ammonium trichloracetate in presence of copper derivatives—a tracer study, 573
Irradiated polyethylene I—Free radical formation, 283
Isobutene, some solvent effects on the cobalt-60 gamma-ray initiated polymerization of, in the presence of zinc oxide, 107

Limitations of the Tobolsky 'two network' theory in the interpretation of stress-relaxation data in rubbers, 125
Limiting viscosity number versus molecular weight relations for polyhexamethylene oxide, 557
Limiting viscosity number versus molecular weight relations for polyoxacyclobutane, 267
Long period spacing, reversible change in, with temperature, 61

Macromolecular Chemistry of Gelatin, review of, 251
Mechanics of Polymer Melt Processing, review of, 638
Mechanisms of Electron Transfer, review of, 639
Methylvinyl silicone rubber, network scission processes in peroxide cured, 99
Methylvinyl silicones, crosslinking of, with organic peroxides, 243
Microscopy, electron diffraction and, of deformed polymer crystals III—Annealing, 135
Model polyethers II—Synthesis by polycondensation of glycols in the presence of alcohols, 217
— III—Acid-catalysed condensation and degradation reactions of hydroxyl-terminated ethers, 223
Molecular forces, structural changes and, in a compressed synthetic polypeptide monolayer, 595
Molecular size distribution, influence of, within a liquid on the viscous flow of the liquid, 91

Network scission processes in peroxide cured methylvinyl silicone rubber, 99
Nicotinamide, polymeric enzyme analogue based on, 479

Observation of crazes in ABS-polymer and high-impact polystyrene under the electron microscope, 421
Organic Compounds with Nitrogen–Nitrogen Bonds, review of, 639

Physics of Non-crystalline Solids, review of, 539
Polyacrylamide solution viscosities, ageing effects in measurements of, 507
Polyamides, infra-red study of interaction of, with iodine in iodine–potassium iodide solution, 199
Polybutene type II/I crystal phase transition, butene-1 copolymers and, 23
[Some] Polyethers, dynamic mechanical properties of, 331
Polyethylene crystals, dissolution and recrystallization of, suspended in various solvents, 603
Poly(ethylene oxide), fractional crystallization of, 85
Polyethylene oxide, proton spin–lattice relaxation in, 426
Polyethylene terephthalate, cold drawing of, 66
Polyethylene terephthalate, temperature dependence of viscoelastic behaviour in, 255
Polyhexamethylene oxide, limiting viscosity number versus molecular weight relations for, 557
Polyisobutene, isothermal fractionation of, 525
Polyisobutylene–solvent systems, [thermodynamics of mixing:] excess volumes in, 151
Poly(isophthaloyl *trans*-2,5-dimethyl-piperazine), effect of ultra-violet irradiation in thermal degradation of, 321
— thermal degradation of, 231
Polymer chain dimensions, temperature dependence of, and second virial coefficients, 513
Polymer dimensions, estimation of unperturbed, from viscosity measurements in non-ideal solvents, 487
— real, comparison between, in solution and the behaviour predicted from models, 459
Polymer fractionation at a lower critical solution temperature phase boundary, 525
Polymeric enzyme analogue based on nicotinamide, 479
Polymer Handbook, review of, 418
Polymerization, initiation of, by ammonium trichloracetate in presence of copper derivatives—a tracer study, 573
Polymerization of some ethylene oxides by the diethylzinc–water system, 1
Polymerization of styrene under pressure, 497
cis-Polymerization by a three-component system containing nickel(0), 419
Polymerization of trifluoracetaldehyde initiated by tertiary bases; effect of temperature on monomer–polymer equilibrium, 541
Polymer Mechanics, Vol. I, No. 1, review of, 535
Polymer single crystals, densities of, reliability of gradient column method for measuring, 195
Polymers of ethylene and propylene oxide, heat capacities of some, 401
Polymers at high temperatures, bulk modulus measurements on, 429
Polymers: Structure and Bulk Properties, review of, 252
[Some] Polymers of substituted acetylenes, 275

Polymethylene copolymers, effect of crystallization temperature upon apparent melting temperature of, 7
— variations in unit-cell dimensions in, 71
Polyoxacyclobutane, limiting viscosity number versus molecular weight relations for, 267
Polypeptide monolayer, structural changes and molecular forces in a compressed synthetic, 595
Polypropylene, isotactic, yield stress behaviour of, 303
Poly(propylene oxide), dilute solution properties of, 167
Polystyrene, glass temperature of, thermodynamic analysis of effect of pressure on, 177
Polystyrene, high-impact, observation of crazes in, under the electron microscope, 421
Poly(terephthaloyl piperazine), thermal degradation of, 231
Poly(terephthaloyl 2-methylpiperazine), thermal degradation of, 231
Polythioacetone, 469
Poly(vinyl chloride), stabilization of, by organotin maleates, 641
Present status of the theory of rubber elasticity, 373
Proceedings of N.R.P.R.A. Jubilee Conference Cambridge 1964, review of, 253
Propylene oxide, heat capacity of, 401
Proteins, formation of new crosslinkages in, by oxidation of the tyrosine residues with potassium nitrosyldisulphonate, 549
Proton acceptor properties and electrical conductance of deeply coloured cyclopentadiene polymers, 465
Proton resonance spectra and tacticity of poly-2-vinylpyridine, 63
Proton spin–lattice relaxation in polyethylene oxide. Spin-diffusion and methyl group rotation, 426

Rapid turbidimetric determinations of theta conditions, 293
Recrystallization, dissolution and, of polyethylene crystals suspended in various solvents, 603
Refinement of crystal and molecular structures of polymers using X-ray data and stereochemical constraints, 157
Regular alkylene ether copolymers, 367
Reliability of gradient column method for measuring densities of polymer single crystals, 195
Reversible change in long period spacing with temperature, 61
Rubber elasticity, present status of the theory of, 373
Rubbers, limitations of the Tobolsky 'two network' theory in the interpretation of stress-relaxation data in, 125

Some solvent effects on the cobalt-60 gamma-ray initiated polymerization of isobutene in the presence of zinc oxide, 107
Stabilization of poly(vinyl chloride) by organotin maleates, 641
Structural changes and molecular forces in a compressed synthetic polypeptide monolayer, 595
Studies on radiation-induced ionic polymerization III—Polymerization of styrene at room temperature, 431
— IV—Polymerization of styrene in solution at room temperature, 451
Styrene, polymerization of, under pressure, 497
— radiation-induced ionic polymerization of, at room temperature, 431
— — in solution at room temperature, 451
Substituted acetylenes, some polymers of, 275
Supermolecular gels in cellulose nitrate solutions, 475
Syndiotactic poly(methyl methacrylate), infra-red absorption characteristics of, from 1 050 cm^{-1} to 1 300 cm^{-1}, 387
Synthesis (of model polyethers) by polycondensation of glycols in the presence of alcohols, 217

Tacticity, proton resonance spectra and, of poly-2-vinylpyridine, 63
Temperature dependence of polymer chain dimensions and second virial coefficients, 513
Temperature dependence of viscoelastic behaviour in polyethylene terephthalate, 255
Testing of Polymers, Vol. I, review of, 535
Thermal degradation of piperazine polyamides II—Poly(terephthaloyl piperazine, poly(terephthaloyl 2-methylpiperazine), and poly(isophthaloyl *trans*-2,5-dimethylpiperazine), 231
— III—Effect of ultra-violet irradiation on poly(isophthaloyl *trans*-2,5-dimethylpiperazine), 321
Thermal stability of amine-cured epoxide polymers, 193
Thermonalytical Methods of Investigation, review of, 536
Thermodynamic analysis of effect of pressure on glass temperature of polystyrene, 177
Thermodynamic data for the system formaldehyde–polyoxymethylene, 640
Thermodynamics of mixing: excess volumes in polyisobutylene–solvent systems, 151
Theta conditions, rapid turbidimetric determinations of, 293
Trifluoracetaldehyde, polymerization of, initiated by tertiary bases, effect of temperature on monomer–polymer equilibrium, 541
Trioxan, influence of dielectric constant on rate of solution polymerization of, 587
Tris(ethylene terephthalate), cyclic, allotrophy of, 583
Toxicity in plastics—a symposium, 586

Variations in unit-cell dimensions in polymethylene copolymers, 71

Vinyl polymers, infra-red–deuteration study of grafting of, into nylon films, 563

Yield stress behaviour of isotactic polypropylene, 303

Author Index

ALLEN, G.: *See* WETTON, R. E. and ALLEN, G.
— *See* BAKER, C. H., CLEMSON, C. S. and ALLEN, G.
— BOOTH, C. and PRICE, C.: The dilute solution properties of poly(propylene oxide), 167
ALLISON, S. W., PINNOCK, P. R. and WARD, I. M.: The cold drawing of polyethylene terephthalate, 66
ANDERSON, H. C.: Thermal stability of amine-cured epoxide polymers, 193
ARNOTT, STRUTHER and WONACOTT, A. J.: The refinement of the crystal and molecular structures of polymers using X-ray data and stereochemical constraints, 157
AUERBACH, I.: Irradiated polyethylene I—Free radical formation, 283

BAKER, C. H. and MANDELKERN, L.: The crystallization and melting of copolymers I—The effect of the crystallization temperature upon the apparent melting temperature of polymethylene copolymers, 7
— — — II—Variations in unit-cell dimensions in polymethylene copolymers, 71
— CLEMSON, C. S. and ALLEN, G.: Polymer fractionation at a lower critical solution temperature phase boundary, 525
BALLARD, D. G. H.: review of *Polymer Handbook*, 418
BALTA, Y. I.: *See* KRIGBAUM, W. R., BALTA, Y. I. and VIA, G. H.
BAMFORD, C. H. and ROBINSON, V. J.: Initiation of polymerization by ammonium trichloracetate in the presence of copper derivatives—a tracer study, 573
BARTLETT, (Miss) J. A. and DALTON, F. L.: Some solvent effects on the cobalt-60 gamma-ray initiated polymerization of isobutene in the presence of zinc oxide, 107
BAWN, C. E. H., COOPER, D. G. T. and NORTH, A. M.: The homogeneous polymerization of butadiene catalysed by rhodium salts, 113
BEAUMONT, R. H., CLEGG, B., GEE, G., HERBERT, J. B. M., MARKS, D. J., ROBERTS, R. C. and SIMS, D.: Heat capacities of propylene oxide and of some polymers of ethylene and propylene oxides, 401
BIANCHI, U.: *See* CUNIBERTI, C. and BIANCHI, U.
BINNS, G. L., FROST, J. S., SMITH, F. B. and YEADON, E. C.: Allotropy of cyclic tris(ethylene terephthalate), 583
BIRD, R. J., MANN, J., POGANY, G. and ROONEY, G.: Electron microscope studies of the fracture of glassy polymers, 307
BIRLEY, A. W.: review of *Mechanics of Polymer Melt Processing*, 638
BLACKADDER, D. A. and SCHLEINITZ, H. M.: The dissolution and recrystallization of polyethylene crystals suspended in various solvents, 603
BOOTH, C. and PRICE, C.: The fractional crystallization of poly(ethylene oxide), 85
— *See* ALLEN, G., BOOTH, C. and PRICE, C.
BRADFIELD, G.: Bulk modulus measurements on polymers at high temperatures, 429
BRUCE, J. MALCOLM and HURST, S. J.: The polymerization of some ethylene oxides by the diethylzinc–water system, 1
BRUCK, S. D.: Thermal degradation of piperazine polyamides II—Poly(terephthaloyl piperazine), poly(terephthaloyl 2-methylpiperazine), and poly(isophthaloyl *trans*-2,5-dimethylpiperazine), 231
— — III—The effect of ultra-violet irradiation on poly(isophthaloyl *trans*-2,5-dimethyl-piperazine), 321
BUSFIELD, W. K.: The polymerization of trifluoracetaldehyde initiated by tertiary bases; the effect of temperature on the monomer–polymer equilibrium, 541

CLEGG, B.: *See* BEAUMONT, R. H. *et alii*
CLEMSON, C. S.: *See* BAKER, C. H., CLEMSON, C. S. and ALLEN, G.
CONNOR, T. M.: Proton spin–lattice relaxation in polyethylene oxide. Spin-diffusion and methyl group rotation, 426
COOPER, D. G. T.: *See* BAWN, C. E. H., COOPER, D. G. T. and NORTH, A. M.
COOPER, W.: review of *Elastomer Stereospecific Polymerization*, 537
CORNET, C. F. and VAN BALLEGOOIJEN, H.: Rapid turbidimetric determinations of theta conditions, 293
COWIE, J. M. G.: Estimation of unperturbed polymer dimensions from viscosity measurements in non-ideal solvents, 487

CUNIBERTI, C. and BIANCHI, U.: Thermodynamics of mixing: excess volumes in polyisobutylene–solvent systems, 151

DALTON, F. L.: *See* BARTLETT, (Miss) J. A. and DALTON, F. L.
DAVID, C.: *See* GEUSKENS, G., LUBIKULU, J. C. and DAVID, C.
DELMAS, G. and PATTERSON, D.: The temperature dependence of polymer chain dimensions and second virial coefficients, 513
DUCK, E. W.: *See* JENKINS, D. K., TIMMS, D. G. and DUCK, E. W.

EARLAND, C. and STELL, J. G. P.: Formation of new crosslinkages in proteins by oxidation of the tyrosine residues with potassium nitrosyldisulphonate, 549
EASTMOND, G. C.: review of *Polymers: Structure and Bulk Properties*, 252
— review of *Physics of Non-crystalline Solids*, 539

FINCH, C. A.: review of *The Macromolecular Chemistry of Gelatin*, 251
— review of *Exposés de Chimie Macromoléculaire. Structure Chimique des Polyosides*, 536
FISCHER, E. W. and HINRICHSEN, G.: On the reliability of the gradient column method for measuring densities of polymer single crystals, 195
FROST, J. S.: *See* BINNS, G. L., FROST, J. S., SMITH, F. B. and YEADON, E. C.
FUJITA, HIROSHI: *See* YAMAMOTO, KAZUHIKO and FUJITA, HIROSHI
— *See* YAMAMOTO, K., TERAMOTO, A. and FUJITA, H.

GEE, G.: The thermodynamic analysis of the effect of pressure on the glass temperature of polystyrene, 177
— The present status of the theory of rubber elasticity, 373
— *See* BEAUMONT, R. H., *et alii*
GEUSKENS, G., LUBIKULU, J. C. and DAVID, C.: Proton resonance spectra and tacticity of poly-2-vinylpyridine, 63
GUARISE, G. B.: Polymerization of styrene under pressure, 497

HAVRILIAK Jr, S. and ROMAN, N.: The infra-red absorption characteristics of syndiotactic poly(methyl methacrylate) from 1 050 cm^{-1} to 1 300 cm^{-1}, 387
HAWORTH, SUSAN: *See* JEFFRIES, R. and HAWORTH, SUSAN
HAYASHI, K.: *See* UENO, K., HAYASHI, K. and OKAMURA, S.
HERBERT, J. B. M.: *See* BEAUMONT, R. H. *et alii*
HILLIER, K. W.: review of *Testing of Polymers*, Vol. I, 535
HINRICHSEN, G.: *See* FISCHER, E. W. and HINRICHSEN, G.
HLADKÝ, E., KUČERA, M. and MAJEROVÁ, K.: Influence of the dielectric constant on the rate of solution polymerization of trioxan, 587
HOBIN, T. P.: Model polyethers III—Acid-catalysed condensation and degradation reactions of hydroxyl-terminated ethers, 223
— Regular alkylene ether copolymers, 367
— and LOWSON, R. T.: Model polyethers II—Synthesis by polycondensation of glycols in the presence of alcohols, 217
HOWELLS, E. R.: review of *Polymer Mechanics*, Vol. I, No. 1, 535
— review of *Thermoanalytical Methods of Investigation*, 536
HUNT, S. E.: *See* LINDSEY, A. S., HUNT, S. E. and SAVILL, N. G.
HURST, S. J.: *See* BRUCE, J. MALCOLM and HURST, S. J.
HYDE, A. J.: A comparison between real polymer dimensions in solution and the behaviour predicted from models, 459

INGRAM, P., KIHO, H. and PETERLIN, A.: Electron diffraction and microscopy of deformed polymer crystals III—Annealing, 135

JEFFRIES, R. and HAWORTH, SUSAN: An infra-red–deuteration study of the grafting of vinyl polymers into nylon films, 563
JENKINS, D. K., TIMMS, D. G. and DUCK, E. W.: *cis*-Polymerization by a three-component system containing nickel(0), 419

KENDRICK, E.: *See* VON ETTINGSHAUSEN, O. G. and KENDRICK, E.
KENWORTHY, J. G.: review of *High Resolution Nuclear Magnetic Resonance Spectroscopy*, Vol. II, 538
KIHO, H.: *See* INGRAM, P., KIHO, A. and PETERLIN, A.
KRIGBAUM, W. R., BALTA, Y. I. and VIA, G. H.: A reversible change in long period spacing with temperature, 61
KUČERA, M.: *See* HLADKÝ, E., KUČERA, M. and MAJEROVÁ, K.

LEDWITH, A.: review of *Organic Compounds with Nitrogen–Nitrogen Bonds*, 639
LINDSEY, A. S., HUNT, S. E. and SAVILL, N. G.: A polymeric enzyme analogue based on nicotinamide, 479
LOAN, L. D.: review of *Proceedings of N.R.P.R.A. Jubilee Conference Cambridge 1964*, 253
LOWSON, R. T.: *See* HOBIN, T. P. and LOWSON, R. T.
LUBIKULU, J. C.: *See* GEUSKENS, G., LUBIKULU, J. C. and DAVID, C.

MACNULTY, B. J.: Some polymers of substituted acetylenes, 275

MAGILL, J. H.: *See* MATSUBARA, I. and MAGILL, J. H.
MAJEROVÁ, K.: *See* HLADKÝ, E., KUČERA, M. and MAJEROVÁ, K.
MALCOLM, B. R.: Structural changes and molecular forces in a compressed synthetic polypeptide monolayer, 595
MANDELKERN, L.: *See* BAKER, C. H. and MANDELKERN, L.
MANN, J.: *See* BIRD, R. J., MANN, J., POGANY, G. and ROONEY, G.
MARKS, D. J.: *See* BEAUMONT, R. H. *et alii*
MATSUBARA, I. and MAGILL, J. H.: An infra-red study of the interaction of polyamides with iodine in iodine–potassium iodide solution, 199
MATSUO, MASATO: Observation of crazes in ABS-polymer and high-impact polystyrene under the electron microscope, 421
MEARES, P.: review of *Crystalline Olefin Polymers*, 251
MELIA, T. P.: Thermodynamic data for the system formaldehyde–polyoxymethylene, 640
MORTON, T. H.: review of *Flammfestmachen von Kunststoffen*, 582
MUFTI, A. S. and POLLER, R. C.: The stabilization of poly(vinyl chloride) by organotin maleates, 641

NARKIS, N. and REBHUN, M.: Ageing effects in measurements of polyacrylamide solution viscosities, 507
NORTH, A. M.: review of *Mechanisms of Electron Transfer*, 639
— *See* BAWN, C. E. H., COOPER, D. G. T. and NORTH, A. M.

OKAMURA, S.: *See* UENO, K., HAYASHI, K. and OKAMURA, S.

PATTERSON, D.: *See* DELMAS, G. and PATTERSON, D.
PETERLIN, A.: *See* INGRAM, P., KIHO, H. and PETERLIN, A.
PINNOCK, P. R. and WARD, I. M.: The temperature dependence of viscoelastic behaviour in polyethylene terephthalate, 255
— *See* ALLISON, S. W., PINNOCK, P. R. and WARD, I. M.
POGANY, G.: *See* BIRD, R. J., MANN, J., POGANY, G. and ROONEY, G.
POLLER, R. C.: *See* MUFTI, A. S. and POLLER, R. C.
POWELL, A.: The influence of the molecular size distribution within a liquid on the viscous flow of the liquid, 91
PRICE, C.: review of *Conformation of Polyethylene and Polypropylene*, 638
— *See* BOOTH, C. and PRICE, C.
— *See* ALLEN, G., BOOTH, C. and PRICE, C.

REBHUN, M.: *See* NARKIS, N. and REBHUN, M.
REYNOLDS, R. J. W.: review of *A History of the Modern British Chemical Industry*, 537
— review of *The Identification of Plastics and Rubbers*, 539
ROBERTS, R. C.: *See* BEAUMONT, R. H. *et alii*
ROBINSON, V. J.: *See* BAMFORD, C. H. and ROBINSON, V. J.
ROETLING, J. A.: Yield stress behaviour of isotactic polypropylene, 303
ROMAN, N.: *See* HAVRILIAK Jr, S. and ROMAN, N.
ROONEY, G.: *See* BIRD, R. J., MANN, J., POGANY, G. and ROONEY, G.

SAVILL, N. G.: *See* LINDSEY, A. S., HUNT, S. E. and SAVILL, N. G.
SCHLEINITZ, H. M.: *See* BLACKADDER, D. A. and SCHLEINITZ, H. M.
SCHURZ, J. and TRITTHART, H.: Supermolecular gels in cellulose nitrate solutions, 475
SIMS, D.: *See* BEAUMONT, R. H. *et alii*
SMITH, F. S.: *See* BINNS, G. L., FROST, J. S., SMITH, F. S. and YEADON, E. C.
STELL, J. G. P.: *See* EARLAND, C. and STELL, J. G. P.

TERAMOTO, A.: *See* YAMAMOTO, K., TERAMOTO, A. and FUJITA, H.
THOMAS, D. K.: Network scission processes in peroxide cured methylvinyl silicone rubber, 99
— Limitations of the Tobolsky 'Two Network' theory in the interpretation of stress-relaxation data in rubbers, 125
— The crosslinking of methylvinyl silicones with organic peroxides, 243
TIMMS, D. G.: *See* JENKINS, D. K., TIMMS, D. G. and DUCK, E. W.
TRITTHART, H.: *See* SCHURZ, J. and TRITTHART, H.
TURNER-JONES, A.: Cocrystallization in copolymers of alpha olefins II—Butene-1 copolymers and polybutene type II/I crystal phase transition, 23

UENO, K., HAYASHI, K. and OKAMURA, S.: Studies on radiation-induced ionic polymerization III—Polymerization of styrene at room temperature, 431
— — — — IV—Polymerization of styrene in solution at room temperature, 451
UPADHYAY, J., WALLACE, J. B. G. and WASSERMANN, A.: Proton acceptor properties and electrical conductance of deeply coloured cyclopentadiene polymers, 465

VAN BALLEGOOIJEN, H.: *See* CORNET, C. F. and VAN BALLEGOOIJEN, H.
VIA, G. H.: *See* KRIGBAUM, W. R., BALTA, Y. I. and VIA, G. H.
VON ETTINGSHAUSEN, O. G. and KENDRICK, E.: Polythioacetone, 469

WALLACE, J. B. G.: *See* UPADHYAY, J., WALLACE, J. B. G. and WASSERMANN, A.

WARD, I. M.: *See* PINNOCK, P. R. and WARD, I. M.
— *See* ALLISON, S. W., PINNOCK, P. R. and WARD, I. M.
WASSERMANN, A.: *See* UPADHYAY, J., WALLACE, J. B. G. and WASSERMANN, A.
WETTON, R. E. and ALLEN, G.: The dynamic mechanical properties of some polyethers, 331
WONACOTT, A. J.: *See* ARNOTT, STRUTHER and WONACOTT, A. J.
YAMAMOTO, KAZUHIKO and FUJITA, HIROSHI: Limiting viscosity number versus molecular weight relations for polyhexamethylene oxide, 557
— TERAMOTO, A. and FUJITA, H.: Limiting viscosity number versus molecular weight relations for polyoxacyclobutane, 267
YEADON, E. C.: *See* BINNS, G. L., FROST, J. S., SMITH, F. S. and YEADON, E. C.